PRACTICAL SYNTHESES OF IRIDIUM COMPLEXES FOR PHOTOCATALYSIS AND THE DEVELOPMENT OF METHODOLOGY TO ACCESS FUNCTIONALIZED AMINO ACIDS

By

KIP TEEGARDIN

Bachelor of Science in Chemistry-Biochemistry
University of Arkansas-Fort Smith
Fort Smith, Arkansas
2012

Submitted to the Faculty of the
Graduate College of the
Oklahoma State University
in partial fulfillment of
the requirements for
the Degree of
DOCTOR OF PHILOSOPHY
December, 2018

PRACTICAL SYNTHESES OF

IRIDIUM COMPLEXES FOR PHOTOCATALYSIS AND THE DEVELOPMENT OF

METHODOLOGY TO ACCESS FUNCTIONALIZED AMINO ACIDS

Dissertation Approved:

Dr. Jimmie Weaver

Dissertation Adviser

Dr. Richard A. Bunce

Dr. Laleh Tahsini

Dr. Christopher Fennell

Dr. Junpeng Deng

ACKNOWLEDGEMENTS

In 2009, I made it my mission to gain an academic degree that will challenge me in every aspect of my life, and in return mold me into a valuable and productive individual. During the course of my academic career, I would like to recognize and acknowledge individuals and organizations that helped make this possible.

I first would like to thank the instructors at University of Arkansas-Fort Smith for guiding me into a STEM field, and thank you again for preparing me for graduate school. Thank you Kappa Alpha Order-Zeta Rho for teaching me about business fundamentals and for all the leadership training along the way. Thank you Todd Phipps for all your help, while I worked as a lab tech, it was the highlight of my time at UAFS. Thank you Dr. Becky and Dr. Belcher for pushing me to apply to graduate school. Most importantly, I would like to recognize Dr. Barabote for the opportunity as a REU student with University of Arkansas. I attempted to apply the advice you gave me in everything I did. You reminded me to maintain a constant learning attitude while in graduate school. Also, I am proud of what we accomplished in a short period of time and I am glad it amounted to a publication.

As a graduate student, I am extremely thankful to have had the chance to work next to some of the most driven yet talented individuals. I was fortunate to be part of a great research team, and I would like to show appreciation to the first members of the Weaver group Aman, Kamal, Sameera and Anu. I cannot thank you enough for all your help and all your words of encouragement. I will never forget the training you gave me Anu. It was a solid

foundation that took me to the next level. Thank you newer members Sonal, Manjula, Jon, Ryne, and Mo. It was beneficial to engage daily in thoughtful discussions about our research. I hope I was of some help to you and to your projects.

Thank you Chen for being one of my greatest friends here at OSU. I will always miss the campus lunches and the weekend get-togethers. Also, thank you for all the chemistry discussions and debate. I am proud of you and I wish you luck in all that you do. I would like to send a special thank you to the Crawfords and my buddy Kyle. You all helped me believe this dream was possible. Thank you Kyle for your input on my 5011, while being the best roommate a guy can have. Thanks Buzz for all the good times back at Bragg. I couldn't be as high speed without you. Thank you Lacey for being a productive undergraduate, and I wish you the best in pharmacy school. I would like to recognize all the staff over the last 5 years for helping me with whatever problem I had. I would like to show appreciation to my committee members for all the tough questions during my 5011, oral exam, and 6011.

Most of all I would like to thank my advisor Dr. Jimmie Weaver for all you have done for me and my family. I chose you as an advisor because I was certain that you were right there to challenge me. You made me aware that I have unique responsibilities as a synthetic chemist with a PhD, and I should be diligent in pursuing every question affecting my project. I learned to consider all other possibilities of my system when acquiring data. You have given me the ability to propose new chemical pathways and the ability to probe such pathways experimentally. Lastly, thank you for never lowering your standards. This steady expectation to achieve the highest of standards will forever with me.

Finally, I would like to thank my parents and the rest of my family for all of your support. This includes my in-laws, which have been like parents to me here in Stillwater.

This includes Gary, Susan, Jennifer, Bill. I have learned so much from you all, and will cherish the memories we shared on the ten of hearts ranch. Mer, thank you for the help with the Virginia move and the efforts to help us transition. Thank you Scorses for the encouragement and the conversations about my future. I know it has been a long road full of burdens, but now hopefully soon we can begin to gain the rewards for all of my efforts.

I would like to acknowledge my mother who always help me to keep focused and my step-father Jason for all the help on all of my pursuits. You both are perfect examples of how a family should become. I would like to thank my father and step-mother for the advice over the years and all of your support. I never had to second guess how important I was to the family. Thank you to my siblings Kayla, Courtney, Samone, Shae, and Britney. You all have made me proud to be your brother for all that you do in your own lives.

I would like to take time to appreciate my wife. Jane has been there during the harshest of times and the best of times. My success depends on you the most, and it takes a special person to put your life on hold for me. You believed in me when everyone around us did not. I want you to know I have the same faith in you, and I hope to grow together in these strides in life. Thank you for giving me Elaina our daughter. It is a privilege watching her grow up and it is fulfilling knowing together we can accomplish anything.

Name: KIP TEEGARDIN

Date of Degree: DECEMBER, 2018

Title of Study: PRACTICAL SYNTHESES OF
IRIDIUM COMPLEXES FOR PHOTOCATALYSIS AND THE
DEVELOPMENT OF METHODOLOGY TO ACCESS
FUNCTIONALIZED AMINO ACIDS

Major Field: CHEMISTRY

Abstract: Incorporation of fluorine into molecules can result in enhanced properties of functional molecules in a variety of fields. As such, there is great interest to synthesize organofluorines. Despite substantial progress, direct fluorination strategies are often unselective. Often the simplest compounds are a challenge to synthesize. This problem is magnified when multiple fluorines are located on one arene. An alternative approach to the synthesis of multifluorinated arenes is to start with a perfluoroarene, in which every possible position has been fluorinated, and then functionalize the undesired C–F bonds. This approach has been pioneered by Swartz, Milstein, and Aizenberg. More recently, the Weaver group has researched new methodology for the selective removal of fluorine from fluorinated arenes. The key C–F fragmentation relies on the visible light mediated photocatalytic electron transfer from a mild tertiary amine reductant. This has been a substantial advancement for the field of C–F functionalization, and has revealed two needs preventing further advancement. Namely, there is a need to increase access to both Ir-based photocatalysts and highly fluorinated building blocks. Notably, thousands of other photocatalytic reactions have emerged utilizing ruthenium and iridium photocatalysts. Since these photocatalysts play a vital role in such reactions, we describe an improved synthesis to a class of homoleptic iridium (III) based complexes that allow rapid access to these compounds in high yields. Using a well-known method, we expanded our photocatalyst library by synthesizing a range of hetereoleptic complexes. Additionally, we report their photophysical and electrochemical properties. Later, we report a modified method, which has been applied to homoleptic complexes to obtain multigram quantities of the photocatalyst in high purity, without the use of a column, and with excellent recovery of excess ligand in high yield, substantially enhancing access to this class of photocatalyst. In an application of these complexes, we developed a photocatalytic reductive coupling of aryl bromides with a broad set of alkenes. We next developed a method that provided fluorinated amino acid building blocks via nucleophilic aromatic substitution of highly fluorinated (hetero)arenes with an oxazolone enolate. Moreover, we demonstrated the utility in a one pot synthesis of medicinally relevant 2-aminohydantoins. We further explored the reactivity of the enolate generated from the alpha amino esters. We showed that the monoanion enolate was a competent nucleophile that could undergo catalytic Michael addition of α-amino esters. We also provided insight into the governing principles, which resulted in an expansion of the scope. The study concludes with a late-stage functionalization of peptidic γ-secretase inhibitor, DAPT, which highlights the power of the method for direct functionalization of biologically relevant peptides.

TABLE OF CONTENTS

Chapter Page

Chapter Page

Chapter Page

LIST OF TABLES

Table Page

LIST OF FIGURES

Figure Page

Figure Page

LIST OF SCHEMES

Scheme Page

Scheme Page

CHAPTER I

INTRODUCTION

1.1 *Strategies for the synthesis of fluorinated aromatics*

Fluorinated compounds are extremely important and are highly valued in a variety of fields, namely, pharmaceuticals,[1] agrochemicals,[2] and industrial applications.[3] This is due to the ability of fluorine to substantially alter the properties of molecules in these various applications.[4] Below **Scheme 1.1** illustrates several examples. Although many applications rely on the use of fluoroaromatics, none are naturally occurring,[4] thus they must be synthesized. In contrast to their importance, there is a relative dearth of useful methods that rapidly yield multifluorinated arenes.

Scheme 1.1 Examples of aryl fluoride applications

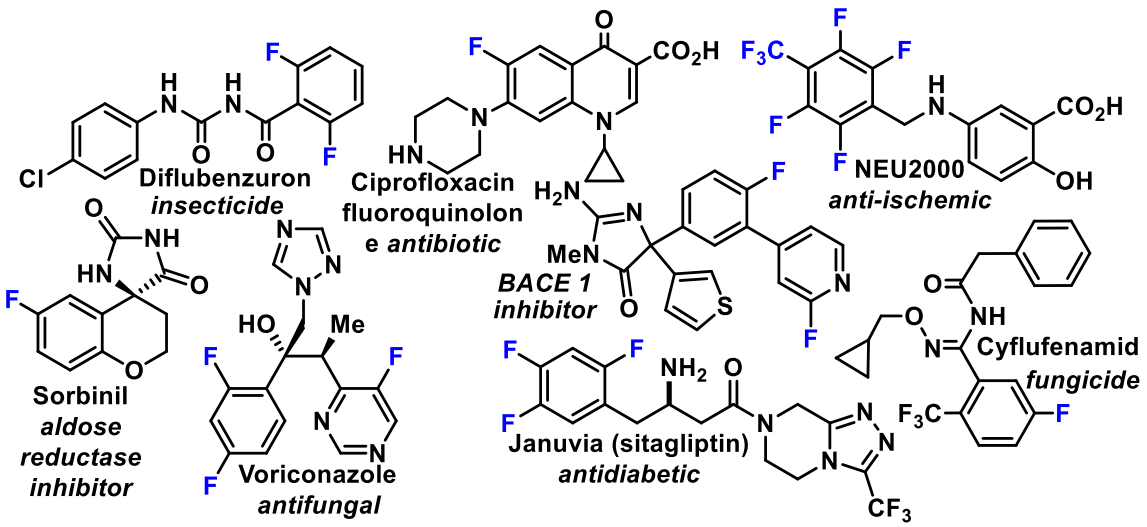

One potential synthetic strategy is the selective installation of fluorine on an arene (**Scheme 1.2**, left). This approach is popular,[5] but often can be challenging to accomplish multifluorination. In most cases, the appropriate functional group must be pre-installed for every fluorination pattern desired and as a consequence the reaction steps become lengthy synthetic sequences (**Scheme 1.2**, right).[5] These apparent drawbacks make it less than ideal to rapidly synthesizing analogs.

Scheme 1.2 Strategies in synthesis of fluorinated aromatics

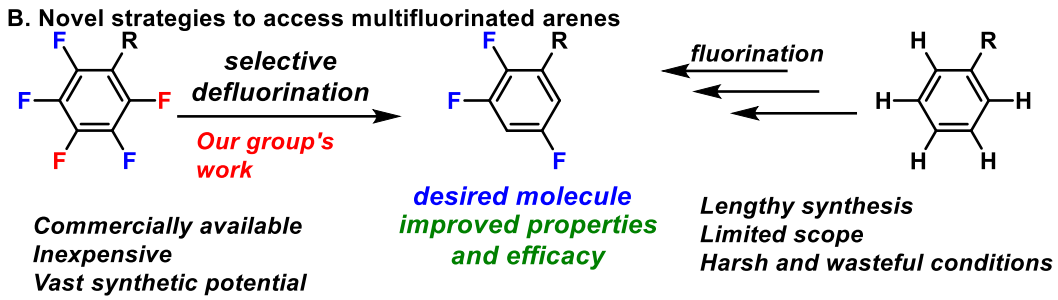

For example, in 2010[6] Codexis and Merck described a synthesis to Januvia, an antidiabetic drug, in high yield with an excellent enantiomeric excess (**Scheme 1.3a)**. However, while not performed by Merck, synthesis of the fluorinated carboxylic acid (**Scheme 1.3b**) became lengthy and cumbersome progressing through a series of harsh and potentially dangerous reactions to yield the starting material for Merck.

Scheme 1.3 Overall synthesis of Januvia

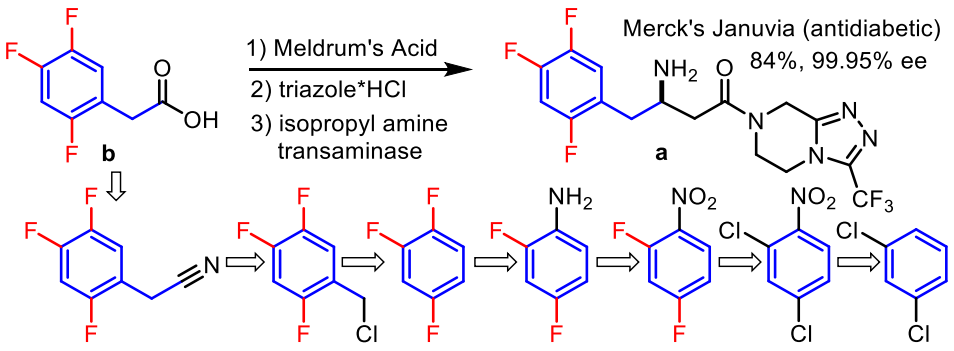

Despite the limitations, a variety of reactions have been developed to synthesize aryl fluorides. Examples include substitution reactions with existing halogenated arenes (**Scheme 1.4a**), cross-coupling reactions with organometallics (**Scheme 1.4b**), and C–H activations *via* fluorination with the help of preexisting directing groups (**Scheme 1.4c**). While beyond the scope of this discussion, Campbell and Ritter discuss C–F bond forming reactions, but this can be reviewed within this article.[7]

Scheme 1.4 Installation of fluorine to an aryl substrate

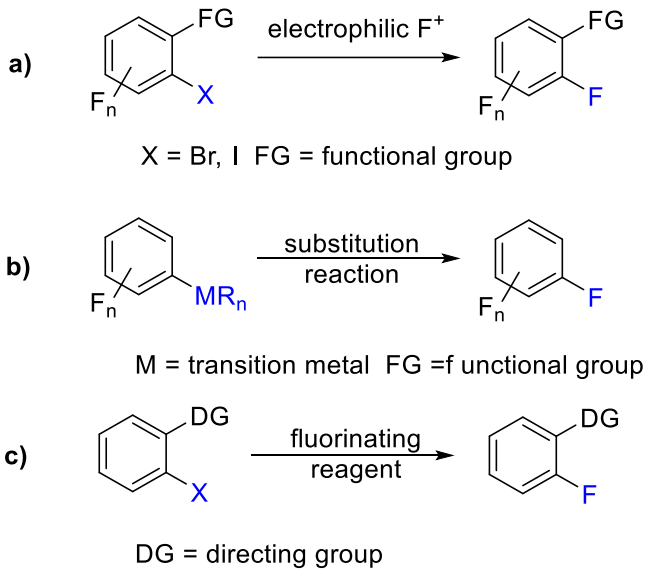

C–F functionalization to prepare highly fluorinated or perfluorinated (hetero)arenes is an attractive alternative to the aforementioned approaches to arylfluorides, and is proving to be exceptionally fruitful. The advantage stems from the fact that perfluorinated arenes are relatively inexpensive and already possess the difficult to install fluorines in the desired locations. The potential advantage of C–F functionalization has been recognized by others, and advancements have been made in the field.[8] Taken in conjunction with recently developed photocatalytic C–F functionalization,[8-10] considerable access to these important motifs are now obtainable.

In regards to C–C bond formation this chemistry possesses many challenges,[11] with unavoidable challenge being that the aryl C–F bond is the shortest and strongest among the halogens (**Figure 1.1**).[12] The C–F bond also presents significant obstacles due to its relative inertness towards traditional transition metal complexes used to activate aryl halides, and active complexes are rare.[5] Complexes with metal centers of Ni, Pt, and Pd can be identified as the major contributors in C–F activation, and usually undergo a catalytic cycle *via* a rate determining oxidative addition step into the C–F bond. Later improvements emerged that are assisted by various directing groups.[9]

Figure 1.1 Selected C–X bond energies and lengths

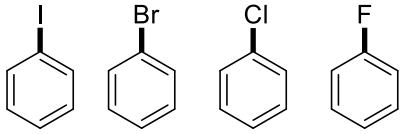

Bond energy (kcal/mol)	**67**	**84**	**97**	**127**
Bond length (Å)	**2.14**	**1.91**	**1.76**	**1.35**

1.2 *Ar_F building blocks and nucleophilic aromatic substitution (S_NAr)*

Another mechanistic topic that is extremely useful is nucleophilic aromatic substitution or S_NAr (**Scheme 1.5**). Generally, this class of substitution consists of an electrophilic aromatic ring which is attacked by a suitable nucleophile. Upon nucleophilic attack, a carbanion intermediate (Meisenheimer complex) is formed, and finally collapses kicking out the halide leaving group, providing the substituted product.

Scheme 1.5 Typical S_NAr mechanism

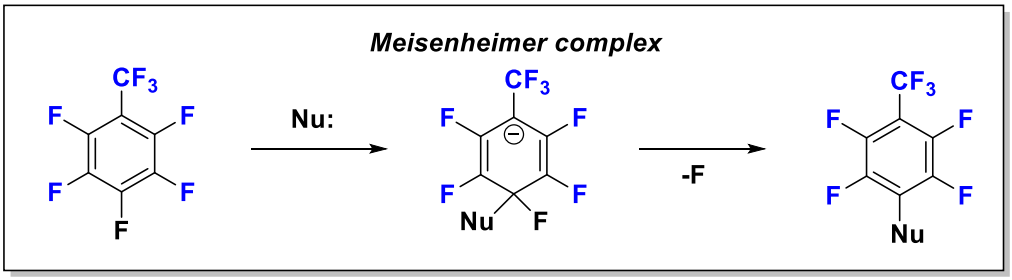

Nucleophilic aromatic substitution has been used to introduce oxygen, nitrogen, carbon, and sulfur based nucleophiles.[13] The key to a successful S_NAr reaction begins with stabilization of the anion, which is electronically influenced by the groups attached to the ring. The electron withdrawing groups on a perfluoroarene for example increase the rate of the reaction by stabilizing the anion both inductively and potentially by resonance, and make the reaction possible. Generally, the S_NAr reactivity of Caryl–X (where X = F, Cl, Br, I) bonds decrease in the order of fluoride > chloride > bromide > iodide, which the opposite is that observed for aliphatic halides in a S_N2 reaction. This trend is thought to reflect the fact that attack of the arene by the nucleophile is the most challenging step, and is accelerated by the small, extremely electronegative fluoride.

While the S_NAr reaction has been extensively explored on many substrates, perfluoroarenes are conspicuously absent from most exploration.[14-17] One potential explanation, is that until recently the remaining C–F bonds of a perfluoroarene would amount to synthetic dead ends, thus, little work was done to explore this reaction of great synthetic potency. Out of the possible nucleophiles, we are most interested in coupling partners that will create new C–C bonds selectively. Our group developed reaction conditions that facilitate per- and polyfluoroarylation of Medrum's acid[18] (**Scheme 1.6**) to generate a completely new class of synthetically versatile fluorinated building blocks. The reaction is controlled by taking advantage of the low nucleophilicity of the resulting arylated enolate salts which allows, for the first time, the selective monoarylation of Meldrum's acid to give access to tertiary carbon centers. While alkylation proved

challenging, quaternarization of the α-carbon could be accomplished by reversing the order of events, i.e. alkylation of Meldrum's acid, followed by arylation. Given the demand for partially fluorinated arenes in various fields, we were satisfied with the results. Later in Chapter IV we will review a reaction we developed shortly after this report appeared involving polyfluoroarylation of oxazolone, an amino acid surrogate, which gives rise to polyfluorinated amino acid derivatives.

Scheme 1.6 Polyfluoroarylation of Meldrum's acid

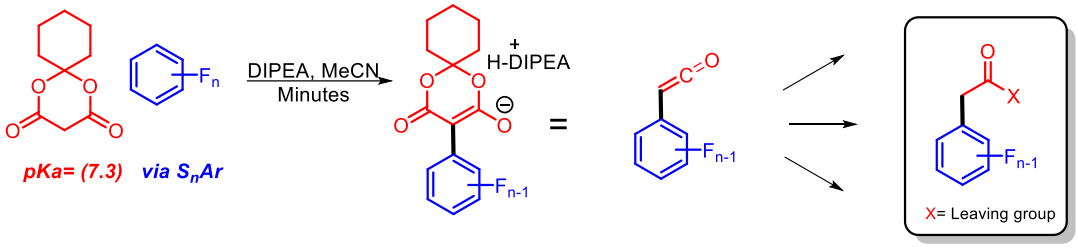

1.3 *Introduction to photocatalysis*

Another mechanistically intriguing mode of reactivity for polyfluorinated arenes is electron transfer facilitated functionalization. These types of mechanisms take advantage of the energetically accessible LUMO which looks primarily like the π* orbital of the polyfluorinated arene. Upon addition of an electron to the π* orbital, an unstable radical anion is formed, which undergoes fragmentation to extrude fluoride and generates an aryl radical plus a fluoride. The initial electron transfer is accomplished *via* photocatalysis, and the next section is a brief introduction to photocatalysis, a description of the electrochemical properties of the photocatalyst, and discussion of how photocatalysis is applied to halogenated arenes to obtain reactive intermediates.

A primary objective of organic chemistry is to discover or invent new methodologies that enable the assembly of molecules of substantial value. Furthermore, any new methodology should be aware of safety, and environmental concerns, and should deliver products with haste. Modern concepts to develop such methodology consist of discovering catalytic mechanisms that will enable a broad range of chemical transformations to take place.[19] Lewis acid catalysis,[20] organocatalysis,[21]

and transition metal catalysis[22] are all examples of such catalytic tools. Among transition metal catalysis, photocatalytic strategies have evolved. Photocatalysis involves the use of visible light to deliver or strip an electron away, also the catalyst can undergo energy transfer events to promote reactivity from common functional groups. For more than 30 years, transition metal complexes have been known to mediate these single-electron transfers (SET) and have led to SET-initiated polymerization reactions,[23] dye-sensitized solar cells,[24] and light emitting diodes.[25] However, it is important to note there are a growing number of examples of visible light absorbing organic dyes that facilitate photocatalysis, but are not the subject of this thesis.[26]

Early reports of transition metal-based photocatalytic mediated organic transformations utilized Ru-based photocatalysts such as *tris*(2,2′-bipyridine) ruthenium(II) or $Ru(bpy)_3^{2+}$, which when excited by visible light undergoes a metal to ligand charge transfer (MLCT) and facilitates one-electron oxidation or reduction of the complex.[27] In 1981, Pac and co-workers[28] utilized a ruthenium photocatalyst in one of the first reports of small organic molecule activation by these type of complexes. In this paper, they reported the reduction of electron deficient alkenes using a stoichiometric reductant. Again in 1990, Fukuzumi[29] described reductive dehalogenation of phenacyl bromide utilizing this complex. Over the last few years, the number of reported organic transformations that utilize transition metal photocatalysts has increased steadily.

Recently in 2008, MacMillian[30] reported direct asymmetric alkylation of aldehydes and Yoon[31] reported [2+2] cycloadditions of enones both utilizing $Ru(bpy)_3Cl_2$ modernizing transition metal photochemistry. In 1985, King and coworkers reported the synthesis and characterization of neutral *fac*-*tris*-phenylpyridinato iridium(III), ($Ir(ppy)_3$), which constitutes the parent photocatalyst[32] of a complimentary class of photocatalysts.[33]

Notably, this complementary group of iridium complexes are *tris*-cyclometalated d-6, 18-electron complexes that are known to be remarkably stable in the ground state. However, upon absorption of photons of the appropriate energy-in the blue region of the visible spectrum, the complexes undergo excitation (**Scheme 1.7**). While an excited singlet state is the initial outcome,

it rapidly relaxes to a long-lived, triplet state.[34] The triplet state has undergone a metal-to-ligand charge transfer. By virtue of charge transfer, it can serve as both a potent oxidant and reductant. By knowing the excited state redox potentials of $E_{1/2}$(Ir+/Ir*) and $E_{1/2}$(Ir*/Ir-) complexes, one can begin to rationally construct novel chemical transformations provided the relevant potentials of substrates are known.

Scheme 1.7 Energy and electron transfer processes in tris-cyclometalated iridium complexes

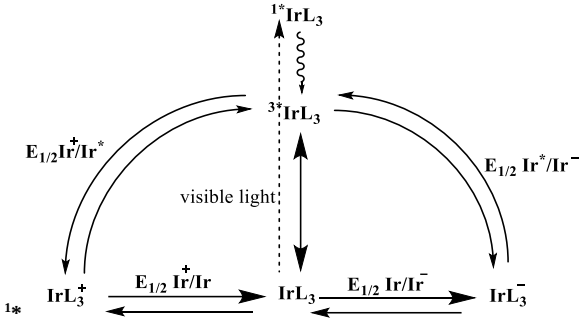

IrL_3 represents the higher energy spin allowed excited state and

$^{3*}IrL_3$ represents the lowest spin forbidden excited state

The neutral tris-homoleptic Ir-complexes have also proved to be of substantial value in synthesis and lighting applications.[35-36] The complex *fac*-Ir(ppy)$_3$ has more reducing power then Ru(bpy)$_3$Cl$_2$ and a longer excited state lifetime.[37] In 2012, Stephenson[37] subsequently presented Ir(ppy)$_3$ as a proficient complex for the dehalogenation of alkyl, alkenyl, and aryl iodides. In 2014, MacMillan also used various neutral complexes, demonstrating that differences in properties result in differences in reactivity.[31] Recently other groups,[38] including our own,[39-46] have utilized *fac*-Ir(ppy)$_3$ and its derivatives, in order to perform a series of other powerful transformations with high catalytic efficiencies. Later in Chapter III, work done by Amandeep Arora and myself, will be described, in which we demonstrate a photocatalytic reductive coupling of aryl bromides with a broad range of alkenes.

In 2014, our group described a photocatalytic hydrodefluorination (HDF) reaction of perfluoroarenes. The method amounted to a convenient way to perform outer-sphere electron

transfers using $Ir(ppy)_3$. Understanding the general mechanism of this reaction, its significance, and the key intermediates, we can start to visualize a vast number of transformations that could undertake by selecting the right coupling partner.

The HDF reaction starts with the absorption of photons by the photocatalyst (**Scheme 1.8,** eq 1). The catalyst is promoted to an excited state and rapidly undergoes intersystem crossing to give the long-lived triplet state. Again, here the photocatalyst can act as both an oxidant or a reductant. In presence of this photoredox catalyst, an electron donation from diisopropylethyl amine (DIPEA, eq 4) while slightly endothermic results in an amine radical cation (eq 6) and a reduced photocatalyst. Compared to the reduced photocatalyst, a perfluoroarene such as pentafluoropyridine (eq 2) has a slight over potential. We postulated the outer sphere electron transfer takes place from the photocatalyst to the arene (eq 3), to form the perfluoroaryl radical anion (not shown). From the meta-stable radical anion, fluoride is expelled generating an aryl radical (eq 5). The aryl radical then abstracts an H-atom from the amine (or amine radical cation) giving the HDF product (eq 7). We further explored other possible synthetic scenarios and imagined how we would control the use of this aryl radical intermediate (eq 8) and supply a new generation of conditions where the aryl radical engages and reacts with various alkenyl, aryl, and alkynyl coupling partners.

Scheme 1.8 Photocatalytic HDF reaction and interception of an aryl radical

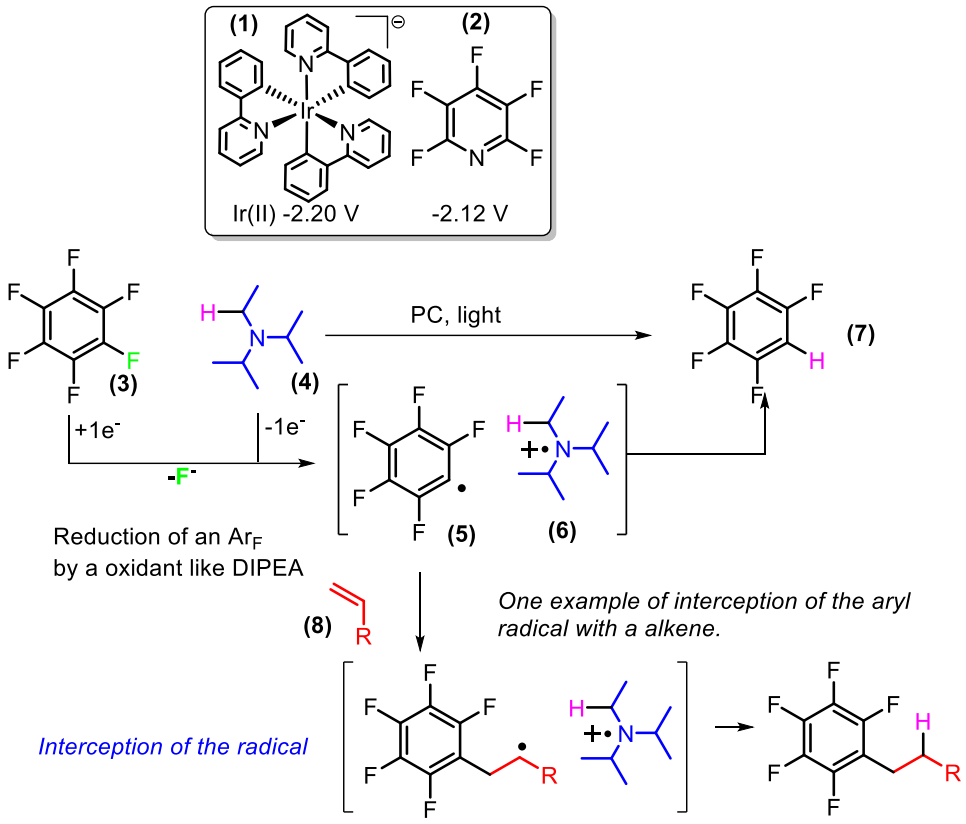

As the exploration of these photocatalysts continue, the new properties they possess will likely expand and give rise to powerful reactions. However, in our own group, we have often found the number of commercially available photocatalysts were low. Arguably, this will limit access to a handful of researchers who have these complexes, which will result in slower advances in the field. Thus, a need exists for a reliable method that delivers these powerful complexes to the organic community as a whole.

Despite a rich history of exploration of the properties of these complexes, syntheses for many the facial homoleptic variants[47] are scattered, and often lack complete chemical, photophysical, and electrochemical characterization. Aware of what was available to the scientific community, we believed it would be valuable to develop a simple and robust method to synthesize homoleptic photocatalysts. This would allow us to adjust the redox potentials and triplet state

energies of the iridium photocatalysts, and potentially give rise to new synthetic transformations that would become possible as a result of greater access to a diverse number of Ir-photocatalysts.

CHAPTER II

FACILE SYNTHESIS OF CYCLOMETALATED IRIDIUM (III) COMPLEXES FOR PHOTOCATALYSIS

2.1 *Introduction of iridium photocatalysts methodology*

A survey of the current literature revealed that there are a number of reported synthetic methods that use more expensive Ir(III) salt, $Ir(acac)_3$[48-50] or alternatively require two steps, first forming the chloro-bridged dimer, and then subsequently breaking the dimer by the addition of the third ligand. This is done even in the case of the *tris*-homoleptic-cyclometalated complexes, which is less than ideal since it requires an additional chemical step just to add the third ligand. Furthermore, a stoichiometric chloride scavenger like AgOTf is often employed[51-52] Konno reported a microwave synthesis of *tris*-cyclometalated iridium complexes, but this required a large excess of ligand (50-100 equiv) which limited the scope of the reaction to readily available ligands such as 2-phenylpyridine.[53] Therefore, working with a post-doc in the group, Dr. Anuradha Singh, we set about to develop a general and simple synthesis that would allow us to acquire the facial homoleptic iridium complexes in high chemical yield *via* a simple and selective one step process.

2.2 *Development of methodology for the synthesis of tris-homoleptic complexes*

In our initial attempt (**Table 2.1**), a glass pressure vial was charged with $IrCl_3$•nH_2O, 2-phenylpyridine, Na_2CO_3 and water and heated at 200 °C for 48 h. Unfortunately, this reaction resulted in extremely low yield (<8%) of the desired complex, $Ir(ppy)_3$. However, it was observed that the reaction was heterogeneous until temperatures reached nearly 200 °C. Concerned that even higher temperatures may be needed to ensure homogeneity, reproducibility, and faster reaction rates the remaining reactions were performed in a Parr reactor for safety purposes, allowing us to safely heat H_2O to 260 °C. Routine optimization of this reaction provided improvement in yields on increasing the equivalents of base from 1.5 to 6, 2-phenylpyridine from 3.3 to 12, and the temperature from 200 to 260 °C. Using optimized conditions (entry 3), the reaction yielded 79% of $Ir(ppy)_3$, **3a**, in just 24 h.

Table 2.1 Optimization of Reaction Conditions

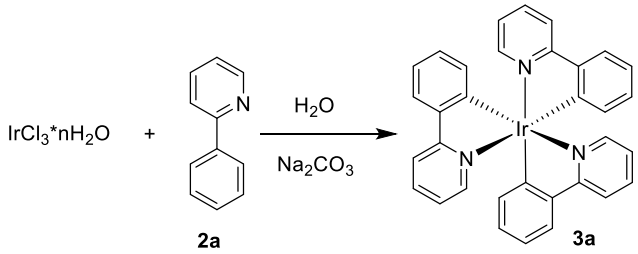

2a **3a**

entry	Na_2CO_3 equiv	equiv of **2a**	temperature	time	% yield
1	1.5 equiv	3.3 equiv	200 ^{0}C	24 h	10%
2	3.0 equiv	6.6 equiv	220 ^{0}C	48 h	22%
3	6.0 equiv	12 equiv	260 ^{0}C	24 h	79%

Pleased with this result, we next attempted to investigate the scope of the method, which required the syntheses of the requisite 2-phenylpyridine ligands **2b-g** (**Scheme 2.1**) which we hoped would lead to catalysts with a range of properties. The ligands were synthesized quite easily via Suzuki coupling of 2-chloropyridine (1 equiv) and the requisite boronic acid (1.2 equiv) with only minor modifications to the literature procedure.[52] Conveniently, the procedure could be performed outside the glovebox. In all cases, the Suzuki coupling reaction led to good yields of

the desired phenylpyridine products and in one case (**2c**) approached quantitative yields. Ligand **2h** (4-(*tert*-butyl)-2-(4-fluorophenyl)pyridine) was synthesized *via* Baran's procedure.[54]

Scheme 2.1 Ligand Synthesis

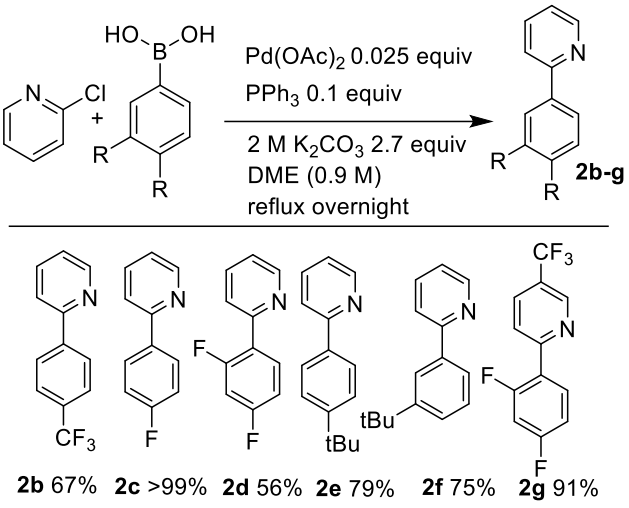

With ligands (**2a-h**) in hand, we returned to the cyclometalation reaction (**Scheme 2.2**). However, under the standard reaction conditions, several of the substrates presented problems. Upon modification of our initial conditions, yields were improved and substantial quantities were obtained. For instance, when 2-(4-*tert*-butyl-phenylpyridine) (**2e**) was subjected to the reaction conditions the expected **3e** was not formed. Rather, **3a** $Ir(ppy)_3$ along with 2-phenylpyridine, **2a**, were the primary products recovered which apparently resulted from the de-*tert*-butylation of either (or both) ligand or Ir-complex at 260 °C. However, by lowering the temperature to 200 °C we were able to suppress de-*tert*-butylation and obtain **3e** in high yield. Moreover, our initial attempts to synthesize **3c** resulted in a mixture of iridium complexes in which partial hydrolysis of fluorine had occurred. Additionally, we observed a migration of fluorine on the ring of the ligand recovered from the reaction mixture.[55] To avoid this problem, reaction with 2-(4-fluorophenyl) pyridine, **2c**, ligand was performed in the absence of sodium carbonate and at lower temperatures (200 °C for 48 h). Surprisingly, using these conditions the reaction proceeded smoothly to achieve **3c** in excellent yield. This experiment suggested that no base is required to

synthesize *tris*-cyclometalated iridium complexes and, to the best of our knowledge, this is the first report that suggests that the base is not necessary for the formation of these complexes. Thus, for the remainder of the fluorinated substrates, the reactions were carried out with no base which allowed us to acquire **3b-e**, and **3h** complexes in moderate to high yields. Compound **3h** was synthesized in 84% yield and was very recently used as a catalyst for the decarboxylative arylation of α-amino acids and α-etheral acids though its synthesis and properties had never been reported.[56] A more modest yield was observed for **3d** but is likely a result of the effectively lowered concentration of **2d**, since only 6 equivalents were used due to smaller quantities on hand. Using standard conditions, new complex, **3f**, was obtained only in trace amounts and addition of base did not prove helpful. In these cases, the major product was the choro-bridged dimer. However, **3f** was finally successfully obtained by subjecting the chloro-bridging dimer to excess ligand in the presence of AgOAc.

Scheme 2.2 Synthesis of facial homoleptic tris-cyclometalated iridium complexes

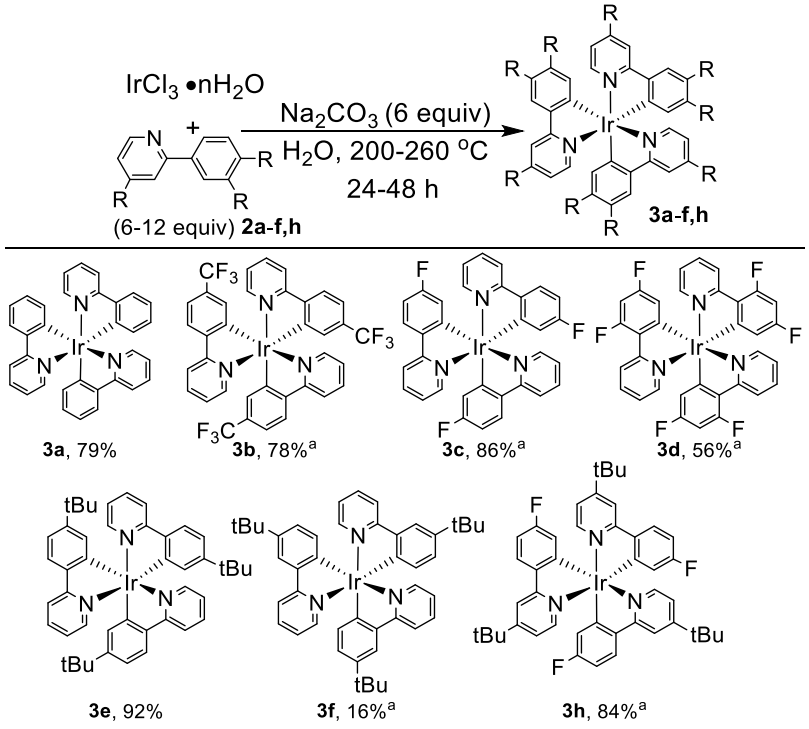

[a]No Na_2CO_3 used.

2.3 *Nonoyama's procedure: expansion of the library to hetereoleptic complexes*

While our initial focus was in the syntheses of the homoleptic iridium complexes, cationic heteroleptic iridium complexes have also proven to be effective photocatalysts and we sought to synthesize a library of cationic complexes as well. In the cationic complexes, the third 2-phenylpyridine ligand is replaced with a 2,2'-bipyridine type ligand (i.e. a neutral ligand). Thus, in order to be able to modify the third ligand, the dichloro-bridged iridium dimer was selectively synthesized according to Nonoyama's procedure,[57] which was then subsequently treated with the third, bipyridyl ligand to afford cationic heteroleptic iridium complexes (**Scheme 2.3**)[58]

Scheme 2.3 Synthesis of cationic iridium complexes

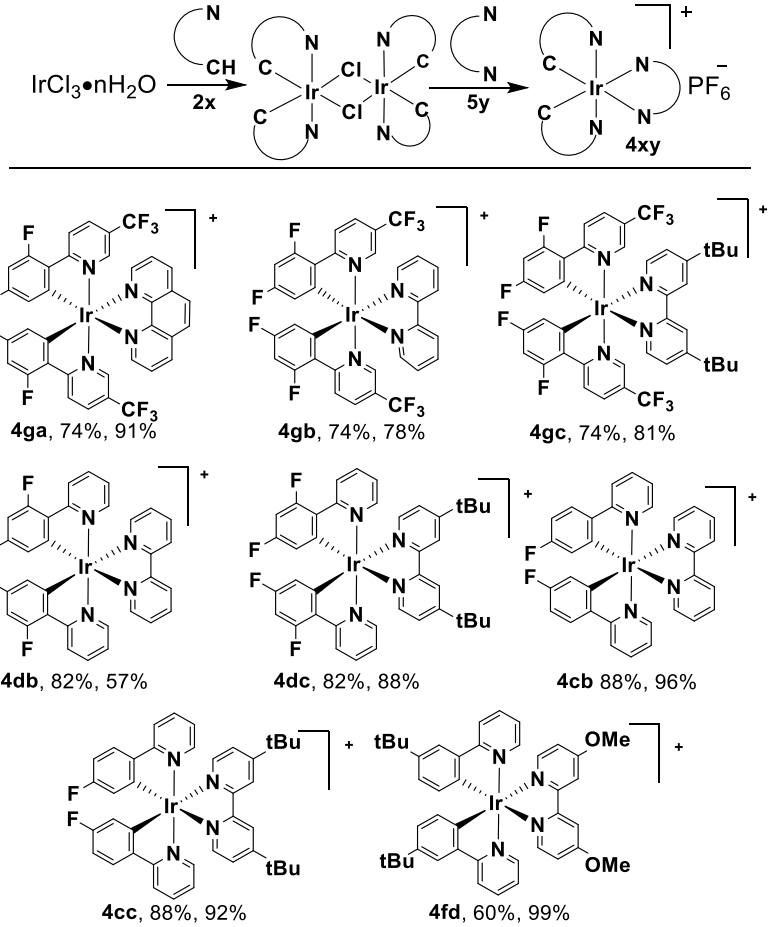

Cationic heteroleptic Ir(III) Complexes 4a-h with PF_6^- counteranion. First step yield followed by second step.

The cyclometalated iridium(III) chloro-bridged dimer $[Ir(ligand)_2Cl]_2$ was prepared by following Nonoyama's procedure[57] in which hydrated iridium(III) chloride was heated with substituted phenylpyridine ligand in a 2:1 methoxyethanol/H_2O mixture at 120 °C. Upon cooling, the chloro-bridging dimer precipitated and was filtered off. The dimer was carried on to the second step without purification. The catalysts were diversified by use of several bipyridine ligands. Finally, anion metathesis was achieved by the addition of aqueous NH_4PF_6. In this manner, complexes **4xy** (**Scheme 2.3**) were synthesized. In some cases, complexes were further purified by recrystallization. This is the first report for complexes **3f**, **4ab**, **4cb** and **4fd**. All synthesized facial homoleptic and cationic heteroleptic complexes were characterized by ^{1}H, ^{13}C, ^{19}F, ^{31}P NMR, LCMS, and new complexes by elemental analysis.

2.4 *Discussion on electrochemical properties*

With iridium complexes in hand, we next turned to the investigation of the photophysical properties of the facial homoleptic **3a-f** and the heteroleptic **4xy** complexes. Absorbance of the facial homoleptic (**Figure 2.1**) and the heteroleptic (**Figure 2.2**) complexes were measured in acetonitrile (10 μM). As depicted in **Figure 2.1** and **2.2** all the complexes show intense UV absorption bands below 325 nm-characteristic of spin allowed transition of ligand (π-π^*)[59] and weaker, broad and unresolved absorption bands in the visible region from 320-480 nm generally assigned as both allowed and spin-forbidden metal to ligand charge transfer (MLCT) transitions.[59]

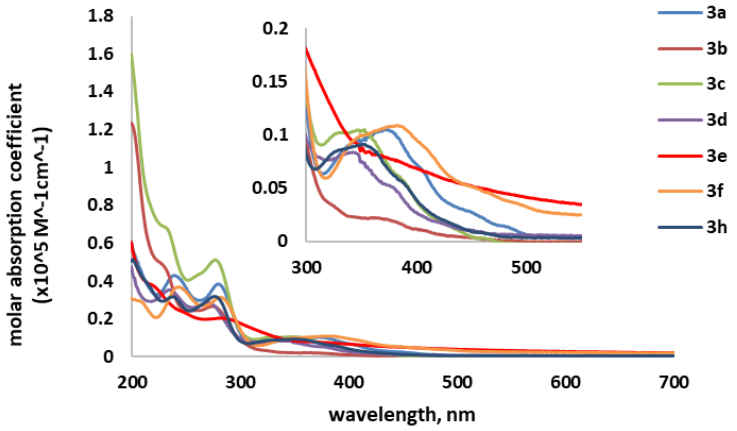

Figure 2.1 Absorbance Spectra: Facial Homoleptic Iridium Complexes: (**3a-f,h**) 10 µM in MeCN.

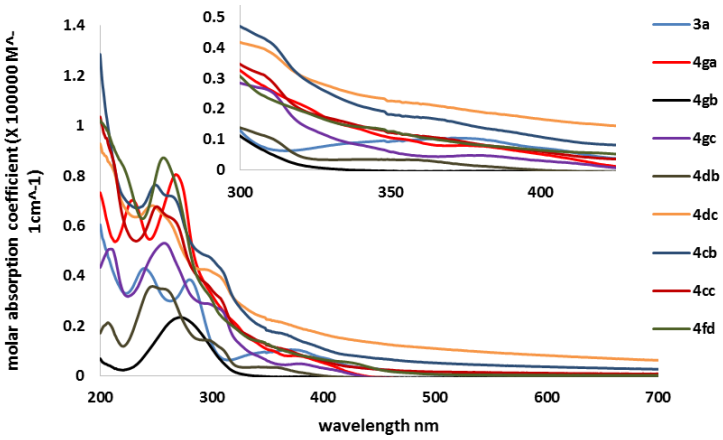

Figure 2.2 Absorbance spectra of 3a and heteroleptic iridium complexes

From a catalysis standpoint, the emission frequency corresponds to the energy available for transfer to substrates, (i.e., the triplet state energy, TSE). The complexes were excited in the region of 370-390 nm which corresponds to the metal-to-ligand charge transfer excitation (**Figure 2.3**).[60] In general, electron-withdrawing substituents on the phenyl ring such as fluorine lower the energy of HOMO resulting in larger HOMO-LUMO gaps and greater emission energies (more blue shifted). Whereas electron-donating substituents such as alkyl groups raise the HOMO energy, resulting in smaller HOMO-LUMO gaps and lower emission energies (more red shifted).[61]

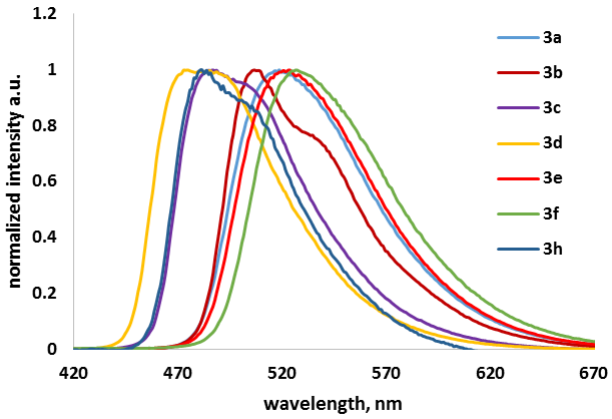

Figure 2.3 Emission spectra of facial homoleptic iridium complexes

Hay and coworkers[62] report time-dependent density functional theory calculations that illustrate, to the first approximation, the HOMO in such complexes is based primarily on the metal and metallated aryl ring, while the LUMO is largely associated with the pyridyl ring (**Scheme 2.4, eqn 1**).[62] Also park illustrated the HOMO-LUMO orbitals of $Ir(dFppy)_3$ studied the electronic properties of the complex using the B3LYP functional and the structural analysis of the optimized geometries.[63] The substituents on the aryl ring tend to affect the HOMO energy to a greater extent than the LUMO (**Scheme 2.4, eqn 2**), while the reverse is true for the pyridyl ring (**Scheme 2.4, eqn 3**).[64] These effects depend greatly on the position of the substituent within the two rings:[64-65] Electron withdrawing groups normally stabilize the orbitals by decreasing the HOMO level and/or electron donating groups on the pyridyl ring increases the LUMO which both results in a larger energy gap i.e. blue shift. Electron donating groups normally destabilize the orbitals by increasing the HOMO level and/or electron withdrawing groups on the pyridyl ring decreases the LUMO both resulting in a smaller energy gap i.e. red shift.

Scheme 2.4A HOMO/LUMO of cyclometalated Ir arylpyridine type of complexes

Scheme 2.4B The effect of substituents on the energies of orbitals

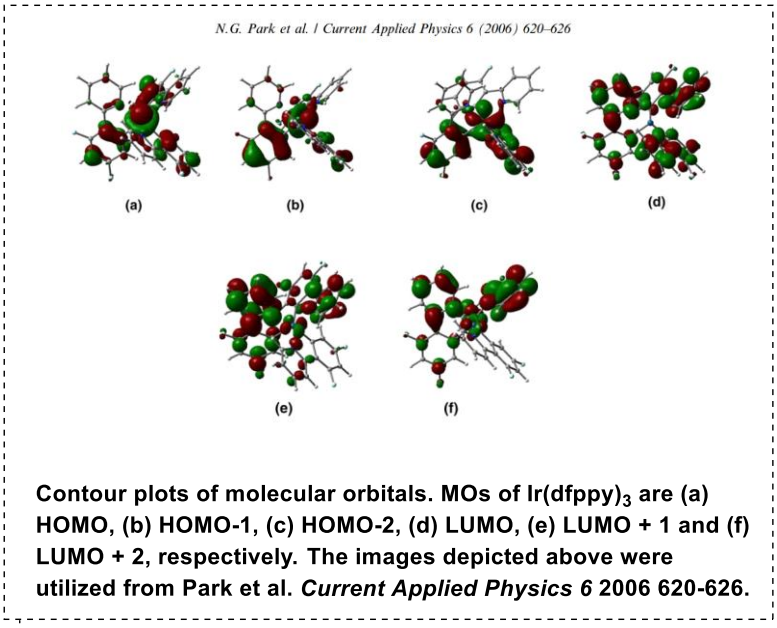

Contour plots of molecular orbitals. MOs of Ir(dfppy)$_3$ are (a) HOMO, (b) HOMO-1, (c) HOMO-2, (d) LUMO, (e) LUMO + 1 and (f) LUMO + 2, respectively. The images depicted above were utilized from Park et al. *Current Applied Physics 6* 2006 620-626.

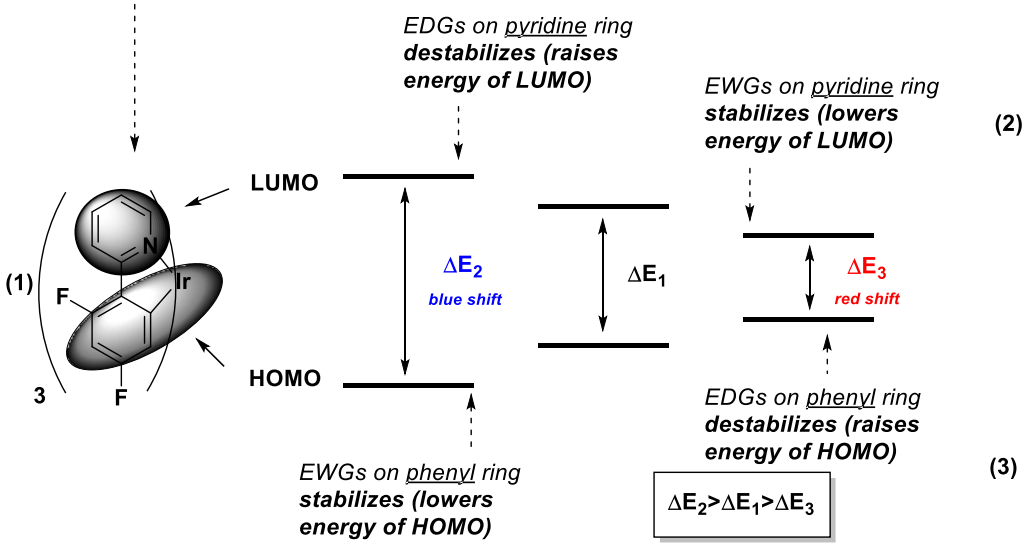

As expected, in complexes that have electron-withdrawing groups (**3b-d** and **3h**) a 10-40 nm hypsochromic shift is observed whereas bathochromic shift of 5-10 nm is observed in alkyl substituted complexes (on the phenyl ring), **3e** and **3f**, when compared to that of Ir(ppy)$_3$ (**3a**).

Furthermore, as the degree of fluorine substitution increases, more blue shifting is observed (**3d** vs. **3c**). Similar trends are observed in the case of heteroleptic cationic iridium complexes (**Figure 2.5**).

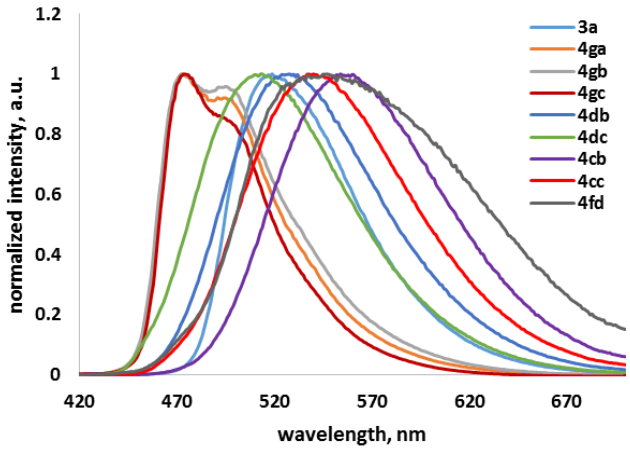

Figure 2.4 Emission spectra of 3a and heteroleptic iridium complexes

Electron withdrawing groups (**4ga, gb, gc**) resulted in a 42-45 nm blue shift with respect to $Ir(ppy)_3$ (**3a**). Complex **4db** shows a 55 nm bathochromic shift relative to more fluorinated complexes **4ga, gb, gc**. Addition of electron donating *tert*-butyl groups on bipyridyl (**4de**) resulted in a 12 nm hypsochromic shift compared to complex **4db**. In the mono-fluoro series, a similar trend was observed (**4cb** and **4cc**). Complexes **4db**, **4cb**, **4cc** and **4fd** depict a 10-42 nm red shift and **4ga**, **4gb**, **4gc**, **4dc** a 2-45 nm blue shift from $Ir(ppy)_3$ (**3a**). Furthermore, among these complexes, complex **4fd** was found to be the most red shifted (*vs*. **3a**) with poor emission which could be due to the methoxy substituents.[66] In most complexes, broad emission spectra were observed which could be due to a significant degree of charge transfer (CT) whereas structured spectra in **4ga** and **4gc** suggest a small CT contribution.[67]

In all complexes emission is from the lowest energy triplet state which is likely formed by mixing of the ^{3}MLCT, ^{3}LC and ^{3}LLCT states[68-69] The emission maximum (λ_{max}) is the triplet state energy, which can be used in photocatalysis for energy transfer processes.[70]

Having investigated the photophysical properties, we next turned to the electrochemical properties of the iridium complexes *via* cyclic voltammetry (CV) which is reported relative to ferrocenium/ferrocene redox couple as shown in **Table 2.2**. The cyclic voltammograms of complexes were collected at a scan rate of 50 mV/s. As anticipated, complexes having electron withdrawing fluorine groups (**3b-d** *vs* **3a**) show higher ground state $E_{ox}^{1/2}$ (Ir^+/Ir) due to lowering of the HOMO energy level. All cationic complexes show higher ground state $E_{ox}^{1/2}$ (Ir^+/Ir) when compared to that of **3a**, and among all complexes **4ga** and **4gc** exhibit the highest ground state $E_{ox}^{1/2}$. Whereas, lower $E_{ox}^{1/2}$ potentials were observed when an electron donating *t*-Bu-substituent was located on the ligand (**3e**, **3f** *v*s. **3a**) as this group is expected to raise the HOMO energy level making it more easily oxidized.[71]

Complexes that have electron withdrawing fluorines on the ligand make them less reducing (smaller negative ground state) $E_{red}^{1/2}$ (Ir/Ir^-) as observed in **3b-d** and **3h** relative to **3a**. Complexes that have an electron donating alkyl group (**3e** *vs.* **3a**) possess a more negative $E_{red}^{1/2}$ (Ir/Ir^-) potential-though **3f** is slightly less reducing than **3a**. Among the cationic complexes **4fd,** is the most reducing as it contains electron rich *t*-Bu- and methoxy substituent on ligands. Furthermore, *t*Bu-bipyridine complexes are more reducing (**4da** *vs*. **4dc**, **4cb** *vs.* **4cc**)

Knowing the excited state redox values is a key element in designing photocatalytic reactions, but the excited state redox potentials cannot be directly evaluated. However, they can be calculated from the electrochemically determined ground state $E_{ox}^{1/2}$ and $E_{red}^{1/2}$ potentials and the energy gap (E_{gap}). E_{gap} values were determined from the CV.

$$E^{1/2}(Ir^+/Ir^*) = E_{ox}^{1/2} - E_{gap}\ eV \qquad \text{(eq 1)}$$

$$E^{1/2}(Ir^*/Ir^-) = E_{gap}\ eV + E_{red}^{1/2} \qquad \text{(eq 2)}$$

We calculated the redox values of the excited state complexes, $E^{1/2}$ (Ir^*/Ir^+) and $E^{1/2}$ (Ir^*/Ir^-) using equations 1 and 2 and the potentials are shown in **Table 2.2**. The table is arranged in descending emission energy values.

Table 2.2 Photophysical and electrochemical data for iridium complexes

complex	λmax	TSE kcal/mol	$E_{1/2}$ ox V	$E_{1/2}$ red V	E gap eV	$E_{1/2}$ (Ir^{+}/Ir^{*})	$E_{1/2}$ (Ir^{*}/Ir^{-})
4gb	473	60.4	1.23	-1.23	2.2	-0.97	0.97
4ga	475	60.2	1.81	-1.25	2.64	-0.83	1.39
4gc	476	60.1	1.77	-1.35	2.77	-1	1.42
3d	476	60.1	0.98	-1.82	2.21	-1.23	0.39
3h	481	59.4	0.926	-1.58	2.2	-1.274	0.62
3c	488	58.6	1	-2.13	2.86	-1.86	0.73
3b	507	56.4	1.11	-2.13	2.76	-1.65	0.63
4dc	516	55.4	1.63	-1.42	2.56	-0.93	1.14
3a	518	55.2	0.78	-2.2	2.75	-1.97	0.55
3e	525	54.5	0.69	-2.27	2.59	-1.9	0.32
3f	528	54.2	0.7	-2.03	2.28	-1.59	0.25
4db	528	54.2	1.66	-1.32	2.46	-0.8	1.14
4cc	540	53	1.49	-1.45	2.52	-1.04	1.07
4cb	556	51.4	1.51	-1.37	2.4	-0.89	1.03
4fd	560	51.2	1.17	-1.5	2.35	-1.12	0.85

In conclusion, we have reported simple synthetic procedures that allow rapid access to an important class of iridium photoredox catalysts. We have successfully developed a simple and general synthesis that provides efficient access to facial *tris*-cyclometalated iridium complexes directly from less expensive $IrCl_3 \bullet nH_2O$. In addition, we applied Nonoyama's method in order to synthesize a number of cationic heteroleptic iridium complexes. Importantly, we have provided the chemical, photophysical, and electrochemical characterization necessary to facilitate catalysis. This should significantly aid in the design of novel chemical transformations via photocatalysis by facilitating access to the catalysts and by providing the relevant photophysical and electrochemical properties necessary to rationally design new synthetic methods.

2.5 *Experimental section*

All reagents were obtained from commercial suppliers (Sigma-Aldrich, Oakwood Chemicals, Alfa Aesar, Strem, and VWR) and used without further purification unless otherwise noted. NMR

spectra were obtained on 400 MHz Bruker Avance III spectrometer and 400 MHz Unity Inova spectrometer. ^{1}H, and ^{13}C, NMR chemical shifts are reported in ppm relative to the residual solvent peak while ^{19}F and ^{31}P NMR are set relative to an external standard. Purifications were carried out using a Teledyne Isco Combiflash Rf 200i flash chromatograph with a Redisep Rf normal phase silica (24 g, 40 g, or 80 g) column with product detection at 254 and 280 nm and by ELSD (evaporative light scattering detector). Substrate synthesis reactions were monitored by thin layer chromatography (TLC) obtained from Sorbent Technology (Silica XHL TLC Plates, w/UV254), glass backed, 250 μm, and were visualized with ultraviolet light. Photophysical properties were studied on Varian Cary Eclipse spectrophotometer and LCMS was taken on Shimadzu liquid chromatograph mass spectrometer (LCMS-2010 E). Electrochemical measurements were performed with CH instruments using a glassy-carbon electrode as a working electrode with a Ag/AgCl reference electrode and a platinum wire as a counter electrode. All sample solutions were prepared in acetonitrile and degassed with nitrogen bubbling for 20 min. prior to voltammetric studies. Tetra-(n-butyl)-ammonium hexafluorophosphate (NBu_4PF_6, 0.1 M in acetonitrile) was used as supporting electrolyte. The HOMO and LUMO energy is calculated from equation eq 3.

$$E_{HOMO/LUMO} = -(E_{onset\ oxi/red}\ \text{vs Fc} + 4.8)\ \text{eV} \qquad \text{(eq 3)}$$

General procedure A for the synthesis of ligands (**2b-2g**)

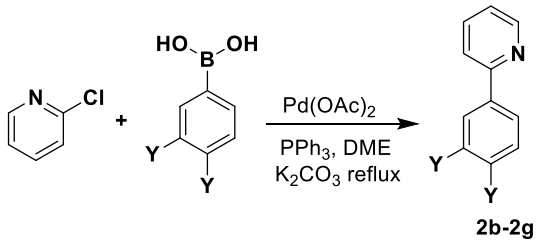

2b-2g

To a two-necked, 100-mL round-bottomed flask equipped with a magnetic stir bar were added 2-chloropyridine (1 equiv), phenylboronic acid (1.2 equiv), triphenylphosphine (0.1 equiv), 2 M

potassium carbonate (2.7 equiv) and 1,2 dimethoxyrthane (0.9 M). The mixture was degassed with Ar for 15 min. $Pd(OAc)_2$ (2.5 mol%) was added to the reaction mixture and degassing was continued for 15 more minutes and then the outlet was removed. The reaction mixture was heated to reflux. The progress of the reaction was monitored by TLC (hexane:EtOAc 90:10). Upon completion (typically 18-24 h), the reaction mixture was cooled to room temperature and extracted with DCM (3 x 20 mL). The combined organic portion was washed with water (3 x 20 mL) and brine (1 x 20 mL), dried over anhydrous sodium sulfate and then concentrated *in vacuo*. The crude material was purified by flash chromatography to obtain pure the ligand.

2b, The general procedure A was followed using 2-chloropyridine (2.0 g, 17.62 mmol), (4-(trifluoromethyl)phenyl)boronic acid (4.08 g, 21.15 mmol), 2 M K_2CO_3 (6.55 g, 47.52 mmol), PPh_3 (461 mg, 1.760 mmol), $Pd(OAc)_2$ (99 mg, 0.4420 mmol) and 1,2 dimethoxyrthane (20 mL). The crude material was purified by flash chromatography using hexane: ethyl acetate (0-5 % EtOAc for 40 cv and ramped to 100 % EtOAc for 40-70 cv and then held at 100% EtOAc 70-80 cv on a 24 g silica column) to afford **2b** in 67% yield (2.60 g, 11.65 mmol) as a white solid. The ^{1}H NMR matched literature values.[55]

2c, General procedure A was followed using 2-chloropyridine (2.0 g, 17.62 mmol), (4-fluorophenyl) boronic acid (2.96 g, 21.15 mmol), 2 M K_2CO_3 (6.55 g, 47.52 mmol), PPh_3 (461 mg, 1.760 mmol), $Pd(OAc)_2$ (99 mg, 0.4420 mmol) and 1,2 dimethoxyrthane (20 mL). The crude material was purified by flash chromatography using hexane:ethyl acetate (0-5 % EtOAc for 40 cv and ramped to 100 % EtOAc for 40-70 cv and then held at 100% EtOAc 70-80 cv on s 24 g silica column) to afford **2c** in quantitative yield (3.0 g, 17.32 mmol) as a white solid. The ^{1}H NMR matched the literature values.[55]

2d, General procedure A was followed using 2-chloropyridine (1.0 g, 8.80 mmol), (2,4-difluorophenyl) boronic acid (1.67 g, 10.56 mmol), 2 M K_2CO_3 (3.28 g, 23.76 mmol), PPh_3 (231 mg, 0.8817 mmol), $Pd(OAc)_2$ (49 mg, 0.2188 mmol) and 1,2 dimethoxyrthane (10 mL). The crude

material was purified by flash chromatography using hexane:ethyl acetate (0-5 % EtOAc for 40 cv and ramped to 100 % EtOAc for 40-70 cv and then held at 100% EtOAc 70-80 cv on a 24 g silica column) to afford **2d** in 56% yield (0.94 g, 4.92 mmol) as a colorless oily liquid. The ^{1}H NMR matched the literature values.[55]

2e, General procedure A was followed using 2-chloropyridine (2.0 g, 17.62 mmol), (4-(tert-butyl) phenylboronic acid (3.76 g, 21.15 mmol), 2 M K_2CO_3 (6.55 g, 47.52 mmol), PPh_3 (461 mg, 1.760 mmol), $Pd(OAc)_2$ (99 mg, 0.4442 mmol) and 1,2 dimethoxyrthane (20 mL). The crude material was purified by flash chromatography using hexane:ethyl acetate (0-5 % EtOAc for 40 cv and ramped to 100 % EtOAc for 40-70 cv and then held at 100% EtOAc 70-80 cv on a 24 g silica column) to afford **2e** in 79% yield (2.93 g, 13.90 mmol) as a colorless oily liquid. The ^{1}H NMR matched the literature values.[55]

2f, General procedure A was followed using 2-chloropyridine (2.0 g, 17.62 mmol), (3-(tert-butyl)phenyl) boronic acid (3.76 g, 21.15 mmol), 2 M K_2CO_3 (6.55 g, 47.52 mmol), PPh_3 (461 mg, 1.760 mmol), $Pd(OAc)_2$ (99 mg, 0.4420 mmol) and 1,2 dimethoxyrthane (20 mL). The crude material was purified by flash chromatography using hexane:ethyl acetate (0-5 % EtOAc for 40 cv and ramped to 100 % EtOAc for 40-70 cv and then held at 100% EtOAc 70-80 cv on a 24 g silica column) to afford **2f** in 79% yield (2.76 g, 13.09 mmol) as a colorless oily liquid. The ^{1}H NMR (Chloroform-*d*, 400 MHz): δ = 8.75 – 8.71 (m, 1H), 8.07 (t, 1H, *J*=1.8 Hz), 7.83 – 7.71 (m, 3H), 7.53 – 7.41 (m, 2H), 7.25 (ddd, 1H, *J*=6.7, 4.8, 2.1 Hz), 1.42 (s, 9H) ppm.

2g, General procedure A was followed using 2-chloro-5-(trifluoromethyl) pyridine (2.0 g, 11.02 mmol), (2,4-difluorophenyl) boronic acid (2.09 g, 13.22 mmol), 2 M K_2CO_3 (4.11g, 29.75 mmol), PPh_3 (288 mg, 1.099 mmol), $Pd(OAc)_2$ (62 mg, 0.2881 mmol) and 1,2 dimethoxyrthane (20 mL). The crude material was purified by flash chromatography using hexane:ethyl acetate (0-5 % EtOAc for 40 cv and ramped to 100 % EtOAc for 40-70 cv and then held at 100% EtOAc 7080

cv on a 24 g silica column) to afford **2g** in 79% yield (2.58 g, 9.961 mmol) as white solid. The ^{1}H NMR matched the literature values.[58]

Procedure for the synthesis of **2h**

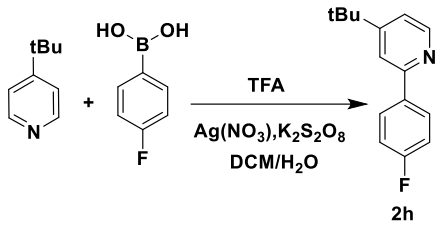

A two necked 250 mL round bottom flask was equipped with a magnetic stir bar, 4-*tert*-butyl pyridine (1.00 g, 7.41 mmol, 1 equiv) and 40 mL of dichloromethane. Trifluoroacetic acid (567 uL, 7.41 mmol 1 equiv), 40 mL of an aqueous silver nitrate solution (0.03 M), 4-fluorophenylboronic acid (1.54 mg, 11.1 mmol, 1.5 equiv), and potassium persulfate (3.09 g, 22.2 mmol, 3 equiv) were separately added. The reaction was stirred vigorously at room temperature for 6 hours and a second addition of silver nitrate (252 mg, 1.48 mmol, 0.2 equiv) and potassium persulfate (3.09 g, 22.2 mmol, 3 equiv) were added. After 18 h, another addition of 4-fluorophenyl boronic acid (515 mg, 3.71 mmol, 0.5 mmol) and potassium persulfate (1.03 g, 7.41 mmol, 1 equiv) were added. The progress of reaction was monitored by TLC (hexane:EtOAc 90:10). Upon completion, the reaction mixture was diluted with a 5% sodium bicarbonate solution and extracted with DCM (3 x 20 mL). The combined organic layer was dried over anhydrous magnesium sulfate and concentrated *in vacuo*. The crude material was purified by flash chromatography using hexane:ethyl acetate (0-5 % EtOAc for 40 cv and ramped to 100 % EtOAc for 40-70 cv and then held at 100% EtOAc 70-80 cv on s 24 g silica column) to afford **2h** in 29% (492 mg, 2.15 mmol) as a colorless oil. The ^{1}H NMR matched the literature values.[54]

General procedure B for the synthesis of homoleptic *fac*- Ir $(C^N)_3$ complexes (**3a-3f,h**)

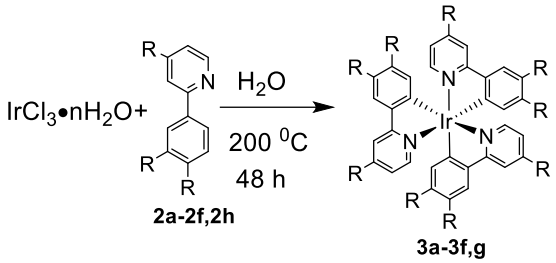

A Parr reactor (1 L model 4533) was charged with iridium (III) chloride (1 equiv), ligand (12 equiv), sodium carbonate (6 equiv) and DI water (0.03 M). The reaction mixture was pressurized (30 psi) and depressurized with Ar (3x) and finally charged again with Ar before sealing. The reaction mixture was heated at 200 °C for 24-48 h. After cooling to room temperature, reaction mixture was extracted with DCM (3 x 20 mL). The combined organic portion was filtered through a celite pad which was then concentrated to the obtain crude product. The pure compound **3a-3f** was obtained by performing flash chromatography. For most complexes, (**3a-3d**) crude samples were dry loaded on silica prior to running the column due to low solubility of the complex. After elution of the ligand with hexane/ethyl acetate the eluting solvent was switched to dichloromethane, which faciliated the elution of the iridium complexes (**3a-3f**).

3a, General procedure B was followed at 260 °C using iridium (III) chloride (192 mg, 0.64 mmol), 2-phenylpyridine (1.19 g, 7.7 mmol), Na_2CO_3 (407 mg, 3.8 mmol), and DI water (850 mL). The crude material was purified by flash chromatography (dry loaded) using hexane:ethyl acetate (0-10 % EtOAc for 40 cv to isolate ligand and then switched to DCM as well as ramped to 100 % DCM for 40-70 cv and then held at 100% DCM 70-80 cv) on a 24 g silica column to afford **3a** in 79% yield (311 mg, 0.47 mmol) as a yellow solid, which matched with the literature.[55] LC/MS M+ (m/z) calculated for $C_{33}H_{24}IrN_3$ 655.16 found, 654.50.

3b, General procedure B was followed except that **no sodium carbonate** was used, using iridium (III) chloride (100 mg, 0.33 mmol), 2-(4-(trifluoromethyl) phenyl) pyridine **2b** (896 mg, 4.0 mmol) and DI water (100 mL). The crude material was purified by flash chromatography (dry loaded) using hexane:DCM (0 % DCM for 16 cv and ramped to DCM 100 % for 16-20 cv and

then held at 100% DCM for 20-23 cv) on an 80 g silica column) to afford **3b** in 78 % yield (221 mg, 0.26 mmol) as a yellow solid. ^{1}H NMR(Chloroform-*d*, 400 MHz): δ = 7.99 (d, 3H, *J*=8.3 Hz), 7.77 – 7.69 (m, 6H), 7.55 (dd, 6H, *J*=6.0, 1.3 Hz), 7.20 – 7.15 (m, 3H), 7.02 (ddd, 3H, *J*=7.1, 5.2, 1.1 Hz), 6.96 (b, 3H) ppm. ^{13}C NMR (Methylene Chloride-d_2, 101 MHz): δ = 165.0, 159.2, 147.5 – 147.4 (m), 147.3, 137.0,132.4 (m), 130.6, 123.9, 123.4, 120.0, 117.3 – 117.2 (m), 100.0. ^{19}F NMR (376 MHz, Chloroform-*d*) δ -62.76 (s). LC/MS (m/z) M+ calculated for $C_{36}H_{21}F_9IrN_3$ 859.12 found: 858.70

3c, the general procedure B was followed except that **no sodium carbonate** was used, using iridium (III) chloride (100 mg, 0.33 mmol), 2-(4-fluorophenyl)pyridine **2c** (678 mg, 3.9 mmol) and DI water (100 mL). The crude material was purified by flash chromatography (dry loaded) using hexane: DCM (0-50 % DCM for 25 cv, held at 50% for 25-35 cv and ramped to 100 % DCM for 35-36 cv and then held at 100% DCM 36-41 cv) on a 40 g silica column to afford **3c** in 78 % yield (202 mg, 0.29 mmol) as a yellow- green solid. ^{1}H NMR(Methylene Chloride-d_2, 400 MHz): δ = 7.88 (d, 3H, *J*=8.2 Hz), 7.72 – 7.64 (m, 6H), 7.52 (ddd, 3H, *J*=5.5, 1.6, 0.8 Hz), 6.94 (ddd, 3H, *J*=7.1, 5.6, 1.3 Hz), 6.63 (td, 3H, *J*=8.7, 2.7 Hz), 6.39 (dd, 3H, *J*=10.3, 2.7 Hz) ppm. ^{13}C NMR(Methylene Chloride-d_2, 101 MHz): δ = 165.3 (d, *J*=5.4 Hz), 163.4 (d, *J*=5.7 Hz), 162.8, 147.2, 140.2, 136.6, 125.8 (d, *J*=9.2 Hz), 122.0, 121.8 (d, *J*=16.4 Hz), 118.9, 107.4 (d, *J*=23.6 Hz) ppm. ^{19}F NMR (376 MHz, Methylene Chloride-d_2) δ -112.33 (ddd, *J* = 10.3, 9.1, 5.7 Hz).). LC/MS (m/z) M+ calculated for $C_{33}H_{21}F_3IrN_3$ 709.13 found, 708.60.

3d, General procedure B was followed except that **no sodium carbonate** was used, using iridium (III) chloride (50 mg, 0.16 mmol), 2-(2,4-difluorophenyl)pyridine **2d** (184 mg, 0.96 mmol) and DI water (100 mL). The crude material was purified by flash chromatography (dry loaded) using hexane:ethyl acetate (0-40% EtOAc for 30 cv, changed EtOAc to DCM and ramped to 100 % DCM for 30-31 cv and then held at 100% DCM 31-39 cv) on a 40 g silica column to afford **3d** in 56 % yield (68 mg, 0.09 mmol) as a pale yellow solid. The NMR specta matched with the

literature.[49] ^{1}H NMR (400 MHz, DMSO-d_6) δ 8.27 (d, 3H, J = 8.6 Hz), 7.95 (t, 3H, J = 7.5 Hz), 7.54 (d, 3H J = 5.1 Hz), 7.26 (t, 3H, J = 6.4 Hz), 6.70 (td, 3H, J = 10.1, 9.2, 5.0 Hz), 6.06 (dd, 3H, J = 8.7, 2.2 Hz). ^{13}C NMR(Methylene Chloride-d_2, 101 MHz): δ = 162.9 (d, J=7.5 Hz), 162.5 (d, J=11.5 Hz), 161.3, 147.2, 137.4, 123.3 (d, J=20.9 Hz), 122.4, 117.8 (dd, J=16.1, 2.8 Hz), 96.6 (t, J=27.2 Hz) ppm. ^{19}F NMR (376 MHz, Methylene Chloride-d_2) δ -109.68 (q, 3F, J = 9.3 Hz), -110.86 (ddd, 3F, J = 12.6, 9.9, 2.3 Hz). LC/MS (m/z) M+ calculated for $C_{33}H_{18}F_6IrN_3$ 763.10 found 763.00.

3e, General procedure B was followed using iridium (III) chloride (100 mg, 0.33 mmol), 2-(4-(tert-butyl)phenyl)pyridine **2e** (844 mg, 4.0 mmol), sodium carbonate (210 mg, 2.0 mmol) and DI water (200 mL). The crude material was purified by flash chromatography using hexane:ethyl acetate (0-20 % EtOAc for 40 cv, switched EtOAc to DCM and ramped to 100 % DCM for 40-60 cv and then held at 100% DCM 60-65 cv) on a 24 g silica column to afford **3e** in 92 % yield (249 mg, 0.30 mmol) as a yellow solid. ^{1}H NMR (400 MHz, Chloroform-d) δ 7.79 (d, 3H, J = 8.2 Hz), 7.60 – 7.48 (m, 9H), 6.93 – 6.86 (m, 6H), 6.83 (ddd, 3H, J = 7.0, 5.6, 1.1 Hz), 1.10 (s, 27H). ^{13}C NMR (101 MHz, Chloroform-d) δ 167.5, 161.5, 152.4, 147.5, 141.6, 136.0, 134.9, 123.5, 121.8, 118.8, 117.2, 34.8, 31.8. LC/MS (m/z) M+ calculated for $C_{45}H_{48}IrN_3$ 823.35 found 822.65.

3f, General procedure B was followed using iridium (III) chloride (25 mg, 0.083 mmol), 2-(3-(tert-butyl) phenyl)pyridine **2f** (200 mg, 0.95 mmol), and DI water (50 mL). The crude material was purified by flash chromatography using hexane:EtOAc (0-10 % EtOAc for 32 cv, switched EtOAc to DCM and ramped to 100 % DCM for 32-42 cv and then held at 100% DCM 42-44 cv) on a 24 g silica column to afford **3f** in 16 % yield (11 mg, 0.013 mmol) as a yellow solid. ^{1}H NMR (400 MHz, Methylene Chloride-d_2) δ 7.99 (dd, 3H, J = 8.3, 5.6 Hz), 7.82 – 7.56 (m, 9H), 6.95 (ddd, 6H, J = 10.2, 6.0, 1.8 Hz), 6.67 (dd, 3H, J = 7.8, 5.7 Hz), 1.35 (s, 27H). ^{13}C NMR (101 MHz, Methylene Chloride-d_2) δ 167.1, 157.3, 147.4, 143.3, 142.4, 136.4, 136.1, 127.6, 122.0,

120.7, 118.9, 34.2, 31.4. Anal. Calcd for $C_{45}H_{48}IrN_3$: C, 65.66; H, 5.88; N, 5.11. Found: C, 64.82; H, 4.98; N, 5.57. LC/MS (m/z) M+ calculated for $C_{45}H_{48}IrN_3$ 823.35 found 822.90.

3h, the general procedure B was followed except that **no sodium carbonate** was used, using iridium (III) chloride (25 mg, 0.083 mmol), 4-(*tert*-butyl)-2-(4-fluorophenyl)pyridine **2h** (230 mg, 1 mmol) and DI water (100 mL). The crude material was purified by flash chromatography (**dry loaded**) using hexane: DCM (0-50 % DCM for 25 cv, held at 50% for 25-35 cv and ramped to 100 % DCM for 35-36 cv and then held at 100% DCM 36-41 cv) on a 40 g silica column to afford **3h** in 84 % yield (61 mg, 0.070 mmol) as a yellowish green solid. ^{1}H NMR (400 MHz, Chloroform-*d*) δ 7.73 – 7.69 (m, 3H), 7.56 (dd, 3H, *J* = 8.6, 5.7 Hz), 7.28 (d, 3H, *J* = 5.9 Hz), 6.83 (dd, 3H, *J* = 5.9, 1.8 Hz), 6.53 (td, 3H, *J* = 8.7, 2.6 Hz), 6.44 – 6.38 (m, 3H), 1.26 (s, 27H). 13C NMR (101 MHz, Chloroform-d) δ 164.0 , 163.0 (d, *J* = 251.5 Hz), 163.0 (d, *J* = 5.6 Hz), 159.1, 145.4, 139.2, 124.2 (d, *J* = 9.1 Hz), 121.3 (d, *J* = 16.1 Hz), 118.3, 114.37, 106.1 (d, *J* = 23.7 Hz), 33.9, 29.5. 19F NMR (376 MHz, Chloroform-d) δ -112.01 (s, 1F). LC/MS (m/z) M+ calculated for $C_{45}H_{45}F_3IrN_3$ 877.32 found 877.20.

General Procedure C for the synthesis of cationic heteroleptic [Ir $(C^N)_2(bpy)]^+$ PF_6^- complexes (**4xy**)

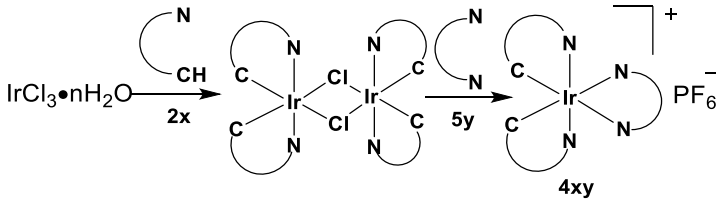

Heteroleptic iridium complexes **4xy** were synthesized in a two-step procedure.[58] In the first step, chloro-bridged dimer was synthesized by charging a two-necked reaction flask with magnetic stir bar, iridium(III) chloride (1 equiv), ligand (2.26 equiv), and a 2:1 v:v mixture of 2-methoxyethanol/water. The mixture was degassed with Ar (*via* Ar bubbling) and heated under reflux at 120 °C with constant stirring overnight. The reaction mixture was cooled to room

temperature and filtered. The precipitate was washed with water (3 x 10 mL), dried in air and taken onto the second step without further purification unless noted. In the second step, the chloro-bridging dimer (1equiv), bipyridyl ligand (2.2 equiv) and ethylene glycol were placed in a two-necked flask and flushed with Ar. The mixture was heated at 150 ºC for 15 h and then cooled. The cooled reaction mixture was washed with hexaned (3 x 10 mL) and mixture was heated to 85 ºC for 5 min. to remove residual hexane. Aqueous ammonium hexafluorophosphate (sat. solution) was added to the reaction mixture causing the iridium-PF_6 salt to precipitate, which was filtered, dried and recrystallized (acetone/ether).

4ga, General procedure C was followed using iridium(III) chloride (178 mg, 0.60 mmol), 2-(2,4-difluorophenyl)-5-(trifluoromethyl)pyridine pyridine **2g** (352 mg, 1.4 mmol) and a 2:1 mixture of 2-methoxyethanol/water (12 mL) to obtain the dimer in 74% yield (326 mg, 0.22 mmol) as yellow solid. **4ga** was synthesized using the dimer (50 mg, 0.034 mmol), phenanthroline (**5a**, 14 mg, 0.075 mmol) and ethylene glycol (2 mL). **4ga** was obtained in 91% yield (64 mg, 0.062 mmol) as yellow crystals after recrystallization from acetone and hexane. ^{1}H NMR (400 MHz, Acetone-d_6) δ 9.01 (dd, 2H, J = 8.3, 1.4 Hz), 8.68 (dd, 2H, J = 5.1, 1.4 Hz), 8.62 (dd, 2H J = 8.8, 2.6 Hz), 8.46 (s, 2H), 8.35 (dd, 2H, J = 8.8, 1.8 Hz), 8.15 (dd, 2H, J = 8.3, 5.1 Hz), 7.92 – 7.83 (m, 2H), 6.92 (ddd, 2H, J = 12.7, 9.3, 2.3 Hz), 6.08 (dd, 2H, J = 8.5, 2.3 Hz). ^{13}C NMR (101 MHz, Acetone-d_6) δ 167.7 (d, J = 6.8 Hz), 164.8 (dd, J = 209.3, 13.1 Hz), 162.2 (dd, J = 212.7, 12.9 Hz), 154.7 (d, J = 7.3 Hz), 152.3, 146.8, 146.4 (q, J = 4.7 Hz), 139.7, 137.2, 131.9, 128.6, 127.4, 127.1 (dd, J = 4.5, 2.6 Hz), 125.2 (d, J = 34.9 Hz), 123.8 (d, J = 20.9 Hz), 114.7 (dd, J = 18.0, 3.0 Hz), 99.4 (apparent t, J = 27.1 Hz). ^{19}F NMR (376 MHz, Acetone-d_6) δ -63.68 (s, 6F), -72.66 (d, 6F, J = 707.3 Hz), -104.86 (q, 2F J = 10.3, 9.3 Hz), -108.12 (td, 2F, J = 12.4, 2.7 Hz). ^{31}P NMR (162 MHz, Acetone-d_6) δ -130.00 – -157.36 (hept, J = 701.46 Hz). Anal. Calcd for $C_{36}H_{18}F_{16}IrN_4P$: C, 41.83; H, 1.76; N, 5.42. Found: C, 41.96; H, 1.89; N, 5.23. LC/MS (m/z) M+ calculated for $C_{36}H_{18}F_{10}IrN_4$ 889.10 found M+, 888.60.

4gb, General procedure C was followed using iridium(III) chloride (178 mg, 0.60 mmol), 2-(2,4-difluorophenyl)-5-(trifluoromethyl)pyridine **2g** (352 mg, 1.4 mmol) and a 2:1 mixture of 2-methoxyethanol/water (12 mL) to the obtain dimer in 74% yield (326 mg, 0.22 mmol) as yellow solid. **4gb** was synthesized using the dimer (100 mg, 0.067 mmol), 2,2'-bipyridyl (**5b**, 23 mg, 0.15 mmol) and ethylene glycol (4 mL). **4b** was obtained in 78 % yield (105 mg, 0.10 mmol) as yellow-green solid. ^{1}H NMR (400 MHz, Acetone-d_6) δ 9.01 (d, 2H, J = 7.6 Hz), 8.64 (dd, 2H, J = 8.8, 2.5 Hz), 8.47 – 8.38 (m, 4H), 8.31 (d, 2H, J = 5.3 Hz), 8.00 (s, 2H), 7.81 (t, 2H, J = 8.0 Hz), 6.87 (ddd, 2H, J = 12.7, 9.3, 2.3 Hz), 5.98 (dd, 2H, J = 8.5, 2.3 Hz). ^{13}C NMR (101 MHz, Acetone-d_6) δ 167.7 (d, J = 6.9 Hz), 164.8 (dd, J = 210.8, 12.9 Hz), 162.2 (dd, J = 214.1, 12.9 Hz), 156.1, 155.2 (d, J = 7.0 Hz), 151.4, 146.2 (q, J = 4.7 Hz), 140.7, 137.5 – 137.1 (m), 129.1, 126.9 (dd, J = 4.3, 2.6 Hz), 125.7, 125.3, 123.9 (d, J = 21.0 Hz), 122.1 (d, J = 271.6 Hz), 114.5 (dd, J = 18.0, 3.0 Hz), 99.4 (apparent t, J = 27.1 Hz). ^{19}F NMR (376 MHz, Acetone-d_6) δ -63.56 (s, 6F), -72.65 (d, 6F, J = 707.3 Hz), -104.62 – -104.81 (m, 2F), -107.74 – -108.15 (m, 2F). ^{31}P NMR (162 MHz, Acetone-d_6) δ -131.24 – -157.38 (hept, J = 707.94 Hz). LC/MS (m/z) M+ calculated for $C_{34}H_{18}F_{10}IrN_4$ 865.10 found M+, 864.50.

4gc, General procedure C was followed using iridium(III) chloride (178 mg, 0.60 mmol), 2-(2,4-difluorophenyl)-5-(trifluoromethyl)pyridine **2g** (352 mg, 1.4 mmol) and a 2:1 mixture of 2-methoxyethanol/water (12 mL) to obtain the dimer in 74% yield (326 mg, 0.22 mmol) as a yellow solid. **4gc** was synthesized using the dimer (100 mg, 0.067 mmol), 4,4'-di-tbutyl-2,2'-bipyridyl (**5c**, 39 mg, 0.147 mmol) and ethylene glycol (4 mL). 4c was obtained in 81% yield (121 mg, 0.11 mmol) as yellow solid. ^{1}H NMR (400 MHz, Acetone-d_6) δ 8.95 (d, 2H, J = 1.8 Hz), 8.63 (dd, 2H, J = 8.8, 2.6 Hz), 8.42 (dd, 2H, J = 8.8, 1.9 Hz), 8.20 (d, 2H, J = 5.9 Hz), 7.85 – 7.81 (m, 4H), 6.88 (ddd, 2H, J = 12.7, 9.3, 2.3 Hz), 5.98 (dd, 2H, J = 8.4, 2.3 Hz), 1.45 (s, 18H). ^{13}C NMR (101 MHz, Acetone-d_6) δ 167.9 (d, J = 7.5 Hz), 165.4, 164.6 (dd, J = 258.5, 12.7 Hz), 162.5 (dd, J = 261.8, 13.1 Hz), 156.0, 155.8 (d, J = 7.0 Hz), 151.1, 145.7 (q, J = 4.8 Hz), 137.2 (d, J = 3.0 Hz),

126.8 (dd, J = 4.4, 2.5 Hz), 126.0, 125.3 (d, J = 35.3 Hz), 123.9 (d, J = 21.0 Hz), 122.6, 122.2 (d, J = 271.7 Hz), 114.5 (dd, J = 17.8, 3.0 Hz), 99.3 (apparent t, J = 27.1 Hz), 35.7, 29.5. ^{19}F NMR (376 MHz, Acetone-d_6) δ -63.69 (s, 6F), -72.68 (d, 6F, J = 707.3 Hz), -104.76 (dt, 2F, J = 11.9, 9.0 Hz), -108.09 (td, 2F, J = 12.4, 2.4 Hz). ^{31}P NMR (162 MHz, Acetone-d_6) δ -131.17 – -157.37 (hept, J = 706.32 Hz). LC/MS (m/z) M+ calculated for $C_{42}H_{34}F_{10}IrN_4$ 977.23 found M+, 977.20.

4db, General procedure C was followed using iridium(III) chloride (89 mg, 0.30 mmol), 2-(2,4-difluorophenyl)pyridine **2d** (130 mg, 0.68 mmol) and a 2:1 mixture of 2-methoxyethanol/water (6 mL) to obtain the dimer in 82% yield (150 mg, 0.12 mmol) as yellow solid. **4db** was synthesized using the dimer (**5b**, 150 mg, 0.12 mmol), 2,2'-bipyridyl (34 mg, 0.22 mmol) and ethylene glycol (6 mL). **4d** was obtained in 57% yield (100 mg, 0.11 mmol) as a yellow solid. ^{1}H NMR (400 MHz, Acetone-d_6) δ 8.89 (d, 2H, J = 8.1 Hz), 8.46 – 8.33 (m, 4H), 8.24 (ddd, 2H, J = 5.4, 1.5, 0.6 Hz), 8.11 – 8.05 (m, 2H), 7.94 (ddd, 2H, J = 5.8, 1.5, 0.7 Hz), 7.77 (ddd, 2H, J = 7.6, 5.5, 1.2 Hz), 7.27 (ddd, 2H, J = 7.4, 5.9, 1.4 Hz), 6.78 (ddd, 2H, J = 12.7, 9.3, 2.4 Hz), 5.82 (dd, 2H, J = 8.5, 2.4 Hz). ^{13}C NMR (101 MHz, Acetone-d_6) δ 164.8 (d, J = 7.1 Hz), 163.5 (dd, J = 39.4, 12.7 Hz), 163.5 (dd, J = 476.4, 12.7 Hz), 156.8, 155.6 (d, J = 6.6 Hz), 152.0, 150.8, 141.2, 140.8, 130.0, 128.9 (dd, J = 4.5, 2.8 Hz), 126.1, 125.2, 124.6 (d, J = 20.2 Hz), 114.7 (dd, J = 17.7, 3.0 Hz), 99.7 (apparent t, J = 27.1 Hz). ^{19}F NMR (376 MHz, Acetone-d_6) δ -72.67 (d, 6F, J = 707.2 Hz), -107.74 – -107.86 (m, 2F), -110.00 – -110.13 (m, 2F). ^{31}P NMR (162 MHz, Acetone-d_6) δ -131.16-157.38 (hept, J = 707.94 Hz). LC/MS (m/z) M+ calculated for $C_{32}H_{20}F_4IrN_4$ 729.13 found M+, 728.55.

4dc, General procedure C was followed using iridium(III) chloride (89 mg, 0.29 mmol), 2-(2,4-difluorophenyl)pyridine **2d** (130 mg, 0.68 mmol) and a 2:1 mixture of 2-methoxyethanol/water (6 mL) to obtain the dimer in 82% yield (150 mg, 0.12 mmol) as a yellow solid. **4dc** was synthesized using the dimer (126 mg, 0.10 mmol), 4,4'-di-*t*butyl-2,2'-bipyridyl (**5c**, 59 mg, 0.22 mmol) and ethylene glycol (6 mL). **4e** was obtained in 88% yield (174 mg, 0.18 mmol) as yellow solid. ^{1}H NMR (400 MHz, Acetone-d_6) δ 8.79 (d, 2H, J = 1.8 Hz), 8.27 (d, 2H, J = 8.4 Hz), 7.98 – 7.90 (m,

4H), 7.76 – 7.72 (m, 2H), 7.62 (dd, 2H, *J* = 5.9, 2.0 Hz), 7.09 (ddd, 2H, *J* = 7.4, 5.9, 1.3 Hz), 6.64 (ddd, 2H, *J* = 12.6, 9.4, 2.4 Hz), 5.65 (dd, 2H, *J* = 8.6, 2.4 Hz), 1.28 (s, 18H). ^{13}C NMR (101 MHz, Acetone-d_6) δ 164.6, 165.4 – 163.8 (m), 162.5 (dd, *J* = 37.2, 12.6 Hz), 160.1 (d, *J* = 12.8 Hz), 155.7, 155.2 (d, *J* = 6.2 Hz), 150.5, 149.6, 139.7, 125.8, 124.1, 123.6 (d, *J* = 20.5 Hz), 122.4, 113.6 (dd, *J* = 17.6, 2.9 Hz), 98.6 (apparent t, *J* = 27.2 Hz), 35.6, 29.5. ^{19}F NMR (376 MHz, Acetone-d_6) δ -72.61 (dd, 6F, *J* = 707.2, 8.6 Hz), -107.90 (q, 2F, *J* = 9.7 Hz), -110.17 (t, 2F, *J* = 11.7 Hz). ^{31}P NMR (162 MHz, Acetone-d_6) δ -130.58 – -157.12 (hept, *J* = 707.94 Hz). LC/MS (m/z) M+ calculated for $C_{40}H_{36}F_4IrN_4$ 841.25 found M+, 840.60.

4cb General procedure C was followed using iridium(III) chloride (89 mg, 0.30 mmol), 2-(4-fluorophenyl)pyridine **2c**, and a 2:1 mixture of 2-methoxyethanol/water (6 mL) to obtain the dimer in 82% yield (150 mg, 0.12 mmol) as a yellow solid. **4f** was synthesized using the dimer (35 mg, 0.031 mmol), 2,2'-bipyridyl (**5b**, 10.5 mg, 0.067 mmol) and ethylene glycol (5 mL). **4cb** was obtained in 94% yield (48 mg, 0.070 mmol) as yellow solid. ^{1}H NMR(400 MHz, Acetone-d_6): δ = 8.87 (d, 2H, *J*= 8.2 Hz), 8.33 (td, 2H, *J*= 8.0, 1.6 Hz), 8.24 (d, 2H, *J*= 8.1 Hz), 8.17 (ddd, 2H, *J*= 5.4, 1.5, 0.7 Hz), 8.05 – 7.95 (m, 4H), 7.83 (ddd, 2H, *J*= 5.8, 1.4, 0.7 Hz), 7.75 (ddd, 2H, *J*= 7.6, 5.5, 1.2 Hz), 7.23 – 7.14 (m, 2H), 6.84 (td, 2H, *J*= 8.9, 2.6 Hz), 5.95 (dd, 2H, *J*= 9.5, 2.6 Hz) ppm ^{13}C NMR(101 MHz, Acetone-d_6): δ = 167.6, 166.0, 157.0, 154.5 (d, *J*= 5.9 Hz), 151.9, 150.3, 141.5 (d, *J*= 2.1 Hz), 140.9, 140.1, 129.8, 128.3 (d, *J*= 9.4 Hz), 126.0, 124.7, 121.2, 118.4 (d, *J*= 17.9 Hz), 110.7 (d, *J*=23.3 Hz) ppm ^{19}F NMR(376 MHz,Acetone-d_6): δ = -72.63 (d, 6F, *J*=707.4 Hz), -110.75 (s, 2F) ppm ^{31}P NMR(162 MHz, Chloroform-*d*): δ = -129.39 – -148.65 (m) ppm. Anal. calcd for $C_{32}H_{22}F_8IrN_4P$: C, 45.88; H, 2.65; N, 6.69. Found: C, 45.75; H, 7.48; N, 7.08. LC/MS (m/z) M+ calculated for $C_{32}H_{22}F_2IrN_4$ 693.14 found, 692.60.

4cc, General procedure C was followed using iridium(III) chloride (89 mg, 0.31 mmol), 2-(4-fluorophenyl)pyridine **2c**, and a 2:1 mixture of 2-methoxyethanol/water (6 mL)to obtain the dimer in 82% yield (150 mg, 0.12 mmol) as yellow solid. **4cc** was synthesized using the dimer (106 mg,

0.10 mmol), 4,4'-di-tbutyl-2,2'-bipyridyl (**5c**, 54 mg, 0.20 mmol) and ethylene glycol (5 mL). **4g** was obtained in 83% yield (158 mg, 0.19 mmol) as yellow solid. ^{1}H NMR(400 MHz, Acetone-d_6): δ = 8.90 (d, 2H, *J*=1.7 Hz), 8.24 (d, 2H, *J*=8.1 Hz), 8.05 – 7.95 (m, 6H), 7.80 – 7.77 (m, 2H), 7.74 (dd, 2H, *J*=5.9, 2.0 Hz), 7.16 (ddd, 2H, *J*=7.3, 5.9, 1.4 Hz), 6.83 (td, 2H, *J*=8.9, 2.6 Hz), 5.94 (dd, 2H, *J*=9.5, 2.6 Hz), 1.41 (s, 18H) ppm ^{13}C NMR (101 MHz, Acetone-d_6) δ 167.7, 165.3, 164.7 (d, *J* = 252.8 Hz), 156.8, 155.1 (d, *J* = 5.8 Hz), 151.4, 150.0, 141.5 (d, *J* = 2.0 Hz), 140.0, 128.2 (d, *J* = 9.4 Hz), 126.7, 124.5, 123.1, 121.1, 118.3 (d, *J* = 17.8 Hz), 110.5 (d, *J* = 23.2 Hz), 36.5 . ^{19}F NMR (376 MHz, Acetone-d_6) δ -72.61 (d, 6F, *J* = 707.4 Hz), -110.86 (s, 2F).^{31}P NMR(Chloroform-*d*, 162 MHz): δ = -139.08 (p, *J*=707.6 Hz) ppm. LC/MS (m/z) M+ calculated for $C_{40}H_{38}F_2IrN_4$ 805.27 found M+, 804.70.

4fd, General procedure C was followed using iridium(III) chloride (178 mg, 0.60 mmol), 2-(3-(*tert*-butyl)phenyl)pyridine **2f** (287 mg, 1.4 mmol), and a 2:1 mixture of 2-methoxyethanol/water (12 mL) to obtain the dimer in 60% yield (232 mg, 0.18 mmol) as a yellow solid. **4fd** was synthesized using the dimer (28 mg, 0.022 mmol), 4,4'-di-methoxy-2,2'-bipyridyl (**5d**, 11 mg, 0.048 mmol) and ethylene glycol (2 mL). **4h** was obtained in > 99% yield (43 mg, 0.044 mmol) as orange solid. ^{1}H NMR (400 MHz, Acetone-d_6) δ 8.35 (d, 2H, *J* = 2.6 Hz), 8.32 (d, 2H, *J* = 8.1 Hz,), 7.99 – 7.92 (m, 4H), 7.91 – 7.87 (m, 2H), 7.83 (d, 2H, *J* = 6.4 Hz), 7.24 (dd, 2H, *J* = 6.4, 2.6 Hz), 7.17 (ddd, 2H, *J* = 7.3, 5.8, 1.4 Hz), 7.02 (dd, 2H, *J* = 8.0, 2.1 Hz), 6.32 (d, 2H, *J* = 8.0 Hz), 4.09 (s, 6H), 1.32 (s, 18H). ^{13}C NMR (101 MHz, Acetone-d_6) δ 168.5, 168.1, 157.7, 151.5, 149.3, 147.3, 144.9, 143.9, 138.4, 131.6, 128.0, 123.4, 121.9, 119.9, 114.1, 111.6, 56.6, 34.2, 31.0. ^{31}P NMR (162 MHz, Acetone-d_6) δ -130.19 – -157.39 (hept, *J* = 707.94 Hz). Anal. calcd for $C_{42}H_{44}F_6IrN_4O_2P$: C, 51.79; H, 4.55; N, 5.75. Found: C, 51.61; H, 4.38; N, 5.94. LC/MS (m/z) M+ calculated for $C_{42}H_{44}IrN_4O_2$ 829.31 found M+, 828.70.

Electrochemical Measurements: Ground state redox potential of all complexes were determined (**Table 2.3**) by CV. Measured $E_{ox}^{1/2}$, $E_{red}^{1/2}$ and E_{gap} (value determined by CV) was utilized to calculate excited state potentials using equation 2 and 3.

$$E_{1/2}\ Ir^{+}/Ir^{*} = E_{1/2\ ox} - E\ gap = \text{(eq 2)}$$

$$E_{1/2}\ Ir^{*}/Ir^{-} = E\ gap + E_{1/2\ red}\ \text{(eq 3)}$$

Table 2.3 Data from electrochemical measurements

complex	λmax	TSE Kcal/mol	$E_{1/2}$ ox V	$E_{1/2}$ red V	E gap eV	$E_{1/2}$ (Ir^{+}/Ir^{*})	$E_{1/2}$ (Ir^{*}/Ir^{-})
4b	473	60.4	1.23	-1.23	2.2	-0.97	0.97
4a	475	60.2	1.81	-1.25	2.64	-0.83	1.39
4c	476	60.1	1.77	-1.35	2.77	-1.0	1.42
3d	476	60.1	0.98	-1.82	2.21	-1.23	0.39
3g	481	59.4	0.93	-1.58	2.2	-1.27	0.62
3c	488	58.6	1.00	-2.13	2.86	-1.86	0.73
3b	507	56.4	1.11	-2.13	2.76	-1.65	0.63
4e	516	55.4	1.63	-1.42	2.56	-0.93	1.14
3a	518	55.2	0.78	-2.2	2.75	-1.97	0.55
3e	525	54.5	0.69	-2.27	2.59	-1.90	0.32
3f	528	54.2	0.70	-2.03	2.28	-1.59	0.25
4d	528	54.2	1.66	-1.32	2.46	-0.80	1.14
4g	540	53.0	1.49	-1.45	2.52	-1.04	1.07
4f	556	51.4	1.51	-1.37	2.40	-0.89	1.03
4h	560	51.2	1.17	-1.50	2.35	-1.12	0.85

Note: TSE=triplet state energy determined from emission spectra

Figure 2.5 Cyclic voltammogram of 3a-3g and 4a-4h

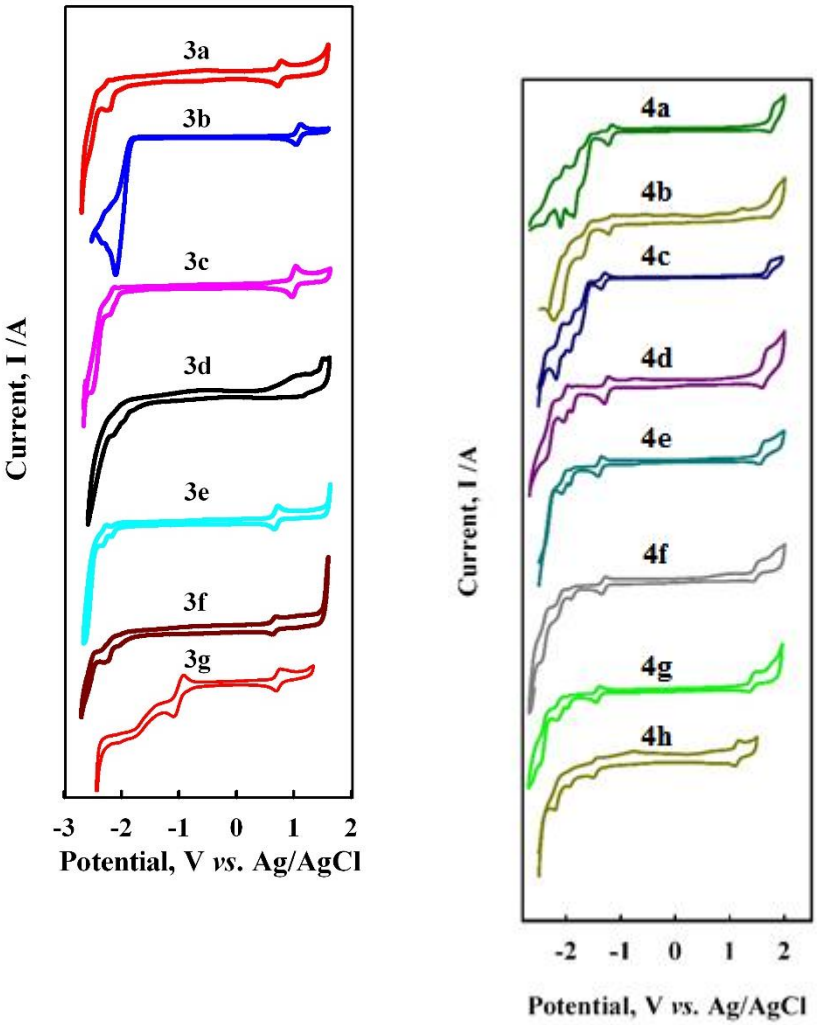

Spectra

Figure 2.6 Chapter II NMR Spectrum Graphs

^{1}H NMR spectrum of **3b**

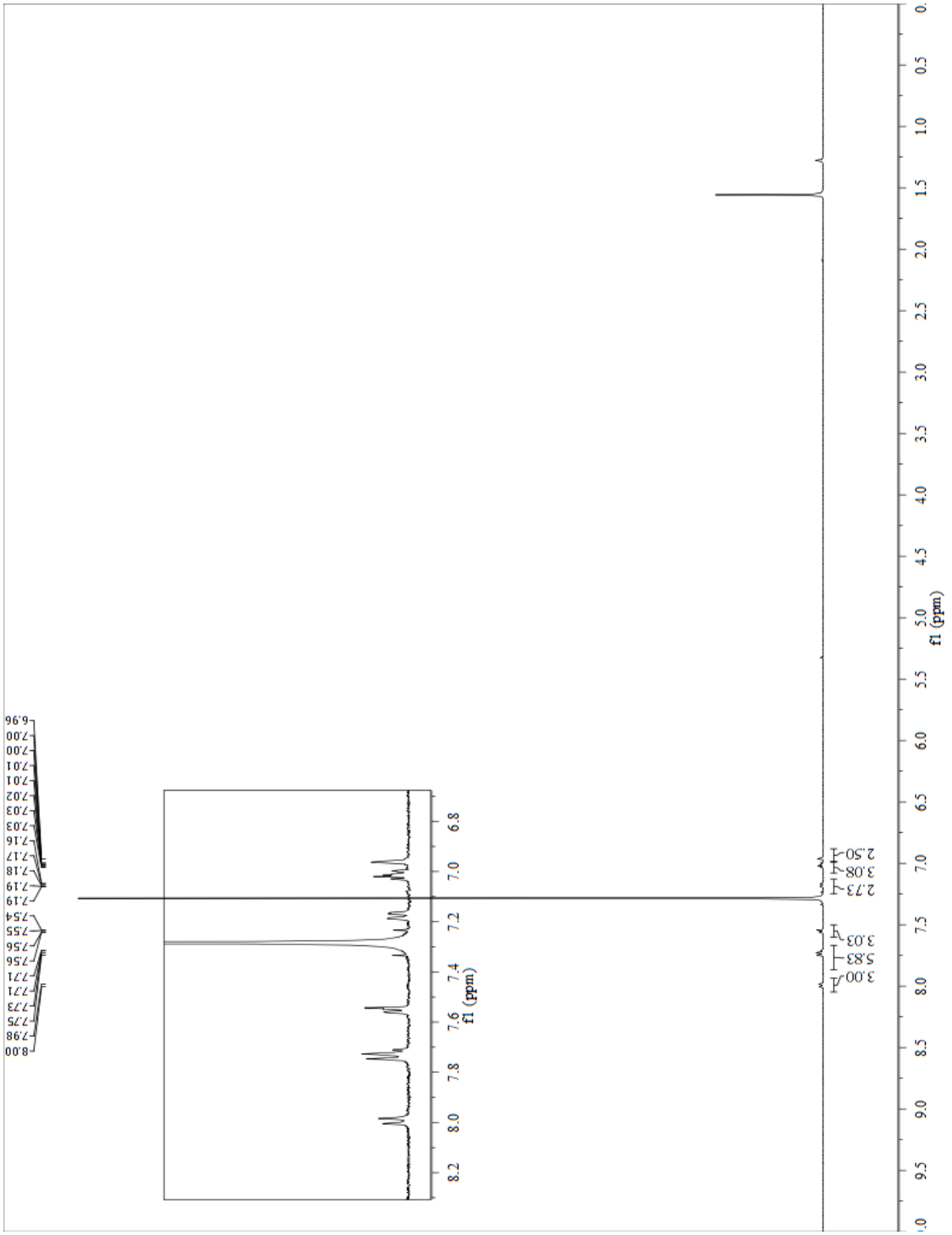

^{13}CNMR spectrum of **3b**

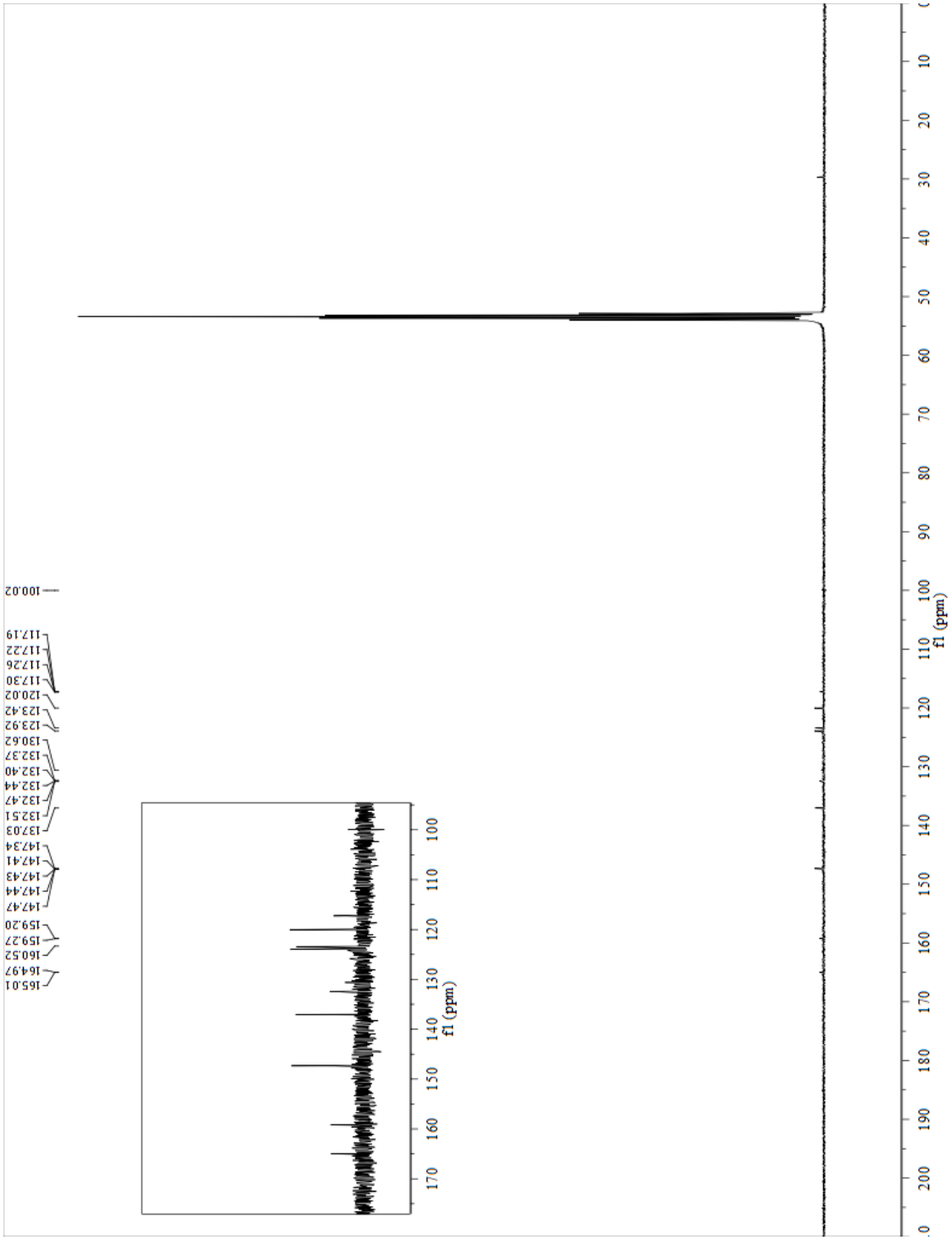

^{19}FNMR spectrum of **3b**

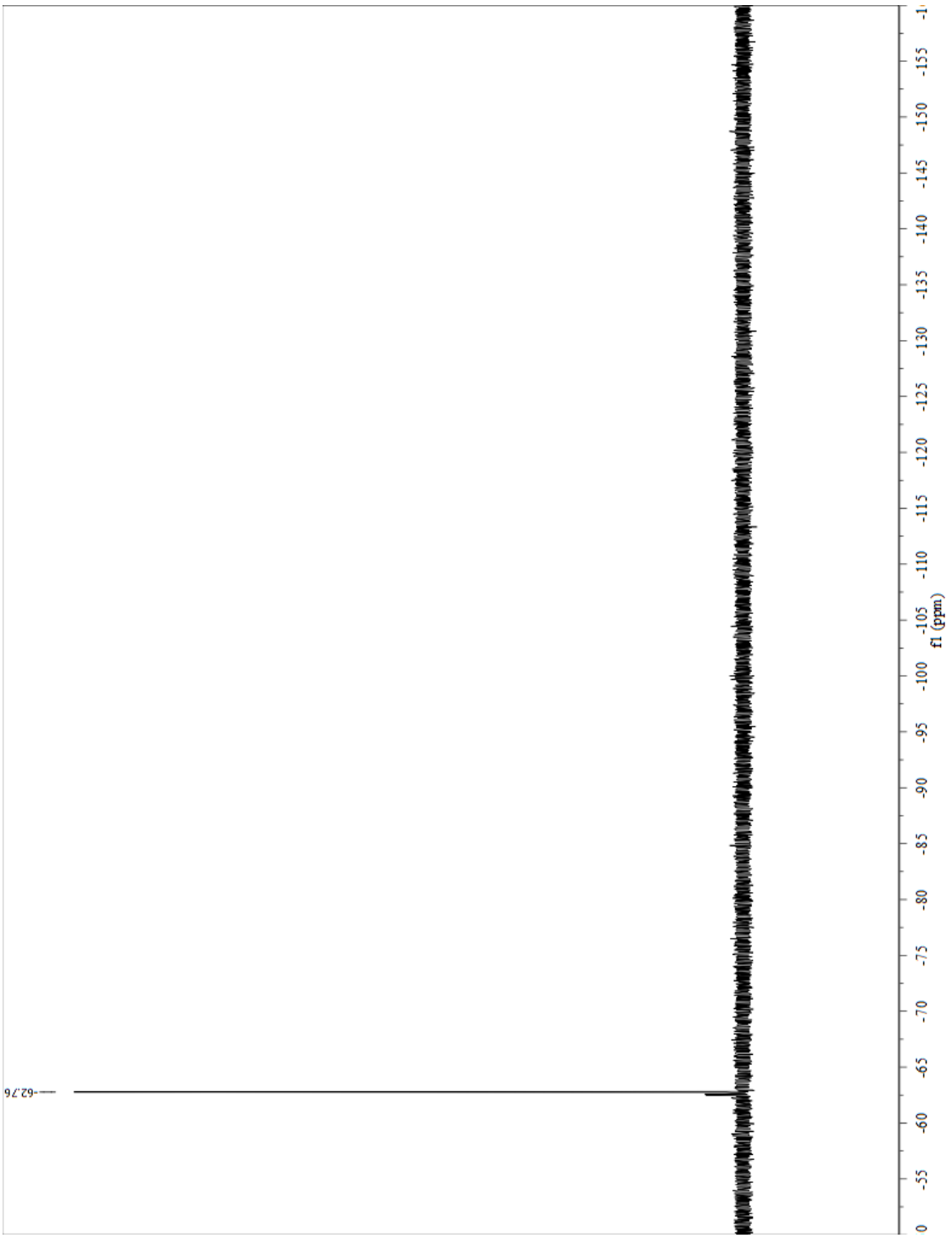

^{1}H NMR spectrum of **3c**

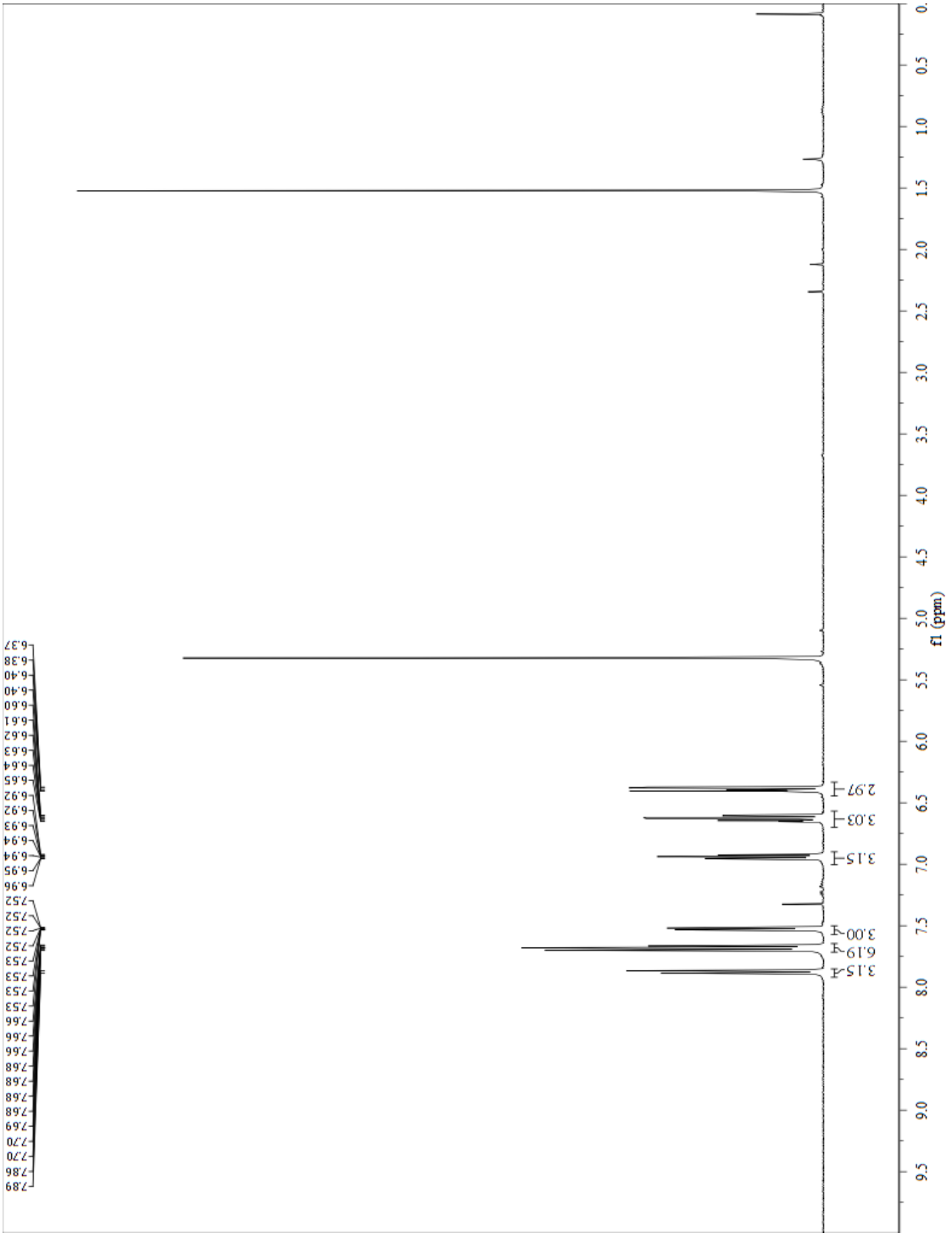

^{13}CNMR spectrum of **3c**

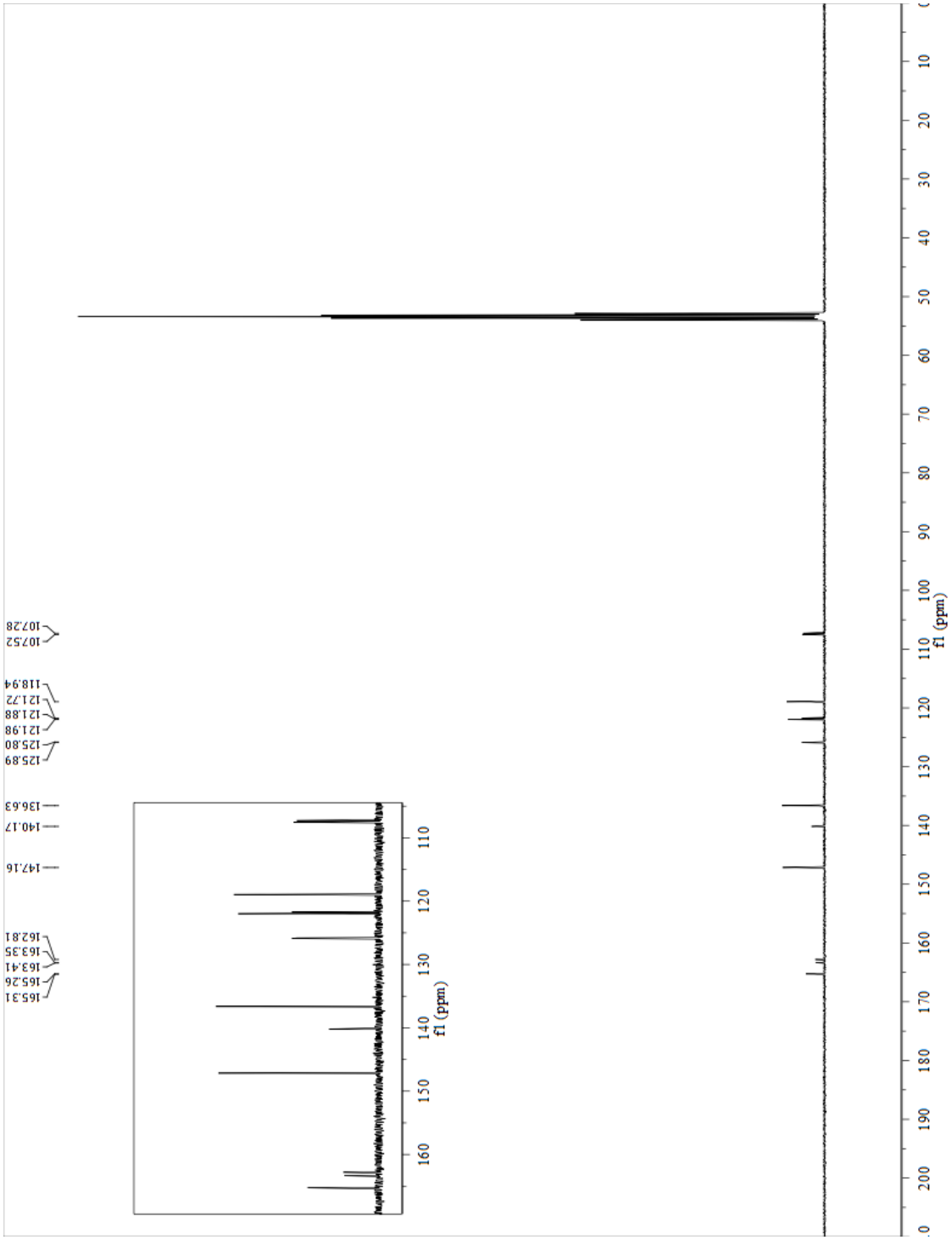

^{19}FNMR spectrum of **3c**

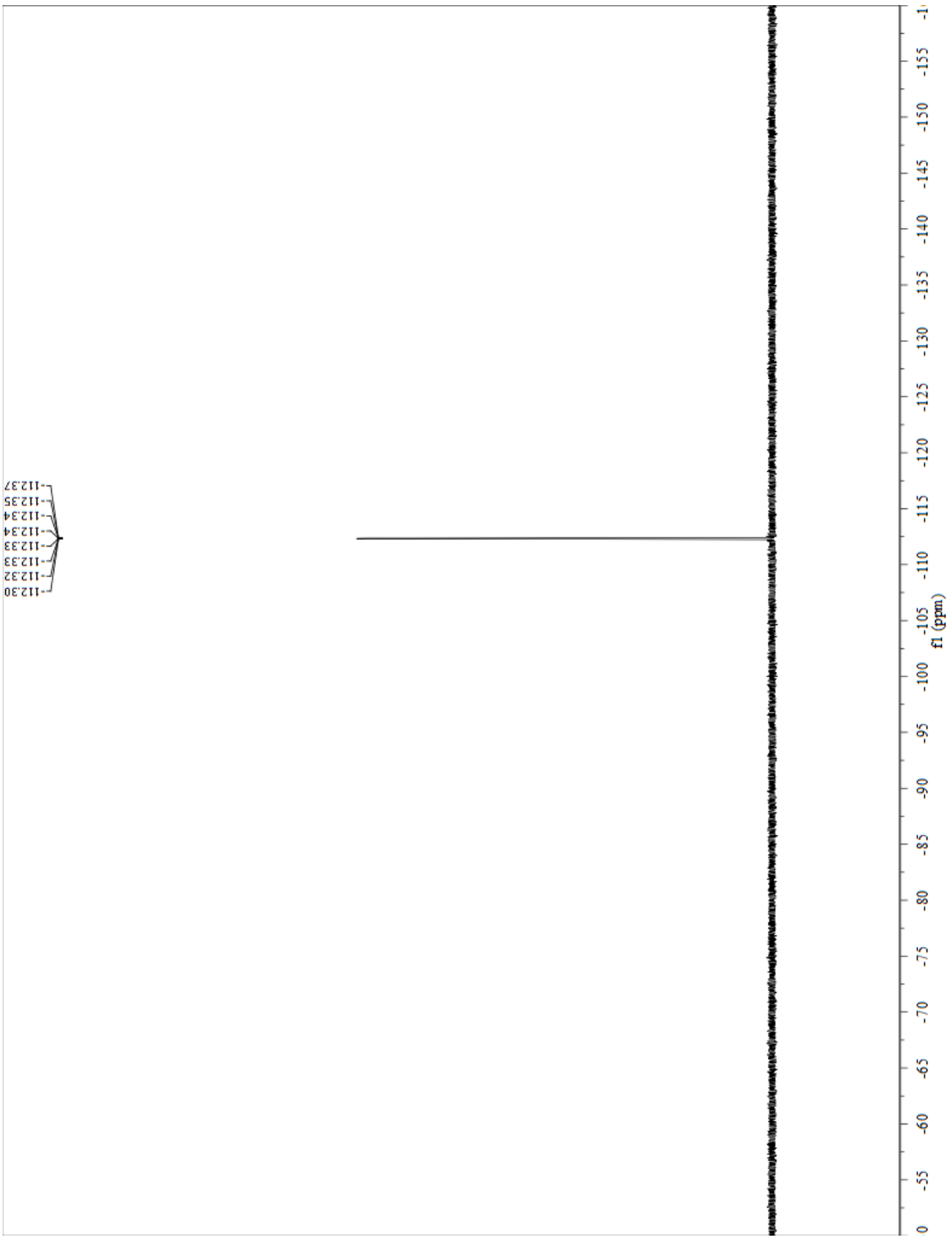

^{1}H NMR spectrum of **3d**

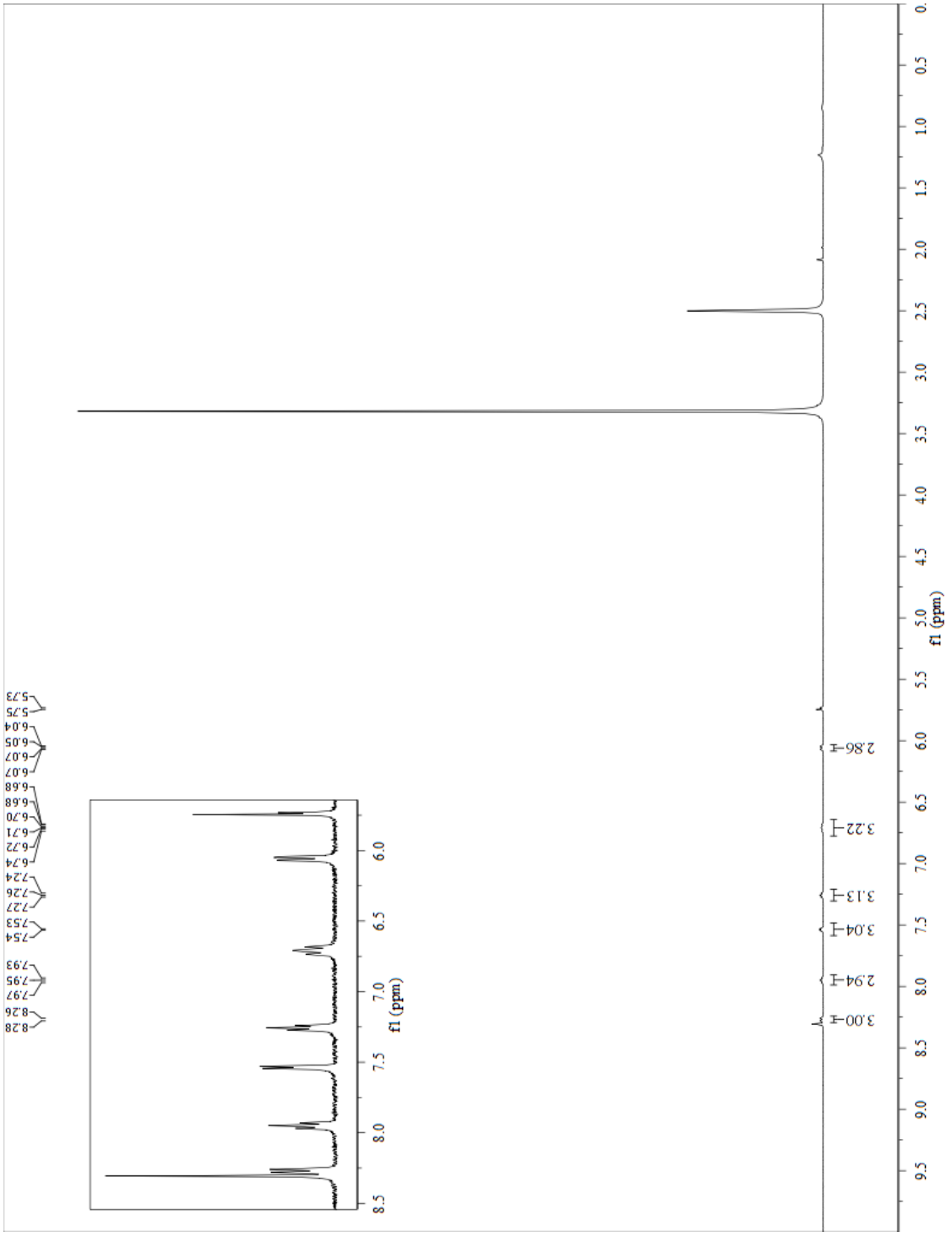

^{13}CNMR spectrum of **3d**

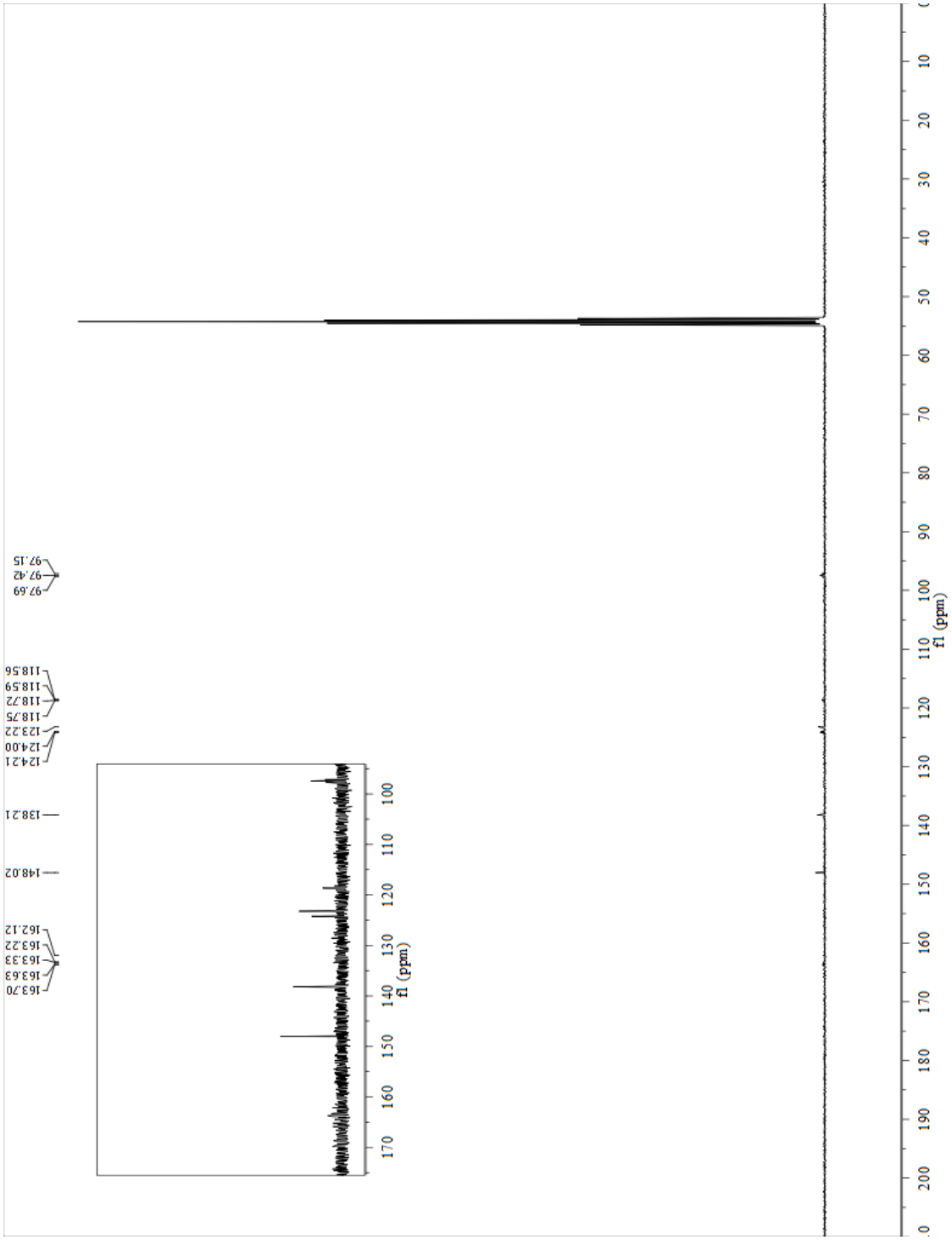

^{19}FNMR spectrum of **3d**

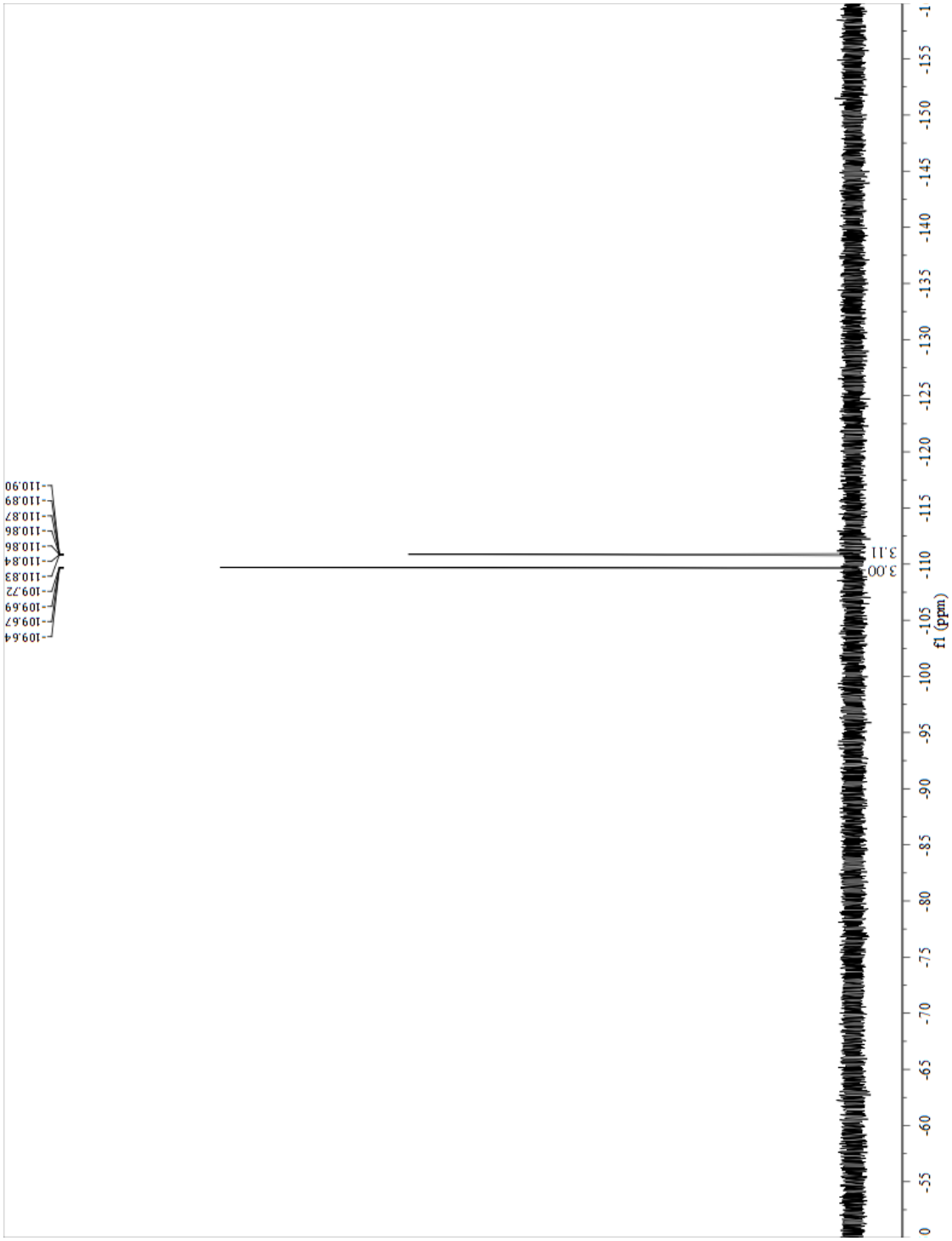

^{1}H NMR spectrum of **3e**

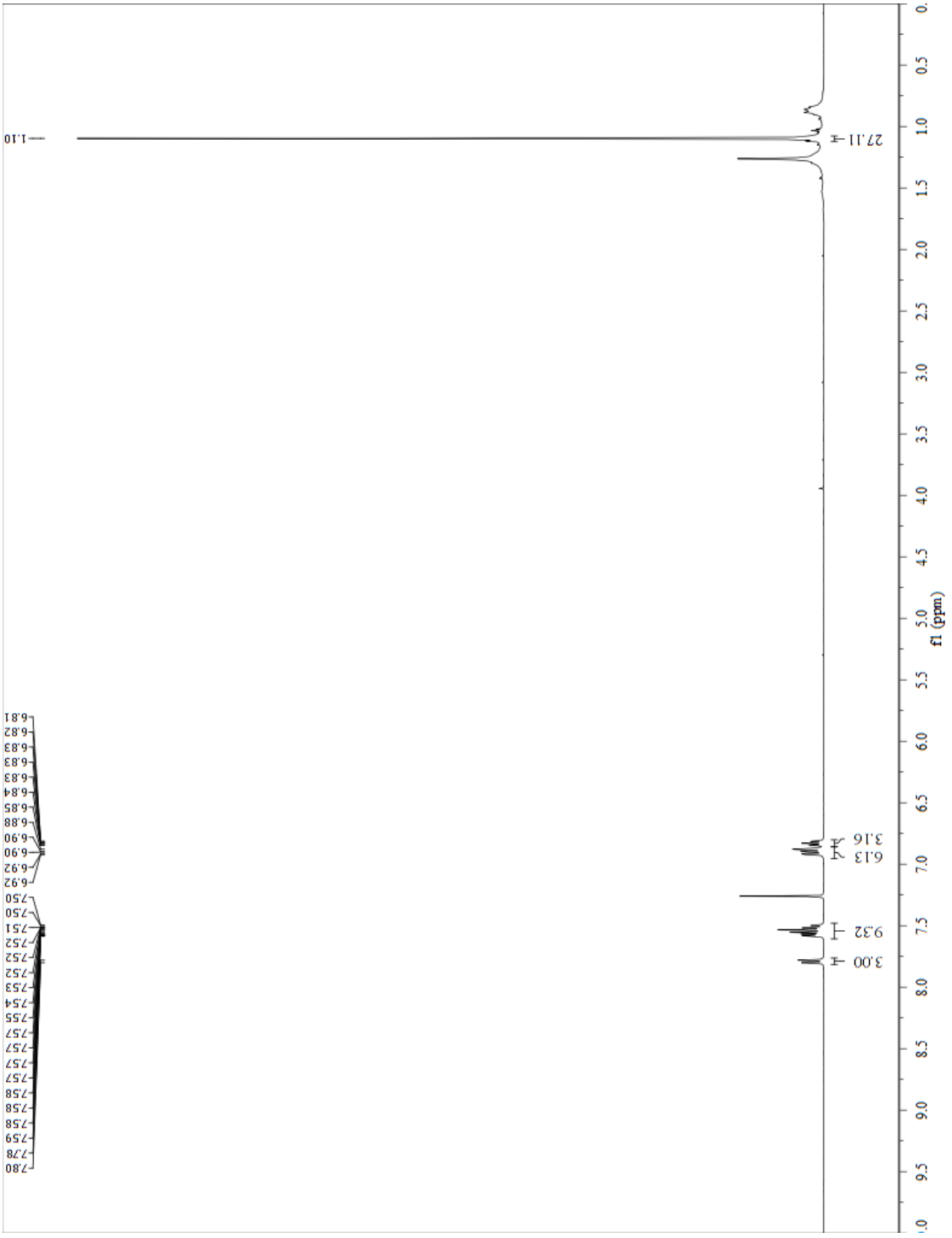

^{13}CNMR spectrum of **3e**

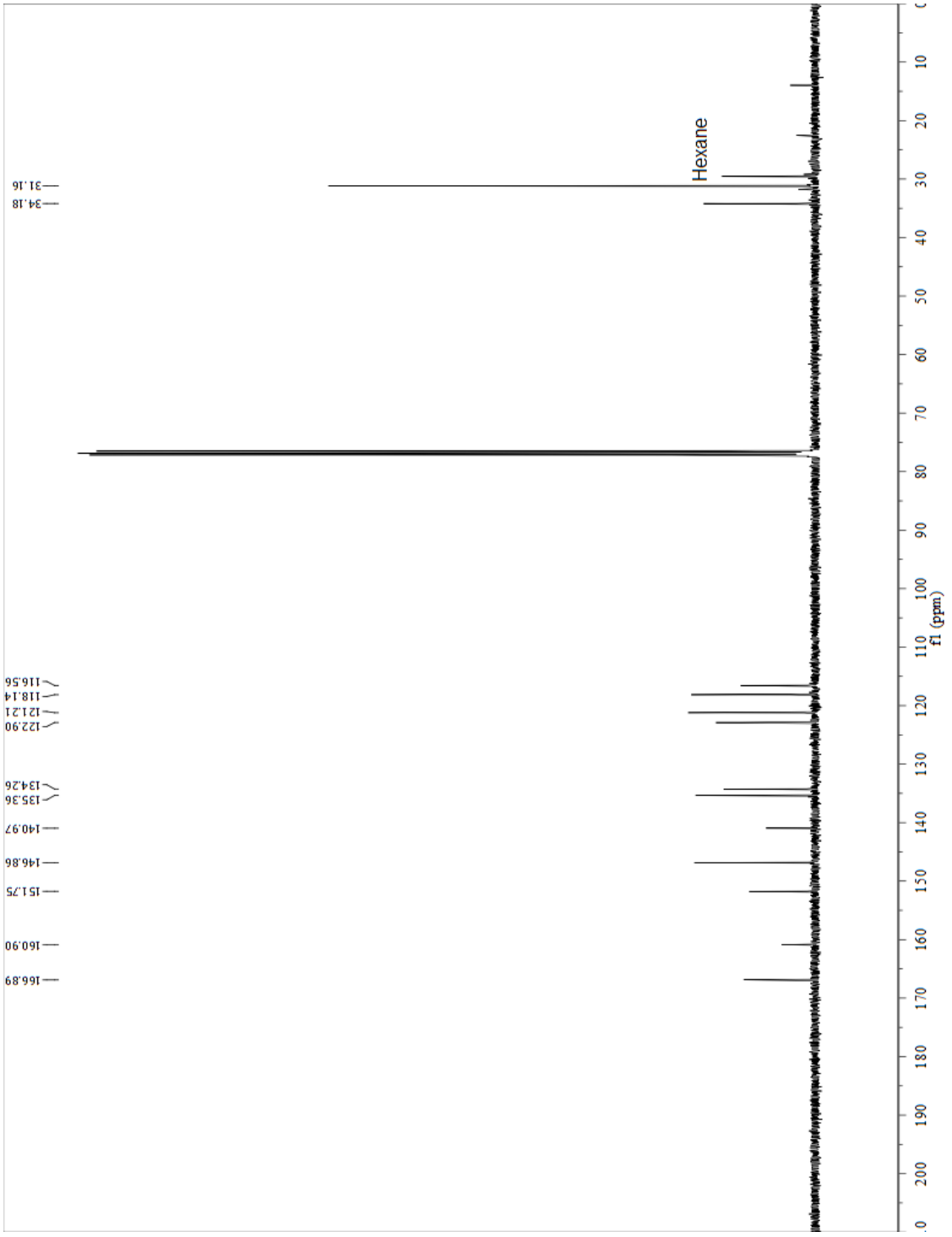

^{1}H NMR spectrum of **3f**

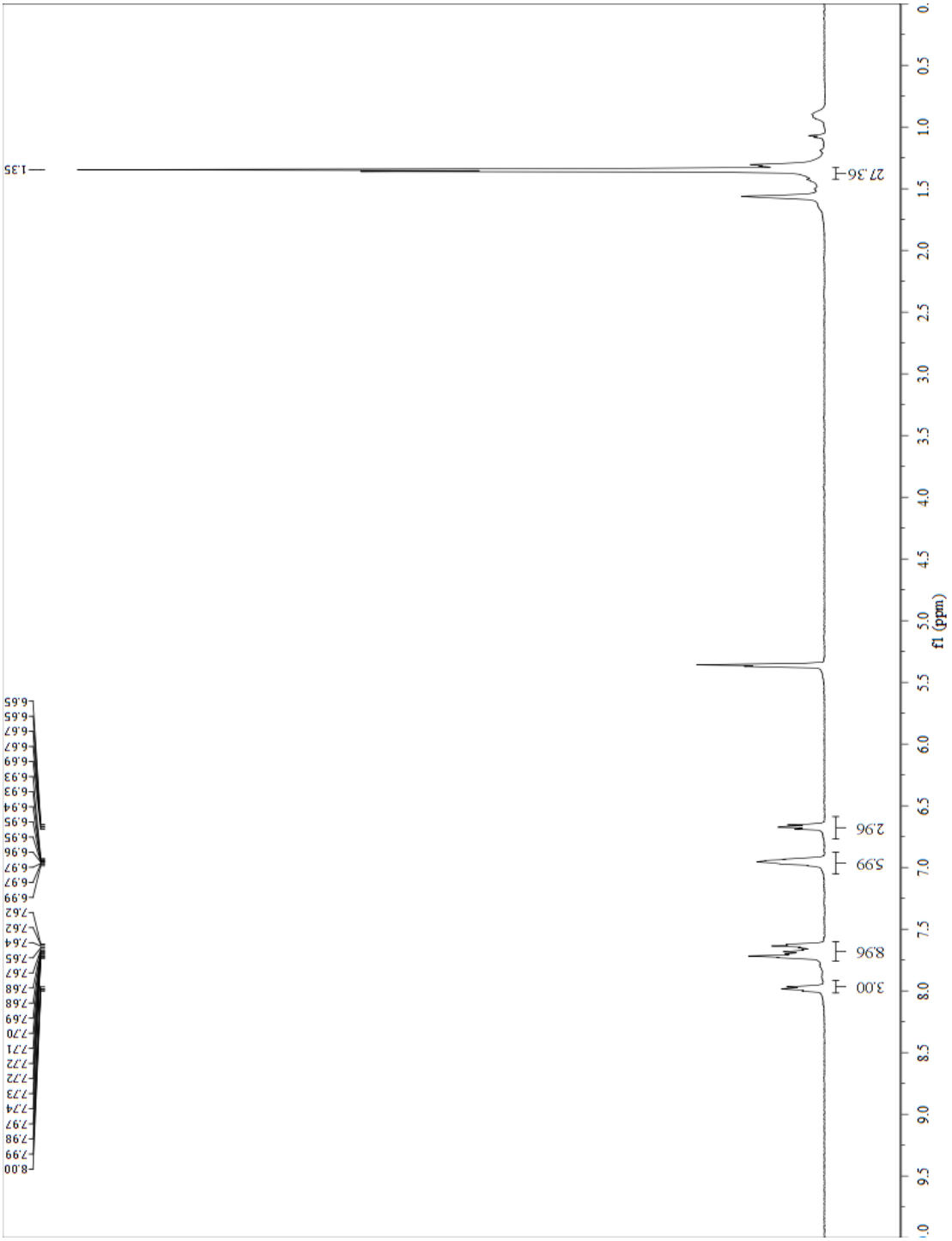

^{13}CNMR spectrum of **3f**

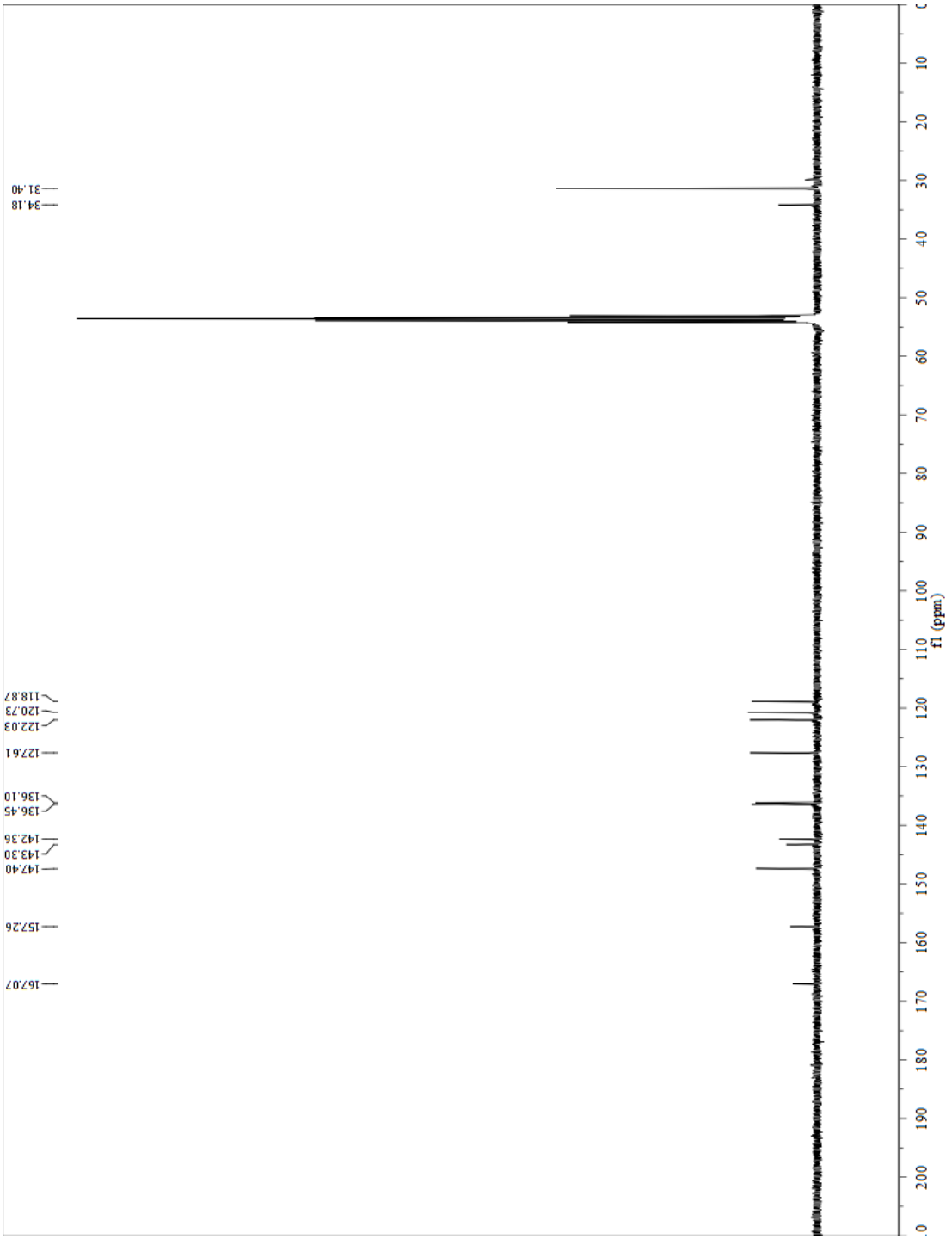

^{1}H NMR spectrum of **3h**

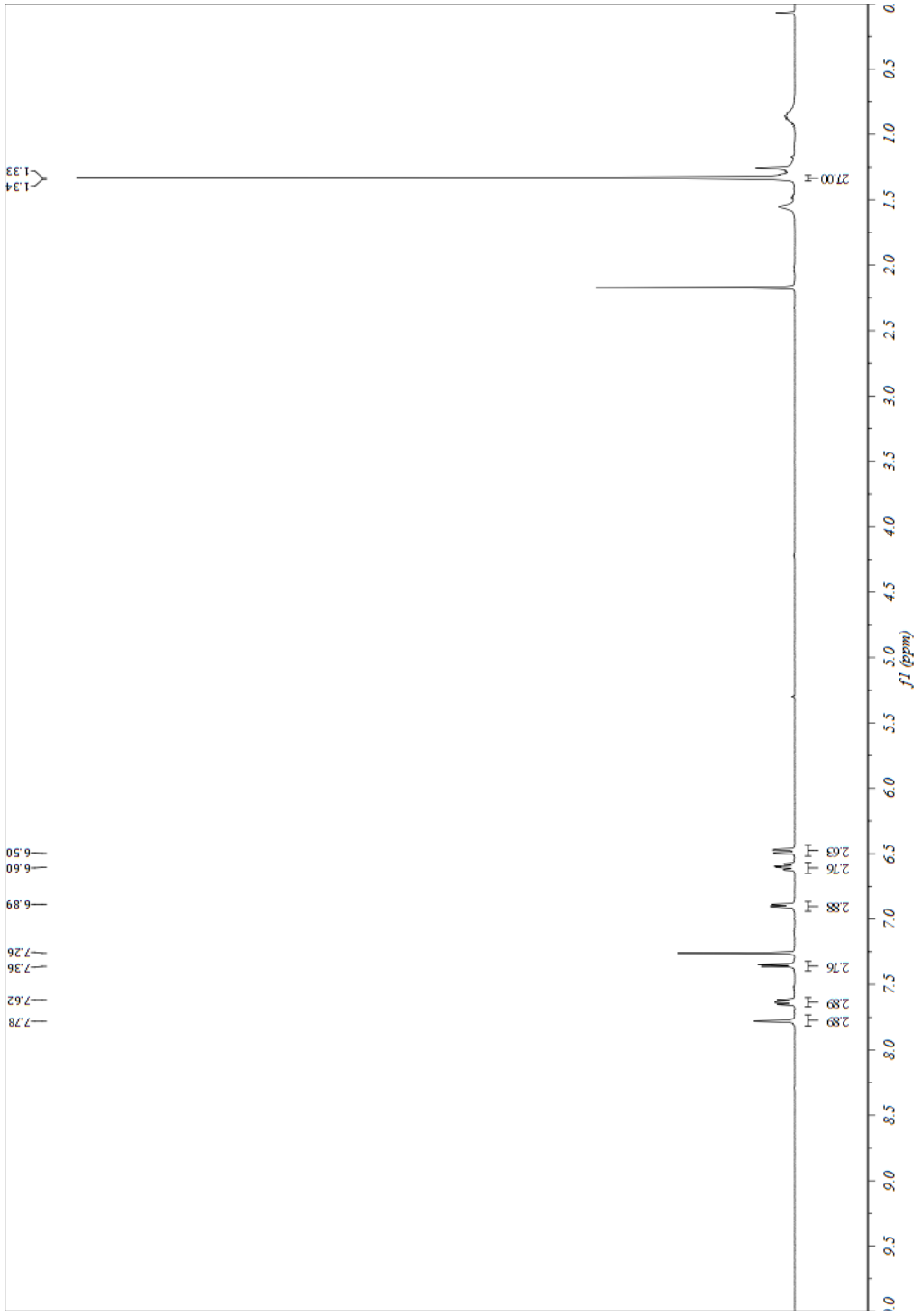

^{13}CNMR spectrum of **3h**

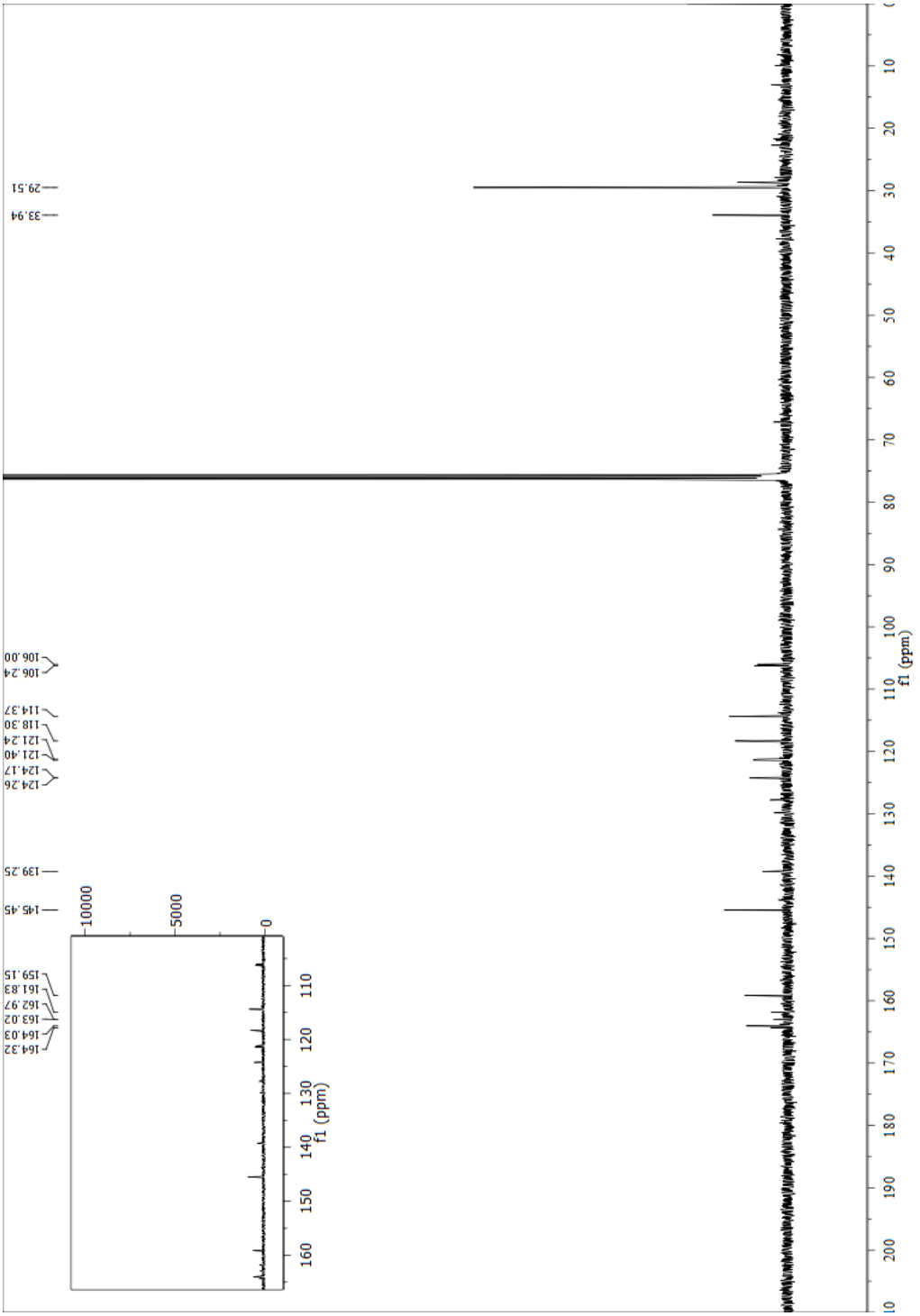

^{19}FNMR spectrum of **3h**

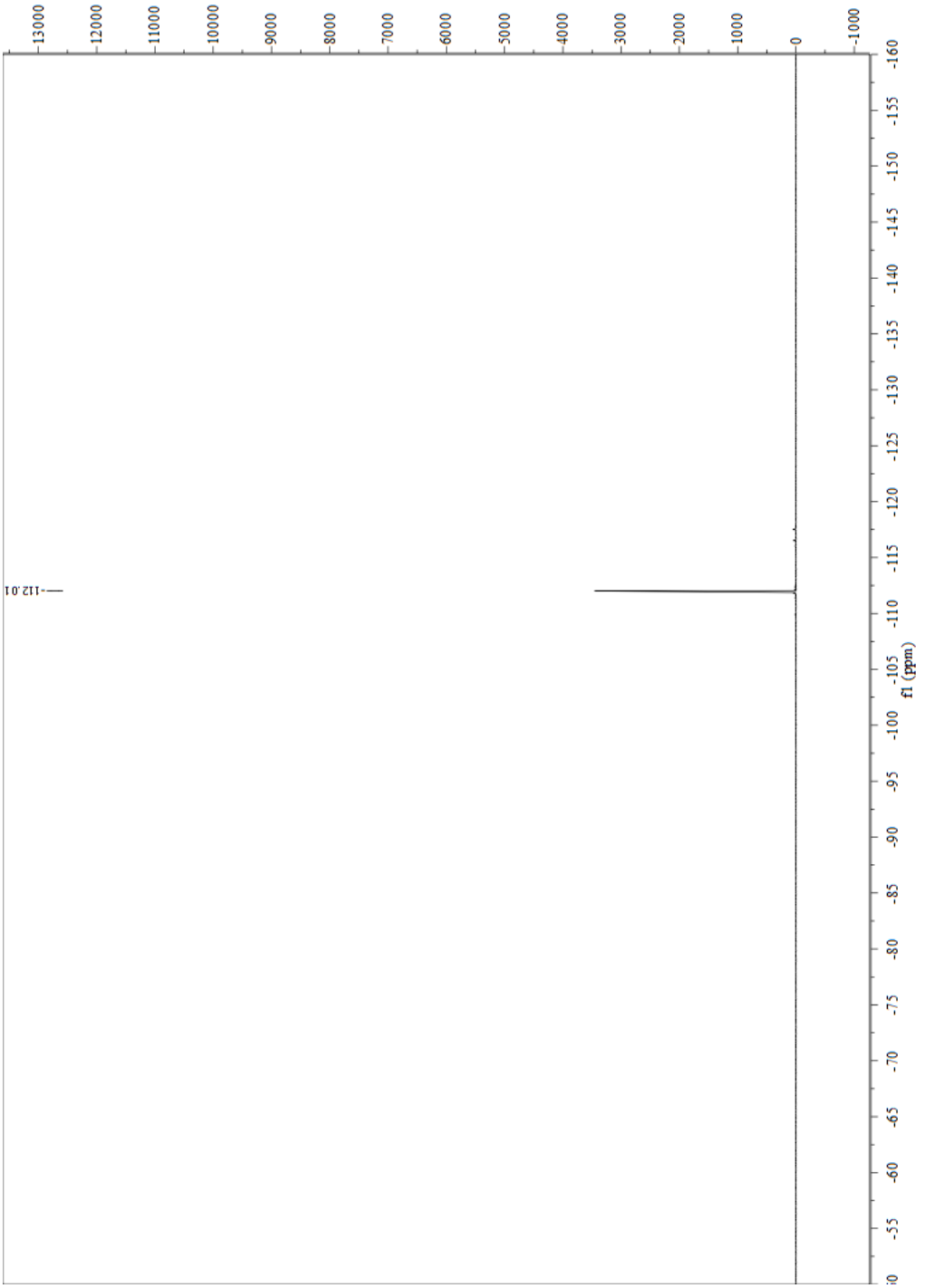

^{1}H NMR spectrum of **4ga**

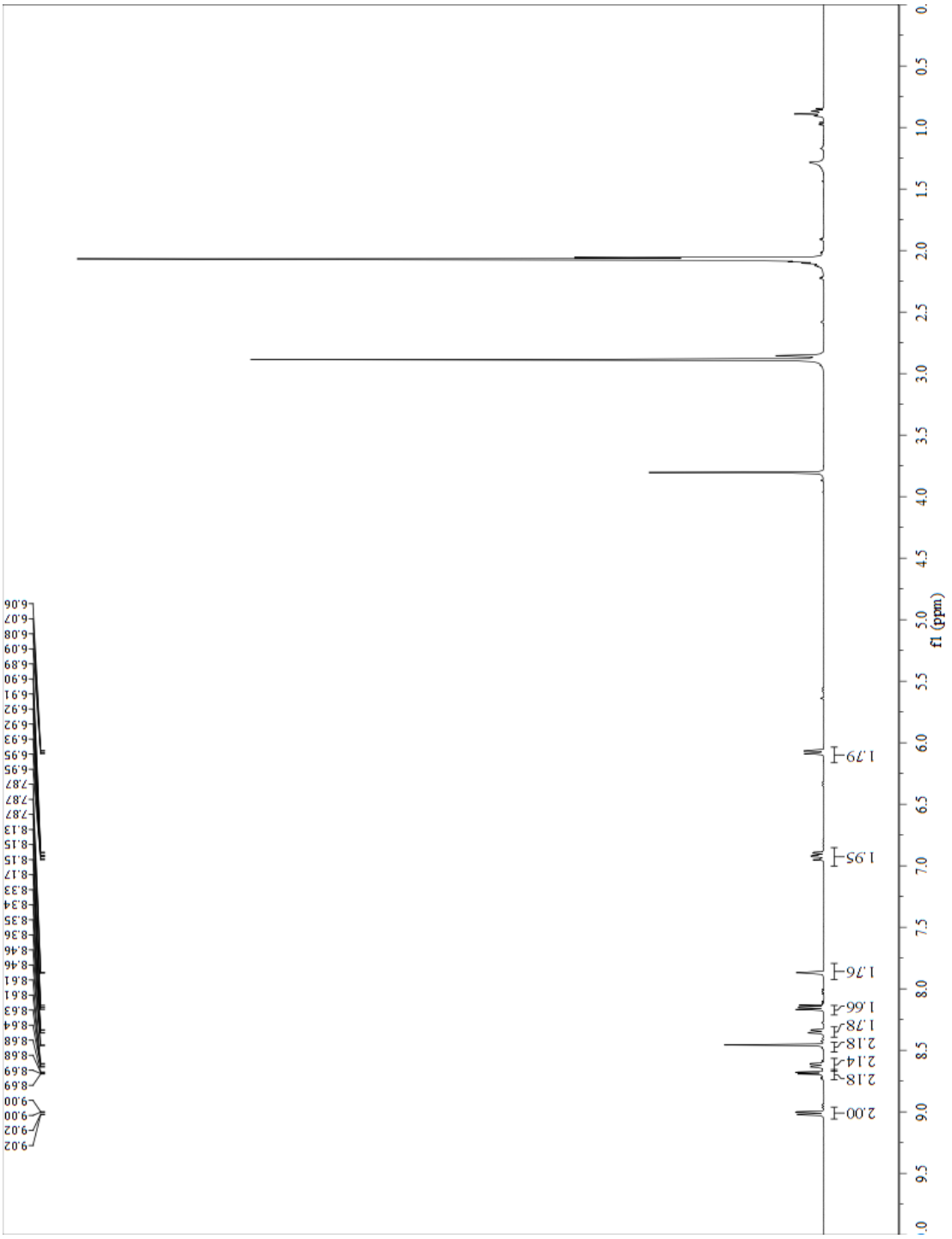

^{13}CNMR spectrum of **4ga**

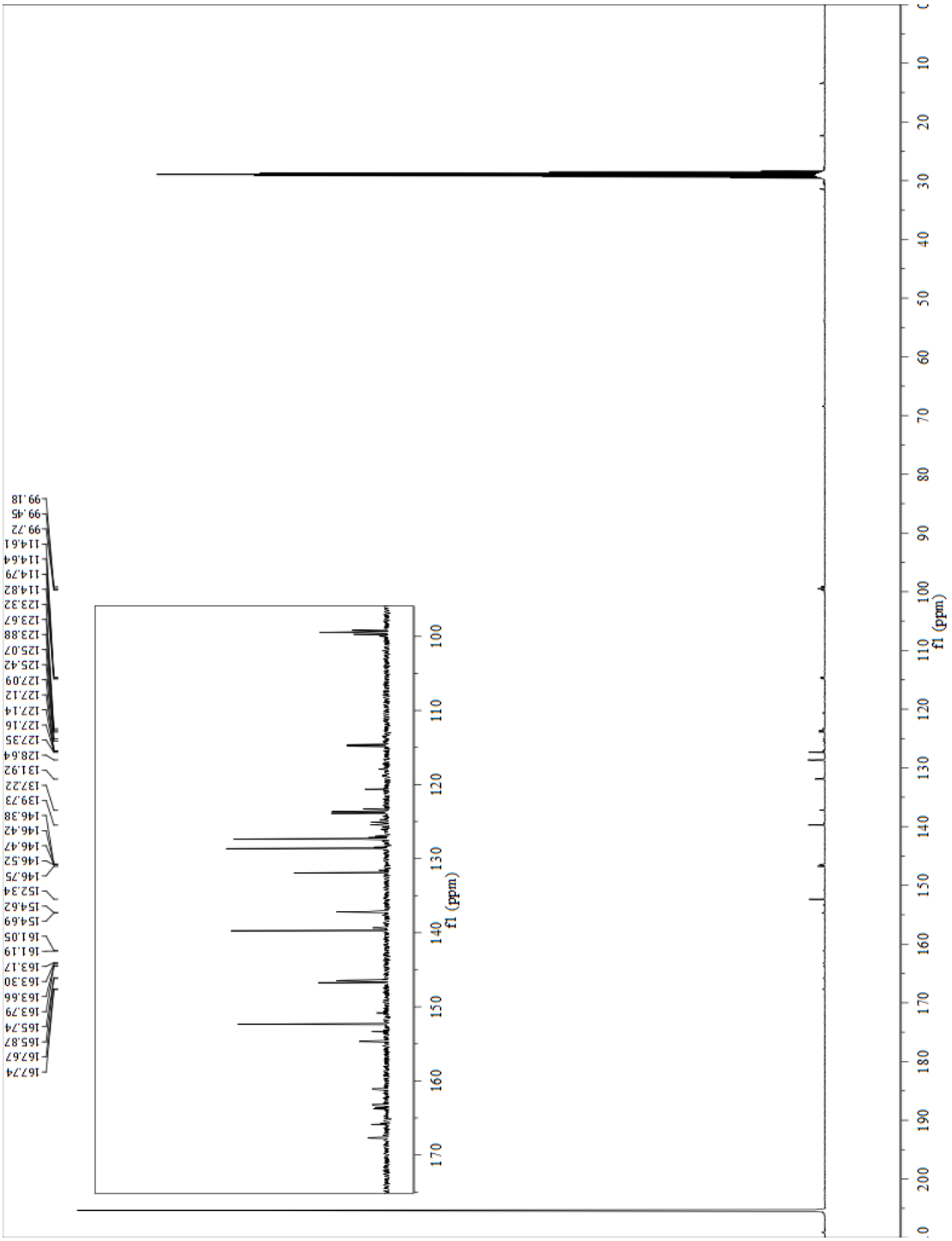

^{19}FNMR spectrum of **4ga**

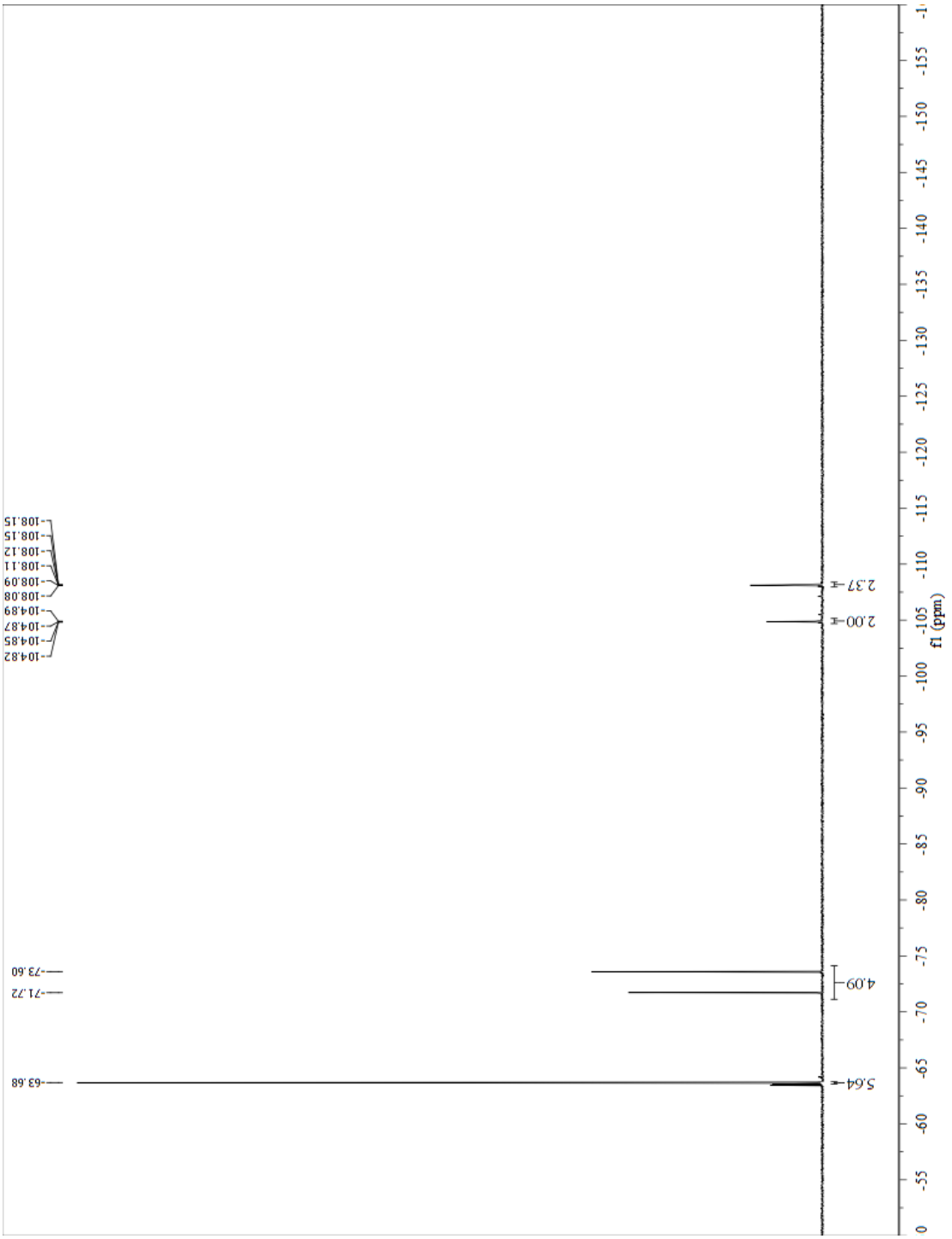

^{31}PNMR spectrum of **4ga**

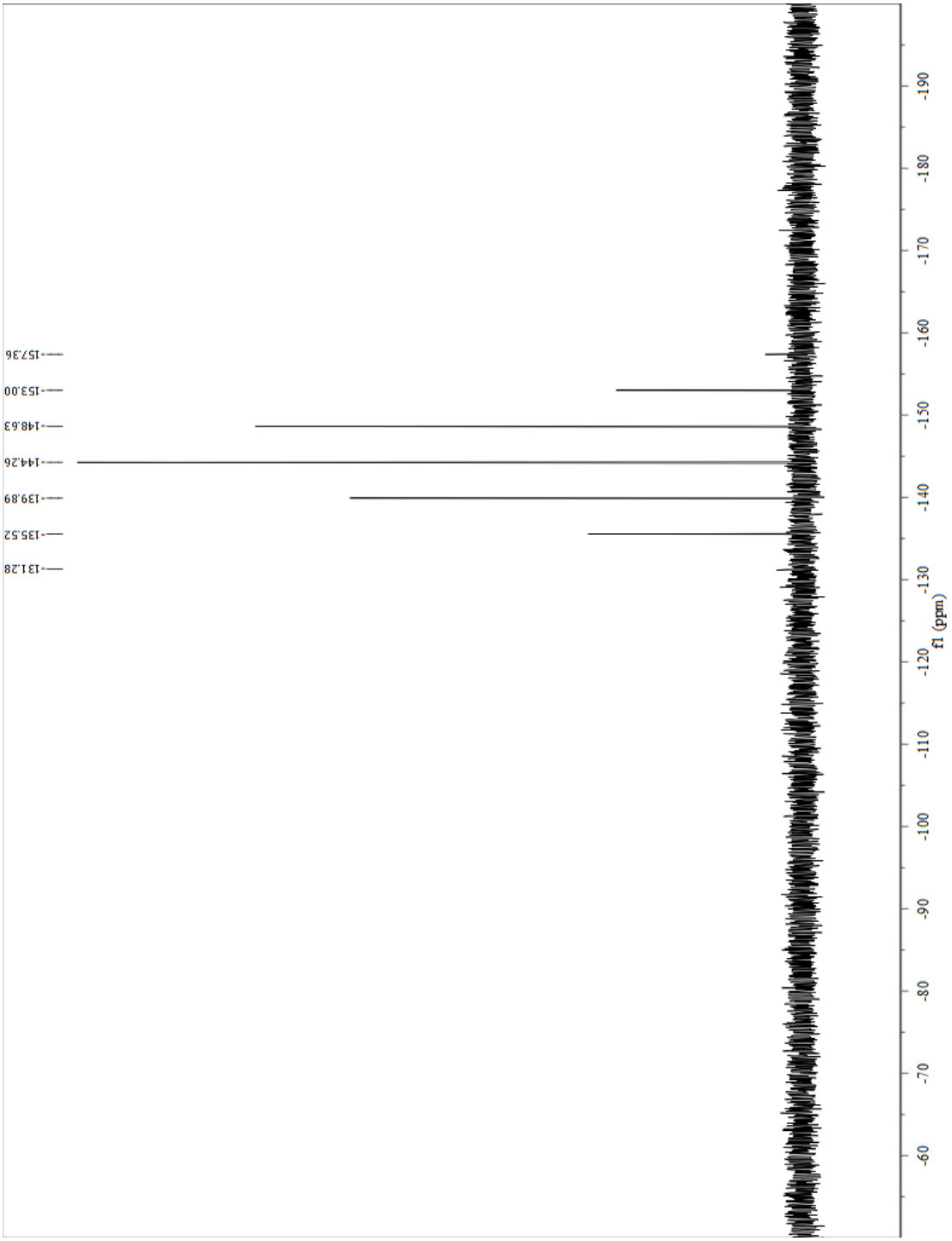

^{1}H NMR spectrum of **4gb**

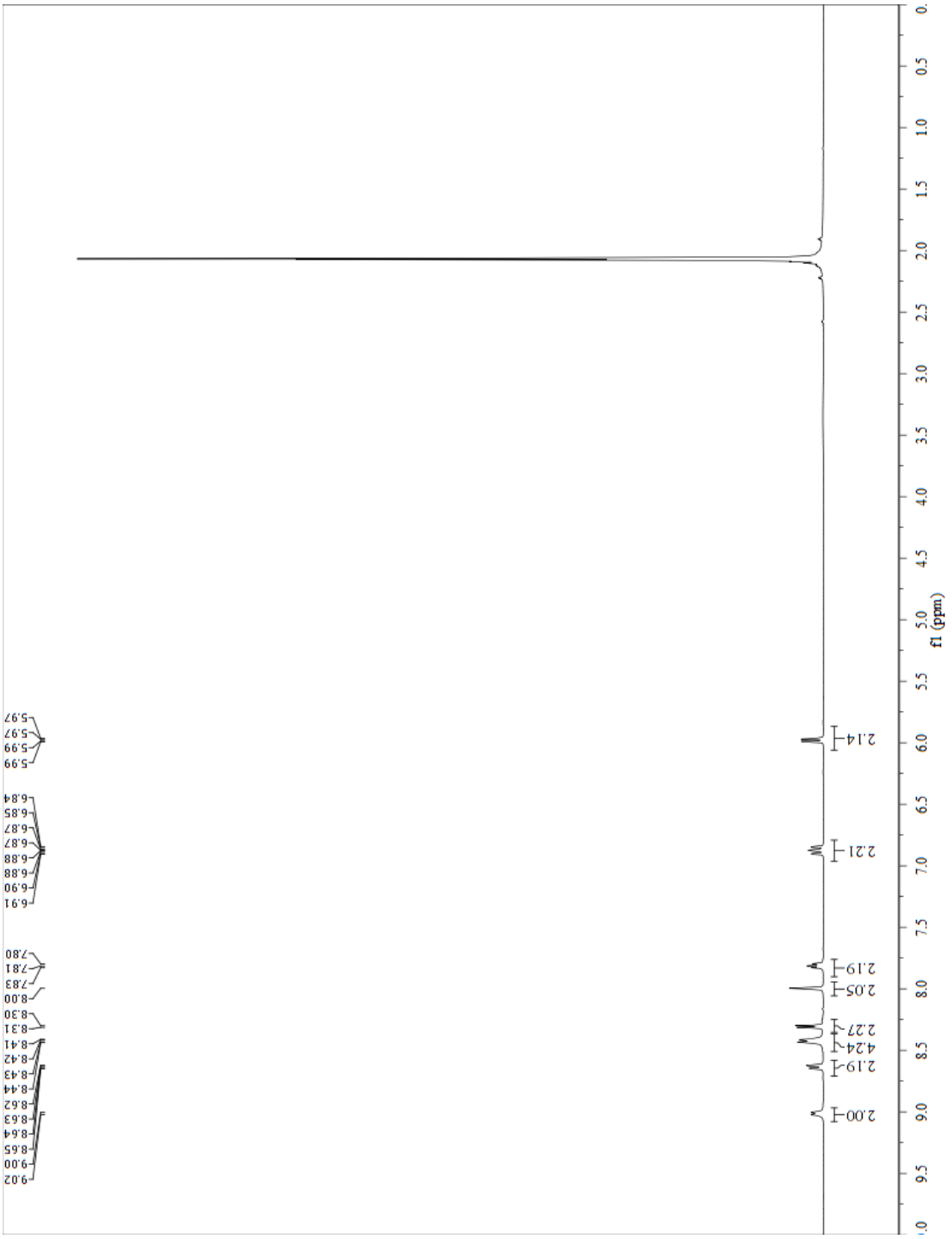

^{13}CNMR spectrum of **4gb**

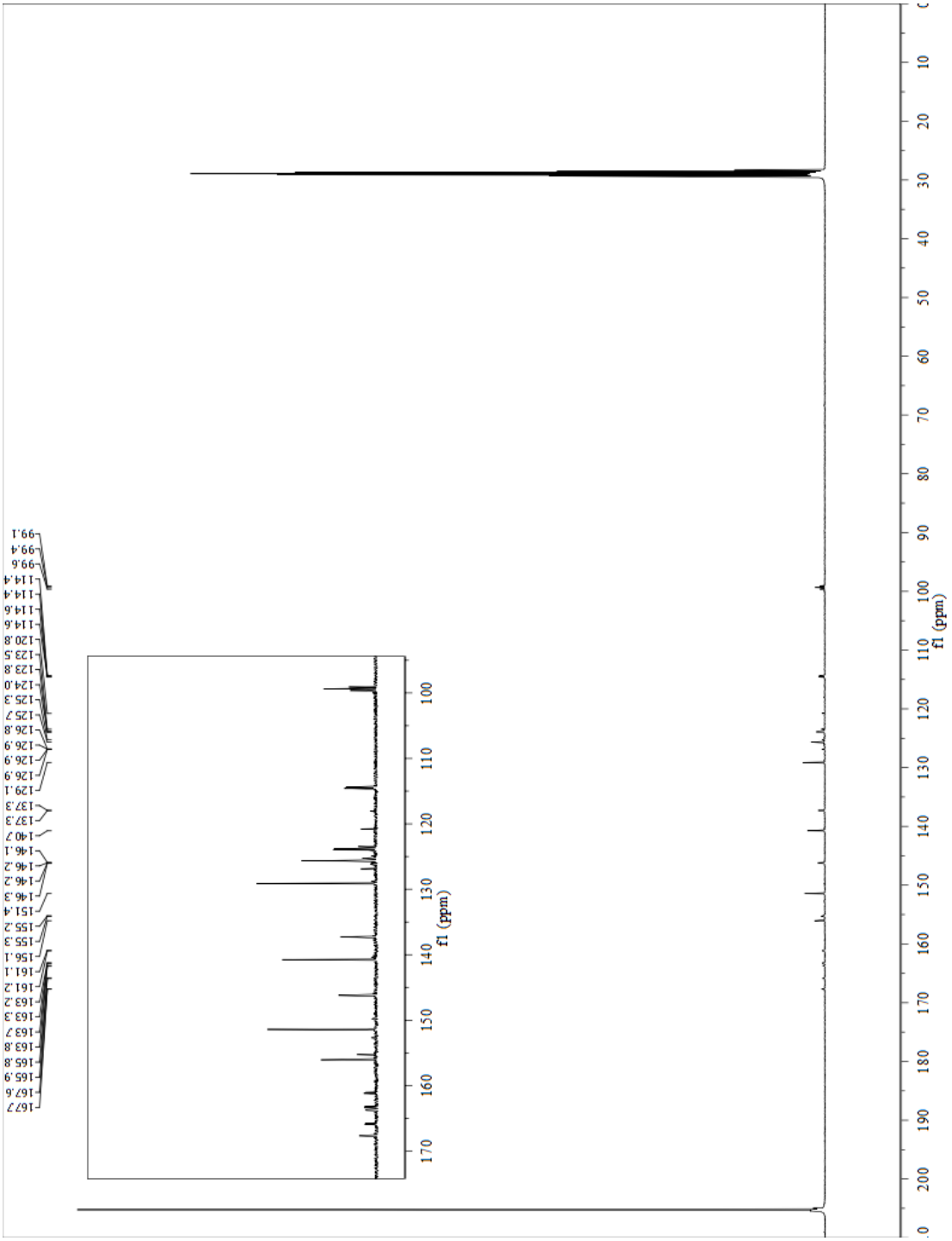

^{19}FNMR spectrum of **4gb**

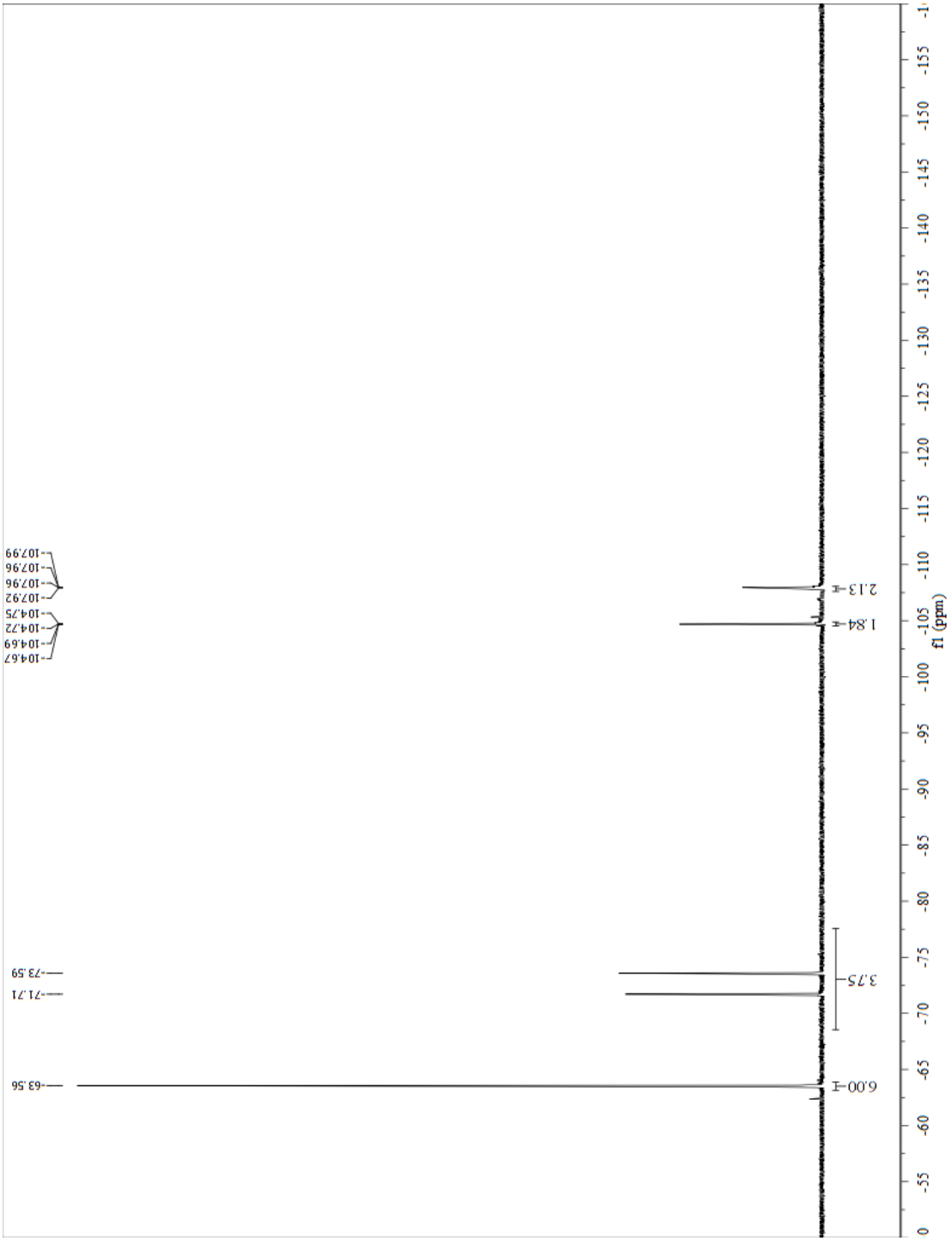

^{31}PNMR spectrum of **4gb**

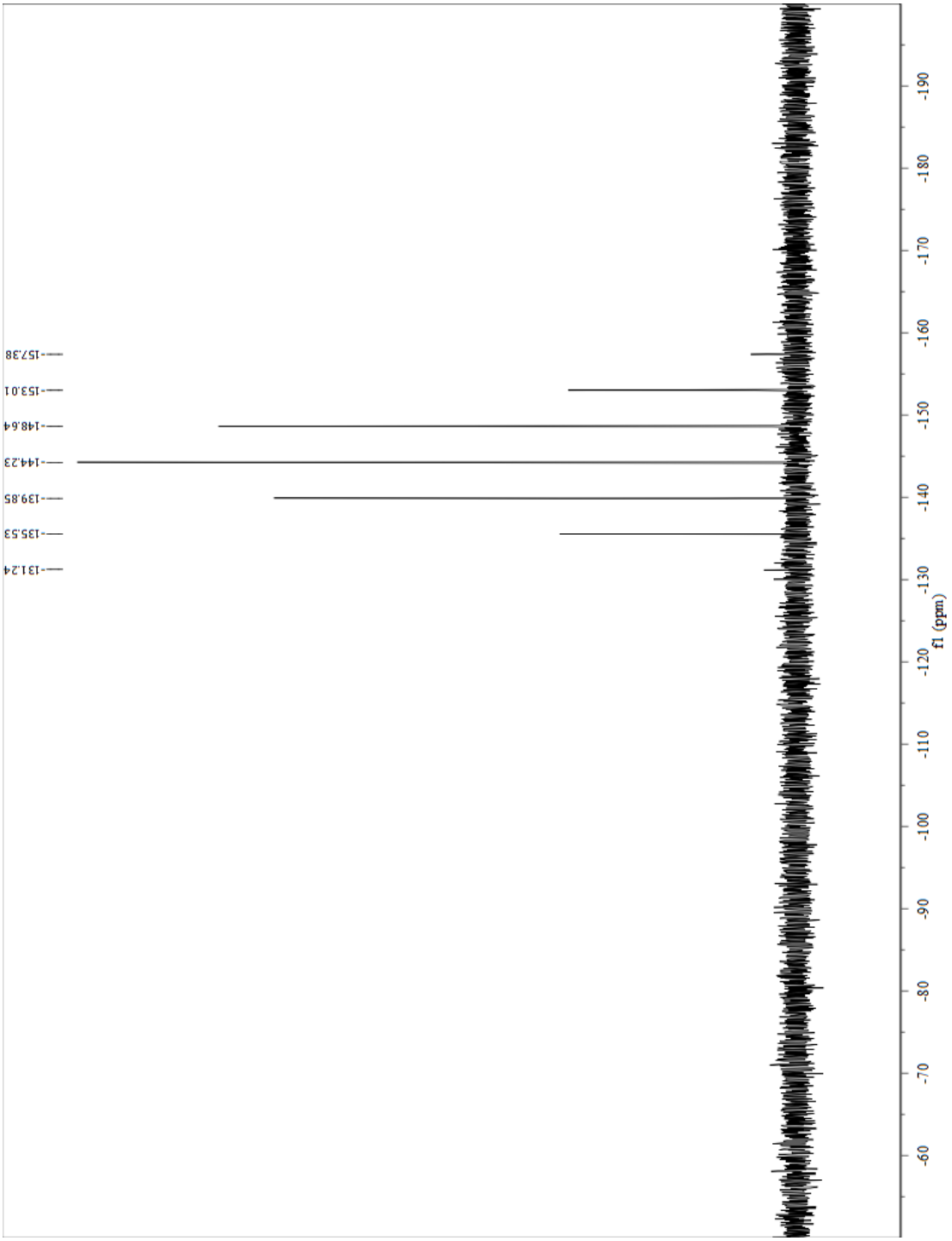

^{1}H NMR spectrum of **4gc**

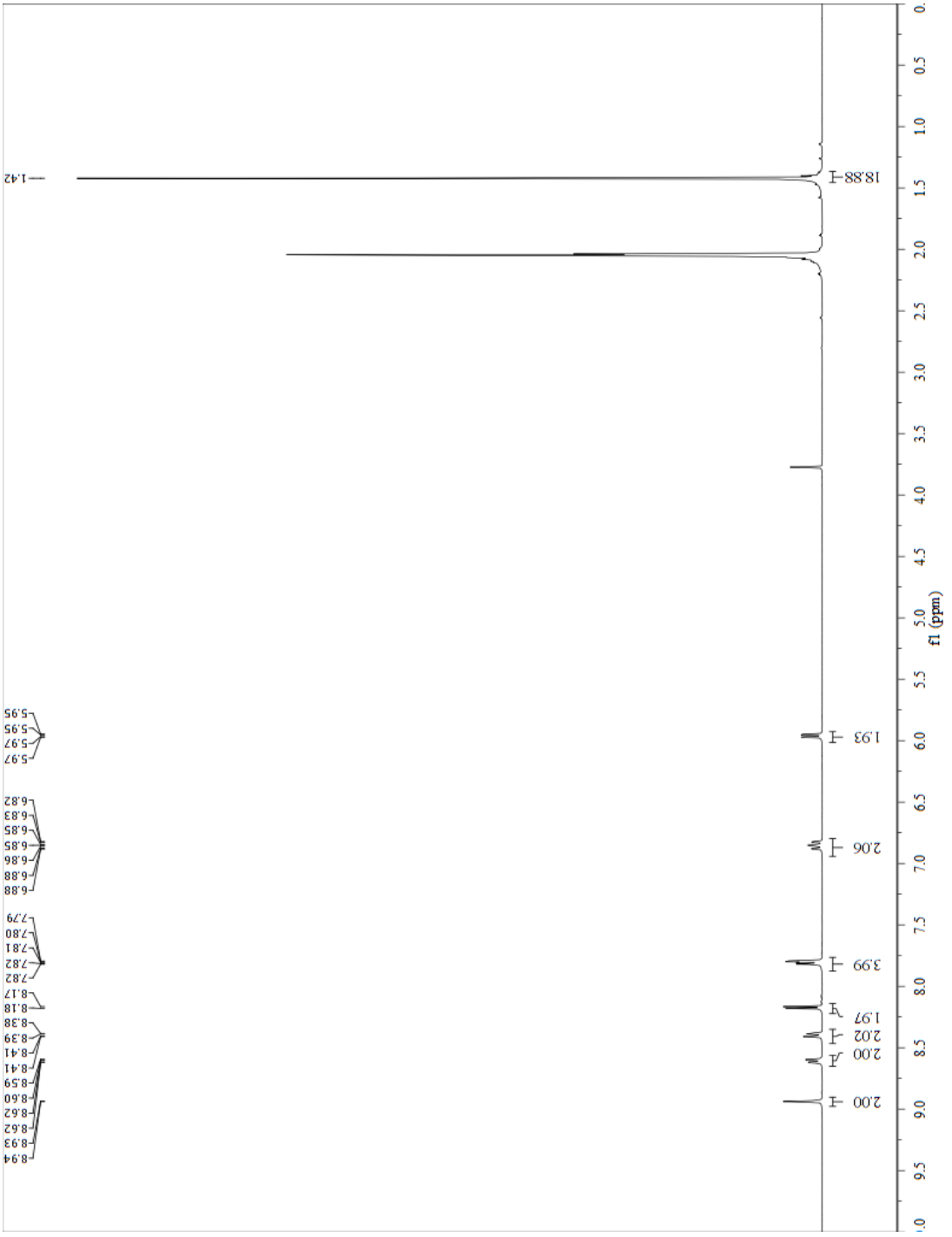

^{13}CNMR spectrum of **4gc**

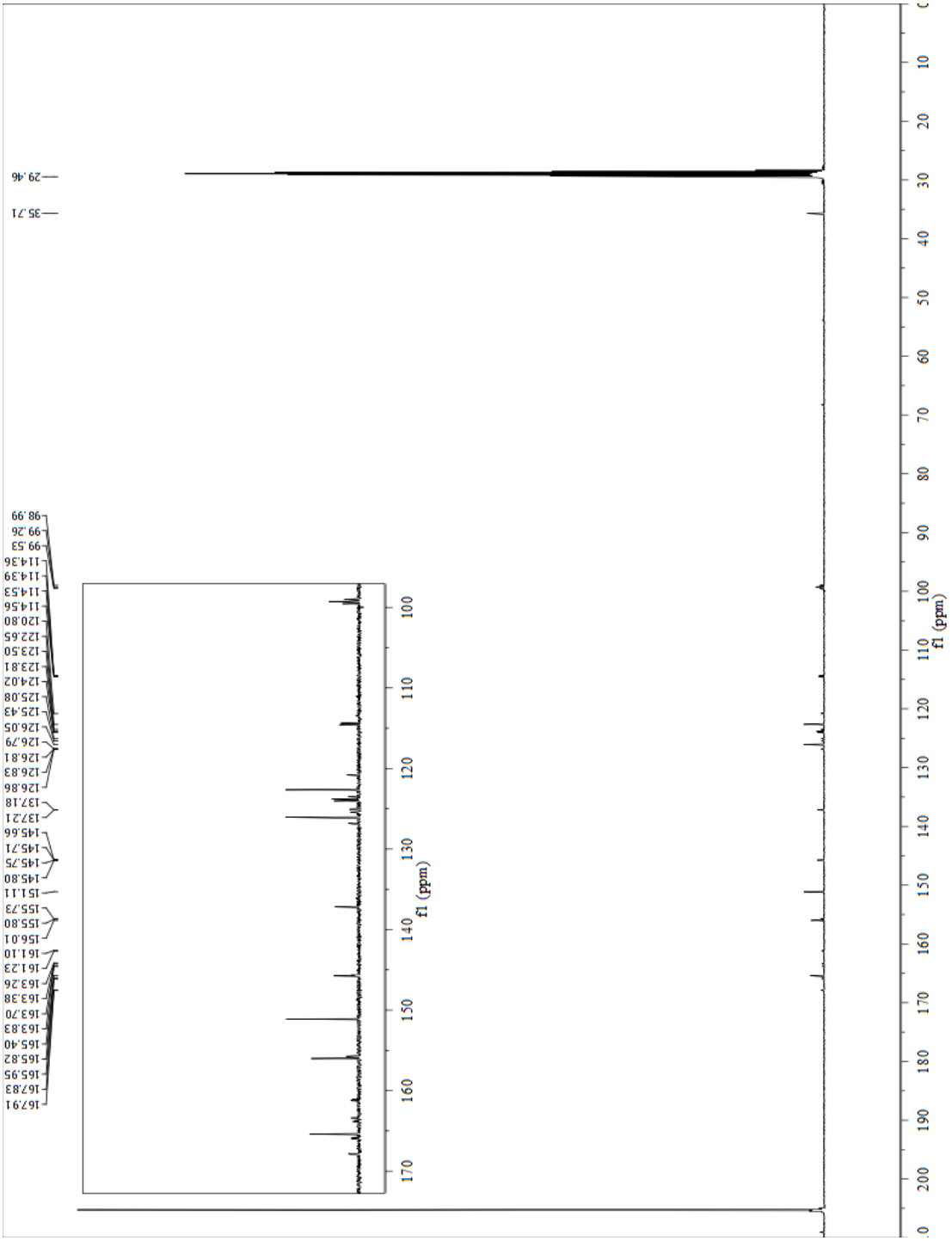

^{19}FNMR spectrum of **4gc**

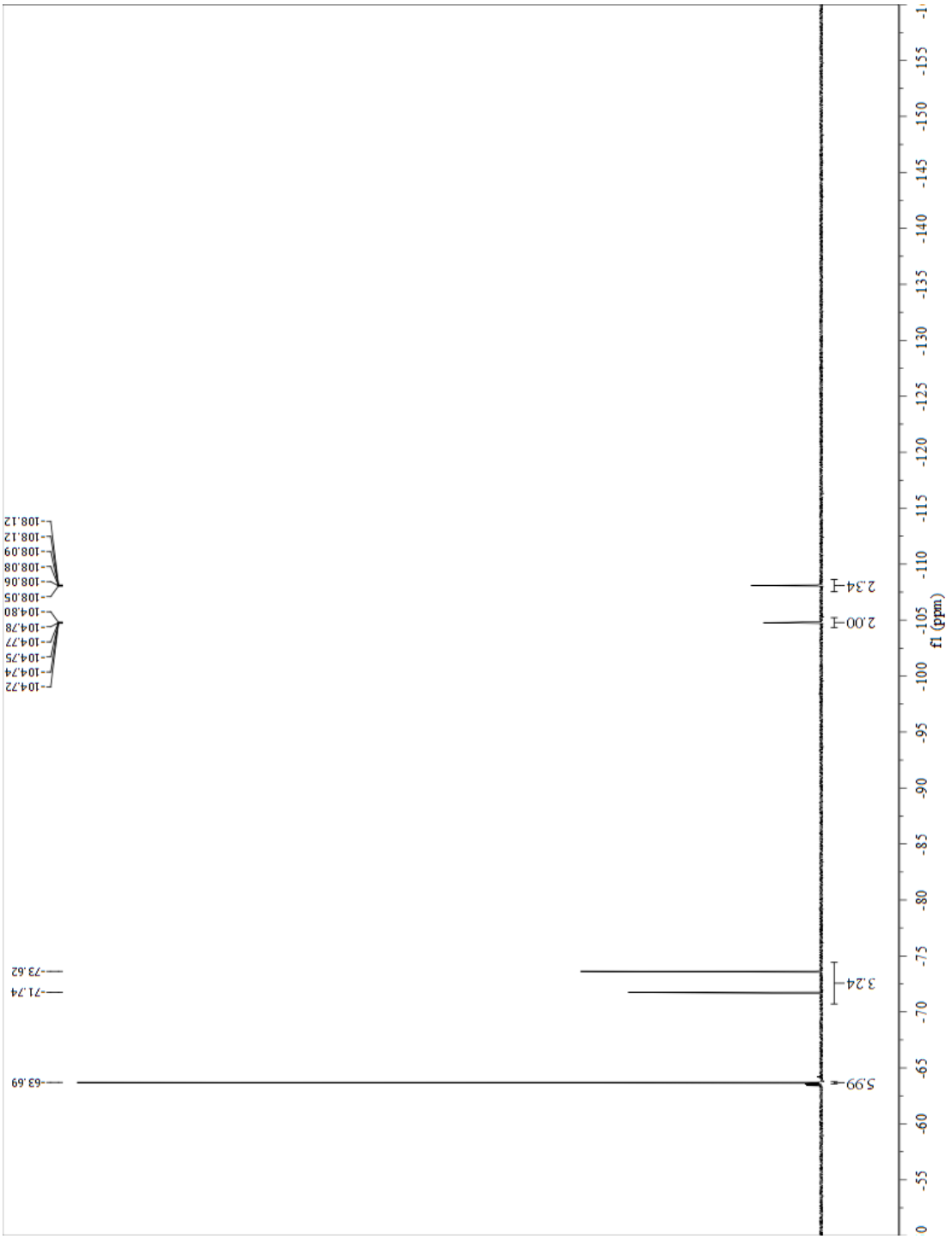

^{31}PNMR spectrum of **4gc**

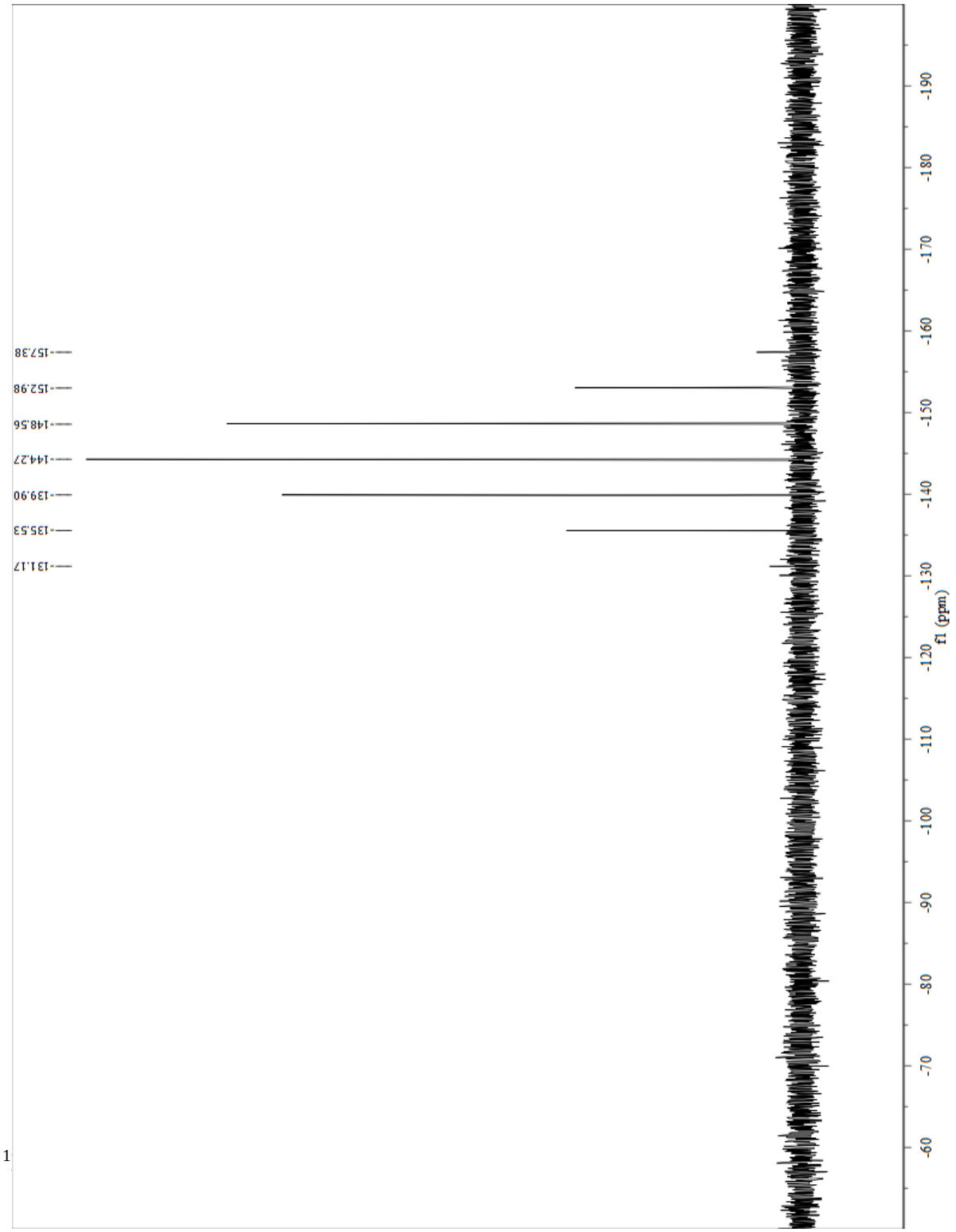

^{1}HNMR spectrum of **4db**

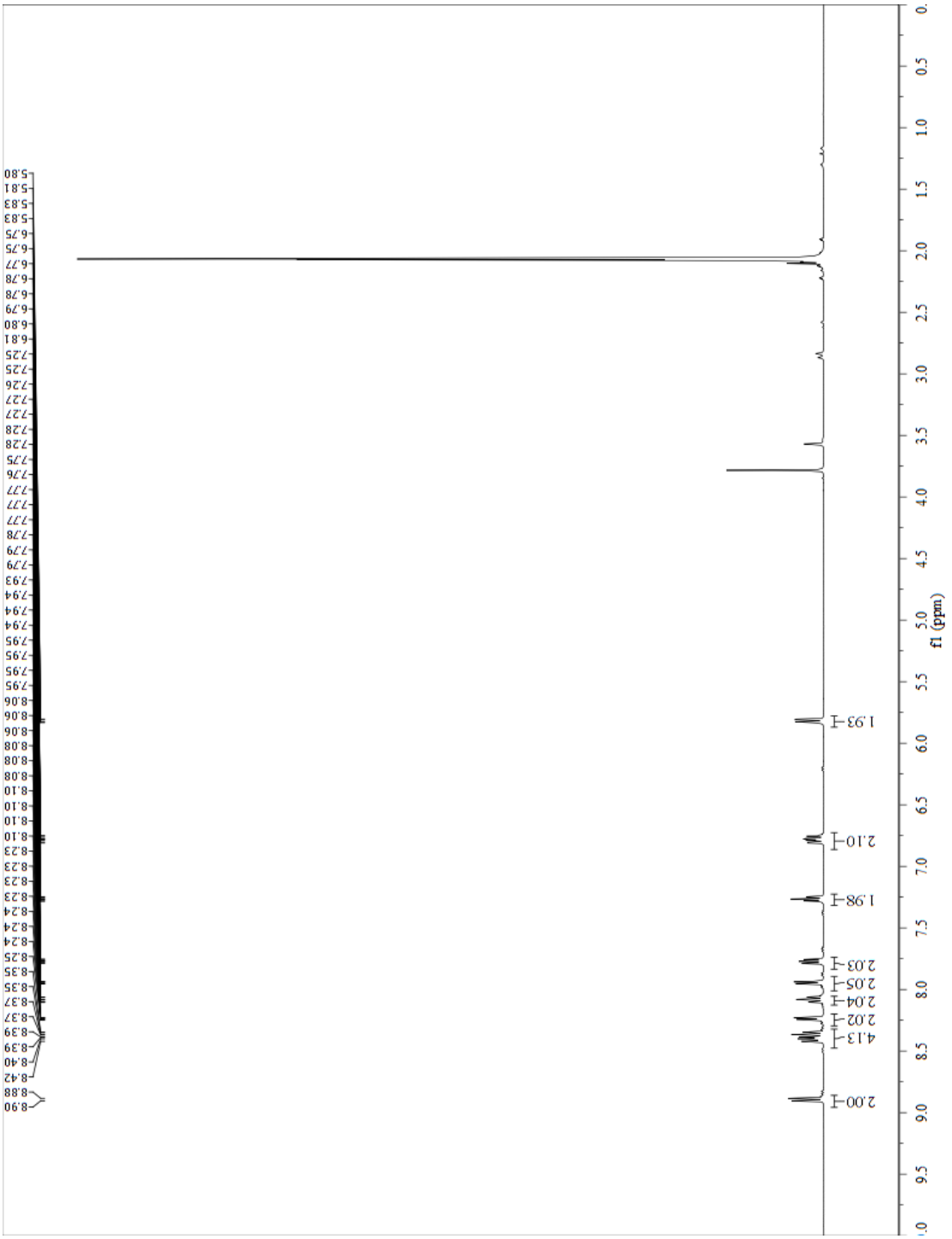

^{13}CNMR spectrum of **4db**

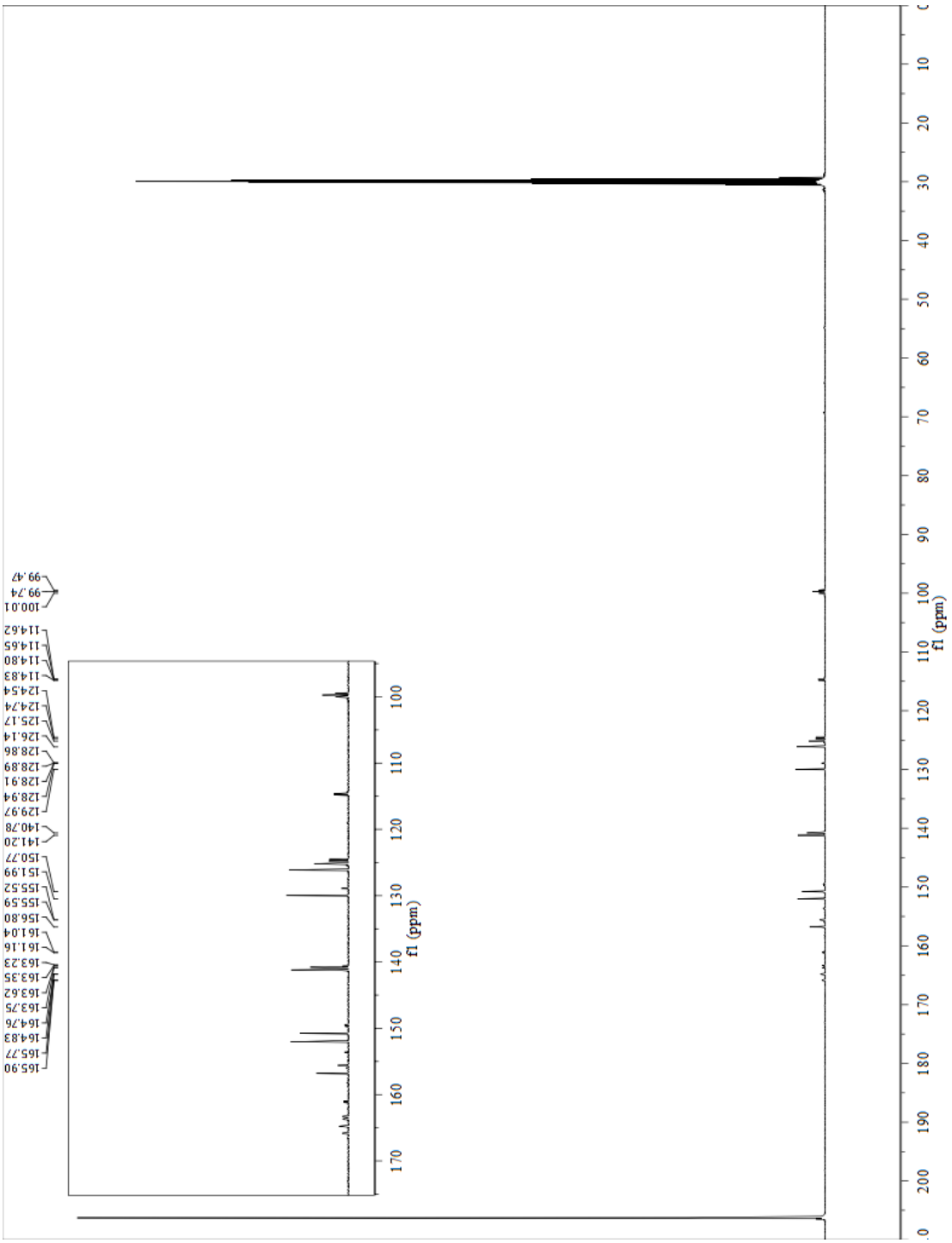

^{19}FNMR spectrum of **4db**

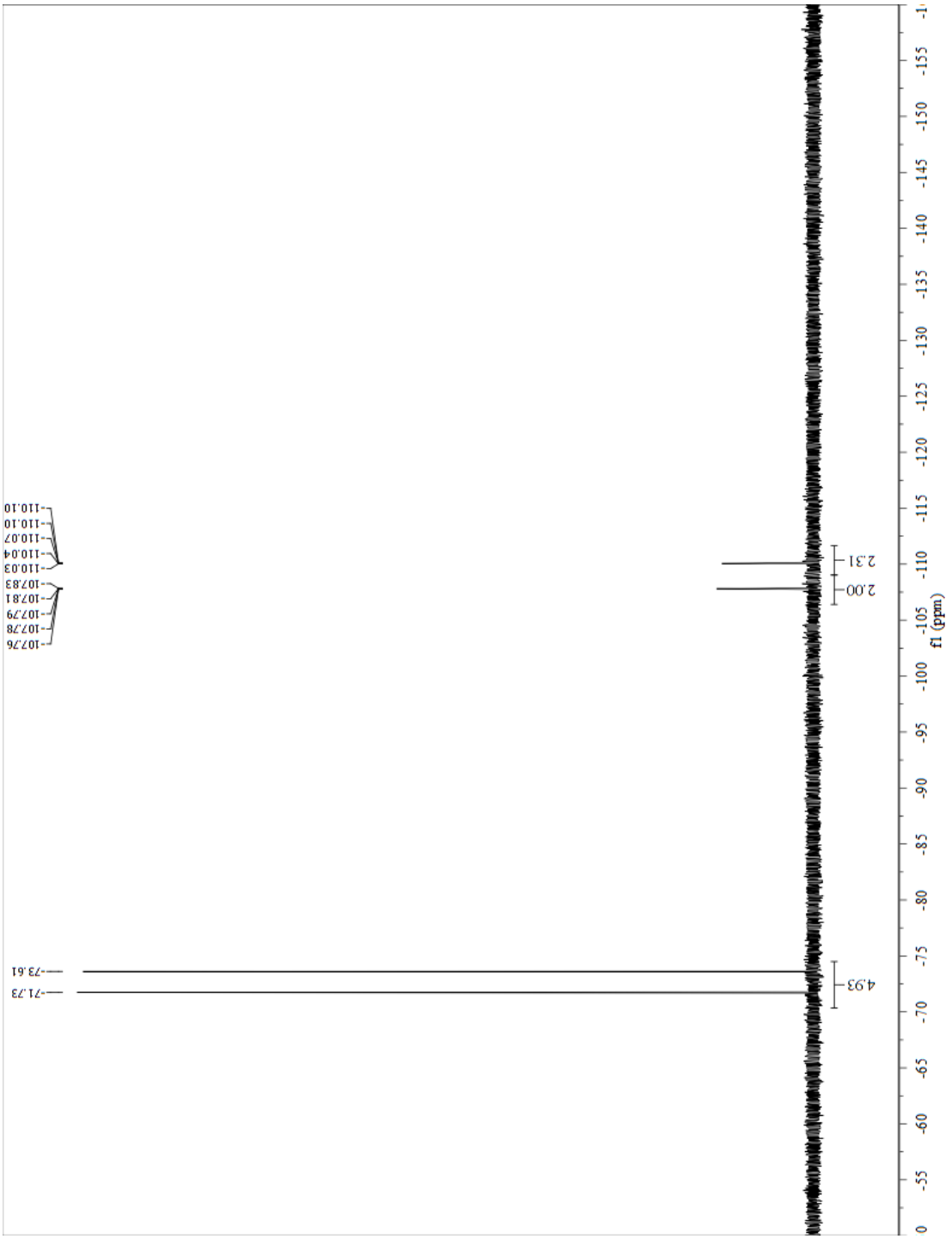

^{31}PNMR spectrum of **4db**

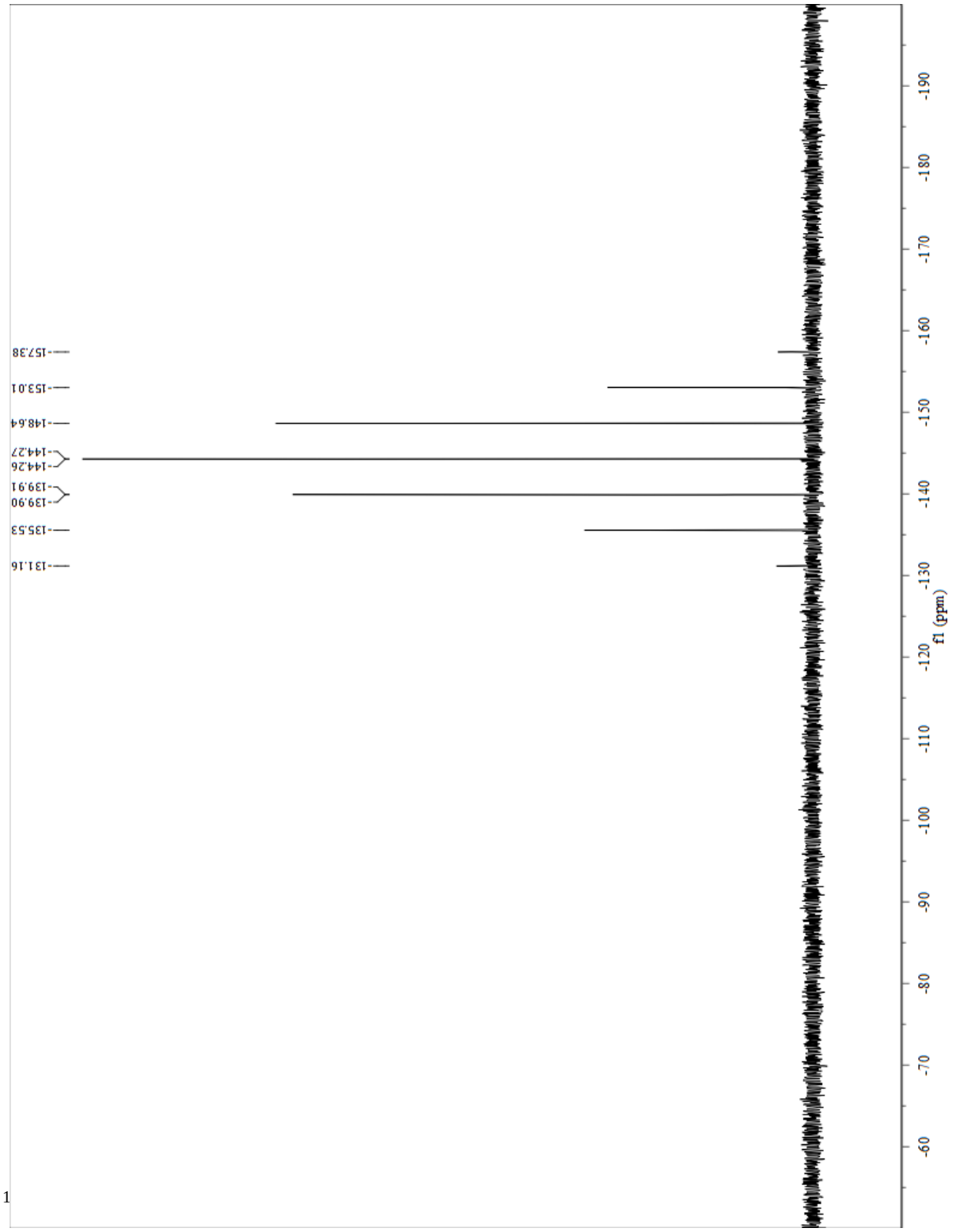

^{1}HNMR spectrum of **4dc**

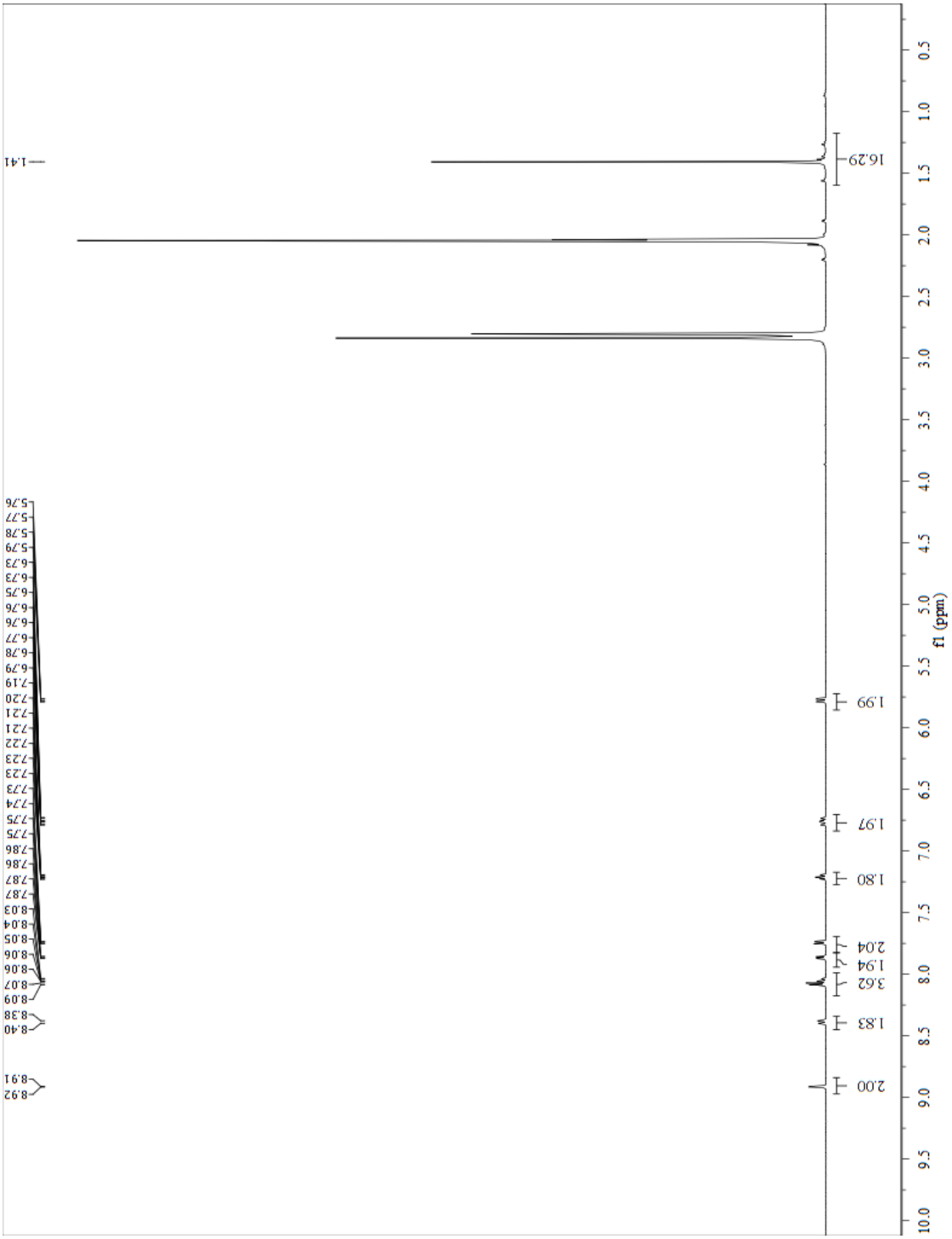

^{13}CNMR spectrum of **4dc**

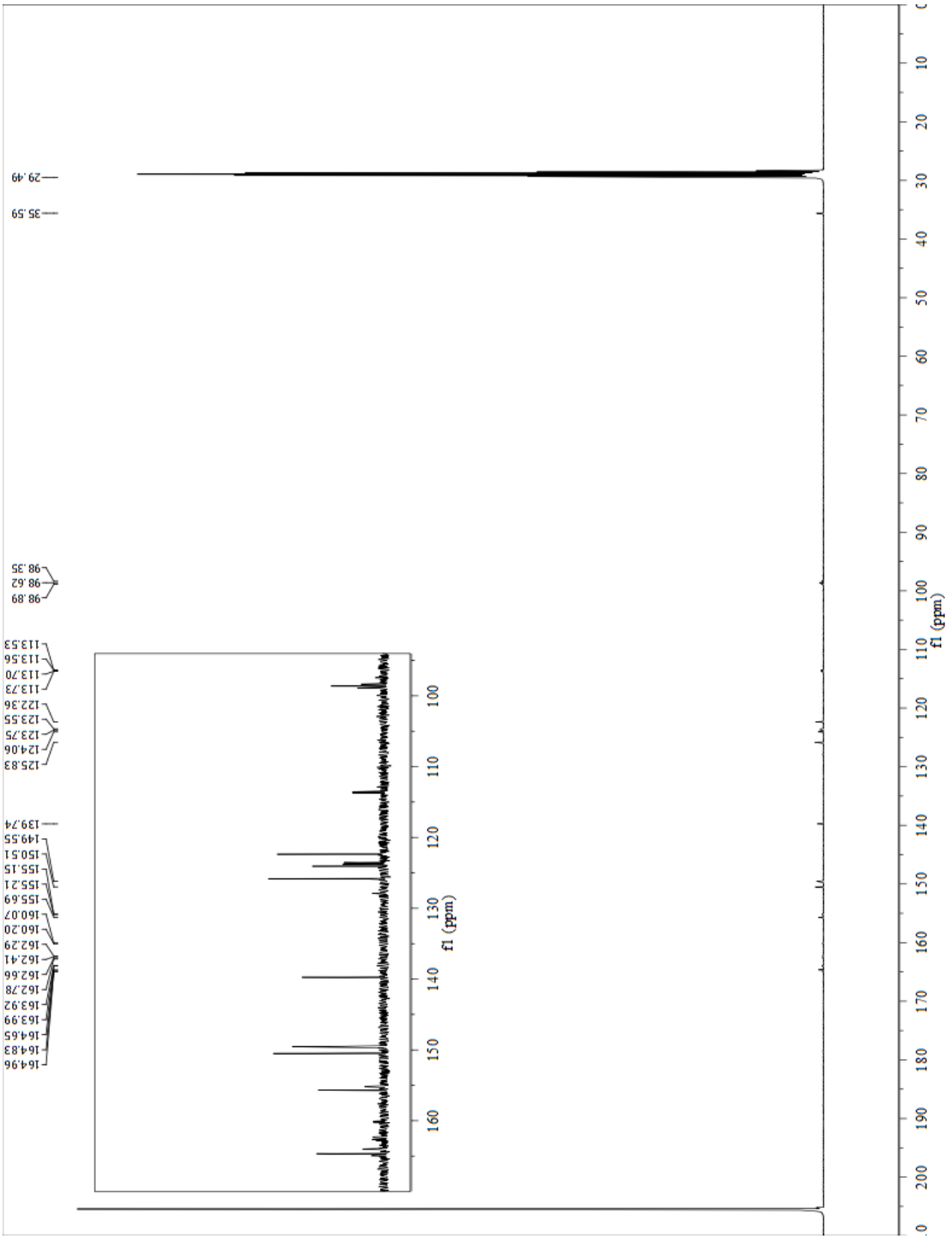

^{19}FNMR spectrum of **4dc**

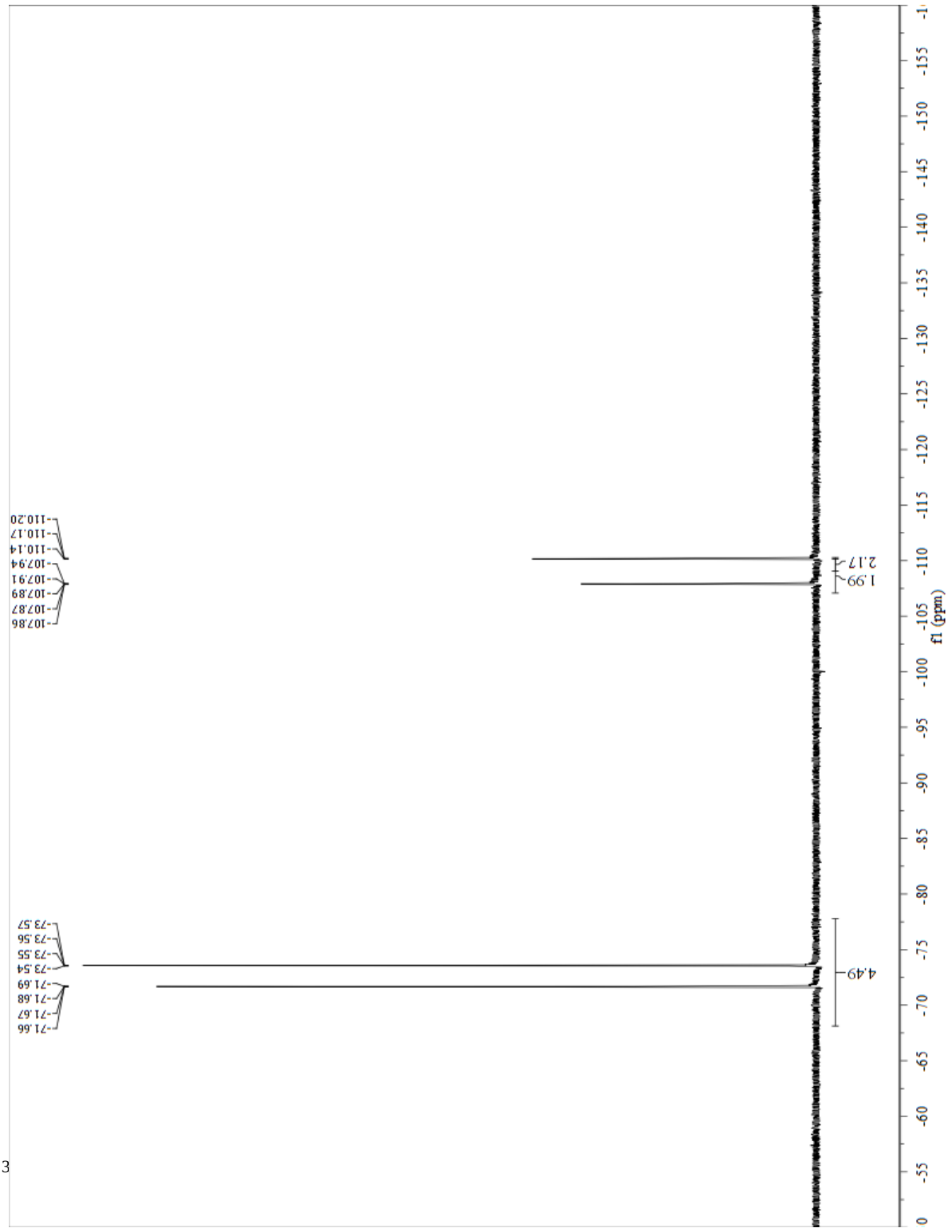

3

^{31}PNMR spectrum of **4dc**

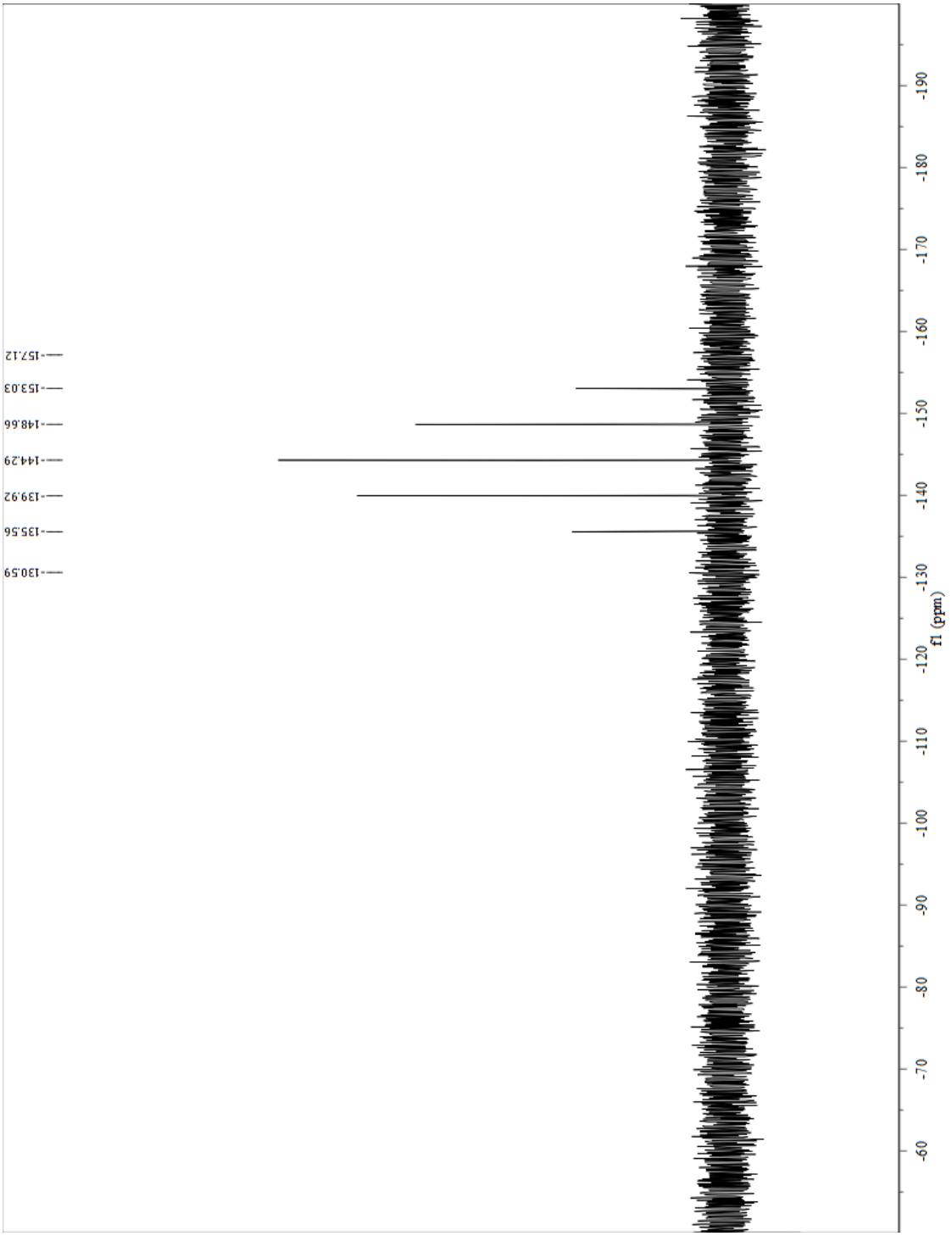

^{1}H NMR spectrum of **4cb**

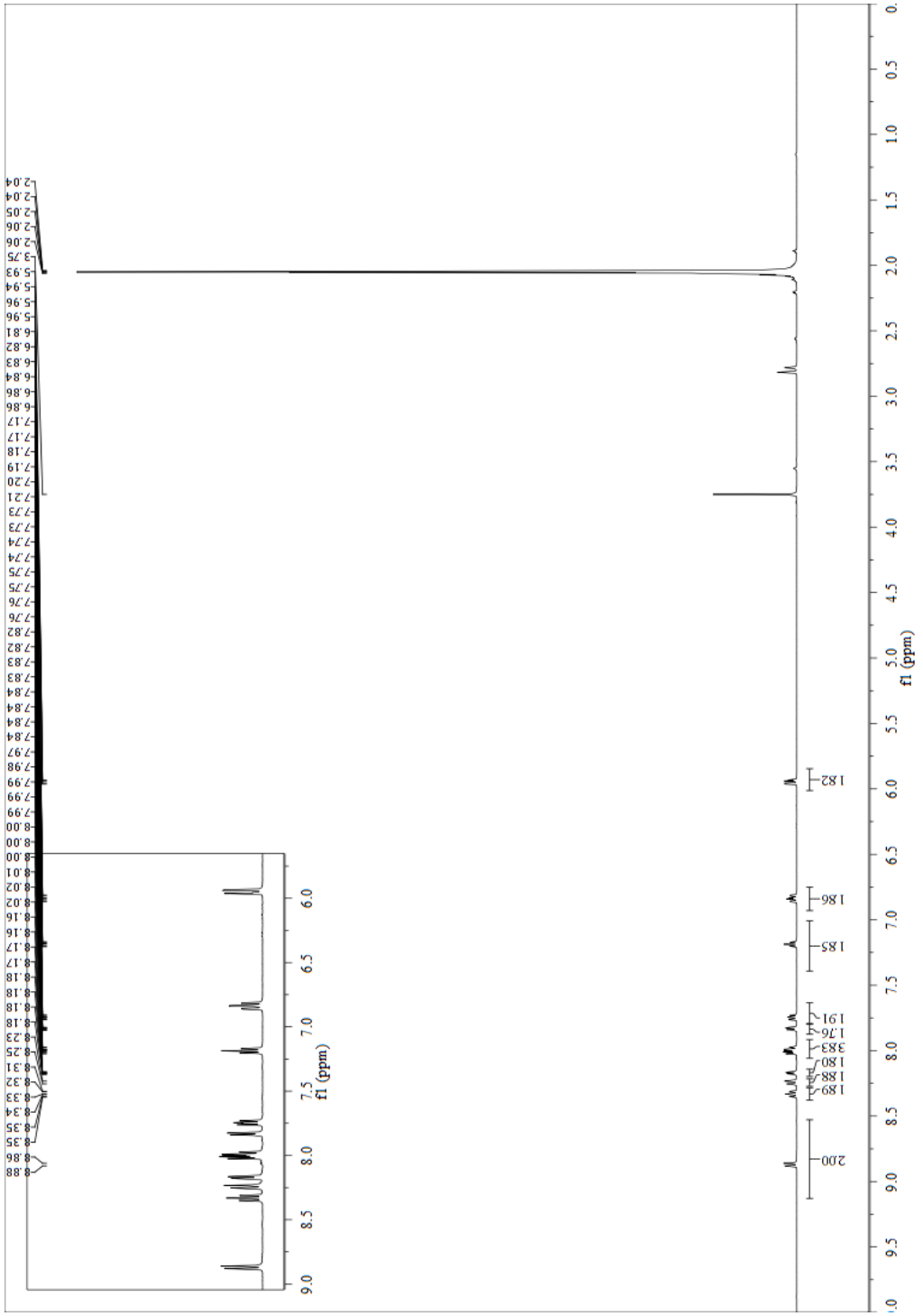

^{13}C NMR spectrum of **4cb**

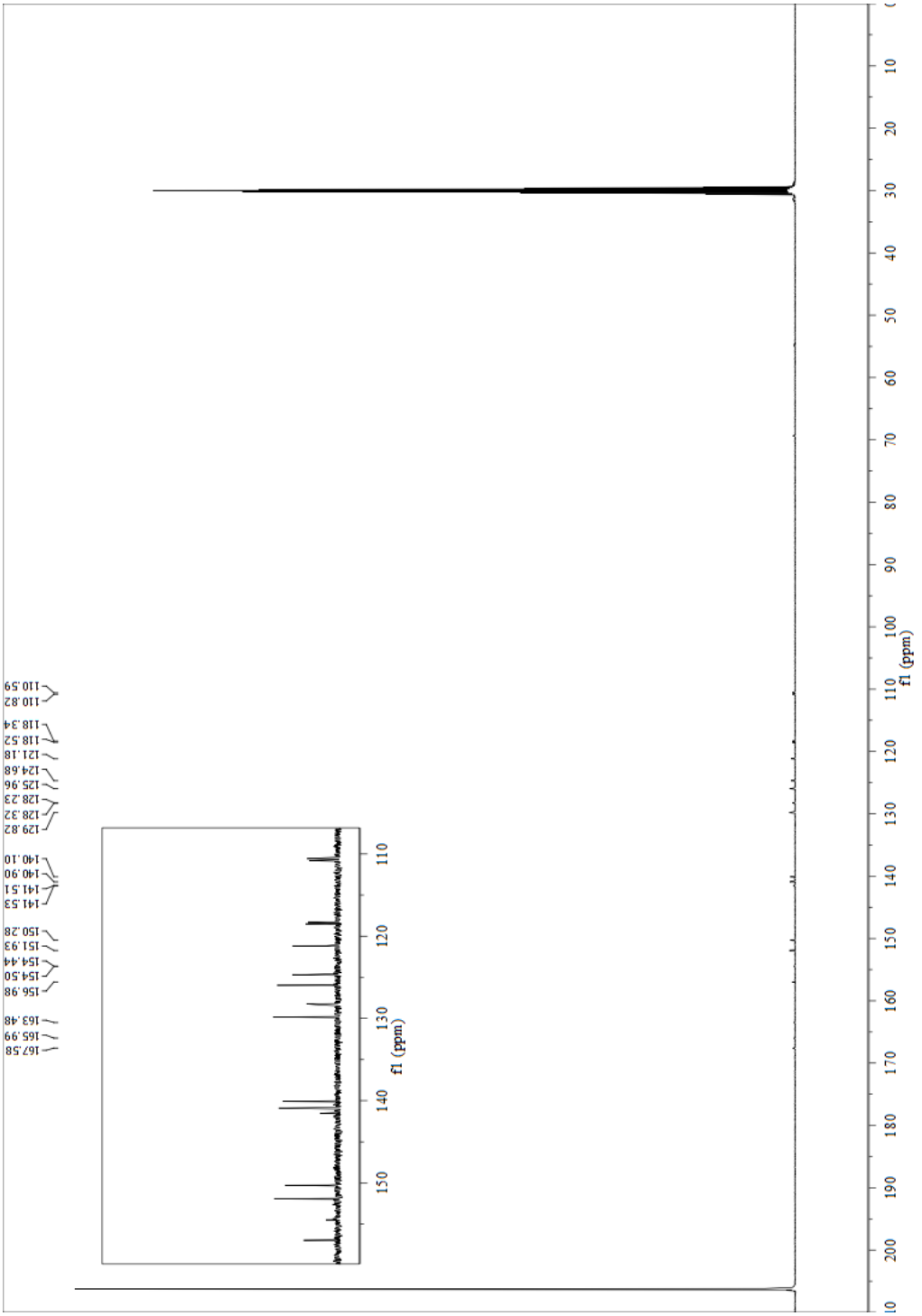

^{19}FNMR spectrum of **4cb**

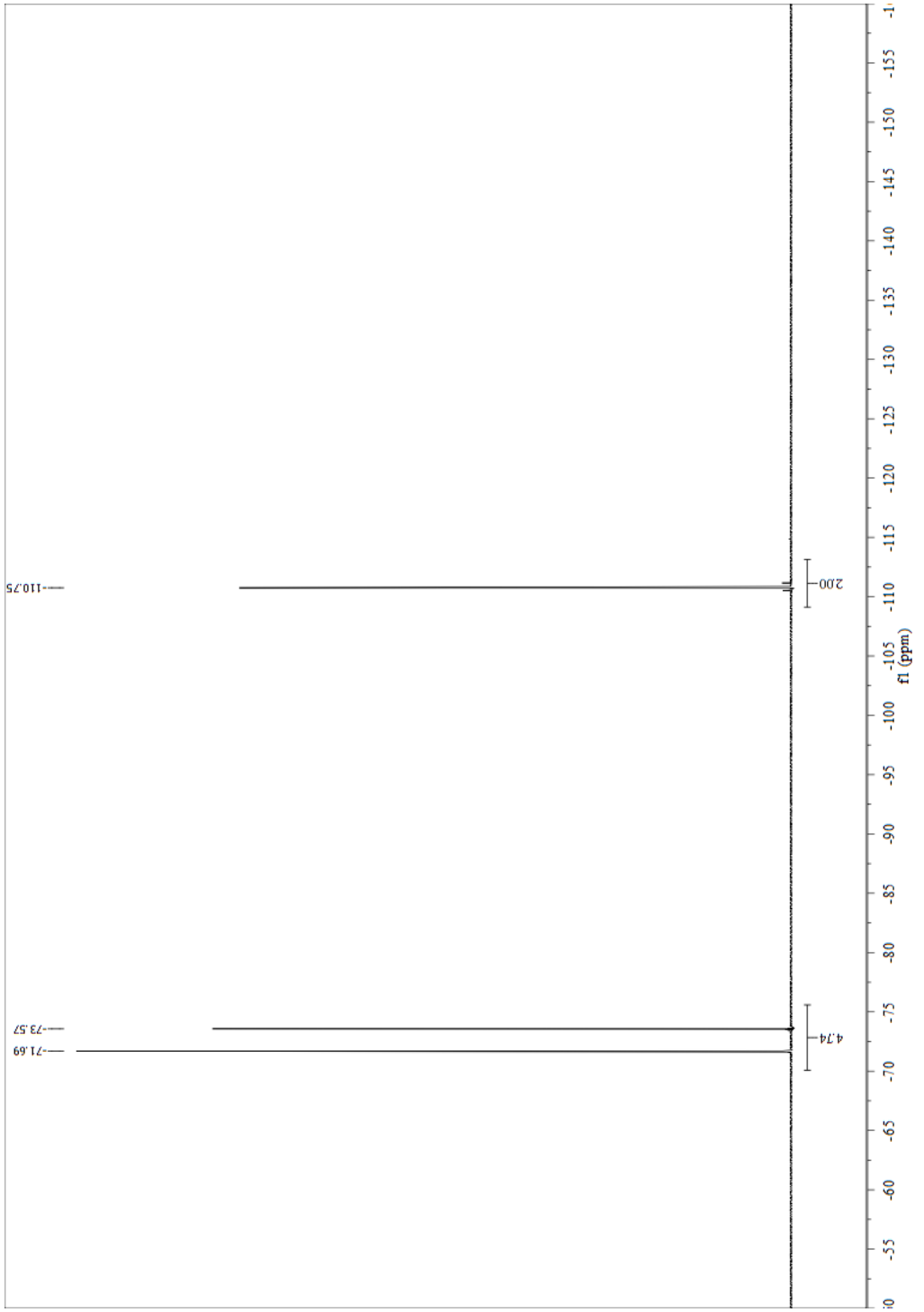

^{31}PNMR spectrum of **4cb**

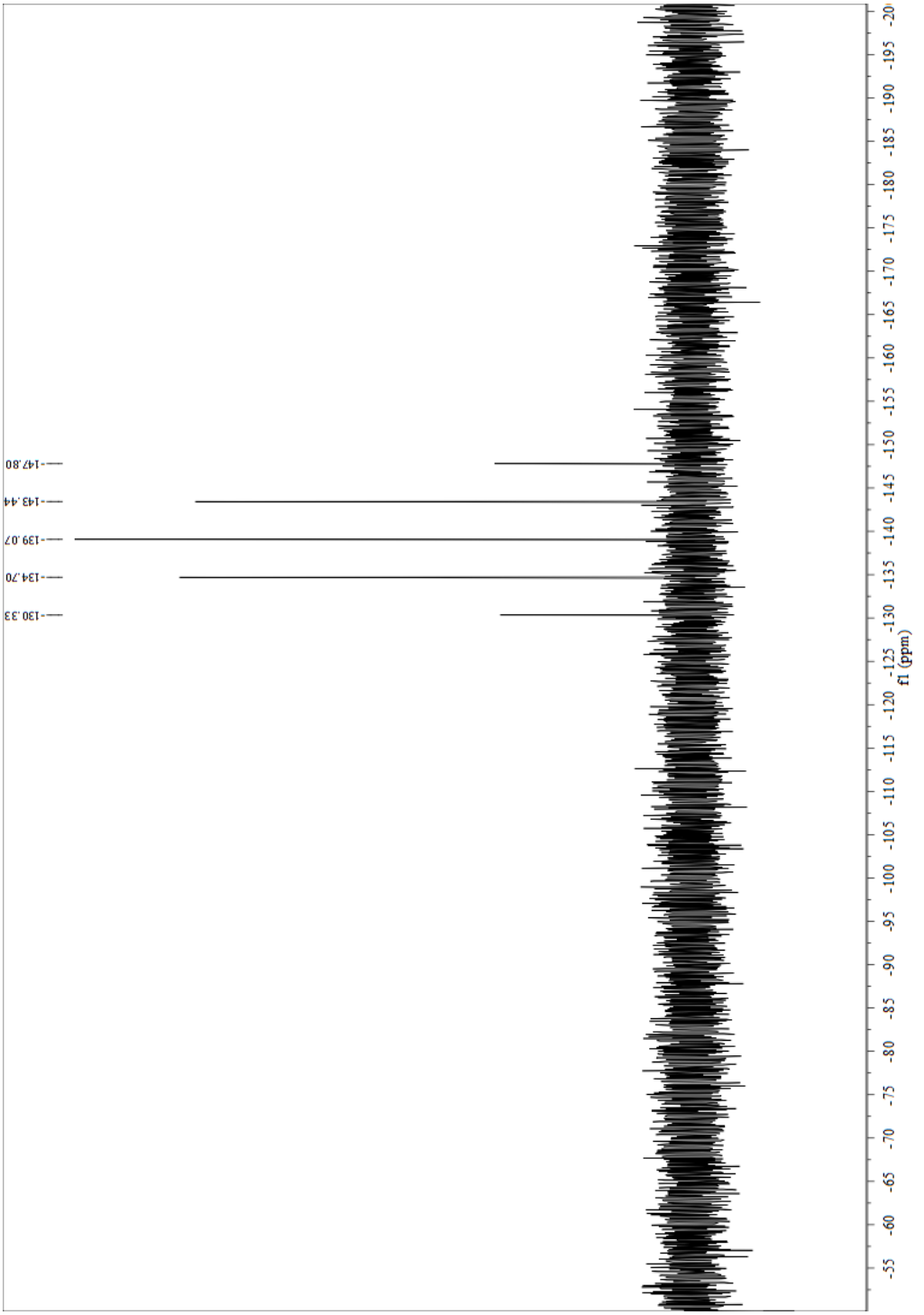

^{1}H NMR spectrum of **4cc**

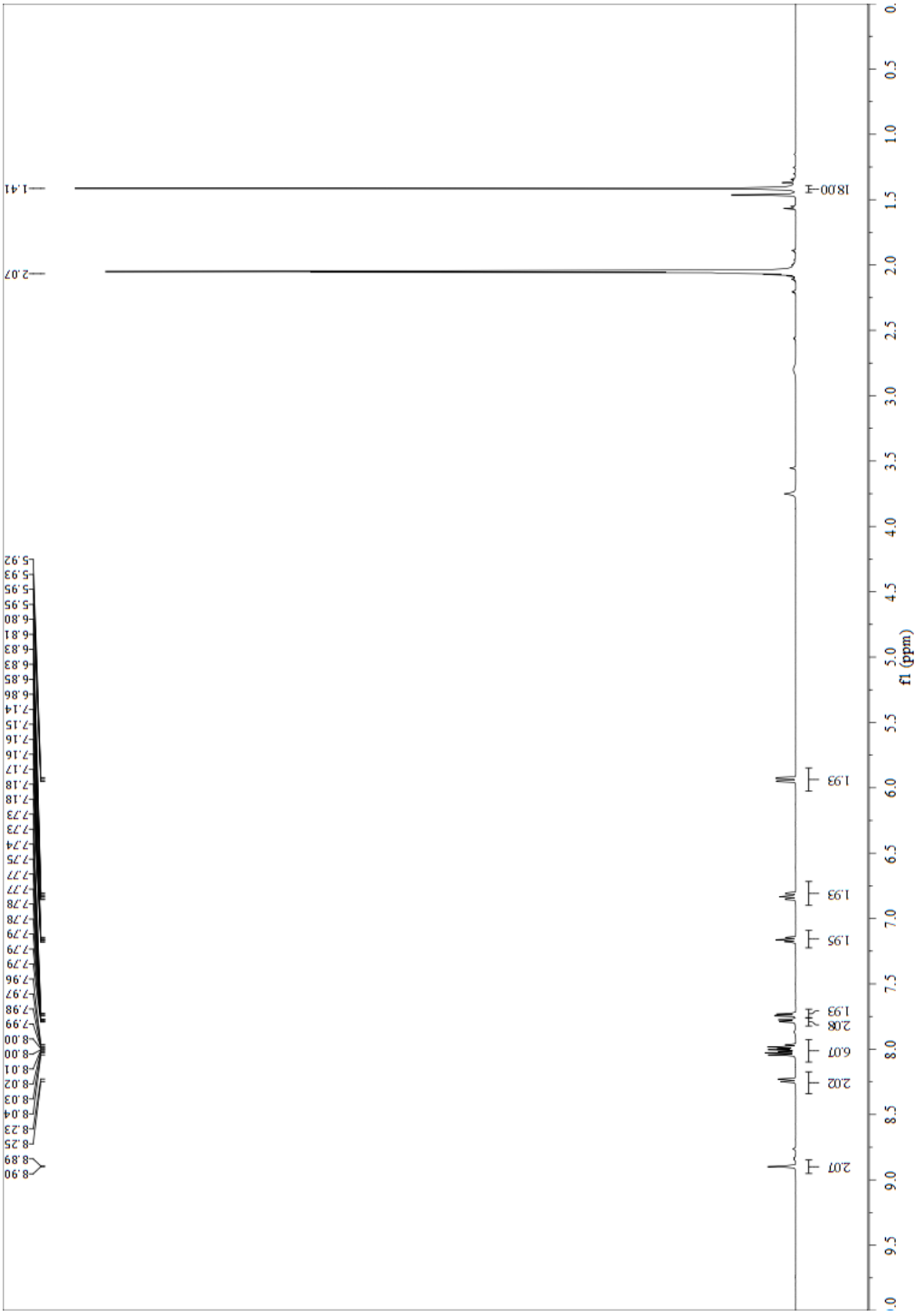

^{13}C NMR spectrum of **4cc**

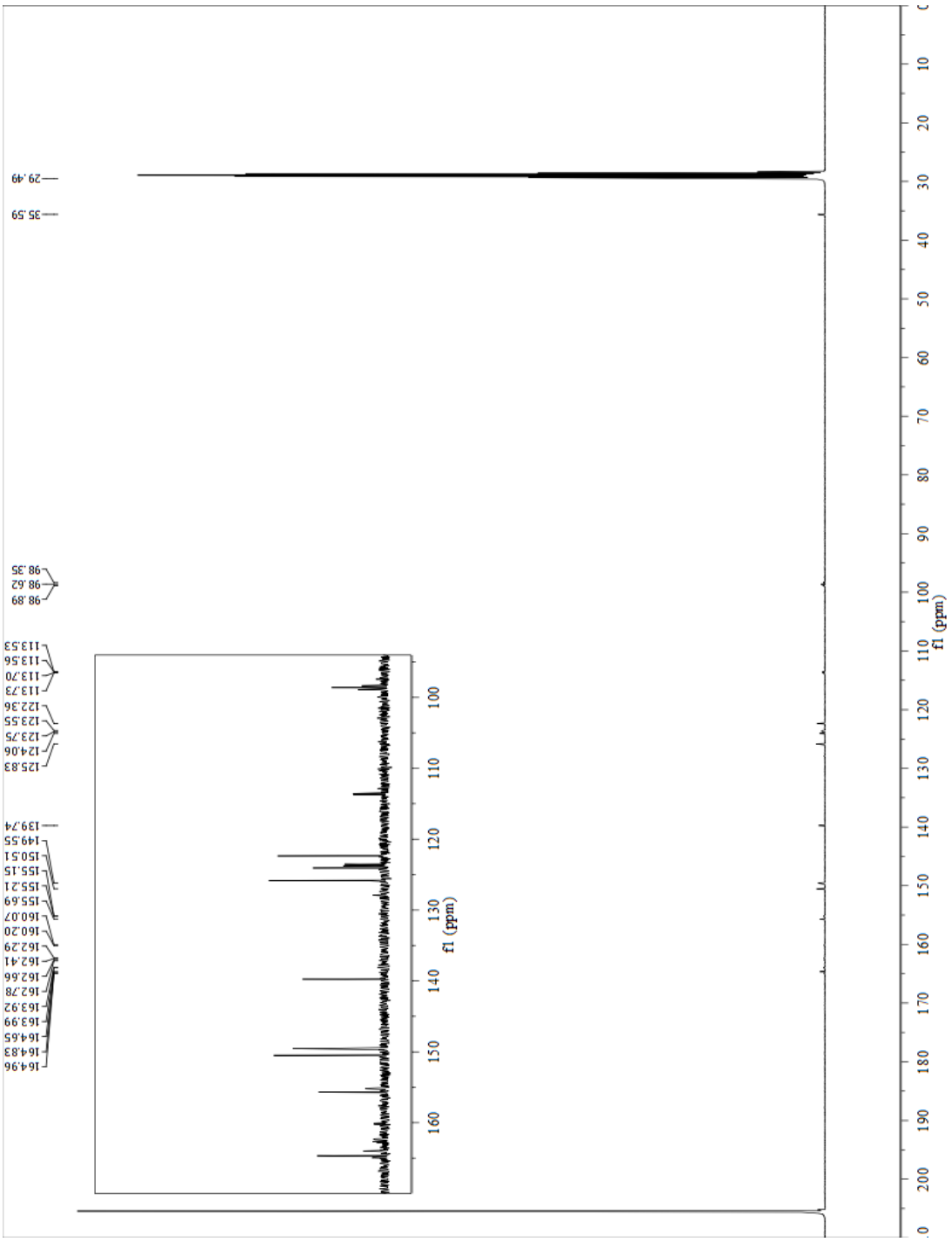

^{19}FNMR spectra of **4cc**

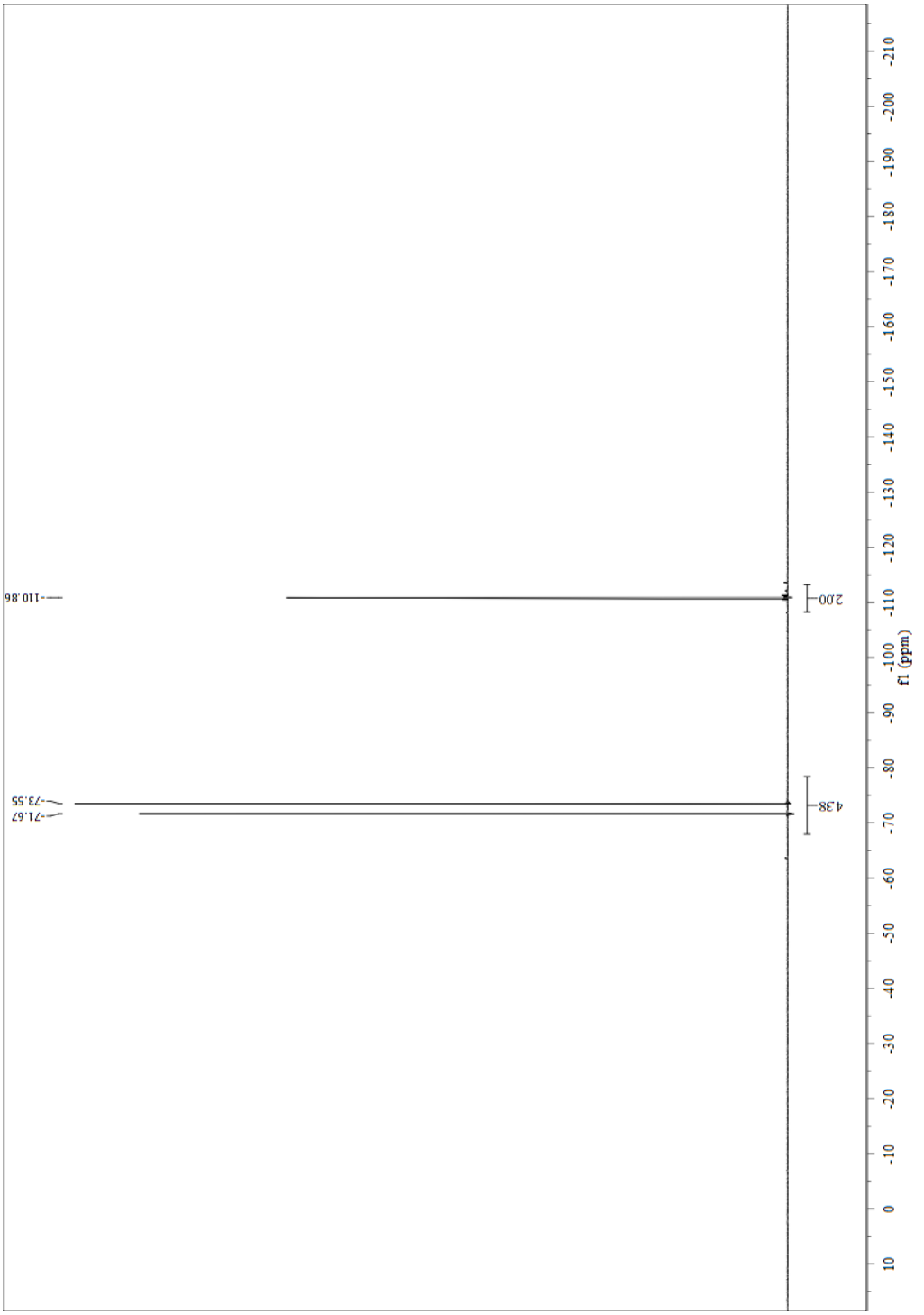

^{31}PNMR spectra of **4cc**

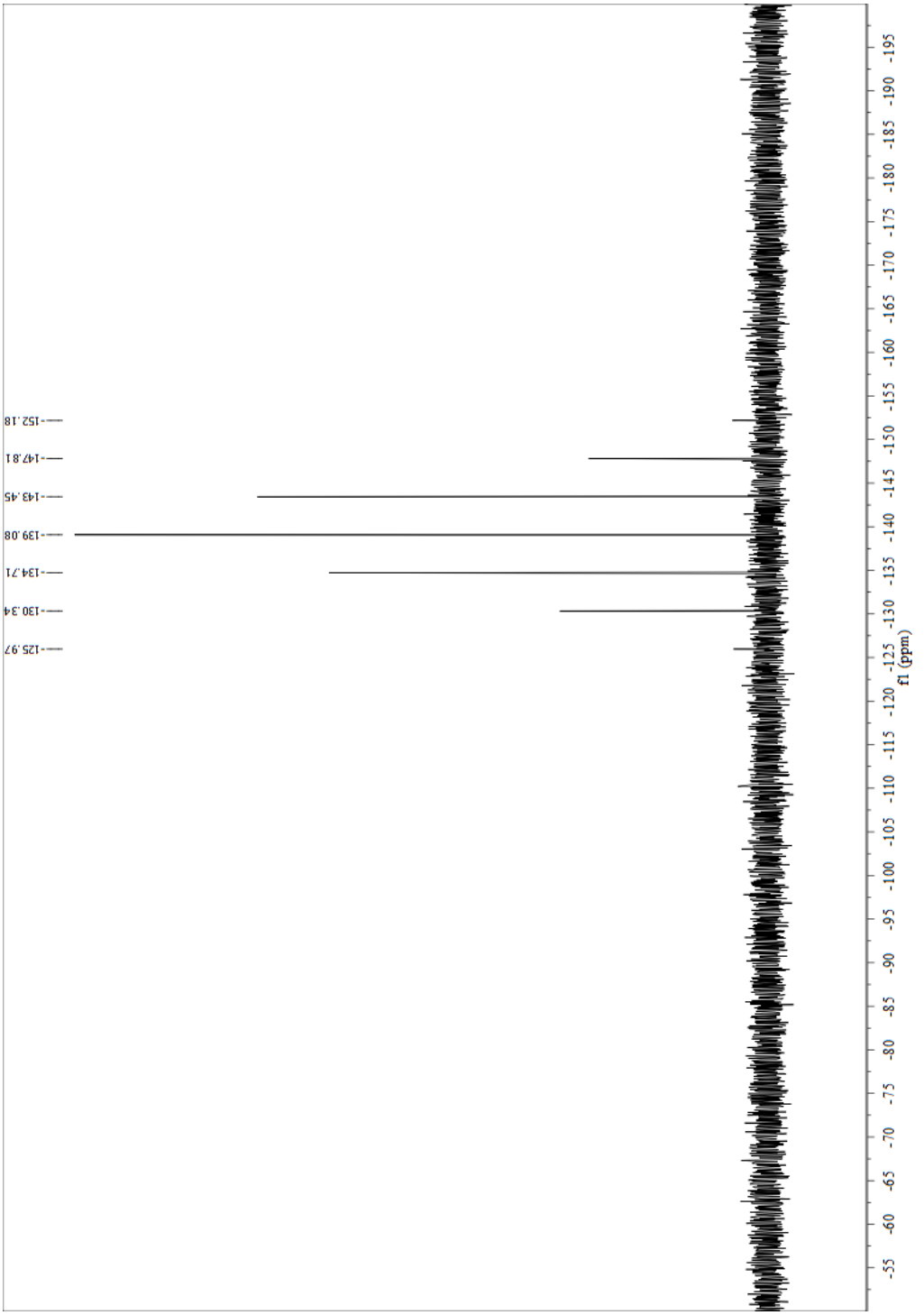

^{1}H NMR spectrum of **4fd**

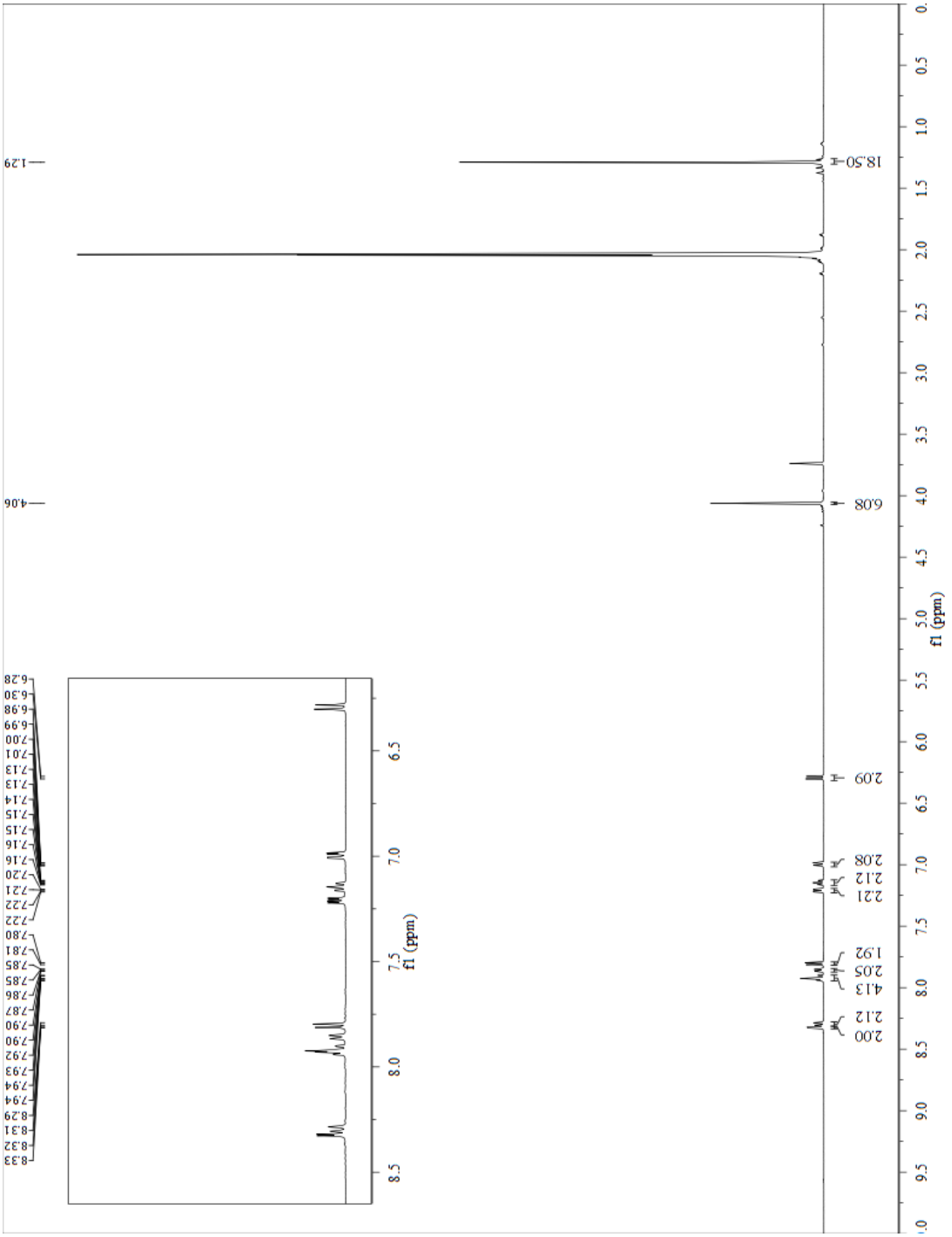

^{13}C NMR spectrum of **4fd**

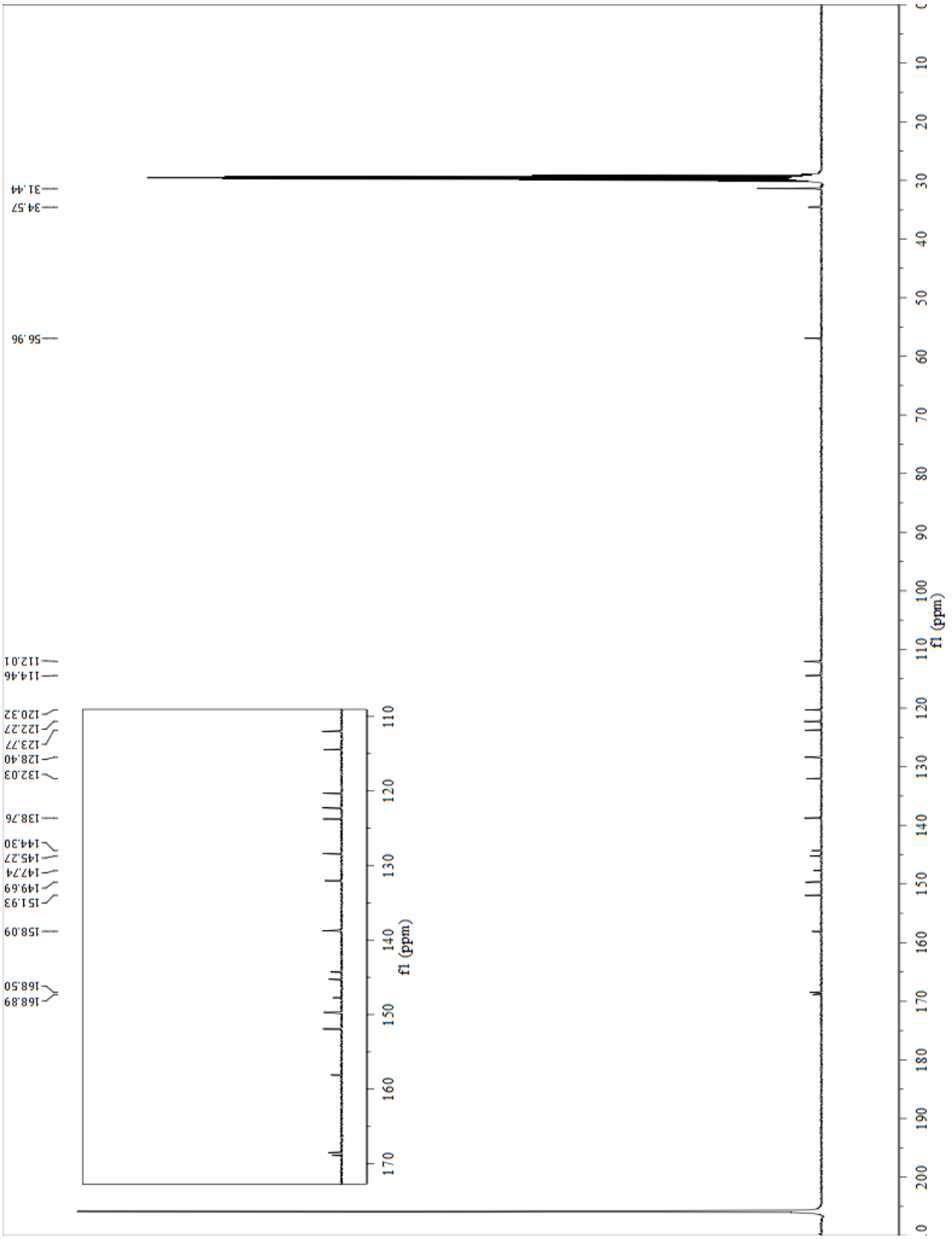

^{31}PNMR spectrum of **4fd**

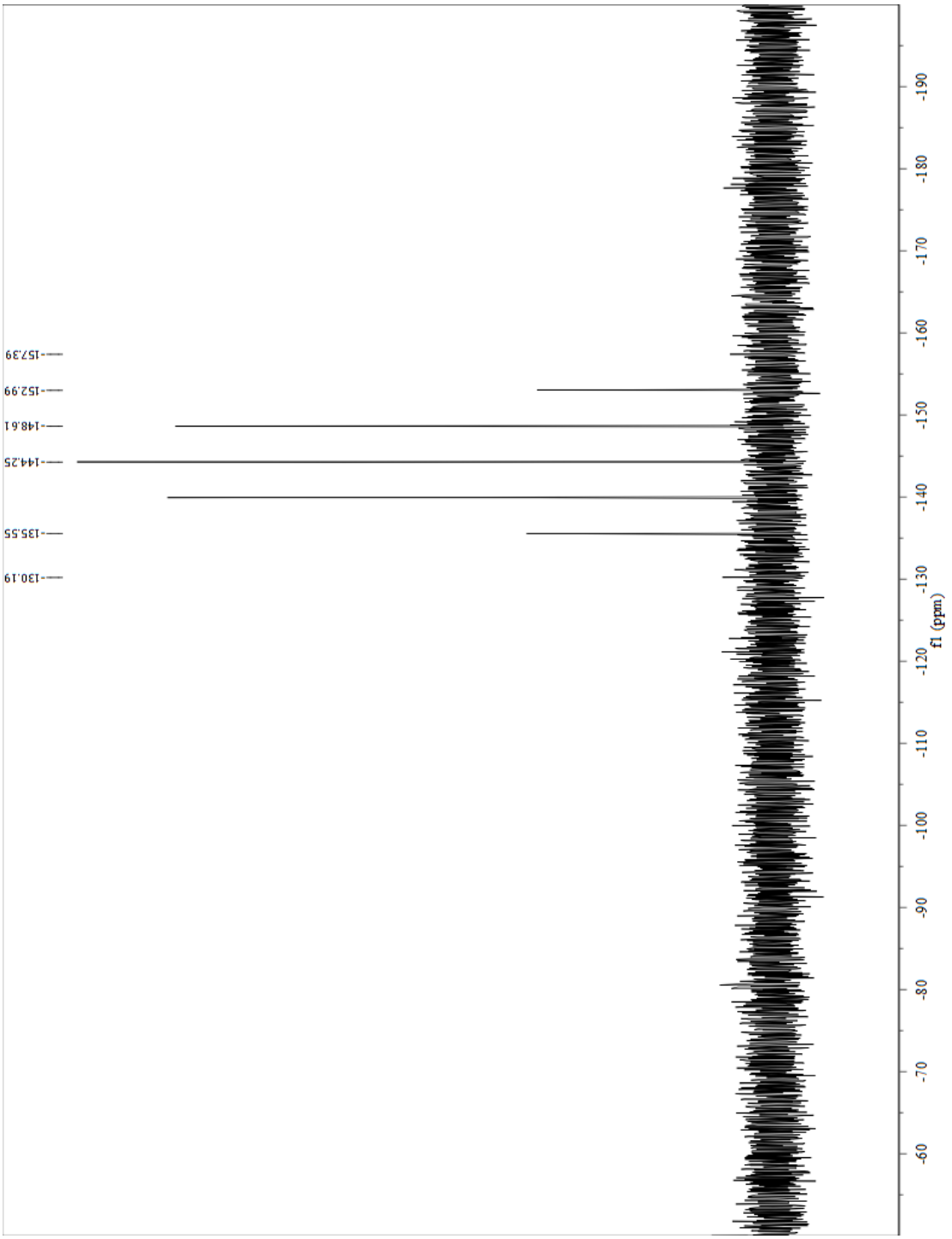

2.6 *Second generation method for homoleptic complexes*

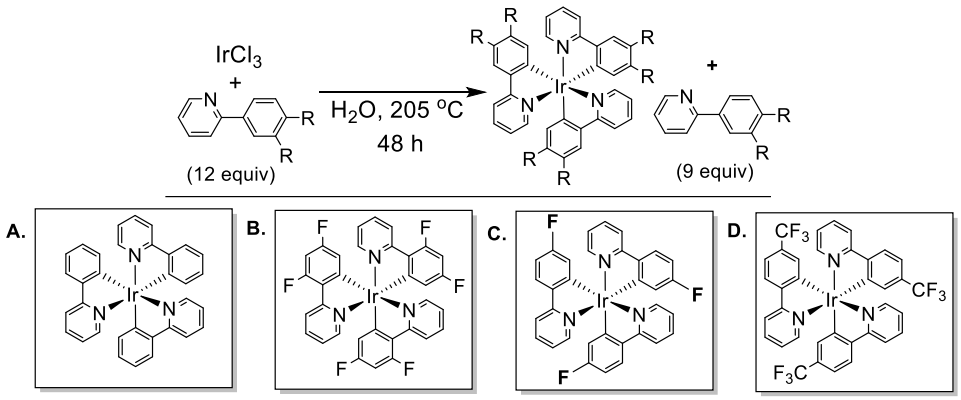

Scheme 2.5 Second generation method for homoleptic iridium complexes

While we and others have used the method described previously to make gram scale quantities of these complexes, there are some notable shortcomings. Namely, purification of the complexes via column chromatography was time intensive, required copious amounts of organic solvents, and was particularly challenging because of the low solubility. Often the isolation of the complex was more challenging than its synthesis. Since this publication, we have worked to improve the method (**Scheme 2.5**), in particular we have focused on making the reaction more scalable. The three main objectives were to maintain high purity of the complex on a gram scale, eliminate chromatography, and recover the excess ligand.

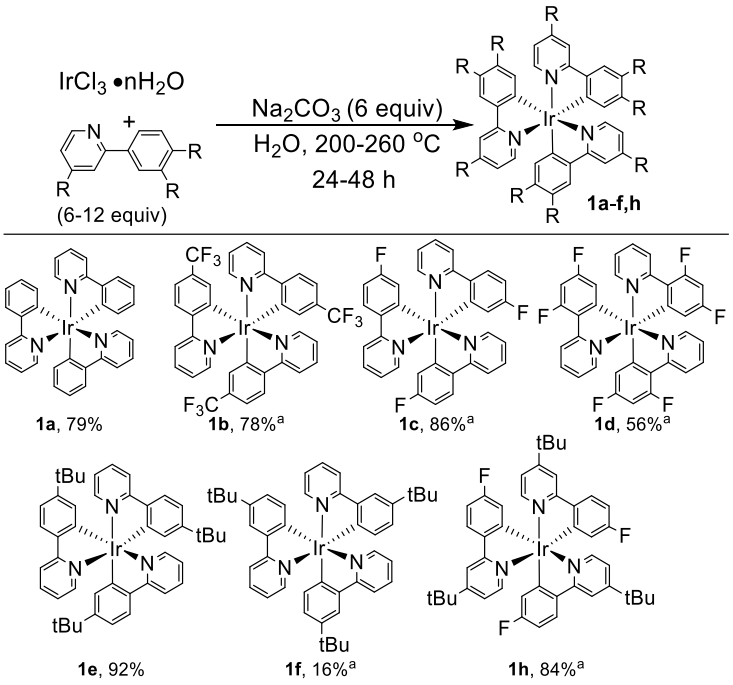

Scheme 2.6 Synthesis of facial-homoleptic iridium complexes

Herein, we report (**Scheme 2.6**) a modified method which has been applied to photocatalysts to obtain multigram quantities of photocatalysts (up to 2.85 g) in high purity (>97%), without the use of a column, and with excellent recovery of excess ligand in good yield (up to 97.0%). The method is demonstrated in the synthesis of **1a** and **1d** as an example. Additionally, while we did not demonstrate the recovery of the organic solvent, it is conceivable that the DCM could also be recovered in high purity. We believe this method to be quite general to this family of photocatalysts. Consequently, this method will facilitate exploration of the chemistry of these Ir-complexes, as well as enable applications, which may require more substantial quantities of Ir-photocatalysts.

A. *Fac-tris(2-phenylpyridinato) iridium(III) (**A**).* Iridium (III) chloride anhydrous (1.30 g, 4.36 mmol, 1 equiv, Note 1), 2-phenylpyridine (7.47 mL, 52.2 mmol, 12.0 equiv, Note 2), and 1.30 L of DI water (0.003 M with respect to $IrCl_3$) is added to a 2 L Parr reactor (Note 3). The

reaction mixture is then pressurized with argon (10.0 PSI, stirred and then depressurized three times and finally charged again with argon before sealing, (Note 4). The reaction mixture is heated to 205 ^{o}C for 48.0 h (Note 5). The reactor is cooled to room temperature with an ice bath, and after cooling, the reactor is opened revealing an insoluble yellow solid on the surfaces and dispersed in the aqueous phase (Note 6). All contents are transferred slowly to a 6 L separatory funnel aided by a large 5 cm glass funnel. The interior of the reactor is mechanically scraped (to extract the yellow material), with metal tongs, cotton balls (25 in total), and 500 mL of DCM from a spray bottle, and again all contents are added to the separatory funnel. (Note 7). While still in the funnel, the cotton is rinsed with 25 mL of DCM from a spray bottle and evenly pressed with tongs to release the yellow material from the cotton (Note 7). After removing the cotton, the solution is then diluted with 2.5 L of DCM (see notes 13 and 14). The separatory funnel is shaken vigorously, allowed to settle and again shaken, and the organic layer (Note 8) is then slowly separated from the aqueous layer (Note 9) and the aqueous layer is further extracted with more DCM (3 x 10 mL), and the organic layers are combined (Note 10). The aqueous layers are kept for future ligand recovery. The combined organic layer is washed with a 1 M HCl solution, with vigorous mixing prior to separation (3 x 900 mL) (Note 11). Each HCl wash is then back extracted with DCM (3 x 10 mL) to insure complete recovery of the product (Note 10). After the final wash (Note 12), the organic layer is filtered slowly (20 min) through a Celite® (35 g) pad on top of a 150 mL medium porosity sintered glass funnel, into a 3 L round-bottom flask, and then dried with 30 g of $MgSO_4$. After filtering the drying reagent using a 4 L Erlenmyer flask fitted with a 5 cm funnel/cotton plug, a homogenous aliquot is removed for NMR analysis (Note 13). Finally, the solvent is removed in batches by transferring to a 2.5 L round-bottomed flask by rotary evaporation (35 °C, 30 mm Hg, 150 rpm) to afford $Ir(ppy)_3$ as a bright yellow solid (Note 14) in 97.5-99.1% yield (2.78 g) in 96.3%-97.5% purity as compared to a standard signal (1,3,5 trimethoxybenzene) in the ^{1}H NMR (see Note 19 for wt % experiments and Note 20 for characterization).

Further purification of $Ir(ppy)_3$ can be performed by adding 2.78 g of the yellow solid to a 1 L round-bottom flask and adding 600 mL of distilled hexanes. The solid material is then sonicated until a uniform slurry is achieved, and 5 mL of dichloromethane is added (Note 15). The liquid is swirled giving a slight yellow tint to the solution indicating successful dissolution of a colored compound, and selective extraction of the impurities. Then the slurry is slowly poured through a 50 mL fine porosity sintered glass funnel to catch the $Ir(ppy)_3$ solid and the filtrate is collected into a 1 L Erlenmeyer flask. The yellow solid is left on the filter to air dry to afford 91.6-93.0% yield (2.61g) in 97.8%-99.1% purity compared to integrations of a standard signal (1,3,5 trimethoxybenzene) in the ^1H NMR (see Note 19 for wt % experiments and Note 20 for characterization).

2-Phenylpyridine recovery: The previously retained aqueous layers are added to a 4 L Erlenmeyer flask with a 60 mm PTFE octagon stir bar. The solution is stirred and slowly brought to pH 10 by adding 119 g of NaOH pellets in 10 portions (Note 16). The solution is added to a 6 L separatory funnel and the ligand is extracted from the salty water with DCM (6 x 1.2 L). The combined organic extracts are added to a 20 L metal canister and are dried with 20 g of $MgSO_4$. After filtering the drying reagent through a 5 cm funnel with a cotton plug into another 20 L canister the solvent is removed in batches by utilizing a continuous rotary evaporation setup (35 °C, 130 mm Hg, 100 rpm, Note 17) to afford 5.90 g 96.4-97.0% (based on excess 9 equiv) of 2-phenylpyridine is recovered in 97.7-98.5% purity compared to a standard signal (trimethoxybenzene) in the ^1H NMR (see Note 19 for wt % experiments and Note 20 for characterization)

B. *Fac-tris(2-(4,6-difluorophenyl)pyridinato) iridium(III) (**A**).* Iridium (III) chloride anhydrous (1.00 g, 3.35 mmol, 1 equiv, Note 1), 2-(4,6-difluoro)phenylpyridine (6.13 mL, 40.2 mmol, 12 equiv) (Note 2), and 1.00 L of DI water (0.003 M with respect to $IrCl_3$) is added to a 2 L Parr reactor (Note 3). The reaction mixture is then pressurized with argon (10.0 PSI, stirred and

then depressurized three times and finally charged again with argon before sealing (Note 4). The reaction mixture is heated to 205 ^{o}C for 48.0 h (Note 5). The reactor is cooled to room temperature with an ice bath, and after cooling the reactor is opened revealing an insoluble yellow solid on the surfaces and dispersed in the aqueous phase (Note 6). All contents are transferred slowly to a 6 L separatory funnel aided by a large 5 cm glass funnel. Then the interior of the reactor is mechanically scraped (to extract the yellow material), with metal tongs, cotton balls (25 in total), and 500 mL of DCM from a 500 mL spray bottle, and again all contents are added to the separatory funnel (Note 7). While still in the funnel, the cotton is rinsed with 25 mL of DCM from a spray bottle and evenly pressed with tongs to release the yellow material from the cotton (Note 7). After removing the cotton, the solution is then diluted with 2.5 L of DCM (see Notes 13 and 14). The separatory funnel is shaken vigorously, allowed to settle and again shaken, the organic layer (Note 8) is then slowly (Note 9) separated from the aqueous layer, the aqueous layer is further extracted with DCM (3 x 10 mL), and the organic layers are combined (Note 10). The aqueous layers are kept for future ligand recovery. The combined organic layer is washed with a 1 M HCl solution with vigorous mixing (4 x 1 L) (Note 11). Each HCl wash is back extracted with DCM (3 x 10 mL) to insure complete recovery of the product (Note 10). After the final wash (Note 12), the organic layer is filtered slowly (20 min) through a Celite® (35 g) pad on top of a 150 mL medium porosity sintered glass funnel, into a 3 L round-bottomed flask, and dried with 50 g of $MgSO_4$. The drying reagent is filtered using a 4 L Erlenmyer flask fitted with a 5 cm funnel/cotton plug. At this point, a homogenous aliquot is removed for NMR analysis (Note 13). Finally, the solvent is removed in batches by transferring to a 2.5 L round-bottomed flask by rotary evaporation (35 °C, 30 mm Hg, 150 rpm) to afford $Ir(diFppy)_3$ as a yellow solid (Note 14) in 90.9% yield (2.32 g) in 90.8% purity compared to a standard signal in the ^{19}F NMR (see Note 19 for wt % experiments and Note 20 for characterization).

Further purification of $Ir(diFppy)_3$ can be performed by adding 2.32 g of the yellow solid to a 1-L round-bottomed flask and adding 600 mL of distilled hexanes. The solid material is sonicated until a uniform slurry is achieved and 5 mL of dichloromethane is added (Note 15). The liquid is swirled giving a slight yellow tint to the solution indicating successful dissolution of a colored compound and selective extraction of the impurities. The product slurry is then slowly filtered through a 50 mL fine porosity sintered glass funnel and the filtrate is collected into a 1 L Erlenmeyer flask. The yellow solid is left on the filter to air dry to afford 71.4% yield (1.82 g) in 97.2% purity compared to integrations of a standard signal in the ^{19}F NMR (see Note 19 for wt % experiments and Note 20 for characterization).

2-(4,6-Difluoro)phenylpyridine recovery: The previously retained aqueous layers are split equally between two 4 L Erlenmeyer flasks containing a 60 mm PTFE octagon stir bar. Each solution is stirred and slowly brought to pH 10 by adding 101 g of NaOH pellets (Note 16). In two batches, each solution is added to a 6 L separatory funnel and the ligand is extracted from the salty water with DCM (6 x 800 mL). The combined organic extracts are added to a 20 L metal canister and are dried with 20 g of $MgSO_4$. After filtering the drying reagent through a 5 cm funnel with a cotton plug into another 20 L canister, the solvent is removed in batches by utilizing a continuous rotary evaporation setup (35 °C, 130 mm Hg, 100 rpm) (Note 17) to afford 5.90 g, 96.8% yield of 2-(4,6-difluoro)phenylpyridine. The purity is determined to be 90.5% pure compared to a standard signal (1,3,5 trimethoxybenzene) in the ^1H NMR (see Note 19 for wt % experiments and Note 20 for characterization).

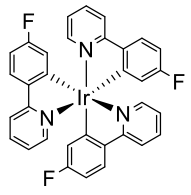

C. *Fac-Tris[5-fluoro-2-(2-pyridinyl-N)phenyl-C]iridium(III)).* Iridium (III) chloride anhydrous (0.47 g , 1.36 mmol, 1 equiv) 2-(4-fluorophenyl)-pyridine (2.83 g, 16.4

mmol, 12.0 equiv) , and 0.41 L of DI water (0.003 M with respect to $IrCl_3$) is added to a 1 L Parr reactor. The reaction mixture is pressurized with argon (10.0 psi), stirred and then depressurized three times, and finally charged again with argon before sealing. The reaction mixture is heated to 205 °C for 48 h. Then the reactor is cooled and after cooling, the reactor is opened revealing an insoluble yellow solid on the surfaces and dispersed in the aqueous phase. All contents are transferred slowly to a 4 L separatory funnel aided by a large 5 cm glass funnel. Then the interior of the reactor is mechanically scraped (to extract the yellow material), with metal tongs, cotton balls, and 250 mL of dichloromethane (DCM) from a spray bottle, and again all contents are added to the separatory funnel.

While still in the funnel, the cotton is rinsed with 25 mL of DCM from a spray bottle and evenly pressed with tongs to release the yellow material from the cotton. After removing the cotton, the solution is then diluted with 1.0 L of DCM. The separatory funnel is shaken vigorously, allowed to settle and again shaken, and the organic layer is then slowly separated from the aqueous layer and the aqueous layer is further extracted with more DCM (3 x 10 mL), and the organic layers are combined. The aqueous layers are kept for future ligand recovery. The combined organic layer is washed with a 1 M HCl solution, with vigorous mixing prior to separation (3 x 500 mL). Each HCl wash is then back extracted with DCM (3 x 10 mL) to insure complete recovery of the product. After the final wash, the organic layer is filtered slowly (20 min) through a Celite® (25 g) pad on top of a 150 mL medium porosity sintered glass funnel, into a 3 L round-bottomed flask, and then dried with 30 g of $MgSO_4$. After filtering the drying reagent using a 4 L Erlenmyer flask fitted with a 5 cm funnel/cotton plug, a homogenous aliquot is removed for NMR analysis. Finally, the solvent is removed in batches by transferring to a 2.5 L round-bottomed flask by rotary evaporation (35 °C, 30 mm Hg, 150 rpm) to afford 963 mg (96%) of $Ir(Fppy)_3$ as a bright yellow solid. 1H NMR(Methylene Chloride-d2, 400 MHz): d δ 7.88 (d, 3H, J = 8.2 Hz), 7.72-7.64 (m, 6H), 7.52 (ddd, 3H, J = 5.5, 1.6, 0.8 Hz), 6.94 (ddd, 3H, J = 7.1, 5.6, 1.3 Hz), 6.63 (td, 3H, J = 8.7,

2.7 Hz), 6.39 (dd, 3H, J = 10.3, 2.7 Hz) ppm. ^{13}C NMR(Methylene Chloride-d2, 101 MHz): d δ 165.3 (d, J = 5.4 Hz), 163.4 (d, J = 5.7 Hz), 162.8, 147.2, 140.2, 136.6, 125.8 (d, J = 9.2 Hz), 122.0, 121.8 (d, J = 16.4 Hz), 118.9, 107.4 (d, J = 23.6 Hz) ppm. ^{19}F NMR (376 MHz, Methylene Chlorided2) d 112.33 (ddd, J = 10.3, 9.1, 5.7 Hz).

2-(4-fluorophenyl)-pyridine recovery The solution is stirred and slowly brought to pH 10 by adding 56 g of NaOH pellets in 10 portions .The solution is added to a 6 L separatory funnel and the ligand is extracted from the salty water with DCM (4 x 900 mL). The combined organic extracts are added to a 20 L metal canister and are dried with 20 g of MgSO4. After filtering the drying reagent through a 5 cm funnel with a cotton plug into another 20 L canister the solvent is removed in batches by utilizing a continuous rotary evaporation setup (35 °C, 130 mm Hg, 100 rpm) to afford 1.55 g 73 % (based on excess 9 equiv) of 2-phenylpyridine is recovered.

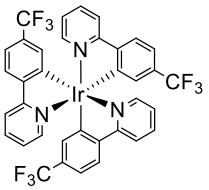

D. *Fac-Tris[2-(2-pyridinyl-N)-5-(trifluoromethyl)phenyl-C]iridium(III).* Iridium (III) chloride anhydrous (1.16 g , 3.89 mmol, 1 equiv) 2-(4-trifluoromethyl phenyl)-pyridine (10.4 g, 46.6 mmol, 12.0 equiv) , and 1.16 L of DI water (0.003 M with respect to $IrCl_3$) is added to a 1 L Parr reactor. The reaction mixture is pressurized with argon (10.0 psi), stirred and then depressurized three times, and finally charged again with argon before sealing. The reaction mixture is heated to 205 °C for 48 h. Then the reactor is cooled and after cooling, the reactor is opened revealing an insoluble yellow solid on the surfaces and dispersed in the aqueous phase. All contents are transferred slowly to a 4 L separatory funnel aided by a large 5 cm glass funnel. Then the interior of the reactor is mechanically scraped (to extract

the yellow material), with metal tongs, cotton balls, and used acetone (100 mL to get residual compound(s) from parr and transfered to a different 250 mL round bottom flask and concentrated down.

The solid was placed on a filter frit, and washed with 1 M HCl to wash away ligand. Yellow solid from frit was taken into 200 mL of acetone and dry loaded with 40 g of silica and column ran with 5-6 column volumes to separate reamaining ligand. The column was then ran with 60:40 Hexanes:EtOAc to pull of dimer and then the solvent system were switched to 100 % DCM to recover the catalyst as a yellow solid in 67.58 % yield 2.26 g. ^{1}H NMR(Chloroform-d, 400 MHz): δ = 7.99 (d, 3H, J = 8.3 Hz), 7.77–7.69 (m, 6H), 7.55 (dd, 6H, J = 6.0, 1.3 Hz), 7.20–7.15 (m, 3H), 7.02 (ddd, 3H, J = 7.1, 5.2, 1.1 Hz), 6.96 (b, 3H) ppm. 13C NMR (Methylene Chloride-d2, 101 MHz): δ = 165.0, 159.2, 147.5–147.4 (m), 147.3, 137.0.132.4 (m), 130.6, 123.9, 123.4, 120.0, 117.3–117.2 (m), 100.0. ^{19}F NMR (376 MHz, Chloroform-d) δ −62.76 (s). LC/MS (m/z) calculated for C36H21F9IrN3 859.12 found M, 858.70.

Notes

1. $IrCl_3$ was obtained from Beantown Chemicals (BTC), available through VWR.
2. 2-Phenylpyridine was obtained from AK scientific and 2-(4,6-difluorophenylpyridine was obtained from Oakwood chemicals.

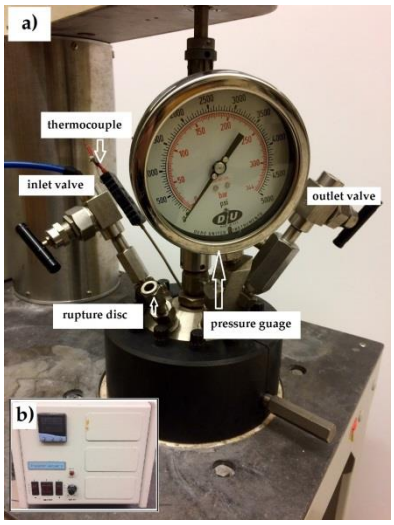

Figure 2.7 Parr reactor

3. A 2 L Parr stirred reactor was fitted with an inlet and outlet valve, a Duro United pressure gauge (0-5000 psi), and a 526HCPH rupture disc was used for the reaction (**Figure 2.7a**). In series with a 4843 controller the reactor was heated with a Parr heater assembly (model no. A1445HC3EE) controlled by a type J thermocouple (15.5 in. length) (**Figure 2.7b**). We have found that the stirring and glass sleeve options are unnecessary for the success of the reaction. We also discovered that headspace in the reactor is very important (1/4 headspace to water). We found that if the same 2 L Parr reactor was loaded with 1.75 L water the reactor leaked and displays a significant amount of pressure. Again, further safety precautions must be taken when changing the headspace to water ratio.
4. If the Parr reactor is not equipped with a stirring mechanism, after pressurizing the reactor with argon one can gently rock the reactor back and forth to mix the contents.
5. The primary cause for incomplete or failed reactions stems from equipment failure. Since the reaction is highly dependent on temperature it is important to insure probes and controllers are working properly, and leak checks are performed on the entire system before every reaction. Insure all valves are free of obstruction and all areas are clean. It is imperative that

the reactor temperature stays above 200 ºC The reactor used in the above reactions had shown significant temperature deviation +/- 5 ºC. So we set our controller to 205 ºC to insure the reactor stays above 200 ºC.

Figure 2.8 An example of the insoluble yellow solid found on the internal components after a successful reaction

6. Suspended dull yellow colored water mixtures is indicative of an unsuccessful reaction, while insoluble yellow colored (**Figure 2.8**) water mixtures are indicative of a successful reaction. For the $Ir(ppy)_3$ catalyst, the primary contaminant after the workup is the chloro-bridging dimer which is a dull yellow color intermediate en-route to the desired product. This was determined by NMR analysis of reaction mixtures after work up.

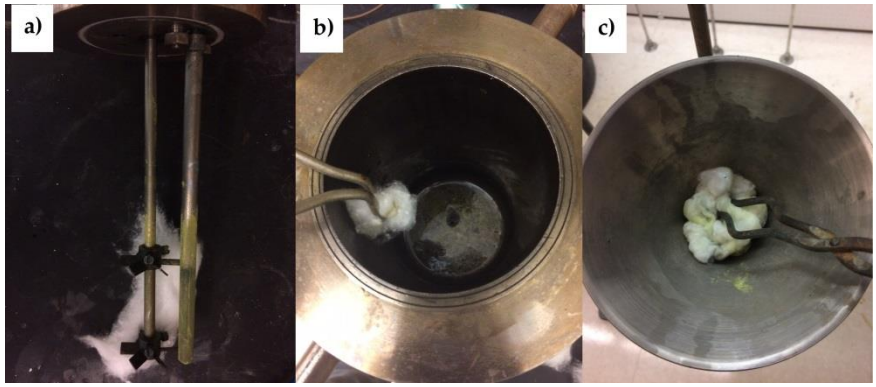

Figure 2.9 Photograph of extraction

7. Yellow solid around the walls, probe shafts, and stirring impellers should be examined for yellow residue and any residue should be scraped or extracted with DCM to insure high accurate yields (**Figure 2.9**).
8. There may be yellow solid that did not dissolve completely into the DCM. This is normal; as the 1 M HCl washes are performed and ligand is removed the catalyst will eventually partition fully into the organic layer.
9. In this large scale workup, the aqueous layer tends to swirl into the organic layer, if separation is done quickly. It is important to insure the separation of the organic layer from the aqueous layer is slow in all separations.
10. There tends to be a small emulsion layer in between the organic and aqueous layers during the workup which contains some black material. Care should be taken to avoid the inclusion of this emulsion layer. The extra DCM rinses serve to fully extract the product that remains in the emulsion and on the walls of the separatory funnel.
11. Because it builds up pressure, it is important to vent the separatory funnel to avoid loss of product and to avoid injury. Some loss of product is apparent when venting the large 6 L separatory funnel through the stopcock, while not the standard technique, venting was performed by securing the separatory funnel back to the ring stand and carefully removing the stopper.
12. Thin-layer chromatography (TLC) was used to insure all ligand was extracted from the organic layer. TLC was performed using Sorbent Technologies Silica Gel XHL normal phase plates and utilizing an eluent system of hexanes/EtOAc (9:1). See Note 18 for Rf values.
13. The solubility of the catalysts is relatively low in dichloromethane (thus a large volume of solvent was used to dilute the compound), yet the impurities (the chloro-bridging dimer and

the excess ligand) are significantly more soluble. Removing an aliquot while the entire mixture is homogenous will insure an accurate NMR analysis.

14. Since the solubility of the catalyst is low in most volatile solvents transferring the material to a smaller container can be laborious and require copious amounts of solvent. It is recommended to scrape the sides of the round-bottomed meticulously and transfer all the material possible as a solid. Then any remaining solid material can be dissolved with solvent and transferred to the smaller container, thus, minimizing the solvent use.
15. To insure high yields of product, the purification step must be performed with care. The amount of DCM that is added to the hexanes can vary depending on the purity of the sample. Lower amounts of DCM are added for purer samples and larger amounts are used for compounds of lower purity. The ratio for the purification technique is typically 1/120 (DCM/Hexanes).
16. One must slowly add the NaOH to avoid excessive heat generation and potential injury. We observed that extraction of ligand becomes difficult, and yields suffer when using a NaOH solution in comparison to direct addition of NaOH pellets. The use of pellets minimizes the aqueous volume into which the ligand may partition.

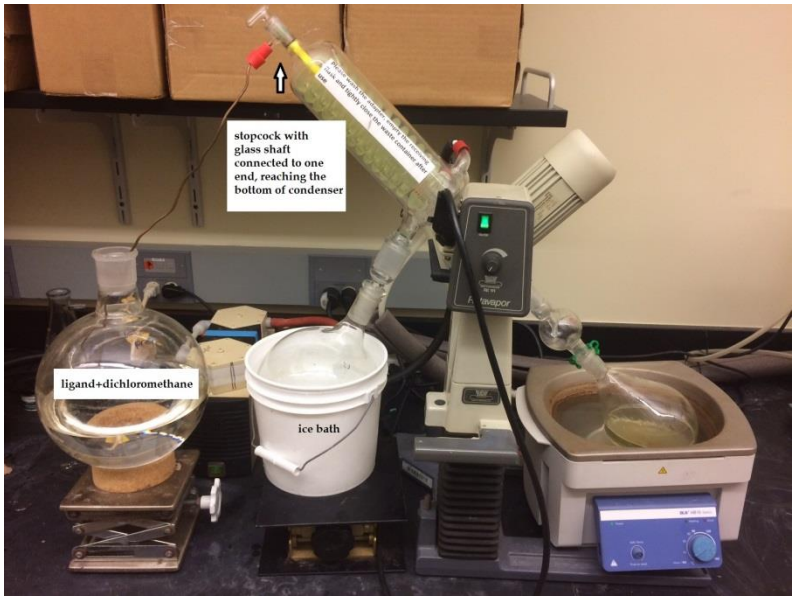

Figure 2.10 Diagram of a continuous rotary evaporation setup

17. See above (**Figure 2.10**) for a diagram for a continuous rotary evaporation setup
18. Rf values are measured using thin layer chromatography (TLC), (obtained from sorbent technologies Silica XHL TLC Plates, w/UV254, glass backed, 250 µm, 20 x 20 cm) see Table below.

Table 2.4 Rf values of the photocatalysts and ligands.

Compound	R_f: 1/9 EtOAc/Hexanes	R_f: 1/1 DCM/Hexanes
Fac-tris(2-phenylpyridinato) iridium(III)	0.028	0.43
2-phenylpyridine	0.31	0.19
Fac-tris(2-(4,6-difluorophenyl)pyridinato) iridium(III)	0.028	0.76
2-(4,6-difluoro)phenylpyridine	0.33	0.23

19. The weight percent was determined by quantitative NMR. The solubility of $I(rppy)_3$ and $Ir(diFppy)_3$ in most deuterated solvents is low, which makes weighing out the necessarily small amounts of dissolvable compound challenging. It is best to accurately weigh out a larger sample (>100 mg of the standard or compound) and dissolve the compound into protio-dichloromethane using a volumetric flask to give an accurate molar solution. Then appropriate volumes of the standard and compound solutions can be mixed. Next, the protio-solvent removed and the mixture redissolved in the appropriate deuterated solvent. A proton NMR spectrum is thus obtained for the mixture with a minimum relaxation delay of 30 s. The weight percent purity of the analyte is calculated by the following equations:

$$Molar\ Ratio = \frac{\frac{I_{cpd}}{{}_{n}Hcpd}}{\frac{I_{std}}{{}_{n}Hstd}}$$

$$wt\% = \frac{mg_{std} \times MW_{std} \times molar\ ratio \times P\text{std}}{mg\text{cpd} \times MW\text{std}}$$

Where,

Wt% = purity of the sample

I_{cpd} = proton integral area of a known peak on the compound being analyzed

${}_{n}H_{cpd}$ = number of hydrogens associated with the compound NMR peak

I_{std} = proton integral area of a known peak on the standard

${}_{n}H_{cpd}$ = number of hydrogens associated with the standard NMR peak

mg_{std} = amount in milligrams of the standard compound weighed for analysis

mg_{cpd} = amount in milligrams of the compound being analyzed

MW_{std} = molecular weight of the standard

MW_{cpd} = molecular weight of the compound being analyzed

P_{std} = wt% purity of the standard expressed as a decimal value. For the purposes of most calculations, a value of 1.00 may be assumed

Wt % of *fac-tris(2-phenylpyridinato) iridium(III)*

(before purification step)

1.0 mL of a 0.004464 M solution (in DCM) of $Irppy_3$ was added to a vial, and then 1.0 mL of 0.04464 M solution (in DCM) of 1,3,5 trimethoxybenzene was added. Then the solution was concentrated and then diluted with CD_2Cl_2 and ^1H NMR was taken. The NMR parameters consisted of a 30 second delay with 128 scans,and a spectrum width of 16 to -4 ppm. Purity calculations with known masses were performed by MestReNova purity/wt % script (see NMR spectra for values).

Wt % of *fac-tris(2-phenylpyridinato) iridium(III)*

(after purification step)

1.0 mL of a 0.007504 M solution (in DCM) of $Ir(ppy)_3$ was added to a vial, and then 0.35 mL of 0.020215 M solution of 1,3,5 trimethoxybenzene was added. Then the solution was concentrated, then diluted with $CDCl_3$, and the ^1H NMR was taken. The NMR parameters consisted of a 30 second delay, with 128 scans, the spectra transmission was moved to the center of the desired signals (irradiated at the 7.1 ppm position) to improve integrals (movetof on VNMRJ software) and a spectrum width of 16 to -4 ppm. Purity calculations with known masses were performed by MestReNova purity/wt % script.

Wt % of *2-phenylpyridine*

152.7 mg of 2-phenylpyridine was added to a vial, and then 173.8 mg of 1,3,5 trimethoxybenzene was added. Then the solution was then diluted with $CDCl_3$ and ^1H NMR was taken. The NMR parameters consisted of a 30 second delay with 16 scans, and a spectrum width of 16 to -4 ppm. Purity calculations with known masses were performed by MestReNova purity/wt % script.

Wt % of *fac-tris(2-(4,6-difluorophenyl)pyridinato) iridium(III)*

(before purification step)

0.50 mL of a $8.391x10^{-4}$ M solution (in DCM) of $Ir(diFppy)_3$ was added to a vial, and then 7.9 uL of 0.05333 M solution of fluorobenzene was added. The solution was added to a NMR tube fitted with a benzene capillary (C_6D_6 sealed into a capillary for locking purposes) and ^{19}F NMR was taken. The NMR parameters consisted of a 30 second delay with 256 scans (insuring a 90 º pulse width), and a spectrum width of -40 to -180 ppm. Purity calculations with known masses were performed by MestReNova purity/wt % script (see NMR spectra for values).

Wt % of *fac-tris(2-(4,6-difluorophenyl)pyridinato) iridium(III)*

(after purification step)

0.50 mL of a 0.0008457 M solution (in DCM) of $Ir(diFppy)_3$ was added to a vial, and then 30 µL of a 0.05333 M solution of fluorobenzene was added. Then the solution was added to a NMR tube fitted with a benzene capillary (C_6D_6 sealed into a capillary for locking purposes) and ^{19}F NMR was taken. The NMR parameters consisted of a 30 second delay, with 1200

scans (insuring a 90 º pulse width), and a spectrum width of -40 to -180 ppm. Purity calculations with known masses were performed by MestReNova purity/wt % script.

Wt % of *2-(4,6-difluoro)phenylpyridine*

28.6 mg of 2-(4,6-difluoro)phenylpyridine was added to a vial, and then 22.28 mg of 1,3,5 trimethoxybenzene was added. Then the solution was diluted with C_6D_6 and ^1H NMR was taken. The NMR parameters consisted of a 30 second delay, with 16 scans, and a spectrum width of 16 to -4 ppm. Purity calculations with known masses were performed by MestReNova purity/wt % script.

20. NMR spectra were obtained on a 400 MHz Bruker Avance III spectrometer and 400 MHz Varian spectrometer. ^1H, ^{19}F and ^{13}C NMR chemical shifts are reported in ppm relative to the residual protio solvent peak (^1H, ^{13}C). IR spectra were recorded on Varian 800 FT-IR. Due to the C-F splitting, carbons that couple with fluorine were reported as multiplets. ^{13}C spectra for the catalysts were taken in protio NMP (best solvent we found to dissolve catalysts), and for locking purposes a sealed capillary with C_6D_6 was added to the NMR tube.

Characterization of compounds

Characterization of *fac-tris(2-phenylpyridinato) iridium(III)*

^1H NMR (400 MHz, Methylene Chloride-d2) δ 9.86 (d, J = 8.2 Hz, 1H), 9.60 (td, J = 8.1, 1.8 Hz, 2H), 9.51 (d, J = 5.5 Hz, 1H), 8.93 – 8.77 (m, 1H), 8.71 (dt, J = 14.1, 7.0 Hz, 1H). ^{13}C NMR (101 MHz, C_6D_6/NMP) δ 166.9, 161.8, 147.8, 144.9, 137.5, 137.3, 129.6, 124.7, 123.3, 120.1, 119.7. FT-IR (neat) cm-1 3035, 1560, 1260, 749.

Characterization of *2-phenylpyridine*

^{1}H NMR (400 MHz, Benzene-d6) δ 8.58 (d, J = 4.7 Hz, 1H), 8.15 (d, J = 7.2 Hz, 1H), 7.32 (d, J = 8.0 Hz, 1H), 7.25 (t, J = 7.5 Hz, 1H), 7.19 – 7.12 (m, 2H), 7.09 (td, J = 7.7, 1.9 Hz, 1H), 6.63 (ddd, J = 7.4, 4.8, 1.0 Hz, 1H). ^{13}C NMR (101 MHz, C6D6) δ 157.7, 150.3, 140.1, 136.6, 129.4, 129.2, 127.5, 122.3, 120.3. FT-IR (neat) cm-1 3061,1579,1293,743.

Characterization of *fac-tris(2-(4,6-difluorophenyl)pyridinato) iridium(III)*

^{1}H NMR (400 MHz, Methylene Chloride-d2) δ 8.31 (d, J = 8.3 Hz, 1H), 7.73 (t, J = 7.8 Hz, 1H), 7.51 (d, J = 5.4 Hz, 1H), 7.04 – 6.91 (m, 2H), 6.42 (ddd, J = 11.7, 9.1, 2.5 Hz, 1H), 6.24 (dd, J = 9.2, 2.4 Hz, 1H). ^{19}F NMR (376 MHz, Chloroform-d) δ -108.64 (q, J = 9.2 Hz), -110.54 (ddd, J = 13.0, 9.8, 2.6 Hz). ^{13}C NMR (101 MHz, Benzene-d6/NMP) δ 165.4 (d, J = 5.6 Hz), 165.3 (d, J = 11.7 Hz), 163.1 (dd, J = 64.4, 11.8 Hz), 162.4 (d, J = 6.8 Hz), 160.8 (d, J = 12.7 Hz), 148.6, 139.2, 128.7, 124.4, 123.7 (d, J = 20.8 Hz), 117.9 (d, J = 16.3 Hz). FT-IR (neat) cm-1 3009, 1555, 1160, 786.

Characterization of *2-(4,6-difluoro)phenylpyridine*

^{1}H NMR (400 MHz, Benzene-d6) δ 8.52 (d, J = 4.0 Hz, 1H), 8.16 (td, J = 8.9, 6.8 Hz, 1H), 7.57 (d, J = 7.1 Hz, 1H), 7.07 (td, J = 7.8, 1.8 Hz, 1H), 6.59 (td, J = 7.9, 3.2 Hz, 2H), 6.52 (ddd, J = 11.4, 8.8, 2.5 Hz, 1H). ^{19}F NMR (376 MHz, Benzene-d6) δ -109.56 (p, J = 8.3 Hz), -112.56 (q, J = 10.7, 9.9 Hz). ^{13}C NMR (101 MHz, Benzene-d6) δ 164.7 (d, J = 12.1 Hz), 162.3 (dd, J = 13.8, 12.0 Hz), 159.9 (d, J = 11.9 Hz), 152.6 (d, J = 2.7 Hz), 150.0, 136.2, 132.8 (dd, J = 9.5, 4.6 Hz), 124.1 (d, J = 11.0 Hz), 122.4, 111.9 (dd, J = 21.0, 3.6 Hz), 104.4 (dd, J = 27.3, 25.4 Hz). FT-IR (neat) cm-1 3086,1567,1138,780.

*2-(4,6-difluoro)phenylpyridine is the only reagent according to vendors should be kept in a sealed air tight vial inside a refrigerator (5 ºC). All other products while neat and in a dark area are benchtop stable. Keeping catalyst in solution for extended amount of time could induce decomposition.

Working with Hazardous Chemicals

The procedures in *Organic Syntheses* are intended for use only by persons with proper training in experimental organic chemistry. All hazardous materials should be handled using the standard procedures for work with chemicals described in references such as "Prudent Practices in the Laboratory" (The National Academies Press, Washington, D.C., 2011; the full text can be accessed free of charge at http://www.nap.edu/catalog.php?record_id=12654). All chemical waste should be disposed of in accordance with local regulations. For general guidelines for the management of chemical waste, see Chapter 8 of Prudent Practices.

In some articles in *Organic Syntheses*, chemical-specific hazards are highlighted in red "Caution Notes" within a procedure. It is important to recognize that the absence of a caution note does not imply that no significant hazards are associated with the chemicals involved in that procedure. Prior to performing a reaction, a thorough risk assessment should be carried out that includes a review of the potential hazards associated with each chemical and experimental operation on the scale that is planned for the procedure. Guidelines for carrying out a risk assessment and for analyzing the hazards associated with chemicals can be found in Chapter 4 of Prudent Practices.

The procedures described in *Organic Syntheses* are provided as published and are conducted at one's own risk. *Organic Syntheses, Inc.*, its Editors, and its Board of Directors do not warrant or guarantee the safety of individuals using these procedures and hereby disclaim any liability for any injuries.

CHAPTER III

REDUCTIVE ALKYLATION OF 2-BROMOAZOLES WITH ALKENES VIA PHOTOCATALYSIS

3.1 *Introduction*

Azoles are a privileged scaffold that have been investigated as therapeutics for numerous diseases[72] additionally 2-alkyl azoles have proven to be remarkable ROCK II inhibitors.[73-75] There are however relatively few rapid syntheses of these targets. Consequently, in order to facilitate thorough SAR studies methods that allow the rapid construction of complex 2-alkyl azoles have grown in demand.

The classic method for making 2-alkyl azoles is *via* cyclodehydration[76] This is still the most commonly used, but it is limited to carboxylic acid derivatives (eqn 1, **Scheme 3.1**). Another drawback of using this method is that it only works with benzo- fused rings not simple azoles. Typically, the scope of this methodology's is limited,and its success depends on the reactivity of the substrates and the availability of the required starting materials. However, in contrast to formation of the heterocycle, cross-coupling has the ability to expedite diversification and recent efforts have provided such strategies. The first is to couple bromoazoles[4] and prefunctionalized

Csp^3–zincates (eqn 2). Alternatively, alkyl-halides[77] and hydrazones[78] have also been used along with 2*H*-benzothiazoles (eqn 3). While these methods have expedited diversification by cross-coupling the partners directly, they still possess limitations. Prefunctionalized zincates must be formed *in situ* which limits the substrates that can be used and the functional group tolerance of the reaction. Also, these preformed organometallics, which are often basic, are difficult to store and handle.

Scheme 3.1 Accessing 2-alkyl benzothiazoles

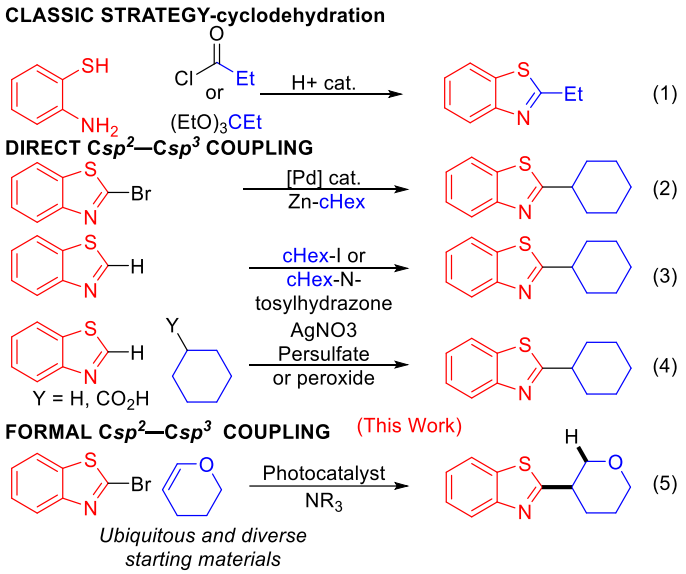

Even more recently, oxidative methods have been used to generate a radical, either by C–H abstraction or by radical decarboxylation (eqn 4) and have proven quite selective for addition of the alkyl radical to the 2-position of an azole.[79-80] However, Csp^3–halides, Csp^3–organometallics or tosyl hydrazones represent a relatively small set of coupling partners that can be used as inputs for the cross-coupling.

Radical addition to alkenes is well known[81] and represents a promising strategy for the reductive alkylation of alkenes. Pioneering work in this area has shown that an aryl bromide can be converted to the aryl radical,[82] most often by use of Bu_3SnH[83] or SmI_2/HMPA.[81, 84] Aside from toxicity issues associated with the organotin and HMPA, the major drawback is the limitation in

scope, which is due to fast over reduction of the desired aryl radical.[81] Consequently, almost all synthetically useful examples of aryl radical addition to unactivated alkenes are intramolecular cyclizations that can outcompete fast reduction.[83]

With the current research possessing limitations, we considered a strategy that would allow direct coupling of an azole or other heteroarene with a desirable partner. We hoped to exploit a mechanistic pathway in which an electron transfer to an azole- or heteroarene-halide iwas achieved via photoredox catalysis, which we anticipated would produce reactive azolyl or heteroaryl intermediates (eqn 5).[85-86] We presumed that these intermediates would engage pi-bonds to form C–C bonds giving rise to the desired products. With this late stage coupling, we further envisioned that this methodology would broaden the overall scope of azole bearing motifs and serve as a unique yet useful strategy for synthesizing these specific types of compounds. Also given the ubiquity of alkenes, this transformation had the immediate potential to significantly alter the types of motifs that could be synthetically accessed by rapid cross-coupling. In 2012, Stephenson and co-workers[33] had shown that a photocatalyst such as $Ir(ppy)_3$, an amine, in the presence of visible light could perform hydrodeiodination of an aryl iodide (**Scheme 3.2**). Much was learned from this example. One being that the amine of the reaction was quenching the photocatalyst and this reduced catalyst was adding electrons to the LUMO of the iodoarene. Secondly, that the amine or formate ion is supplying the H-atom.

Scheme 3.2 Dehalogenation of aryl iodides

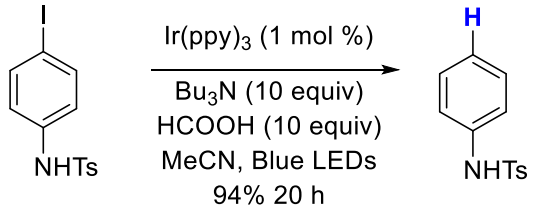

In 2014, MacMillan and coworkers demonstrated that 2-chlorobenzothiazoles could be coupled with 1-phenylpyrrolidine forming a C–C bond (**Scheme 3.3**). While the mechanism was not clear, it did suggest that these halogenated azoles were capable of also accepting electrons photocatalyically resulting in the formation of a desirable C–C bond.

Scheme 3.3 Photocatalytic aryl carbinamine formation

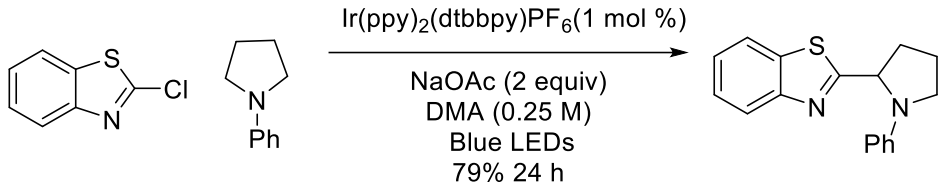

Previously, Arora and co-workers in our group[41] proposed that 2-chloroazoles upon the delivery of a single electron transfer (SET) results in the generation of the chloro azolyl radical anions (**Scheme 3.4**),and the bond-forming reactive intermediate can be applied to the C–H functionalization of tertiary amines aliphatic amines to synthesize α-azolyl carbinamines.[87]

Scheme 3.4 Coupling of tertiary aliphatic amines with 2-chloroazoles

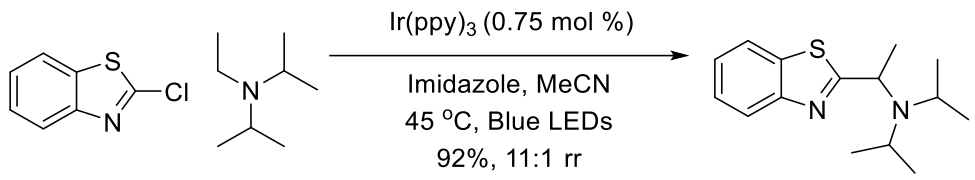

The work depicted here in this chapter suggests that the halogen at the 2-position displays contrasting reactivity, thereby giving substantial control over the reaction. In contrast to this, 2-bromoazoles as well and other related heteroaryl bromides, undergo rapid mesolytic fragmentation of bromide and give rise to the relatively long-lived azolyl or heteroaryl radical intermediates which appear to be responsible for C–C bond formation, as opposed to the radical anions in the case of chlorides.

The LUMO of the haloarene is the π* orbital.[88-89] After delivery of the electron and formation of the radical anion, an intramolecular electron transfer takes place from the π* to the σ* orbital resulting in C–X fragmentation.[12, 90-92] If the π-type radical anion is planar such monomolecular fragmentation is forbidden, since the orbitals are orthogonal (**Figure 3.1A**). The leaving group and its effect on the rate of fragmentation is depicted in **Figure 3.1B**. The larger and less electronegative atoms lower the σ* energy and in return promote facile fragmentation. For bimolecular reactions to be possible, the πRA must be generated and long-lived. Electronegative atoms or heteroatoms within the ring stabilize or lower the energy of the π*-orbital (LUMO).[19]

Figure 3.1 Energy diagrams for radical anion fragmentation

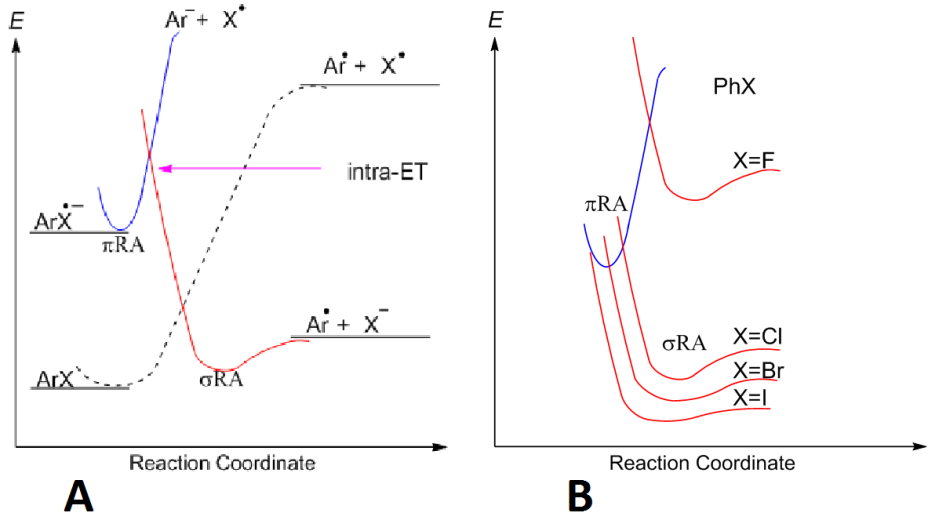

3.2 *Optimization studies*

Initial experiments consisted of optimizing the reaction conditions. The next set of tables illustrate the results of the experiments. Initially solvent was examined for the reaction in **Table 3.1.** Various solvents were screened including polar protic, polar aprotic, and non-polar solvents. The reaction performs best under polar aprotic conditions and CH_3CN was chosen as the solvent

choice due to the overall reduction was low. Next, temperature was investigated and 45 ^{o}C was the optimal temperature (**Table 3.2**). It is important to note; that the table depicts that regioselectivity is thermalyl dependent, giving the best rr (6:1, 70%). The next table displays concentration dependence, at 0.25 M the reduction is also at the lowest (**Table 3.3**). Finally, in **Table 3.4** a catalyst screen was performed and out of the catalyst screen $Ir(ppy)_3$ proved to be the optimal catalyst.

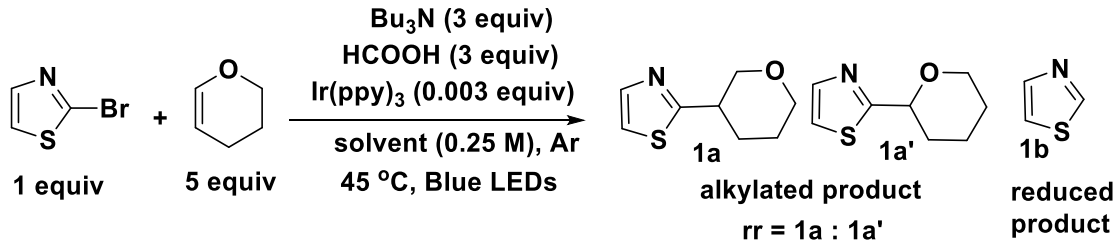

Table 3.1 Solvent screening

Entry	Solvent	NMR Conversion	Reduction	Alkylated product (rr = 1a : 1a')
1	Dichloromethane	100%	37%	63% (5:1) + unidentified side product
2	DMA	100%	60%	40% (6:1)
3	DMF	100%	58%	42% (5:1)
4	DMSO	68%	23%	45% (4:1)
5	THF	50%	35%	15% (4:1)
6	Toluene	0 %	na	na

7	MeOH	19%	7%	12% (3:1)
8	Nitromethane	0%	na	na
9	NMP	100%	72%	28% (7:1)
10	**CH_3CN**	**100%**	**30%**	**70% (6:1)**

rr = regioisomeric ratio

na = not applicable

CH_3CN was chosen as the solvent for further optimization.

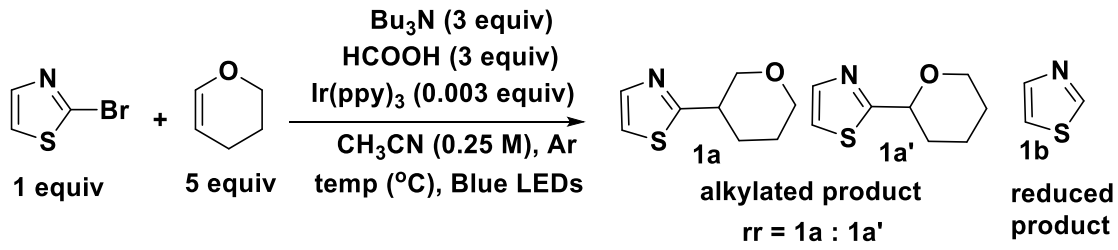

Table 3.2 Effect of temperature

Entry	Temperature (°C)	NMR conversion	Reduction	Alkylated Product (rr = 1a : 1a')
1	30 °C	100%	51%	49% (4:1)
2	**45 °C**	**100%**	**34%**	**66% (6:1)**
3	60 °C	100%	40%	40% (5:1) + unidentified side product

45°C was chosen as the temperature for further optimization.

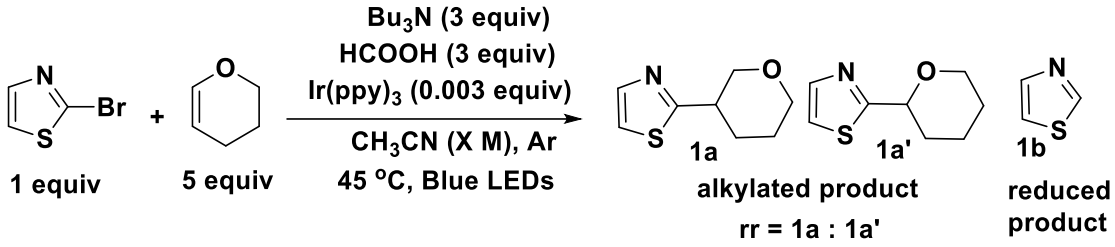

Table 3.3 Effect of Concentration

Entry	Concentration	NMR conversion	Reduction	Alkylated product (rr = 1a : 1a')
1	0.10 M	100%	55%	45% (5:1)
2	0.15 M	100%	52%	48% (4:1)
3	0.20 M	100%	47%	53% (5:1)
4	**0.25 M**	**100%**	**38%**	**62% (5:1)**
5	0.30 M	100%	40%	60% (5:1)
6	0.35 M	100 %	42%	58%(5:1)
7	0.40 M	100%	48%	52% (5:1)

0.25 M was chosen as the concentration for the reaction

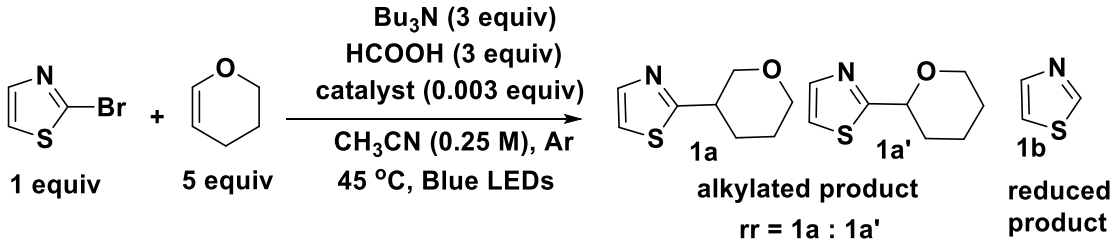

Table 3.4 Catalysts screening

Entry	Catalyst	NMR conversion	Reduction	Alkylated product (rr = 1a : 1a')
1	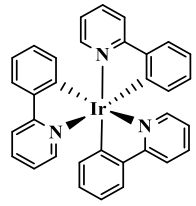	**100%**	**33%**	**67% (5:1)**
2	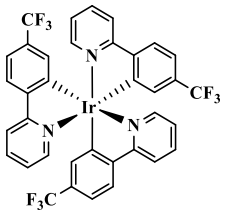	67%	32%	35% (4:1)
3	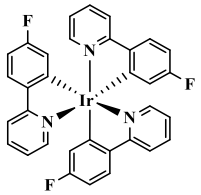	75%	38%	37% (5:1)
4	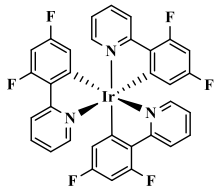	33%	17%	16% (4:1)
5	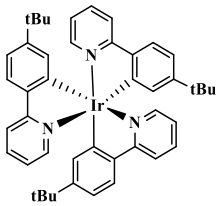	68%	37%	31% (4:1)

6	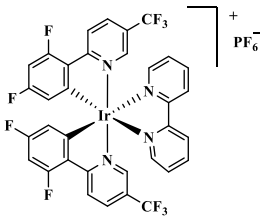	100%	42%	58% (4:1)
7	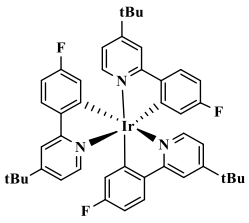	100%	47%	53% (4:1)
8	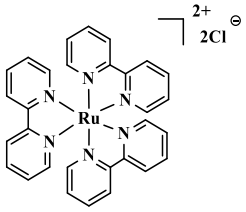	0%	na	na
9	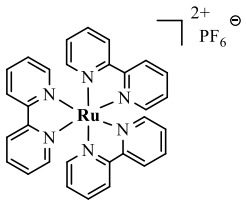	18%	11%	7% (na)
10	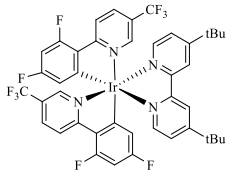	100%	37%	63% (4:1)

Ir(ppy)$_3$ was chosen as the catalyst for the reaction

With initial results in hand, we decided to look at other factors that could affect the overall reactivity. Previously, the Weaver group showed that 2-chloroazoles[39] could be used to functionalize the α-C–H of tertiary aliphatic amines. However, after experimentation, addition of

electron-rich dihydropyran to 2-chlorothiazole (entry 3, **Table 3.5**) yielded only reduced azole (**1b**) and carbinamine (**1c**) as the major products. Whereas, the use of the 2-bromothiazole resulted in a complete change in reactivity (entry 2) in which the reductively coupled product was the major C–C-product and the carbinamine (**1c**) was not observed. Based on the work of Bunnett[15] and Rossi[93] who have shown that radical anions will fragment a bromide faster than the corresponding chloride, it is reasonable to think that the observed change in reactivity is due to the nature of the reactive intermediates involved. Specifically, we postulated that 2-chloroazoles underwent C–C formation *via* the radical anion while 2-bromoazoles underwent C–C formation *via* the azolyl radical. We next sought to increase the amount of C–C bond forming product to reduction product (i.e., **1a+1a'** vs. **1b**). Exchanging the ethyl of DIPEA for an isobutyl group (entry 3 vs. 2) resulted in a significant increase in the desired product, albeit at the expense of reaction time. Furthermore, we observed that the product ratio was not constant throughout the course of the reaction (entry 4 vs. 5), with relative increases of **1a** as the reaction progressed. We suspected that this might be a result of acidic species generated under the reaction conditions that could be reducing the amount of free amine in solution and possibly accelerating the formation of the desired product via a proton coupled electron transfer.[94] Thus, we explored some acidic additives and found that the best mixture was NBu_3/HCOOH (1:1) (entry 7).

Table 3.5 Optimization of Reaction Conditions

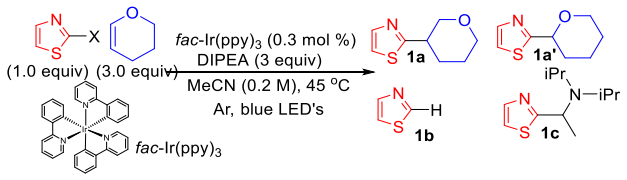

entry	X	modifications	conv[a]	1a:1a':1b:1c[b]	time
1.	Cl		100%	0:0:31:69	23 h
2.	Br	none	100%	38:10:52:0	22 h

3.	Br	used (iPr)$_2$NiBu instead of DIPEA	100%	52:13:35:0	2 d
4.	Br	used NBu$_3$ instead of DIPEA	24%	17:8:75:0	2 h
5.	Br	used NBu$_3$ instead of DIPEA	69%	30:8:62:0	23 h
6.	Br	used (iPr)$_2$NiBu w/ HCO_2H (1:1)	100%	44:6:50:0	22 h
7.	Br	used NBu$_3$ w/ HCO_2H (1:1)	100%	51:8:41:0	22 h
8.	Br	entry 7, but 1.2 equiv alkene	100%	17:3:80:0	22 h
9.	Br	entry 7, but 2.0 equiv alkene	100%	26:6:67:0	22 h
10.	Br	entry 7, but 3.0 equiv alkene	100%	39:9:52:0	22 h
11.	Br	entry 7, but 5.0 equiv alkene	100%	57:13:32:0	22 h
12.	Br	entry 11, at 0.25 M	100%	65:10:25:0	22 h
13.	Br	same as entry 12, with 20% v:v H_2O	100%	60:10:30:0	22 h
14.	Br	entry 12, no Ir(ppy)$_3$	0%		22 h
15.	Br	entry 12, no light or amine	0%		22 h

a. Conversion determined by ^{1}H NMR. b. product ratio determined by GCMS.

We next explored the concentration of alkene. Consistent with a process in which there is a competition for reduction and alkylation of the azolyl radical, increased concentration of alkene led to more alkylated products (**1a** + **1a'** entries 8-11). Further concentrating the reaction also led to a slight improvement. In an attempt to check the operational flexibility of the reaction, we added water, which resulted in only a slight decrease of the desired products. Finally, control experiments (entries 14 and 15) indicated that photocatalyst, light, and amine were all necessary components of the reaction. In retrospect, 2-bromothiazole was an ideal substrate for optimization since we have empirically observed it to have the greatest tendency to undergo reduction of all the azoles that we have studied. In other words, it provided a highly sensitivity substrate facilitating optimization of the reaction conditions. Using 0.3 mol% *fac*-tris-(2-phenylpyridine) ($Ir(ppy)_3$), a 1:1 mix of amine and formic acid (3 equiv), and 5 equivalents of alkenes, we began to explore the scope of the reaction.

3.3 *Substrate scope*

Initially, we reacted a series of thiazoles with dihydropyran. We obtained a 65% yield with a 6:1 regioisomeric ratio (rr) for simple 2-bromothiazole (**1a**, **Scheme 3.5**). In most cases, substitution of the thiazole increased the selectivity (**1a** vs. **2a**-**7a**). Products **5a** and **6a** highlight an important feature of electron-addition induced fragmentation events which can be very selective and in these cases display perfect chemoselectivity for the 2-bromo over the 4-bromo and 5-bromo positions. The reaction works well for benzothiazole (**7a**). However, the inclusion of a 5-chloro or 5,7-difluoro slightly reduces the regioselectivity (**8a**, and **9a**). In contrast to thiazoles, we do not observe competitive reduction of 2-bromobenzimidazoles (**10a**) and consequently, yields are higher. Additionally, under these conditions 2-bromooxazole (**11a**) does not undergo reductive alkylation and highlights the impact that the nature of the heterocycle has on the reaction.

Next, we evaluated the nature of the alkene that could participate in the reductive alkylation. In general, we found the addition to be remarkably sensitive to the substitution pattern of the alkene. Specifically, the addition typically occurred at the less substituted carbon to provide the alkylated azoles in high regioselectivity. The reaction works for mono-substituted- (**13a**), 1,1-disubstuted (**16a, 18a**, **21a**, **22a**, **24** and **26a**), 1,2-disubstituted (**5a-10a**, **17a**, **19a**, **20a**, **23a**), trisubstituted- (**12a**, **14a**, **15a**), and bridged-alkenes (**17a-23a**). A number of functional groups that likely would be sensitive to basic organometallics work well in this method, including free alcohols (**12a**, **15a**), acetates (**16a**), esters (**23a**), and enones (**24a**). Believing that we were forming an azolyl radical, we were pleased to see that weaker bonds, such as benzylic (**26a**), allylic (**25a**, **26a**) as well as acetal C–H's (**13a**) were well tolerated. Furthermore, we saw no addition to the phenyl rings (**14a**, **26a**), suggesting a preference for π-electrons of alkenes over those of arenes.

Scheme 3.5 Scope of the reductive alkylation

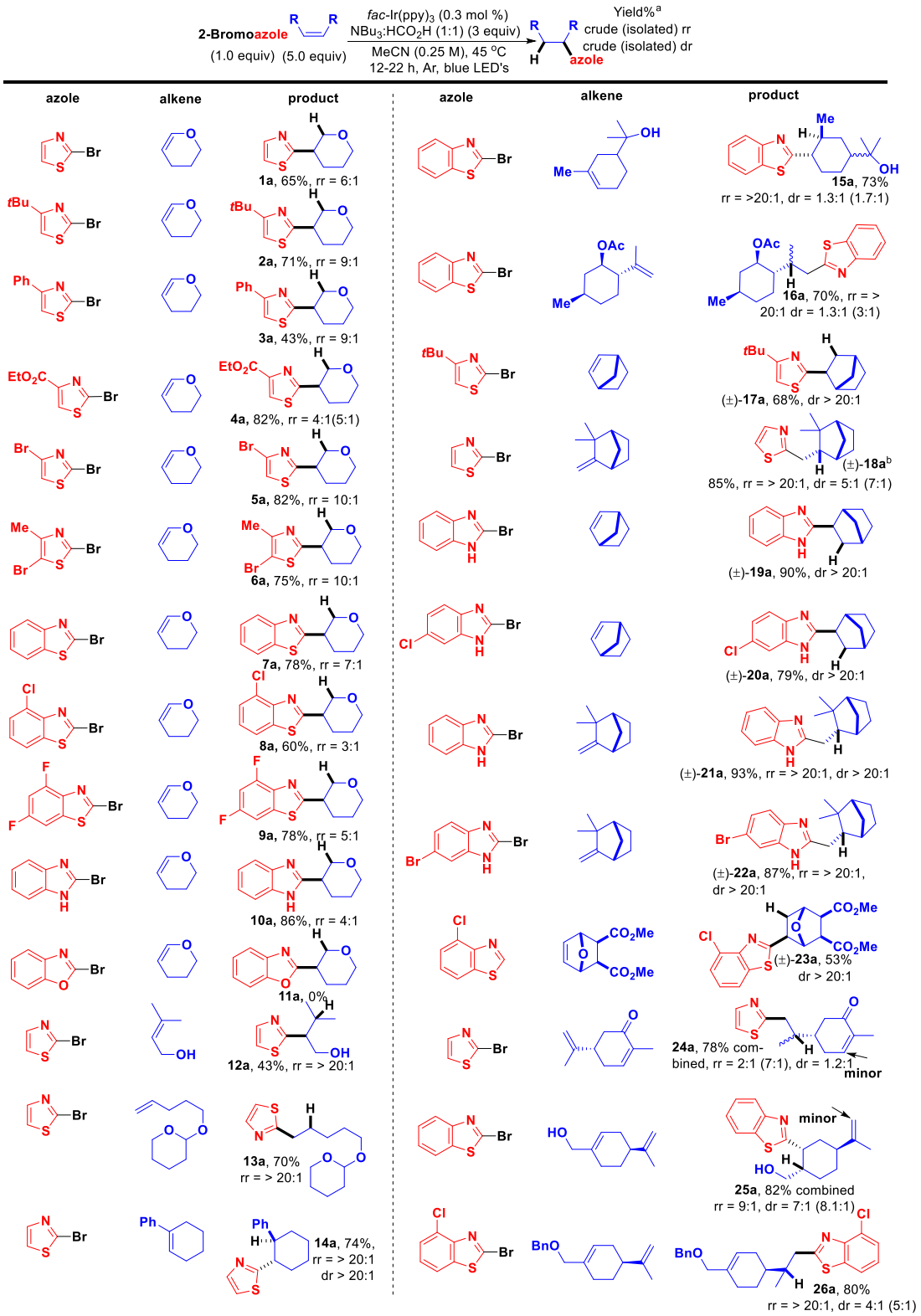

Additionally, in more complex molecules containing multiple alkenes we observed synthetically useful selectivities (**24a**-**26a**). Interestingly, comparison of perillyl alcohol derivatives (**25a**, **26a)** suggests that the presence of the free hydroxyl group can alter the inherent regioselectivity.

When these reaction conditions were applied to terpenoids containing a vinyl cyclobutane motif, we observed clean, reductive ring opening in good yields, high regioselectivity and diastereoselectivity. Addition of difluorobenzothiazole to α-pinene provided a 68% yield of an enantio- and diastereomerically pure trisubstituted cyclohexene (eqn 6**, Scheme 3.6**). The reaction of caryophyllene oxide afforded a single stereoisomeric product in good yield (eqn 7) with the epoxide functional group remaining unchanged. The selectivity of the ring opening event suggests that reductive azolylation of vinyl cyclobutanes may be a general and convenient method for the formal allylic substitution with concomitant ring enlargement.

Scheme 3.6 Ring opening of vinylcyclobutanes

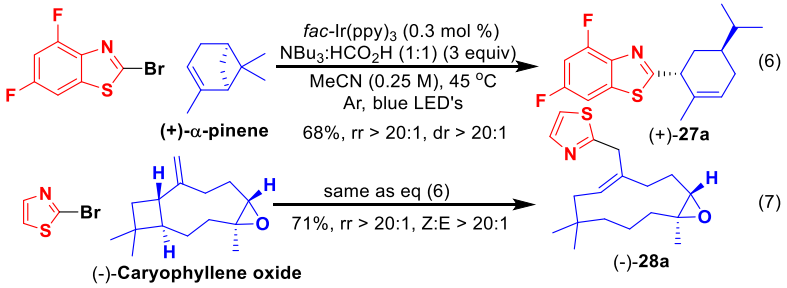

The ability to easily and directly expand the carbon framework of an alkene situated within a complex molecule presents an exciting possibility as a late stage functional group handle. Thus, we examined the thiazolylation of unprotected cholesterol, which gave a single stereoisomeric product (eqn 8, **Scheme 3.7**).

Next, we wanted to address a scenario in which the alkene was more precious than the azole. Thus, we were forced to look at the underlying problematic reduction that necessitated the

use of an excess of 2-bromothiazole. The amine is the stoichiometric reductant and is essential to the reaction. We speculated that it could also be facilitating undesired reduction of the bromoazole.

Scheme 3.7 Thiazolation of cholesterol

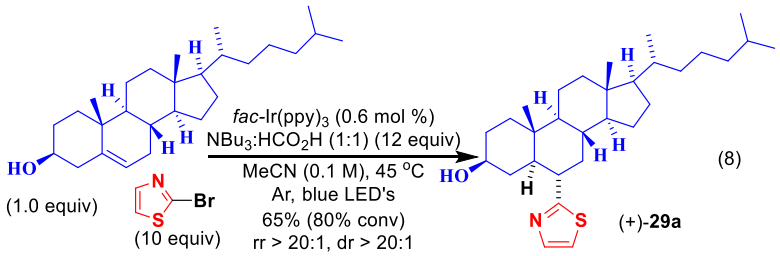

3.4 *Reduction pathway studies: lowering parasitic HAT*

We speculated that the rate of the undesired reduction reaction might depend upon the concentration of the amine and we probed this by keeping the amine concentration artificially low via iterative addition of amine. We decided it was best to experiment to approve reaction conditions further.

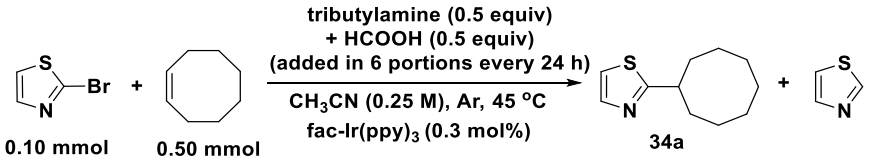

In the experiment, a 5 mm NMR tube capped with NMR septum (Ace glass, part no. 9096-25) was charged *fac*-tris(2-phenyl pyridinato-C^2, *N*) Iridium(III) (Ir(ppy)3) (0.4 mL [0.75 mM stock solution of catalyst in MeCN]). 2-bromothiazole (15 mg, 0.10 mmol) and cyclooctene (11.5 mg, 0.50 mmol) as well as tributylamine (9 mg, 0.05 mmol) and formic acid (2 mg, 0.05 mmol) were added in the beginning of reaction. A sealed glass capillary containing C_6D_6 was placed in NMR tube for locking purposes. Then the reaction tube was degassed via Ar bubbling for 10 min. and then the exit needle and Ar line were removed and reaction tube was sealed with parafilm. The NMR tube was placed in a light bath (as described above) and the lower portion of the tube

was submerged under the water bath which was maintained at 45 ^{o}C. ^{1}H NMR was recorded after 24 h, followed by addition of 0.05 mmol of tributylamine and 0.05 mmol of formic acid. Then the reaction mixture was again degassed and placed in the light bath. After an additional 24 h, the ^{1}H NMR was once again recorded. This incremental addition of tributylamine and formic acid was repeated until a total of 0.3 mmol of tributylamine and formic acid were added to the reaction. The results have been tabulated, below (**Table 3.6**).

Table 3.6 Iterative addition of amine

Entry	Total mmol of formic acid	Total mmol of tributylamine	NMR conversion	Reduction	Alkylated product
1	0.05	0.05	0%	na	na
2	1	1	0%	na	na
3	1.5	1.5	20%	9%	11%
4	2.0	2.0	36%	17%	19%
5	2.5	2.5	74%	32%	42%
6	**3.0**	**3.0**	**100%**	**48%**	**52%**
7	Single addition of HCOOH (3.0 mmol)	Single addition of Bu_3N (3.0 mmol)	100%	72%	28%

By comparison, when a single addition of tributylamine (3.0 equiv) and formic acid (3.0 equiv) is initially added, all at once, the reaction undergoes 100% conversion, out of which 72% is reduction and 28% is alkylated product **34a** (entry 7) in 12 h (reaction time) while incremental addition leads to a 48% reduction and 52% alkylated product (entry 6). This experiment suggests

that the rate of reduction of the azole has a greater amine concentration dependency than the alkylated product and encouraged further exploration of this question.

Alternatively, we could take advantage of the poor solubility of tertiary amine with long alkyl chains (in MeCN), which can provide a convenient method for keeping a low concentration over time. Thus we evaluated the solubility of various amines derivatives, which is given below (**Figure 3.2**).

Figure 3.2 Experimentally determined solubility of several amines at 23 ˚C

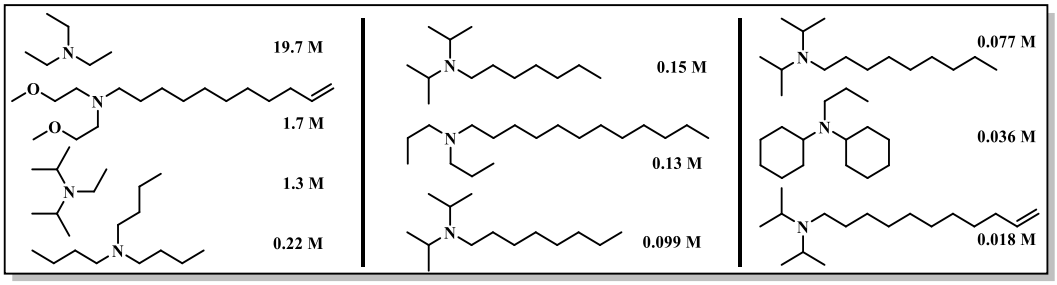

(*i*Pr)$_2$N*n*-Oct amine was chosen for second round of optimization.

Based on the previous experiment, we believed that maintaining a low concentration of amine in solution could improve product ratio. Furthermore, we speculated that a lower amine concentration might require a more oxidizing photocatalyst to compensate for the decreased concentration of amine. The next set of experiments (**Table 3.7**) tested several photocatalysts while using the less soluble amine. **Ir(ppy)$_3$** and **(Cat-1)** were selected for further optimization, which have been summarized and discussed next (**Table 3.8**).

Table 3.7 Second round of optimization studies

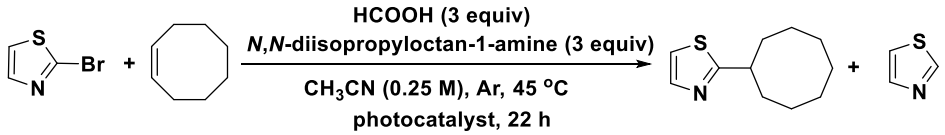

Entry	Catalyst	NMR conversion in 22 h	Reduction	Alkylated product
1	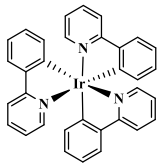	**84%**	**54%**	**30%**
2	cat - 1 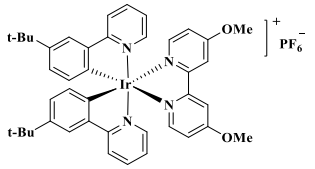	**48%**	**27%**	**21%**
3	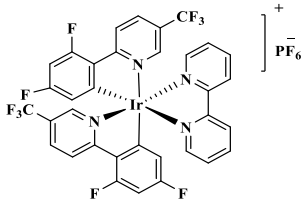	43%	22%	21%
4	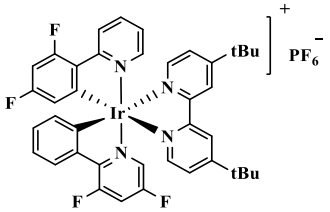	48%	22%	26%
5	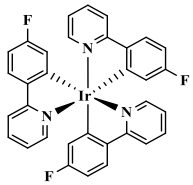	25%	9%	16%
6	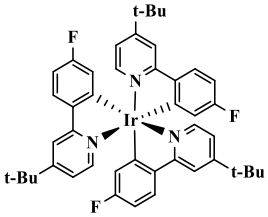	5%	5%	na

Lowering the concentration of free amine did indeed decrease the undesired reduction pathway, since the reduction was likely directly dependent on the amine concentration. Iterative addition of the amine improved the product ratio (entry 2 vs. 1) and supported our hypothesis.

Table 3.8 Amine Dependent Reduction Pathway Study

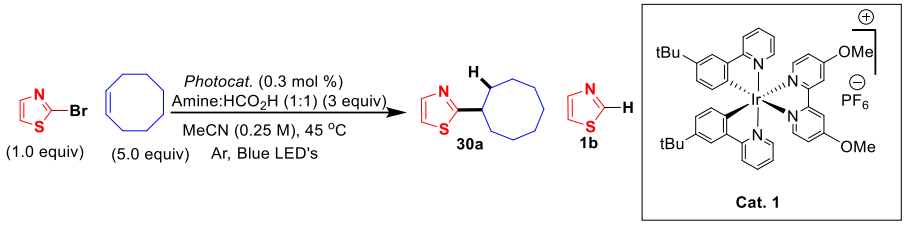

entry	cat.	amine	conv	**30a**:**1b**
1.	$Ir(ppy)_3$	Bu_3N	100%	25:75
2.	$Ir(ppy)_3$	Bu_3N*****	100%	52:48
3.	$Ir(ppy)_3$	$(iPr)_2N$*n*-Oct	84%	36:64
4.	**Cat. 1**	Bu_3N	100%	22:78
5.	**Cat. 1**	$(iPr)_2N$*n*-Oct	48%	44:56

***(iterative incremental addition)**

We were pleased to find that the use of the less soluble amine did lead to an improved ratio of the desired product (entry 3 vs. 1). We also recognized that decreasing the amine concentration might affect the rate of the photocatalytic reaction. We found that several more oxidizing photocatalysts resulted in increased alkylated product ratios, with Cat-1[55] providing the fastest reaction among these catalysts.

Using 2 sets of conditions, **conditions A**-tributylamine (3 equiv), HCOOH (3 equiv), *fac*-Ir(ppy)$_3$ (0.3 mol%) in 14 h and **conditions B**-*N*, *N*-diisopropyloctan-1-amine (3 equiv), HCOOH (3 equiv), cat-1 (0.3 mol%) in 5 days, we investigated the effect of changing the equivalents of alkene (**Table 3.9**).

Table 3.9 Effect of change in equiv of alkene

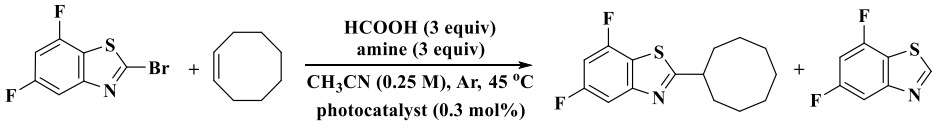

Entry	Reactions conditions	Equiv of Alkene	NMR conversion	Reduction	Alkylated product
1	**Cond. A**	1.2 equiv	100%	82%	18%
2	**Cond. B**	1.2 equiv	100%	56%	44%
3	**Cond. A**	2.4 equiv	100%	67%	33%
4	**Cond. B**	2.4 equiv	100%	32%	68%
5	**Cond. A**	5 equiv	100%	39%	61%
6	**Cond. B**	5 equiv	100%	20%	80%

Comparison of the two sets of conditions (**Conditions A** and **B)** at various alkene loadings, showed significant enhancements in the desired product formation by using the less soluble amine and more oxidizing catalyst (**Cat-1**) (**conditions B**), albeit at the expense of longer reaction time.

Using our modified conditions, we investigated more valuable 2-bromo-4,6-difluorobenzothiazole as well as several of the poorer yielding substrates from Table 2 (**Scheme 3.8**). In all cases, we observed increases in yield. We expect that these conditions will be ideal in cases where the azole is more precious and reaction time is not.

Scheme 3.8 Reduction minimizing conditions

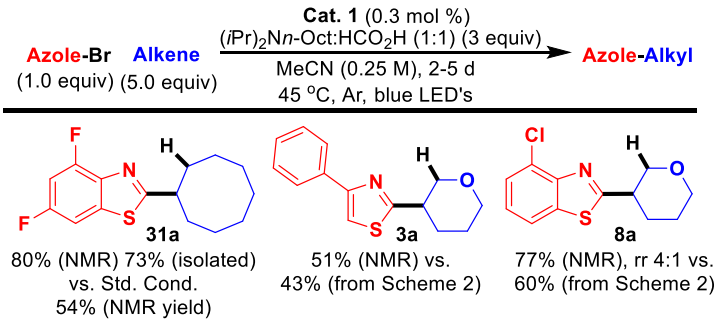

Finally, we suspected that this type of reactivity should be possible with other reducible bromoarenes. In our initial attempt, we subjected electron deficient bromopyrimidnes and benzenes to unoptimized conditions **(Scheme 3.9)**. We found that all underwent reductive alkylation, allowing isolation of the alkylated pyrimidine (**32a**) and benzenes (**33a, 34a**). Importantly, these preliminary results suggest that photocatalytic reductive alkylation may be a general strategy for Csp^2–Csp^3 cross-coupling. Furthermore, it warrants development of substrate specific conditions, which will likely be unique given the significant electronic differences between the aromatic motifs.

Scheme 3.9 Reductive alkylation as a general strategy

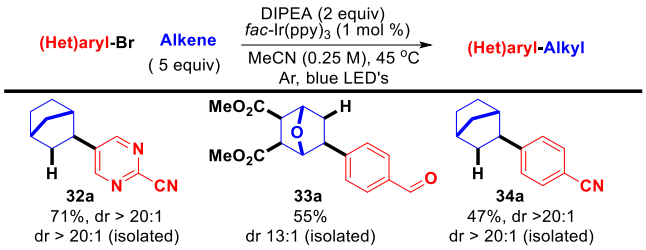

3.5 *Mechanistic findings*

In regards to the mechanism fluorescence quenching experiments were conducted (**Figure 3.3A-F**). The results suggest that as an individual component 2-bromothiazole provides the fastest quenching (**Table 3.10**). The nonlinearity of the slope when bromoazole is used is interesting (**Figure 3.3A**). However, the rate of quenching is significantly reduced when other reaction components are included with the bromoazole (**Figure 3.3E and F**) and make interpretation of the quenching event uncertain given the relatively small differences in rates of quenching event and leave open the possibility of multiple types of quenching events occurring simultaneously.

Figure 3.3A $Ir(ppy)_3$ emission quenching by 2-bromothiazole (Q)

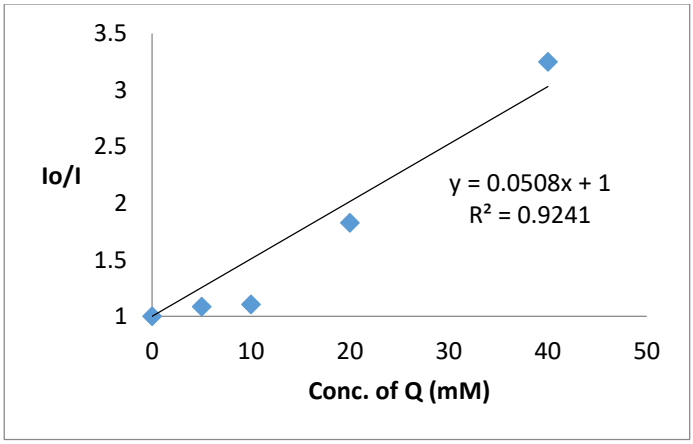

Figure 3.3B $Ir(ppy)_3$ emission quenching by dihydropyran (Q)

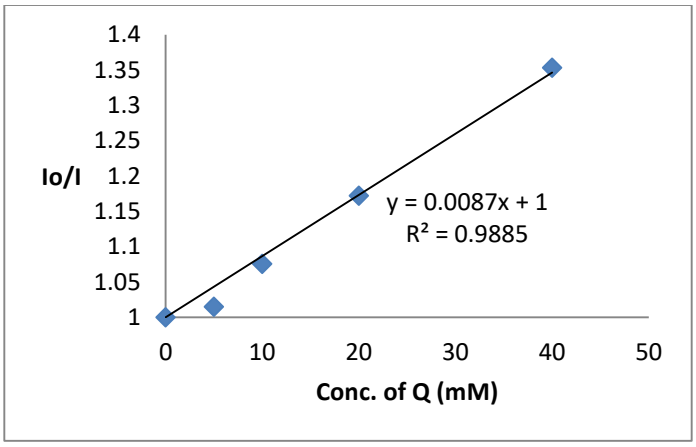

Figure 3.3C $Ir(ppy)_3$ emission quenching by tributylamine (Q)

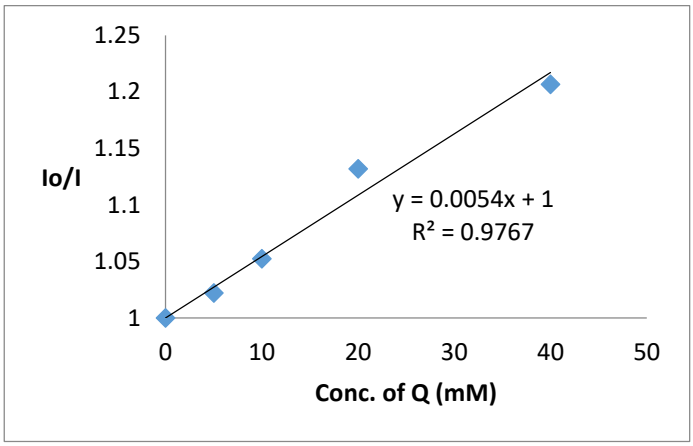

Figure 3.3D $Ir(ppy)_3$ emission quenching by tributylamine and formic acid (1:1) (Q)

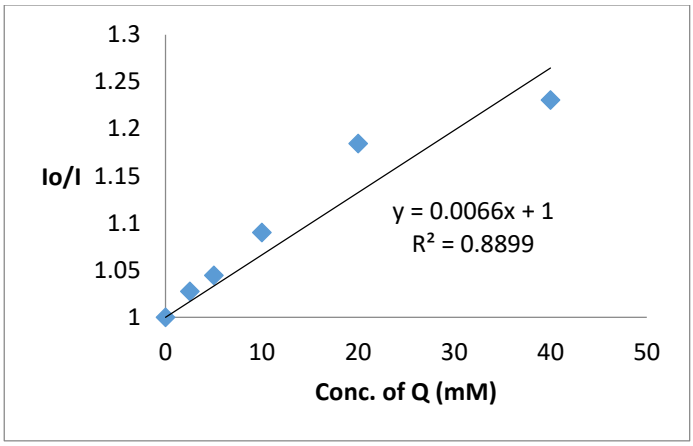

Figure 3.3E $Ir(ppy)_3$ emission quenching by 2-bromothiazole and formic acid (1:3) (Q)

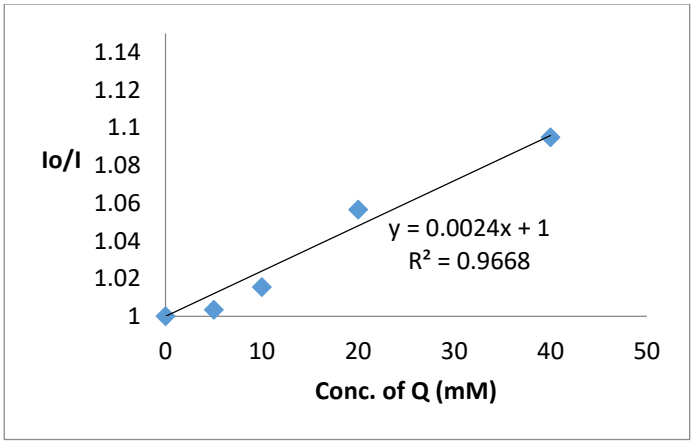

Figure 3.3F $Ir(ppy)_3$ emission quenching by 2-bromothiazole and tributylamine with formic acid (1:3:3) (Q)

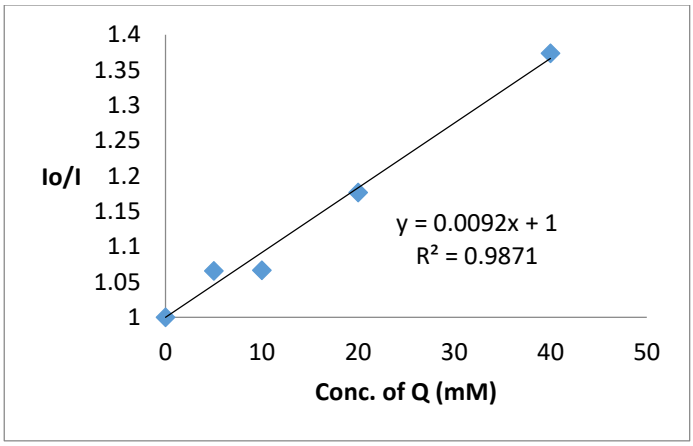

Table 3.10 Tabulated slopes of potential quenchers

Quencher (Q)	Slope
2-Bromothiazole	0.0508
Dihydropyran	0.0087
Tributylamine	0.0054
Tributylamine and formic acid (1:1)	0.0066
2-Bromothiazole and formic acid (1:3)	0.0024
2-Bromothiazole and tributylamine with formic acid(1:3:3)	0.0092

During our investigation, we speculated that problematic reduction might depend upon amine concentration in the reaction mixture. To address this problem, we began by considering the mechanism (**Scheme 3.10**). We posited that upon absorption of a photon in the visible region, the $Ir(ppy)_3$ is capable of being quenched either oxidatively by the bromoazole or reductively by the amine, followed by electron transfer to the azole. In either scenario, the ultimate outcome being the formation of the radical anion (***int-A***). The radical anion is expected to undergo bromide

extrusion to give an azoyl radical (***int-B***) [90] The azoyl radical (***int-B***) then undergoes addition to the alkene with a significant preference for the less substituted terminus to give the more stable alkyl radical (***int-C***). The alkyl radical ultimately undergoes HAT (hydrogen atom transfer) to give the alkylated azole. It was envisioned that the undesired reduced azole arose from a parasitic propagation reaction. In this scenario, the azoyl radical (***int-B***) undergoes HAT from the amine to give the reduced azole and an α-amino radical (***int-D***). Based on the work of Scaiano,[95] we believed that ***int-D*** may play an active role in the reaction. Specifically, we suspected that it may be transferring an electron to the bromoazole to give an imminium and another radical anion and completing the parasitic pathway. Several experiments were designed to test this hypothesis.

Scheme 3.10 Possible mechanism

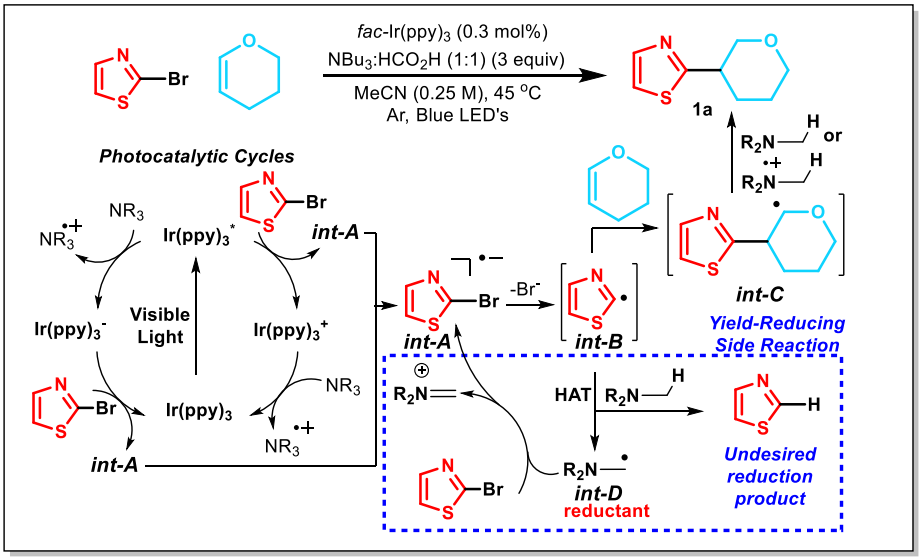

Our postulated mechanism assumed that the H-atom source was the amine and not the formate. However, given that formate has been used as an H-atom source within related photocatalytic work,[96] we assessed the H-atom source by performing several photocatalytic reactions using deuterium labeled reagents. GC-MS was used to determine the ratio of M+1/M$^+$

for each of reactions below via selected ion monitoring (SIM) mode. Increases in the M+1 peak are due to deuterium incorporation.

The first experiment evaluated the solvent as the source of H-atoms by changing the solvent from CH_3CN to CD_3CN in the reaction (eqn 1). Absorption intensity of each of the M^+ and M+1 of **1a** was determined by using SIM mode on GCMS.

Table 3.11 Deuterium from solvent

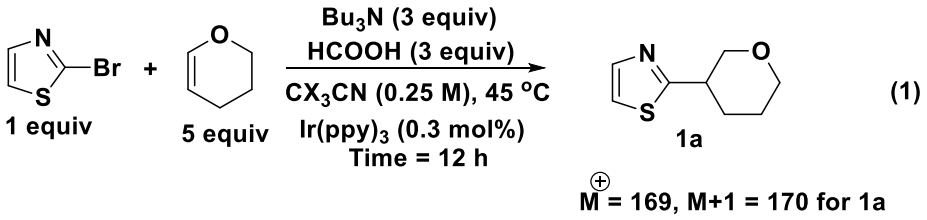

X = H

Entry	Selected ion	m/z	Abs. int.	M+1/M^+
1	M+1	170	410	
2	M^+	169	798	0.339 ($H_{solvent}$)

X = D

3	M+1	170	313	
4	M^+	169	589	0.347 ($D_{solvent}$)

The ratio of $D_{solvent}$/ $H_{solvent}$ = 2.3%. Thus, the solvent was playing only a minor role in providing H-atoms.

The second experiment demonstrates effect of changing HCOOH to DCOOD in the reaction (eqn 2). Absorption intensity of each of the M^+ and M+1 of **2a** is determined as described above.

Table 3.12 Deuterium from acid

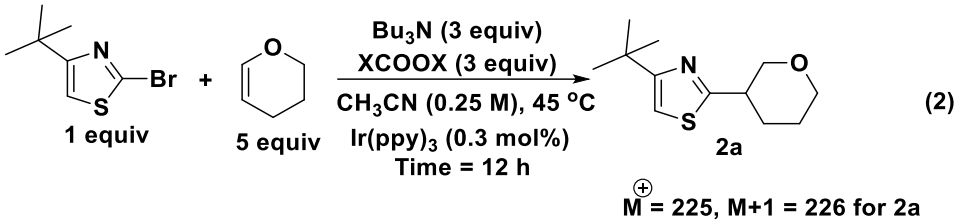

(2)

X = H

Entry	Selected ion	m/z	Abs. int.	$M+1/M^+$
1	M+1	226	5098	
2	M^+	225	23541	0.1780 (H_{acid})

X = D

3	M+1	226	4556	
4	M^+	225	20982	0.1784 (D_{acid})

The ratio of $D_{solvent}/ H_{solvent}$ = 0.2%. It appears that the role of the formic acid is not as a deuterium source, since very little was found to be incorporated. The formic acid is likely functioning as a Bronsted acid.

The third experiment demonstrates effect of changing HCOOH to DCOOD in the reaction (eqn 3). Absorption intensity of each of the M^+ and M+1 of **SI-1** is determined as described above.

Table 3.13 Deuterium from amine

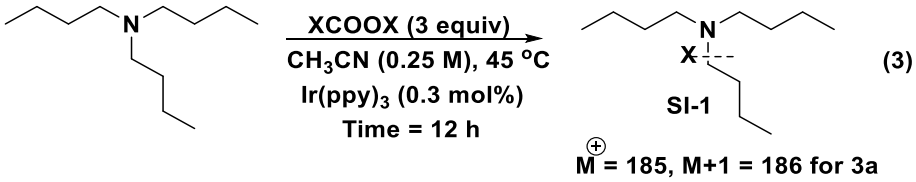

(3)

X = H

Entry	Selected ion	m/z	Abs. int.	M+1/M^+
1	M+1	186	7554	
2	M^+	185	48136	0.1356 (H_{amine})

X = D

3	M+1	186	14118	
4	M^+	185	61589	0.1864 (D_{amine})

The ratio of $D_{solvent}$/ $H_{solvent}$ = 37.5%. It is an interesting observation that under these conditions (note, the absence of the bromoazole) significant H-atom scrambling occurs.

We conclude that the amine is infact serving as the primary reductant while the solvent serves to provide a small percentage of the H-atom. Additionally, in the absence of the substrate significant deuterium incorporation is seen in the amine.

Demonstrating that this is indeed possible, MacMillan and coworkers[97] two years later exploited this reaction mechanism to incorporate deuterium and tritium into pharmaceutical compounds (**Scheme 3.11**). This method was applied to 18 drug molecules and incorporation of

deuterium and tritium were observed. The report supports our proposed mechanism and portrays the overall utility of photoredox catalyzed reactions.

Scheme 3.11 Photoredox-catalyzed deuteration and tritiation of pharmaceutical compounds

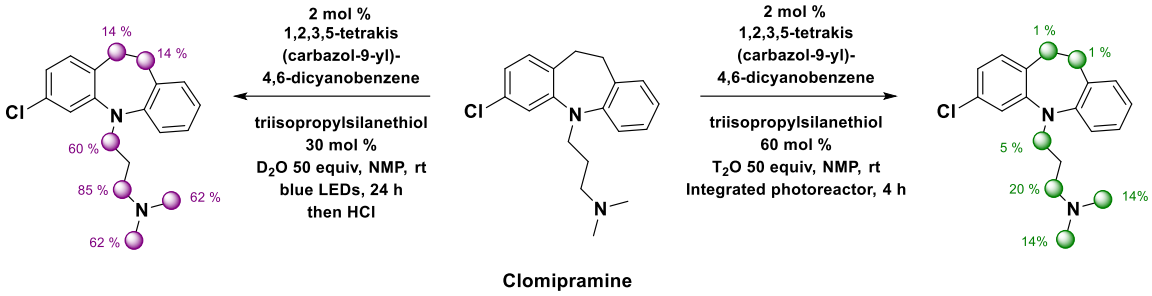

In conclusion, we have shown that photocatalysis has the ability to deliver Csp^2–Csp^3 cross-coupled products directly from 2-bromoazoles and unactivated alkenes. The ability to utilize alkenes directly as a surrogate for the corresponding alkyl group is a powerful synthetic strategy. In addition, the scope of the azole is general for thiazoles, benzothiazoles, and benzimidazoles, and in many cases, couples with excellent selectivity for the less substituted terminus of the alkene. The optional use of either alkene or azole as the limiting reagent is an attractive feature that should further enhance the utility. We have shown that this concept can be extended to other bromoarenes to generate both aryl and heteroaryl radicals in a controlled fashion, giving a sufficiently long-lived radical that it is capable of undergoing intermolecular C–C bond formation. Further exploration will expand the scope of the photocatalytic reductive coupling.

3.6 *Experimental section*

All reagents were obtained from commercial suppliers (Aldrich, VWR, TCI Chemicals, and Oakwood Chemicals) and used without further purification unless otherwise noted. 2-

bromoazoles were purchased from Sigma-Aldrich, except 2-bromobenzo[d]thiazole, 2-bromo-4-chlorobenzo[d]thiazole, 2-bromo-4,6-difluorobenzo[d]thiazole, 2,5-dibromo-4-methylthiazole, ethyl 2-bromothiazole-4-carboxylate, 2,6-dibromo-1H-benzo[d]imidazole and 2-bromo-6-chloro-1H-benzo[d]imidazole which were synthesized according to literature procedures.[98, 2, 3] Alkenes **A-1**[4], **A-2**[5] and **A-3**[6] were synthesized according to literature procedure and all other corresponding alkenes were purchased from Sigma-Aldrich, Oakwood Chemicals, and VWR. *N*,*N*-diisopropyloctan-1-amine was synthesized according to a literature procedure.[7] Tributylamine was purchased from VWR and *N*,*N*-diisopropylethylamine from Sigma-Aldrich. Photocatalyst fac-*tris*(2-phenyl pyridinato-C^2, *N*)iridium(III) ($Ir(ppy)_3$) and all other photocatalysts were synthesized according to the literature procedure.[8] Reactions were monitored by thin layer chromatography (TLC), (obtained from sorbent technology Silica XHL TLC Plates, w/UV254, glass backed, 250 µm, 20 x 20 cm) and were visualized with ultraviolet light, potassium permanganate stain, GC-MS (QP 2010S, Shimadzu equipped with auto sampler) and ^{1}H NMR.

Photocatalytic reactions were set up in a light bath as described below. Blue LEDs (in the form of strips *i.e.*, 18 LEDs/ft from Solid Apollo) were wrapped around the walls of glass crystallization dish and secured with masking tape and then wrapped with aluminum foil. A lid which rest on the top was fashioned from cardboard and holes were made such that reaction tubes (5mm NMR tube) were held firmly in the cardboard lid which was placed on the top of bath. Water was added to the bath such that the tubes were submerged in the water which was maintained at 45 ^{o}C with the aid of a sand bath connected to a thermostat.

Isolations were carried out using Teledyne Isco Combiflash Rf 200i flash chromatograph with Redisep Rf normal phase silica (4 g, 12 g, 24 g, 40 g) with product detection at 254 and 288 nm and evaporative light scattering detection. NMR spectra were obtained on a 400 MHz Bruker Avance III spectrometer and 600 MHz Unity Inova spectrometer. ^{1}H and ^{13}C NMR chemical shifts are reported in ppm relative to the residual protio solvent peak (^{1}H, ^{13}C). IR spectra were recorded on Varian 800 FT-IR. Melting points were determined on Stuart Digital (SMP10), Melting point-apparatus, 120 VAC. Mass spectra (HRMS) analysis was performed on LTQ-OrbitrapXL by Thermo Scientific ltd. Quenching studies were performed on Varian Carey Eclipse fluorescence spectrophotometer. Optical rotation was measured on an Autopol V polarimeter by Rudolph Research Analytical.

General procedure A for synthesis of 2-bromothiazoles and 2-bromobenzothiazoles[99]

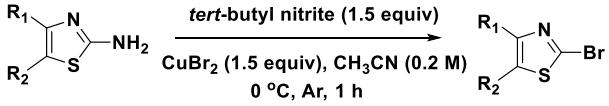

The aminoazole (1.0 equiv) and $CuBr_2$ (1.5 equiv) in CH_3CN was added to a round bottom flask and cooled to 0 ^{0}C under argon. Next, *tert*-butyl nitrite (1.5 equiv) was added drop wise to the reaction flask. The reaction mixture was stirred at 0 ^{o}C for 1 h and then at room temperature for another 20 minutes until full consumption of the starting material. The reaction was monitored by TLC. After consumption of the starting material, the mixture was diluted with H_2O (15 mL) and acidified with 12 N HCl (until pH<1 by indicator paper) then extracted with CH_2Cl_2 (3×20

mL). The organic layers were combined and dried with $MgSO_4$. The crude product was concentrated *in vacuo* and purified via normal phase chromatography.

S-1

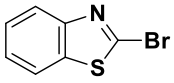

The **general procedure A** was followed using benzothiazol-2-amine (3.00 g, 19.0 mmol), *tert*-butyl nitrite (3.09 g, 29.0 mmol), $CuBr_2$ (6.36 g, 29.0 mmol) and 95.0 mL of MeCN to afford **S-1** in 63% yield after isolation (2.60 g, 12.0 mmol) as an orange solid. The substrate was purified via automated flash chromatography using EtOAc in hexanes (0% to 100%) with product eluting at 8% on a 40 g silica column.

S-2

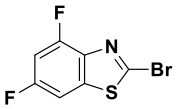

The **general procedure A** was followed using 4,6-difluorobenzothiazol-2-amine (100 mg, 0.54 mmol), *tert*-butyl nitrite (83.1 mg, 0.81 mmol), $CuBr_2$ (180 mg, 0.81 mmol) and 2.6 mL of MeCN to afford **S-2** in 65% yield after isolation (87.0 mg, 0.35 mmol) as white solid. The substrate was purified via automated flash chromatography using EtOAc in hexanes (0% to 100%) with product eluting at 10% on 4 g silica column.

S-3

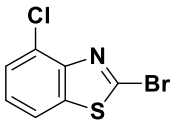

The **general procedure A** was followed using 4-chlorobenzothiazol-2-amine (500 mg, 2.72 mmol), *tert*-butyl nitrite (420 mg, 4.08 mmol), $CuBr_2$ (910 mg, 4.08 mmol) and 13.5 mL of MeCN to afford **S-3** in 52% yield after isolation (349 mg, 1.41 mmol) as white solid. The substrate was purified via automated flash chromatography using EtOAc in hexanes (0% to 100%) with product eluting at 12% on a 24 g silica column.

S-4

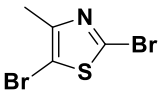

The **general procedure A** was followed using 4-methylthiazol-2-amine (500 mg, 4.38 mmol), *tert*-butyl nitrite (678 mg, 6.58 mmol), $CuBr_2$ (1.47 g, 6.58 mmol) and 22.0 mL of MeCN to afford **S-4** in 68% yield after isolation (766 mg, 2.98 mmol) as colorless oil. The substrate was purified via automated flash chromatography using EtOAc in hexanes (0% to 100%) with product eluting at 8% on a 24 g silica column.

S-5

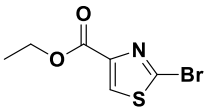

The **general procedure A** was followed using ethyl 2-aminothiazole-4-carboxylate (200 mg, 1.16 mmol), $CuBr_2$ (389 mg, 1.74 mmol), isoamyl nitrite (204 mg, 1.74 mmol) and 5.8 mL of MeCN to afford **S-5** in 70% yield (192 mg, 0.81 mmol) as colorless oil. The substrate was purified via automated flash chromatography using EtOAc in hexanes (0% to 100%) with product eluting at 12% on a 24 g silica column. ^{1}H-NMR and GC-MS matched previous literature.[100]

General procedure B for synthesis of 2-bromobenzoimidazoles[101]

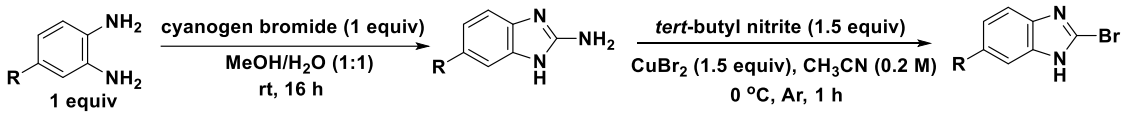

(Step 1) To a round bottom flask equipped with a magnetic stir bar containing 1:1 mix of H_2O and MeOH, cyanogen bromide (1.0 equiv of 5 M solution in MeCN) and benzodiamine (1.0 equiv) was added. The reaction was stirred for 16 h at room temperature and monitored by TLC. After full consumption of the starting material, the reaction mixture was concentrated and extracted with EtOAc. The organic layer was then washed with a saturated $NaHCO_3$ solution. The organic layer was dried with $MgSO_4$, concentrated *in vacuo,* and purified via normal phase chromatography.

(Step 2) The aminoazole (1.0 equiv) and $CuBr_2$ (1.5 equiv) were added to a round bottom flask and cooled to 0 °C and the flask was flushed with argon. Next, *tert*-butyl nitrite (1.5 equiv) was added drop wise to the flask. After consumption of starting material, as monitored by TLC, the mixture was diluted with H_2O (20 mL) and acidified with 12 N HCl (until pH<1 by indicator paper), then extracted with CH_2Cl_2 (3×20 mL). The combined organic layers were dried over $MgSO_4$ and concentrated *in vacuo* and purified via normal phase chromatography.

S-5

(Step 1) The **general procedure B** was followed using 4-bromobenzene-1,2-diamine (2.00 g, 16.9 mmol), cyanogen bromide (2.2 mL, 5 M in MeCN, 16.9 mmol), H_2O (30 mL) and MeOH (30 mL). Upon completion, the reaction was worked up (**general procedure B,** step 1) and purified via automated flash chromatography using MeOH in CH_2Cl_2 (0% to 40%) with product eluting at 11% on a 40 g silica column to afford 6-bromo-1H-benzoimidazol-2-amine in 80% yield (1.82 g, 8.59 mmol). **(Step 2)** Using 6-bromo-1H-benzoimidazol-2-amine (1.82 g, 8.59 mmol), *tert*-butyl nitrite (1.07 g, 12.9 mmol), $CuBr_2$ (2.87 g, 12.9 mmol) and 43.0 mL MeCN to afford **S-5** in 63% (1.50 g, 5.4 mmol). The substrate was purified via automated flash chromatography using EtOAc in hexanes (0% to 100%) with product eluting at 9% on a 40 g silica column.

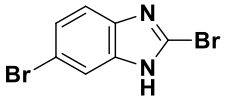

S-6

(Step 1) The **general procedure B** was followed using 4-chlorobenzene-1,2-diamine (3.00 g, 21.0 mmol), cyanogen bromide (4.2 mL, 5 M in MeCN, 21.0 mmol) H_2O (40 mL), and MeOH (40 mL). Upon completion, the reaction was worked up (**general procedure B,** step 1) and purified via automated flash chromatography using MeOH in CH_2Cl_2 (0% to 40%) with product eluting at 12% on a 40 g silica column to afford 6-chloro-1H-benzoimidazol-2-amine in 81% yield (2.86 g, 17.1 mmol). **(Step 2)** Using 6-chloro-

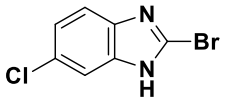

1H-benzoimidazol-2-amine (2.86 g, 17.1 mmol), *tert*-butyl nitrite (2.64 g, 25.6 mmol), $CuBr_2$ (5.73 g, 25.6 mmol) and MeCN (85.5 mL) to afford **S-6** in 38 % (1.51 g, 6.47 mmol). The substrate was purified via automated flash chromatography using EtOAc in hexanes (0% to 100%) with product eluting at 10% on a 40 g silica column.

Synthesis of alkenes (A-16, A-23, A-26)

Procedure C-1 for the synthesis of alkene A-16[102]

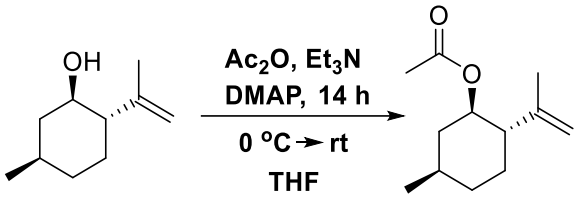

(1*R*, 2*S*, 5*R*)-5-methyl-2-(prop-1-en-2-yl)cyclohexan-1-ol (500 mg, 3.1 mmol) was combined with acetic anhydride (373 mg, 3.66 mmol), triethylamine (555 mg, 5.49 mmol), and DMAP (1.86 mg, 0.015 mmol) in THF (6.1 mL, 0.5 M) at 0 °C. The reaction mixture was maintained at 0 °C for 1 h and then was allowed to stir at room temperature overnight. TLC analysis (30% EtOAc in hexanes) revealed full consumption of the starting material. The solvent was removed by rotary evaporation, and the resulting material was diluted with EtOAc and washed with water and brine and dried over $MgSO_4$ resulting in a 92% (550 mg, 2.8 mmol) yield as a colorless oil.

Procedure C-2 for the synthesis of alkene A-23[103]

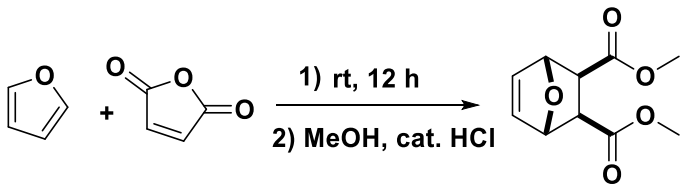

(Step 1) Furan (18 mL, 172 mmol) and maleic anhydride (5.10 g, 52.0 mmol) were added to a round bottom flask and the reaction mixture was stirred at room temperature. After 12 h, the slurry was filtered and the white solid was recrystallized using acetone, affording 49% yield of the cycloaddition adduct (4.2 g, 25.3 mmol). (Step 2) 40 mL of MeOH and catalytic amount of 12 N HCl (86 µL, 1.02 mmol) was added to cycloaddition adduct from the first step (1.71 g, 10.2 mmol). After 3 h, the mixture was concentrated and the substrate was purified via automated flash chromatography using EtOAc in hexanes (0% to 100%) with product eluting at 50% on a 40 g silica column, yielding 50% (1.09 g, 5.14 mmol) as a white solid.

Procedure C-3 for the synthesis of alkene A-26[104]

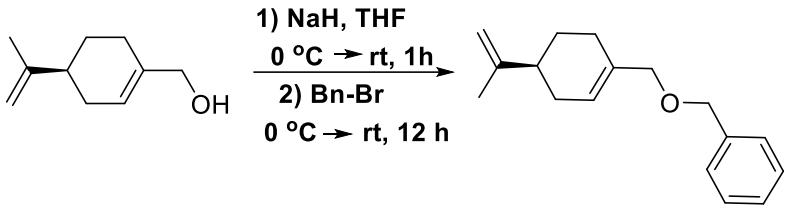

(*S*)-peryllylalchol (800 mg, 5.26 mmol) in THF (10 mL, 0.52 M) was added quickly to a vigorously stirring suspension of NaH (163 mg, 6.83 mmol) at 0 °C. After the reaction was stirred for 60 min at rt, the reaction mixture was cooled to 0 °C and Bn-Br (988 mg, 5.78 mmol) was added drop-wise via syringe (over 30 minutes) and allowed to warm to rt. After stirring for 12 h, the reaction was quenched with sat. NH_4Cl (70 mL) and water (40 mL) and was extracted with Et_2O (2 x 80 mL). The combined organic extracts were dried over $MgSO_4$ and concentrated under reduced pressure to yield 94% (1200 mg, 4.95 mmol) as a colorless oil.

Procedure D for the synthesis of amine[105]

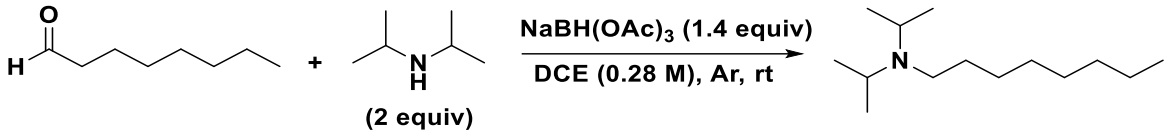

An oven dried round bottomed flask equipped with a magnetic stir bar and an Ar inlet was charged with diisopropylamine (788 mg, 7.8 mmol) and octyl aldehyde (500 mg, 3.9 mmol) in 1,2-dichloroethane (DCE) (14 mL, 0.28 M), then sodium triacetoxyborohydride ($NaBH(OAc)_3$) (1.2 g, 5.5 mmol) was added. The reaction was monitored by GC-MS. After the complete consumption of the aldehyde, the reaction mixture was quenched by adding saturated aqueous $NaHCO_3$ (15 mL) and extracted with ethyl acetate (3×20 mL). The combined organic layer was dried over $MgSO_4$. The solvent was evaporated to give the free base, yielding 92% (766 mg, 3.6 mmol) as colorless oil.

Emission Quenching Experiment

Emission intensities were recorded on Varian Carey Eclipse fluorescence spectrophotometer. All solutions of $Ir(ppy)_3$ in MeCN were excited at 370 nm and the emission intensities were observed at 520 nm. In this experiment, a 0.5 μM solution of $Ir(ppy)_3$ in MeCN was added to the appropriate amount of the quencher (Q) in a 1.0 cm quartz cuvette. After degassing each solution with a stream of argon for 15 minutes, the emission spectra were recorded.

Photocatalytic reductive coupling

General procedure E for the photocatalytic reductive alkylation of bromoazoles with alkenes **(limiting azole)**

A 5 mm NMR tube fitted with a NMR septum was charged with *fac*-tris(2-phenyl pyridinato-C^2, *N*) Iridium(III) ($Ir(ppy)_3$) (0.003 equiv, X mL of 0.75 mM stock solution of catalyst in MeCN,

where X mL of MeCN is used to make 0.25 M with respect to the 2-bromoazoles), 2-bromoazoles (1 equiv), alkene (5 equiv), tributylamine (3 equiv) and formic acid (3 equiv) and the reaction mixture was degassed via Ar bubbling for 10 min and then the exit needle and Ar line were removed and reaction tube was sealed with parafilm. The tube was placed in a light bath (description above) and the lower portion of the tube was submerged under the water bath which was maintained at 45 ^{o}C. The reaction was monitored by ^{1}H NMR or GC-MS. After the complete consumption of aryl bromide, CH_3CN was removed via rotovap and the residue was treated with water (2 mL) and extracted with CH_2Cl_2 (2 x 5 mL). The organic portions were combined and dried over anhydrous $MgSO_4$. The crude product was concentrated *in vacuo* and purified via normal phase chromatography.

General procedure F for the photocatalytic reductive alkylation of bromoazoles with alkenes **(limiting alkene)**

This procedure is identical to **general procedure E** except with following changes, where, 2-bromoazole (10 equiv), alkene (1 equiv), tributylamine (12 equiv) and formic acid (12 equiv) were used in MeCN (0.25 M with respect to 2-bromoazole).

General procedure G for the photocatalytic reductive alkylation of bromoazoles with alkenes **(Reduction minimizing conditions)**

This procedure is identical to **general procedure E** except with following changes, where Iridium(+1)(4,4´-dimethoxy-2,2´bipyridine)bis[4-*tert*-butyl-2-(4-*tert*-butylpyridinal)phenyl]**(cat-1)** (0.003 equiv, X mL of 0.75 mM stock solution of catalyst in MeCN, where X mL of MeCN is used to make 0.25 M with respect to the 2-bromoazoles) and 2-bromoazole (1 equiv), alkene (5 equiv), *N*,*N*-diisopropyloctan-1-amine (3 equiv) and formic acid (3 equiv) were used.

General procedure H for the photocatalytic reductive alkylation for heteroaromatic bromide with alkene

This procedure is identical to **general procedure E** except with following changes, where *fac*-tris(2-phenyl pyridinato-C^2, *N*) Iridium(III) ($Ir(ppy)_3$) (0.003 equiv, X mL of 0.65 mM stock solution of catalyst in MeCN, where X mL of MeCN is used to make 0.25 M with respect to heteroaromatic bromide), heteroaromatic bromide (1 equiv), alkene (5 equiv), *N*-ethyl-*N*-isopropylpropan-2-amine (DIPEA) (2 equiv) were used. The reaction was monitored by NMR or GCMS. After the complete consumption of heteroaromatic bromide, CH_3CN was removed via rotovap and the residue was treated with saturated aqueous $NaHCO_3$ solution (5 mL) and extracted with CH_2Cl_2 (2 x 5 mL). The organic portions were combined and dried over anhydrous $MgSO_4$. The crude product was concentrated *in vacuo* and purified via normal phase chromatography.

1a 2-(tetrahydro-2H-pyran-3-yl)thiazole

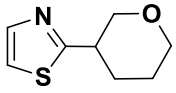

The **general procedure E** was followed using 2-bromothiazole (15 mg, 0.09 mmol), 3,4-dihydro-2H-pyran (38 mg, 0.46 mmol), tributylamine (51 mg, 0.27 mmol), formic acid (13 mg, 0.27 mmol) and 0.36 mL of stock solution of $Ir(ppy)_3$ in MeCN was used to afford **1a** in 65% yield (10 mg, 0.059 mmol), rr 6:1 (based on crude ^{1}H NMR) as an oil. After the completion of the reaction, 12 h, the substrate was purified via automated flash chromatography using EtOAc in hexanes (0% to 100%) with product eluting at 10% on a 12 g silica column. ^{1}H NMR (400 MHz, $CDCl_3$) δ 7.72 (d, J = 3.3 Hz, 1H), 7.23 (d, J = 3.3 Hz, 1H), 4.19 (ddd, J = 11.2, 4.1, 1.8 Hz, 1H), 3.96 (dt, J = 12.3, 3.4 Hz, 1H), 3.59 (dd, J = 11.2, 9.8 Hz, 1H), 3.56–3.46 (m, 1H), 3.38–3.27 (m, 1H), 2.30–2.21 (m, 1H), 1.96–1.83 (m, 1H), 1.83–1.70 (m, 2H). ^{13}C NMR (101 MHz, $CDCl_3$) δ 171.3, 142.2, 117.8, 72.1, 68.0, 40.6, 30.0, 25.1. FT-IR

(neat) cm^{-1} 2933, 2848, 1434, 1085. HRMS (ESI) $C_8H_{11}NOS$ calcd. $[M+H]^+$ 170.0635 observed 170.0629.

2a 4-(tert-butyl)-2-(tetrahydro-2H-pyran-3-yl)thiazole

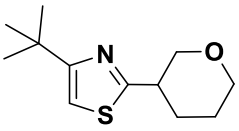

The **general procedure E** was followed using 2-bromo-4-(tert-butyl)thiazole (25 mg, 0.11 mmol), 3,4-dihydro-2H-pyran (46 mg, 0.55 mmol), tributylamine (63 mg, 0.34 mmol), formic acid (16 mg, 0.34 mmol) and 0.45 mL of stock solution of $Ir(ppy)_3$ in MeCN was used to afford **2a** in 71% yield (18 mg, 0.079 mmol), rr 9:1 (based on crude ^1H NMR) and isolated as rr 10:1 mixture as a yellow oil. After the completion of the reaction, 14 h, the substrate was purified via automated flash chromatography using EtOAc in hexanes (0% to 100%) with product eluting at 12% on a 4 g silica column. ^1H NMR (400 MHz, $CDCl_3$) δ 6.74 (s, 1H), 4.17 (ddd, J = 11.1, 4.0, 1.7 Hz, 1H), 3.94 (dt, J = 11.0, 3.8 Hz, 1H), 3.58–3.43 (m, 2H), 3.35–3.23 (m, 1H), 2.29–2.18 (m, 1H), 1.90–1.66 (m, 3H), 1.31 (s, 9H). ^{13}C NMR (101 MHz, $CDCl_3$) δ 170.2, 166.2, 109.0, 72.4, 68.2, 41.1, 34.7, 30.3, 30.0, 25.4. FT-IR (neat) cm^{-1} 2957, 2866, 1513, 1150. HRMS (ESI) $C_{12}H_{19}NOS$ calcd. $[M+H]^+$ 226.1261 observed 226.1253. **Note** - The regioisomer is marked in all ^1H NMR and ^{13}C NMR spectra as ◍.

3a 4-phenyl-2-(tetrahydro-2H-pyran-3-yl)thiazole

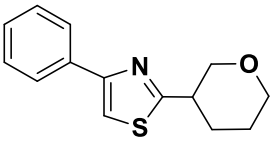

The **general procedure E** was followed using 2-bromo-4-phenylthiazole (25 mg, 0.10 mmol), 3,4-dihydro-2H-pyran (44 mg, 0.52 mmol), tributylamine (58 mg, 0.31 mmol), formic acid (14 mg, 0.31 mmol), and 0.40 mL of stock solution of $Ir(ppy)_3$ in MeCN was used to afford **3a** in 43% yield (10 mg, 0.043 mmol), rr 9:1 (based on crude **^{1}H** NMR) as yellow oil. After the completion of the reaction, 13 h, the substrate was purified via automated flash chromatography using EtOAc in hexanes (0% to 100%) with product eluting at 3% on a 12 g silica column. ^1H NMR (400 MHz,

$CDCl_3$) δ 7.90 (d, J = 1.4 Hz, 1H), 7.88 (t, J = 1.3 Hz, 1H), 7.42 (t, J = 7.5 Hz, 2H), 7.36 (s, 1H), 7.32 (t, J = 7.4 Hz, 1H), 4.25 (ddd, J = 11.2, 4.1, 1.7 Hz, 1H), 3.97 (dt, J = 11.1, 3.1 Hz, 1H), 3.65 (dd, J = 11.1, 9.8 Hz, 1H), 3.58–3.50 (m, 1H), 3.43–3.32 (m, 1H), 2.35–2.24 (m, 1H), 2.01–1.88 (m, 1H), 1.85–1.73 (m, 2H). ^{13}C NMR (101 MHz, $CDCl_3$) δ 171.3, 155.1, 134.6, 128.7, 128.0, 126.4, 111.8, 72.3, 68.2, 41.1, 30.2, 25.3. FT-IR (neat) cm^{-1} 2925, 2859, 1492, 1090. HRMS (ESI) $C_{14}H_{15}NOS$ calcd. $[M+H]^+$ 246.0948 observed 246.0935.

4a ethyl 2-(tetrahydro-2H-pyran-3-yl)thiazole-4-carboxylate

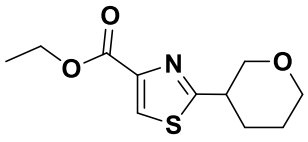

The **general procedure E** was followed using ethyl 2-bromothiazole-4-carboxylate (25 mg, 0.11 mmol), 3,4-dihydro-2H-pyran (44 mg, 0.53 mmol), tributylamine (58 mg, 0.32 mmol), formic acid (14 mg, 0.32 mmol), and 0.42 mL of stock solution of $Ir(ppy)_3$ in MeCN was used to afford **4a** in 82% yield (22 mg, 0.090 mmol), rr 4:1(based on crude ^1H NMR) and isolated as mix of rr 5:1 as yellow oil. After the completion of the reaction, 14 h, the substrate was purified via automated flash chromatography using EtOAc in hexanes (0% to 100%) with product eluting at 16% on a 12 g silica column. **Note** - Another regioisomer is marked as ‖ in spectra. ^1H NMR (400 MHz, $CDCl_3$) δ 8.08 (s, 1H), 4.42 (q, *J* = 7.1 Hz, 2H), 4.16 (ddd, *J* = 11.5, 4.0, 1.7 Hz, 1H), 3.92 (dt, *J* = 11.4, 4.0 Hz, 1H), 3.63 (dd, *J* = 11.2, 9.0 Hz, 1H), 3.60–3.50 (m, 1H), 3.47–3.35 (m, 1H), 2.24 (m, 1H), 1.98–1.84 (m, 1H), 1.75 (m, 2H), 1.40 (t, *J* = 7.1 Hz, 3H). ^{13}C NMR (101 MHz, $CDCl_3$) δ 172.4, 161.4, 146.9, 126.7, 71.9, 68.2, 61.5, 41.0, 30.0, 24.8, 14.4. FT-IR (neat) cm^{-1} 2933, 2851, 1735, 1722, 1100. HRMS (ESI) $C_{11}H_{15}NO_3S$ calcd. $[M+H]^+$ 242.0845 observed 242.0839.

5a 4-bromo-2-(tetrahydro-2H-pyran-3-yl)thiazole

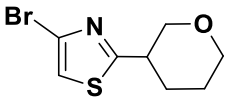

The **general procedure E** was followed using 2,4-dibromothiazole (25 mg, 0.10 mmol), 3,4-dihydro-2H-pyran (44 mg, 0.52 mmol), tributylamine (57 mg, 0.31 mmol), formic acid (14 mg, 0.31 mmol), and 0.40 mL of stock solution of $Ir(ppy)_3$ in MeCN was used to afford **5a** in 82% yield (19 mg, 0.082 mmol), rr 10:1 (based on crude ^{1}H NMR) as yellow oil. After the completion of the reaction, 12 h, the substrate was purified via automated flash chromatography using EtOAc in hexanes (0% to 100%) with product eluting at 2% on a 4 g silica column. ^{1}H NMR (400 MHz, $CDCl_3$) δ 7.12 (s, 1H), 4.14 (ddd, J = 11.2, 4.1, 1.7 Hz, 1H), 3.92 (dt, J = 11.3, 3.3 Hz, 1H), 3.59 (dd, J = 11.2, 9.4 Hz, 1H), 3.56–3.47 (m, 1H), 3.34–3.25 (m, 1H), 2.25–2.16 (m, 1H), 1.95–1.81 (m, 1H), 1.80–1.69 (m, 2H). ^{13}C NMR (101 MHz, $CDCl_3$) δ 172.6, 124.6, 115.9, 71.9, 68.1, 40.9, 29.8, 24.9. FT-IR (neat) cm^{-1} 2933, 2841, 1470, 1053, 670. HRMS (ESI) $C_8H_{10}BrNOS$ calcd. $[M+Na]^+$ 269.9559 observed 269.9551.

6a 5-bromo-4-methyl-2-(tetrahydro-2H-pyran-3-yl)thiazole

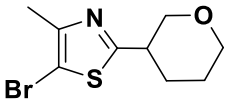

The **general procedure E** was followed using 2,5-dibromo-4-methylthiazole (25 mg, 0.097 mmol), 3,4-dihydro-2H-pyran (41 mg, 0.49 mmol), tributylamine (54 mg, 0.29 mmol), formic acid (13 mg, 0.29 mmol), and 0.40 mL of stock solution of $Ir(ppy)_3$ in MeCN was used to afford **6a** in 75% yield (19 mg, 0.073 mmol, including both isomers), rr 10:1 (based on crude ^{1}H NMR) as an oil. After the completion of the reaction, 12 h, the substrate was purified via automated flash chromatography using EtOAc in hexanes (0% to 100%) with product eluting at 12% on a 12 g silica column. ^{1}H NMR (400 MHz, $CDCl_3$) δ 4.10 (dd, J = 11.8, 4.2 Hz, 1H), 3.91 (dt, J = 11.6, 3.9 Hz, 1H), 3.62–3.45 (m, 2H), 3.21 (td, J = 9.0, 4.4 Hz, 1H), 2.36 (s, 3H), 2.24–2.12 (m, 1H), 1.90–1.79 (m, 1H), 1.78–1.68 (m, 2H). ^{13}C NMR (101 MHz, $CDCl_3$) δ 170.6, 151.0, 103.0, 71.9, 68.2, 41.3, 29.7, 25.0, 15.6. FT-IR (neat) cm^{-1} 2927, 2849, 1541, 1103, 695, HRMS (ESI) $C_9H_{12}BrNOS$ calcd. $[M+H]^+$ 261.9896 observed 261.9891.

7a 2-(tetrahydro-2H-pyran-3-yl)benzo[d]thiazole

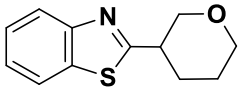

The **general procedure E** was followed using 2-benzobromothiazole (25 mg, 0.12 mmol), 3,4-dihydro-2H-pyran (49 mg, 0.58 mmol), tributylamine (65 mg, 0.35 mmol), formic acid (16 mg, 0.39 mmol), 0.48 mL of stock solution of $Ir(ppy)_3$ in MeCN was used to afford **7a** in 78% yield (20 mg, 0.093 mmol), rr 7:1 (based on crude ^1H NMR) as yellow oil. After the completion of the reaction, 12 h, the substrate was purified via automated flash chromatography using EtOAc in hexanes (0% to 100%) with product eluting at 11% on a 12 g silica column. ^1H NMR (400 MHz, $CDCl_3$) δ 7.99 (d, J = 8.0 Hz, 1H), 7.86 (d, J = 7.9 Hz, 1H), 7.46 (t. J = 8.1 Hz, 1H), 7.36 (t, J = 8.2 Hz, 1H), 4.30–4.22 (m, 1H), 4.02–3.94 (m, 1H), 3.72 (dd, J = 11.2, 9.7 Hz, 1H), 3.60–3.51 (m, 1H), 3.45–3.36 (m, 1H), 2.34-2.31 (m, 1H), 2.06–1.92 (m, 1H), 1.80 (m, 2H). ^{13}C NMR (101 MHz, $CDCl_3$) δ 172.1, 153.1, 134.5, 126.0, 124.9, 122.7, 121.6, 71.8, 68.2, 41.7, 30.0, 25.2. FT-IR (neat) cm^{-1} 2939, 2839, 1513, 1095. HRMS (ESI) $C_{12}H_{13}NOS$ calcd. $[M+H]^+$ 220.0791 observed 220.0787.

8a 4-chloro-2-(tetrahydro-2H-pyran-3-yl)benzo[d]thiazole

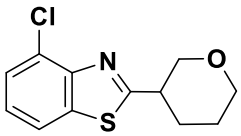

The **general procedure E** was followed using 2-bromo-4-chlorobenzo[d]thiazole (25 mg, 0.10 mmol), 3,4-dihydro-2H-pyran (42 mg, 0.51 mmol), tributylamine (56 mg, 0.30 mmol), formic acid (14 mg, 0.30 mmol), and 0.40 mL of stock solution of $Ir(ppy)_3$ of MeCN was used to afford **8a** in 60% yield (15 mg, 0.060 mmol), rr 3:1 (based on crude ^1H NMR) as an oil. After the completion of the reaction, 24 h, the substrate was purified via automated flash chromatography using EtOAc in hexanes (0% to 100%) with product eluting at 13% on a 12 g silica column. ^1H NMR (400 MHz, $CDCl_3$) δ 7.76 (d, J = 8.0 Hz, 1H), 7.48 (d, J = 7.8 Hz, 1H), 7.29 (t, J = 8.0 Hz, 1H), 4.25 (ddd, J = 11.5, 4.2, 1.8 Hz, 1H), 3.96 (dt, J = 11.1, 3.9 Hz, 1H), 3.72 (dd, J = 11.3, 9.3 Hz, 1H), 3.66–3.53

(m, 1H), 3.57–3.44 (m, 1H), 2.38–2.26 (m, 1H), 2.08–1.91 (m, 1H), 1.86–1.72 (m, 2H). ^{13}C NMR (101 MHz, $CDCl_3$) δ 173.4, 150.0, 136.1, 127.6, 126.3, 125.4, 120.1, 71.8, 68.2, 41.8, 30.0, 25.0. FT-IR (neat) cm^{-1} 2941, 2842, 1524, 1117, 827. HRMS (ESI) $C_{12}H_{12}ClNOS$ calcd. $[M+H]^+$ 254.0401 observed 254.0394.

9a 4,6-difluoro-2-(tetrahydro-2H-pyran-3-yl)benzo[d]thiazole

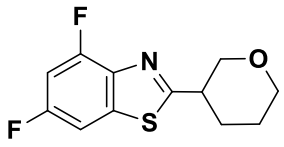

The **general procedure E** was followed using 2-bromo-4,6-difluorobenzo[d]thiazole (25 mg, 0.10 mmol), 3,4-dihydro-2H-pyran (42 mg, 0.50 mmol), tributylamine (55 mg, 0.30 mmol), formic acid (14 mg, 0.30 mmol), and 0.40 mL of stock solution of $Ir(ppy)_3$ of MeCN was used to afford **9a** in 78% yield (20 mg, 0.078 mmol), rr 5:1 (based on crude ^{1}H NMR) as an oil. After the completion of the reaction, 18 h, the substrate was purified via automated flash chromatography using EtOAc in hexanes (0% to 100%) with product eluting at 11% on a 12 g silica column. ^{1}H NMR (400 MHz, $CDCl_3$) δ 7.35 (d, J = 7.5 Hz, 1H), 6.98 (t, J = 10.7 Hz, 1H), 4.23 (ddd, J = 11.7, 4.0, 1.8 Hz, 1H), 3.96 (dt, J = 11.5, 4.0 Hz, 1H), 3.77–3.70 (m, 1H), 3.63–3.53 (m, 1H), 3.48–3.37 (m, 1H), 2.35–2.24 (m, 1H), 2.06–1.94 (m, 1H), 1.84–1.73 (m, 2H). ^{13}C NMR (101 MHz, $CDCl_3$) δ 172.8, 160.4 (dd, J = 247.3, 10.4 Hz), 155.4 (dd, J = 259.0, 13.4 Hz), 139.2 (dd, J = 13.3, 2.6 Hz), 137.9 (dd, J = 12.7, 5.0 Hz), 104.1 (dd, J = 26.4, 4.7 Hz), 102.5 (dd, J = 28.3, 21.9 Hz). 72.0, 68.7, 42.1, 30.3, 25.4. ^{19}F NMR (376 MHz, $CDCl_3$) δ -113.0 (td, J = 8.4, 5.5 Hz), -117.7–118.2 (m). FT-IR (neat) cm^{-1} 2927, 2852, 1612, 1438, 1100. HRMS (ESI) calcd. $C_{12}H_{11}F_2NOS$ $[M+H]^+$ 256.0603 observed 256.0592

10a 2-(tetrahydro-2H-pyran-3-yl)-1H-benzo[d]imidazole

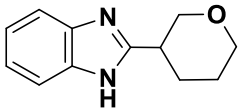

The **general procedure E** was followed using 2-bromo-1H-benzo[d]imidazole (25 mg, 0.13 mmol), 3,4-dihydro-2H-pyran (53 mg, 0.63 mmol), tributylamine (70 mg, 0.38 mmol), formic acid (17 mg, 0.38 mmol), and 0.50 mL of stock solution of $Ir(ppy)_3$ of MeCN was used to afford **10a** in 86% yield (22 mg, 0.108 mmol), rr 4:1 (based on crude ^1H NMR) as white solid. m.pt 235-238 ^oC. After the completion of the reaction, 24 h, the substrate was purified via automated flash chromatography using EtOAc in hexanes (column was buffered with 1% Et_3N in hexane before running) (0% to 100%) with product eluting at 11% on a 24 g silica column. ^1H NMR (400 MHz, Methanol-d_4) δ 7.53–7.46 (m, 2H), 7.18 (dt, J = 6.1, 3.7 Hz, 2H), 4.12 (ddd, J = 11.6, 4.2, 1.8 Hz, 1H), 3.93 (dt, J = 11.3, 3.8 Hz, 1H), 3.69 (t, J = 10.6 Hz, 1H), 3.54 (dt, J = 11.4, 6.8 Hz, 1H), 3.34–3.27 (m, 1H), 3.17 (tt, J = 10.3, 4.1 Hz, 1H), 2.25–2.16 (m, 1H), 2.05–1.92 (m, 1H), 1.75 (dp, J = 7.7, 4.0 Hz, 2H). ^{13}C NMR (101 MHz, CD_3OD) δ 155.2, 122.0, 78.2, 77.9, 77.5, 76.8, 70.5, 67.8, 37.0, 28.0, 25.0. FT-IR (neat) cm^{-1} 2931, 2858, 1454, 1109. HRMS (ESI) calcd. $C_{12}H_{14}N_2O$ $[M+H]^+$ 203.1179 observed 203.1173

12a 3-methyl-2-(thiazol-2-yl)butan-1-ol

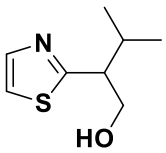

The **general procedure E** was followed using 2-bromothiazole (50 mg, 0.30 mmol) (E)-3-methylbut-1-en-1-ol (129 mg, 1.50 mmol), tributylamine (167 mg, 0.90 mmol), formic acid (41 mg, 0.90 mmol), and 1.2 mL of stock solution of $Ir(ppy)_3$ of MeCN was used to afford **12a** in 43% yield (22 mg, 0.13 mmol) rr >20:1 (based on crude ^1H NMR) as yellow oil. After the completion of the reaction, 12 h, the substrate was purified via automated flash chromatography using EtOAc in hexanes (column was buffered 1% Et_3N in hexanes before running) (0% to 100%) with product eluting at 26% on a 12 g silica column. ^1H NMR (400 MHz, $CDCl_3$) δ 7.73 (d, J = 3.3 Hz, 1H), 7.23 (d, J = 3.4 Hz, 1H), 4.05 (dt, J = 11.1, 6.7 Hz, 1H), 3.92 (ddd, J = 11.2, 5.5, 3.4 Hz, 1H), 3.26–3.16 (m, 1H), 2.96 (td, J = 7.0, 3.4 Hz,

1H), 2.23 (h, J = 6.9 Hz, 1H), 1.04 (d, J = 6.8 Hz, 3H), 0.91 (d, J = 6.8 Hz, 3H). ^{13}C NMR (101 MHz, $CDCl_3$) δ 172.8, 142.1, 117.9, 63.2, 52.0, 30.4, 20.9, 20.2. FT-IR (neat) cm^{-1} 3342, 2962, 2872, 1512 HRMS (ESI) $C_8H_{13}NOS$ calcd. $[M+H]^+$ 172.0791 observed 172.0788.

13a 2-(5-((tetrahydro-2H-pyran-2-yl)oxy)pentyl)thiazole

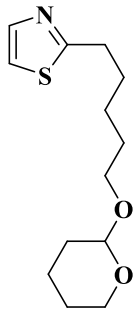

The **general procedure E** was followed using 2-bromothiazole (25 mg, 0.15 mmol), 2-(pent-4-en-1-yloxy)tetrahydro-2H-pyran (130 mg, 0.76 mmol), tributylamine (85 mg, 0.46 mmol), formic acid (21 mg, 0.46 mmol), and 0.60 mL of stock solution of $Ir(ppy)_3$ in MeCN was used to afford **13a** in 70% yield (27 mg, 0.11 mmol) rr>20:1 (based on crude ^{1}H NMR) as yellow oil. After the completion of the reaction, 12 h, the substrate was purified via automated flash chromatography using EtOAc in hexanes (column was buffered with 1% Et_3N in hexane before running) (0% to 100%) with product eluting at 4% on a 12 g silica column. ^{1}H NMR (400 MHz, $CDCl_3$) δ 7.67 (d, *J* = 3.3 Hz, 1H), 7.18 (d, *J* = 3.3 Hz, 1H), 4.56 (dd, *J* = 4.6, 2.6 Hz, 1H), 3.85 (ddd, *J* = 11.0, 7.5, 3.4 Hz, 1H), 3.74 (dt, *J* = 9.6, 6.7 Hz, 1H), 3.54–3.44 (m, 1H), 3.39 (dt, *J* = 9.6, 6.5 Hz, 1H), 3.04 (t, *J* = 7.8 Hz, 2H), 1.90–1.77 (m, 3H), 1.72–1.61 (m, 3H), 1.59–1.46 (m, 6H). ^{13}C NMR (101 MHz, $CDCl_3$) δ 171.4, 142.0, 118.0, 98.9, 67.3, 62.4, 33.2, 30.8, 29.9, 29.4, 25.8, 25.5, 19.7. FT-IR (neat) cm^{-1} 2938, 2865, 1507, 1032. HRMS (ESI) $C_{13}H_{21}NO_2S$ calcd. $[M+Na]^+$ 278.1185 observed 278.1183.

14a 2-(2-phenylcyclohexyl)thiazole

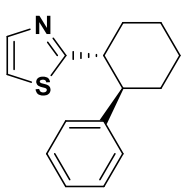

The **general procedure E** was followed using 2-bromothiazole (25 mg, 0.15 mmol), 2,3,4,5-tetrahydro-1,1'-biphenyl (120 mg, 0.76 mmol), tributylamine (85 mg, 0.46 mmol), formic acid (21 mg, 0.46 mmol) and 0.60 mL of stock solution of $Ir(ppy)_3$ in MeCN solution was used to afford **14a** in 74% yield (27 mg, 0.11 mmol),

rr>20:1 (based on crude ^{1}H NMR), dr>20:1 (based on crude ^{1}H NMR) as colorless oil. After the completion of the reaction, 14 h, the substrate was purified via automated flash chromatography using EtOAc in hexanes (0% to 100%) with product eluting at 0.5% on a 12 g silica column. ^{1}H NMR (400 MHz, $CDCl_3$) δ 7.77 (t, J = 3.6 Hz, 1H), 7.40 (d, J = 3.5 Hz, 1H), 7.31 (d, J = 6.7 Hz, 1H), 7.28–7.21 (m, 1H), 7.19–7.12 (m, 3H), 3.97–3.86 (m, 1H), 3.31 (dt, J = 11.5, 4.1 Hz, 1H), 2.49–2.37 (m, 1H), 2.35–2.27 (m, 1H), 2.25–2.07 (m, 3H), 2.04–1.94 (m, 1H), 1.85–1.76 (m, 1H), 1.74–1.62 (m, 1H). ^{13}C NMR (101 MHz, $CDCl_3$) δ 171.7, 144.1, 141.5, 128.0, 127.8, 126.0, 117.6, 46.4, 45.3, 31.3, 26.7, 25.9, 21.8. FT-IR (neat) cm^{-1} 2925, 2859, 1681, 1444. HRMS (ESI) $C_{15}H_{17}NS$ calcd. $[M+H]^+$ 244.1154 observed 244.1151.

15a 2-(tetrahydro-2H-pyran-3-yl)benzo[d]thiazole

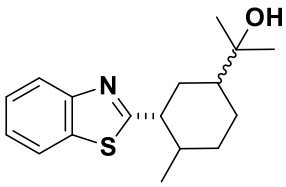

The **general procedure E** was followed using 2-benzobromothiazole (25 mg, 0.12 mmol), 2-(4-methylcyclohex-3-en-1-yl)propan-2-ol (90 mg, 0.58 mmol), tributylamine (65 mg, 0.35 mmol), formic acid (16 mg, 0.35 mmol) and 0.50 mL of stock solution of $Ir(ppy)_3$ in MeCN was used to afford **15a** in 73% yield (25 mg, 0.087 mmol, including both diastereomers), rr >20:1 (based on crude ^{1}H NMR), dr 1.3:1 (based on crude ^{1}H NMR) and isolated as dr 1.7:1 as pale oil. After the completion of the reaction, 12 h, the substrate was purified via automated flash chromatography using EtOAc in hexanes (0% to 100%) with product eluting at 10% (diastereomer **a**) and 11% (diastereomer **b**) on a 24 g silica column. Diastereomer **a**- ^{1}H NMR (400 MHz, $CDCl_3$), δ 8.00 (d, *J* = 8.1 Hz, 1H), 7.84 (d, *J* = 7.8 Hz, 1H), 7.44 (t, *J* = 7.6 Hz, 1H), 7.34 (t, *J* = 7.5 Hz, 1H), 3.66 (dq, *J* = 4.6, 2.3 Hz, 1H), 2.14 (dq, *J* = 13.3, 2.7 Hz, 1H), 2.06–1.95 (m, 2H), 1.89 (ddt, *J* = 10.6, 6.4, 3.7 Hz, 2H), 1.64 (td, *J* = 13.0, 5.2 Hz, 3H), 1.43 (d, *J* = 2.4 Hz, 1H), 1.17 (s, 3H), 1.15 (s, 3H), 0.92 (d, *J* = 6.2 Hz, 3H). ^{13}C NMR (101 MHz, $CDCl_3$) δ 172.7, 152.9, 134.9, 125.7, 124.6, 122.8, 121.2, 72.7, 45.6, 42.9, 35.2, 32.6, 29.9, 27.2, 27.2, 27.0, 19.9. Diastereomer **b** - ^{1}H NMR (400 MHz, $CDCl_3$,)

δ 7.98 (d, J = 8.0 Hz, 1H), 7.85 (d, J = 7.9 Hz, 1H), 7.44 (t, 1H), 7.34 (t, J = 8.1 Hz, 1H), 2.80 (td, J = 11.2, 3.4 Hz, 1H), 2.39–2.11 (m, 2H), 1.95 (ddt, J = 17.6, 11.8, 2.7 Hz, 2H), 1.88–1.73 (m, 2H), 1.53–1.43 (m, 3H), 1.19 (s, 6H), 0.87 (d, J = 6.4 Hz, 3H). ^{13}C NMR (101 MHz, $CDCl_3$) δ 176.6, 153.0, 134.6, 125.8, 124.6, 122.6, 121.6, 72.6, 51.0, 48.8, 38.0, 35.8, 35.2, 27.2, 27.1, 26.9, 20.3. FT-IR (neat) cm^{-1} 3546, 2959, 2857, 1504. HRMS (ESI) $C_{17}H_{23}NOS$ calcd. $[M+H]^+$ 290.1573 observed 290.1569. **Note** - The diastereomer is marked in all ^{1}H NMR and ^{13}C NMR spectra.as ◍. The stereochemical assignment is based on detailed analysis of coupling constants.

16a (1R,2S,5R)-2-(1-(benzo[d]thiazol-2-yl)propan-2-yl)-5-methylcyclohexyl acetate

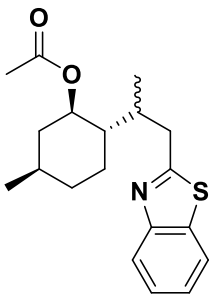

The **general procedure E** was followed using 2-benzobromothiazole (25 mg, 0.12 mmol), (1R,2S,5R)-5-methyl-2-(prop-1-en-2-yl)cyclohexyl acetate (110 mg, 0.58 mmol), tributylamine (65 mg, 0.35 mmol), formic acid (16 mg, 0.35 mmol), and 0.45 mL of stock solution of $Ir(ppy)_3$ in MeCN was used to afford **16a** in 70% yield (28 mg, 0.084 mmol), rr >20:1 (based on crude ^{1}H NMR), dr 1.25:1 (based on crude ^{1}H NMR) and isolated as dr 3:1 mixture as yellow oil. After the completion of the reaction, 22 h, the substrate was purified via automated flash chromatography using EtOAc in hexanes (0% to 100%) with product eluting at 12% on a 40 g silica column. ^{1}H NMR [mix of diastereomers] (400 MHz, $CDCl_3$) δ 7.95 (d, *J* = 8.3 Hz, 1H), 7.83 (d, *J* = 8.1 Hz, 1H), 7.44 (t, *J* = 7.7 Hz, 1H), 7.34 (t, *J* = 7.6 Hz, 1H), 4.83 (td, *J* = 10.9, 4.1 Hz, 1H), 3.20 (dd, *J* = 14.2, 3.7 Hz, 1H), 2.82 (dd, *J* = 14.0, 10.9 Hz, 1H), 2.44–2.21 (m, 2H), 2.14 (s, 3H), 1.77 (dd, *J* = 32.2, 14.6 Hz, 3H), 1.67–1.47 (m, 4H), 0.98 (d, *J* = 6.9 Hz, 3H), 0.92 (d, *J* = 6.6 Hz, 3H). ^{13}C NMR (101 MHz, $CDCl_3$) δ 171.9, 170.5, 153.0, 135.2, 125.6, 124.4, 122.4, 121.3, 73.4, 46.7, 40.7, 37.2, 34.5, 34.1, 31.2, 26.7, 25.5, 21.7, 16.9. FT-IR (neat) cm^{-1} 2922, 2841,1732, 1520. HRMS (ESI) calcd. $C_{19}H_{25}NO_2S$ $[M+H]^+$ 332.1679 observed 332.1673. **Note** - The diastereomer is marked in ^{1}H NMR and ^{13}C NMR spectra as ◍.

17a 2-((1S,2S,4R)-bicyclo[2.2.1]heptan-2-yl)-4-(tert-butyl)thiazole

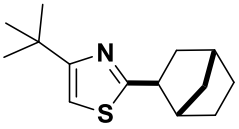

The **general procedure E** was followed using 2-bromo-4-(tert-butyl)thiazole (25 mg, 0.11 mmol), norbornene (53 mg, 0.57 mmol), tributylamine (63 mg, 0.34 mmol), formic acid (16 mg, 0.34 mmol), and 0.45 mL of stock solution of $Ir(ppy)_3$ in MeCN was used to afford **17a** in 68% yield (18 mg, 0.075 mmol), rr>20:1 (based on crude ^1H NMR), dr>20:1 (based on crude ^1H NMR) as colorless oil. After the completion of the reaction, 15 h, the substrate was purified via automated flash chromatography using EtOAc in hexanes (0% to 100%) with product eluting at 2% on a 24 g silica column. ^1H NMR (400 MHz,$CDCl_3$) δ 6.69 (s, 1H), 3.08 (dd, *J* = 8.6, 5.3 Hz, 1H), 2.46 (s, 1H), 2.36 (s, 1H), 2.01–1.90 (m, 1H), 1.86–1.74 (m, 1H), 1.69–1.50 (m, 5H), 1.40 (tt, *J* = 9.1, 2.8 Hz, 1H), 1.32 (s, 9H). ^{13}C NMR (101 MHz, $CDCl_3$) δ 174.0, 164.1, 106.6, 44.5, 42.5, 37.1, 34.6, 34.2, 32.8, 28.1, 27.8, 26.9. FT-IR (neat) cm^{-1} 2928, 2851. HRMS (ESI) $C_{14}H_{21}NS$ calcd. $[M+H]^+$ 236.1467 observed 236.1460. Stereochemistry is assigned analogy to literature.[9]

18a 2-(((1S,4R)-3,3-dimethylbicyclo[2.2.1]heptan-2-yl)methyl)thiazole

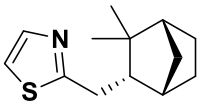

The **general procedure F** was followed using 2-bromothiazole (288 mg, 1.8 mmol) camphene (24 mg , 0.18 mmol), tributylamine (400 mg, 2.2 mmol), formic acid (101 mg, 2.2 mmol), and 0.72 mL of stock solution of $Ir(ppy)_3$ in MeCN was used to afford **18a** in 85% yield (34 mg, 0.15 mmol), rr>20:1 (based on crude ^1H NMR), 4:1 [(reduced:oxidized), based on crude ^1H NMR], dr 5:1 (based on crude ^1H NMR) and isolated as mixture of diastereomers with dr 7:1 and 7:1 (reduced : oxidized) mixture, as a pale oil. After the completion of the reaction, 20 h, the substrate was purified via automated flash chromatography using EtOAc in hexanes (0% to 100%) with product eluting at 8% on a 24 g silica column. ^1H NMR [mix of diastereomers and oxidized product] (400 MHz,$CDCl_3$) δ 7.65 (d, J = 3.3 Hz, 1H),

7.16 (d, J = 3.3 Hz, 1H), 3.08–2.92 (m, 2H), 2.07 (s, 1H), 2.01–1.91 (m, 1H), 1.78 (s, 1H), 1.63 (t, J = 9.8 Hz, 1H), 1.54–1.44 (m, 1H), 1.33–1.26 (m, 2H), 1.15 (dd, J = 13.2, 7.0 Hz, 2H), 1.00 (s, 3H), 0.88 (s, 3H). ^{13}C NMR (101 MHz, $CDCl_3$) δ 171.6, 142.0, 117.8, 51.1, 49.2, 41.2, 37.4, 36.9, 32.2, 30.8, 24.6, 21.6, 20.3. FT-IR (neat) cm^{-1} 2904, 2872, 1460. HRMS (ESI) $C_{13}H_{19}NS$ calcd. $[M+H]^+$ 222.1311 observed 222.1318. Diastereoselectivity is based on detailed analysis of coupling constants. **Note** – The diastereomer and oxidized product is marked in the ^{1}H NMR and ^{13}C NMR spectra as ○ and ▭.

19a 2-(bicyclo[2.2.1]heptan-2-ylmethyl)-1H-benzo[d]imidazole

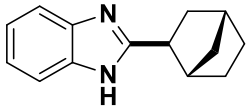

The **general procedure E** was followed using 2-bromo-1H-benzo[d]imidazole (25 mg, 0.13 mmol), norbornene (60 mg, 0.63 mmol), tributylamine (70 mg, 0.38 mmol), formic acid (17.3 mg, 0.38 mmol), and 0.50 mL of stock solution of $Ir(ppy)_3$ in MeCN was used to afford **19a** in 90% yield (25 mg, 0.12 mmol), rr>20:1 (based on crude ^{1}H NMR), dr>20:1 (based on crude ^{1}H NMR) as white solid, m.pt 242–245 °C. After the completion of the reaction, 24 h, the substrate was purified via automated flash chromatography using EtOAc in hexanes (column was buffered with 1% Et_3N in hexane before running) (0% to 100%) with product eluting at 12% on a 24 g silica column. ^{1}H NMR (400 MHz, $CDCl_3$) δ 7.56 (dd, J = 5.2, 3.0 Hz, 2H), 7.21 (dd, J = 5.8, 3.0 Hz, 2H), 2.99 (dd, J = 8.7, 5.2 Hz, 1H), 2.65–2.59 (m, 1H), 2.41 (s, 1H), 2.24–2.13 (s, 1H), 1.79 (ddd, J = 12.3, 9.2, 2.5 Hz, 1H), 1.69–1.54 (m, 3H), 1.42–1.27 (m, 3H). ^{13}C NMR (101 MHz, $CDCl_3$) δ 158.7, 137.9, 122.3, 114.6, 42.7, 41.9, 36.6, 36.3, 36.2, 29.7, 28.7. FT-IR (neat) cm^{-1} 2931, 2830, HRMS(ESI) calcd. $C_{14}H_{16}N_2$ $[M+H]^+$ 213.1387 observed 213.1379. Stereochemistry is assigned based on **17a**.

20a 2-(bicyclo[2.2.1]heptan-2-ylmethyl)-6-chloro-1H-benzo[d]imidazole

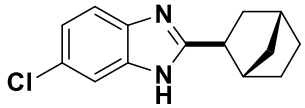

The **general procedure E** was followed using 2-bromo-6-chloro-1H-benzo[d]imidazole (25 mg, 0.11 mmol), norbornene (51 mg, 0.54 mmol), tributylamine (60 mg, 0.32 mmol), formic acid (15 mg, 0.32 mmol), and 0.45 mL of stock solution of $Ir(ppy)_3$ in MeCN was used to afford **20a** in 79% yield (21 mg, 0.087 mmol), dr >20:1 (based on crude ^1H NMR) as white solid. m.pt. 223 - 225 ^oC. After the completion of the reaction, 24 h, thesubstrate was purified via automated flash chromatography using EtOAc in hexanes (column was buffered with 1% Et_3N in hexane before running) (0% to 100%) with product eluting at 12% on a 24 g silica column. ^1H NMR (400 MHz, CD_3OD) δ 7.44 (s, 1H), 7.40 (d, J = 11.0 Hz, 1H), 7.12 (dd, J = 8.6, 2.0 Hz, 1H), 3.29 (p, J = 1.7 Hz, 1H), 2.94 (ddd, J = 8.8, 5.8, 2.9 Hz, 1H), 2.52 (dd, J = 4.0, 1.7 Hz, 1H), 2.37 (d, J = 4.2 Hz, 1H), 2.09–2.00 (m, 1H), 1.75 (ddd, J = 12.1, 9.1, 2.4 Hz, 1H), 1.69–1.60 (m, 1H), 1.60–1.54 (m, 1H), 1.46–1.38 (m, 1H), 1.34–1.21 (m, 2H). ^{13}C NMR (101 MHz, CD_3OD) δ 162.0, 128.5, 123.4, 79.6, 79.6, 79.3, 78.9, 43.9, 43.1, 37.6, 37.2, 36.9, 30.7, 29.7. FT-IR (neat) cm^{-1} 2931, 2858, 780. HRMS (ESI) calcd. $C_{14}H_{15}ClN_2$ $[M+H]^+$ 247.0997 observed 247.0994. Stereochemistry is assigned based on **17a**.

21a 2-((3,3-dimethylbicyclo[2.2.1]heptan-2-yl)methyl)-1H-benzo[d]imidazole

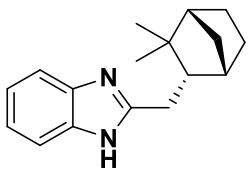

The **general procedure E** was followed using 2-bromo-1H-benzo[d]imidazole (25 mg, 0.13 mmol), (+)-camphene (86 mg, 0.63 mmol), tributylamine (70 mg, 0.38 mmol), formic acid (17.3 mg, 0.38 mmol), and 0.52 mL of stock solution of $Ir(ppy)_3$ in MeCN was used to afford **21a** in 93% yield (31 mg, 0.12 mmol), rr >20:1 (based on crude ^1H NMR), dr>20:1 (based on crude ^1H NMR) as white solid, m.pt 197–200 ^oC. After the completion of the reaction, 24 h, the substrate was purified via automated flash chromatography using EtOAc in hexanes (column was buffered with 1% Et_3N in hexane before running) (0% to 100%) with product eluting at 17% on a 24 g silica column. ^1H NMR (400 MHz, Methanol-d_4) δ 7.47 (dd, *J*=5.9, 3.2 Hz, 1H), 7.16 (dd, *J*=6.0, 3.2 Hz, 1H), 3.30

(dt, *J*=3.0, 1.5 Hz, 0H), 2.94–2.77 (m, 1H), 2.09 (ddd, *J* = 10.2, 6.5, 3.6 Hz, 1H), 1.78 (s, 0H), 1.75–1.56 (m, 2H), 1.36–1.24 (m, 2H), 1.18 (d, *J*=9.6 Hz, 1H), 1.01 (s, 1H), 0.91 (s, 1H). ^{13}C NMR (101 MHz, CD_3OD) δ 155.5, 138.0, 121.7, 113.8, 49.5, 49.1, 41.4, 36.8, 36.4, 31.1, 25.8, 24.2, 20.6, 19.7. FT-IR (neat) cm^{-1} 3086, 2964, 1635, 1591. HRMS (ESI) calcd. $C_{17}H_{22}N_2$ [M+H]$^+$ 255.1856 observed 255.1849. Diastereoselectivity is based on detailed analysis of coupling constants.

22a 6-bromo-2-((3,3-dimethylbicyclo[2.2.1]heptan-2-yl)methyl)-1H-benzo[d]imidazole

The **general procedure E** was followed using 2,6-dibromo-1H-benzo[d]imidazole (25 mg, 0.10 mmol), (+)-camphene (61 mg, 0.45 mmol), tributylamine (50 mg, 0.27 mmol), formic acid (13 mg, 0.27 mmol), and 0.36 mL of stock solution of $Ir(ppy)_3$ in MeCN was used to afford **22a** in 87% yield (29 mg, 0.087 mmol), rr>20:1 (based on crude ^{1}H NMR), dr>20:1 (based on crude ^{1}H NMR) as white solid. m.pt 200–203 ºC. After the completion of the reaction, 12 h, the substrate was purified via automated flash chromatography using EtOAc in hexanes (column was buffered with 1% Et_3N in hexanes before running) (0% to 100%) with product eluting at 12% on a 4 g silica column. ^{1}H NMR (400 MHz, $CDCl_3$) δ 7.67 (d, J = 1.8 Hz, 1H), 7.38 (d, J = 8.4 Hz, 1H), 7.31 (dd, J = 8.5, 1.9 Hz, 1H), 2.90 (dd, J = 7.8, 4.9 Hz, 2H), 2.05 (dt, J = 10.6, 3.0 Hz, 2H), 1.74 (s, 1H), 1.52 (t, J = 9.6 Hz, 2H), 1.42 (t, J = 8.2 Hz, 1H), 1.29–1.19 (m, 2H), 1.13 (d, J = 9.7 Hz, 1H), 0.82 (s, 6H). ^{13}C NMR (101 MHz, $CDCl_3$) δ 156.7, 140.1, 137.4, 125.2, 117.6, 115.8, 115.1, 49.7, 48.8, 41.3, 37.2, 36.9, 31.9, 26.7, 24.6, 21.6, 20.2. FT-IR (neat) cm^{-1} 3021, 2954, 1625, 1596, 650. HRMS (ESI) calcd. $C_{17}H_{21}BrN_2$ [M+H]$^+$ 333.0962 observed 333.0961. Diastereoselectivity is based on detailed analysis of coupling constants.

23a dimethyl 5-(4-chlorobenzo[d]thiazol-2-yl)-7-oxabicyclo[2.2.1]heptane-2,3-dicarboxylate

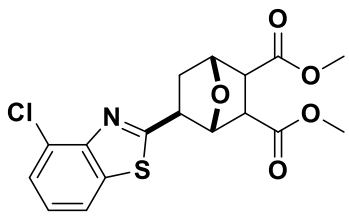

The **general procedure E** was followed using 2-bromo-4-chlorobenzo[d]thiazole (25 mg, 0.10 mmol), dimethyl 7-oxabicyclo[2.2.1]hept-5-ene-2,3-dicarboxylate (106 mg, 0.51 mmol), tributylamine (56 mg, 0.30 mmol), formic acid (14 mg, 0.30 mmol), and 0.40 mL of stock solution of $Ir(ppy)_3$ in MeCN was used to afford **23a** in 53% yield (19 mg, 0.053 mmol), rr >20:1 (based on crude ^{1}H NMR), dr>20:1 (based on crude ^{1}H NMR) as an oil. After the completion of the reaction, 14 h, the substrate was purified via automated flash chromatography using EtOAc in hexanes (0% to 100%) with product eluting at 17% on a 12 g silica column. ^{1}H NMR (400 MHz, $CDCl_3$) δ 7.76 (d, J = 8.0 Hz, 1H), 7.48 (d, J = 7.7 Hz, 1H), 7.30 (t, J = 8.0 Hz, 1H), 5.12 (d, J = 5.4 Hz, 1H), 5.10 (s, 1H), 3.77 (dd, J = 8.8, 4.5 Hz, 1H), 3.70 (d, J = 8.7 Hz, 6H), 3.18 (q, J = 9.6 Hz, 2H), 2.29 (dd, J = 13.2, 8.8 Hz, 1H), 2.17 (dq, J = 15.0, 5.0 Hz, 1H). ^{13}C NMR (101 MHz, $CDCl_3$) δ 175.4, 170.9, 170.6, 149.2, 136.9, 127.5, 126.4, 125.6, 120.3, 83.3, 78.5, 52.4, 52.3, 51.8, 51.3, 47.8, 39.5. FT-IR (neat) cm^{-1} 2946, 1742, 1200, 1163. HRMS (ESI) calcd. $C_{17}H_{16}ClNO_5S$ $[M+H]^+$ 382.0510 observed 382.0506. Stereochemistry is assigned based on **19a**.

24a **Major** - (S)-2-methyl-5-(1-(thiazol-2-yl)propan-2-yl)cyclohex-2-en-1-one and **Minor** - (5R)-2-methyl-5-(prop-1-en-2-yl)-3-(thiazol-2-yl)cyclohexan-1-one (minor)

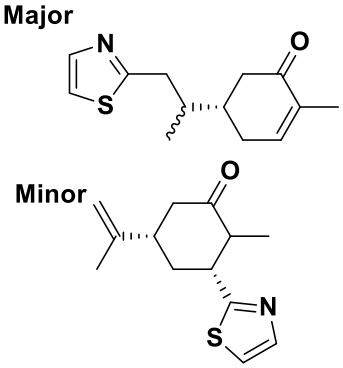

The **general procedure E** was followed using 2-bromothiazole (25 mg, 0.15 mmol), 2-methyl-5-(prop-1-en-2-yl)cyclohex-2-en-1-one (110 mg, 0.76 mmol), tributylamine (85 mg, 0.46 mmol), formic acid (21 mg, 0.46 mmol), and 0.65 mL of stock solution of $Ir(ppy)_3$ in MeCN was used to afford **24a** in 78% yield [28 mg (20 mg (major also contains small amount of minor) and 8 mg (minor, mix of diastereomers), 0.12 mmol], rr 2:1 (major : minor) (based on crude ^{1}H NMR), dr (major) 1.2:1 (based on crude ^{1}H NMR). After the completion of the reaction, 19 h, the substrate was purified via automated flash chromatography using EtOAc in hexanes (0% to 100%) with minor product eluting at 12% and major product eluting at 17% on a 24 g silica column. **Major isomer**-^{1}H NMR, [mix. of diastereomers and minor isomer] (400 MHz, $CDCl_3$) δ 7.67 (t, J = 3.0 Hz, 1H), 7.19 (t, J = 3.1 Hz, 1H), 6.73 (dq, J = 5.8, 1.7 Hz, 1H), 3.10 (ddd, J = 14.4, 9.2, 5.2 Hz, 1H), 2.86 (dt, J = 14.5, 8.3 Hz, 1H), 2.59–2.47 (m, 1H), 2.45–2.33 (m, 1H), 2.30–2.16 (m, 2H), 2.15–2.00 (m, 2H), 1.75 (dd, J = 2.6, 1.3 Hz, 3H), 0.94 (dd, J = 6.5, 2.6 Hz, 3H). ^{13}C NMR (101 MHz, $CDCl_3$) δ 199.7, 199.7, 144.7, 144.6, 142.2, 142.2, 135.3, 135.3, 118.1, 118.1, 117.8, 113.5, 42.2, 40.5, 39.6, 39.4, 38.1, 37.9, 37.3, 37.2, 30.2, 28.0, 15.7, 15.6, 15.5, 15.5. **Note** - The diastereomer and regioisomer are marked as ⬮ in spectra. **Minor Isomer** -^{1}H NMR, [mixture of diastereomers] (400 MHz, $CDCl_3$) δ 7.70 (d, J = 3.4 Hz, 1H), 7.18 (d, J = 3.3 Hz, 1H), 4.74 (d, J = 21.5 Hz, 2H), 3.91 (dt, J = 6.0, 4.0 Hz, 1H), 2.80–2.72 (m, 1H), 2.68 (ddd, J = 14.4, 4.1, 1.2 Hz, 1H), 2.51–2.42 (m, 1H), 2.37–2.27 (m, 1H), 2.18–2.11 (m, 2H), 1.70 (s, 3H), 0.97 (d, J = 6.7 Hz, 3H). ^{13}C NMR (101 MHz, $CDCl_3$) δ 210.3, 169.6, 147.2, 142.8, 117.9, 110.2, 47.3, 45.5, 40.3, 35.8, 29.4, 22.7, 14.1. **Note** - The diastereomer is marked as ⬮ in spectra. FT-IR (neat) cm^{-1} 2962, 1706, 1666, 1655. HRMS (ESI) calcd. $C_{13}H_{17}NOS$ $[M+H]^+$ 236.1104 observed 236.1102.

25a ((1S,2R,4S)-2-(benzo[d]thiazol-2-yl)-4-(prop-1-en-2-yl)cyclohexyl)methanol

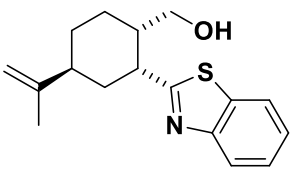

The **general procedure E** was followed using 2-benzobromothiazole (25 mg, 0.12 mmol), (4-(prop-1-en-2-yl)cyclohex-1-en-1-yl)methanol (89 mg, 0.58 mmol), tributylamine (65 mg, 0.35 mmol), formic acid (16 mg, and 0.50 mL of stock solution of $Ir(ppy)_3$ in MeCN was used to afford **25a** in 82% yield (28 mg, 0.097 mmol), rr 9:1 (based on crude ^1H NMR), dr 7:1 (based on crude ^1H NMR) and isolated as dr 8.1:1 (mixture) as pale oil. After the completion of the reaction, 21 h, the substrate was purified via automated flash chromatography using EtOAc in hexanes (0% to 100%) with product eluting at 8% on a 12 g silica column. ^1H NMR (400 MHz, $CDCl_3$) δ 7.96 (d, J = 8.1 Hz, 1H), 7.86 (d, J = 7.9 Hz, 1H), 7.46 (t, J = 7.7 Hz, 1H), 7.37 (t, J = 7.5 Hz, 1H), 4.75 (s, 2H), 3.88 (s, 1H), 3.73–3.61 (m, 1H), 3.56–3.41 (m, 1H), 2.47 (t, J = 12.3 Hz, 1H), 2.29 (d, J = 14.0 Hz, 1H), 2.17–2.02 (m, 1H), 1.92 (d, J = 12.7 Hz, 1H), 1.83 (td, J = 13.5, 4.9 Hz, 1H), 1.76 (s, 3H), 1.61 (q, J = 14.1, 13.1 Hz, 2H), 1.45–1.30 (m, 1H). ^{13}C NMR (101 MHz, $CDCl_3$) δ 174.0, 152.0, 149.5, 134.5, 126.1, 125.0, 122.6, 121.4, 109.0, 65.2, 43.3, 41.9, 40.4, 36.5, 31.0, 24.6, 21.0. FT-IR (neat) 3435, 2985, 2854cm^{-1}. HRMS (ESI) $C_{17}H_{21}NOS$ calcd. $[M+H]^+$ 288.1417 observed 288.1414. Diastereoselectivity is based on detailed analysis of coupling constants.

<u>26a</u> 2-(2-(4-((benzyloxy)methyl)cyclohex-3-en-1-yl)propyl)-4-chlorobenzo[d]thiazole

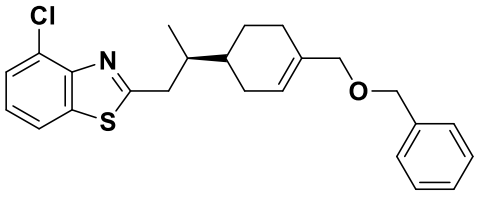

The **general procedure E** was followed using 2-bromo-4-chloro-1H-benzo[d]thiazole (25 mg, 0.10 mmol), (4-(prop-1-en-2-yl)cyclohex-1-en-yl)methoxy)methyl)benzene (120 mg, 0.51 mmol), tributylamine (56 mg, 0.30 mmol), formic acid (14 mg, 0.30 mmol), and 0.40 mL of stock solution of $Ir(ppy)_3$ in MeCN solution was used to afford **26a** in 80% yield (33 mg, 0.08 mmol), rr >20:1 (based on crude ^1H NMR), dr 4:1 (based on crude ^1H NMR) and isolated dr 5:1 (mixture) as an oil. After the completion of the reaction, 17 h, the substrate was purified via automated flash

chromatography using EtOAc in hexanes (0% to 100%) with product eluting at 12% on a 12 g silica column. ^{1}H NMR (400 MHz, $CDCl_3$) [mix of diastereomers] δ 7.96 (d, J = 8.1 Hz, 1H), 7.86 (d, J = 7.9 Hz, 1H), 7.46 (t, J = 7.7 Hz, 1H), 7.37 (t, J = 7.5 Hz, 1H), 4.75 (s, 2H), 3.88 (s, 1H), 3.73–3.61 (m, 1H), 3.56–3.41 (m, 1H), 2.47 (t, J = 12.3 Hz, 1H), 2.29 (d, J = 14.0 Hz, 1H), 2.17–2.02 (m, 1H), 1.92 (d, J = 12.7 Hz, 1H), 1.83 (td, J = 13.5, 4.9 Hz, 1H), 1.76 (s, 3H), 1.61 (q, J = 14.1, 13.1 Hz, 2H), 1.45–1.30 (m, 2H). ^{13}C NMR (101 MHz, $CDCl_3$) δ 174.0, 152.0, 149.5, 134.5, 126.1, 125.0, 122.6, 121.4, 109.0, 65.2, 43.3, 41.9, 40.4, 36.5, 31.0, 24.6, 21.0. FT-IR (neat) cm^{-1}. HRMS (ESI) $C_{24}H_{26}NClOS$ calcd. $[M+H]^+$ 412.1496 observed 412.1492. The diastereomer is marked as ⬮ in spectra.

27a 4,6-difluoro-2-(5-isopropyl-2-methylcyclohex-2-en-1-yl)benzo[d]thiazole

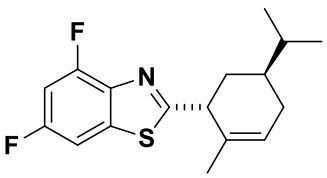

The **general procedure E** was followed using 2-bromo-4,6-difluorobenzo[d]thiazole (25 mg, 0.10 mmol), alpha-pinene (68 mg, 0.50 mmol), tributylamine (56 mg, 0.30 mmol), formic acid (14 mg, 0.30 mmol), and 0.40 mL of stock solution of $Ir(ppy)_3$ in MeCN was used to afford **27a** in 68% yield (21 mg, 0.068 mmol), rr >20:1 (isolated) as yellow oil. After the completion of the reaction, 16 h, the substrate was purified via automated flash chromatography using EtOAc in hexanes (0% to 100%) with product eluting at 4% on a 12 g silica column. ^{1}H NMR (400 MHz, $CDCl_3$) δ 7.32 (d, J = 7.5 Hz, 1H), 6.96 (t, J = 9.7 Hz, 1H), 5.76 (s, 1H), 3.89 (d, J = 6.1 Hz, 1H), 2.21 (d, J = 17.8 Hz, 2H), 2.08 (d, J = 13.1 Hz, 1H), 1.73 (s, 3H), 1.57 (s, 2H), 1.44 (dt, J = 12.7, 6.4 Hz, 1H), 0.84 (dd, 6H). ^{13}C NMR (101 MHz, $CDCl_3$) δ 176.8 (d, J = 3.0 Hz), 159.6 (dd, J = 246.8, 10.4 Hz), 154.7 (dd, J = 258.7, 13.4 Hz),138.8 (dd, J = 13.2, 2.5 Hz), 138.1 (dd, J = 12.6, 5.1 Hz), 132.0, 126.6 103.3 (dd, J = 26.2, 4.7 Hz), 101.5 (dd, J = 28.3, 21.9 Hz).45.0, 34.7, 33.2, 31.9, 28.6, 22.4, 19.7, 19.1. ^{19}F NMR (376 MHz, $CDCl_3$) δ -113.6 (dd, *J* = 7.9 Hz), -117.8–-118.3 (m). FT-

IR (neat) cm^{-1} 2956, 1617, 1585. HRMS (ESI) $C_{17}H_{19}F_2NS$ calcd $[M+H]^+$ 308.1279 observed 308.1278. $[\alpha]_D^{20}$ = +87.17 (c 0.016, $CHCl_3$).

28a 2-(((1S,11S,Z)-7,7,11-trimethyl-12-oxabicyclo[9.1.0]dodec-4-en-4-yl)methyl)thiazole

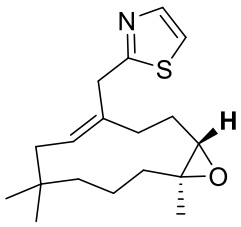

The **general procedure E** was followed using 2-bromothiazole (25 mg, 0.15 mmol) (-) caryophylleneoxide (170 mg, 0.76 mmol), tributylamine (85 mg, 0.46 mmol), formic acid (21 mg, 0.46 mmol), and 0.65 mL of stock solution of $Ir(ppy)_3$ in MeCN solution was used to afford **28a** in 71% yield (32 mg, 0.106 mmol) rr >20:1 (based on crude ^1H NMR), Z:E>20:1 as colorless oil. After the completion of the reaction, 19 h, the substrate was purified via automated flash chromatography using EtOAc in hexanes (0% to 100%) with product eluting at 14% on a 12 g silica column. ^1H NMR (400 MHz, $CDCl_3$) δ 7.67 (d, J = 3.3 Hz, 1H), 7.19 (d, J = 3.3 Hz, 1H), 5.49 (dd, J = 11.1, 2.6 Hz, 1H), 3.93 (d, J = 15.1 Hz, 1H), 3.52 (d, J = 15.2 Hz, 1H), 2.82 (dd, J = 11.1, 1.8 Hz, 1H), 2.50–2.38 (m, 1H), 2.36–2.21 (m, 2H), 2.18–1.97 (m, 2H), 1.83 (dt, J = 15.2, 2.7 Hz, 1H), 1.66–1.39 (m, 4H), 1.27 (s, 3H), 1.23 (d, J = 2.7 Hz, 1H), 1.12 (dd, J = 10.9, 7.2 Hz, 1H), 0.98 (s, 3H), 0.89 (s, 3H). ^{13}C NMR (101 MHz, $CDCl_3$) δ 170.3, 142.9, 134.8, 128.4, 119.2, 63.2, 63.1, 41.3, 38.9, 38.0, 35.5, 33.6, 33.5, 30.0, 28.7, 24.8, 19.0, 18.4. FT-IR (neat) cm^{-1} 2952, 1595, 850. HRMS (ESI) $C_{18}H_{27}NOS$ calcd $[M+H]^+$ 306.1886 observed 306.1877. $[\alpha]^D_{20}$ = -490.7 (c 0.013, $CHCl_3$). Stereochemistry is assigned based on NOE, HSQC and COSY.

29a(3S,8S,9S,10R,13R,14S,17R)-10,13-dimethyl-17-((R)-6-methylheptan-2-yl)-6-(thiazol-2-yl)hexadecahydro-1H-cyclopenta[a]phenanthren-3-ol

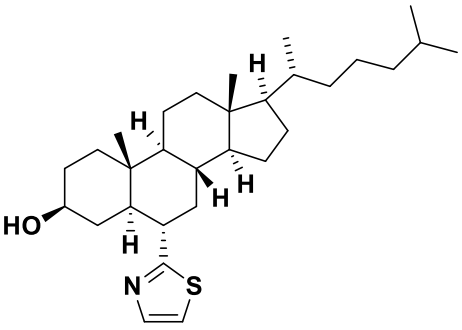

The **general procedure F** was followed using 2-bromothiazole (110 mg, 0.65 mmol) cholesterol (25 mg, 0.064 mmol), tributylamine (140 mg, 0.77 mmol), formic acid (35 mg, 0.77 mmol), $Ir(ppy)_3$ (0.006 equiv, 0.64 mL of 0.6 mM stock solution of catalyst in MeCN, where 0.64 mL of MeCN is used to make 0.1 M with respect to cholesterol) was used to afford **29a** in 65% yield (19 mg, 0.042 mmol). After the completion of the reaction, 24 h, the substrate was purified via automated flash chromatography using EtOAc in hexanes (0% to 100%) with product eluting at 60% on a 12 g silica column as yellow oil. (**Note** – reaction went only up to 80% conversion with respect to cholesterol) rr >20:1 (based on crude ^{1}H NMR) dr> 20:1 (based on crude ^{1}H NMR). ^{1}H NMR (599 MHz, $CDCl_3$) δ 7.66 (d, J = 3.3 Hz, 1H), 7.17 (d, J = 3.3 Hz, 1H), 3.63 (tt, J = 11.0, 4.6 Hz, 1H), 3.26–3.19 (m, 1H), 2.34 (ddd, J = 13.8, 3.5, 1.8 Hz, 1H), 2.16–2.05 (m, 2H), 1.98 (ddt, J = 12.6, 5.2, 2.7 Hz, 2H), 1.89–1.82 (m, 1H), 1.82–1.75 (m, 1H), 1.72–1.62 (m, 3H), 1.57–1.47 (m, 3H), 1.45–1.37 (m, 2H), 1.34 (dd, J = 7.4, 4.0 Hz, 2H), 1.33–1.28 (m, 3H), 1.27–1.23 (m, 2H), 1.18–1.12 (m, 3H), 1.11–1.05 (m, 2H), 1.03–0.95 (m, 3H), 0.91 (d, J = 6.5 Hz, 3H), 0.87 (d, J = 2.8 Hz, 3H), 0.86 (d, J = 2.8 Hz, 3H), 0.71 (s, 3H), 0.51 (s, 3H). ^{13}C NMR (101 MHz, $CDCl_3$) δ 173.3, 141.5, 117.2, 71.9, 56.3, 56.1, 55.2, 47.6, 42.6, 42.5, 39.8, 39.4, 38.7, 37.9, 36.7, 36.0, 36.0, 35.7, 32.1, 31.3, 28.1, 27.8, 24.0, 23.7, 22.6, 22.4, 21.0, 18.5, 14.5, 12.1. FT-IR (neat) cm^{-1} 3465, 2933, 1680. HRMS (ESI) $C_{30}H_{49}NOS$ calcd $[M+H]^+$ 472.3607 observed 472.3608. $[\alpha]_D^{20}$ = + 5.54 (c 0.011, $CHCl_3$). Diastereoselectivity is based on detailed analysis of coupling constants.

30a 2-cyclooctylthiazole

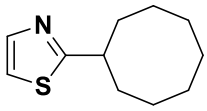

The **general procedure E** was followed using 2-bromothiazole (25 mg, 0.15 mmol) cis-cyclooctene (84 mg, 0.75 mmol), tributylamine (85 mg, 0.46 mmol), formic acid (21 mg, 0.46 mmol), and 0.65 mL of stock solution of $Ir(ppy)_3$ in MeCN solution was used to afford **30a** in 23% yield (7 mg, 0.035 mmol) as yellow oil. After the completion of the reaction, 12 h, the substrate was purified via automated flash chromatography using EtOAc in hexanes (0% to 100%) with product eluting at 7% on a 12 g silica column. ^{1}H NMR (400 MHz, $CDCl_3$) δ 7.66 (d, J = 3.3 Hz, 1H), 7.16 (d, J = 3.3 Hz, 1H), 3.37–3.22 (m, 1H), 2.16–2.03 (m, 2H), 1.96–1.84 (m, 2H), 1.83–1.70 (m, 2H), 1.66–1.57 (m, 8H). ^{13}C NMR (101 MHz, $CDCl_3$) δ 178.4, 141.8, 117.3, 42.7, 32.9, 27.1, 26.0, 25.3. FT-IR (neat) cm^{-1} 2872, 2920. HRMS (ESI) $C_{11}H_{17}NS$ calcd. $[M+H]^+$ 196.1154 observed 196.1150.

31a 2-cyclooctyl-4,6-difluorobenzo[d]thiazole

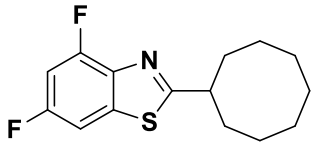

The **general procedure G** was followed using 2-bromo-4,6-difluorobenzo[d]thiazole (25 mg, 0.10 mmol), cyclooctene (55 mg, 0.50 mmol), *N*,*N*-diisopropyloctan-1-amine (55 mg, 0.30 mmol), formic acid (14 mg, 0.30 mmol), and 0.40 mL of stock solution of **cat-1** in MeCN was used to afford **31a** in 73% yield (20 mg, 0.073 mmol) as yellow oil. After the completion of the reaction, 48 h, the substrate was purified via automated flash chromatography using EtOAc in hexanes (0% to 100%) with product eluting at 3% on a 12 g silica column. ^{1}H NMR (400 MHz, $CDCl_3$) δ 6.62 (dd, J = 19.8, 7.9 Hz, 1H), 6.47 (qd, J = 10.4, 2.5 Hz, 1H), 4.11–3.88 (m, 1H), 2.64 (ddt, J = 85.9, 7.8, 3.3 Hz, 2H), 2.27–2.06 (m, 2H), 1.90–1.75 (m, 2H), 1.77–1.65 (m, 1H), 1.66–1.48 (m, 7H). ^{13}C NMR (101 MHz, $CDCl_3$) δ 157.0 (ddd, *J* = 241.0, 23.8, 10.7 Hz), 148.7 (dt, *J* = 244.1, 12.6 Hz), 133.8–127.8 (m), 104.7 (ddd, *J* = 26.3, 12.6, 3.5 Hz), 99.9 (ddd, *J* = 27.2, 22.6, 2.5 Hz), 94.1, 92.7, 48.7, 48.4, 31.6, 31.2, 28.7, 28.1, 24.9, 24.2. ^{19}F NMR (376 MHz, $CDCl_3$) δ -120.7 (dt, *J* =

30.0, 8.6 Hz), -128.6 (dd, J = 188.2, 10.2 Hz). FT-IR (neat) cm^{-1} 3025, 2927, 2852, 1612, 1438, 1385. HRMS (ESI) $C_{15}H_{17}F_2NS$ calcd $[M+NH_4]^+$ 299.1388 observed 299.1387.

32a 5-((1R,4S)-bicyclo[2.2.1]heptan-2-yl)pyrimidine-2-carbonitrile

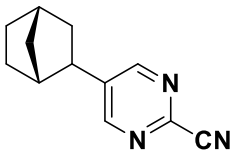

The **general procedure H** was followed using 5-bromopyrimidine-2-carbonitrile (25 mg, 0.14 mmol), norbornene (64 mg, 0.68 mmol), *N*,*N*-diisopropylethylamine (21 mg, 0.30 mmol), and 0.56 mL of stock solution of $Ir(ppy)_3$ in MeCN was used to afford **32a** in 71% yield (21 mg, 0.10 mmol), dr > 20:1 (based on crude ^1H NMR) as an oil. After the completion of the reaction, 48 h, the substrate was purified via automated flash chromatography using EtOAc in hexanes (0% to 100%) with product eluting at 6% on a 12 g silica column. ^1H NMR (400 MHz, $CDCl_3$) δ 8.68 (s, 2H), 2.81 (dd, J = 9.0, 5.5 Hz, 1H), 2.48 (t, J = 4.1 Hz, 1H), 2.43 (dd, J = 3.9, 1.6 Hz, 1H), 1.90 (ddd, J = 11.7, 8.9, 2.2 Hz, 1H), 1.75–1.57 (m, 3H), 1.48–1.38 (m, 2H), 1.37–1.27 (m, 2H). ^{13}C NMR (101 MHz, $CDCl_3$) δ 156.7, 143.0, 142.6, 115.8, 43.2, 37.0, 36.3, 30.3, 28.5. FT-IR (neat) cm^{-1} 1400, 2225, 2800, 2950.

33a dimethyl (1R,4S,5R)-5-(4-formylphenyl)-7-oxabicyclo[2.2.1]heptane-2,3-dicarboxylate

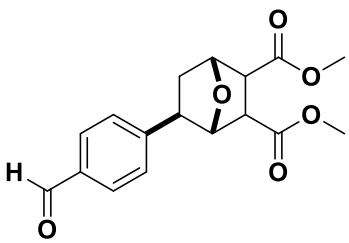

The **general procedure H** was followed using 4-bromobenzaldehyde (50 mg, 0.27 mmol), dimethyl (1R,4S)-7-oxabicyclo[2.2.1]hept-5-ene-2,3-dicarboxylate (180 mg, 0.85 mmol), *N*,*N*-diisopropylethylamine (70 mg, 0.54 mmol), and 1.35 mL of stock solution of $Ir(ppy)_3$ in MeCN was used to afford **33a** in 55% yield (47 mg, 0.149 mmol), dr > 20:1 (based on crude ^1H NMR) as an oil. After the completion of the reaction, 72 h, the substrate was purified via automated flash chromatography using EtOAc in hexanes (column was buffered with 0.5% Et_3N in hexanes before running) (0% to 100%) with product eluting at

32% on a 4 g silica column.. ^{1}H NMR (400 MHz, Acetone-d_6) δ 10.00 (s, 1H), 7.91–7.79 (m, 2H), 7.57–7.47 (m, 2H), 4.99 (d, *J* = 5.3 Hz, 1H), 4.71 (s, 1H), 3.61 (s, 3H), 3.58 (s, 3H), 3.36–3.24 (m, 3H), 2.32 (dd, *J* = 12.6, 8.9 Hz, 1H), 1.81 (dt, *J* = 12.6, 5.1 Hz, 1H). ^{13}C NMR (101 MHz, Acetone-d_6) δ 368.9, 348.4, 348.2, 330.1, 312.5, 306.9, 305.3, 261.5, 255.8, 229.0, 228.6, 228.4, 224.7, 217.4. FT-IR (neat) cm^{-1} 2725, 2820, 1720, 1679, 1133.

34a 4-((1S,4R)-bicyclo[2.2.1]heptan-2-yl)benzonitrile

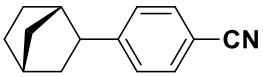

The **general procedure H** was followed using 4-bromobenzonitrile (75 mg, 0.41 mmol), norbornene (193 mg, 2.1 mmol)), *N*,*N*-diisopropylethylamine (106 mg, 0.82 mmol), and 1.7 mL of stock solution of Ir(ppy)$_3$ in MeCN was used to afford 3**4a** in 47% yield (38 mg, 0.19 mmol), dr>20:1 as an oil. After the completion of the reaction, 72 h, the substrate was purified via automated flash chromatography using EtOAc in hexanes (0% to 100%) with product eluting at 5% on a 12 g silica column. ^{1}H NMR (400 MHz, $CDCl_3$) δ 7.56 (d, J = 8.2 Hz, 2H), 7.30 (d, J = 8.1 Hz, 2H), 2.78 (t, J = 6.8 Hz, 1H), 2.38 (s, 2H), 1.82 (t, J = 10.8 Hz, 1H), 1.66–1.53 (m, 3H), 1.47 (d, J = 9.9 Hz, 1H), 1.37 (t, J = 9.0 Hz, 1H), 1.30 (d, J = 8.7 Hz, 1H), 1.23 (d, J = 10.1 Hz, 1H). ^{13}C NMR (101 MHz, $CDCl_3$) δ 153.3, 132.2, 128.0, 119.4, 109.3, 47.7, 42.7, 39.3, 37.0, 36.3, 30.6, 28.9. FT-IR (neat) cm^{-1} 2949, 2874, 2226, 1608.

Improvement of percentage yield of substrate 3a and 8a with new modified conditions (Conditions B)

3a 4-phenyl-2-(tetrahydro-2H-pyran-3-yl)thiazole

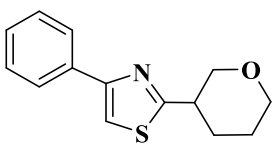

The **Conditions B** were followed using 2-bromo-4-phenylthiazole (25 mg, 0.10 mmol), 3,4-dihydro-2H-pyran (42 mg, 0.50 mmol), *N*,*N*-diisopropyloctan-1-amine (64 mg, 0.30 mmol), formic acid (14 mg, 0.30 mmol), 0.40 mL of stock solution of cat-1 in MeCN. After 3 days, 1,3,5-trimethoxybenzene

(8.4 mg, 0.05 mmol) was added as an internal standard and the yield of **3a** was calculated as 51% (based on ^{1}H NMR) with a rr 9:1 (based on crude ^{1}H NMR). **Note** – In comparison to **3a** (with **Conditions A**) the yield improved from 43% to 51%.

8a 4-chloro-2-(tetrahydro-2H-pyran-3-yl)benzo[d]thiazole

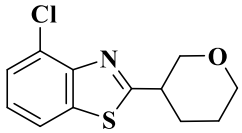

The **Conditions B** were followed using 2-bromo-4-chlorobenzo[d]thiazole (25 mg, 0.10 mmol), 3,4-dihydro-2H-pyran (42 mg, 0.50 mmol), *N*,*N*-diisopropyloctan-1-amine (64 mg, 0.30 mmol), formic acid (14 mg, 0.30 mmol), and 0.40 mL of stock solution of cat-1 in MeCN. After 4 days, 1,3,5-trimethoxybenzene (8.4 mg, 0.05 mmol) was added as an internal standard and the yield of **8a** was calculated as 77% yield (based on ^{1}H NMR) and rr 4:1 (based on crude ^{1}H NMR). **Note** In comparison to **8a** (with **Conditions A**) the yield improved from 60% to 77% with slight improvement of rr 3:1 (with **Conditions A**) to rr 4:1.

Spectra

Figure 3.4 Chapter III NMR Spectrum Graphs

^{1}H NMR (400 MHz, $CDCl_3$) of **1a** - 2-(tetrahydro-2H-pyran-3-yl)thiazole

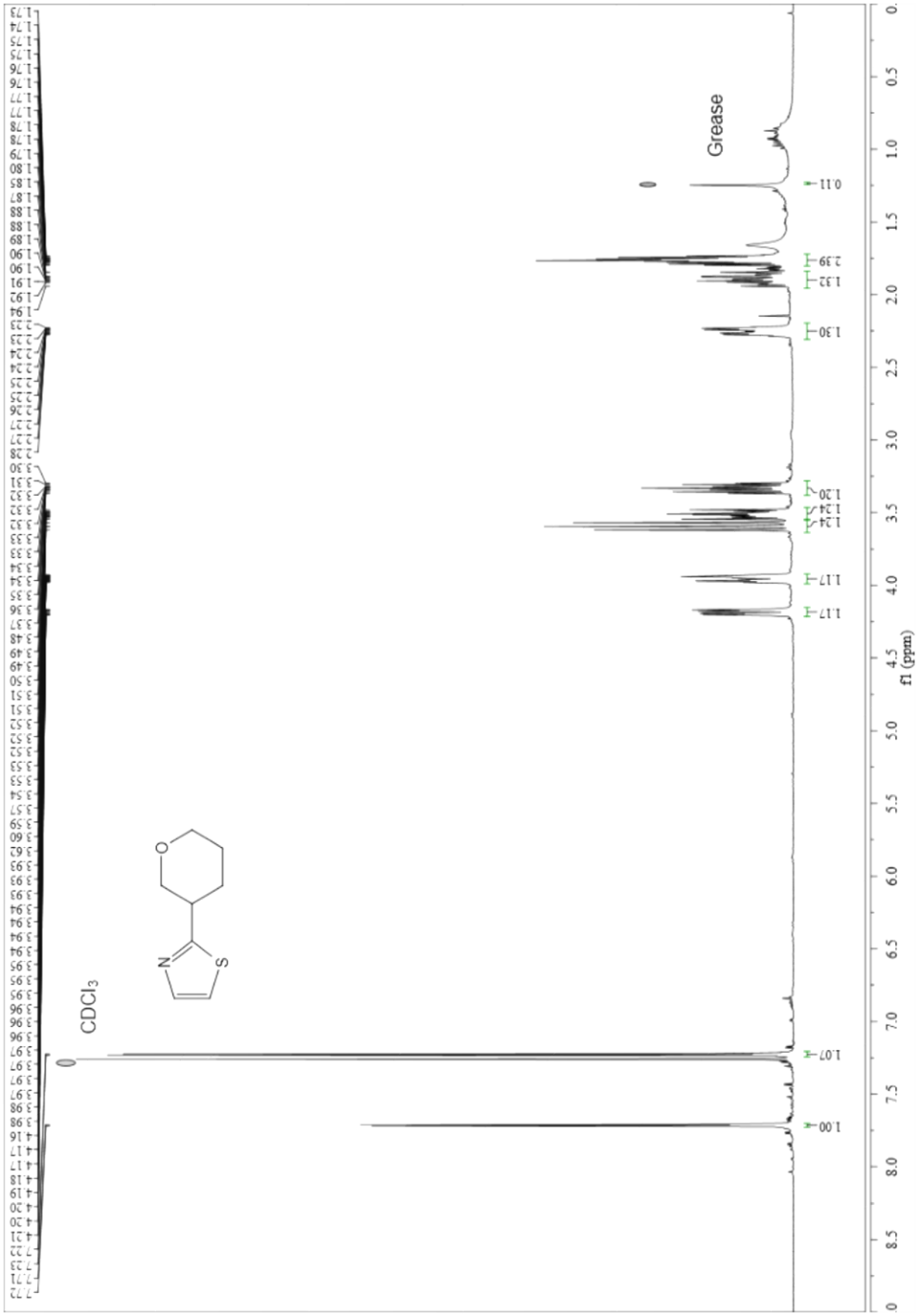

^{13}C NMR (101 MHz, $CDCl_3$) of **1a**-2-(tetrahydro-2H-pyran-3-yl)thiazole

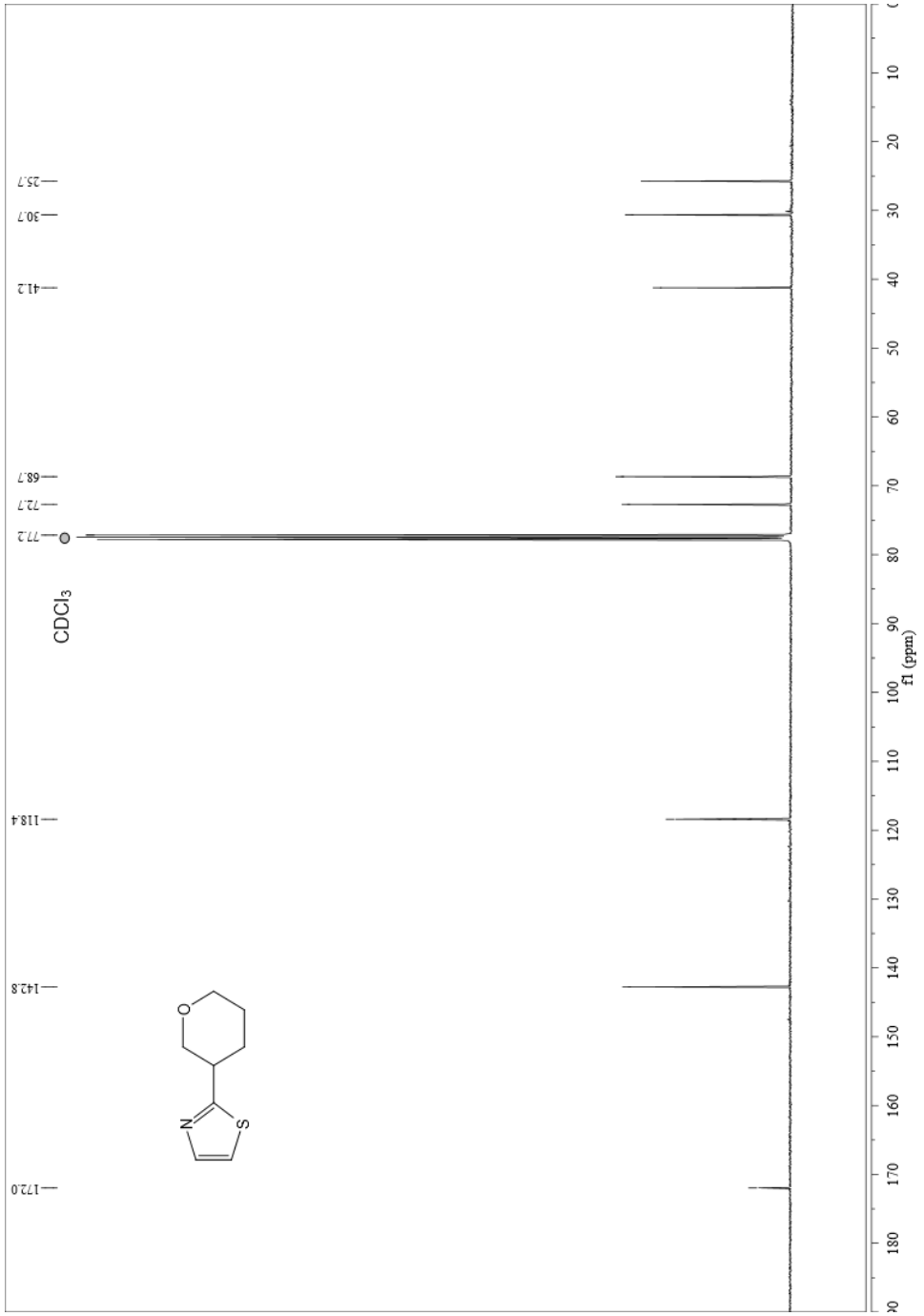

^{1}H NMR (400 MHz, $CDCl_3$) of **2a** 4-(tert-butyl)-2-(tetrahydro-2H-pyran-3-yl)thiazole

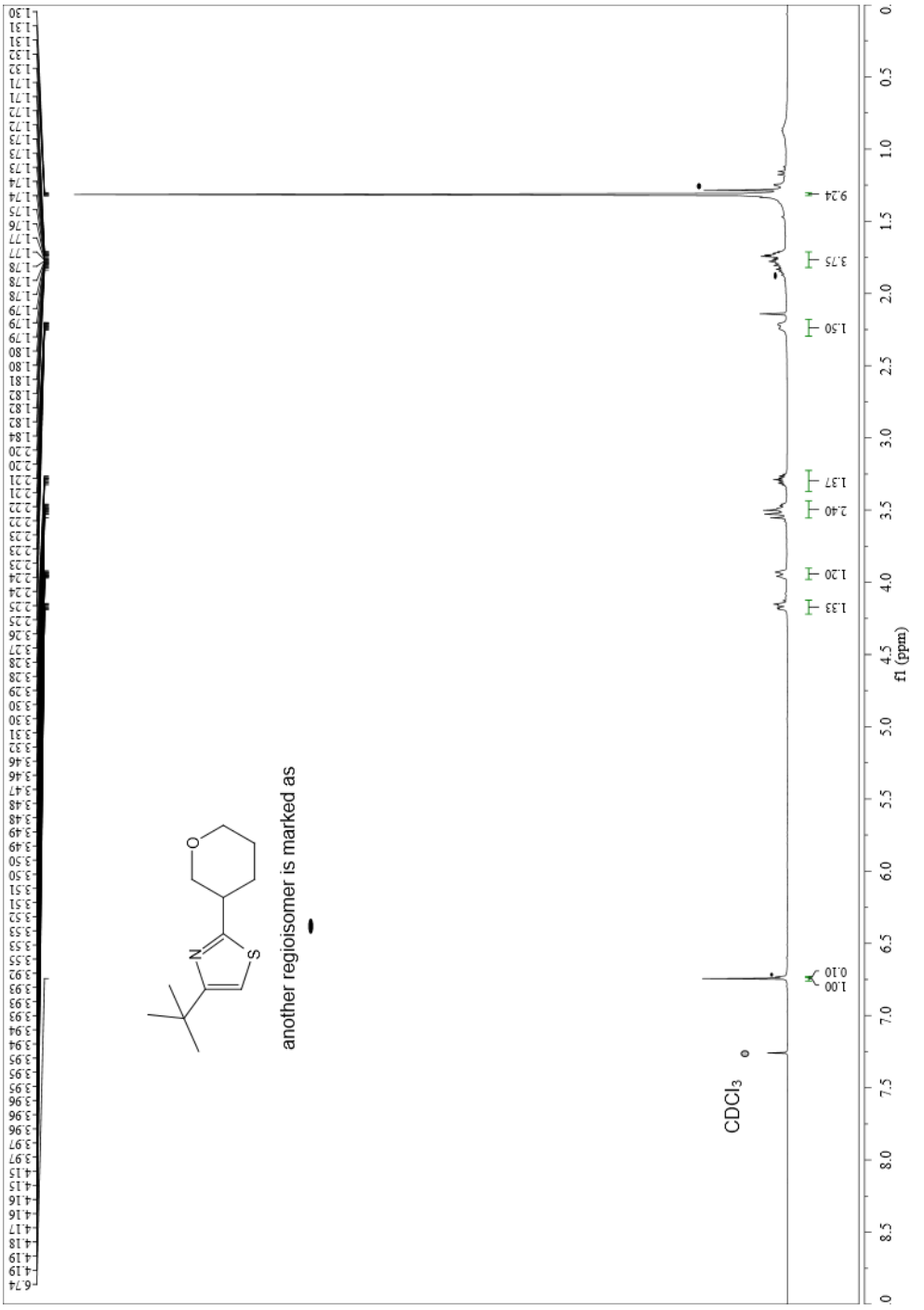

^{13}C NMR(101 MHz, $CDCl_3$) of **2a** 4-(tert-butyl)-2-(tetrahydro-2H-pyran-3-yl)thiazole

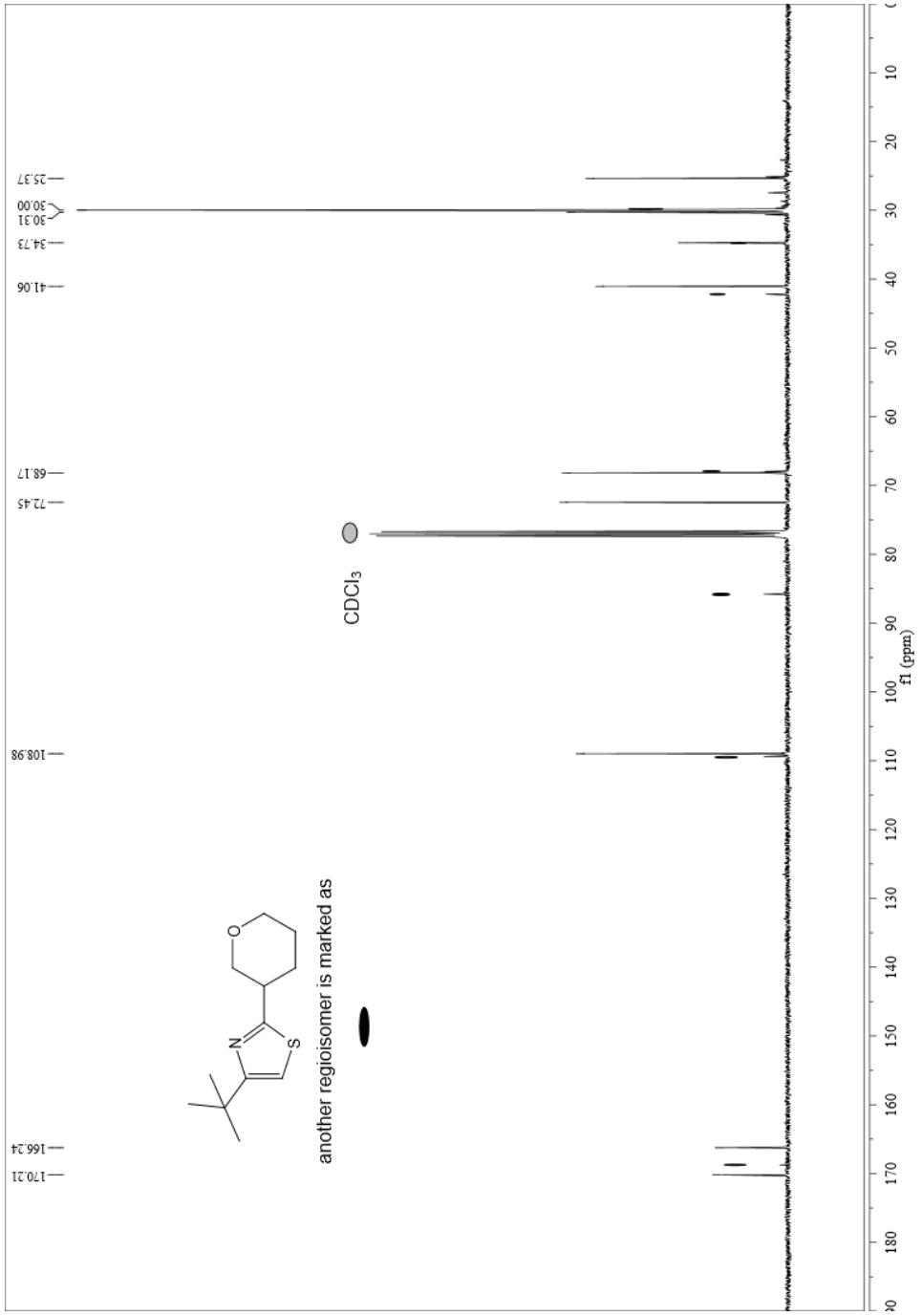

^{1}H NMR(400 MHz, $CDCl_3$) of **3a** 4-phenyl-2-(tetrahydro-2H-pyran-3-yl)thiazole

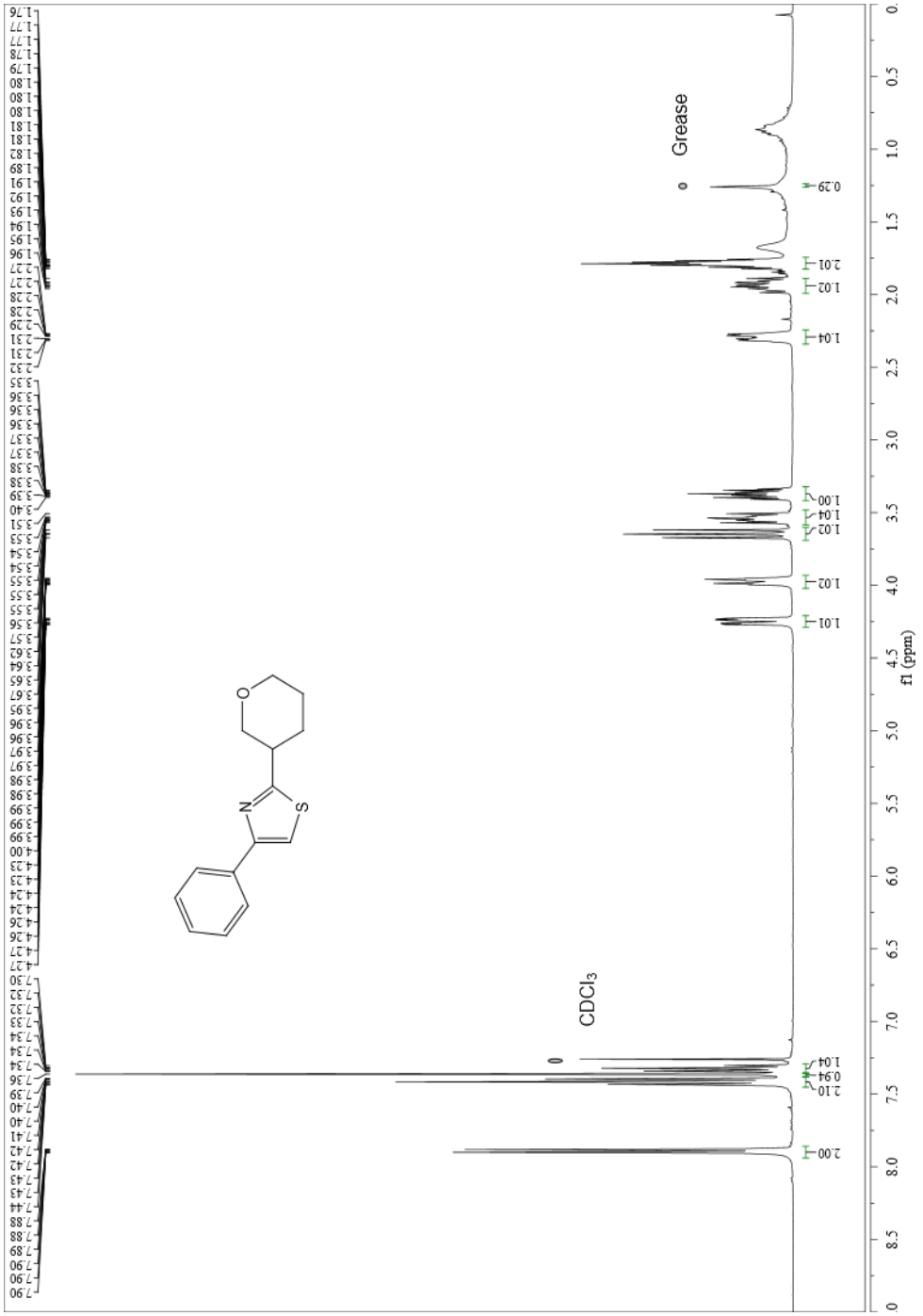

^{13}C NMR (101 MHz, $CDCl_3$) of **3a** 4-phenyl-2-(tetrahydro-2H-pyran-3-yl)thiazole

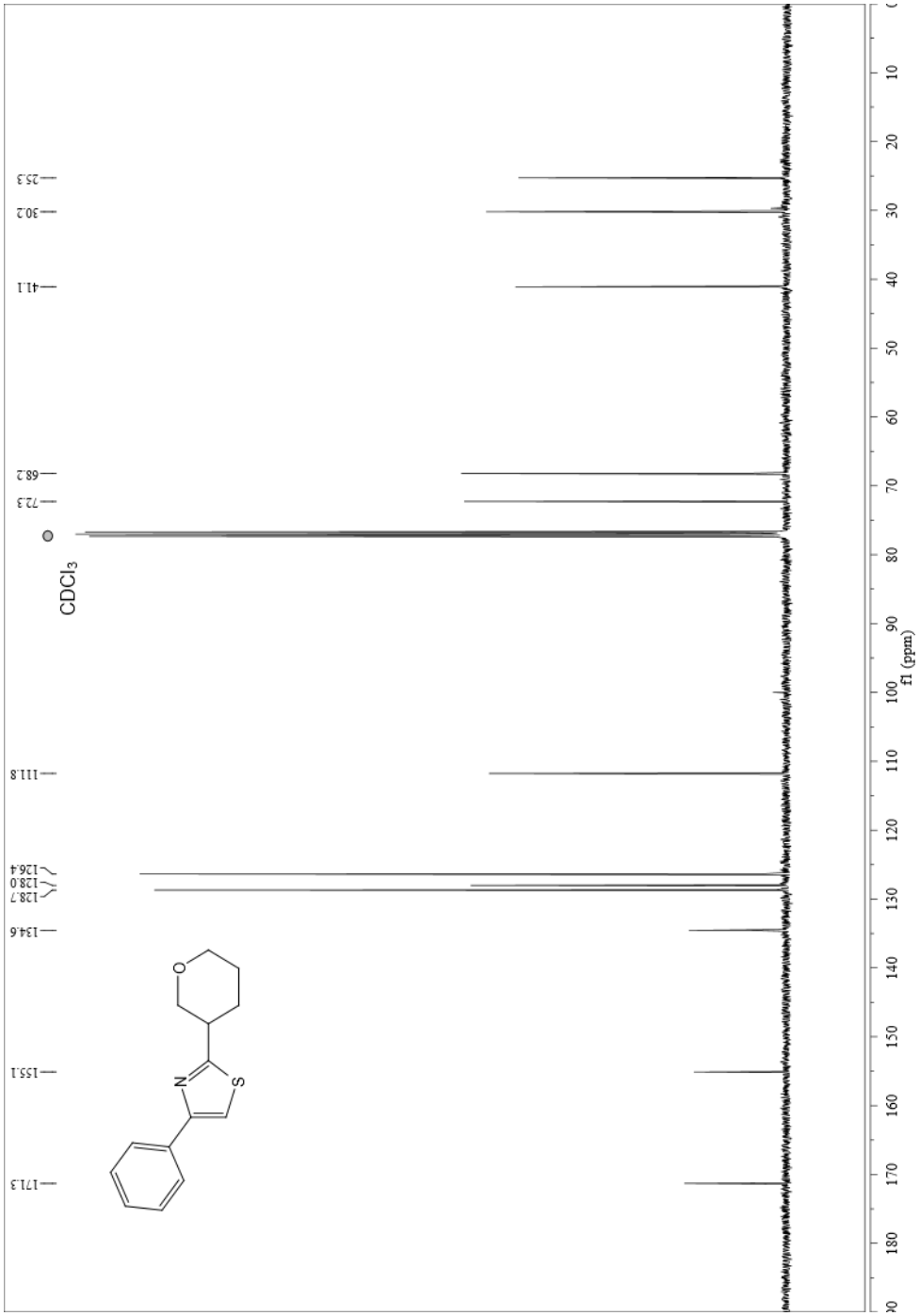

^{1}H NMR (400 MHz, $CDCl_3$) of **4a** ethyl 2-(tetrahydro-2H-pyran-3-yl)thiazole-4-carboxylate

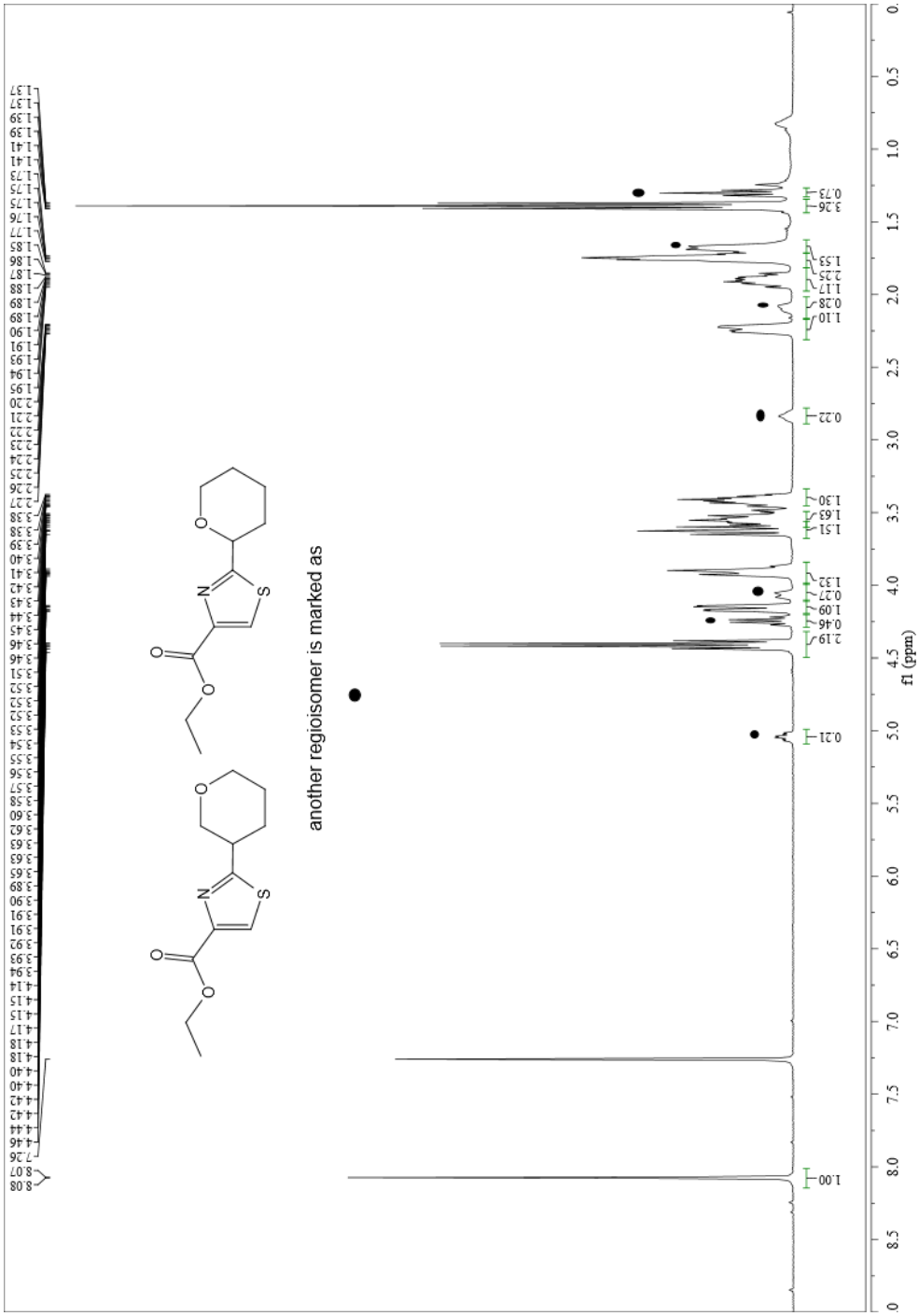

^{13}C NMR (101 MHz, $CDCl_3$) of **4a** ethyl 2-(tetrahydro-2H-pyran-3-yl)thiazole-4-carboxylate

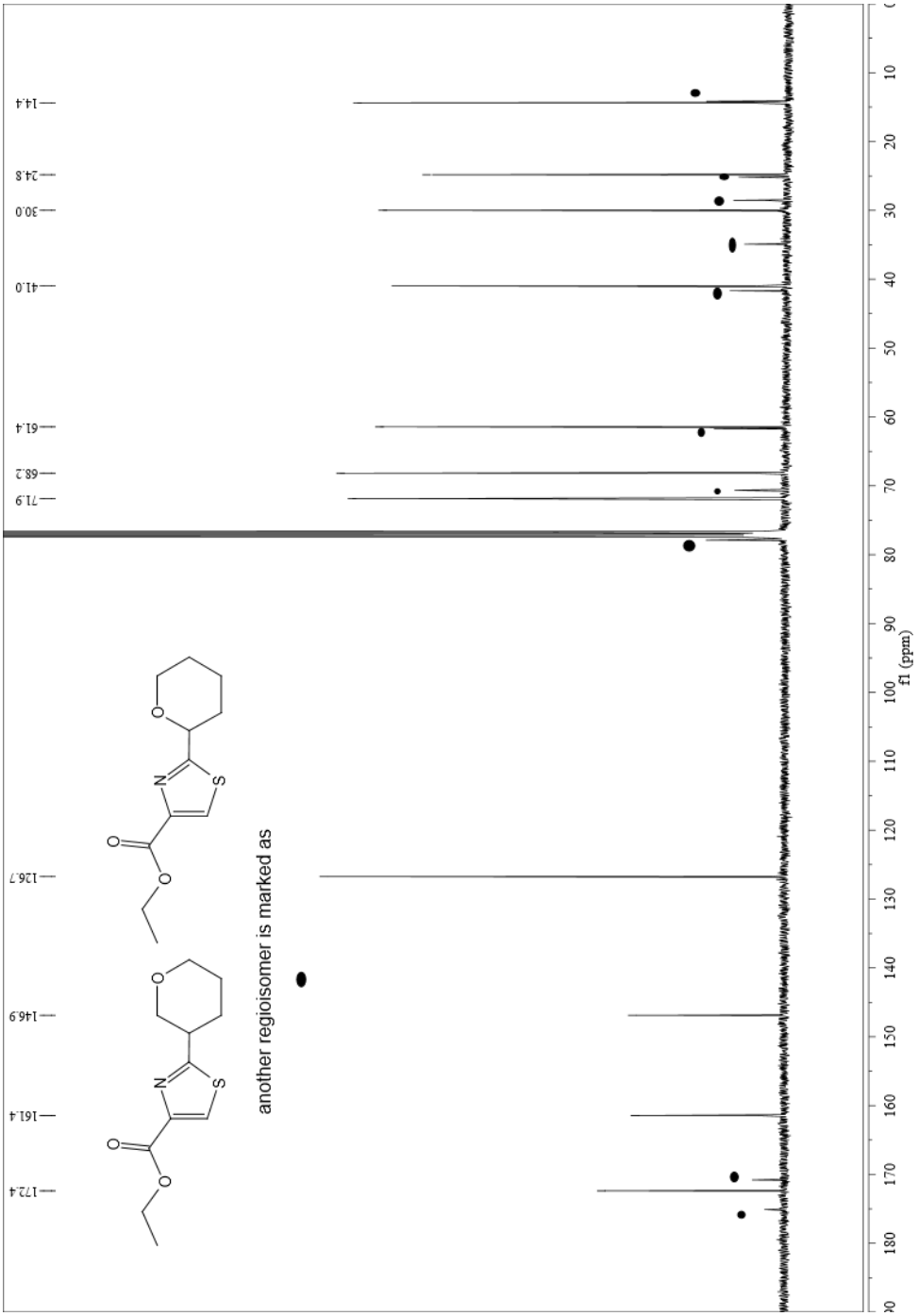

^{1}H NMR (400 MHz, $CDCl_3$) of **5a** 4-bromo-2-(tetrahydro-2H-pyran-3-yl)thiazole

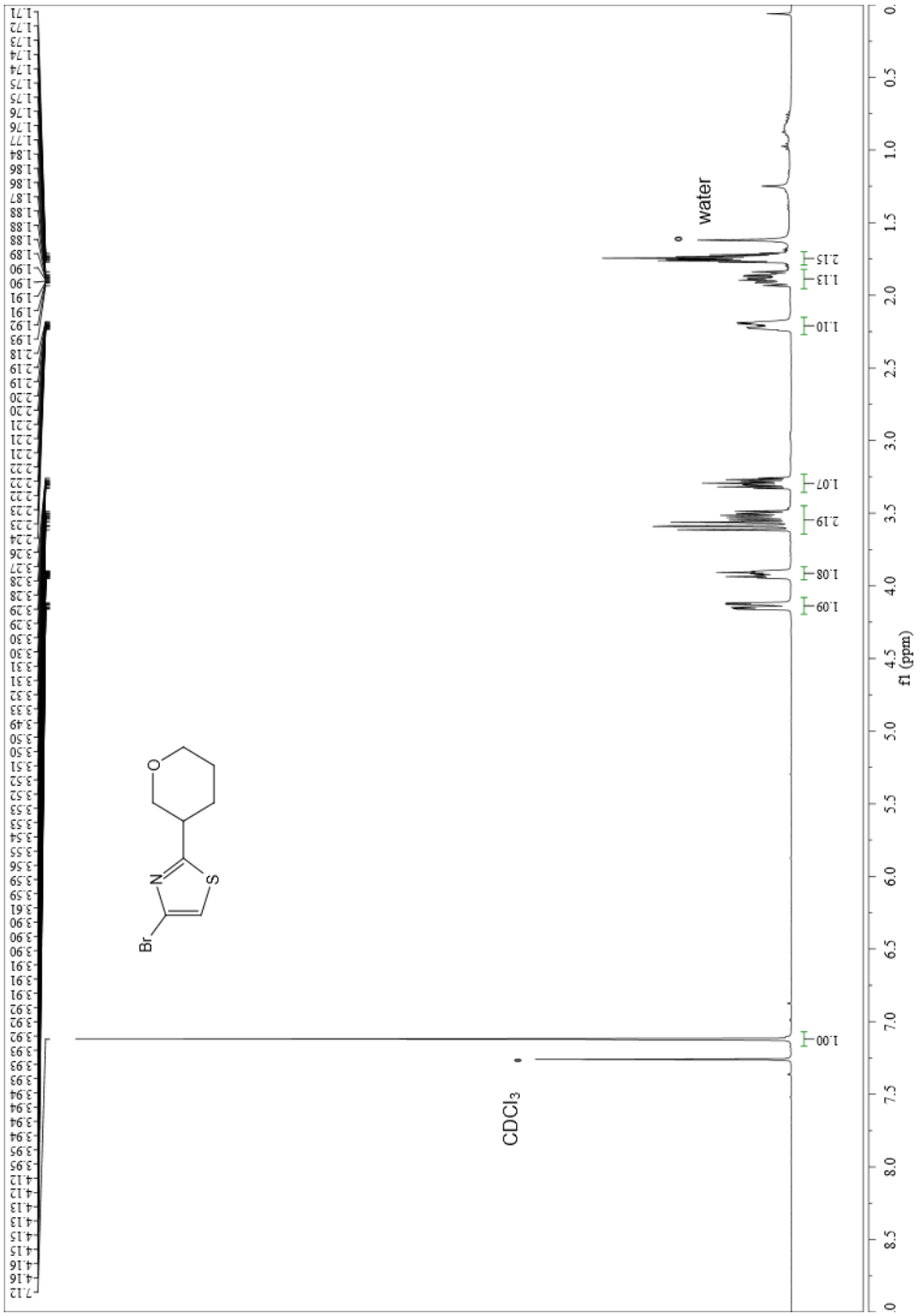

^{13}C NMR (101 MHz, $CDCl_3$) of **5a** 4-bromo-2-(tetrahydro-2H-pyran-3-yl)thiazole

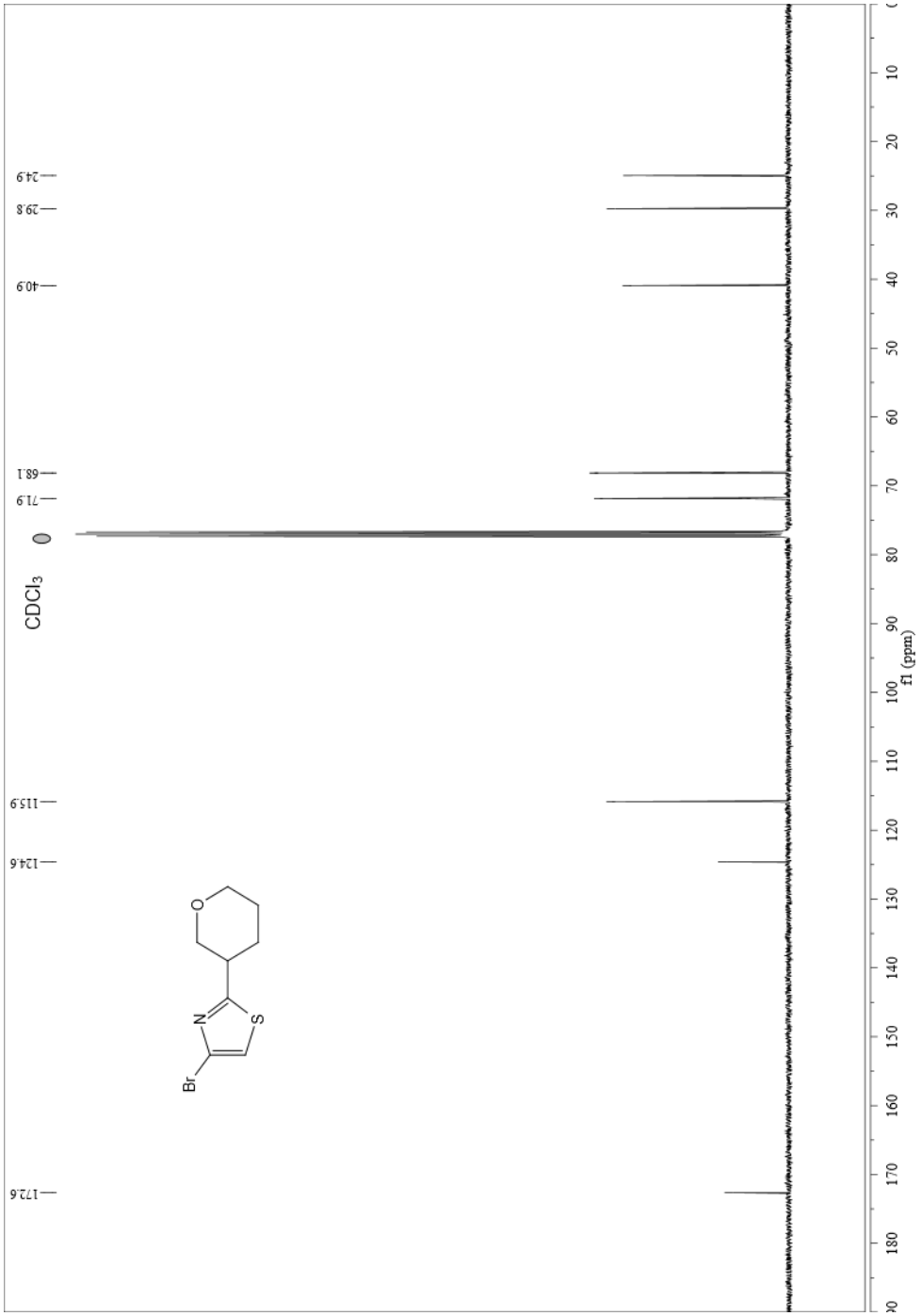

^{1}H NMR (400 MHz, $CDCl_3$) of **6a** 5-bromo-4-methyl-2-(tetrahydro-2H-pyran-3-yl)thiazole

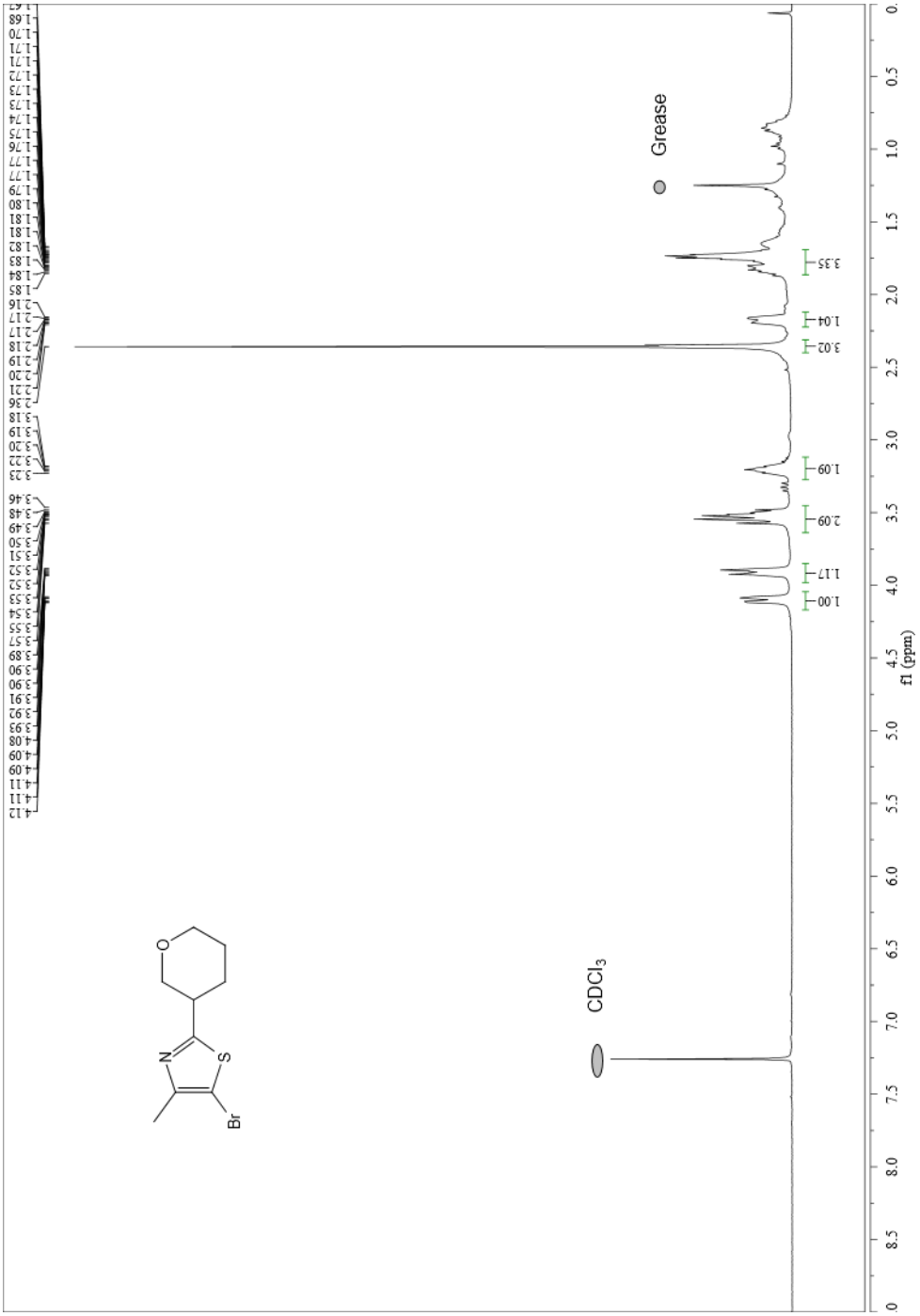

^{13}C NMR (101 MHz, $CDCl_3$) of **6a** 5-bromo-4-methyl-2-(tetrahydro-2H-pyran-3-yl)thiazol

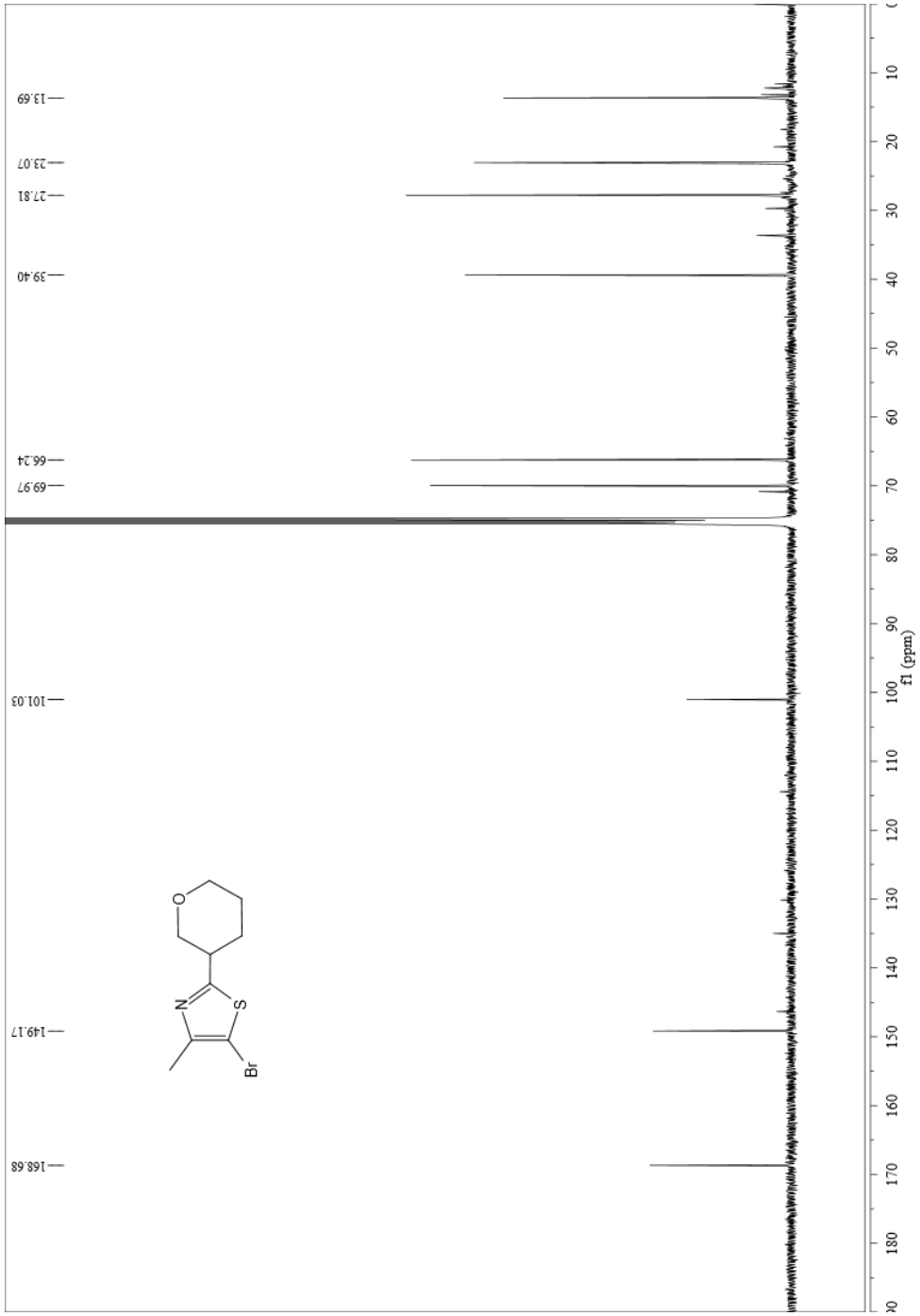

^{1}H NMR (400 MHz, $CDCl_3$) of **7a** 2-(tetrahydro-2H-pyran-3-yl)benzo[d]thiazole

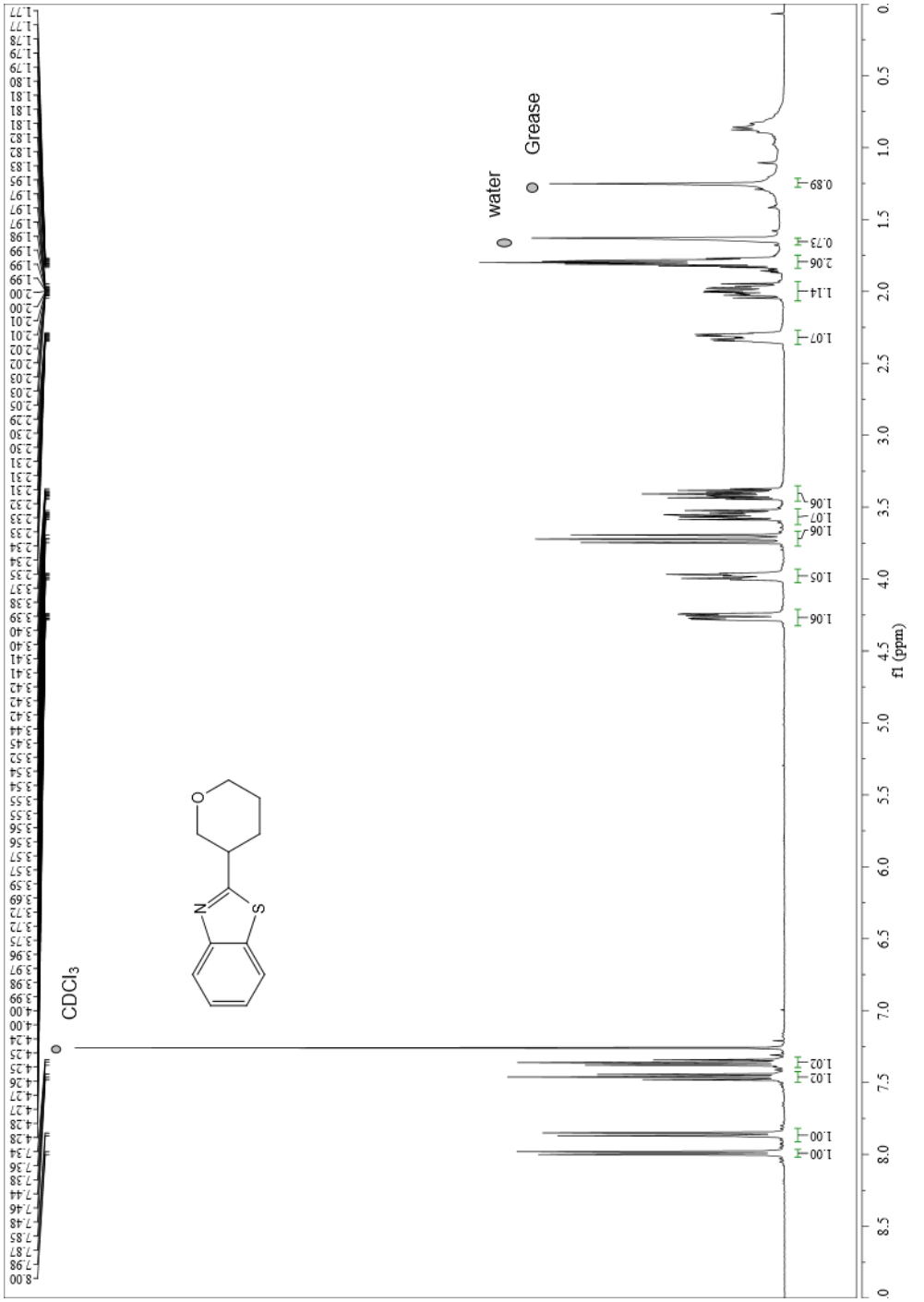

^{13}C NMR (101 MHz, $CDCl_3$) of **7a** 2-(tetrahydro-2H-pyran-3-yl)benzo[d]thiazole

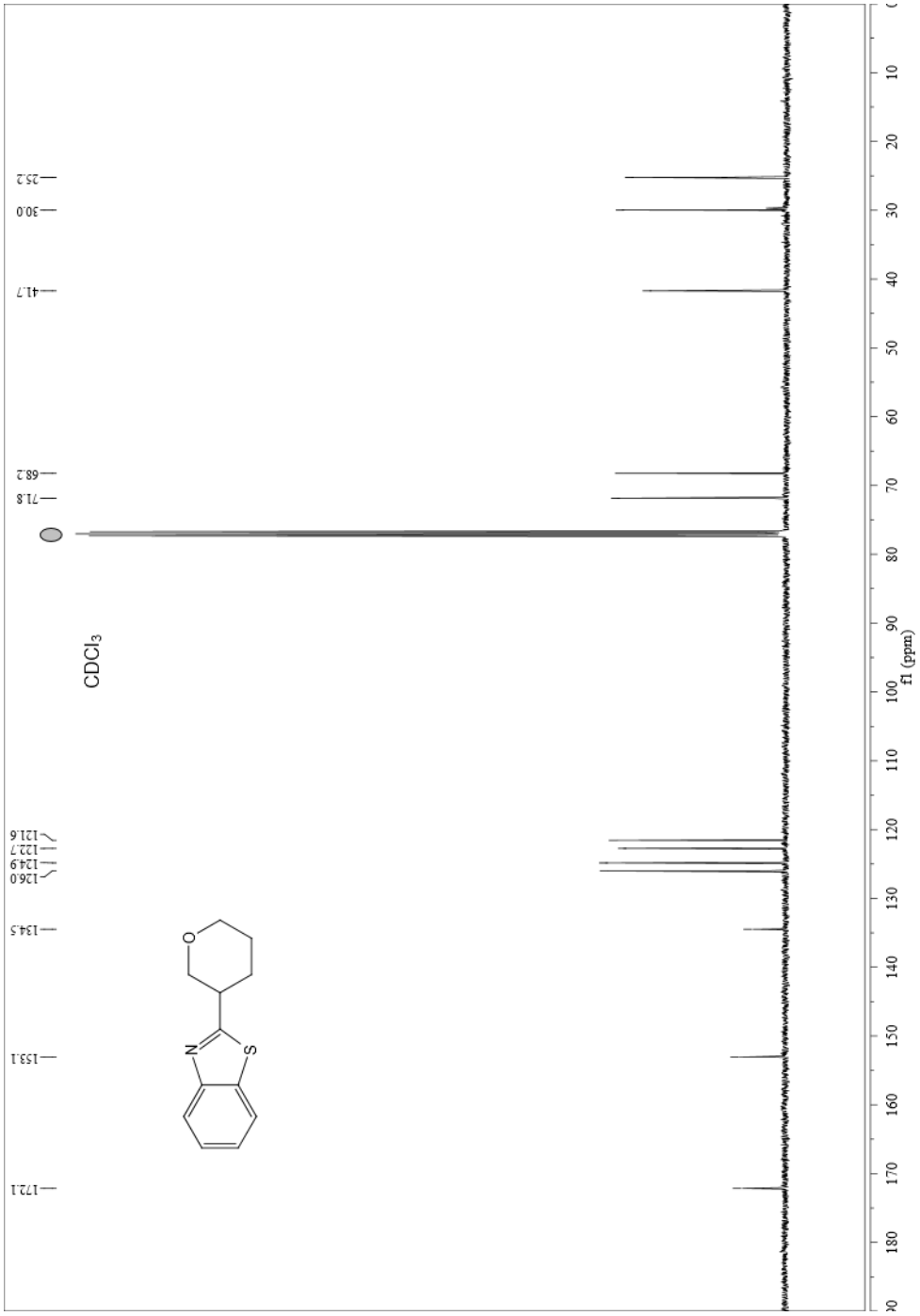

^{1}H NMR (400 MHz, $CDCl_3$) of **8a** 4-chloro-2-(tetrahydro-2H-pyran-3-yl)benzo[d]thiazole

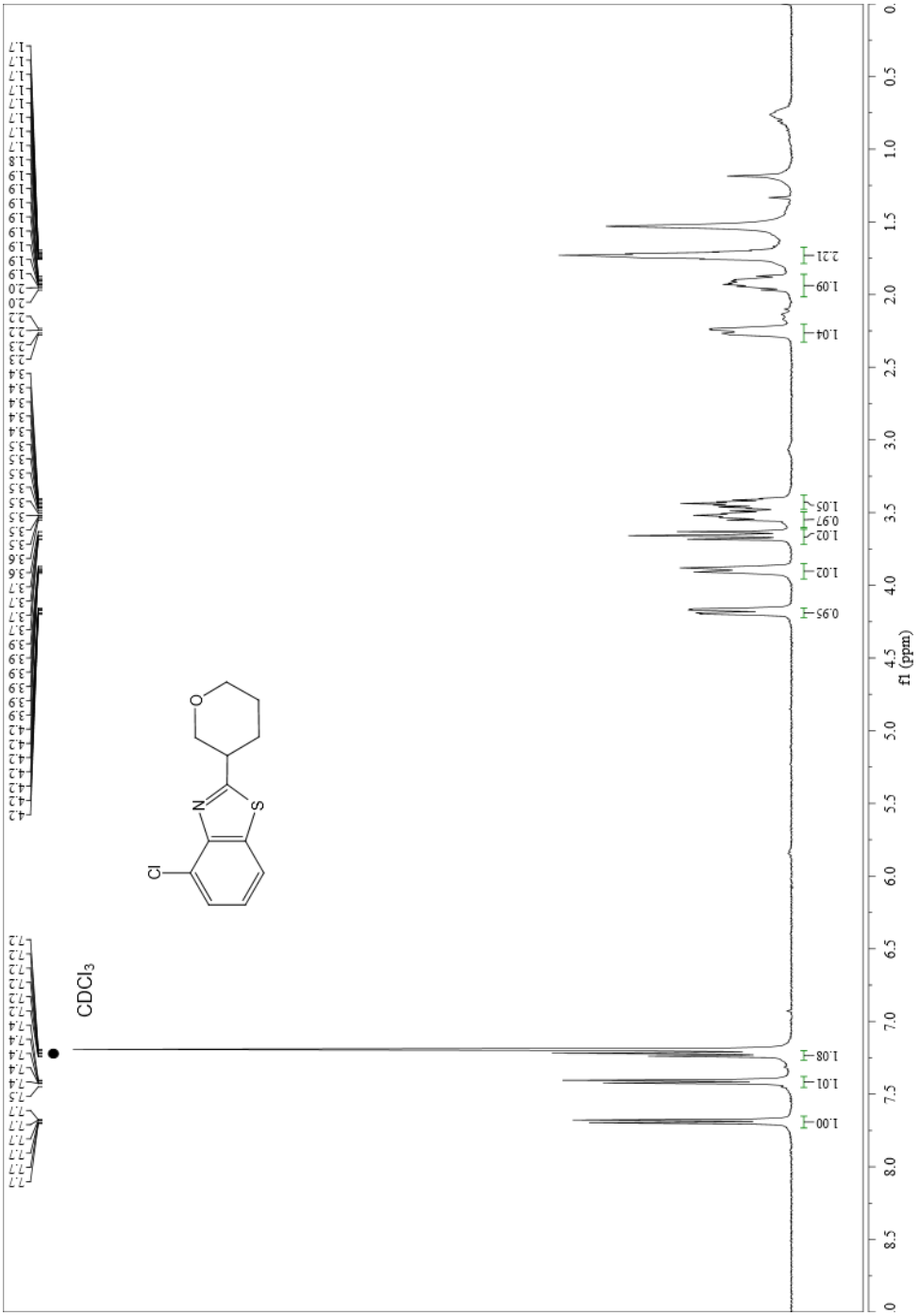

^{13}C NMR (101 MHz, $CDCl_3$) of **8a** 4-chloro-2-(tetrahydro-2H-pyran-3-yl)benzo[d]thiaz

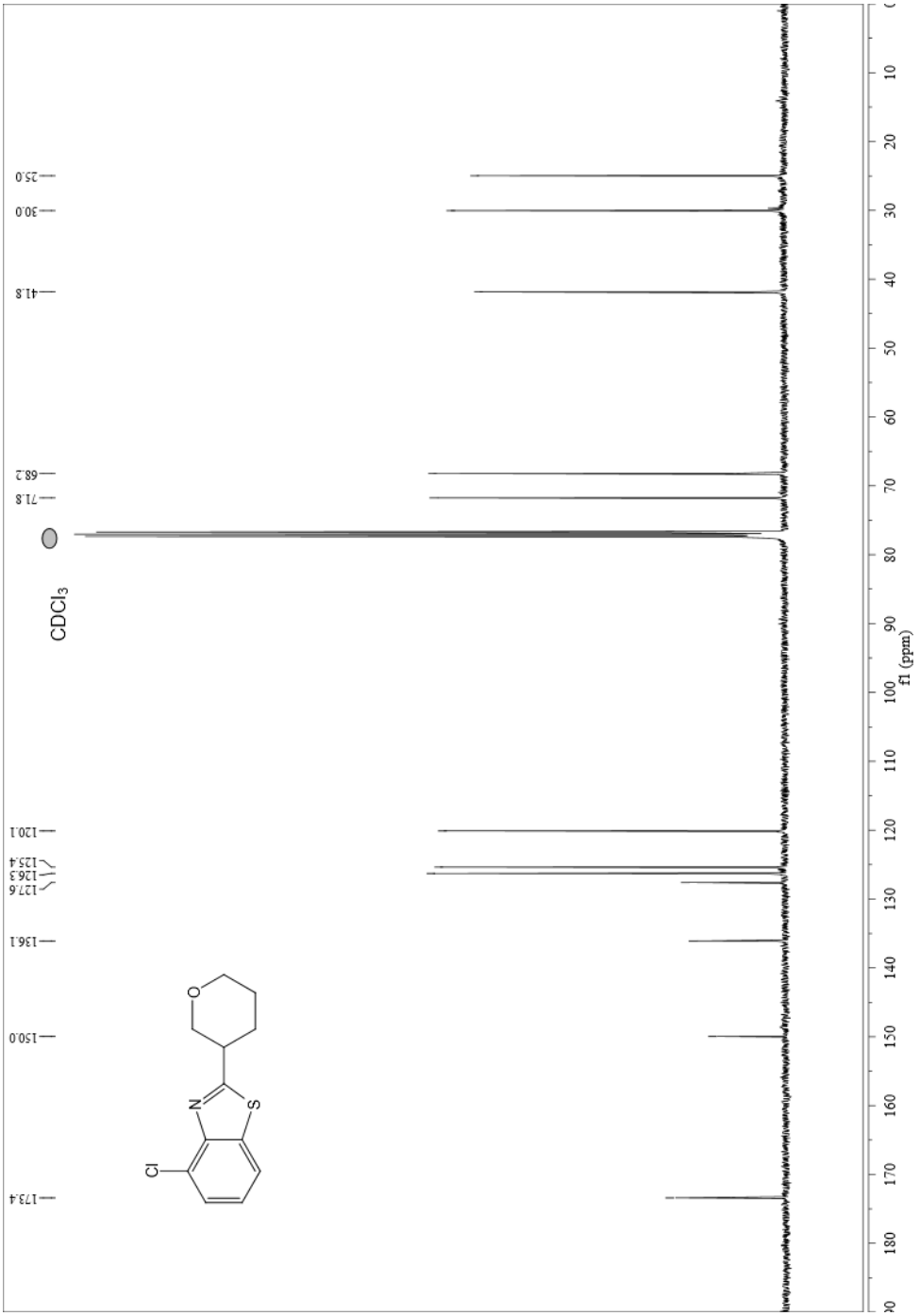

^{1}H NMR (400 MHz, $CDCl_3$) of **9a** 4,6-difluoro-2-(tetrahydro-2H-pyran-3-yl)benzo[d]thiazole

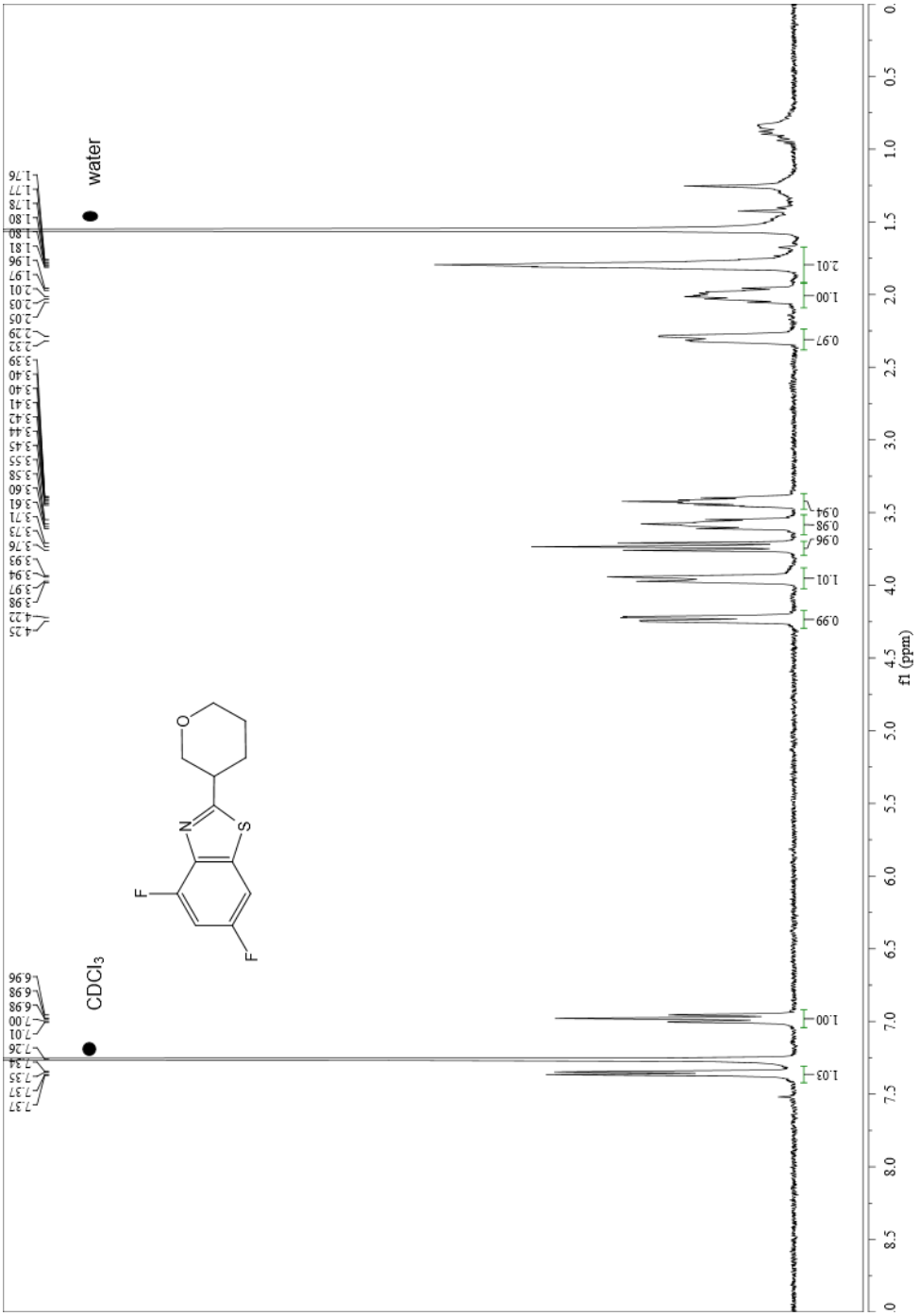

^{13}C NMR (101 MHz, $CDCl_3$) of **9a** 4,6-difluoro-2-(tetrahydro-2H-pyran-3-yl)benzo[d]thiazole

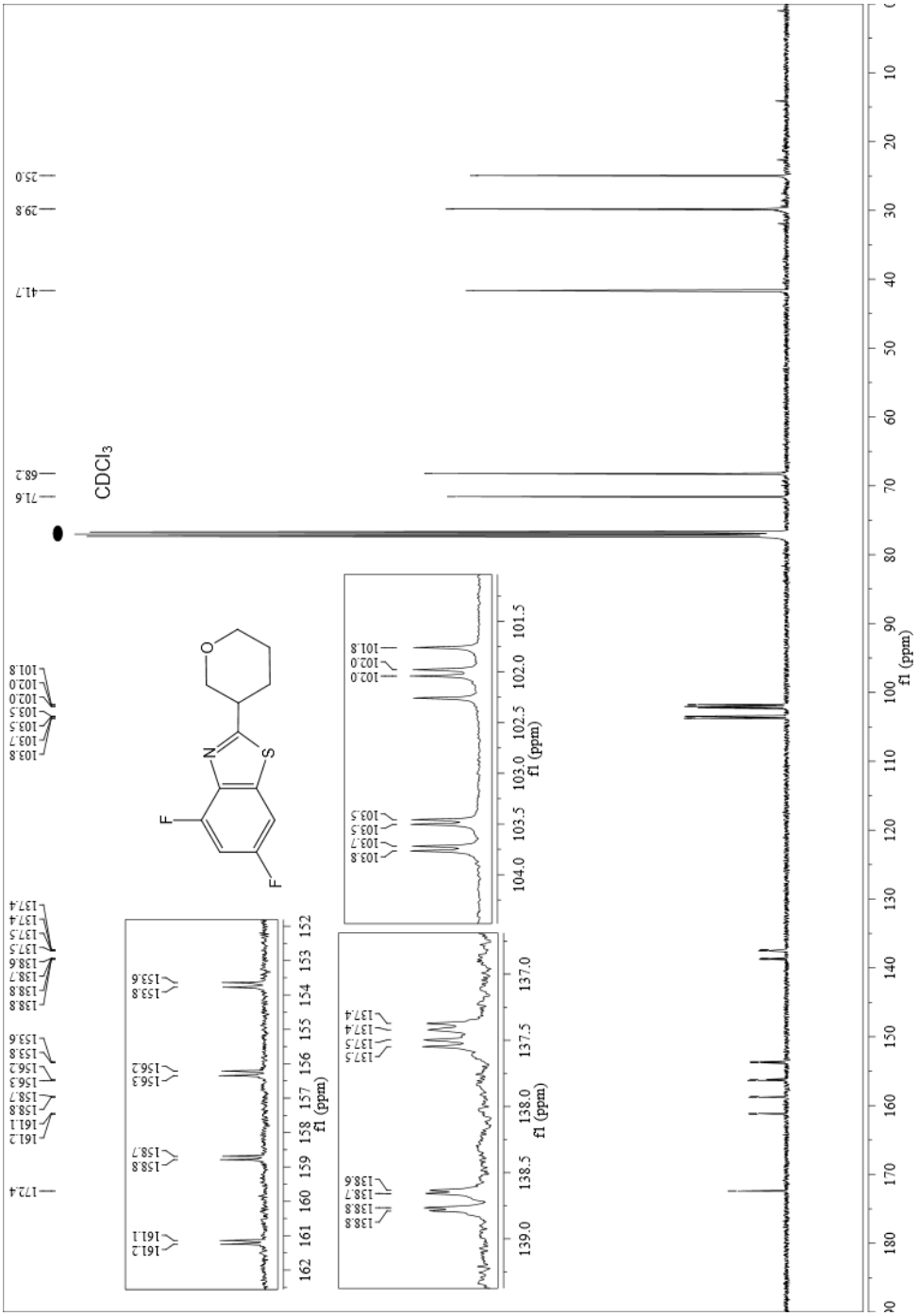

^{19}F NMR (376 MHz, $CDCl_3$) of **9a** 4,6-difluoro-2-(tetrahydro-2H-pyran-3-yl)benzo[d]thiazol

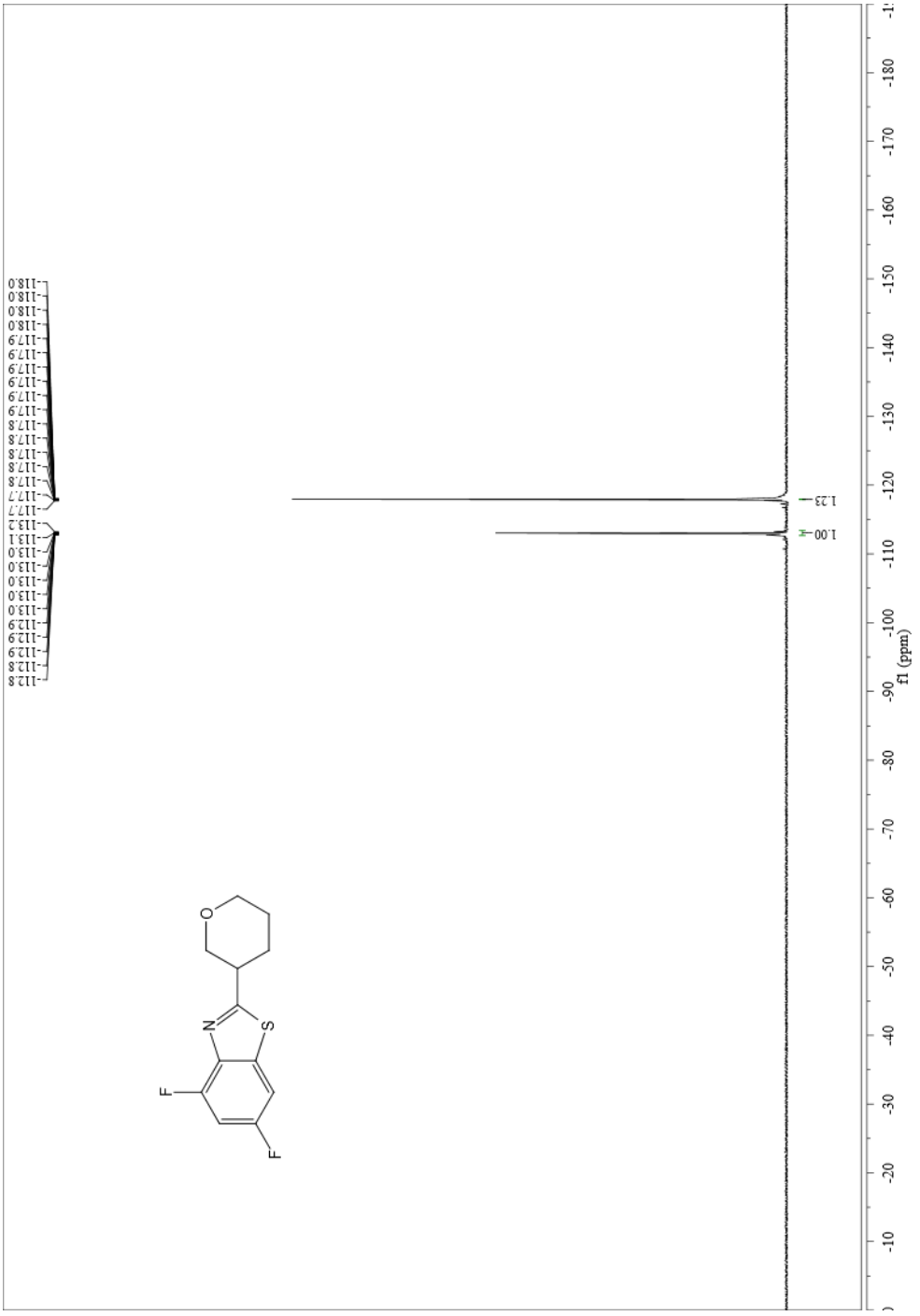

^{1}H NMR (400 MHz, CD_3OD) of **10a** 2-(tetrahydro-2H-pyran-3-yl)-1H-benzo[d]imidazole

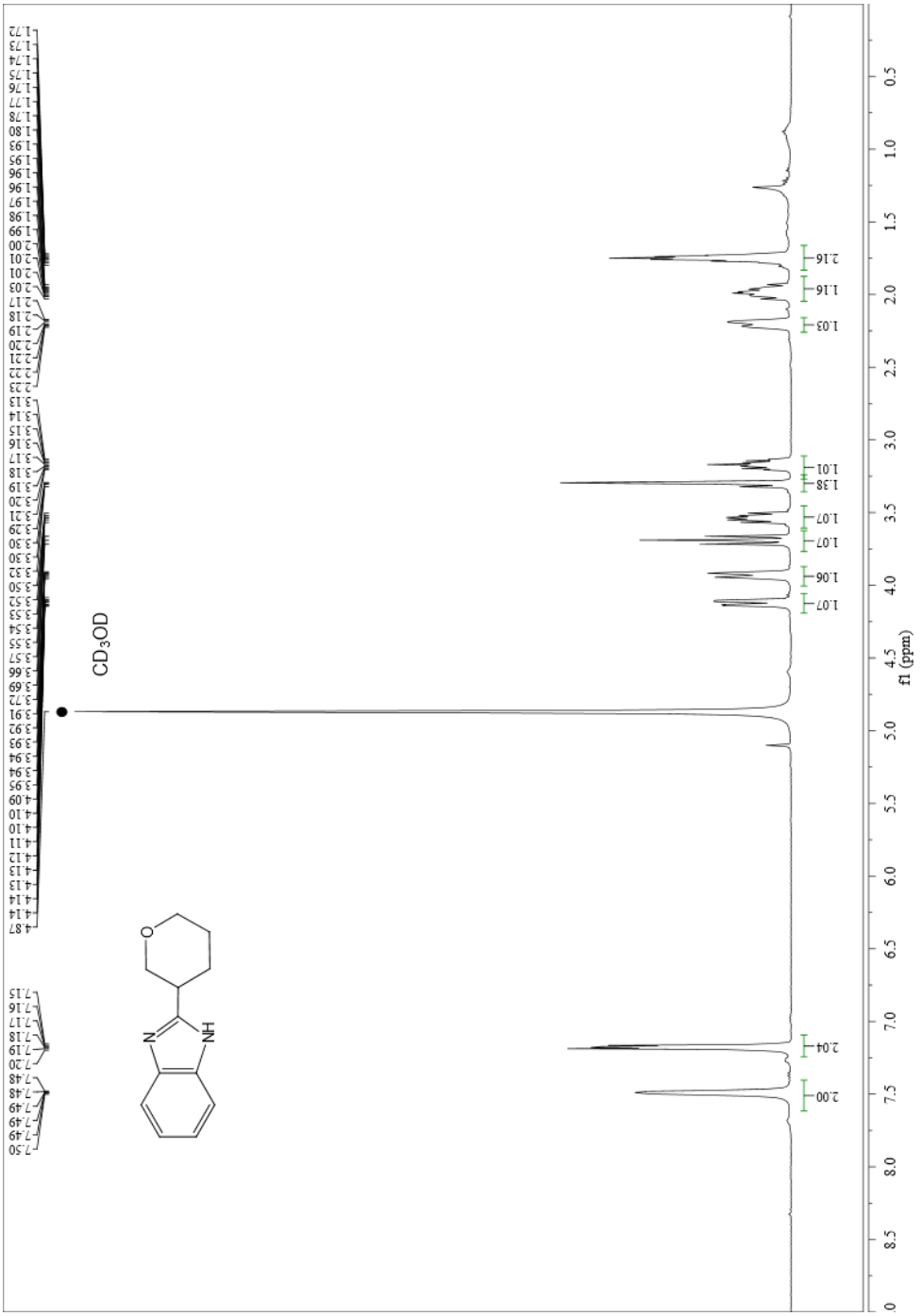

^{13}C NMR (101 MHz, CD_3OD) of **10a** 2-(tetrahydro-2H-pyran-3-yl)-1H-benzo[d]imidazole

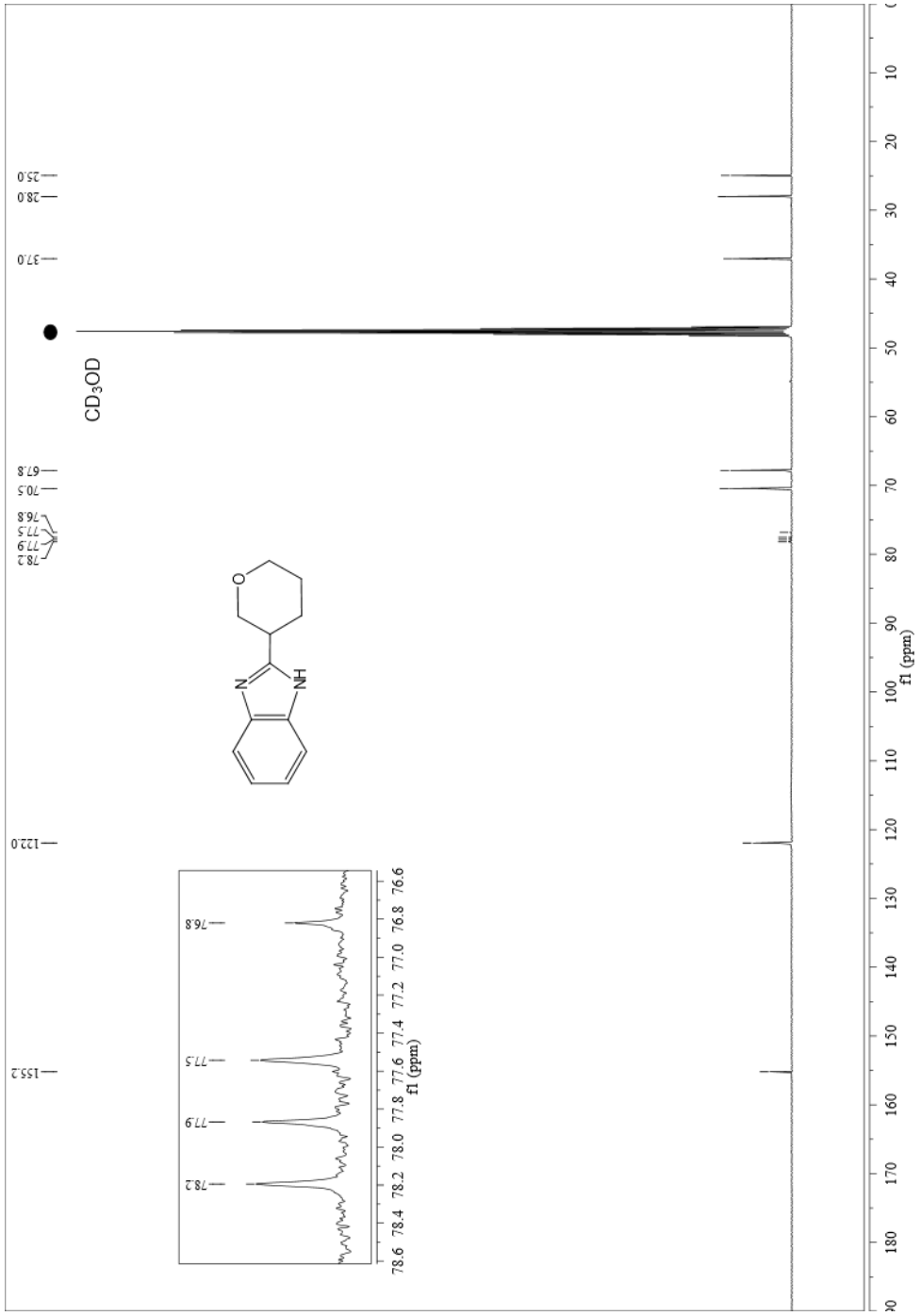

^{1}H NMR (400 MHz, $CDCl_3$) of **12a** 3-methyl-2-(thiazol-2-yl)butan-1-ol

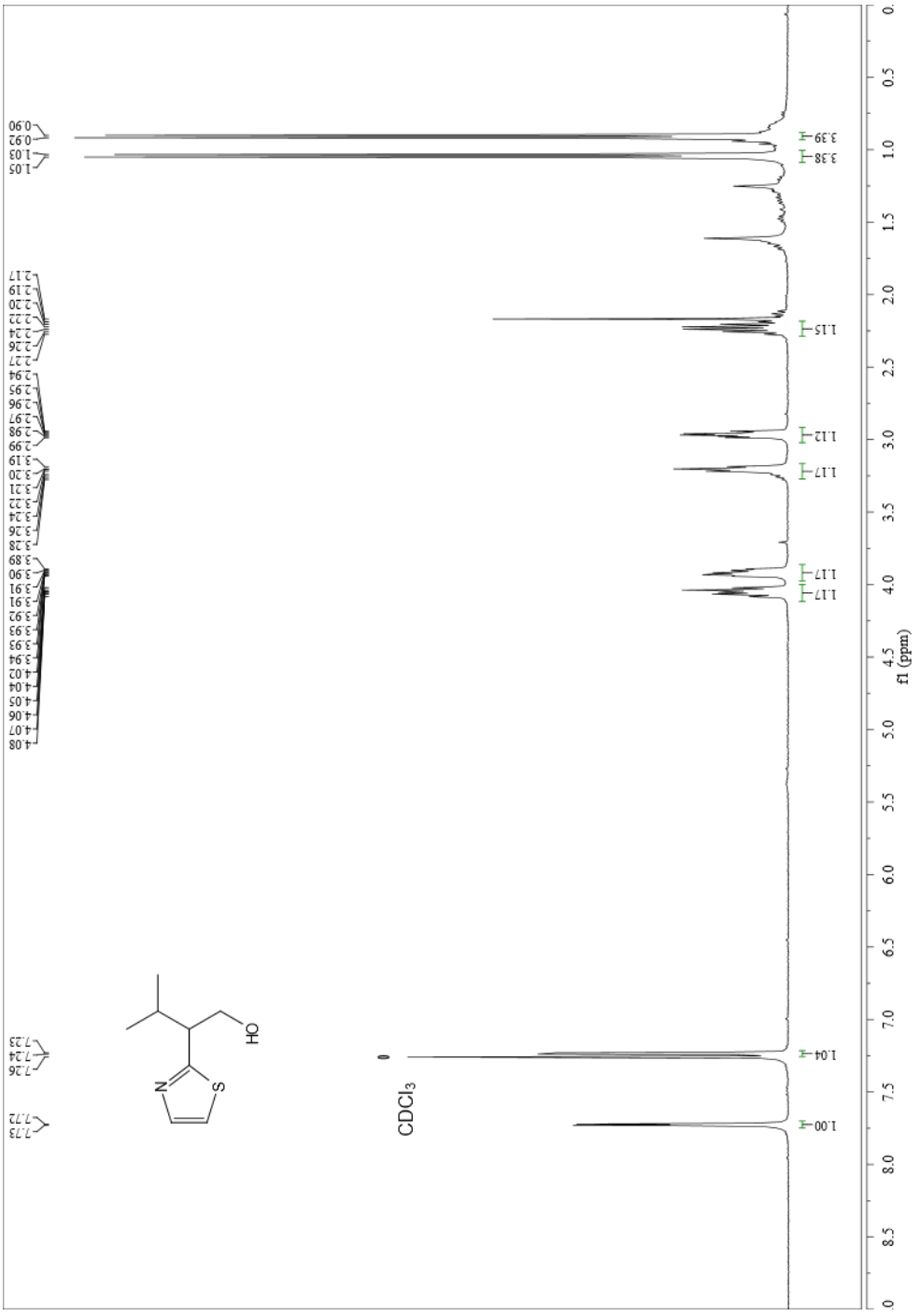

^{13}C NMR (101 MHz, $CDCl_3$) of **12a** 3-methyl-2-(thiazol-2-yl)butan-1-ol

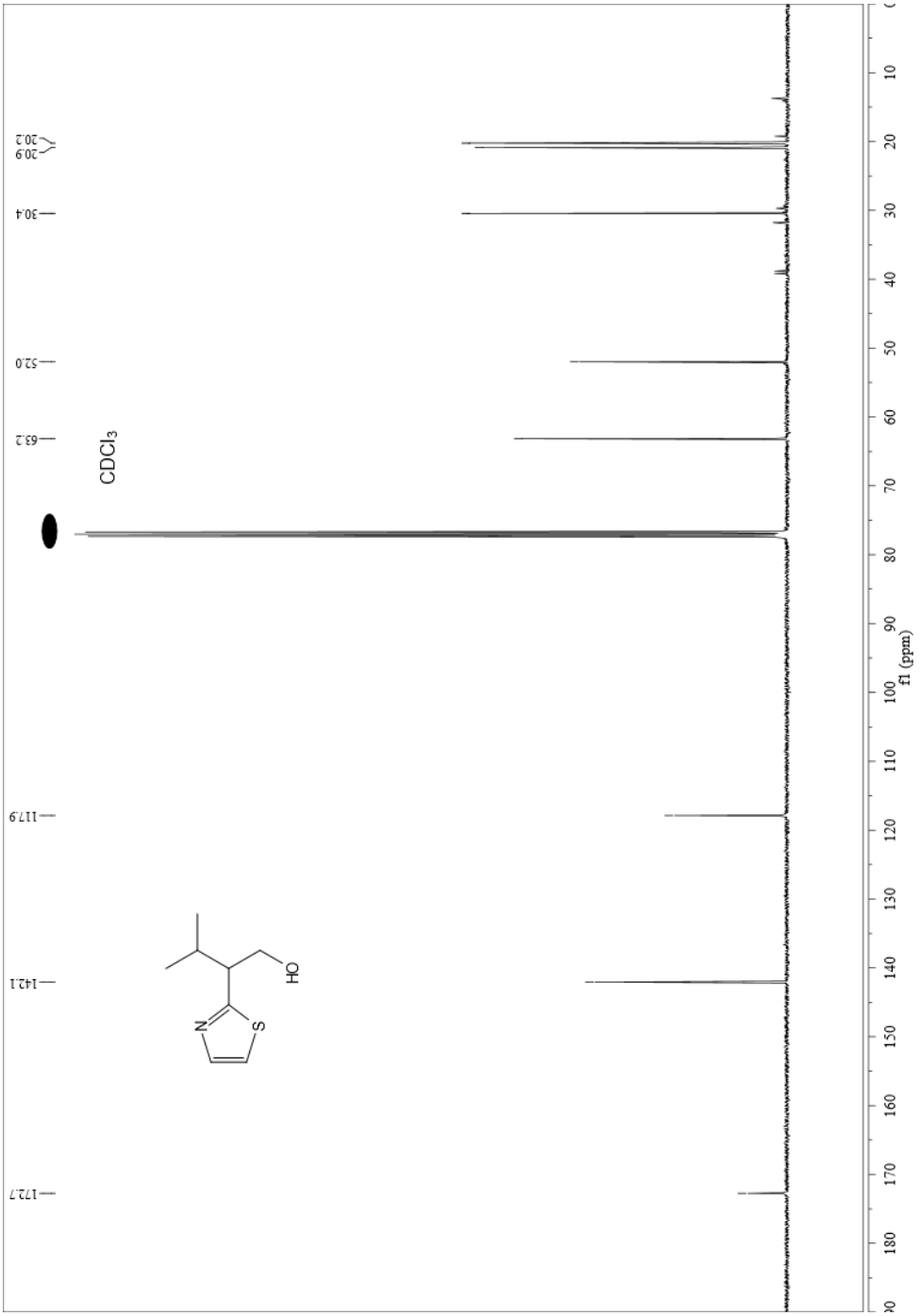

^{1}H NMR (400 MHz, $CDCl_3$) of **13a** 2-(5-((tetrahydro-2H-pyran-2-yl)oxy)pentyl)thiazole

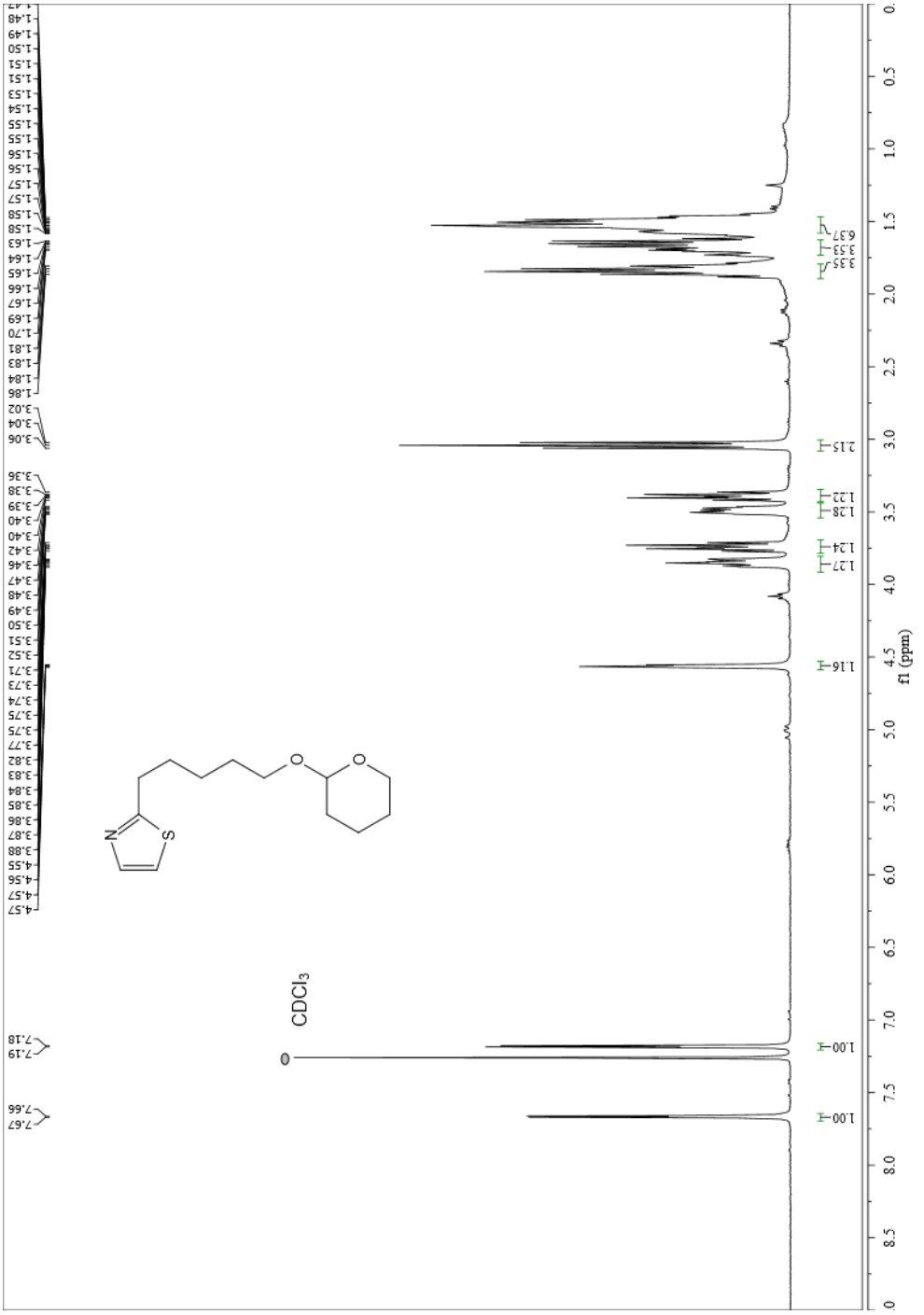

^{13}C NMR (101 MHz, $CDCl_3$) of **13a** 2-(5-((tetrahydro-2H-pyran-2-yl)oxy)pentyl)thiazole

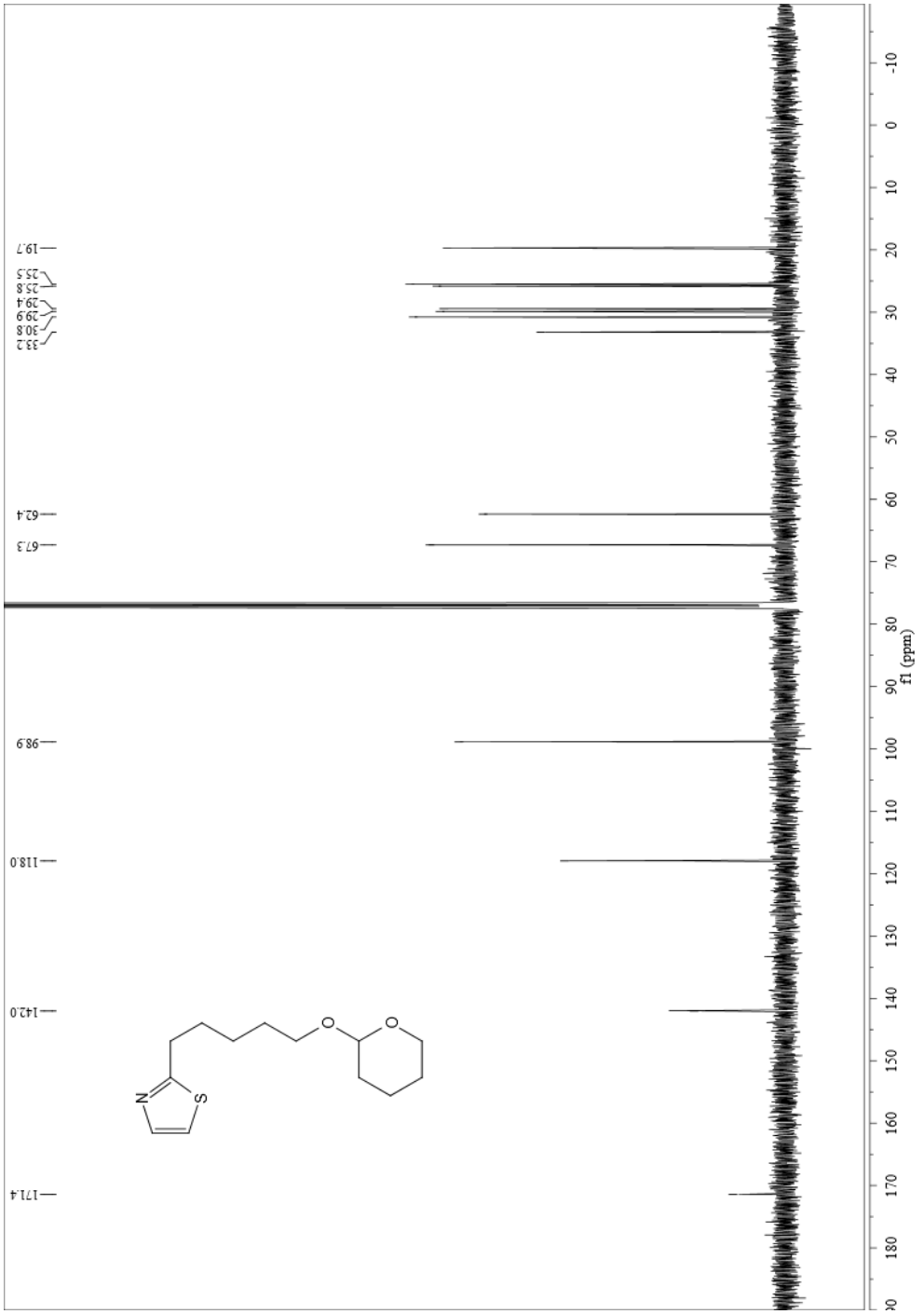

^{1}H NMR (400 MHz, $CDCl_3$) of **14a** 2-(2-phenylcyclohexyl)thiazole

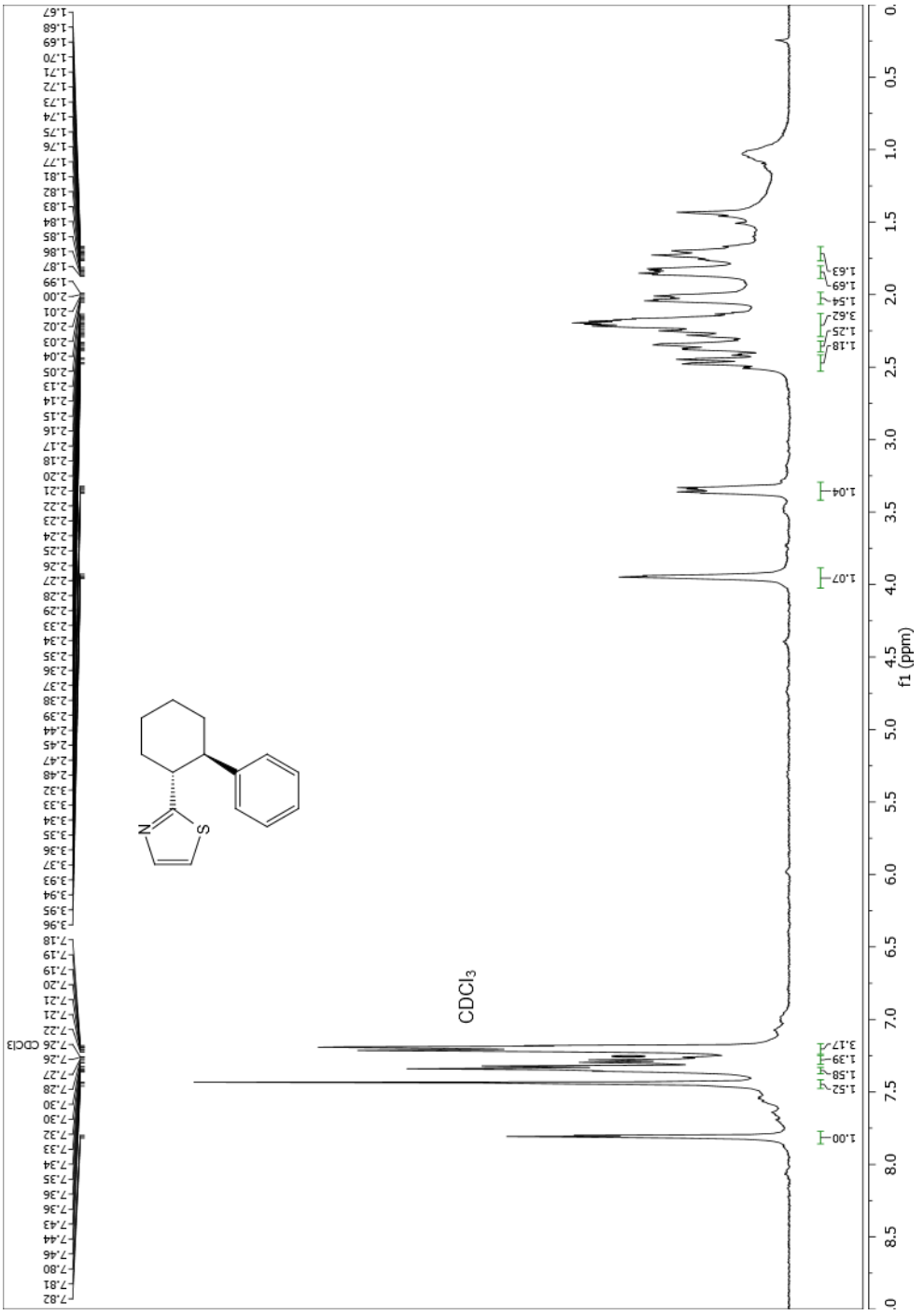

^{13}C NMR (101 MHz, $CDCl_3$) of **14a** 2-(2-phenylcyclohexyl)thiazole

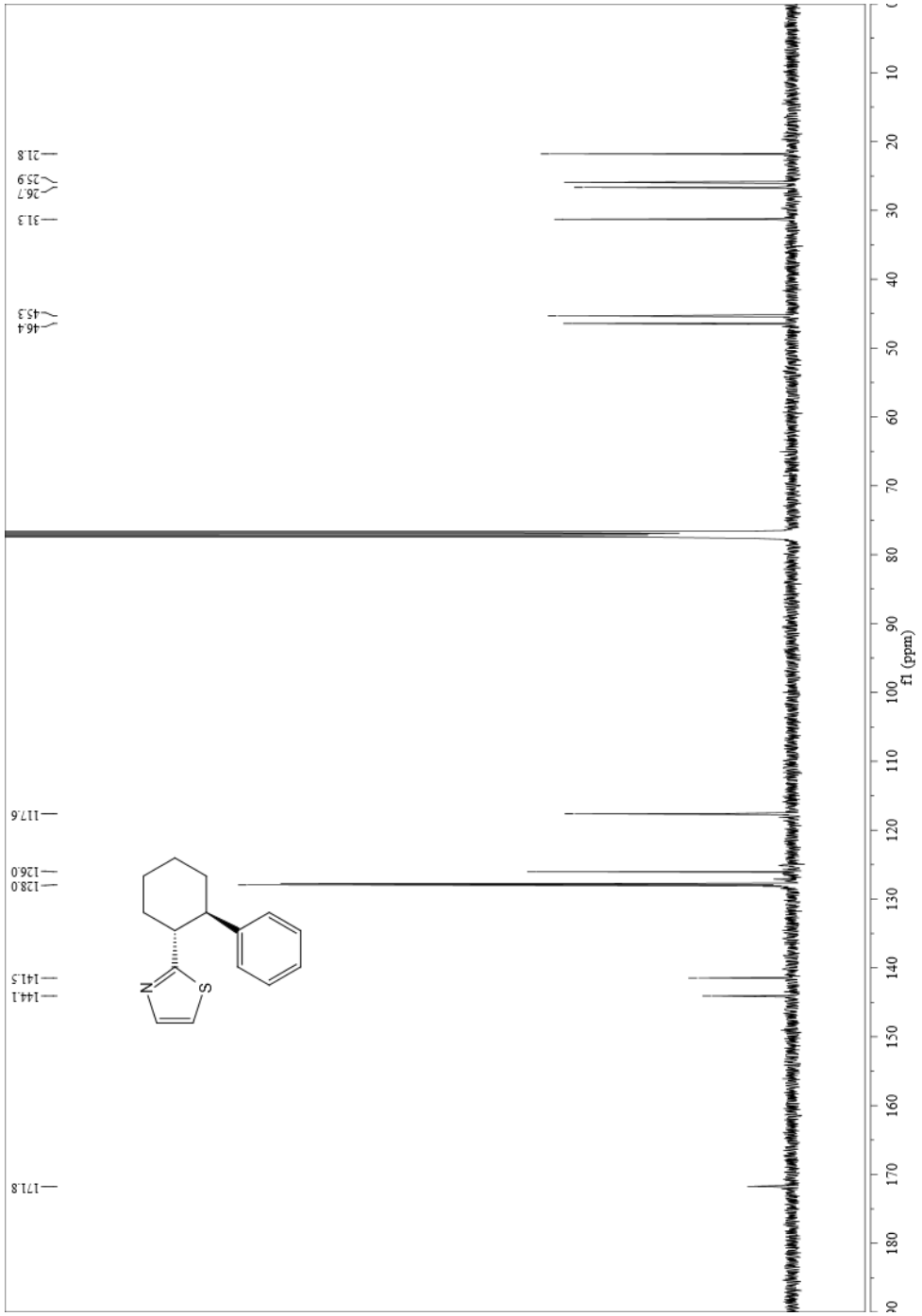

^{1}H NMR of **15a** (Diastereomer a) 2-(tetrahydro-2H-pyran-3-yl)benzo[d]thiazole

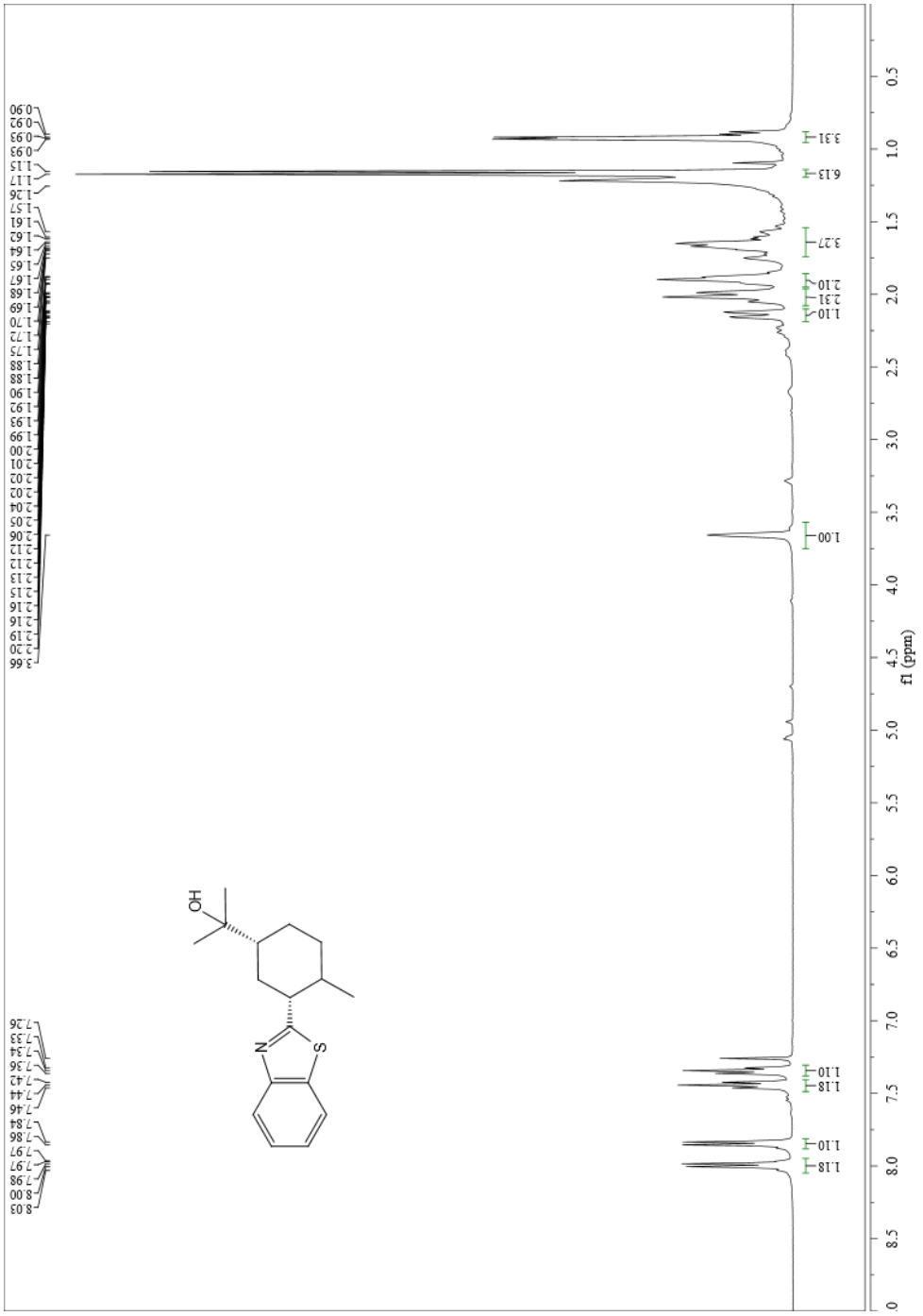

^{13}C NMR of **15a** (Diastereomer a) 2-(tetrahydro-2H-pyran-3-yl)benzo[d]thiazole

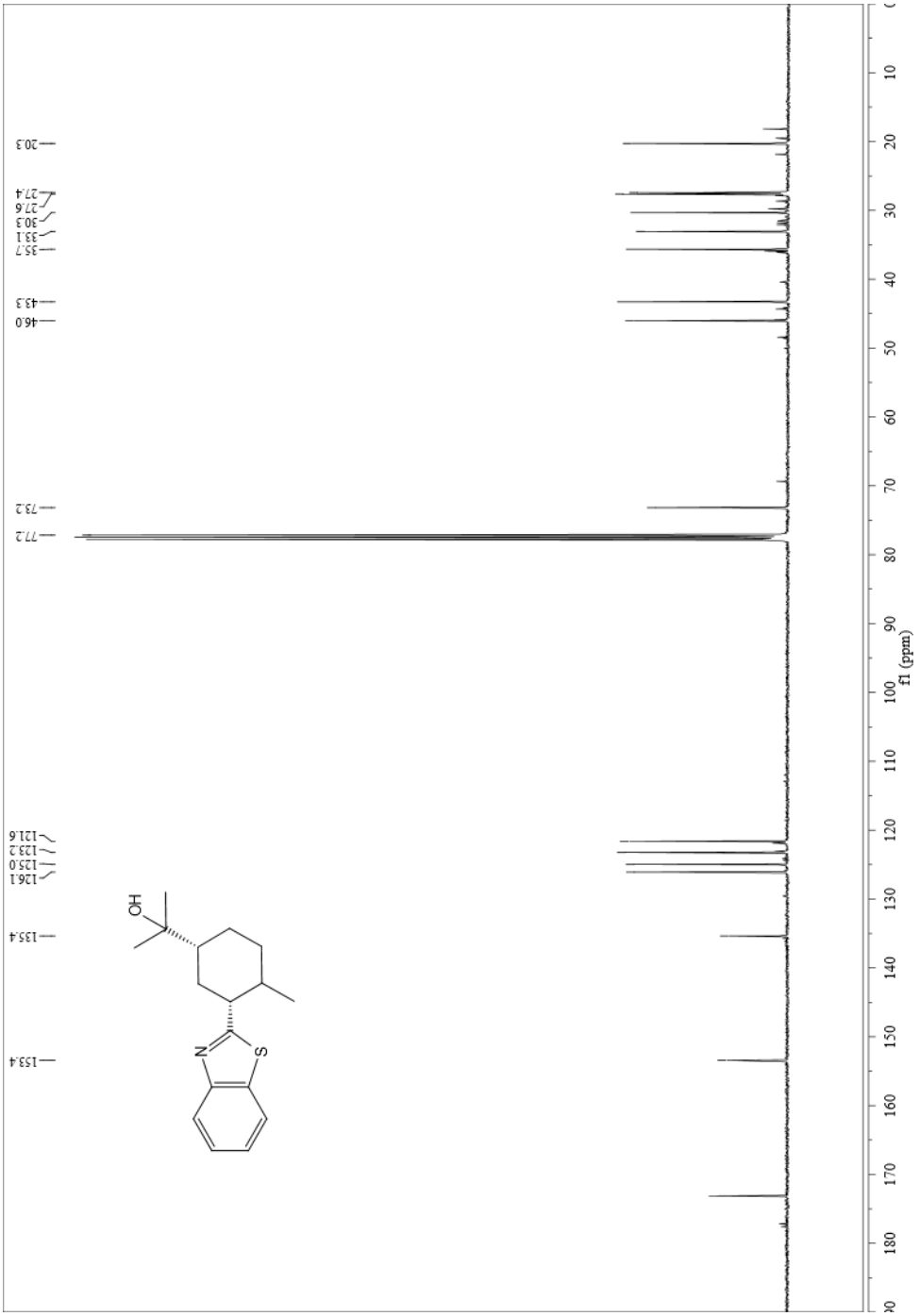

^{1}H NMR of **15a** (Diastereomer b) 2-(tetrahydro-2H-pyran-3-yl)benzo[d]thiazole

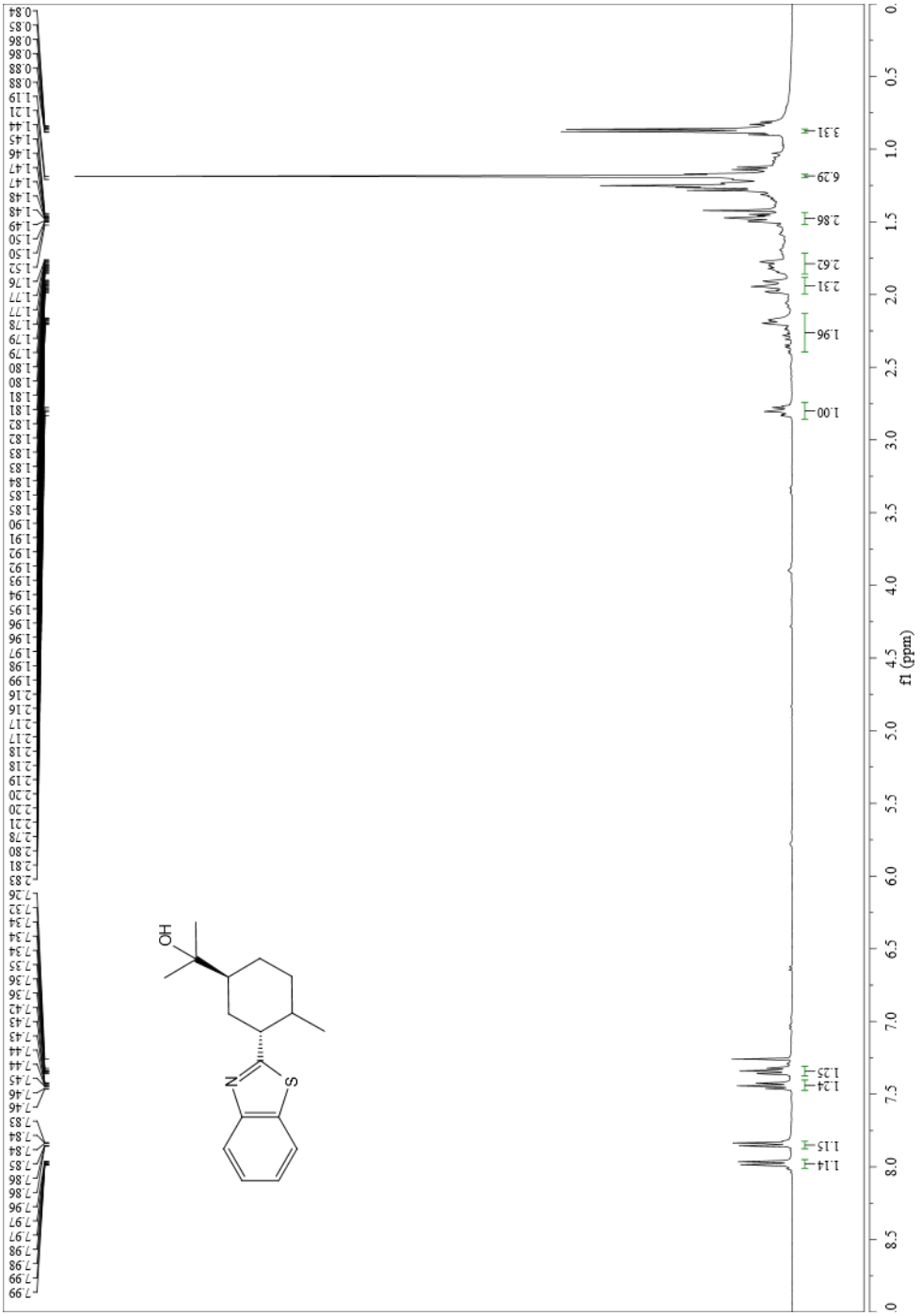

^{13}C NMR (101 MHz, $CDCl_3$) of **15a** (Diastereomer b) 2-(tetrahydro-2H-pyran-3-yl)benzo[d]thia

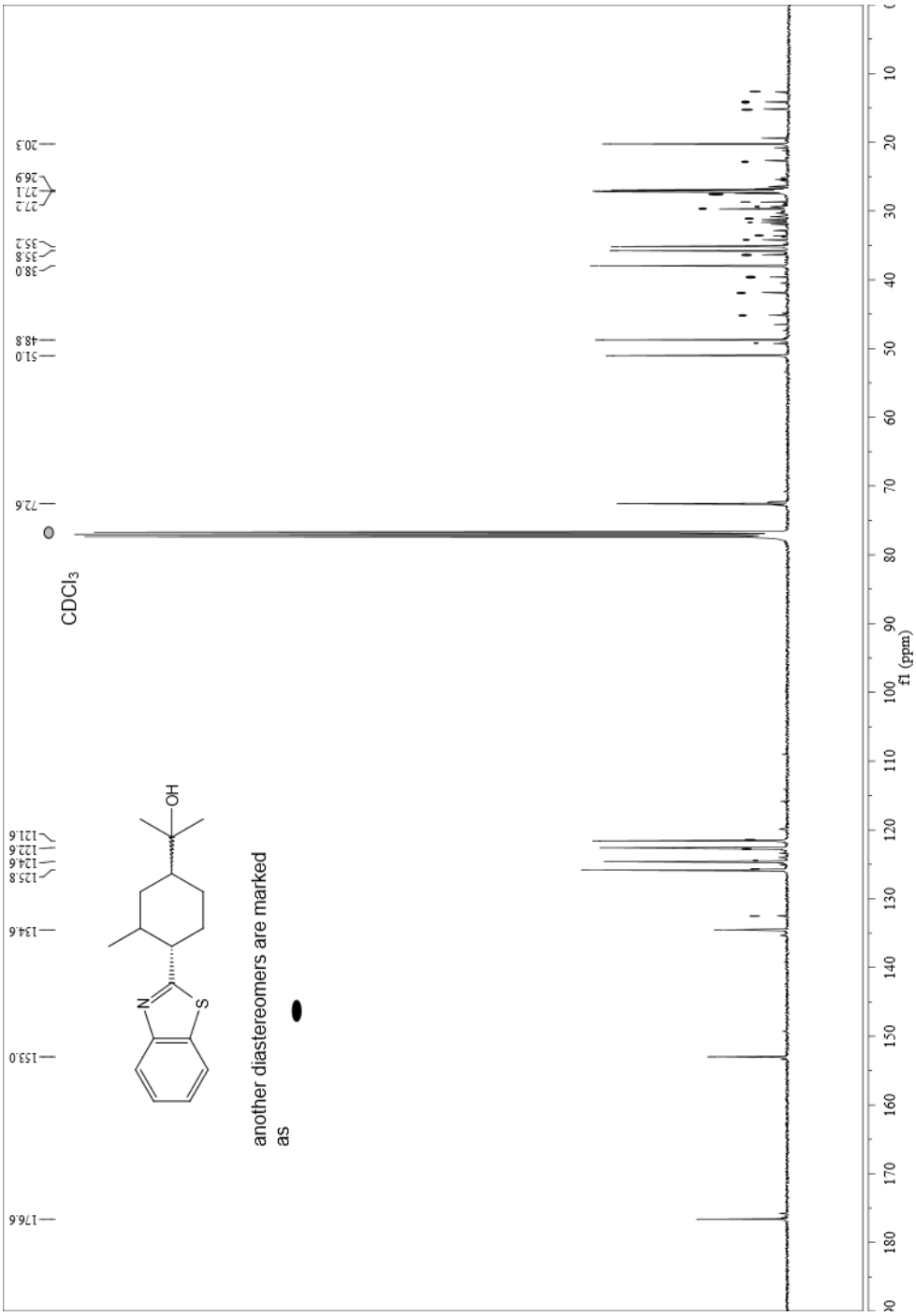

^{1}H NMR (400 MHz, $CDCl_3$) of **16a** (1R,2R,5R)-2-((R)-1-(benzo[d]thiazol-2-yl)propan-2-yl)-5-methylcyclohexyl acetate

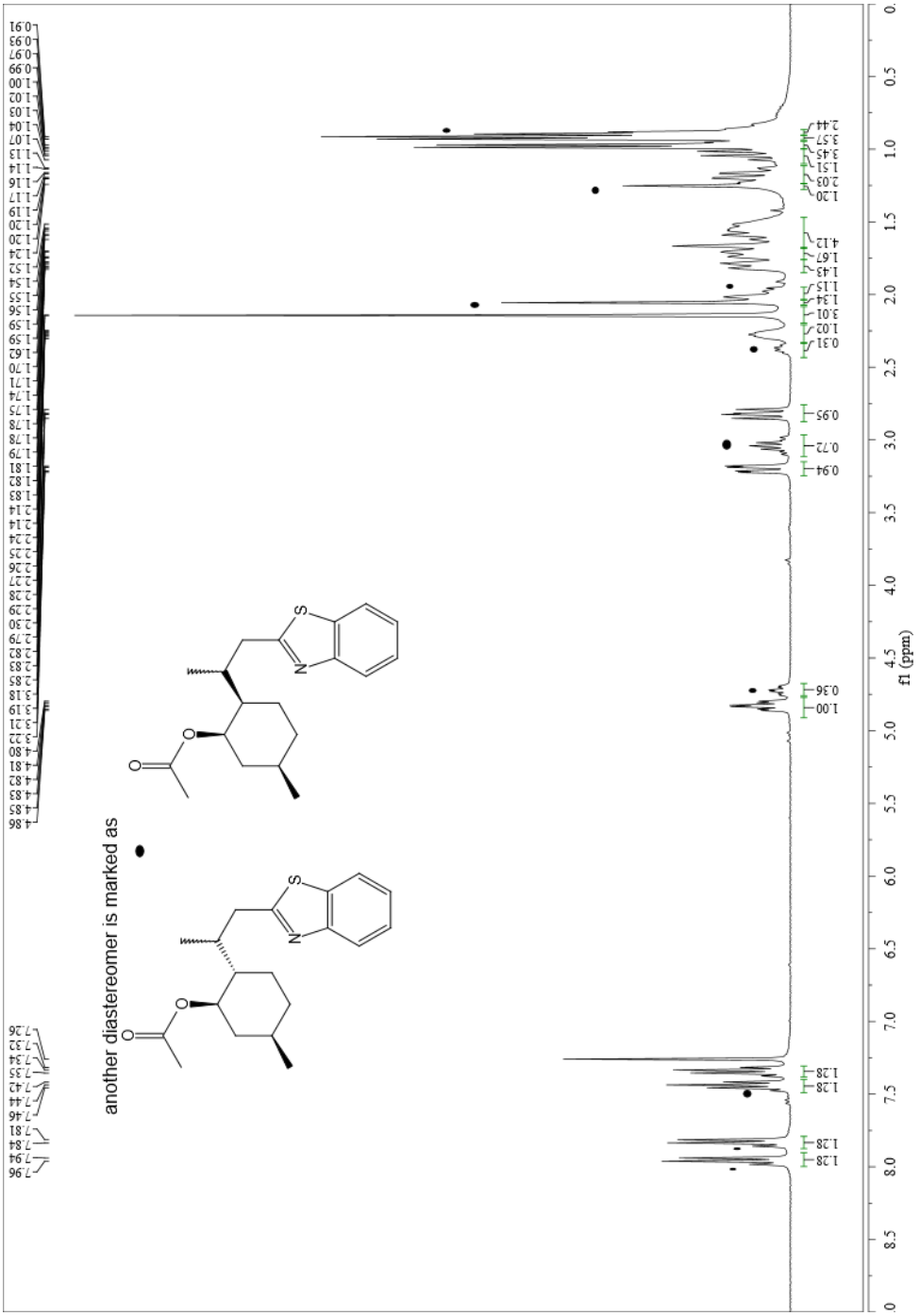

^{13}C NMR (101 MHz, $CDCl_3$) of **16a** (1R,2R,5R)-2-((R)-1-(benzo[d]thiazol-2-yl)propan-2-yl)-5-methylcyclohexyl acetate

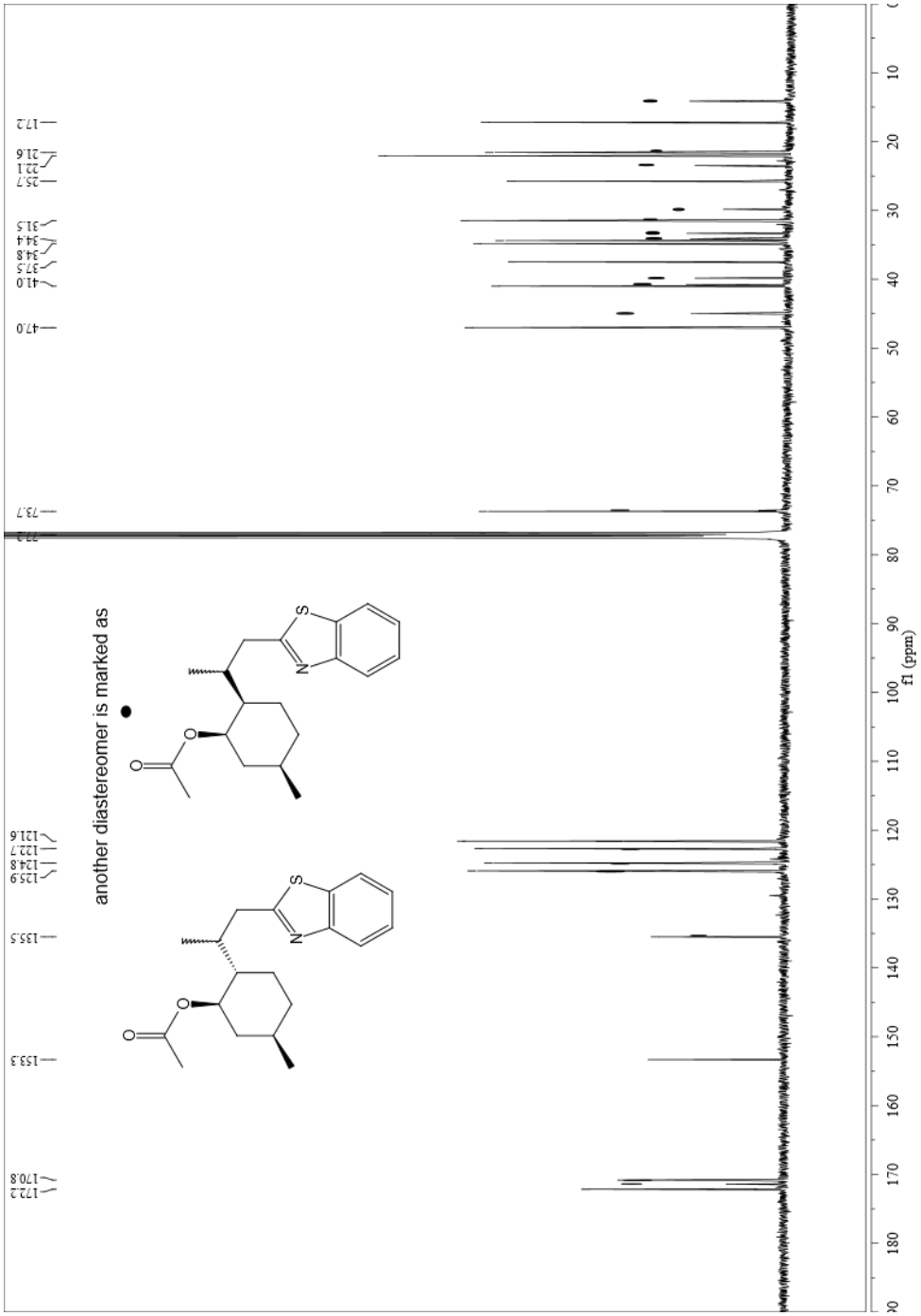

GC of **16a** (1R,2R,5R)-2-((R)-1-(benzo[d]thiazol-2-yl)propan-2-yl)-5-methylcyclohexyl acetate

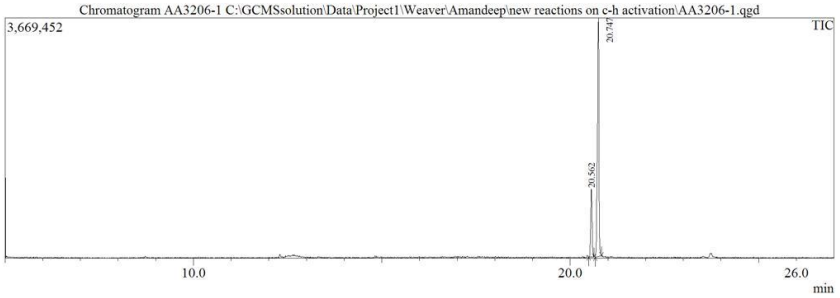

Peak Report TIC

Peak#	R.Time	I.Time	F.Time	Area	Area%	Height	Height%	A/H	Mark	Name
1	20.562	20.492	20.633	2714785	20.41	1038942	22.21	2.61	MI	
2	20.747	20.658	20.825	10584907	79.59	3639025	77.79	2.90	MI	
				13299692	100.00	4677967	100.00			

Spectrum

Line#:1 R.Time:20.6(Scan#:1868)
MassPeaks:106
RawMode:Single 20.6(1868) BasePeak:43(179469)
BG Mode:None

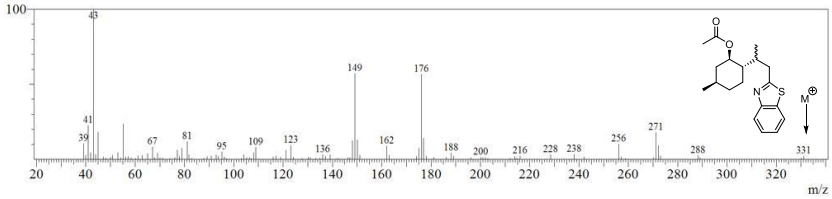

Line#:2 R.Time:20.7(Scan#:1888)
MassPeaks:149
RawMode:Single 20.7(1888) BasePeak:43(387940)
BG Mode:None

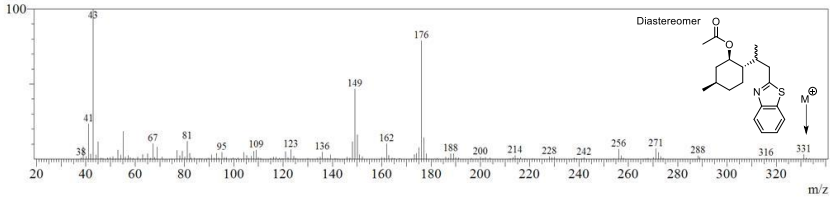

^{1}H NMR (400 MHz, $CDCl_3$) of **17a** 2-(bicyclo[2.2.1]heptan-2-yl)-4-(tert-butyl)thiazole

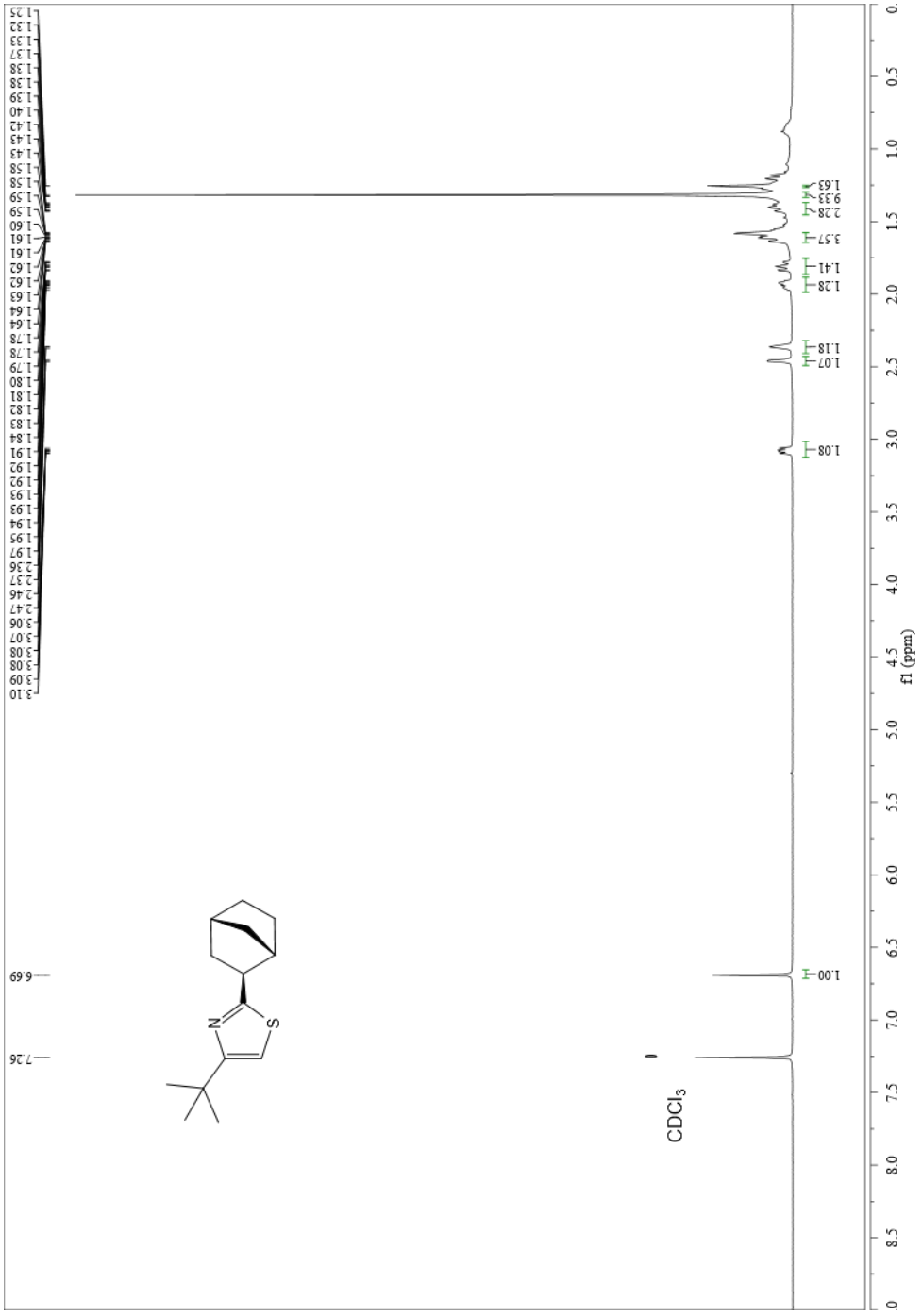

^{13}C NMR (101 MHz, $CDCl_3$) of **17a** 2-(bicyclo[2.2.1]heptan-2-yl)-4-(tert-butyl)thiazole

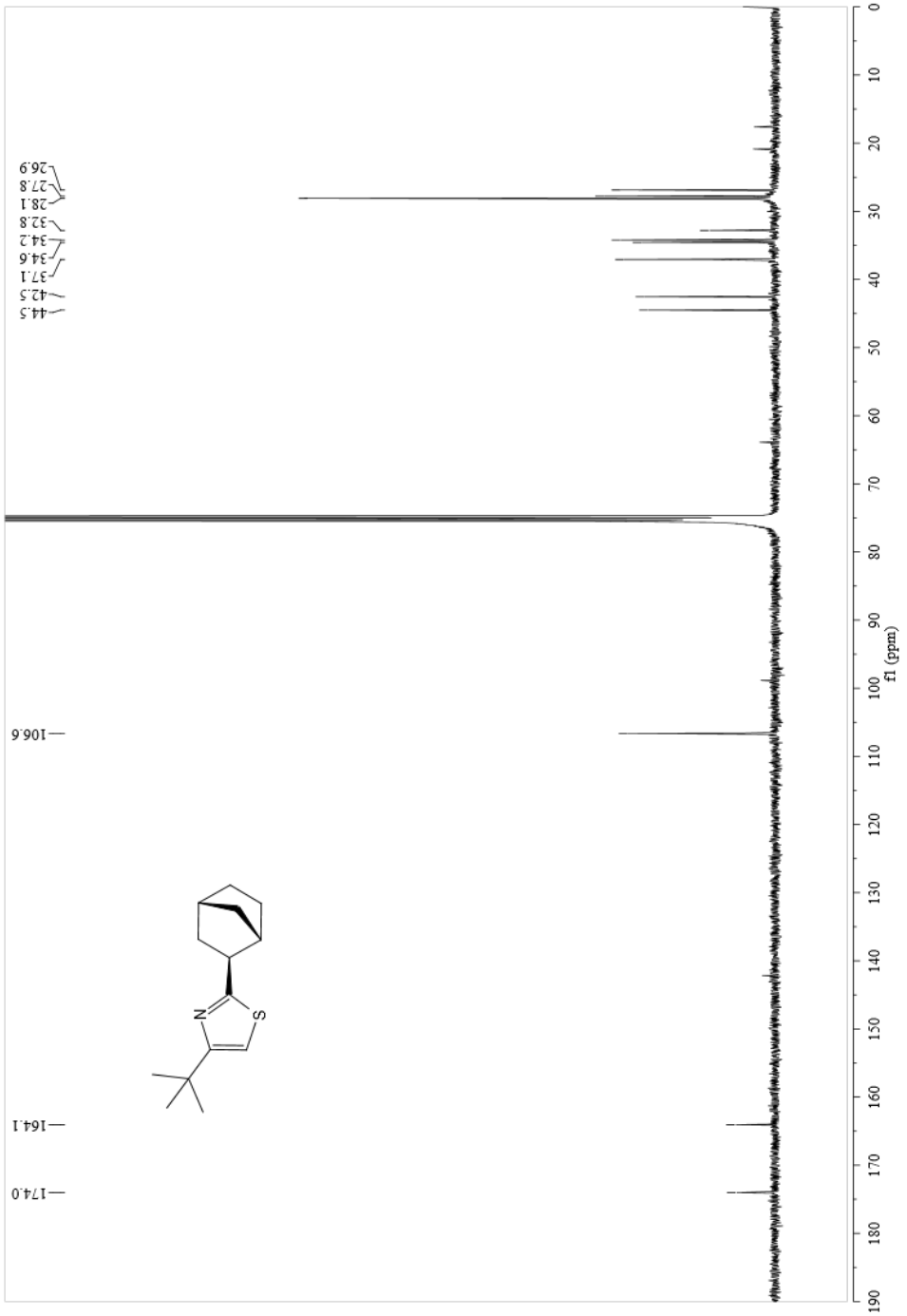

^{1}H NMR (400 MHz, $CDCl_3$) of **18a** 2-(((1S,4R)-3,3-dimethylbicyclo[2.2.1]heptan-2-yl)methyl)thiazole

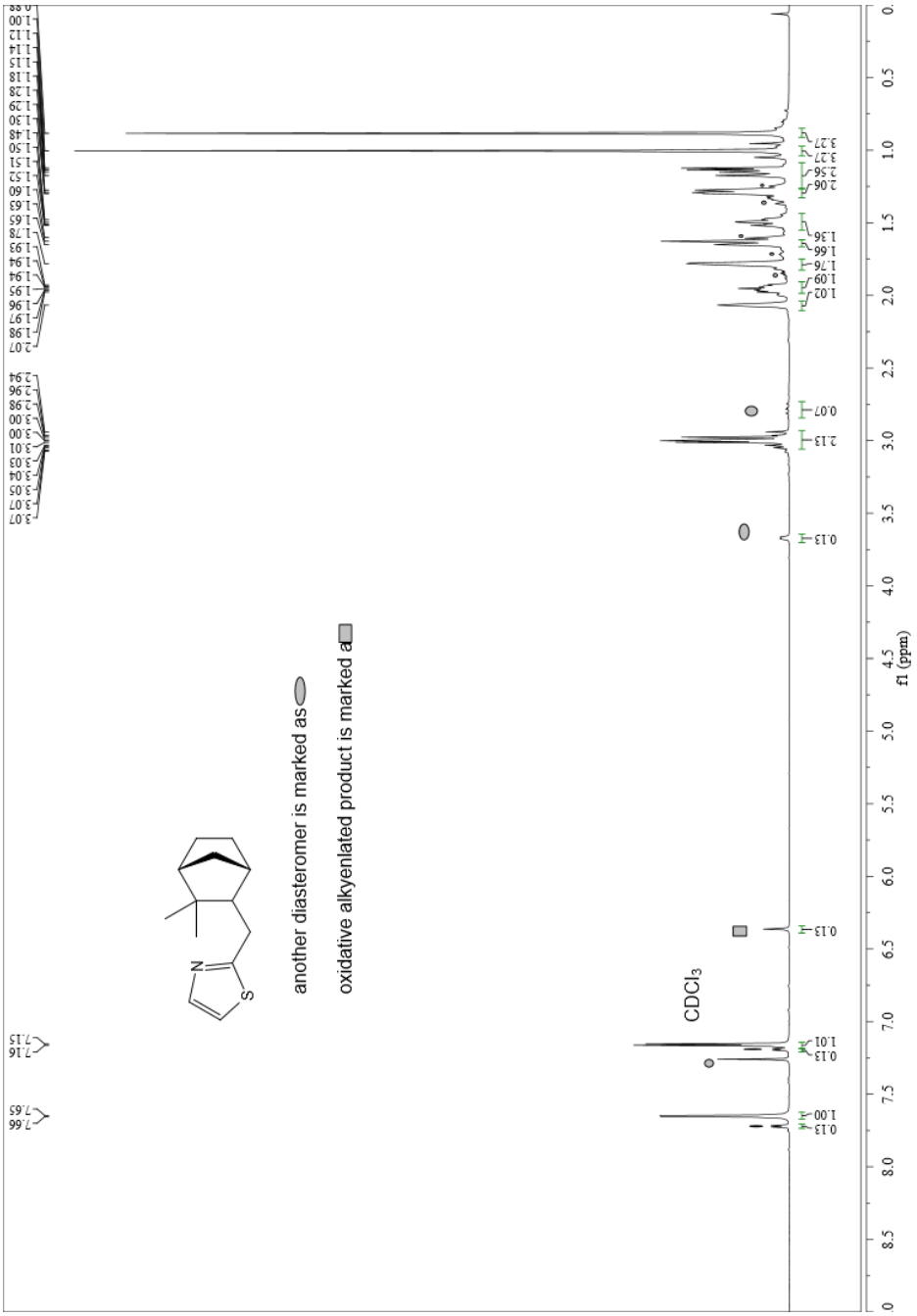

^{13}C NMR (101 MHz, $CDCl_3$) of **18a** 2-(((1S,4R)-3,3-dimethylbicyclo[2.2.1]heptan-2-yl)methyl)thiazole

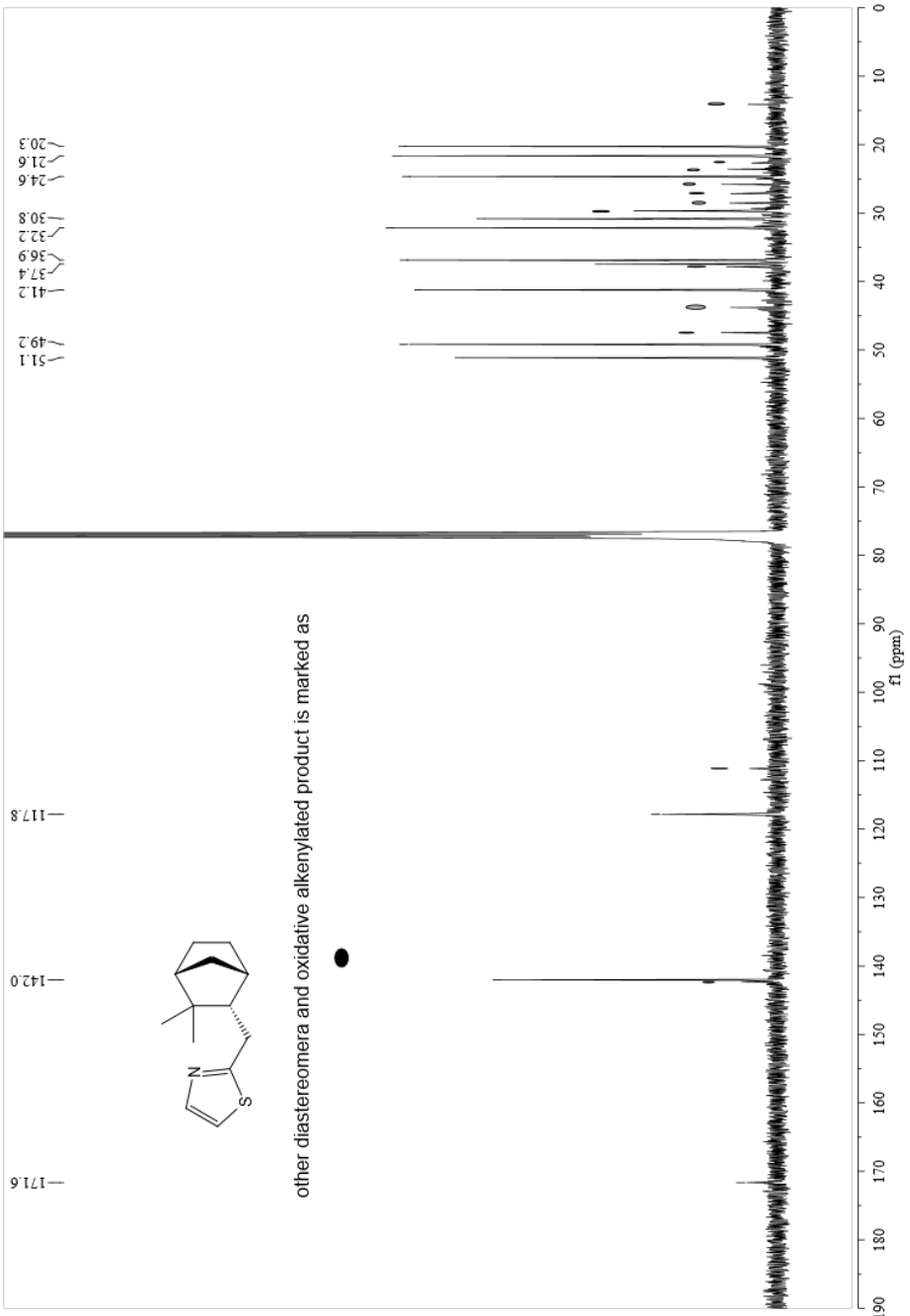

^{13}C of **18a** 2-(((1S,4R)-3,3-dimethylbicyclo[2.2.1]heptan-2-yl)methyl)thiazole

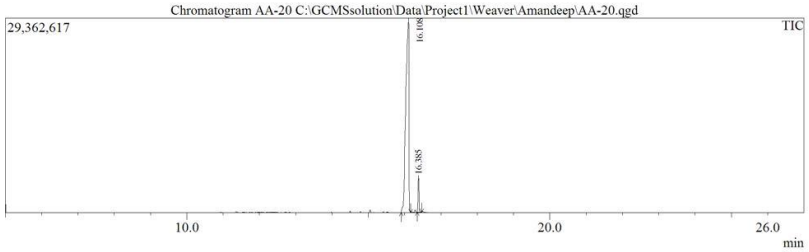

Peak Report TIC

Peak#	R.Time	I.Time	F.Time	Area	Area%	Height	Height%	A/H	Mark	Name
1	16.108	15.900	16.167	173468410	94.50	29322175	83.99	5.91	MI	
2	16.385	16.342	16.467	10105309	5.50	5588343	16.01	1.80	MI	
				183573719	100.00	34910518	100.00			

Spectrum

Line#:1 R.Time:16.0(Scan#:1324)
MassPeaks:161
RawMode:Single 16.0(1324) BasePeak:41(1792897)
BG Mode:None

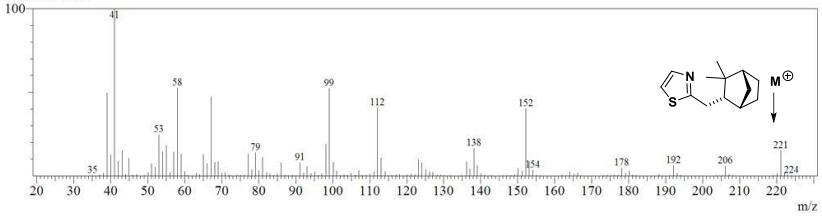

Line#:2 R.Time:16.4(Scan#:1366)
MassPeaks:157
RawMode:Single 16.4(1366) BasePeak:41(339510)
BG Mode:None

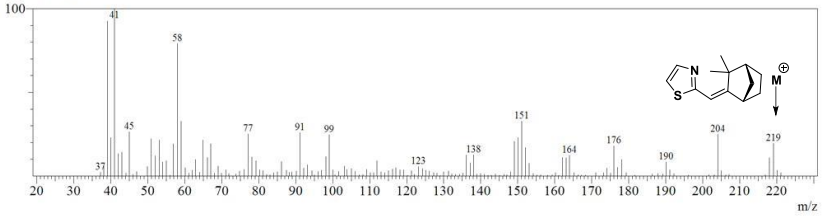

G

^{1}H NMR (400 MHz, $CDCl_3$) of **19a** 2-(bicyclo[2.2.1]heptan-2-ylmethyl)- 1H-benzo[d]imidazole

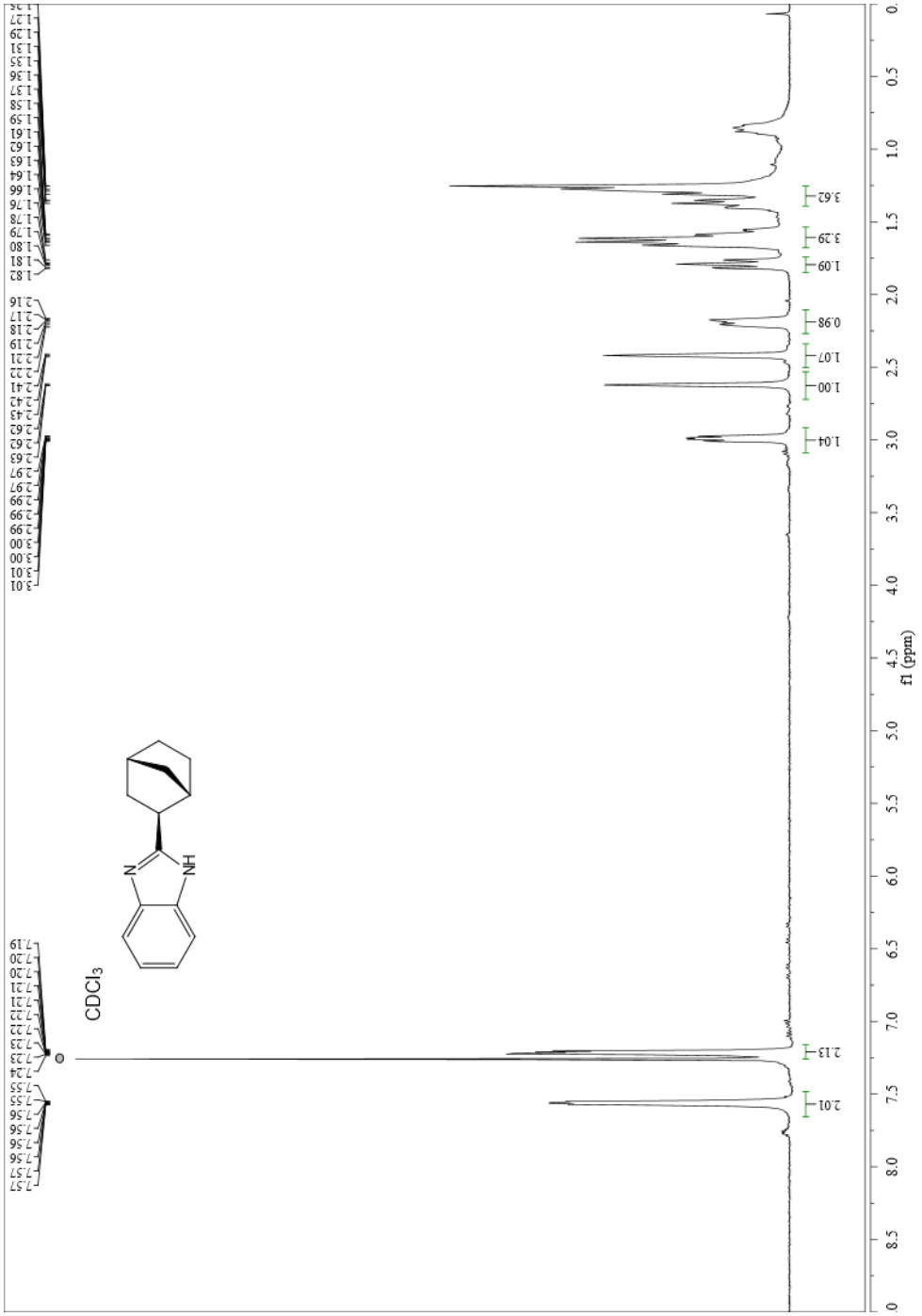

^{13}C NMR (101 MHz, $CDCl_3$) of **19a** 2-(bicyclo[2.2.1]heptan-2-ylmethyl)-1H-benzo[d]imidazole

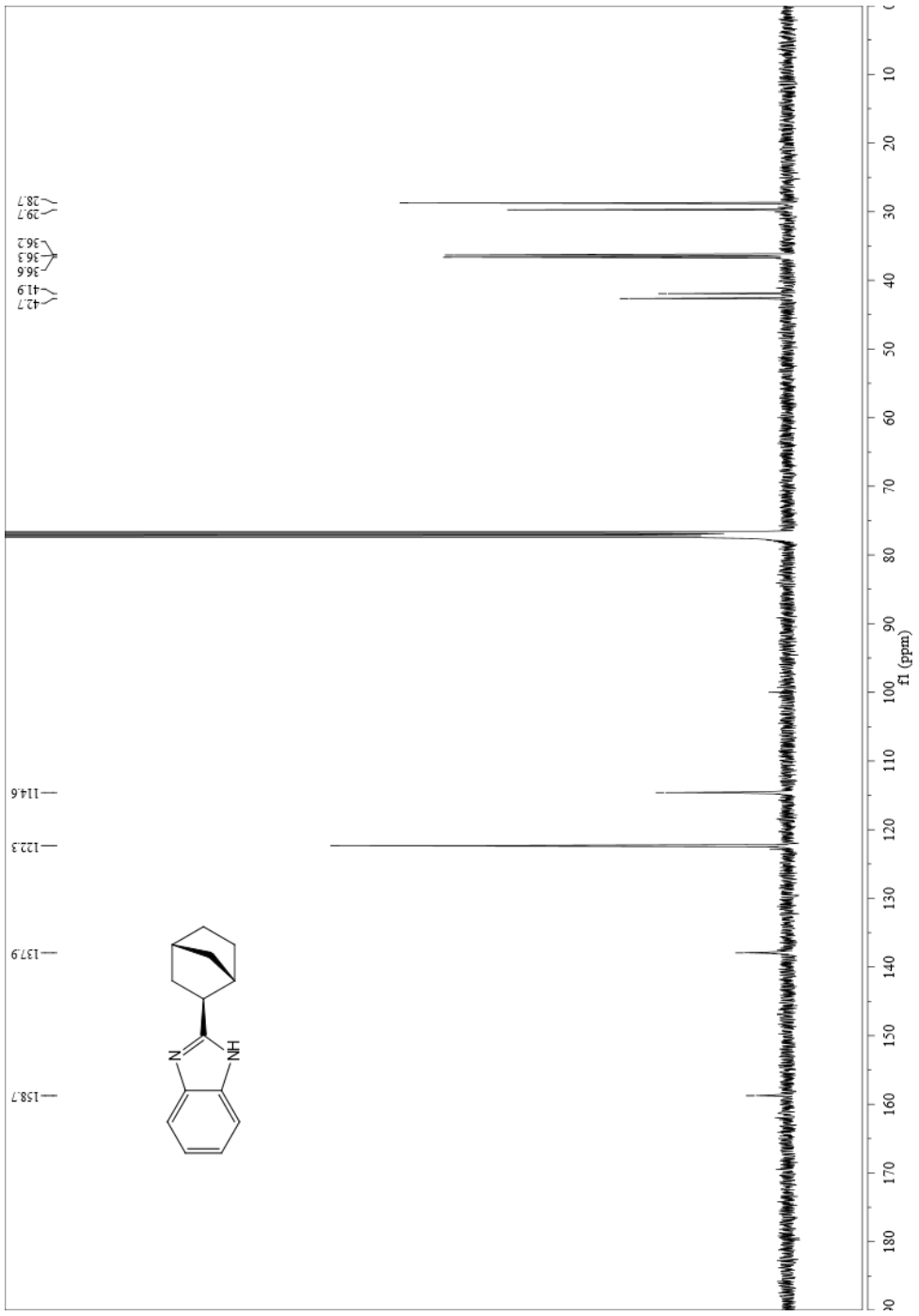

^{1}H NMR (400 MHz, CD_3OD) of **20a** 2-(bicyclo[2.2.1]heptan-2-ylmethyl)-6-chloro-1H-benzo[d]imidazole

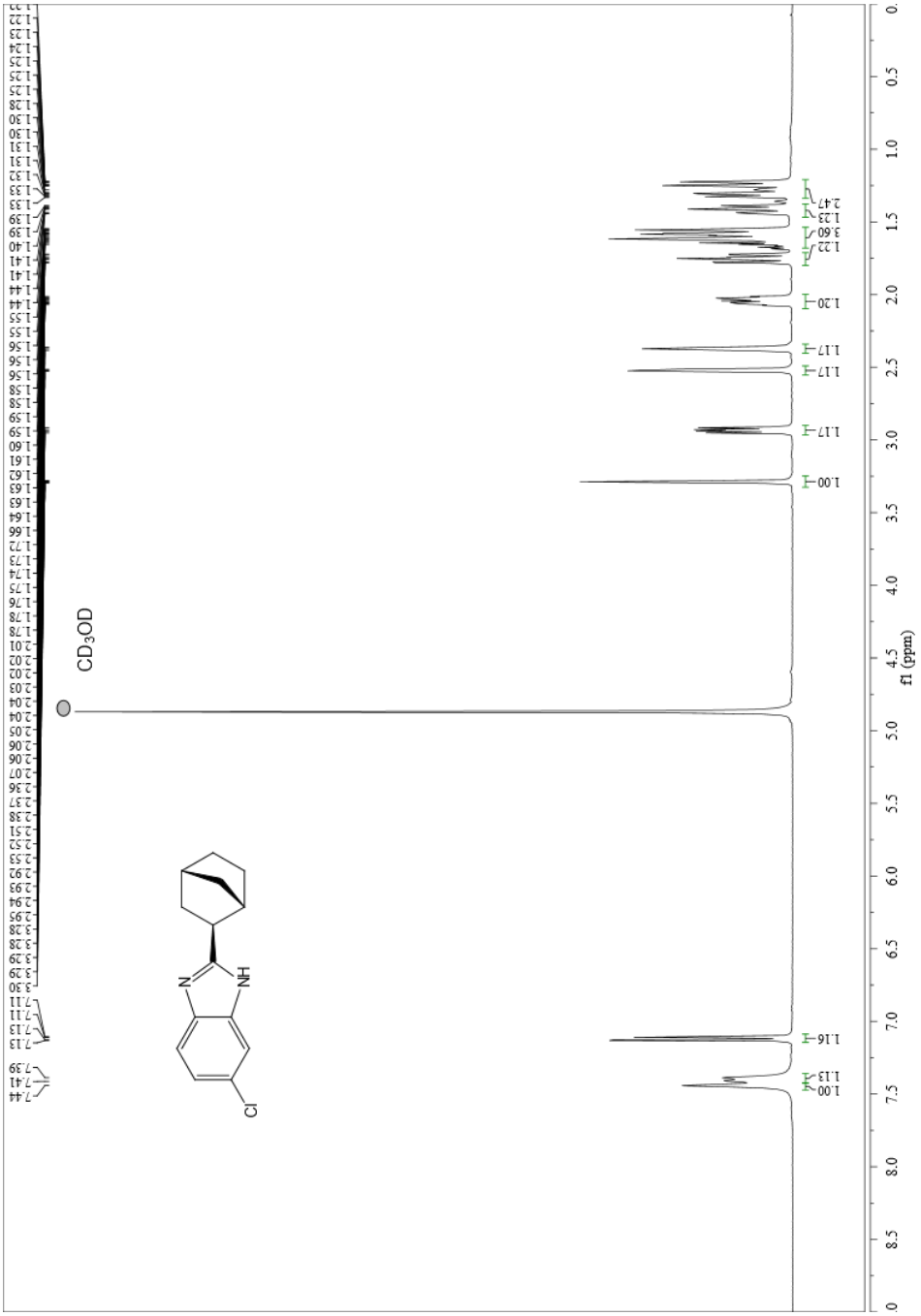

^{13}C NMR (101 MHz, CD_3OD) of **20a** 2-(bicyclo[2.2.1]heptan-2-ylmethyl)-6-chloro-1H-benzo[d]imidazole

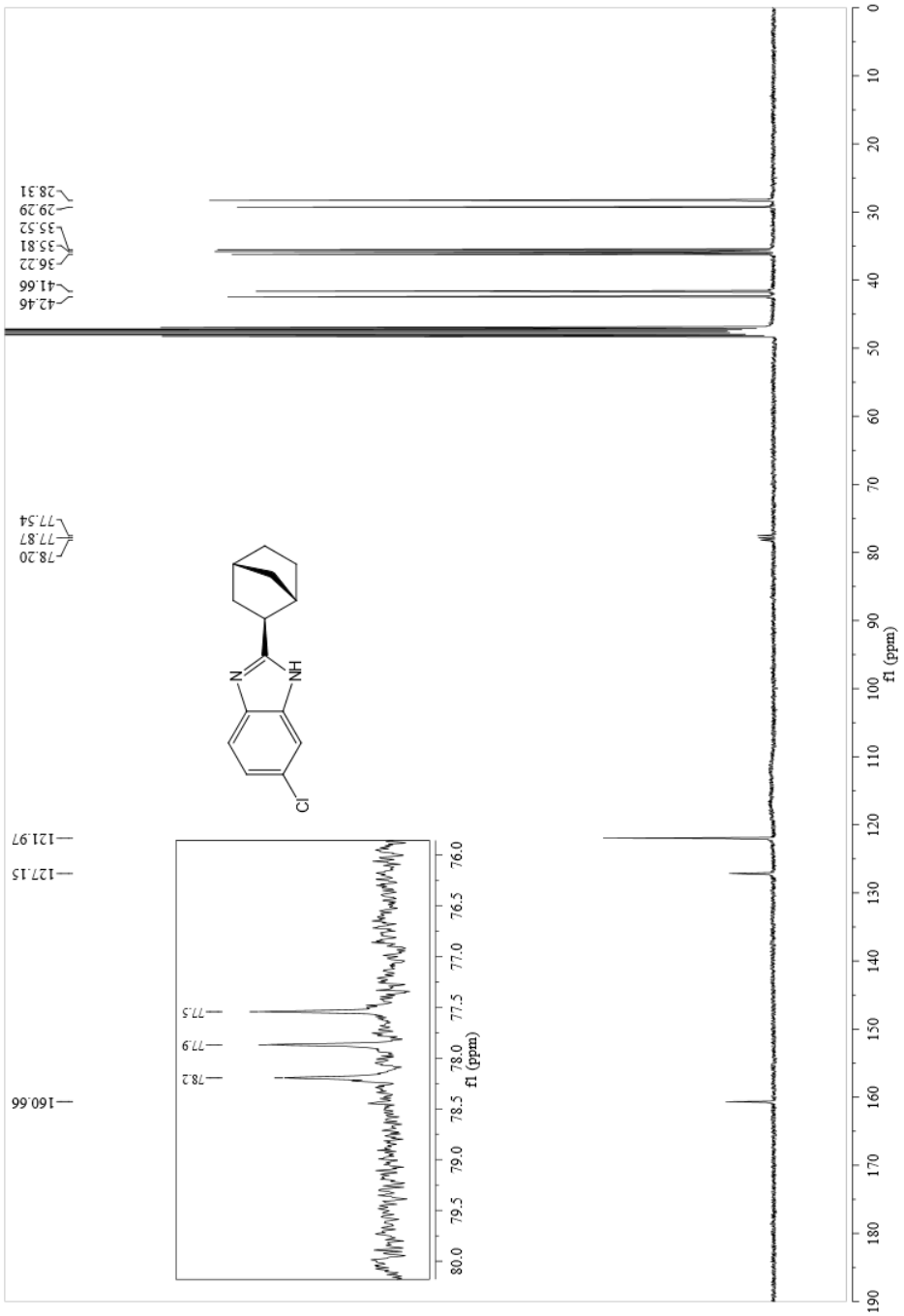

^{1}H NMR (400 MHz, CD_3OD) of **21a** 2-((3,3-dimethylbicyclo[2.2.1]heptan-2-yl)methyl)-1H-benzo[d]imidazole

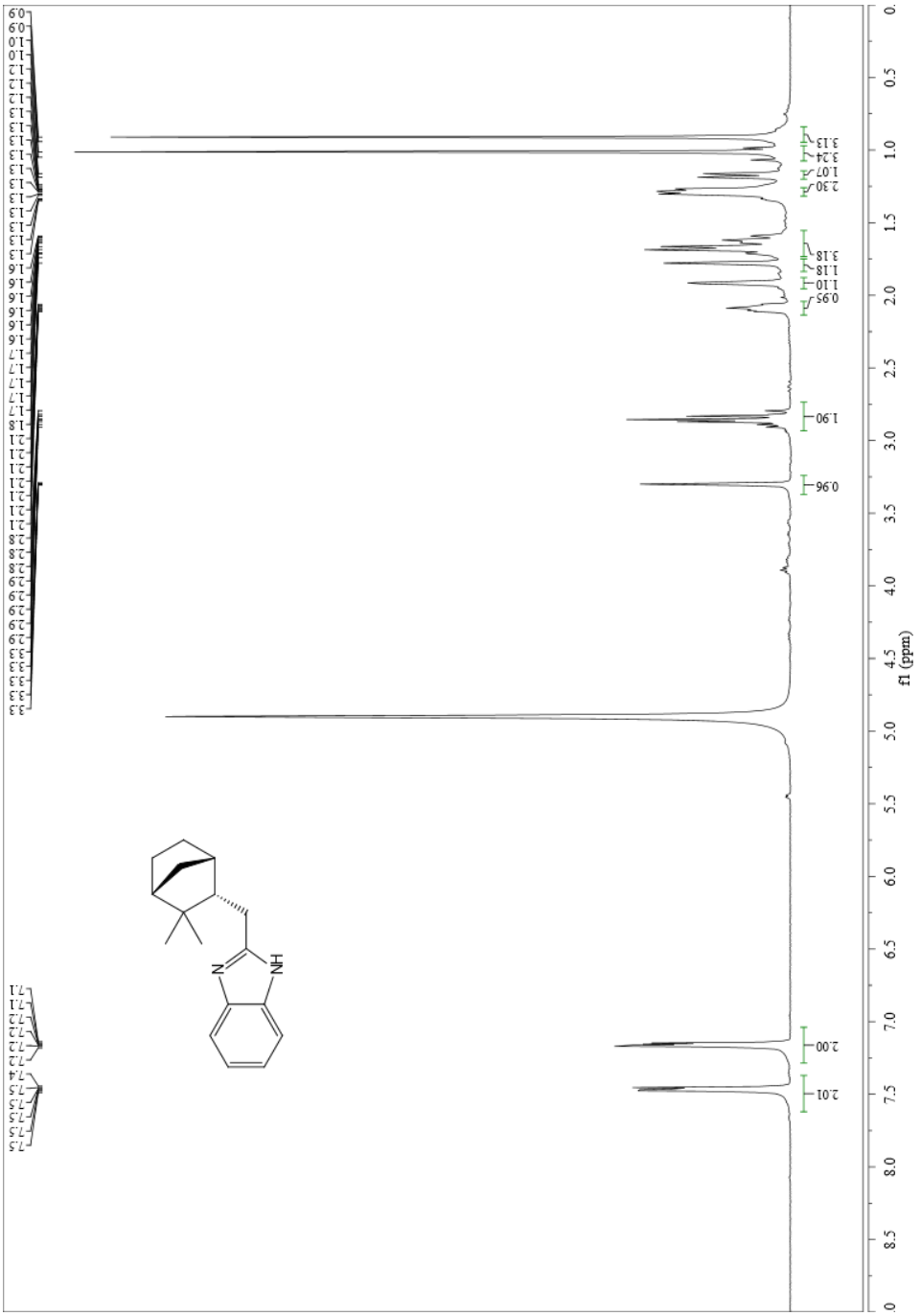

^{13}C NMR (101 MHz, CD_3OD) of **21a** 2-((3,3-dimethylbicyclo[2.2.1]heptan-2-yl)methyl)-1H-benzo[d]imidazole

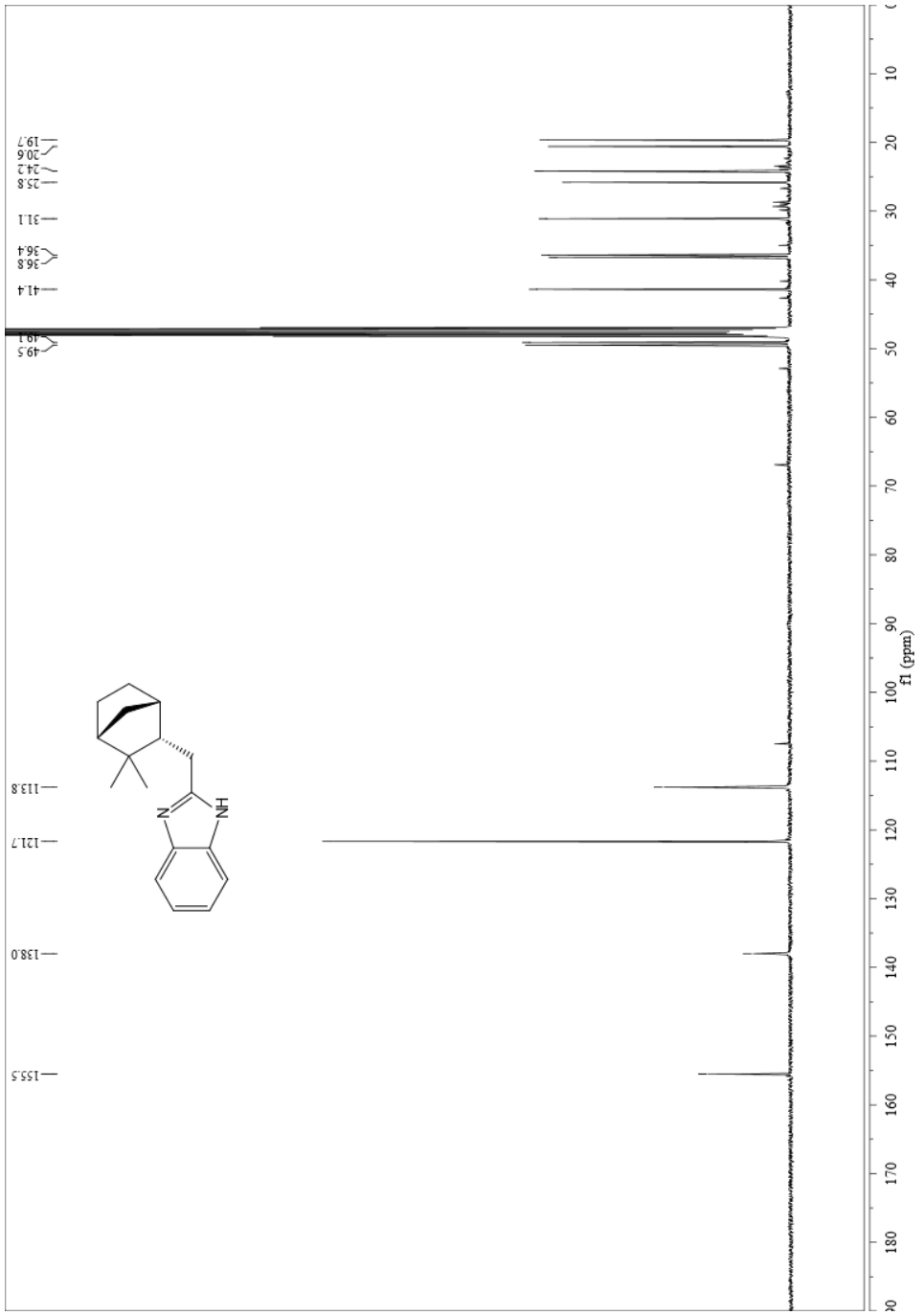

^{1}H NMR (400 MHz, $CDCl_3$) of **22a** 6-bromo-2-((3,3-dimethylbicyclo[2.2.1]heptan-2-yl)methyl)-1H-benzo[d]imidazole

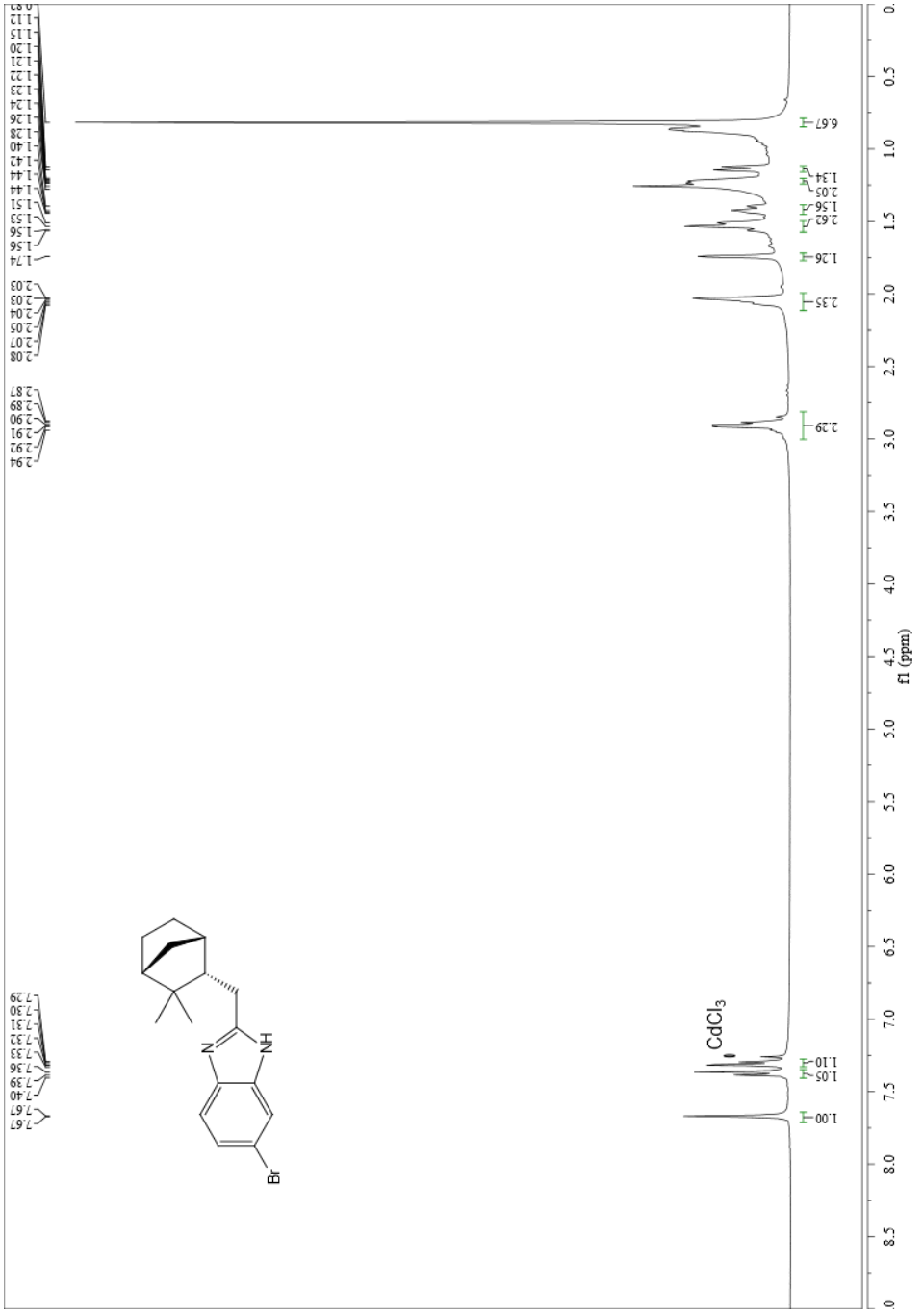

^{13}C NMR (101 MHz, $CDCl_3$) of **22a** 6-bromo-2-((3,3-dimethylbicyclo[2.2.1]heptan-2-yl)methyl)-1H-benzo[d]imidazole

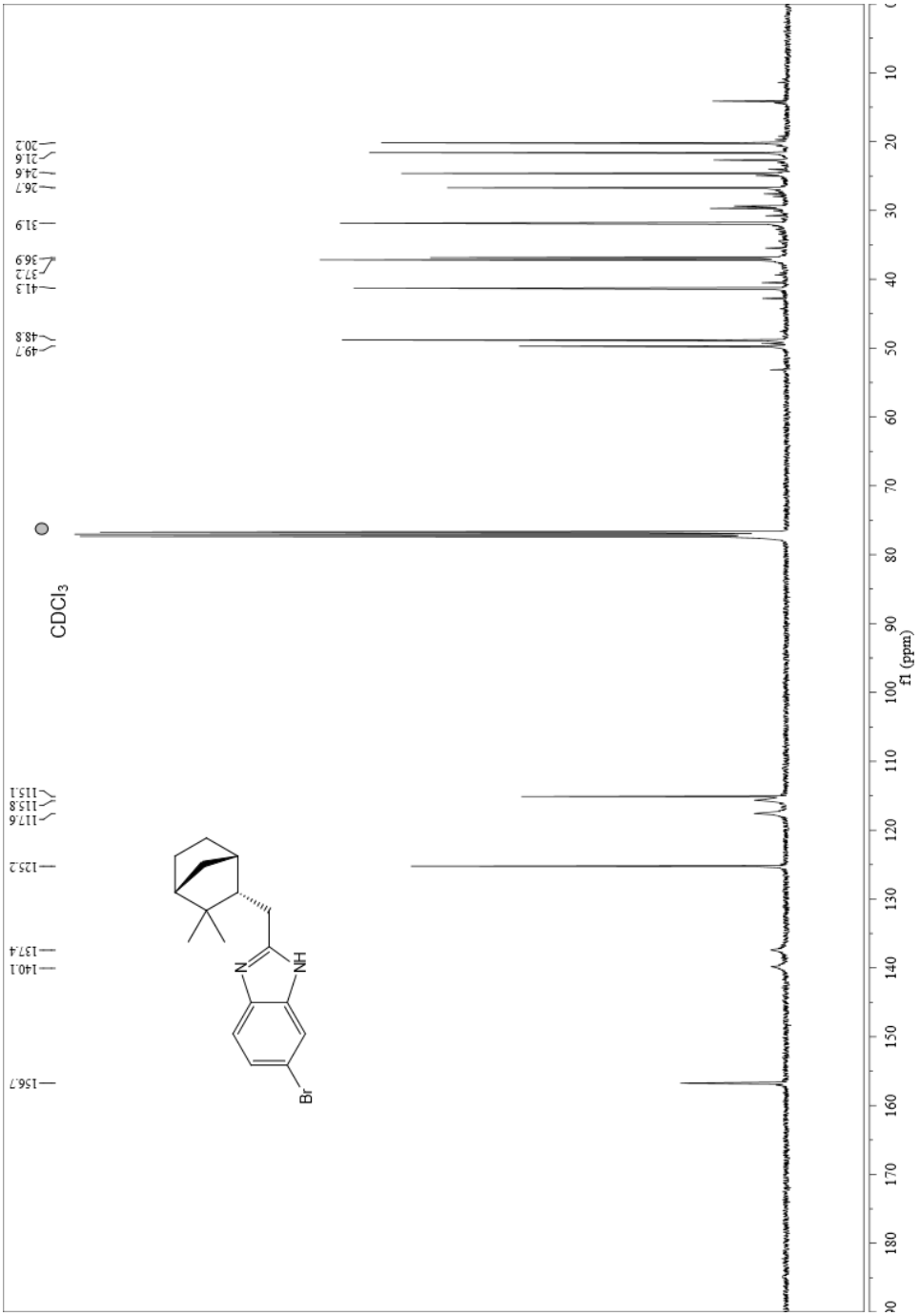

^{1}H NMR, (400 MHz, $CDCl_3$), of **23a** dimethyl 5-(4-chlorobenzo[d]thiazol-2-yl)-7-oxabicyclo[2.2.1]heptane-2,3-dicarboxylate

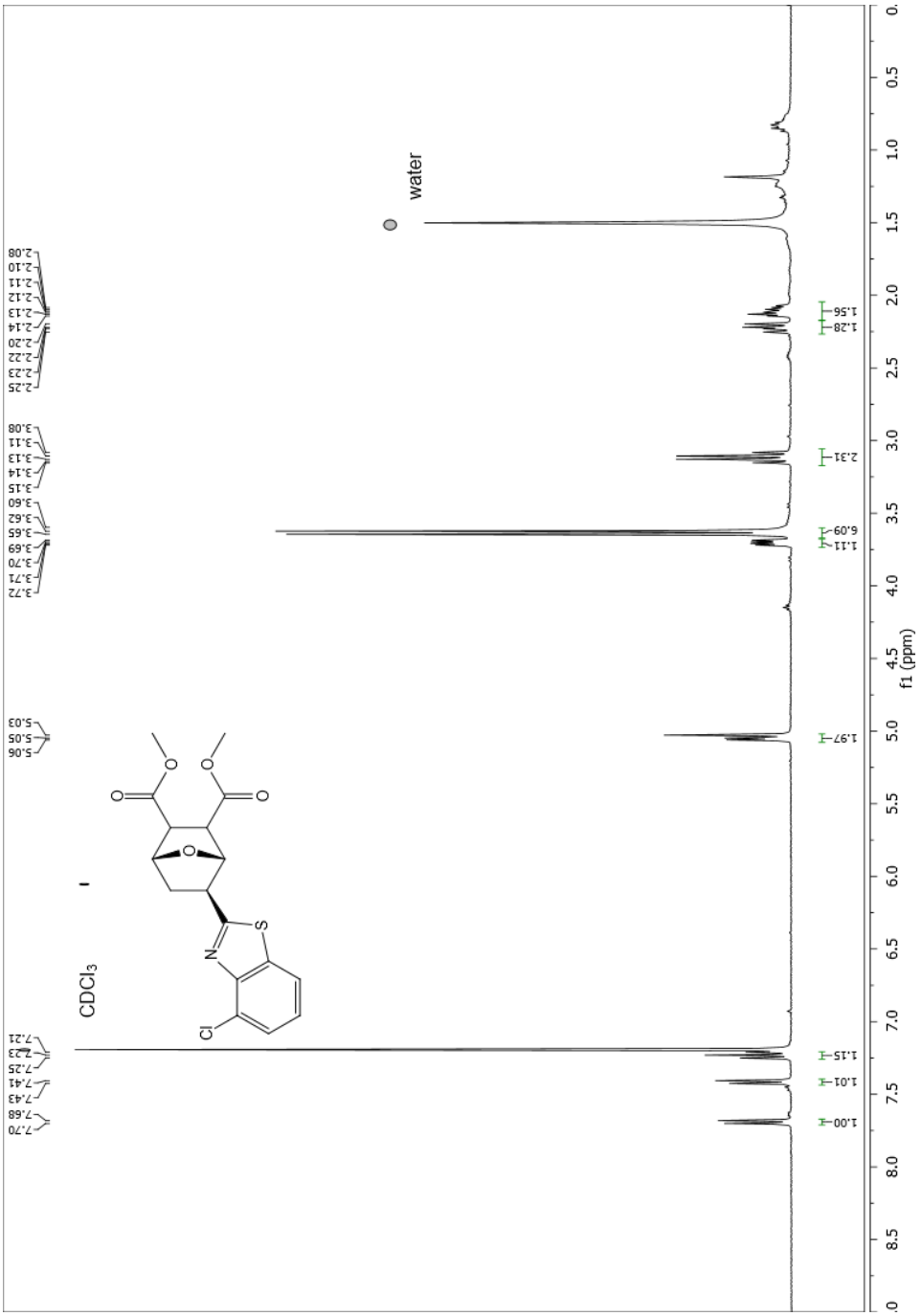

^{13}C NMR (101 MHz, $CDCl_3$) of **23a** dimethyl 5-(4-chlorobenzo[d]thiazol-2-yl)-7-oxabicyclo[2.2.1]heptane-2,3-dicarboxylate

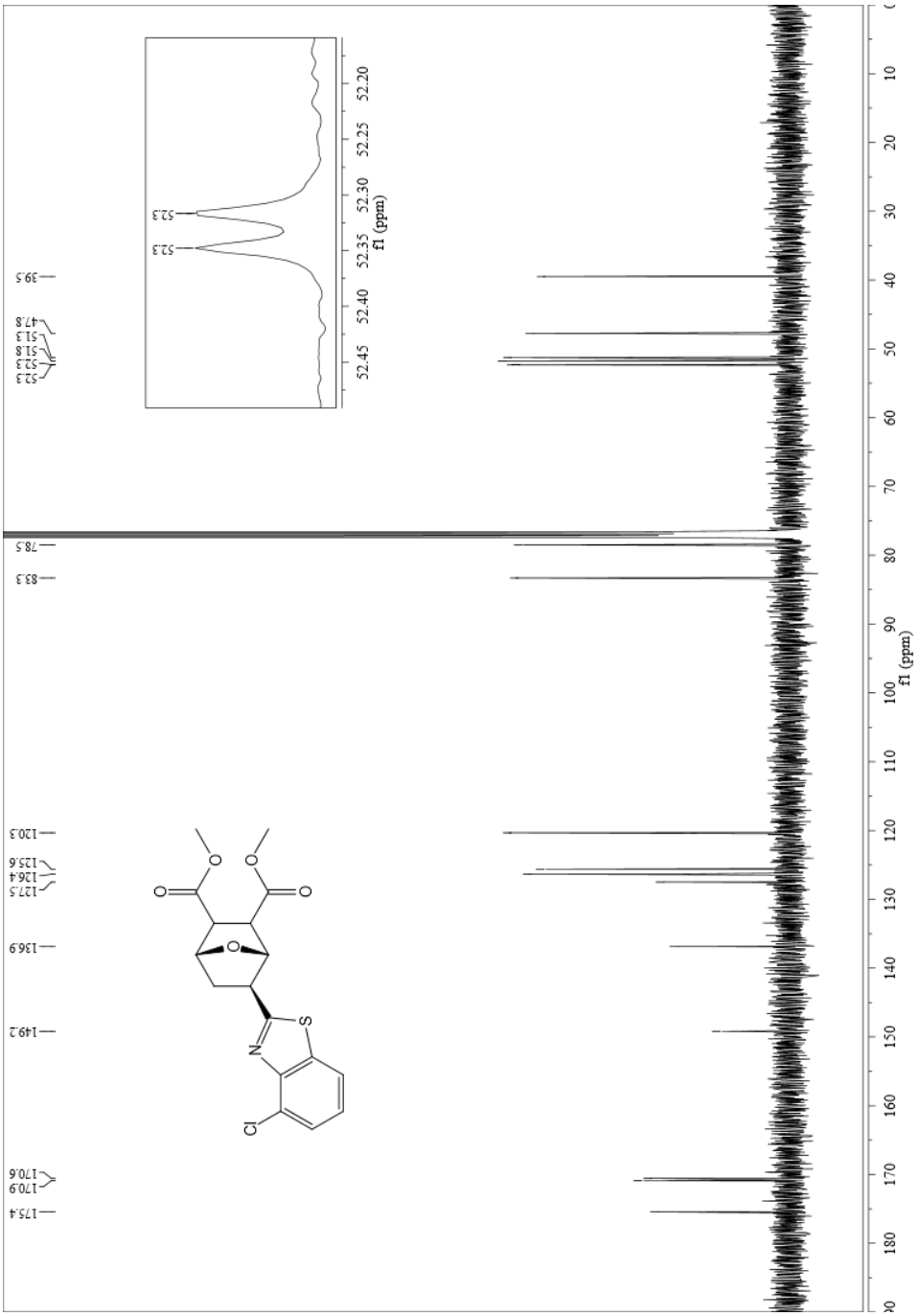

^{1}H NMR (400 MHz, $CDCl_3$) of **24a** (Major) 2-methyl-5-(1-(thiazol-2-yl)propan-2-yl)cyclohex-2-en-1-one and B) 2-methyl-5-(prop-1-en-2-yl)-3-(thiazol-2-yl)cyclohexan-1-o

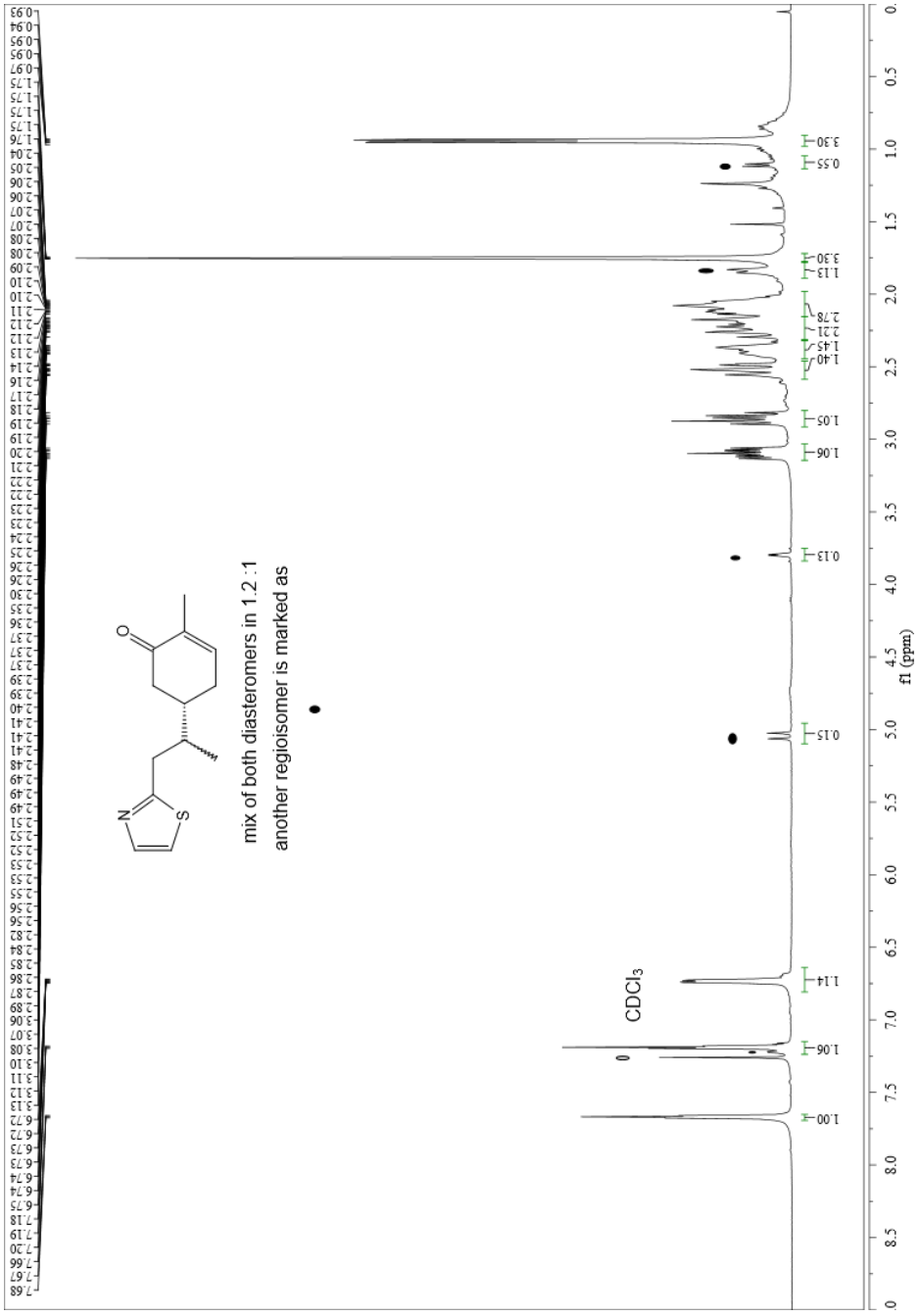

^{13}C NMR (101 MHz, $CDCl_3$) of **24a** (Major) 2-methyl-5-(1-(thiazol-2-yl)propan-2-yl)cyclohex-2-en-1-one and B) 2-methyl-5-(prop-1-en-2-yl)-3-(thiazol-2-yl)cyclohexan-1-one

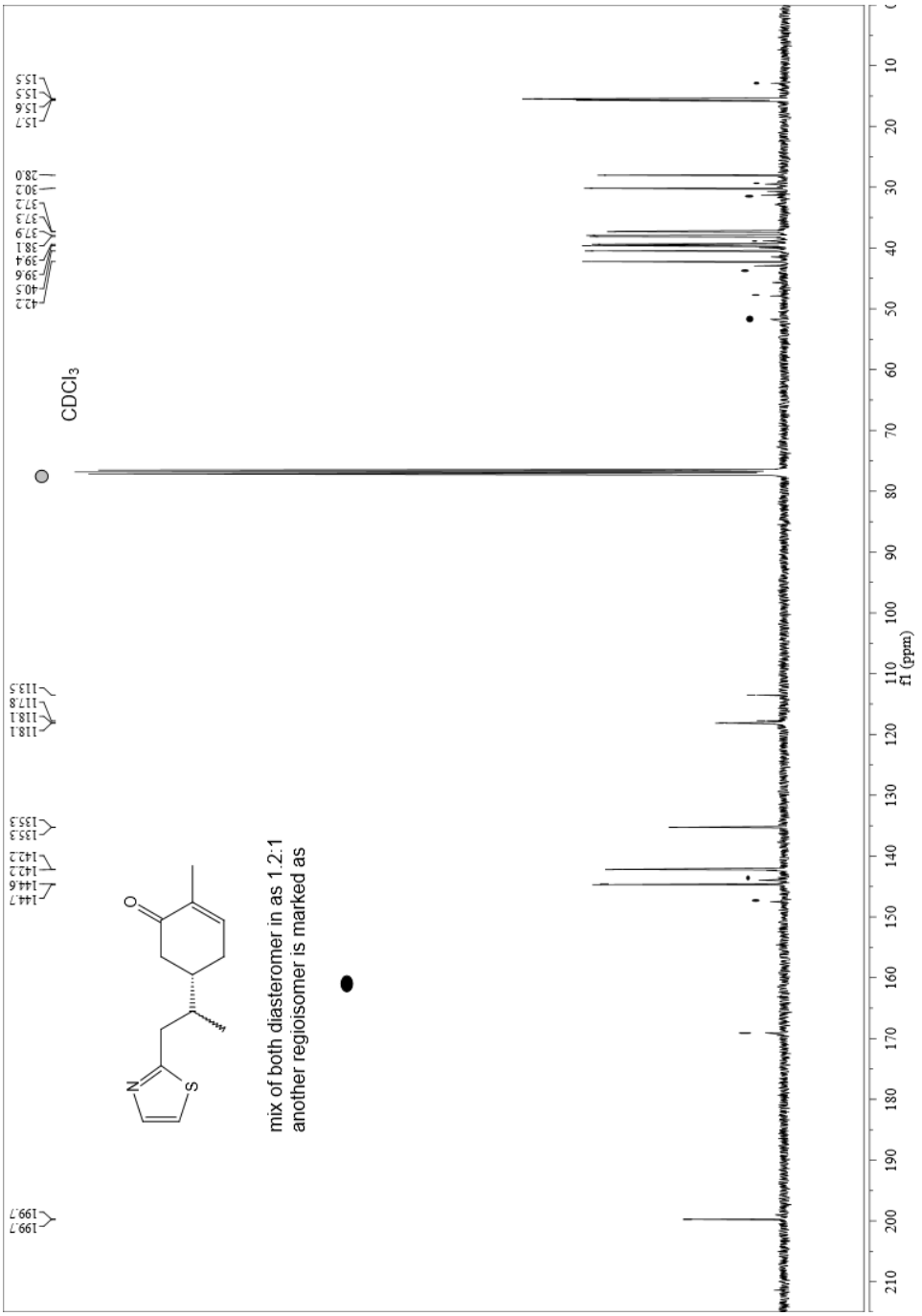

GC of **24a** (Major) 5R)-2-methyl-5-(prop-1-en-2-yl)-3-(thiazol-2-yl)cyclohexan-1-one

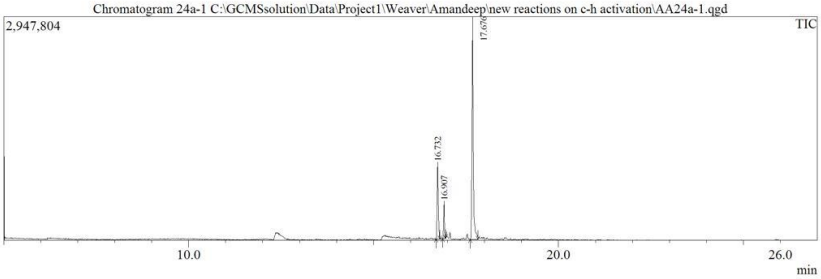

Peak Report TIC

Peak#	R.Time	I.Time	F.Time	Area	Area%	Height	Height%	A/H	Mark	Name
1	16.732	16.692	16.792	2152574	21.78	1013447	22.83	2.12	MI	
2	16.907	16.867	16.950	786775	7.96	494055	11.13	1.59	MI	
3	17.676	17.617	17.825	6945002	70.26	2932388	66.05	2.36	MI	
				9884351	100.00	4439890	100.00			

Spectrum

Line#:1 R.Time:16.7(Scan#:1408)
MassPeaks:98
RawMode:Single 16.7(1408) BasePeak:126(125254)
BG Mode:None

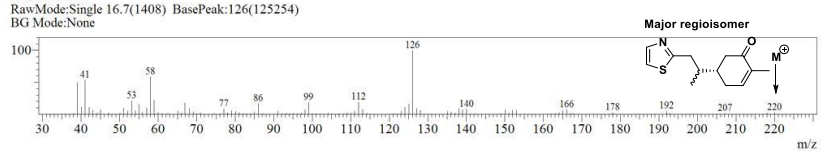

Line#:2 R.Time:16.9(Scan#:1429)
MassPeaks:75
RawMode:Single 16.9(1429) BasePeak:126(46836)
BG Mode:None

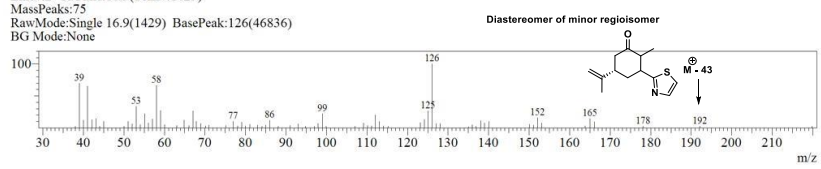

Line#:3 R.Time:17.7(Scan#:1522)
MassPeaks:107
RawMode:Single 17.7(1522) BasePeak:99(427613)
BG Mode:None

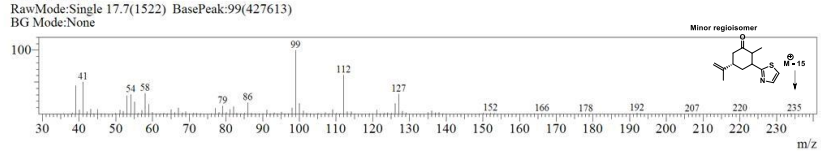

^{1}H NMR (400 MHz, $CDCl_3$) of **24a** (Minor) 5(R)-2-methyl-5-(prop-1-en-2-yl)-3-(thiazol-2-yl)cyclohexan-1-one

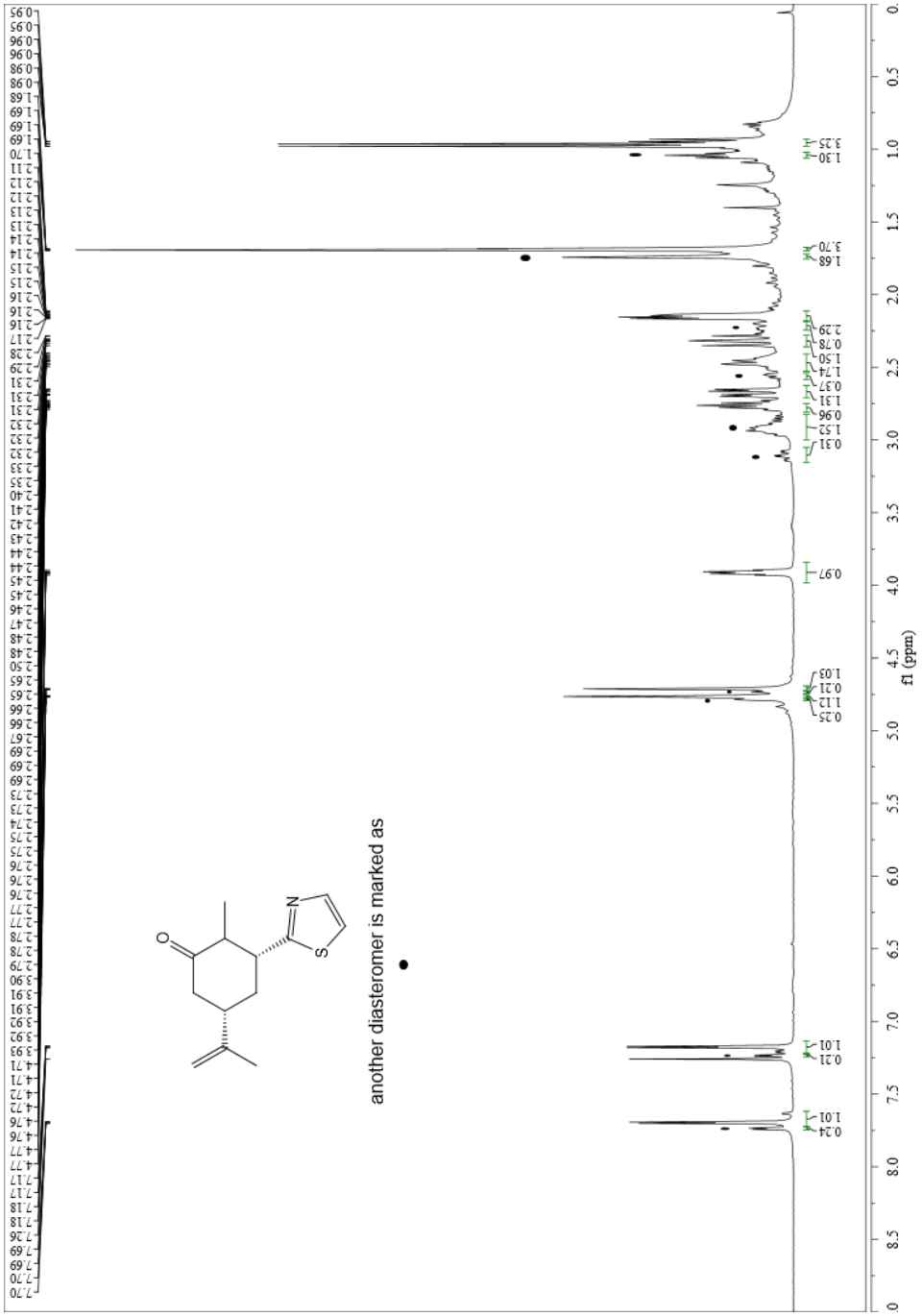

^{13}C NMR (101 MHz, $CDCl_3$) of **24a** (Minor) 5(R)-2-methyl-5-(prop-1-en-2-yl)-3-(thiazol-2-yl)cyclohexan-1-one

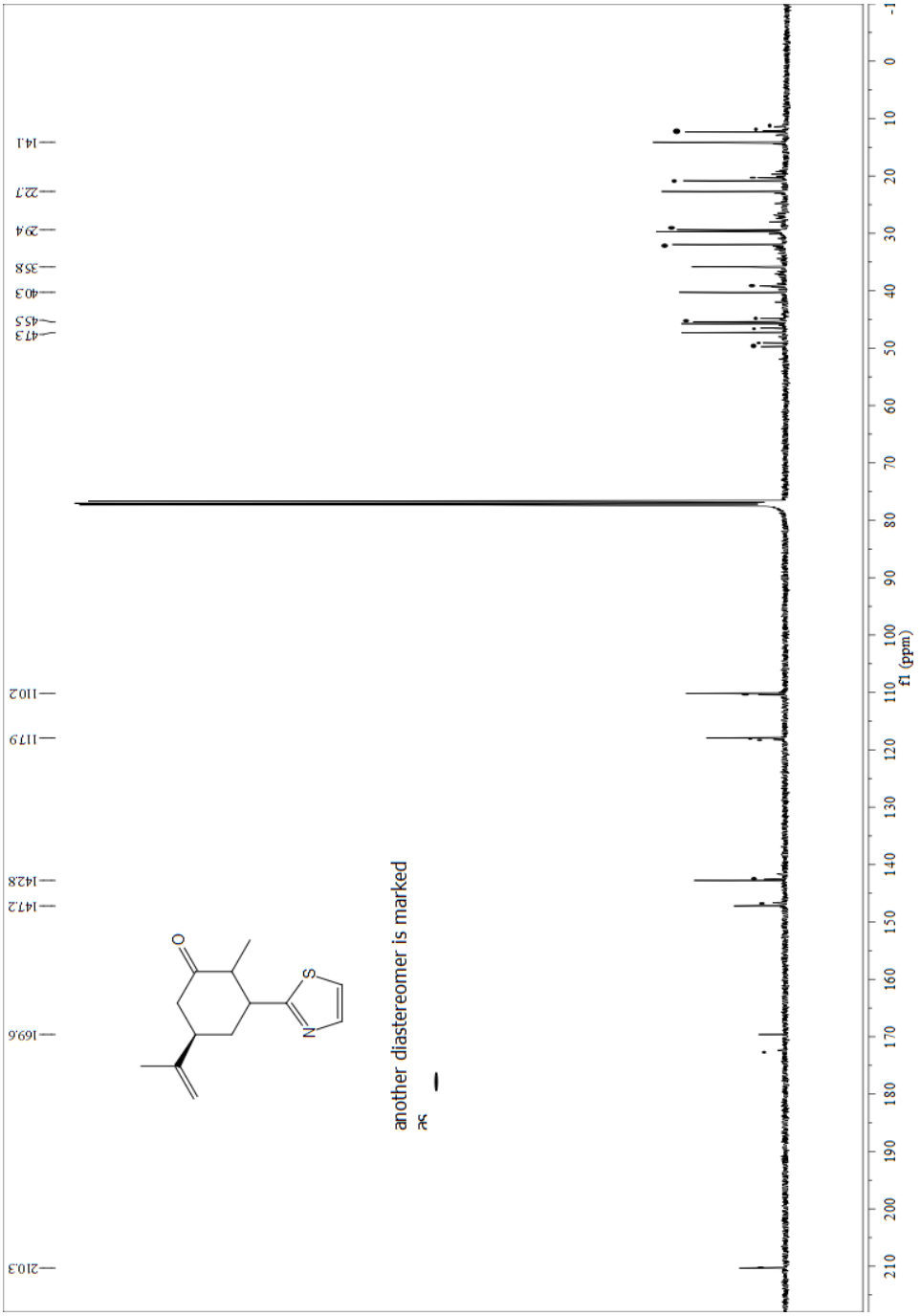

GC of **24a** (Minor) 5R)-2-methyl-5-(prop-1-en-2-yl)-3-(thiazol-2-yl)cyclohexan-1-one

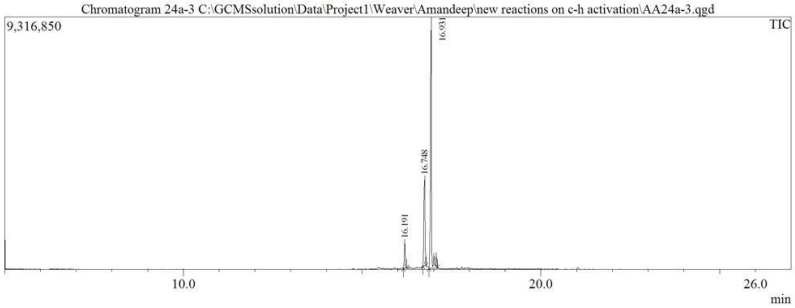

Peak Report TIC

Peak#	R.Time	I.Time	F.Time	Area	Area%	Height	Height%	A/H	Mark	Name
1	16.191	16.158	16.250	1710578	5.79	1063505	7.80	1.60	MI	
2	16.748	16.700	16.792	7865669	26.62	3315661	24.32	2.37	MI	
3	16.931	16.867	17.108	19970990	67.59	9257042	67.89	2.15	MI	
				29547237	100.00	13636208	100.00			

Spectrum

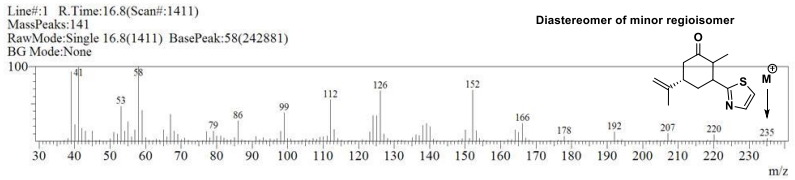

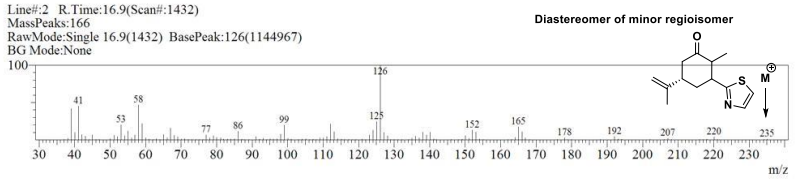

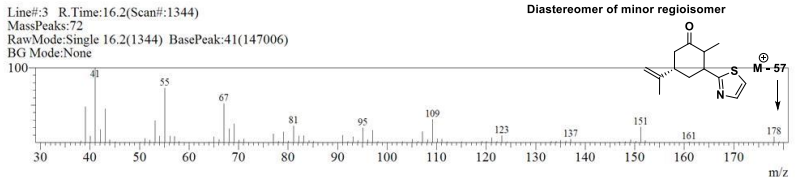

^{1}H NMR (400 MHz, $CDCl_3$) of **25a** (2-(benzo[d]thiazol-2-yl)-4-(prop-1-en-2-yl)cyclohexyl)methanol

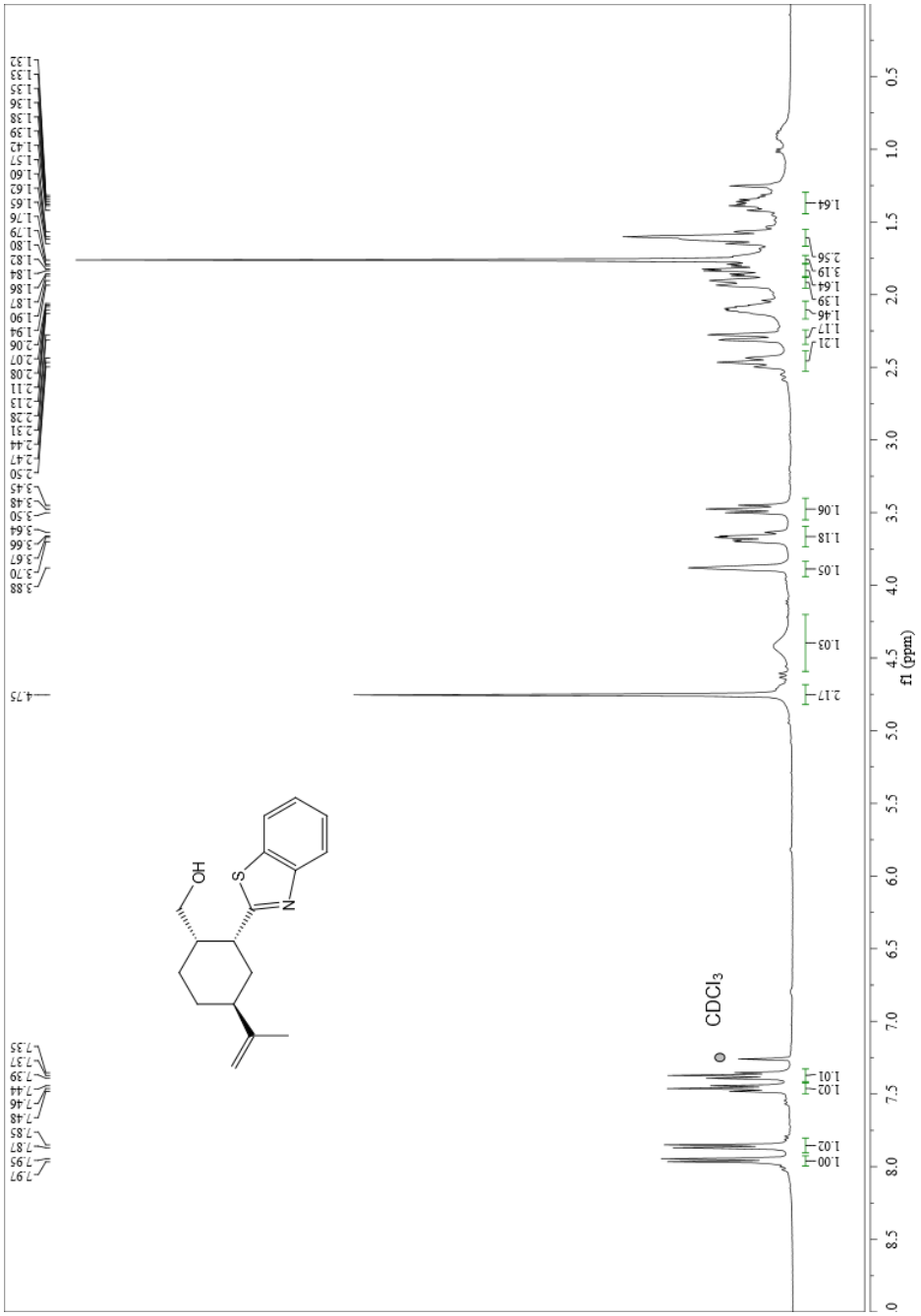

^{13}C NMR (101 MHz, $CDCl_3$) of **25a** (2-(benzo[d]thiazol-2-yl)-4-(prop-1-en-2-yl)cyclohexyl)methanol

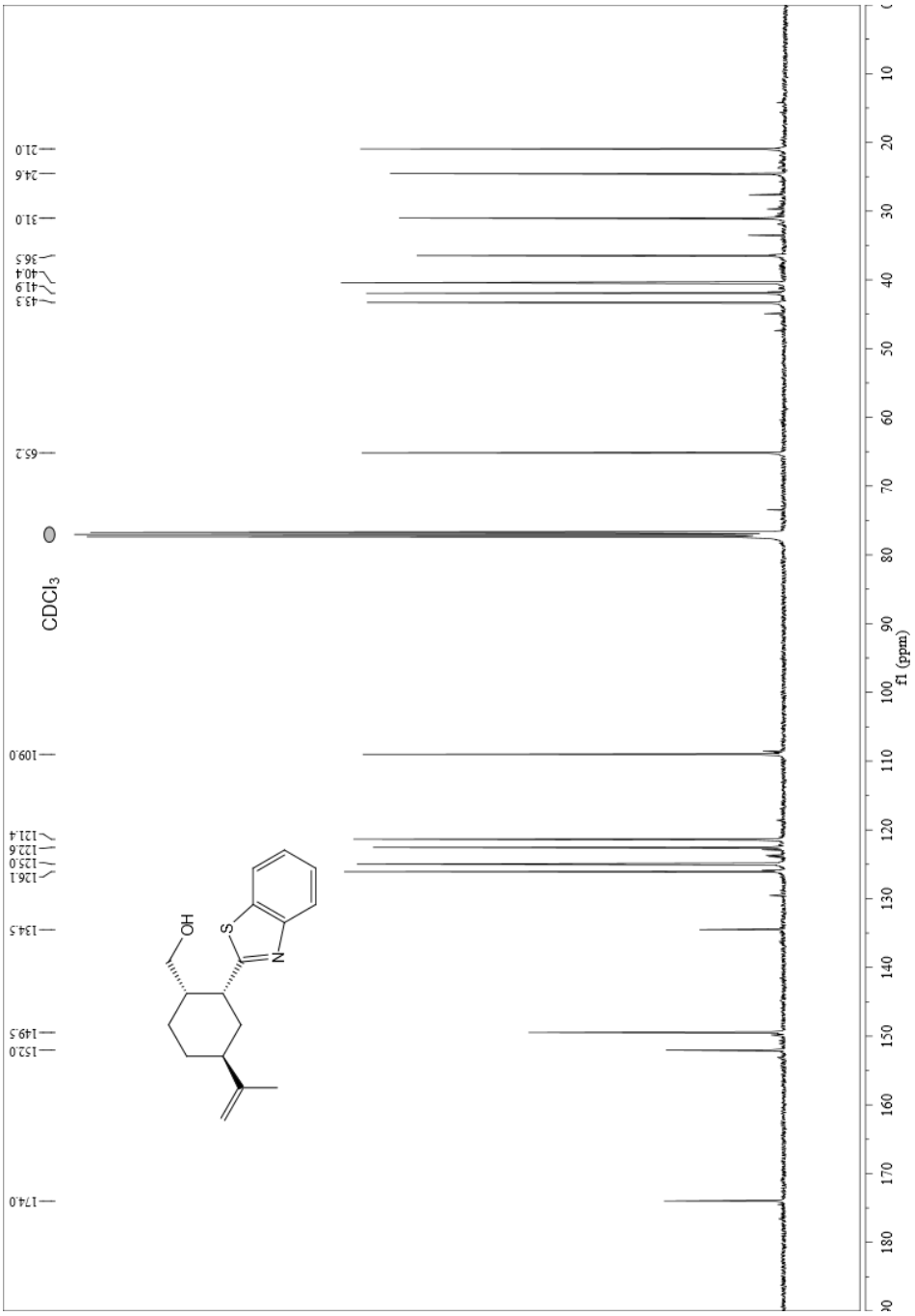

^{1}H NMR (400 MHz, $CDCl_3$) of **26a** 2-(2-(4-((benzyloxy)methyl)cyclohex-3-en-1-yl)propyl)-4-chlorobenzo[d]thiazole

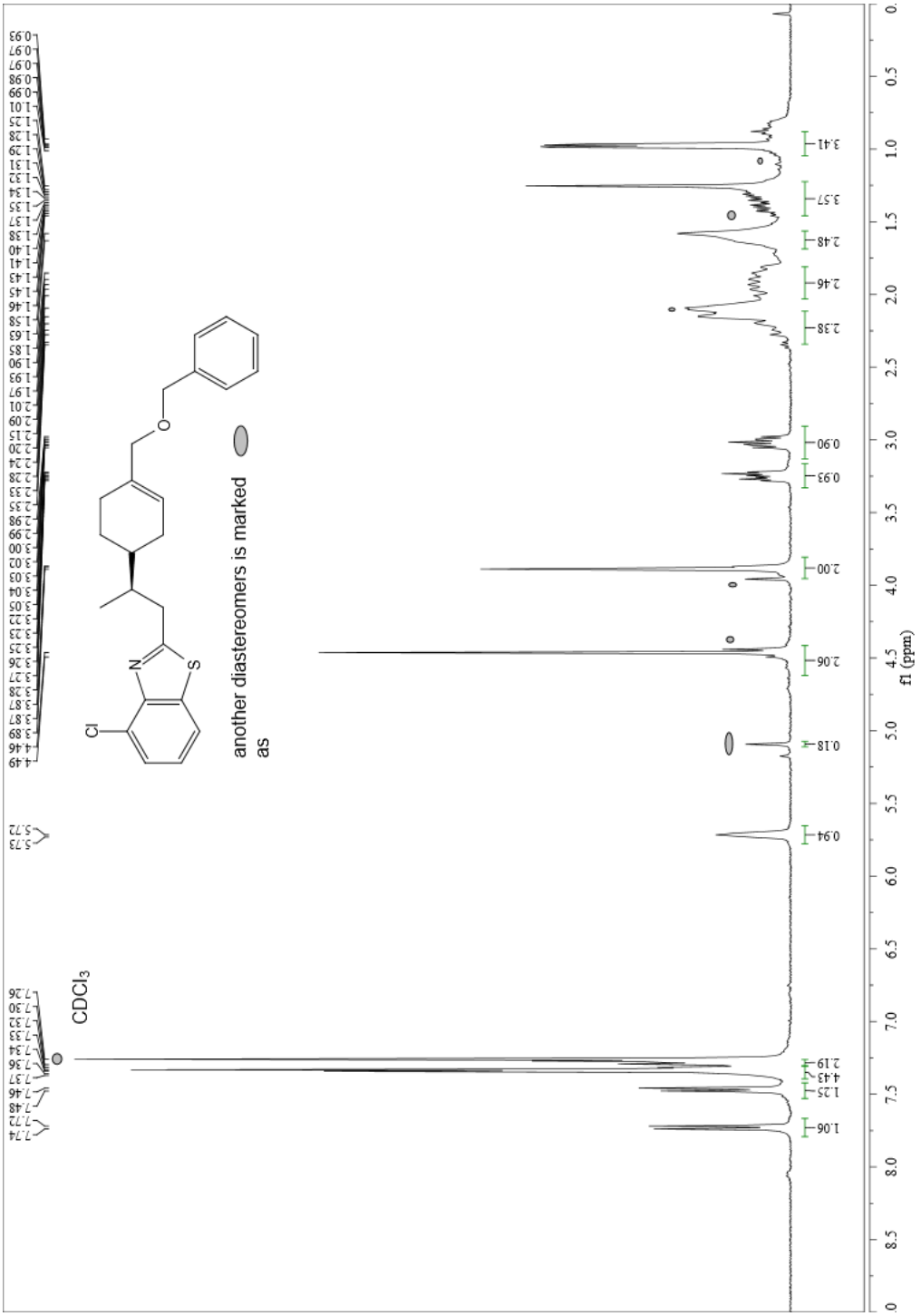

^{13}C NMR (101 MHz, $CDCl_3$) of **26a** 2-(2-(4-((benzyloxy)methyl)cyclohex-3-en-1-yl)propyl)-4-chlorobenzo[d]thiazole

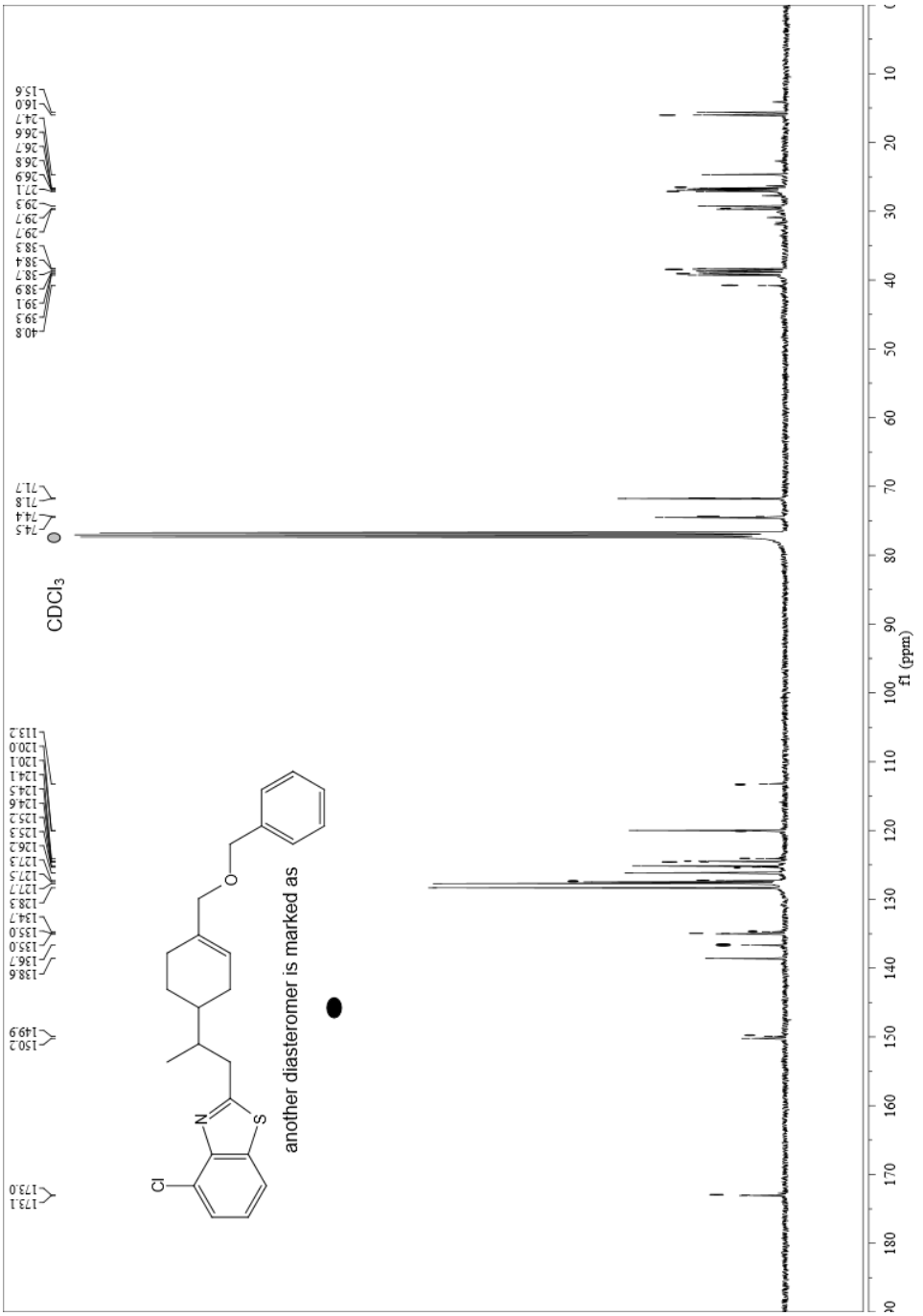

^{1}H NMR (400 MHz, $CDCl_3$) of **27a** 4,6-difluoro-2-(5-isopropyl-2-methylcyclohex-2-en-1-yl)benzo[d]thiazol

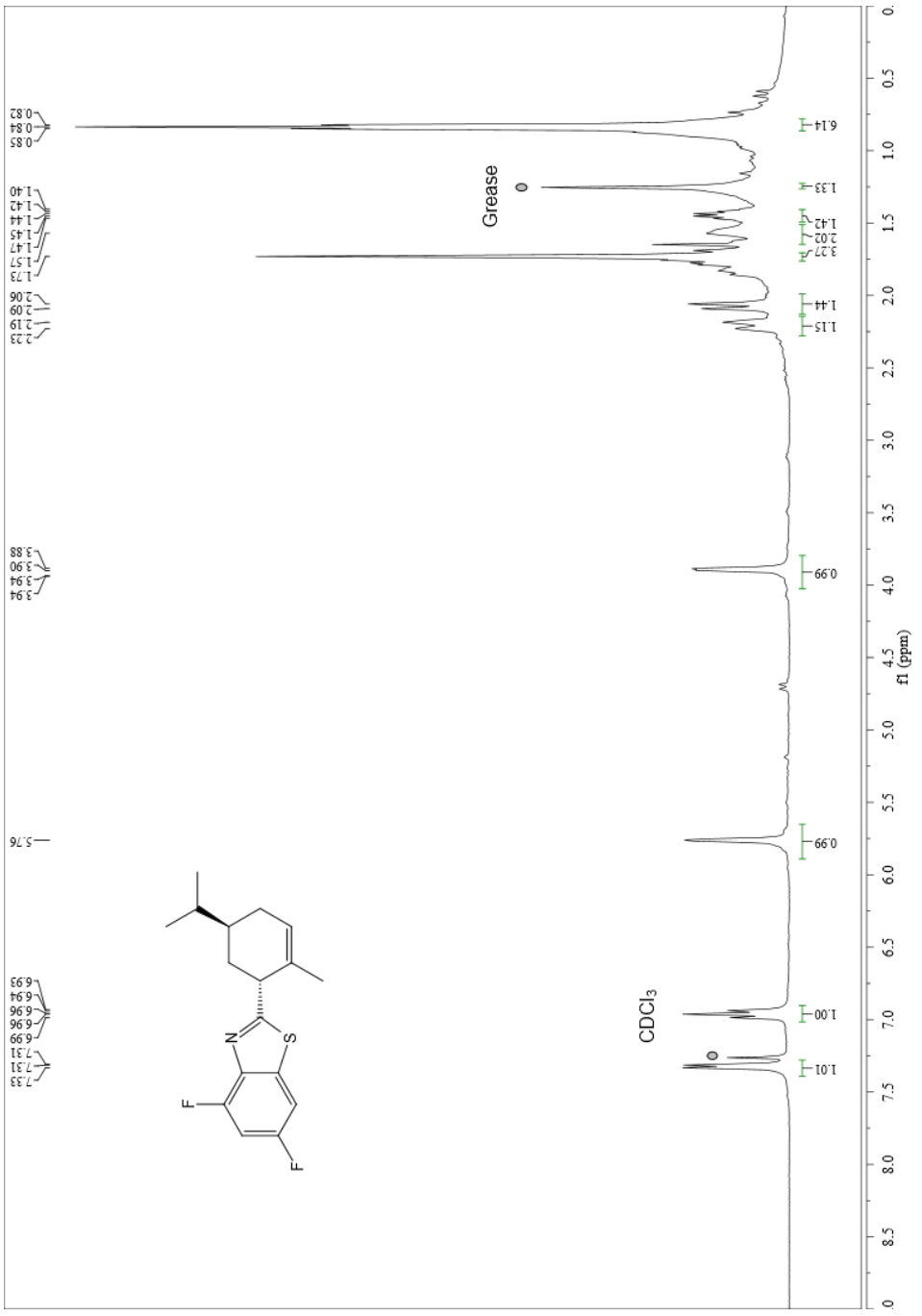

^{13}C NMR (101 MHz, $CDCl_3$) of **27a** 4,6-difluoro-2-(5-isopropyl-2-methylcyclohex-2-en-1-yl)benzo[d]thiazole

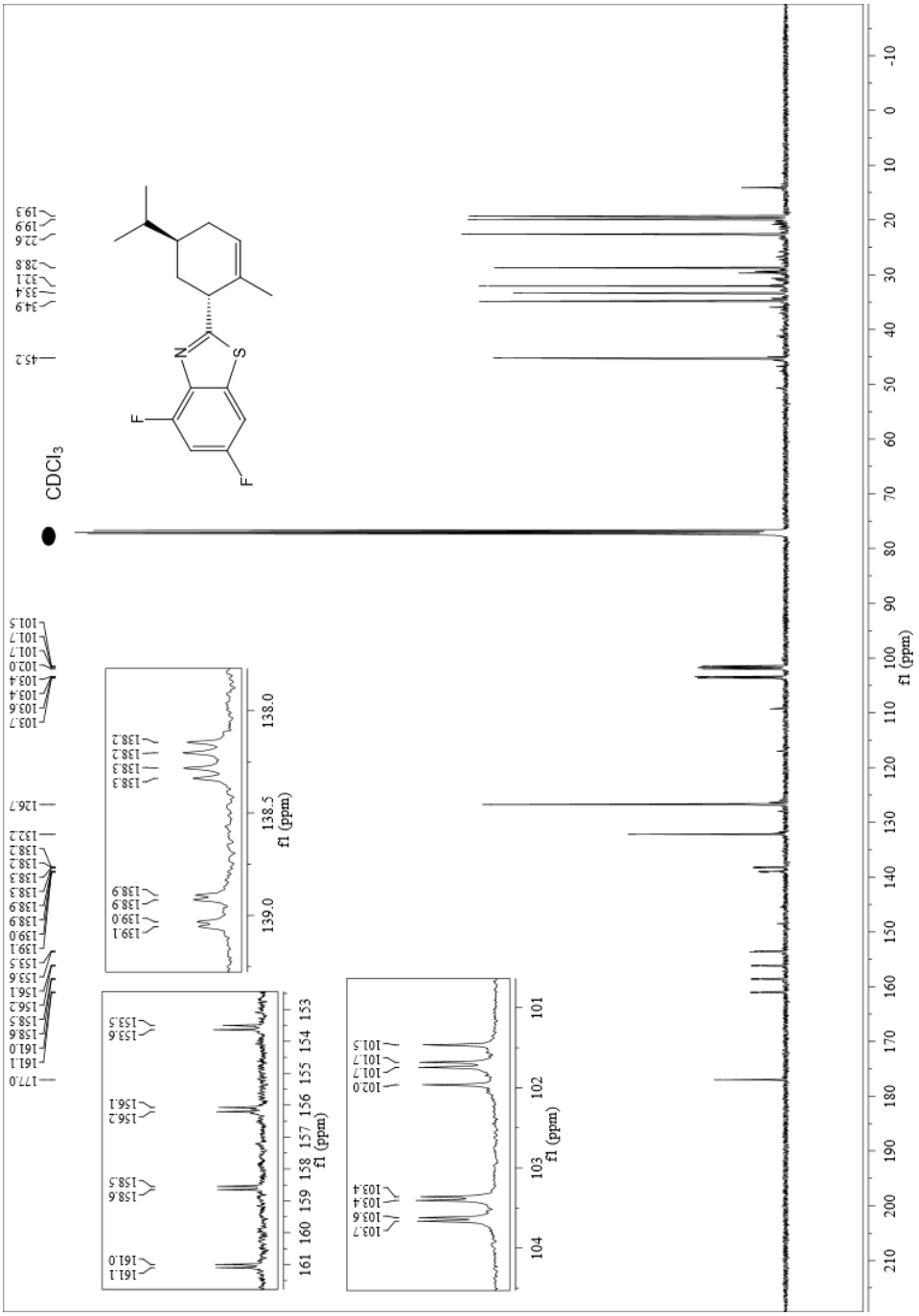

^{19}F NMR (376 MHz, $CDCl_3$) of **27a** 4,6-difluoro-2-(5-isopropyl-2-methylcyclohex-2-en-1-yl)benzo[d]thiazole

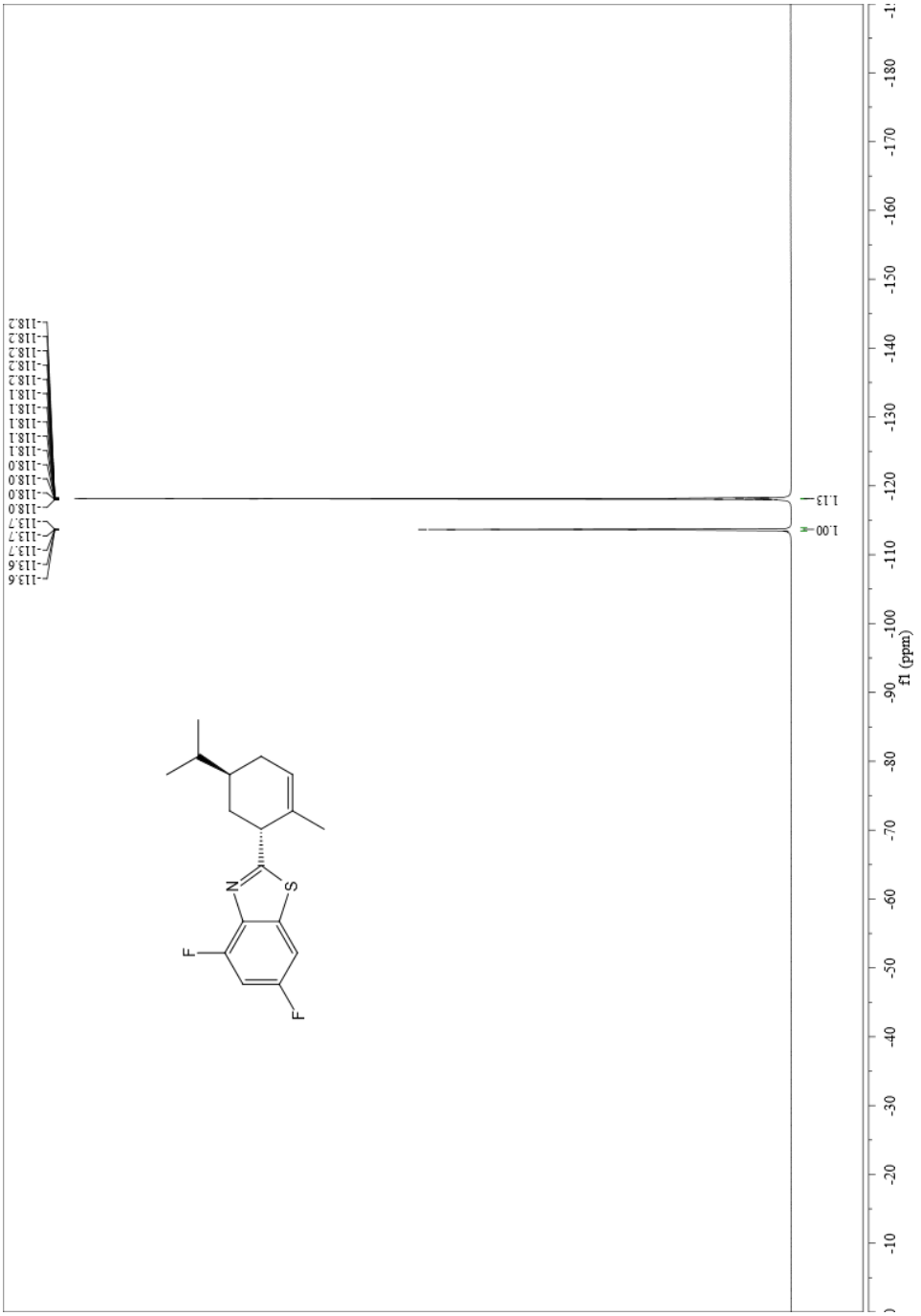

^{1}H NMR (400 MHz, $CDCl_3$) of **28a** 2-(((1S,11S,Z)-7,7,11-trimethyl-12-oxabicyclo[9.1.0]dodec-4-en-4-yl)methyl)thiazole

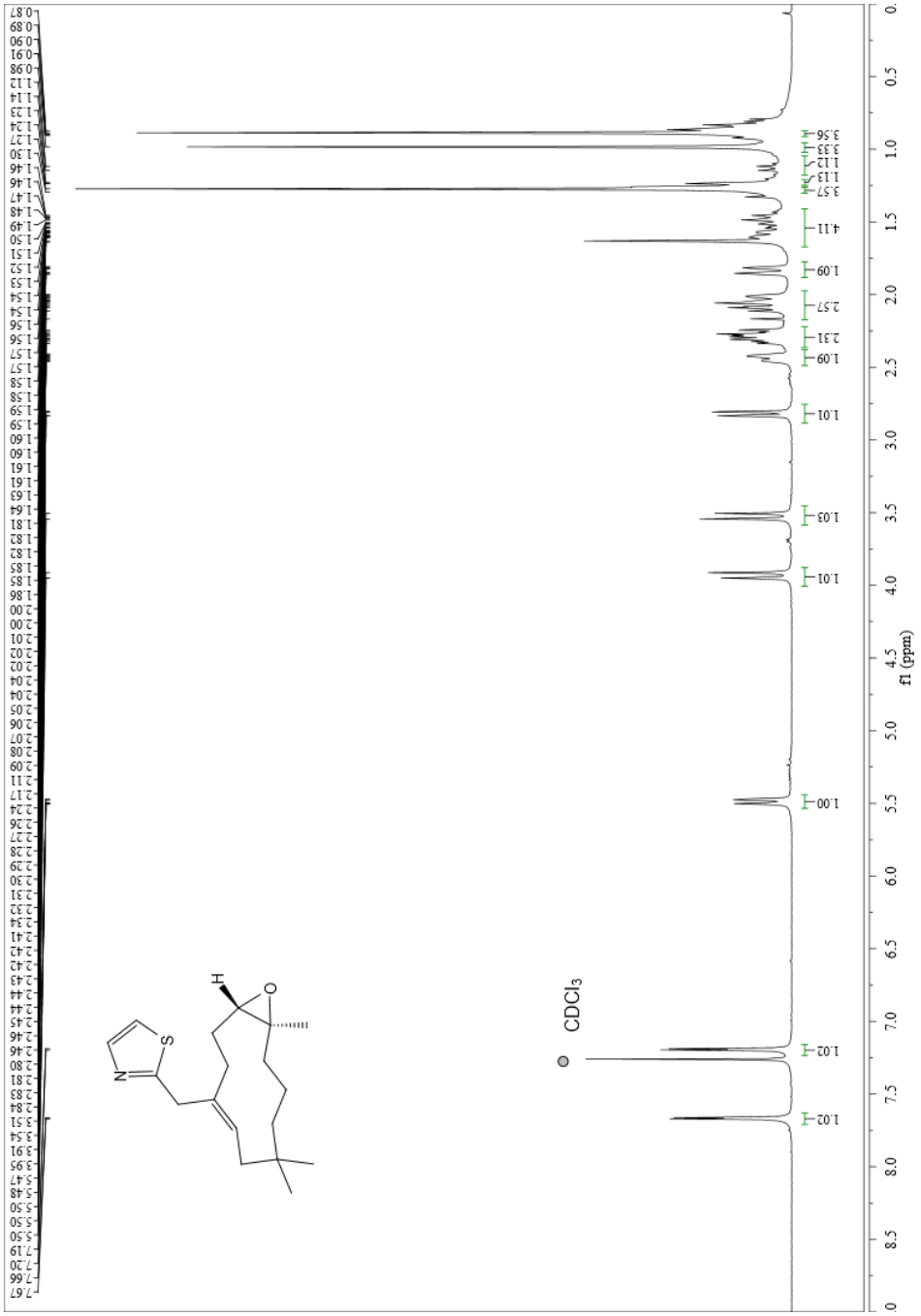

^{13}C NMR (101 MHz, $CDCl_3$) of **28a** 2-(((1S,11S,Z)-7,7,11-trimethyl-12-oxabicyclo[9.1.0]dodec-4-en-4-yl)methyl)thiazole

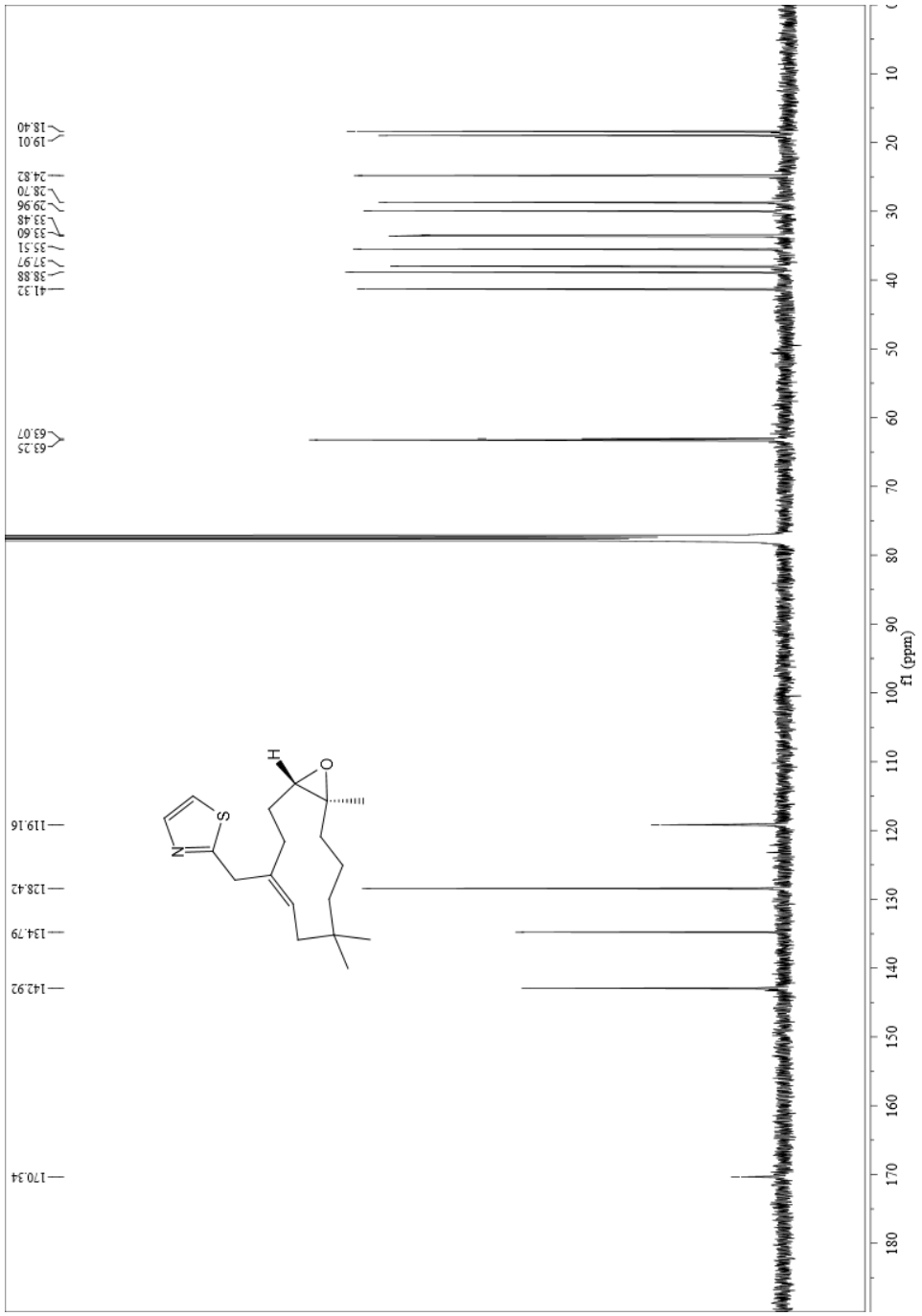

^{1}H NMR (599 MHz, $CDCl_3$) of **29a** (3S,8S,9S,10R,13R,14S,17R)-10,13-dimethyl-17-((R)-6-methylheptan-2-yl)-6-(thiazol-2-yl)hexadecahydro-1H-cyclopenta[a]phenanthren-3-ol

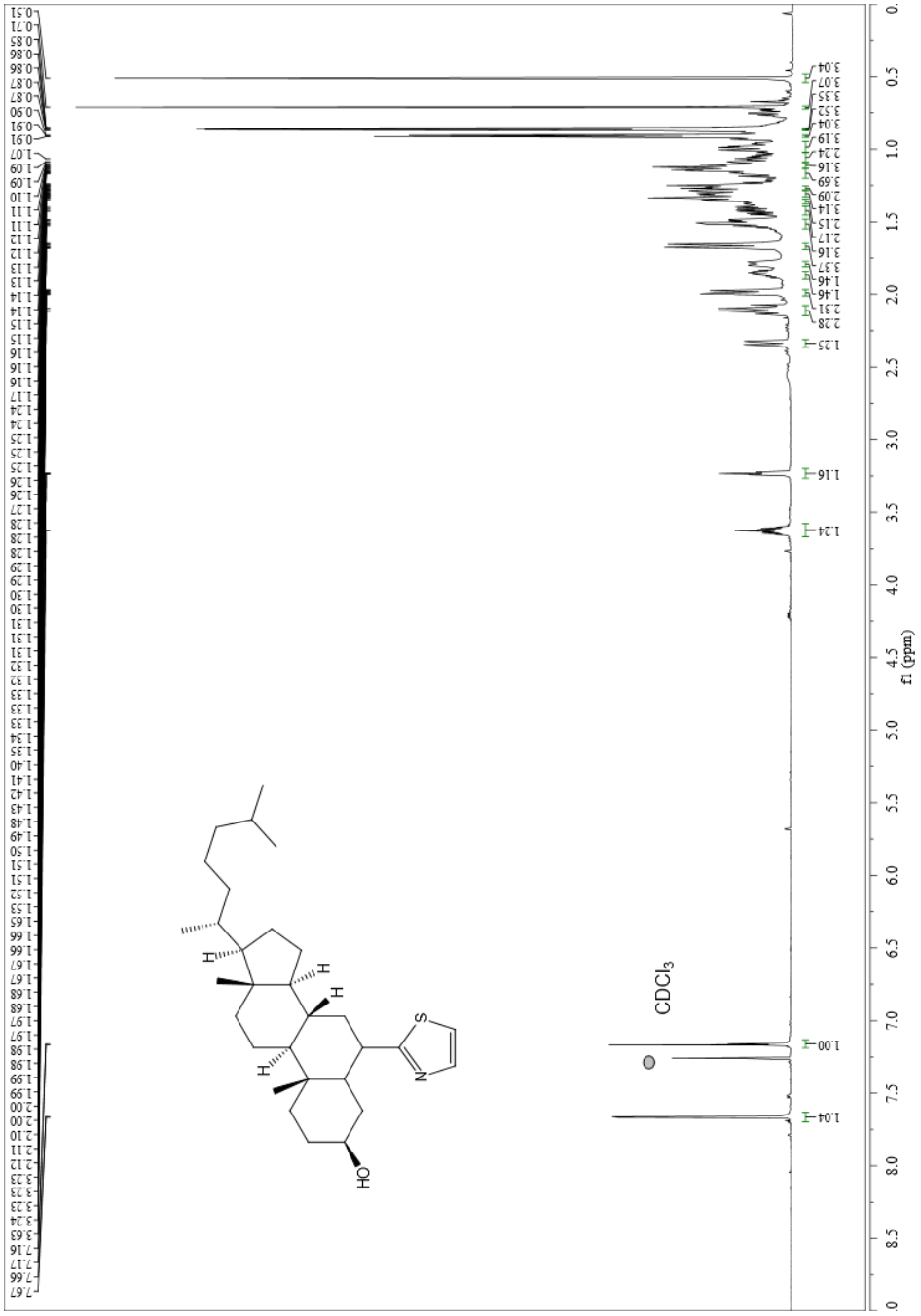

^{13}C NMR (101 MHz, $CDCl_3$) of **29a** (3S,8S,9S,10R,13R,14S,17R)-10,13-dimethyl-17-((R)-6-methylheptan-2-yl)-6-(thiazol-2-yl)hexadecahydro-1H-cyclopenta[a]phenanthren-3-ol

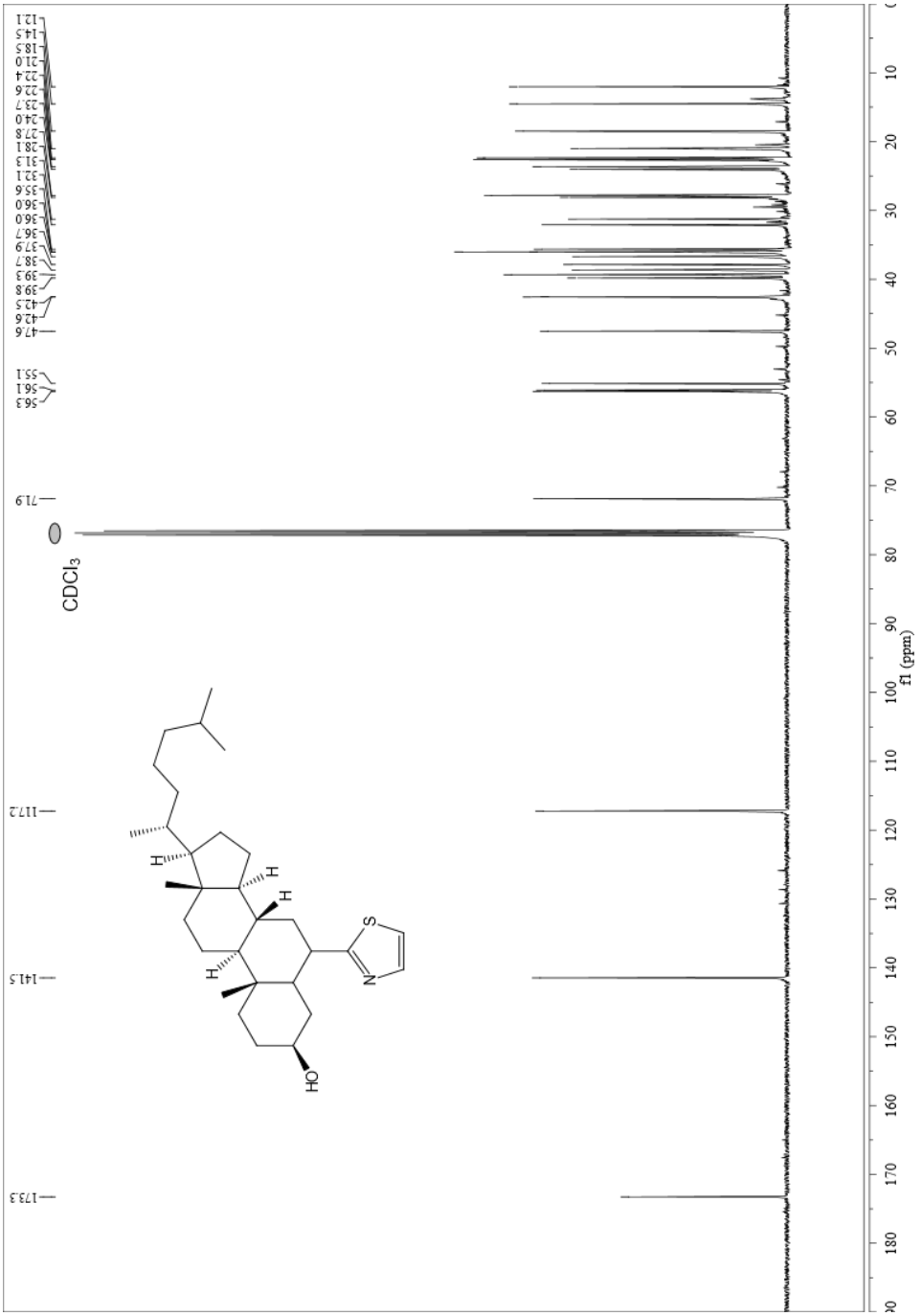

^{1}H NMR (400 MHz, $CDCl_3$) of **30a** 2-cyclooctylthiazole

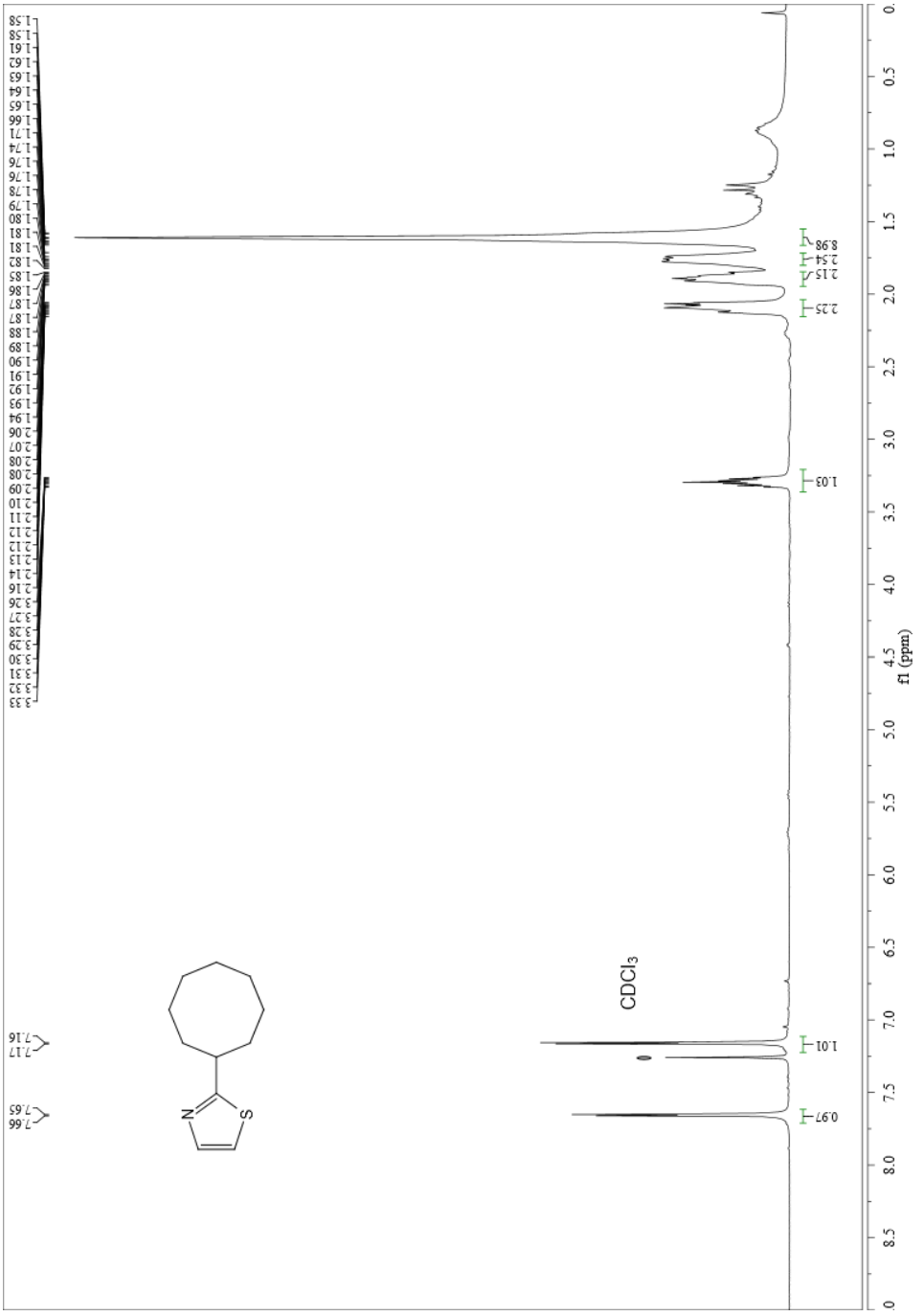

^{13}C NMR (101 MHz, $CDCl_3$) of **30a** 2-cyclooctylthiazole

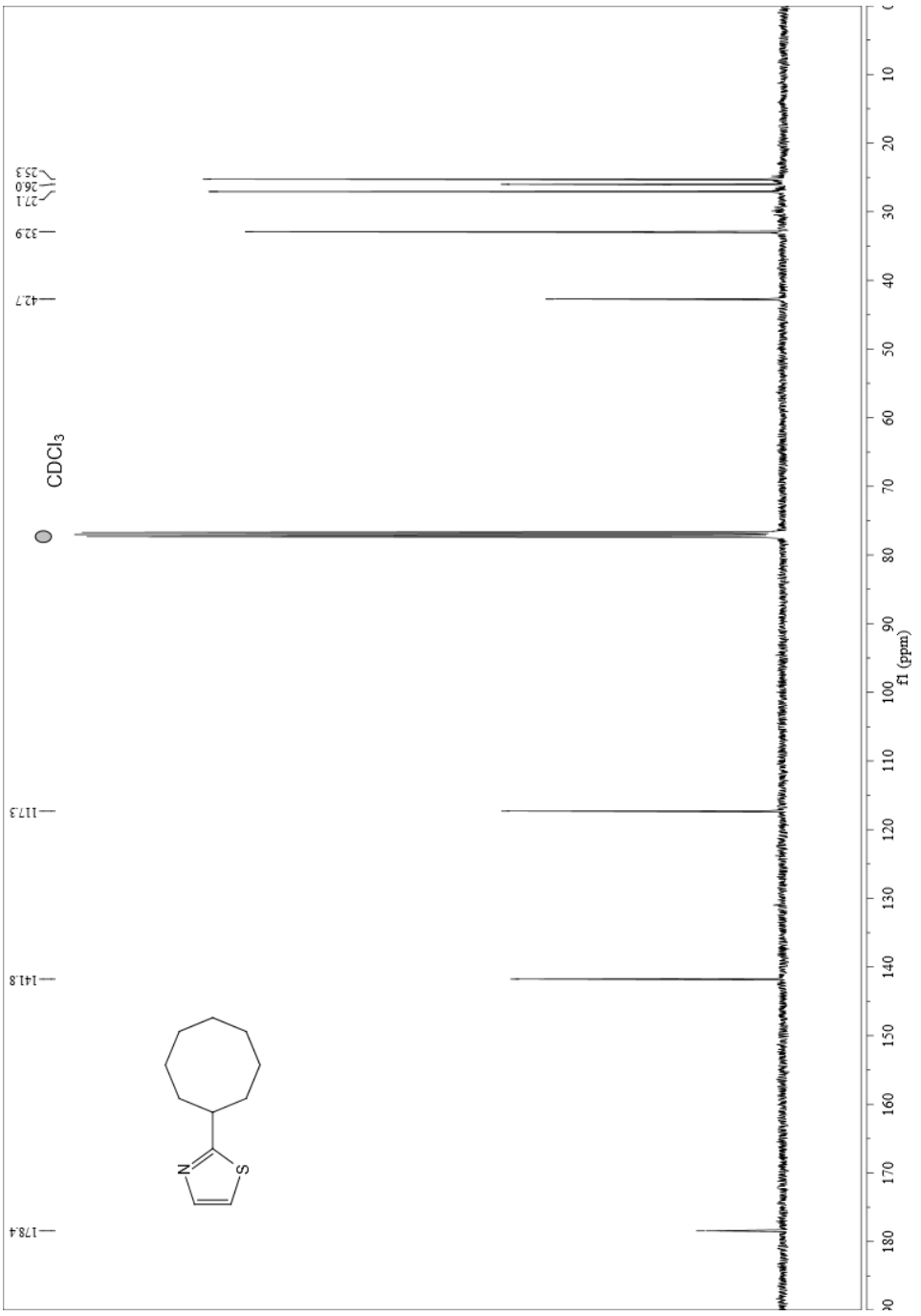

^{1}H NMR (400 MHz, $CDCl_3$) of **31a** 2-cyclooctyl-4,6-difluorobenzo[d]thiazole

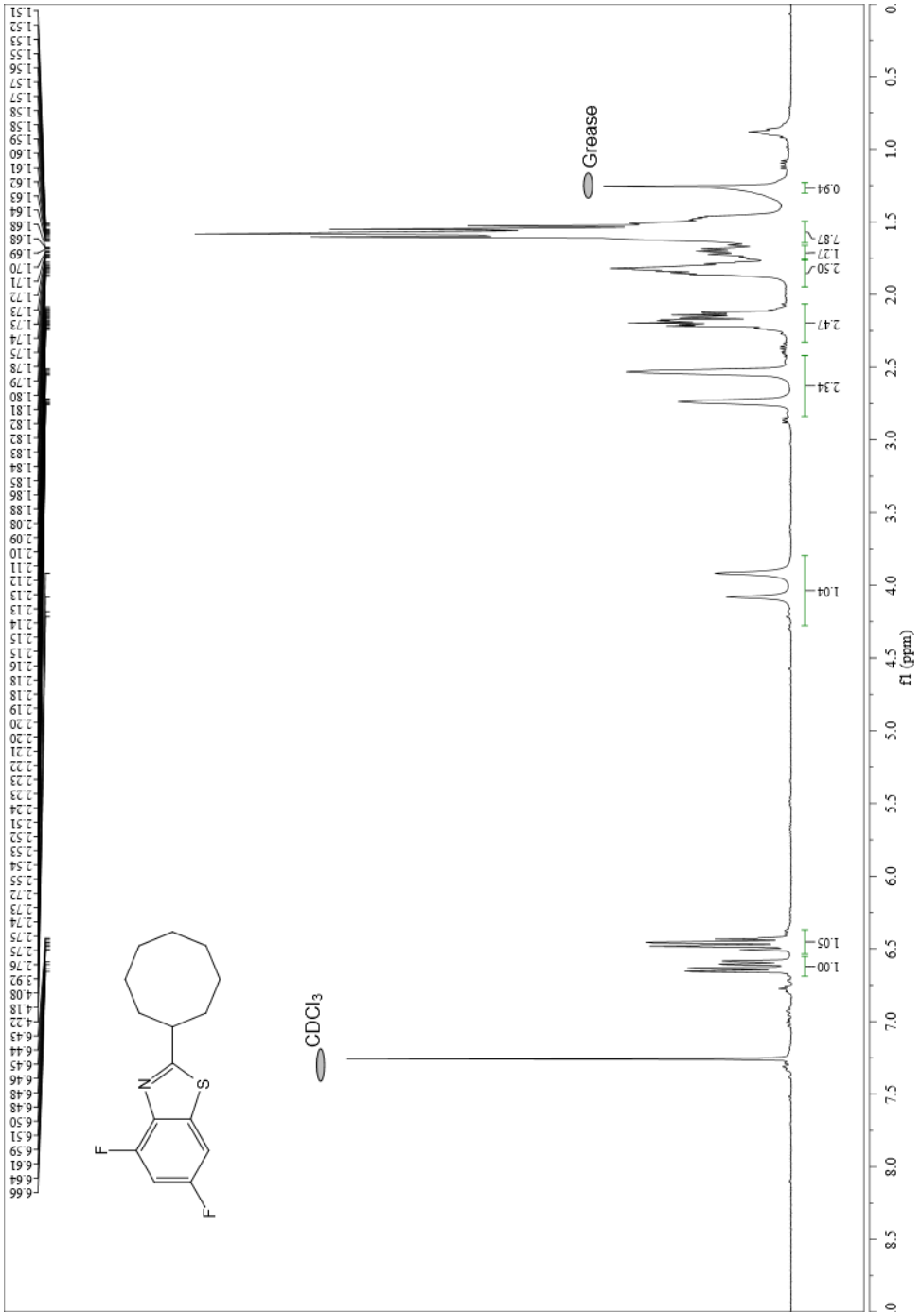

^{13}C NMR (101 MHz, $CDCl_3$) of **31a** 2-cyclooctyl-4,6-difluorobenzo[d]thiazole

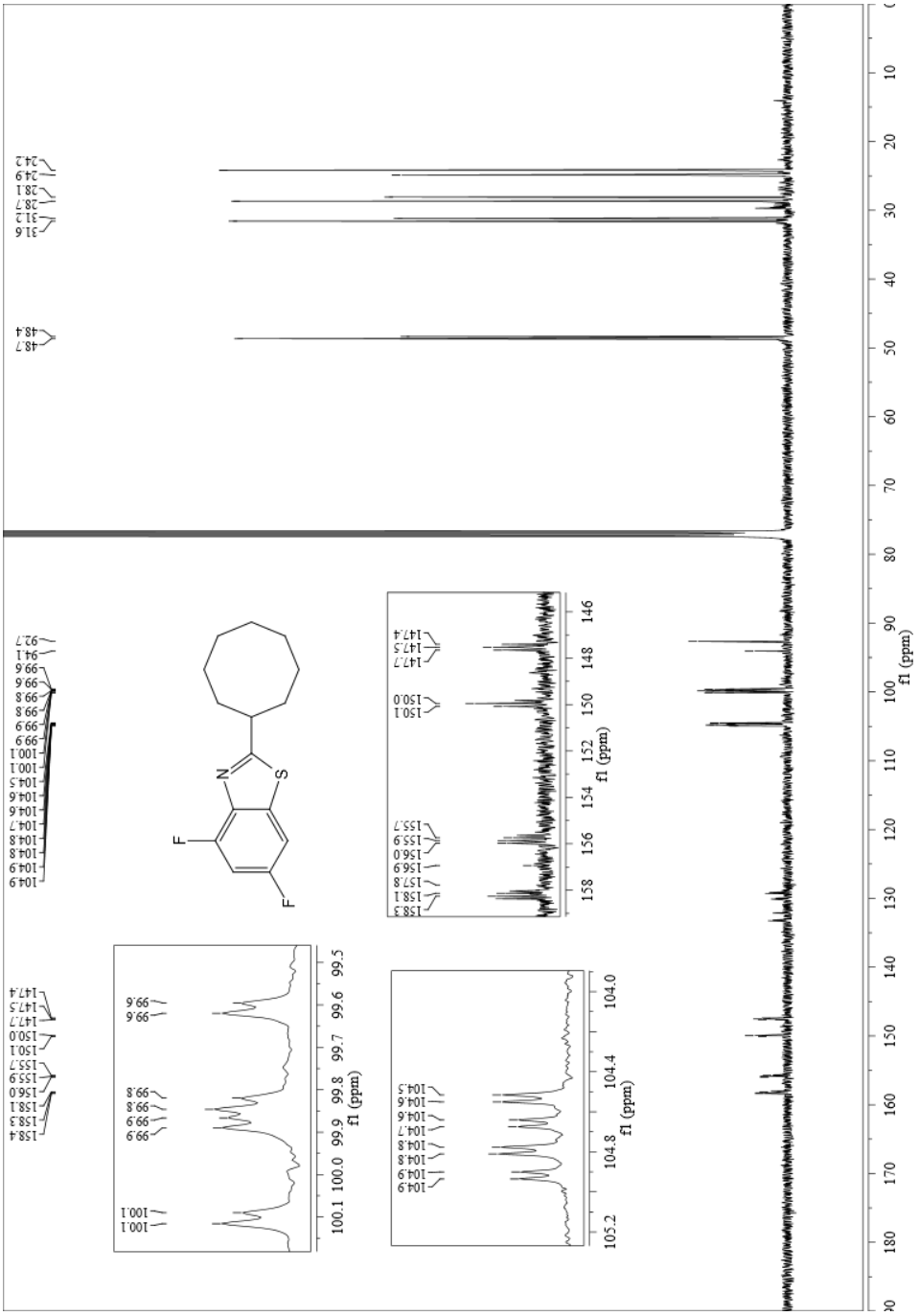

^{19}F NMR (376 MHz, $CDCl_3$) of **31a** 2-cyclooctyl-4,6-difluorobenzo[d]thiazole

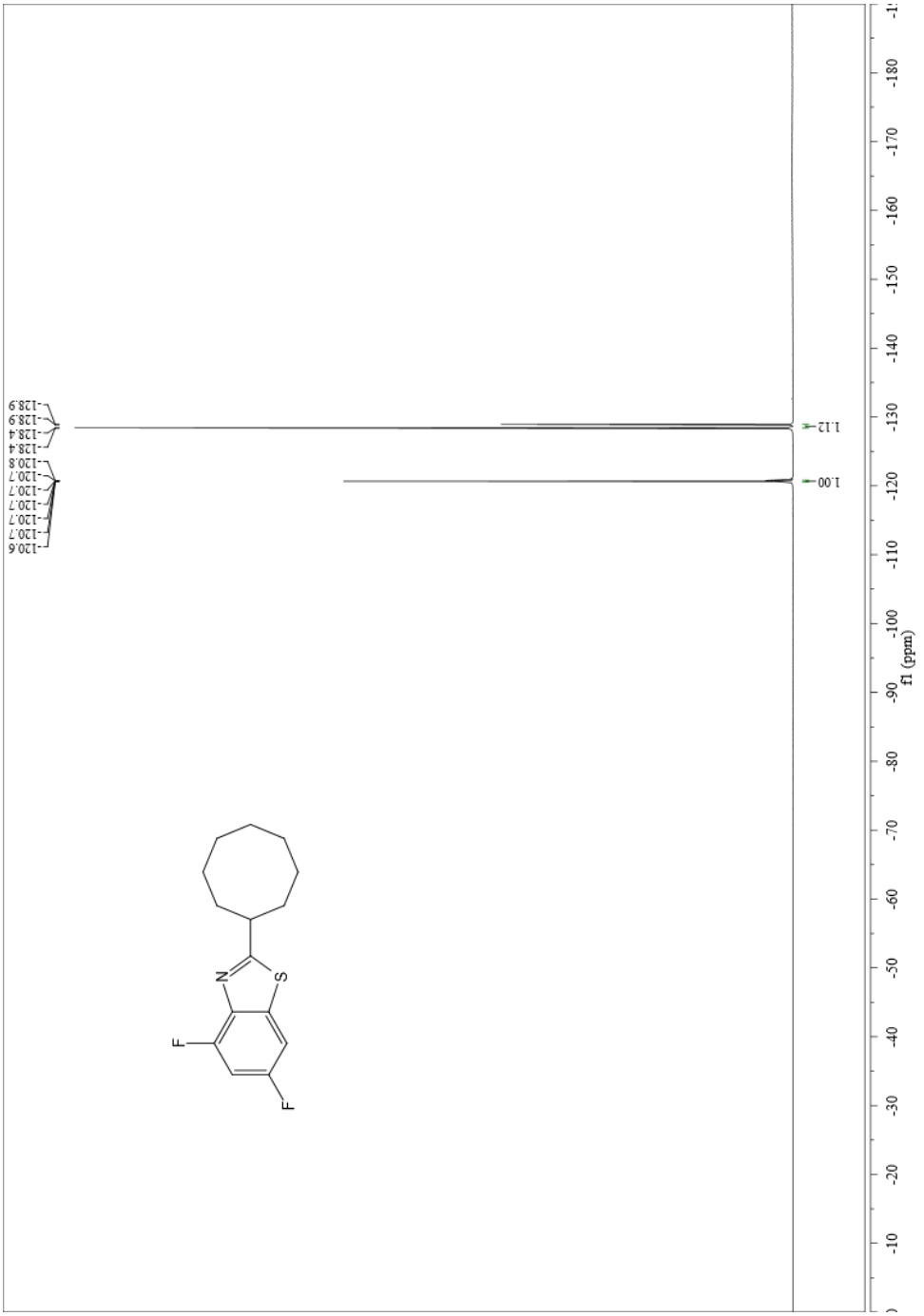

^{1}H NMR (400 MHz, $CDCl_3$) of **32a** 5-((1R,4S)-bicyclo[2.2.1]heptan-2-yl)pyrimidine-2-carbonitrile

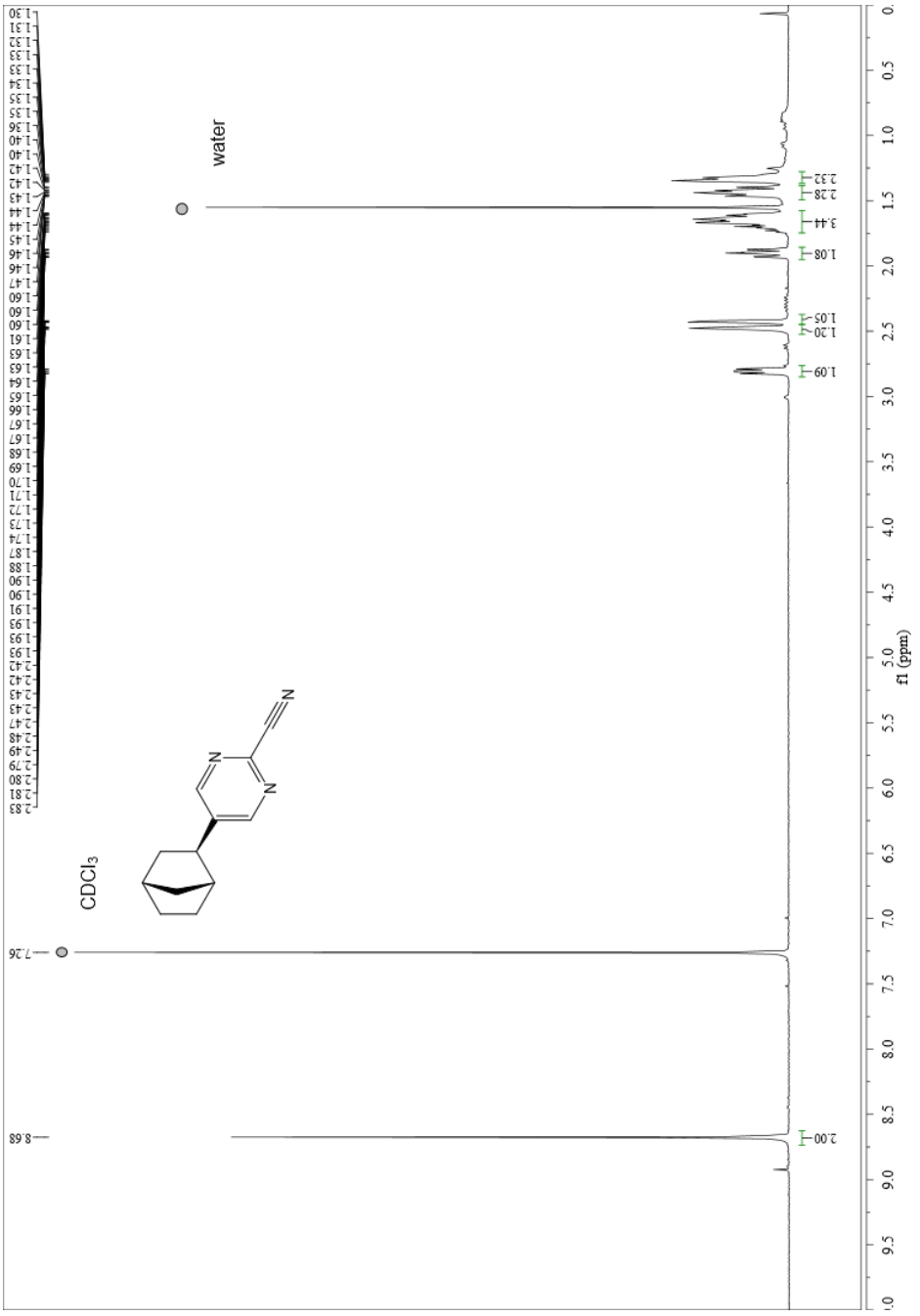

^{13}C NMR (101 MHz, $CDCl_3$) of **32a** 5-((1R,4S)-bicyclo[2.2.1]heptan-2-yl)pyrimidine-2-carbonitrile

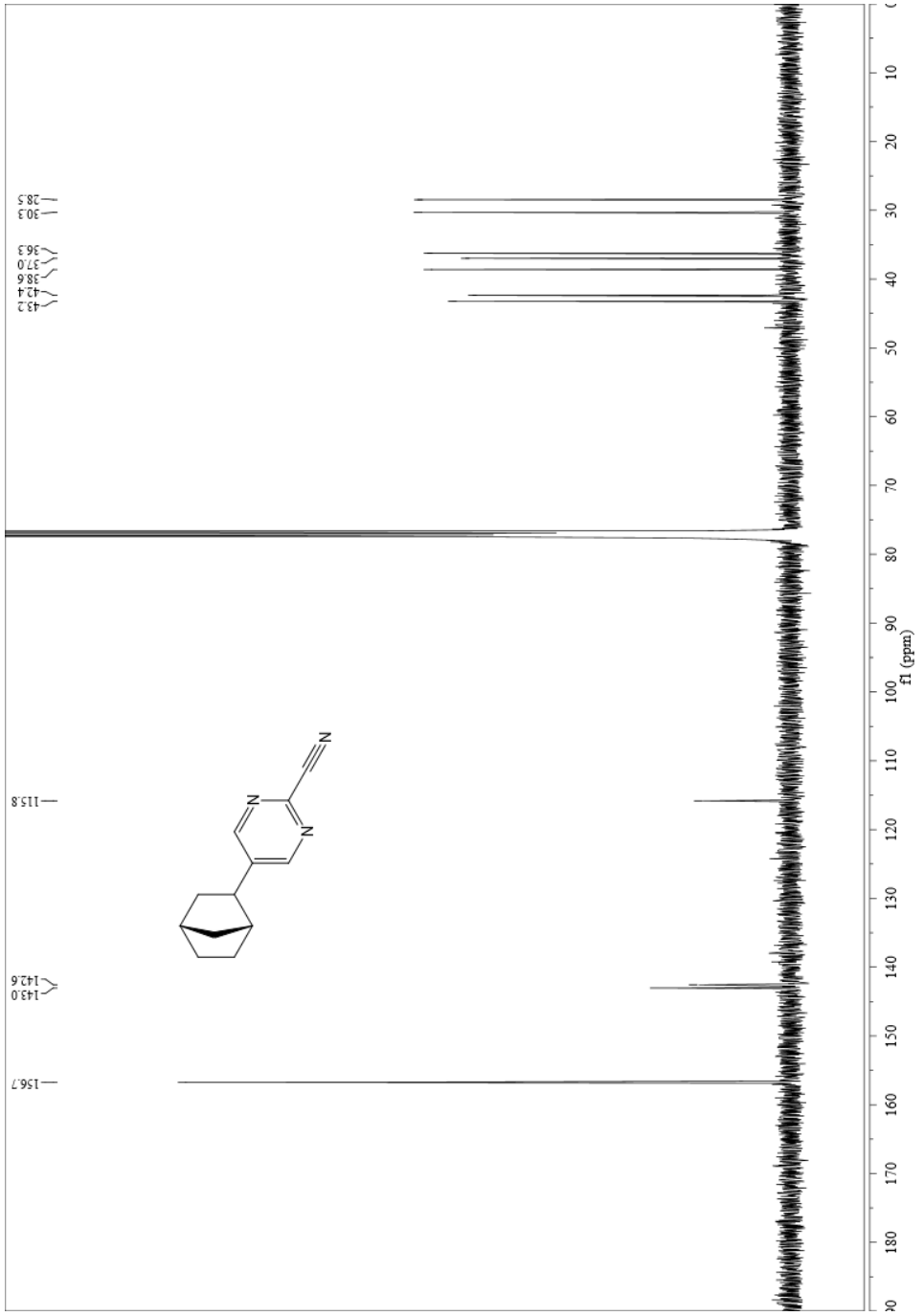

^{1}H NMR (400 MHz, CD_3OCD_3) of **33a** dimethyl (1R,4S,5R)-5-(4-formylphenyl)-7-oxabicyclo[2.2.1]heptane-2,3-dicarboxylate

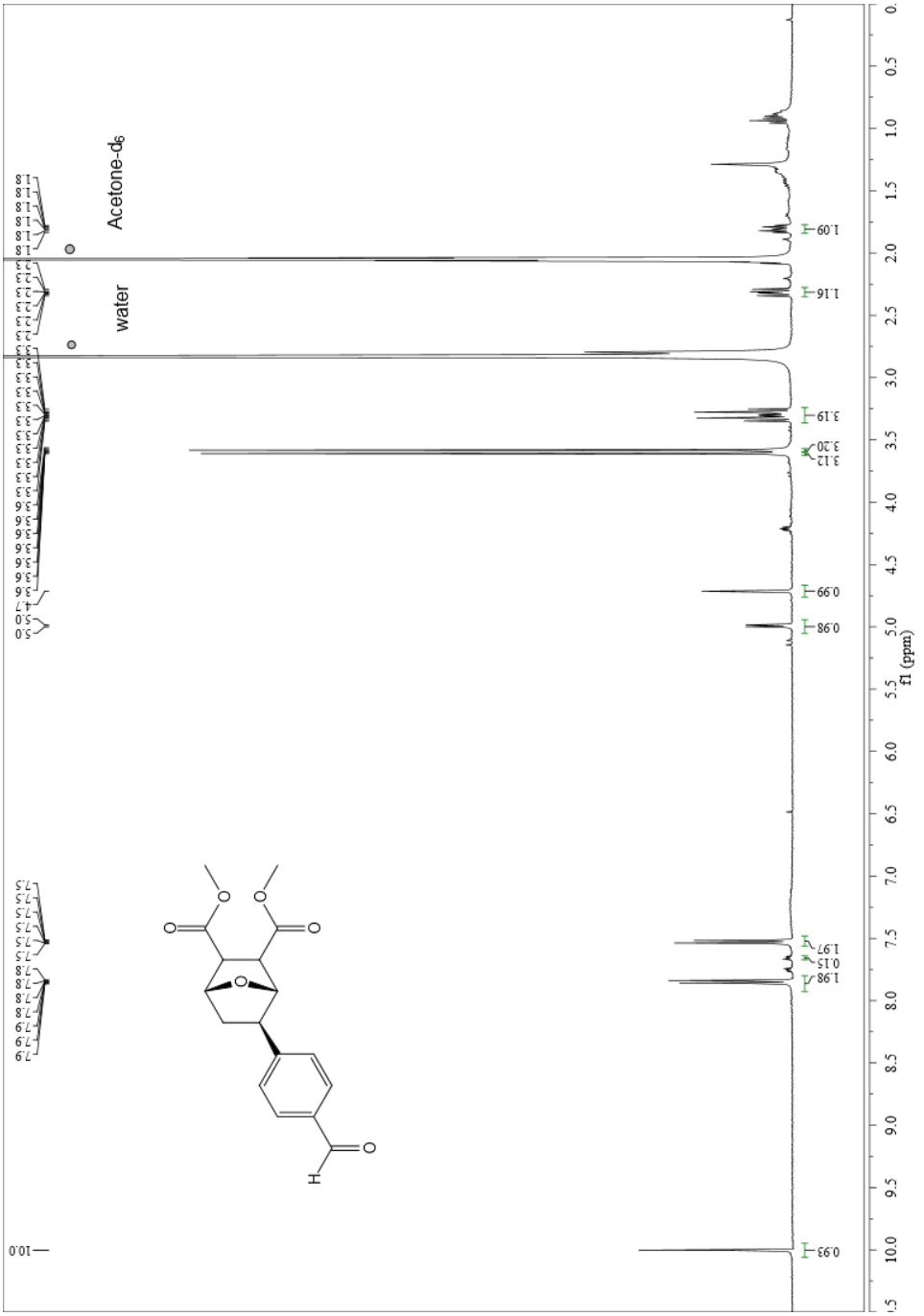

^{13}C NMR (400 MHz, CD_3OCD_3) of **33a** dimethyl (1R,4S,5R)-5-(4-formylphenyl)-7-oxabicyclo[2.2.1]heptane-2,3-dicarboxylate

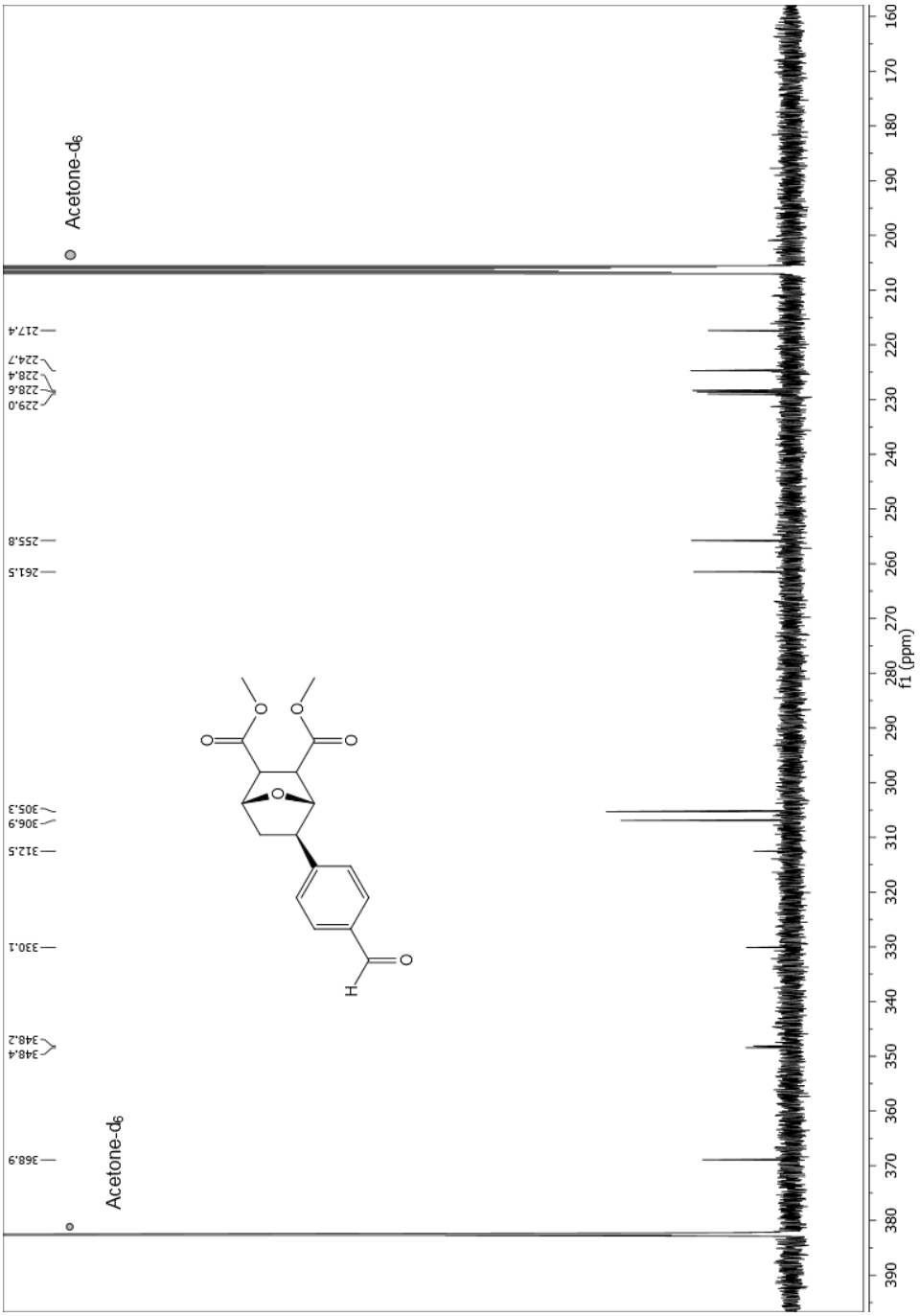

^{1}H NMR (400 MHz, $CDCl_3$) of **34a** 4-((1S,4R)-bicyclo[2.2.1]heptan-2-yl)benzonitrile

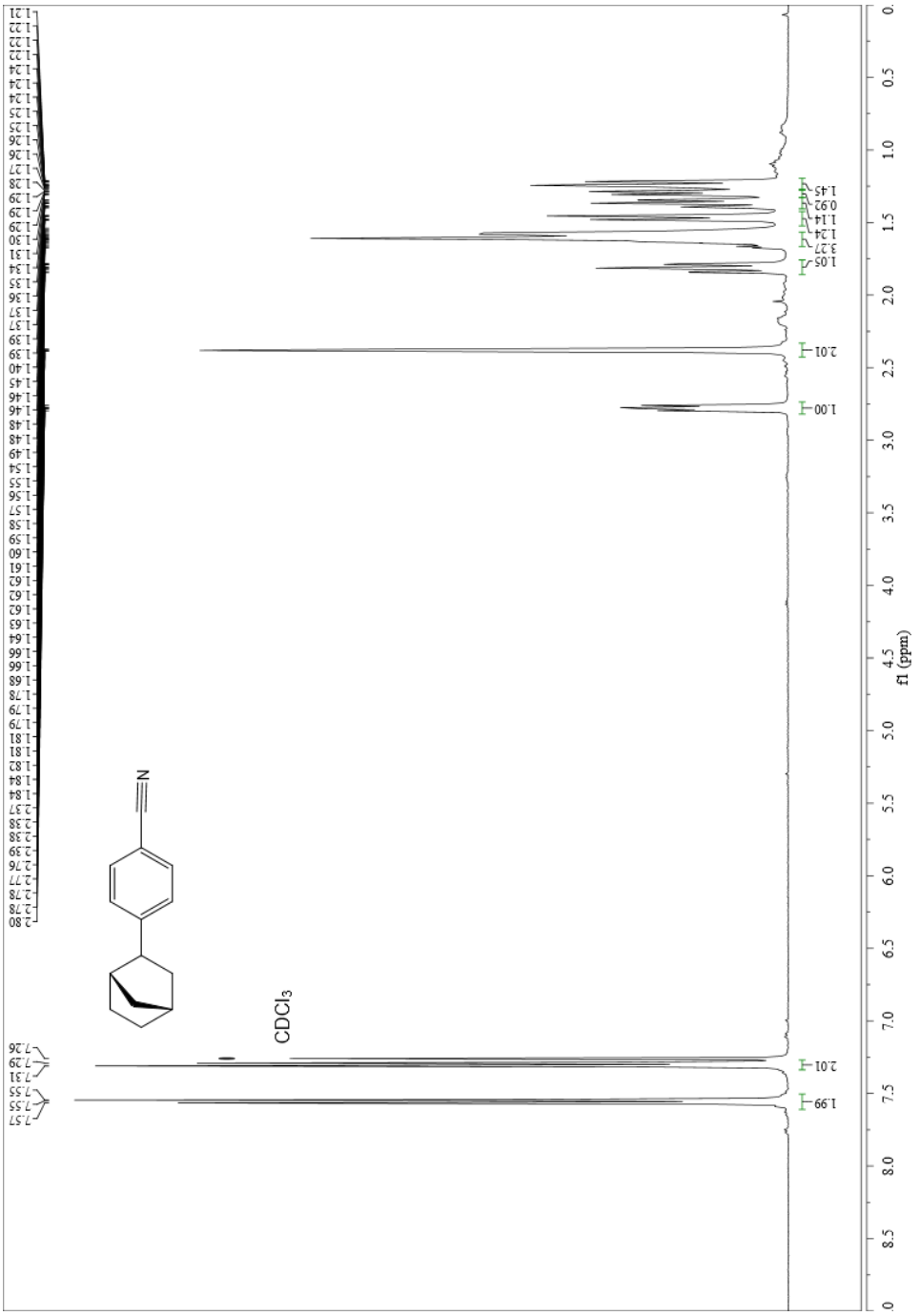

^{13}C NMR(101 MHz, $CDCl_3$) of **34a** 4-((1S,4R)-bicyclo[2.2.1]heptan-2-yl)benzonitrile

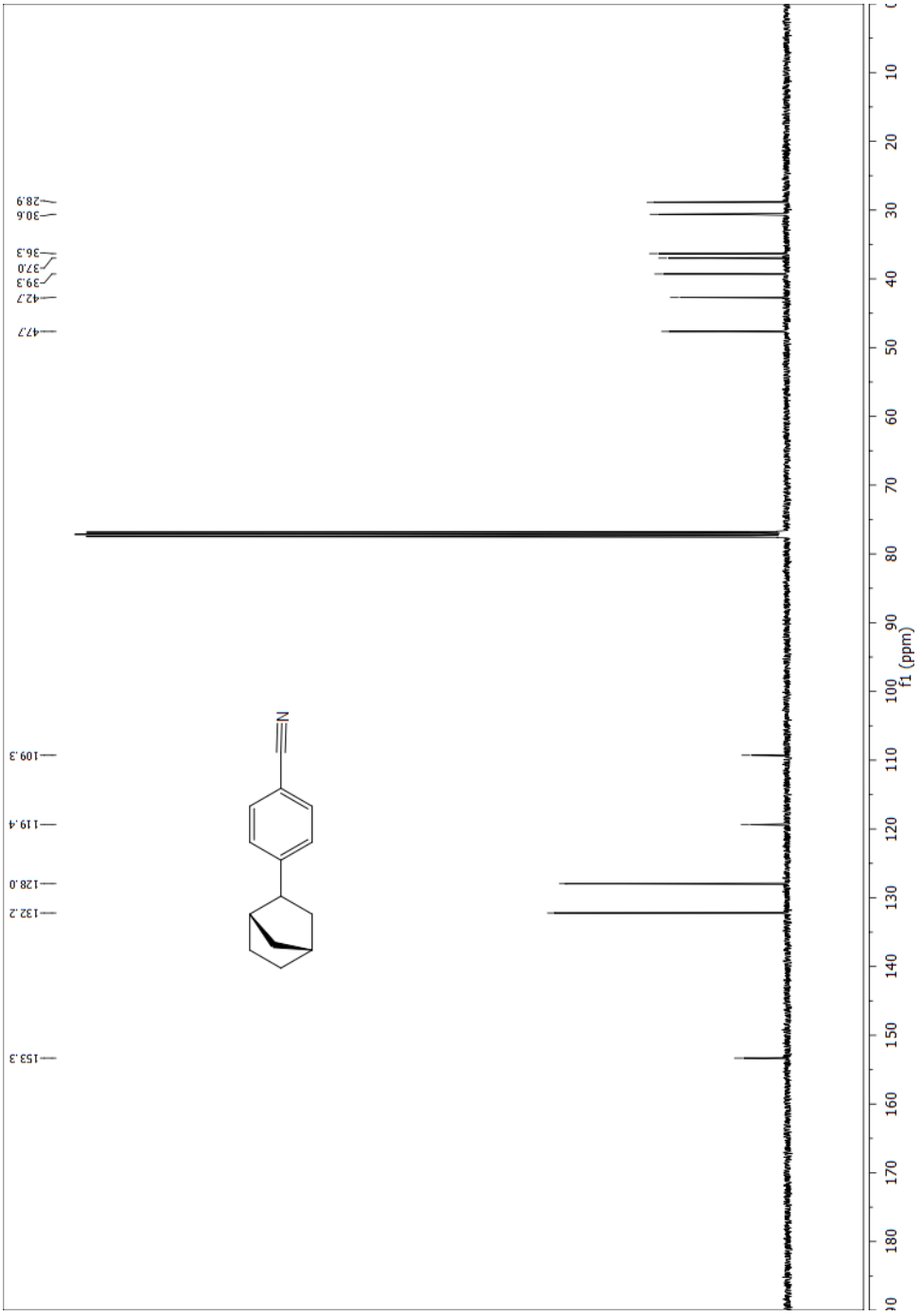

^{1}H NMR (400 MHz, $CDCl_3$) of **11c** 1-(benzo[d]oxazol-2-yl)-N,N-dibutylbutan-1-amine

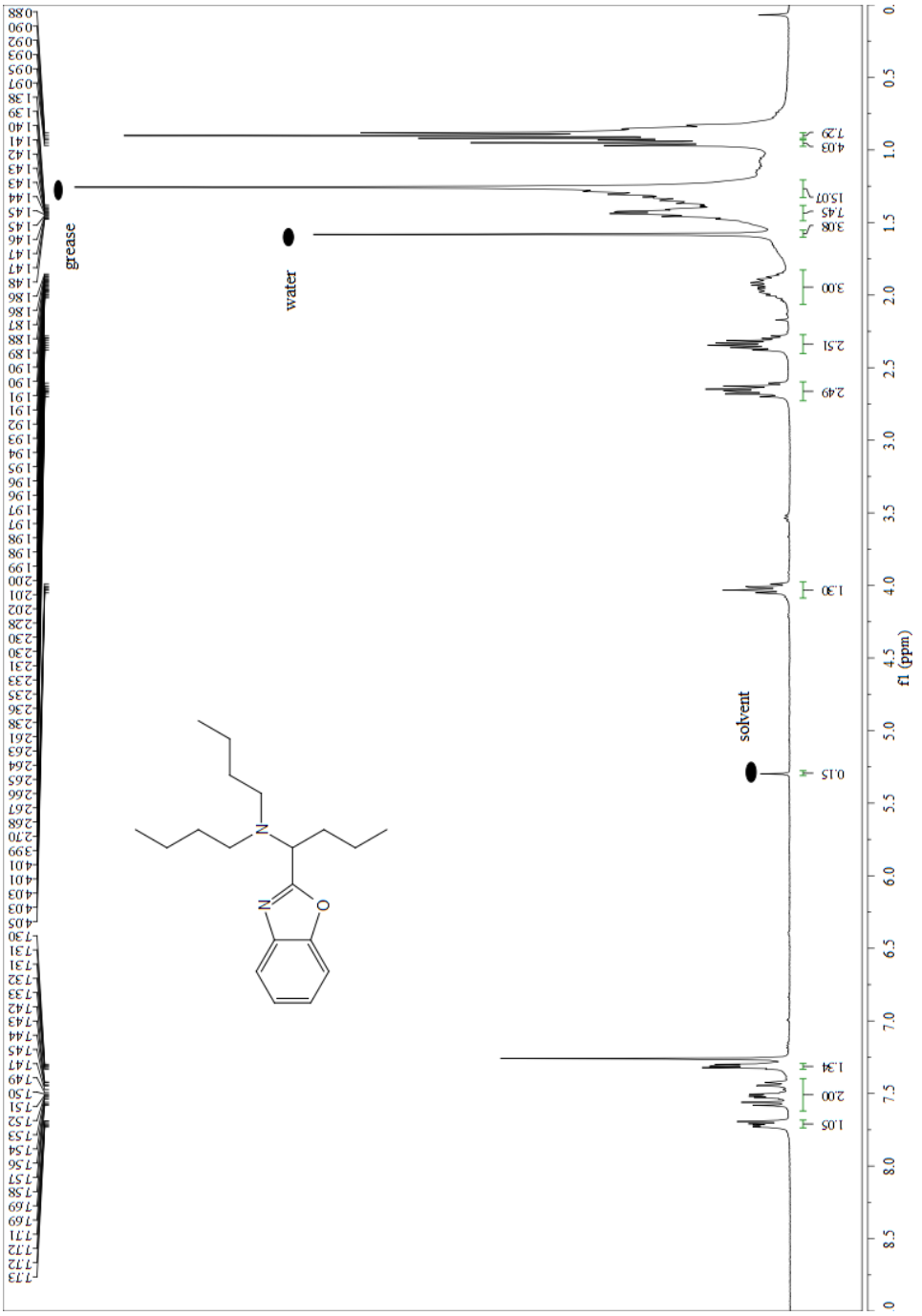

CHAPTER IV

POLYFLUOROARYLATION OF OXAZOLONES: ACCESS TO FLUORINATED AMINO ACIDS

4.1 *Introduction*

Amino acids and derivatives are indispensable building blocks within organic chemistry. The addition of an oxazolone enolate to an electrophile is a common strategy to elaborate the alpha amino acid motif.[106-109] α-Arylation of the oxazolone enolate has been accomplished via Ag-mediated arylation with diaryliodonium salts (**Scheme 4.1**, eqn 1),[109] Pd-catalyzed cross-coupling of aryl-bromides (eqn 2),[110] and pyridine addition via nucleophilic addition to *N*-tosylated pyridines (eqn 3).[106] However, these methods do little to access amino acids that possess highly fluorinated arenes, since the requisite fluorinated starting materials are not available. Additionally, while these methods proved useful for accessing tertiary carbons, secondary carbons were never obtained. In other words, it was important that the product be fully substituted at the alpha position, likely due to the fact that the product was more reactive than the starting material. We posited that the oxazolone enolate might undergo uncatalyzed substitution of the perfluoroarenes (eqn 5), via nucleophilic aromatic substitution (S_NAr), and because the product was anticipated to

form a more stable anion, we anticipated diminishment of its nucleophilicity when compared to the starting material, allowing clean formation of the product without over arylation. Importantly, if successful, this would provide rapid and facile access to non-natural multifluoroarylated amino acids.

Scheme 4.1. Arylation of oxazolones

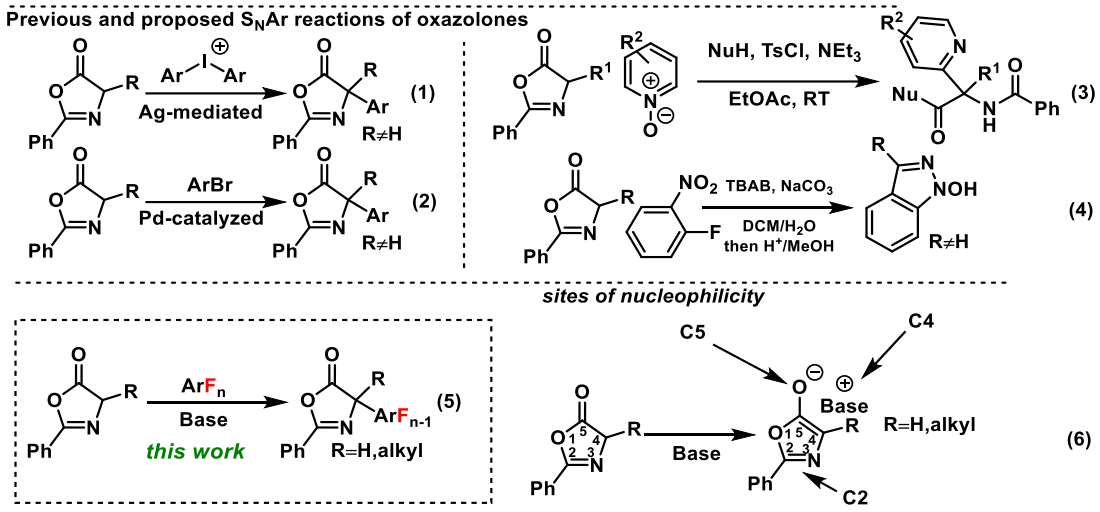

The oxazolone enolate is a versatile nucleophile which can conceivably undergo addition at C2, C4, and even the C5-oxygen bond (eqn 6).[111] The only example of S_NAr-type reactions with oxazolones is the addition to 2-nitroarenes, which undergoes subsequent cyclization with the nitro functional group to give indazole products (eqn 4).[112] Though the reaction leads to a different product, it suggests that oxazolone enolate might be a competent nucleophile in the addition to perfluoroarenes (eqn 5).

4.2 *Optimization studies*

We started our investigation using 2-phenyloxazol-5(4H)-one (**1**, **Table 4.1**) derived from glycine with pentafluoropyridine and diisopropylamine (DIPEA) in acetonitrile which were optimal conditions in the analogous addition of Meldrum's acid enolate.[18] Initially, we ran the

reaction at 45 °C (entry 1) but found the reaction gave full conversion at room temperature, giving complete conversion to the C4-arylation product within just 20 min (entry 2). Owing to the relatively fast addition, we were able to lower the amount of the arene to 1.025 equiv (entry 3) without any detectable diminishment of conversion. Previously, we have observed DIPEA can undergo a slow *N*–substitution/dealkylation sequence when subjected to highly electrophilic perfluoroarenes at elevated temperatures.[113] Consequently, by keeping the amount of excess perfluoroarene low (0.025 equiv) and reactions at room temperature, the amine substituted product was not observed. A solvent screen (entries 2-7) revealed polar aprotic solvents work best, while ethereal, hydrocarbon, and halogenated solvents gave little to no conversion (entries 5-7). To facilitate reaction scale up, we simultaneously reduced the arene loading and concentrated the reaction to 1 M (entry 8) which smoothly proceeded to full conversion. Next, we evaluated a less activated arene, octafluorotoluene (**b**), instead of pentafluoropyridine (entry 9), but unfortunately, it gave very low conversion under these conditions.

However, upon switching to stronger base, tetramethyl guanidine (TMG-H^+, $pKa_{(MeCN)}$ = 23.3 compared to ~18.8 for DIPEA-H^+).[114] We observed complete conversion, even at -20 °C (entry 10). Lower temperatures were necessary to avoid TMG addition to the perfluoroarenes (not shown).

Table 4.1. Optimization of Reaction Conditions

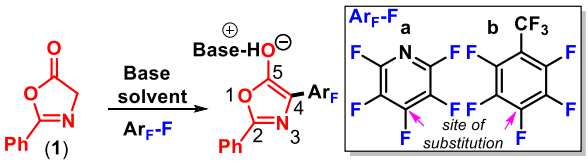

entry	conditions	Arene (equiv)	Amine (equiv)	T (°C)	% conv
1.	0.3 M ACN	**a** (2)	DIPEA (3)	45	100
2.	0.3 M ACN	**a** (2)	DIPEA (3)	22	100

3.	0.3 M DMF	**a** (2)	DIPEA (3)	22	100
4.	0.3 M DMSO	**a** (2)	DIPEA (3)	22	100
5.	0.3 M THF	**a** (2)	DIPEA (3)	22	24
6.	0.3 M Tol	**a** (2)	DIPEA (3)	22	<5
7.	0.3 M DCM	**a** (2)	DIPEA (3)	22	25
8.	1 M ACN	**a** (1.025)	DIPEA (3)	22	100
9.	1 M ACN	**b** (2)	DIPEA (3)	22	<5
10.	1 M ACN	**b** (2)	TMG (2.4)	-20	100
11.	1 M ACN	**b** (1.025)	TMG (2.05)	-20	100
12.	1 M ACN	**a** (1.025)	TMG (2.05)	-20	100

a. Conversion determined by ^{19}F NMR after 30 min.

It is puzzling why the same acid (i.e. oxazolone) would require a stronger base as a function of electrophile. One potential explanation for this observation is that the ammonium enolate is the minor product of an equilibrium (**Scheme 4.2A**). Due to the decreased electrophilicity of octafluorotoluene, the rate of attack by the enolate is significantly retarded.

Scheme 4.2 A. Equilibria of oxazolone under basic conditions B. π-stacking events of pentafluoropyridine and octafluorotoluene

A. Equilibria of oxazolone under basic conditions

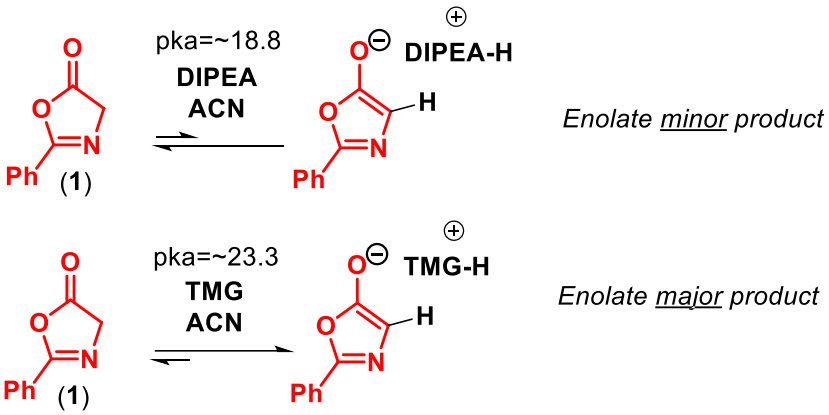

B. π-stacking events of pentafluoropyridine and octafluorotoluene

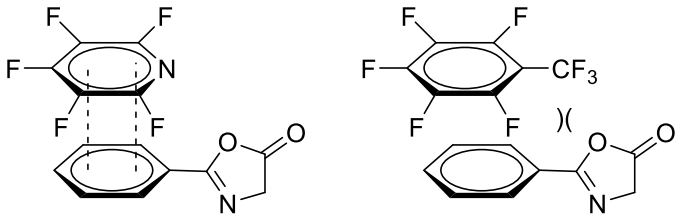

The use of a stronger base accelerates the reaction by shifting the equilibrium in favor of the enolate. An alternative possibility is that pentafluoropyridine undergoes a π-stacking event (**Scheme 4.2B**)[115],[116] with the phenyl ring of the oxazolone, which could result in an acidification of the C4-H. In contrast, when octafluorotoluene is used, it is less prone to undergo this acidifying, π-stacking event, presumably due to the steric bulk of the trifluoromethyl group, and thus requires a stronger base to generate the requisite enolate.

Thus, with the use of tetramethylguanidine (TMG) at -20 °C, we were able achieve full conversion of **1**, using just 1.025 equivalents of octafluorotoluene (b, entry 11). When we applied these reaction conditions to pentafluoropyridine (a, entry 12) we observed quantitative conversion to the product by ^{19}F NMR, suggesting that the TMG conditions would have a broader scope.

4.3 *Substrate scope*

With the optimal conditions in hand (entry 12), we were prepared to explore the scope. Typically, oxazolones are not easily isolated due to their predisposition for ring opening, and instead are usually derivatized immediately to a more stable molecule.[107] This is easily accomplished under acidic conditions, since the oxazolone behaves as an activated ester. We explored the ring opening of the oxazolone with alcohols to form perfluoroaryl *N*-benzoyl protected esters (**Scheme 4.3**). We found protonation of the oxazolone under anhydrous conditions was the key to high yield and that this was best accomplished using catalytic amounts trifluoroacetic acid in dry alcohol.

Scheme 4.3 Arylation and esterification of oxazolone

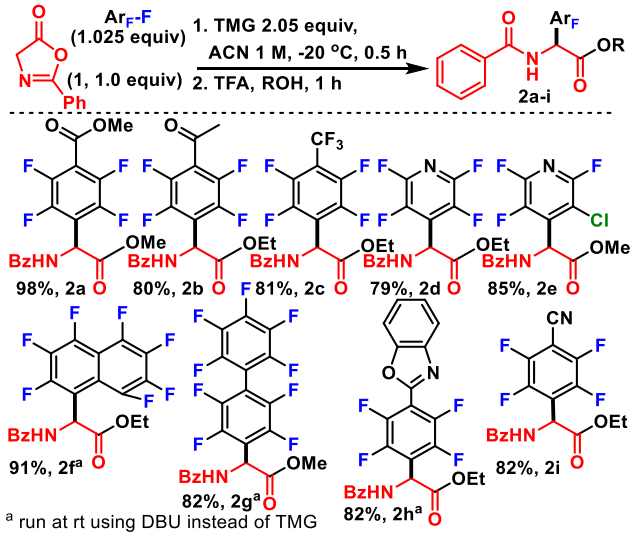

The scope of the one pot perfluoroarylation and esterification of the oxazolone was explored. Generally, the reaction scope was very good and worked well with many of the commercially available perfluoroarenes. No undesired reactivity was observed with esters (**2a**) or

ketones (**2b**). Less activated octafluorotoluene, octafluoronapthalene, and decafluorobiphenyl all reacted to give the expected product in excellent yields (**2c**, **2f**, and **2g**). Both benzoxazoles (**2h**) and benzonitriles (**2i**) underwent arylation and esterification in good yield. Comparison of pyridine products **2d** and **2e** revealed the preference for substitution of the 4-fluoro over that of 3-chloro leaving group. This is consistent with a S_NAr reaction, and is expected, as fluorine is the preferred nucleofuge and attack of the 4-position maximizes delocalization of the charge in the Meisenheimer complex.

However, substitution of 4-chlorotetrafluoropyridine (**Scheme 4.4**) leads primarily to substitution of the chloride, rather than substituting at the 2-fluoro position, to give **2d** as the major product. This suggests, in this case, that the regioselectivity is primarily dictated by the electronics of the arene rather than the nucleofuge.

Scheme 4.4 Arylation and esterification of oxazolone

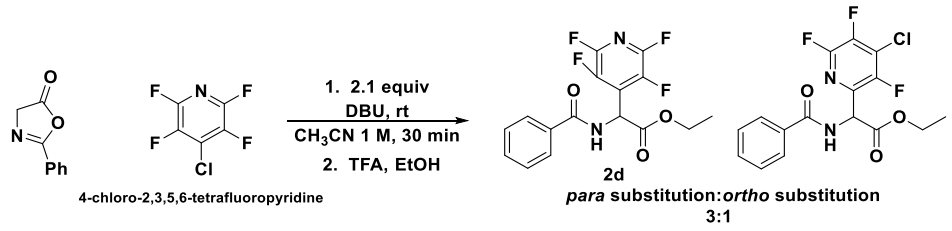

Next, we explored the ring opening of oxazolones with water, which would provide direct access to non-natural *N*-benzoyl protected amino acids in a rapid and facile manner (**Scheme 4.5A**). We were pleased to see that the perfluoroarylated oxazolone intermediates could be efficiently hydrolyzed (**3a**-**3e**). Since facilitating access to more elaborate fluorinated building blocks was our primary objective, we also developed chromatography-free conditions (**Scheme 4.5B**) that were amenable to scaling, and allowed us to synthesize the amino acids derivatives on a gram scale with minimal effort. After initial removal of MeCN, the crude acids were extracted with $CHCl_3$, washed with acidic brine, and stripped of solvent in vacuo. Next, the acid was washed

with hexanes and trace dichloromethane to selectively extract the impurities and yield pure acids. This process was applied successfully on a gram scale for several substrates (**3a-3c**), suggesting the method may be useful for making more sizeable quantities of the *N*- benzoyl protected acids.

Scheme 4.5 Telescope reaction to synthesize multifluoroaryl amino acids

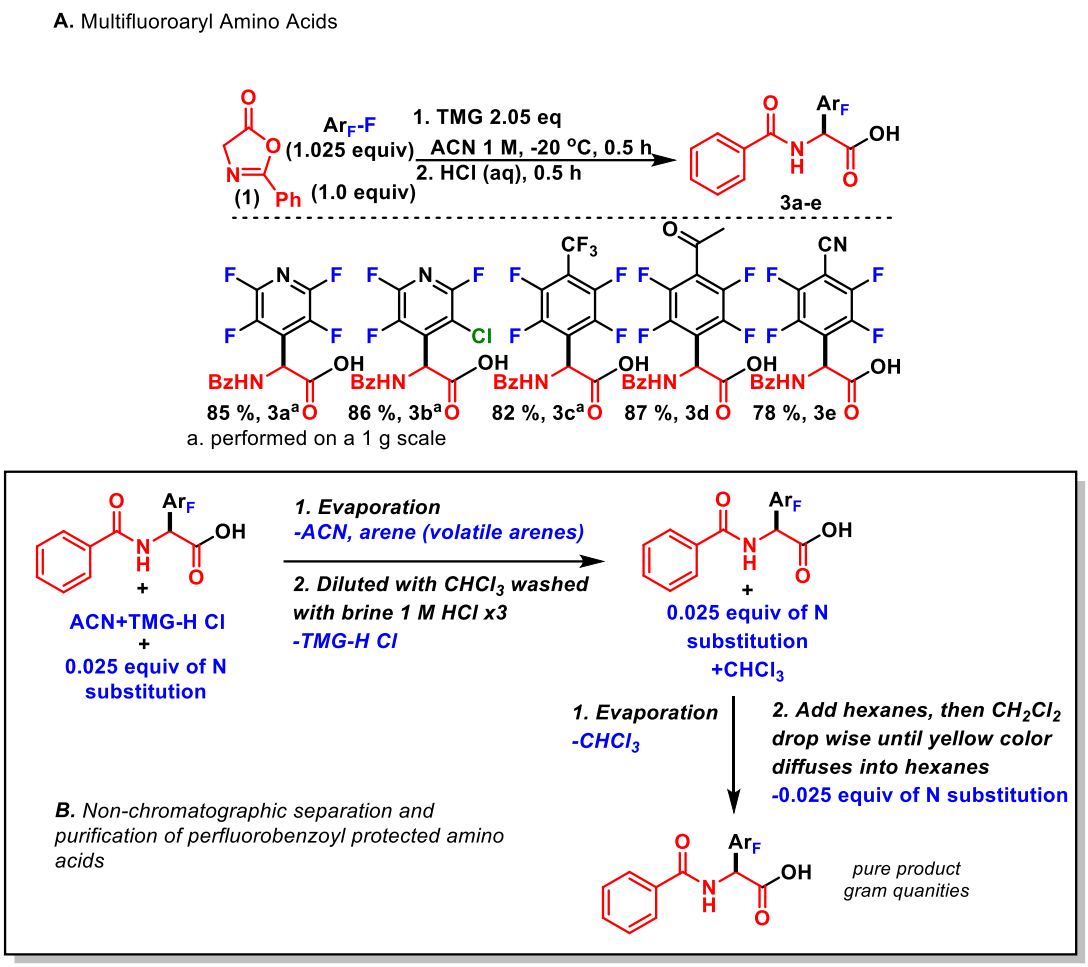

4.4 *Debenzoylation of amino acids and Schiff base mediated decarboxylation*

Next, we probed the deprotection of the *N*-benzoyl groups in hopes of accessing the free amino acids. Unfortunately, in the case of pyridine derived (**3a**), standard deprotection conditions of refluxing in concentrated HCl led to the deprotected and decarboxylated ammonium salts. The amino acid derivatives apparently underwent a thermal decarboxylation, however it was not clear

whether debenzoylation occurred prior to or following decarboxylation. Fortunately, after lowering the reaction temperature to 60 °C, we found that the amino acids underwent smooth debenzoylation, but did not undergo decarboxylation.

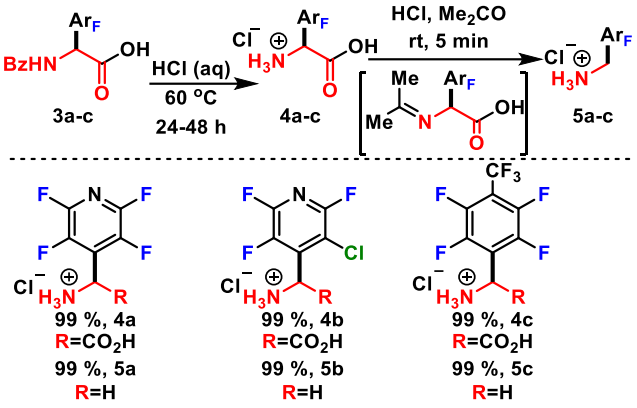

Scheme 4.6 Debenzoylation of Amino Acids and Schiff Base Mediated Decarboxylation

Thus, by subjecting acids (3a-c, **Scheme 4.6**) to aqueous HCl carefully heated to 60 °C, we acquired the unprotected amino acids in quantitative yields. Upon exposure to acetone the amino acid salts (4a-c) undergo rapid and quantitative decarboxylative protonation. Presumably, this takes place through a transiently formed Schiff base, which facilitates the decarboxylation and then undergoes hydrolysis to form (**5a-c**).[117] Given the high yielding and facile nature of each step, the addition of oxazolone to perfluoroarenes is an attractive strategy to access highly fluorinated benzylic amine derivatives such as **5a-c**.

As mentioned above, upon refluxing the benzoyl protected amino acids (**3a-c**) in HCl, the outcome was the deprotected and decarboxylated product. Two possible pathways are conceivable and are shown in **Scheme 4.7**. By doping the reaction of **3a** with isolated **4a**, it is possible to NMR doping experiments were performed, in which the isolated hydrochloride salts of amino acids (**4a-c**) were added to the refluxing HCl conditions. This confirmed that debenzoylation occurs prior to decarboxylation.

Scheme 4.7 Reaction pathways of decarboxylation

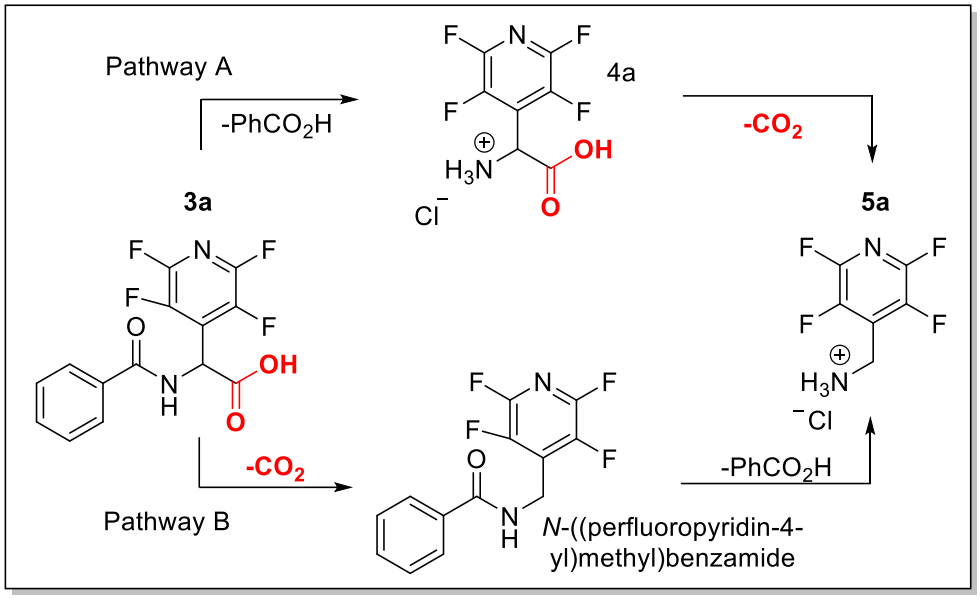

During our investigation, we found that under the standard deprotection conditions (refluxing the benzoyl protected amino acid (**3a**) in concentrated HCl) led to the deprotected and decarboxylated ammonium salt (**5a**). While the nature of the final product was apparent, the reaction sequence was not clear. In other words, did debenzoylation precede decarboxylation (**Scheme 4.7**, Pathway A) or did it proceed decarboxylation (**Scheme 4.7**, Pathway B).

Figure 4.1 Stacked spectra of starting material, product (amino acid)

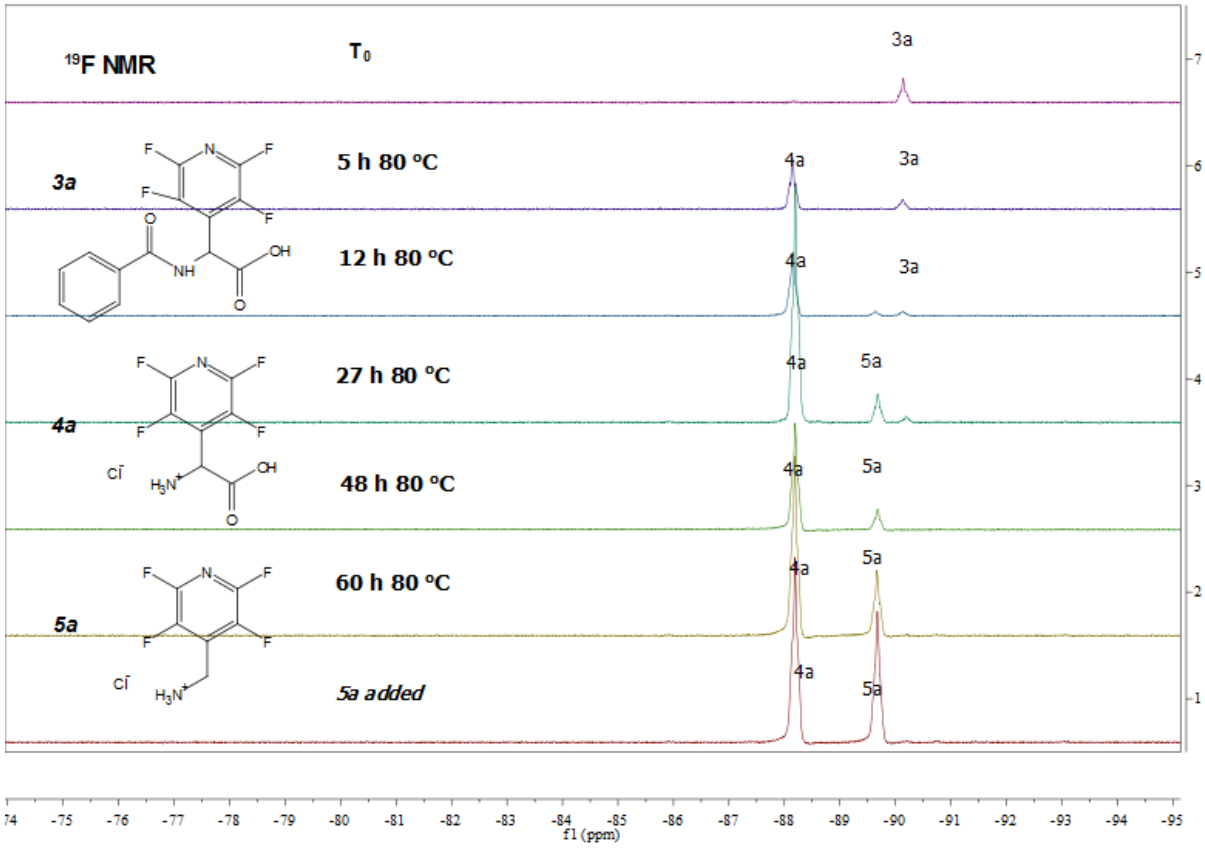

To probe the reaction, 20 mg of 3a (0.061 mmol) and 0.50 mL of 12 M HCl was added to a NMR tube and the T_0 ^{19}F NMR was collected (**Figure 4.6**, spectrum 7). The reaction was run at 80 °C and ^{19}F NMR data was collected at 5 h, 12 h, 27 h, 48 h, and 60 h (spectra 2-6, respectively). After the last time point, the NMR tube was doped with previously isolated **5a** (5 mg) and the ^{19}F NMR was taken which confirmed the identity of the second species, and by elimination, the structure of **3a** as well.

Figure 4.2 ^{19}F NMR after workup

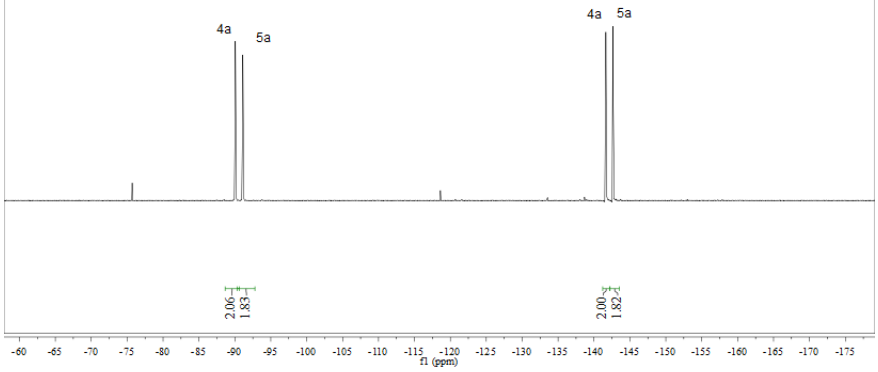

Figure 4.3 ^{1}H NMR after workup

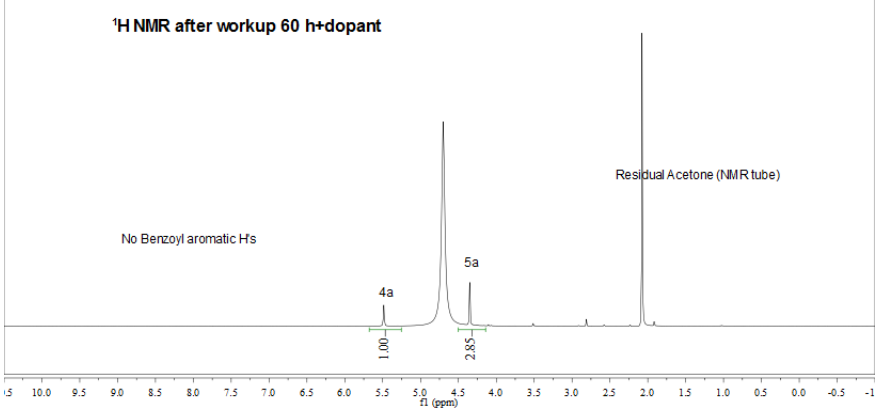

The progression of the reaction is displayed in **Figure 4.1** and after 5 h the conversion of starting material to a new intermediate is apparent and the peak chemical shifts at -88 ppm. With prolonged heat, a second intermediate is formed with a chemical shift of -89.5 ppm. Yet, the doping of the NMR reaction revealed **5a** to be the final product shifting at -89.5 ppm. After a typical workup (see general procedure G) of the incomplete reaction (where starting material is consumed and only partial conversion of the intermediate to the **5a** product), the ^{19}F NMR (**Figure 4.2**) and the ^{1}H NMR (**Figure 4.3**) revealed that the intermediate *N*-((perfluoropyridin-4-

yl)methyl)benzamide was neither of the intermediates observed due to the lack of benzoyl aromatic signals. The first intermediate was found to be **4a** (seen at -88 ppm) matching of what one would expect in the ^{1}H NMR (s, 1H) ^{19}F NMR δ -89.95 – -90.40 (m), -141.50 – -142.06 (m). With this evidence, we eliminated pathway B (**Scheme 4.7**) as the reaction pathway and concluded that the most logical route is pathway A, where the benzoyl protected amino acids undergo deprotection and then thermally decarboxylate giving the benzylic amine. This finding is consistent with TGA experiments (section **4.5)** which show that for **3b** and **4b,** which differ by the deprotection of the *N*-benzoyl group, that the amide (**3b**) is less prone to thermal decarboxylation than the corresponding ammonium acid (**4b**).\

4.5 *Thermal gravimetric analysis*

Having generated a strategy to access a novel class of fluorinated amino acids and our own experience with the unexpected decarboxylation of the amino acid derivatives, we thought it appropriate to explore the thermal stability of several derivatives. Thus, we performed thermal gravimetric analysis on several of the products we had formed (**Scheme 4.8**). As expected the benzoyl protected esters (2d) were thermally stable and gradually sublimed. However, the benzoyl protected acids 3a-c all underwent decarboxylation at 108 ^{o}C, 132 ^{o}C, and 159 ^{o}C, respectively. The differences in decarboxylation temperature seem to reflect the stability of a benzylic anion, however, it may also correlate to basicity of the amide motif. Comparison of 3b and 4b shows that the HCl salts actually undergo a more facile thermal decarboxylation than the *N*-benzoylated substrate, and is consistent with our previous findings in **Scheme 4.6**. However, 4c failed to undergo decarboxylation and instead gradually sublimed. It may be possible that the 4c is sufficiently acidic that it instead sublimed through a small equilibrium of neutral (or potentially zwitterionic) amino acid.

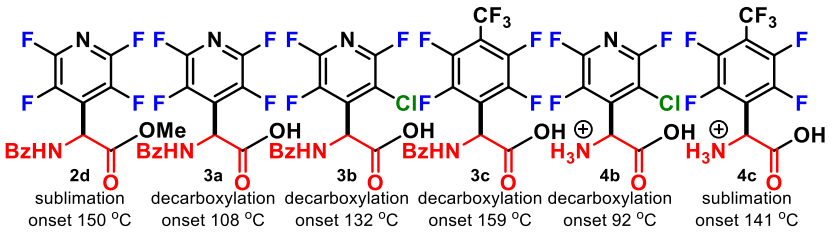

Scheme 4.8 Thermalgravimetric Analysis of α-Multifluoroaryl Amino Acid Derivatives.

Next, we evaluated the perfluoroarylations of substituted oxazolones, which yield fully substituted, non-natural amino acid derivatives (**Scheme 4.9**). Upon additional substitution of the oxazolone, the carbonyl is permanently formed, which is prone to opening by nucleophiles, including TMG.

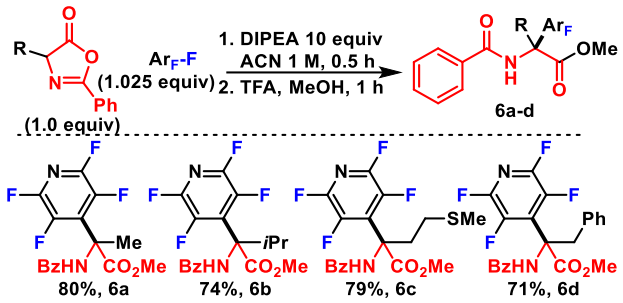

Scheme 4.9 Fully substituted amino acid esters

We were pleased to see that even the substituted oxazolone enolate underwent selective C4-addition to give the desired amino acids, rather than C2-addition, which has been observed for substituted oxazolones.[111, 118] However, in order to be able to derivatize in the second step, we found it necessary to utilize DIPEA as the base. Perfluoroarylated amino acid esters were derived from alanine, valine, methionine, and phenylalanine in good yield (6a-d).

4.6 *One pot multicomponent synthesis of 2-aminohydantoins*

When we utilized TMG as the base, we found that after arylation the TMG would undergo nucleophilic ring opening to form *N*-acylated guanidines, which upon heating in HCl underwent

debenzoylation and cyclization with extrusion of dimethyl amine **(Scheme 4.10)**. This sequence yields 2-aminohydantoins which are currently being studied[119-125] as possible inhibitors of BACE1, an enzyme believed to play a central role in the formation β-amyloid formation associated with Alzheimer's disease. Traditionally, 2-aminohydantoins have been synthesized by adding an activated carbon to the *N*-terminus which then serves to bridge the *N*- and *C*-termini of the amino acid. In contrast, the guanidine serves in place of the activated carbon and is attached to the *C*-terminus. To our knowledge, this cyclization approach is novel and demonstrates the potential for a one-pot, three component coupling that could be used to rapidly explore the chemical space surrounding this important motif.

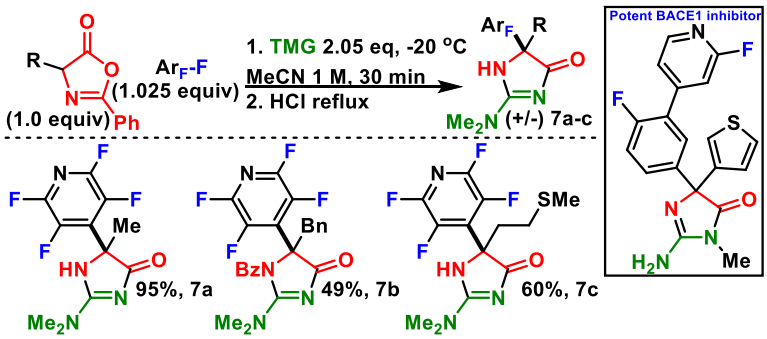

Scheme 4.10 One pot multicomponent synthesis of 2-amino hydantoins

In summary, we have shown that the oxazolone enolate is capable of nucleophilic aromatic substitution and can be utilized to rapidly form non-natural fluorinated amino acid derivatives. Importantly, the reaction is highly selective both in terms of C–F and oxazolone regioselectivity. Furthermore, we have provided conditions that allow transformation of the product to valuable building blocks, namely, *N*-Bz esters, *N*-Bz acids, acid-HCl salts, and by way of Schiff-base decarboxylation, the benzylic amines. Furthermore, we have reported the behavior of these compounds towards thermal decarboxylation, which indicate that the compounds should be stable at room temperature. Finally, we demonstrate the utility of the reaction and its product

by demonstrating its use in a 3-component reaction, which allows rapid access 2-aminohydantoins, a biologically relevant motif.

4.7 *Experimental section*

General Experimental:

All reagents were obtained from commercial suppliers (Aldrich, VWR, TCI Chemicals, and Oakwood Chemicals) and used without further purification unless otherwise noted. *N*-benzoyl alanine was purchased from Oakwood Chemicals and all other *N*-benzoyl amino acids were synthesized according to literature procedures.[126] Oxazolones were synthesized according to literature procedure.[127] Reactions were monitored by thin layer chromatography (TLC), (obtained from sorbent technology Silica XHL TLC Plates, w/UV254, glass backed, 250 µm, 20 x 20 cm) and were visualized with ultraviolet light, potassium permanganate stain, GC-MS (QP 2010S, Shimadzu equipped with auto sampler) and ^{1}H NMR ^{19}F NMR.

Isolations were carried out using Teledyne Isco Combiflash Rf 200i flash chromatograph with Sorbent normal phase silica (standard grade) (4 g, 12 g, 24 g, or 40 g) with product detection at 254 and 288 nm and evaporative light scattering detection. NMR spectra were obtained on a 400 MHz Bruker Avance III spectrometer and 400 MHz Varian spectrometer. ^{1}H, ^{19}F and ^{13}C NMR chemical shifts are reported in ppm relative to the residual protio solvent peak (^{1}H, ^{13}C). IR spectra were recorded on Varian 800 FT-IR. Due to the C-F splitting, carbons that couple with fluorine were reported as multiplets. Melting points were determined on Stuart Digital (SMP10) melting point apparatus. High resolution mass spectrometry (HRMS) analysis was performed on LTQ-OrbitrapXL by Thermo Scientific ltd.

General procedure A for synthesis of *N*-benzoyl amino acids[1]

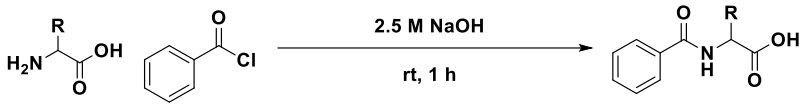

Benzoyl chloride **(1.2 equiv**) was added incrementally in 4 portions over **30** minutes to a solution of the amino acid (**1 equiv)** and 2.5 M NaOH **(3.8 equiv**) in distilled water. After the addition was complete, the ice bath was removed, and the reaction was quenched by the dropwise addition of concentrated aqueous hydrochloric acid until **pH 1** was reached, which resulted in precipitation of the product. The solid product was isolated by filtration and then recrystallized from water. The resulting crystals were air dried to give the desired *N*-benzoyl amino acid, which showed no trace of benzoic acid by 1H NMR.

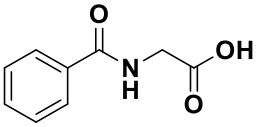

S-1 in 93% yield after isolation (10.86 g, 60.9 mmol) as a white solid. The **general procedure A** was followed using glycine (5.00 g, 66.6 mmol), benzoyl chloride (9.30 mL, 79.2 mmol), 2.5 M NaOH (100 mL, 251 mmol). ^{1}H-NMR matched that previously reported in the literature.[126]

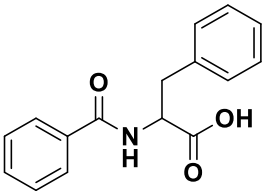

S-2 in 79% yield after isolation (3.20 g, 11.9 mmol) as a white solid. The **general procedure A** was followed using phenyl alanine (2.50 g, 15.1mmol), benzoyl chloride (2.11 mL, 18.1 mmol), 2.5 M NaOH (23.0 mL, 57.4 mmol). ^{1}H-NMR matched that previously reported in the literature.[128]

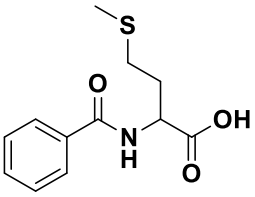

S-3 in 66% yield after isolation (2.80 g, 11.1 mmol) as a white solid. The **general procedure A** was followed using methionine (2.50 g, 16.8 mmol), benzoyl chloride (2.34 mL, 20.1 mmol), 2.5% NaOH (25.5 mL, 63.8 mmol). ^{1}H-NMR matched that previously reported in the literature.[129]

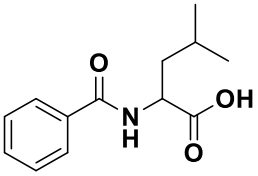

S-4 in 67% yield after isolation (2.41 g, 10.2 mmol) as a white solid. The **general procedure A** was followed using leucine (2.00 g, 15.2 mmol), benzoyl chloride (2.12 mL, 18.3 mmol), 2.5% NaOH (23.1 mL, 57.8 mmol). ^{1}H-NMR matched that previously reported in the literature.[128]

General procedure B: for synthesis of oxazolones

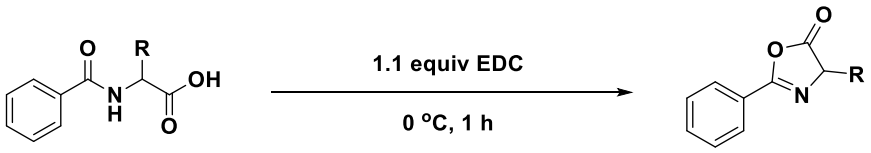

To a flame dried round bottom flask a suspension of *N*-benzoyl amino acid (1 equiv) in dry CH_2Cl_2 (0.07 M), under an argon atmosphere, at 0 ºC, was added EDC HCl (1.1 equiv). The materials were stirred at 0 ºC for 1 hour. The reaction mixture was diluted with an equal volume of CH_2Cl_2, and washed successively with water, saturated aqueous $NaHCO_3$, and water (each 1/2 the volume of the organic phase), then dried over $MgSO_4$ and concentrated under reduced pressure. (Note: the oxazolones are moisture and thermally sensitive reagents. As a precaution the oxazolones were stored under argon at 5 ºC until use).

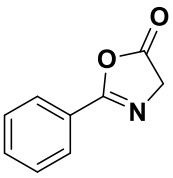

S-5 in 80% yield after isolation (1.80 g, 11.1 mmol) as a pale white solid. The **general procedure B** was followed using *N*-benzoyl glycine (2.50 g, 14.0 mmol), EDC (2.38 g, 15.3 mmol), CH_2Cl_2 (200 mL). ^{1}H-NMR matched that previously reported in the literature.[127]

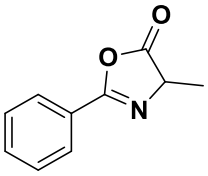

S-6 in >95% yield after isolation (907 mg, 5.18 mmol) as a white solid. The **general procedure B** was followed using *N*-benzoyl alanine (1.00 g, 5.18 mmol), EDC (884 mg, 5.69 mmol), CH_2Cl_2 (74 mL). ^{1}H-NMR matched that previously reported in the literature.[127]

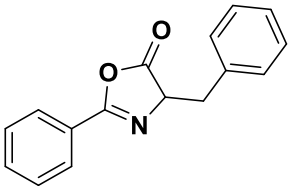

S-7 in 87% yield after isolation (806 mg, 3.21 mmol) as a white solid. The **general procedure B** was followed using *N*-benzoyl phenylalanine (990 mg, 3.68 mmol), EDC (628 mg, 4.04 mmol), CH_2Cl_2 (52.5 mL). ^{1}H-NMR matched that previously reported in the literature.[127]

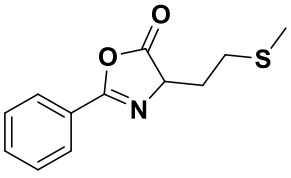

S-8 in 74% yield after isolation (1.1 g, 4.68 mmol) as a pale white solid. The **general procedure B** was followed using *N*-benzoyl methionine (1.6 g, 6.32 mmol), EDC (1.08 g, 6.95 mmol), CH_2Cl_2 (90.2 mL). H-NMR matched that previously reported in the literature.[129]

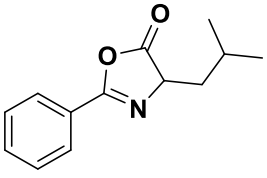

S-9 in 95% yield after isolation (553 mg, 2.45 mmol) as a pale white solid. The **general procedure B** was followed using *N*-benzoyl leucine (610 mg, 2.59 mmol), EDC (443 mg, 2.85 mmol), CH_2Cl_2 (37.0 mL). ^{1}H-NMR matched that previously reported in the literature.[128]

Synthesis of 2-(perfluorophenyl)benzo[d]oxazole

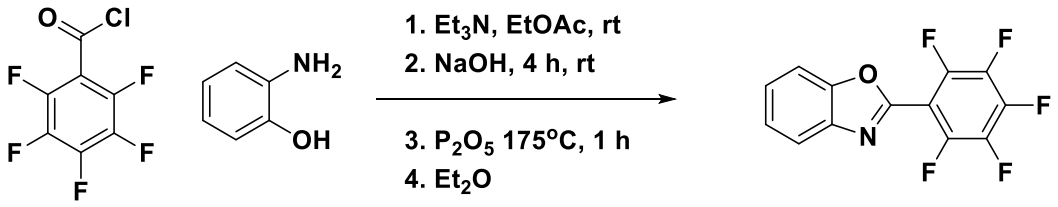

2-(perfluorophenyl)benzo[d]oxazole as a white solid in 33% yield. 2-(perfluorophenyl)benzo[d]oxazole was prepared by following the literature procedure.[40] Triethylamine (1.7 g, 16.9 mmol) was added dropwise to a solution of 2-aminophenol (1.4 g, 12.7 mmol) and pentafluorobenzoyl chloride (3.2 g, 14.1 mmol) in ethyl acetate (50 mL). The mixture was refluxed overnight and then aq NaOH (1M, 30 mL) was added and stirred for 3 hours at room temperature. The resulting mixture was extracted with EtOAc (5 × 20 mL) and washed with H_2O (25 mL) and brine (25 mL). The organic layer was dried over anhydrous $MgSO_4$ to yield 4 g of intermediate. Next, P_2O_5 (4.0 g, 28 mmol) was added to the intermediate and then heated at 175 ^oC for 1 hour. After the mixture had cooled to room temperature, ice water (50 mL) was added and mixture was extracted with EtOAc (5 × 20 mL). The combined organic layers were washed with aq NaOH (0.25 M, 50 mL), followed by water, brine and dried over anhydrous $MgSO_4$ and then concentrated *in vacuo* to afford the crude product. The resultant crude residue was purified by automated flash chromatography (hexane:EtOAc 90:10) to give the product (1.2 g, 4.2 mmol), which matches with NMR spectra of product reported in the literature.[130]

Halogen selectivity experiment:

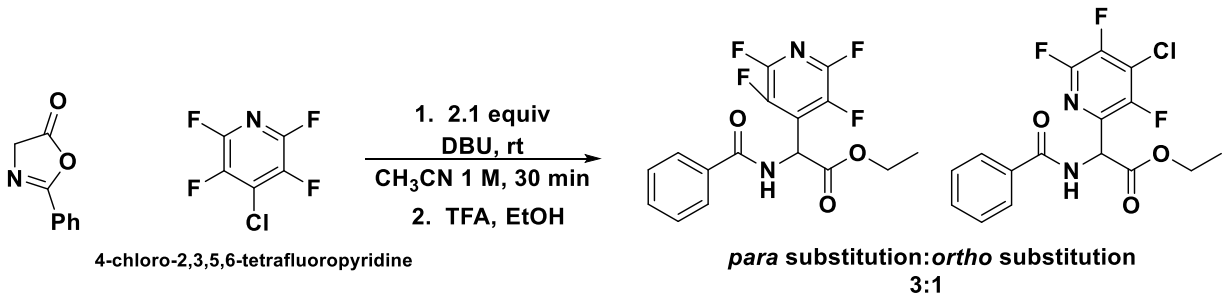

Under an argon atmosphere, oxazolone (50 mg, 0.310 mmol, 1 equiv), 4-chloro-2,3,5,6-tetrafluoropyridine (69 mg, 0.372 mmol, 1.2 equiv), and CH_3CN (0.310 mL, 1 M) were added to small test tube, which was fitted with a septum. Then a steady stream of 1,8-diazabicyclo(5.4.0)undec-7-ene (95 uL, 0.651 mmol, 2.1 equiv) was added down the side of the test tube glass. The mixture was allowed to react for 30 min. The reaction was quenched by the addition of a trifluoroacetic acid/ethanol) solution (47.4 uL, 0.620 mmol, 2 equiv/0.620 mL of ethanol). The solution was concentrated and then diluted with $CHCl_3$ (5 mL) which was then washed with 1 M HCl brine solution (2.5 mL x 3). The organic layer was dried with $MgSO_4$, filtered, and concentrated to give the crude product, which was purified by column chromatography. The *para/ortho* product ratio was determined by integrations of peaks in the ^{1}H and ^{19}F NMR.

Synthesis of perfluoroaryl-*N*-benzoyl amino acids/esters

General procedure C for synthesis of *N*-benzoyl perfluoroaryl-amino esters **2a**,**2b**,**2c**,**2d**,**2e**,**2i**.

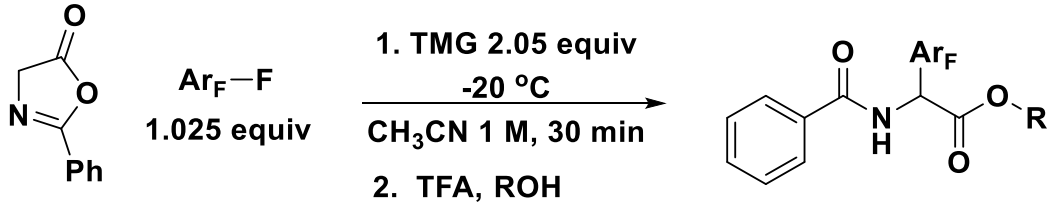

Under an argon atmosphere, oxazolone (**1 equiv**), Ar_F–F (**1.025 equiv**), and CH_3CN **(1 M)** were added to small test tube, which was fitted with a septum and cooled to -20 ºC. Then a steady stream of tetramethylguanidine (**2.05 equiv**) was added down the side of the test tube glass which facilitated the cooling of the TMG solution prior to dissolution. The mixture was allowed to react for 30 min, then the cooling bath was removed, and the reaction was left to warm to room temperature. The reaction was quenched by the addition of a trifluoroacetic acid/alcohol (methanol or ethanol) solution (**2 equiv**/double volume)**.** The solution was concentrated and then diluted with $CHCl_3$ which was then washed with 1 M HCl brine solution (half the volume of organic layer x 3). The organic layer was dried with $MgSO_4$, filtered, and concentrated to give the crude product, which was purified by column chromatography.

General procedure D for synthesis of *N*-benzoyl perfluoroaryl-amino esters **2f**, **2g**, and **2h**.

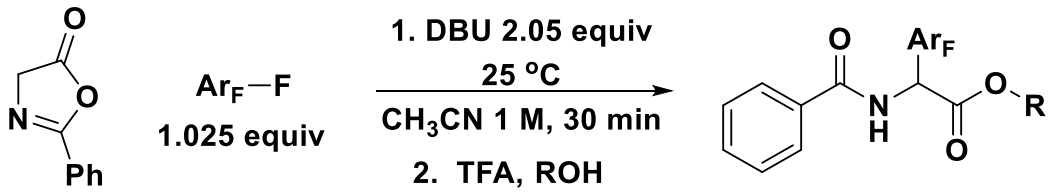

Under an argon atmosphere, oxazolone (**1 equiv**), Ar_F–F (**1.025 equiv**), and CH_3CN **(1 M)** were added to small test tube, which was fitted with a septum. Then a steady stream of 1,8-diazabicyclo(5.4.0)undec-7-ene (**2.05 equiv**) was added down the side of the test tube glass. The mixture was allowed to react for 30 min. The reaction was quenched by the addition of a trifluoroacetic acid/alcohol (methanol or ethanol) solution (**2 equiv**/double volume). The solution was concentrated and then diluted with $CHCl_3$ which was then washed with 1 M HCl brine solution

(half the volume of organic layer x 3). The organic layer was dried with $MgSO_4$, filtered, and concentrated to give the crude product, which was purified by column chromatography.

General procedure E for synthesis of *N*-benzoyl perfluoroaryl-amino acids **3a, 3b, 3c, 3d, and 3e**.

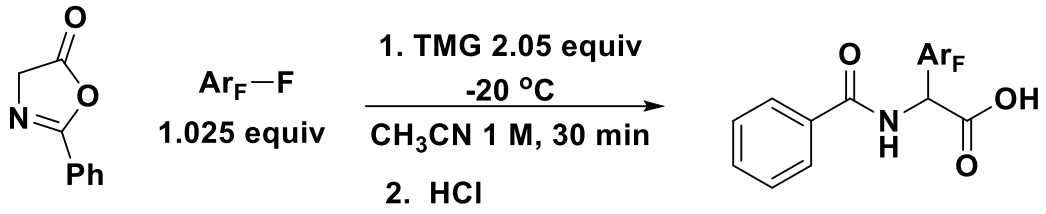

Under an argon atmosphere, oxazolone (**1 equiv**), Ar_F–F (**1.025 equiv**), and CH_3CN **(1 M)** were added to small test tube, which was fitted with a septum and cooled to -20 ºC. Then a steady stream of tetramethylguanidine (**2.05 equiv**) was added down the side of the test tube glass which facilitated the cooling of the TMG solution. The reaction was left to react for 30 min and then the cooling bath was removed, and the reaction was allowed to warm to room temperature and subsequently quenched by the addition of 6 M HCl. The solution was concentrated and extracted with $CHCl_3$, and then the organic layer was washed with half volumes of a 1 M HCl-brine solution x 3. The organic layer was dried with $MgSO_4$ and concentrated giving crude product. Purification of the crude product can be accomplished without chromatography by adding hexanes to a round bottom flask containing the crude product then carefully adding dichloromethane dropwise until the hexanes becomes yellow and a colorless solid is left behind. The solid was filtered and air dried to yield the pure acid.

General procedure F for synthesis of *N*-benzoyl perfluoroaryl-amino esters **6a**, **6b, 6c**, and **6d**.

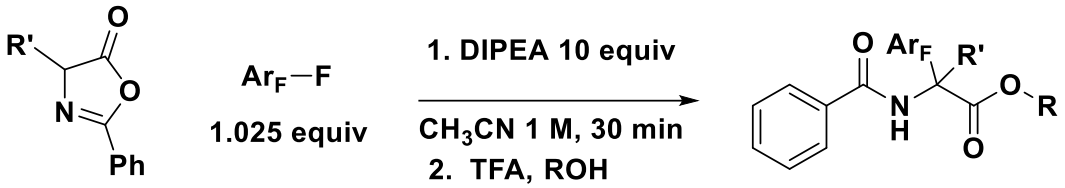

Under an argon atmosphere, oxazolone (**1 equiv**), Ar_F-F (**1.025 equiv**), CH_3CN (**1 M**) were added to small test tube which was fitted with a septum. Then a steady stream of DIPEA (**10 equiv**) was added to mixture. While stirring vigorously (note: the reaction mixture is biphasic), the reaction was left to react for 30 min. After 30 min. the bottom layer was separated and quenched by the addition of a trifluoroacetic acid/alcohol (methanol or ethanol) solution (**20 equiv**/**20 equiv**). The solution was concentrated and then diluted with $CHCl_3$ which was then washed with 1 M HCl-brine solution (half the volume of organic layer x 3). The organic layer was dried with $MgSO_4$, filtered, and concentrated to give the crude product, which was purified by column chromatography.

2a methyl 4-(1-benzamido-2-methoxy-2-oxoethyl)-2,3,5,6-tetrafluorobenzoate

Colorless oil,98.5% yield (122 mg, 0.305 mmol).

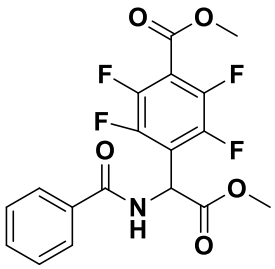

The **general procedure C** was followed using 2-phenyloxazol-5(4H)-one (50.0 mg, 0.310 mmol), 2,3,4,5,6 pentafluorobenzoate (67.4 mg, 0.318 mmol), tetramethylguanidine (73.2 mg, 0.636 mmol), 0.310 mL of MeCN and trifluoroacetic acid (70.7 mg, 0.620 mmol)/methanol (0.620 mL) was used to afford **2a.** FT-IR (neat) cm^{-1} 1743, 1754, 1680, 1085. ^{1}H NMR (400 MHz, Chloroform-*d*) δ 7.80 (d, *J* = 7.3 Hz, 2H), 7.54 (t, *J* = 7.4 Hz, 1H), 7.45 (t, *J* = 7.6 Hz, 2H), 7.36 (d, *J* = 6.5 Hz, 1H), 6.22 (d, *J* = 6.7 Hz, 1H), 3.96 (s, 3H), 3.83 (s, 3H). ^{19}F NMR (376 MHz, Chloroform-*d*) δ -138.64 – -139.00 (m), -141.86 (q, *J* = 11.5 Hz). ^{13}C

NMR (101 MHz, Chloroform-*d*) δ 168.9, 167.0, 160.3, 146.4 (ddt, *J* = 37.7, 15.2, 4.8 Hz), 143.9 (ddt, *J* = 44.6, 15.2, 4.9 Hz), 133.2, 132.8, 129.2, 127.6, 119.9 (t, *J* = 15.6 Hz), 113.3 (t, *J* = 16.1 Hz), 54.3, 53.8, 47.5. HRMS (ESI) $C_{18}H_{13}F_4NO_5$ calcd. $[M+K]^+$ 438.0361 observed 438.0337.

2b ethyl 2-(4-acetyl-2,3,5,6-tetrafluorophenyl)-2-benzamidoacetate

Colorless oil, 80% yield (98.5 mg, 0.248 mmol).

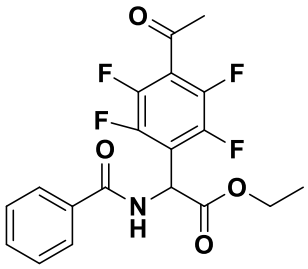

The **general procedure C** was followed using 2-phenyloxazol-5(4H)-one (50 mg, 0.310 mmol), 2',3',4',5',6' pentafluoroacetophenone (66.8 mg, 0.318 mmol), tetramethylguanidine (73.2 mg, 0.636 mmol), trifluoroacetic acid (70.7 mg, 0.620 mmol)/ethanol (0.620 mL) and 0.310 mL of MeCN was used to afford **2b.** FT-IR (neat) cm^{-1} 1730, 1756, 1655, 1105. ^1H NMR (400 MHz, Chloroform-*d*) δ 7.80 (d, *J* = 7.1 Hz, 2H), 7.53 (t, *J* = 7.4 Hz, 1H), 7.44 (t, *J* = 7.5 Hz, 2H), 7.39 (d, *J* = 6.4 Hz, 1H), 6.17 (d, *J* = 6.4 Hz, 1H), 4.32 (dq, J = 10.8, 3.7 Hz, 2H), 2.60 (t, *J* = 1.6 Hz, 3H), 1.26 (t, *J* = 7.1 Hz, 3H). ^{19}F NMR (376 MHz, Chloroform-*d*) δ -141.34 (dd, *J* = 22.3, 13.2 Hz), -141.72 (ddd, *J* = 21.9, 13.4 Hz. ^{13}C NMR (101 MHz, Chloroform-*d*) δ 192.3, 168.4, 167.0, 146.1 (dd, *J* = 116.6, 6.9 Hz), 144.4 – 142.5 (m), 133.2, 132.7, 129.2, 127.6, 120.1 (t, *J* = 16.9 Hz), 119.7 (t, *J* = 15.6 Hz), 63.7, 47.7, 32.8, 14.4. HRMS (ESI) $C_{19}H_{15}F_4NO_4$ calcd. $[M+Na]^+$ 420.0829 observed 420.0810.

2c ethyl 2-benzamido-2-(2,3,5,6-tetrafluoro-4-(trifluoromethyl)phenyl)acetate

White solid, 81% yield (106 mg, 0.251 mmol).

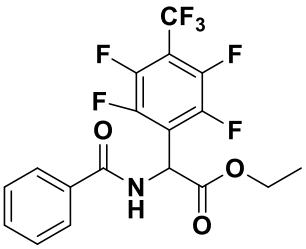

The **general procedure C** was followed using 2-phenyloxazol-5(4H)-one (50 mg, 0.310 mmol), octafluorotoluene (38 mg, 0.318 mmol), tetramethylguanidine (73.2 mg, 0.636 mmol), trifluoroacetic acid (70.7 mg, 0.620 mmol)/ethanol (0.620 mL) and 0.310 mL of MeCN was used to afford **2c.** FT-IR (neat) cm^{-1} 2496, 1756, 1659, 1095. ^{1}H NMR (400 MHz, Chloroform-*d*) δ 7.81 (d, *J* = 7.8 Hz, 2H), 7.54 (t, *J* = 7.4 Hz, 1H), 7.49 – 7.35 (m, 3H), 6.18 (d, *J* = 6.3 Hz, 1H), 4.32 (qd, *J* = 10.8, 3.7 Hz, 2H), 1.28 (t, *J* = 7.1 Hz, 3H). ^{19}F NMR (376 MHz, Chloroform-*d*) δ -56.48 (t, *J* = 21.7 Hz), -139.84 (ddt, *J* = 30.4, 21.7, 11.5 Hz), -140.84 (td, *J* = 15.6, 5.6 Hz). ^{13}C NMR (101 MHz, Chloroform-*d*) δ 167.7, 166.7, 145.9 (dd, *J* = 113.0, 15.4 Hz), 143.3 (dd, *J* = 121.4, 15.4 Hz), 132.6, 132.4, 128.8, 127.2, 121.0 (t, *J* = 15.4 Hz), 120.6 (d, *J* = 274.7 Hz), 110.7 – 109.0 (m), 63.5, 47.3, 13.9. HRMS (ESI) $C_{18}H_{12}F_7NO_3$ calcd. $[M+]^+$ 423.0700 observed 423.0698.

2d ethyl 2-benzamido-2-(perfluoropyridin-4-yl)acetate

Pale white solid,79% yield (87 mg, 0.245 mmol).

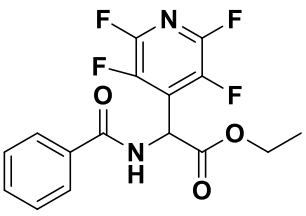

The **general procedure C** was followed using 2-phenyloxazol-5(4H)-one (50 mg, 0.310 mmol), pentafluoropyridine (53.8 mg, 0.318 mmol), tetramethylguanidine (73.2 mg, 0.636 mmol), trifluoroacetic acid (70.7 mg, 0.620 mmol)/ethanol (0.620 mL) and 0.310 mL of MeCN was used to afford **2d.** FT-IR (neat) cm^{-1} 1756, 1669, 1630, 1090. ^{1}H NMR (400 MHz, Acetonitrile-d_3) δ 7.83 (d, *J* = 8.1 Hz, 2H), 7.78 (d, *J* = 6.0 Hz, 1H), 7.58 (t, *J* = 7.4 Hz, 1H), 7.48 (t, *J* = 7.6 Hz, 2H), 6.27 (d, *J* = 7.2 Hz, 1H), 4.26 (q, *J* = 7.1 Hz, 2H), 1.23 (t, *J* = 7.1 Hz, 3H). ^{19}F

NMR (376 MHz, Acetonitrile-d_3) δ -92.87 – -93.35 (m), -144.21 – -144.65 (m). ^{13}C NMR (101 MHz, Acetonitrile-d_3) δ 167.9, 167.7, 145.7 – 142.9 (m), 141.7 (dd, *J* = 258.7, 35.3 Hz), 133.9, 133.2, 131.3 (t, *J* = 14.9 Hz), 129.6, 128.4, 63.9, 48.2, 14.1. HRMS (ESI) $C_{16}H_{12}F_4N_2O_3$ calcd. $[M+K]^+$ 395.0416 observed 395.0405.

2e methyl 2-benzamido-2-(3-chloro-2,5,6-trifluoropyridin-4-yl)acetate

Yellow solid, 85% yield (178 mg, 0.487 mmol).

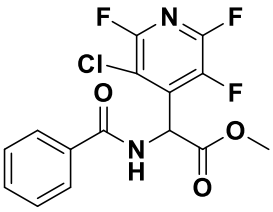

The **general procedure C** was followed using 2-phenyloxazol-5(4H)-one (100 mg, 0.621mmol), 3-chloro-2,4,5,6 tetrafluoropyridine (118.0mg, 0.636 mmol), tetramethylguanidine (145 mg, 1.27 mmol), trifluoroacetic acid (141 mg, 1.24 mmol)/methanol (1.24 mL) and 0.621 mL of MeCN was used to afford **2e.** FT-IR (neat) cm^{-1} 1731, 1640, 1680, 1085. ^{1}H NMR (400 MHz, Chloroform-*d*) δ 7.83 (d, *J* = 7.6 Hz, 2H), 7.58 (t, *J* = 7.2 Hz, 1H), 7.48 (m, *J* = 17.0, 9.2 Hz, 3H), 6.37 (d, *J* = 5.7 Hz, 1H), 3.88 (s, 3H). ^{19}F NMR (376 MHz, Chloroform-*d*) δ -72.87 (dd, *J* = 27.8, 12.3 Hz), -87.48 (dd, *J* = 21.4, 12.5 Hz), -143.98 – -144.42 (m). ^{13}C NMR (101 MHz, Chloroform-*d*) δ 168.2, 167.1, 151.6 (dq, *J* = 244.4, 12.0, 3.0 Hz), 147.6 (ddd, *J* = 248.6, 17.4, 13.5 Hz), 142.1 (ddd, *J* = 260.7, 27.2, 6.4 Hz), 139.8 (d, *J* = 12.3 Hz), 132.9, 132.9, 129.3, 127.7, 113.6 (d, *J* = 41.9 Hz), 54.5, 50.40. HRMS (ESI) $C_{15}H_{10}ClF_3N_2O_3$ calcd. $[M+Na]^+$ 381.0224 observed 381.0203.

2f ethyl 2-benzamido-2-(perfluoronaphthalen-1-yl)acetate

Yellow oil, 82% yield (69.2 mg, 0.254 mmol).

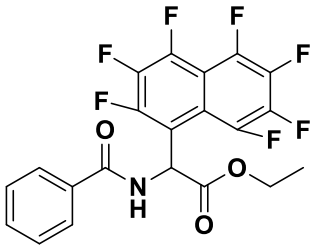

The **general procedure D** was followed using 2-phenyloxazol-5(4H)-one (50 mg, 0.310 mmol), octafluoronapalene (86.5 mg, 0.318 mmol), 1,8-diazabicyclo(5.4.0)undec-7-ene (96.7 mg, 0.636 mmol), trifluoroacetic acid (141 mg, 1.24 mmol)/ethanol (0.620 mL) and 0.310 mL of MeCN was used to afford **2f.** FT-IR (neat) cm^{-1} 2943, 2849, 1760, 1677, 1085. ^{1}H NMR (400 MHz, Chloroform-*d*) δ 7.74 (d, *J* = 7.2 Hz, 2H), 7.46 (t, *J* = 7.4 Hz, 1H), 7.37 (m, *J* = 7.5 Hz, 3H), 6.25 (d, *J* = 6.5 Hz, 1H), 4.23 (dq, *J* = 10.8, 7.1 Hz, 2H), 1.18 (t, *J* = 7.1 Hz, 3H). ^{19}F NMR (376 MHz, Chloroform-*d*) δ -120.69 (dd, *J* = 68.3, 18.5 Hz), -138.91 (d, *J* = 16.6 Hz), -143.22 (dt, *J* = 68.3, 16.8 Hz), -145.79 (dt, *J* = 61.8, 17.5 Hz), -148.06 (dt, *J* = 57.6, 18.0 Hz), -152.40 (t, *J* = 18.5 Hz), -154.99 (t, *J* = 20.3 Hz). ^{13}C NMR (101 MHz, Chloroform-*d*) δ 168.8, 167.1, 151.3 (d, *J* = 266.9 Hz), 148.1 – 145.1 (m), 147.8 – 144.9 (m), 143.1 (d, *J* = 54.7 Hz), 142.5 – 139.5 (m), 142.0 – 140.2 (m), 138.6 (dd, *J* = 118.3 Hz), 133.3, 132.7, 129.2, 127.6, 115.8 (t, *J* = 18.0 Hz), 111.9 (t, *J* = 13.0 Hz), 108.7 – 108.1 (m), 63.7, 47.7, 14.4. HRMS (ESI) $C_{21}H_{12}F_7NO_3$ calcd. $[M+K]^+$ 498.0337 observed 498.0309.

2g methyl 2-benzamido-2-(perfluoro-[1,1'-biphenyl]-4-yl)acetate

Colorless oil, 82% yield (265 mg, 0.508 mmol).

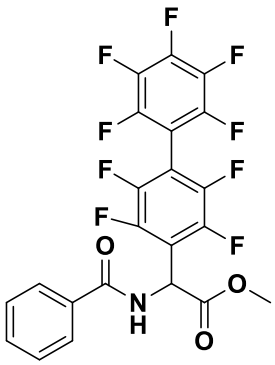

The **general procedure D** was followed using 2-phenyloxazol-5(4H)-one (100 mg, 0.621mmol), decafluorobiphenyl (212.7 mg, 0.637 mmol), 1,8-diazabicyclo(5.4.0)undec-7-ene (193 mg, 1.27 mmol),trifluoroacetic acid (141 mg, 1.24 mmol)/methanol (1.24 mL) and 0.621 mL of MeCN was used to afford **2g.** FT-IR (neat) cm^{-1} 2950, 1744, 1634, 1085. ^{1}H NMR (400 MHz, Chloroform-*d*) δ 7.85 (d, *J* = 7.1 Hz, 2H), 7.56 (t, *J* = 7.4 Hz, 1H), 7.48 (t, *J* = 7.5 Hz, 2H), 7.38 (d, *J* = 6.8 Hz, 1H), 6.31 (d, *J* = 6.8 Hz, 1H), 3.88 (s, 3H). ^{19}F NMR (376 MHz, Chloroform-*d*) δ -136.95 (dtt, *J* = 14.0, 6.0, 2.7

Hz), -137.40 (h, *J* = 10.4 Hz), -141.84 (q, *J* = 11.4 Hz), -149.85 (t, *J* = 21.0 Hz), -160.38 (tt, *J* = 21.2, 5.4 Hz). ^{13}C NMR (101 MHz, Chloroform-*d*) δ 169.1, 167.1, 147.1 – 145.5 (m), 146.4 – 143.5 (m), 143.3 (dt, *J* = 14.4, 3.9 Hz), 139.6 (d, *J* = 8.5 Hz), 137.2 (dd, *J* = 14.0, 5.8 Hz), 133.2, 132.9, 129.3, 127.7, 119.1 (t, *J* = 15.6 Hz), 107.1 (t, *J* = 16.2 Hz), 102.4 (t, *J* = 16.8 Hz), 54.4, 47.5. HRMS (ESI) $C_{23}H_{12}F_9NO_3$ calcd. $[M+H]^+$ 508.0590 observed 508.0545.

2h ethyl 2-benzamido-2-(4-(benzo[d]oxazol-2-yl)-2,3,5,6-tetrafluorophenyl)acetate

Pale white solid, 82% yield (120 mg, 0.254 mmol).

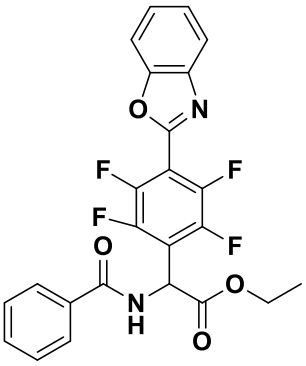

The **general procedure D** was followed using 2-phenyloxazol-5(4H)-one (50 mg, 0.310 mmol), 2-(perfluorophenyl)benzo[d]oxazole (90.6 mg, 0.318 mmol), 1,8-diazabicyclo(5.4.0)undec-7-ene (96.7 mg, 0.636 mmol), trifluoroacetic acid (70.7 mg, 0.620 mmol)/ethanol (0.620 mL) and 0.310 mL of MeCN was used to afford **2h.** FT-IR (neat) cm^{-1} 2950, 1749, 1634, 1140, 1085, 1052. ^{1}H NMR (400 MHz, Chloroform-*d*) δ 7.89 (d, *J* = 8.8 Hz, 1H), 7.84 (d, *J* = 8.5 Hz, 2H), 7.65 (d, *J* = 8.4 Hz, 1H), 7.55 (t, *J* = 7.4 Hz, 1H), 7.51 – 7.37 (m, 5H), 6.26 (d, *J* = 6.6 Hz, 1H), 4.33 (dq, *J* = 7.7, 3.6 Hz, 2H), 1.28 (t, *J* = 7.1 Hz, 3H). ^{19}F NMR (376 MHz, Chloroform-*d*) δ -139.98 – -140.48 (m), -142.52 – -143.05 (m).

^{13}C NMR (101 MHz, Chloroform-*d*) δ 168.5, 167.1, 153.3, 150.9, 145.8 (ddt, *J* = 250.1, 14.3, 5.3 Hz), 145.5 (ddt, *J* = 260.3, 15.6, 4.1 Hz), 141.6, 133.3, 132.8, 129.2, 127.7, 127.0, 125.6, 121.4, 119.9 (t, *J* = 15.8 Hz), 111.5, 108.9 (t, *J* = 13.5 Hz), 63.8, 47.8, 14.4. HRMS (ESI) $C_{24}H_{16}F_4N_2O_4$ calcd. $[M+Na]^+$ 495.0938 observed 495.0911.

2i ethyl 2-benzamido-2-(4-cyano-2,3,5,6-tetrafluorophenyl)acetic acid

Yellow oil,79% yield (93.1 mg, 0.245 mmol).

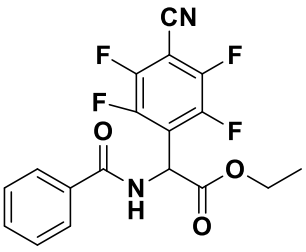

The **general procedure A** was followed using 2-phenyloxazol-5(4H)-one (50 mg, 0.310 mmol), 2,3,4,5,6 pentaflurobenzonitrile (61.4 mg, 0.318 mmol), tetramethylguanidine (73.2 mg, 0.636 mmol), trifluoroacetic acid (72.5 mg, 0.636 mmol)/ethanol (0.620 mL) and 0.310 mL of MeCN was used to afford **2i.** FT-IR (neat) cm^{-1} 2933, 2250, 1714, 1083. ^{1}H NMR (400 MHz, Chloroform-*d*) δ 7.72 (d, *J* = 7.4 Hz, 2H), 7.47 (t, *J* = 7.4 Hz, 1H), 7.43 – 7.29 (m, 3H), 6.08 (d, *J* = 5.9 Hz, 1H), 4.24 (qd, *J* = 10.7, 5.4 Hz, 2H), 1.20 (t, *J* = 7.1 Hz, 3H). ^{19}F NMR (376 MHz, Chloroform-*d*) δ -131.74 (td, *J* = 16.4, 6.7 Hz), -139.49 (td, *J* = 16.3, 6.6 Hz).

^{13}C NMR (101 MHz, Chloroform-*d*) δ 167.3, 166.7, 148.5 – 146.1 (m), 148.6 – 145.7 (m), 145.9 – 143.4 (m), 132.5, 132.4, 128.8, 127.2, 123.4 (t), 107.1, 63.6, 47.5, 13.9. HRMS (ESI) $C_{18}H_{12}F_4N_2O_3$ calcd. $[M+Na]^+$ 403.0676 observed 403.0654.

3a 2-benzamido-2-(perfluoropyridin-4-yl)acetic acid

White solid,85% yield (1.73 g, 5.27 mmol).

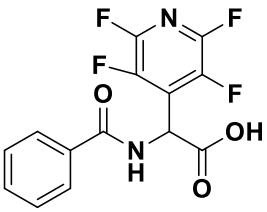

The **general procedure E** was followed using 2-phenyloxazol-5(4H)-one (1.00 g, 6.20 mmol), pentafluoropyridine (1.08 g, 6.36 mmol), tetramethylguanidine (1.46 g, 12.71 mmol), and 6.20 mL of MeCN was used to afford **3a.** FT-IR (neat) cm^{-1} 3643, 2250, 1715, 1106. ^{1}H NMR (400 MHz, Acetonitrile-d_3) δ 7.95 – 7.73 (m, 3H), 7.60 (t, *J* = 7.4 Hz, 1H), 7.50 (t, *J* = 7.6 Hz, 2H), 6.26 (d, *J* = 6.9 Hz, 1H). ^{19}F NMR (376 MHz, CD_3CN) δ -93.07, -144.38. ^{13}C NMR (101 MHz, Acetonitrile-d_3) δ 168.3, 167.7, 151.9 (dd, *J* = 240.4, 9.7 Hz), 148.1 (dq, *J* = 244.4, 17.6, 13.9 Hz), 142.8 (ddd, *J* = 258.2, 27.4, 6.2 Hz), 141.1 (d, *J* = 12.7 Hz), 133.8, 133.2, 129.6, 128.4,

114.4 (dd, *J* = 35.3, 6.5 Hz), 50.8. HRMS (ESI) $C_{14}H_8F_4N_2O_3$ calcd. $[M+K]^+$ 367.0103 observed 367.0083.

3b 2-benzamido-2-(3-chloro-2,5,6-trifluoropyridin-4-yl)acetic acid

Pale white solid, 86% yield (1.84 g, 5.33 mmol).

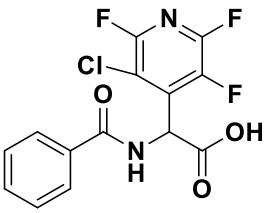

The **general procedure E** was followed using 2-phenyloxazol-5(4H)-one (1.00 g, 6.20 mmol), 3-chloro-2,4,5,6 tetrafluoropyridine (1.18 g, 6.36 mmol), tetramethylguanidine (1.46 g, 12.71 mmol), and 6.20 mL of MeCN was used to afford **3b.** FT-IR (neat) cm^{-1} 3604, 1722, 1664, 1085. ^1H NMR (400 MHz, Acetonitrile-d_3) δ 7.82 (d, *J* = 7.4 Hz, 2H), 7.74 (d, *J* = 5.9 Hz, 1H), 7.57 (t, *J* = 7.4 Hz, 1H), 7.47 (t, *J* = 7.6 Hz, 2H), 6.34 (d, *J* = 6.6 Hz, 1H). ^{19}F NMR (376 MHz, Acetonitrile-d_3) δ -76.02 (dd, *J* = 27.3, 12.5 Hz), -91.08 (dd, *J* = 21.1, 13.2 Hz), -144.77 (t, *J* = 24.3 Hz). ^{13}C NMR (101 MHz, Acetonitrile-d_3) δ 168.3, 167.7, 151.9 (dd, *J* = 240.4, 9.7 Hz), 148.1 (dq, *J* = 244.4, 17.6, 13.9 Hz), 142.8 (ddd, *J* = 258.2, 27.4, 6.2 Hz), 141.1 (d, *J* = 12.7 Hz), 133.8, 133.2, 129.6, 128.4, 114.4 (dd, *J* = 35.3, 6.5 Hz), 50.8. HRMS (ESI) $C_{14}H_8ClF_3N_2O_3$ calcd. $[M+Na]^+$ 367.0068 observed 367.0047.

3c 2-benzamido-2-(2,3,5,6-tetrafluoro-4-(trifluoromethyl)phenyl)acetic acid

White solid, 82% yield (2.00 g, 5.06 mmol).

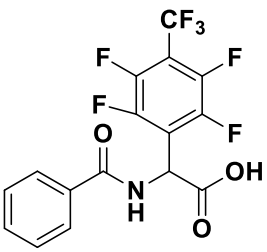

The **general procedure E** was followed using 2-phenyloxazol-5(4H)-one (1.00 g, 6.20 mmol), octafluorotoluene (1.50 g, 6.36 mmol), tetramethylguanidine (1.46 g, 12.71 mmol), and 0.620 mL of MeCN was used to afford **3c.** FT-IR (neat) cm^{-1} 3590, 1743, 1653, 1076. ^1H NMR (400 MHz, Acetonitrile-d_3) δ 7.82 (d, *J* = 7.1 Hz, 2H), 7.74 (d, *J* = 6.5

Hz, 1H), 7.62 – 7.53 (m, 1H), 7.47 (t, *J* = 7.6 Hz, 2H), 6.22 (d, *J* = 7.0 Hz, 1H). ^{19}F NMR (376 MHz, Acetonitrile-d_3) δ -57.30 (t, *J* = 21.8 Hz), -141.58 (td, *J* = 15.6, 6.2 Hz), -142.47 – -142.84 (m). ^{13}C NMR (101 MHz, Acetonitrile-d_3) δ 168.5, 133.5, 167.3, 147.5 – 144.4 (m), 144.7 (dd, *J* = 256.6, 17.1 Hz), 132.7, 129.1, 127.9, 122.1 (t, *J* = 16.2 Hz), 47.3, 121.5 (d, *J* = 273.6 Hz), 110.5 – 108.3 (m). HRMS (ESI) $C_8H_{11}NOS$ calcd. $[M+Na]^+$ 418.0285 observed 418.0276.

3d 2-(4-acetyl-2,3,5,6-tetrafluorophenyl)-2-benzamidoacetic acid

Colorless oil, 87% yield (99.6 mg, 0.270 mmol).

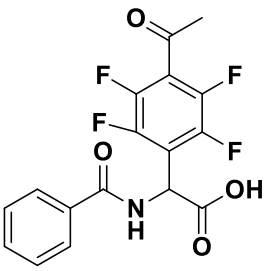

The **general procedure E** was followed using 2-phenyloxazol-5(4H)-one (50 mg, 0.310 mmol), 2',3',4',5',6' pentafluoroacetophenone (66.8 mg, 0.318 mmol), tetramethylguanidine (118.0mg, 0.636 mmol), and 0.310 mL of MeCN was used to afford **3d.** FT-IR (neat) cm^{-1} 3640, 1721, 1630, 1006. ^{1}H NMR (400 MHz, Acetonitrile-d_3) δ 7.84 (d, *J* = 7.3 Hz, 2H), 7.77 (d, *J* = 6.5 Hz, 1H), 7.58 (t, *J* = 7.4 Hz, 1H), 7.49 (t, *J* = 7.6 Hz, 2H), 6.14 (d, *J* = 6.7 Hz, 1H), 2.60 (s, 3H). ^{19}F NMR (376 MHz, Acetonitrile-d_3) δ -143.02 (dd, *J* = 21.5, 12.8 Hz), -143.63 (dd, *J* = 21.5, 12.9 Hz). ^{13}C NMR (101 MHz, Acetonitrile-d_3) δ 193.2, 169.6, 167.6, 147.5 – 144.4 (m), 143.4 (dt, *J* = 14.8, 5.4 Hz), 134.1, 132.9, 129.5, 128.3, 120.7 (t, *J* = 16.4 Hz), 120.3 (t, *J* = 17.1 Hz), 47.9, 32.6.

HRMS (ESI) $C_{17}H_{11}F_4NO_4$ calcd. $[M+]^+$ 369.0624 observed 369.0601.

3e 2-benzamido-2-(4-cyano-2,3,5,6-tetrafluorophenyl)acetic acid

Yellow oil, 78% yield (85.1 mg, 0.241 mmol).

The **general procedure E** was followed using 2-phenyloxazol-5(4H)-one (50 mg, 0.310 mmol),

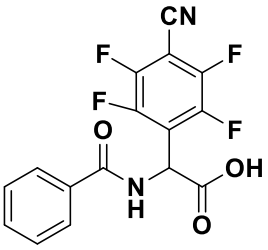

2,3,4,5,6 pentaflurobenzonitrile (63.4 mg, 0.318 mmol), tetramethylguanidine (118.0 mg, 0.636 mmol), and 0.310 mL of MeCN was used to afford **3e.** FT-IR (neat) cm^{-1} 3590, 2255, 1707, 1674. ^{1}H NMR (400 MHz, Acetonitrile-d_3) δ 7.82 (d, J = 7.3 Hz, 2H), 7.75 (d, J = 6.2 Hz, 1H), 7.57 (t, J = 7.4 Hz, 1H), 7.47 (t, J = 7.6 Hz, 2H), 6.23 (d, J = 6.9 Hz, 1H). ^{19}F NMR (376 MHz, Acetonitrile-d_3) δ -134.83 (td, J = 15.8, 6.5 Hz), -140.78 (td, J = 15.8, 6.5 Hz). ^{13}C NMR (101 MHz, Acetonitrile-d_3) δ 168.6 , 167.7 , 148.1 (ddt, J = 259.1, 16.5, 3.9 Hz), 147.5 – 144.4 (m), 147.4 – 144.2 (m), 133.8 , 133.1 , 129.5 , 128.4 , 124.3 (t, J = 16.2 Hz), 108.5 , 47.8. HRMS (ESI) $C_{16}H_8F_4N_2O_3$ calcd. $[M+Na]^+$ 403.0676 observed 403.0701.

6a methyl 2-benzamido-2-(perfluoropyridin-4-yl)propanoate

Colorless oil, 80% yield (81.2 mg, 0.228 mmol).

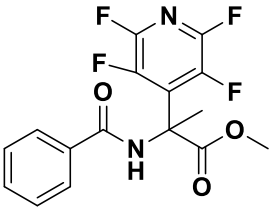

The **general procedure F** was followed using 4-methyl-2-phenyloxazol-5(4H)-one (50.0 mg, 0.285 mmol), pentafluoropyridine (49.5 mg, 0.293 mmol), *N*,*N*-diisopropylethylamine (368 mg, 2.85 mmol), trifluoroacetic acid (650 mg, 5.7 mmol)/methanol (0.230 mL) and 0.285 mL of MeCN was used to afford **6a.** FT-IR (neat) cm^{-1} 2833, 1740, 1634, 1095. ^{1}H NMR (400 MHz, Chloroform-*d*) δ 7.81 (s, 1H), 7.77 (d, J = 7.2 Hz, 2H), 7.54 (t, J = 7.4 Hz, 1H), 7.46 (t, J = 7.5 Hz, 2H), 3.89 (s, 3H), 2.22 (t, J = 3.3 Hz, 3H). ^{19}F NMR (376 MHz, Chloroform-*d*) δ -90.86 – -91.11 (m), -140.47 – -140.85 (m). ^{13}C NMR (101 MHz, Chloroform-*d*) δ 172.4, 166.2, 146.4 (dt, J = 180.2 Hz), 141.6 (dd, J = 261.0 Hz), 133.5, 132.8, 132.1 (t, J = 3.3 Hz), 129.2, 127.5, 59.7, 54.9, 23.7. HRMS (ESI) $C_{16}H_{12}F_4N_2O_3$ calcd. $[M+Na]^+$ 379.0676 observed 379.0698.

6b methyl 2-benzamido-4-methyl-2-(perfluoropyridin-4-yl)pentanoate

Colorless oil, 74% yield (136 mg, 0.340 mmol).

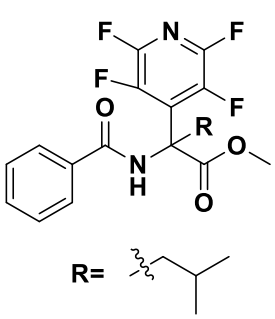

The **general procedure F** was followed using 4 4-isobutyl-2-phenyloxazol-5(4H)-one (100 mg, 0.460 mmol), pentafluoropyridine (79.7 mg, 0.472 mmol), *N*,*N*-diisopropylethylamine (595 mg, 4.6 mmol), trifluoroacetic acid (1040 mg, 9.2 mmol)/methanol (0.372 mL) and 0.460 mL of MeCN was used to afford **6b.** FT-IR (neat) cm^{-1} 2893, 1711, 1637, 1105. ^{1}H NMR (400 MHz, Chloroform-*d*) δ 7.80 (s, 1H), 7.76 (d, *J* = 8.3 Hz, 2H), 7.54 (t, *J* = 7.4 Hz, 1H), 7.46 (t, *J* = 7.8 Hz, 2H), 3.87 (s, 2H), 3.40 – 2.14 (m, 2H), 1.74 – 1.50 (m, 1H), 0.96 (d, *J* = 6.6 Hz, 2H), 0.93 (d, *J* = 6.7 Hz, 2H).

^{19}F NMR (376 MHz, Chloroform-*d*) δ -90.47 – -91.21 (m), -138.40 – -140.05 (m). ^{13}C NMR (101 MHz, Chloroform-*d*) δ 170.6, 165.4, 145.4 – 142.3 (m), 140.6 (ddd, *J* = 261.1, 27.0, 5.2 Hz), 132.9, 132.4 (t, *J* = 10.4 Hz), 128.7, 126.8, 62.9, 53.9, 40.9, 24.4, 23.9, 23.7. HRMS (ESI) $C_{19}H_{18}F_4N_2O_3$ calcd. $[M+H]^+$ 399.1326 observed 399.1299.

6c methyl 2-benzamido-4-(methylthio)-2-(perfluoropyridin-4-yl)butanoate

Colorless oil, in 79% yield (69.7 mg, 0.167 mmol).

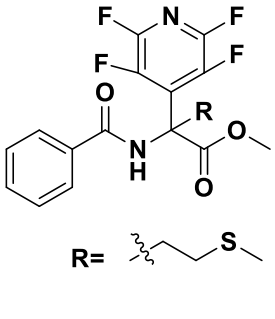

The **general procedure F** was followed using 4-(2-(methylthio)ethyl)-2-phenyloxazol-5(4H)-one (50.0 mg, 0.212 mmol), pentafluoropyridine (36.8 mg, 0.218 mmol), *N*,*N*-diisopropylethylamine (274 mg, 2.12 mmol), trifluoroacetic acid (483 mg, 4.24 mmol)/methanol (0.171 mL) and 0.212 mL of MeCN was used to afford **6c.** FT-IR (neat) cm^{-1} 2799, 1739, 1655, 1005. ^{1}H NMR (400 MHz, Chloroform-*d*) δ 7.81 (s, 1H), 7.77 (d, *J* = 8.5 Hz, 2H), 7.56 (t, *J* = 7.4 Hz, 1H), 7.47 (t, *J* = 7.6 Hz, 2H), 3.89 (s, 3H), 3.65 – 3.52 (m, 1H), 2.67 (dt, *J* =

14.2, 5.8 Hz, 1H), 2.61 – 2.50 (m, 1H), 2.39 – 2.27 (m, 1H), 2.09 (s, 3H). ^{19}F NMR (376 MHz, Chloroform-*d*) δ -90.31 – -90.85 (m), -139.48 (t, *J* = 19.6 Hz). ^{13}C NMR (101 MHz, Chloroform-*d*) δ 170.5, 166.2, 145.9 – 142.9 (m), 141.4 (dd, *J* = 261.5, 35.0 Hz), 133.3, 132.9, 132.0 (t, *J* = 10.4 Hz), 129.3, 127.5, 63.1, 54.9, 33.4, 28.8, 16.2. HRMS (ESI) $C_{18}H_{16}F_4N_2O_3S$ calcd. $[M+H]^+$ 417.0891 observed 417.0862.

6d methyl 7-benzamido-8,9,11-trifluoro-6,7-dihydro-1l4-1,5-(metheno)fluoronino[2,3-c]pyridine-7-carboxylate

Colorless oil, 71% yield (61.1 mg, 0.141 mmol).

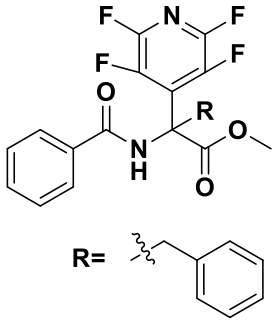

The **general procedure F** was followed using 4-benzyl-2-phenyloxazol-5(4H)-one (50.0 mg, 0.199 mmol), pentafluoropyridine (34.5 mg, 0.204 mmol), *N*,*N*-diisopropylethylamine (257 mg, 1.99 mmol), trifluoroacetic acid (453 mg, 3.98 mmol)/methanol (0.161 mL) and 0.199 mL of MeCN was used to afford **6d.** FT-IR (neat) cm^{-1} 3080, 1715, 1674, 1040. ^{1}H NMR (400 MHz, Chloroform-*d*) δ 7.65 (d, *J* = 8.1 Hz, 2H), 7.48 (dd, *J* = 13.9, 6.5 Hz, 2H), 7.39 (t, *J* = 7.6 Hz, 2H), 7.20 (d, *J* = 7.1 Hz, 3H), 6.94 (d, *J* = 7.5 Hz, 2H), 4.57 (d, *J* = 13.5 Hz, 1H), 3.76 (s, 3H), 3.51 (d, *J* = 13.5 Hz, 1H). ^{19}F NMR (376 MHz, Chloroform-*d*) δ -93.05 (ddd, *J* = 23.2, 14.8, 7.7 Hz), -144.30 – -144.54 (m). ^{13}C NMR (101 MHz, Chloroform-*d*) δ 169.76, 166.49, 144.47 (dt, *J* = 244.2, 17.1 Hz), 141.44 (dd, *J* = 260.8, 23.6 Hz), 134.4, 133.6, 132.9, 132.4 (t, *J* = 10.8 Hz), 130.5, 129.3, 129.0, 128.3, 127.5, 64.4, 54.5, 39.4. HRMS (ESI) $C_{22}H_{16}F_4N_2O_3$ calcd. $[M+H]^+$ 433.1170 observed 433.1140.

General procedure G for the deprotection of perfluoroaryl-*N*-benzoyl amino acids

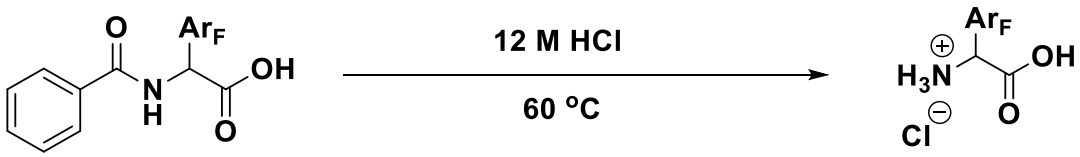

The *N*-benzoyl amnio acid (1.0 equiv) and 12 M HCl (0.01 M) was added to a round bottom flask and heated to 60 ^{0}C. The reaction was monitored by ^{19}F NMR and after consumption of the starting material the mixture was diluted with a half volume of H_2O and washed with equal volumes of toluene x3. The aqueous layer was concentrated *in vacuo* to give the product.

4a carboxy(perfluoropyridin-4-yl)methanaminium chloride

White solid, 99% yield (59 mg, 0.228 mmol).

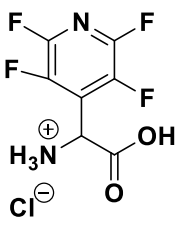

The **general procedure G** was followed using 2-benzamido-2-(perfluoropyridin-4-yl)acetic acid (75 mg, 0.228 mmol) and 23.4 mL of 12 M HCl to afford **4a.** FT-IR (neat) cm^{-1} 3670, 3300, 1724, 1065. ^{1}H NMR (400 MHz, Deuterium Oxide) δ 5.52 (s, 1H). ^{19}F NMR (376 MHz, Deuterium Oxide) δ -89.95 – -90.40 (m), -141.50 – -142.06 (m). ^{13}C NMR (101 MHz, Deuterium Oxide) δ 167.55, 143.47 (dt, *J* = 245.5, 16.5 Hz), 140.43 (dd, *J* = 260.6, 35.0 Hz), 125.36 (t, *J* = 16.6 Hz), 46.42. HRMS (ESI) $C_7H_5F_4N_2O_2Cl$ calcd. $[M+]^+$ 259.9976 observed 259.9964.

4b carboxy(3-chloro-2,5,6-trifluoropyridin-4-yl)methanaminium chloride

White solid, in 99% yield (119 mg, 0.431 mmol).

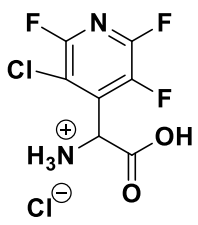

The **general procedure G** was followed using 2-benzamido-2-(3-chloro-2,5,6-trifluoropyridin-4-yl)acetic acid (150 mg, 0.435 mmol) and 43.5 mL of 12 M HCl to afford **4b.** FT-IR (neat) cm^{-1} 3683, 3300, 1715, 1034. ^{1}H NMR (400 MHz, Deuterium Oxide) δ 5.43 (s, 1H). ^{19}F NMR (376 MHz, Deuterium Oxide) δ -72.70 – -141.42 (m), -84.21 – -93.07 (m), -141.39 . ^{13}C NMR (101 MHz, Deuterium Oxide) δ 167.2, 151.0 (dd, *J* = 243.5, 10.3 Hz), 147.0 (dt, *J* = 246.8, 14.6 Hz), 141.5 (dd, *J* = 260.3, 31.8 Hz), 134.5 (d, *J* = 12.7 Hz), 114.1 (dd, *J* = 35.1, 4.9 Hz), 48.9. HRMS (ESI) $C_7H_5F_3N_2O_2Cl_2$ calcd.$[M+]^+$ 275.9680 observed 275.9672.

4c carboxy(2,3,5,6-tetrafluoro-4-(trifluoromethyl)phenyl)methanaminium chloride

White solid, 99% yield (41.1 mg, 0.125 mmol).

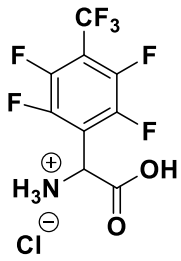

The **general procedure G** was followed using 2-benzamido-2-(2,3,5,6-tetrafluoro-4-(trifluoromethyl)phenyl)acetic acid (50 mg, 0.127 mmol) and 12.7 mL of 12 M HCl to afford **4c.** FT-IR (neat) cm^{-1} 3677, 3309, 1725, 1101. ^{1}H NMR (400 MHz, Acetonitrile-d_3) δ 3.63 (s, 1H). ^{19}F NMR (376 MHz, Acetonitrile-d_3) δ -57.28 , -136.68 – -138.28 (m), -140.91 . ^{13}C NMR (101 MHz, Acetonitrile-d_3) δ 165.4, 146.8 – 144.9 (m), 144.3 – 142.2 (m), 128.8 – 126.4 (m), 121.7, 115.5 – 114.6 (m), 47.6. HRMS (ESI) $C_9H_5F_7NO_2Cl$ calcd.$[M+]^+$ 326.9897 observed 326.9888.

General procedure H for the decarboxylation of perfluoroaryl amino acids

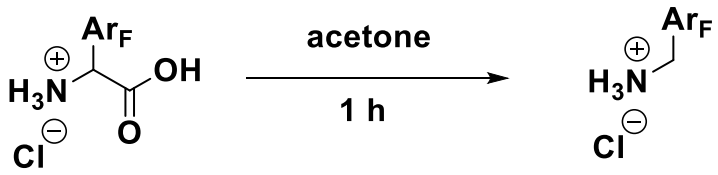

The amino acid (**1.0** equiv) and acetone 1 M was added to a round bottom flask with a magnetic stir bar was left to stir for 1 hour. The reaction was monitored by ^{19}F NMR and after consumption of the starting material; the mixture was concentrated *in vacuo* to give the product.

5a (perfluoropyridin-4-yl)methanaminium chloride

White solid, 99% yield (12.4 mg, 0.0572 mmol)

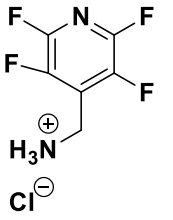

The **general procedure H** was followed using carboxy(perfluoropyridin-4-yl)methanaminium chloride (15mg, 0.0576 mmol) and 57.6 uL of acetone to afford **5a.** FT-IR (neat) cm^{-1} 3603, 3287, 3044, 1015. ^{1}H NMR (400 MHz, Deuterium Oxide) δ 4.36 (s, 1H). ^{19}F NMR (376 MHz, Deuterium Oxide) δ -91.12 (dq, *J* = 28.3, 13.1 Hz), -142.50 – -142.83 (m). ^{13}C NMR (101 MHz, Deuterium Oxide) δ ^{13}C NMR (101 MHz, Deuterium Oxide) δ 144.8 – 141.6 (m), 140.7 (dd, *J* = 259.7, 34.7 Hz), 125.4 (t, *J* = 15.9 Hz), 31.1. HRMS (ESI) $C_6H_5F_4N_2Cl$ calcd. $[M+]^+$ 216.0077 observed 216.0054.

5b (3-chloro-2,5,6-trifluoropyridin-4-yl)methanaminium chloride

White solid, 99% yield (16.9 mg, 0.0725 mmol).

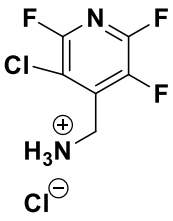

The **general procedure H** was followed using carboxy(3-chloro-2,5,6-trifluoropyridin-4-yl)methanaminium chloride (25.0 mg, 0.0725 mmol) and 72.5 uL of acetone to afford **5b.** FT-IR (neat) cm^{-1} 3632, 3250, 3033, 1055. ^{1}H NMR (400 MHz, Deuterium Oxide) δ 4.51 (s, 1H). ^{19}F NMR (376 MHz, Deuterium Oxide) δ -74.14 (dd, *J* = 27.7, 12.4 Hz), -88.82 (dd, *J* = 21.4, 12.4 Hz), -140.28 – -147.60 (m). ^{13}C NMR (101 MHz, Deuterium Oxide) δ 151.0 (ddd, *J* = 242.5, 11.9, 2.9 Hz), 147.1 (ddd, *J* = 246.8,

17.6, 13.2 Hz), 141.9 (ddd, *J* = 259.0, 27.0, 6.4 Hz), 135.3 (d, *J* = 14.2 Hz), 114.1 (dd, *J* = 34.7, 6.8 Hz), 34.1. HRMS (ESI) $C_6H_5ClF_3N_2Cl$ calcd. $[M+]^+$ 231.9782 observed 231.9799.

5c (2,3,5,6-tetrafluoro-4-(trifluoromethyl)phenyl)methanaminium chloride

White solid, 99% yield (10.7 mg, 0.027 mmol).

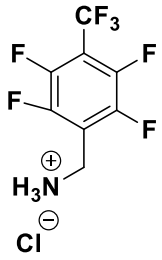

The **general procedure H** was followed using carboxy(2,3,5,6-tetrafluoro-4-(trifluoromethyl)phenyl)methanaminium chloride (15 mg, 0.038 mmol) and 38 uL of acetone to afford **5c.** FT-IR (neat) cm^{-1} 3609, 3277, 3064, 1077. ^1H NMR (400 MHz, DMSO-d_6) δ 4.24 (s, 1H). ^{19}F NMR (376 MHz, Deuterium Oxide) δ -57.69 (t, *J* = 21.5 Hz), -139.33 (dt, *J* = 17.2, 9.5 Hz), -139.69 – -140.09 (m). ^{13}C NMR (101 MHz, DMSO-d_6) δ 145.8 (d, *J* = 251.7 Hz), 143.6 (dt, *J* = 259.4, 18.4 Hz), 121.0 (d, *J* = 276.2 Hz), 118.7 (d, *J* = 35.9 Hz), 108.9, 30.6.

HRMS (ESI) $C_8H_5F_7NCl$ calcd. $[M+]^+$ 282.9999 observed 283.0023.

Synthesis of 2-aminohydantoins

General procedure I for synthesis of 2-aminohydantoins

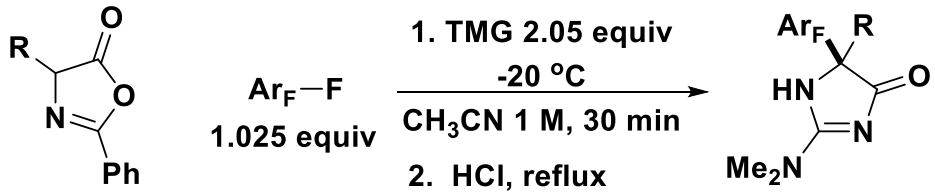

Under an argon atmosphere, oxazolone **(1 equiv**), Ar_F–F **(1.025 equiv),** CH_3CN **(1 M)** were added to small test tube, which was fitted with a septum and cooled to -20 ºC. Then a steady stream of

tetramethylguanidine **(1.025 equiv)** was added to mixture down the side of the test tube glass which facilitated cooling of the TMG solution. The reaction was left to react for 30 min and then the cooling bath was removed. After, the reaction had warmed to room temperature, then a solution of 12 M aqueous hydrochloric acid (0.1 M) was added and refluxed for 24-48 h. The solution was diluted with a half volume of water and made neutral with $NaHCO_3$. The aqueous layer was extracted with EtOAc x 3 and the organic layer was dried with $MgSO_4$ and concentrated giving crude product. Purification of the crude product was purified by normal phase column chromatography.

7a 2-(dimethylamino)-5-methyl-5-(perfluoropyridin-4-yl)-1,5-dihydro-4H-imidazol-4-one

White solid, 95% yield (314 mg, 1.08 mmol).

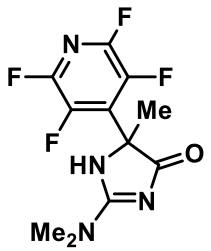

The **general procedure I** was followed using 4-methyl-2-phenyloxazol-5(4H)-one (200 mg, 1.14 mmol), pentafluoropyridine (66.8 mg, 1.17 mmol), tetramethylguanidine (135 mg, 1.17 mmol), 11.4 mL HCl, and 1.14 mL of MeCN was used to afford **7a.** FT-IR (neat) cm^{-1} 3203, 2967, 1730, 1035. ^1H NMR (400 MHz, DMSO-d_6) δ 8.99 (s, 1H), 3.11 (s, 3H), 2.98 (s, 3H), 1.75 (s, 3H).

^{19}F NMR (376 MHz, CD_3CN) δ -143.03, -143.64. ^{19}F NMR (376 MHz, DMSO-d_6) δ -92.57 – -93.01 (m), -140.20 – -140.83 (m). ^{13}C NMR (101 MHz, DMSO-d_6) δ 185.8, 169.9, 145.0 – 141.5 (m), 142.6 – 138.8 (m), 133.1 (t, J = 10.6 Hz), 64.5, 38.1, 36.2, 23.9. HRMS (ESI) $C_{11}H_{10}F_4N_4O$ calcd. $[M+K]^+$ 329.0422 observed 329.0456.

7b 5-benzoyl-2-(dimethylamino)-5-(perfluoropyridin-4-yl)-1,5-dihydro-4H-imidazol-4-one

Yellow oil, in 49% yield (37.1 mg, 0.0975 mmol).

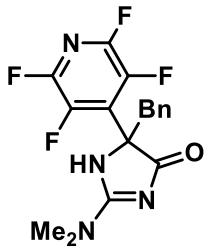

The **general procedure** I was followed using 4-benzyl-2-phenyloxazol-5(4H)-one (50 mg, 0.199 mmol), pentafluoropyridine (34.5 mg, 0.204 mmol), tetramethylguanidine (23.5 mg, 0.204 mmol), 1.99 mL HCl, and 0.199 mL of MeCN was used to afford **7b.** FT-IR (neat) cm^{-1} 3222, 2957, 1710, 1005. ^{1}H NMR (400 MHz, DMSO-d_6) δ 8.69 (s, 1H), 7.23 (s, 5H), 3.51 (q, J = 13.0 Hz, 2H), 2.86 (s, 3H), 2.72 (s, 3H). ^{19}F NMR (376 MHz, DMSO-d_6) δ -92.27 – -92.81 (m), -138.65 – -138.98 (m). ^{13}C NMR (101 MHz, DMSO-d_6) δ 183.2, 169.7, 145.23 – 142.16 (m), 142.13 – 138.90 (m), 133.76, 132.87 (t, J = 10.9 Hz), 130.5, 127.6, 126.9, 78.6, 69.3, 37.7, 35.9. HRMS (ESI) $C_{17}H_{14}F_4N_4O$ calcd. $[M+H]^+$ 367.1177 observed 367.1150.

7c 2-(dimethylamino)-5-(2-(methylthio)ethyl)-5-(perfluoropyridin-4-yl)-1,5-dihydro-4H-imidazol-4-one

Yellow solid, 60% yield (45.6 mg, 0.127 mmol).

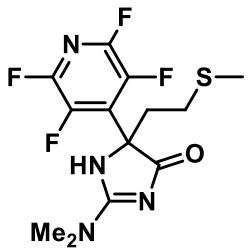

The **general procedure** was followed using 4-(2-(methylthio)ethyl)-2-phenyloxazol-5(4H)-one (50 mg, 0.212 mmol), pentafluoropyridine (36.8 mg, 0.218 mmol), tetramethylguanidine (25.1 mg,0.218 mmol), 2.12 mL HCl, and 0.212 mL of MeCN was used to afford **7c.** FT-IR (neat) cm^{-1} 2897, 2860, 1734, 1091. ^{1}H NMR (400 MHz, DMSO-d_6) δ 8.71 (s, 1H), 3.11 (s, 3H), 3.01 (s, 3H), 2.56 (d, J = 2.7 Hz, 1H), 2.46 – 2.26 (m, 2H).

^{19}F NMR (376 MHz, DMSO-d_6) δ -92.35 – -92.61 (m), -139.85 – -140.08 (m). ^{13}C NMR (101 MHz, DMSO-d_6) δ 183.7, 170.3, 145.5 – 142.6 (m), 142.4 – 138.9 (m), 132.5 (t, J = 11.0 Hz), 68.8, 38.6, 36.7, 36.2, 27.8, 15.1. HRMS (ESI) $C_{13}H_{14}F_4N_4OS$ calcd. $[M+H]^+$ 351.0897 observed 351.0866.

NMR spectra

Figure 4.4 Chapter IV NMR Spectrum Graphs

^{1}H NMR (400 MHz, Chloroform-*d*) **2a**

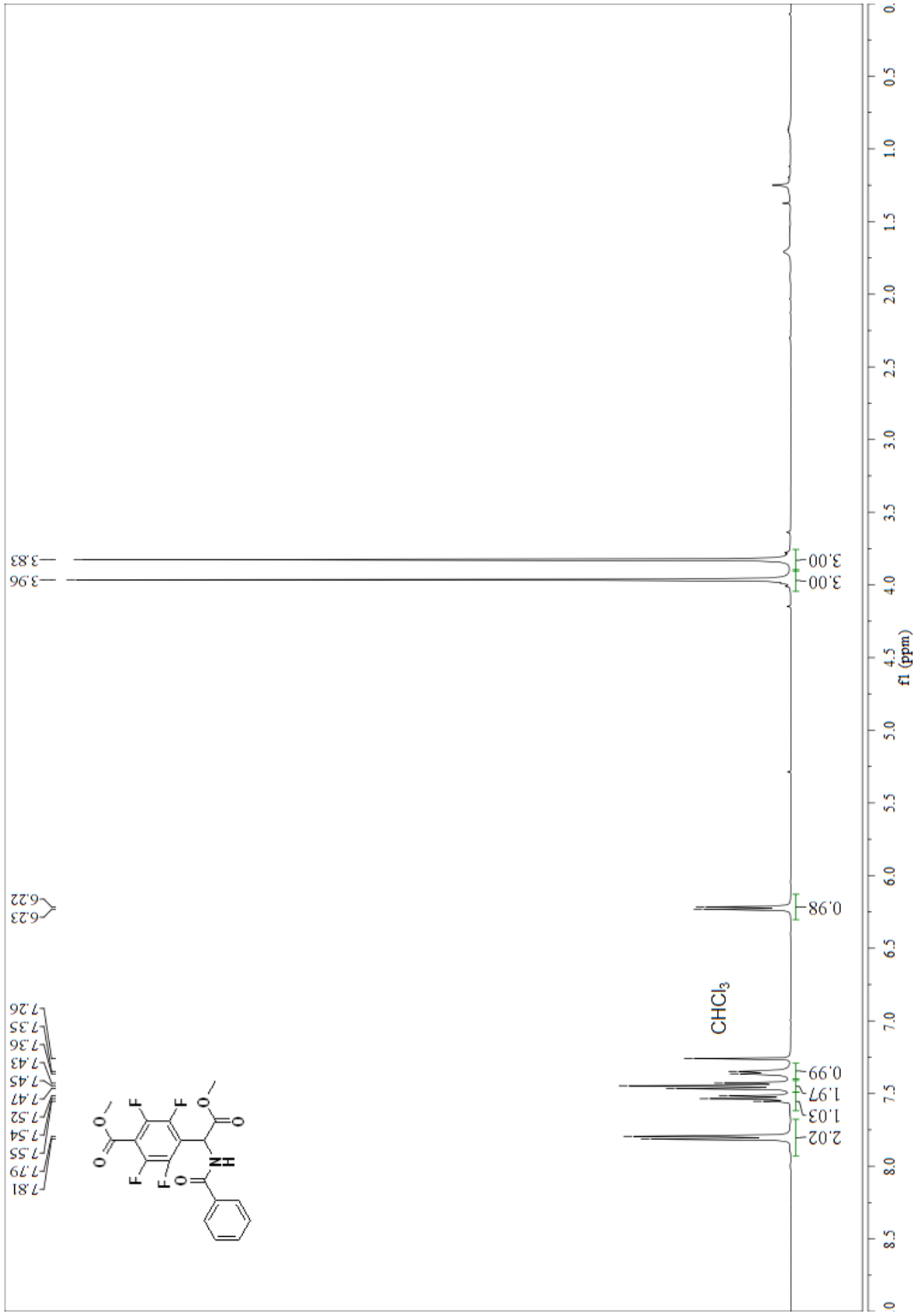

^{19}F NMR (376 MHz, Chloroform-*d*) **2a**

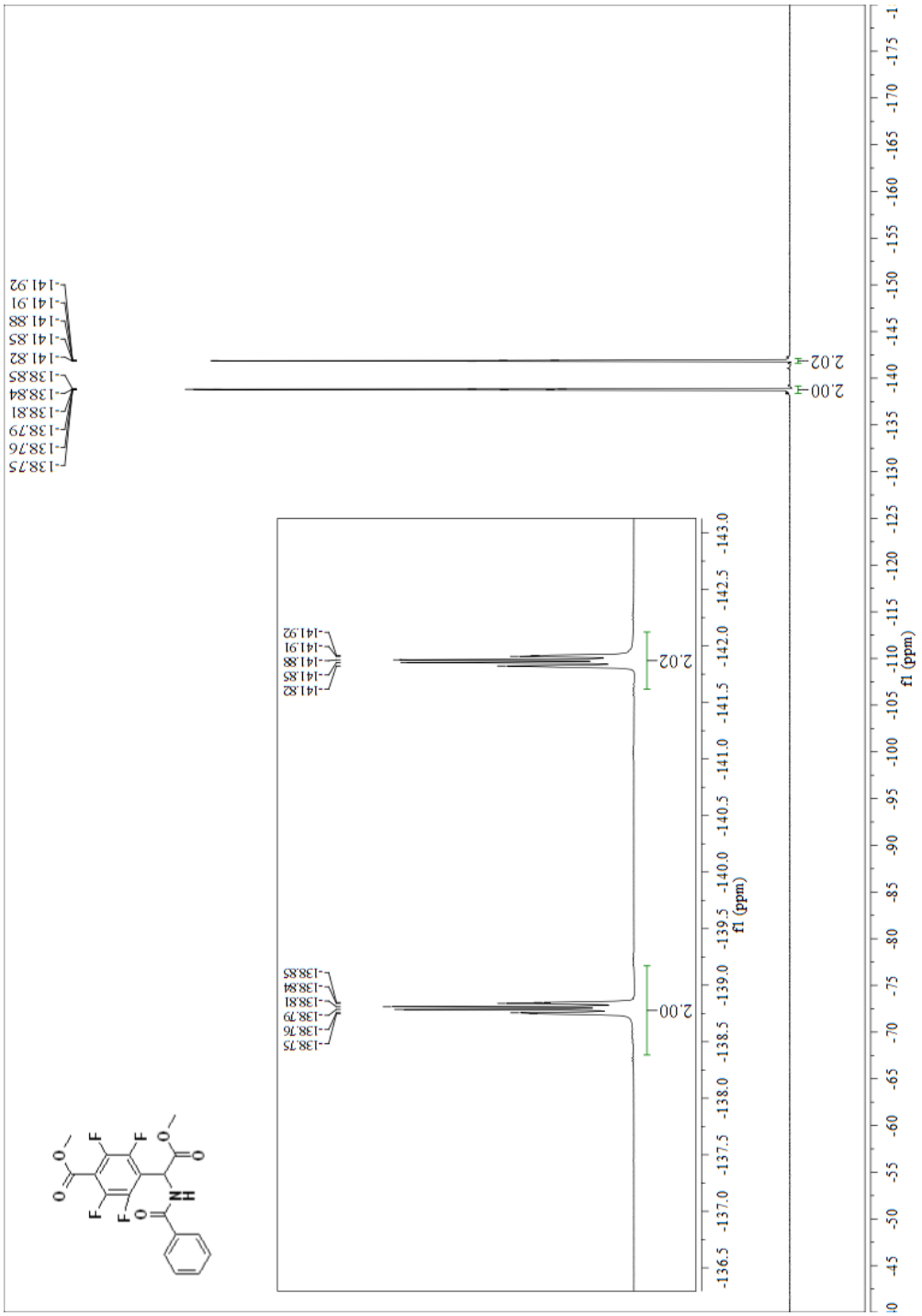

^{13}C NMR (101 MHz, Chloroform-*d*) **2a**

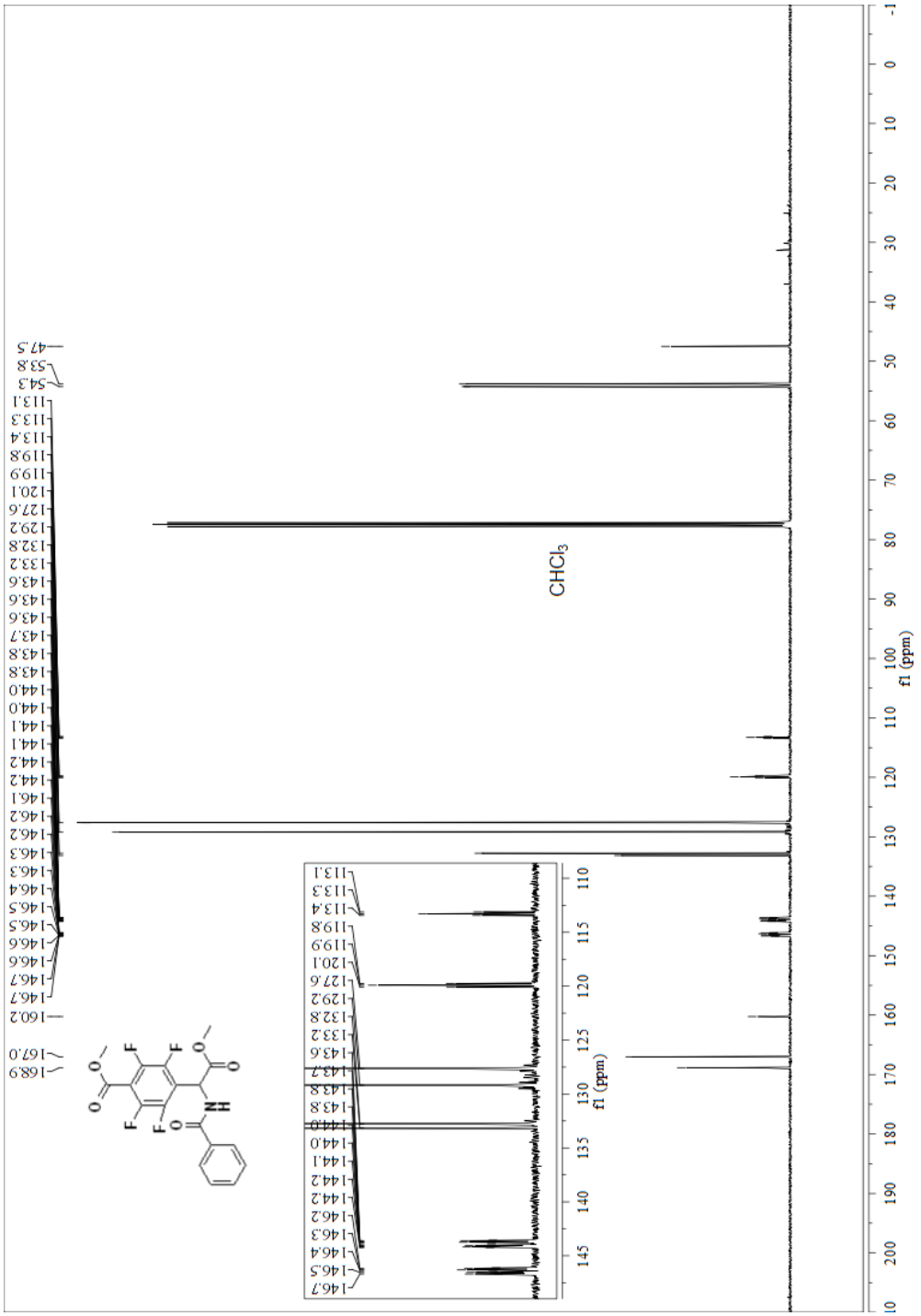

^{1}H NMR (400 MHz, Chloroform-*d*) **2b**

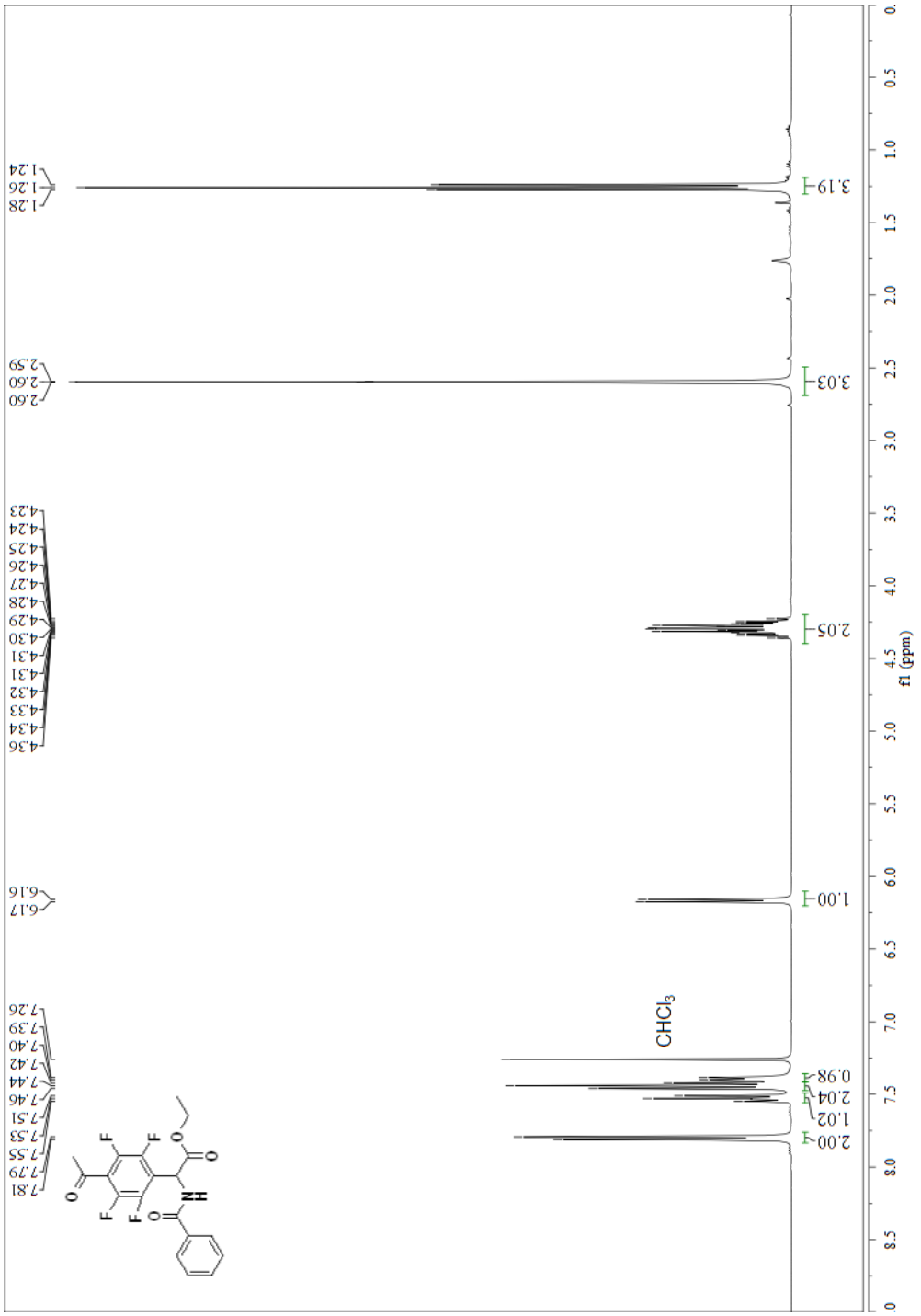

^{19}F NMR (376 MHz, Chloroform-*d*) **2b**

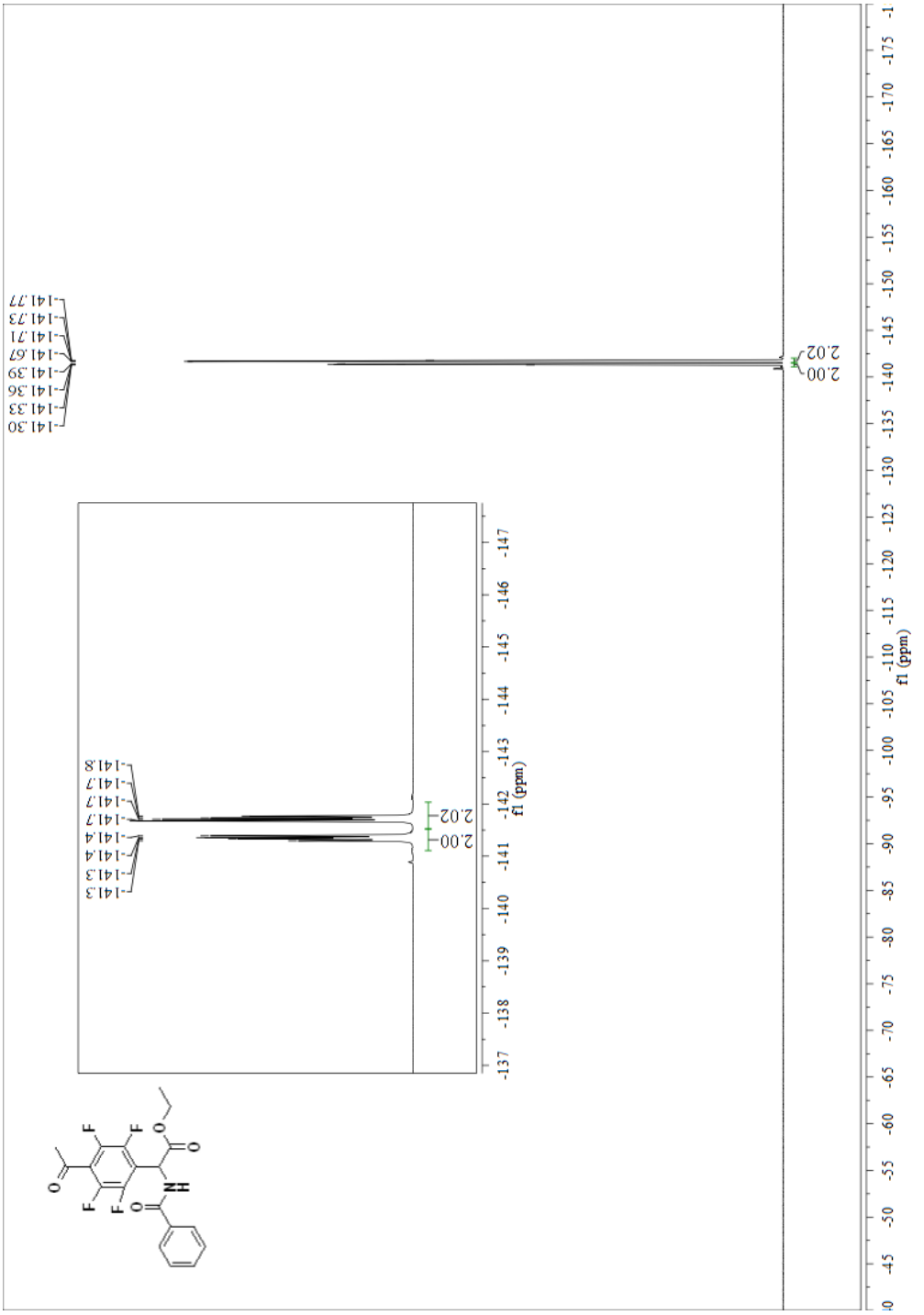

^{13}C NMR (101 MHz, Chloroform-*d*) **2b**

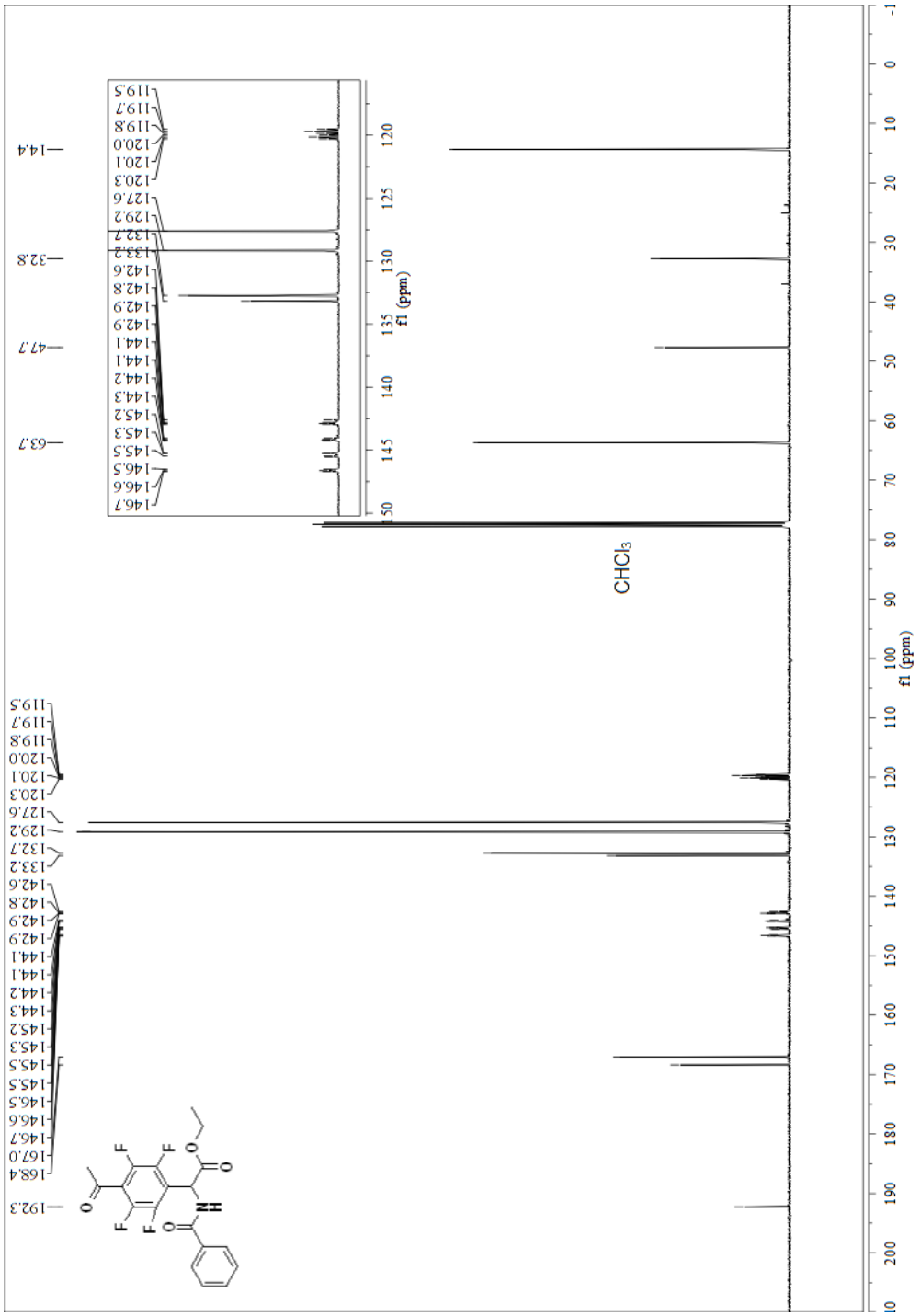

^{1}H NMR (400 MHz, Chloroform-*d*) **2c**

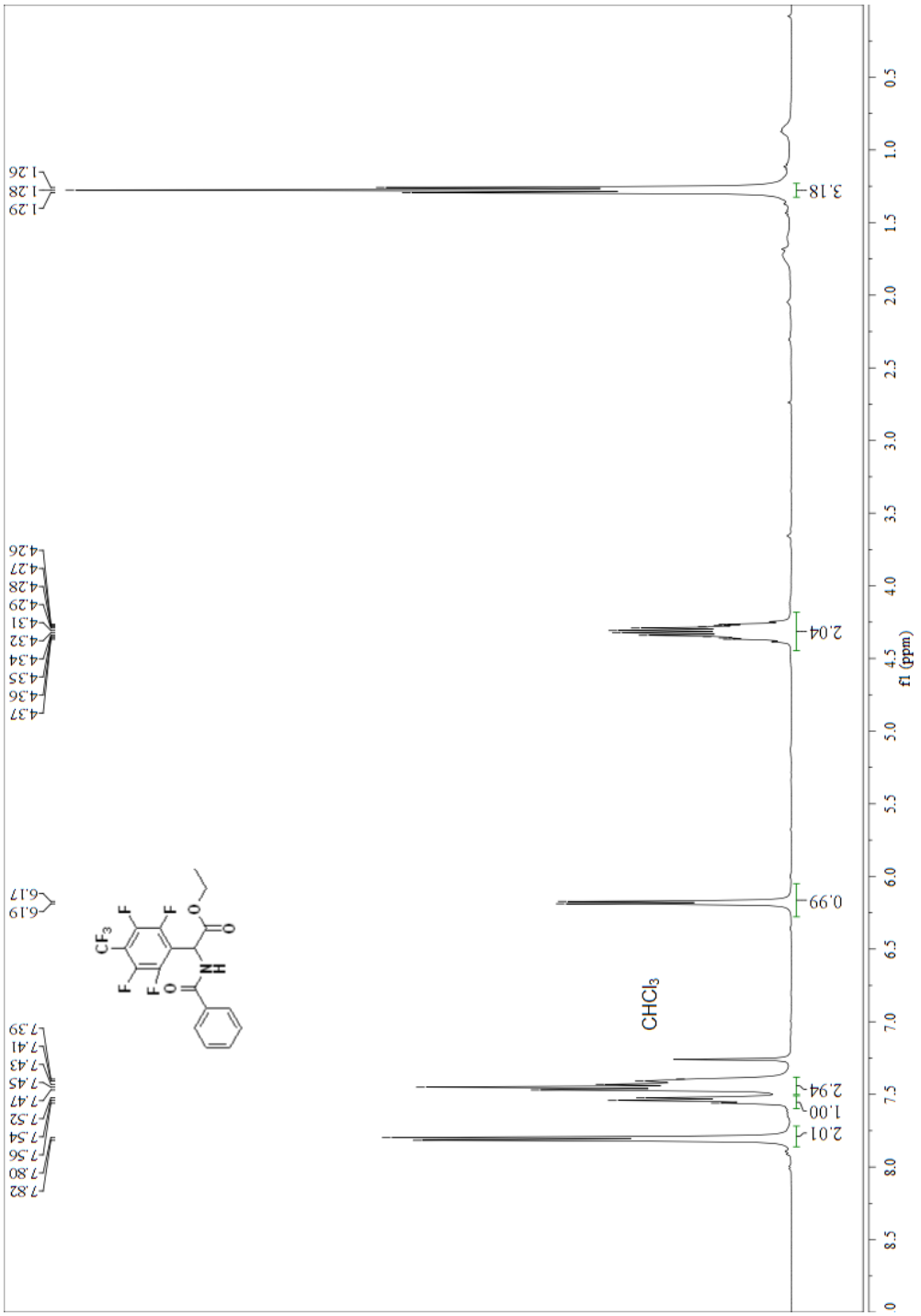

^{19}F NMR (376 MHz, Chloroform-*d*) **2c**

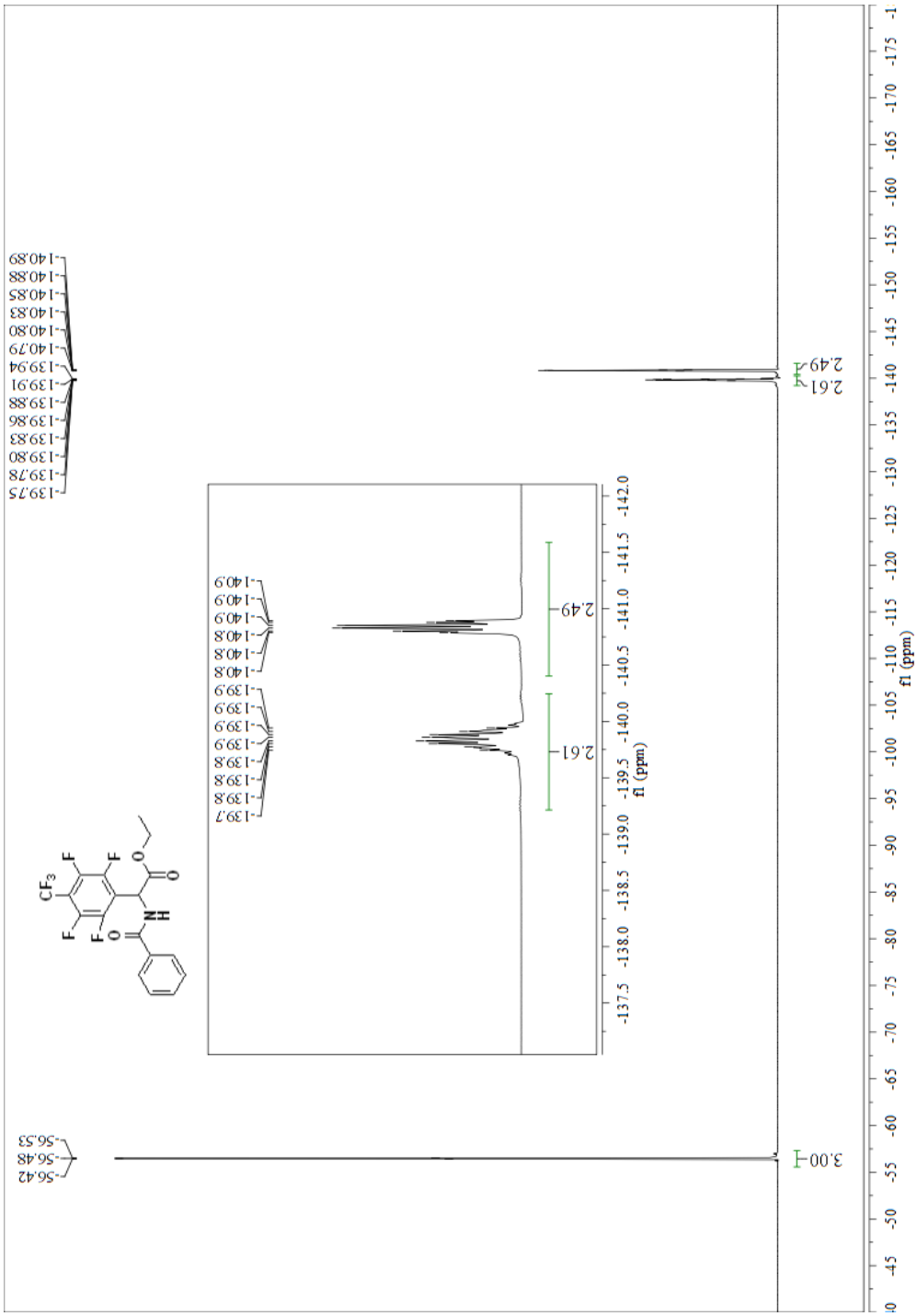

^{13}C NMR (101 MHz, Chloroform-*d*) **2c**

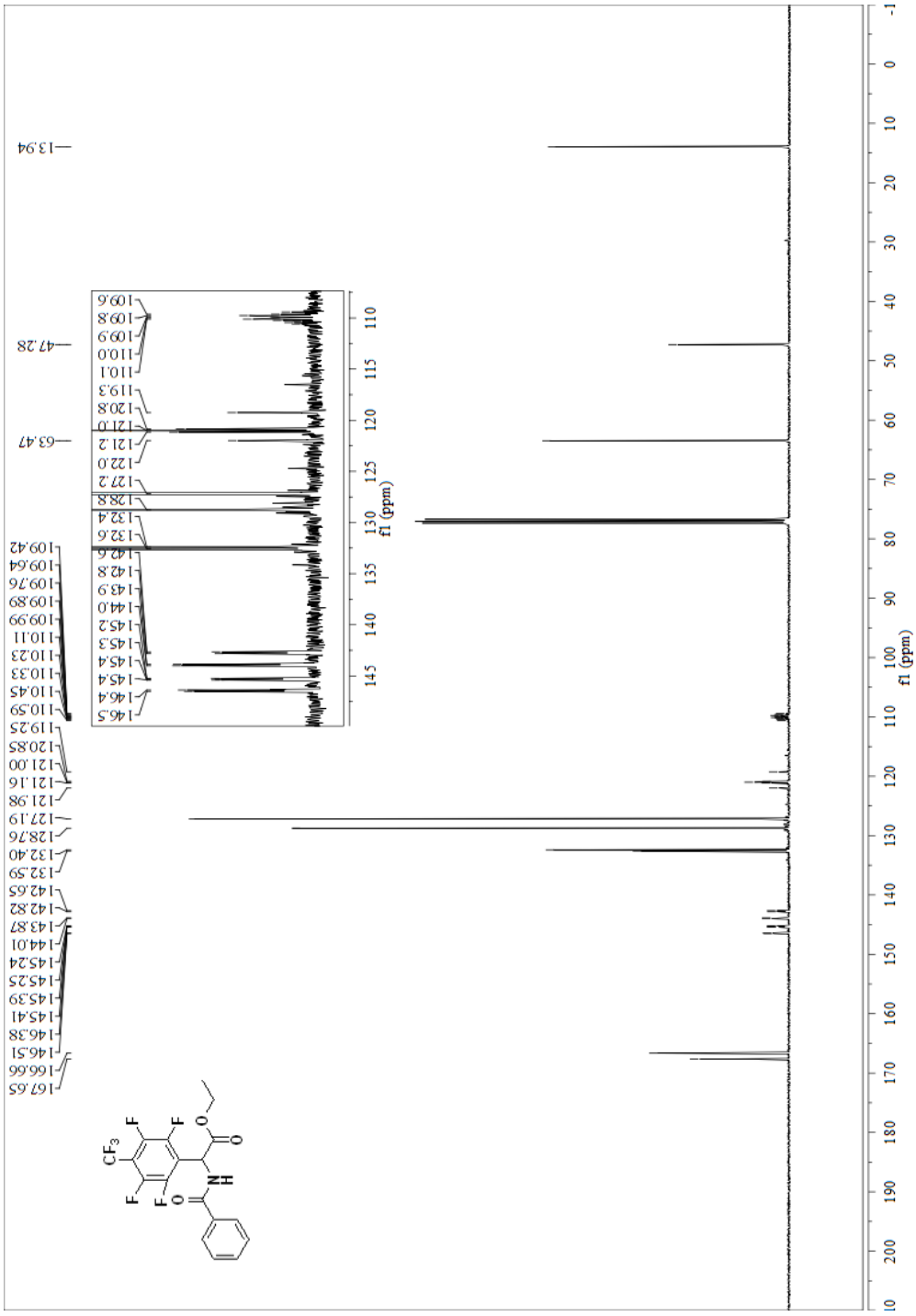

^{1}H NMR (400 MHz, Acetonitrile-d_3) **2d**

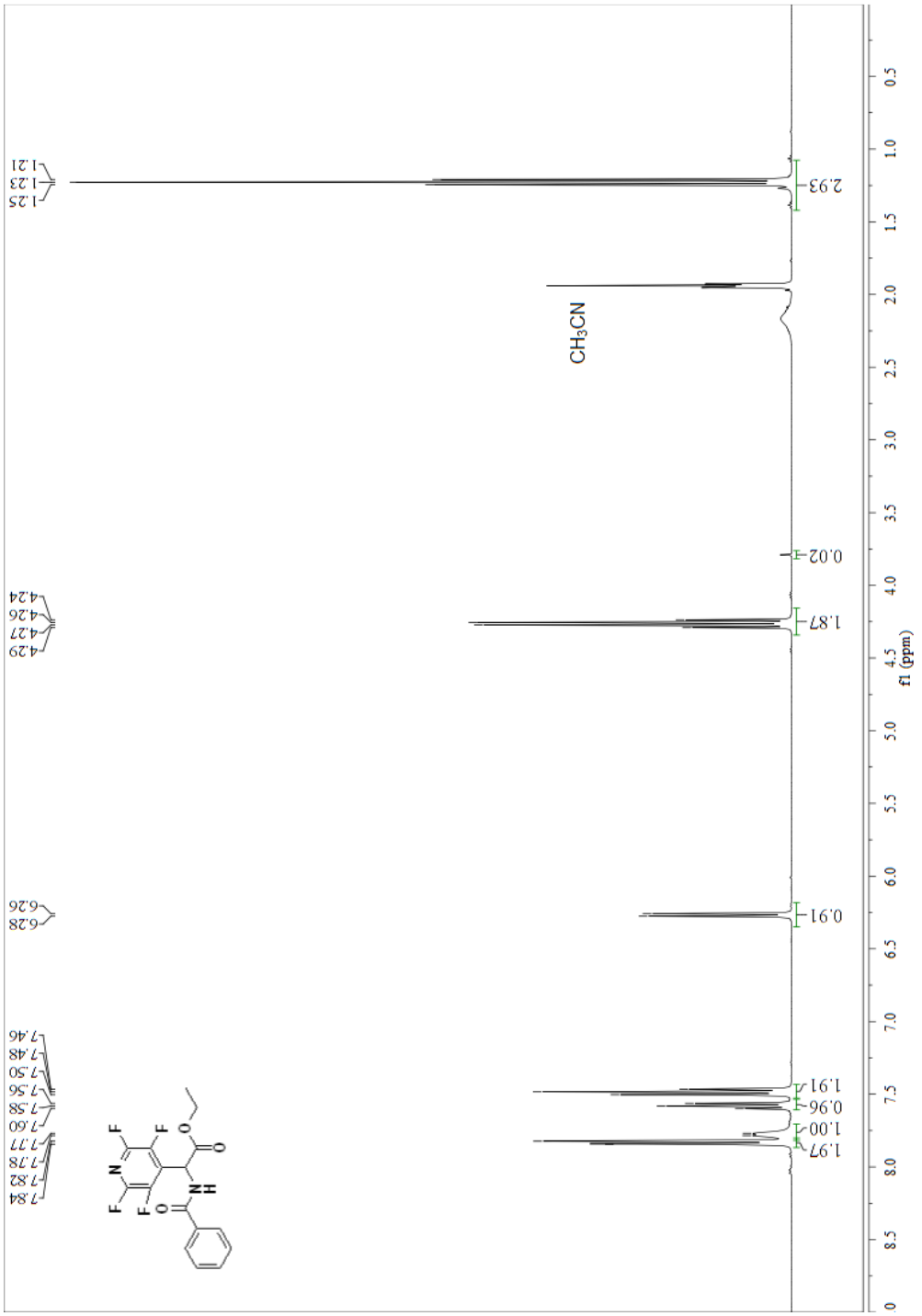

^{19}F NMR (376 MHz, Acetonitrile-d_3) **2d**

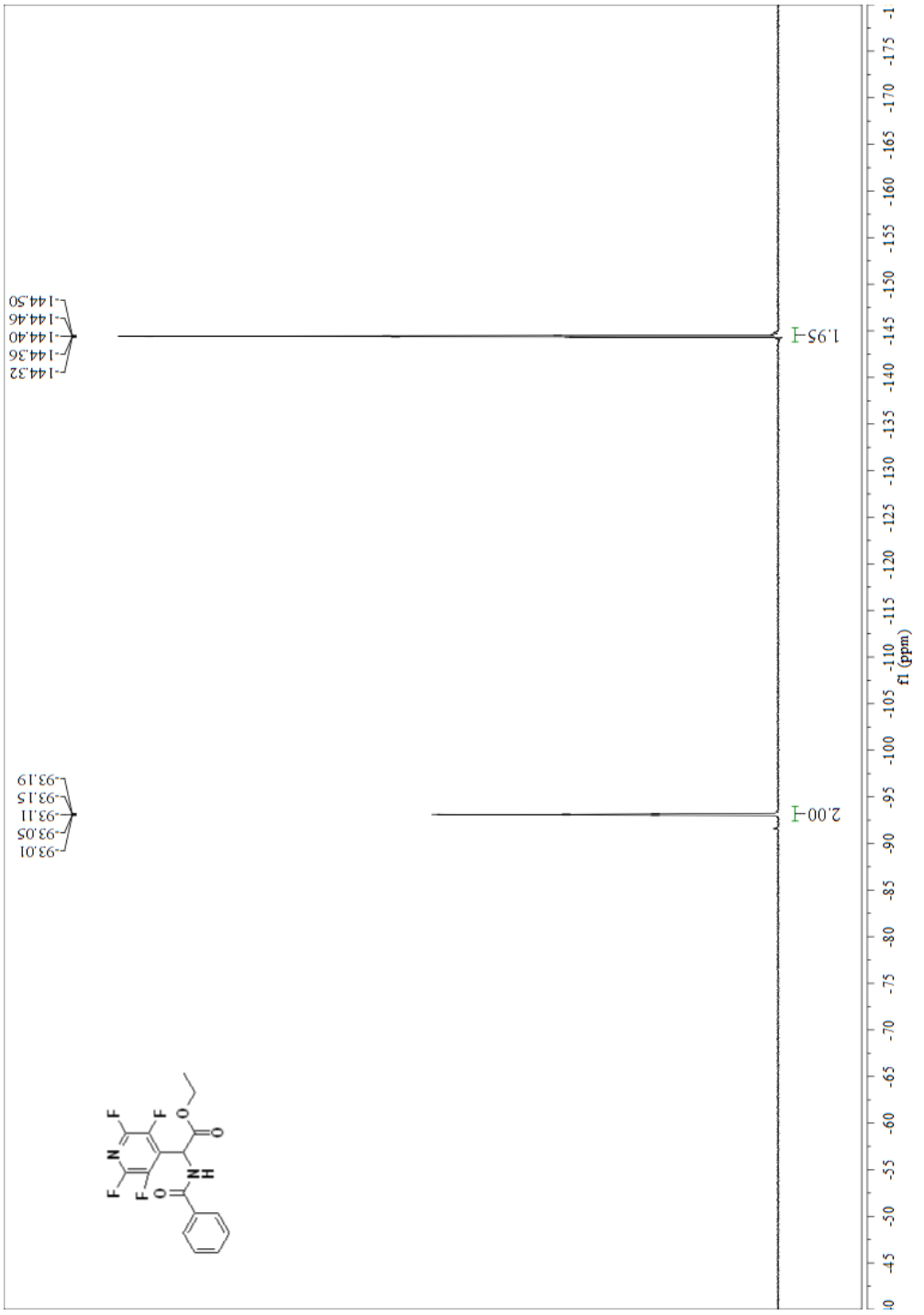

^{13}C NMR (101 MHz, Acetonitrile-d_3) **2d**

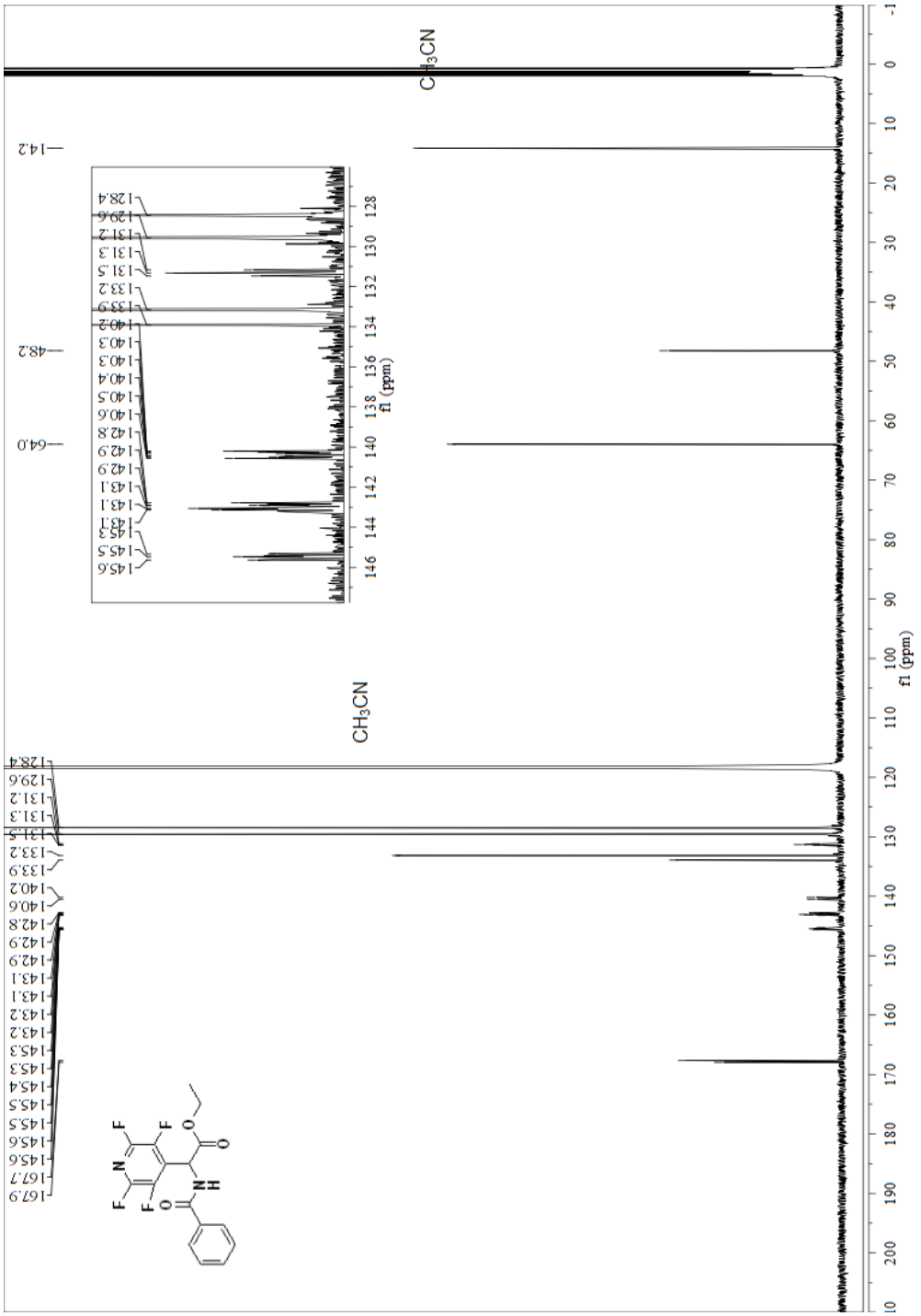

^{1}H NMR (400 MHz, Chloroform-*d*) **2e**

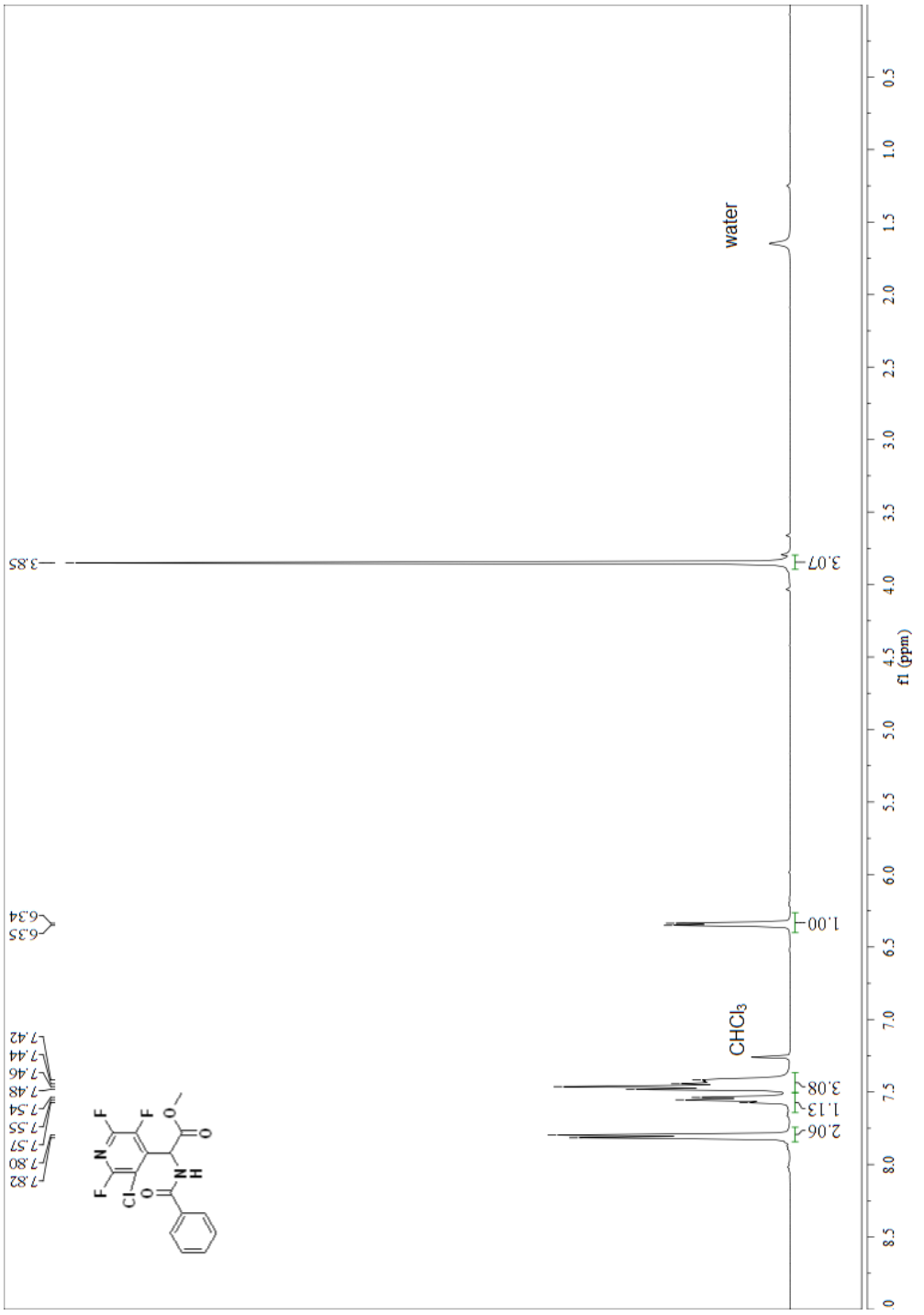

^{19}F NMR (376 MHz, Chloroform-*d*) **2e**

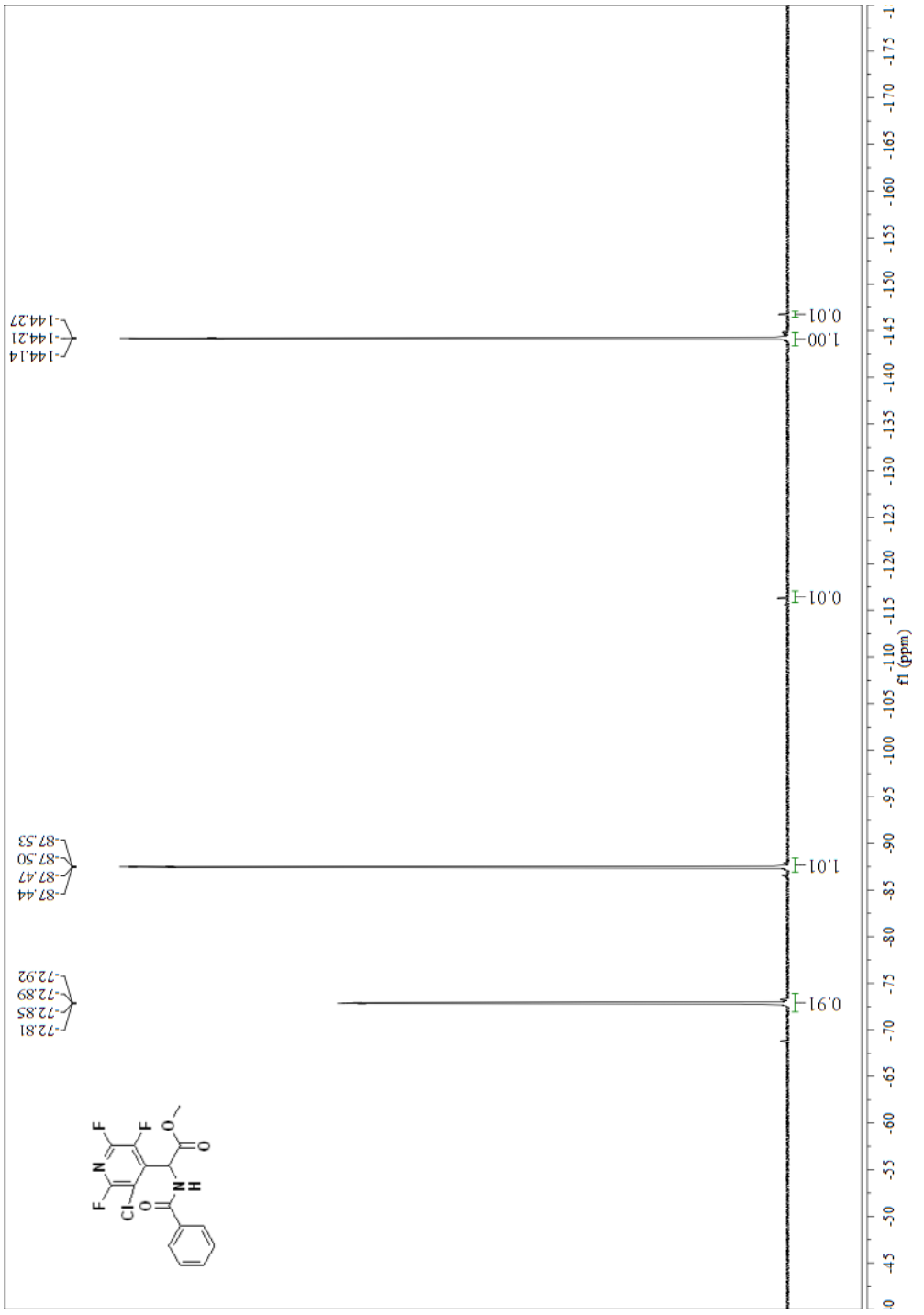

^{13}C NMR (101 MHz, Chloroform-*d*) **2e**

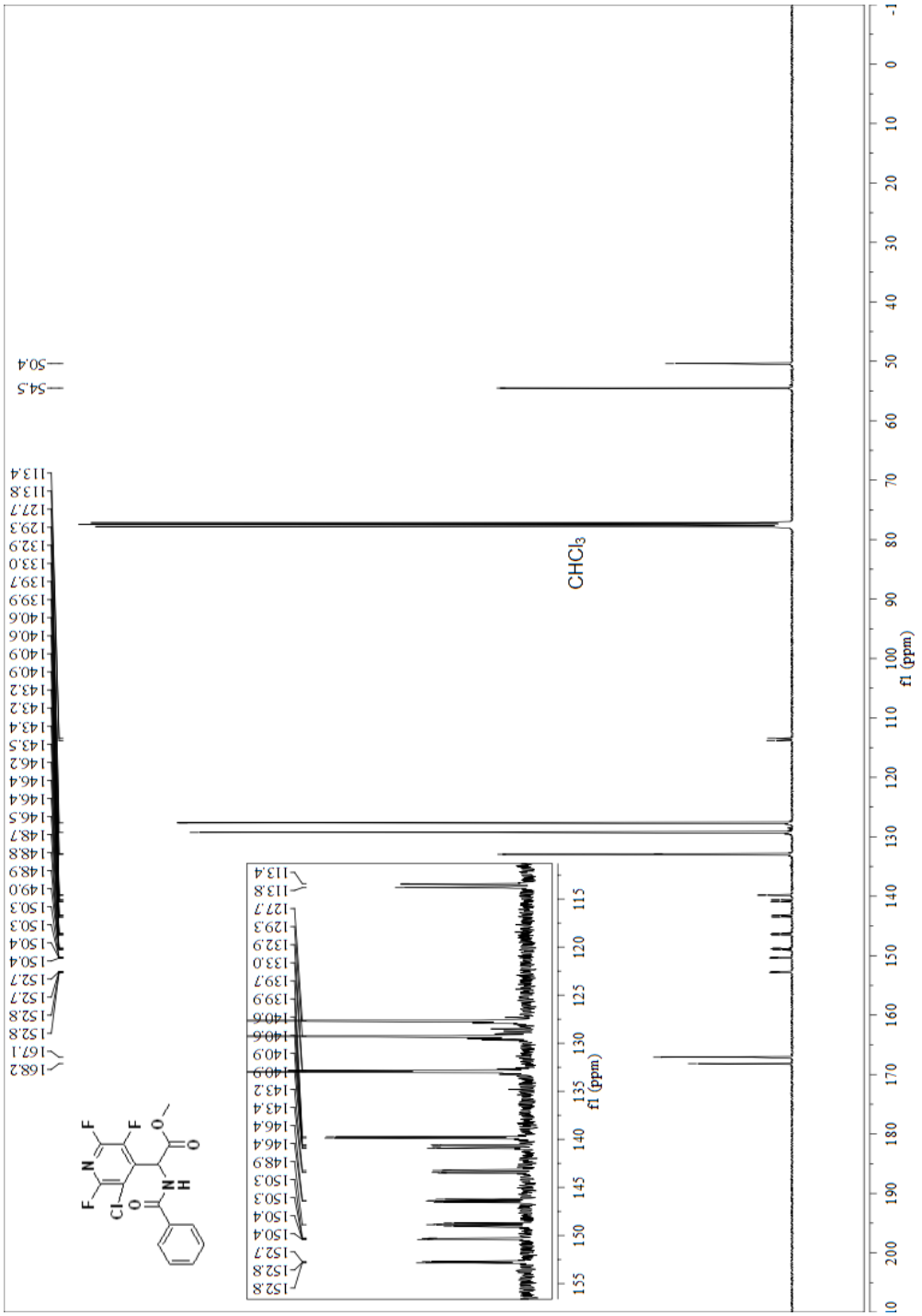

^{1}H NMR (400 MHz, Chloroform-*d*) **2f**

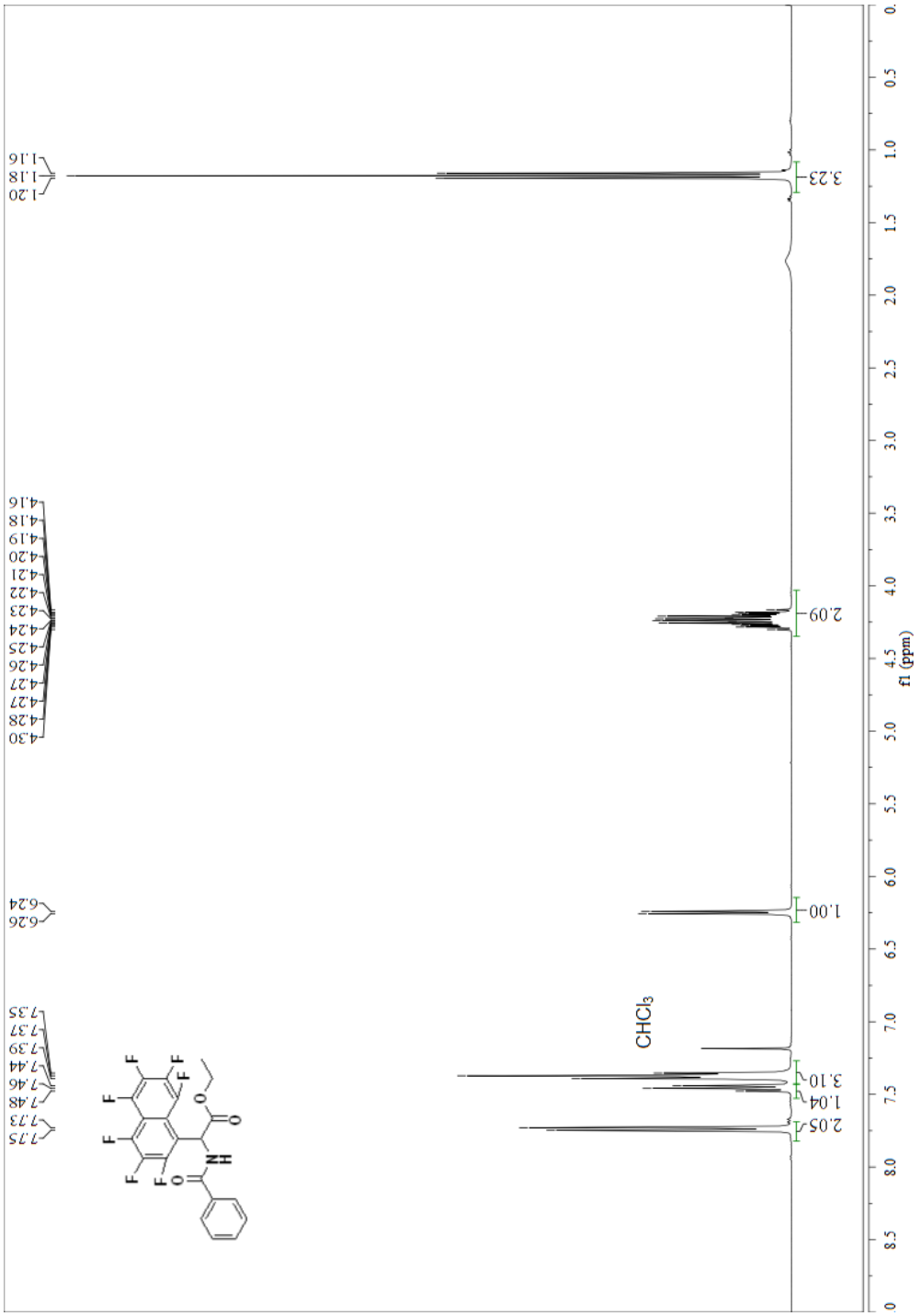

^{19}F NMR (376 MHz, Chloroform-*d*) **2f**

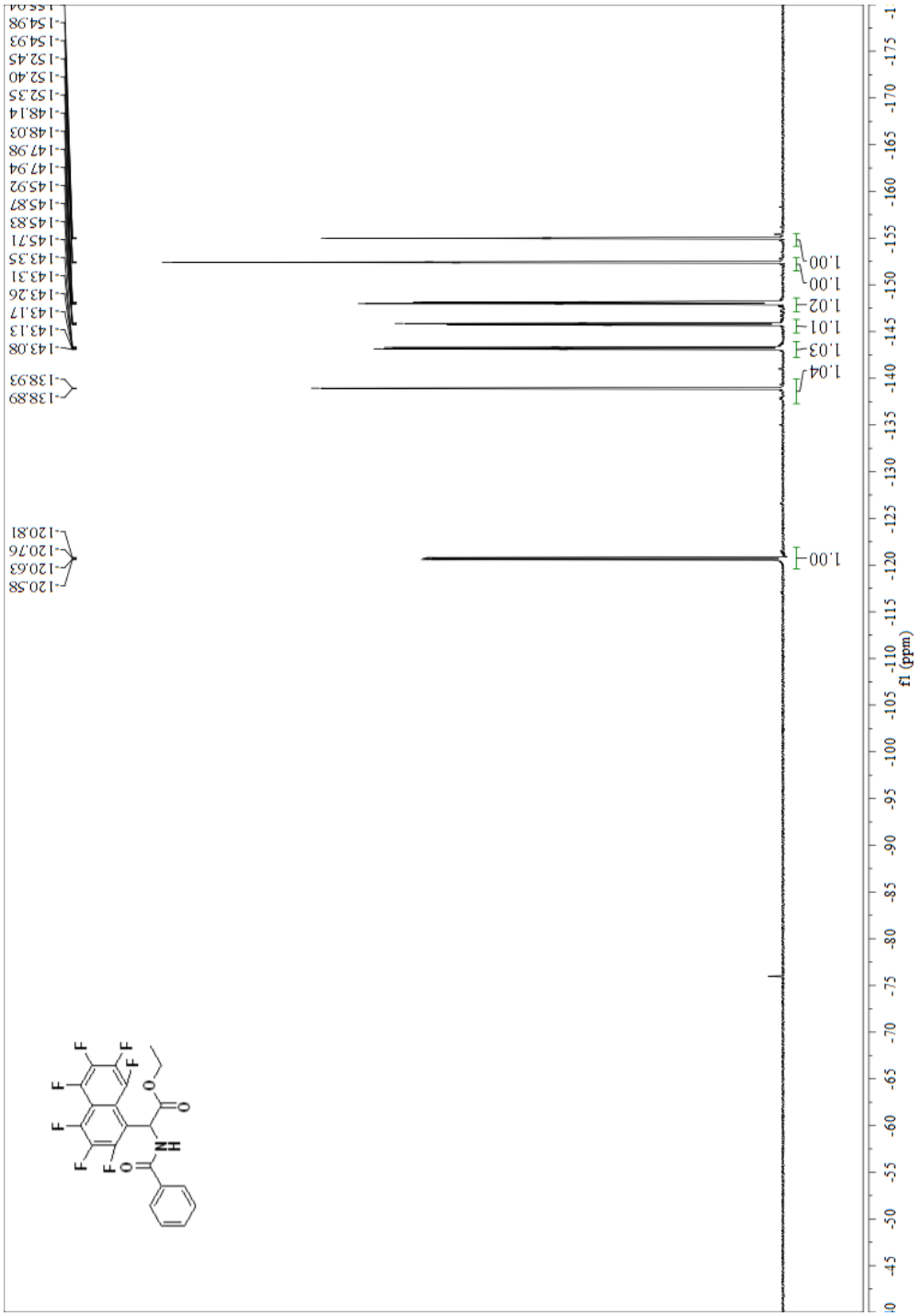

^{13}C NMR (101 MHz, Chloroform-*d*) **2f**

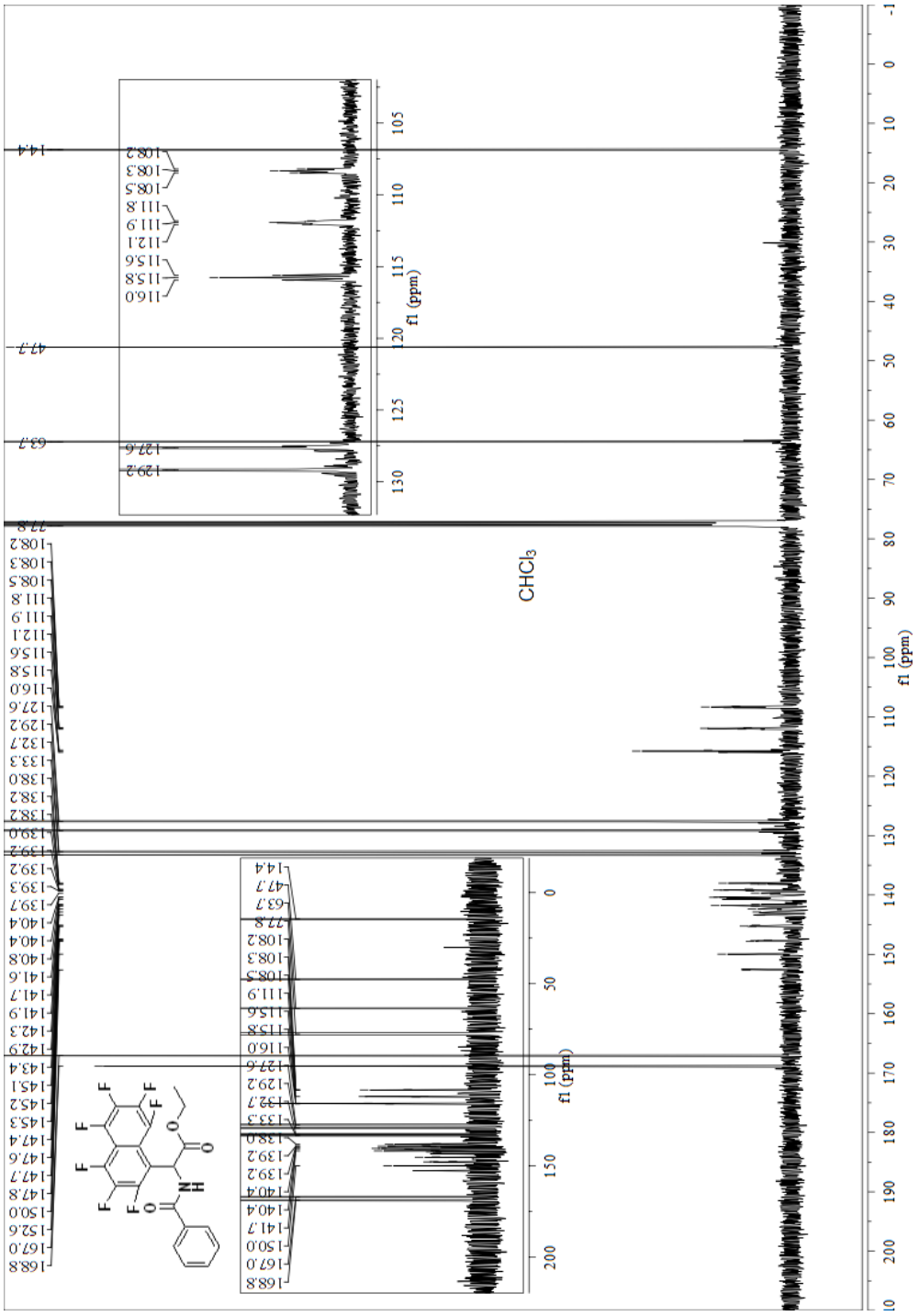

^{1}H NMR (400 MHz, Chloroform-*d*) **2g**

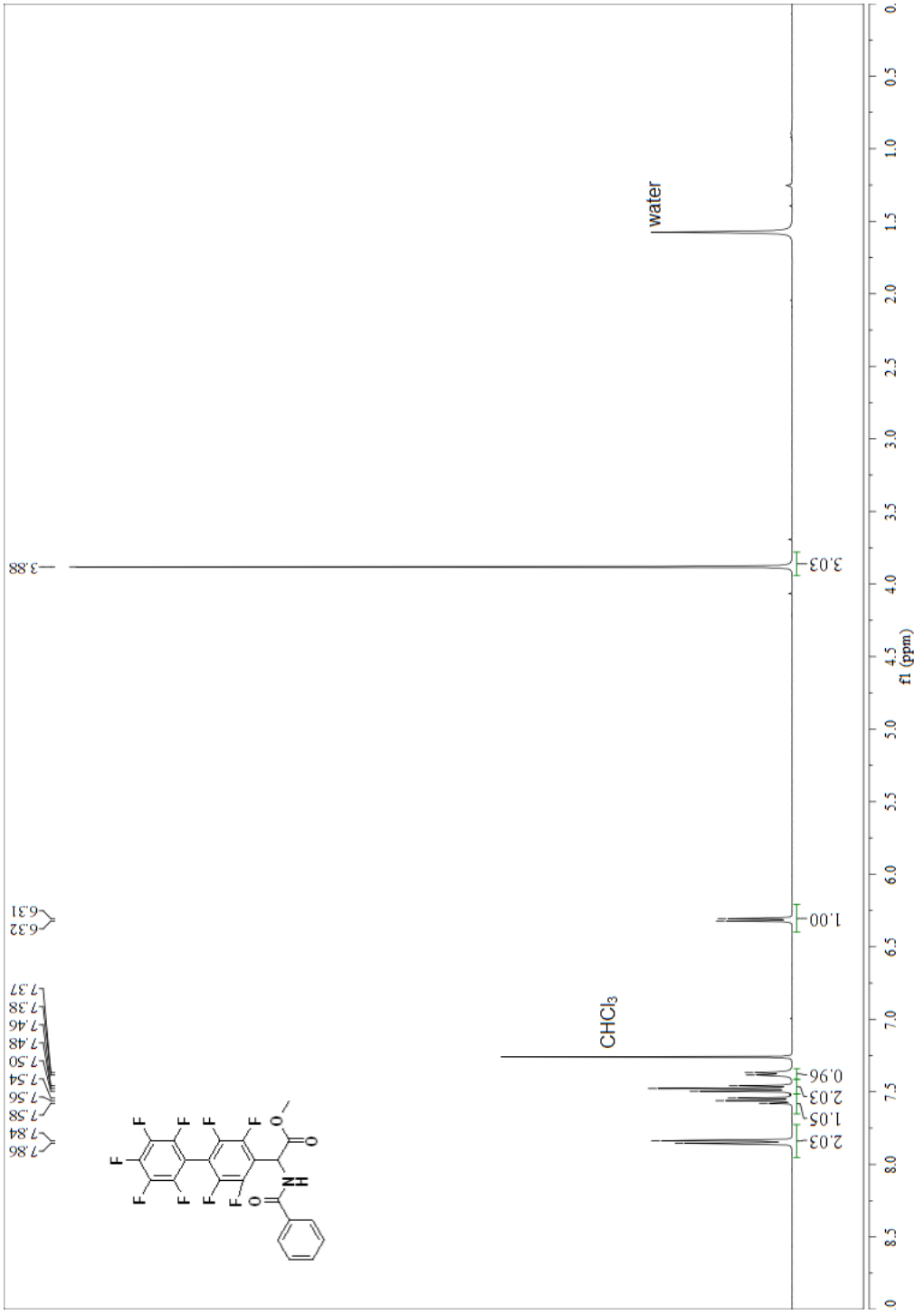

^{19}F NMR (376 MHz, Chloroform-*d*) **2g**

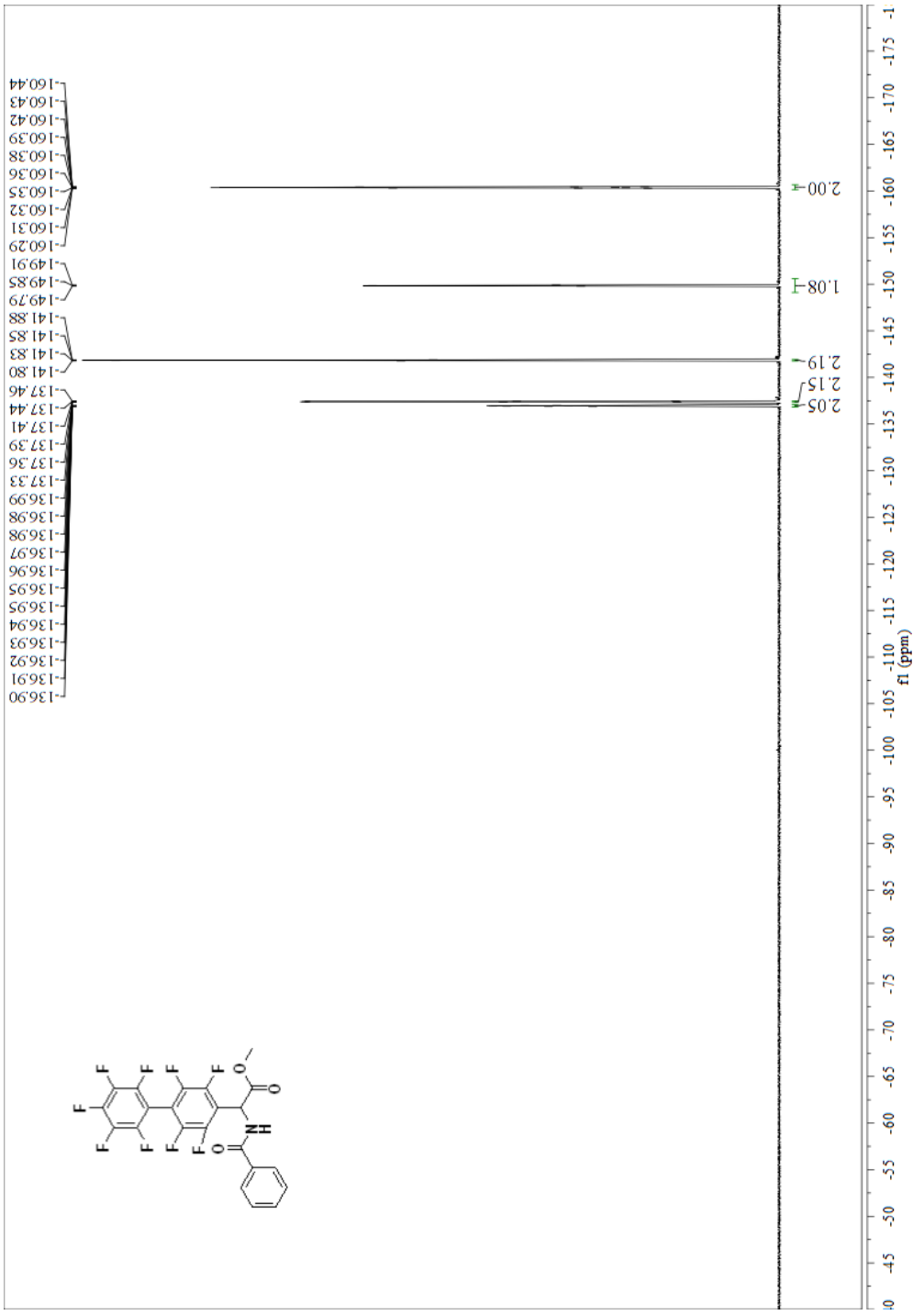

^{13}C NMR (101 MHz, Chloroform-*d* **2g**

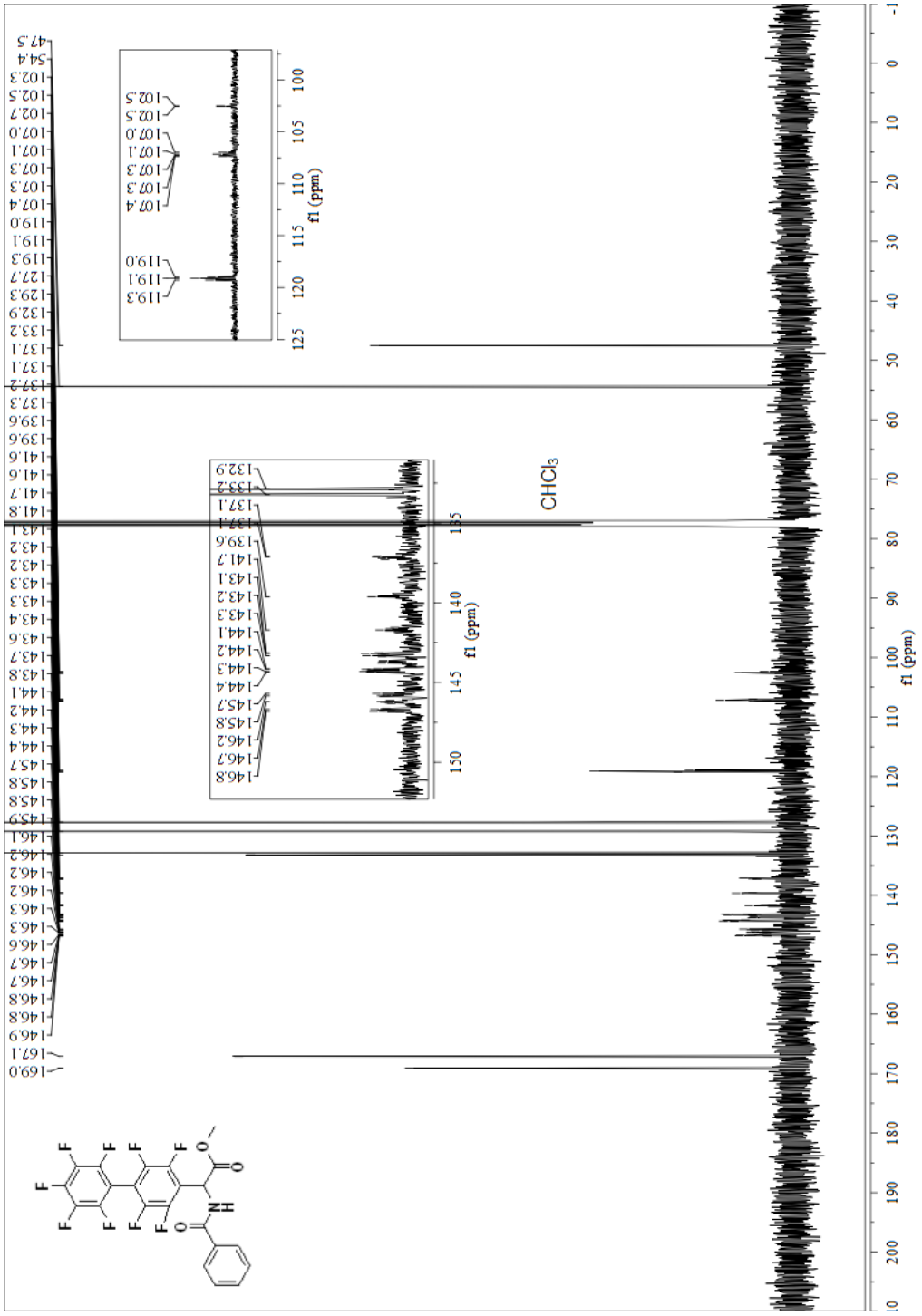

[1]H NMR (400 MHz, Chloroform-*d*) **2h**

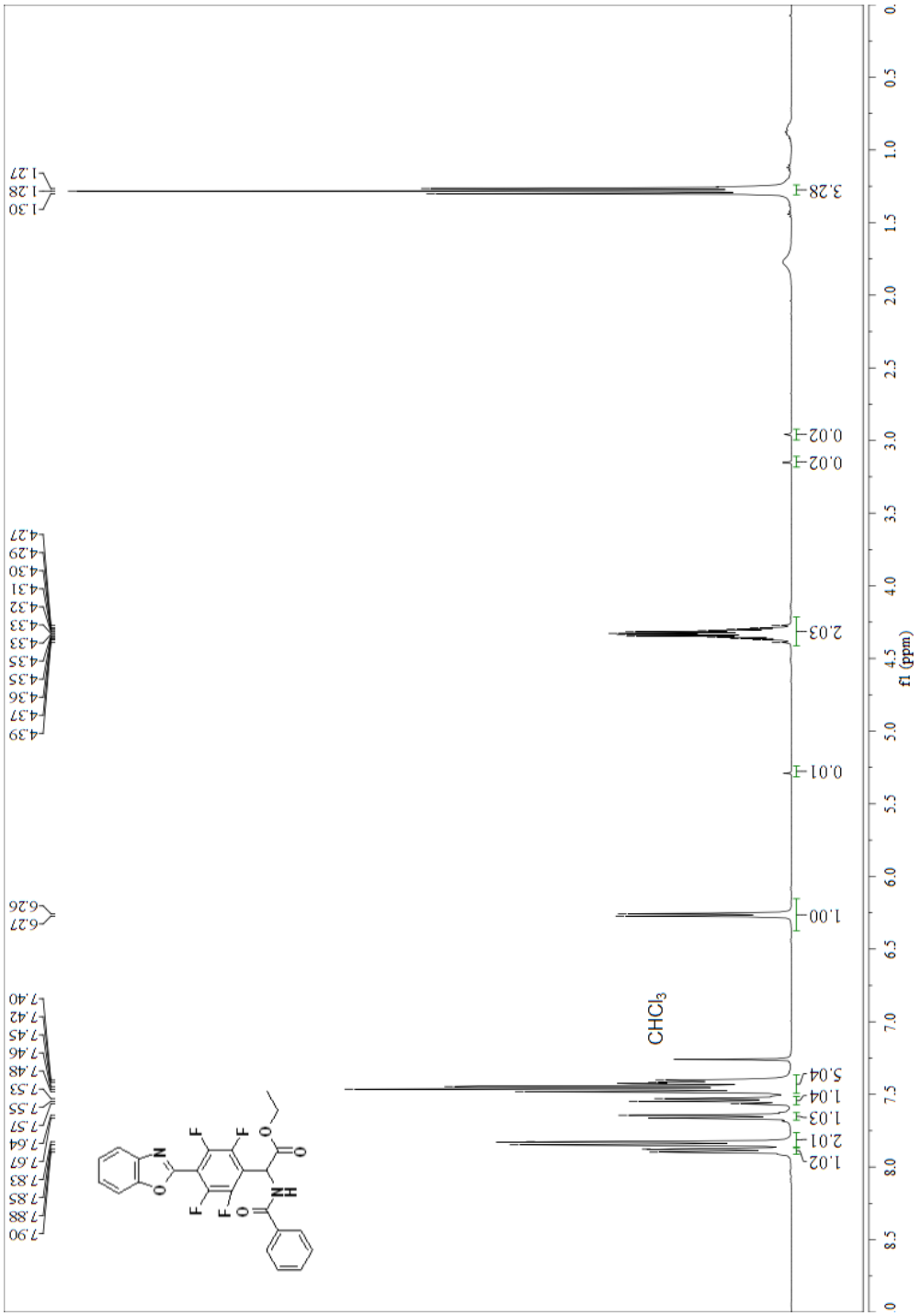

^{19}F NMR (376 MHz, Chloroform-*d*) **2h**

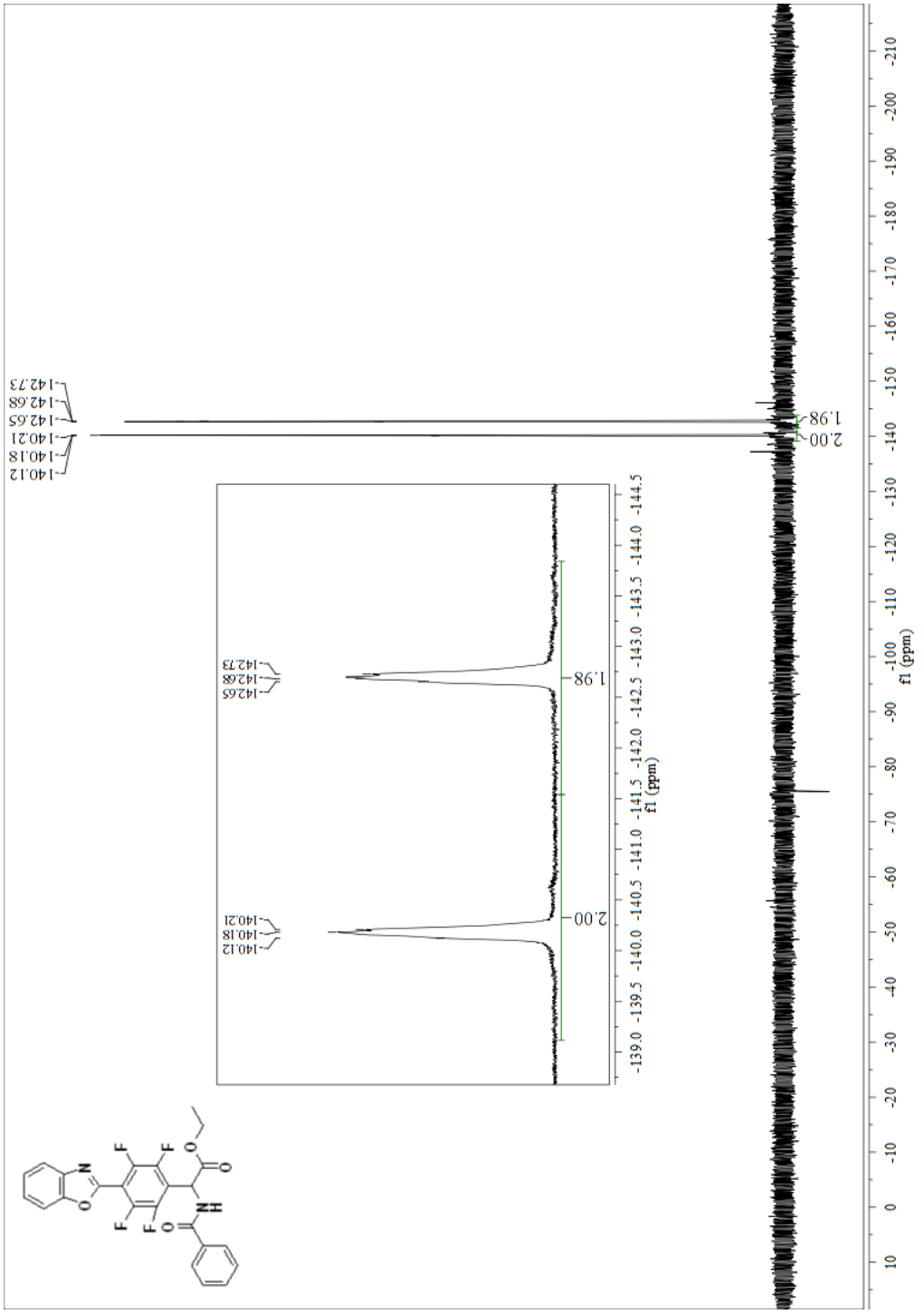

^{13}C NMR (101 MHz, Chloroform-*d*) **2h**

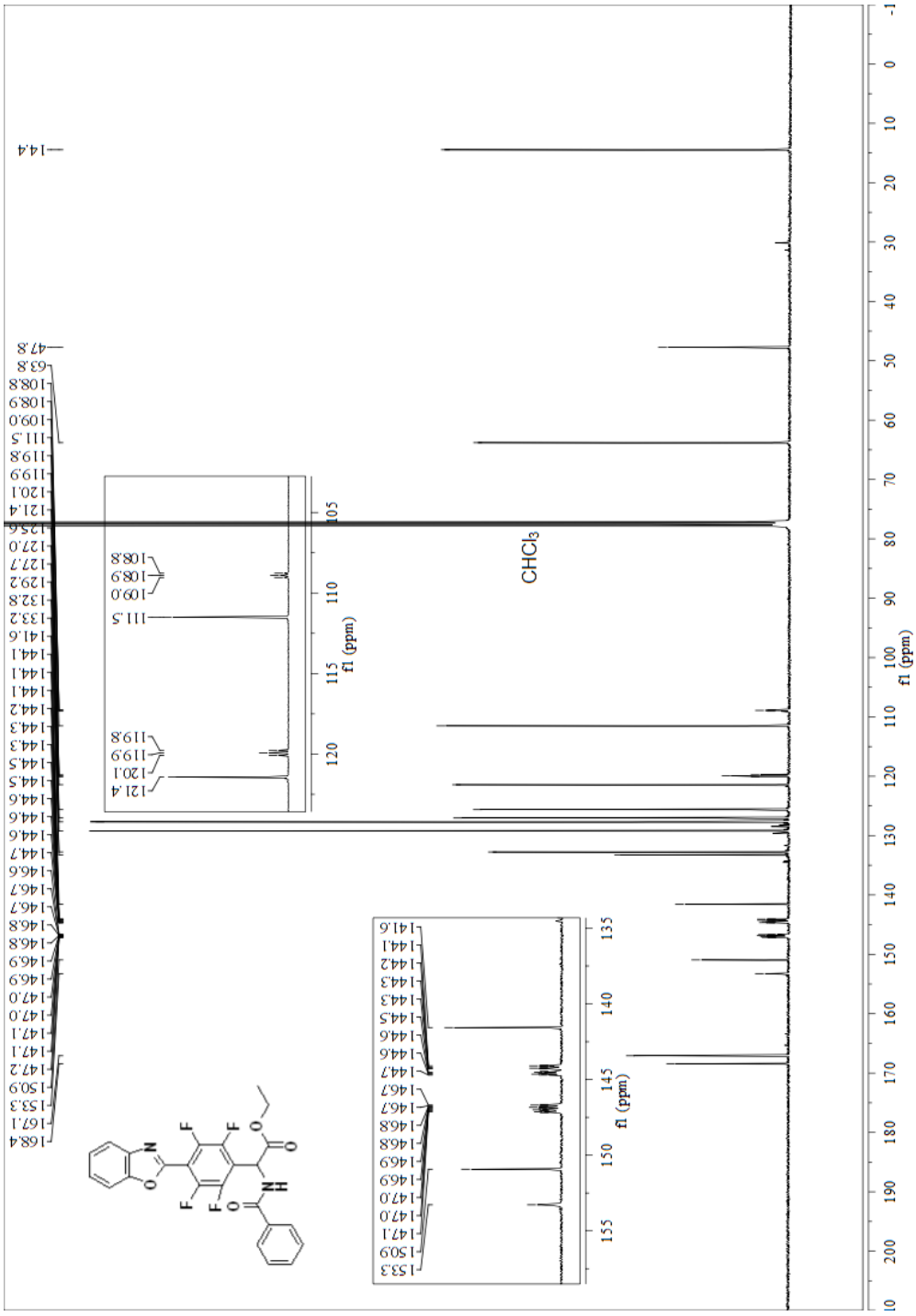

^{1}H NMR (400 MHz, Chloroform-*d*) **2i**

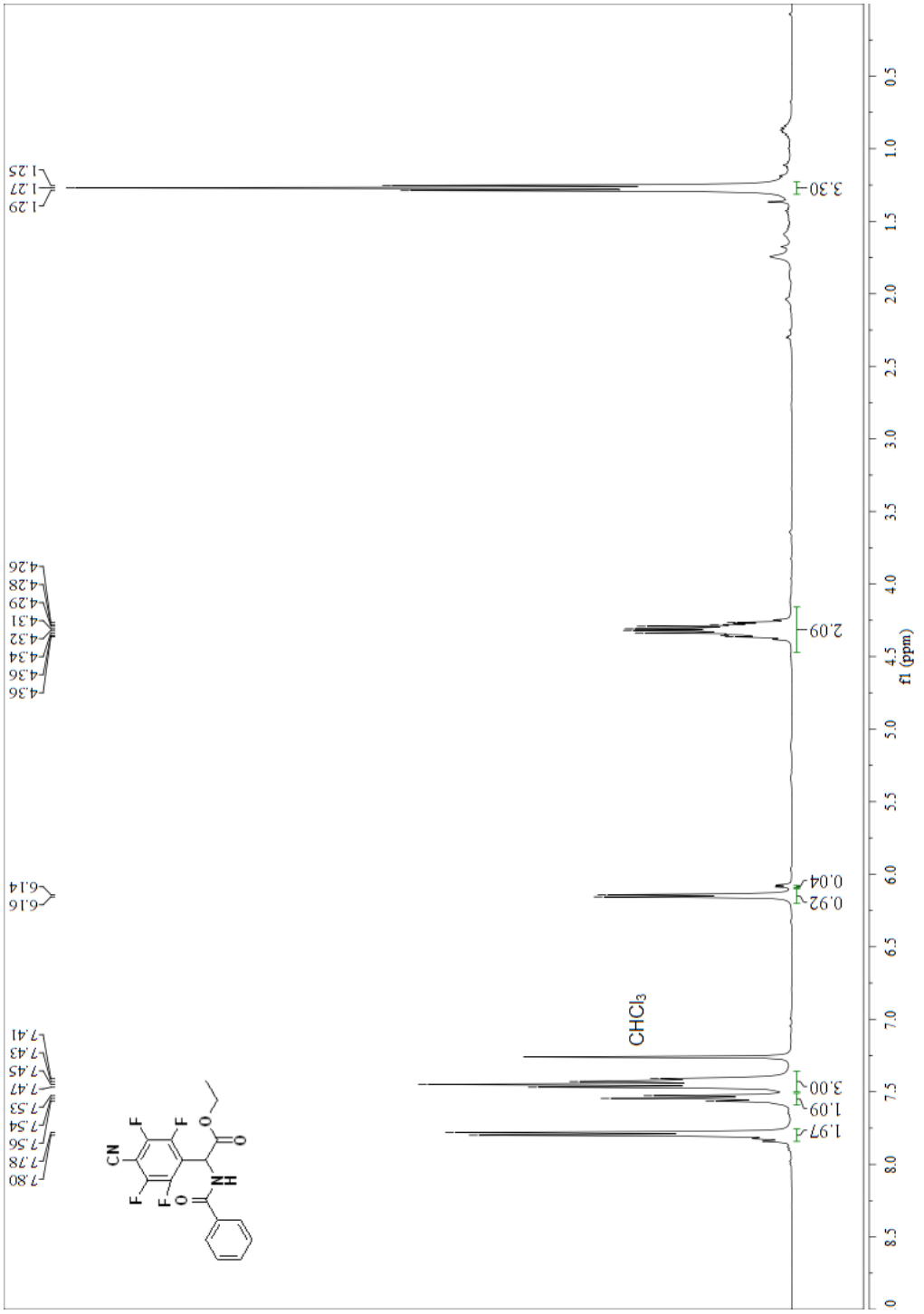

^{19}F NMR (376 MHz, Chloroform-*d*) **2i**

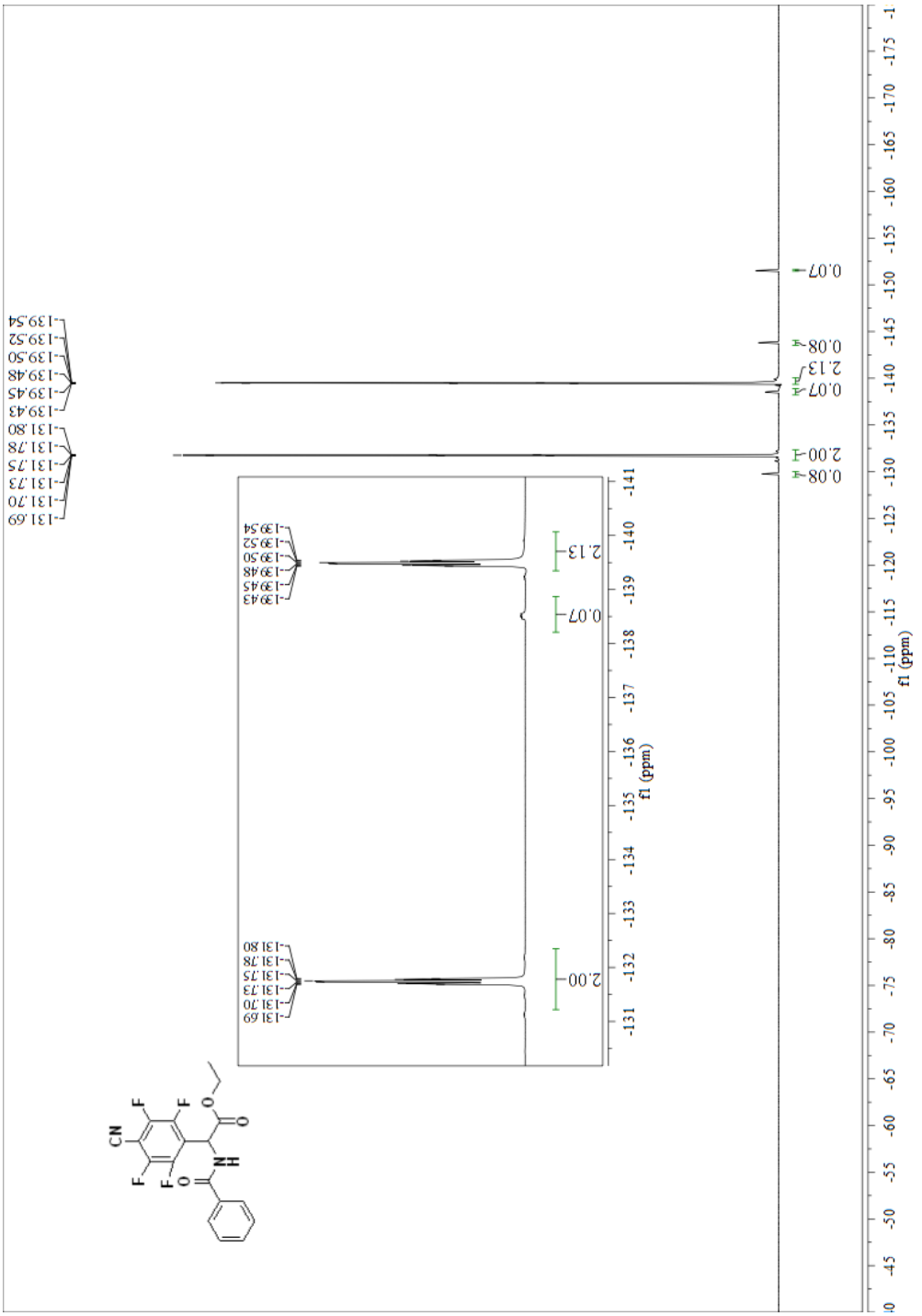

^{13}C NMR (101 MHz, Chloroform-*d*) **2i**

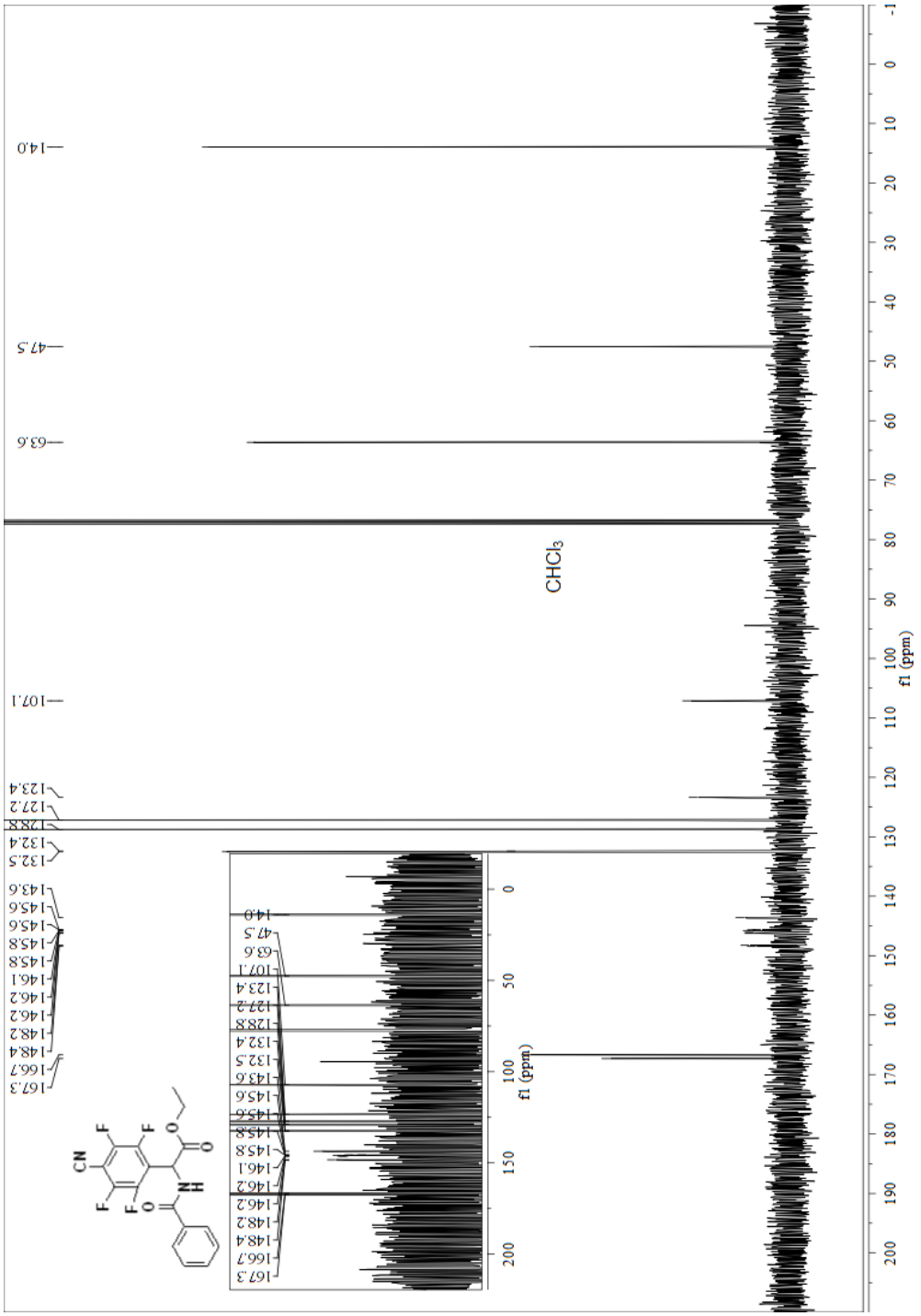

^{1}H NMR (400 MHz, Acetonitrile-d_3) **3a**

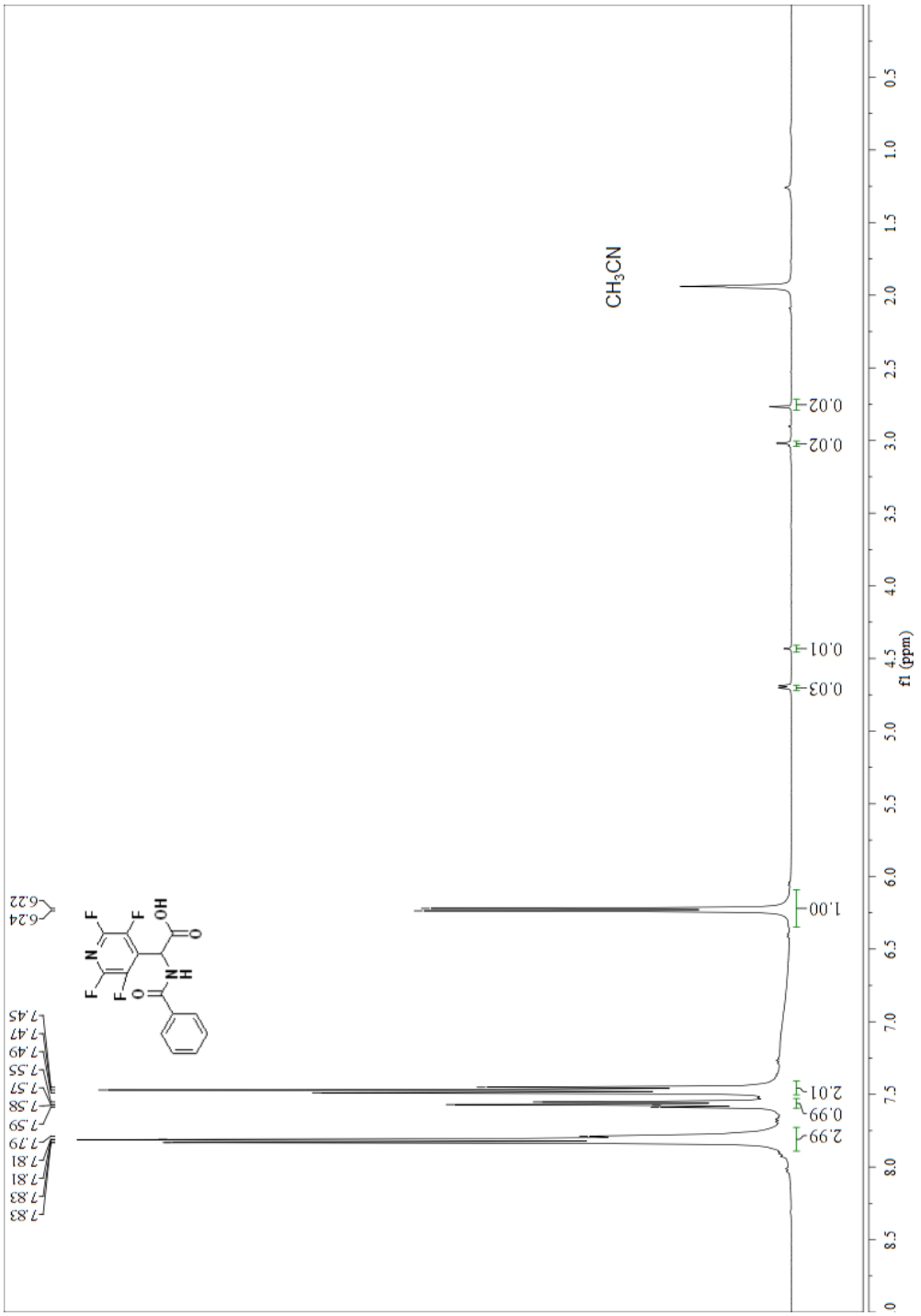

^{19}F NMR (376 MHz, Acetonitrile-d_3) **3a**

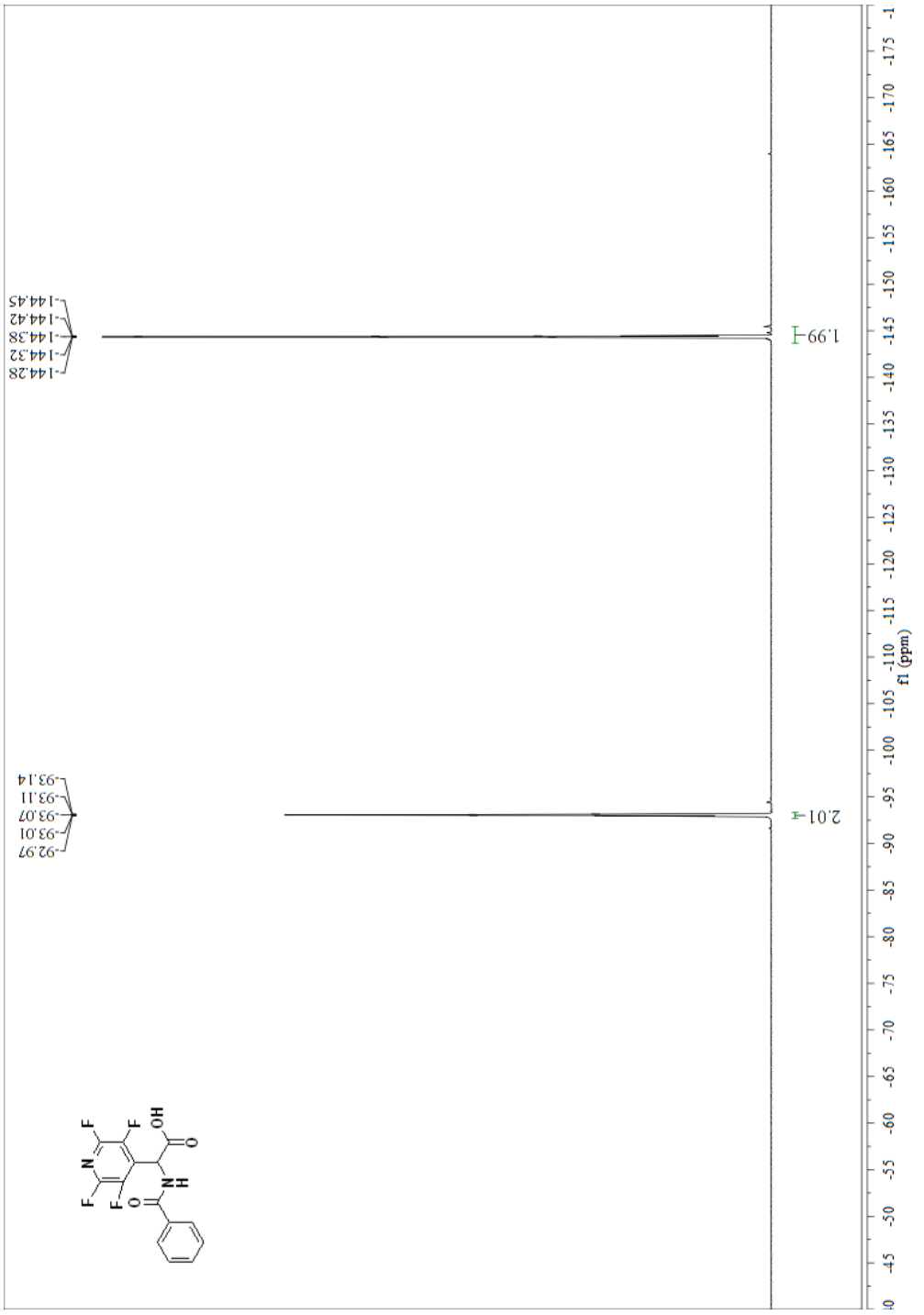

^{13}C NMR (101 MHz, Acetonitrile-d_3) **3a**

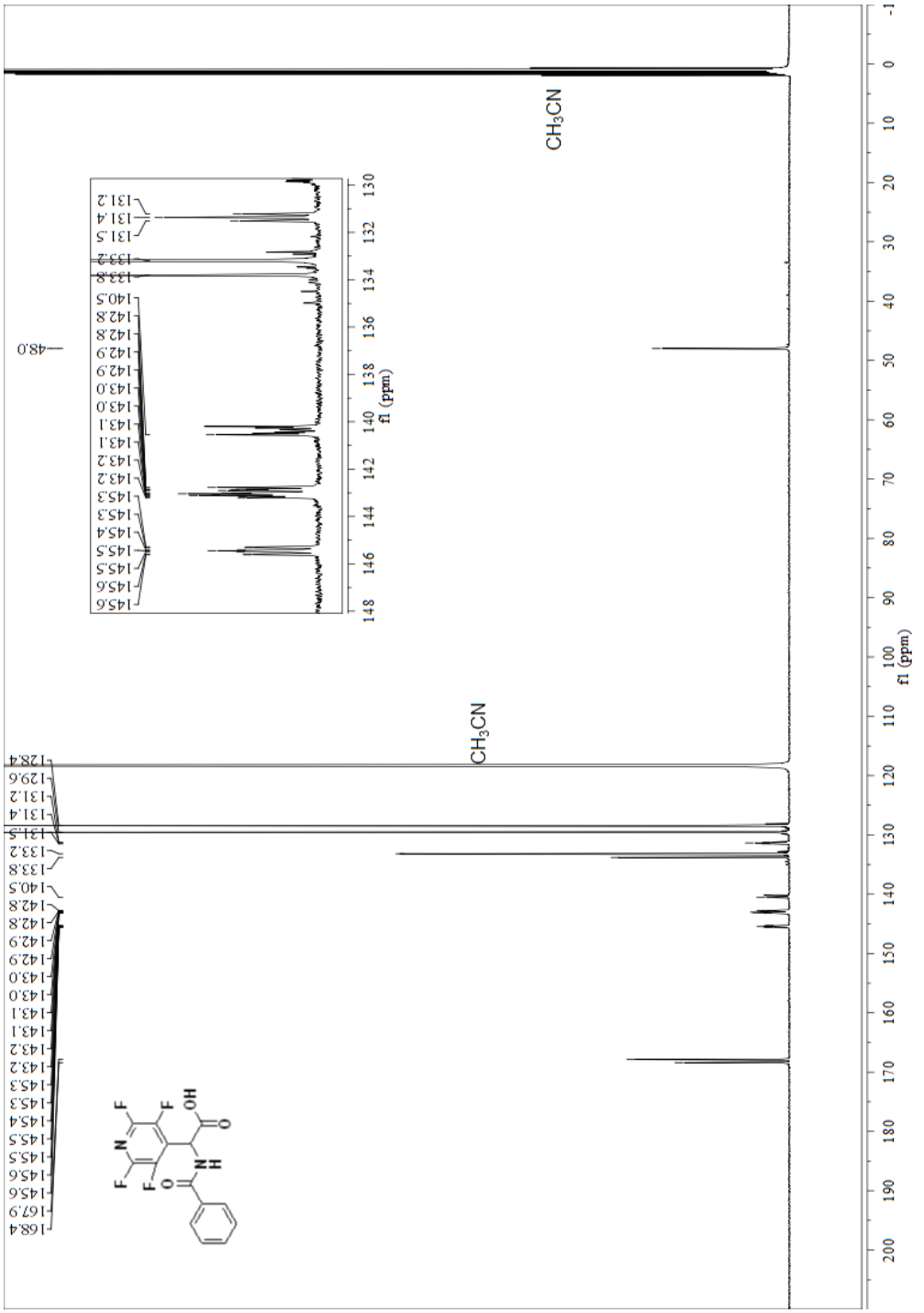

^{1}H NMR (400 MHz, Acetonitrile-d_3) **3b**

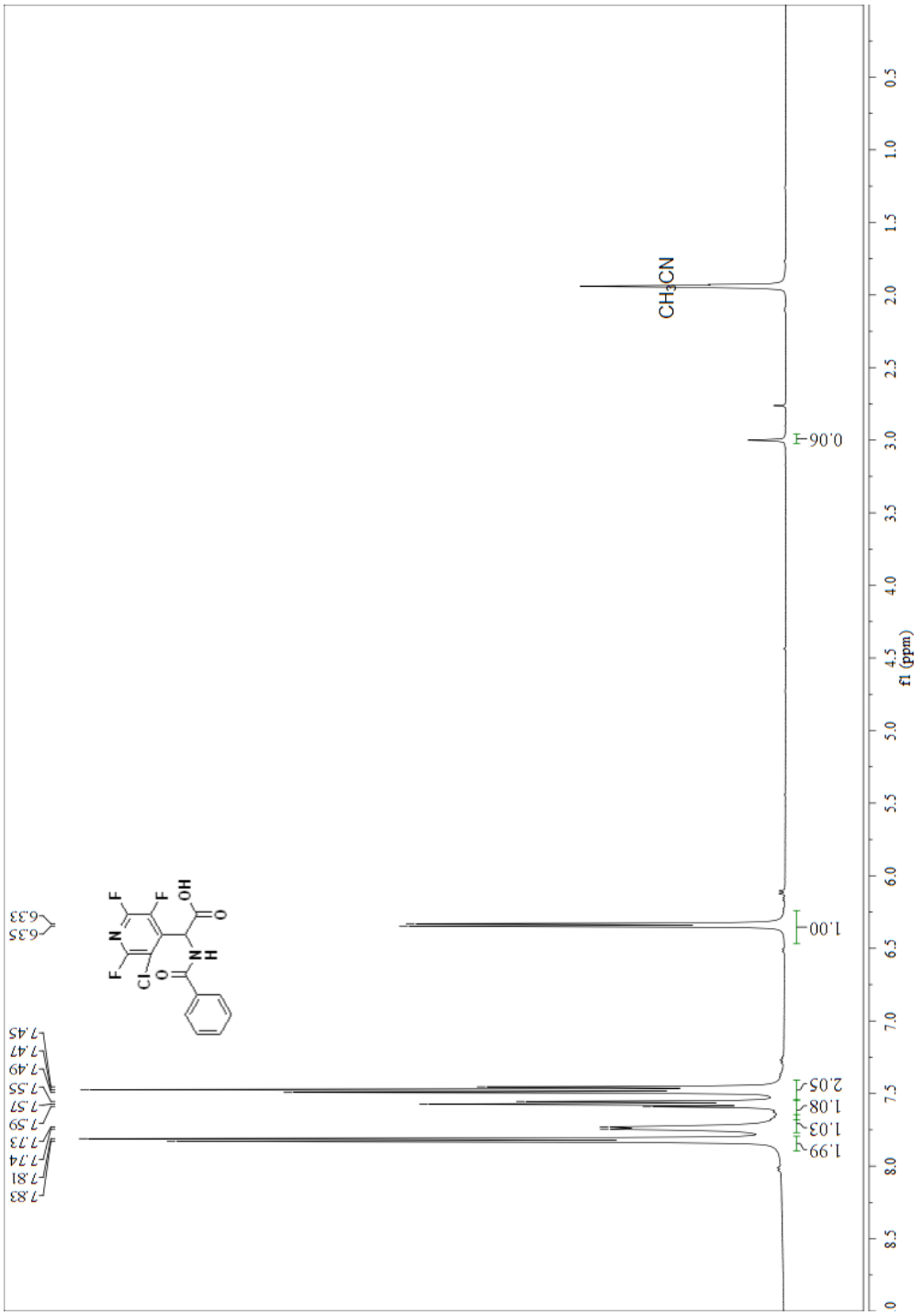

^{19}F NMR (376 MHz, Acetonitrile-d_3) **3b**

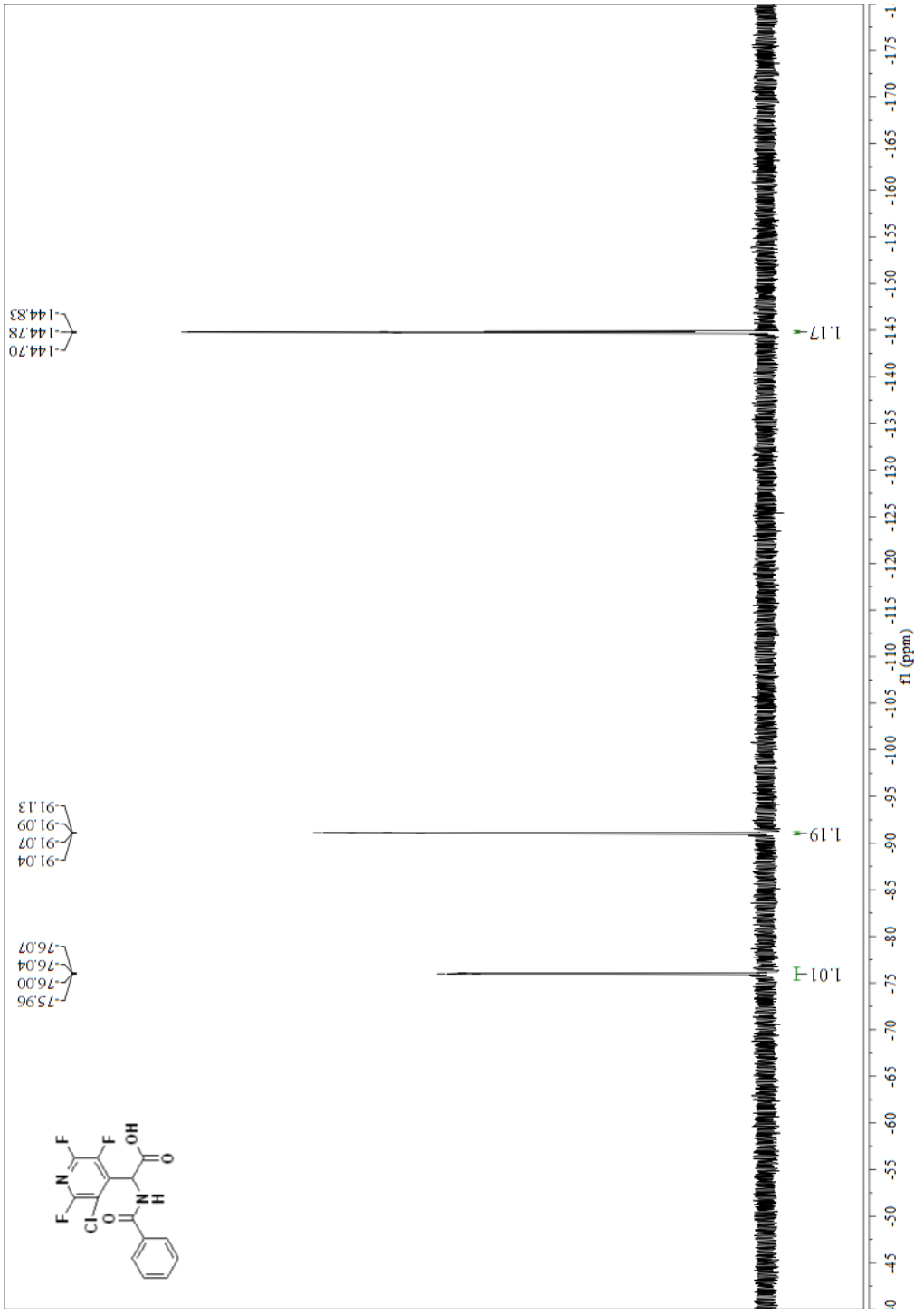

^{13}C NMR (101 MHz, Acetonitrile-d_3) **3b**

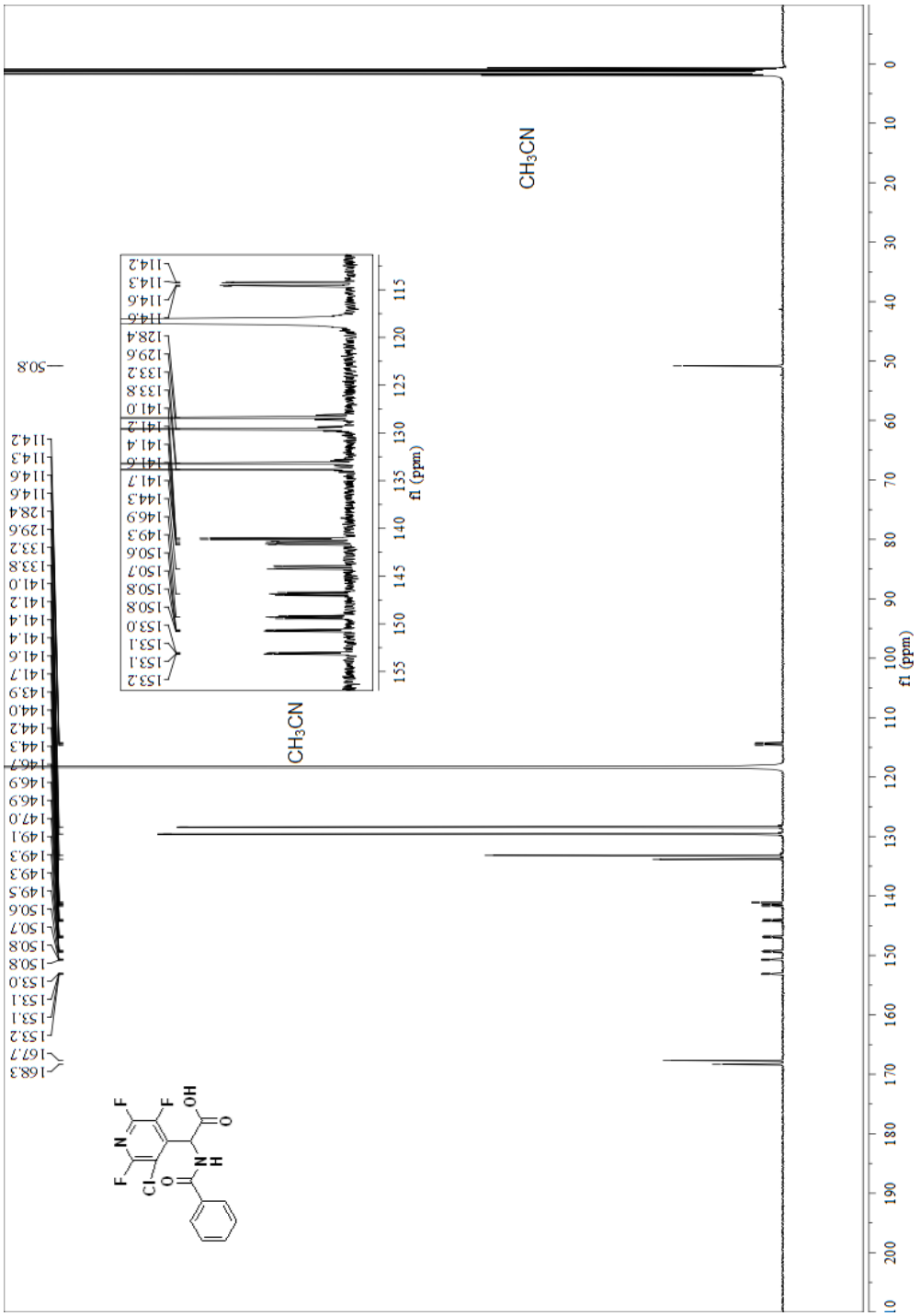

^{1}H NMR (400 MHz, Acetonitrile-d_3) **3c**

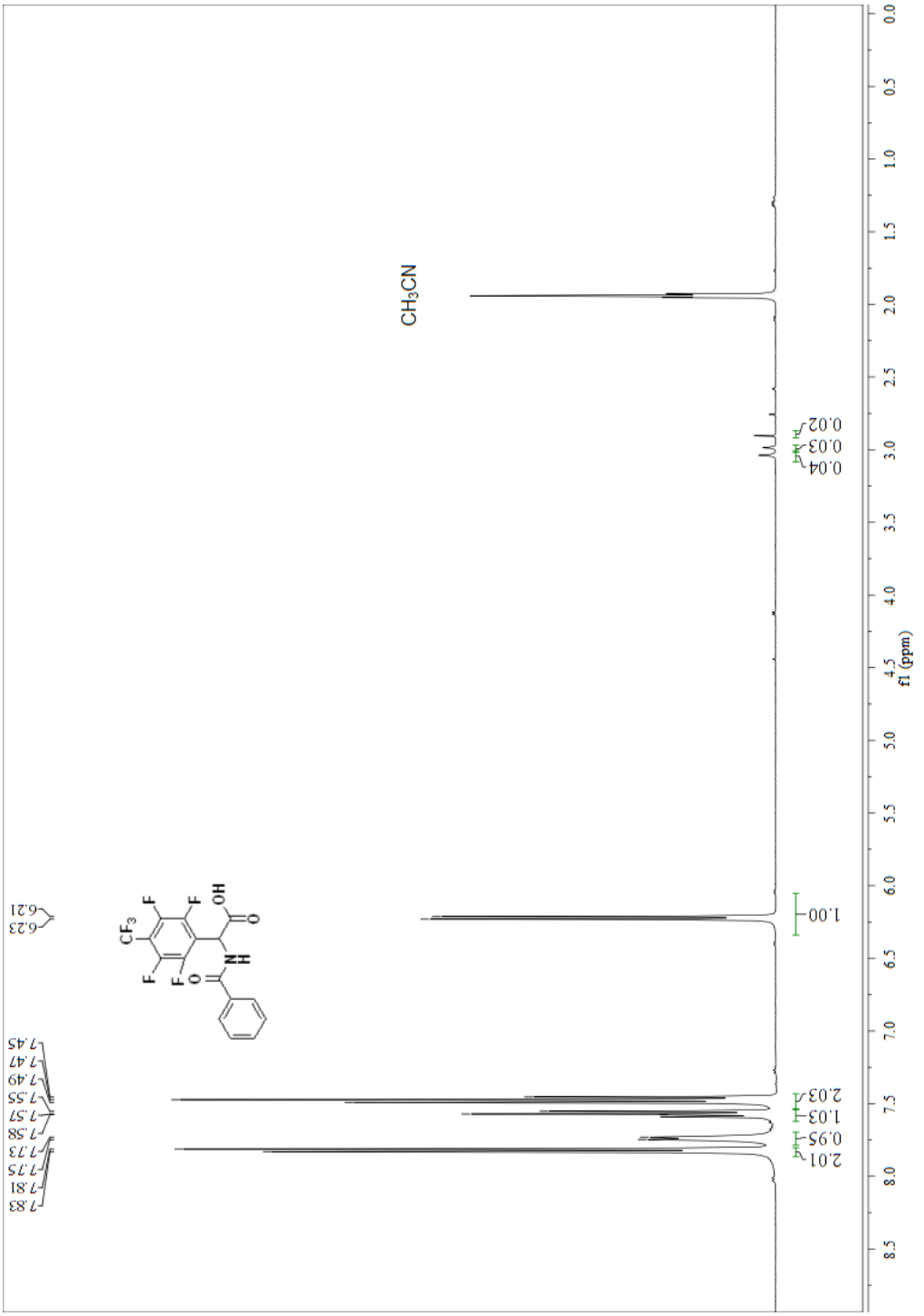

^{19}F NMR (376 MHz, Acetonitrile-d_3) **3c**

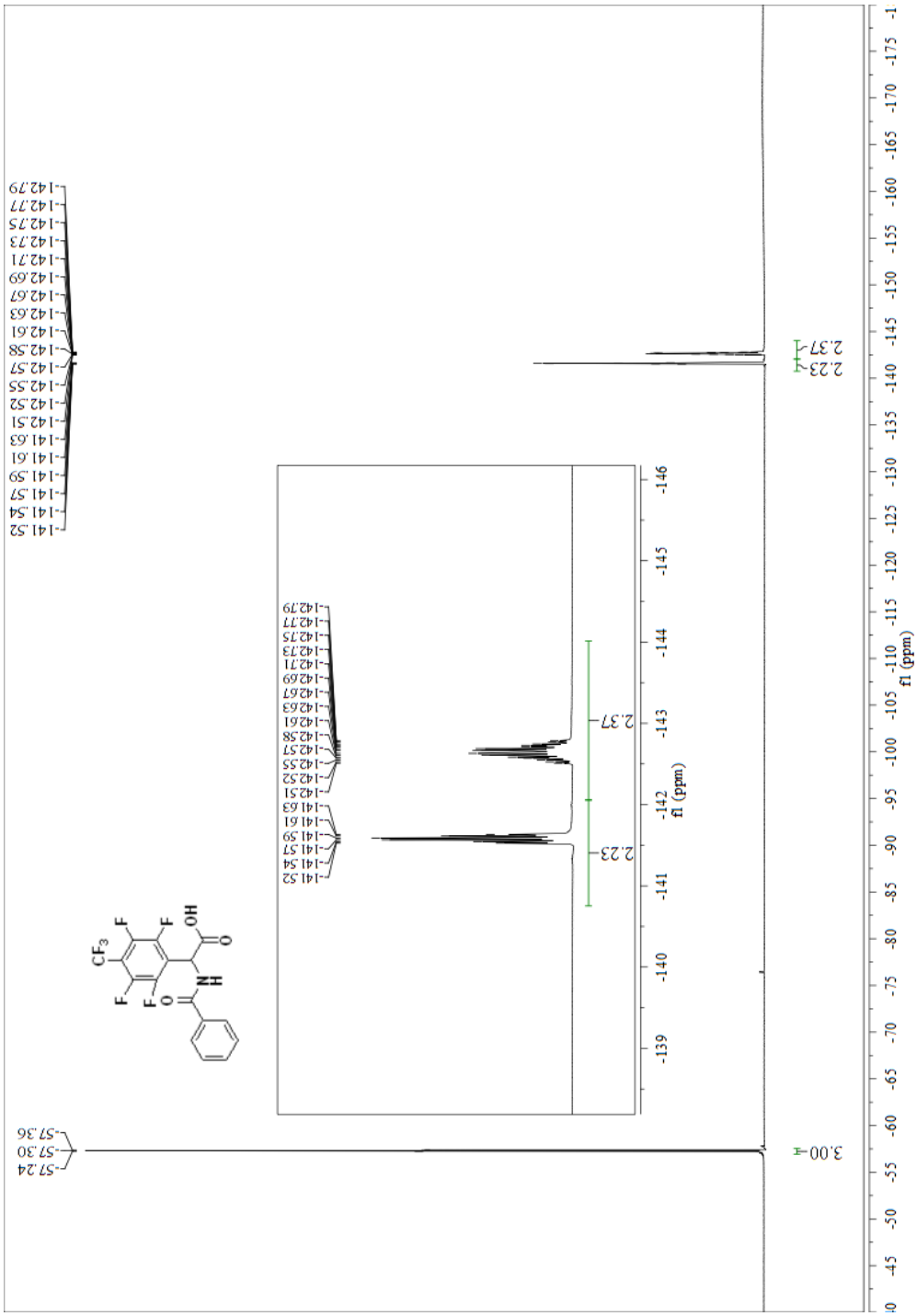

^{13}C NMR (101 MHz, Acetonitrile-d_3) **3c**

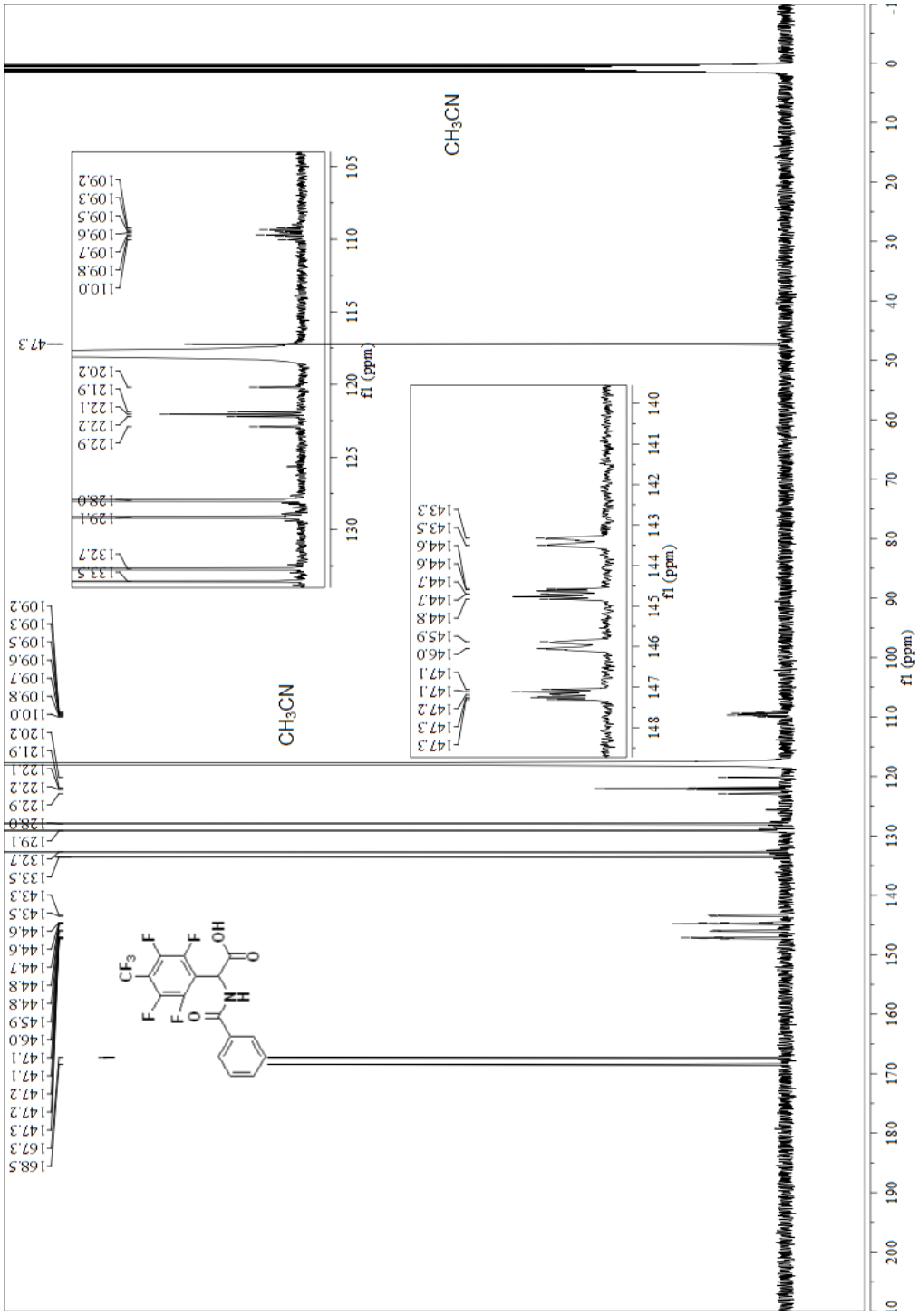

^{1}H NMR (400 MHz, Acetonitrile-d_3) **3d**

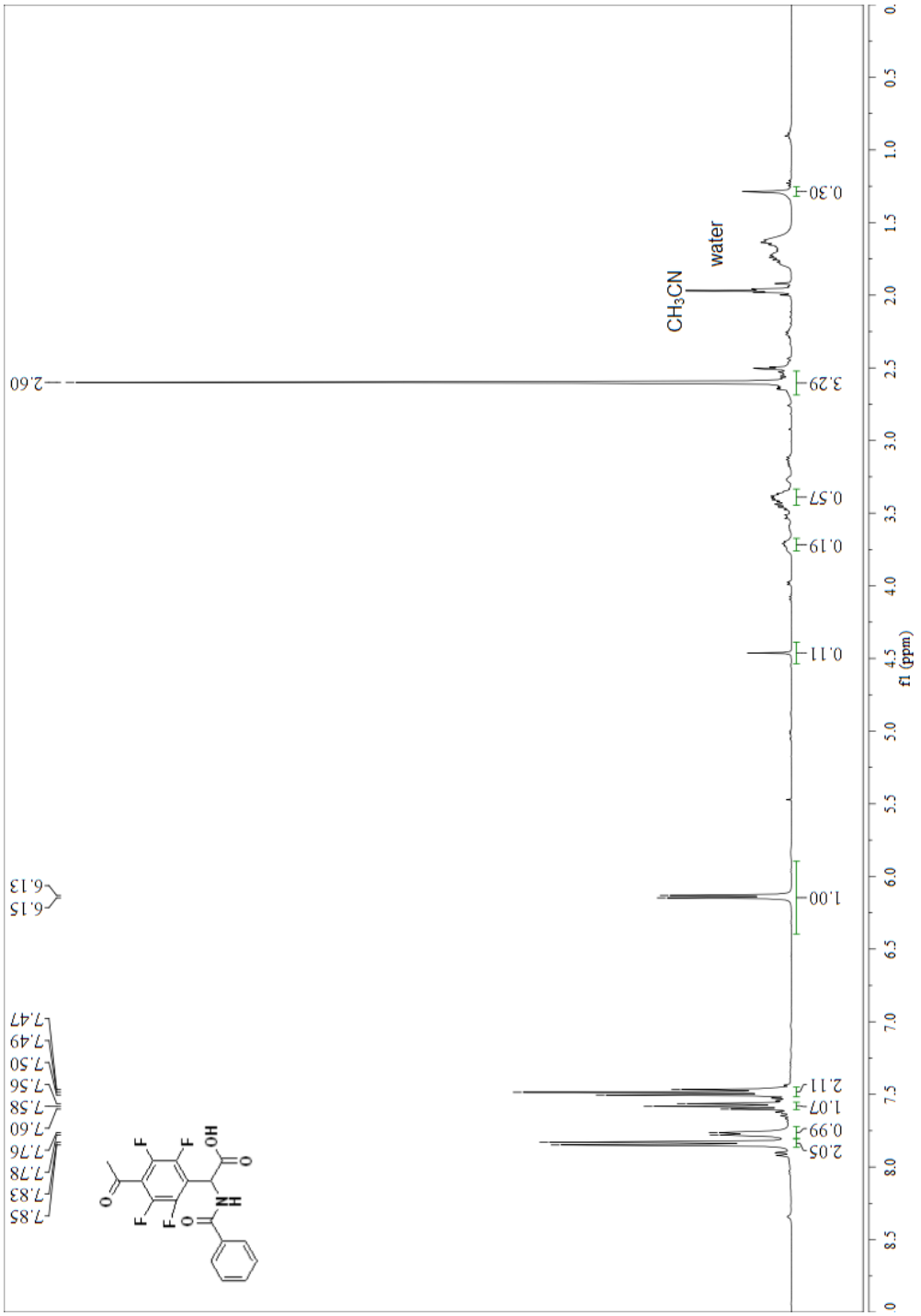

^{19}F NMR (376 MHz, Acetonitrile-d_3) **3d**

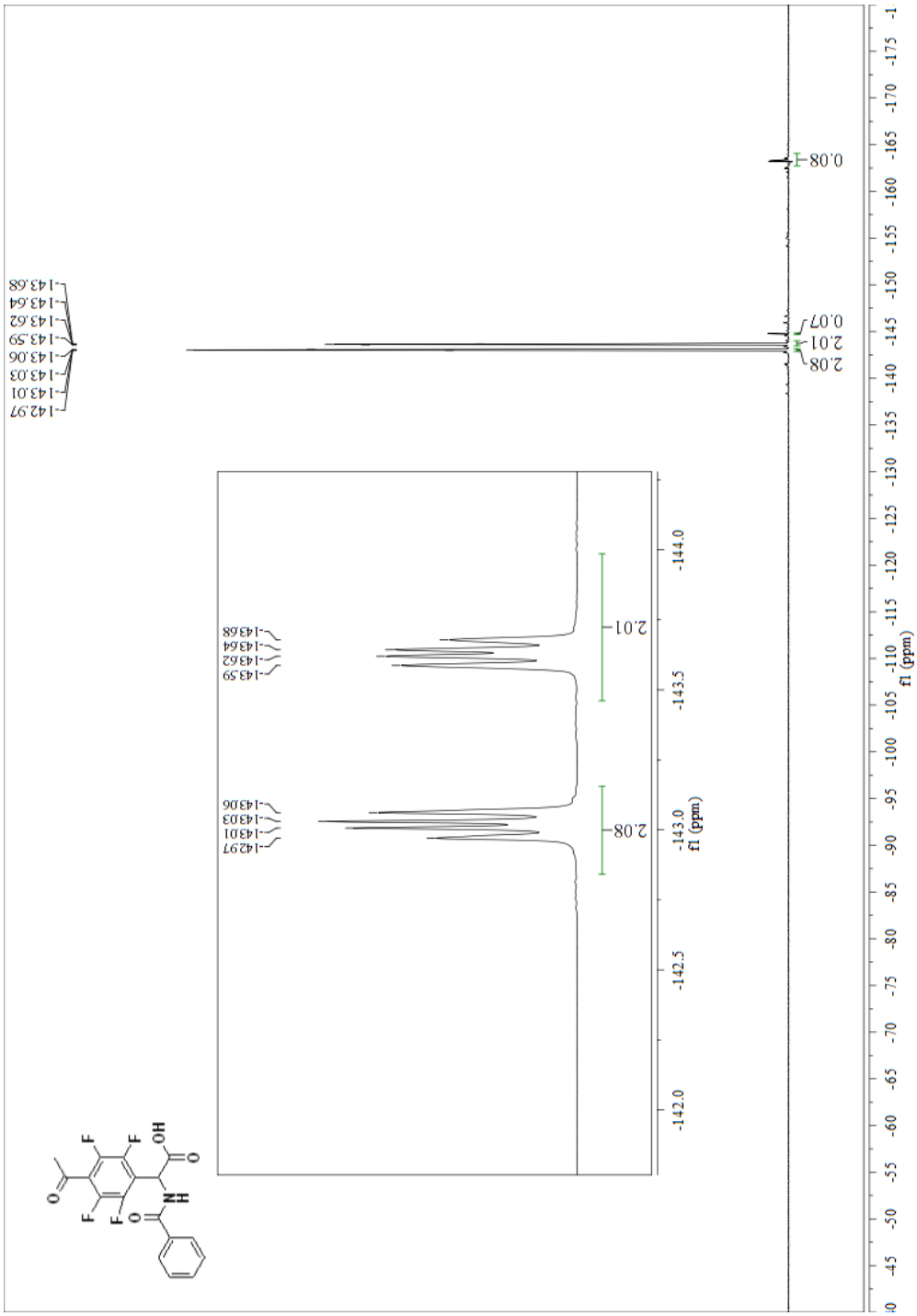

^{13}C NMR (101 MHz, Acetonitrile-d_3) **3d**

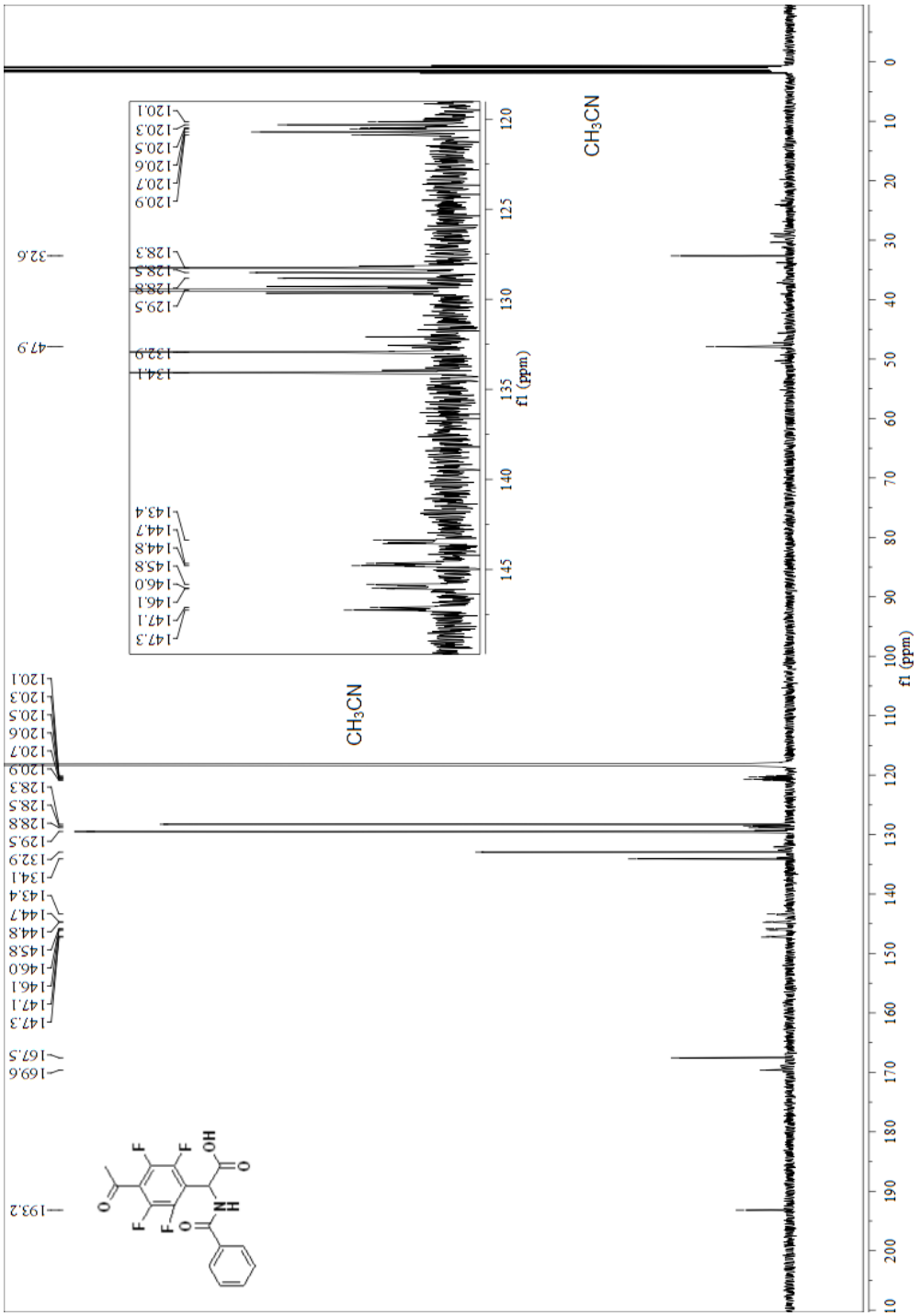

^{1}H NMR (400 MHz, Acetonitrile-d_3) **3e**

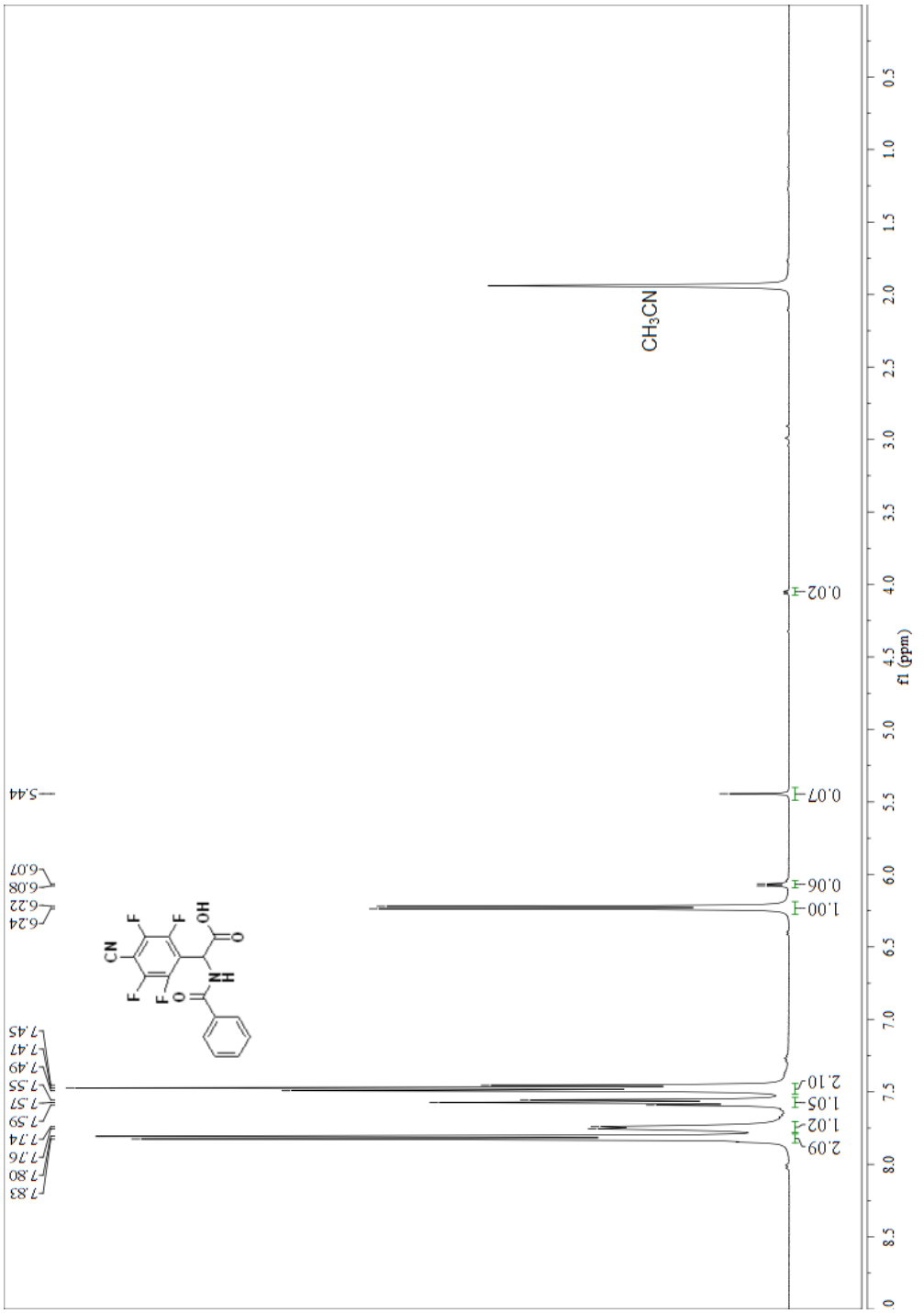

^{19}F NMR (376 MHz, Acetonitrile-d_3) **3e**

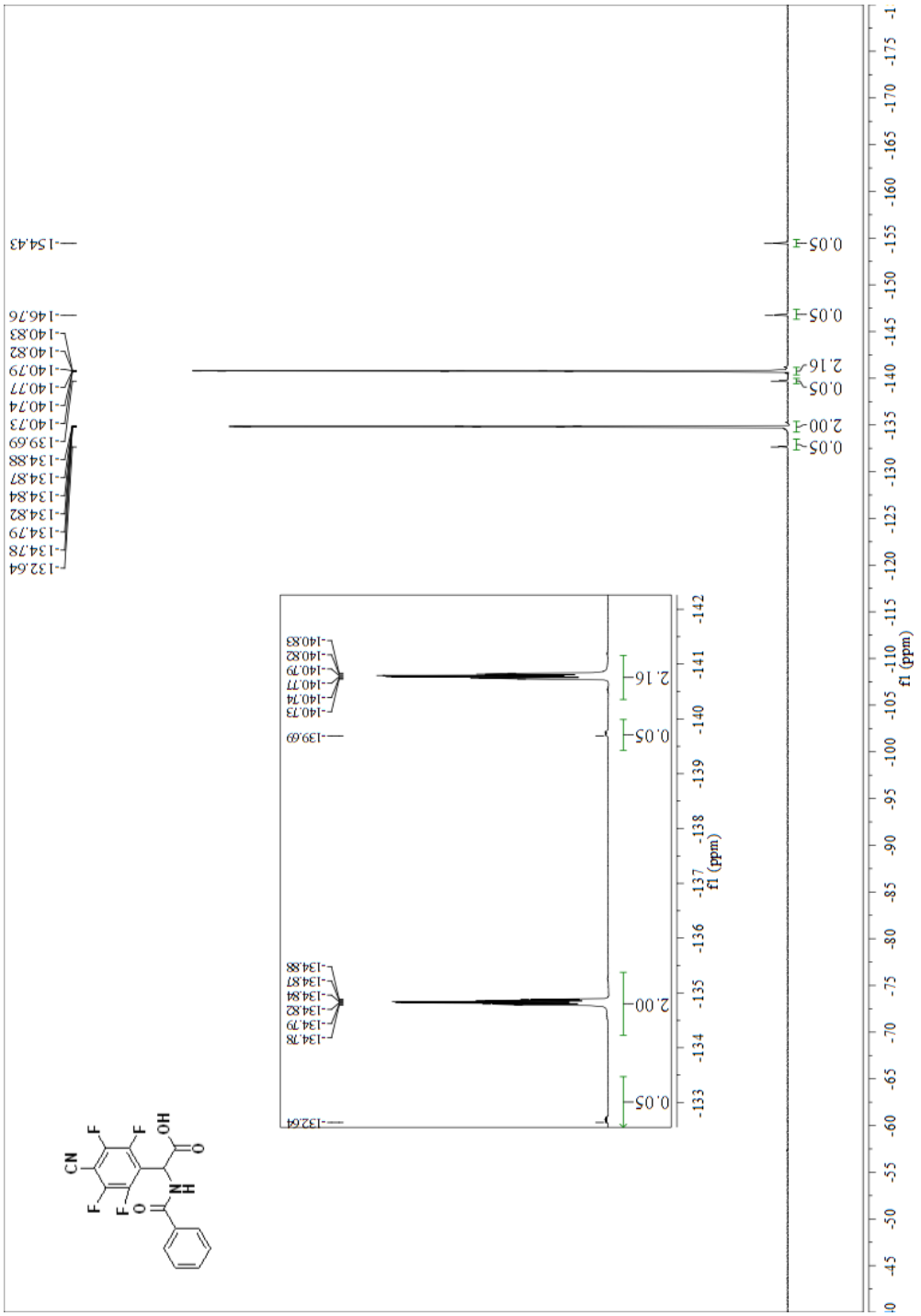

^{13}C NMR (101 MHz, Acetonitrile-d_3) **3e**

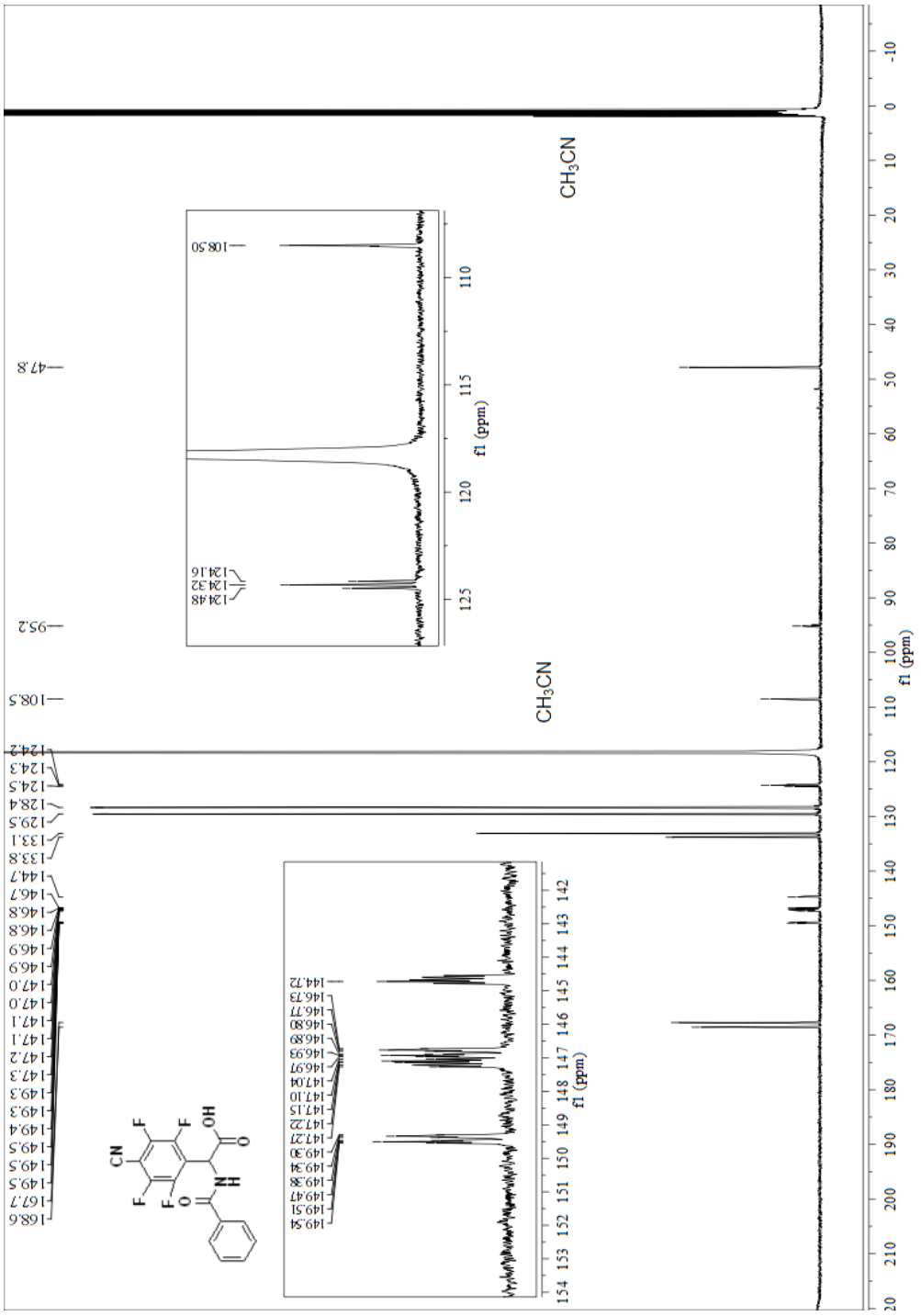

^{1}H NMR (400 MHz, D_2O) **4a**

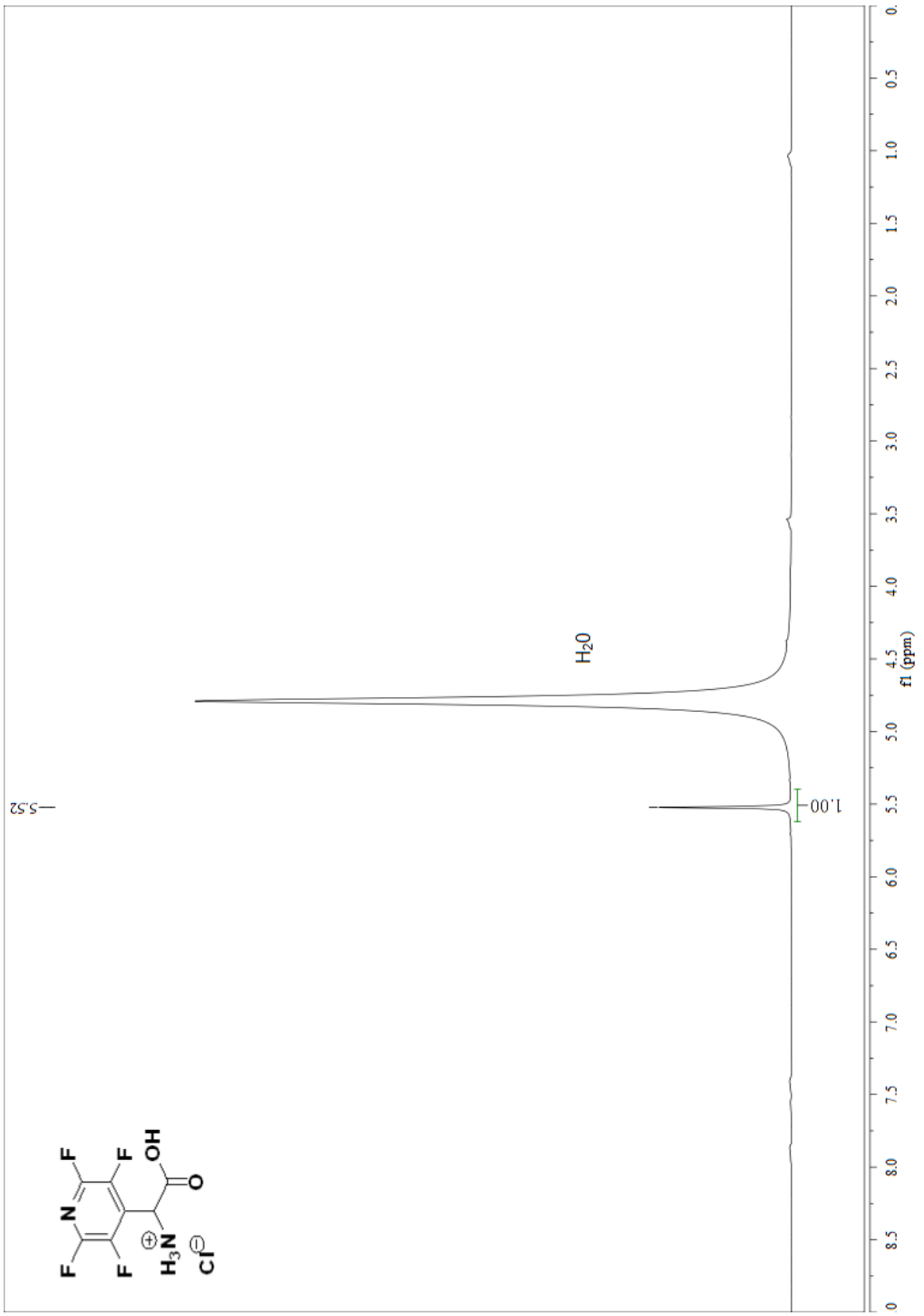

^{19}F NMR (376 MHz, D_2O) **4a**

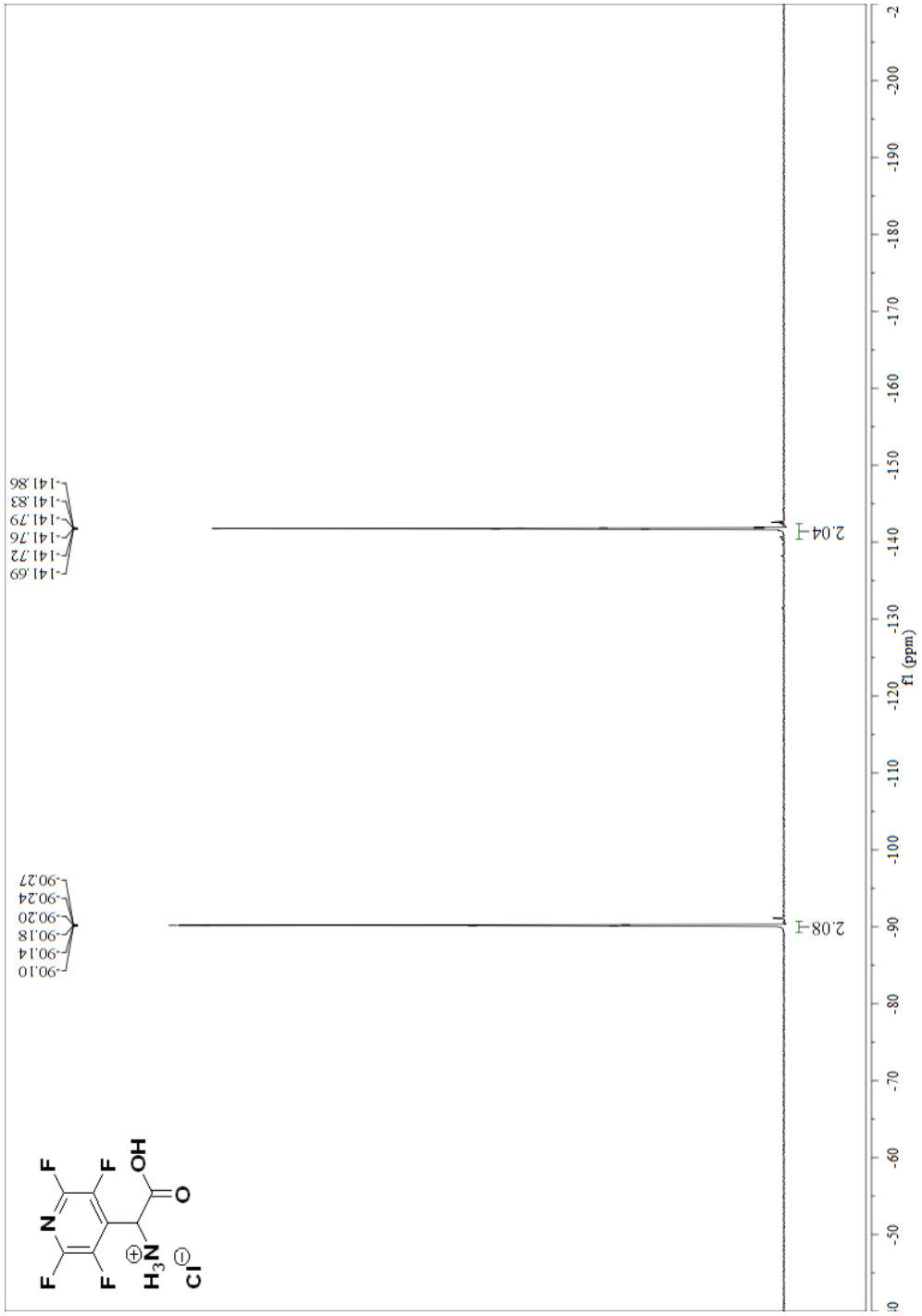

^{13}C NMR (101 MHz, D_2O) **4a**

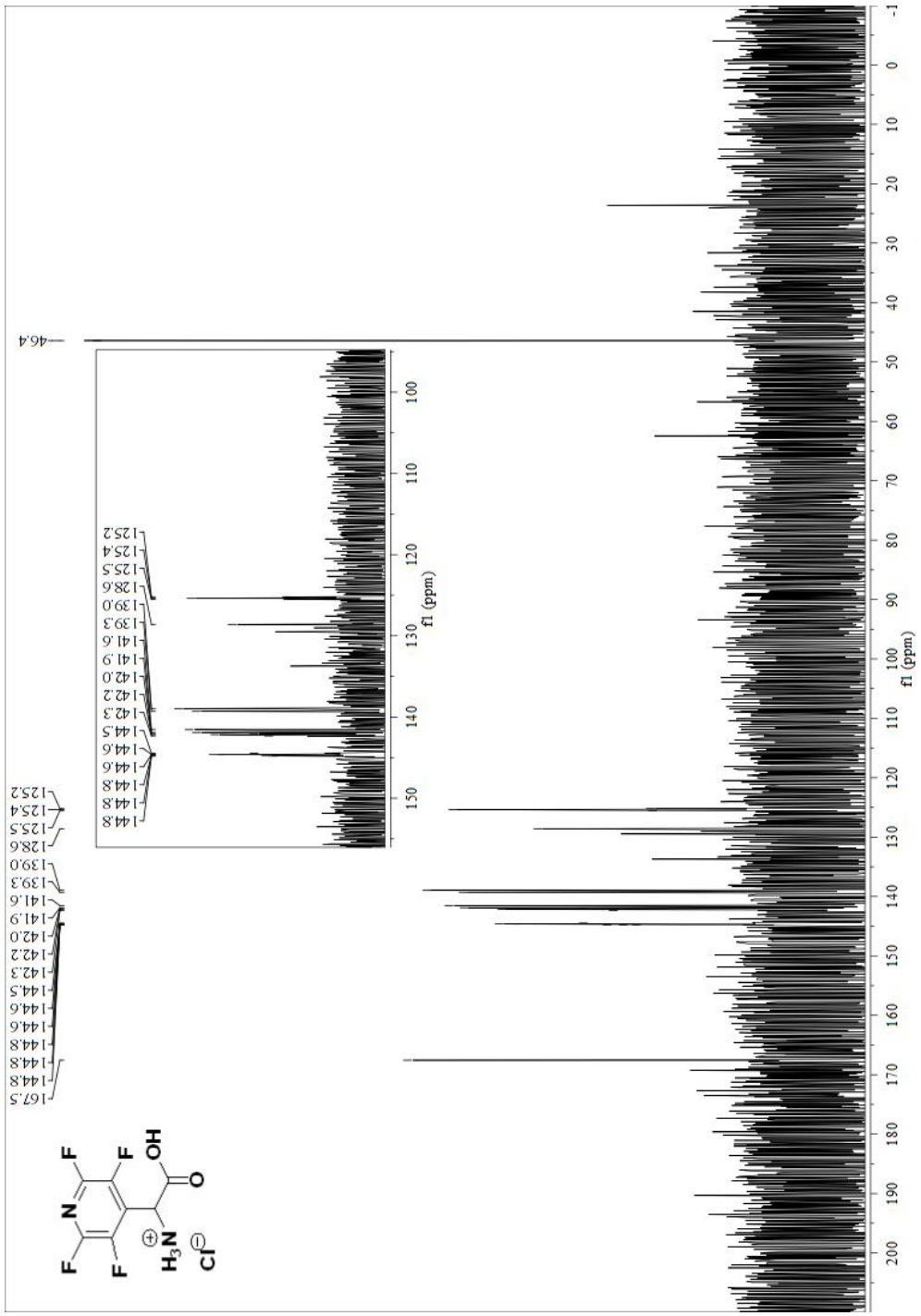

^{1}H NMR (400 MHz, D_2O) **4b**

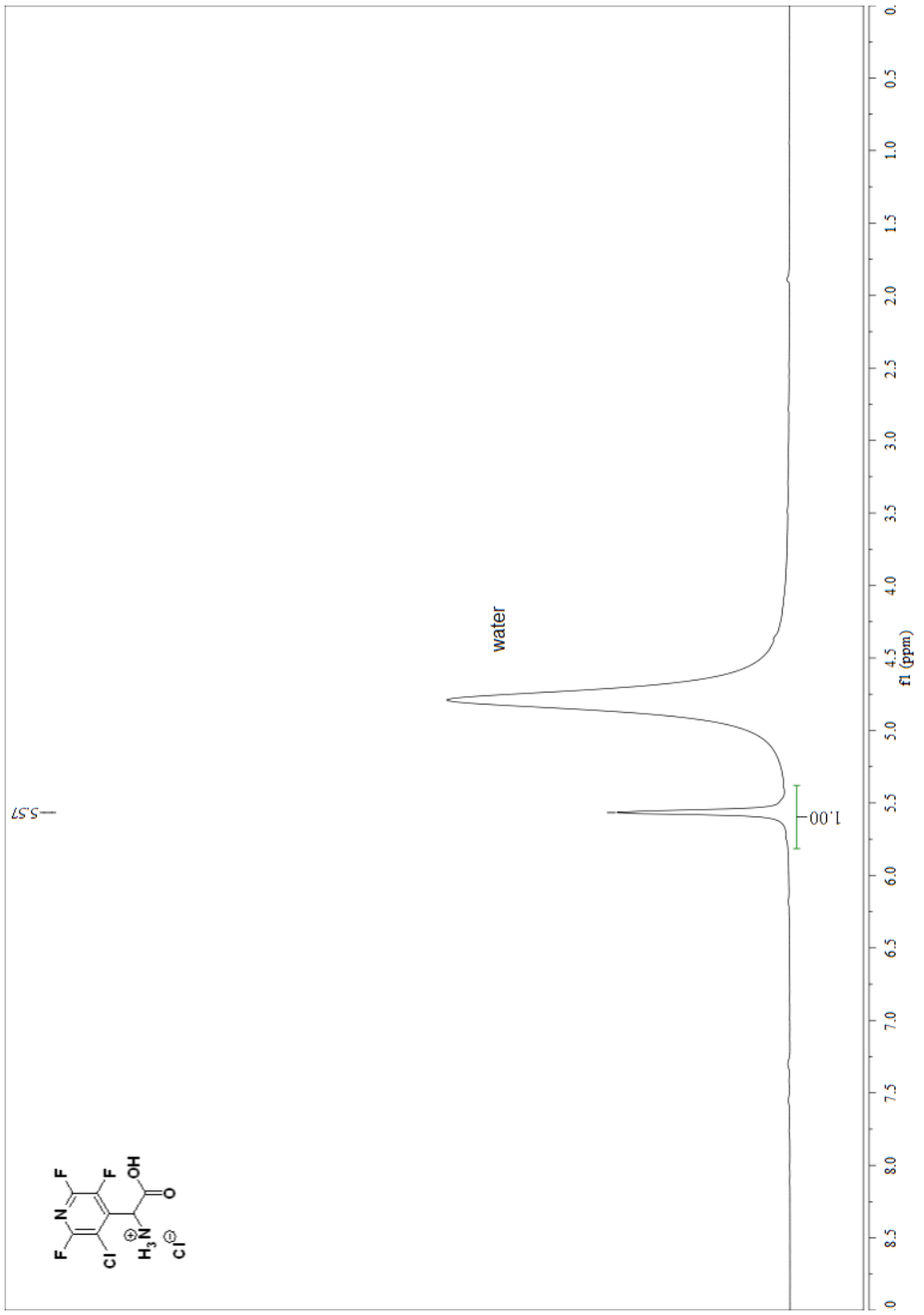

^{19}F NMR (376 MHz, D_2O) **4b**

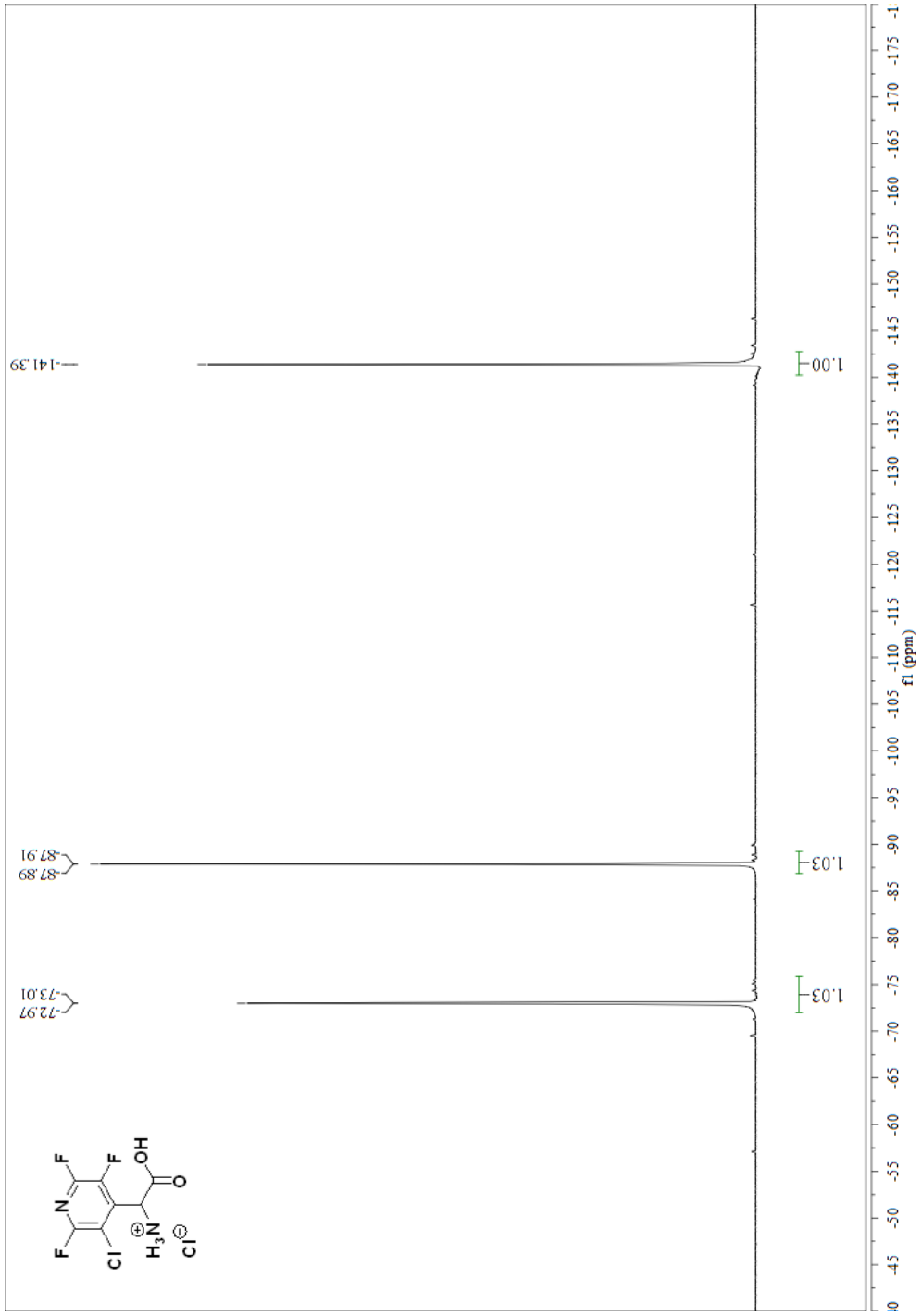

^{13}C NMR (101 MHz, D_2O) **4b**

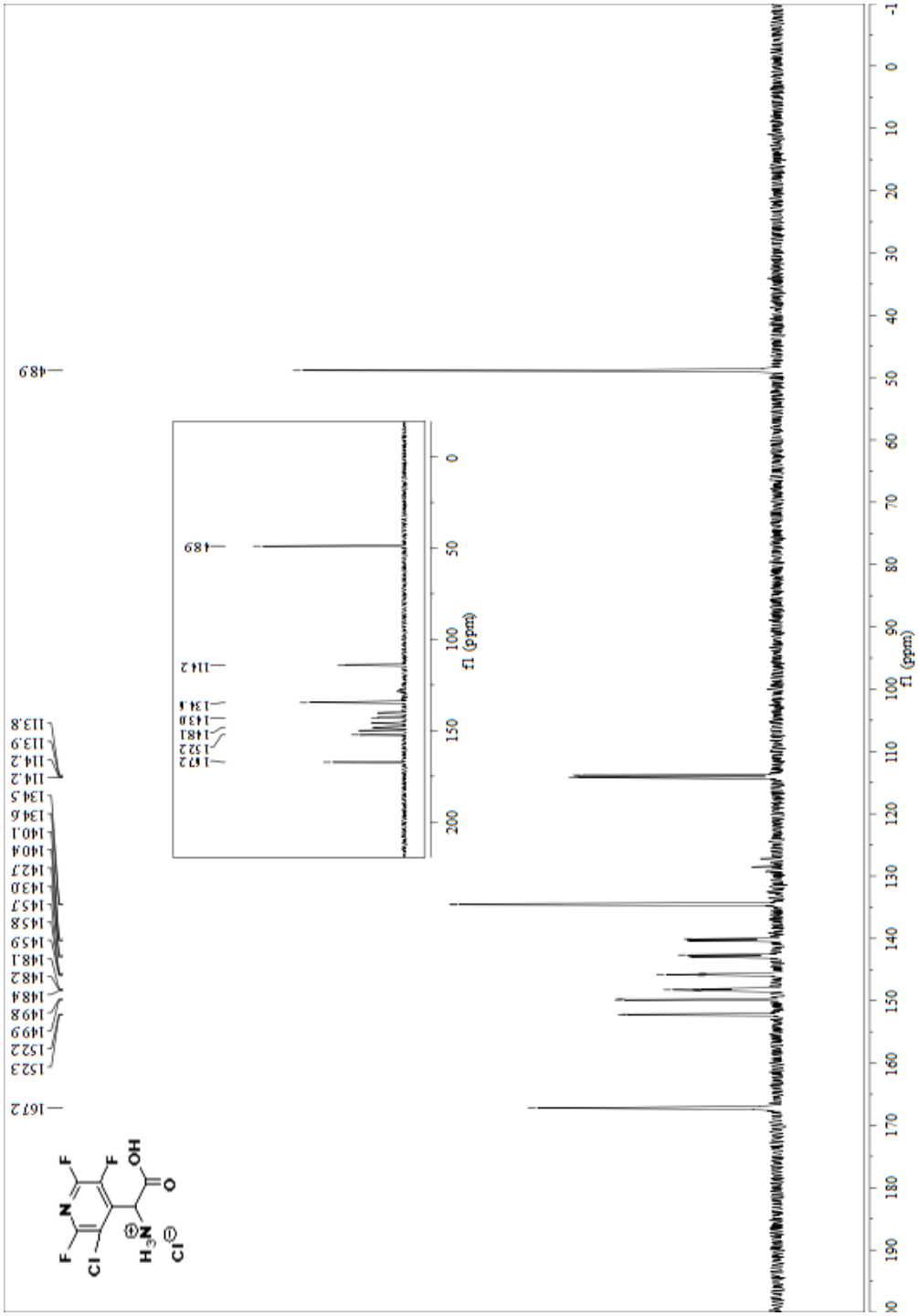

^{1}H NMR (400 MHz, Acetonitrile-d_3) **4c**

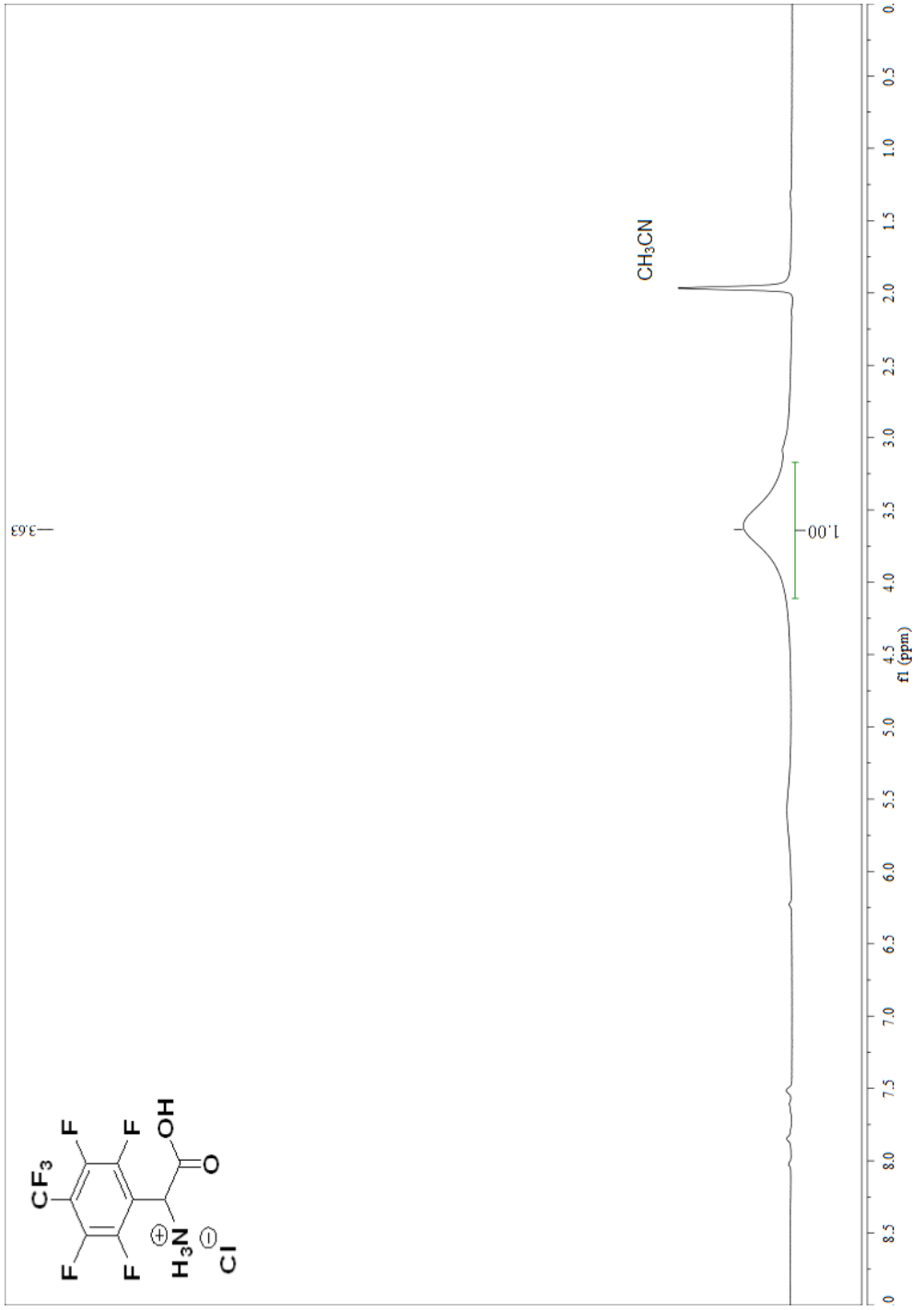

^{19}F NMR (376 MHz, Acetonitrile-d_3) **4c**

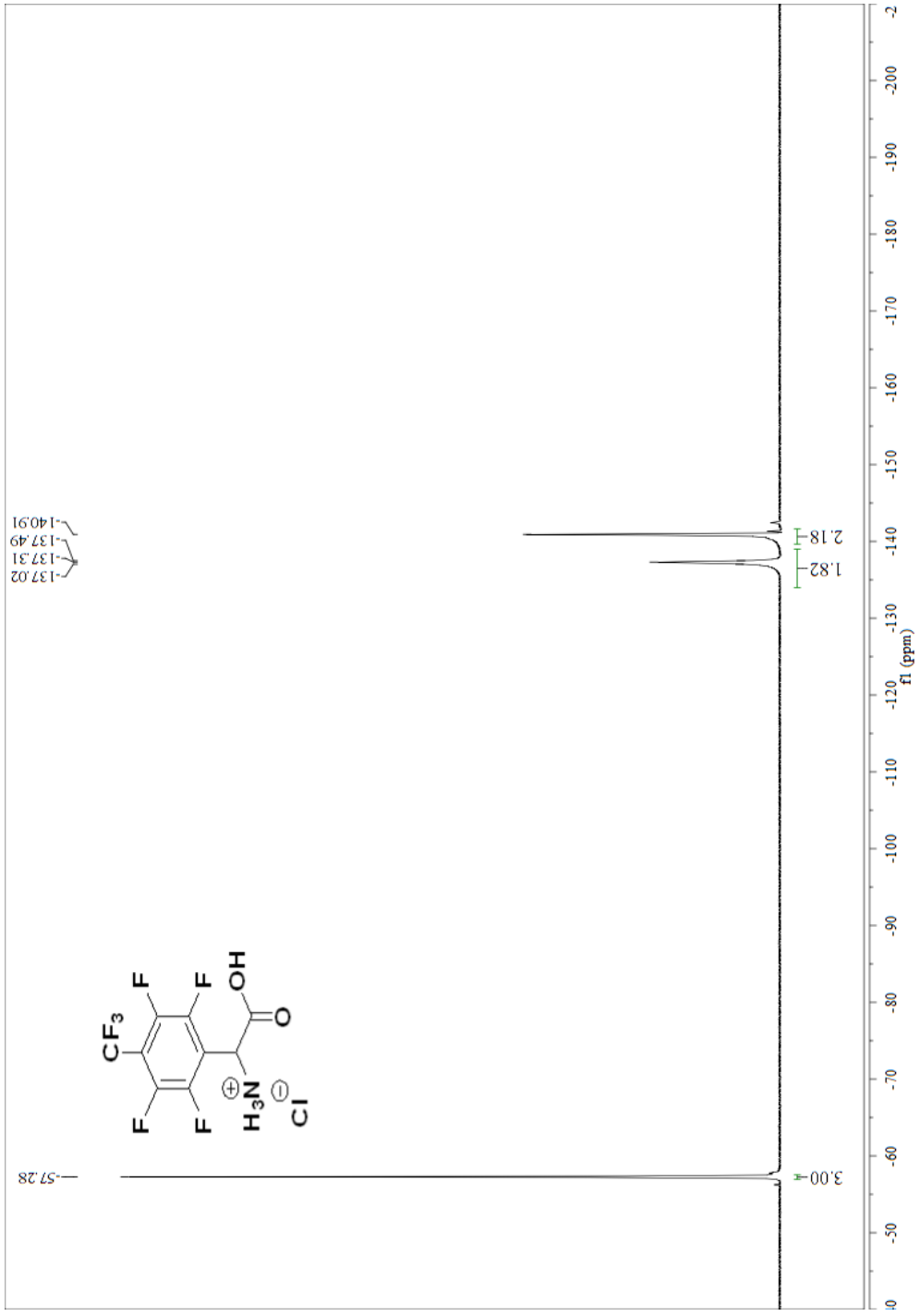

^{13}C NMR (101 MHz, Acetonitrile-d_3) **4c**

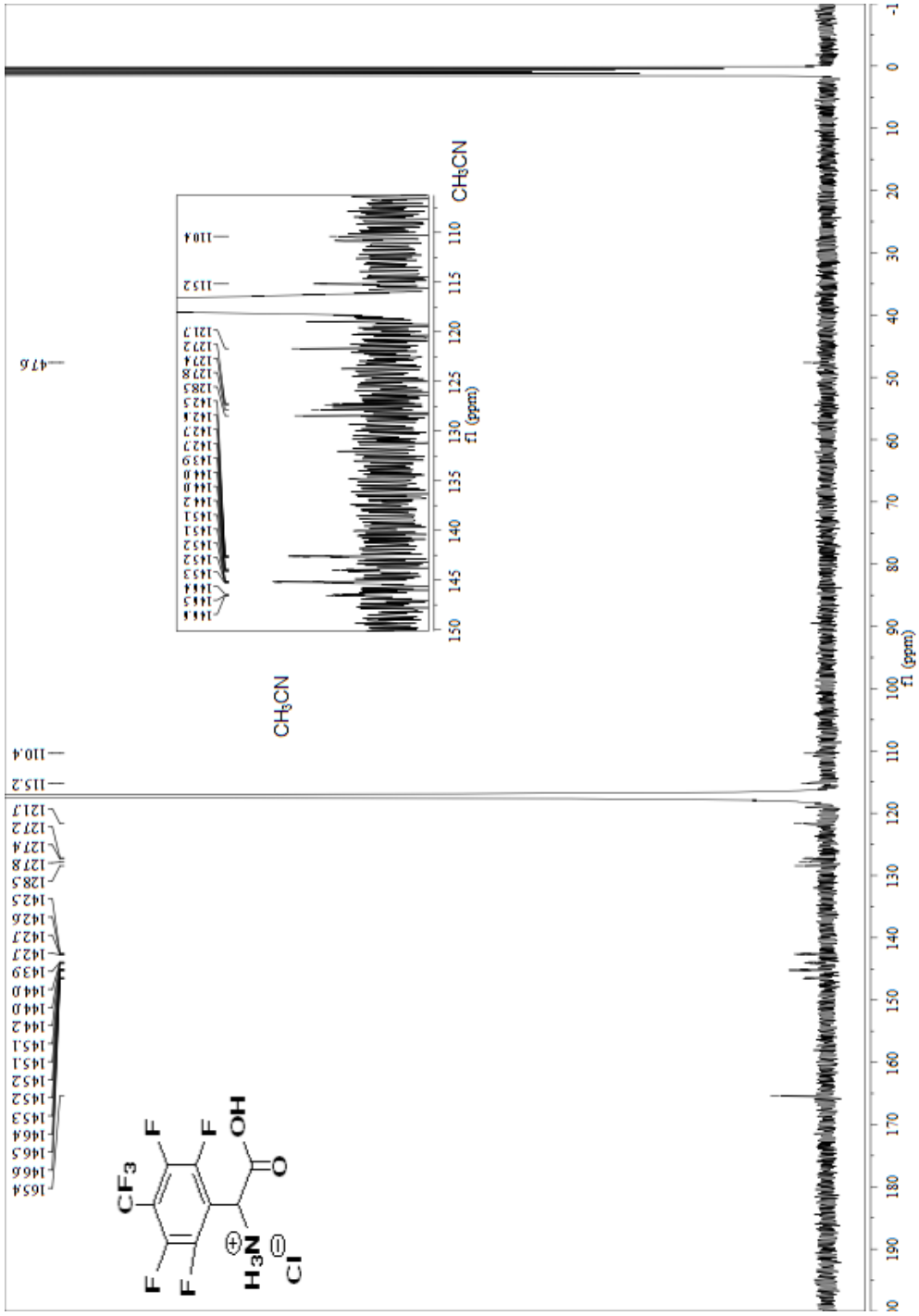

^{1}H NMR (400 MHz, D_2O) **5a**

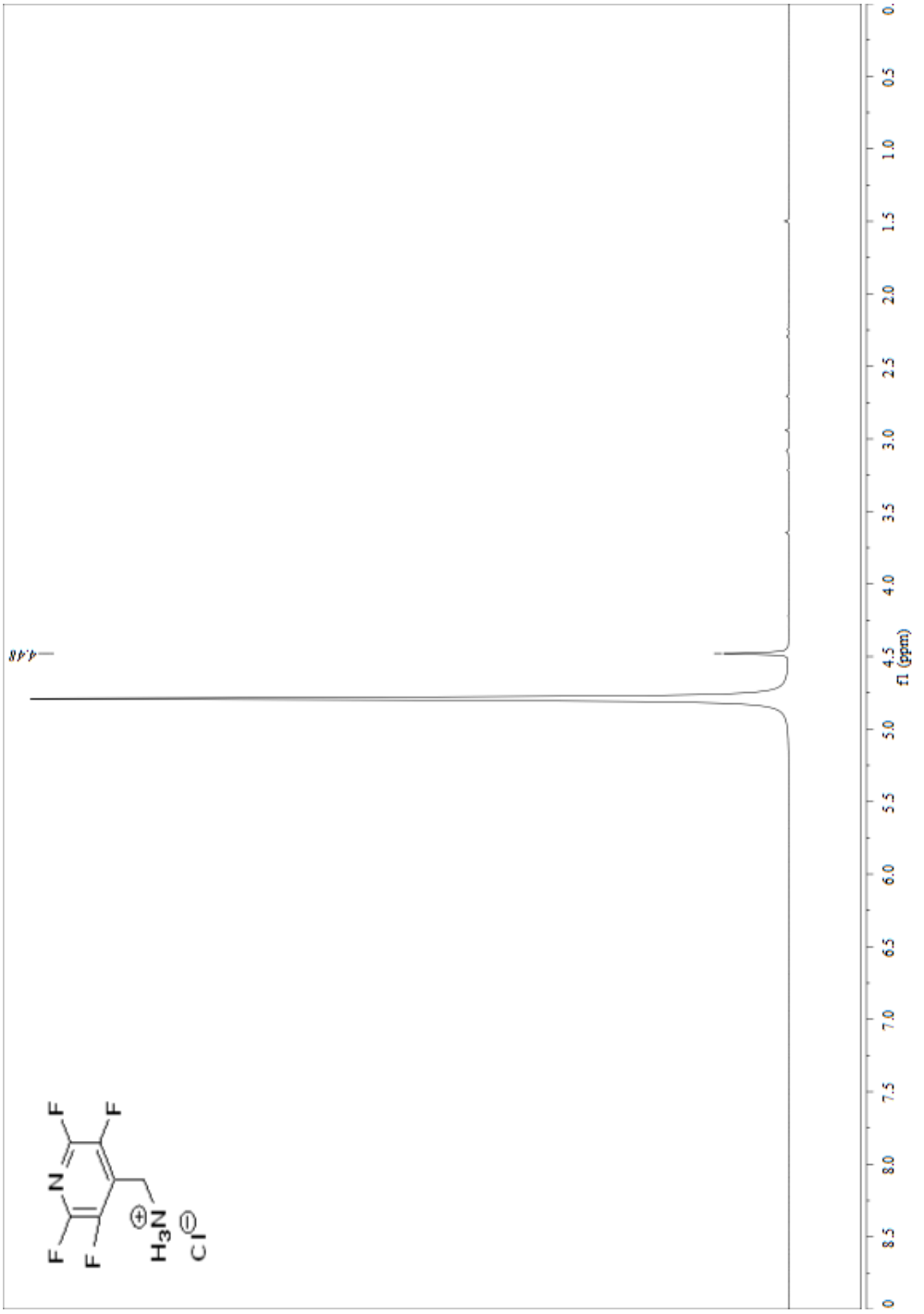

^{19}F NMR (376 MHz, D_2O) **5a**

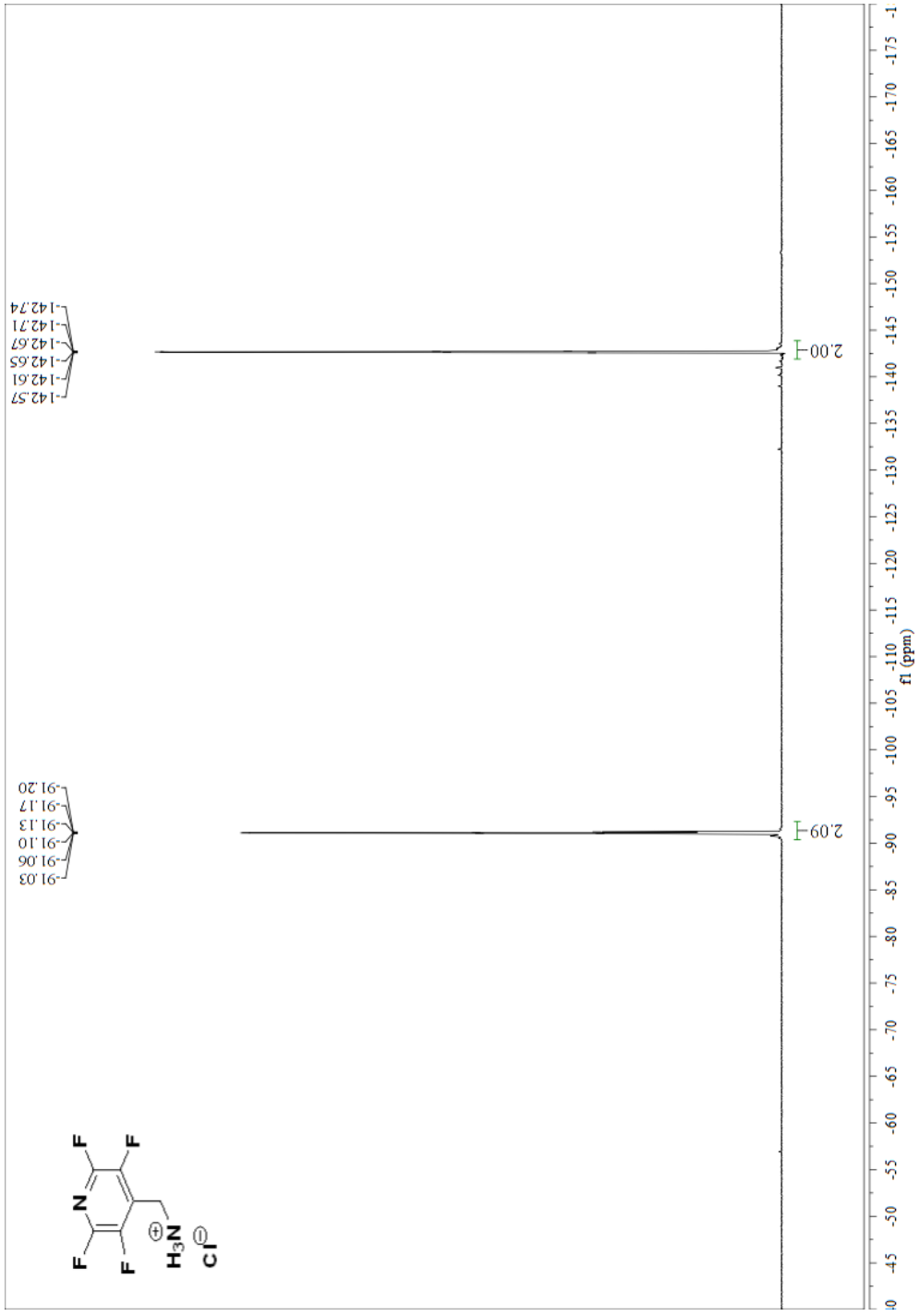

^{13}C NMR (101 MHz, D_2O) **5a**

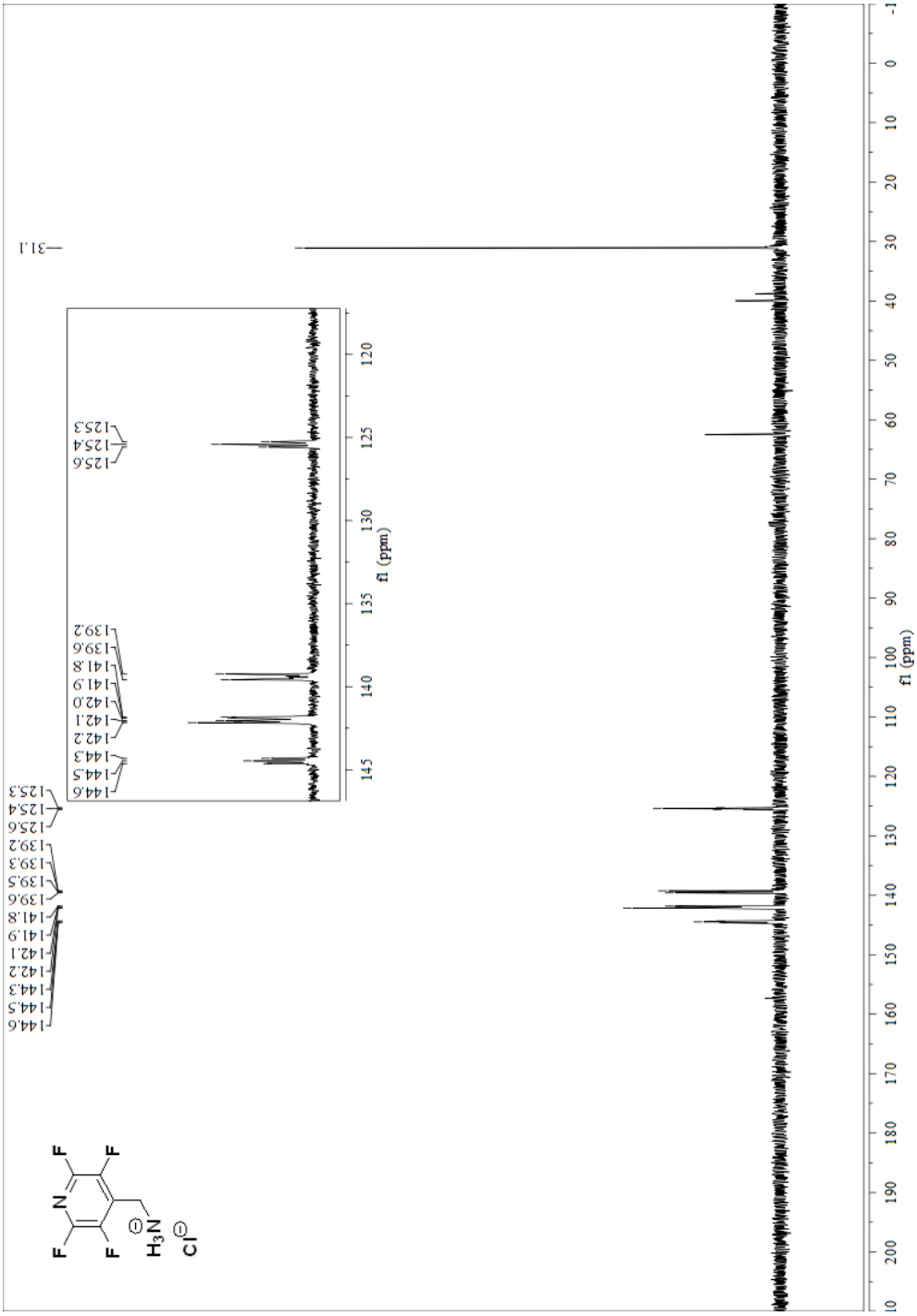

^{1}H NMR (400 MHz, D_2O) **5b**

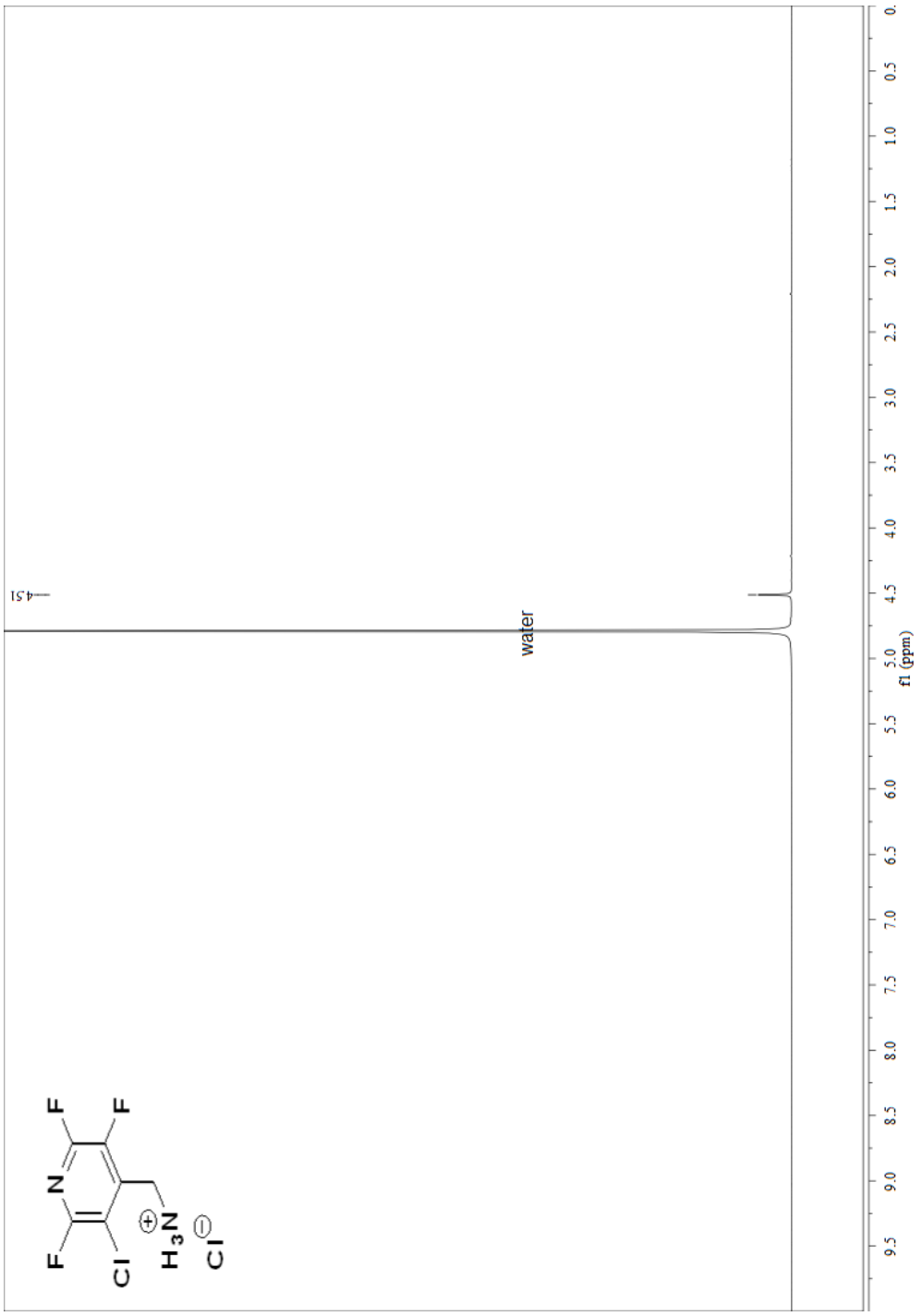

^{19}F NMR (376 MHz, D_2O) **5b**

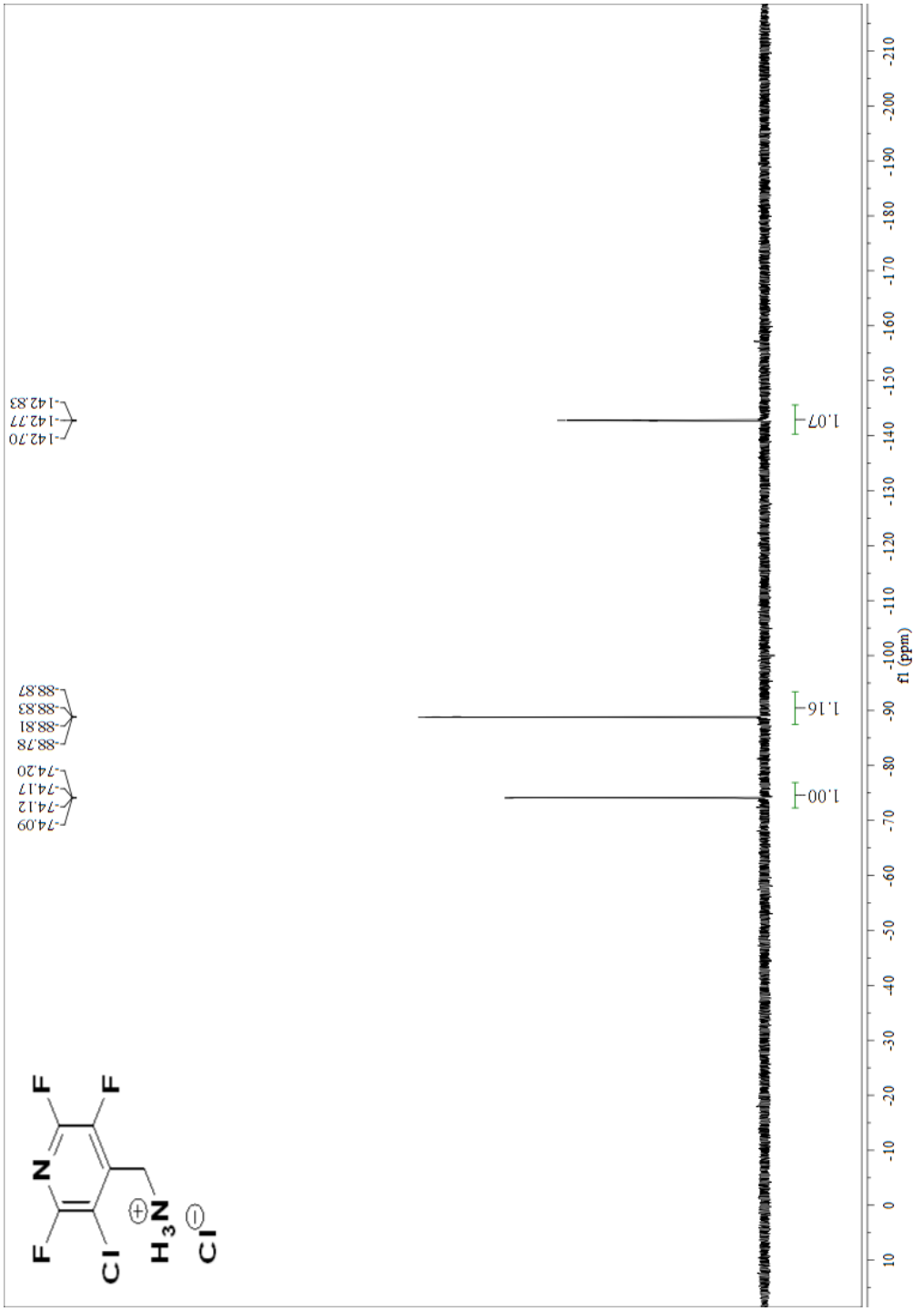

^{13}C NMR (101 MHz, D_2O) **5b**

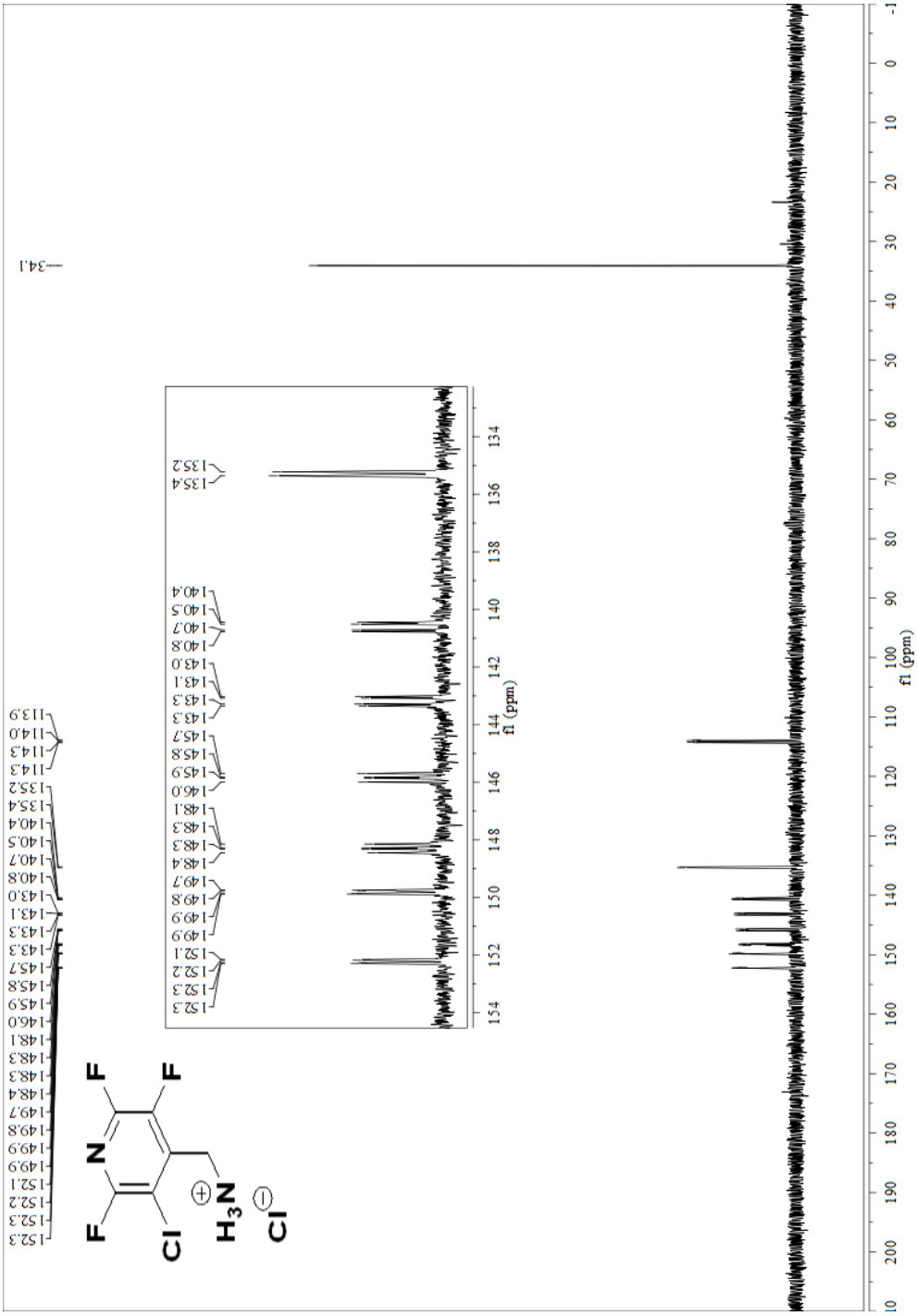

^{1}H NMR (400 MHz, DMSO-d_6) **5c**

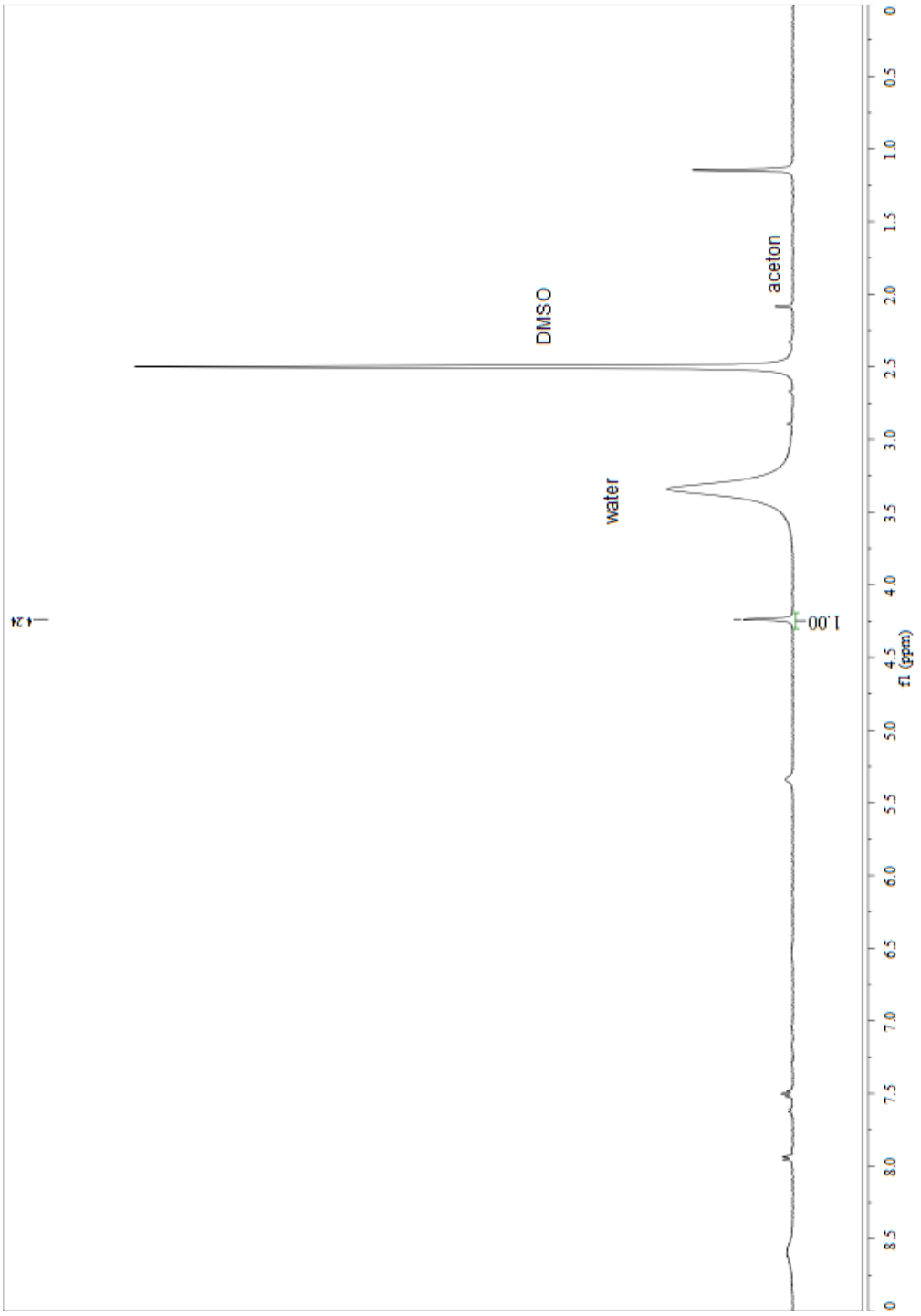

^{19}F NMR (376 MHz, DMSO-d_6) **5c**

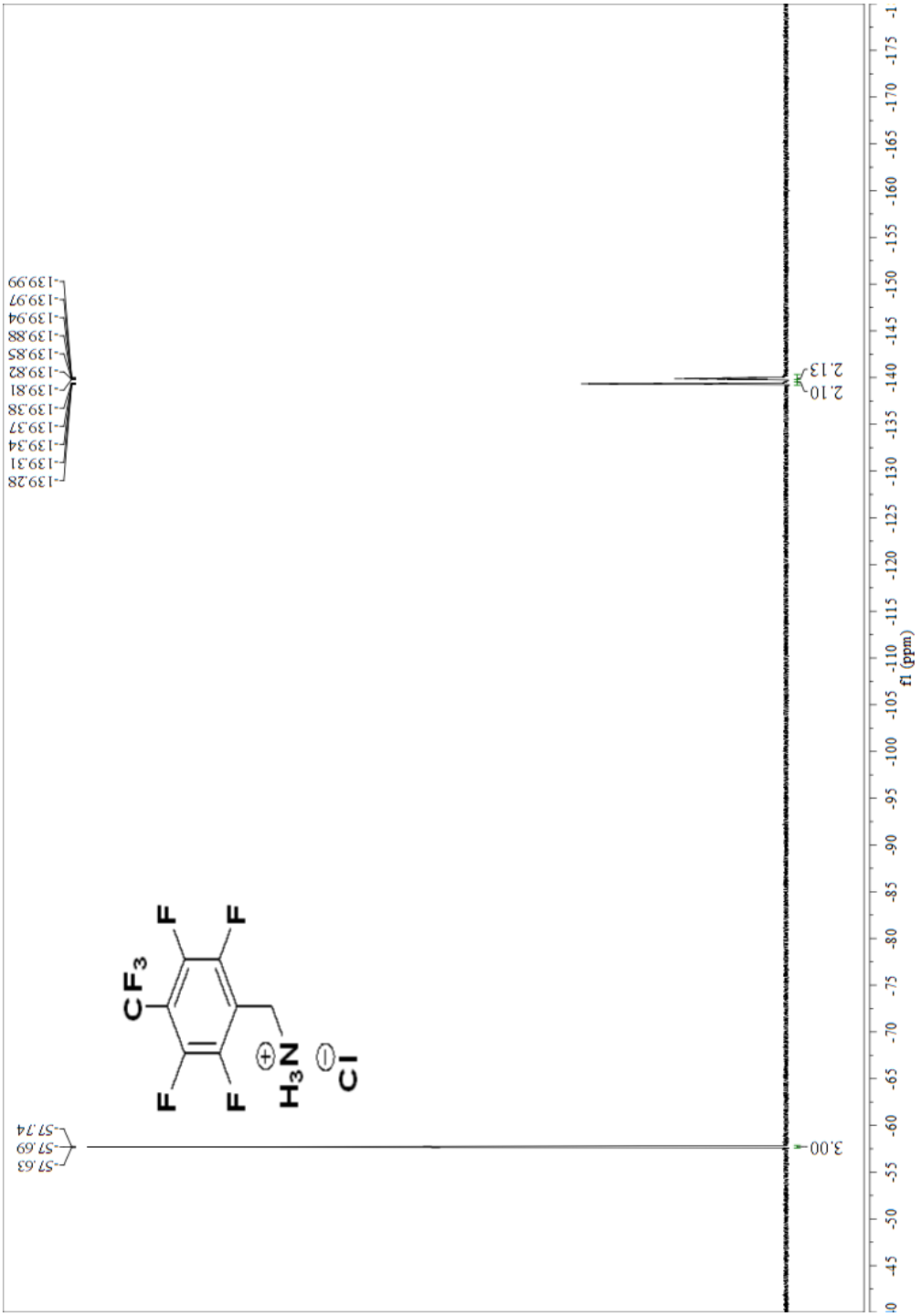

^{13}C NMR (101 MHz, DMSO-d_6) **5c**

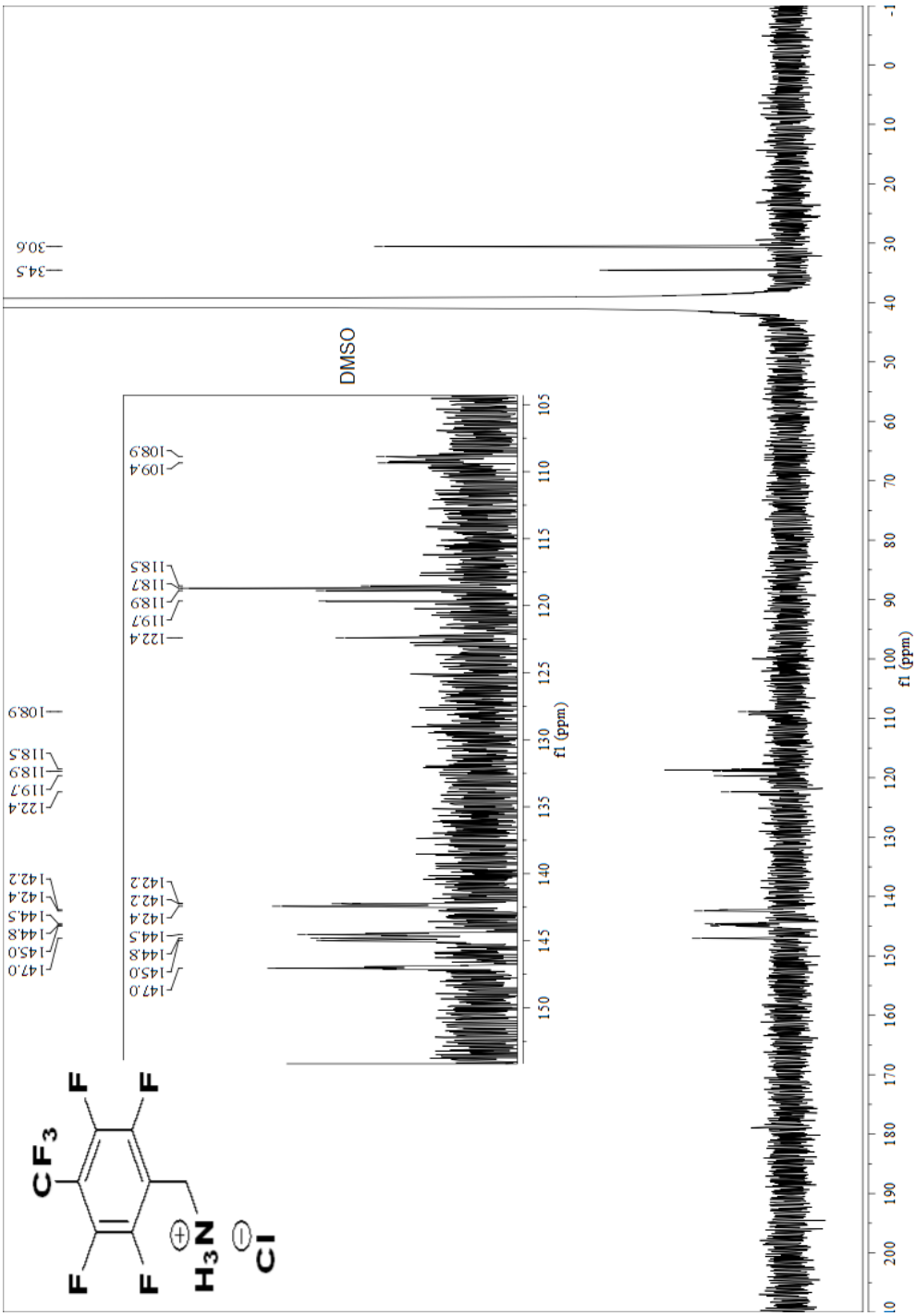

^{1}H NMR (400 MHz, Chloroform-*d*) **6a**

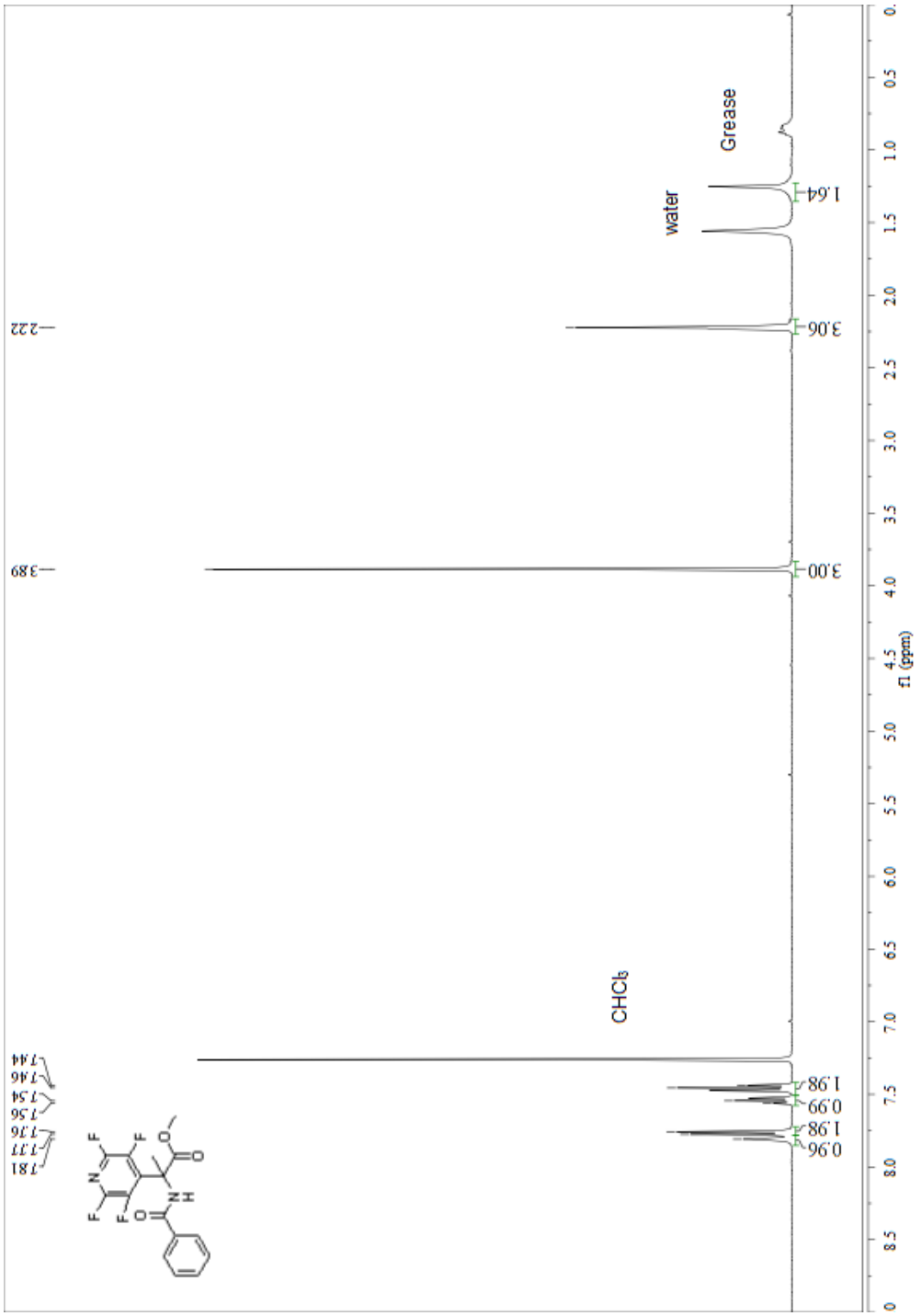

^{19}F NMR (376 MHz, Chloroform-*d*) **6a**

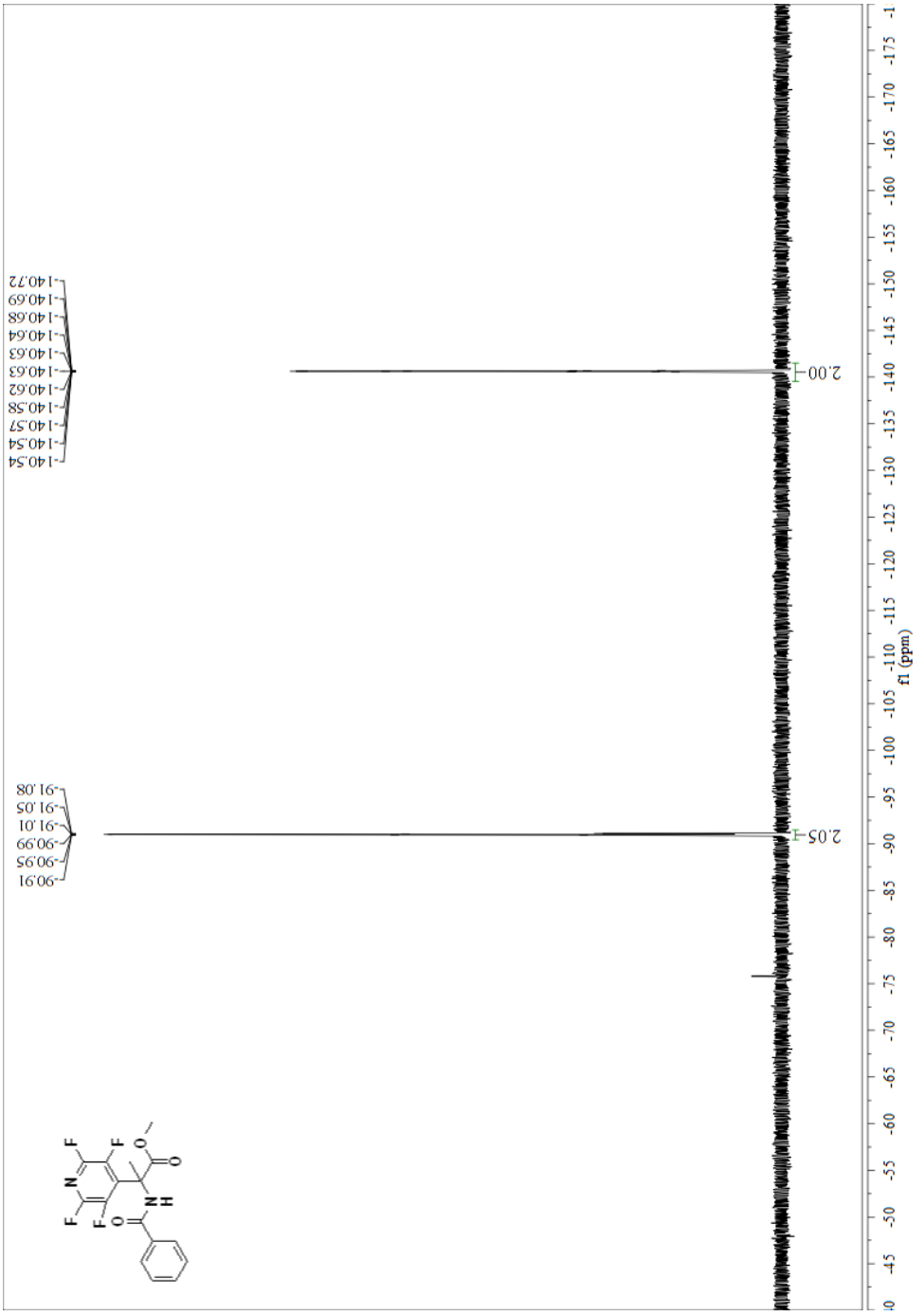

^{13}C NMR (101 MHz, Chloroform-*d*) **6a**

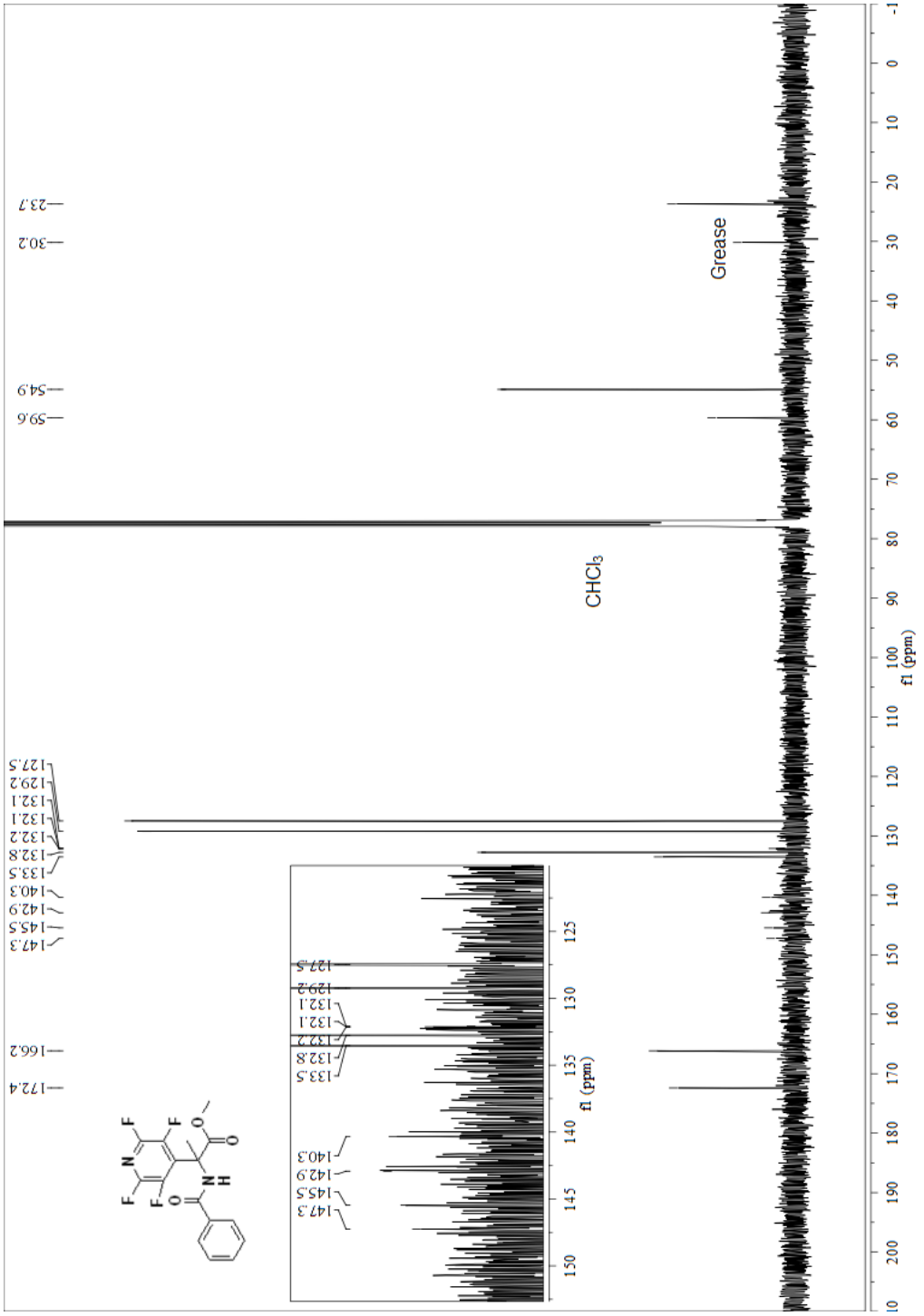

^{1}H NMR (400 MHz, Chloroform-*d*) **6b**

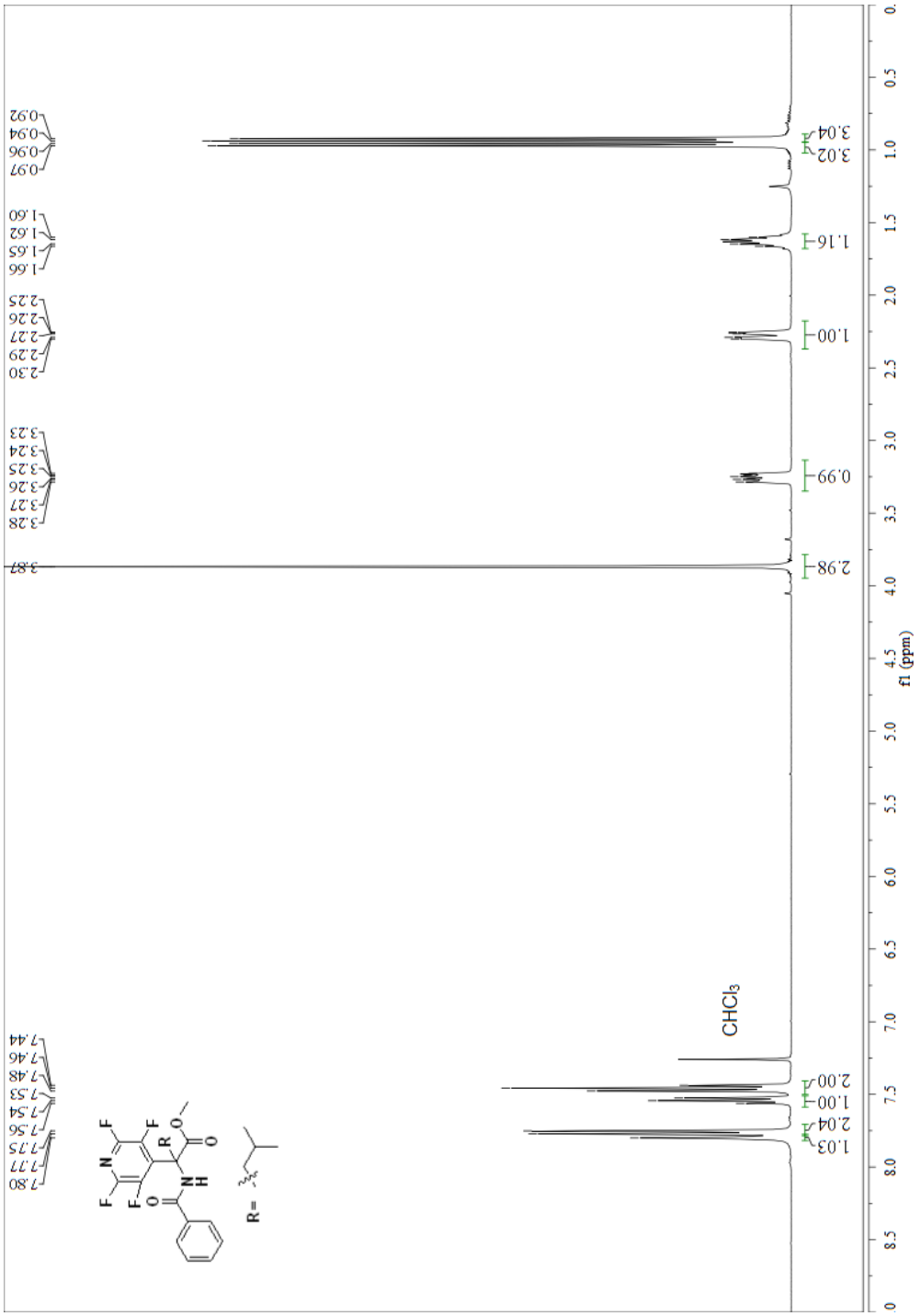

^{19}F NMR (376 MHz, Chloroform-*d*) **6b**

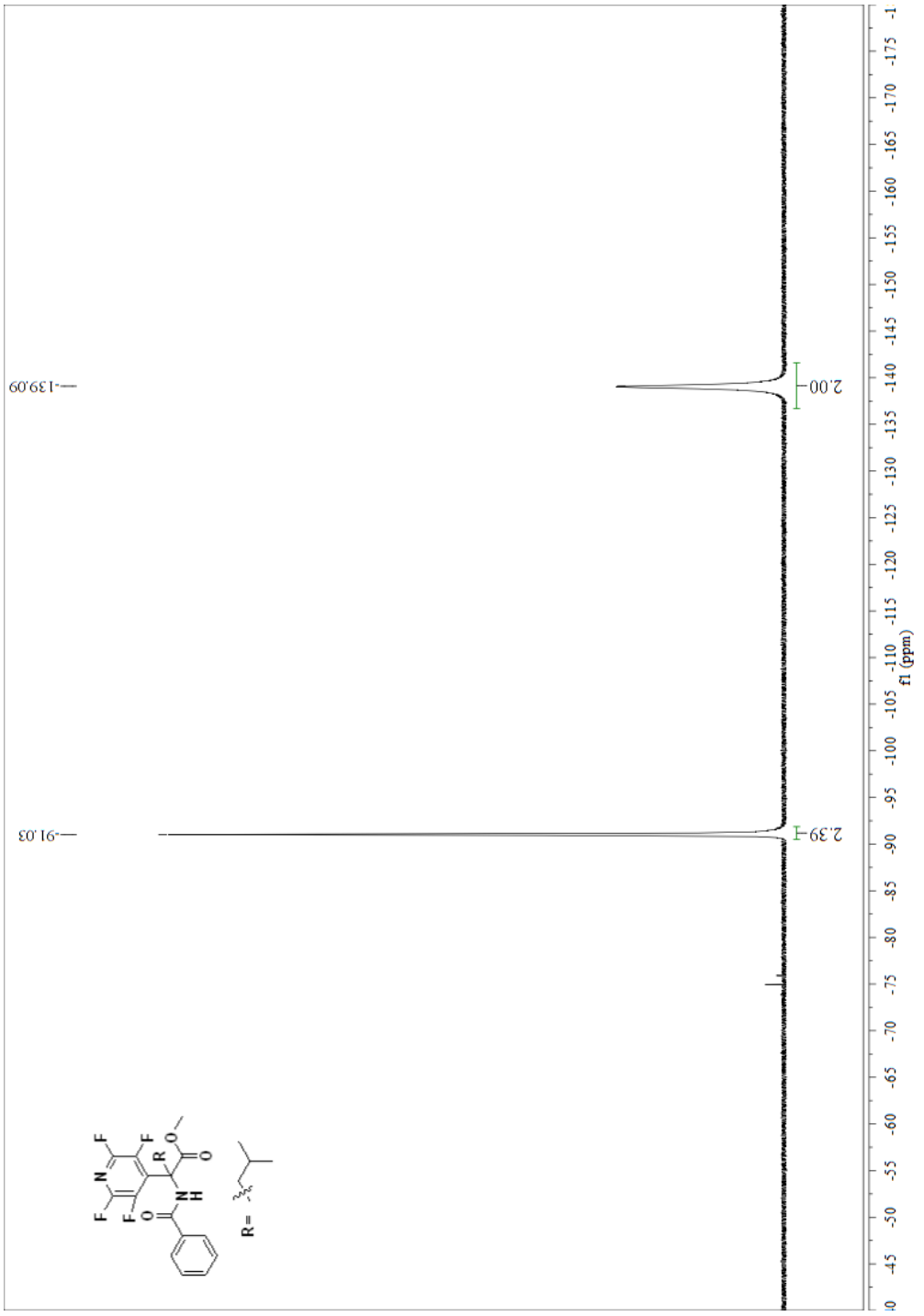

^{13}C NMR (101 MHz, Chloroform-*d*) **6b**

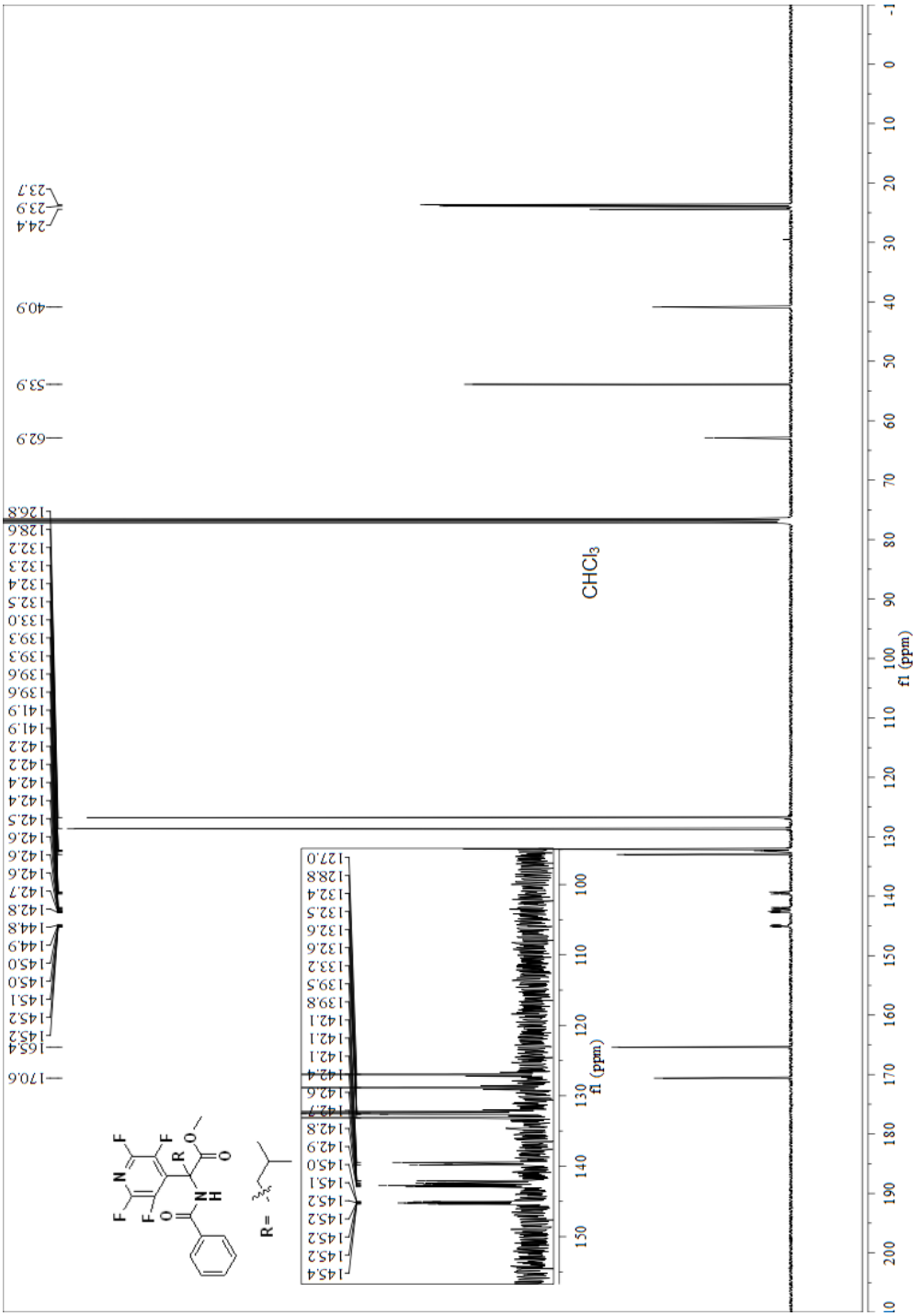

^{1}H NMR (400 MHz, Chloroform-*d*) **6c**

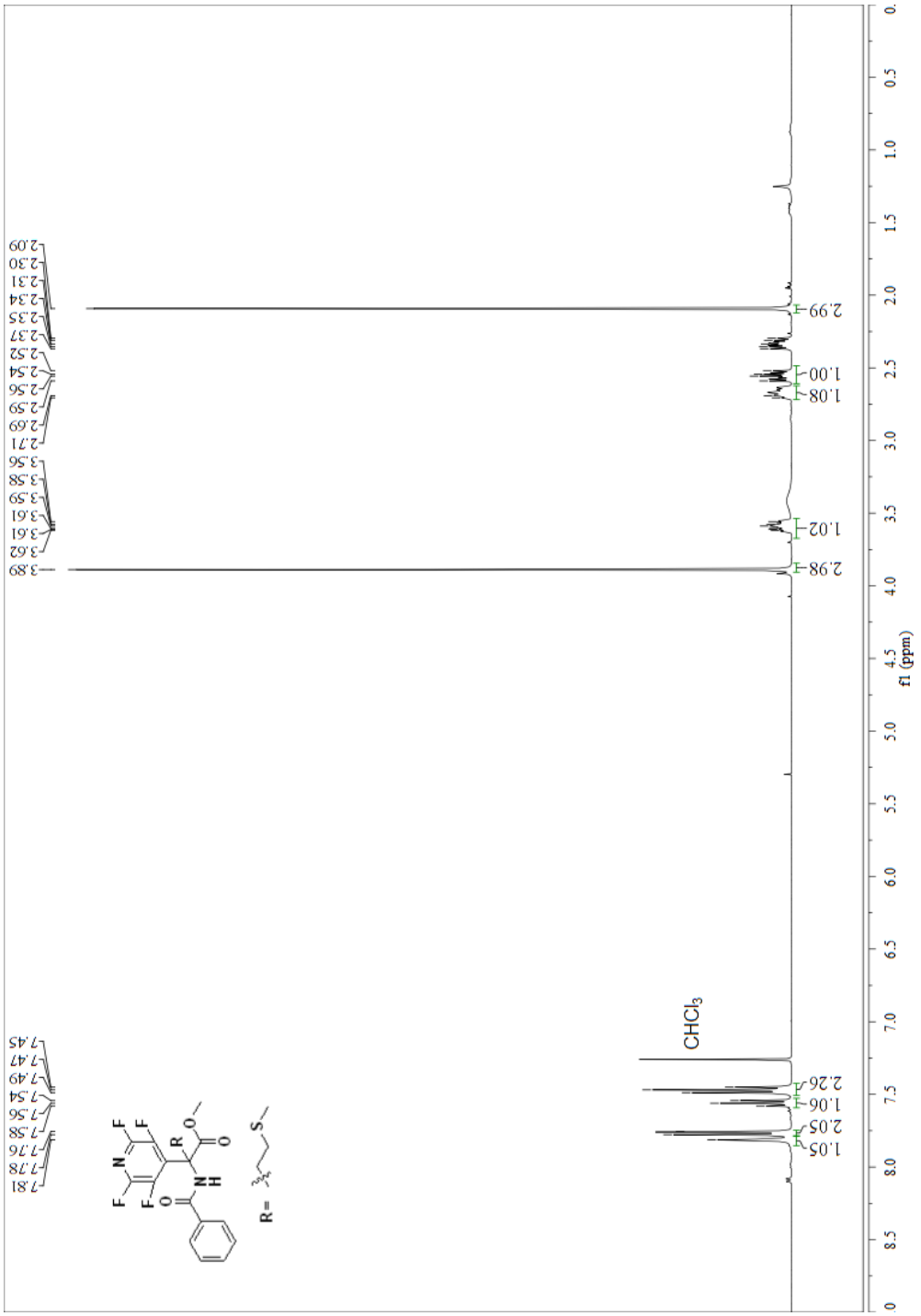

^{19}F NMR (376 MHz, Chloroform-*d*) **6c**

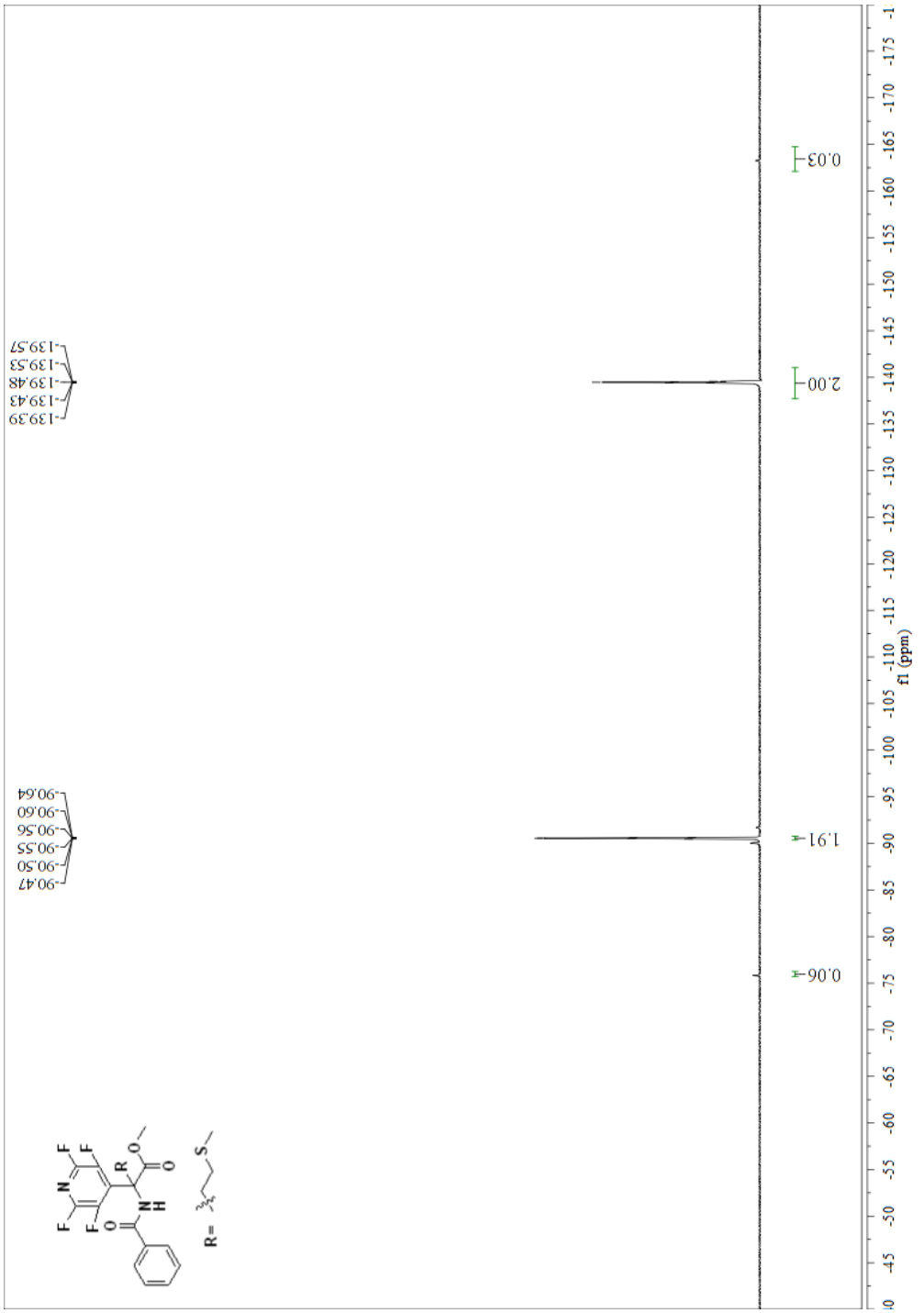

^{13}C NMR (101 MHz, Chloroform-*d*) **6c**

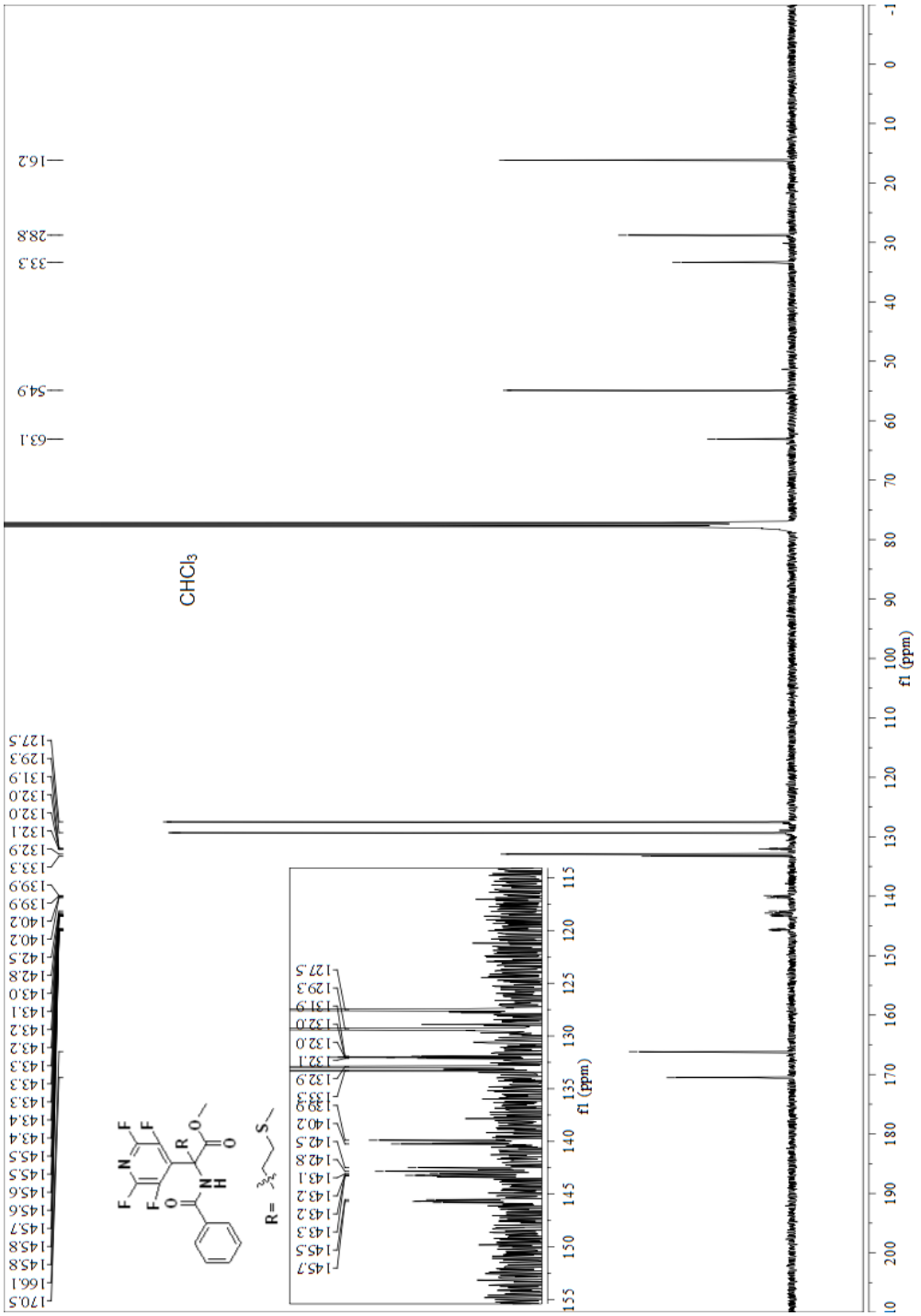

^{1}H NMR (400 MHz, Chloroform-*d*) **6d**

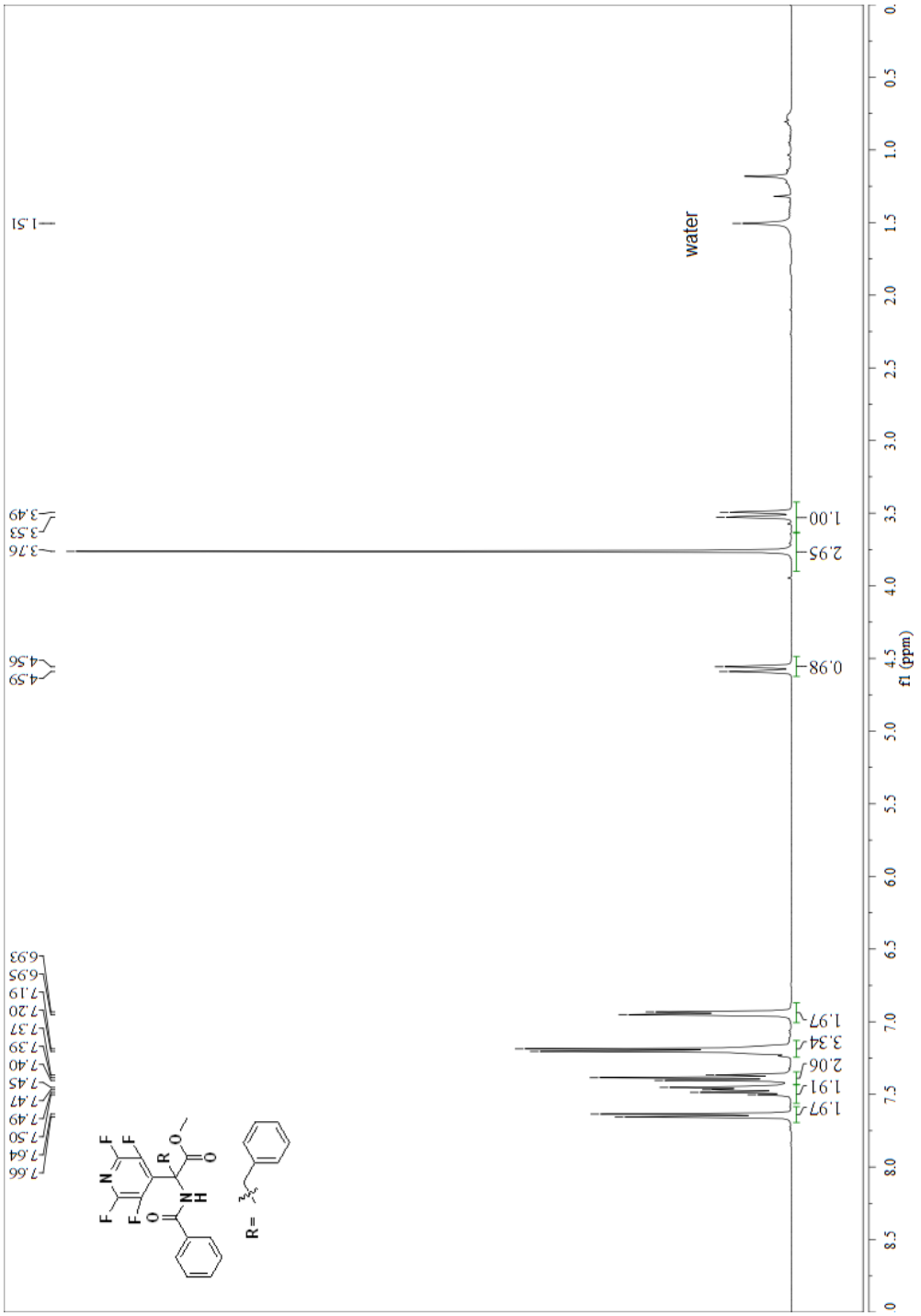

^{19}F NMR (376 MHz, Chloroform-*d*) **6d**

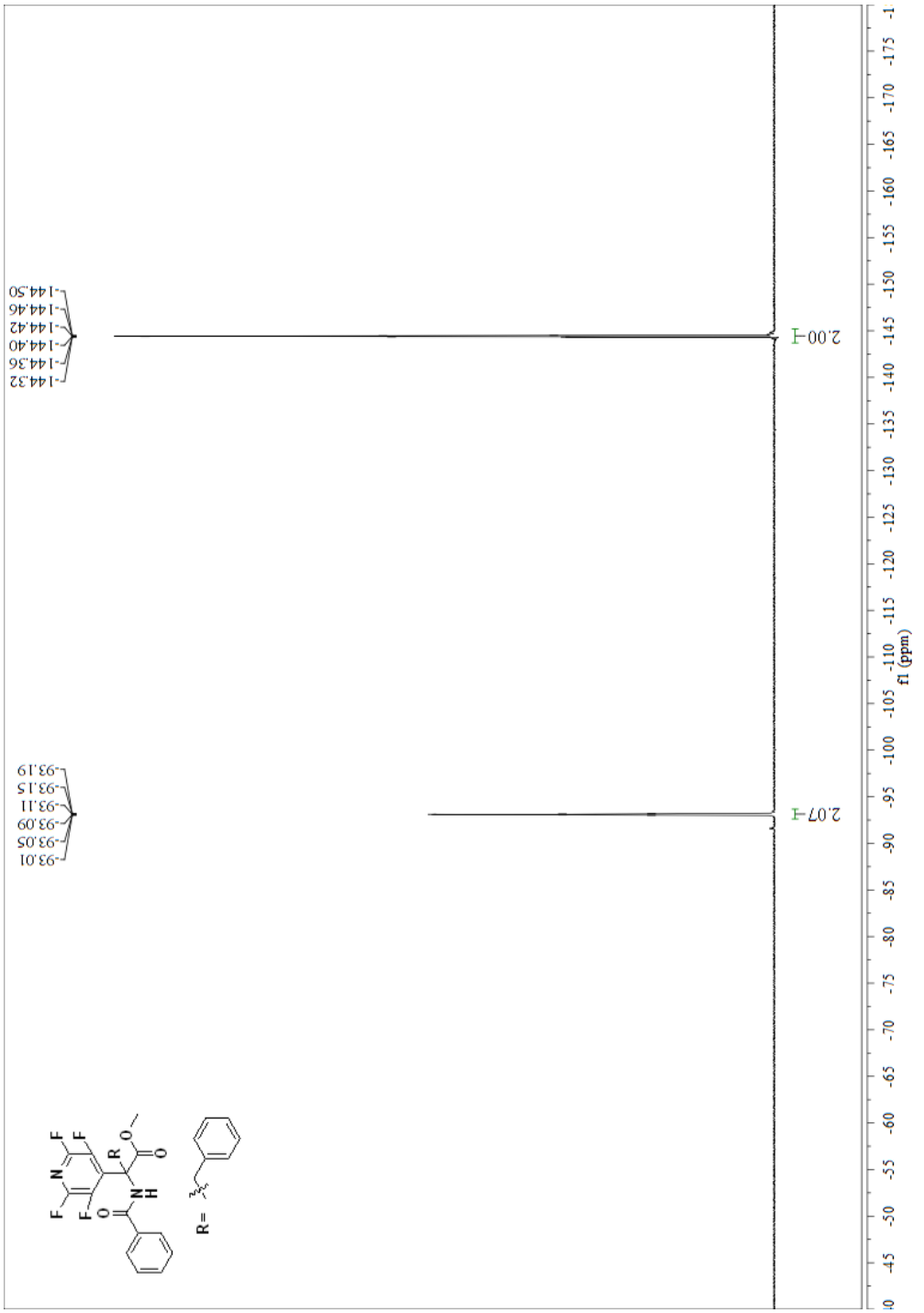

^{13}C NMR (101 MHz, Chloroform-*d*) **6d**

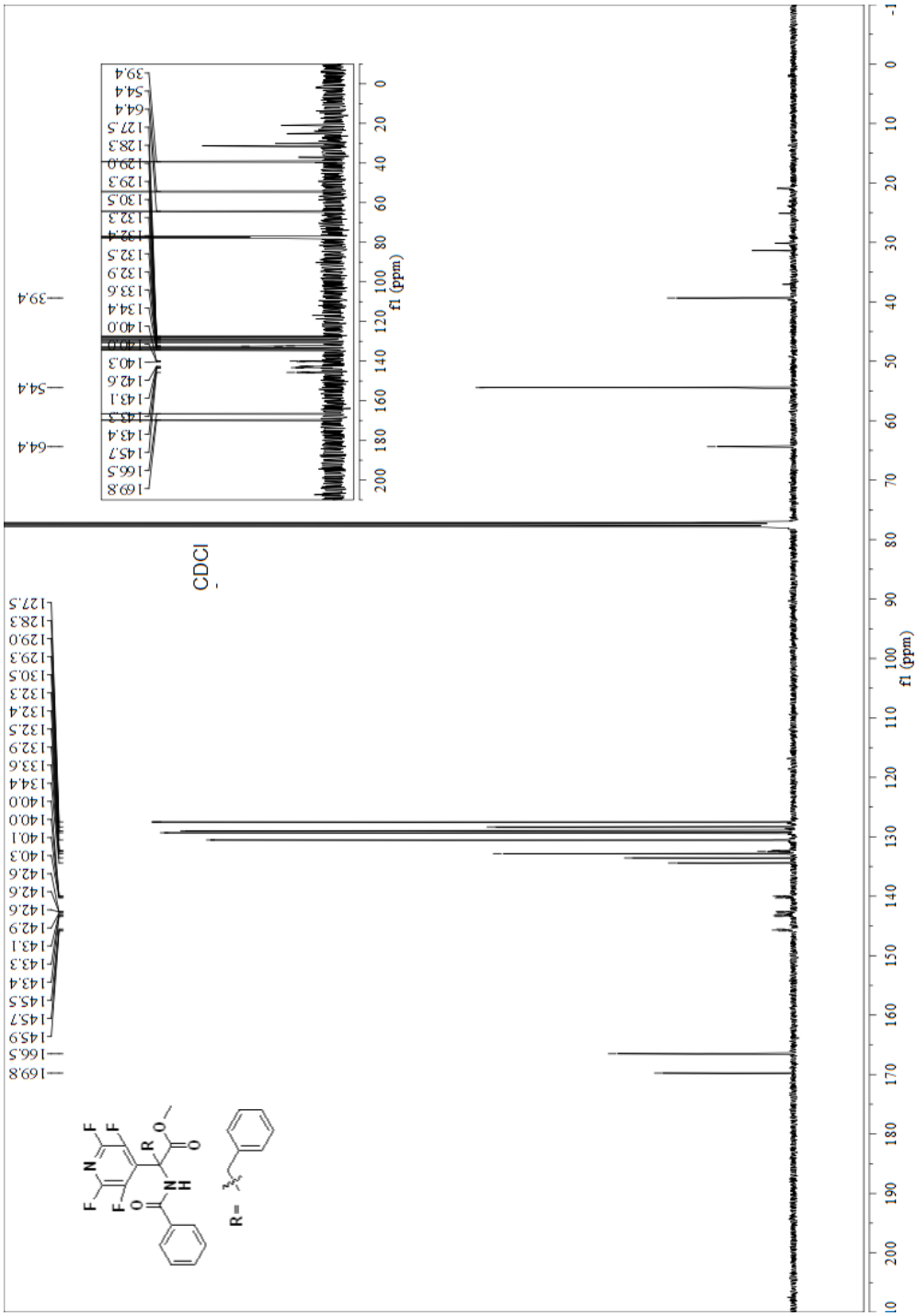

^{1}H NMR (400 MHz, DMSO-d_6) **7a**

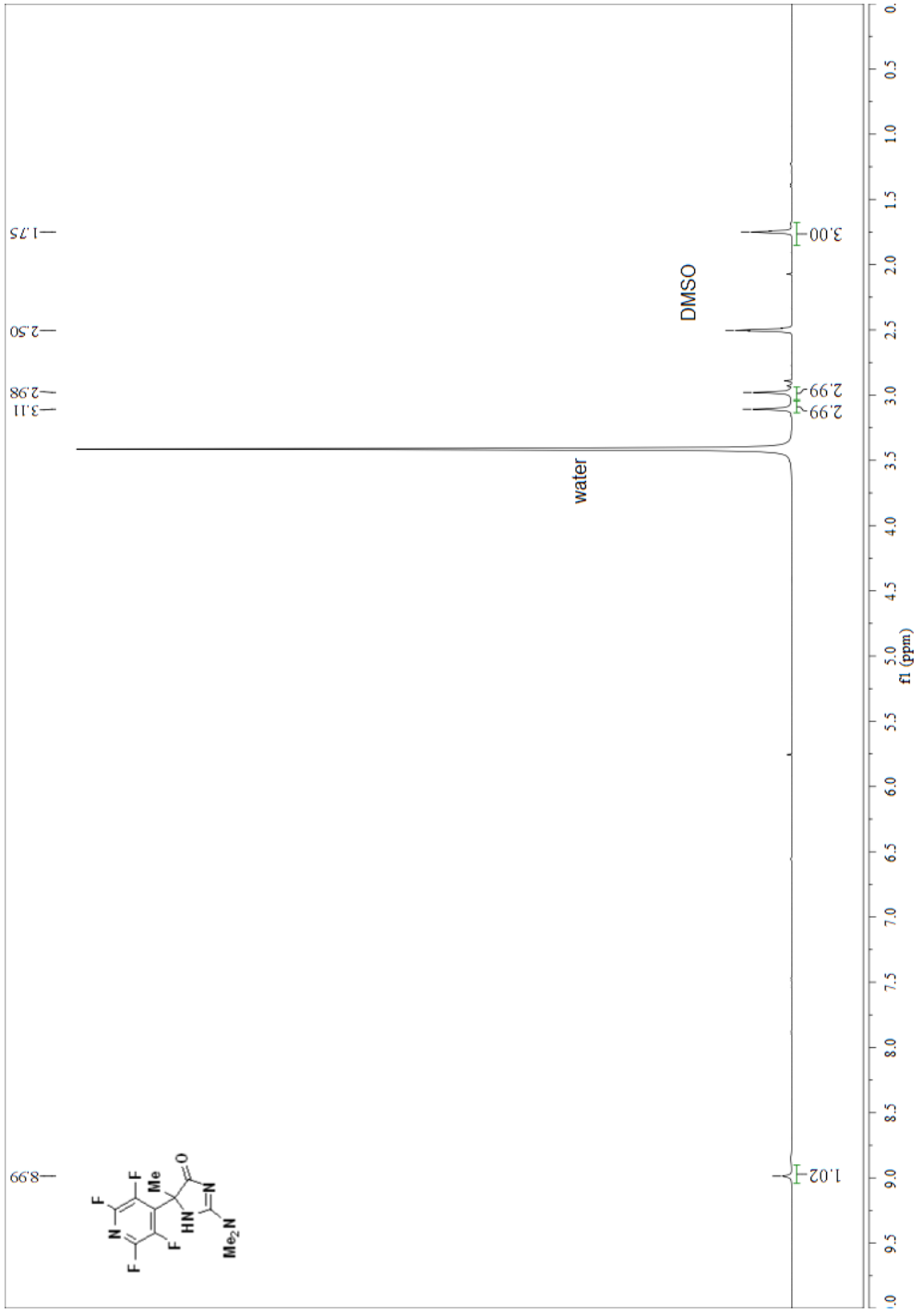

^{19}F NMR (376 MHz, DMSO-d_6) **7a**

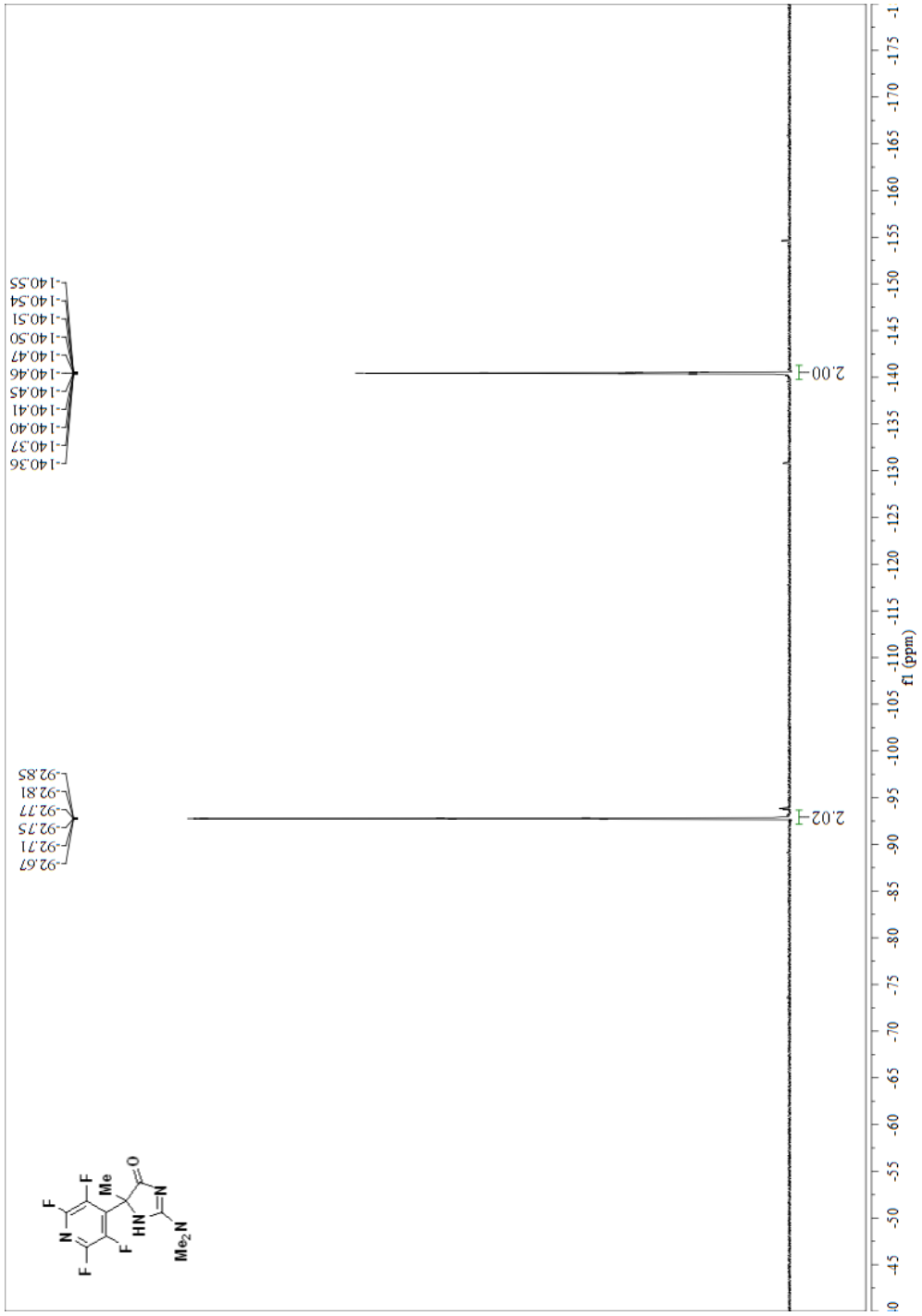

^{13}C NMR (101 MHz, DMSO-d_6) **7a**

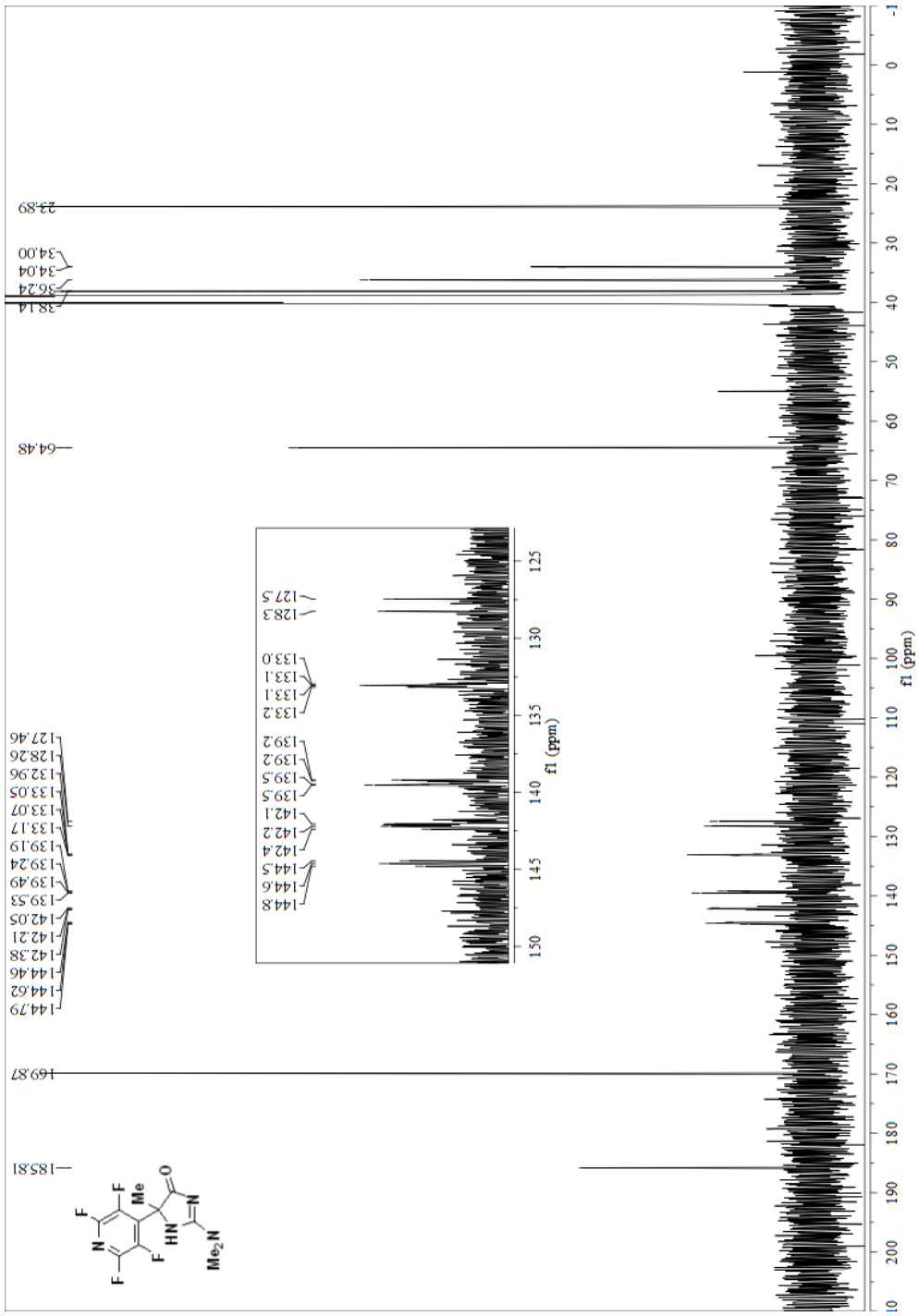

^{1}H NMR (400 MHz, DMSO-d_6) **7b**

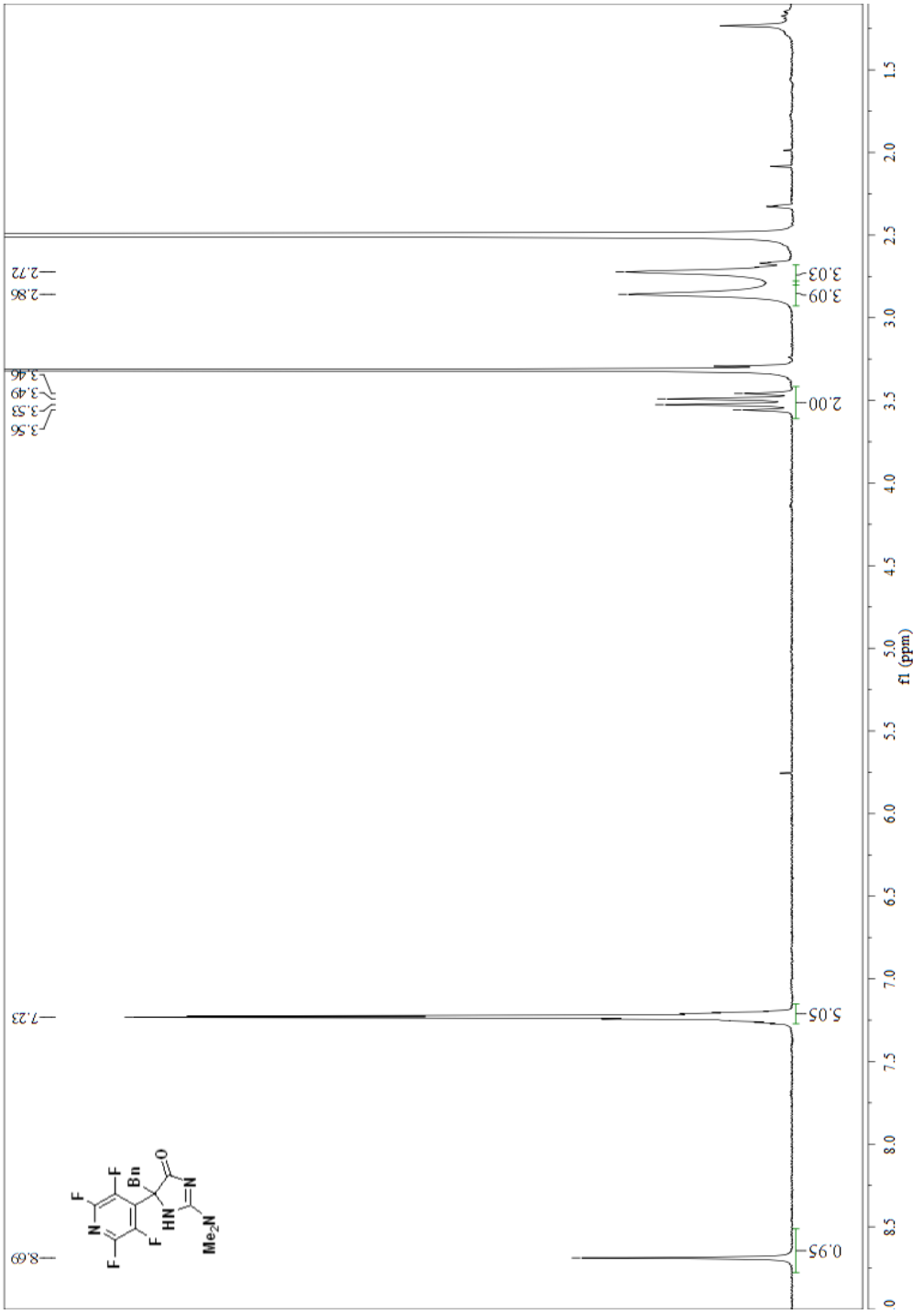

^{19}F NMR (376 MHz, DMSO-d_6) **7b**

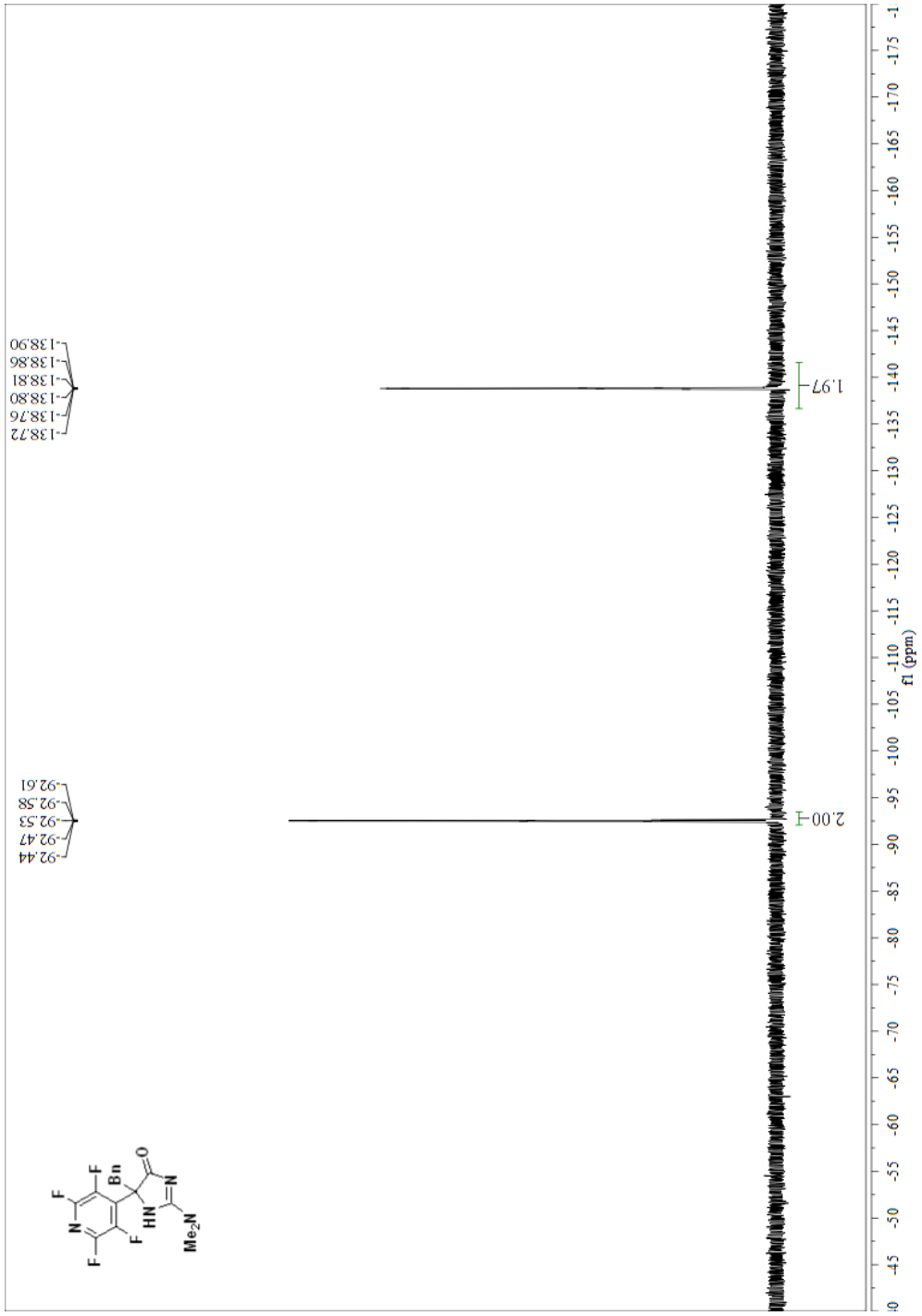

^{13}C NMR (101 MHz, DMSO-d_6) **7b**

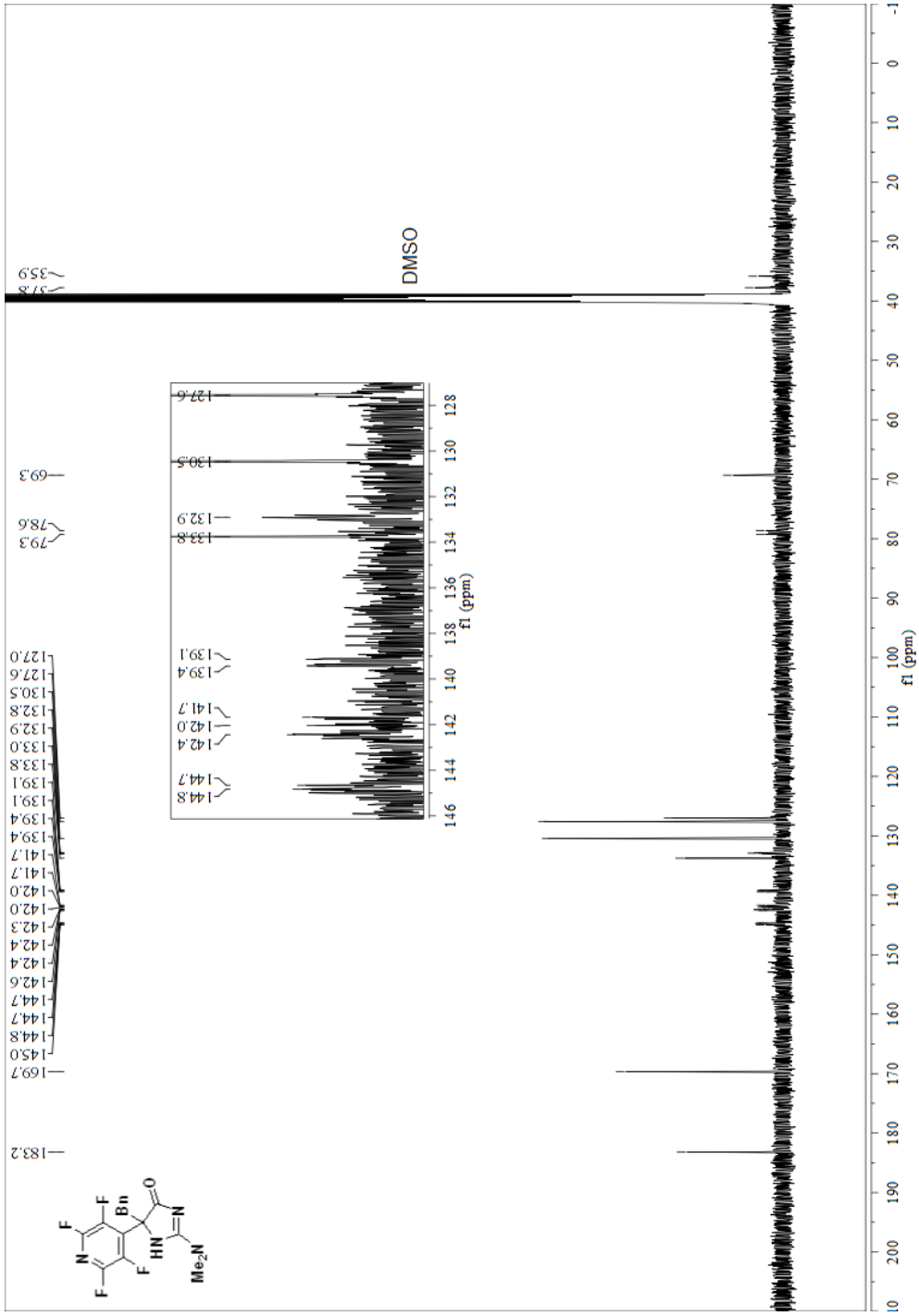

^{1}H NMR (400 MHz, DMSO-d_6) **7c**

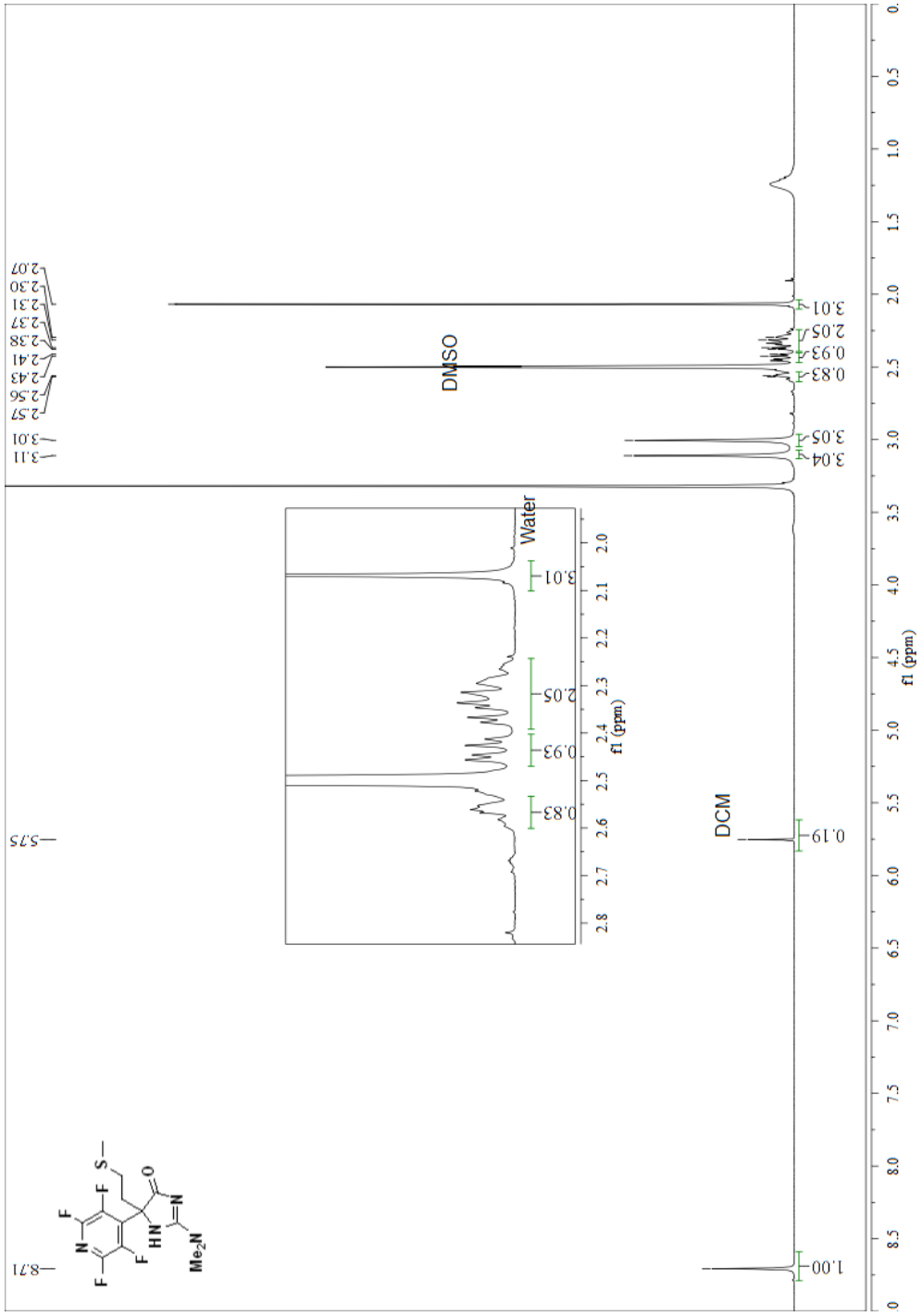

^{19}F NMR (376 MHz, DMSO-d_6) **7c**

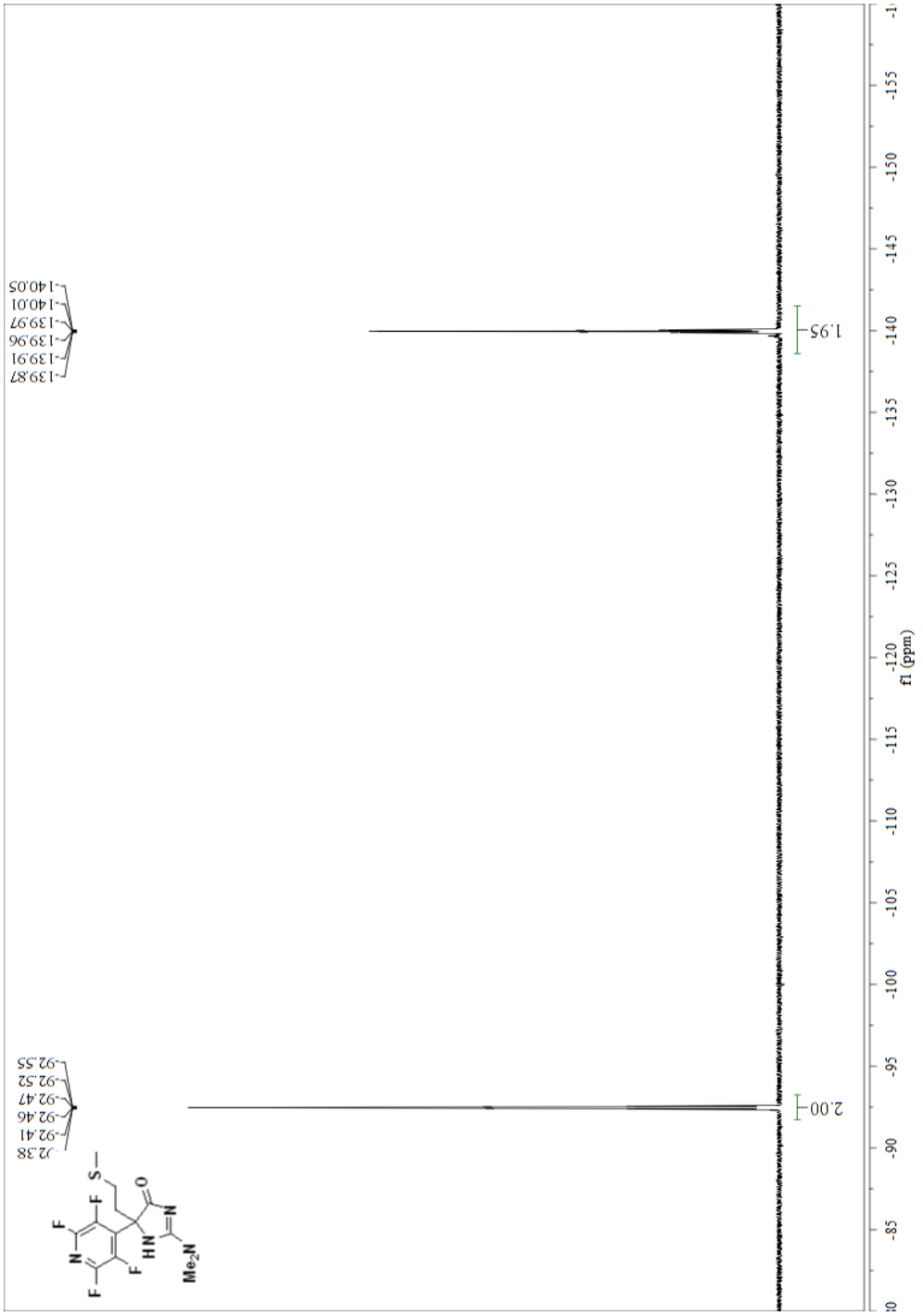

^{13}C NMR (101 MHz, DMSO-d_6) **7c**

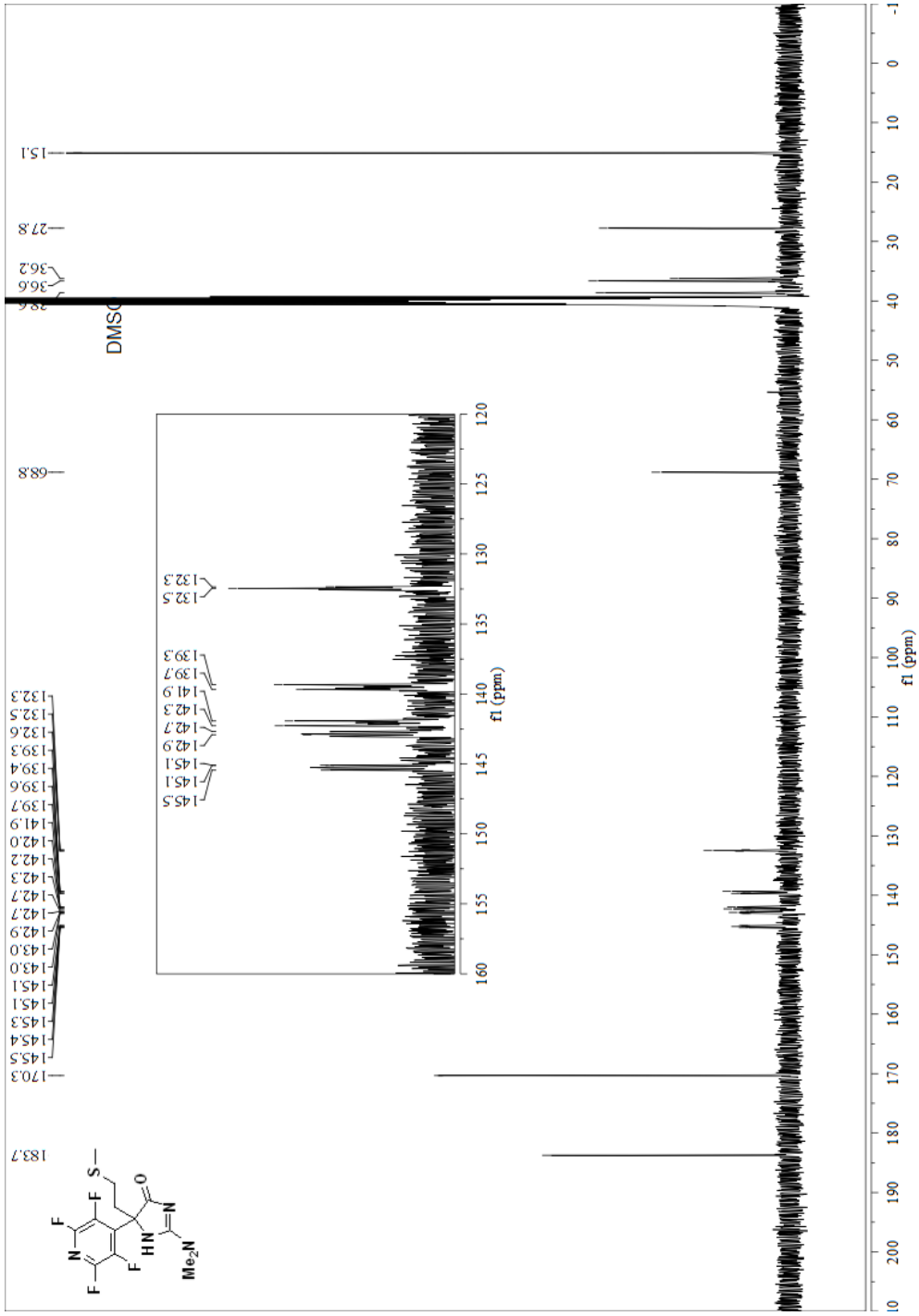

CHAPTER V

FACILE FORMATION OF NON-NATURAL α,α-DISUBSTITUTED AMINO ESTERS VIA CATALYTIC MICHAEL ADDITION

5.1 *Historical background*

With their immense importance to the human condition, it is not surprising that methodology aimed. Not surprisingly, methodology aimed at derivatizing α-amino acids has received much attention.[131-135] To perform selective carbon framework modifications of amino acids, one must contend with the presence of N–H units that are more acidic than the latent C–H. The use of a Schiff base is one strategy to alkylate an amino ester (**Scheme 5.1A**)[136] this removes the acidic N–H proton and acidifies the C–H, facilitating formation of the requisite enolate.[137-143] Nature accesses the requisite enolate via the cyclized/dehydrated aromatic oxazolone, using it to epimerize α-stereocenters.[144] Indeed, the oxazolone enolate will react with a number of electrophiles, including Michael acceptors[107, 118, 128, 145-148] and is a common strategy for amino acid derivatization (**Scheme 5.1B**).[149] We became curious if a more direct route might be possible, specifically,

whether the enolate could be directly utilized without the need for an enolate surrogate (**Scheme 5.1C**).While Michael addition to an amino ester enolate has not been explored (**Scheme 5.1E**), the *C*-alkylation with alkyl halides (**Scheme 5.1C-D**) has been extensively utilized.[150-154] However, despite its use in the literature, key mechanistic questions remain unanswered especially concerning the degree of deprotonation of the requisite enolate involved in the alkylation.[150-152, 155-157]

In 1976, Krapcho proposed that under basic conditions *N*-acyl or carbamate protected amino esters must react through a dianion intermediate[158] (**Scheme 5.1C**). This logically stems from the fact that alkylation occurs at the less acidic α-carbon rather than at the more acidic N–H, and therefore must take place through the dianion in which the less stable carbanion reacts first. In 1985, Hoye[159] proposed an alternative mechanism in which the substrate first undergoes a kinetic deprotonation of the N–H with stoichiometric base, followed by a proton transfer from the C–H to generate the reactive monoanionic enolate (**Scheme 5.1D**). We reasoned if Hoye's hypothesis were true, then addition of an amino ester to a Michael acceptor could regenerate the base, making the reaction catalytic (**Scheme 5.1E**).

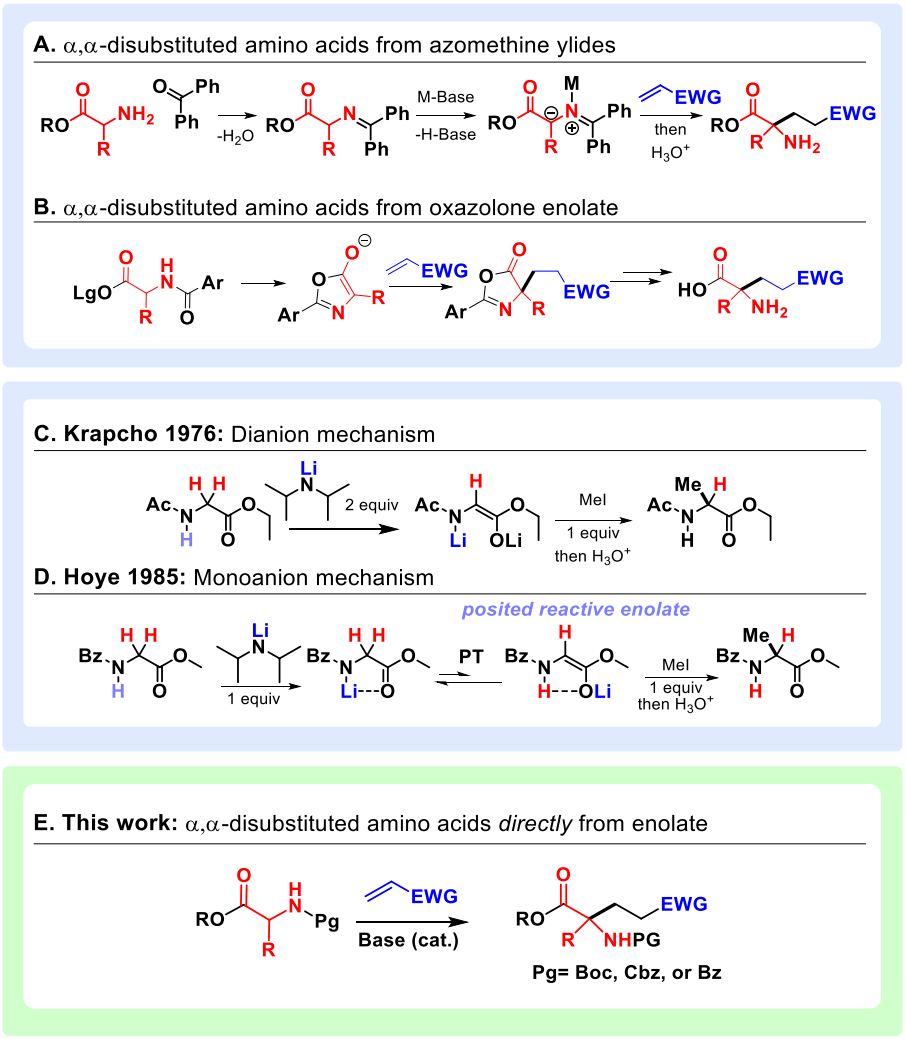

Scheme 5.1. The use of enolates and equivalents to access α,α-disubstituted amino acids

5.2 *Optimization studies*

We initiated our investigation using the conveniently synthesized *N*-benzoyl perfluoropyridinyl glycine (**A**, **Table 5.1)**.[160] We anticipated that the perfluoroaryl unit would acidify the αC–H and tilt the equilibrium towards the enolate. To **A** we added Hünigs base (DIPEA, 3 equiv) and methyl vinyl ketone (MVK, 3 equiv) in acetonitrile (0.5 M) (entry 1). Within 36 h we observed complete conversion of the starting material to a product alkylated at the carbon rather than at the nitrogen, and were able to isolate it in near quantitative yield.

Table 5.1. Optimization of Reaction Conditions

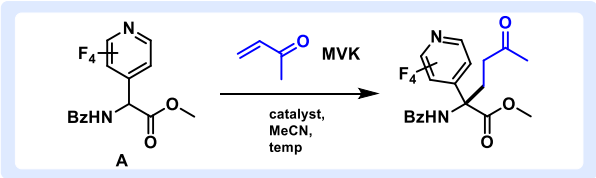

entry	MVK (equiv)	Base	Mol%	T (°C)	Time (h)	% conv.[a]	% NMR yield[b]
1.	3	DIPEA	300	22	36	100	>99
2.	3	TMG	105	-20	1	100	>99
3.	3	DBU	105	-20	1	71	64
4.	3	NaOH	105	-20	1	100	92
5.	1.05	TMG	105	-20	1	100	>99
6.	1.05	TMG	10	-20	1	100	>99
7.	1.05	TMG	1.0	-20	1	100	>99
8.	1.05	TMG	0.1	45	48	<3	<3
9.	1.05	MTBD	0.1	-20	1	100	>99
10.	1.05	MTBD	0.1	22	1	100	>99

a. Conversion determined by ^{19}F NMR. b. Yields determined by ^{19}F NMR relative to trifluoroacetic acid as internal standard.

While full conversion was achieved, the rate was rather modest. Switching to a stronger base such as tetramethylguanidine (TMG) (TMG-H$^+$, pKa in MeCN = 23.3 vs. ~18.8 for DIPEA-H$^+$)[114] or NaOH, substantially increased the rates, and the reaction completed within 1 h (Table 5.1, entries 2-4). Despite its enhanced basicity, DBU (pKa in MeCN = 24.3)[161] failed to give comparable rates and over time led to unidentified by-products in ^{19}F NMR spectra. Using TMG, we next attempted to lower the base loading and run the reaction catalytically. We observed complete conversion using catalyst loadings of both 10 and 1 mol% (entries 6 and 7). However, upon dropping the loading to 0.1 mol% TMG, no product was observed (entry 8). This lack of

reactivity could potentially be due to trace acidic impurities in the reaction mixture. However, we have previously observed TMG undergoing *N*–substitution of aromatic fluorides when subjected to highly electrophilic perfluoroaryl derivatives and could also explain the observation.[162-163] Upon switching to the bulky bicyclic superbase, MTBD (7-methyl-1,5,7-triazabicyclo[4.4.0]dec-5-ene, pKa 25.4 in MeCN),[164] the catalytic activity was completely restored using just 0.1 mol% both at room temperature and -20 ºC (entries 9-10).

5.3 *Substrate scope*

Satisfied, we next investigated the substrate scope of the Michael acceptor (Scheme 5.2A). The reaction is quite general and, in addition to MVK (2a), will abide many commercially available mono-substituted Michael acceptors. Both ethyl and *t*-butyl acrylates (2b and 2c) gave excellent yields, though a subtle difference was observed, potentially due to the greater steric demand of the *t*-butyl acrylate. Acrylonitrile gave nearly quantitative yield (2d), as did unsaturated sulfones (2e and 2f). Diactivated fumaronitrile also underwent addition, giving a diastereomeric ratio of 1.5/1 (2g). Resubjecting the product to the catalyst and solvent resulted in the erosion of the dr to 1.2/1, suggesting that selectivity may be challenging to maintain. Additionally, *N*-phenylmaleimide (2h) worked under these conditions, albeit at a noticeably diminished rate compared to the mono-substituted alkenes, but nonetheless resulted in high yield of a mixture of diastereomers, which could be partially resolved upon isolation. It is worth noting that reaction with nitroalkenes failed to give the product and instead appeared to react with the base. Additionally, many α-substituted alkenes and electrophiles failed to react appreciably with 1a (Table 5.2).

Scheme 5.2. Exploration of the Michael acceptor, α-substituent, and the amino protecting group

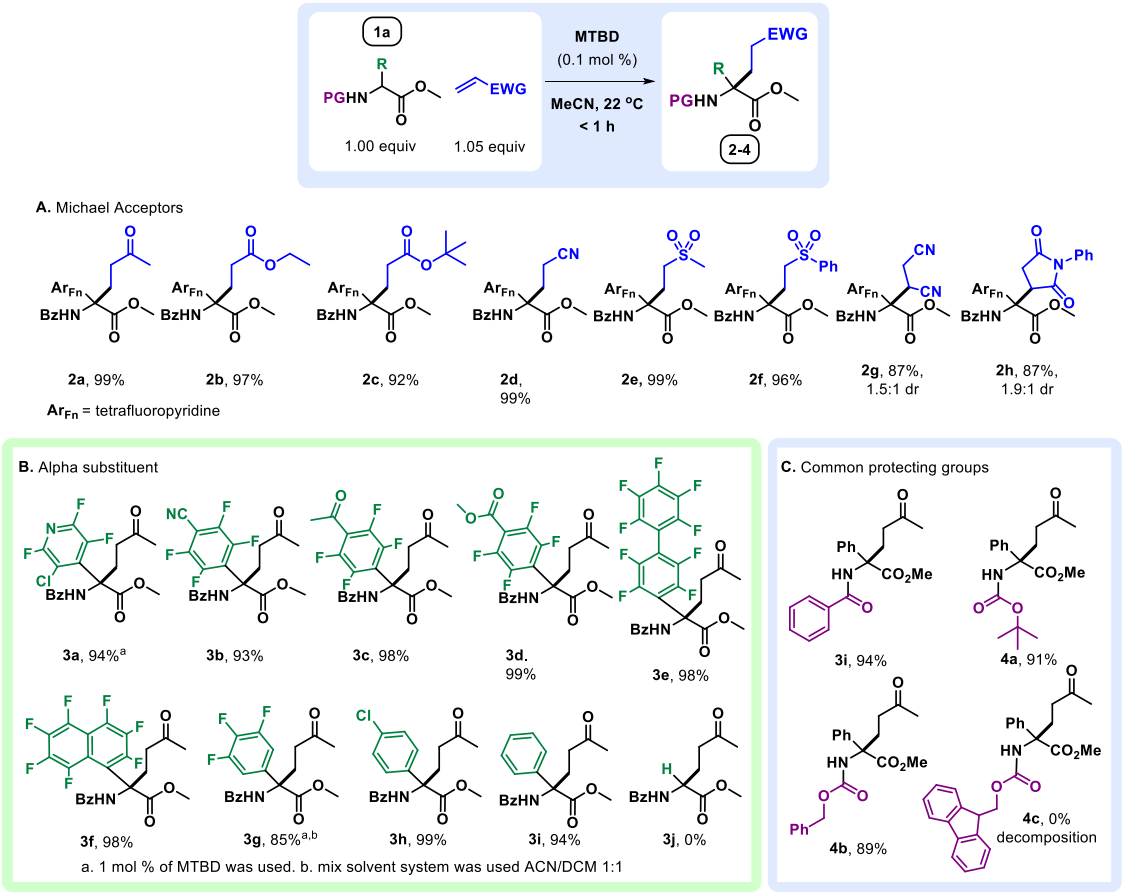

Table 5.2 List of failed Michael acceptors and other electrophiles

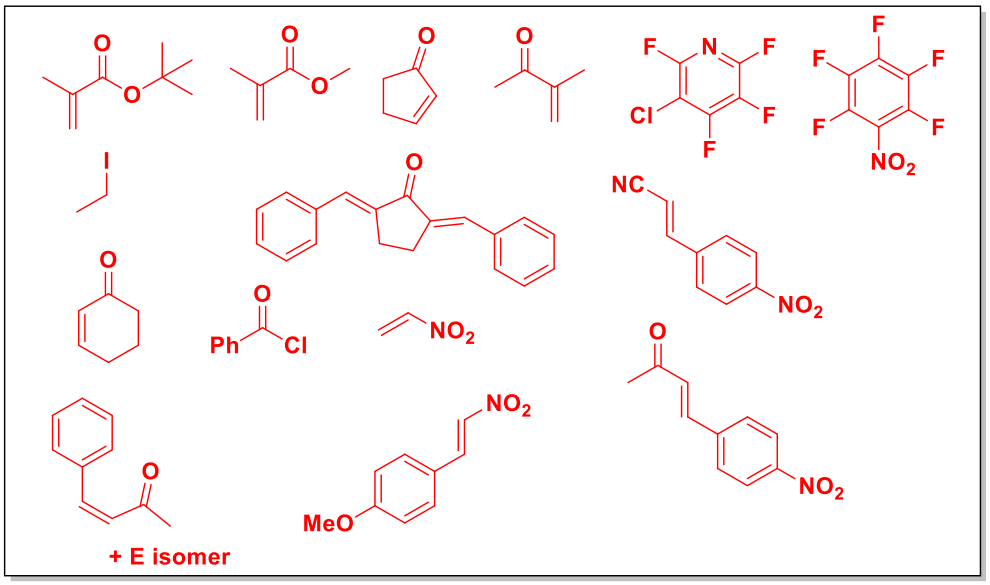

Next, we explored the scope of the aryl side chain (Scheme 5.2B). More acidic substrates (3a and 3b) underwent smooth addition. It is noteworthy that Touzin[136] observed that *N,N*-dimethyl-α-amino ester enolates readily undergo 1,2-addition to ketones, whereas we exclusively observed 1,4-addition to α,β-unsaturated ketones (2a, and 3a-3h). In fact, not even in the case of activated perfluoroaryl ketones (3c), did we observe 1,2-addition. Perfluoroarylesters (3d) and less stabilized enolates like perfluorobiphenyl, perfluoronapthalene amino esters (3e and 3f), and even trifluorophenyl glycine (3g), 4-Cl-phenyl glycine (3h), and phenylglycine (3i) worked well and gave excellent yields. However, attempts to use benzoyl protected glycine (3j) failed to produce any product, even with elevated temperatures and higher catalyst loading.

Next, to make the reaction more broadly useful, we investigated the nitrogen protecting groups standard to peptide coupling for the phenyl glycine methyl ester (Scheme 5.2C). We found that both *N*-Boc (4a) and *N*-Cbz (4b) protecting groups facilitated smooth addition, giving similar yields to the *N*-benzoyl group. Not surprisingly, when we attempted to use the base-labile *N*-Fmoc protected phenyl glycine the substrate underwent decomposition (4c).

5.4 *DFT calculations*

Next, we turned our attention to the reaction mechanism. While Hoye's mono-anion/proton shift mechanism seemed consistent (**Scheme 5.1D**), with certain substrates we qualitatively observed a rate dependence on the loading of the electrophile which appeared to be greater than first order. We wondered if the first step of the reaction might be an aza-Michael addition (**Scheme 5.3**)., which effectively removes the more acidic N–H, allowing the base to deprotonate the αC–H. This would generate the requisite enolate, which would then undergo Michael addition, revealing the product via a retro-aza-Michael reaction.

Scheme 5.3 Retro-aza-Michael reaction

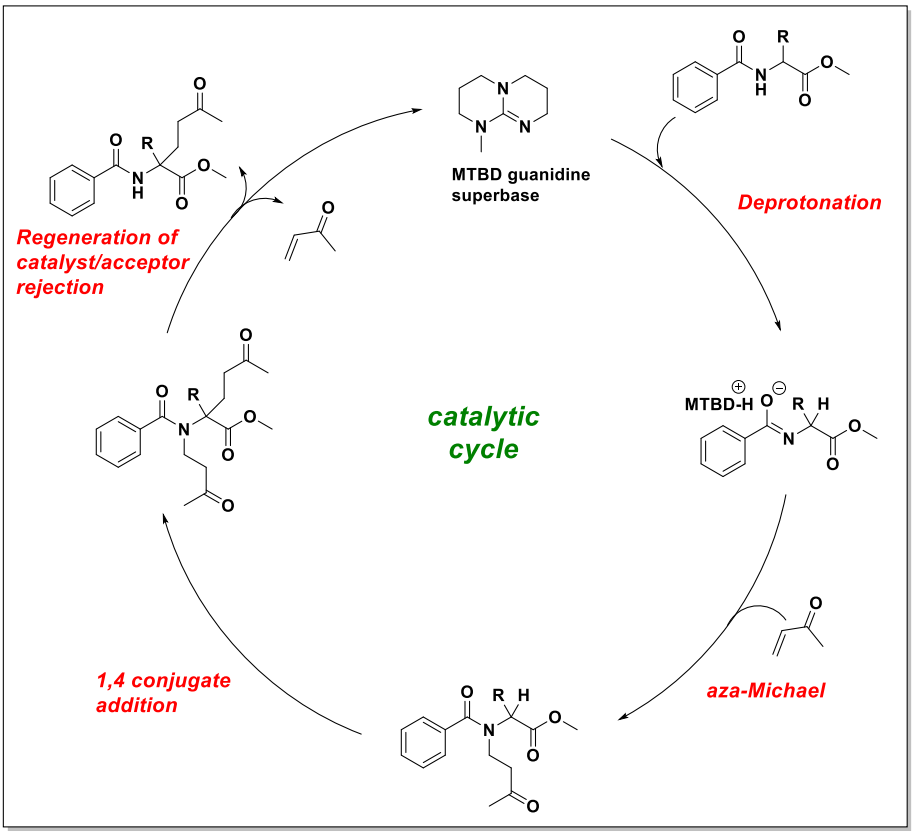

In order to probe the idea of temporarily masking the acidic proton, we minimized the geometries and calculated energies (**Table 5.4**) using DFT (B3LYP/6-311+G(2d,p)). The *N*-alkylated species (***comp*-B, Table 5.4**) was endothermic by 1.7 kcal/mol when compared to the starting materials, but +9.5 kcal/mol when compared to the *C*-alkylated final product (***comp*-C**). The endothermic nature of the *N*-alkylation is reasonable, considering that there are no examples in the literature of the product of an aza-Michael addition to an α-amino acid derivative, perhaps due to the loss of a stabilizing H-bond in the product.

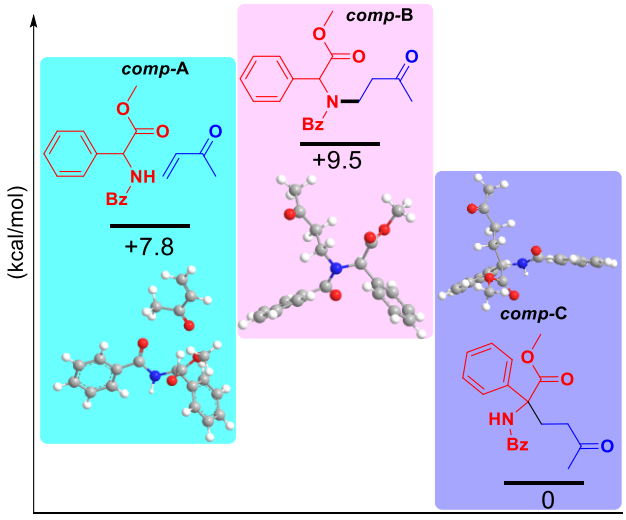

Table 5.3 DFT calculations: B3LYP/6-311+G(2d,p) optimized geometries for starting materials and products.

Below are various searches (**Search 1-3**) conveying reactions of aza-michael type observed in literature and SciFinder searches were performed on the latest online version. After conducting a search on SciFiner consisting of a amide and a Michael accepotr, it was found that indeed an Aza-Micheal type of reaction is known and well explored (**Search 1**). The first search (**Search 1**) clearly shows the aza-Micheal to form a tertiary nitrogen is possible. However, looking at the subset of products that consisted of an alpha-amino carbonyl motif that (similar to our products), no products were found (**Search 2**). Moreover, when starting with an alpha-amino carbonyl (**Search 3**) 71 hits were observed. Most of these examples were either irrelevant or unique multistep cases. These searches give support to the endothermic nature of N-alkylation products.

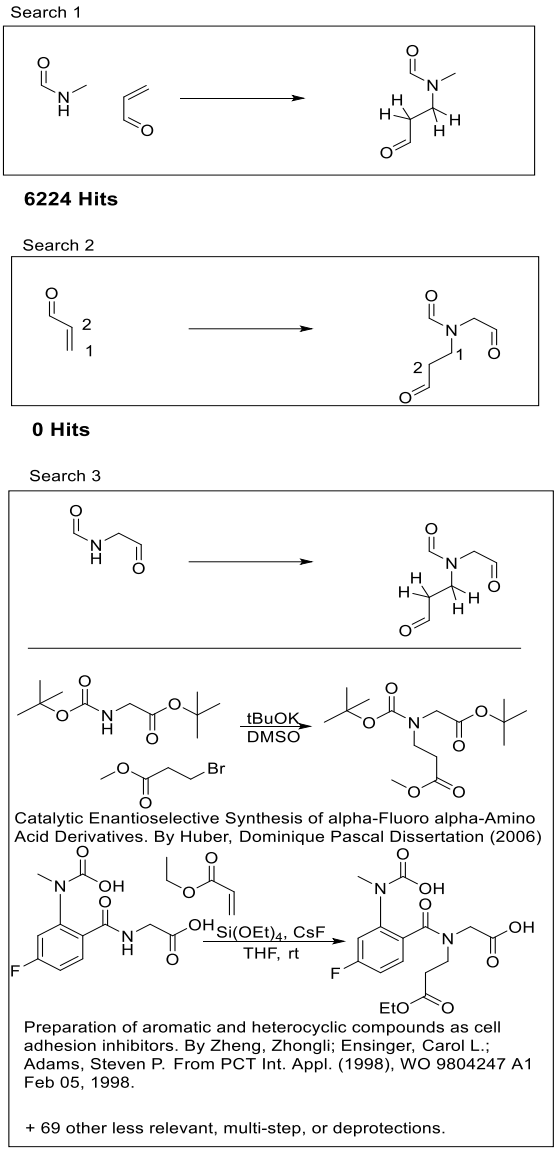

Thus, our calculations explained why the *N*-alkylated product was never observed, but suggested ***comp*-A** and ***comp*-B** were energetically close enough to allow for transient *N*-alkylation. To probe this scenario, we subjected unreactive *N*-Bz glycine methyl ester (**Scheme 5.2B, 3j**) to modified conditions, allowing us to study the proposed first step, reversible *N*-alkylation (eq 1).

5.5 *(retro)aza-Michael reaction study*

Upon exposure of the protected glycine (**Scheme 5.3**, A) to MTBD and CD_3OD, rapid deuterium incorporation was observed at *N* (*int*-1). Then, protio-MVK was added to the reaction mixture. As expected, no *N*- (*int*-2) or *C*-alkylation (3j) was observed. Decisively, we did not observe deuterium scrambling into the MVK (D-MVK), which would support transient and reversible *N*-alkylation. Thus, we concluded that the Aza-Micheal/C-Micheal/retro-aza-Micheal mechanism was not operative, and that Hoye's mechanism was likely operative in our system.

Scheme 5.4 (retro)aza-Michael reaction study

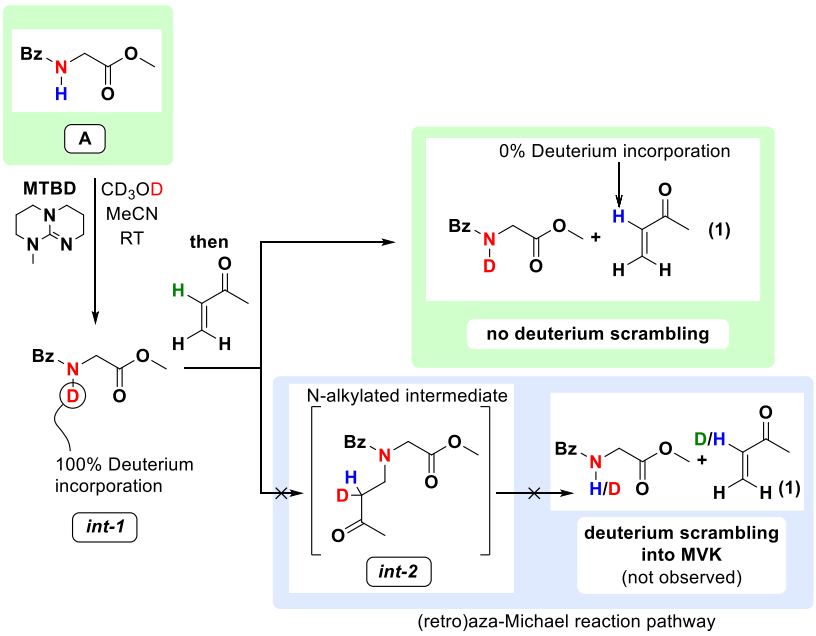

5.6 *Michael reaction of natural amino esters*

The implication was that substrates that underwent C–C bond formation were doing so because the lowered pKa of the αC–H allowed sufficient quantities of the reactive enolate to form. However, substrates devoid of acidifying functional groups, such as simple glycine and other α-alkyl amino esters were not sufficiently acidic to form the requisite enolate. To test this, we

examined commercially available Boc-protected trifluoroalanine methyl ester, which indeed gave 4d (eqn 2) in 83% isolated yield.

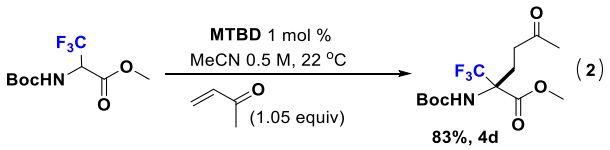

We postulated that we could selectively acidify the αC–H over the N–H by making the ester component more electron withdrawing. The *N*-Bz trifluoroethyl esters of several natural amino acids, which were otherwise, unreactive (**Scheme 5.4**), provided the necessary acidification of the C–H to turn on reactivity. Admittedly, the reactions are more sluggish than previous substrates, and required both higher catalyst loadings and higher temperatures, but nonetheless reached full conversion at room temperature. Attempted reaction of the methyl ester indicated the essential nature of the trifluoroethyl ester component (5a vs 5b). The trifluoroethyl esters facilitated both the desired reaction, but were also found to be prone to hydrolysis (from adventitious H_2O). We found that switching the solvent from MeCN to DCM was essential to prevent hydrolysis.

Scheme 5.5 Michael reaction of natural amino esters

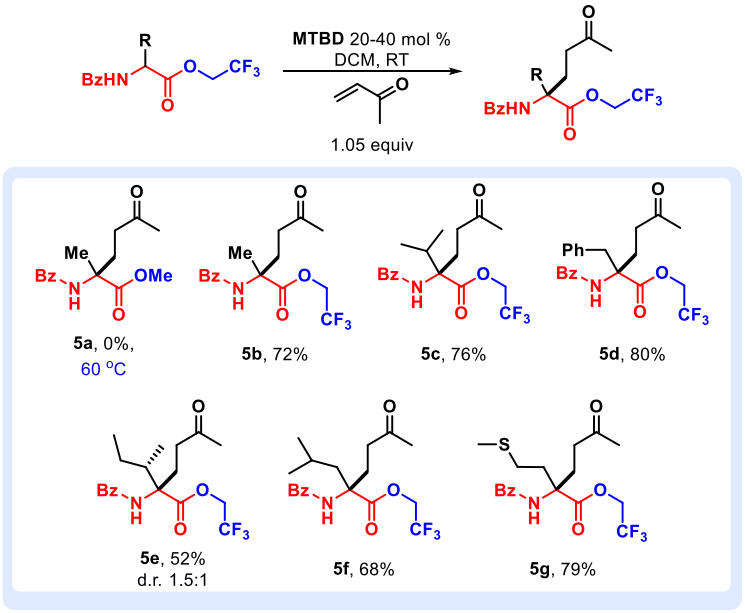

Scheme 5.6 Failed experiments

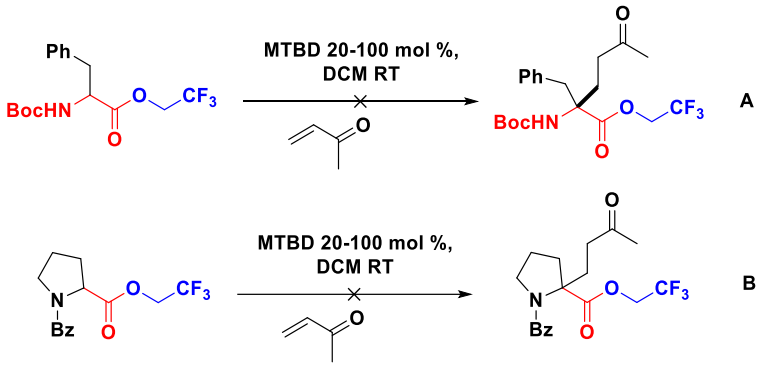

The *N*-Bz trifluoroethyl esters of several natural amino acids provided the necessary acidification of the C–H to turn on reactivity but when *N*-Boc-Phe trifluoroethyl ester was attempted the reaction gave no conversion (**Scheme 5.5A**). We are unsure of the reason why this reaction failed and it is even more puzzeling since previously *N*-Boc protected amino acids did convert to product. Further investigation of this reaction would be worthwile.

Probing if the NH of the reaction was important we applied the reaction conditions to proline which displays no NH. We were surprised to find out that the N-Bz-pro trifluoroethyl ester

failed to react (**Scheme 5.5B**). We speculated this could be due to stabilization of the carbonyl with the adjacent NH, but again this is a question we have yet to probe.

5.7 *Late-stage modification of peptides*

Having established the importance of the α-substituent in facilitating the reaction, we speculated we could use the difference in reactivity between α-aryl and α-alkyl amino acids to perform selective modification of peptides possessing such units. We synthesized dipeptide Boc-Ala-Phg-OMe to test our hypothesis and after subjecting the dipeptide to our reaction conditions (**Scheme 5.6**, eqn 3), we were pleased to observe a single regioisomer in which *C*-alkylation occurred exclusively at the phenyl glycine subunit in good yield (6a, 73% yield, 92% BRSM). The reaction took place with little stereoinduction (dr 1.2/1), leaving open the possibility of external control. Intrigued by this result we thought it would be worthwhile to apply our reaction conditions to the dipeptide Boc-Phe-Phg-OMe (**Scheme 5**, eq 4), where the amino acid subunits are reversed, and the phenyl glycine contains an amide instead of a methyl ester. We were pleased to observe the product where *C*-alkylation occurred exclusively at the phenyl glycine subunit but the rate was sluggish and the yield was significantly lower (6b, 38% yield dr 1.6/1, 69% BRSM). Earlier attempts to try to selectively alkylate peptides through multianion approaches were often fraught with solubility issues when dealing with polylithiated peptides at low temperatures.[165-166] The monoanion approach circumvents this issue altogether.[165, 167] We next examined the dipeptide DAPT which is a γ-secretase inhibitor[168] and has been shown *in vivo* to selectively inhibit the formation α-amyloid[168] involved in Alzheimer's disease.[168] More generally, it is thought to indirectly inhibit NOTCH, an important α-secretase substrate[169] involved in autoimmune and proliferative diseases.[169] Exposing DAPT to just 1.05 equivalents of MVK and 50 mol% MTBD led to full conversion to give 6c in 90% yield. Similarly, the reaction was sluggish compared to the simple phenylglycine derivative. One potential reason for this is the addition of H-bond donors, which could stabilize, and therefore, retard the attack of the requisite carbanion on the

electrophile. Additionally, it is expected that there will be greater populations of unproductive aza-anions that must funnel to the reactive enolate.

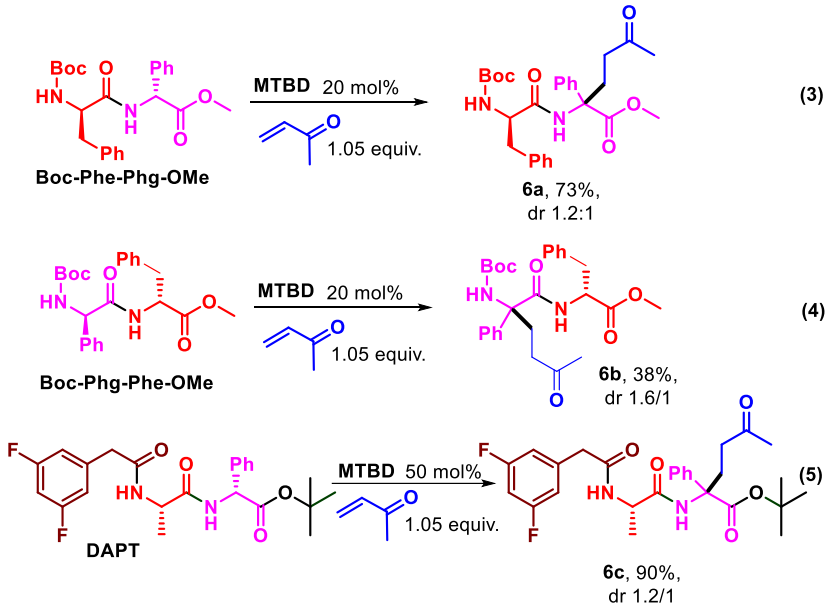

Scheme 5.7 Late-stage modification of peptides

A deuterium labeling study indicated that both N–Hs exchanged, as did the αC–H of the phenylglycine unit. No scrambling was observed at the corresponding alanine αC–H. The phenyl glycine methine integrations decreased displaying evidence of deuterium incorporation at the α-carbon of the phenyl glycine subunit. Integrations observed: **0.51**, 1.05, 3.00 (Phg-H, Ala-H, Phg-OMe) see the labeled spectrum below.

Figure 5.1 Deuterium labeling study Phg vs. Ala

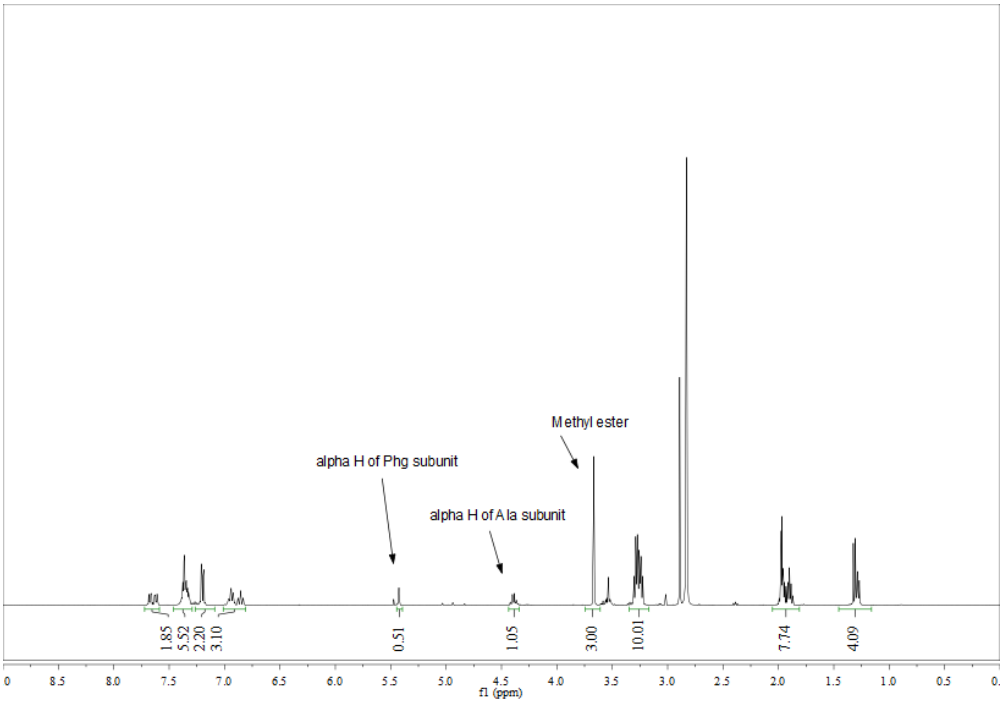

In conclusion, we have investigated the direct activation of useful amino acid derivatives. In contrast to current alkylation strategies, we have demonstrated the ability to access the enolate through a strategy that involves funneling of a monoanion to the reactive carbanion. The operational simplicity, high chemo-selectivity, and the fast rate of the reaction make it particularly attractive for further development. This reaction significantly expands access to non-natural amino acids derivatives, as we have demonstrated strategies to elaborate both natural, non-natural amino esters, and the ability to selectively functionalize the more acidic residues within small peptides.

5.8 *Experimental section*

General Experimental:

All reagents were obtained from commercial suppliers (Aldrich, VWR, TCI Chemicals, and Oakwood Chemicals) and used without further purification unless otherwise noted. Reactions were monitored by thin layer chromatography (TLC), (obtained from sorbent technology Silica XHL TLC Plates, w/UV254, glass backed, 250 µm, 20 x 20 cm) and were visualized with ultraviolet light, potassium permanganate stain, GC-MS (QP 2010S, Shimadzu equipped with auto sampler) and ^{19}F and ^{1}H NMR.

Isolations were carried out using Teledyne Isco Combiflash Rf 200i flash chromatograph with Sorbtech normal phase silica (4 g, 12 g, 24 g, 40 g) with product detection at 254 and 288 nm and evaporative light scattering detection. NMR spectra were obtained on a 400 MHz Bruker Avance III spectrometer and 400 MHz Varian spectrometer. ^{1}H, ^{19}F and ^{13}C NMR chemical shifts are reported in ppm relative to the residual protio solvent peak or TMS signal. IR spectra were recorded on Varian 800 FT-IR. Mass spectra (HRMS) analysis was performed on LTQ-OrbitrapXL by Thermo Scientific ltd using a Heated-electrospray ionization (H-ESI) source.

Synthesis of N-acyl/carbamate amino esters

II.i Procedures for the esterification of amino acids[170]

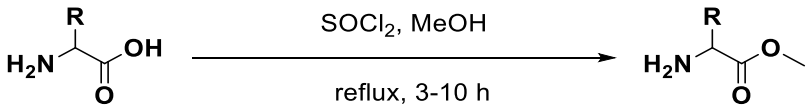

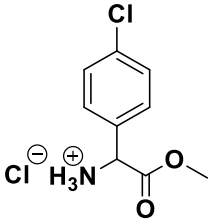

S-1: 1-(4-Chlorophenyl)-2-methoxy-2-oxoethanaminium chloride. *p*-Chlorophenylglycine (1 g, 5.39 mmol) was dissolved in MeOH (5 mL). The solution was cooled to 0 °C and thionyl chloride (0.78 mL, 10.8 mmol) was added dropwise. The reaction mixture was heated under reflux for 3 h.

Cooling to rt followed by concentration in vacuo afforded the title compound as a white solid (1.27 g, quant.). Spectral data matched the literature values.[170]

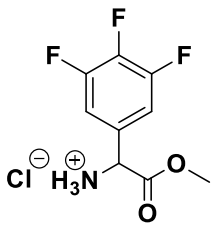

S-2: 1-(3,4,5-trifluoropheny)-2-methoxy-2-oxoethanaminium chloride. 3,4,5-trifluorophenylglycine (2.0 g, 9.7 mmol) was dissolved in MeOH (30 mL). The solution was cooled to 0 ◦C and thionyl chloride (1.4 mL, 19.5 mmol) was added dropwise. The reaction mixture was heated under reflux for 3 h. Cooling to rt followed by concentration in vacuo afforded the title compound as a crude semi-white solid (2.3 g, 93%). The crude compound was moved to next step without further purification.

***N*-Acylation/protection of amino acids/esters**

-General procedure A for the preparation of *N*-benzoyl-α-amino acids[160]

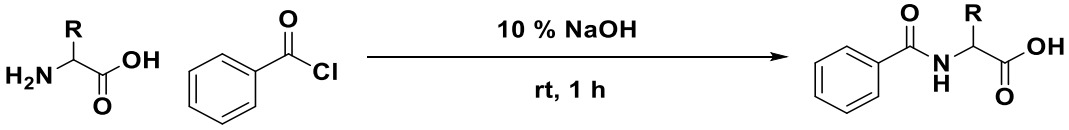

Benzoyl chloride **(1.2 equiv**) was added in 4 portions over **30** minutes to a **0 ºC** solution of the amino acid (**1 equiv)** and 10 % NaOH **(3.8 equiv**) in distilled water (open to air). After the addition was complete, the ice bath was removed, and the reaction was quenched by the dropwise addition of concentrated aqueous hydrochloric acid until **pH 1** was reached, which resulted in the precipitation of the product. The solid was isolated by filtration and then recrystallized from water. The resulting crystals were air dried to give the desired ***N*-**benzoyl amino acid, which showed no trace of benzoic acid by ^{1}H NMR. If benzoic acid was detected, the compound was stirred in cool (0 ^{o}C) 1 M benzene (or toluene in relation to starting material)for 1 h,, and isolated by filtration.

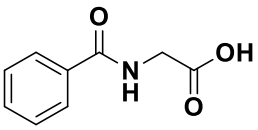

***N*-benzoyl glycine**: The **general procedure A** was followed using glycine (5.00 g, 66.6 mmol), benzoyl chloride (9.30 mL, 79.2 mmol), 10 % NaOH (100 mL, 251 mmol) to afford the title compound in 93% yield after isolation (10.86 g, 60.9 mmol) as a white solid. ^{1}H-NMR matched previous literature.[126]

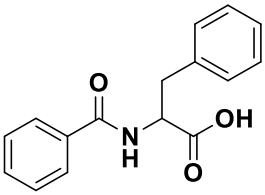

***N*-benzoyl phenyl alanine**: The **general procedure A** was followed using phenyl alanine (2.50 g, 15.1mmol), benzoyl chloride (2.11 mL, 18.1 mmol), 10 % NaOH (23.0 mL, 57.4 mmol) to afford the title compound in 79% yield after isolation (3.2 g, 11.9 mmol) as a white solid. ^{1}H-NMR matched previous literature.[128]

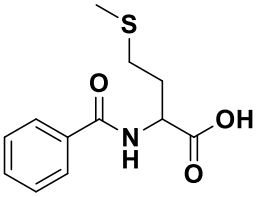

***N*-benzoyl methionine**: The **general procedure A** was followed using methionine (2.50 g, 16.8 mmol), benzoyl chloride (2.34 mL, 20.1 mmol), 10 % NaOH (25.5 ml, 63.8 mmol) to afford the title compound in 79% yield after isolation (3.2 g, 11.9 mmol) as a white solid.

^{1}H-NMR matched previous literature.[129]

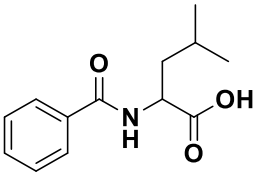

***N*-benzoyl leucine**: The **general procedure A** was followed using leucine (2.00 g, 15.2 mmol), benzoyl chloride (2.12 mL, 18.3 mmol), 10 % NaOH (23.1 ml, 57.8 mmol) to afford the title compound in 67% yield after isolation (2.4 g, 10.2 mmol) as a white solid. ^{1}H-NMR matched previous literature.[128]

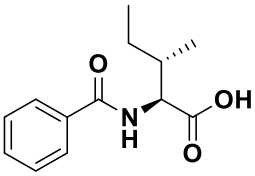

***N*-benzoyl L-isoleucine**: The **general procedure A** was followed using L-isoleucine (300 mg, 2.3 mmol), benzoyl chloride (0.32 mL, 2.7 mmol), 10 % NaOH (23.1 mL, 8.7 mmol) to afford the title compound in 43% yield after isolation (247 mg, 0.99 mmol) as a white solid. ^{1}H-NMR matched previous literature.[171]

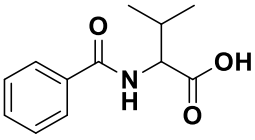

***N*-benzoyl Valine**: The **general procedure A** was followed using leucine (1 g, 8.5 mmol), benzoyl chloride (1.2 mL, 10 mmol), 10 % NaOH (10 mL, 25.5 mmol) to afford the title compound in 88% yield after isolation (1.64 g, 7.5 mmol) as a white solid. ^{1}H-NMR matched previous literature.[128]

-General procedure B for the preparation of *N*-benzoyl-α-amino esters[172]

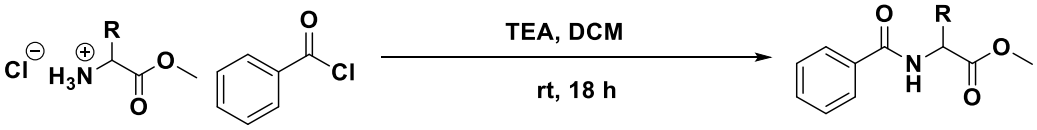

A solution of benzoyl chloride (**1 equiv**) in CH_2Cl_2 (**2 M**) was added dropwise to a suspension of the glycine methyl ester hydrochloride (**1 equiv**) and triethylamine (2.2 equiv) in CH_2Cl_2 (**0.5 M**) at 0 ^{o}C. The reaction mixture was stirred at room temperature for 18 h, it was washed with equal volumes of aq. HCl (**3 x 1 M**), saturated aq. $NaHCO_3$ (**3x**) and saturated aq. NaCl, successively. Next the organic extract was dried (over $MgSO_4$) and concentrated under reduced pressure. Then, the crude amide was purified via column chromatography.

- General procedure C for the preparation of *N*-benzoyl-α-amino esters[173]

N-Benzoyl amino acid (**1 equiv**), alcohol (**3 equiv**), EDC (**1.5 equiv**), DMAP (**1 equiv**) were dissolved in anhydrous DCM (**0.2 M**) and the reaction was stirred for 16 h at room temperature

under an argon atmosphere. The workup consisted of diluting solution with DCM and quenching with equal amount of water. The organic layer was separated and washed with equal amount of sat. $NaHCO_3$ (**3x**), 0.01 M HCl (**2x**) (this step was omitted when synthesizing trifluoroethyl esters), and water twice. The organic layer was separated, and the solution was concentrated under vacuum. Flash column chromatography was used to purify the desired compound.

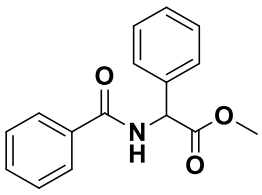

Methyl 2-benzamido-2-phenylacetate. The **general procedure B** was followed using the glycine methyl ester hydrochloride (1.00 g, 4.81 mmol), benzoyl chloride (0.560 mL, 4.81 mmol), triethylamine (1.48 mL, 10.6 mmol) to afford the title compound in 90% yield after isolation (1.17 g, 4.34 mmol) as a white solid. ^{1}H-NMR matched previous literature.[174]

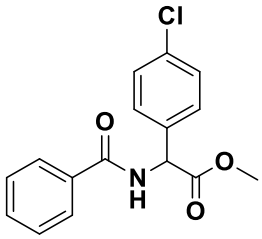

methyl 2-benzamido-2-(4-chlorophenyl)acetate. The **general procedure B** was followed using the 1-(4-Chlorophenyl)-2-methoxy-2-oxoethanaminium chloride (1.5 g, 6.35 mmol), benzoyl chloride (0.740 mL, 6.35 mmol), triethylamine (1.97 mL, 13.97 mmol) to afford the title compoound in 83% yield after isolation (1.6 g, 5.37 mmol) as a white solid. ^{1}H NMR (400 MHz, Chloroform-*d*) δ 7.84 (d, *J* = 7.1 Hz, 2H), 7.55 (t, *J* = 8.0 Hz, 1H), 7.46 (t, *J* = 7.9 Hz, 2H), 7.43 – 7.33 (m, 4H), 7.29 (d, *J* = 6.3 Hz, 1H), 5.77 (d, *J* = 6.7 Hz, 1H), 3.79 (s, 3H).^{13}C NMR (101 MHz, Chloroform-*d*) δ 171.3, 166.6, 135.3, 134.6, 133.4, 132.1, 129.2, 128.8, 128.7, 127.3, 56.31, 53.2.

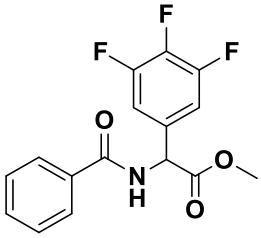

methyl 2-benzamido-2-(3,4,5-trifluorophenyl)acetate. The **general procedure B** was followed using the 1-(3,4,5-trifluoropheny)-2-methoxy-2-oxoethanaminium chloride. (0.700 mg, 2.74 mmol), benzoyl chloride (0.318 mL, 2.74 mmol), triethylamine (0.841 mL, 6.03 mmol) to afford the title compound in 71% yield after isolation (628 mg, 1.95 mmol) as a white solid. ^{1}H-NMR matched previous literature. ^{19}F NMR (376 MHz, Chloroform-

d) δ -131.81 – -134.40 (m), -160.07 (tt, *J* = 20.4, 6.4 Hz). ^{1}H NMR (400 MHz, Chloroform-*d*) δ 7.85 (d, *J* = 7.1 Hz, 2H), 7.57 (t, *J* = 7.4 Hz, 1H), 7.47 (t, *J* = 7.5 Hz, 2H), 7.41 (d, *J* = 6.2 Hz, 1H), 7.12 (dd, *J* = 7.9, 6.4 Hz, 2H), 5.72 (d, *J* = 6.4 Hz, 1H), 3.82 (s, 3H). ^{13}C NMR (101 MHz, Chloroform-*d*) δ ^{13}C NMR (101 MHz, Chloroform-*d*) δ 170.5, 166.7, 151.5 (ddd, *J* = 251.4, 10.2, 3.9 Hz), 139.9 (dt, *J* = 253.0, 15.3 Hz), 133.1, 132.4, 128.9, 128.5, 127.8 – 126.4 (m), 113.3 – 110.1 (m), 55.9 (d, *J* = 1.8 Hz), 53.6.

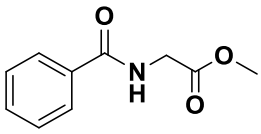

methyl benzoylglycinate. The **general procedure C** was followed using the *N*-benzoyl glycine (250 mg, 1.40 mmol), methanol (0.170 mL, 4.19 mmol), EDC (401 mg, 2.09 mmol), DMAP (170 mg, 1.40 mmol), and 7 mL of CH_2Cl_2 to afford the title compound in 73% yield after isolation (197 mg, 1.02 mmol) as a white solid. ^{1}H-NMR matched previous literature.[175]

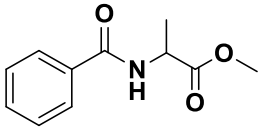

methyl benzoylalaninate. The **general procedure C** was followed using the *N*-benzoyl alanine (300 mg, 1.55 mmol), methanol (0.188 mL, 4.66 mmol), EDC (447 mg, 2.33 mmol), DMAP (190 mg, 1.55 mmol), and 7.8 mL of CH_2Cl_2 to afford the title compound in 82% yield after isolation (264 mg, 1.27 mmol) as a white solid. ^{1}H-NMR matched previous literature.[176]

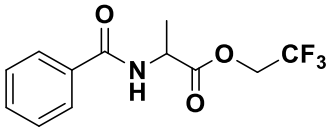

2,2,2-trifluoroethyl benzoylalaninate. The **general procedure C** was followed using the *N*-benzoyl alanine (500 mg, 2.59 mmol), trifluroethanol (0.586 mL, 7.76 mmol), EDC (744 mg, 3.88 mmol), DMAP (316 mg, 2.59 mmol), and 13 mL of CH_2Cl_2 to afford the title compound in 54% yield after isolation (290 m g, 1.40 mmol) as a white solid. ^{19}F NMR (376 MHz, Chloroform-*d*) δ -73.85 (t, *J* = 8.3 Hz). ^{1}H NMR (400 MHz, Chloroform-*d*) δ 7.80 (d, *J* = 7.0 Hz, 2H), 7.53 (t, *J* = 7.4 Hz, 1H), 7.46 (t, *J* = 7.4 Hz, 2H), 6.58 (d, *J* = 6.9 Hz, 1H), 4.90 (p, *J* = 7.2 Hz, 1H), 4.67 (dq, *J* = 12.6, 8.3 Hz, 1H), 4.48 (dq, *J* = 12.6, 8.3 Hz, 1H), 1.58 (d, *J* = 7.3 Hz, 3H).^{13}C NMR (101 MHz,

Chloroform-*d*) δ 172.2, 167.6, 133.9, 132.3, 129.0, 127.9 – 127.3 (m), 123.1 (q, *J* = 277.3 Hz), 61.3 (q, *J* = 36.9 Hz), 48.8, 18.4.

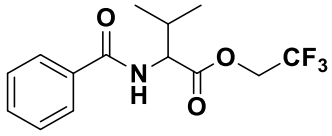

2,2,2-trifluoroethyl benzoylvalinate. The **general procedure C** was followed using the *N*-benzoyl valine (600 mg, 2.71 mmol), trifluroethanol (0.614 mL, 8.13 mmol), EDC (780 mg, 4.07 mmol), DMAP (331 mg, 2.71 mmol), and 14 mL of CH_2Cl_2 to afford the title compound in 67% yield after isolation (551 mg, 1.82 mmol) as a white solid. ^{19}F NMR (376 MHz, Methylene Chloride-d_2) δ -74.05 (t, *J* = 8.5 Hz). ^{1}H NMR (400 MHz, Methylene Chloride-d_2) δ 7.79 (d, *J* = 8.0 Hz, 2H), 7.54 (d, *J* = 7.5 Hz, 1H), 7.47 (t, *J* = 7.4 Hz, 2H), 6.52 (d, *J* = 8.5 Hz, 1H), 4.79 (dd, *J* = 8.5, 5.1 Hz, 1H), 4.59 4.76 – 4.40 (m, 2H), 2.31 (hept, *J* = 6.9, 5.1 Hz, 1H), 1.03 (dd, *J* = 9.5, 6.9 Hz, 6H). ^{13}C NMR (101 MHz, Methylene Chloride-d_2) δ 171.2, 167.8, 134.6, 132.4, 129.2, 127.6, 123.5 (q, *J* = 277.2 Hz), 61.2 (d, *J* = 36.7 Hz), 58.1, 31.8, 19.3, 18.2.

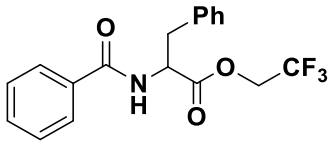

2,2,2-trifluoroethyl benzoylphenylalaninate. The **general procedure C** was followed using the *N*-benzoyl phenylalanine (1000 mg, 3.71 mmol), trifluroethanol (0.841 mL, 11.1 mmol), EDC (1068 mg, 5.57 mmol), DMAP (454 mg, 3.71 mmol), and 14 mL of CH_2Cl_2 to afford the title compound in 61% yield after isolation (796 m g, 2.27 mmol) as a white solid. ^{19}F NMR (376 MHz, Chloroform-*d*) δ -73.48 (t, *J* = 8.3 Hz). ^{1}H NMR (400 MHz, Chloroform-*d*) δ 7.71 (d, *J* = 7.1 Hz, 2H), 7.52 (t, *J* = 7.4 Hz, 1H), 7.43 (t, *J* = 7.9 Hz, 2H), 7.36 – 7.27 (m, 3H), 7.16 (d, *J* = 6.5 Hz, 2H), 6.46 (d, *J* = 7.7 Hz, 1H), 5.18 (dt, *J* = 7.8, 5.9 Hz, 1H), 4.66 – 4.41 (m, 2H), 3.39 – 3.20 (m, 2H).

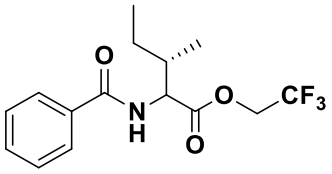

2,2,2-trifluoroethyl benzoyl-iso-leucinate. The **general procedure C** was followed using the *N*-benzoyl iso-leucine (250 mg, 1.06 mmol) as one diastereomer, trifluroethanol (0.319 mL, 3.19 mmol), EDC (306 mg, 1.59 mmol), DMAP (130 mg, 1.06 mmol), and 5.3 mL of CH_2Cl_2 to afford the title compound in 78% yield after isolation (263 mg, 0.83 mmol) as a white solid. ^{19}F NMR (376 MHz, Methylene Chloride-d_2) δ -74.03 (t, *J* = 8.3 Hz), -74.09 (d, *J* = 8.4 Hz). ^{1}H NMR (400 MHz, Methylene Chloride-d_2) δ 7.78 (dt, *J* = 8.3, 1.2 Hz, 4H), 7.58 – 7.52 (m, 2H), 7.47 (tt, *J* = 8.3, 0.9 Hz, 4H), 6.54 (d, *J* = 7.9 Hz, 1H), 6.49 (d, *J* = 8.3 Hz, 1H), 4.96 (dd, *J* = 8.7, 4.2 Hz, 1H), 4.83 (dd, *J* = 8.4, 5.2 Hz, 1H), 4.68 (dqd, *J* = 12.7, 8.5, 1.4 Hz, 2H), 4.49 (dqd, *J* = 12.7, 8.5, 2.0 Hz, 2H), 2.17 – 1.98 (m, 2H), 1.61 – 1.44 (m, 5H), 1.38 – 1.23 (m, 2H), 1.06 – 0.93 (m, 12H). ^{13}C NMR (101 MHz, Methylene Chloride-d_2) δ 171.57, 171.18, 167.83, 167.65, 134.65, 134.59, 132.36, 129.18, 127.59 – 127.53 (m), 124.89, 122.14, 119.38, 61.16 (qd, *J* = 36.7, 6.0 Hz), 57.40, 56.23, 38.38, 38.16, 26.83, 25.84, 15.83, 15.00, 12.01, 11.82. d.r.-1.6/1.

2,2,2-trifluoroethyl benzoylleucinate. The **general procedure C** was followed using the *N*-

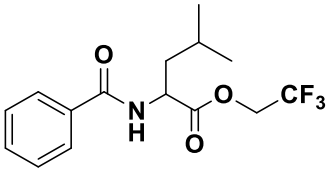

benzoyl leucine (1000 mg, 4.250 mmol), trifluroethanol (1.275 mL, 12.75 mmol), EDC (1222 mg, 6.37 mmol), DMAP (519 mg, 4.25 mmol), and 21 mL of CH_2Cl_2 to afford the title compound in 88% yield after isolation (1187 mg, 3.74 mmol) as a white solid. ^{19}F NMR (376 MHz, Methylene Chloride-d_2) δ -74.15 (t, *J* = 8.5 Hz). ^{1}H NMR (400 MHz, Methylene Chloride-d_2) δ 7.79 (d, *J* = 7.1 Hz, 2H), 7.54 (t, *J* = 7.4 Hz, 1H), 7.47 (d, *J* = 7.7 Hz, 2H), 6.57 (d, *J* = 8.1 Hz, 1H), 4 4.92 – 4.77 (m, 1H), 4.64 (dq, *J* = 12.7, 8.5 Hz, 1H), 2.00 – 1.53 (m, 3H), 1.06 – 0.94 (m, 6H). ^{13}C NMR (101 MHz, Methylene Chloride-d_2) δ 172.2, 167.7, 134.4, 132.4, 129.2, 127.6, 125.4 – 119.1 (m), 61.3 (q, *J* = 36.7 Hz), 51.7, 41.5, 25.6, 23.1, 22.1.

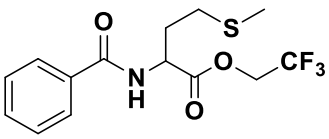

2,2,2-trifluoroethyl benzoylmethioninate. The **general procedure C** was followed using the *N*-benzoyl leucine (1000 mg, 3.95 mmol), trifluroethanol (0.894 mL, 11.84 mmol), EDC (1135 mg, 5.92 mmol), DMAP (482 mg, 3.95 mmol), and 20 mL of CH_2Cl_2 to afford the title compound in 61% yield after isolation (807 mg, 2.41 mmol) as a white solid. ^{19}F NMR (376 MHz, Chloroform-*d*) δ -73.65 (t, *J* = 8.4 Hz). ^{1}H NMR (400 MHz, Chloroform-*d*) δ 7.82 (d, *J* = 7.1 Hz, 2H), 7.54 (t, *J* = 7.4 Hz, 1H), 7.46 (t, *J* = 7.4 Hz, 2H), 6.98 (d, *J* = 7.4 Hz, 1H), 5.03 (td, *J* = 7.4, 5.0 Hz, 1H), 4.49 (dq, *J* = 12.6, 8.3 Hz, 1H), 4.49 (dq, *J* = 12.6, 8.3 Hz, 1H), 2.69 – 2.56 (m, 2H), 2.32 (ddd, *J* = 14.5, 7.3, 5.0 Hz, 1H), 2.20 (dt, *J* = 14.4, 7.0 Hz, 1H), 2.13 (s, 3H). ^{13}C NMR (101 MHz, Chloroform-*d*) δ 170.7, 167.3, 133.4, 132.0, 128.7, 127.1, 122.7 (q, *J* = 277.4 Hz), 61.0 (q, *J* = 36.9 Hz), 52.1, 30.9, 30.0, 15.5.

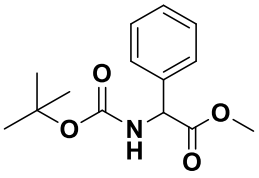

methyl 2-((tert-butoxycarbonyl)amino)-2-phenylacetate. To a solution of glycine methyl ester hydrochloride (500 mg, 2.48 mmol), triethylamine (0.864 mL, 6.20 mmol, 2.5 equiv), and a mixture of THF and H_2O (2.5/2.5 mL), Boc_2O (650 mg, 2.98 mmol, 1.2 equviv) was gradually added at 0 °C. After strirring for 15 h at rt, the mixture was concentrated in vacuo to a rid the mixture of THF. After extractions of ethyl acetate (3 x 50 mL), the combined organic layer was washed with aqueous HCl (0.1 M, 40 mL), water (40 mL), and saturated aqueous NaCl solution (20 mL), dried over $MgSO_4$, filtered and concentrated in vacuo to afford the title compound as a white solid (631 mg, 96%). The procedure and spectral data corresponds to that reported in the literature.[177-178]

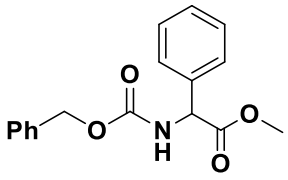

methyl 2-(((benzyloxy)carbonyl)amino)-2-phenylacetate A solution of glycine methyl ester hydrochloride (500 mg, 2.48 mmol) and Et_3N (0.864 mL, 6.20 mmol, 2.5 equiv) in CH_2Cl_2 (5 mL) was added dropwise to a solution of benzyl chloroformate (0.425 mL, 2.98 mmol, 1.2 equiv) in CH_2Cl_2 (20

mL) at 0 °C. The solution was warmed to room temperature and stirred over night. Then, the reaction was quenched by the addition of water (20 mL). The organic layer was seperated and then dried over anhydrous $MgSO_4$. Evaporation and column chromatography on silica gel afforded corresponding the title compound as white solid (623 mg, 84%). The procedure and spectral data corresponds to that reported in the literature.[179-180]

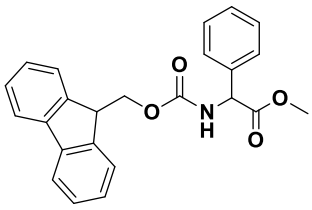

Methyl 2-((((9H-fluoren-9-yl)methoxy)carbonyl)amino)-2-phenylacetate. A solution of glycine methyl ester hydrochloride (300 mg, 1.49 mmol) and Et_3N (0.518 mL, 3.72 mmol, 2.5 equiv) in CH_2Cl_2 (5 mL) was added dropwise to a solution of fluorenyl chloroformate (0.463 mL, 1.79 mmol, 1.2 equiv) in CH_2Cl_2 (20 mL) at 0 °C. The solution was warmed to room temperature and stirred overnight. Then, the reaction was quenched by the addition of water (20 mL). The organic layer was seperated and then dried over anhydrous $MgSO_4$. Evaporation and column chromatography on silica gel afforded corresponding the title compound as white solid (340 mg, 59%). The procedure and spectral data corresponds to that reported in the literature.[181]

Synthesis of perfluoro-*N*-benzoyl amino esters

(*see our previous work for more details in regards to synthesizing fluorinated non-natural amino acids via arylation of oxazolones*)[160]

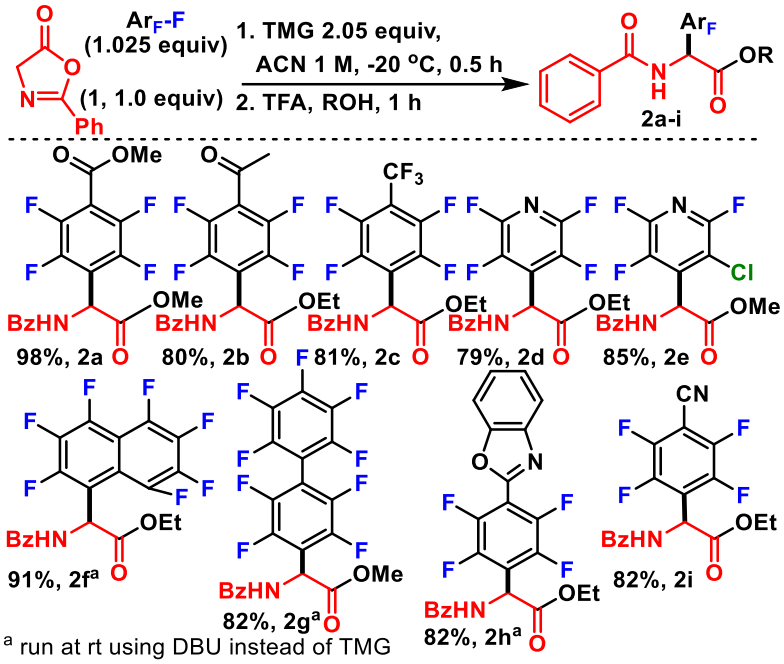

Synthesis of 5-(4H)-oxazolone

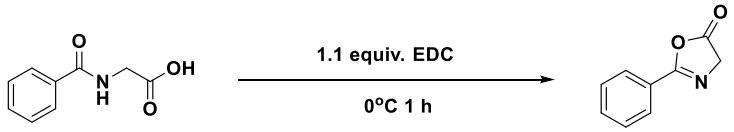

To a suspension of *N*-benzoyl glycine (2.50 g, 14.0 mmol) in dry CH_2Cl_2 (200 mL) under argon at 0 °C was added EDC HCl (2.38 g, 15.3 mmol). The materials were stirred at 0 °C for 1 hour. The reaction mixture was diluted with an equal volume of CH_2Cl_2, and washed successively with water, saturated aqueous $NaHCO_3$, and water (each 1/2 the volume of the organic phase), then dried over $MgSO_4$ and concentrated under reduced pressure to afford the title compound in 80 % yield after isolation (1.80 g, 11.1 mmol) as a pale white solid. ^{1}H-NMR spectrum matched that previously reported in the literature.[160]

General procedure D for synthesis of *N*-benzoyl perfluoro-amino esters

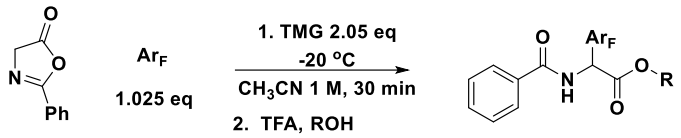

Under an inert atmosphere oxazolone **(1 equiv**), Ar_{Fn} **(1.025 equiv),** CH_3CN **(1 M)** was added to small test tube and cooled to -20 ºC. Then a steady stream of tetramethylguandine **(2.05 equiv)** was added to mixture down the side of the test tube glass. The reaction was left to react for 30 min. After the reaction was complete, the cooling bath was removed, and the reaction was left to warm to room temperature, then quenched by the addition of a trifluoroacetic acid/alcohol solution (2 equiv and double the volume of the MeCN). The solution was concentrated and brought into $CHCl_3$ then the organic layer was washed with half volumes of a 1 M HCl brine solution (3x). The organic layer was dried with $MgSO_4$ and concentrated to give the crude product. The crude product was purified by column chromatography.

General procedure E for synthesis of *N*-benzoyl perfluoro-amino esters

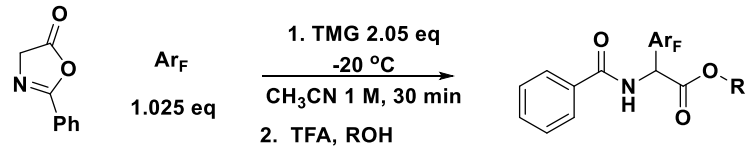

Under an inert atmosphere oxazolone **(1 equiv**), Ar_F **(1.025 equiv),** CH_3CN **(1 M)** was added to small test tube at room temperature. Then a steady stream of 1,8-Diazabicyclo(5.4.0)undec-7-ene **(2.05 equiv)** was added to mixture down the side of the test tube glass. The reaction was left to react for 30 min. After the reaction was complete, the cooling bath was removed, and the reaction was left to warm to room temperature, then quenched by the addition of a trifluoroacetic acid/alcohol solution (2 equiv and double the volume of the MeCN). The solution was

concentrated and brought into $CHCl_3$ then the organic layer was washed with half volumes of a 1 M HCl brine solution (3x). The organic layer was dried with $MgSO_4$ and concentrated giving crude product. The crude product was purified by column chromatography.

2a methyl 4-(1-benzamido-2-ethoxy-2-oxoethyl)-2,3,5,6-tetrafluorobenzoate

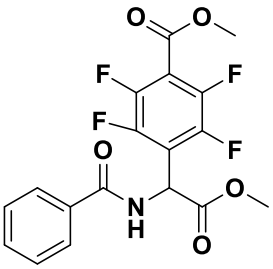

The **general procedure D** was followed using 2-phenyloxazol-5(4H)-one (300 mg, 1.86 mmol), 2,3,4,5,6 pentafluorobenzoate (431 mg, 1.91 mmol), tetramethylguanidine (0.487 ml, 3.81 mmol), 1.86 mL of MeCN and trifluoroacetic acid (0.284 mL, 3.72 mmol) in methanol (3.72 mL) was used to afford the titled compound in 90% yield (668 mg, 1.67 mmol). NMR data matched previous literature value.[160]

2b methyl 2-(4-acetyl-2,3,5,6-tetrafluorophenyl)-2-benzamidoacetate

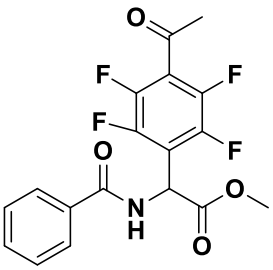

The **general procedure D** was followed using 2-phenyloxazol-5(4H)-one (150 mg, 0.931 mmol), 2',3',4',5',6' pentafluoroacetophenone (200 mg, 0.954 mmol), tetramethylguanidine (239 µL, 1.91 mmol), trifluoroacetic acid (142 µL, 1.86 mmol) in methanol (1.86 mL) and 0.931 mL of MeCN was used to afford the titled compound in 71 % yield (253 mg, 0.661 mmol). ^{19}F NMR (376 MHz, Chloroform-*d*) δ -141.06 – -141.36 (m), -141.59 – -141.77 (m). ^{1}H NMR (400 MHz, Chloroform-*d*) δ 7.81 (d, *J* = 7.1 Hz, 2H), 7.55 (t, *J* = 7.4 Hz, 1H), 7.46 (t, *J* = 7.5 Hz, 2H), 7.36 (d, *J* = 6.4 Hz, 1H), 6.21 (d, *J* = 6.5 Hz, 1H), 3.84 (s, 3H), 2.61 (t, *J* = 1.6 Hz, 3H). ^{13}C NMR (101 MHz, Chloroform-*d*) δ 191.9, 168.6, 166.8, 146.8 – 144.8 (m), 143.9 (dt, *J* = 13.6, 4.7 Hz), 142.8 – 142.4 (m), 132.8, 132.5, 128.9, 127.3, 120.3 – 118.7 (m), 53.9, 47.2, 32.5.

2d methyl 2-benzamido-2-(perfluoropyridin-4-yl)acetate

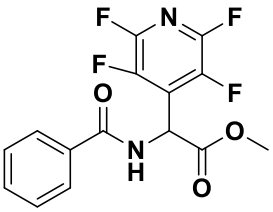

The **general procedure D** was followed using 2-phenyloxazol-5(4H)-one (300 mg, 1.86 mmol), pentafluoropyridine (323 mg, 1.91 mmol), tetramethylguanidine (0.487 µL, 3.81 mmol), trifluoroacetic acid (0.284 mL, 3.72 mmol) in methanol (3.72 mL) was used to afford the titled compound in 69% yield (439 mg, 1.28 mmol). ^{19}F NMR (376 MHz, Chloroform-*d*) δ -88.79 – -90.87 (m), -142.46 – -145.85 (m). ^{1}H NMR (400 MHz, Chloroform-*d*) δ 7.80 (d, *J* = 7.1 Hz, 2H), 7.57 – 7.48 (m, 2H), 7.44 (t, *J* = 7.6 Hz, 2H), 6.22 (d, *J* = 6.3 Hz, 1H), 3.85 (s, 3H). ^{13}C NMR (101 MHz, Chloroform-*d*) δ 167.7, 166.8, 143.4 (dddd, *J* = 246.3, 16.0, 12.6, 2.8 Hz), 141.9 – 138.9 (m), 132.5 (d, *J* = 11.1 Hz), 129.9 (tt, *J* = 14.1, 2.4 Hz), 128.8, 127.3, 54.7, 47.4.

2e methyl 2-benzamido-2-(3-chloro-2,5,6-trifluoropyridin-4-yl)acetate

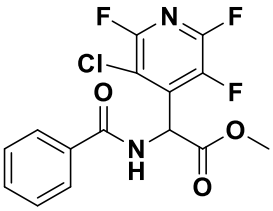

The **general procedure D** was followed using 2-phenyloxazol-5(4H)-one (100 mg, 0.621 mmol), 3-chloro-2,4,5,6 tetrafluoropyridine (118.0 mg, 0.636 mmol), tetramethylguanidine (145 mg, 1.27 mmol), trifluoroacetic acid (95 µL, 1.24 mmol) in methanol (1.24 mL) and 0.621 mL of MeCN was used to afford **2e** in 85% yield (178 mg, 0.487 mmol). NMR data matched previous literature values.[160]

2f methyl 2-benzamido-2-(perfluoronaphthalen-1-yl)acetate

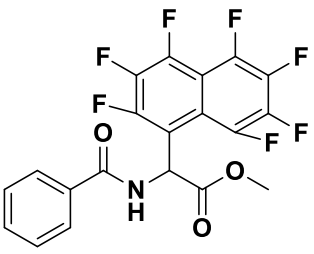

The **general procedure E** was followed using 2-phenyloxazol-5(4H)-one (50 mg, 0.310 mmol), octafluoronapalene (86 mg, 0.318 mmol), 1,8-diazabicyclo(5.4.0)undec-7-ene (96.7 mg, 0.636 mmol), trifluoroacetic acid (95 µL, 1.24 mmol) in ethanol (0.620 mL) and

0.310 mL of MeCN was used to afford **2f** in 82% yield (69.2 mg, 0.254 mmol). ^{19}F NMR (376 MHz, Chloroform-*d*) δ -120.66 (dd, *J* = 68.1, 18.4 Hz), -138.68 – -139.91 (m), -142.74 – -143.82 (m), -145.84 (dtd, *J* = 57.6, 16.7, 4.6 Hz), -148.02 (dtt, *J* = 57.7, 18.1, 4.7 Hz), -152.03 – -153.02 (m), -154.60 – -155.85 (m). ^{1}H NMR (400 MHz, Chloroform-*d*) δ 7.80 (d, *J* = 7.1 Hz, 2H), 7.55 – 7.47 (m, 1H), 7.43 (t, *J* = 7.5 Hz, 2H), 6.36 (d, *J* = 6.6 Hz, 1H), 3.84 (s, 3H). ^{13}C NMR (101 MHz, Chloroform-*d*) δ 168.9, 166.8, 150.9 (d, *J* = 260.5 Hz), 146.1 (d, *J* = 252.4 Hz), 142.8 (d, *J* = 41.3 Hz), 141.9, 141.4 (t, *J* = 15.1 Hz), 140.9 – 139.7 (m), 138.3 (dt, *J* = 118.8, 15.2 Hz), 132.8, 132.4, 128.8, 127.3, 115.2 (t, *J* = 17.7 Hz), 111.6, 108.0 (t, *J* = 13.7 Hz), 53.9, 47.2 (dt, *J* = 3.9, 2.1 Hz).

2g methyl 2-benzamido-2-(perfluoro-[1,1'-biphenyl]-4-yl)acetate

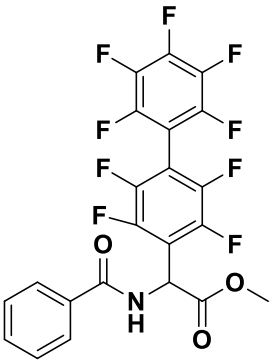

The **general procedure E** was followed using 2-phenyloxazol-5(4H)-one (100 mg, 0.621 mmol), decafluorobiphenyl (212.7 mg, 0.637 mmol), 1,8-diazabicyclo(5.4.0)undec-7-ene (193 mg, 1.27 mmol), trifluoroacetic acid (95 µL, 1.24 mmol) in methanol (1.24 mL) and 0.621 mL of MeCN was used to afford **2g** in 82% yield (265 mg, 0.508 mmol). NMR data matched previous literature values.[160]

2i methyl 2-benzamido-2-(4-cyano-2,3,5,6-tetrafluorophenyl)acetic acid

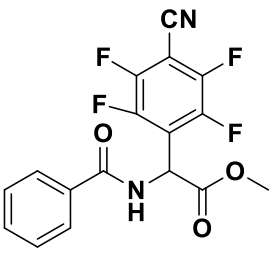

The **general procedure D** was followed using 2-phenyloxazol-5(4H)-one (300 mg, 1.86 mmol), 2,3,4,5,6 pentaflurobenzonitrile (240 µL, 1.91 mmol), tetramethylguanidine (0.487 ml, 3.81 mmol), 1.86 mL of MeCN and trifluoroacetic acid (0.284 mL, 3.72 mmol) in methanol (3.72 mL) was used to afford the titled compound in 66% yield (668 mg, 1.67 mmol). ^{19}F NMR (376 MHz, Chloroform-*d*) δ -128.70 – -134.21 (m), -139.47 (td, *J* = 16.5, 6.8

Hz). ^{1}H NMR (400 MHz, Chloroform-*d*) δ 7.79 (d, *J* = 8.1 Hz, 2H), 7.55 (t, *J* = 7.4 Hz, 1H), 7.45 (t, *J* = 7.6 Hz, 2H), 7.41 (d, *J* = 6.0 Hz, 1H), 6.18 (d, *J* = 6.1 Hz, 1H), 3.85 (s, 3H). ^{13}C NMR (101 MHz, Chloroform-*d*) δ 167.9, 166.8, 148.8 – 145.4 (m), 146.6 – 143.2 (m), 132.6, 132.4, 128.9, 127.3, 123.2 (t, *J* = 15.3 Hz), 107.19 (t, *J* = 3.7 Hz), 94.65 (tt, *J* = 17.0, 2.8 Hz), 54.18, 47.46 (p, *J* = 2.1 Hz).

Michael reaction: synthesis of α,α-disubstituted amino acid derivatives

General procedure F for synthesis of Michael adducts

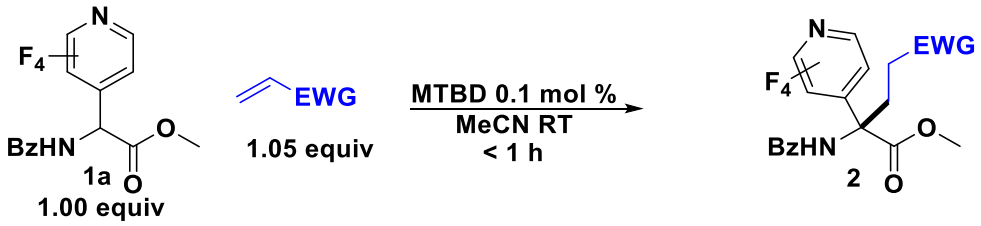

Under an inert atmosphere the methyl 2-benzamido-2-(perfluoropyridin-4-yl)acetate **(1 equiv**), Michael acceptor **(1.05 equiv),** CH_3CN **(0.5 M)** was added to a small test tube. Then MTBD **(0.001 equiv** made from a stock solution**)** was added to mixture and stirred vigorously. The reaction was monitored by ^{19}F NMR until the starting material was consumed. After the reaction was complete, the reaction was quenched with acetic acid (1 equiv). The solution was then concentrated and a half volume of brine solution was added. The salty water was extracted with CH_2Cl_2 (3x) and the combined organic extracts were washed with half volumes of a 1 M HCl brine solution (3x), and a final wash with tap water. The organic layer was dried with $MgSO_4$ and concentrated giving crude product. The crude product was purified further by column chromatography.

General procedure G for synthesis of *N*-benzoyl-Aryl-Michael adducts

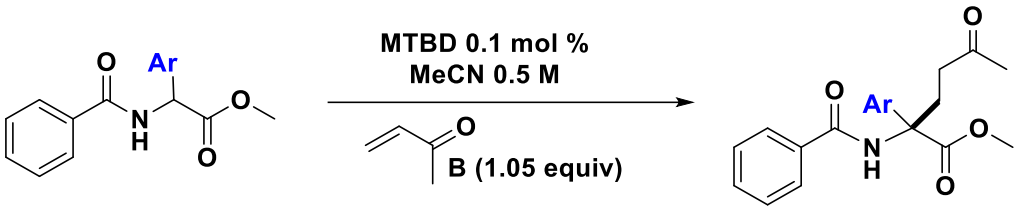

Under an inert atmosphere the amino ester substrate **(1 equiv**), methylvinyl ketone **(1.05 equiv),** CH_3CN **(0.5 M)** was added to a small test tube. Then MTBD **(0.001-0.01 equiv** made from a stock solution**)** was added to mixture and stirred vigorously. The reaction was monitored by ^{19}F NMR/^{1}H NMR until the starting material was consumed. After the reaction was complete, the reaction was quenched with acetic acid (1 equiv). The solution was then concentrated and a half volume of brine solution was added. The salty water was extracted with CH_2Cl_2 (3x) and the combined organic extracts were washed with half volumes of a 1 M HCl brine solution (3x) and a final wash with tap water. The organic layer was dried with $MgSO_4$ and concentrated giving crude/pure product. The crude product was purified further by column chromatography.

General procedure H for synthesis of *N*-boc/cbz-Aryl-Michael adducts

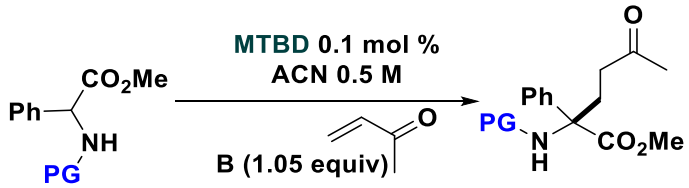

Under an inert atmosphere the protected phenyl glycine substrate **(1 equiv**), methylvinyl ketone **(1.05 equiv)**, CH_3CN **(0.5 M)** was added to a small test tube. Then MTBD **(0.001 equiv** made from a stock solution**)** was added to mixture and stirred vigorously. The reaction was monitored

by ^{19}F NMR/^{1}H NMR until the starting material was consumed. After the reaction was complete, the reaction was quenched with acetic acid (1 equiv). The solution was then concentrated and a half volume of brine solution was added. The salty water was extracted with CH_2Cl_2 (3x) and the combined organic extracts were washed with half volumes of a 1 M HCl brine solution (3x) and a final wash with tap water. The organic layer was dried with $MgSO_4$ and concentrated giving crude/pure product. The crude product was purified further by column chromatography.

General procedure I for synthesis of *N*-benzoyl Michael adducts (natural amino esters)

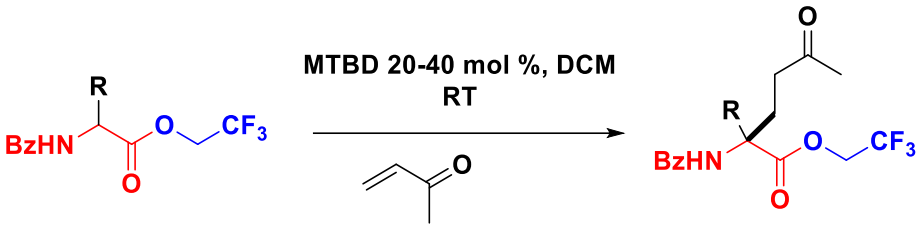

Under a dry inert atmosphere, the amino ester substrate **(1 equiv**), methylvinyl ketone **(1.05 equiv)**, dry DCM **(0.5 M)** was added to a small test tube. Then MTBD **(0.10-0.40 equiv)** was added to mixture and stirred vigorously. The reaction was monitored by ^{19}F NMR/^{1}H NMR until the starting material was consumed. The organic solution was then dried with $MgSO_4$ and concentrated giving crude product. The crude product was purified further by column chromatography.

2a methyl-2-benzamido-5-oxo-2-(perfluoropyridin-4-yl)hexanoate

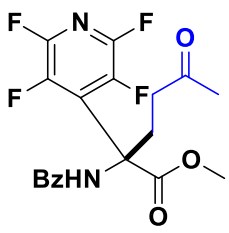

The **general procedure F** was followed using methyl 2-benzamido-2-(perfluoropyridin-4-yl)acetate (150 mg, 0.438 mmol), methyl vinyl ketone (38.4 µL, 0.460 mmol), 0.880 mL of a 0.0005 M MTBD/CH_3CN solution (0.0004383 mmol of MTBD) to afford the title compound in 99% yield (179 mg, 0.430 mmol). ^{19}F NMR (376 MHz, Chloroform-*d*) δ -90.52 – -90.94 (m), -137.70 – -142.09

(m). ^{1}H NMR (400 MHz, Chloroform-*d*) δ 7.81 – 7.72 (m, 3H), 7.56 (t, *J* = 7.4 Hz, 1H), 7.47 (t, *J* = 7.5 Hz, 2H), 3.84 (s, 3H), 3.43 (dddt, *J* = 14.1, 6.9, 4.8, 2.1 Hz, 1H), 2.82 (dddt, *J* = 14.2, 6.9, 4.3, 2.2 Hz, 1H), 2.59 (dt, *J* = 18.2, 6.7 Hz, 1H), 2.47 (dt, *J* = 18.3, 7.0 Hz, 1H), 2.14 (s, 3H). ^{13}C NMR (101 MHz, Chloroform-*d*) δ 206.7, 170.8, 166.1, 144.4 (dt, *J* = 244.7, 18.2 Hz), 141.4 (dd, *J* = 261.2, 34.6 Hz), 133.2, 132.9, 132.4 – 131.9 (m), 129.3, 127.5, 54.9, 38.4, 30.4, 27.7, 2.4. FT-IR (neat) cm-1 1743, 1754, 1680, 1085. HRMS (ESI) $C_{19}H_{16}F_4N_2O_4$ calcd. $[M+Na]^+$ 435.0938 observed 435.0908.

2b 5-ethyl 1-methyl-2-benzamido-2-(perfluoropyridin-4-yl)pentanedioate

The **general procedure F** was followed using methyl 2-benzamido-2-(perfluoropyridin-4-

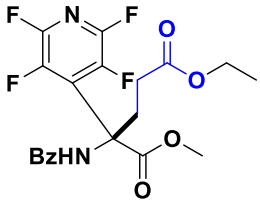

yl)acetate (50 mg, 0.146 mmol), ethyl acrylate (18.0. µL, 0.153 mmol), 0.293 mL of a 0.0005 M MTBD/CH_3CN solution (0.0001463 mmol of MTBD) to afford the title compound in 97% yield (63 mg, 0.140 mmol). ^{19}F NMR (376 MHz, Chloroform-*d*) δ -88.61 – -92.72 (m), -136.58 – -141.53 (m). ^{1}H NMR (400 MHz, Chloroform-*d*) δ 7.80 – 7.73 (m, 3H), 7.55 (t, *J* = 7.4 Hz, 1H), 7.46 (t, *J* = 7.5 Hz, 2H), 4.08 (q, *J* = 7.1 Hz, 2H), 3.86 (s, 3H), 3.56 (dddd, *J* = 14.7, 8.6, 6.6, 2.1 Hz, 1H), 2.79 (dddd, *J* = 16.7, 8.6, 4.5, 2.2 Hz, 1H), 2.44 (ddd, *J* = 16.8, 7.9, 6.6 Hz, 1H), 2.29 (ddd, *J* = 16.7, 8.3, 6.7 Hz, 1H), 1.22 (t, *J* = 7.1 Hz, 3H). ^{13}C NMR (101 MHz, Chloroform-*d*) δ 172.4, 170.6, 166.1, 146.0 – 142.9 (m), 142.9 – 139.5 (m), 133.2, 132.9, 132.0 (t, *J* = 10.4 Hz), 129.3, 127.5, 62.9, 61.4, 54.9, 29.5, 29.1, 14.5. FT-IR (neat) cm-1 3412, 1748, 1730, 1508, 1270. HRMS (ESI) $C_{20}H_{18}F_4N_2O_5$ calcd. $[M+Na]^+$ 465.1044 observed 465.1027.

2c 5-(tert-butyl) 1-methyl-2-benzamido-2-(perfluoropyridin-4-yl)pentanedioate

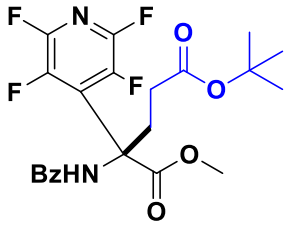

The **general procedure F** was followed using methyl 2-benzamido-2-(perfluoropyridin-4-yl)acetate (50 mg, 0.146 mmol), methyl vinyl ketone (22.5 µL, 0.153 mmol), 0.293 mL of a 0.0005 M MTBD/CH_3CN solution (0.000146 mmol of MTBD) to afford the title compound in 92% yield (63 mg, 0.130 mmol). ^{19}F NMR (376 MHz, Chloroform-*d*) δ -88.33 – -93.28 (m), -139.54 (h, *J* = 13.8 Hz). ^{1}H NMR (400 MHz, Chloroform-*d*) δ 7.83 (s, 1H), 7.76 (d, *J* = 8.0 Hz, 2H), 7.52 (t, *J* = 7.4 Hz, 1H), 7.43 (tt, *J* = 8.1, 1.4 Hz, 2H), 3.84 (s, 3H), 3.45 (dt, *J* = 14.7, 7.5 Hz, 1H), 2.75 (dt, *J* = 14.4, 7.1 Hz, 1H), 2.45 – 2.31 (m, 1H), 2.21 (dt, *J* = 16.9, 7.5 Hz, 1H), 1.40 (s, 9H). ^{13}C NMR (101 MHz, Chloroform-*d*) δ 171.7, 170.5, 166.1, 144.3 (dt, *J* = 243.6, 15.7 Hz), 142.8 – 139.1 (m), 133.2, 132.8, 132.2 (t, *J* = 10.4 Hz), 129.2, 127.5, 81.6, 62.9, 54.8, 30.4, 28.9, 28.4. FT-IR (neat) cm-1 3430, 1727, 1702, 1595, 1310. HRMS (ESI) $C_{22}H_{22}F_4N_2O_5$ calcd. $[M+H]^+$ 471.1538 observed 471.1530.

2d methyl-2-benzamido-4-cyano-2-(perfluoropyridin-4-yl)butanoate

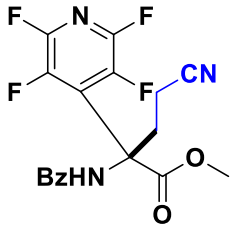

The **general procedure F** was followed using methyl 2-benzamido-2-(perfluoropyridin-4-yl)acetate (100 mg, 0.292 mmol), acrylonitrile (20.1 µL, 0.307 mmol), 0.584 mL of a 0.0005 M MTBD/CH_3CN solution (0.000292 mmol of MTBD) to afford the title compound in 99% yield (114 mg, 0.29 mmol). ^{19}F NMR (376 MHz, Chloroform-*d*) δ -87.49 – -92.37 (m), -137.14 – -143.28 (m). ^{1}H NMR (400 MHz, Chloroform-*d*) δ 7.76 (d, *J* = 1.3 Hz, 3H), 7.57 (t, *J* = 7.4 Hz, 1H), 7.48 (t, *J* = 7.6 Hz, 2H), 3.95 (s, 3H), 3.72 (dtt, *J* = 14.2, 7.0, 2.0 Hz, 1H), 2.79 (dtd, *J* = 14.2, 8.3, 2.2 Hz, 1H), 2.50 (dt, *J* = 17.4, 6.7 Hz, 1H), 2.38 (dt, *J* = 17.4, 7.2 Hz, 1H). ^{13}C NMR (101 MHz, Chloroform-*d*) δ 169.6, 166.1, 145.7 – 142.6 (m), 140.9 (dd, *J* = 261.4, 35.1 Hz), 132.9, 132.4, 130.9 (t, *J* = 11.2 Hz), 129.1, 127.2, 118.2, 62.1, 55.1, 29.5, 12.4. FT-IR (neat) cm-1 3270, 2248, 1762, 1515, 1295. HRMS (ESI) $C_{18}H_{13}F_4N_3O_3$ calcd. $[M+H]^+$ 396.0966 observed 396.0963.

2e methyl-2-benzamido-4-(methylsulfonyl)-2-(perfluoropyridin-4-yl)butanoate

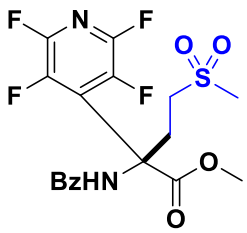

The **general procedure F** was followed using methyl 2-benzamido-2-(perfluoropyridin-4-yl)acetate (75 mg, 0.219 mmol), methyl vinyl sulfone (24 mg, 0.230 mmol), 0.438 mL of a 0.0005 M MTBD/CH_3CN solution (0.000219 mmol of MTBD) to afford the title compound in 99% yield (97 mg, 0.22 mmol). ^{19}F NMR (376 MHz, Chloroform-*d*) δ -86.03 – -92.09 (m), -138.05 – -142.09 (m). ^{1}H NMR (400 MHz, Chloroform-*d*) δ 7.79 – 7.72 (m, 3H), 7.59 (t, *J* = 7.4 Hz, 1H), 7.49 (t, *J* = 7.6 Hz, 2H), 3.93 (s, 3H), 3.81 (td, *J* = 14.2, 13.0, 4.9 Hz, 1H), 3.16 (ddd, *J* = 14.0, 10.8, 5.1 Hz, 1H), 3.04 – 2.77 (m, 5H). ^{13}C NMR (101 MHz, Chloroform-*d*) δ 169.7, 166.1, 154.1 – 145.0 (m), 143.7 – 139.1 (m), 133.0, 132.3, 131.6 (t, *J* = 10.2 Hz), 129.2, 127.2, 62.0, 55.2, 49.9, 40.6, 27.3. FT-IR (neat) cm-1 3208, 1761, 1517, 1328, 1282. HRMS (ESI) $C_{18}H_{16}F_4N_2O_5S$ calcd. $[M+Na]^+$ 471.0608 observed 471.0597.

2f methyl-2-benzamido-2-(perfluoropyridin-4-yl)-4-(phenylsulfonyl)butanoate

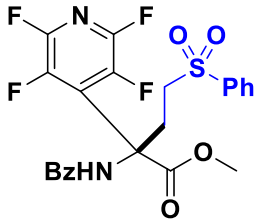

The **general procedure F** was followed using methyl 2-benzamido-2-(perfluoropyridin-4-yl)acetate (50 mg, 0.146 mmol), phenyl vinyl sulfone (26 mg, 0.153 mmol), 0.29 mL of a 0.0005 M MTBD/CH_3CN solution (0.0001461 mmol of MTBD) to afford the title compound in 99% yield (72 mg, 0.14 mmol). ^{19}F NMR (376 MHz, Chloroform-*d*) δ -86.31 – -93.00 (m), -136.30 – -142.65 (m). ^{1}H NMR (400 MHz, Chloroform-*d*) δ 7.88 (d, *J* = 7.3 Hz, 2H), 7.70 – 7.61 (m, 4H), 7.59 – 7.51 (m, 3H), 7.45 (t, *J* = 7.6 Hz, 2H), 3.87 (s, 3H), 3.66 – 3.57 (m, 1H), 3.20 (ddd, *J* = 14.2, 10.8, 5.1 Hz, 1H), 3.03 – 2.90 (m, 1H), 2.81 (ddd, *J* = 15.5, 12.7, 3.5 Hz, 1H). ^{13}C NMR (101 MHz, Chloroform-*d*) δ 169.9, 165.9, 150.0 – 145.2 (m), 143.7 – 139.6 (m), 138.8, 134.7, 133.1, 133.0,

132.0 – 130.9 (m), 130.0, 129.3, 128.1, 127.6, 60.9, 32.2, 23.2, 14.4. FT-IR (neat) cm^{-1} 3409, 1750, 1506, 1308, 1145. HRMS (ESI) $C_{23}H_{18}F_4N_2O_5S$ calcd. $[M+H]^+$ 511.0945 observed 511.0949.

2g methyl 2-benzamido-3,4-dicyano-2-(perfluoropyridin-4-yl)butanoate

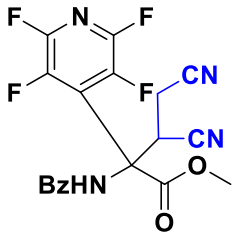

The **general procedure F** was followed using methyl 2-benzamido-2-(perfluoropyridin-4-yl)acetate (50 mg, 0.146 mmol), fumanitrile (12 mg, 0.153 mmol), 0.29 mL of a 0.0005 M MTBD/CH_3CN solution (0.0001461 mmol of MTBD) to afford the title compound (d.r. 1.5:1) in 87% yield (53 mg, 0.130 mmol). ^1H NMR (400 MHz, Chloroform-*d*) δ 7.94 (s, 1H), 7.81 – 7.72 (m, 8H), 7.64 – 7.57 (m, 3H), 7.49 (ddd, *J* = 8.1, 6.7, 1.2 Hz, 6H), 5.39 (t, *J* = 5.8 Hz, 1H), 5.23 (t, *J* = 6.4 Hz, 2H), 4.08 (s, 6H), 4.06 (s, 3H), 3.16 – 2.67 (m, 6H). ^{13}C NMR (101 MHz, Chloroform-*d*) δ 167.2, 166.9, 166.6, 166.2, 145.9 – 142.5 (m), 142.4 – 138.8 (m), 133.6, 133.4, 131.7, 131.4, 129.3, 129.2, 128.1 – 127.5 (m), 127.4, 127.4, 115.2, 114.8, 114.6, 114.5, 62.5, 62.2, 55.9, 55.8, 34.1 (t, *J* = 4.7 Hz), 31.5 (t, *J* = 4.4 Hz), 18.8 (t, *J* = 3.5 Hz), 17.4. FT-IR (neat) cm-1 3376, 2999, 1752, 1505, 1316. HRMS (ESI) $C_{19}H_{12}F_4N_4O_3$ calcd. $[M+H]^+$ 421.0918 observed 421.0910.

2h methyl 2-benzamido-2-(2,5-dioxo-1-phenylpyrrolidin-3-yl)-2-(perfluoropyridin-4-yl)acetate

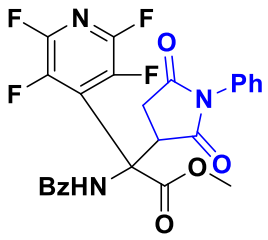

The **general procedure F** was followed using methyl 2-benzamido-2-(perfluoropyridin-4-yl)acetate (50 mg, 0.146 mmol), N-Phenylmaleimide (27 mg , 0.153 mmol), 0.29 mL of a 0.0005 M MTBD/CH_3CN solution (0.0001461 mmol of MTBD) to afford the title compound (d.r. 1.9:1 based on crude ^{19}F NMR) in 87% yield (66 mg, 0.130 mmol) when considering both diastermers, however we were able to separate one diastermer for

characterization. ^{19}F NMR (376 MHz, Chloroform-*d*) δ -86.86 – -93.28 (m), -139.58 (dt, *J* = 35.9, 17.9 Hz). ^{1}H NMR (400 MHz, Chloroform-*d*) δ 7.86 (s, 1H), 7.79 (d, *J* = 7.2 Hz, 2H), 7.61 (d, *J* = 7.4 Hz, 1H), 7.54 – 7.37 (m, 5H), 7.20 (d, *J* = 7.1 Hz, 2H), 4.97 (dd, *J* = 9.8, 5.0 Hz, 1H), 3.97 (s, 3H), 3.62 (dd, *J* = 19.0, 5.0 Hz, 1H), 3.20 (dd, *J* = 19.0, 9.7 Hz, 1H). ^{13}C NMR (101 MHz, Chloroform-*d*) δ 174.4, 174.1, 168.6, 167.6, 146.4 – 143.1 (m), 142.8 – 139.0 (m), 133.4, 132.7, 131.7, 129.7, 129.5, 129.4, 128.9 (d, *J* = 10.0 Hz), 127.6, 126.6, 63.4, 55.7, 46.9, 32.5. FT-IR (neat) cm^{-1} 3390, 1751, 1646, 1501, 1270. HRMS (ESI) $C_{25}H_{17}F_4N_3O_5$ calcd. $[M+H]^+$ 516.1177 observed 516.1184.

3a methyl-2-benzamido-2-(3-chloro-2,5,6-trifluoropyridin-4-yl)-5-oxohexanoate

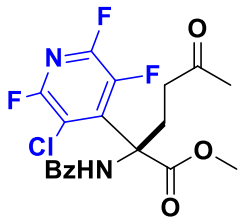

The **general procedure G** was followed using substrate (75 mg, 0.209 mmol), methyl vinyl ketone (18.3 µL, 0.220 mmol), 0.42 mL of a 0.005 M MTBD/CH_3CN solution (0.002094 mmol of MTBD) to afford the title compound in 94% yield (84 mg, 0.20 mmol). ^{19}F NMR (376 MHz, Chloroform-*d*) δ -73.82 (dd, *J* = 26.5, 13.0 Hz), -87.39 (dd, *J* = 22.4, 13.0 Hz), -136.78 (ddt, *J* = 27.3, 22.2, 5.5 Hz). ^{1}H NMR (400 MHz, Chloroform-*d*) δ 7.80 – 7.74 (m, 2H), 7.70 (s, 1H), 7.56 (t, *J* = 7.4 Hz, 1H), 7.47 (t, *J* = 7.5 Hz, 2H), 3.80 (s, 3H), 3.47 (ddd, *J* = 12.0, 6.8, 5.1 Hz, 1H), 2.87 (ddd, *J* = 14.2, 12.7, 6.6 Hz, 1H), 2.55 (q, *J* = 6.9, 1.3 Hz, 2H), 2.13 (s, 3H). ^{13}C NMR (101 MHz, Chloroform-*d*) δ 206.5, 171.3, 165.7, 147.2 (d, *J* = 15.3 Hz), 145.4 (d, *J* = 16.5 Hz), 143.8 (dd, *J* = 183.2, 14.8 Hz), 133.3, 128.9, 127.2, 121.4 (t, *J* = 12.0 Hz), 119.4 – 119.0 (m), 62.6, 54.4, 38.3, 32.6, 30.1, 27.7. FT-IR (neat) cm-1 1754, 1739, 1676, 1100. HRMS (ESI) $C_{19}H_{16}ClF_3N_2O_4$ calcd. $[M+H]^+$ 429.0823 observed 429.0818.

3b methyl-2-benzamido-2-(4-cyano-2,3,5,6-tetrafluorophenyl)-5-oxohexanoate

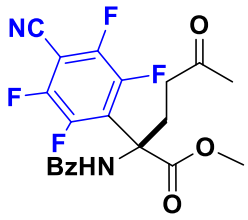

The **procedure G** was followed using substrate (75 mg, 0.205 mmol), methyl vinyl ketone (18.0 µL, 0.215 mmol), 0.41 mL of a 0.0005 M MTBD/CH_3CN solution (0.0002048 mmol of MTBD) to afford the title compound in 93% yield (83 mg, 0.20 mmol). ^{19}F NMR (376 MHz, Chloroform-*d*) δ -132.44 (td, *J* = 15.1, 7.0 Hz), -135.22 (dq, *J* = 15.9, 6.9 Hz).^{1}H NMR (400 MHz, Chloroform-*d*) δ 7.74 – 7.64 (m, 3H), 7.49 (t, *J* = 7.4 Hz, 1H), 7.40 (t, *J* = 7.5 Hz, 2H), 3.76 (s, 3H), 3.34 (dtt, *J* = 14.0, 6.7, 2.1 Hz, 1H), 2.73 (dtt, *J* = 14.1, 6.9, 4.5, 2.2 Hz, 1H), 2.39 (dt, *J* = 18.3, 7.0 Hz, 1H), 2.39 (dt, *J* = 18.2, 7.0 Hz, 1H)2.07 (s, 3H). ^{13}C NMR (101 MHz, Chloroform-*d*) δ 206.6, 171.0, 166.1, 148.9 (dt, *J* = 18.1, 3.8 Hz), 147.7 – 144.5 (m), 133.2, 132.9, 129.3, 127.5, 125.7 (t, *J* = 11.7 Hz), 107.6 (t, *J* = 3.6 Hz), 94.5, 63.1 (d, *J* = 2.4 Hz), 54.9, 38.4 (t, *J* = 1.8 Hz), 30.4, 27.9 (t, *J* = 6.6 Hz). FT-IR (neat) cm-1 3412, 2246, 1747, 1718, 1581, 1303. HRMS (ESI) $C_{21}H_{16}F_4N_2O_4$ calcd. $[M+H]^+$ 437.1119 observed 437.1123.

3c methyl-2-(4-acetyl-2,3,5,6-tetrafluorophenyl)-2-benzamido-5-oxohexanoate

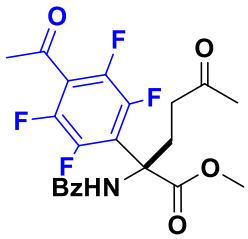

The **procedure G** was followed using substrate (90 mg, 0.235 mmol), methyl vinyl ketone (20.5 µL, 0.247 mmol), 0.47 mL of a 0.0005 M MTBD/CH_3CN solution (0.0002348 mmol of MTBD) to afford the title compound in 98% yield (104 mg, 0.230 mmol). ^{19}F NMR (376 MHz, Chloroform-*d*) δ -137.37 (dd, *J* = 21.1, 11.4 Hz), -141.87 (dd, *J* = 21.2, 11.2 Hz). ^{1}H NMR (400 MHz, Chloroform-*d*) δ 7.84 – 7.73 (m, 3H), 7.55 (t, *J* = 7.4 Hz, 1H), 7.46 (t, *J* = 7.5 Hz, 2H), 3.81 (s, 3H), 3.53 – 3.36 (m, 1H), 2.81 (dtt, *J* = 14.3, 7.0, 2.3 Hz, 1H), 2.60 (t, *J* = 1.7 Hz, 3H), 2.55 (m, 1H), 2.48 – 2.39 (m, 1H), 2.13 (s, 3H). ^{13}C NMR (101 MHz, Methylene Chloride-d_2) δ 206.8, 192.4, 171.6, 165.9, 148.3 – 145.5 (m), 145.4 – 143.1 (m), 134.1, 132.6, 129.2 (d, *J* = 4.1 Hz), 127.6 (d, *J* = 4.2 Hz), 122.5 – 121.6 (m), 119.9 (d, *J* = 31.1 Hz), 63.1, 54.7, 38.6, 32.8, 30.3, 28.2.

FT-IR (neat) cm-1 3306, 1762, 1715, 1533, 1184. HRMS (ESI) $C_{22}H_{19}F_4NO_5$ calcd. $[M+H]^+$ 454.1272 observed 454.1269.

3d methyl-4-(2-benzamido-1-methoxy-1,5-dioxohexan-2-yl)-2,3,5,6-tetrafluorobenzoate

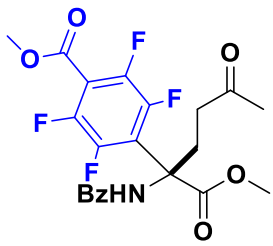

The **procedure G** was followed using substrate (50 mg, 0.125 mmol), methyl vinyl ketone (11.0 µL, 0.131 mmol), 0.25 mL of a 0.0005 M MTBD/CH_3CN solution (0.0001252 mmol of MTBD) to afford the title compound in 99% yield (58 mg, 0.124 mmol). ^{19}F NMR (376 MHz, Chloroform-*d*) δ -137.55 (dt, *J* = 16.2, 8.2 Hz), -139.33 – -139.83 (m). ^1H NMR (400 MHz, Chloroform-*d*) δ 7.80 – 7.73 (m, 3H), 7.53 (t, *J* = 7.4 Hz, 1H), 7.45 (t, *J* = 7.5 Hz, 2H), 3.95 (s, 3H), 3.80 (s, 3H), 3.43 (dddd, *J* = 16.3, 8.6, 6.1, 2.1 Hz, 1H), 2.88 – 2.72 (m, 1H), 2.57 (dt, *J* = 18.1, 6.8 Hz, 1H), 2.57 (dt, *J* = 18.1, 6.8 Hz, 1H), 2.12 (s, 3H). ^{13}C NMR (101 MHz, Chloroform-*d*) δ 206.5, 171.2, 165.7, 160.0, 146.6 (ddt, *J* = 98.8, 16.4, 5.2 Hz), 144.1 (ddt, *J* = 103.8, 16.7, 5.2 Hz), 133.3, 132.4, 128.9, 127.1, 121.8 (t, *J* = 12.0 Hz), 112.3 (t, *J* = 16.0 Hz), 62.6, 54.3, 53.4, 38.2, 30.0, 27.7 (t, *J* = 6.4 Hz).FT-IR (neat) cm^{-1} 2933, 2848, 1434, 1085. FT-IR (neat) cm-1 3240, 1744, 1732, 1709, 1517, 1250. HRMS (ESI) $C_{22}H_{19}F_4NO_6$calcd. $[M+H]^+$ 470.1221 observed 470.1214.

3e methyl-2-benzamido-5-oxo-2-(perfluoro-[1,1'-biphenyl]-4-yl)hexanoate

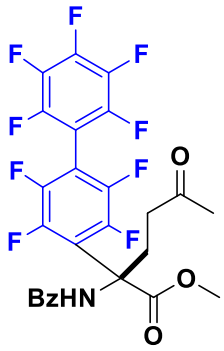

The **procedure G** was followed using substrate (62 mg, 0.122 mmol), methyl vinyl ketone (10.7 µL, 0.128 mmol), 0.24 mL of a 0.0005 M MTBD/CH_3CN solution (0.0001222 mmol of MTBD) to afford the title compound in 98% yield (69 mg, 0.120 mmol). ^{19}F NMR (376 MHz, Chloroform-*d*) δ -136.42 – -136.89 (m), -137.52 (dt, *J* = 14.3, 7.6 Hz), -138.31 (dt, *J* = 19.3, 9.3 Hz), -150.13 (tt, *J* = 20.9, 3.2 Hz), -159.19 – -162.48 (m). ^{1}H NMR (400 MHz, Chloroform-*d*) δ 7.89 – 7.75 (m, 3H), 7.55 (t, *J* = 7.4 Hz, 1H), 7.47 (t, *J* = 7.5 Hz, 2H), 3.85 (s, 3H), 3.51 (dt, *J* = 14.2, 6.9 Hz, 1H), 2.85 (dddd, *J* = 16.3, 7.0, 4.4, 2.0 Hz, 1H), 2.46 (dt, *J* = 18.0, 7.1 Hz, 1H), 2.46 (dt, *J* = 18.0, 7.1 Hz, 1H), 2.15 (s, 3H).^{13}C NMR (101 MHz, Chloroform-*d*) δ 206.6, 171.4, 165.7, 145.9 (d, *J* = 9.1 Hz), 145.6 – 144.5 (m), 145.3 – 142.8 (m), 141.3, 138.0 (d, *J* = 255.6 Hz), 133.4, 132.4, 128.9, 127.2, 120.9 (t, *J* = 12.0 Hz), 106.3 (t, *J* = 18.1 Hz), 102.3, 64.5 – 59.8 (m), 54.4, 38.3 (d, *J* = 1.8 Hz), 30.1, 27.7 (t, *J* = 6.4 Hz). FT-IR (neat) cm-1 3417, 1745, 1719, 1530, 1276. HRMS (ESI) $C_{26}H_{16}F_9NO_4$ calcd. $[M+H]^+$ 578.1008 observed 578.1000.

3f methyl-2-benzamido-5-oxo-2-(perfluoronaphthalen-1-yl)hexanoate

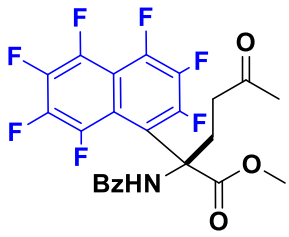

The **procedure G** was followed using substrate (69 mg, 0.155 mmol), methyl vinyl ketone (13.6 µL, 0.163 mmol), 0.31 mL of a 0.0005 M MTBD/CH_3CN solution (0.0001550 mmol of MTBD) to afford the title compound in 98% yield (78 mg, 0.152 mmol). ^{19}F NMR (376 MHz, Chloroform-*d*) δ -115.07 (dd, *J* = 78.1, 17.1 Hz), -134.52 (d, *J* = 15.4 Hz), -142.70 (dtt, *J* = 77.8, 16.5, 4.3 Hz), -146.41 (dtd, *J* = 56.5, 16.9, 4.7 Hz), -148.46 (dtt, *J* = 56.5, 16.9, 4.7 Hz), -151.37 – -153.74 (m),153.74 – -158.34 (m). ^{1}H NMR (400 MHz, Chloroform-*d*) δ 7.85 (s, 1H), 7.77 (d, *J* = 7.1 Hz, 2H), 7.54 (t, *J* = 7.4 Hz, 1H), 7.45 (t, *J* = 7.5 Hz, 2H), 3.82 (s, 3H), 3.54 (dt, *J* = 12.0, 7.0 Hz, 1H), 2.90 (dddd, *J* = 16.3, 6.7, 4.5, 2.2 Hz, 1H), 2.69 – 2.41 (m, 2H), 2.15 (s, 3H). ^{13}C NMR (101 MHz, Chloroform-*d*) δ 206.6, 171.7, 165.7, 152.7, 150.2, 148.5, 146.1, 143.3, 142.4,

141.3, 140.6, 140.2, 138.8, 137.8, 133.4, 132.4, 128.9, 127.2, 118.1 – 116.5 (m), 62.8, 54.3, 38.4, 30.1, 27.9. FT-IR (neat) cm-1 3270, 1765, 1712, 1512, 1246. HRMS (ESI) $C_{24}H_{16}F_7NO_4$ calcd. $[M+H]^+$ 516.1040 observed 516.1031.

3g methyl-2-benzamido-5-oxo-2-(3,4,5-trifluorophenyl)hexanoate

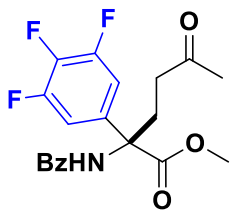

The **procedure G** was followed using substrate (100 mg, 0.309 mmol), methyl vinyl ketone (27.1 µL, 0.325 mmol), 0.62 mL of a 0.005 M MTBD/CH_3CN solution (0.003093 mmol of MTBD) to afford the title compound in 85% yield (103 mg, 0.263 mmol). ^{19}F NMR (376 MHz, Chloroform-*d*) δ -130.73 – -135.68 (m), -160.84 (tt, *J* = 20.6, 6.3 Hz). ^1H NMR (400 MHz, Chloroform-*d*) δ 8.01 (s, 1H), 7.86 (d, *J* = 7.2 Hz, 2H), 7.57 (t, *J* = 7.3 Hz, 1H), 7.50 (t, *J* = 7.5 Hz, 2H), 7.14 (dd, *J* = 8.9, 6.4 Hz, 2H), 3.77 (s, 3H), 3.05 – 2.95 (m, 1H), 2.79 (ddd, *J* = 14.1, 8.1, 6.3 Hz, 1H), 2.62 (ddd, *J* = 17.9, 8.1, 6.0 Hz, 1H), 2.29 (ddd, *J* = 17.9, 8.5, 6.3 Hz, 1H), 2.14 (s, 3H).^{13}C NMR (101 MHz, Chloroform-*d*) δ 207.5, 172.4, 165.8, 151.2 (ddd, *J* = 249.9, 10.0, 4.0 Hz), 139.4 (dt, *J* = 252.7, 15.3 Hz), 136.0 (td, *J* = 6.8, 4.4 Hz), 133.4, 132.4, 128.9, 127.2, 111.4 – 110.6 (m), 64.4, 54.1, 38.8, 30.1, 28.6. FT-IR (neat) cm-1 3405, 1739, 1717, 1530, 1239. HRMS (ESI) $C_{20}H_{18}F_3NO_4$ calcd. $[M+H]^+$ 394.1261 observed 394.1254.

3h methyl-2-benzamido-2-(4-chlorophenyl)-5-oxohexanoate

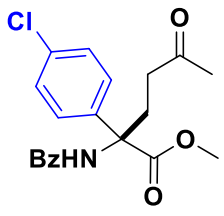

The **procedure G** was followed using substrate (100 mg, 0.329 mmol), methyl vinyl ketone (28.8 µL, 0.346 mmol), 0.66 mL of a 0.0005 M MTBD/CH_3CN solution (0.0003293 mmol of MTBD) to afford the title compound in 99% yield (122 mg, 0.326 mmol). ^1H NMR (400 MHz, Chloroform-*d*) δ 7.96 (s, 1H), 7.86 (d, *J* = 7.3 Hz, 2H), 7.54 (t, *J* = 7.3 Hz, 1H), 7.45 (dd, *J* = 21.0,

8.2 Hz, 4H), 7.30 (d, *J* = 8.7 Hz, 2H), 3.73 (s, 3H), 3.10 (ddd, *J* = 14.5, 9.2, 5.7 Hz, 1H), 3.10 (ddd, *J* = 14.5, 9.2, 5.7 Hz, 1H), 2.60 (ddd, *J* = 17.6, 8.8, 5.7 Hz, 1H), 2.28 (ddd, *J* = 17.6, 9.2, 5.9 Hz, 1H), 2.12 (s, 3H).^{13}C NMR (101 MHz, Chloroform-*d*) δ 207.7, 173.1, 165.7, 137.9, 133.9, 133.8, 132.1, 128.8, 128.8, 127.6, 127.1, 64.8, 53.8, 38.9, 30.1, 28.3. FT-IR (neat) cm^{-1} 3315, 1737, 1702, 1525, 695. HRMS (ESI) $C_{20}H_{20}ClNO_4$ calcd. $[M+H]^+$ 374.1154 observed 374.1151.

3i methyl-2-benzamido-5-oxo-2-phenylhexanoate

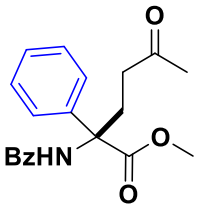

The **procedure G** was followed using substrate (25 mg, 0.093 mmol), methyl vinyl ketone (8.1 µL, 0.097 mmol), 0.19 mL of a 0.0005 M MTBD/CH_3CN solution (0.0000928 mmol of MTBD) to afford the title compound in 94% yield (30 mg, 0.087 mmol). ^{1}H NMR (400 MHz, Chloroform-*d*) δ 7.89 – 7.81 (m, 3H), 7.53 (t, *J* = 7.3 Hz, 1H), 7.50 – 7.42 (m, 4H), 7.34 (t, *J* = 7.5 Hz, 2H), 7.28 (t, *J* = 7.2 Hz, 1H), 3.72 (s, 3H), 3.18 (ddd, *J* = 14.9, 9.7, 5.5 Hz, 1H), 2.92 (ddd, *J* = 14.5, 9.4, 5.7 Hz, 1H), 2.60 (ddd, *J* = 17.4, 9.3, 5.5 Hz, 1H), 2.27 (ddd, *J* = 17.4, 9.7, 5.7 Hz, 1H), 2.11 (s, 3H). ^{13}C NMR (101 MHz, Chloroform-*d*) δ 207.9, 173.5, 165.7, 139.2, 134.2, 132.0, 128.8, 128.8, 128.1, 127.2, 126.1, 65.3, 53.7, 39.1, 30.0, 28.2. FT-IR (neat) cm^{-1} 3356, 1744, 1709, 1561. HRMS (ESI) $C_{20}H_{21}NO_4$ calcd. $[M+H]^+$ 340.1543 observed 340.1549.

4a methyl-2-((tert-butoxycarbonyl)amino)-5-oxo-2-phenylhexanoate

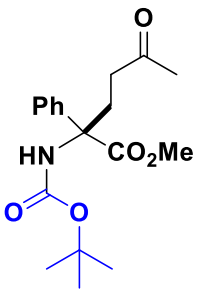

The **procedure G** was followed using substrate (150 mg, 0.565 mmol), methyl vinyl ketone (50.0 µL, 0.594 mmol), 1.13 mL of a 0.0005 M MTBD/CH_3CN solution (0.0005654 mmol of MTBD) to afford the title compound in 92% yield (174 mg, 0.520 mmol). ^{1}H NMR (400 MHz, Methylene Chloride-d_2) δ 7.43 (d, *J* = 7.6 Hz, 2H), 7.35 (t, *J* = 7.4 Hz, 2H), 7.28 (t, *J* = 7.2 Hz, 1H), 6.06

(s, 1H), 3.64 (s, 3H), 2.75 (m, 2H), 2.51 (ddd, *J* = 17.2, 9.7, 5.4 Hz, 1H), 2.26 (ddd, *J* = 17.2, 10.2, 5.6 Hz, 1H), 2.10 (s, 3H), 1.33 (s, 9H).^{13}C NMR (101 MHz, Methylene Chloride-d_2) δ 207.8, 173.4, 154.3, 140.9, 128.9, 128.3, 126.5, 80.2, 65.0, 53.7, 39.1, 30.2, 29.1, 28.5. FT-IR (neat) cm-1 3424, 2976, 1709. HRMS (ESI) $C_{18}H_{25}NO_5$ calcd. $[M+H]^+$ 336.1802 observed 336.1805.

4b methyl-2-(((benzyloxy)carbonyl)amino)-5-oxo-2-phenylhexanoate

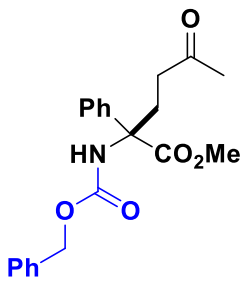

The **procedure G** was followed using substrate (25 mg, 0.084 mmol), methyl vinyl ketone (7.3 µL, 0.088 mmol), 0.17 mL of a 0.0005 M MTBD/CH_3CN solution (0.0000835 mmol of MTBD) to afford the title compound in 89% yield (27 mg, 0.074 mmol). ^{1}H NMR (400 MHz, Chloroform-*d*) δ 7.46 – 7.40 (m, 2H), 7.37 – 7.28 (m, 8H), 6.37 (s, 1H), 5.02 (q, *J* = 12.3 Hz, 2H), 3.66 (s, 3H), 2.96 (s, 1H), 2.82 (td, *J* = 9.5, 9.0, 5.0 Hz, 1H), 2.38 (m, 2H), 2.11 (s, 3H). ^{13}C NMR (101 MHz, Chloroform-*d*) δ 207.5, 172.9, 154.1, 139.6, 136.5, 128.8, 128.6, 128.3, 128.2, 128.2, 125.9, 66.8, 64.7, 53.6, 38.8, 30.0, 28.1. FT-IR (neat) cm-1 3361, 3060, 3030, 1740, 1716. HRMS (ESI) $C_{21}H_{23}NO_5$ calcd. $[M+Na]^+$ 392.1468 observed 392.1462.

4d methyl-2-((tert-butoxycarbonyl)amino)-5-oxo-2-(trifluoromethyl)hexanoate

The **procedure G** was followed using substrate (100 mg, 0.389 mmol), methyl vinyl ketone (34.0

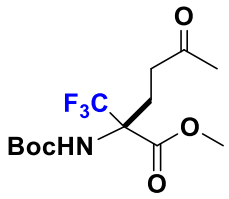

µL, 0.408 mmol), 0.78 mL of a 0.0005 M MTBD/CH_3CN solution (0.0003888 mmol of MTBD) to afford the title compound in 83% yield (106 mg, 0.323 mmol). ^{19}F NMR (376 MHz, Methylene Chloride-d_2) δ -74.70. ^{1}H NMR (400 MHz, Methylene Chloride-d_2) δ 5.61 (s, 1H), 3.80 (s, 3H), 2.72 – 2.52 (m, 2H), 2.49 – 2.38 (m, 1H), 2.31 (ddd, *J* = 14.9, 8.7, 6.2 Hz, 1H), 2.12 (s, 3H), 1.41 (s, 9H). ^{13}C NMR (101 MHz, Methylene Chloride-d_2) δ 207.2, 167.6, 153.9, 124.9 (q, *J* = 287.5 Hz), 81.3, 65.2 (q, *J* = 28.1 Hz),

54.1, 37.9, 30.2, 28.4, 24.8. FT-IR (neat) cm-1 3425, 1740, 1723, 1537. HRMS (ESI) $C_{13}H_{20}F_3NO_5$calcd. $[M+H]^+$ 328.1366 observed 328.1366.

5b 2,2,2-trifluoroethyl-2-benzamido-2-methyl-5-oxohexanoate

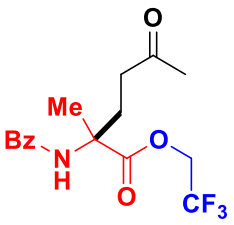

The **procedure H** was followed using substrate (40 mg, 0.145 mmol), methyl vinyl ketone (12.7 µL, 0.153 mmol), 0.290 mL of CH_2Cl_2, and MTBD (12.7 µL, 0.153 mmol, 20 mol %) to afford the title compound in 72% yield (36 mg, 0.100 mmol). ^{19}F NMR (376 MHz, Chloroform-*d*) δ -73.69 (t, *J* = 8.4 Hz). ^{1}H NMR (400 MHz, Chloroform-*d*) δ 7.81 (d, *J* = 7.1 Hz, 2H), 7.60 (s, 1H), 7.51 (d, *J* = 6.0 Hz, 1H), 7.45 (t, *J* = 7.3 Hz, 2H), 4.81 – 4.29 (m, 2H), 2.69 (qdd, *J* = 18.9, 7.6, 5.2 Hz, 2H), 2.36 (ddd, *J* = 14.8, 7.8, 5.2 Hz, 1H), 2.19 (s, 3H), 2.18 – 2.11 (m, 1H), 1.71 (s, 3H). ^{13}C NMR (101 MHz, Chloroform-*d*) δ 209.8, 172.2, 166.8, 133.8, 131.9, 128.8, 127.2, 123.0 (q, *J* = 277.4, 277.3 Hz), 61.2 (q, *J* = 36.6 Hz), 59.3, 38.7, 31.5, 30.1, 23.2. FT-IR (neat) cm-1 3445, 1733, 1718, 1598. HRMS (ESI) $C_{16}H_{18}F_3NO_4$ calcd. $[M+H]^+$ 346.1261 observed 346.1254.

5c 2,2,2-trifluoroethyl-2-benzamido-2-isopropyl-5-oxohexanoate

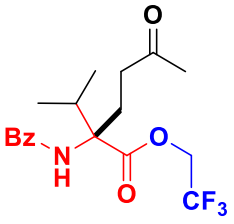

The **procedure H** was followed using substrate (150 mg, 0.495mmol), methyl vinyl ketone (43.3 µL, 0.519 mmol), 1.00 mL of CH_2Cl_2, and MTBD (21.3 µL, 0.148 mmol,30 mol %) to afford the title compound in 76% yield (140 mg, 0.376mmol). ^{19}F NMR (376 MHz, Methylene Chloride-d_2) δ -73.76 (t, *J* = 8.5 Hz). ^{1}H NMR (400 MHz, Methylene Chloride-d_2) δ 7.76 (d, *J* = 7.2 Hz, 2H), 7.53 (t, *J* = 6.7 Hz, 1H), 7.45 (t, *J* = 7.4 Hz, 2H), 6.97 (s, 1H), 4.60 (qq, *J* = 8.6, 4.2 Hz, 2H), 2.79 – 2.58 (m, 2H), 2.57 – 2.45 (m, 1H), 2.45 – 2.27 (m, 2H), 2.05 (s, 3H), 1.07 (d, *J* = 7.0 Hz, 3H), 0.98 (d, *J* = 6.9 Hz, 3H). ^{13}C NMR (101 MHz, Methylene Chloride-d_2) δ 208.2, 172.2, 166.8, 135.2, 132.2, 129.2, 127.4, 120.8 (q, *J* =277.3, 277.3 Hz), 67.4, 61.6 (q, *J* = 36.7 Hz), 39.2, 34.4,

30.2, 26.9, 18.2, 17.8. FT-IR (neat) cm-1 3423, 1741, 1720, 1560. HRMS (ESI) $C_{18}H_{22}F_3NO_4$ calcd. $[M+H]^+$ 374.1574 observed 374.1581.

5d 2,2,2-trifluoroethyl-2-benzamido-2-benzyl-5-oxohexanoate

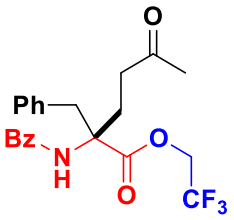

The **procedure H** was followed using substrate (120 mg, 0.342 mmol), methyl vinyl ketone (30.0 µL, 0.359 mmol), 1.00 mL of CH_2Cl_2, and MTBD (9.8 µL, 0.0684 mmol,20 mol %) to afford the title compound in 76% yield (115 mg, 0.273 mmol). ^{19}F NMR (376 MHz, Chloroform-*d*) δ -73.27 (t, *J* = 8.5 Hz). ^1H NMR (400 MHz, Chloroform-*d*) δ 7.82 (d, *J* = 7.0 Hz, 2H), 7.64 (t, *J* = 7.4 Hz, 1H), 7.55 (t, *J* = 7.5 Hz, 2H), 7.34 – 7.29 (m, 3H), 7.17 – 7.13 (m, 2H), 7.12 (s, 1H), 4.68 (q, *J* = 8.4 Hz, 2H), 3.77 (d, *J* = 13.8 Hz, 1H), 3.58 (d, *J* = 13.8 Hz, 1H), 2.86 (dt, *J* = 14.2, 7.0 Hz, 1H), 2.64 (m, 2H), 2.36 (dt, *J* = 14.4, 6.7 Hz, 1H), 2.21 (s, 3H). ^{13}C NMR (101 MHz, Chloroform-*d*) δ 208.2, 171.9, 167.0, 135.7, 134.3, 132.0, 130.2, 128.9, 128.5, 127.3, 127.1, 122.9 (q, *J* =277.2, 277.3 Hz), 64.5, 61.7 (q, *J* = 36.8 Hz), 40.2, 38.5, 29.9, 29.6. FT-IR (neat) cm-1 3451, 1743, 1725, 1527. HRMS (ESI) $C_{22}H_{22}F_3NO_4$ calcd. $[M+H]^+$ 422.1574 observed 422.1570.

5e 2,2,2-trifluoroethyl-2-benzamido-2-isobutyl-5-oxohexanoate

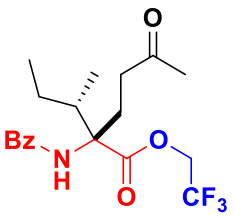

The **procedure H** was followed using substrate (100 mg, 0.315 mmol), methyl vinyl ketone (27.6 µL, 0.313 mmol), 0.600 mL of CH_2Cl_2, and MTBD (10.0 µL, 0.0894 mmol, 20 mol %) to afford the title compound (d.r. 1.5:1) in 52% yield (63 mg, 0.164 mmol). ^1H NMR (400 MHz, Methylene Chloride-d_2) δ 7.68 (dt, *J* = 6.9, 1.3 Hz, 4H), 7.50 – 7.42 (m, 2H), 7.44 – 7.34 (m, 5H), 7.33 – 7.27 (m, 1H), 6.91 (s, 1H), 6.85 (s, 1H), 4.51 (qd, *J* = 8.5, 1.9 Hz, 4H), 2.77 – 2.61 (m, 3H), 2.57 – 2.37 (m, 3H), 2.37 – 2.15 (m, 6H), 1.98 (s, 6H), 0.98 (d, *J* = 6.9 Hz, 3H), 0.94 – 0.67 (m, 12H). ^{13}C

NMR (101 MHz, Methylene Chloride-d_2) δ 208.2, 208.2, 172.4, 172.3, 166.7, 166.6, 135.2, 132.2, 129.5, 129.5, 129.2, 129.1, 127.4, 126.6 (d, J = 10.3 Hz), 125.7 (d, J = 162.6 Hz), 67.6, 67.4, 61.6 (qd, J = 36.8, 1.4 Hz, two carb ons), 46.8, 41.7, 41.3, 40.4, 39.3, 39.2, 30.2, 26.99, ,26.95, 26.3, 25.1, 24.7, 14.3, 13.9, 13.0. HRMS (ESI) $C_{19}H_{24}F_3NO_4$ calcd. $[M+H]^+$ 388.1730 observed 388.1722.

5f 2,2,2-trifluoroethyl-2-benzamido-2-isobutyl-5-oxohexanoate

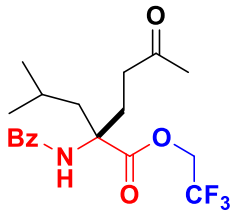

The **procedure H** was followed using substrate (150 mg, 0..473 mmol), methyl vinyl ketone (41.4 µL, 0.496 mmol), 1.00 mL of CH_2Cl_2, and MTBD (27.2 µL, 0.189 mmol,20 mol %) to afford the title compound in 68% yield (125 mg, 0.321 mmol). ^{19}F NMR (376 MHz, Chloroform-d) δ -73.27 (t, J = 8.5 Hz). ^{1}H NMR (400 MHz, Methylene Chloride-d_2) δ 7.77 (d, J = 7.2 Hz, 2H), 7.53 (t, J = 7.3 Hz, 1H), 7.45 (t, J = 7.4 Hz, 2H), 7.14 (s, 1H), 4.58 (q, J = 8.4 Hz, 2H), 2.74 (ddd, J = 14.5, 8.7, 6.0 Hz, 1H), 2.53 – 2.39 (m, 2H), 2.31 (ddd, J = 17.8, 8.7, 6.1 Hz, 1H), 2.17 (ddd, J = 14.5, 8.5, 6.1 Hz, 1H), 2.05 (s, 3H), 1.93 (dd, J = 14.4, 6.9 Hz, 1H), 1.72 – 1.55 (m, 1H), 0.90 (d, J = 6.7 Hz, 3H), 0.83 (d, J = 6.6 Hz, 3H). ^{13}C NMR (101 MHz, Methylene Chloride-d_2) δ 208.0, 173.8, 166.6, 135.1, 132.2, 129.2, 127.4, 123.5(q, J =277.2, 277.3 Hz), 63.9, 61.9 (q, J = 36.8 Hz), 43.7, 38.6, 30.4, 30.2, 25.3, 24.1, 23.4. HRMS (ESI) $C_{19}H_{24}F_3NO_4$ calcd. $[M+H]^+$ 388.1730 observed 388.1738.

5g 2,2,2-trifluoroethyl-2-benzamido-2-(2-(methylthio)ethyl)-5-oxohexanoate

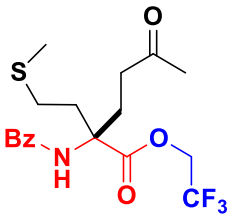

The **procedure H** was followed using substrate (100 mg, 0.298 mmol), methyl vinyl ketone (26.1 µL, 0.313 mmol), 0.600 mL of CH_2Cl_2, and MTBD (12.8 µL, 0.0894 mmol,30 mol %) to afford the title compound in 79% yield (96 mg, 0.235 mmol). ^{19}F NMR (376 MHz, Methylene Chloride-d_2) δ -73.85 (t, *J* = 8.5 Hz). ^{1}H NMR (400 MHz, Methylene Chloride-d_2) δ 7.71 (d, *J* = 7.3 Hz, 2H), 7.47 (t, *J* = 7.3 Hz, 1H), 7.39 (t, *J* = 7.5 Hz, 2H), 7.24 (s, 1H), 4.52 (q, *J* = 8.4 Hz, 2H), 2.59 (ddd, *J* = 14.5, 10.1, 6.9 Hz, 2H), 2.52 – 2.23 (m, 5H), 2.15 – 2.06 (m, 1H), 2.01 (s, 3H), 1.97 (s, 3H). ^{13}C NMR (101 MHz, Methylene Chloride-d_2) δ 208.4, 172.6, 166.8, 134.6, 132.4, 129.2, 127.5, 123.0 (q, *J* =277.2, 277.3 Hz), 63.5, 61.9 (q, *J* = 36.7 Hz), 38.6, 34.9, 30.2, 29.8, 29.1, 15.8. FT-IR (neat) cm-1 3421, 1752, 1726, 1608. HRMS (ESI) $C_{18}H_{22}F_3NO_4S$ calcd. $[M+H]^+$ 406.1294 observed 406.1303.

-Synthesis of peptides Boc-Phe-Phg-OMe and DAPT

Boc-Phe-Phg-OMe (methyl 2-((R)-2-((tert-butoxycarbonyl)amino)-3-phenylpropanamido)-2-phenylacetate)

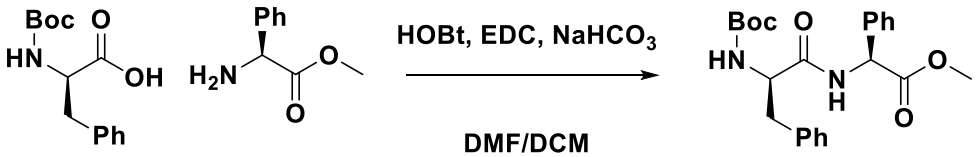

N-Boc phenyl alanine (500 mg, 1.89 mmol), phenyl glycine methyl ester HCl (380 mg,1.89 mmol), EDC (432 mg, 2.26 mmol), HOBt (346 mg , 2.26 mmol) and $NaHCO_3$ (380 mg, 2.88 mmol) were dissolved in anhydrous DMF/DCM (9.43 mL 20/80 v/v) at 0 °C and the reaction was stirred for 16 h at room temperature under inert atmosphere. The workup consisted of concentrating the solution, diluting with EtOAc 20 mL, and adding with an equal amount of water. The organic layer was separated and then washed with equal amount of sat. $NaHCO_3$ (x3), 1 M HCl (x2), and water. The organic layer was again separated and the solution was concentrated

under vacuum. Flash column chromatography was used to purify the desired compound giving a yeild 60% (467 mg, 1.13 mmol). ^{1}H NMR (400 MHz, Chloroform-*d*) δ 7.33 – 7.29 (m, 3H), 7.24 – 7.18 (m, 5H), 7.11 (dd, *J* = 7.3, 2.1 Hz, 2H), 6.88 – 6.71 (m, 1H), 5.50 (d, *J* = 7.1 Hz, 1H), 5.04 (s, 1H), 4.40 (s, 1H), 3.70 (s, 3H), 3.04 (d, *J* = 7.0 Hz, 2H), 1.40 (s, 9H).

DAPT, N-[N-(3,5-Difluorophenacetyl)-L-alanyl]-S-phenylglycine t-butyl ester

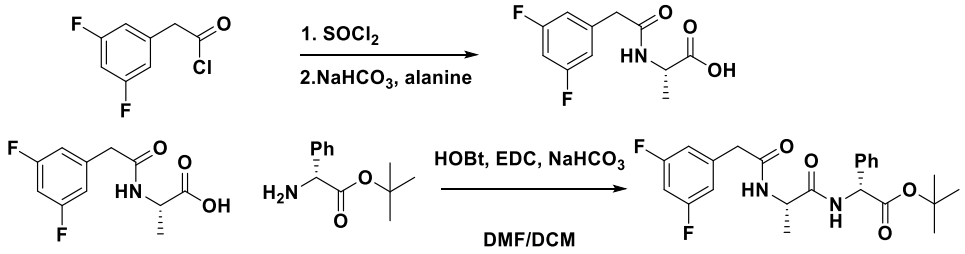

Synthesis of (3,5-difluorophenyl)acetyl chloride- 2-(3,5-difluorophenyl)acetic acid (3.00 g, 17.4 mmol) was added to 35 mL of DCM and 6 mL of $SOCl_2$ and left to react until by ^{19}F the starting material was consumed. Then the solution was concentrated and used without further purification.[182] Synthesis of (2-(3,5-difluorophenyl)acetyl)-L-alanine-2-(3,5-difluorophenyl)acetyl chloride (1.49 g, 16.8 mmol) was added alternately in 4 portions over 30 minutes to a solution of alanine (3.18 g, 16.8 mmol) in 20 mL of a 10 % $NaHCO_3$. After the addition was complete the reaction was left to react for 2 h. After 2 h, the reaction was quenched by the dropwise addition of concentrated aqueous hydrochloric acid until **pH 1,** which resulted in the formation of a precipitate. The solid was isolated by filtration and then trituration from DCM/Hexanes. The resulting crystals were filtered and air dried to give the desired acid in 62% (2.5 g, 10.3 mmol). Synthesis of DAPT, N-[N-(3,5-Difluorophenacetyl)-L-alanyl]-S-phenylglycine t-butyl ester- 2-(3,5-difluorophenyl)acetyl)-L-alanine (300 mg, 1.23 mmol) from the above procedure, phenyl glycine tert-butyl ester HCl (331 mg,1.36 mmol), EDC (259 mg, 1.36 mmol), HOBt (208 mg , 1.36 mmol) and $NaHCO_3$ (155 mg, 1.85 mmol) were dissolved in

anhydrous DMF/DCM (9.43 mL 20/80 v/v) at 0 ºC and the reaction was stirred for 16 hr at room temperature under inert atmosphere. The workup consisted of concentrating solution, diluting with EtOAc 20 mL, and an equal amount of water. The organic layer was separated and washed with equal amount of sat. $NaHCO_3$ (x3), 1 M HCl (x2), and water. The organic layer was again separated and the solution was concentrated under vacuum. Flash column chromatography was used to purify the desired compound at 79% (421 mg, 0.973 mmol).Characterization data matched that was seen in literature.[182]

-Late stage functionliaztion of peptides Boc-Phe-Phg-OMe and DAPT

General Procedure A: Under an dry inert atmosphere the peptide (**1 equiv**), methylvinyl ketone **(1.05 equiv),** MeCN **(0.5 M)** was added to a small test tube. Then MTBD **(0.10-0.50 equiv)** was added to mixture and stirred vigorously. The reaction was monitored by ^{19}F NMR/^{1}H NMR until the starting material was consumed. The organic solution was then dried with $MgSO_4$ and concentrated giving crude product. The crude product was purified further by column chromatography.

6a Boc-Phe-Phg-OMe, methyl-2-2-((tert-butoxycarbonyl)amino)-3-phenylpropanamido)-5-oxo-2-phenylhexanoate

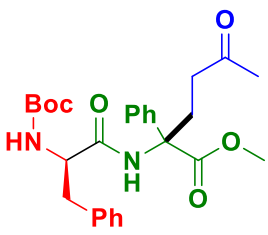

The **procedure A** was followed using substrate (25 mg, 0.0601 mmol), methyl vinyl ketone (5.3 µL, 0.0640 mmol), 0.120 mL of ACN, and MTBD (0.87 µL, 0.0060608 mmol, 20 mol %) to afford the title compound in 73% yield (21 mg, 0.044 mmol). ^{1}H NMR (400 MHz, Chloroform-*d*) δ 7.40 (s, 1H), 7.29 – 7.15 (m, 19H), 7.14 – 7.10 (m, 3H), 4.88 (dd, *J* = 16.1, 7.1 Hz, 2H), 4.32 (p, *J* = 7.5 Hz, 2H), 3.58 (s, 3H), 3.56 (s, 3H), 3.07 – 2.85 (m, 6H), 2.65 (ddd, *J* =

14.5, 10.3, 5.2 Hz, 2H), 2.32 (ddd, *J* = 16.1, 10.4, 5.1 Hz, 1H), 2.15 (ddd, *J* = 15.7, 10.2, 5.1 Hz, 1H), 2.09 – 2.04 (m, 1H), 2.02 (s, 2H), 1.99 (s, 3H), 1.94 (ddd, *J* = 16.9, 10.6, 5.3 Hz, 1H), 1.39 (s, 9H), 1.38 (s, 9H). ^{13}C NMR (101 MHz, Chloroform-*d*) δ 207.6, 207.6, 172.9, 172.8, 169.9, 169.7, 139.1, 138.8, 136.7, 136.6, 129.6, 129.6, 128.9, 128.7, 128.7, 128.1, 128.1, 127.1, 125.9, 65.0, 64.9, 56.2, 53.5, 53.5, 38.7, 38.5, 37.6, 37.5, 30.1, 29.9, 28.4, 27.6, 27.3. FT-IR (neat) cm-1: 3327, 3061, 1760, 1635. HRMS (ESI) $C_{27}H_{34}N_2O_6$ calcd. $[M+H]^+$ 483.2490 observed 483.2499.

6b Boc-Phg-Phe-OMe derivative, methyl 2-((tert-butoxycarbonyl)amino)-5-oxo-2-phenylhexanoyl)-D-phenylalaninate

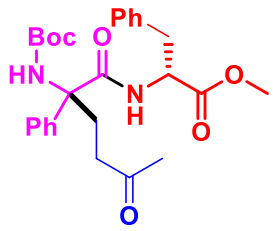

The **procedure A** was followed using substrate (135 mg, 0.328 mmol), methyl vinyl ketone (28.7 µL, 0.344 mmol), 0.655 mL of ACN, and MTBD (10.1 µL, 0.0655 mmol, 20 mol %) to afford the title compound in 33% yield (58 mg, 0.120 mmol). ^{1}H NMR (400 MHz, Methylene Chloride-d_2) δ 7.42 – 7.27 (m, 10H), 7.21 (dq, J = 8.6, 2.9, 2.1 Hz, 2H), 7.17 – 7.12 (m, 1H), 7.08 (t, J = 7.4 Hz, 2H), 7.03 – 6.94 (m, 2H), 6.63 (s, 2H), 6.46 (s, 1H), 6.28 (s, 1H), 6.15 (s, 1H), 4.70 (ddd, J = 13.0, 7.8, 5.3 Hz, 2H), 3.85 – 3.67 (m, 1H), 3.66 (s, 3H), 3.57 (s, 2H), 3.17 – 3.01 (m, 1H), 2.89 (dd, J = 6.0, 3.5 Hz, 3H), 2.86 – 2.65 (m, 3H), 2.43 – 2.30 (m, 2H), 2.10 (s, 4H), 2.04 (s, 2H), 1.37 – 1.28 (m, 32H). ^{13}C NMR (101 MHz, Methylene Chloride-d_2) δ 208.4, 208.1, 172.3, 171.9, 171.7, 171.7, 154.4, 154.4, 142.1, 136.7, 135.9, 131.3, 129.7, 129.6, 129.4, 129.4, 129.2, 129.1, 128.3, 128.3, 127.5, 127.4, 126.4, 126.4, 80.2, 80.0, 64.7, 64.6, 52.8, 52.7, 38.8, 38.6, 38.2, 37.9, 30.4, 30.4, 30.3, 29.9, 29.9, 29.5, 28.8, 28.6, 28.6, 28.5. FT-IR (neat) cm-1: 3403, 3077, 1770, 1635. HRMS (ESI) $C_{27}H_{34}N_2O_6$ calcd. $[M+H]^+$ 483.2490 observed 483.2499.

6c DAPT deravative, tert-butyl-2-2-(2-(3,5-difluorophenyl)acetamido)propanamido)-5-oxo-2-phenylhexanoate

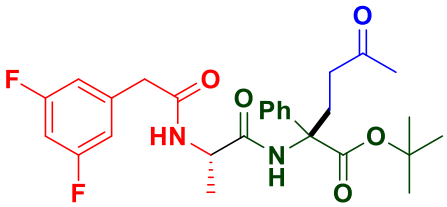

The **procedure A** was followed using substrate (100 mg, 0.231 mmol), methyl vinyl ketone (20.2 µL, 0.243 mmol), 0.120 mL of ACN, and MTBD (16.60 µL, 0.116 mmol, 50 mol %) to afford the title compound in 90% yield (105 mg, 0.208 mmol). ^{19}F NMR (376 MHz, Methylene Chloride-d_2) δ -110.39 – -110.46 (m), -110.47 – -110.53 (m). ^{1}H NMR (400 MHz, Methylene Chloride-d_2) δ 7.52 (s, 1H), 7.46 (s, 1H), 7.40 – 7.18 (m, 9H), 6.84 (ddt, *J* = 6.7, 4.3, 2.1 Hz, 3H), 6.73 (tdd, *J* = 9.1, 5.2, 2.5 Hz, 2H), 6.34 (dd, *J* = 12.6, 7.0 Hz, 2H), 4.45 (td, *J* = 7.0, 3.6 Hz, 2H), 3.49 (s, 3H), 3.48 (s, 1H), 2.90 (dddd, *J* = 14.1, 10.8, 5.1, 3.3 Hz, 2H), 2.67 (ddd, *J* = 13.8, 10.5, 5.0 Hz, 2H), 2.43 (dddd, *J* = 17.5, 10.6, 5.1, 2.0 Hz, 2H), 2.23 – 2.11 (m, 3H), 2.08 (s, 1H), 2.06 (s, 1H), 1.32 (dd, *J* = 7.0, 4.8 Hz, 5H), 1.29 (d, *J* = 1.0 Hz, 16H). ^{13}C NMR (101 MHz, Methylene Chloride-d_2) δ 207.9, 207.7, 171.5, 171.5, 170.9, 170.9, 169.9, 169.8, 140.3, 140.3, 139.4 (td, *J* = 9.7, 5.5 Hz), 128.9, 128.1 (d, *J* = 1.3 Hz), 126.3, 113.6 – 112.1 (m), 103.0 (td, *J* = 25.3, 4.1 Hz), 83.8 (d, *J* = 3.3 Hz), 65.5 (d, *J* = 2.6 Hz), 50.1, 49.9, 43.2, 43.15, 4.99, 38.9, 30.2, 30.2, 27.9, 27.8, 27.7, 18.4 (d, *J* = 2.3 Hz). FT-IR (neat) cm-1 3431, 1502, 1254. HRMS (ESI) $C_{27}H_{32}F_2N_2O_5$ calcd. $[M+K]^+$ 541.1911 observed 541.1922.

-Deuterium studies/experiments

Retro-Michael experiment

Phenyl glycine methyl ester substrate **(**10 mg, 0.0518 mmol,1 equiv) was added to a NMR tube fitted with a C_6D_6 capillary (for NMR locking purposes) and a ^{1}H NMR experiment was conducted as a baseline (**Figure 5.2**). Then MTBD **(**7.9 mg, 0.0518 mmol, 1 equiv**)** was added to mixture and ^{1}H NMR experiment was conducted observing the N-H of the ester has been completely deprotonated (**Figure 5.3**). Then MeOD **(**100 µL, 0.518 mmol,100 equiv) was added and the mixture was left to react for 1 h, then the solution was concentrated removing the excess MeOD. ^{1}H NMR indicated that the glycine ester nitrogen was either deutrerated, more likely bonded to MTBD-D which is indicated by the broadening of MTBD signal (**Figure 5.4**). Next, methylvinyl ketone **(**4.3 µL, 0.0518 mmol, 1 equiv**)** was added and left to react for 6 h, and a final ^{1}HNMR was performed, which showed no incorporation of deuterium in the methylvinyl ketone nor a return of the ester's N-H (**Figure 5.5**), indicating the lack of a transient N-alkylation event.

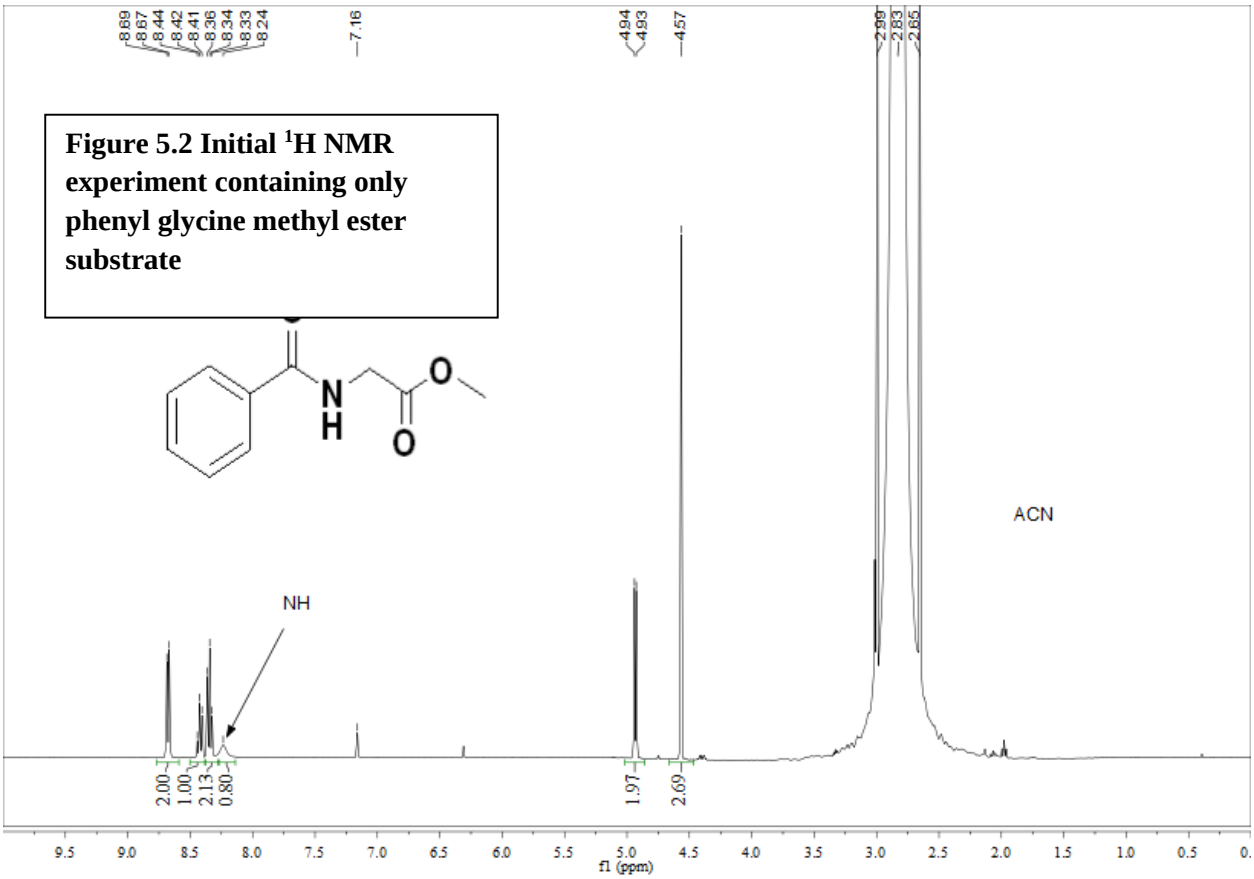

Figure 5.2 Initial ^{1}H NMR experiment containing only phenyl glycine methyl ester substrate

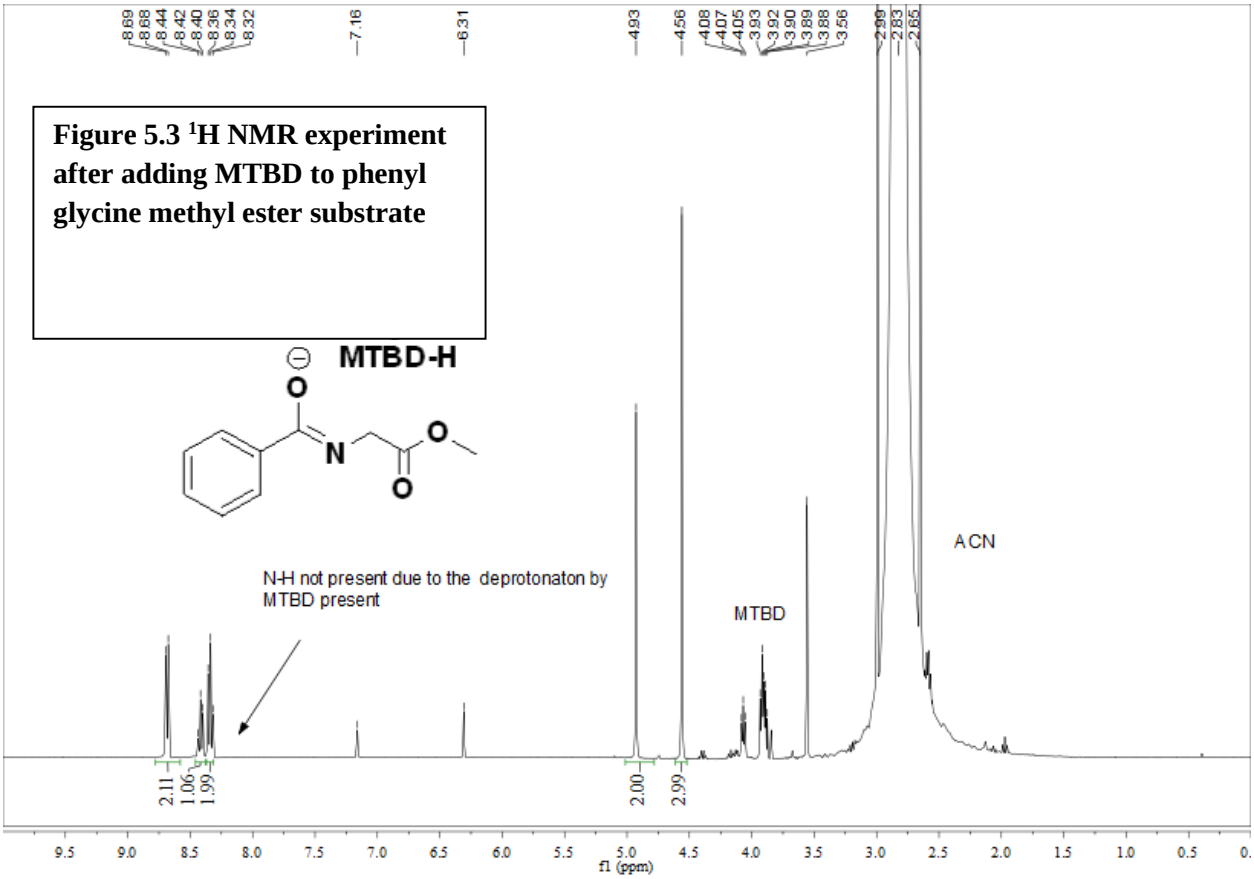

Figure 5.3 ^{1}H NMR experiment after adding MTBD to phenyl glycine methyl ester substrate

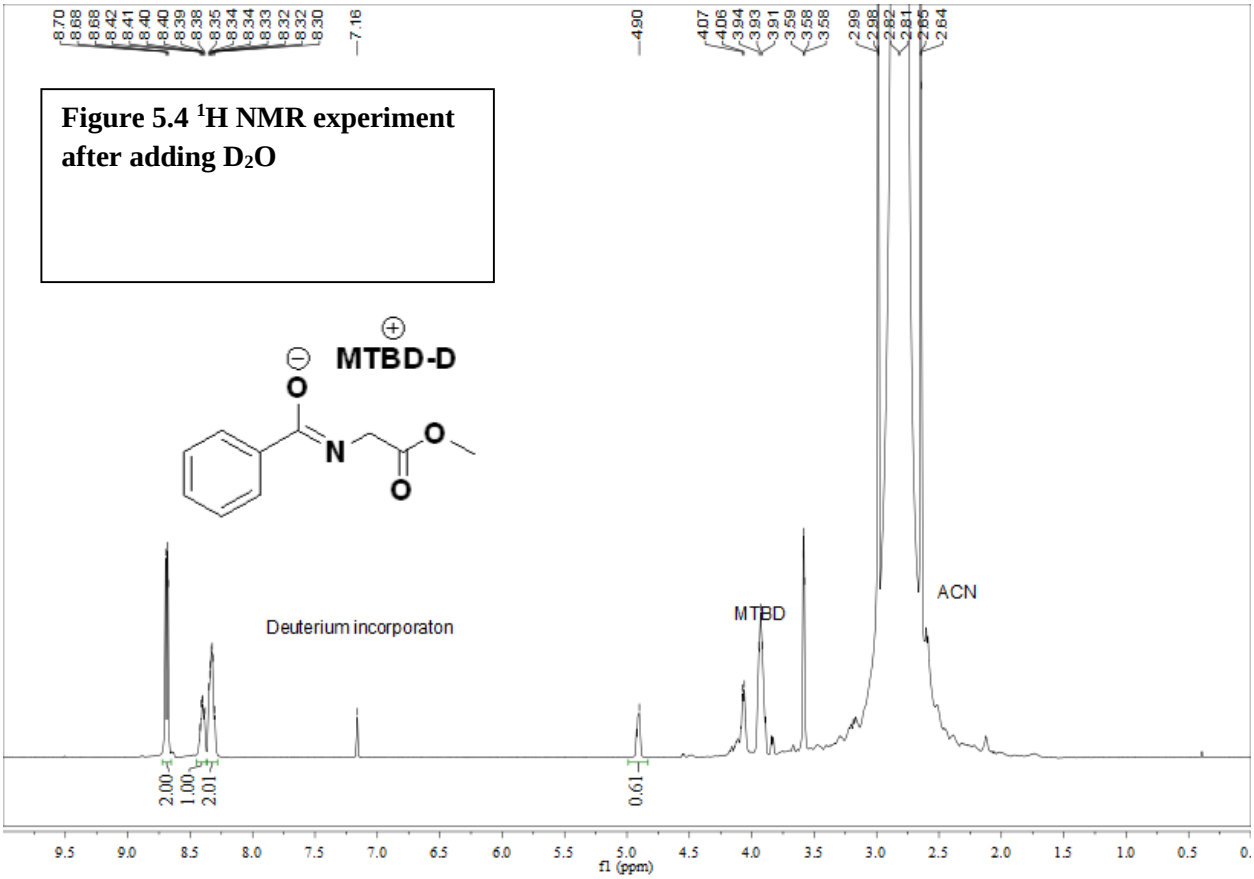

Figure 5.4 ^{1}H NMR experiment after adding D_2O

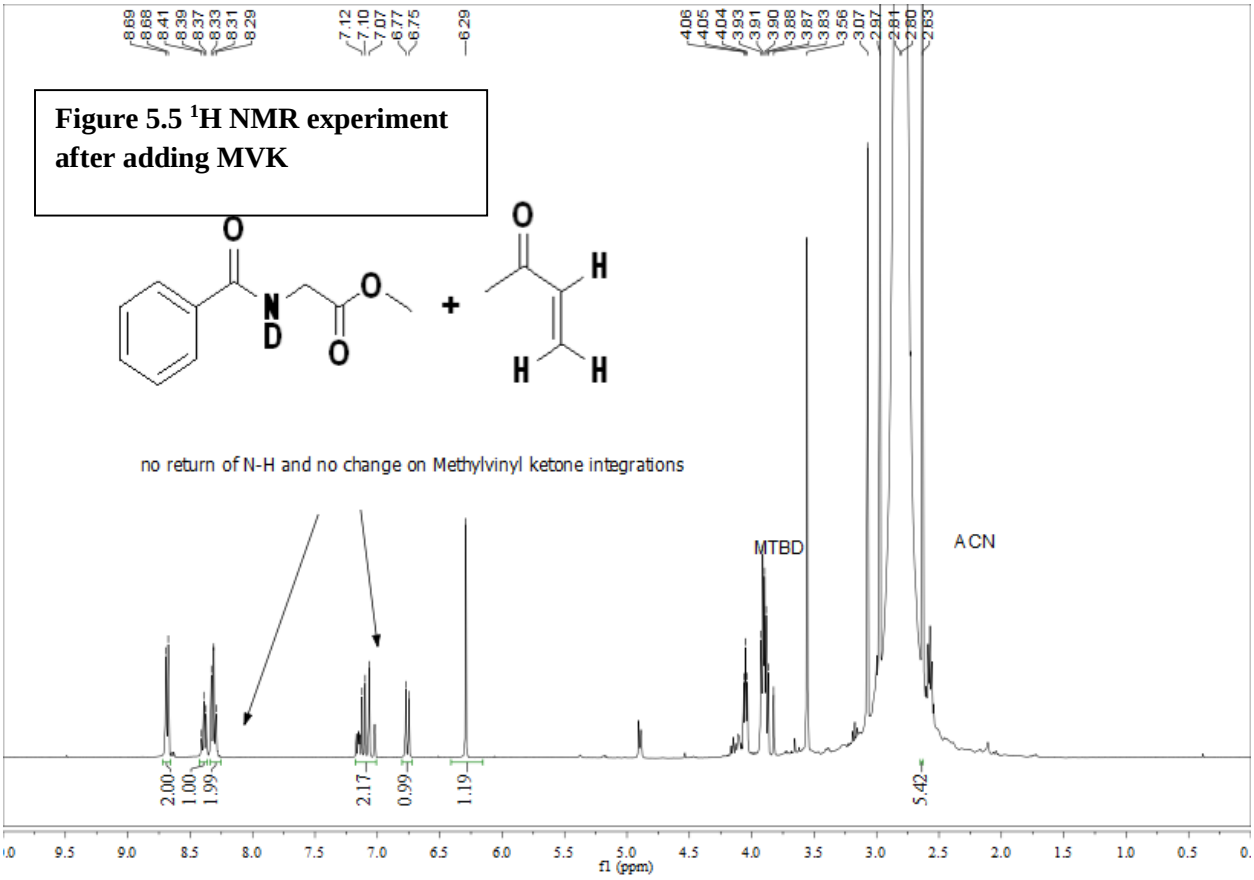

Peptide deuterium experiment

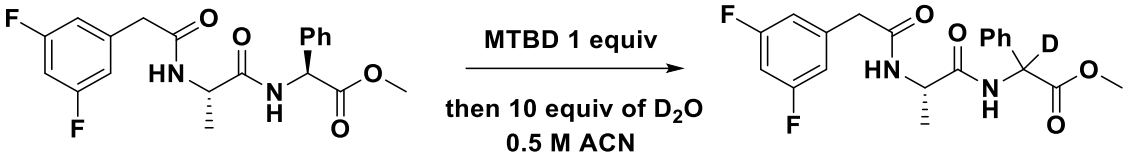

To a dry NMR tube, MTBD (7.8 mg, 0.051 mmol) was added to a solution of the peptide (20 mg, 0.051 mmol) in acetonitrile (0.3 mL). Then D_2O (9.25 µL, 0.51 mmol) was added and the experiment was left to react for 24 h and monitored by ^1H NMR.

DFT references

M. J. Frisch, G. W. Trucks, H. B. Schlegel, G. E. Scuseria,
M. A. Robb, J. R. Cheeseman, G. Scalmani, V. Barone, B. Mennucci,
G. A. Petersson, H. Nakatsuji, M. Caricato, X. Li, H. P. Hratchian,
A. F. Izmaylov, J. Bloino, G. Zheng, J. L. Sonnenberg, M. Hada,
M. Ehara, K. Toyota, R. Fukuda, J. Hasegawa, M. Ishida, T. Nakajima,
Y. Honda, O. Kitao, H. Nakai, T. Vreven, J. A. Montgomery, Jr.,
J. E. Peralta, F. Ogliaro, M. Bearpark, J. J. Heyd, E. Brothers,
K. N. Kudin, V. N. Staroverov, T. Keith, R. Kobayashi, J. Normand,
K. Raghavachari, A. Rendell, J. C. Burant, S. S. Iyengar, J. Tomasi,
M. Cossi, N. Rega, J. M. Millam, M. Klene, J. E. Knox, J. B. Cross,
V. Bakken, C. Adamo, J. Jaramillo, R. Gomperts, R. E. Stratmann,
O. Yazyev, A. J. Austin, R. Cammi, C. Pomelli, J. W. Ochterski,
R. L. Martin, K. Morokuma, V. G. Zakrzewski, G. A. Voth,
P. Salvador, J. J. Dannenberg, S. Dapprich, A. D. Daniels,
O. Farkas, J. B. Foresman, J. V. Ortiz, J. Cioslowski,
and D. J. Fox, Gaussian, Inc., Wallingford CT, 2010.

NMR spectra

Figure 5.6 Chapter V NMR Spectrum Graphs

^{1}H NMR (400 MHz, Chloroform-*d*) **2a**

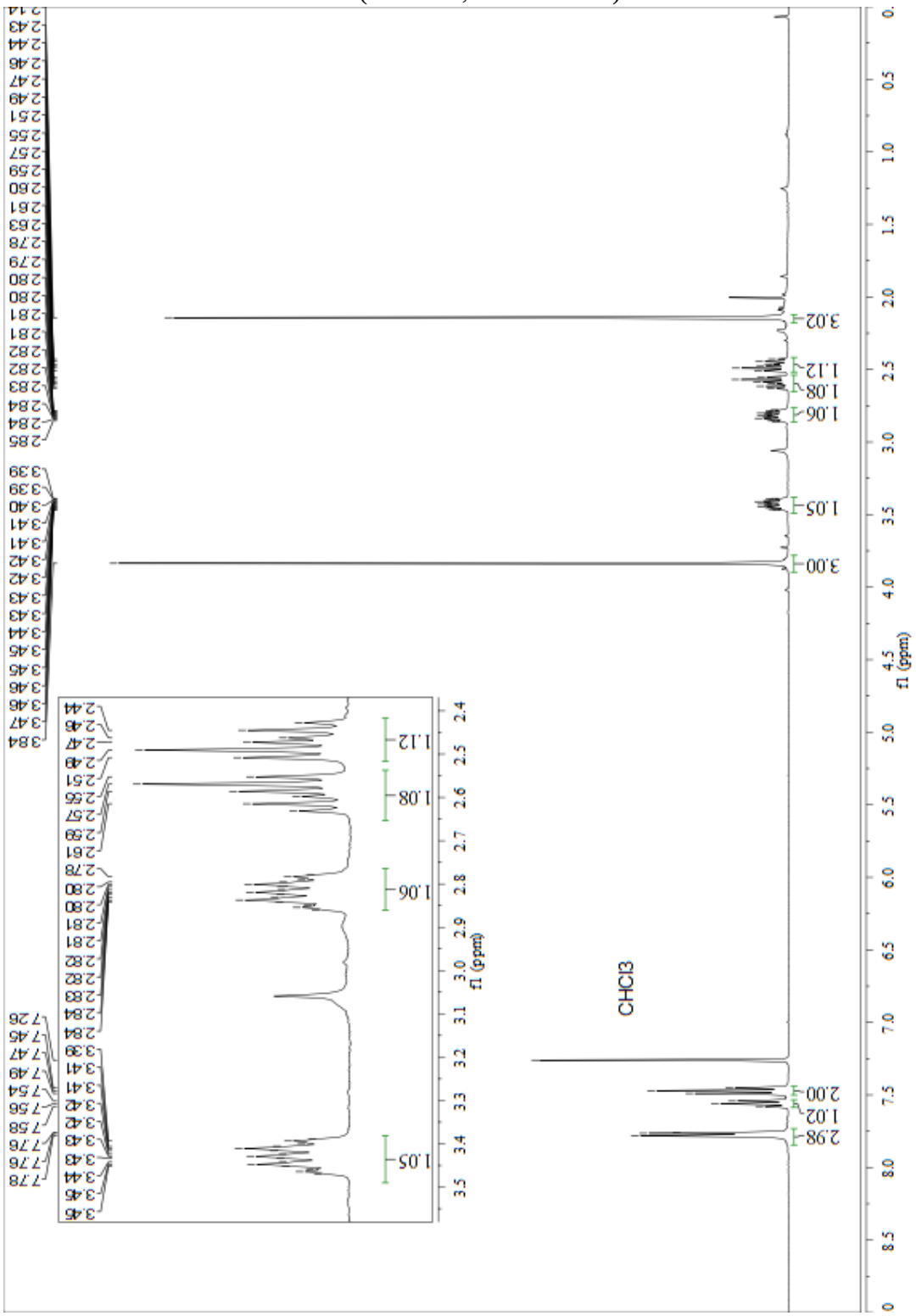

^{19}F NMR (376 MHz, Chloroform-*d*) **2a**

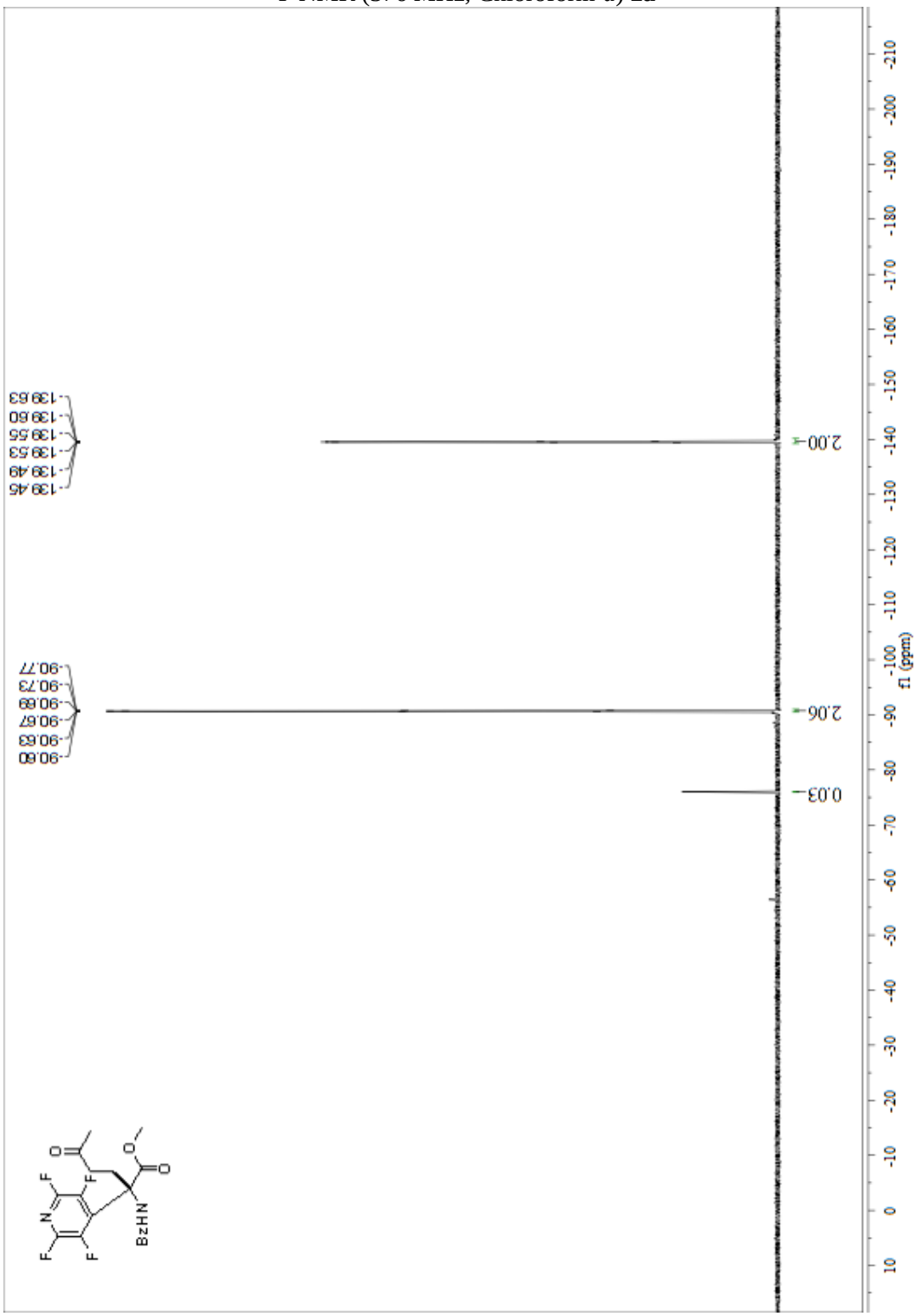

^{13}C NMR (101 MHz, Chloroform-*d*) **2a**

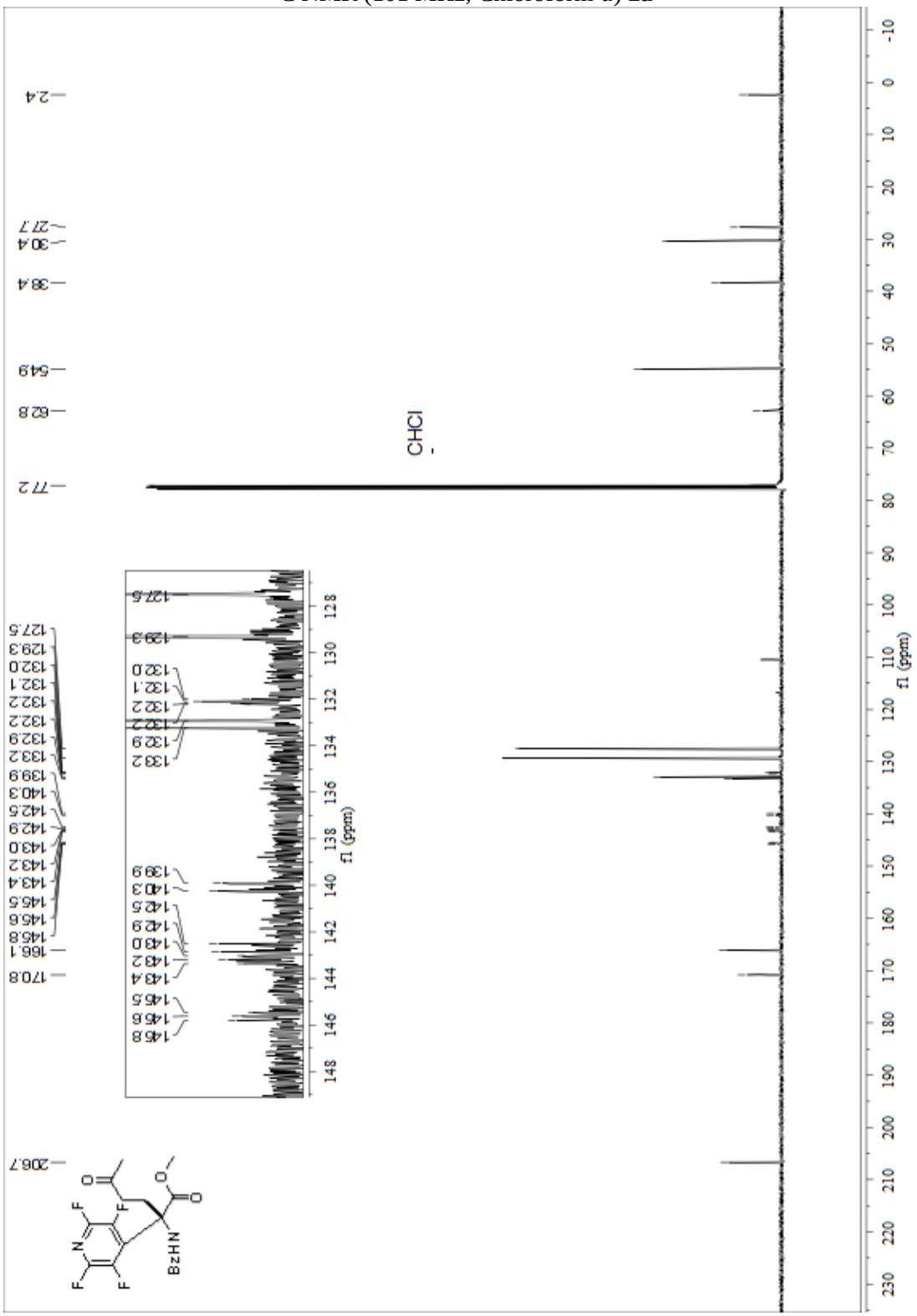

HSQC 2d NMR (400 MHz, Chloroform-*d*) **2a**

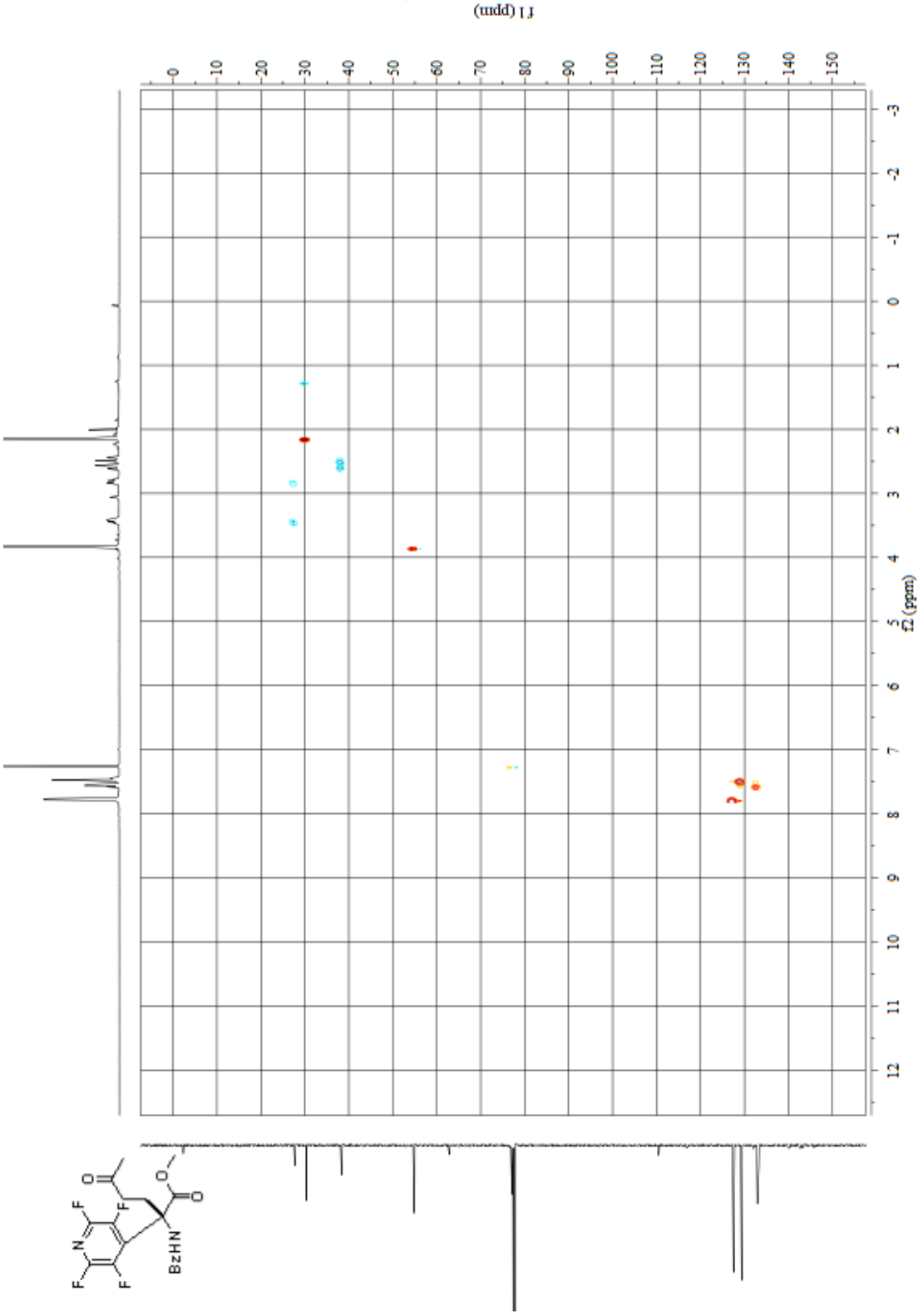

^{1}H NMR (400 MHz, Chloroform-*d*) **2b**

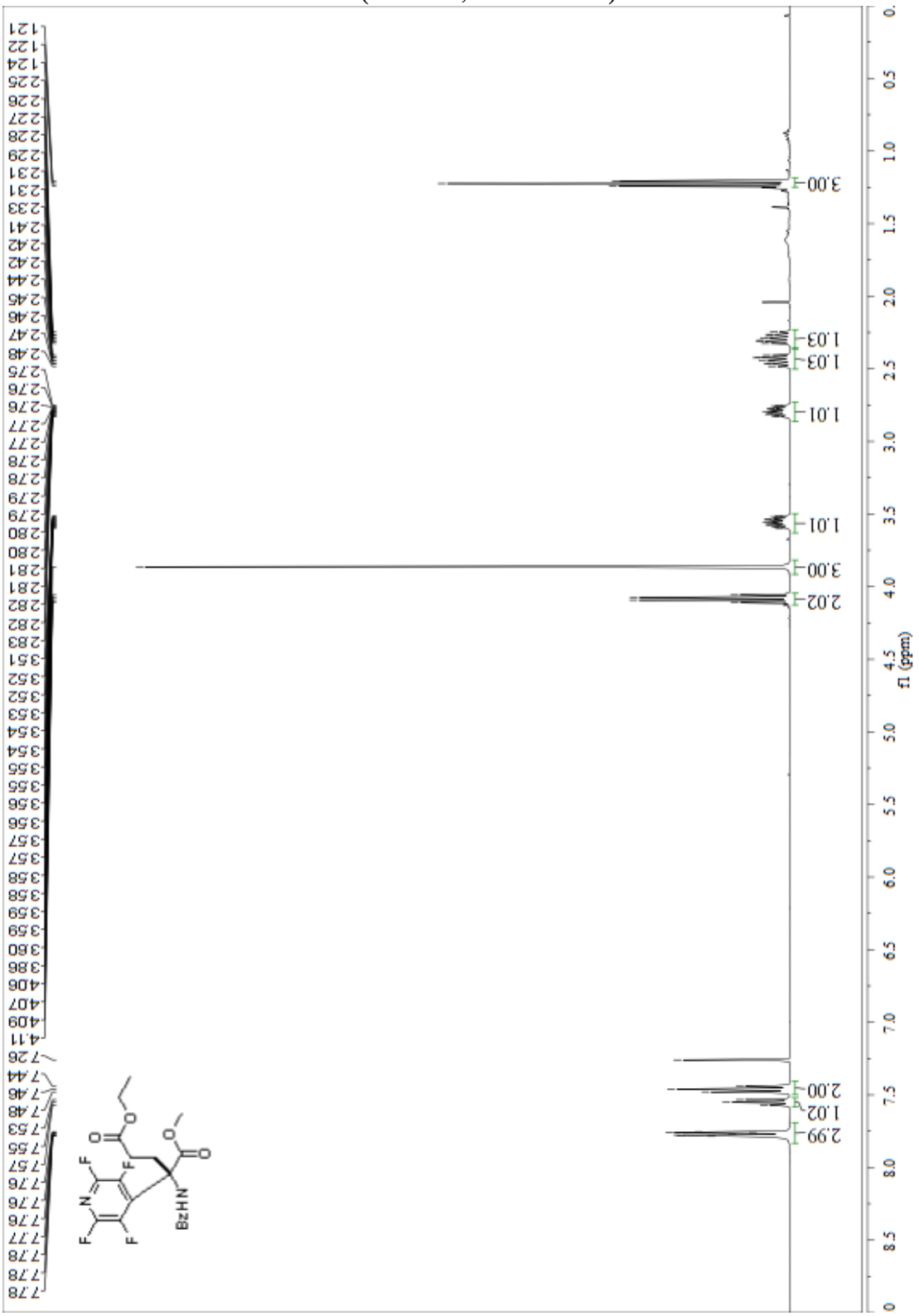

^{19}F NMR (376 MHz, Chloroform-*d*) **2b**

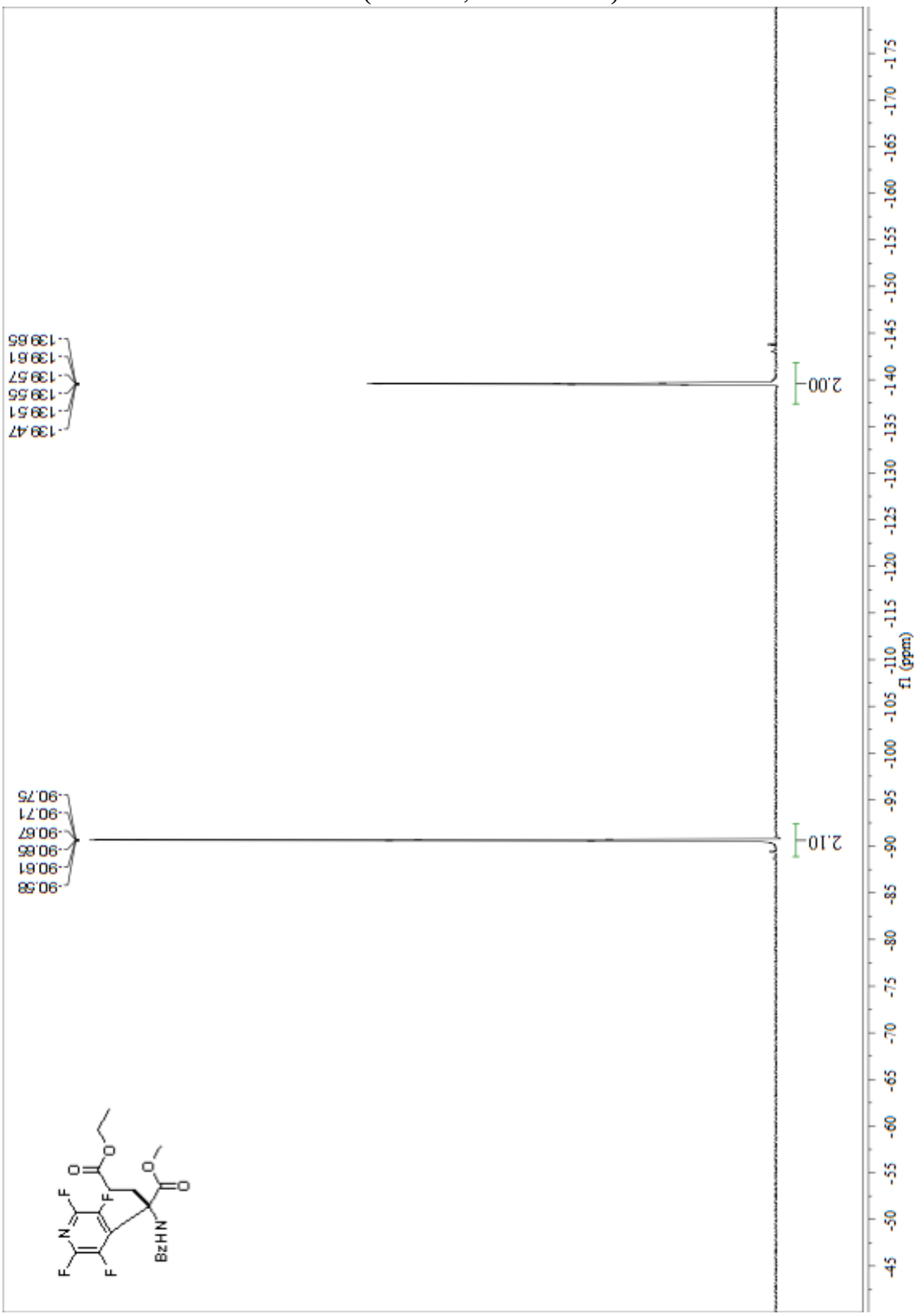

^{13}C NMR (101 MHz, Chloroform-*d*) **2b**

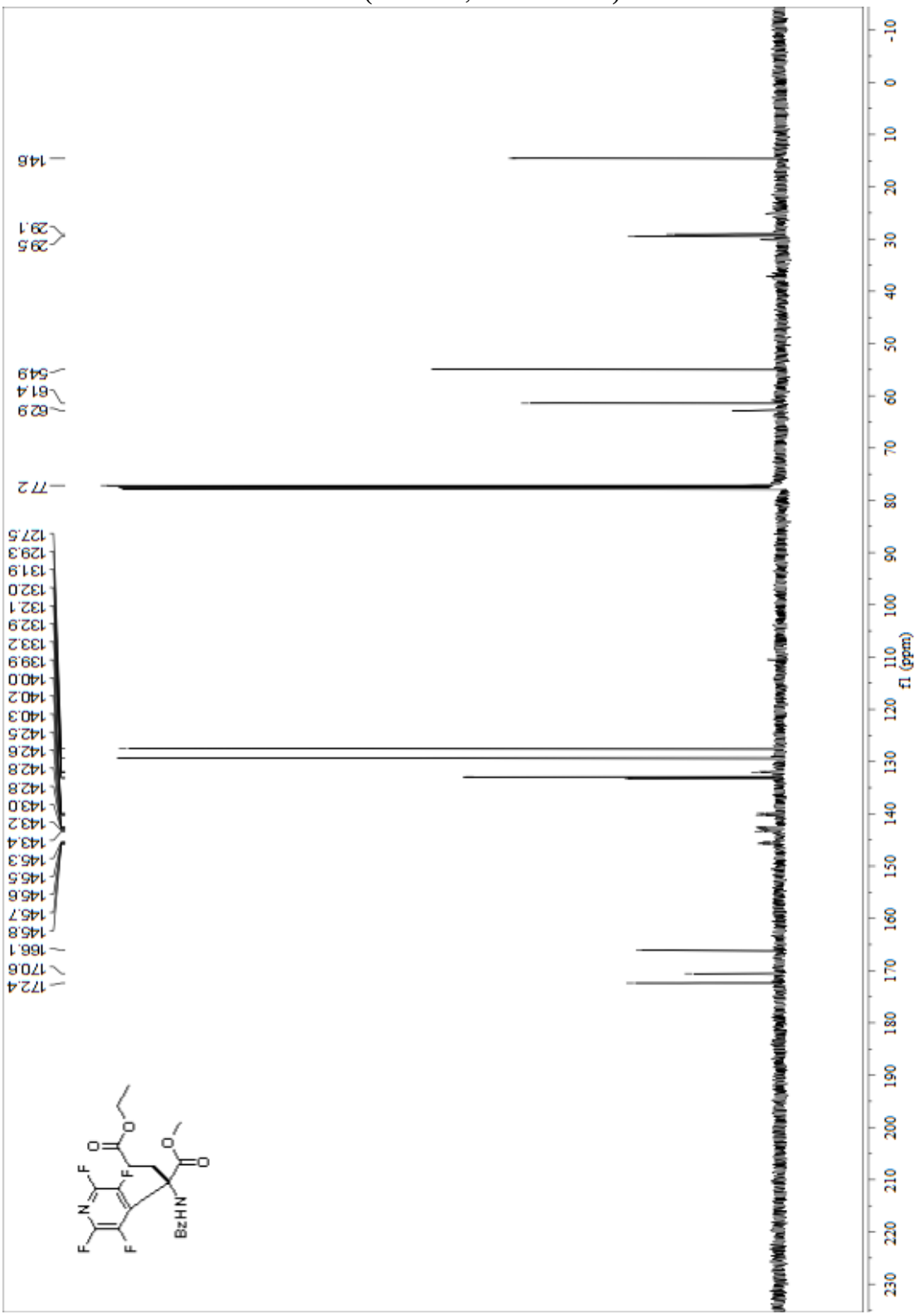

^{1}H NMR (400 MHz, Chloroform-*d*) **2c**

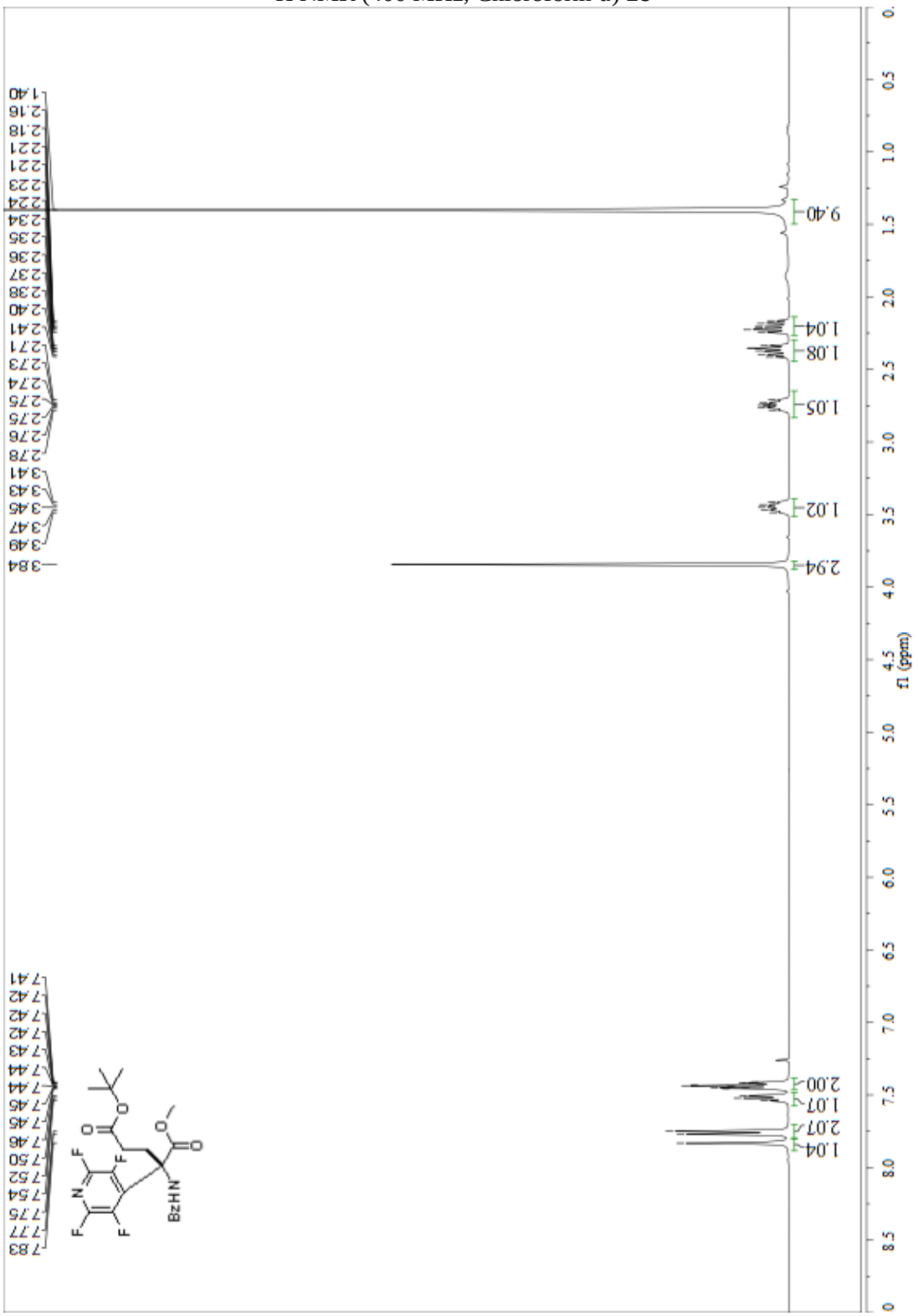

^{19}F NMR (376 MHz, Chloroform-*d*) **2c**

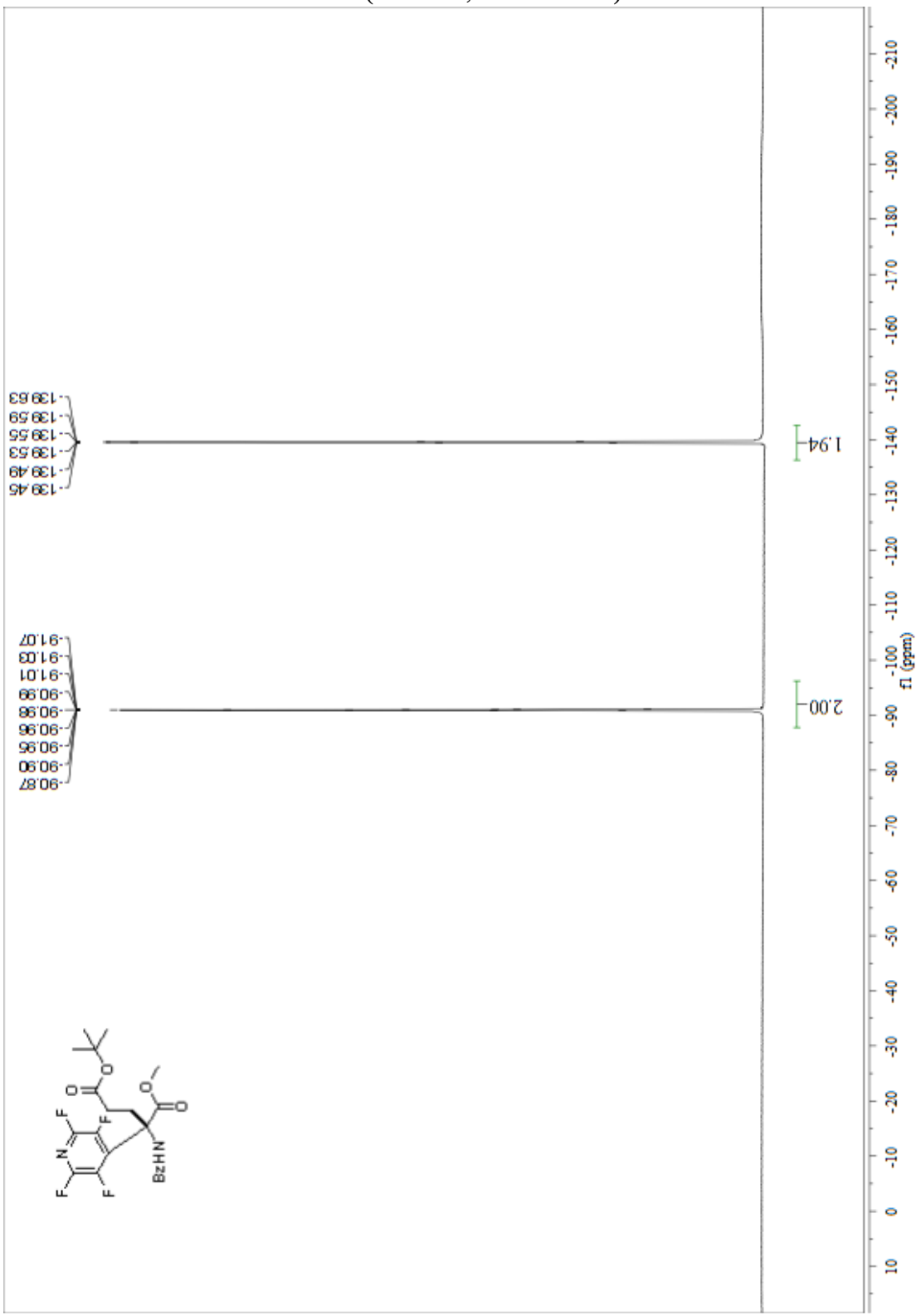

^{13}C NMR (101 MHz, Chloroform-*d*) **2c**

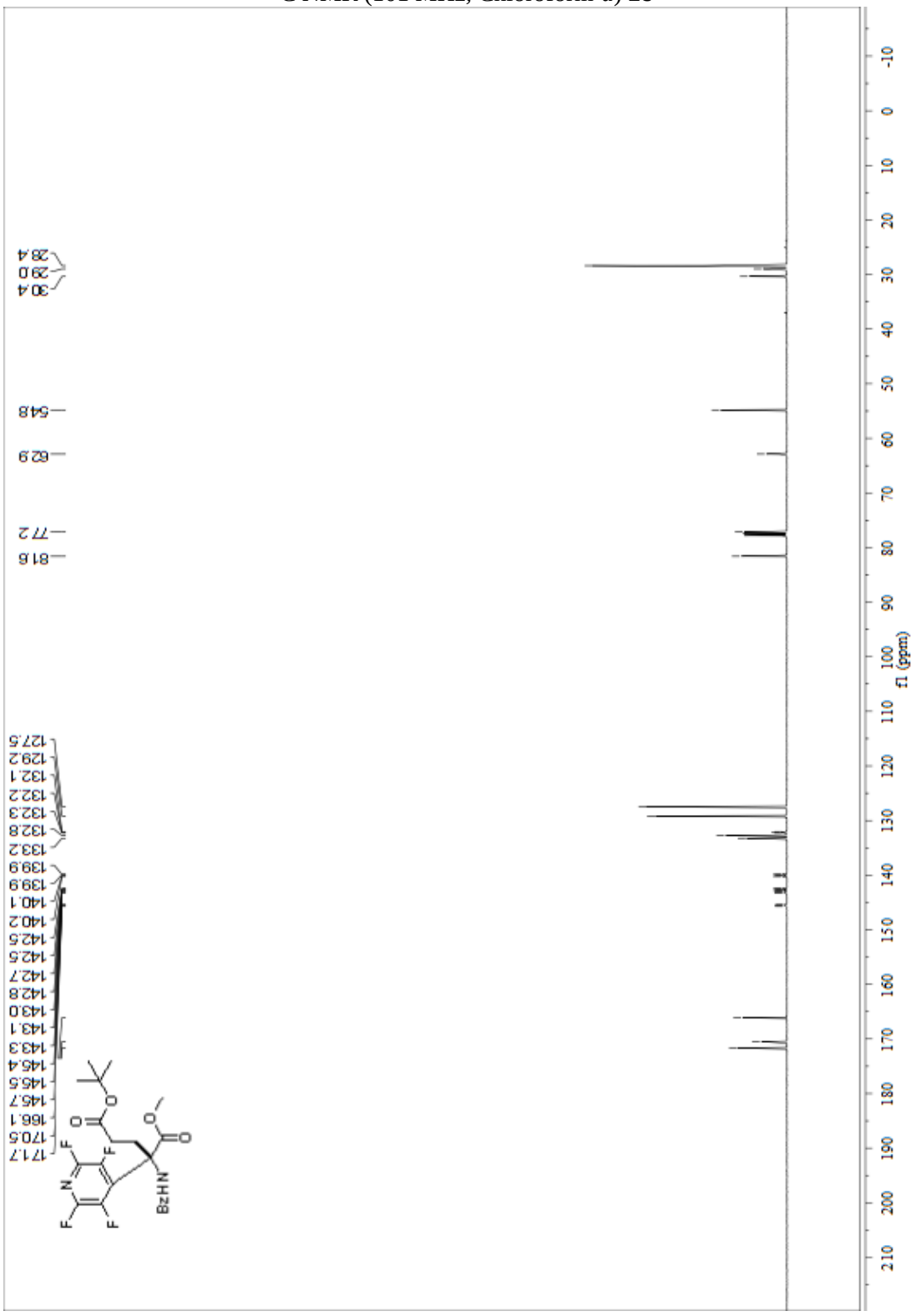

^{1}H NMR (400 MHz, Chloroform-*d*) **2d**

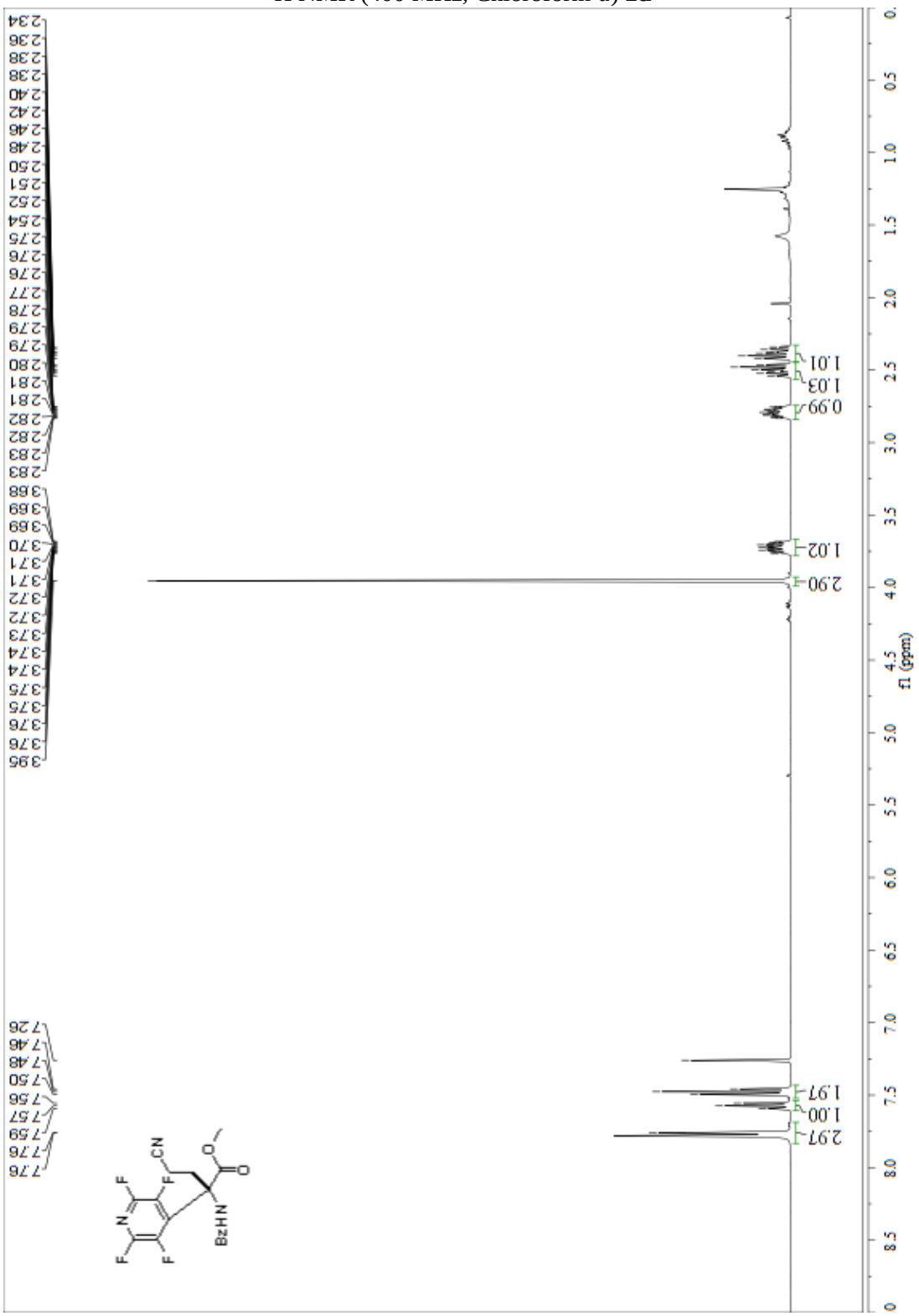

^{19}F NMR (376 MHz, Chloroform-*d*) **2d**

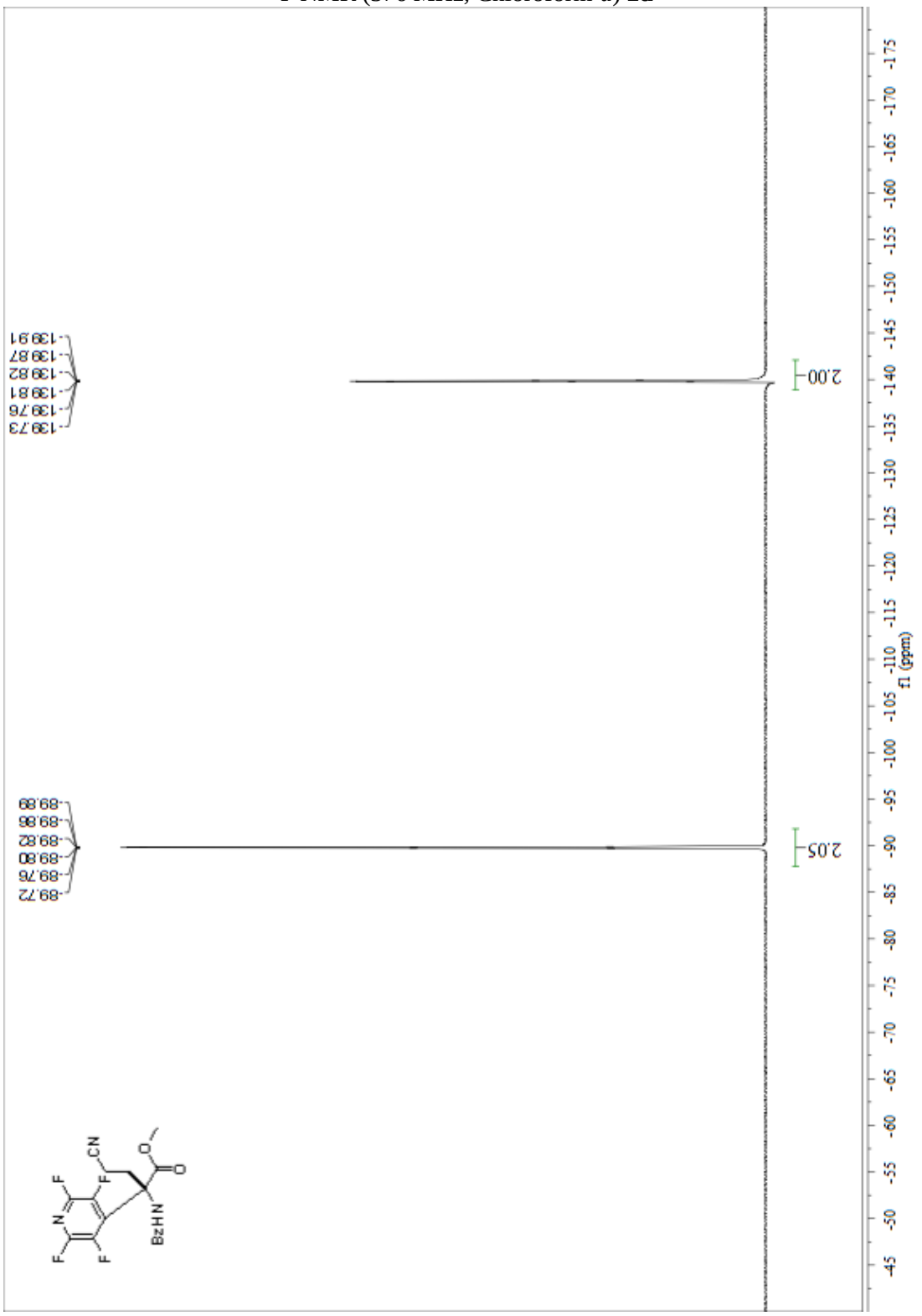

^{13}C NMR (101 MHz, Chloroform-*d*) **2d**

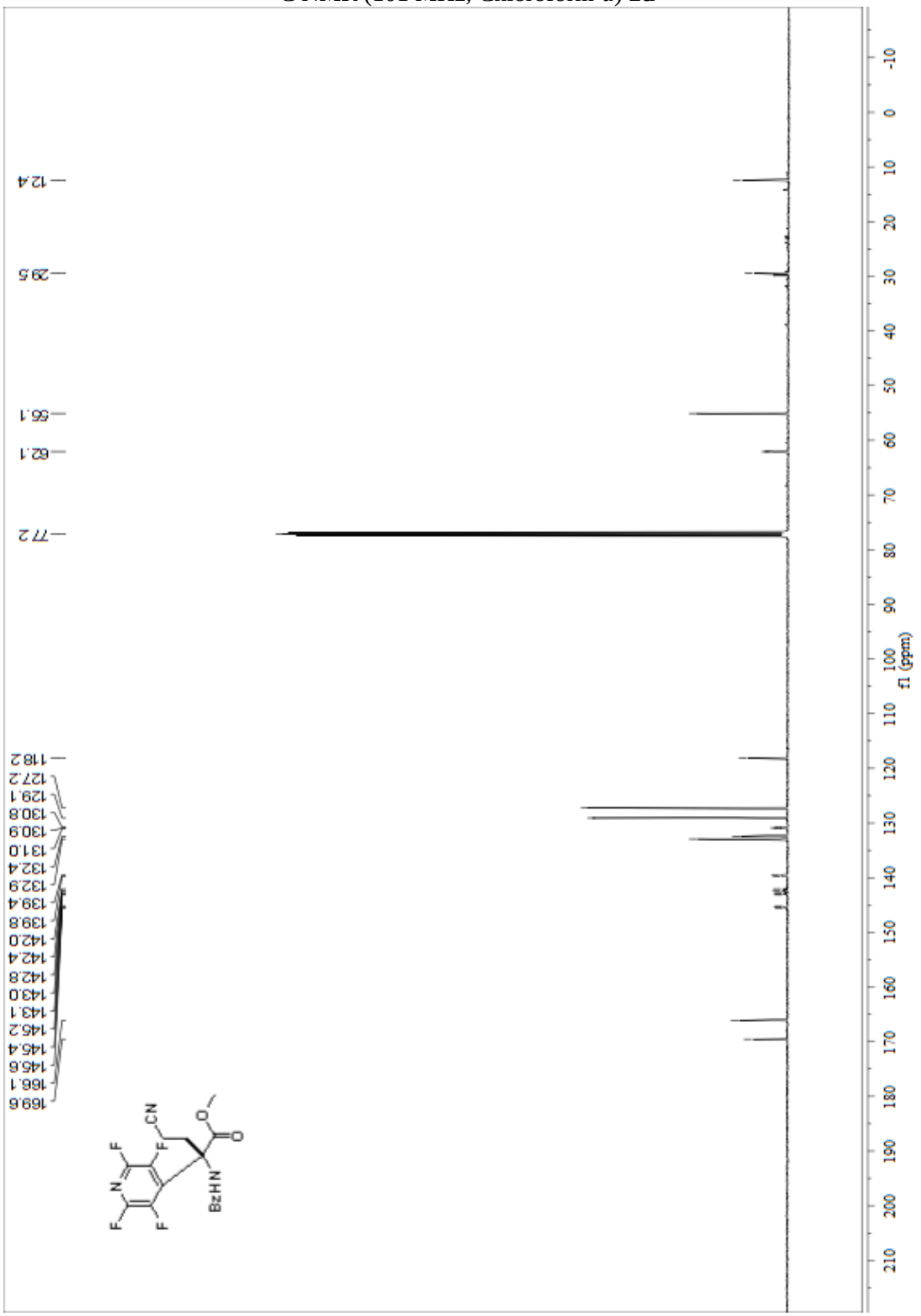

^{1}H NMR (400 MHz, Chloroform-*d*) **2e**

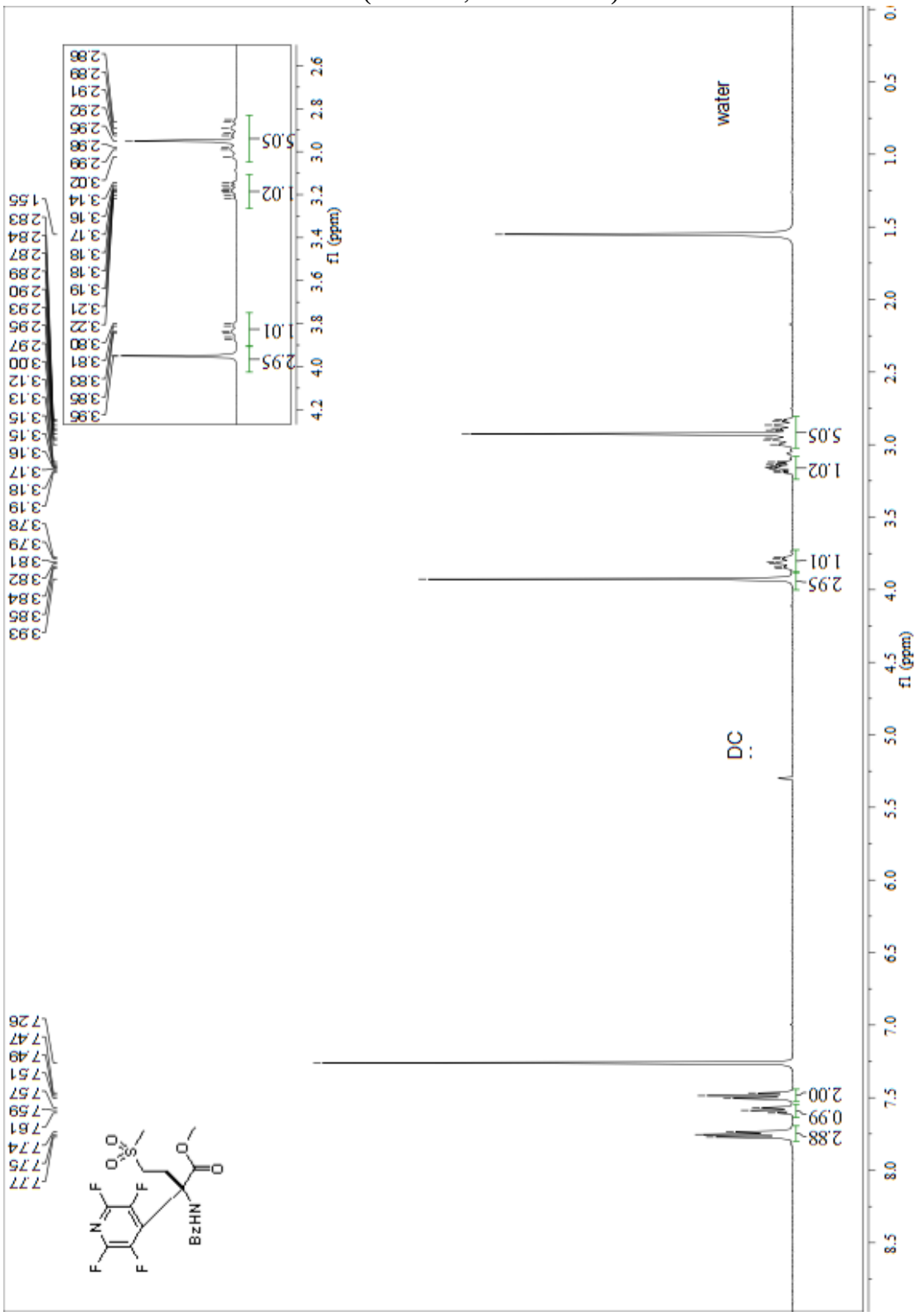

^{19}F NMR (376 MHz, Chloroform-*d*) **2e**

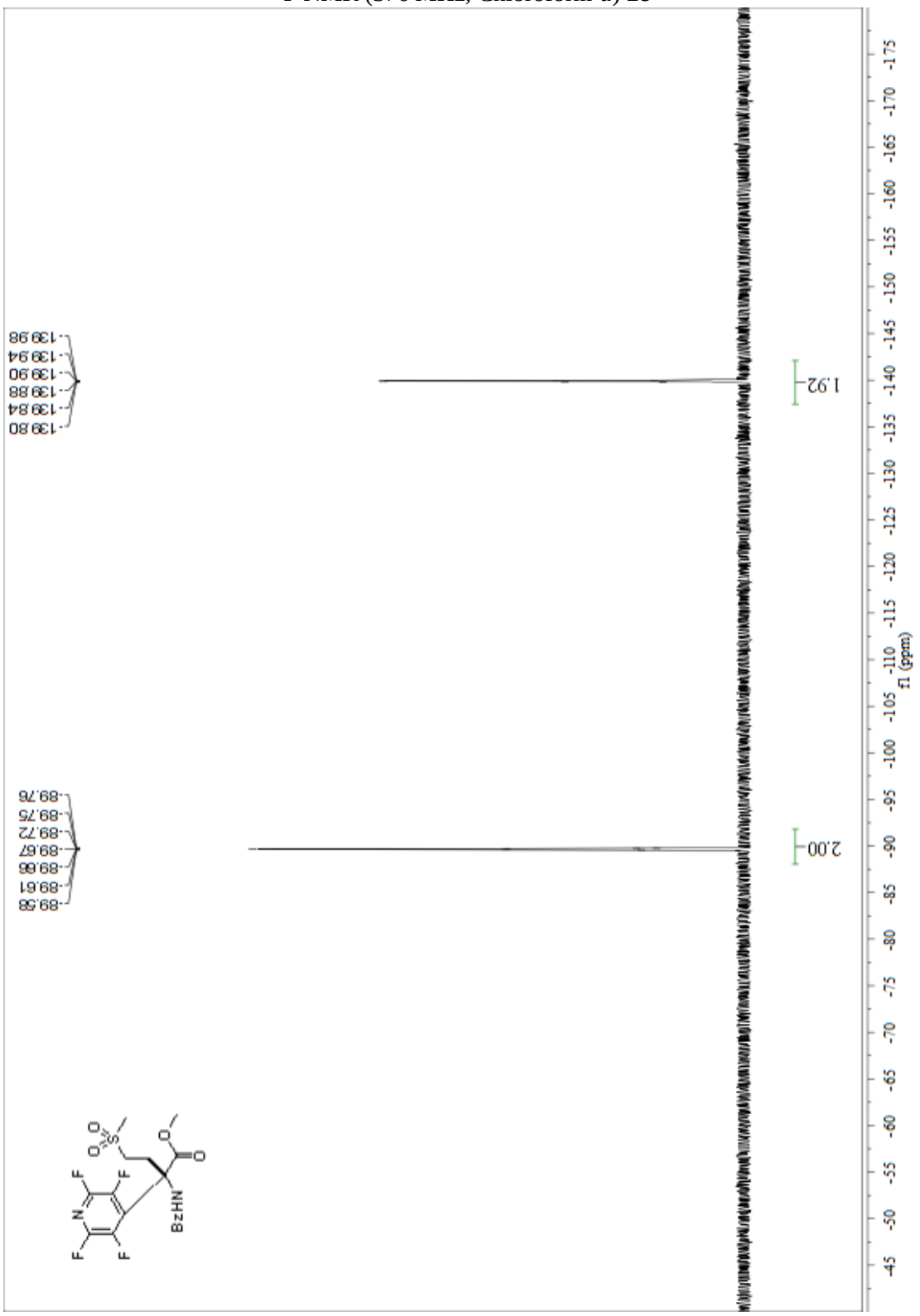

^{13}C NMR (101 MHz, Chloroform-*d*) **2e**

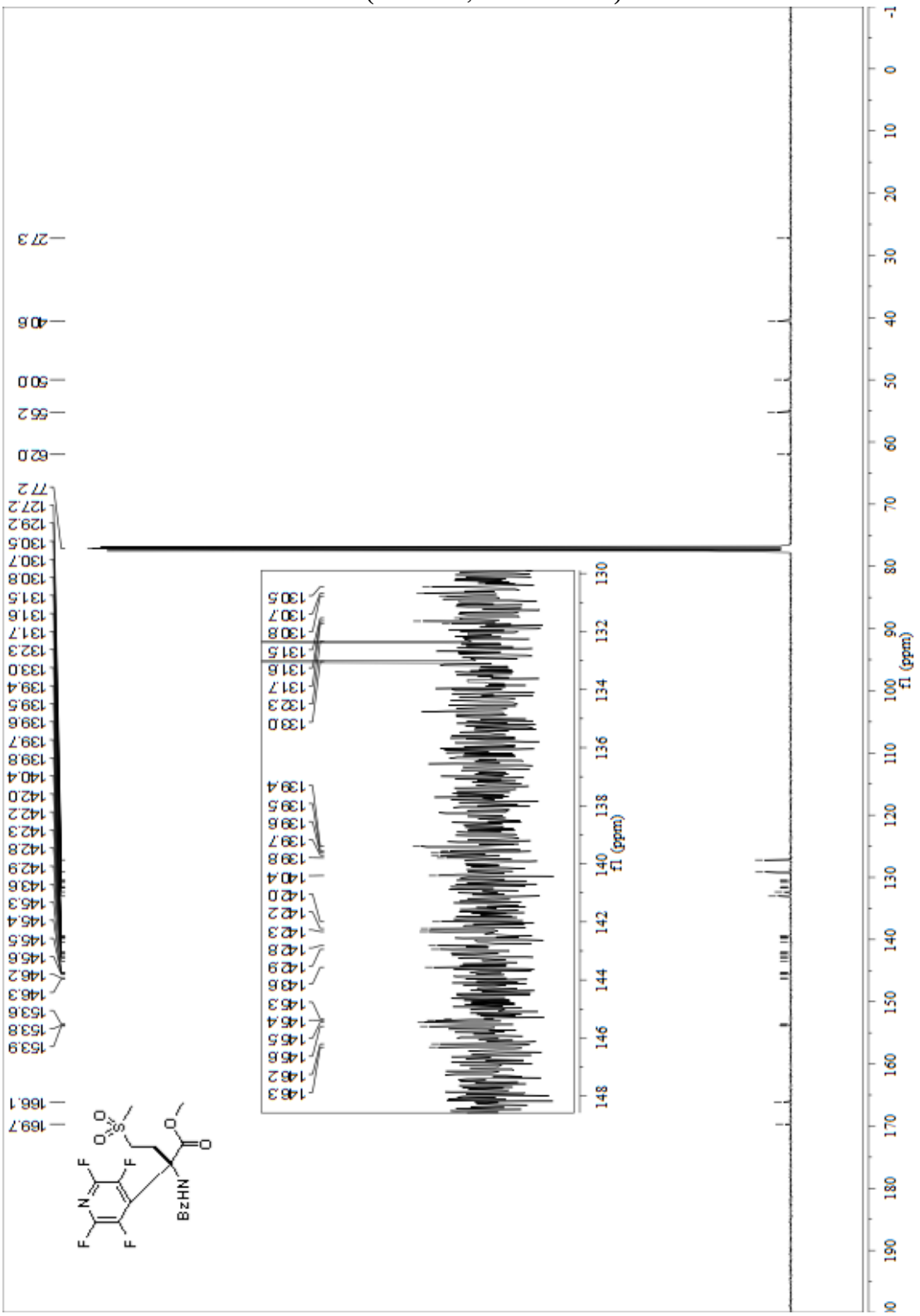

^{1}H NMR (400 MHz, Chloroform-*d*) **2f**

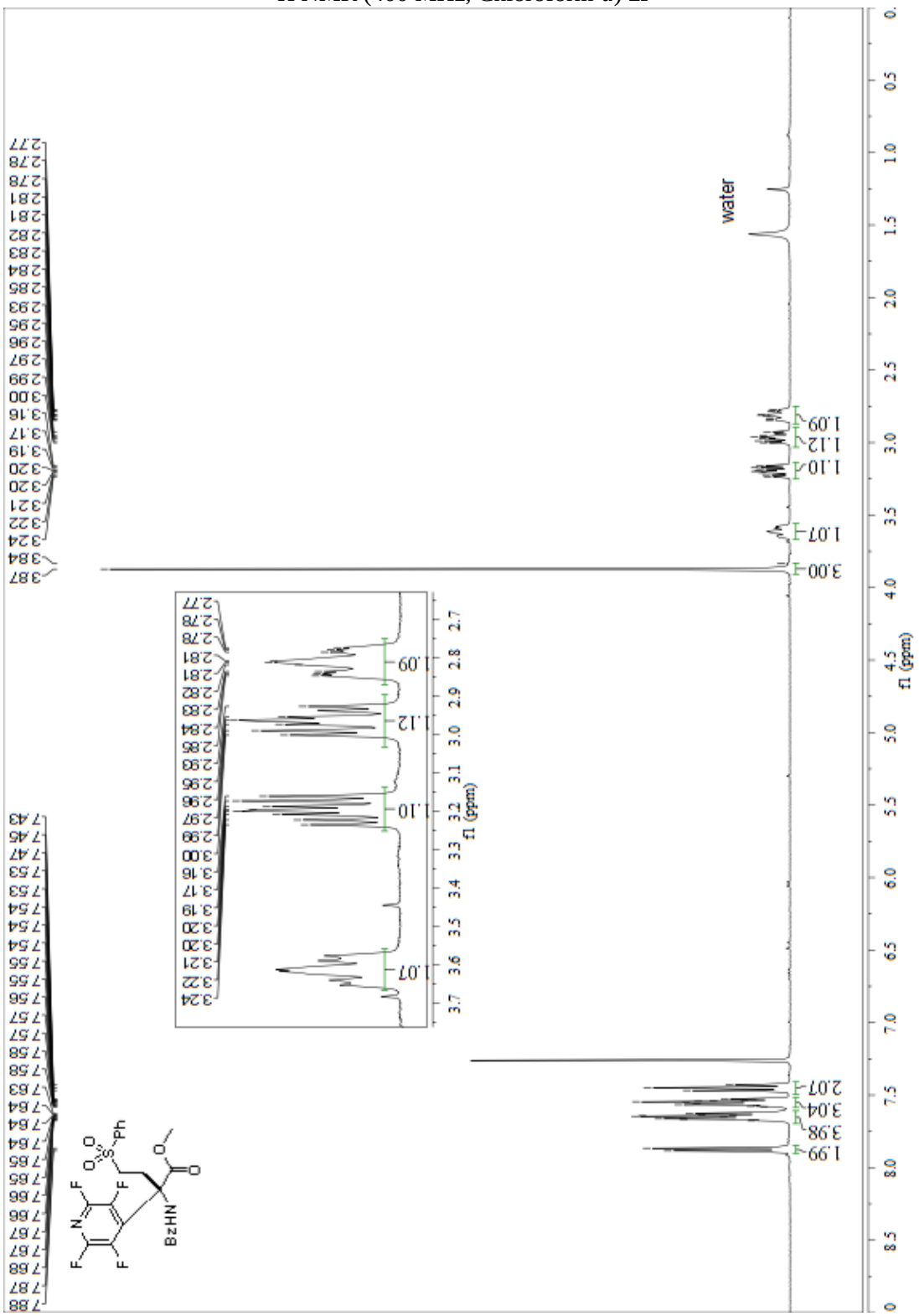

^{19}F NMR (376 MHz, Chloroform-*d*) **2f**

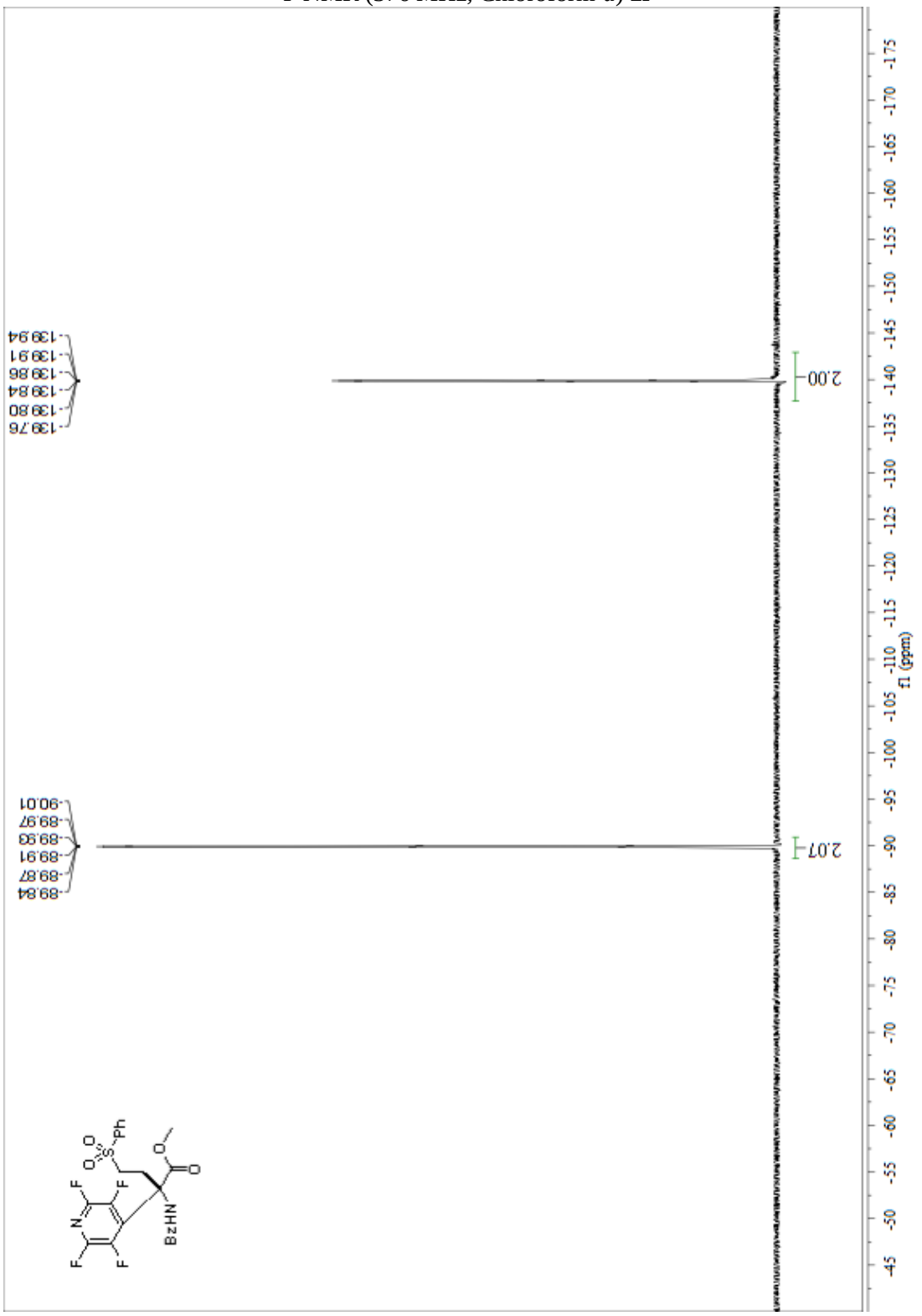

^{13}C NMR (101 MHz, Chloroform-*d*) **2f**

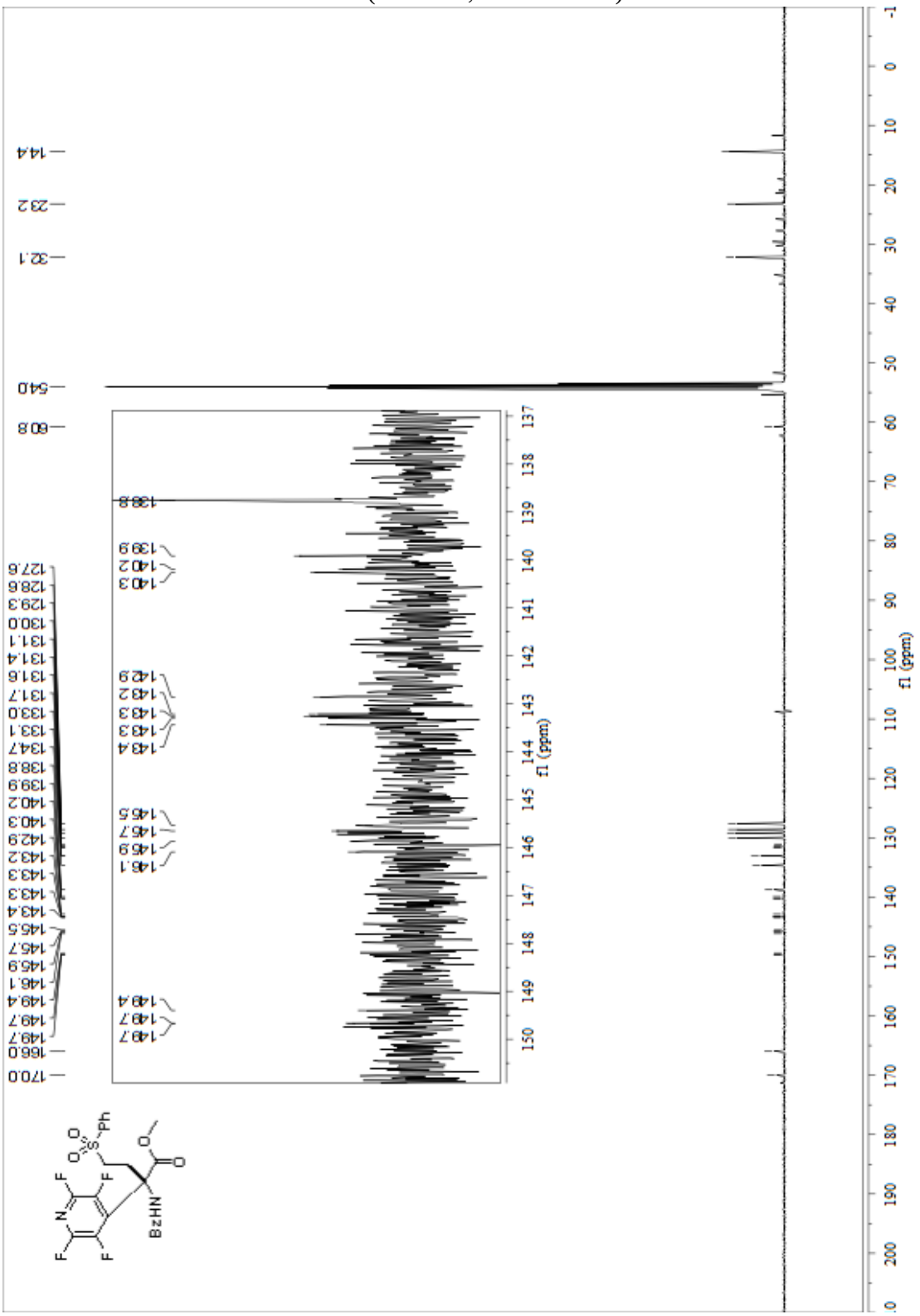

[1]H NMR (400 MHz, Chloroform-*d*) **2g**

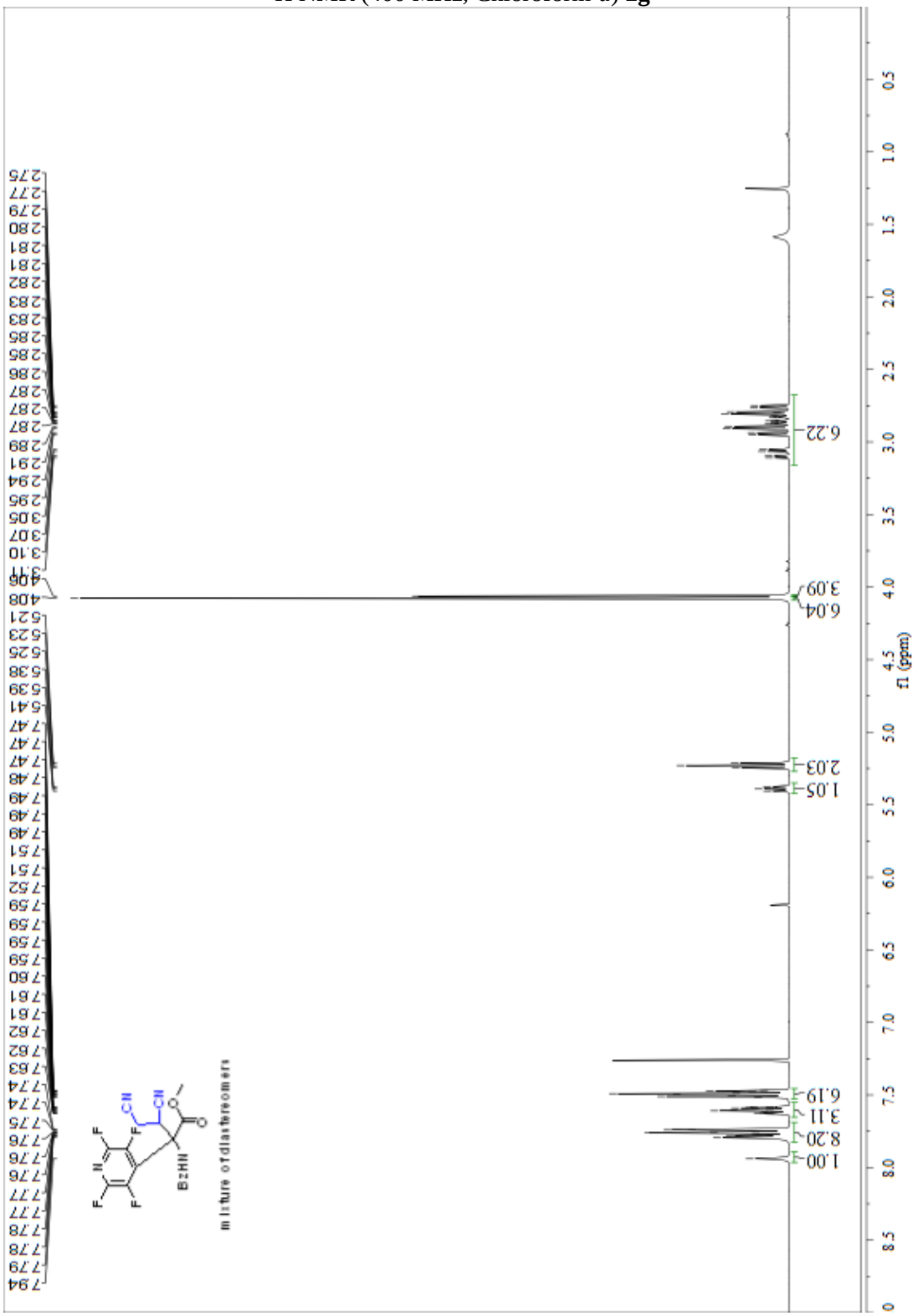

^{19}F NMR (376 MHz, Chloroform-*d*) **2g**

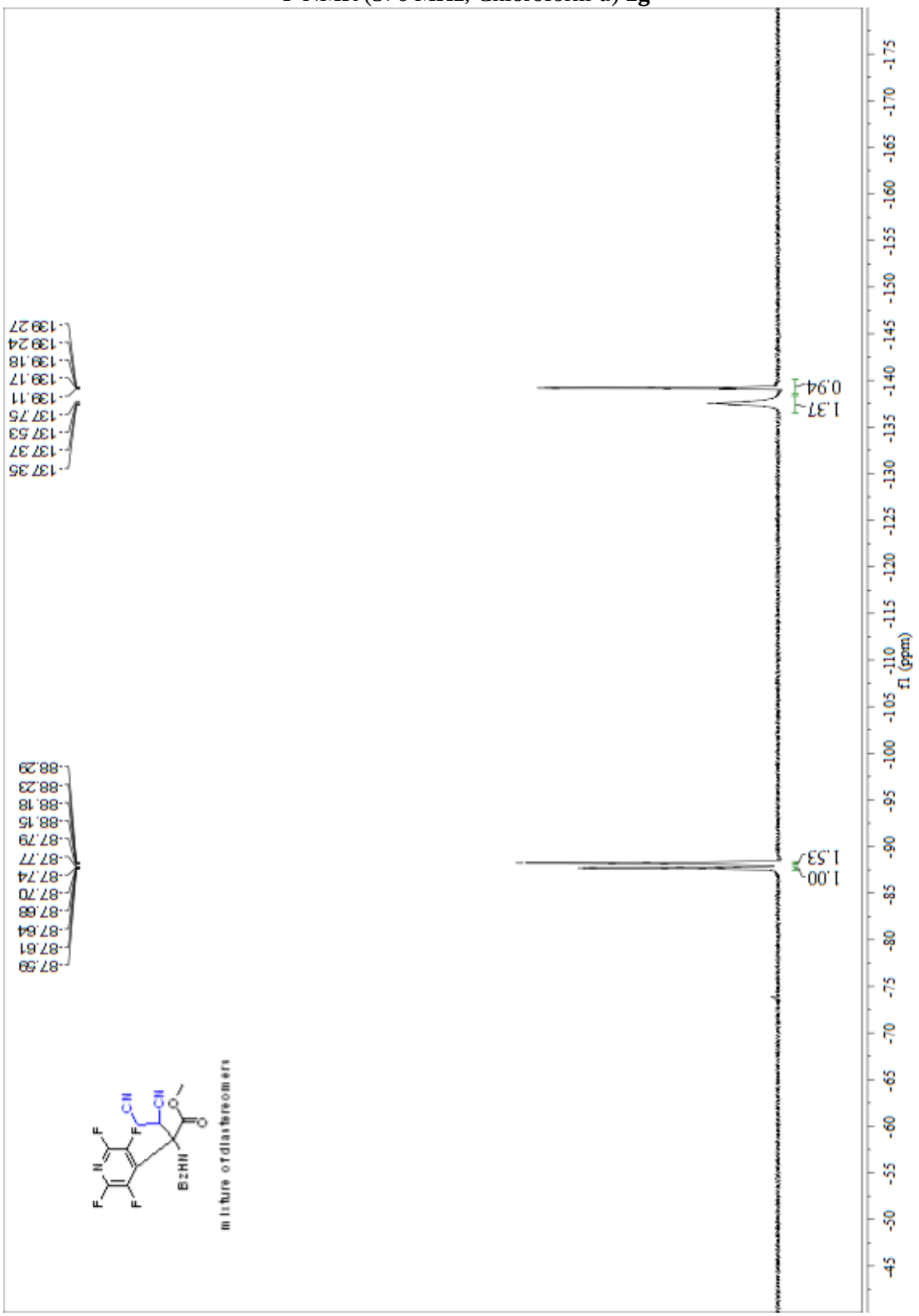

^{13}C NMR (101 MHz, Chloroform-*d*) **2g**

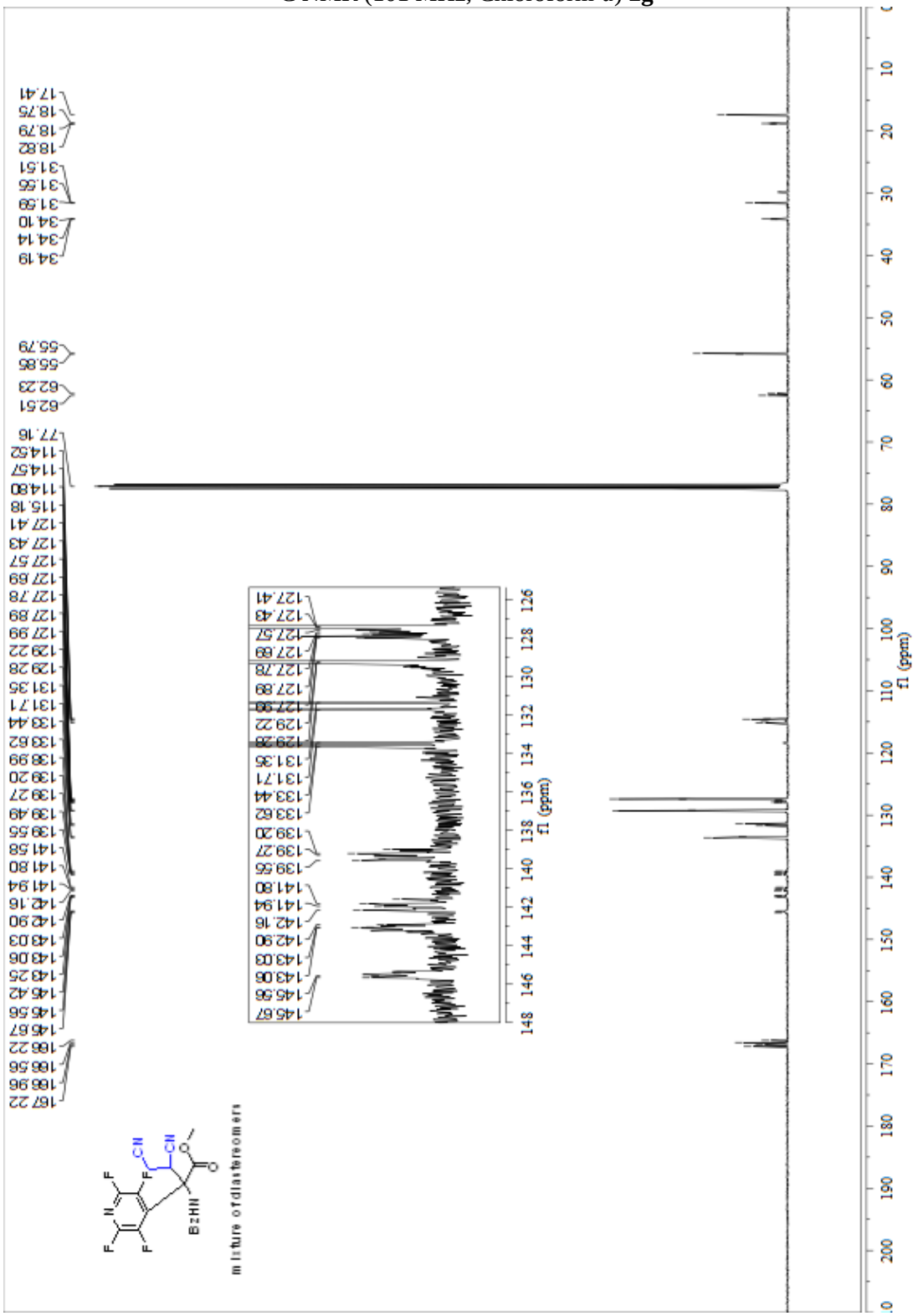

^{1}H NMR (400 MHz, Chloroform-*d*) **2h**

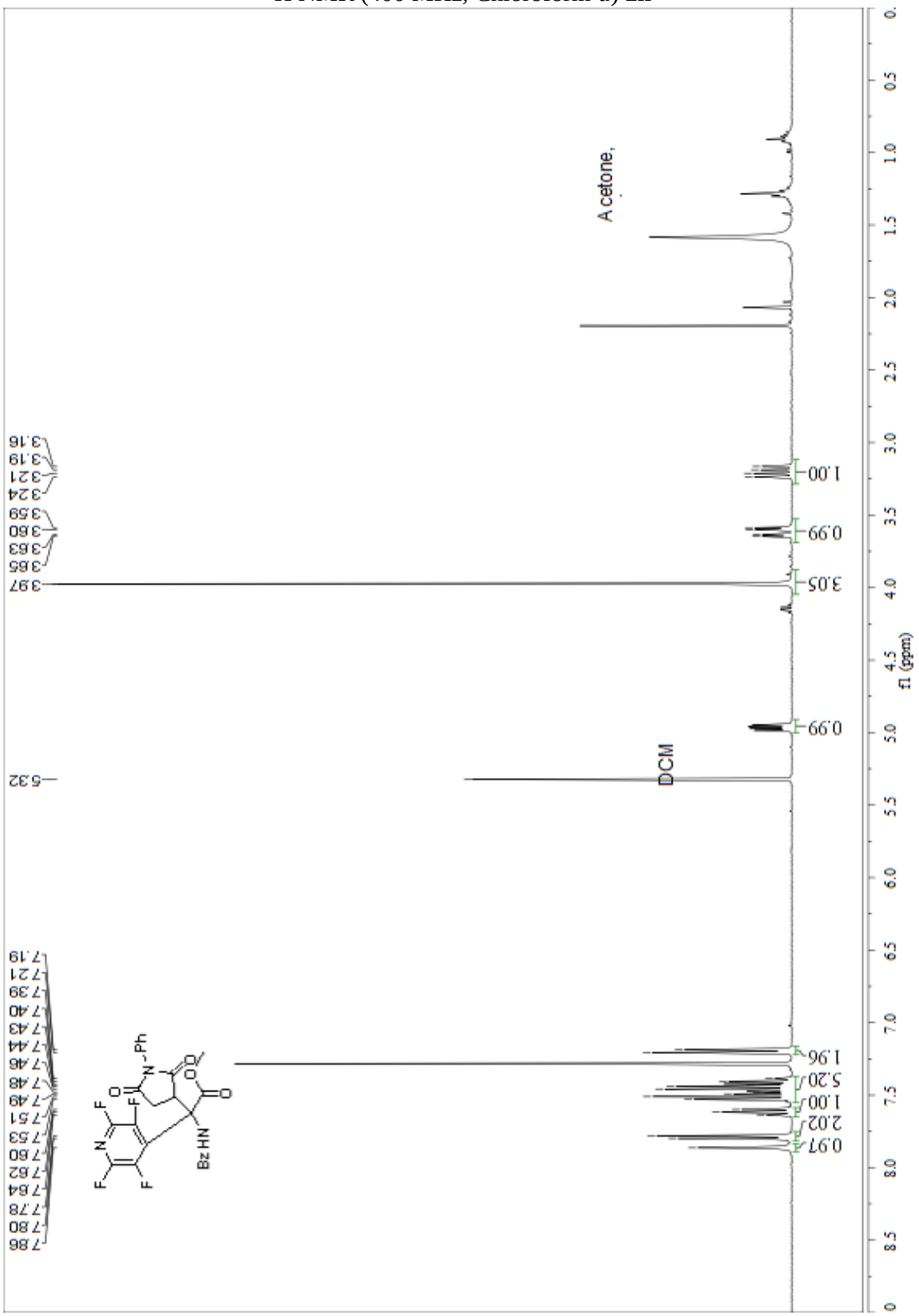

^{19}F NMR (376 MHz, Chloroform-*d*) **2h**

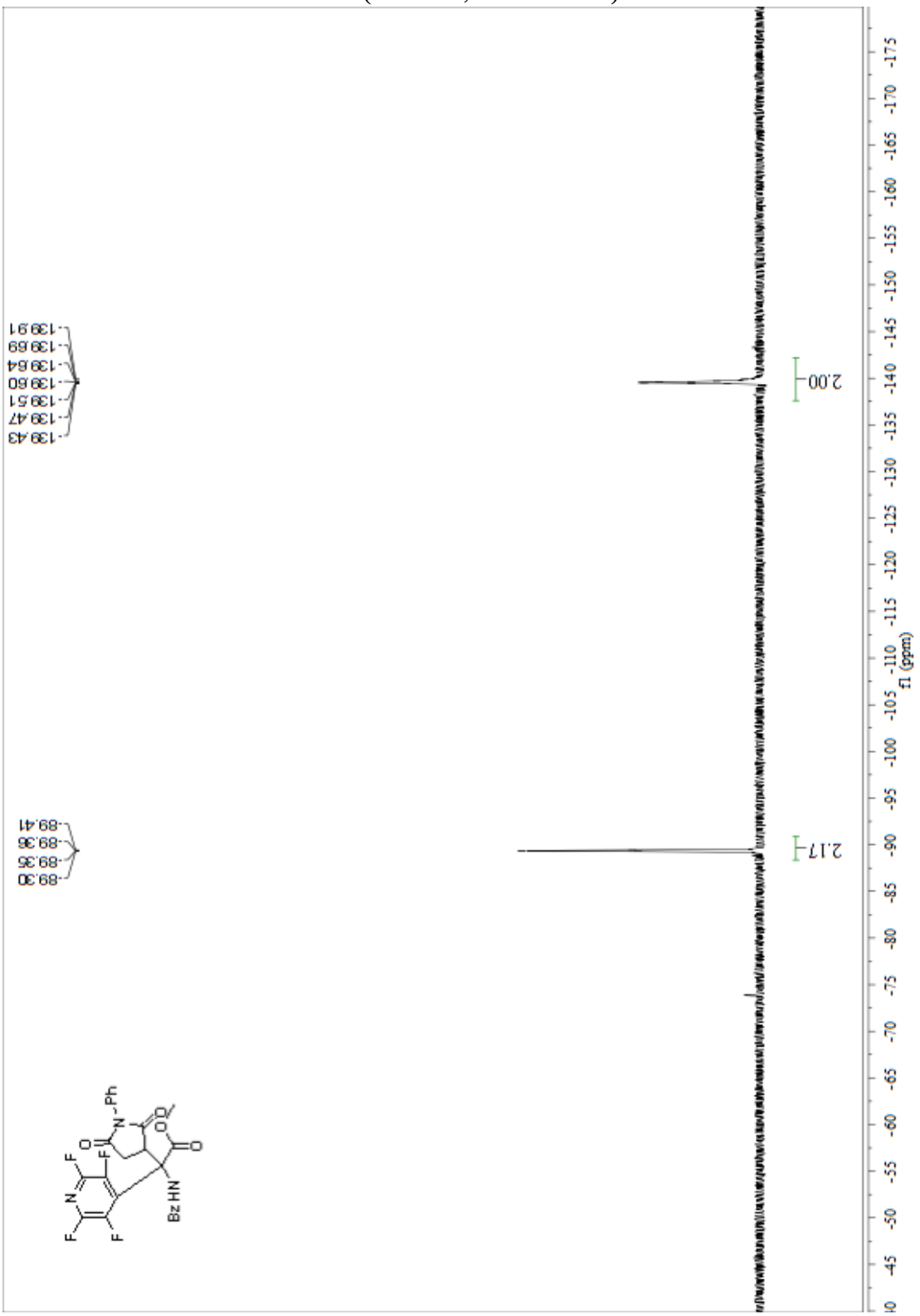

^{13}C NMR (101 MHz, Chloroform-*d*) **2h**

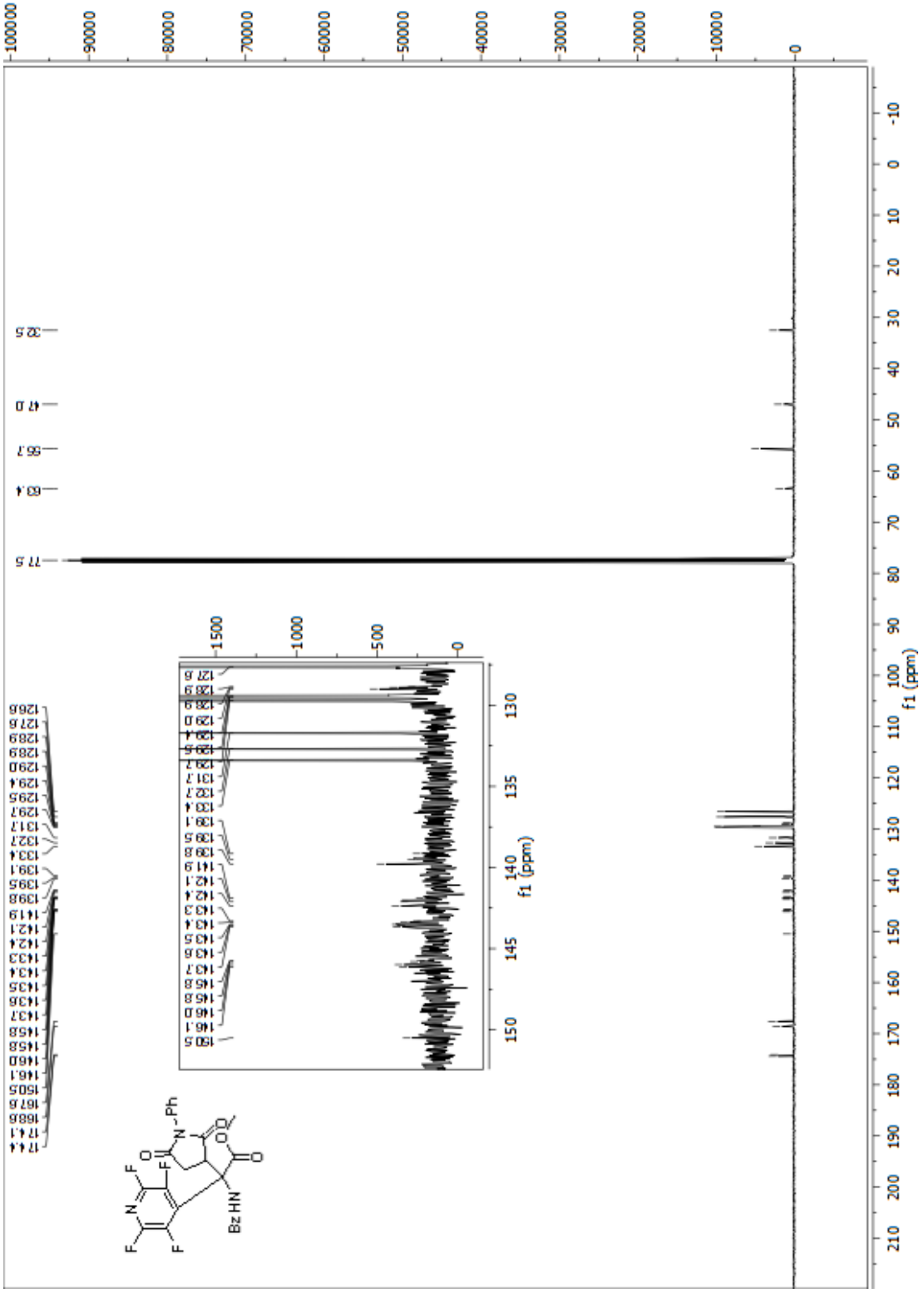

^{1}H NMR (400 MHz, Chloroform-*d*) **3a**

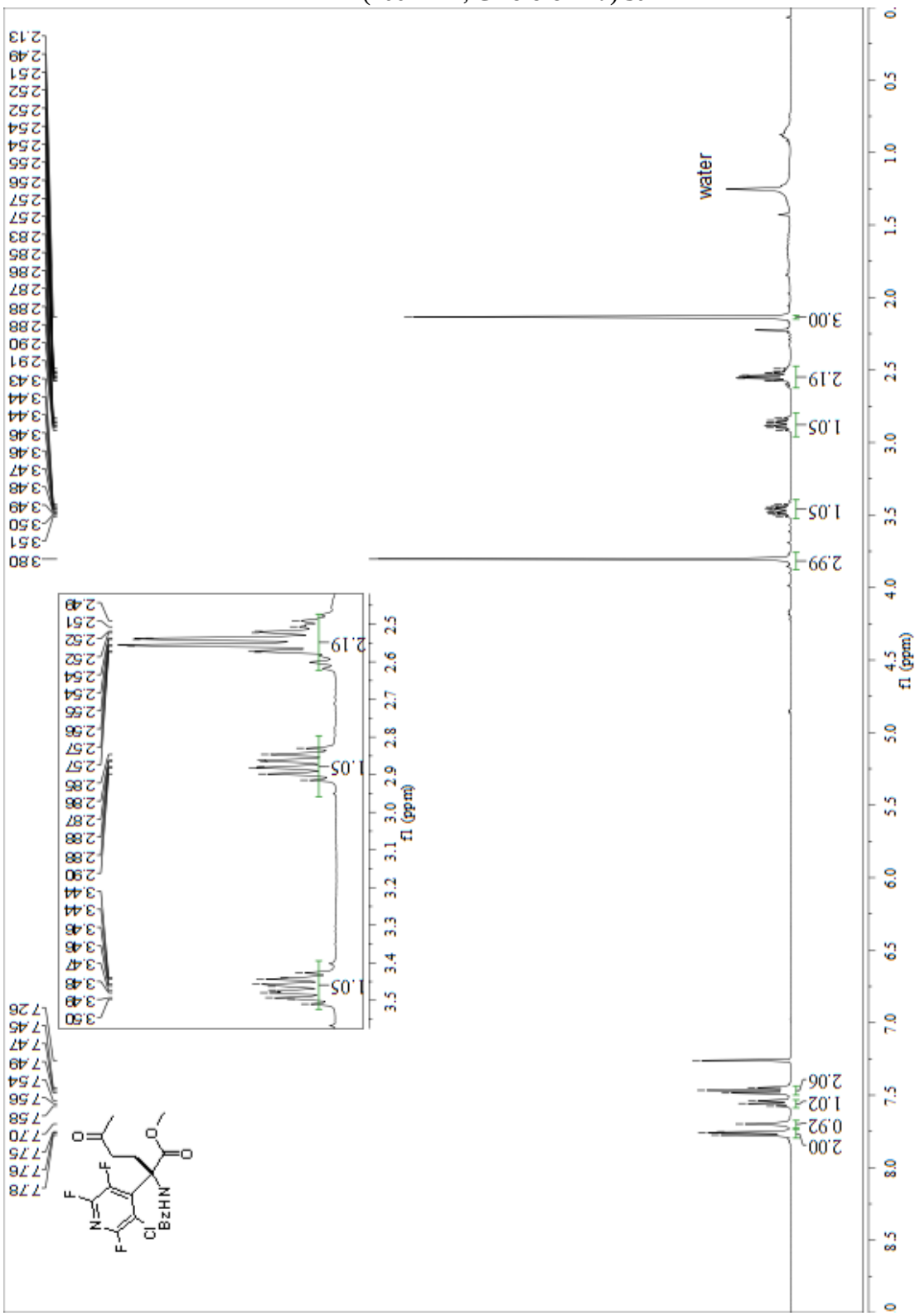

^{19}F NMR (376 MHz, Chloroform-*d*) **3a**

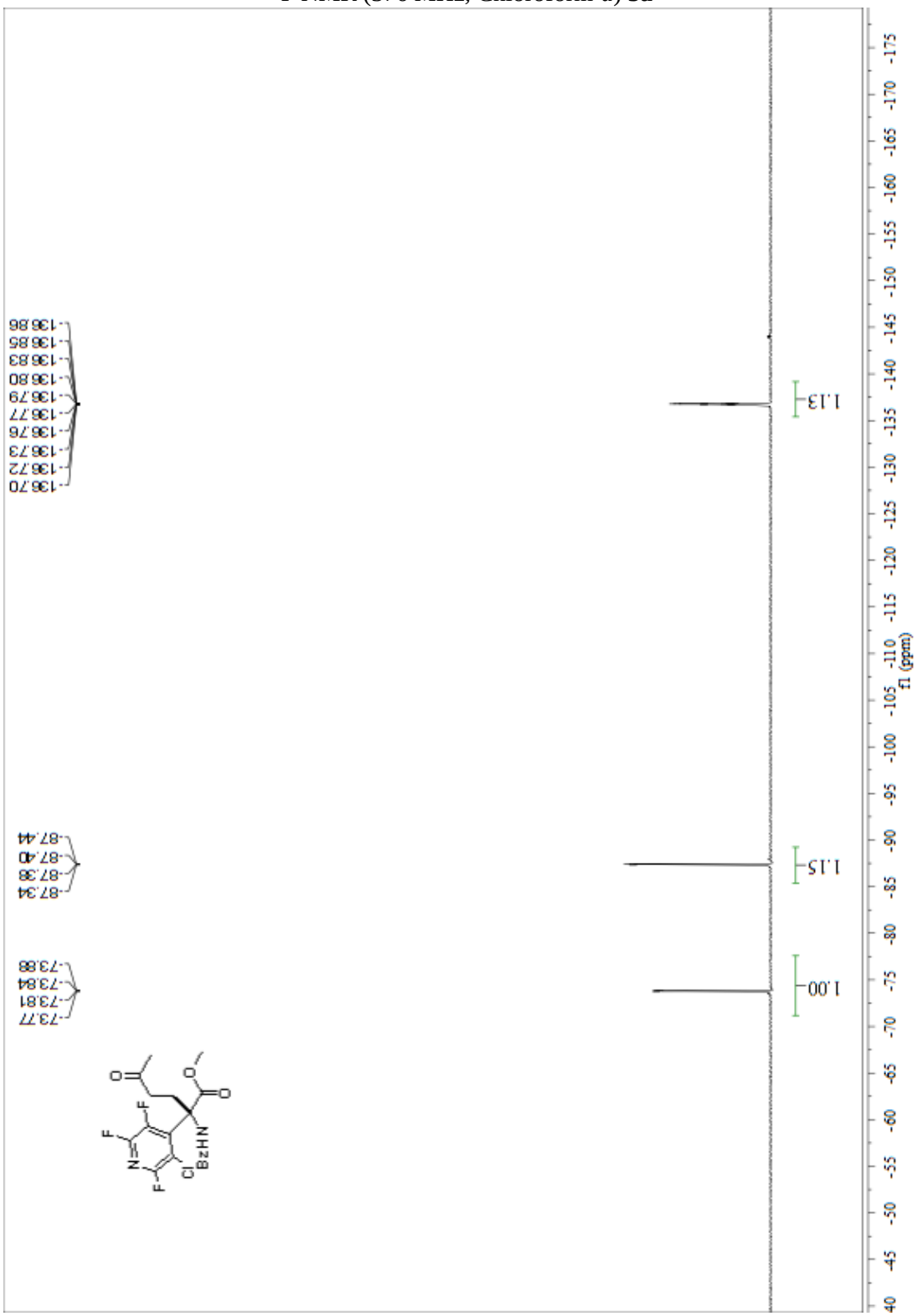

^{13}C NMR (101 MHz, Chloroform-*d*) **3a**

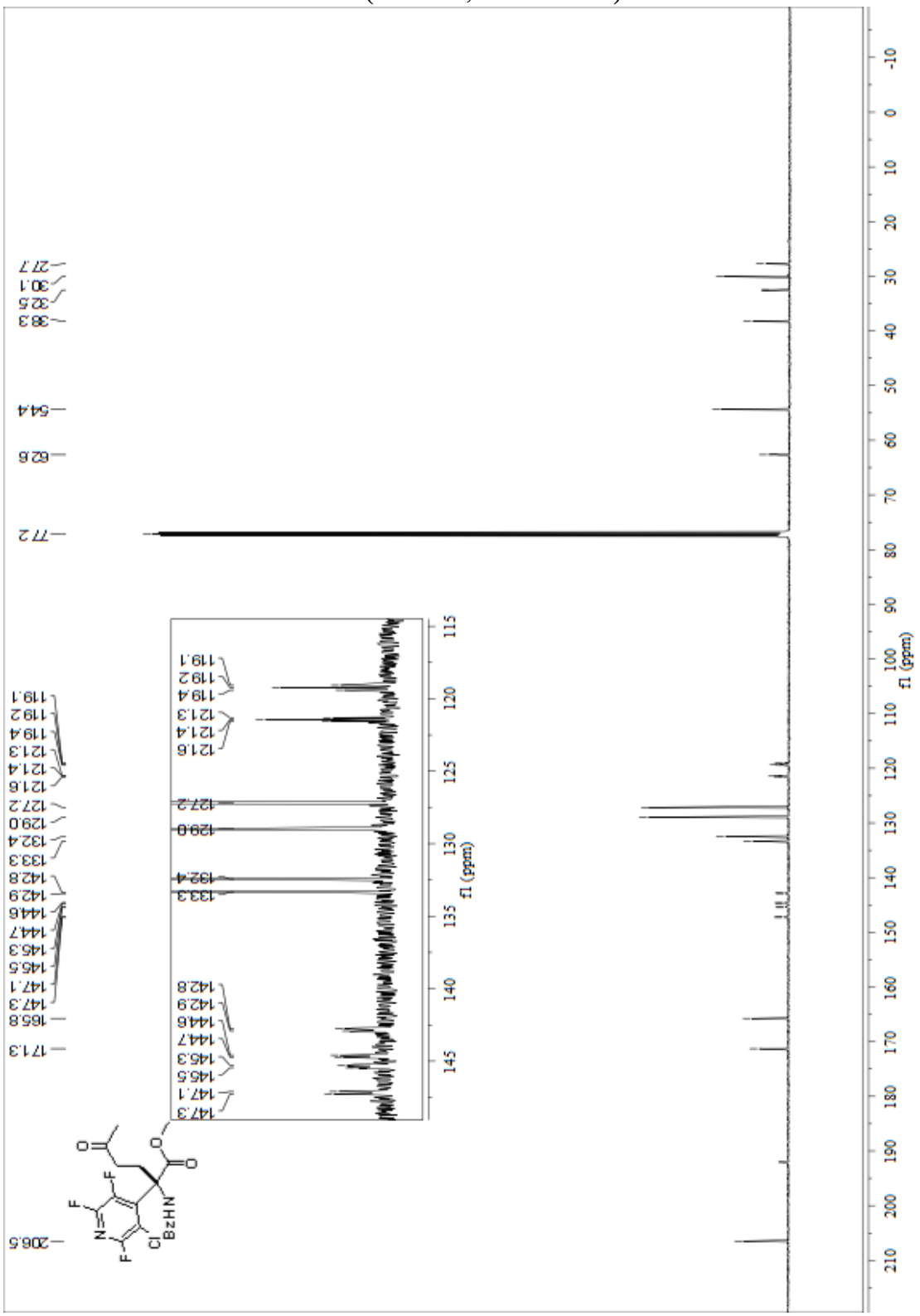

^{1}H NMR (400 MHz, Chloroform-*d*) **3b**

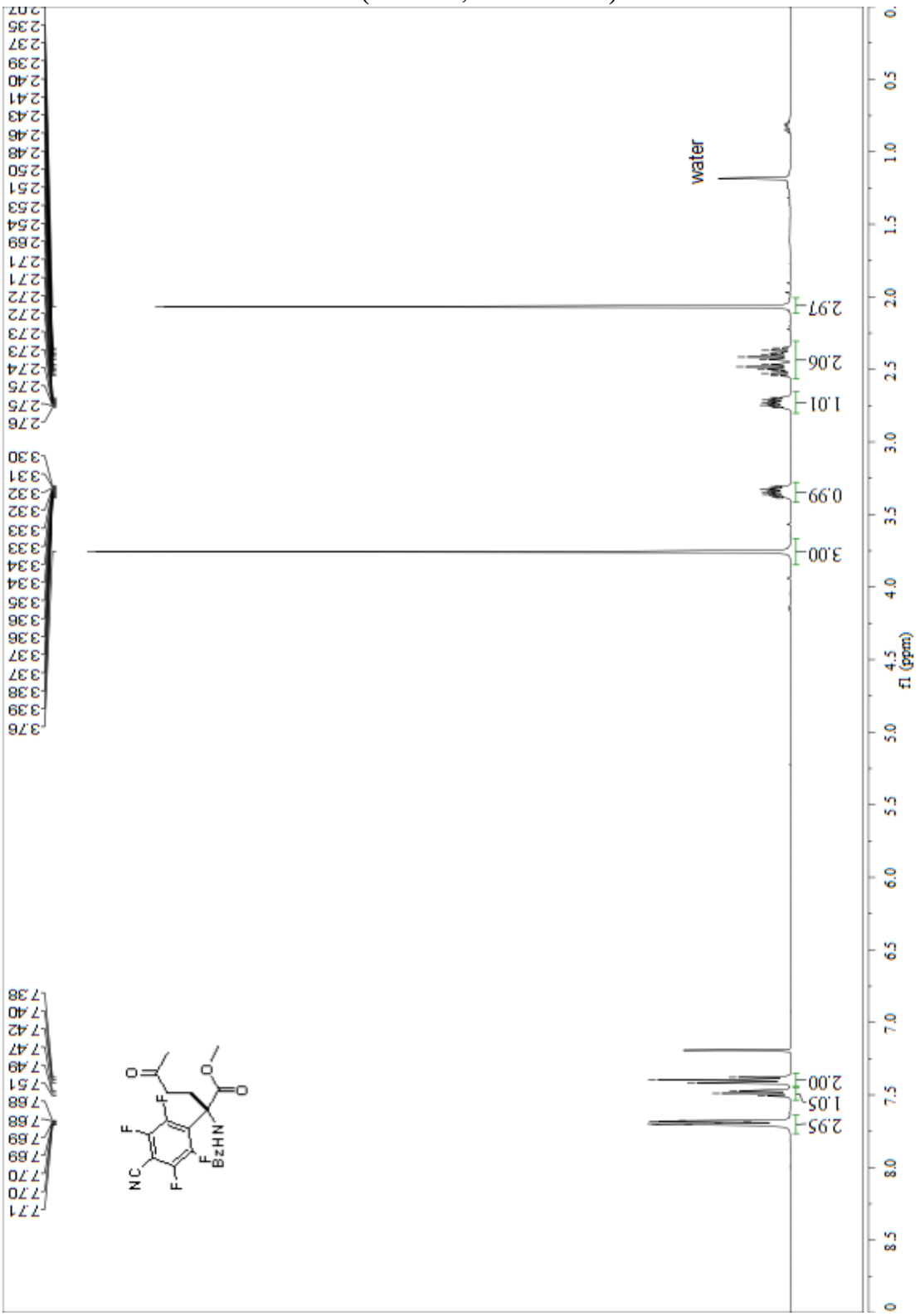

^{19}F NMR (376 MHz, Chloroform-*d*) **3b**

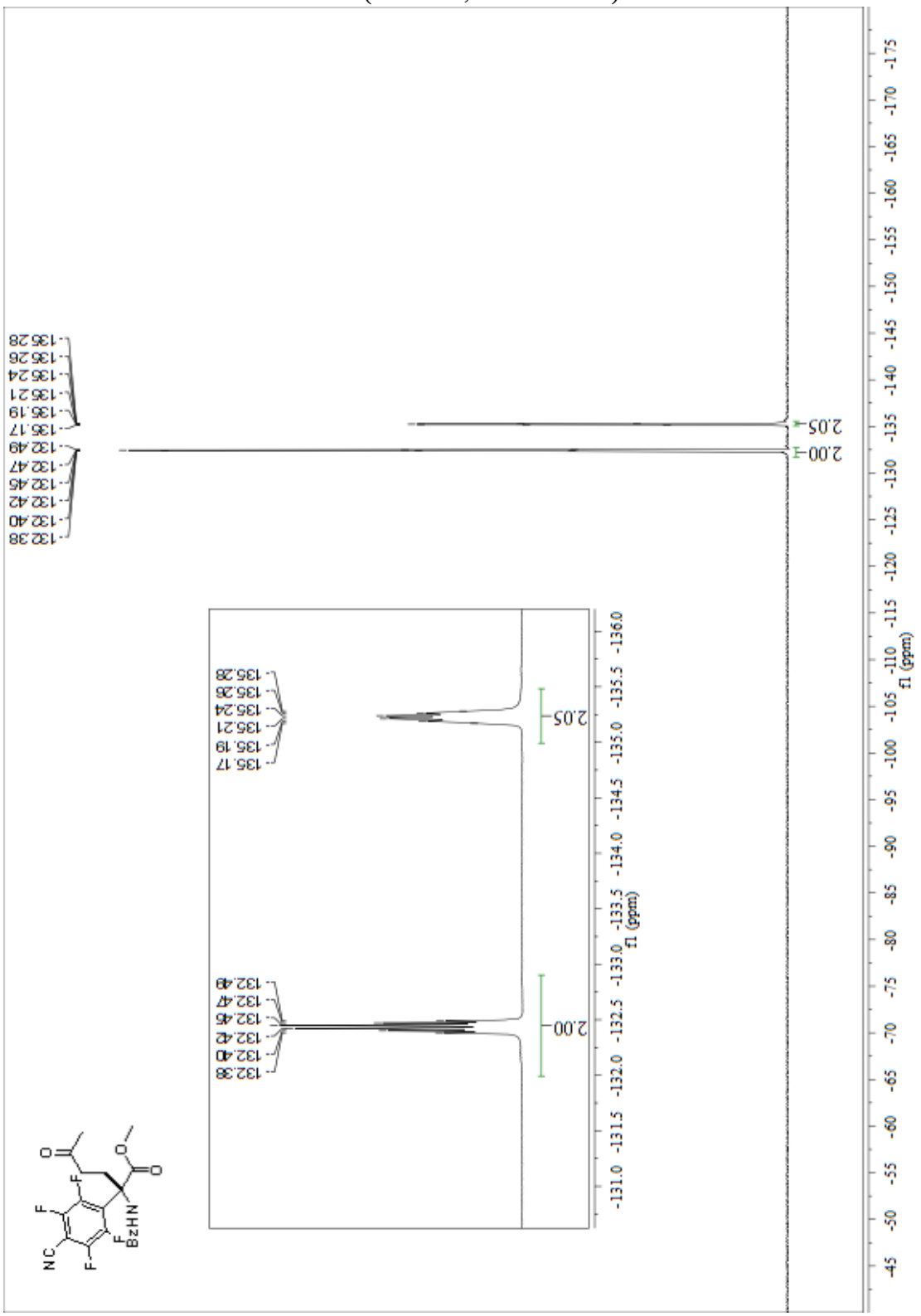

^{13}C NMR (101 MHz, Chloroform-*d*) **3b**

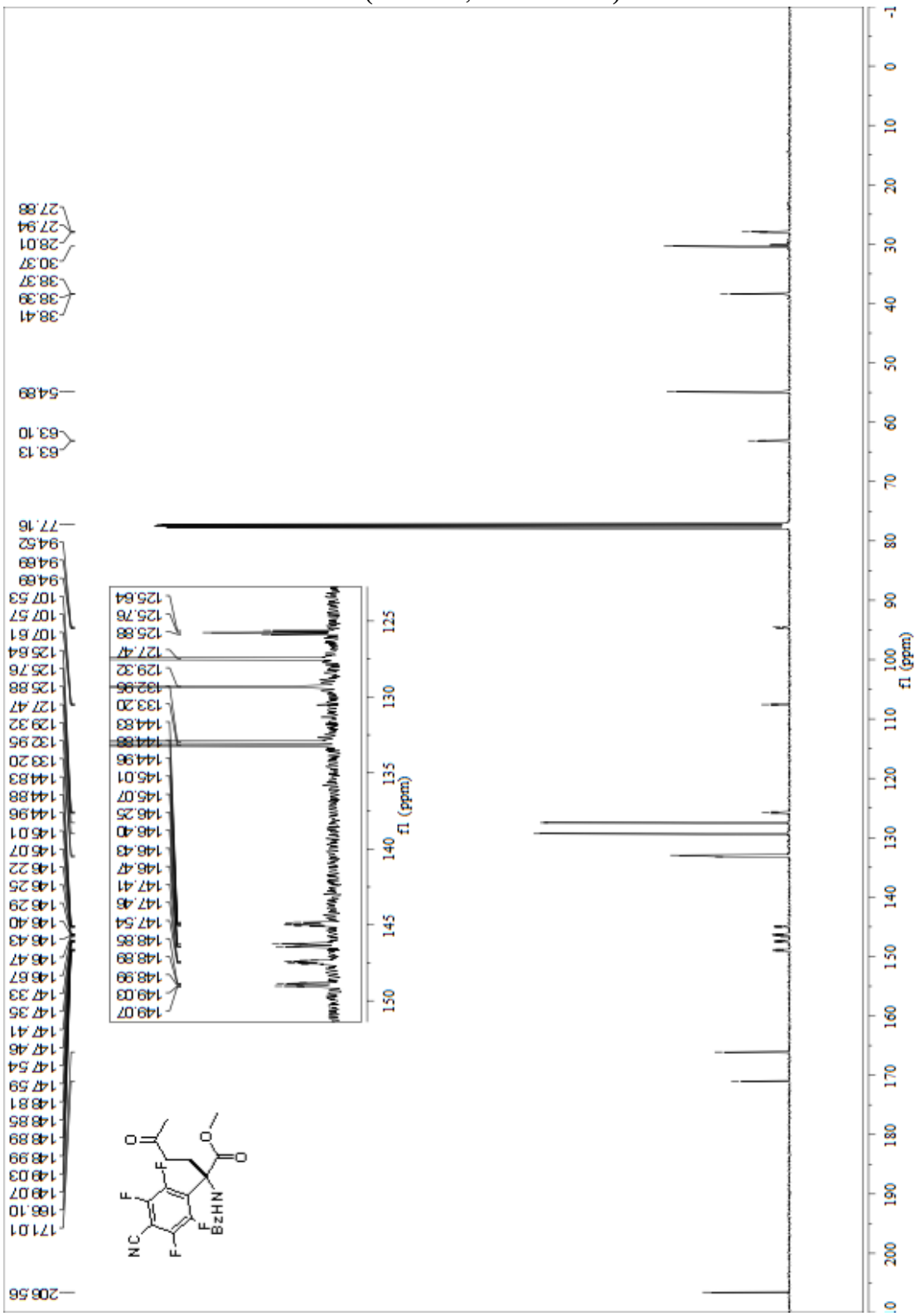

^{1}H NMR (400 MHz, Chloroform-*d*) **3c**

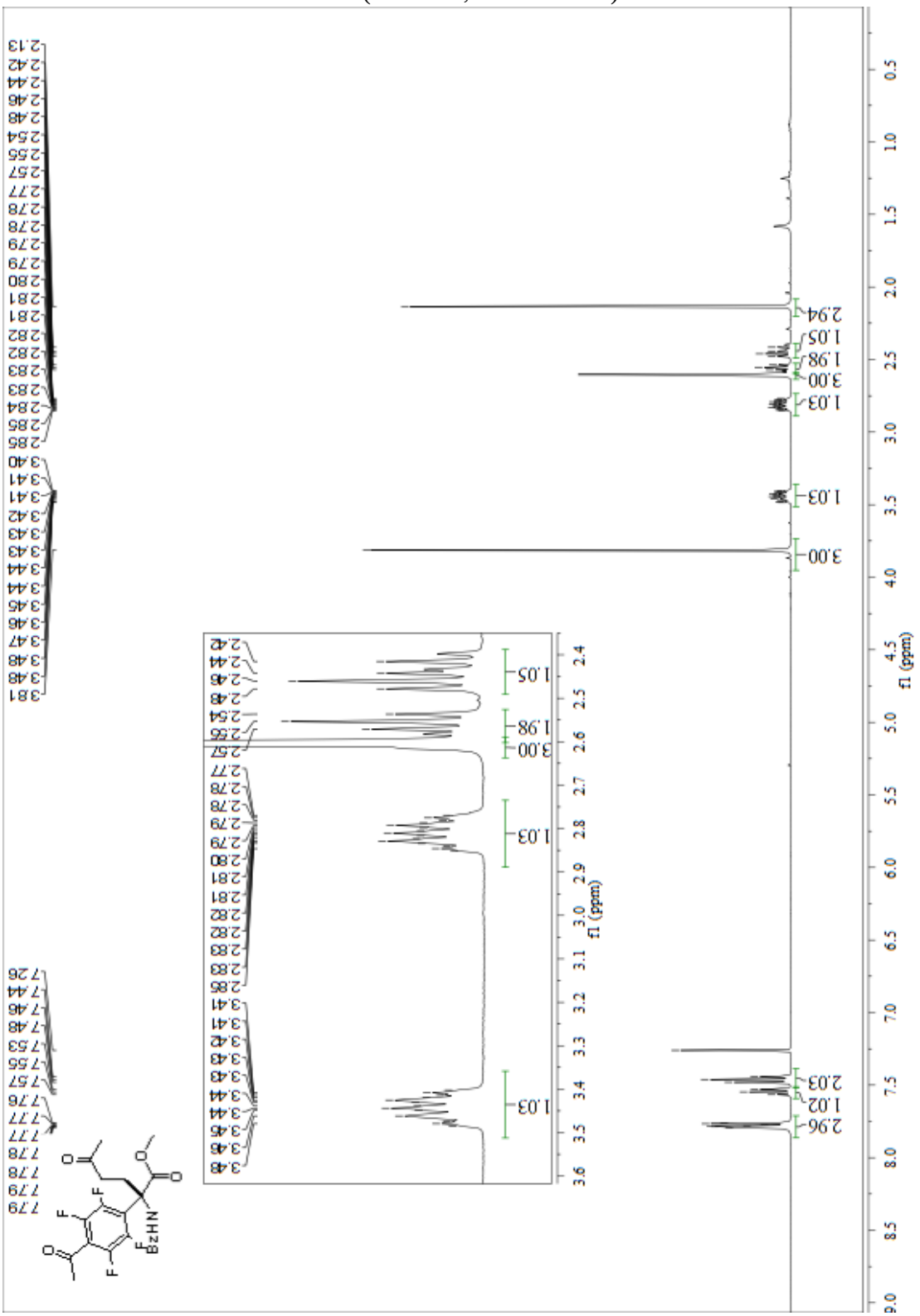

^{19}F NMR (376 MHz, Chloroform-*d*) **3c**

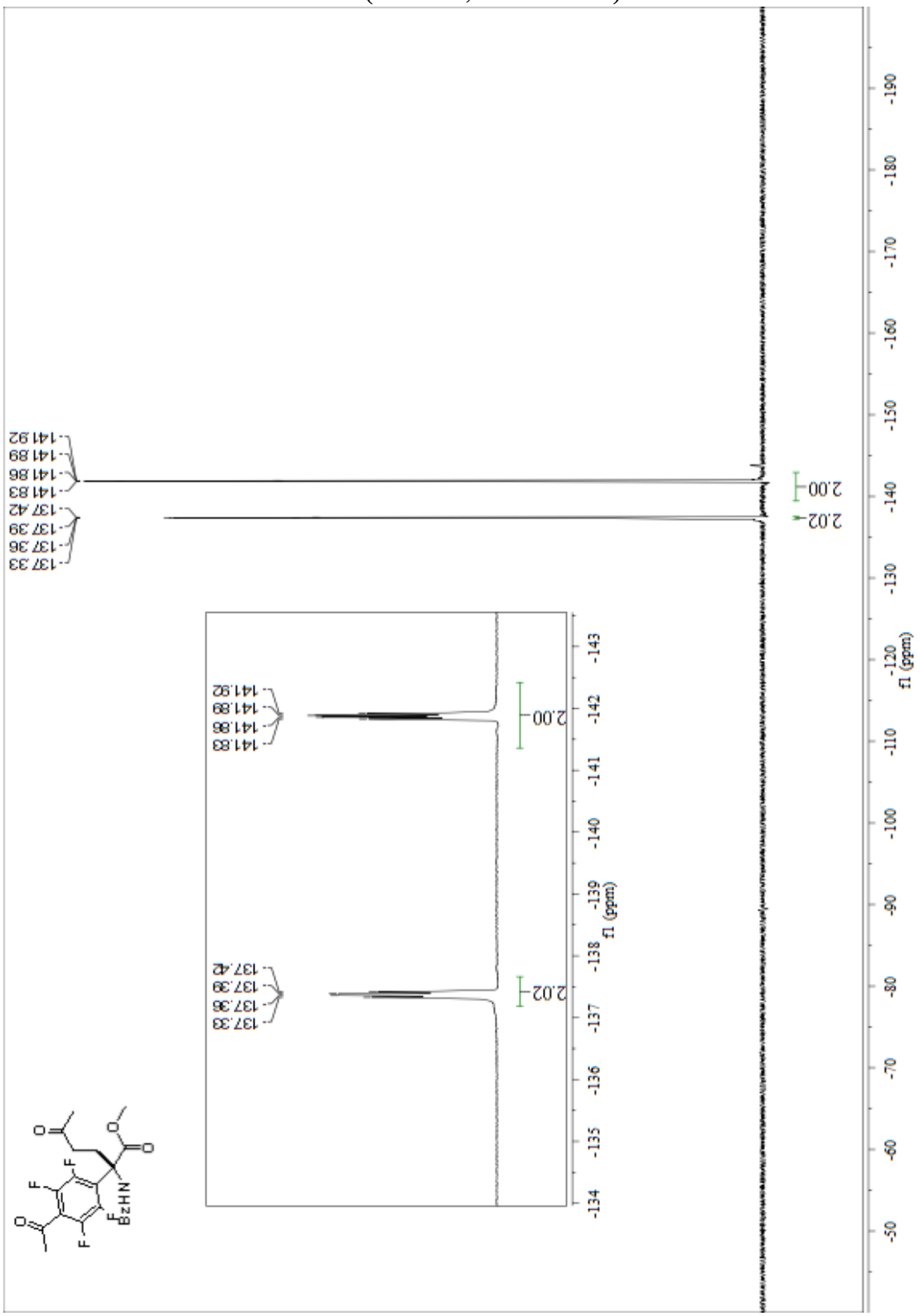

^{13}C NMR (101 MHz, Chloroform-*d*) **3c**

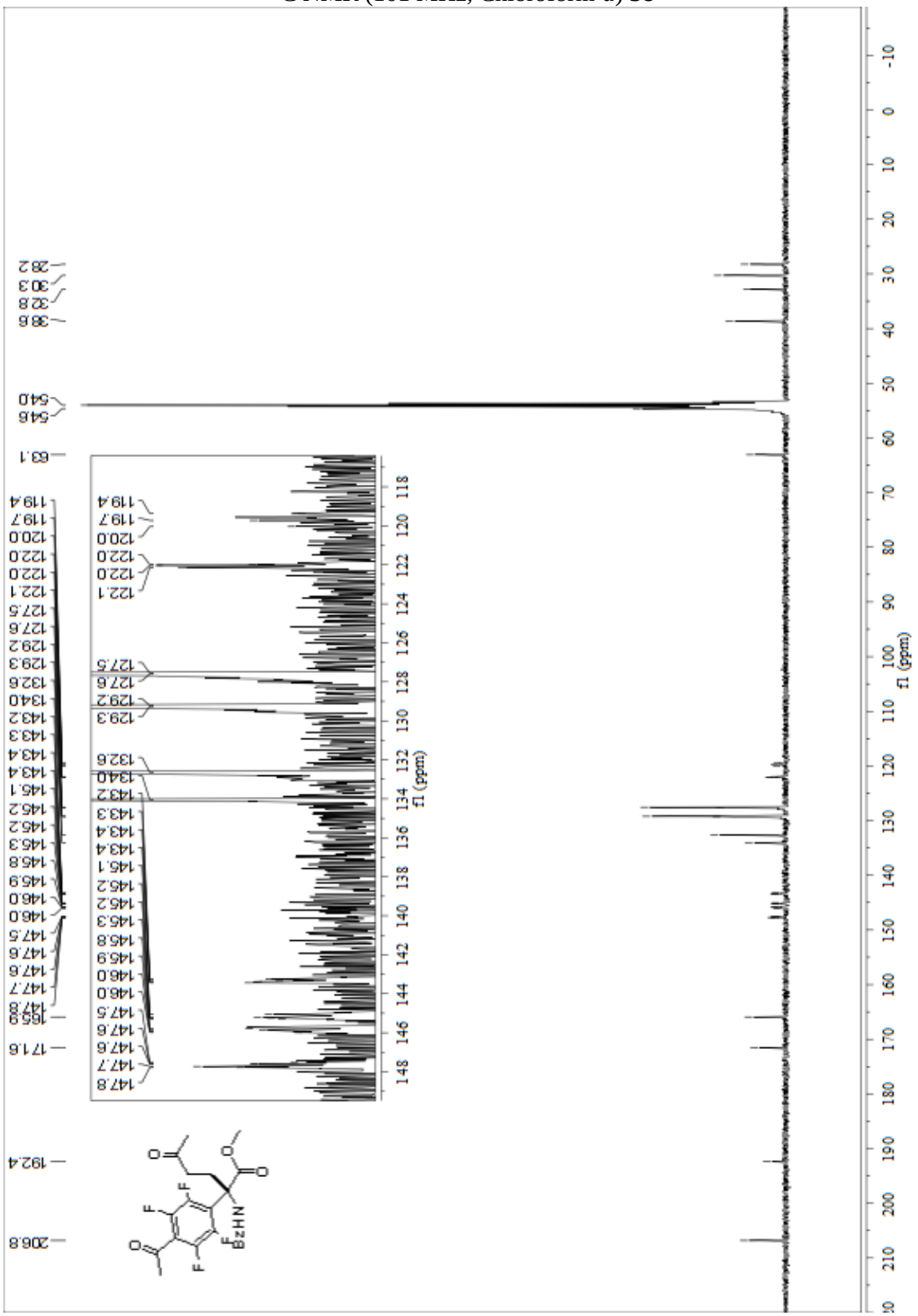

[1]H NMR (400 MHz, Chloroform-*d*) **3d**

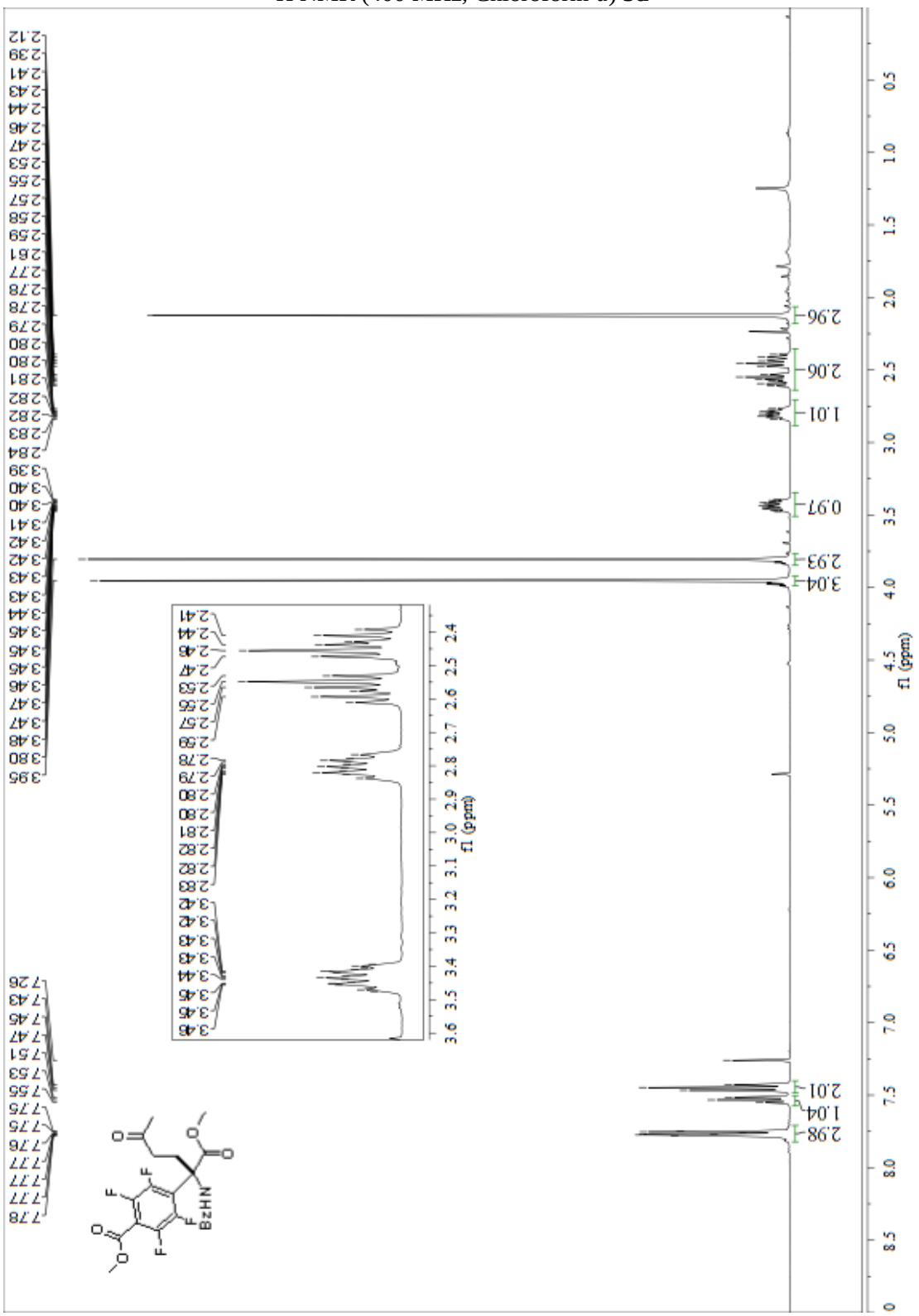

^{19}F NMR (376 MHz, Chloroform-*d*) **3d**

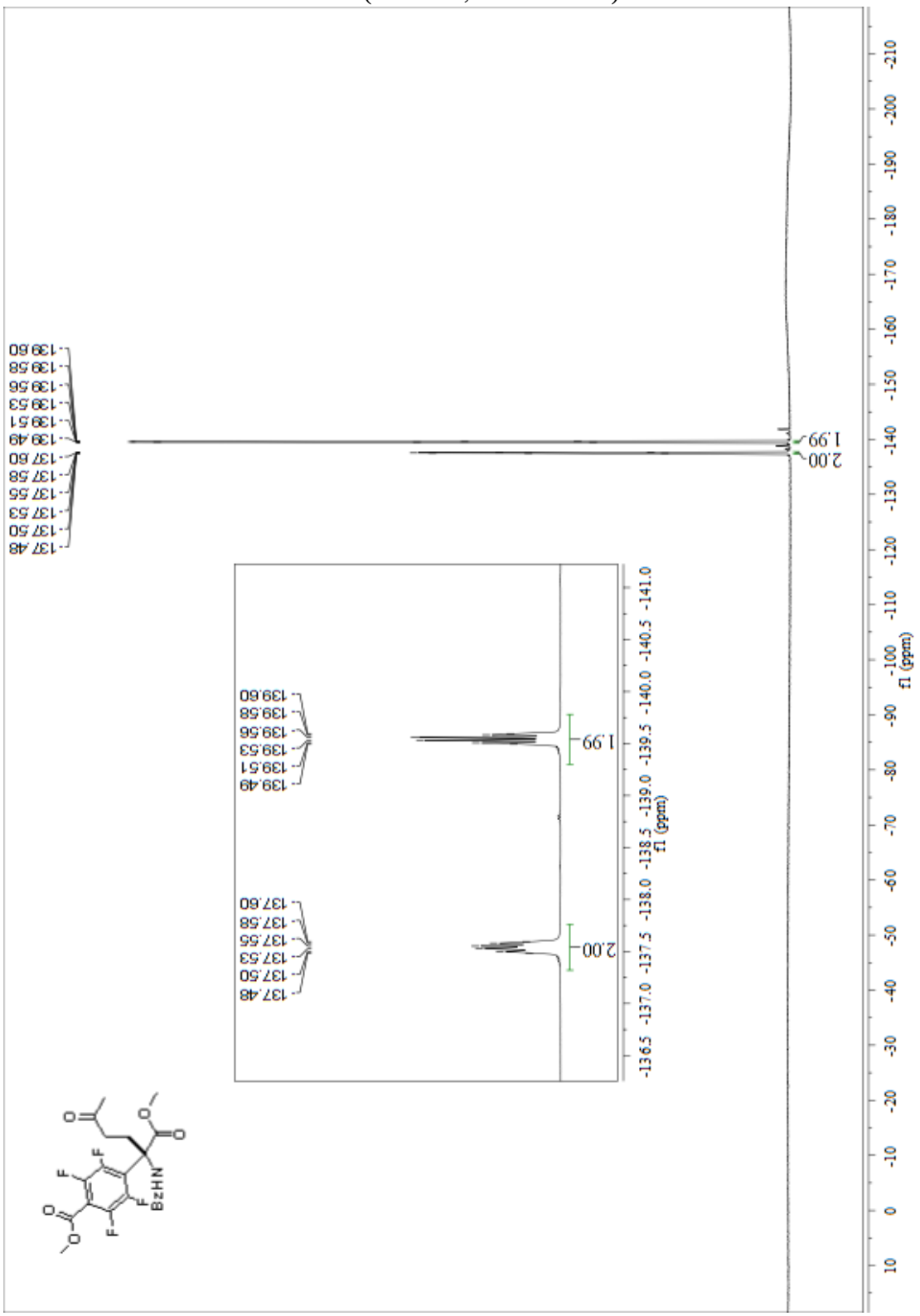

^{13}C NMR (101 MHz, Chloroform-*d*) **3d**

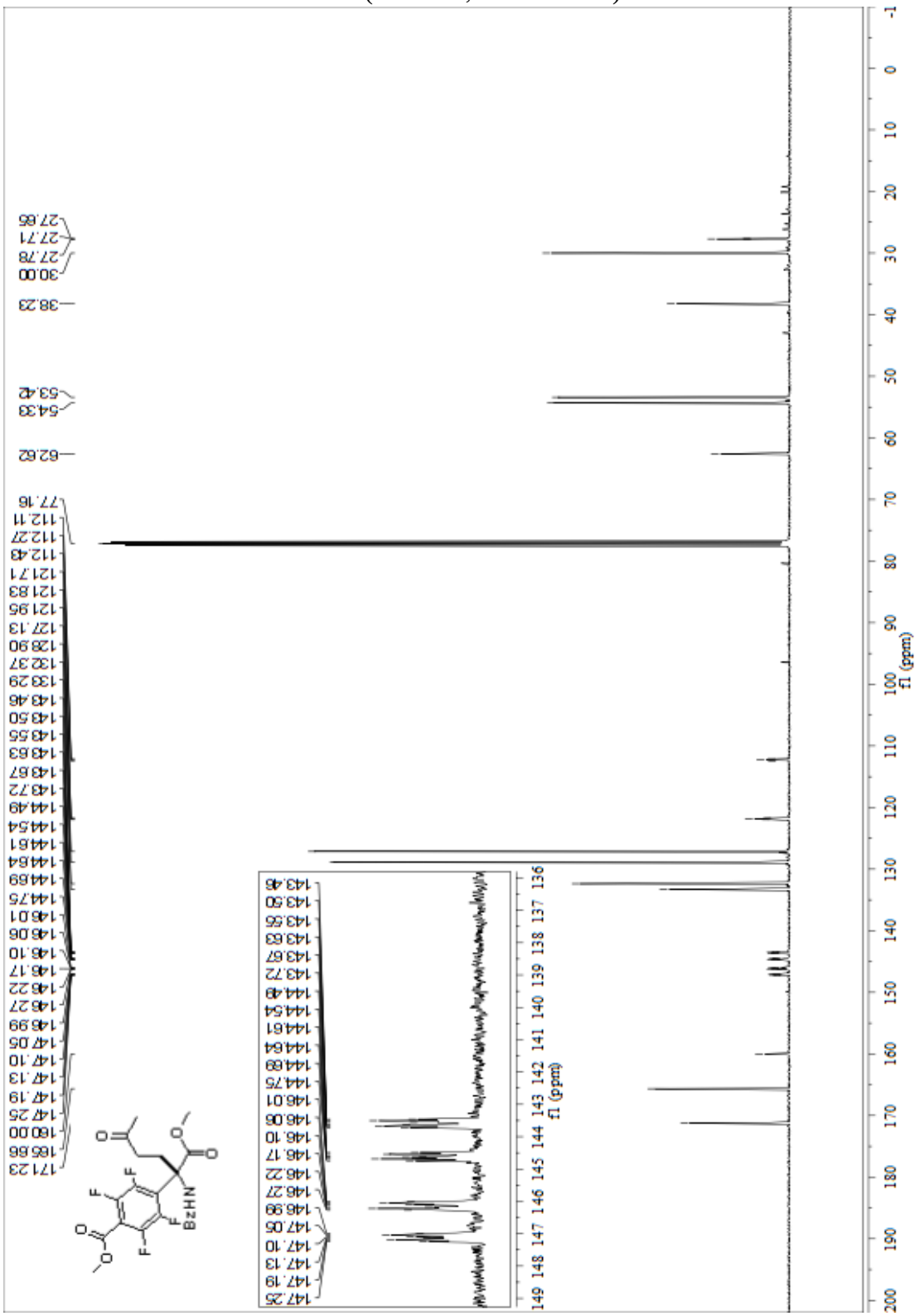

^{1}H NMR (400 MHz, Chloroform-*d*) **3e**

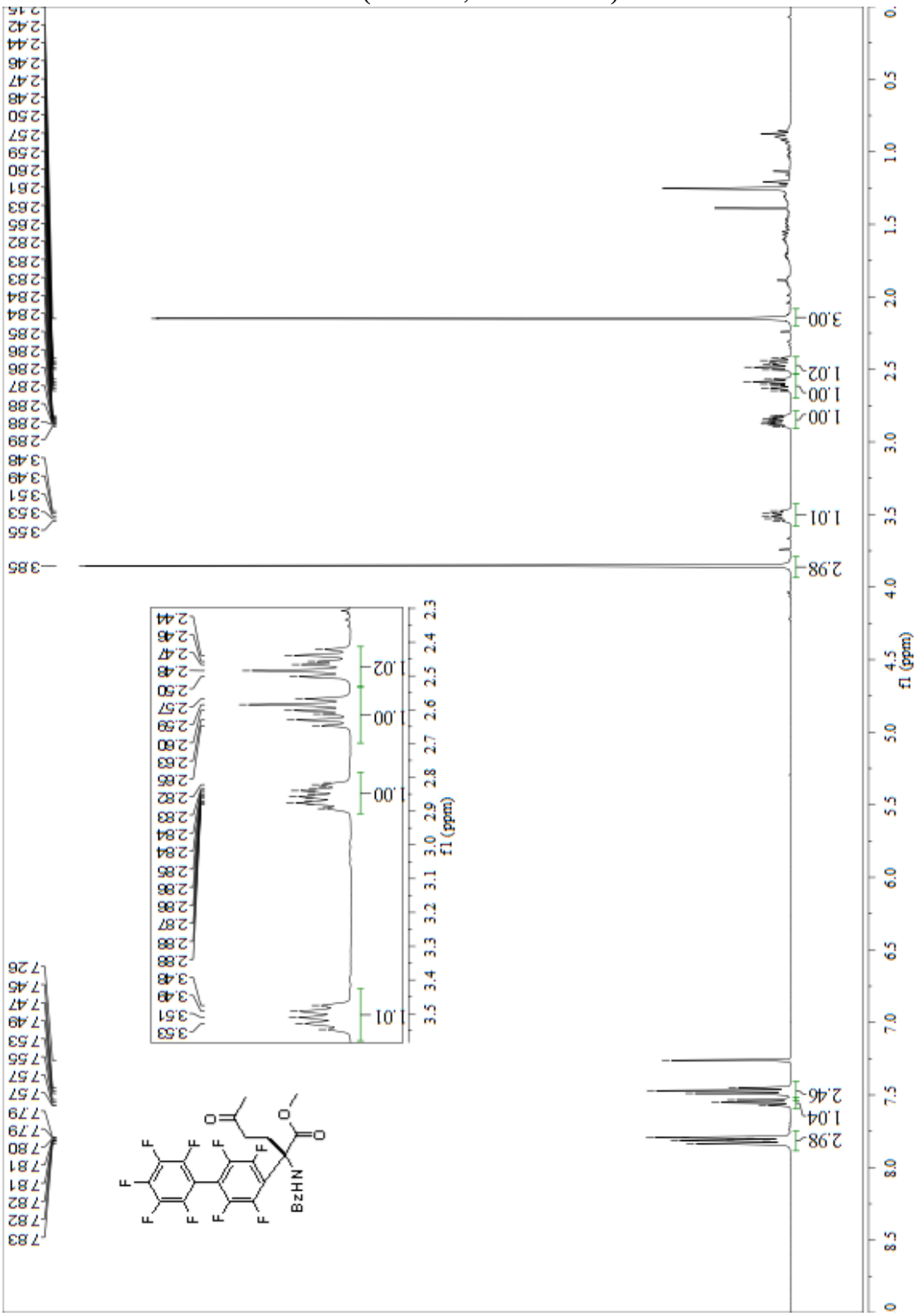

^{19}F NMR (376 MHz, Chloroform-*d*) **3e**

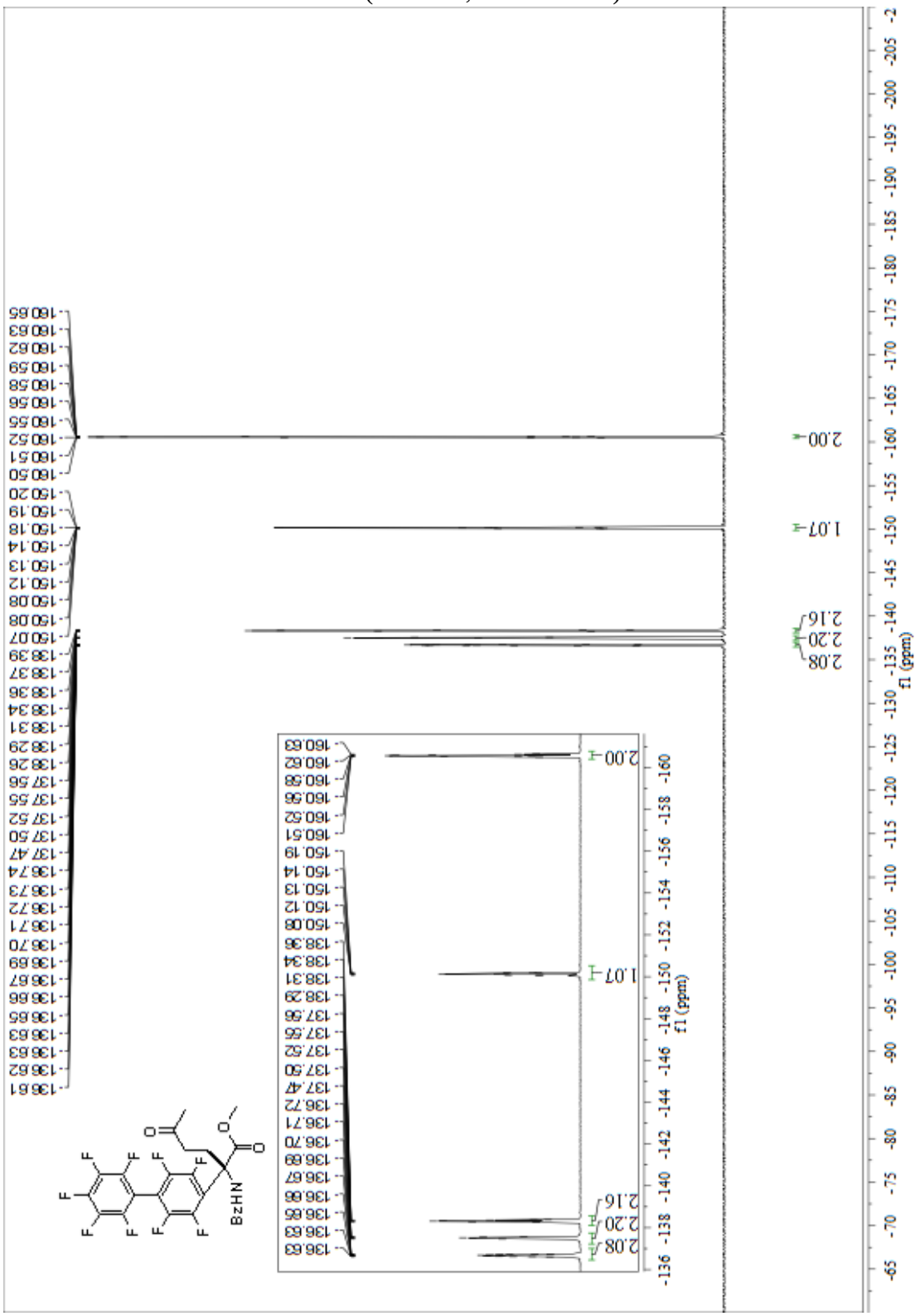

^{13}C NMR (101 MHz, Chloroform-*d*) **3e**

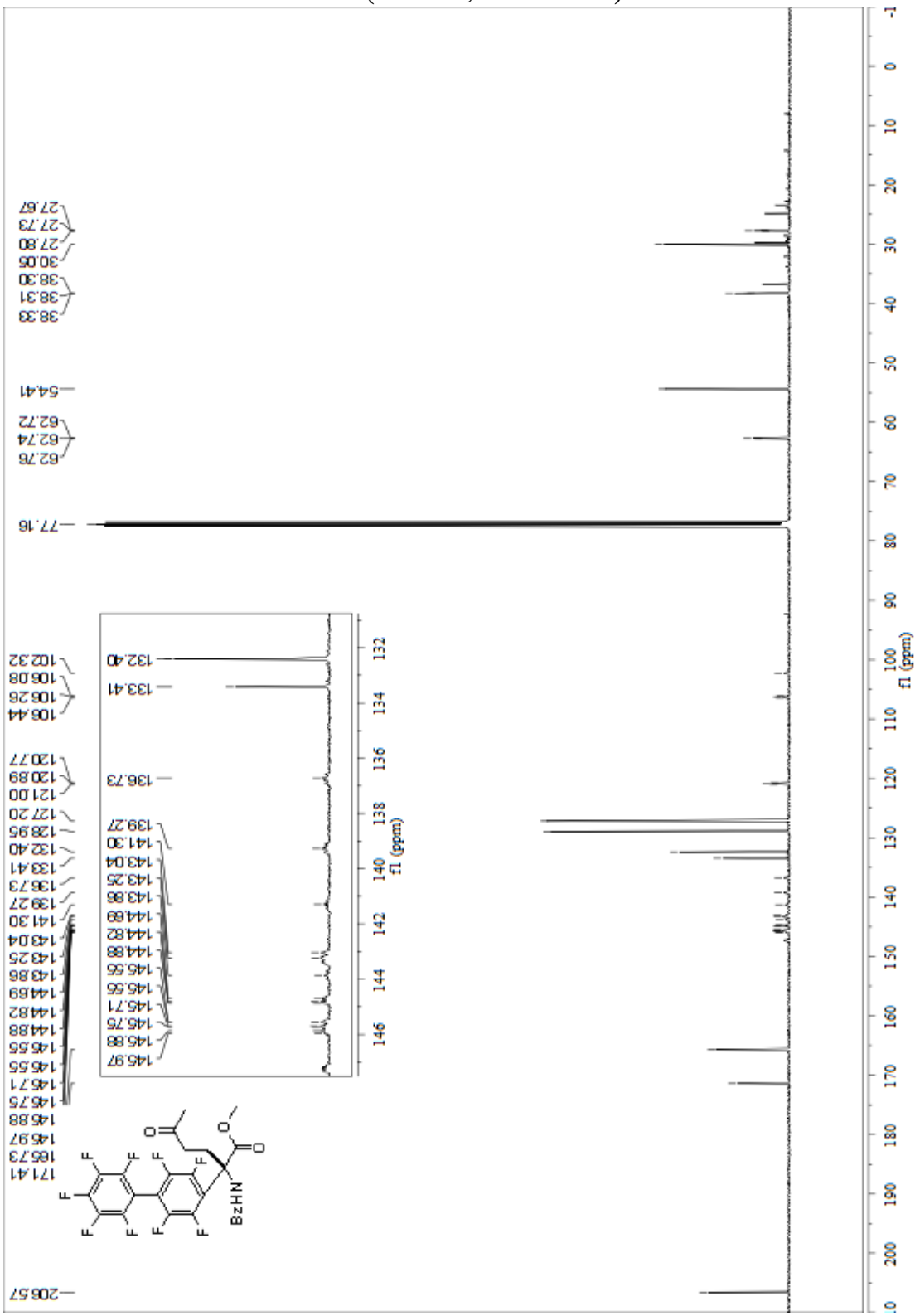

^{1}H NMR (400 MHz, Chloroform-*d*) **3f**

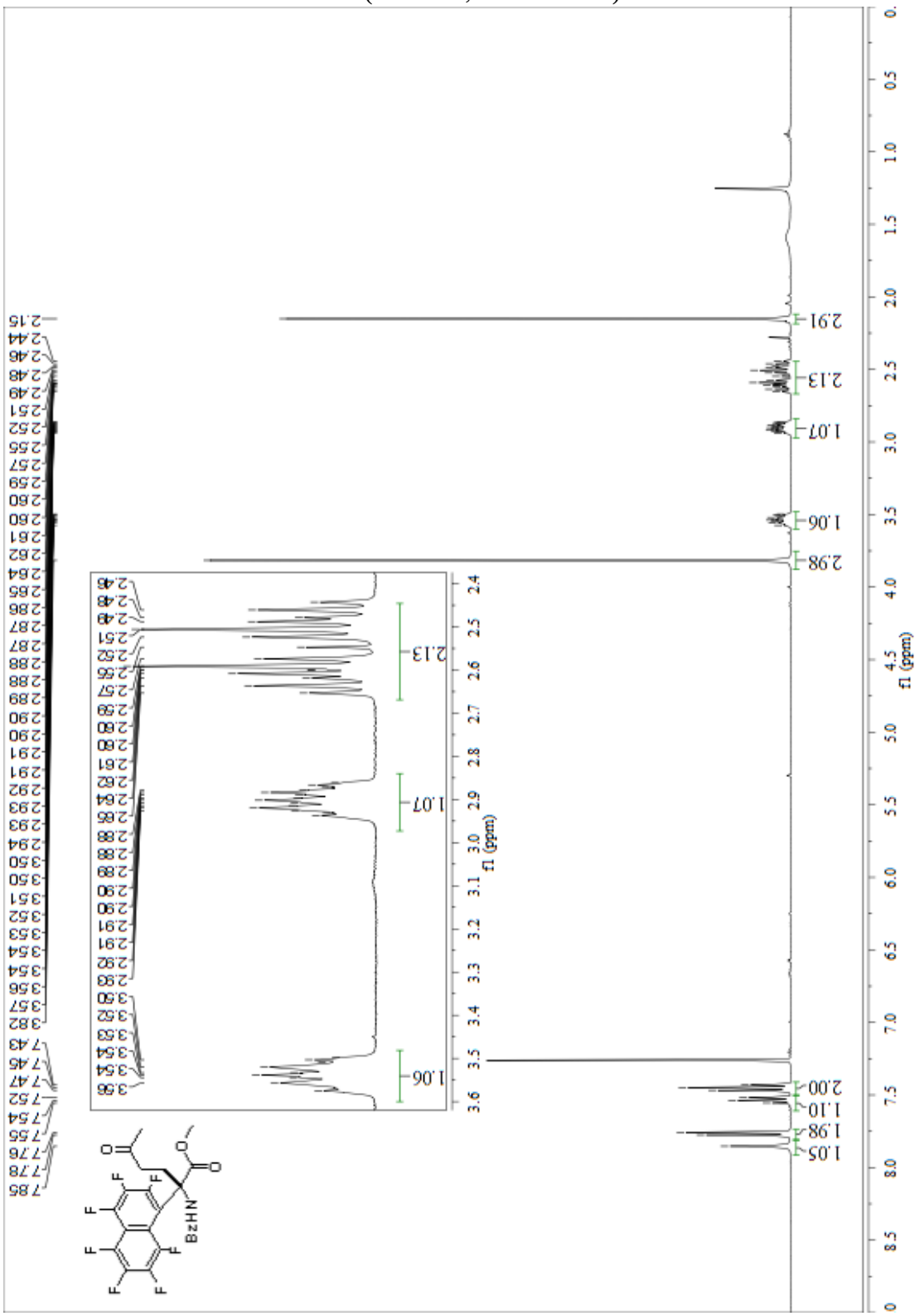

^{19}F NMR (376 MHz, Chloroform-*d*) **3f**

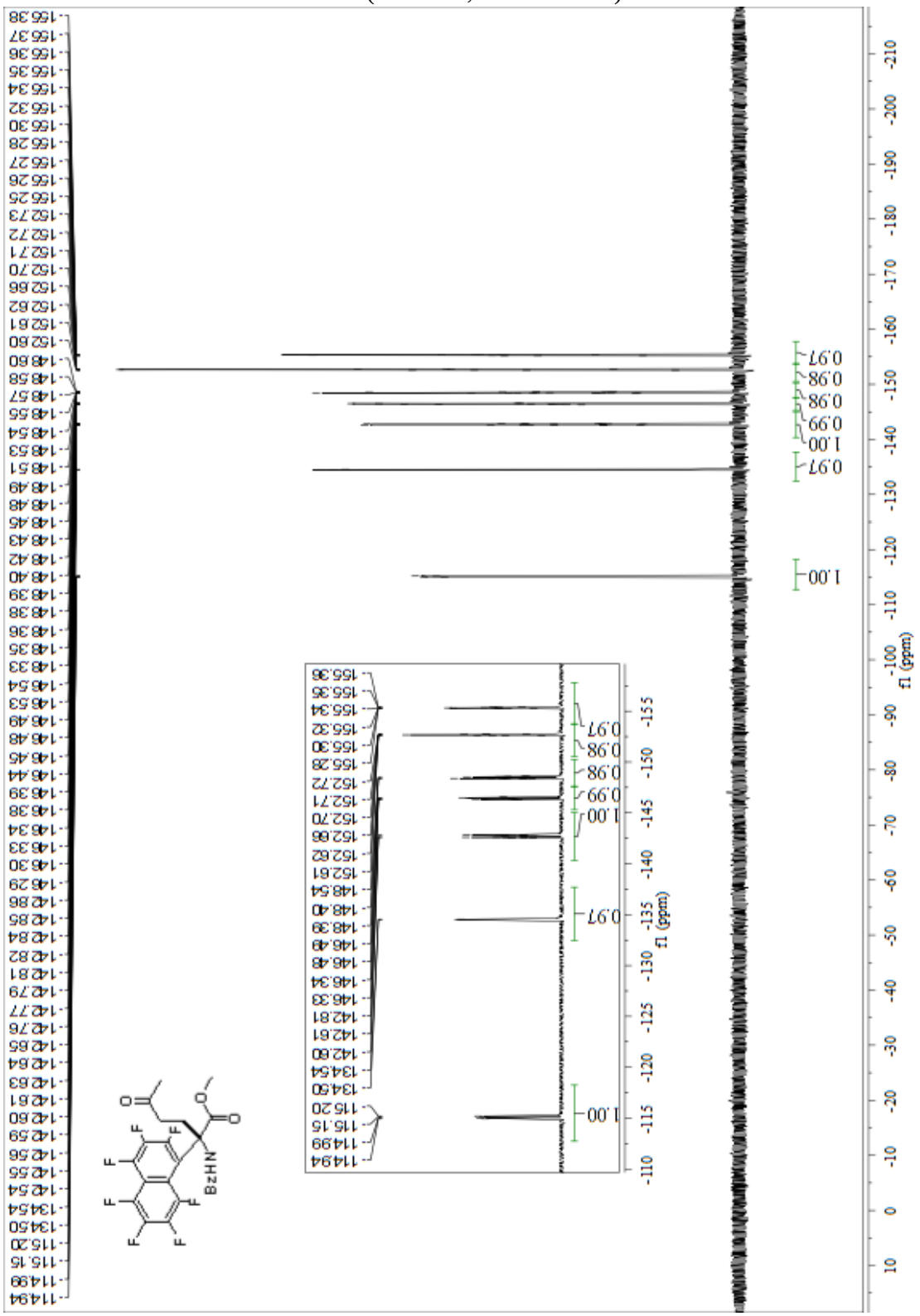

^{13}C NMR (101 MHz, Chloroform-*d*) **3f**

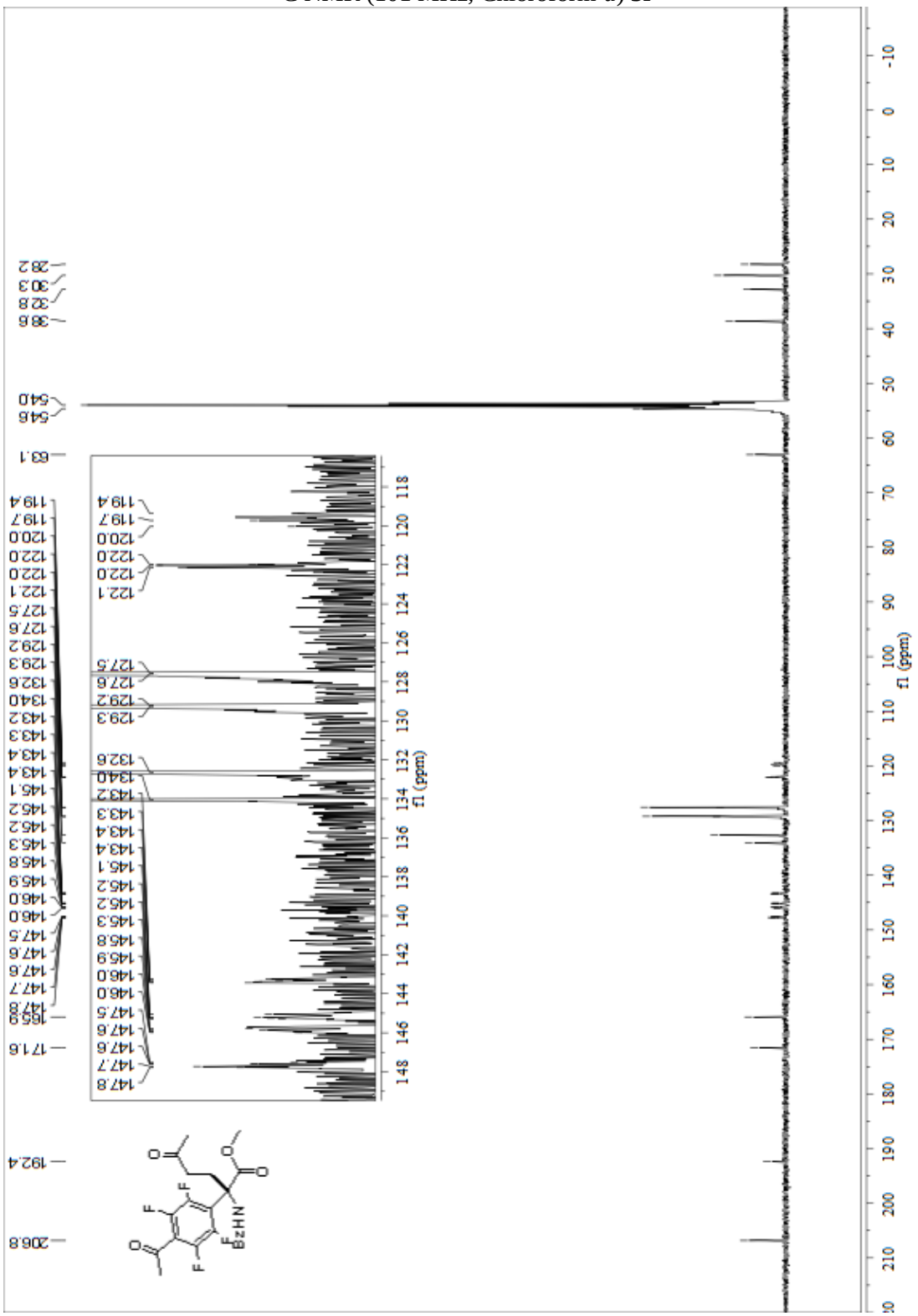

^{1}H NMR (400 MHz, Chloroform-*d*) **3g**

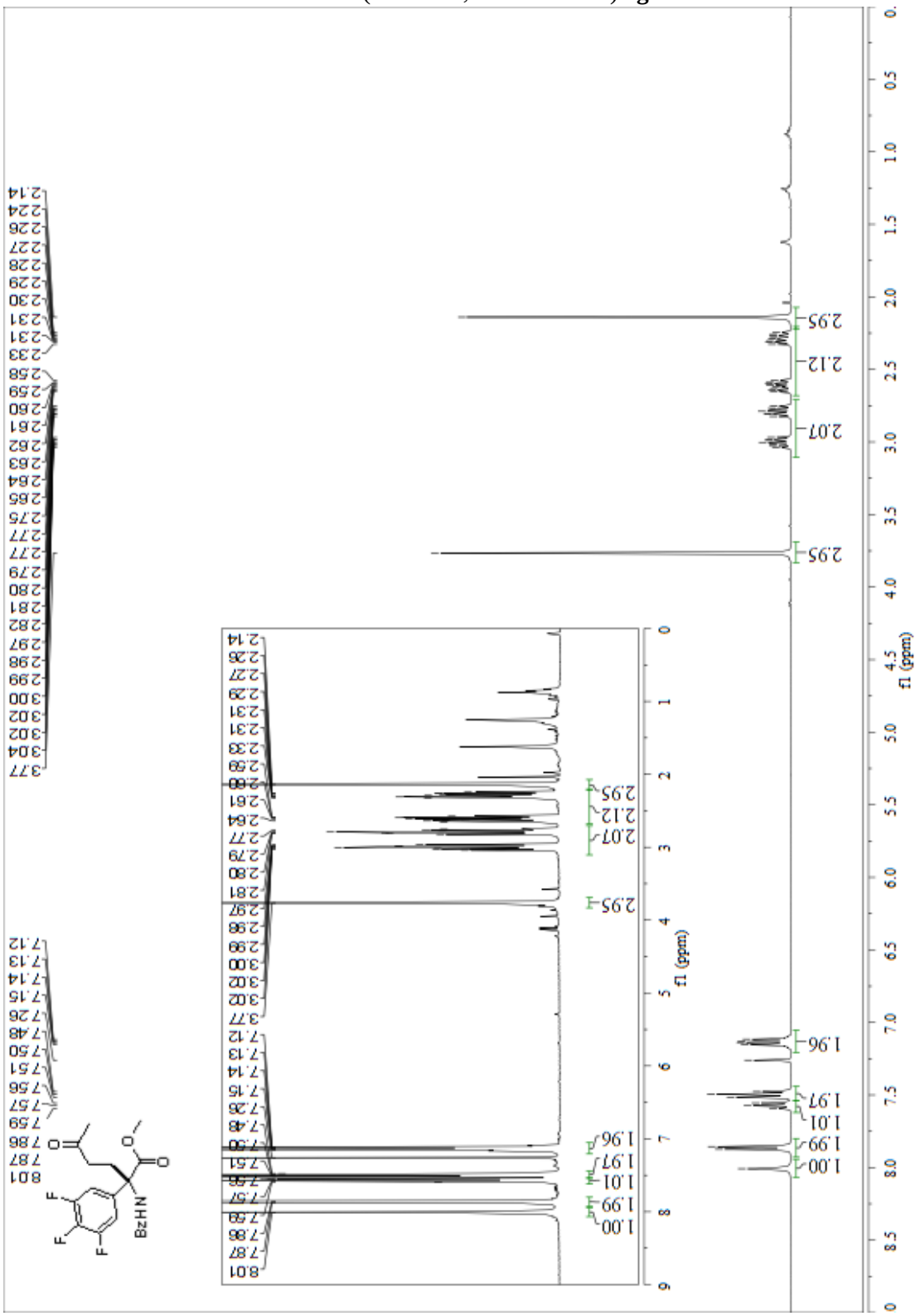

^{19}F NMR (376 MHz, Chloroform-*d*) **3g**

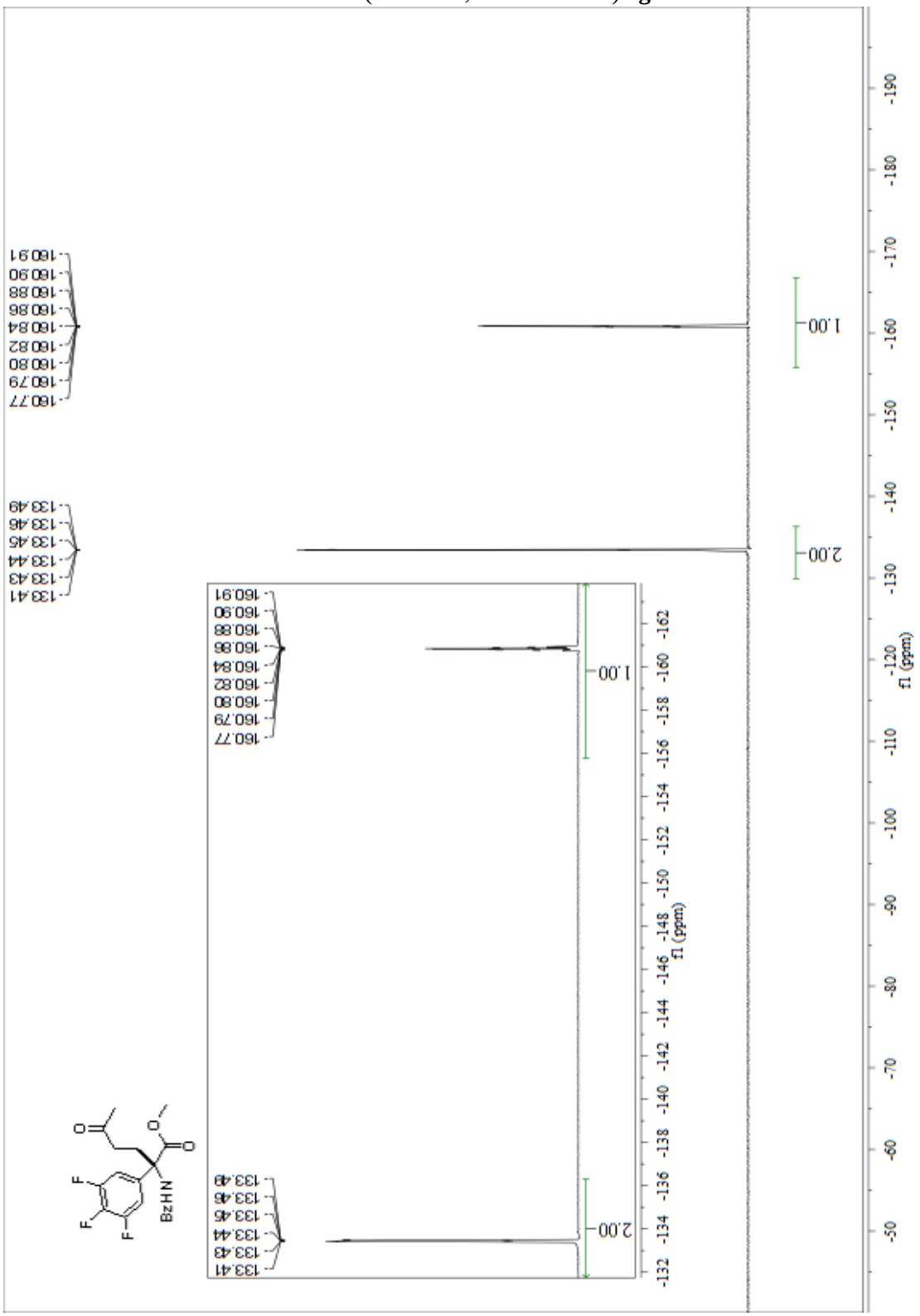

^{13}C NMR (101 MHz, Chloroform-*d*) **3g**

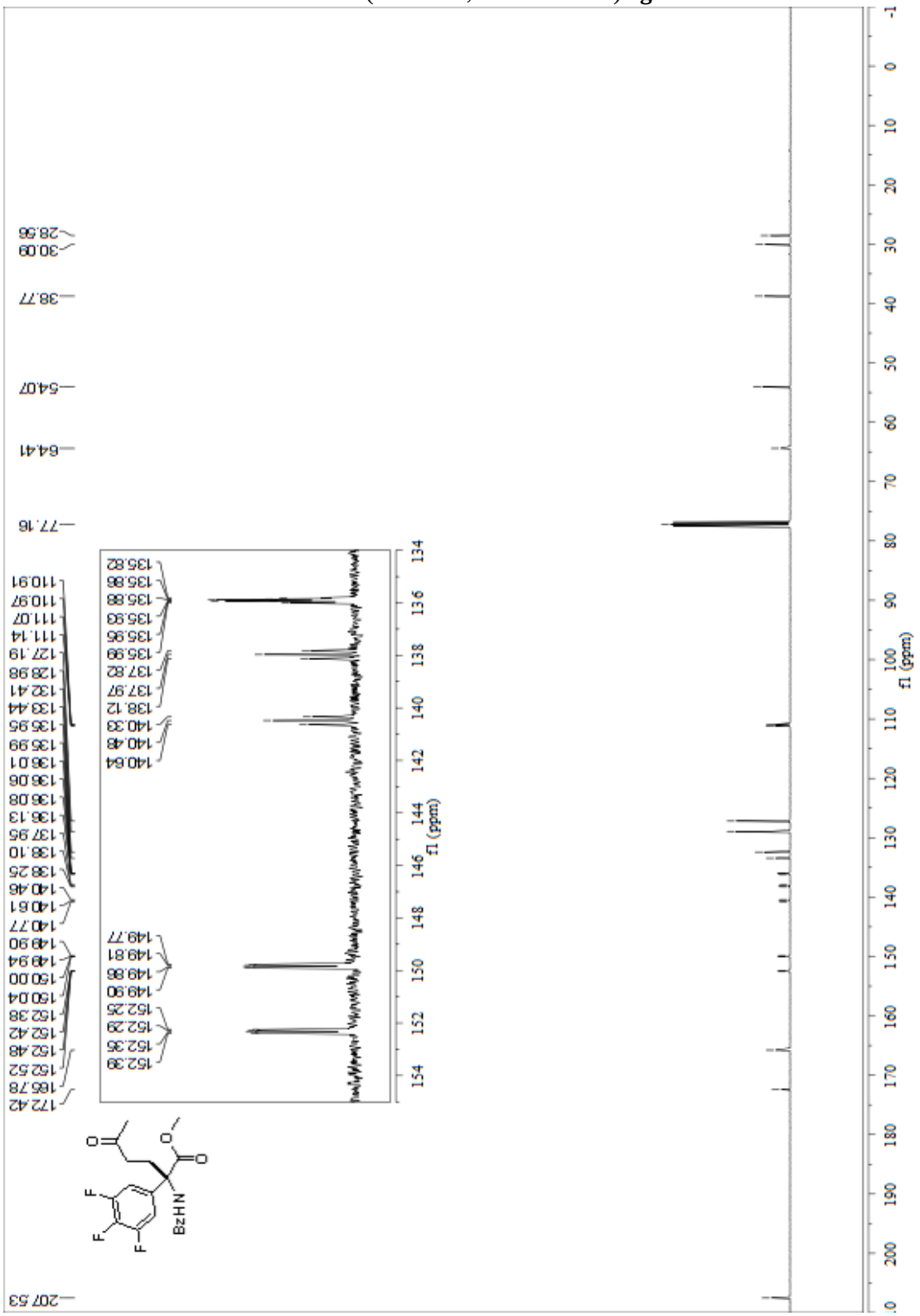

^{1}H NMR (400 MHz, Chloroform-*d*) **3h**

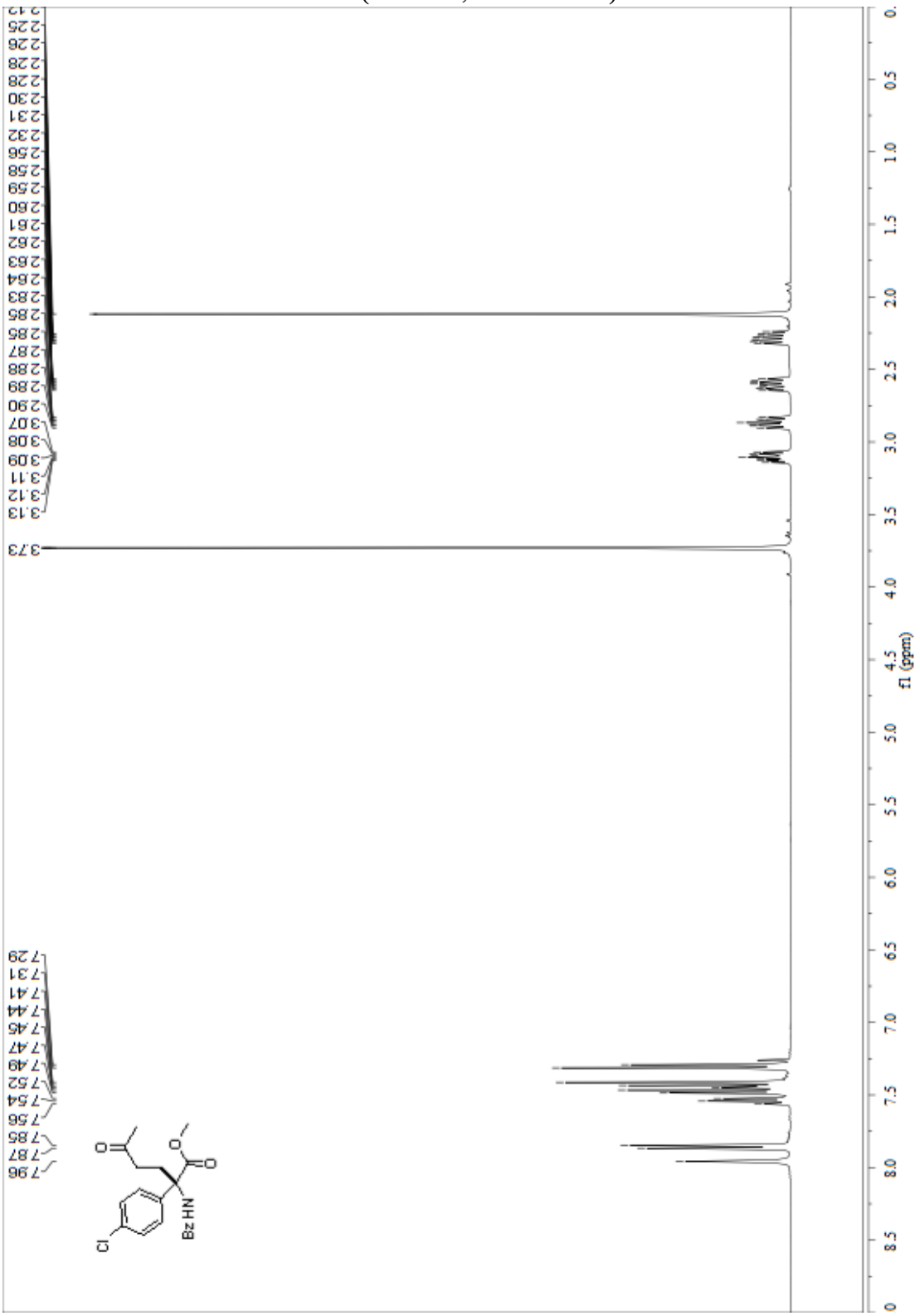

^{13}C NMR (101 MHz, Chloroform-*d*) **3h**

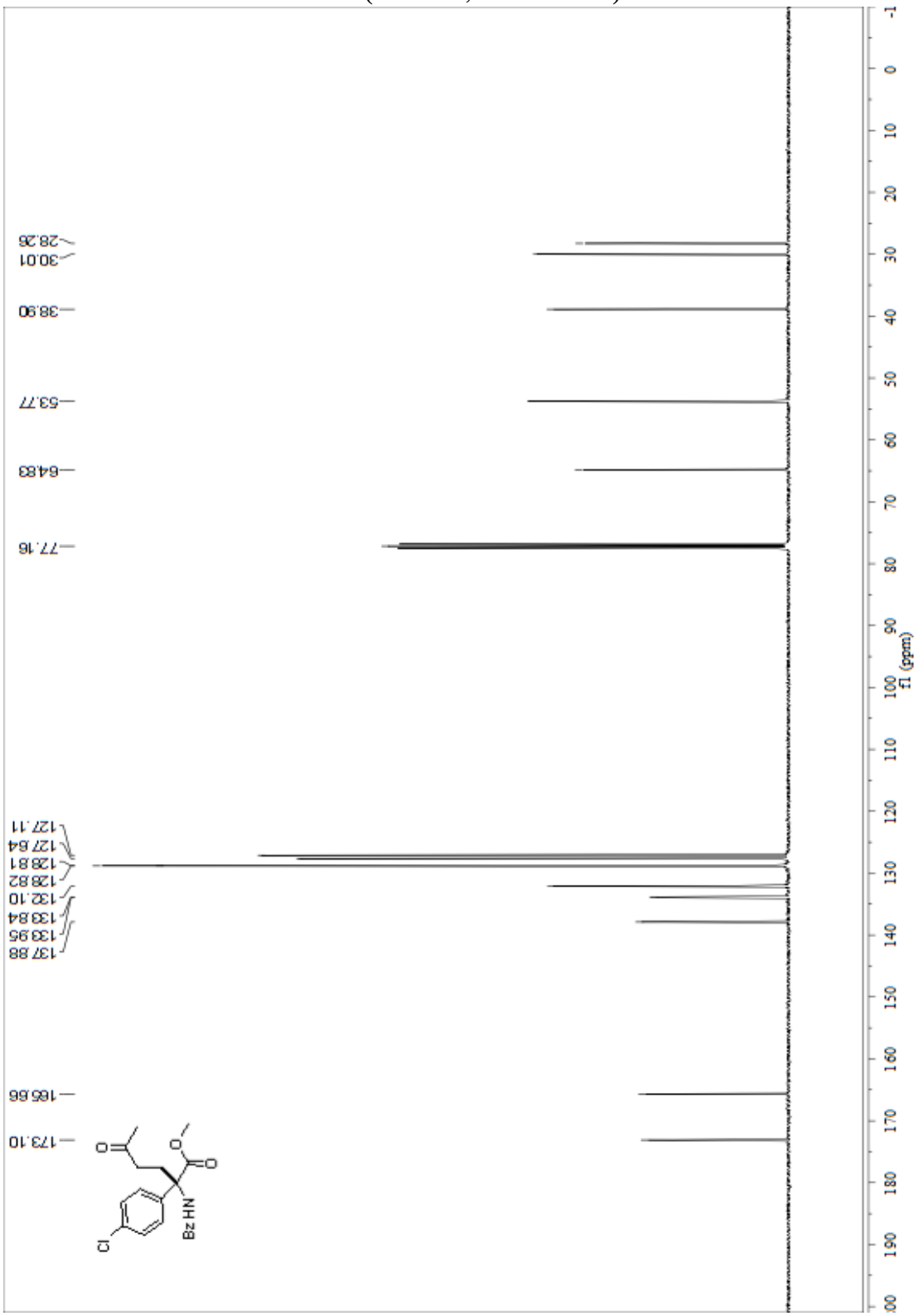

^{1}H NMR (400 MHz, Chloroform-*d*) **3i**

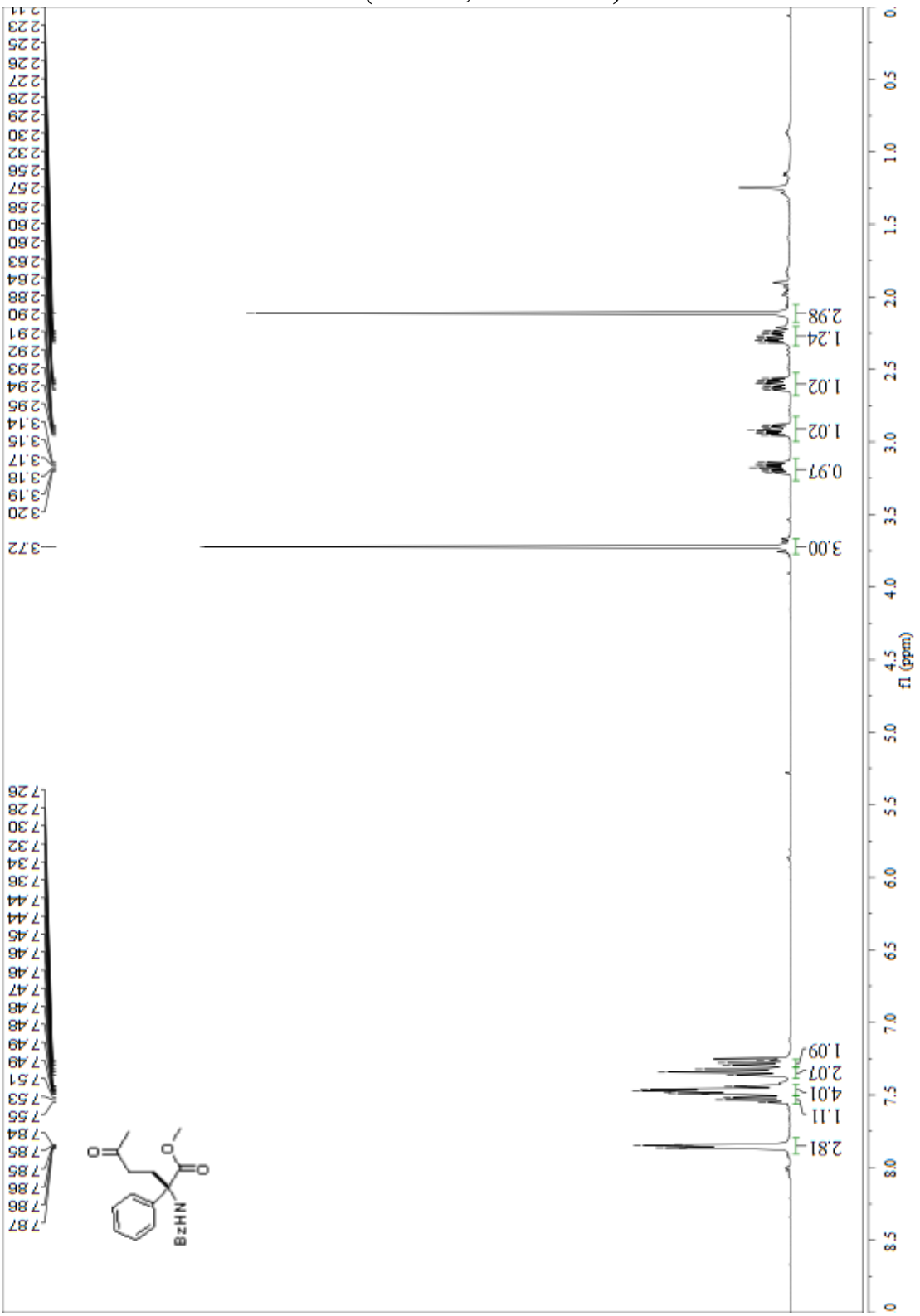

^{13}C NMR (101 MHz, Chloroform-*d*) **3i**

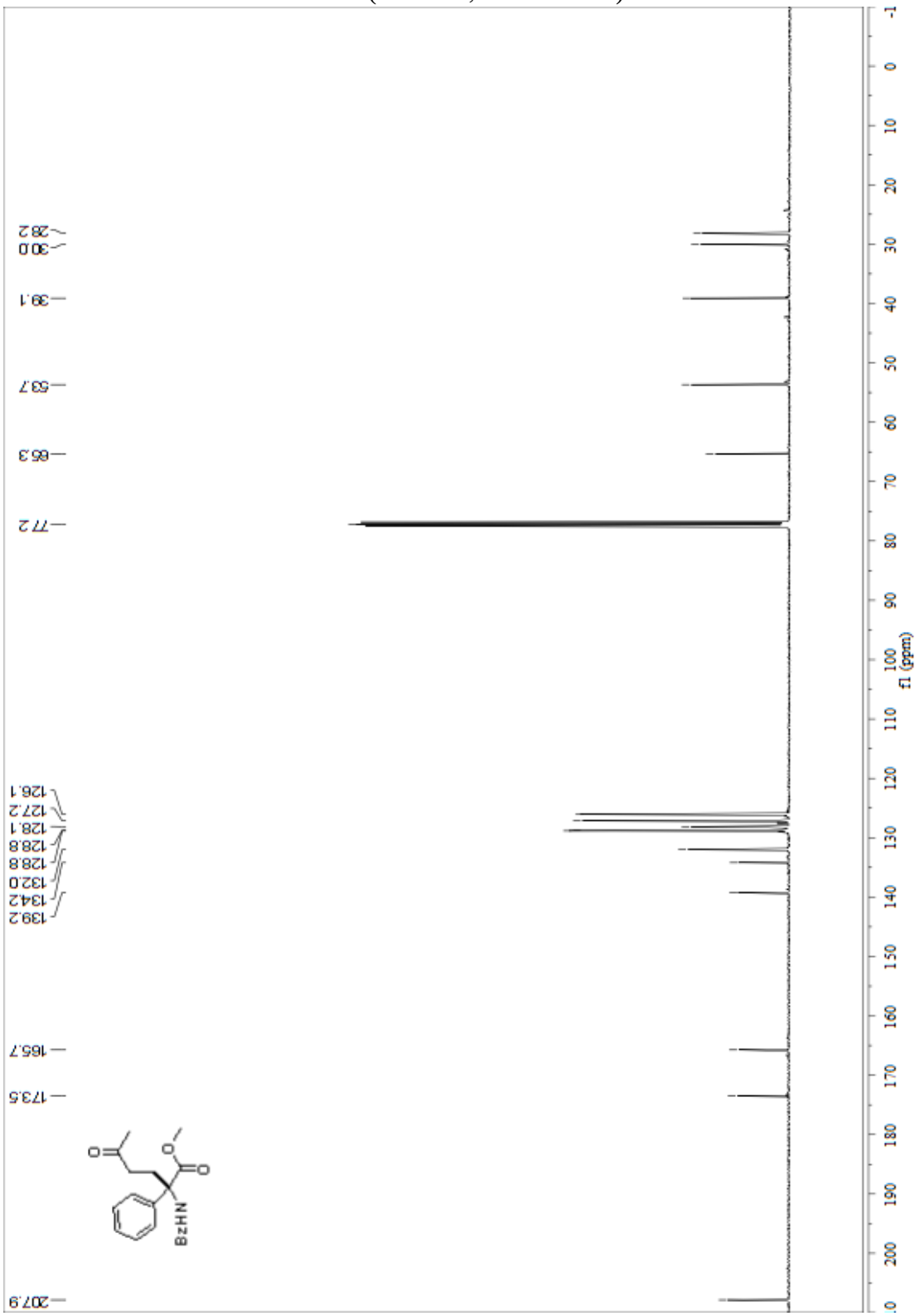

^{1}H NMR (400 MHz, Methylene Chloride-*d*) **4a**

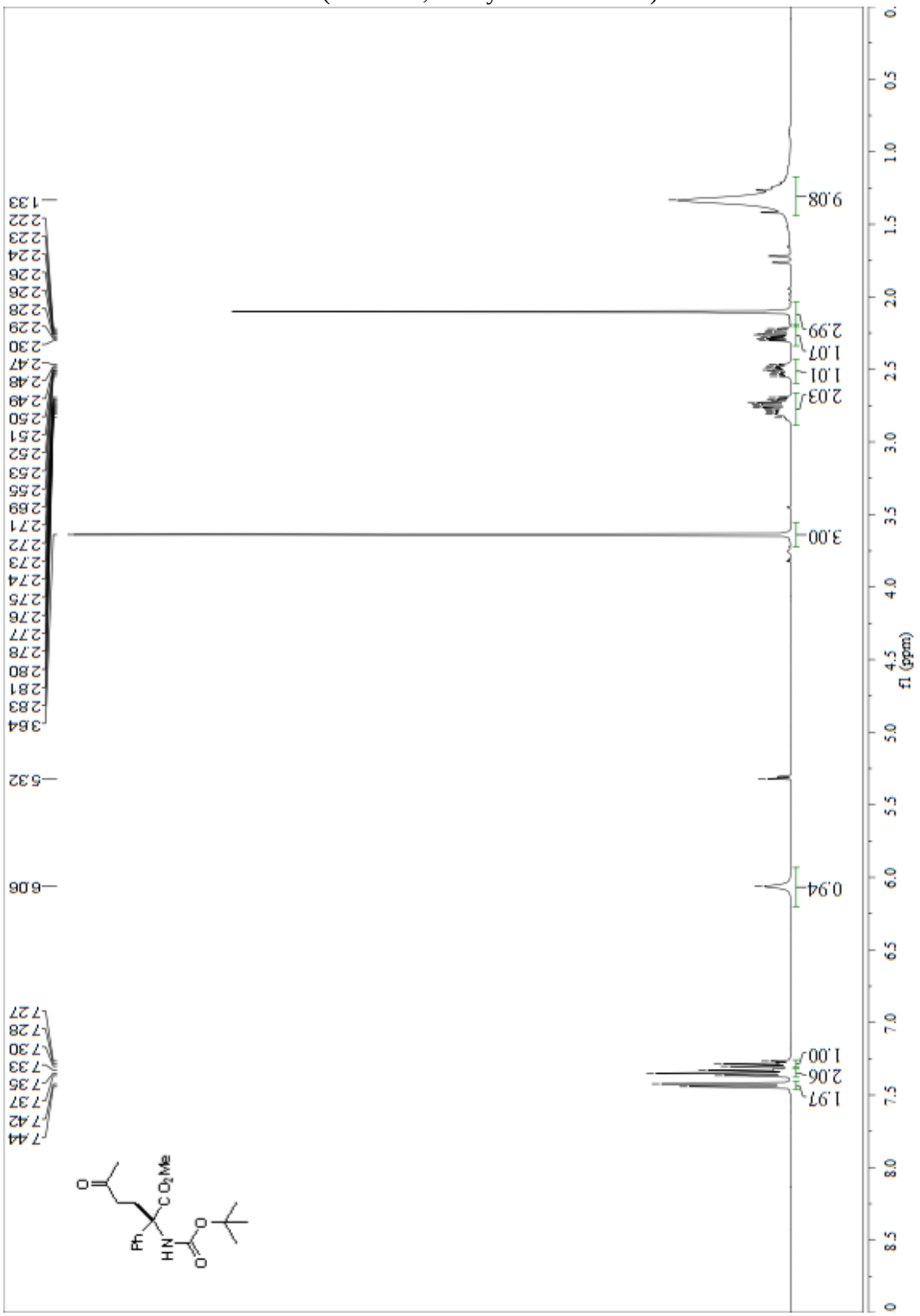

^{13}C NMR (101 MHz, Methylene Chloride -*d*) **4a**

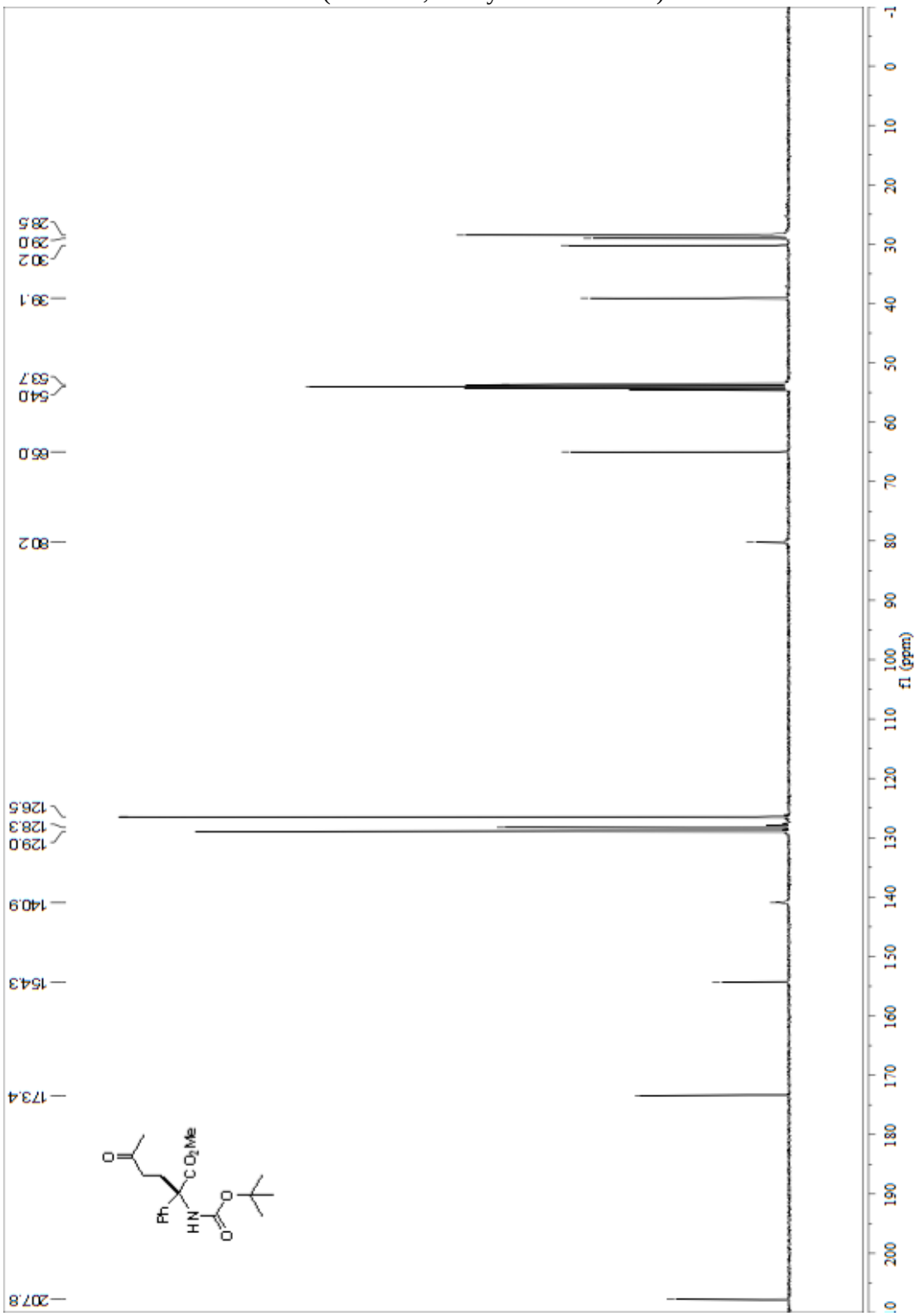

^{1}H NMR (400 MHz, Chloroform-*d*) **4b**

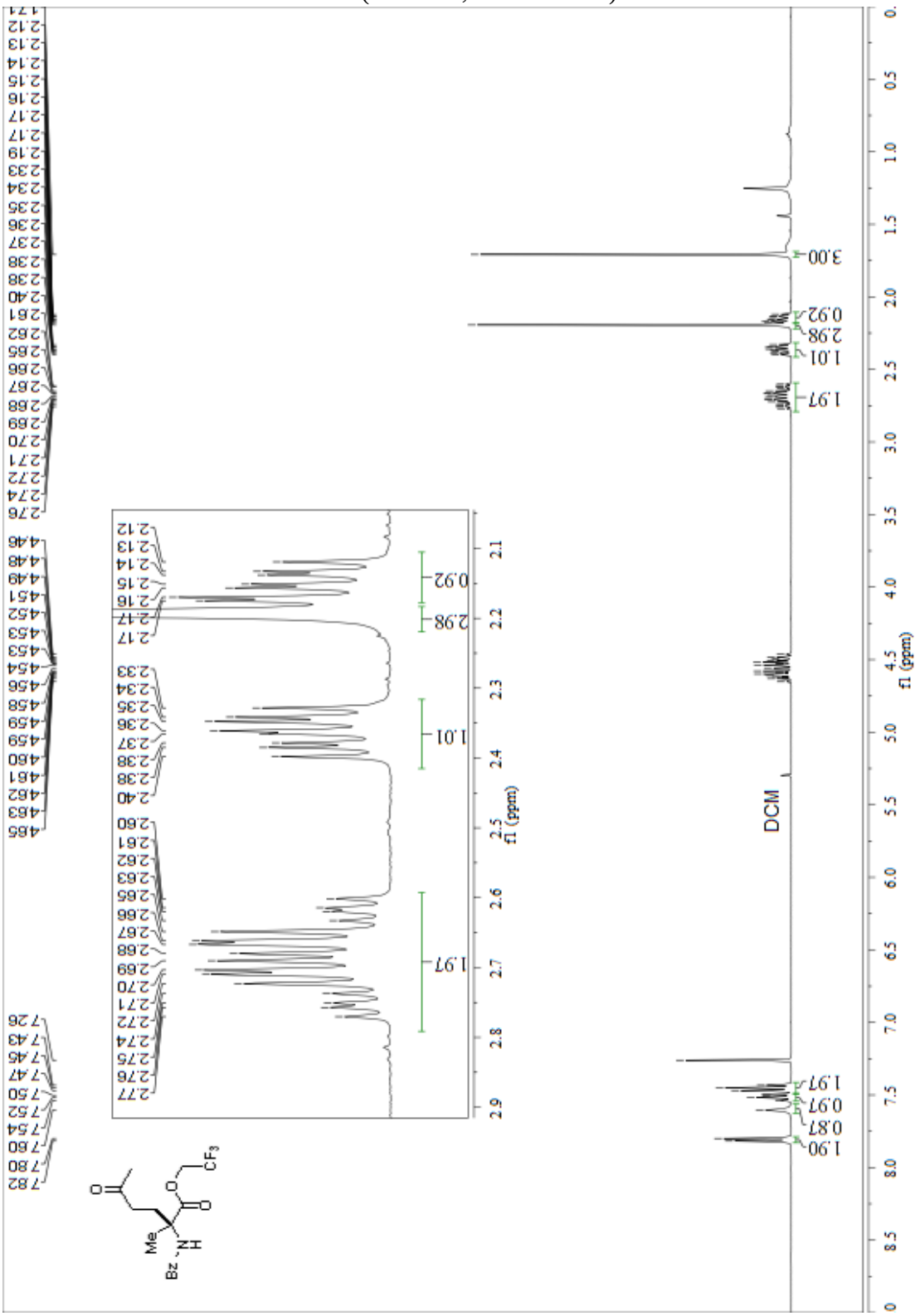

^{13}C NMR (101 MHz, Chloroform-*d*) **4b**

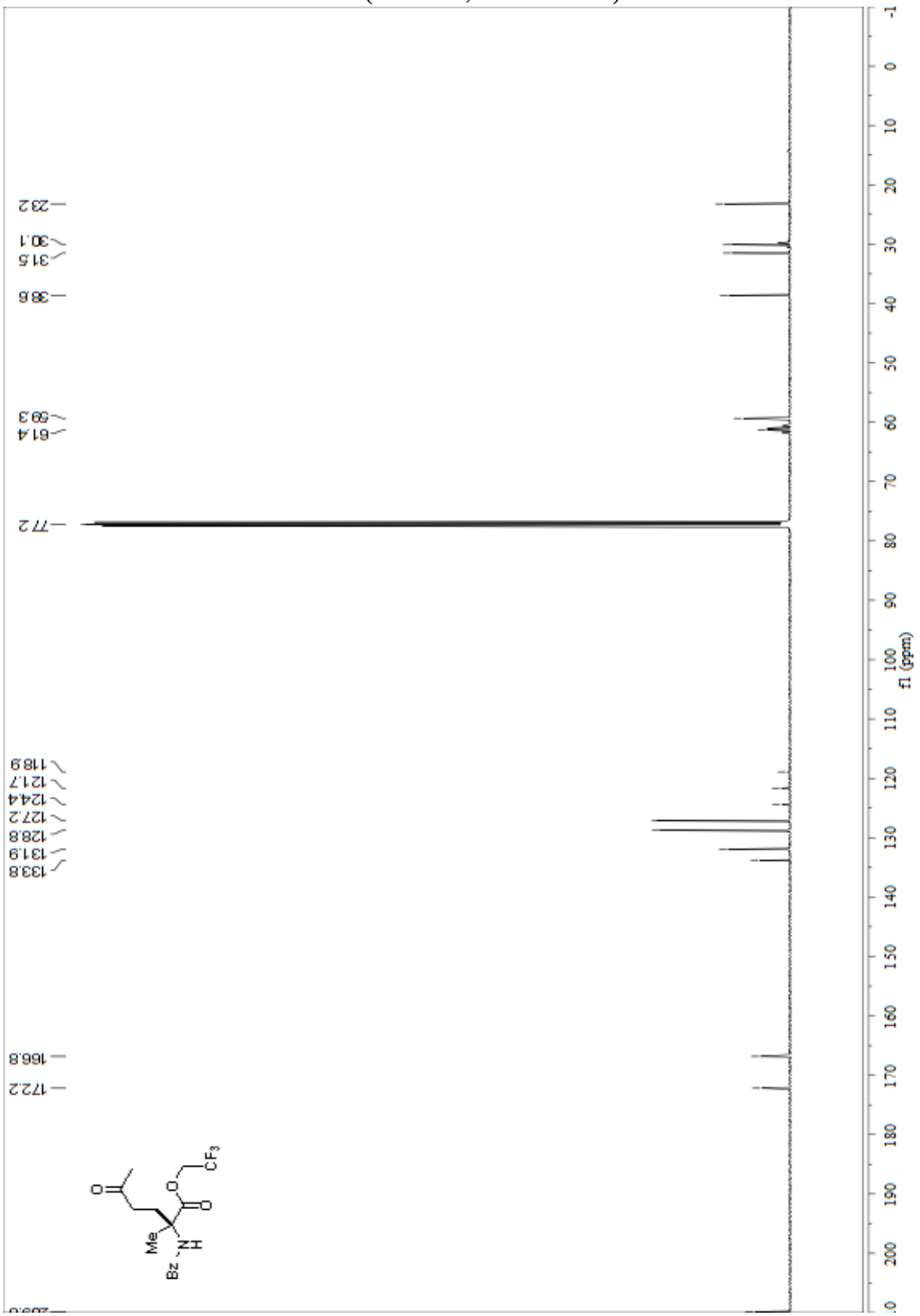

^{1}H NMR (400 MHz, Methylene Chloride-*d*) **4d**

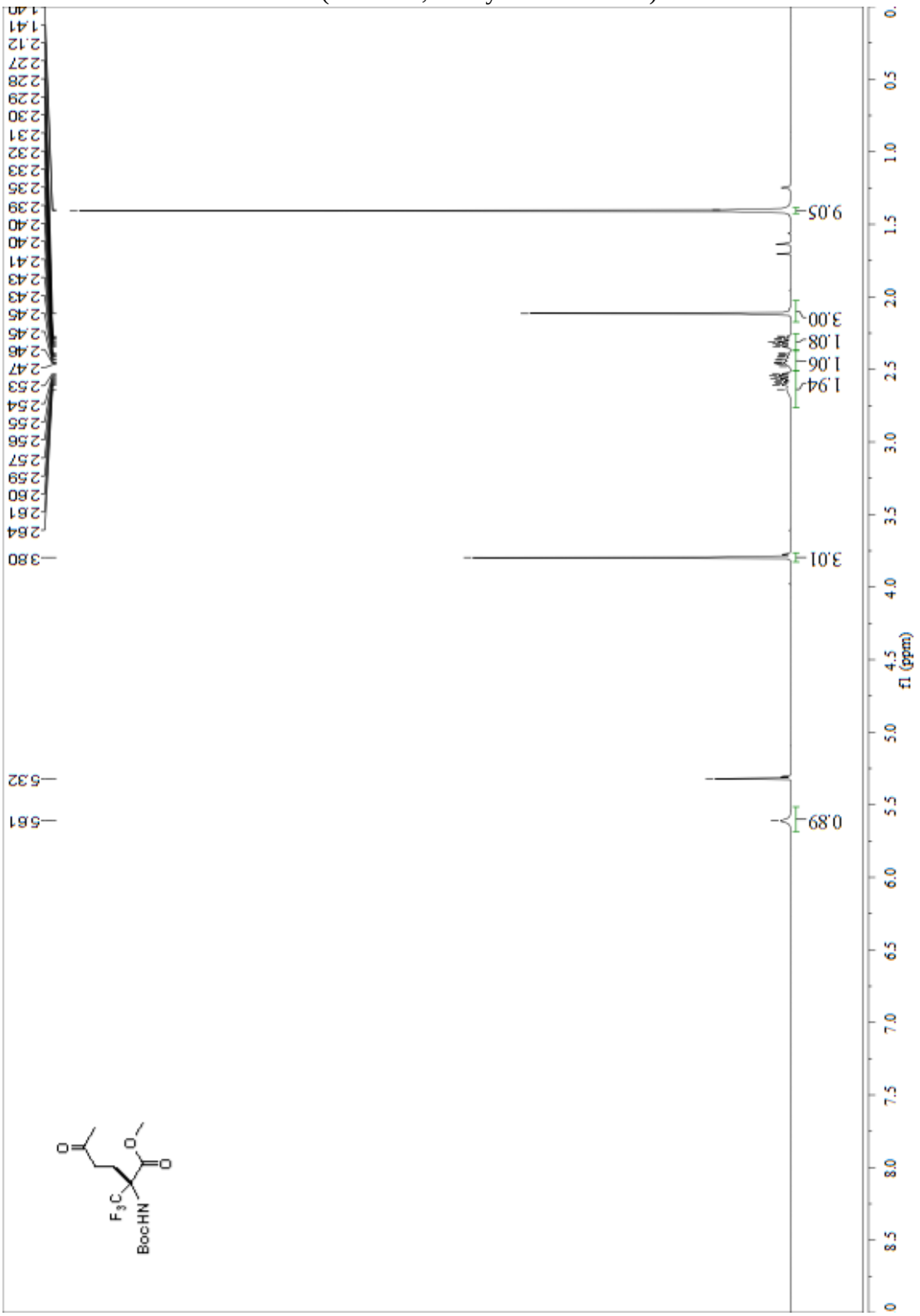

^{19}F NMR (376 MHz, Methylene Chloride-*d*) **4d**

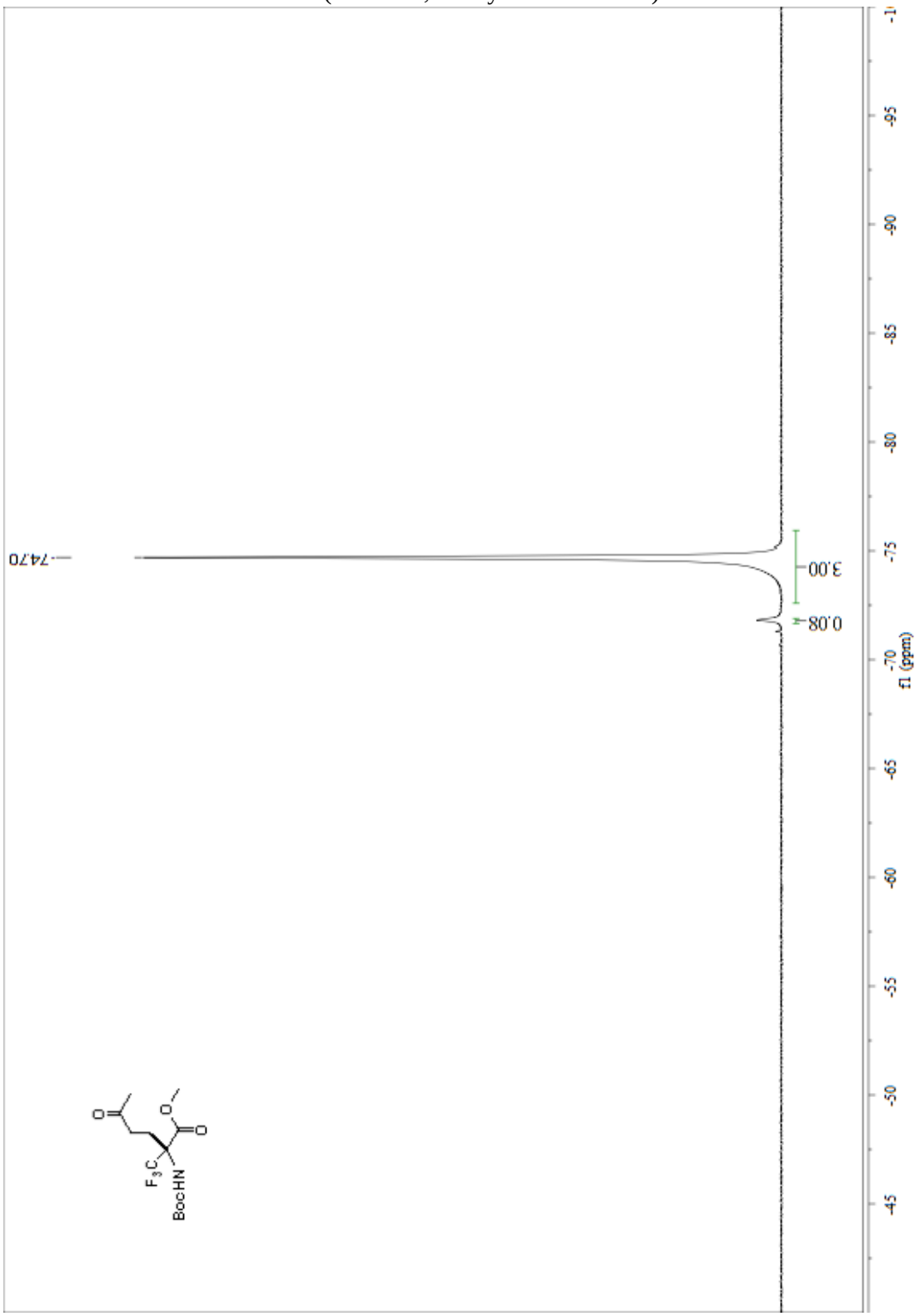

^{13}C NMR (101 MHz, Methylene Chloride-*d*) **4d**

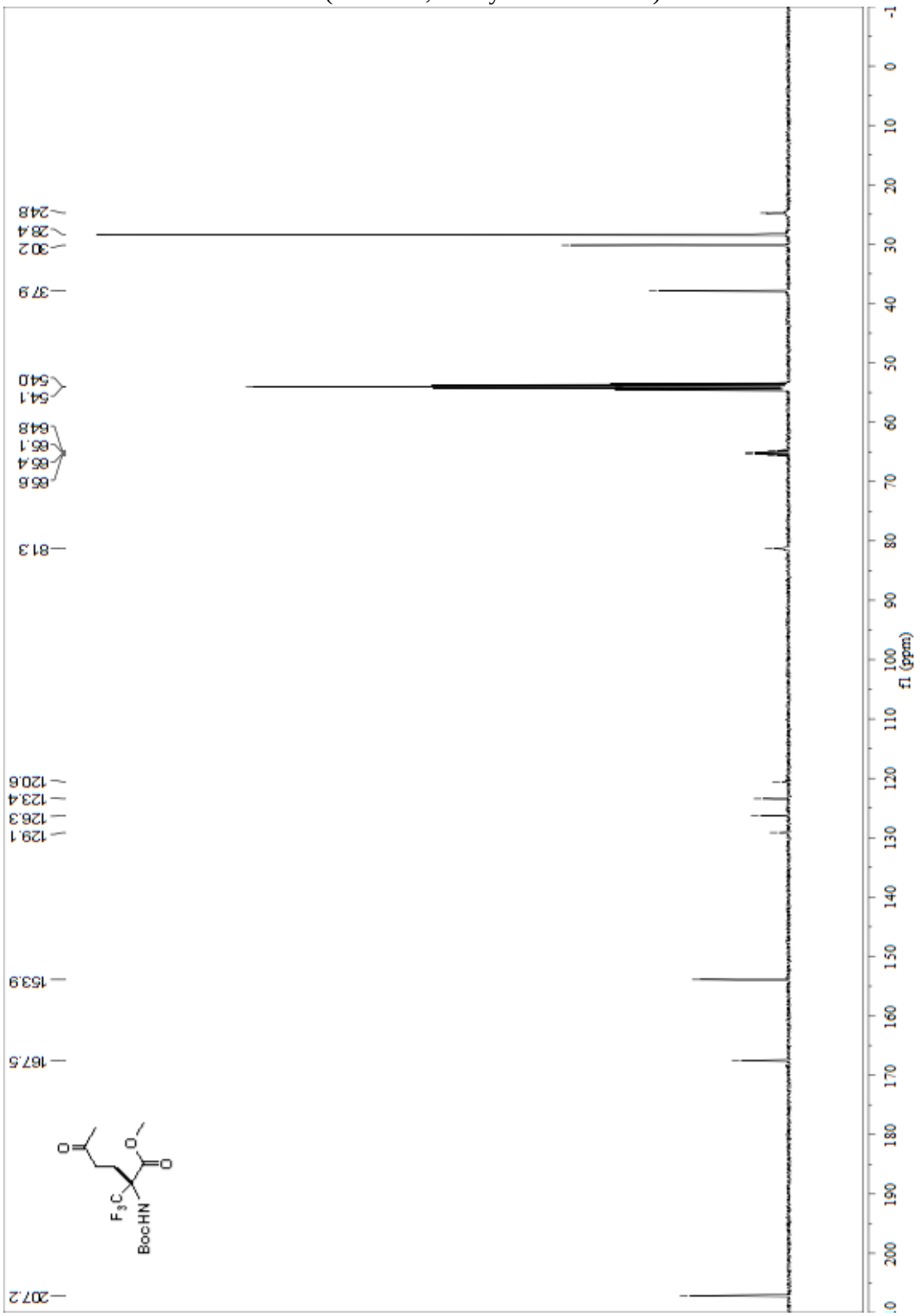

^{1}H NMR (400 MHz, Chloroform-*d*) **5b**

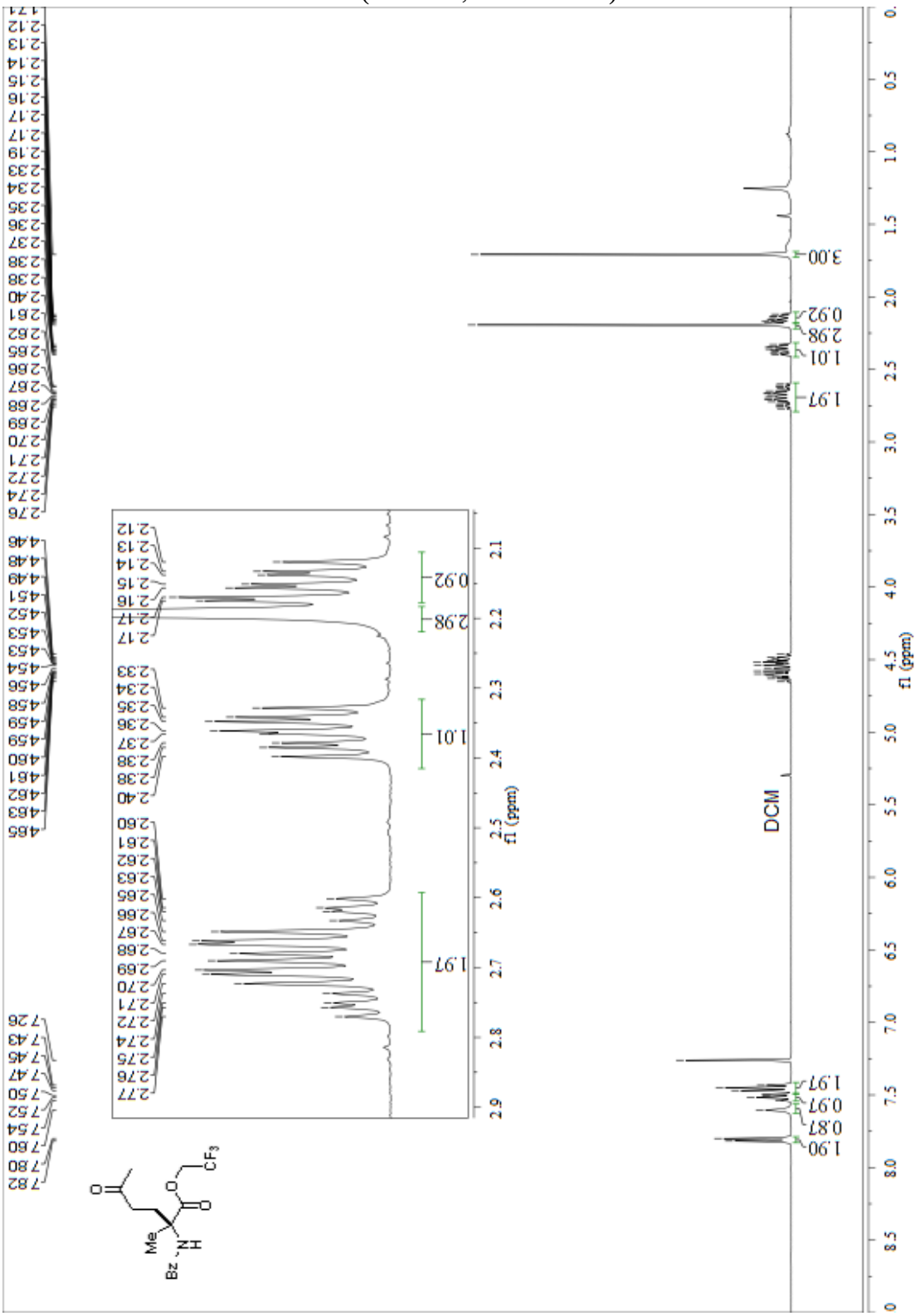

^{19}F NMR (376 MHz, Chloroform-*d*) **5b**

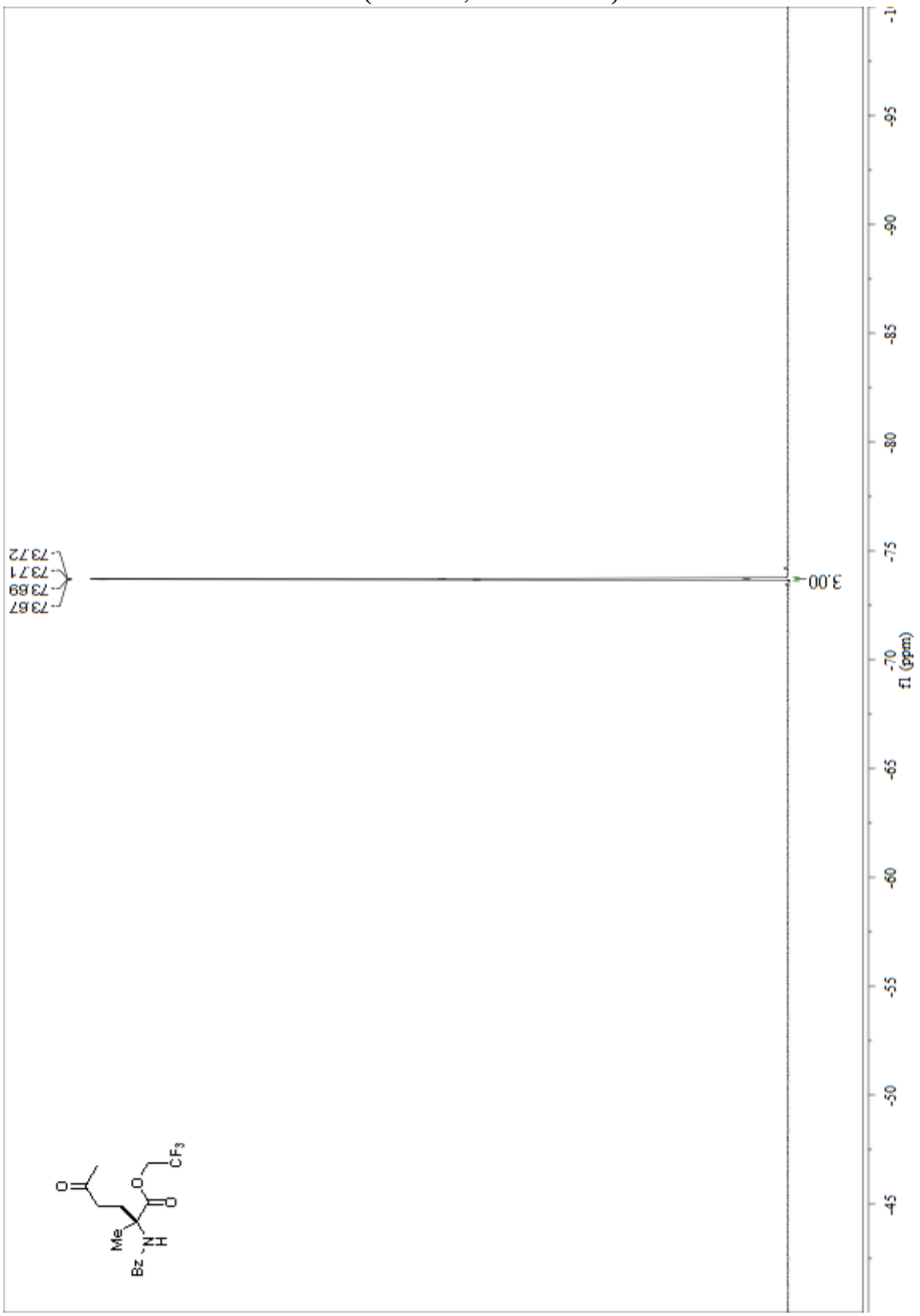

^{13}C NMR (101 MHz, Chloroform-*d*) **5b**

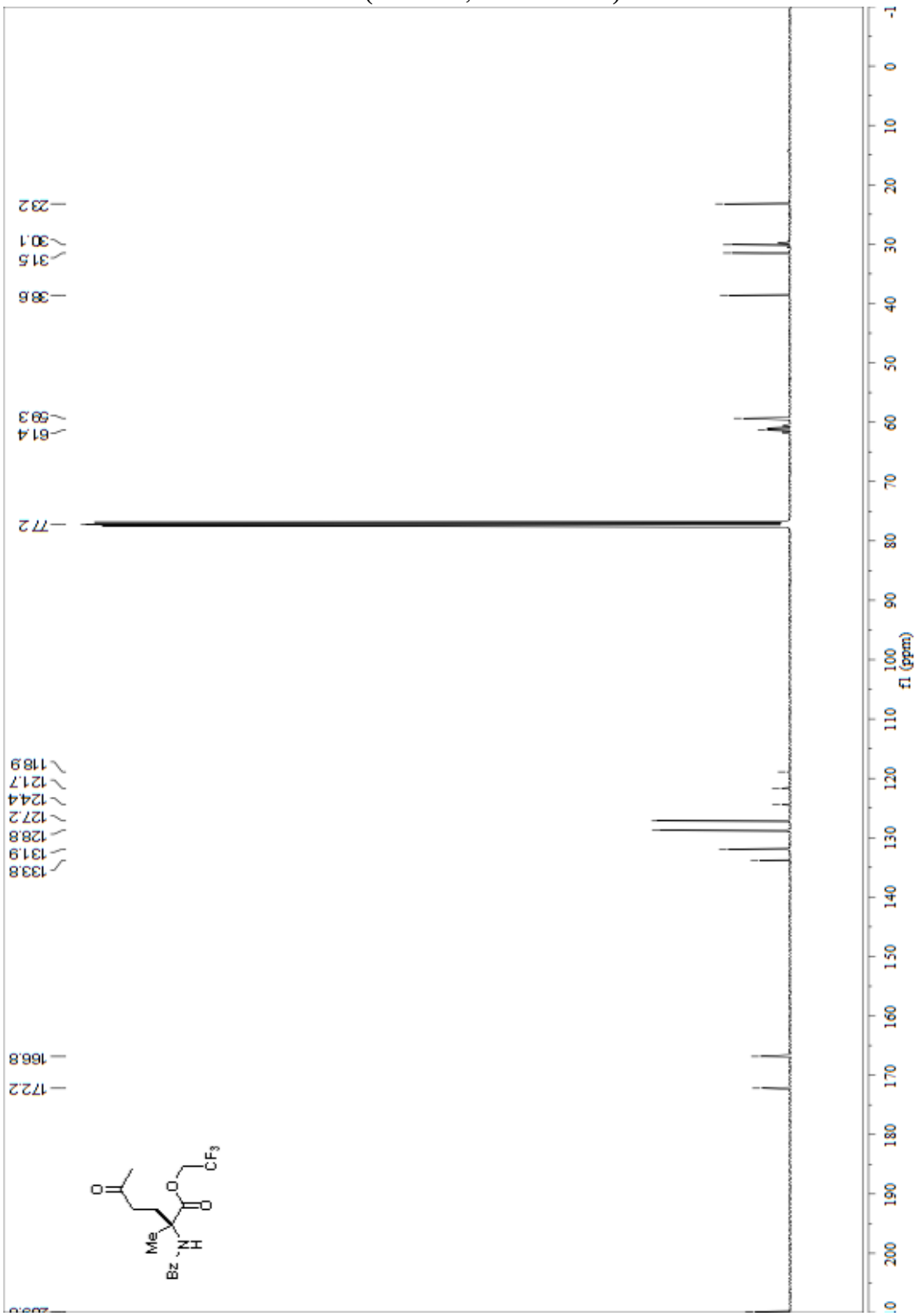

[1]H NMR (400 MHz, Methylene Chloride -*d*) **5c**

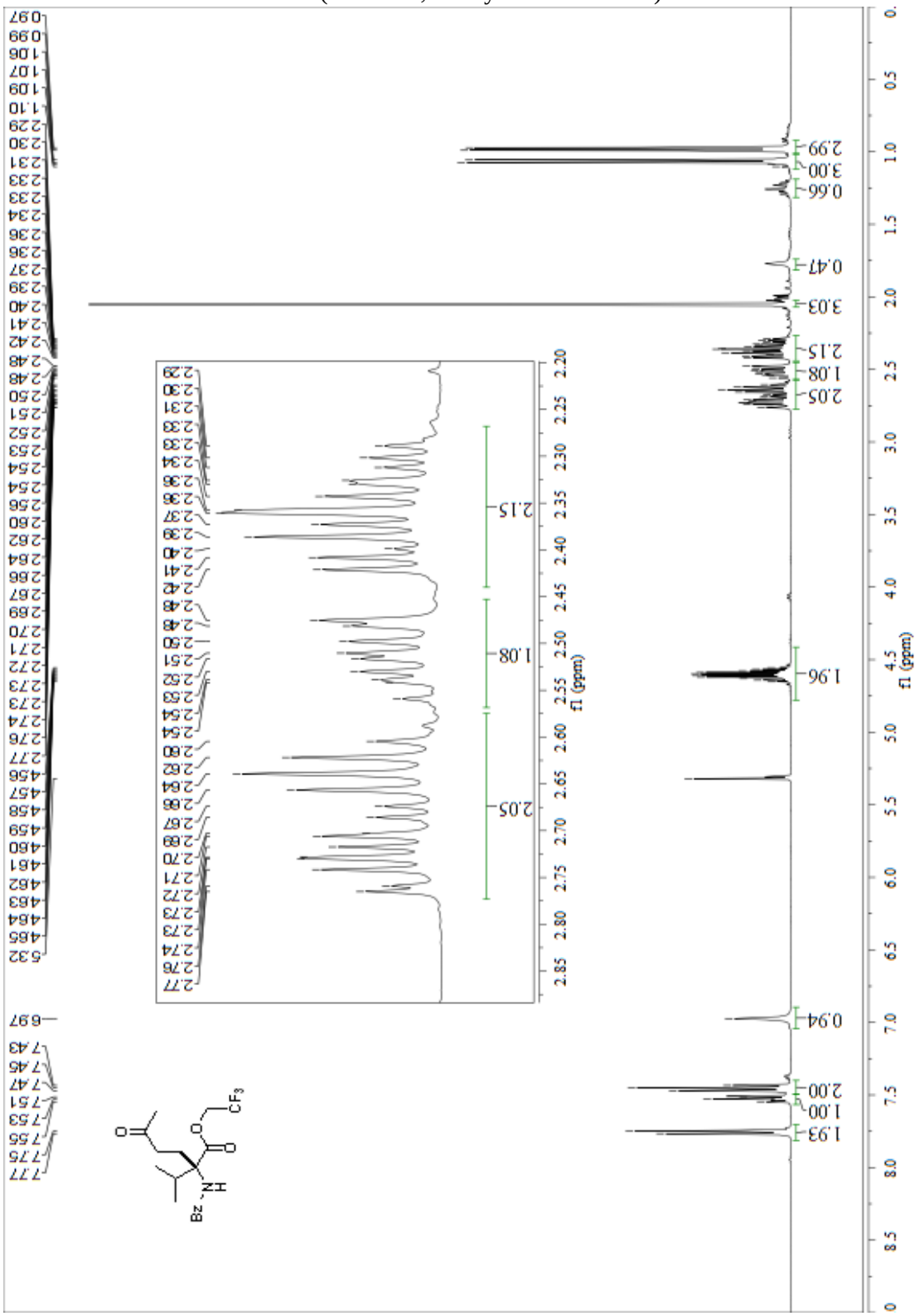

^{19}F NMR (376 MHz, Methylene Chloride -*d*) **5c**

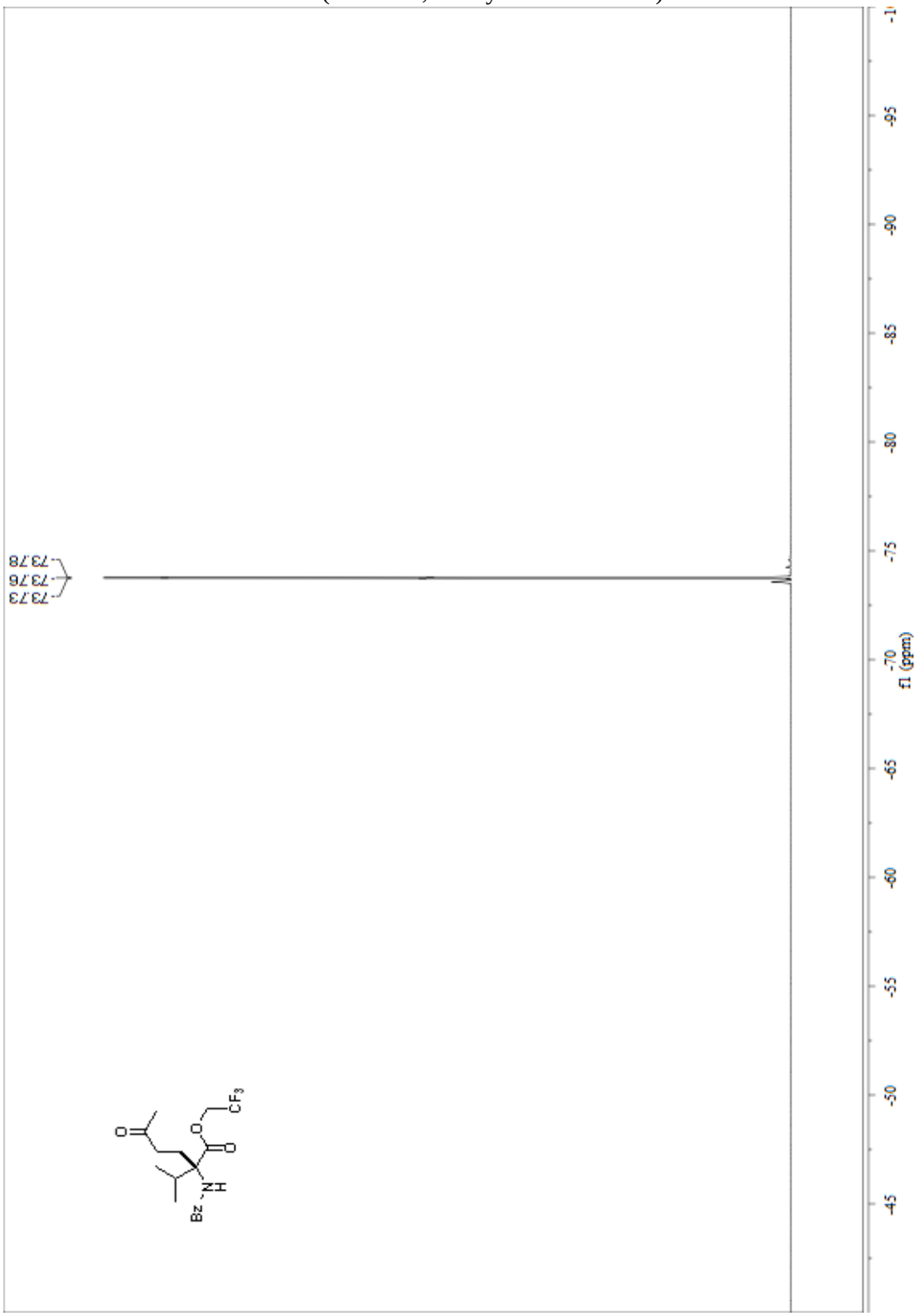

^{13}C NMR (101 MHz, Methylene Chloride -*d*) **5c**

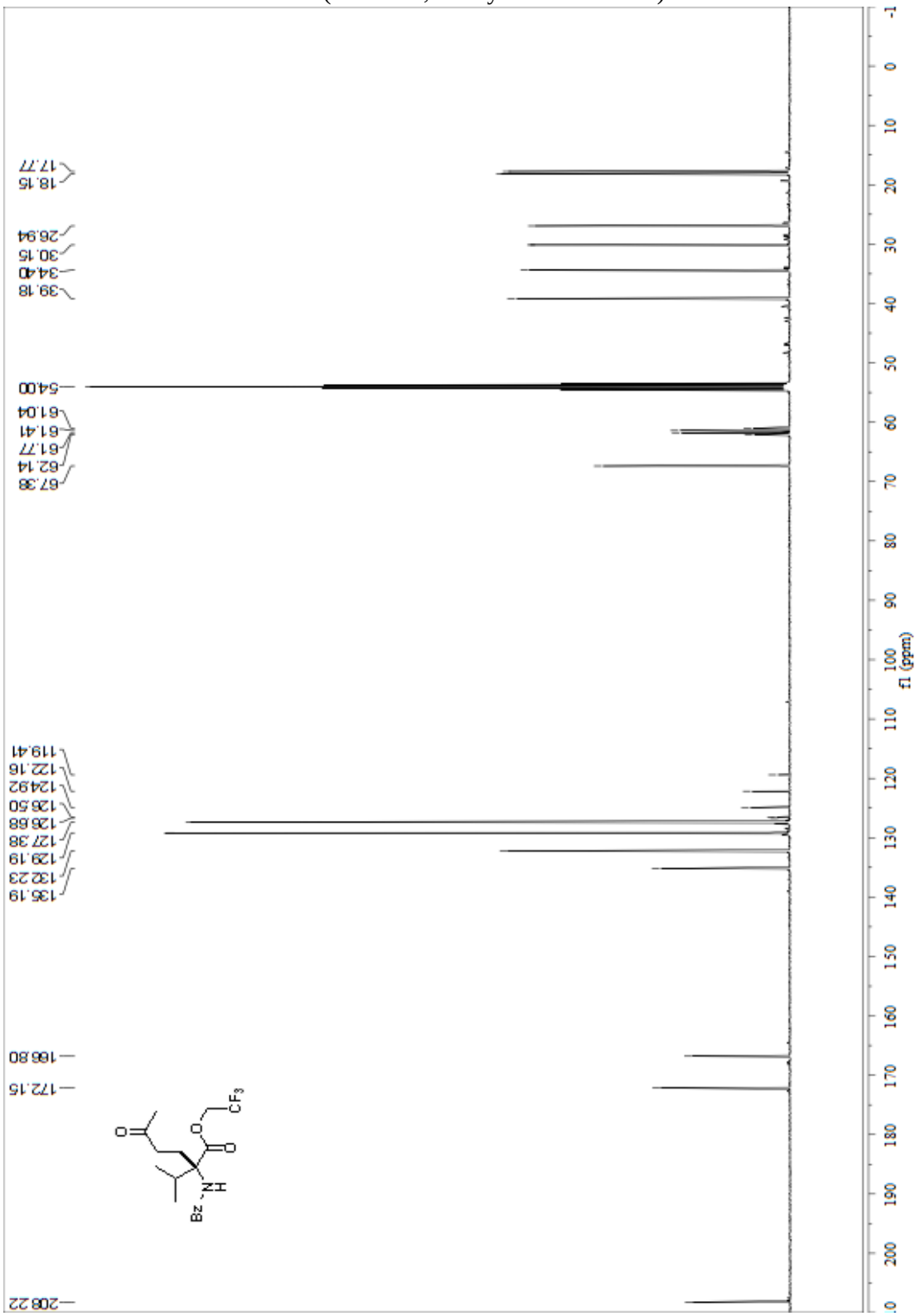

^{1}H NMR (400 MHz, Chloroform-*d*) **5d**

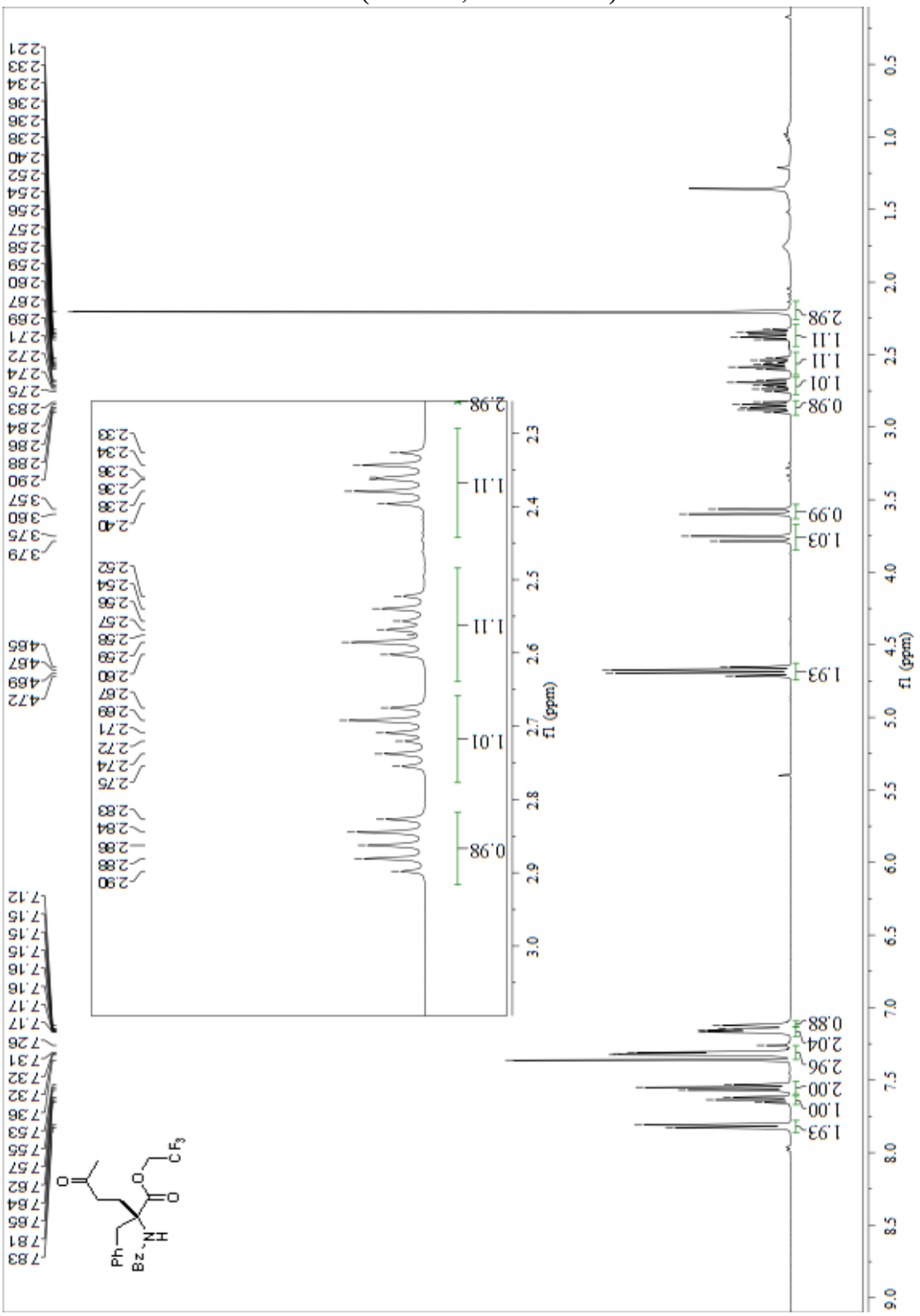

^{19}F NMR (376 MHz, Chloroform-*d*) **5d**

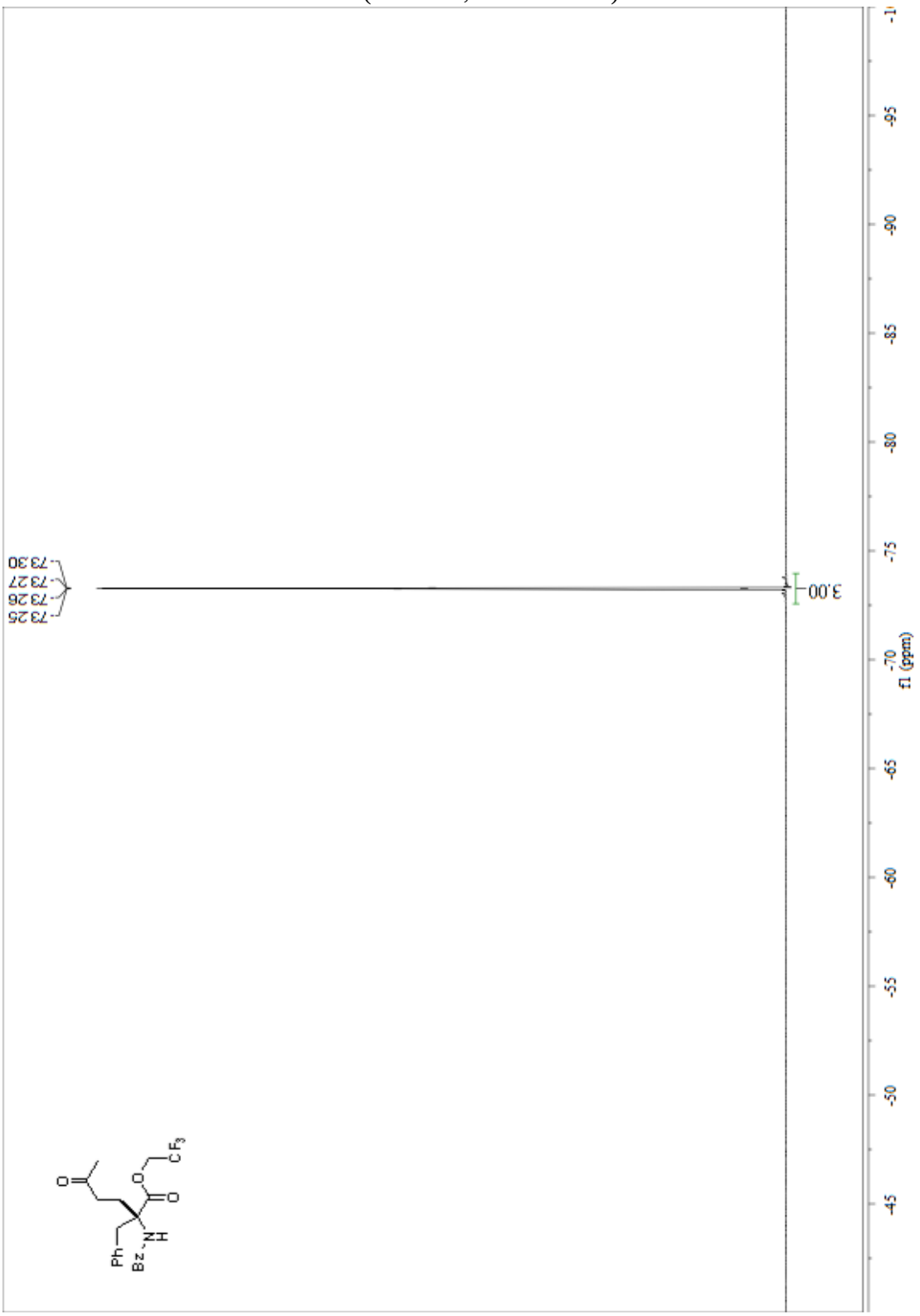

^{13}C NMR (101 MHz, Chloroform-*d*) **5d**

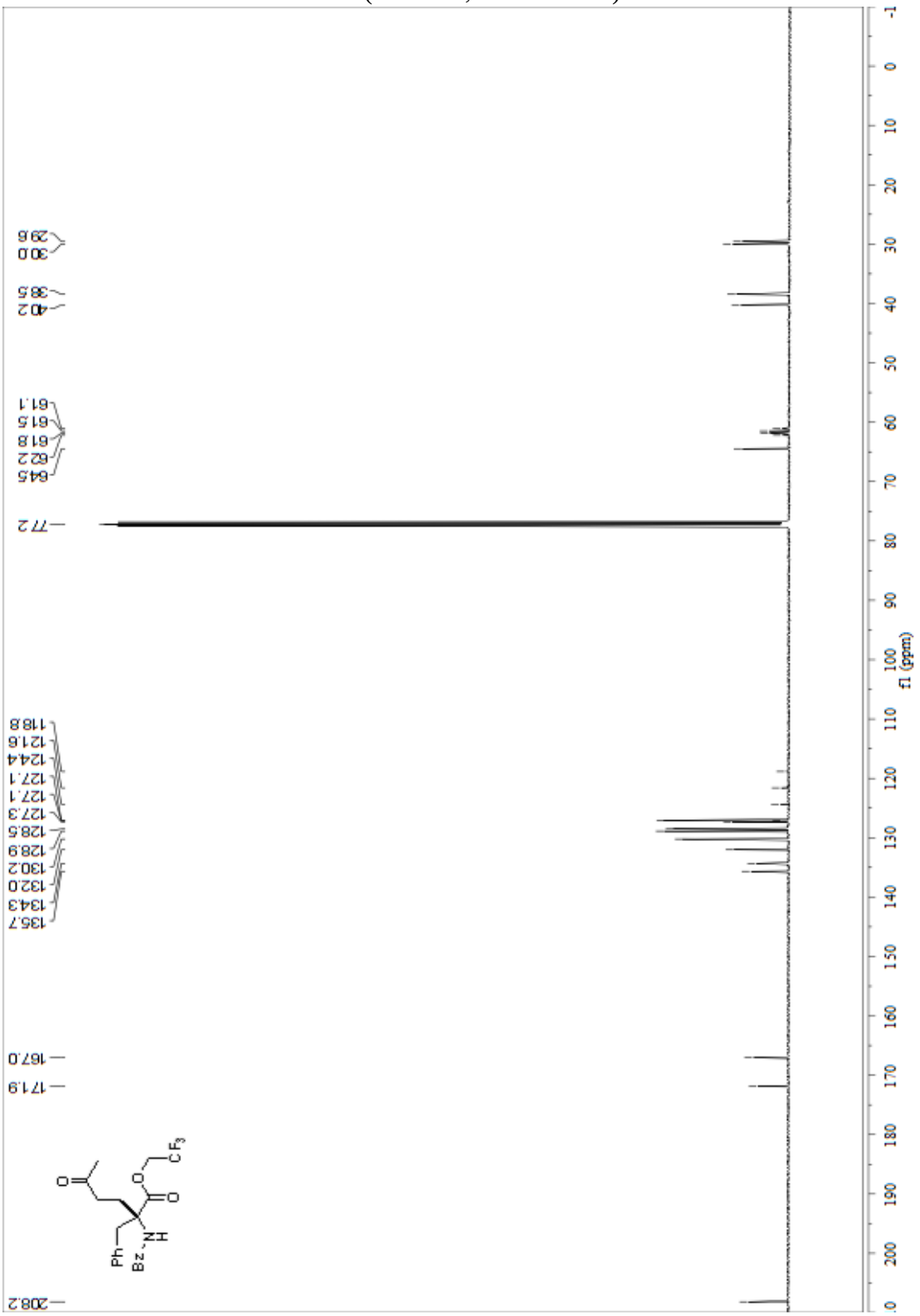

^{1}H NMR (400 MHz, Methylene Chloride-*d*) **5e**

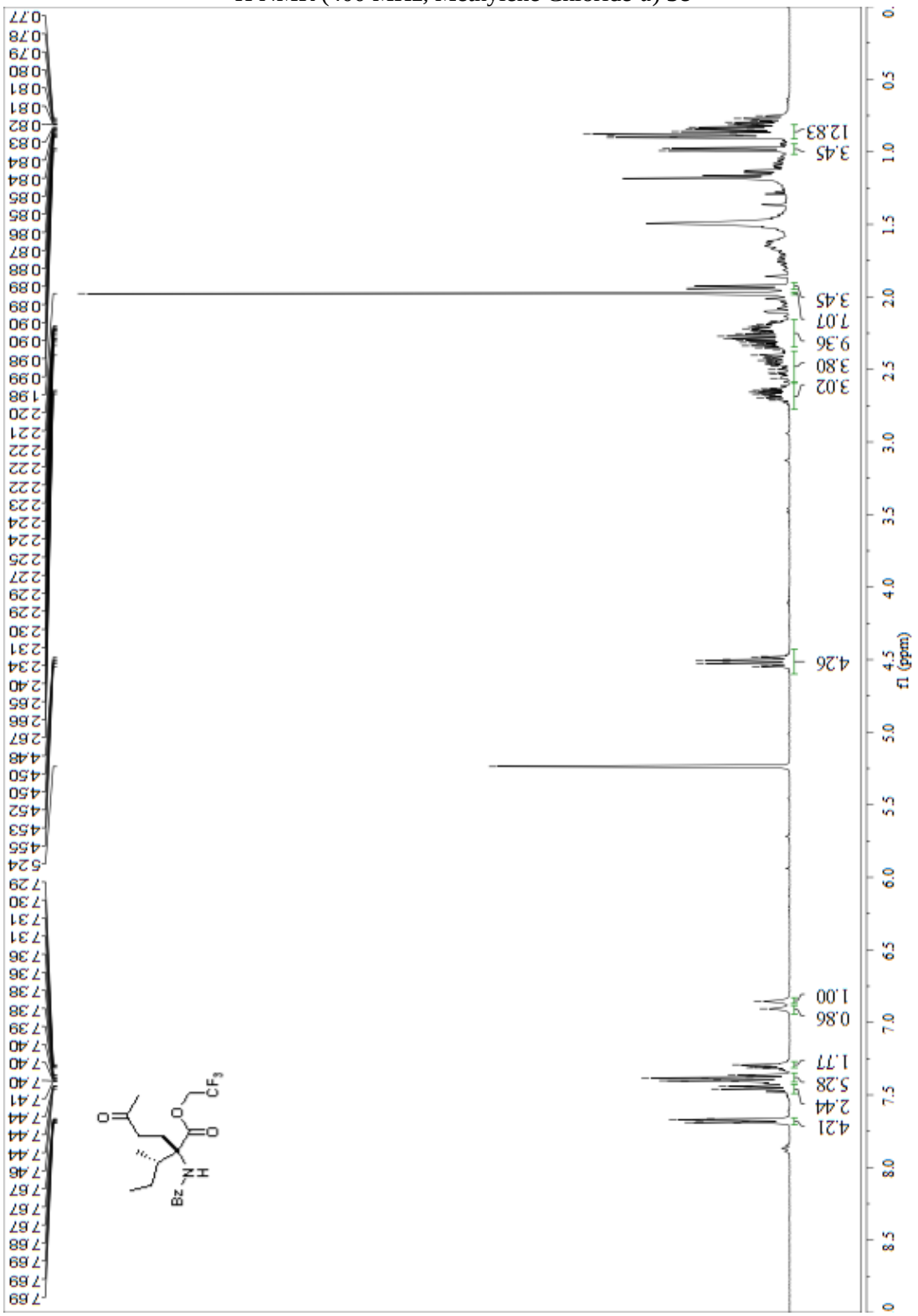

^{19}F NMR (376 MHz, Methylene Chloride -*d*) **5e**

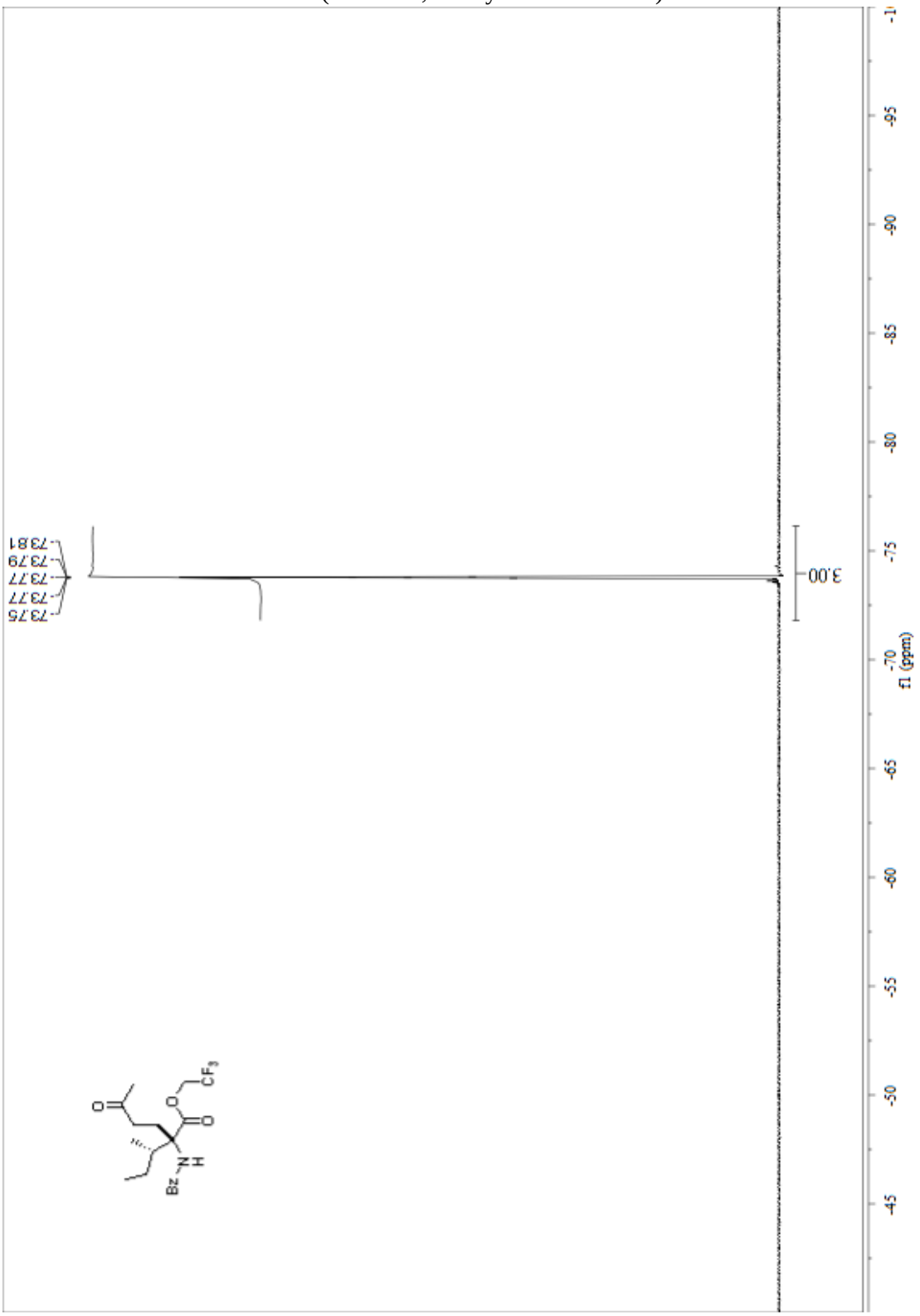

^{13}C NMR (101 MHz Methylene Chloride-*d*) **5e**

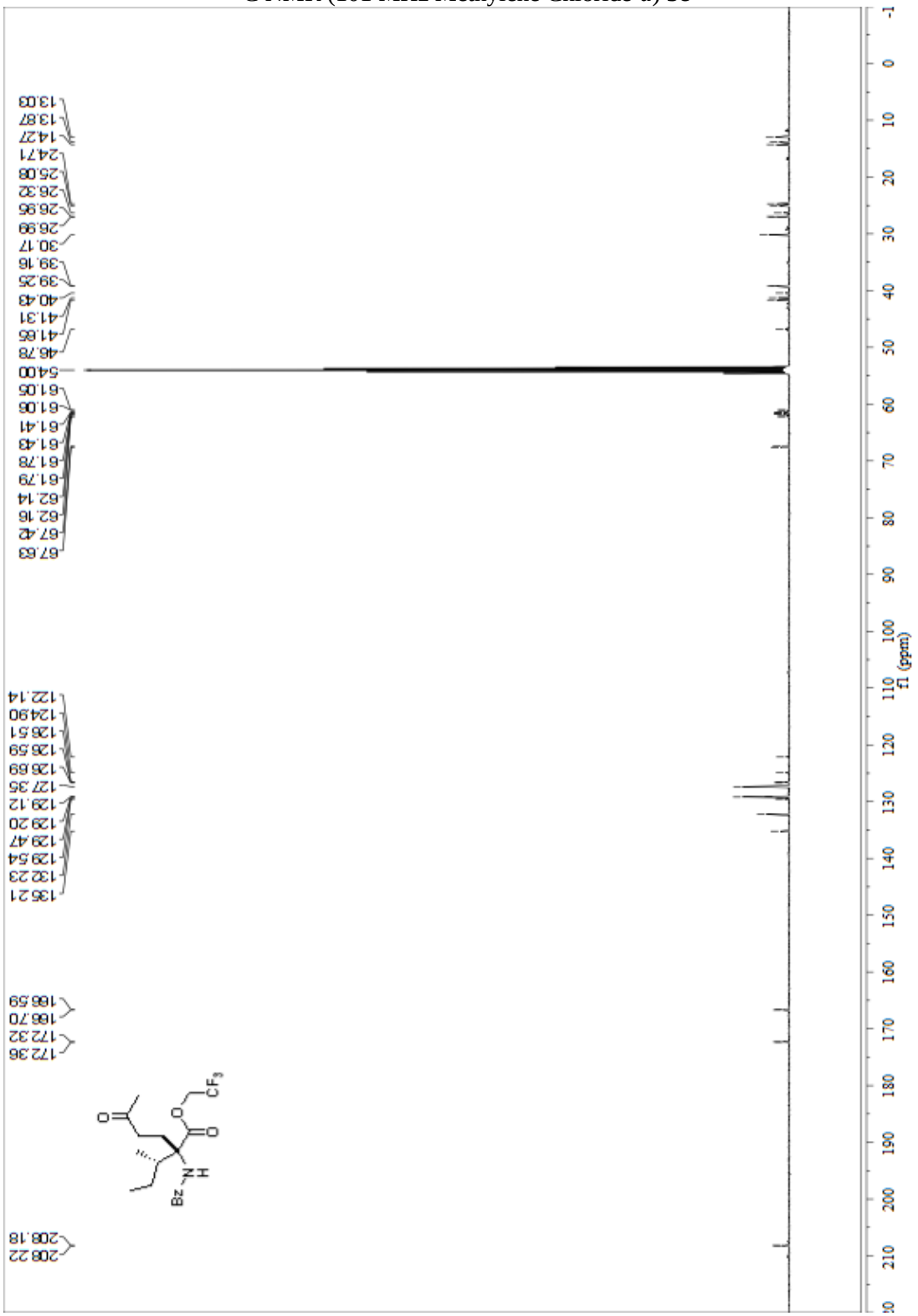

[1]H NMR (400 MHz, Methylene Chloride-*d*) **5f**

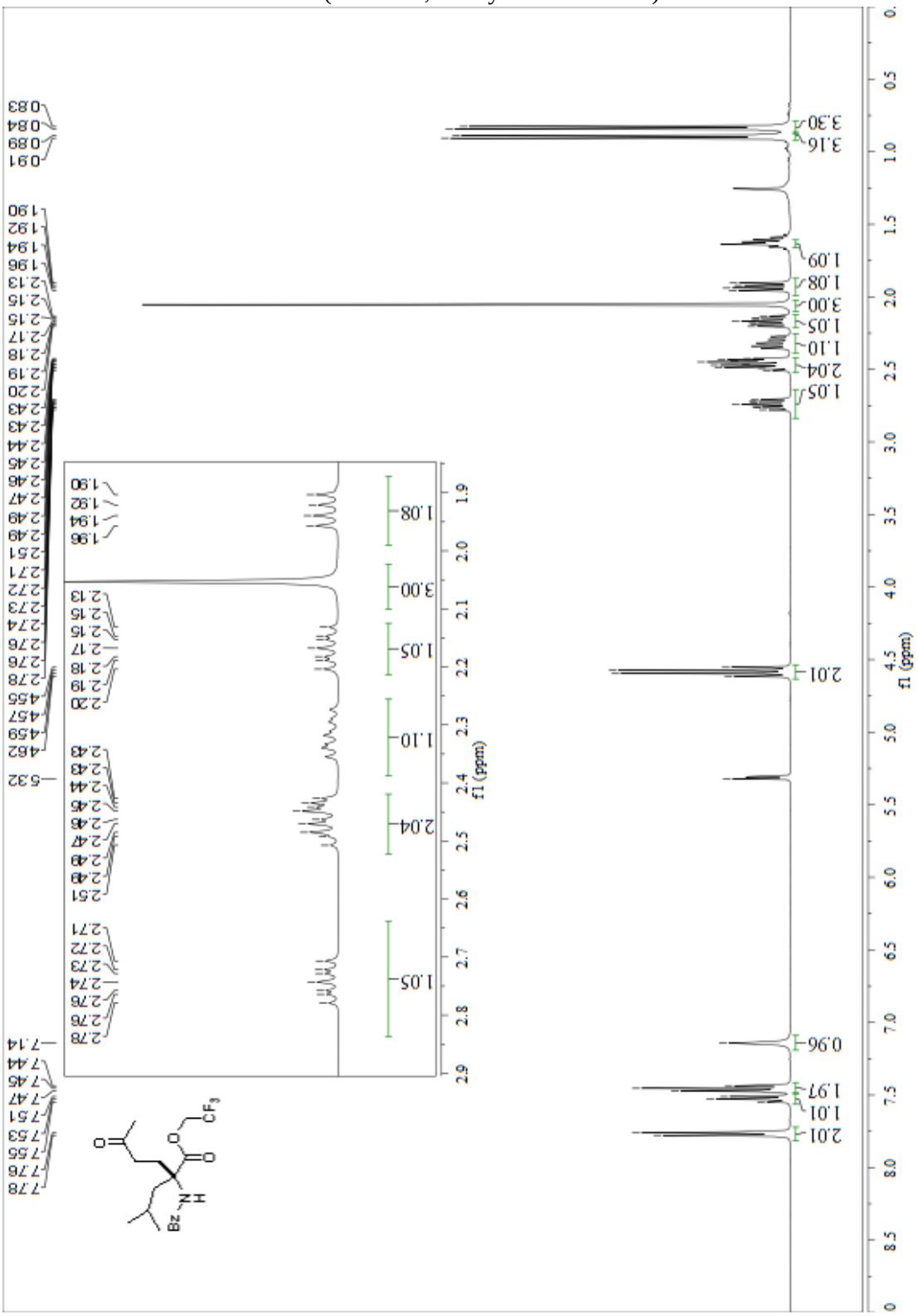

^{19}F NMR (376 MHz, Methylene Chloride-*d*) **5f**

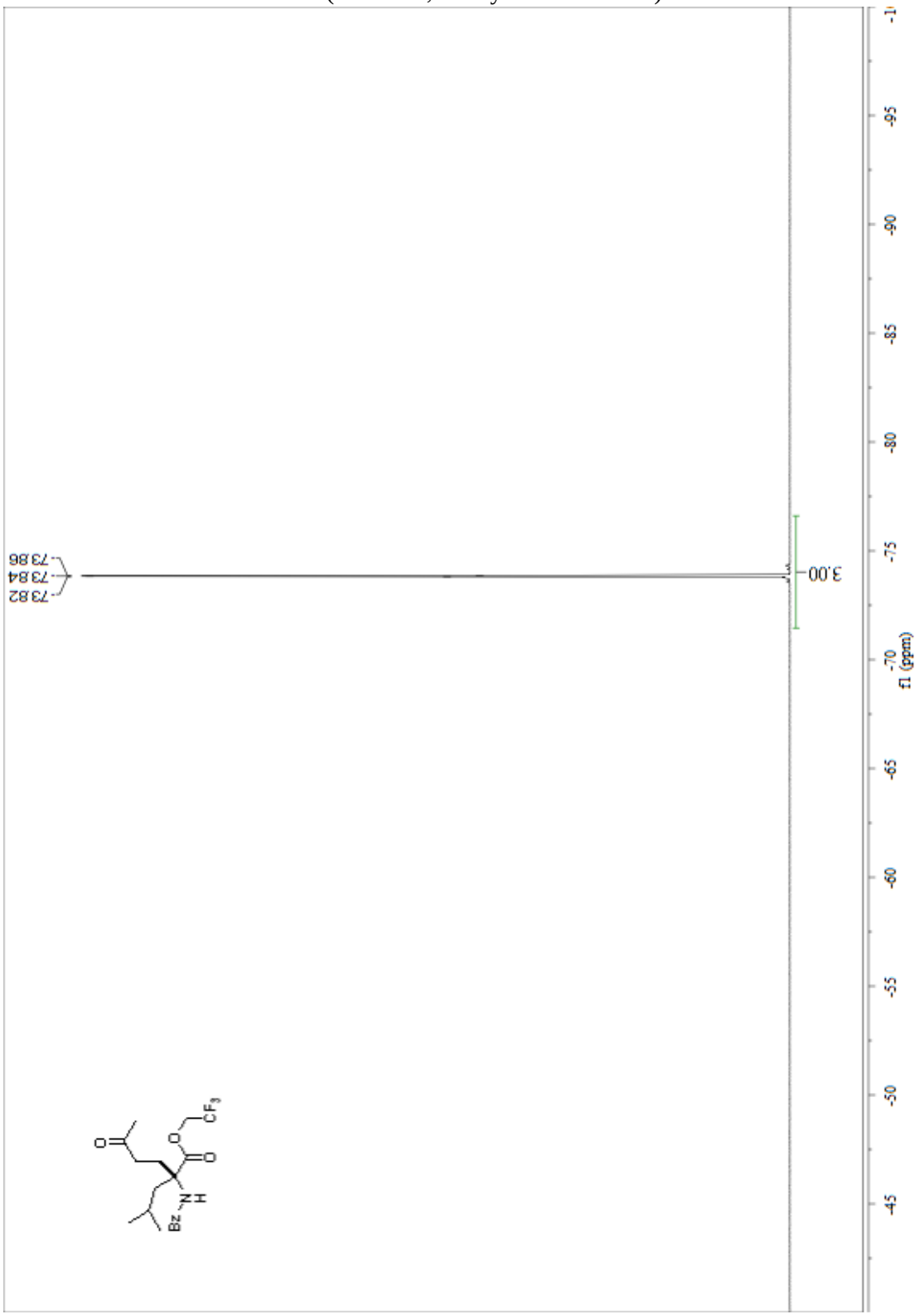

^{13}C NMR (101 MHz, Methylene Chloride-*d*) **5f**

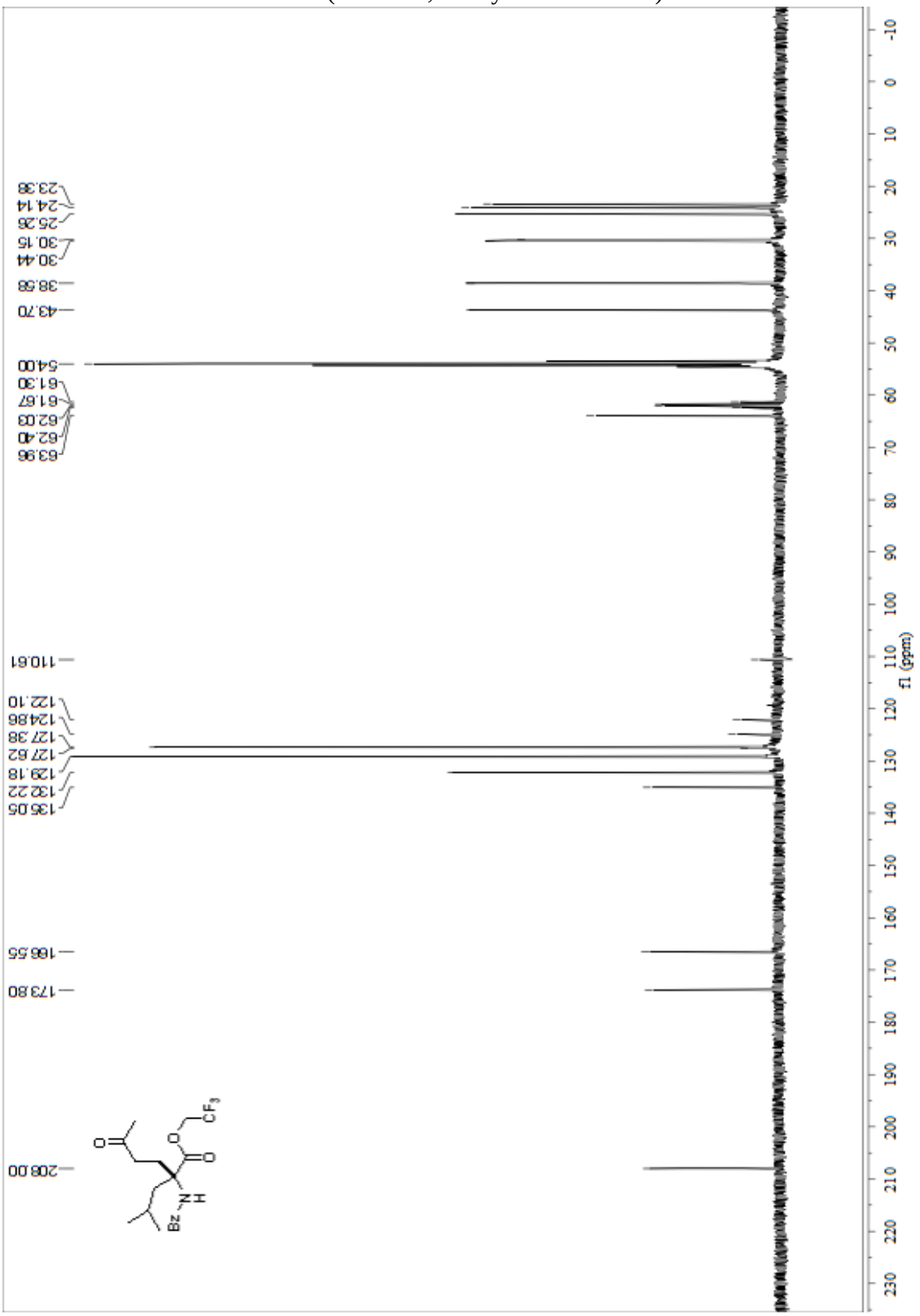

[1]H NMR (400 MHz, Methylene Chloride-*d*) **5g**

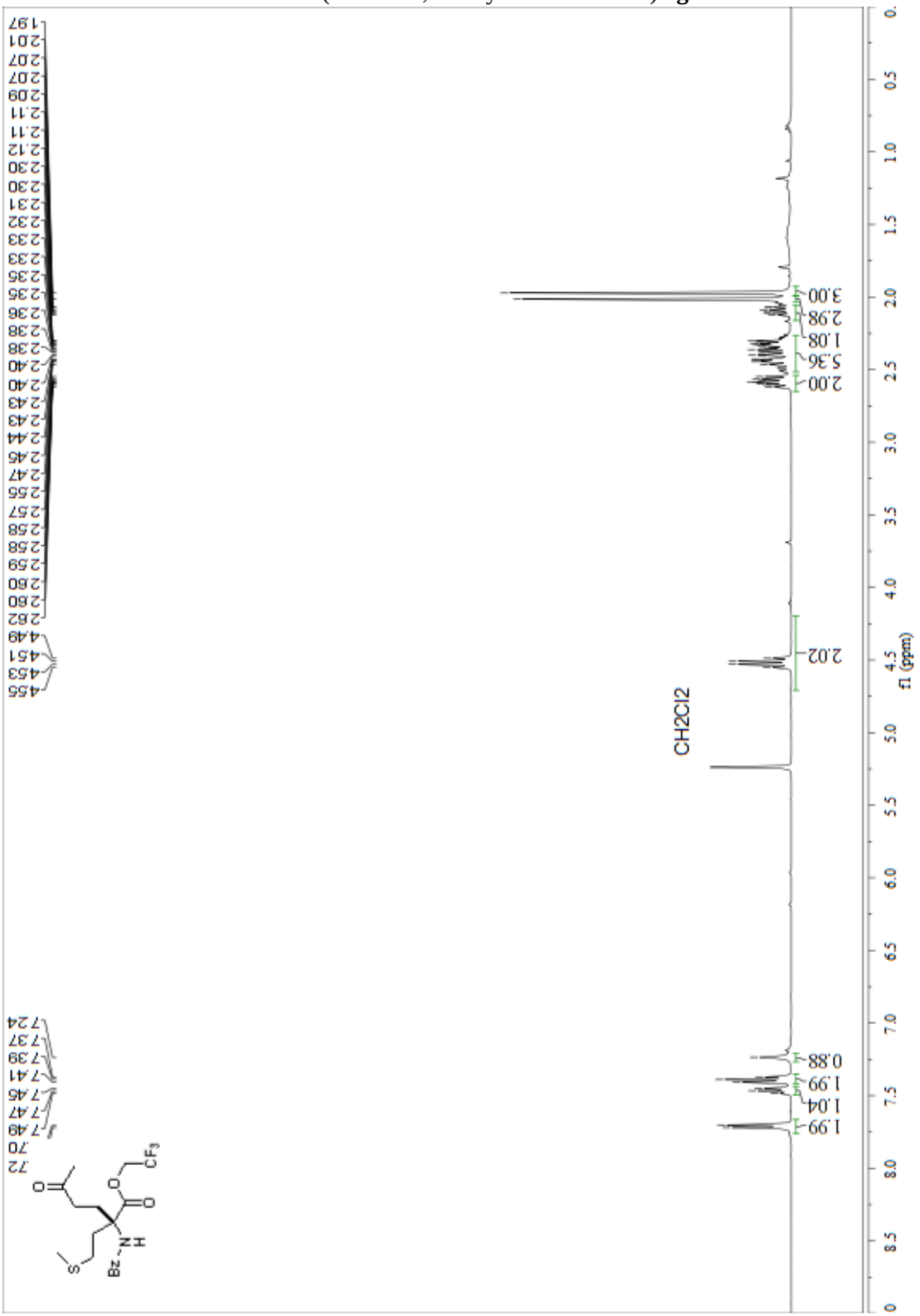

^{19}F NMR (376 MHz, Methylene Chloride-*d*) **5g**

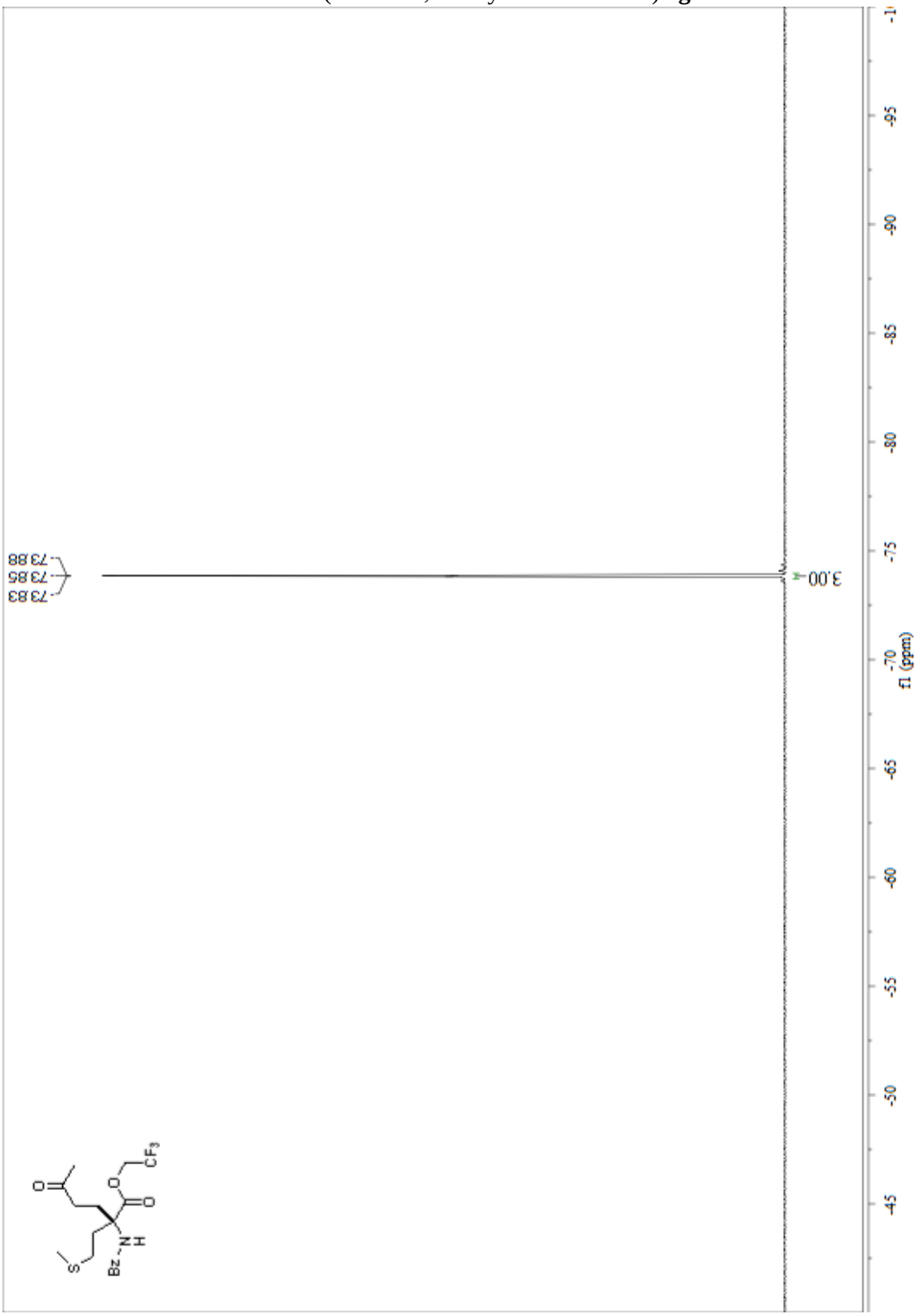

^{13}C NMR (101 MHz, Chloroform-*d*) **5g**

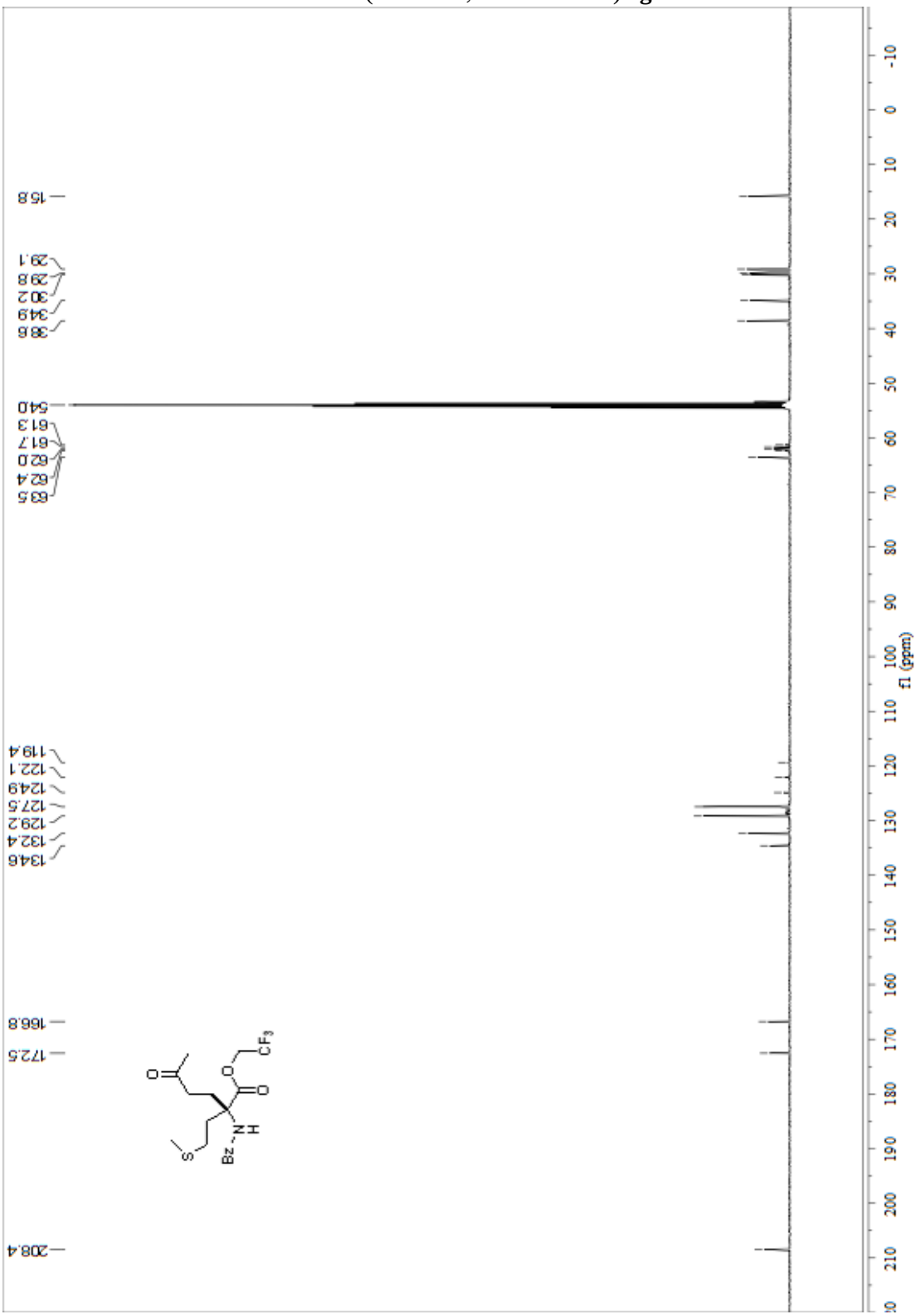

^{1}H NMR (400 MHz, Chloroform-*d*) **6a**

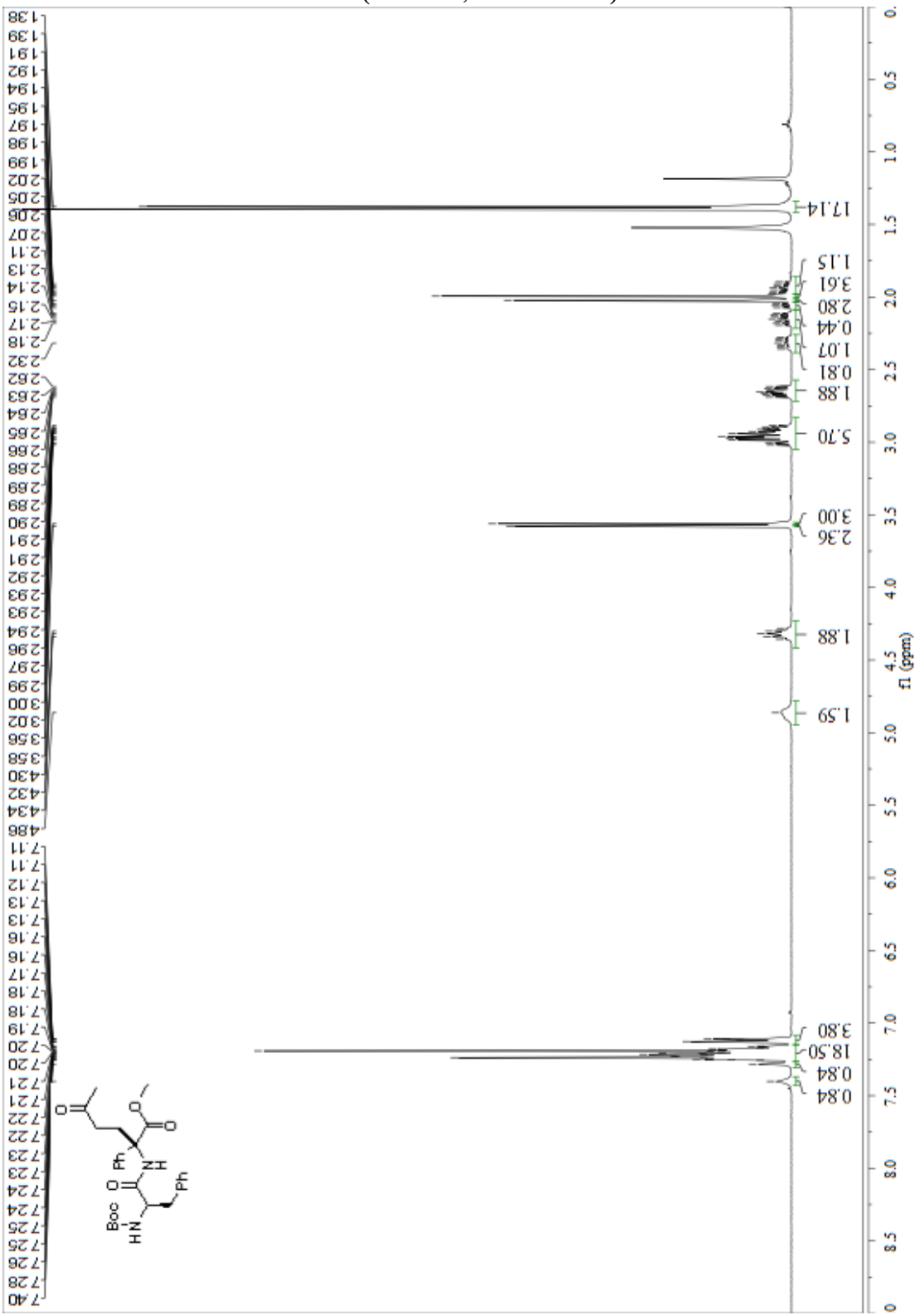

^{13}C NMR (101 MHz, Methylene Chloride -*d*) **6a**

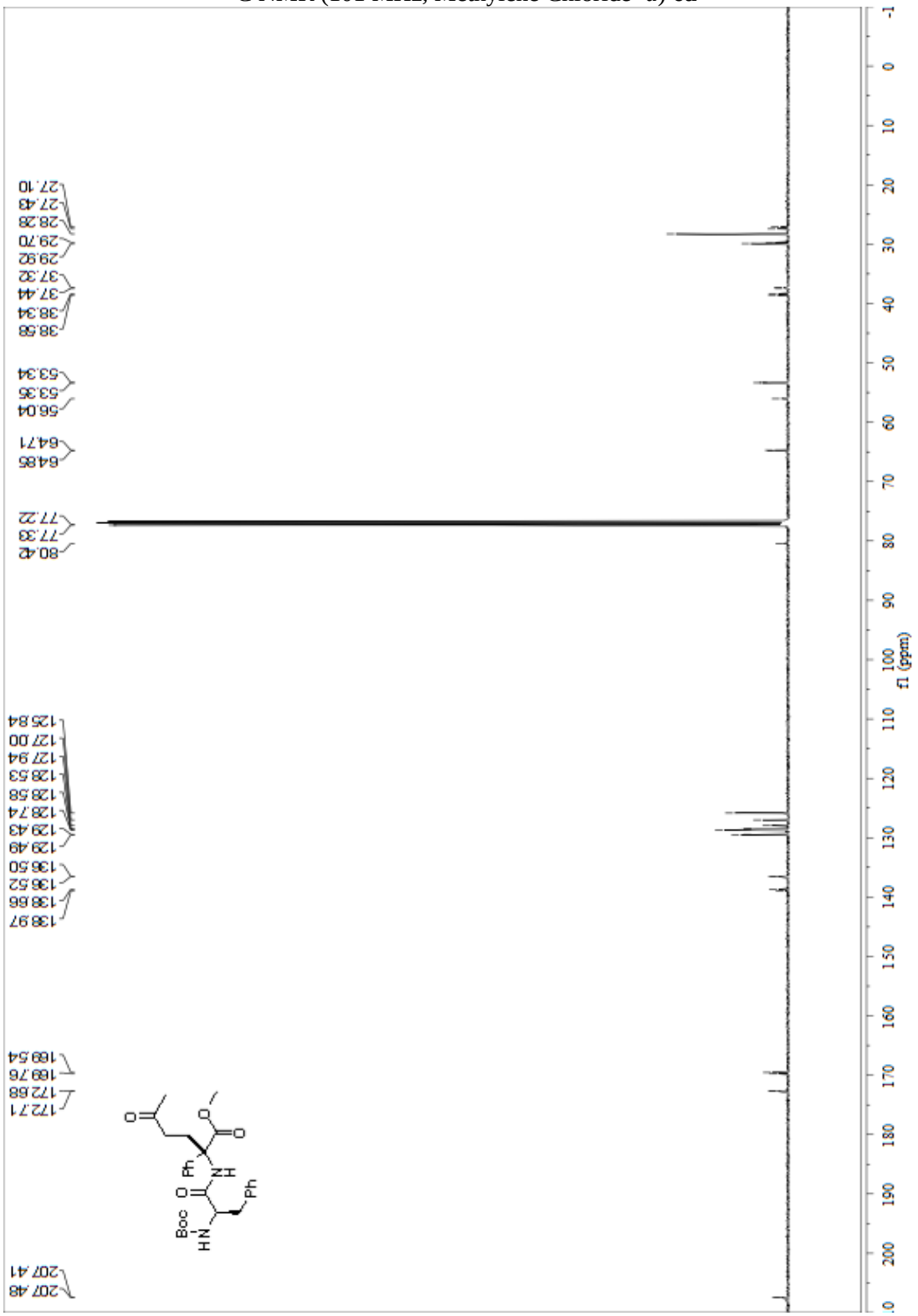

HSQC 2d NMR (400 MHz, Methylene Chloride-*d*) **6a**

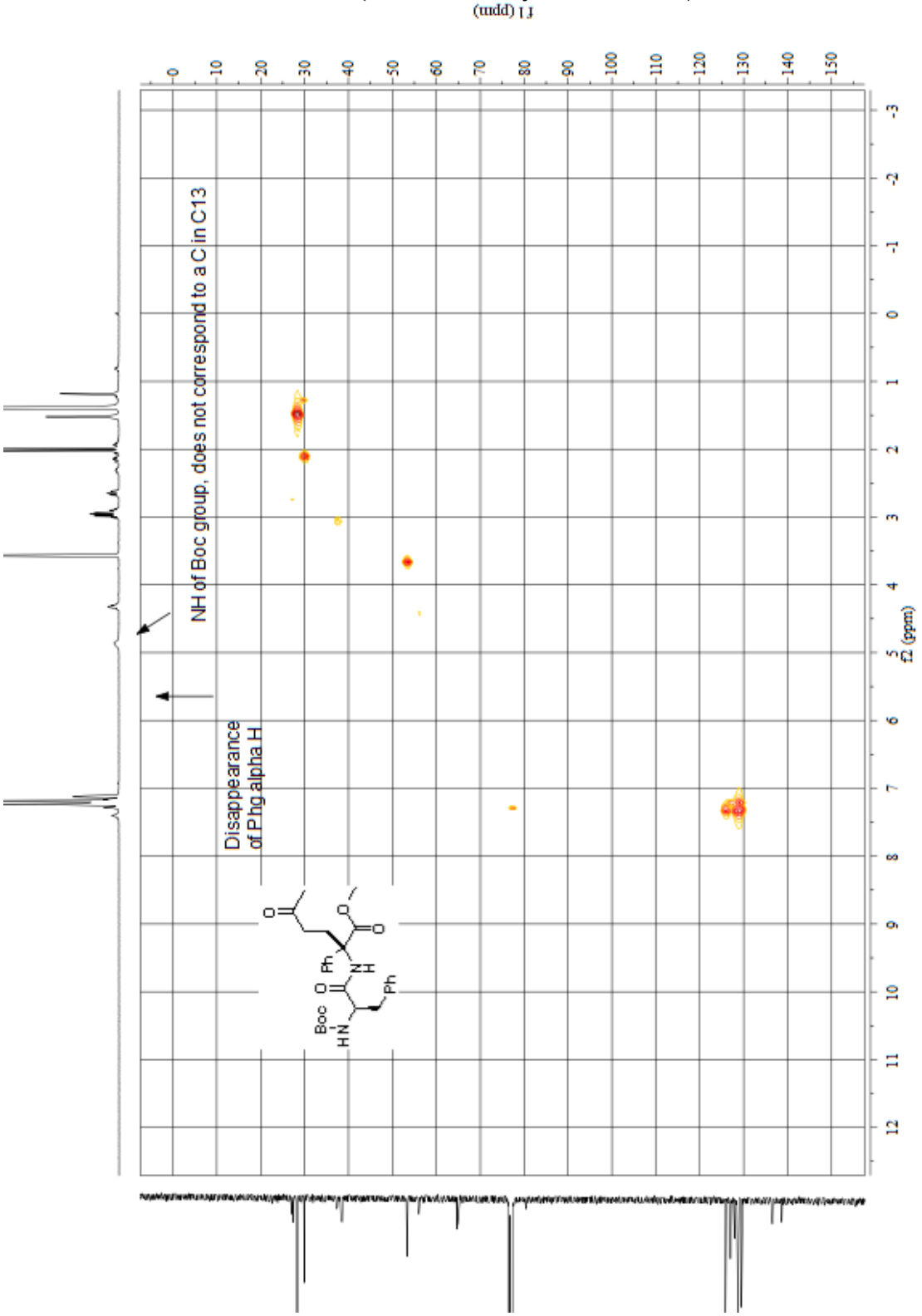

[1]H NMR (400 MHz, Methylene Chloride) **6b**

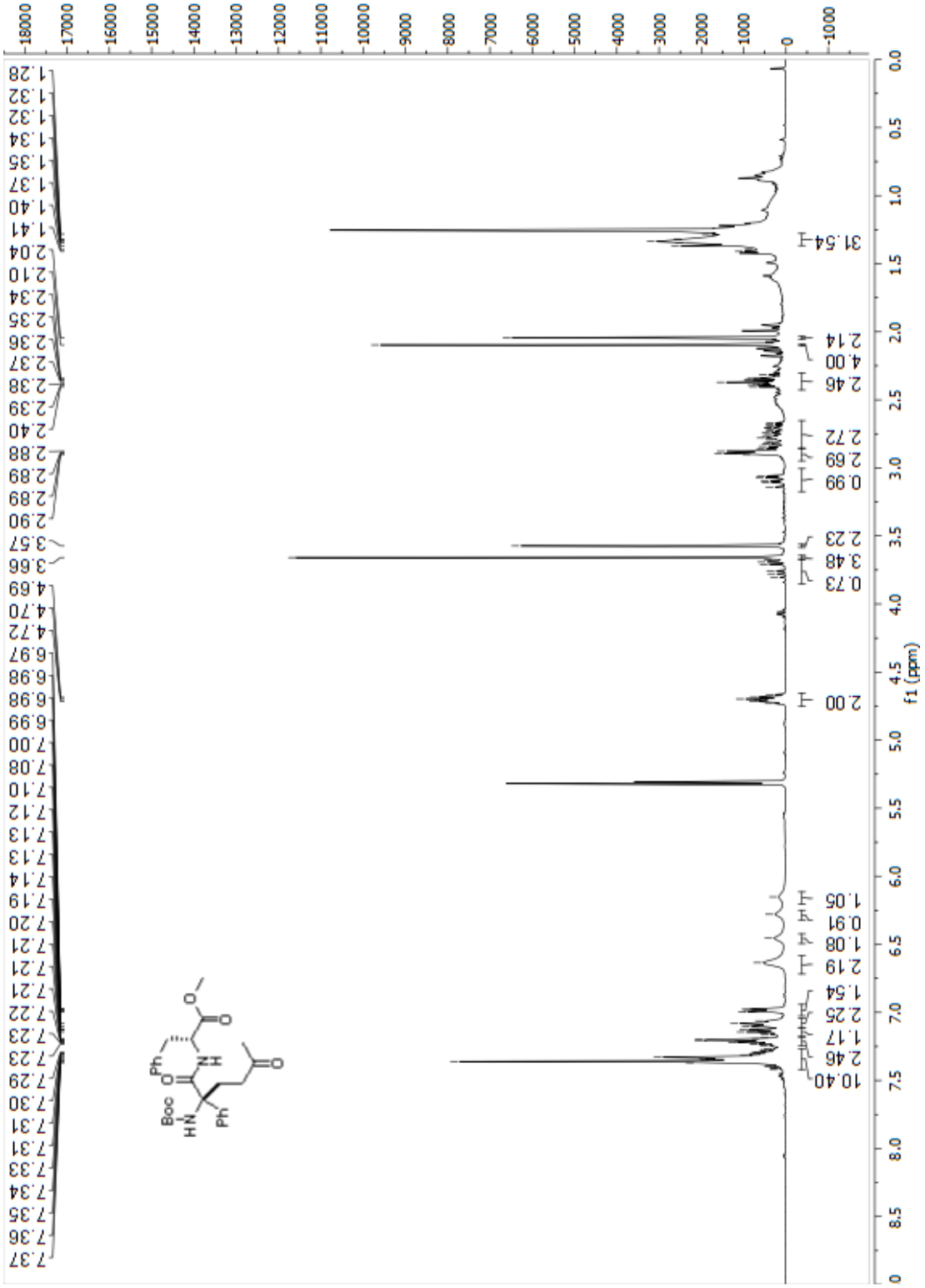

^{13}C NMR (101 MHz, Methylene Chloride -*d*) **6b**

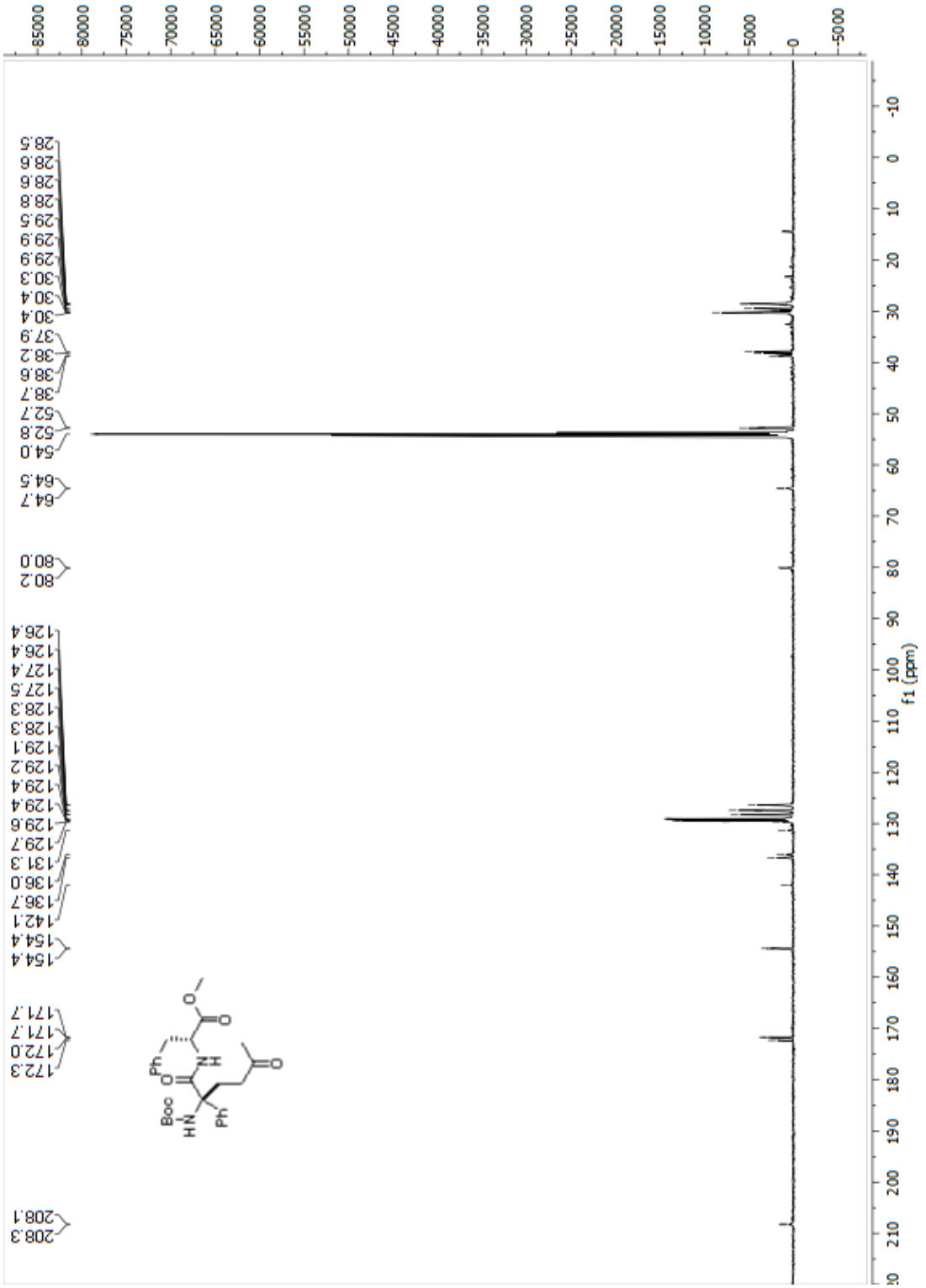

HSQC 2d NMR (400 MHz, Methylene Chloride-*d*) **6b**

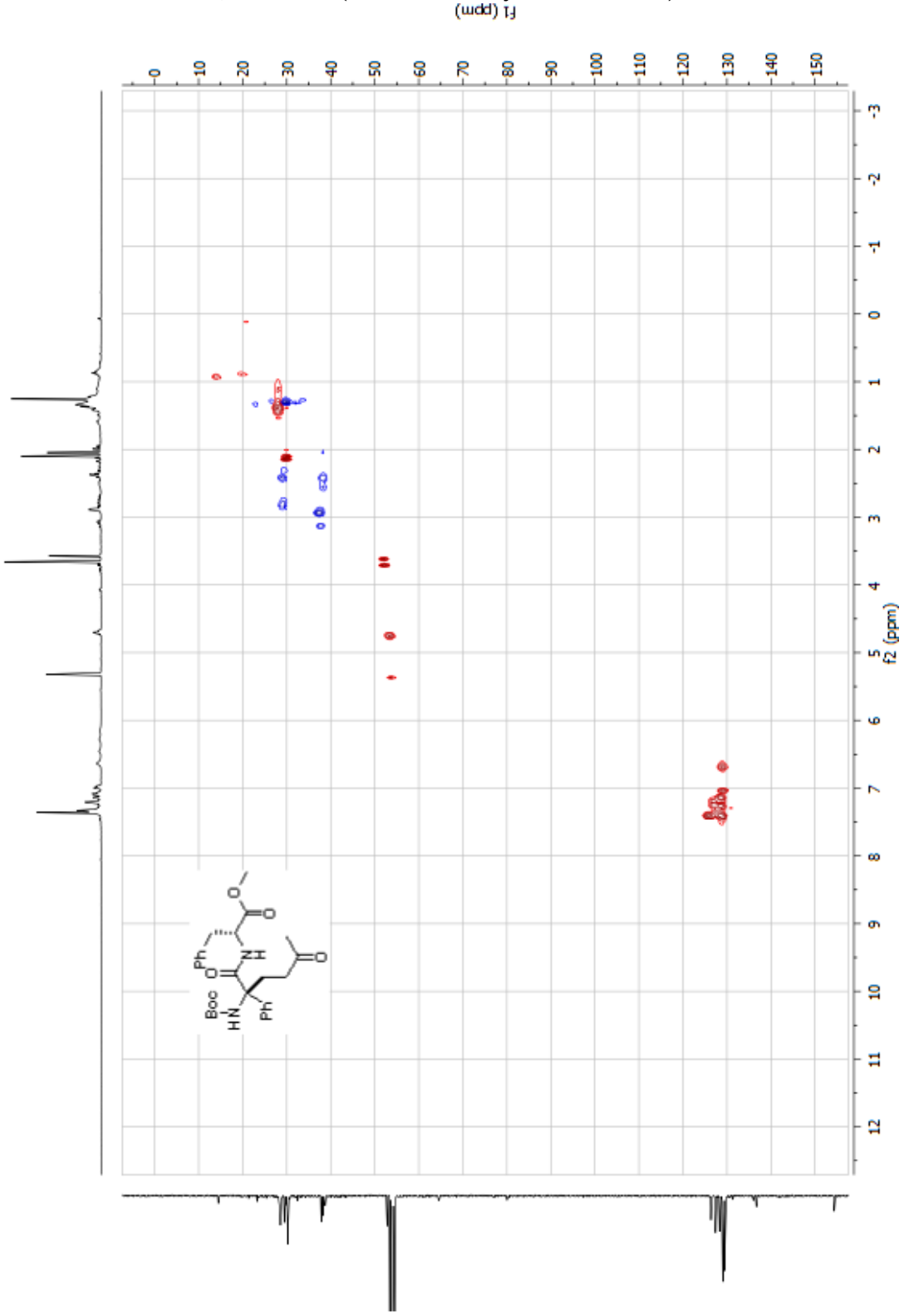

[1]H NMR (400 MHz, Methylene Chloride-*d*) **6c**

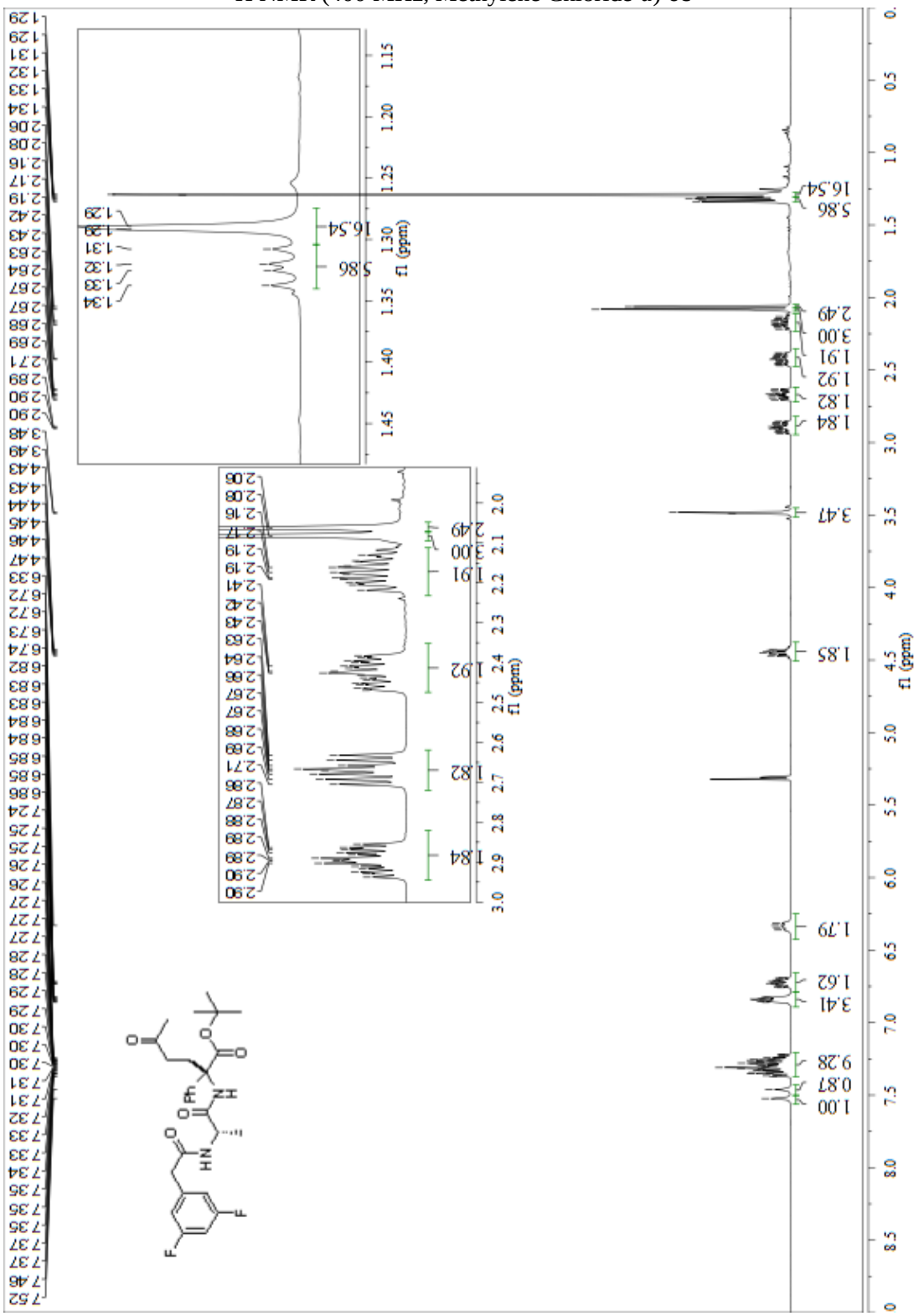

^{19}F NMR (376 MHz, Methylene Chloride-*d*) **6c**

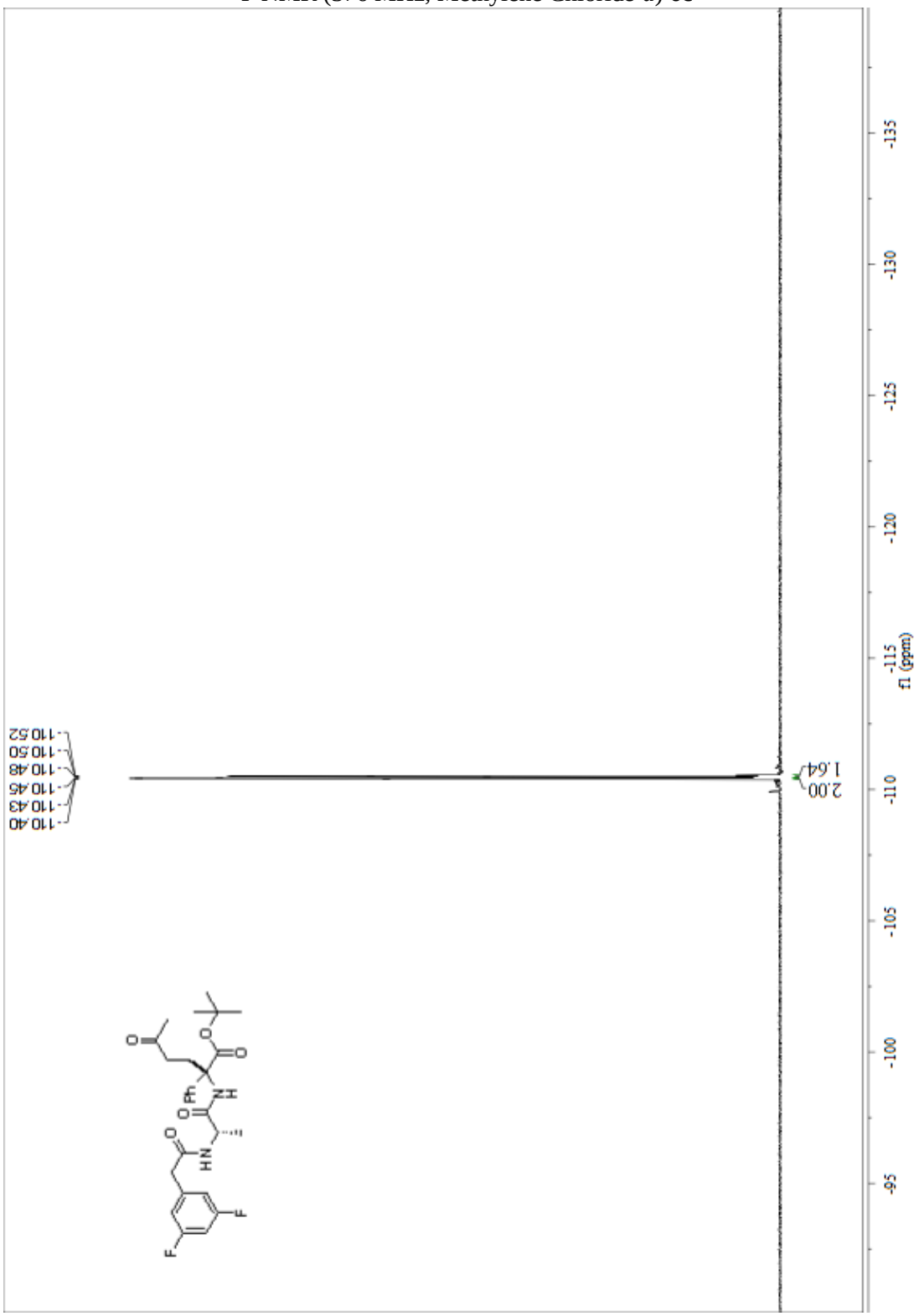

^{13}C NMR (101 MHz Methylene Chloride-*d*) **6c**

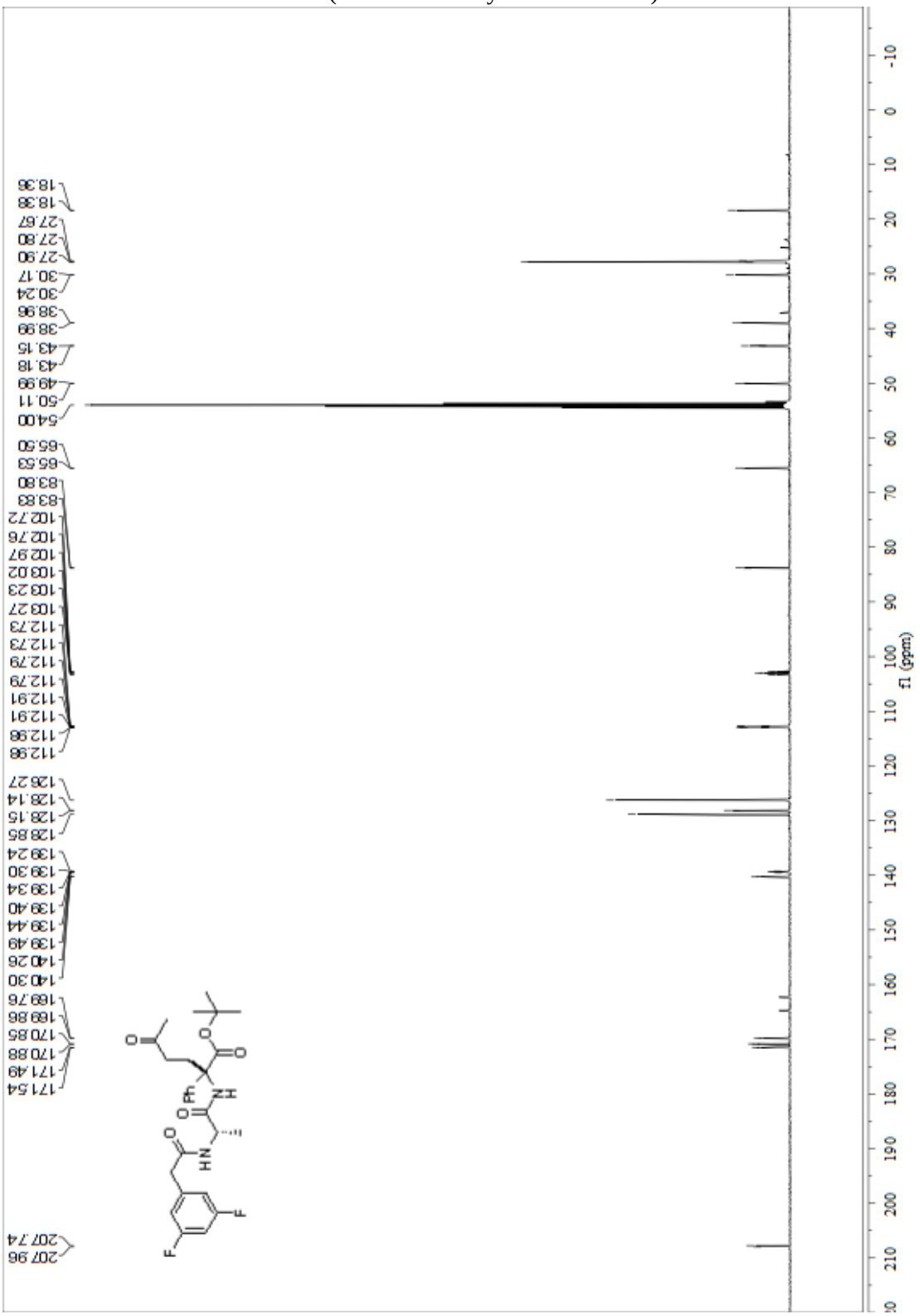

HSQC 2d NMR (400 MHz, Methylene Chloride-*d*) **6c**

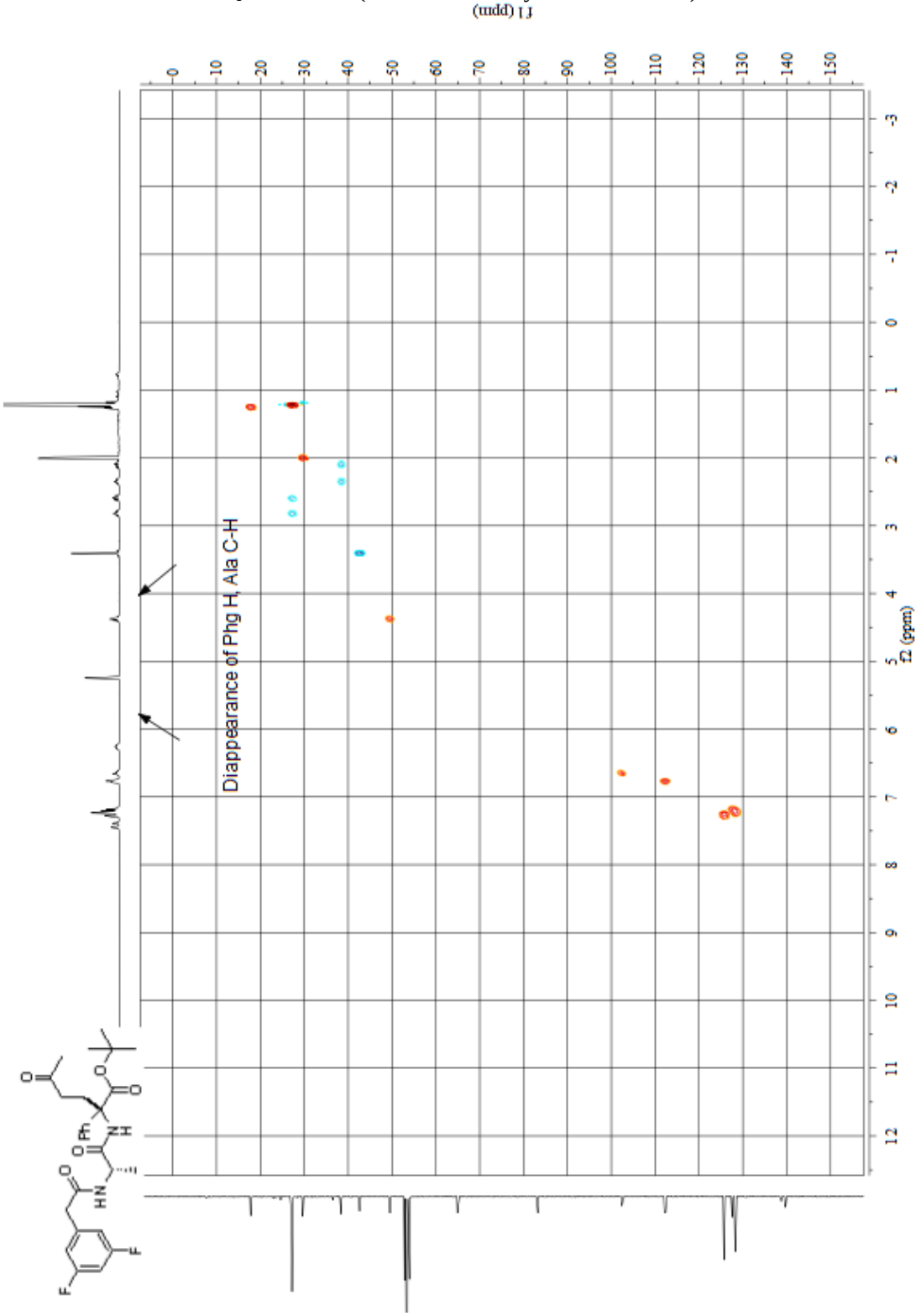

^{1}H NMR (400 MHz, Chloroform-*d*) **6a**

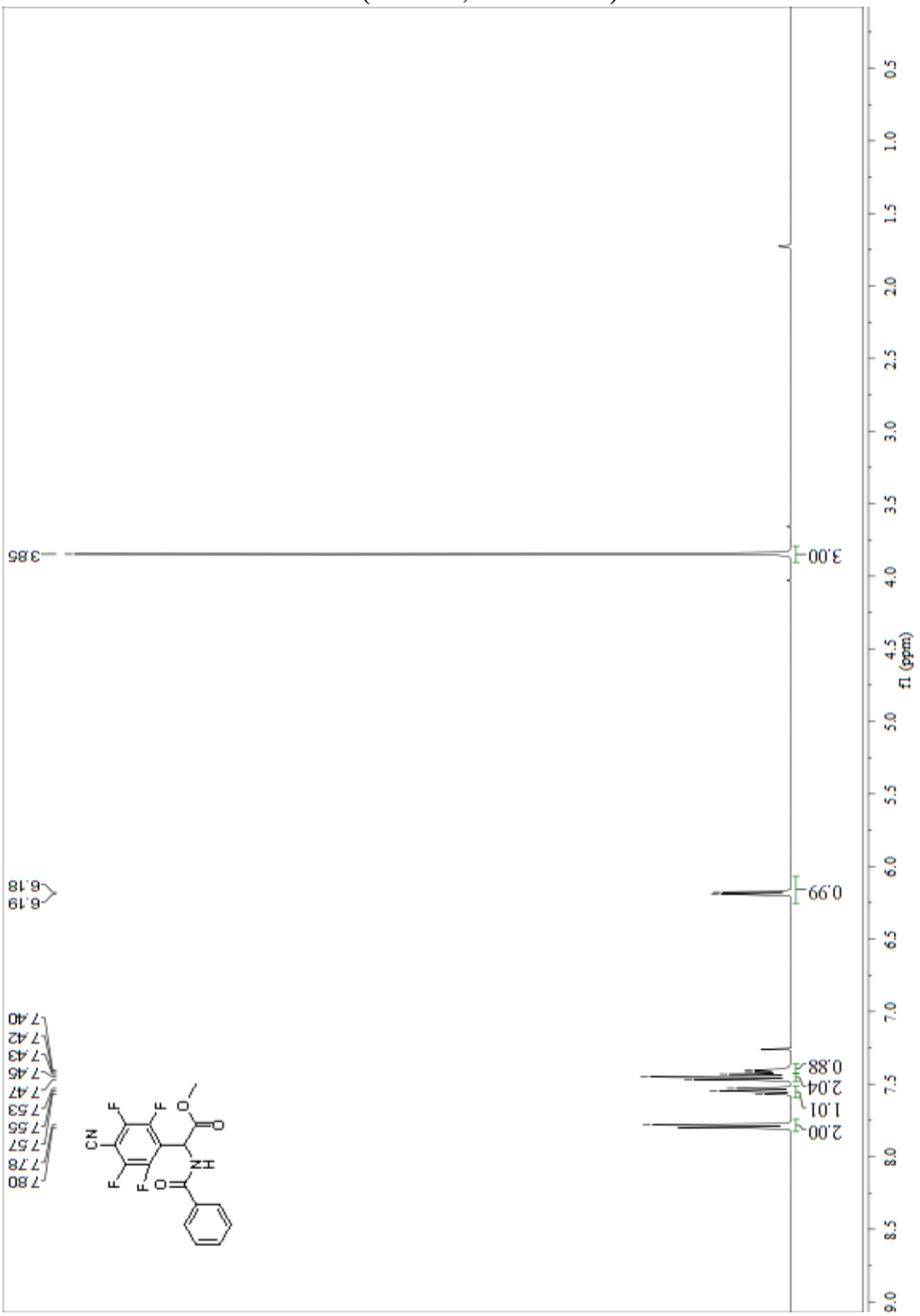

^{19}F NMR (376 MHz, , Chloroform-*d*) **6b**

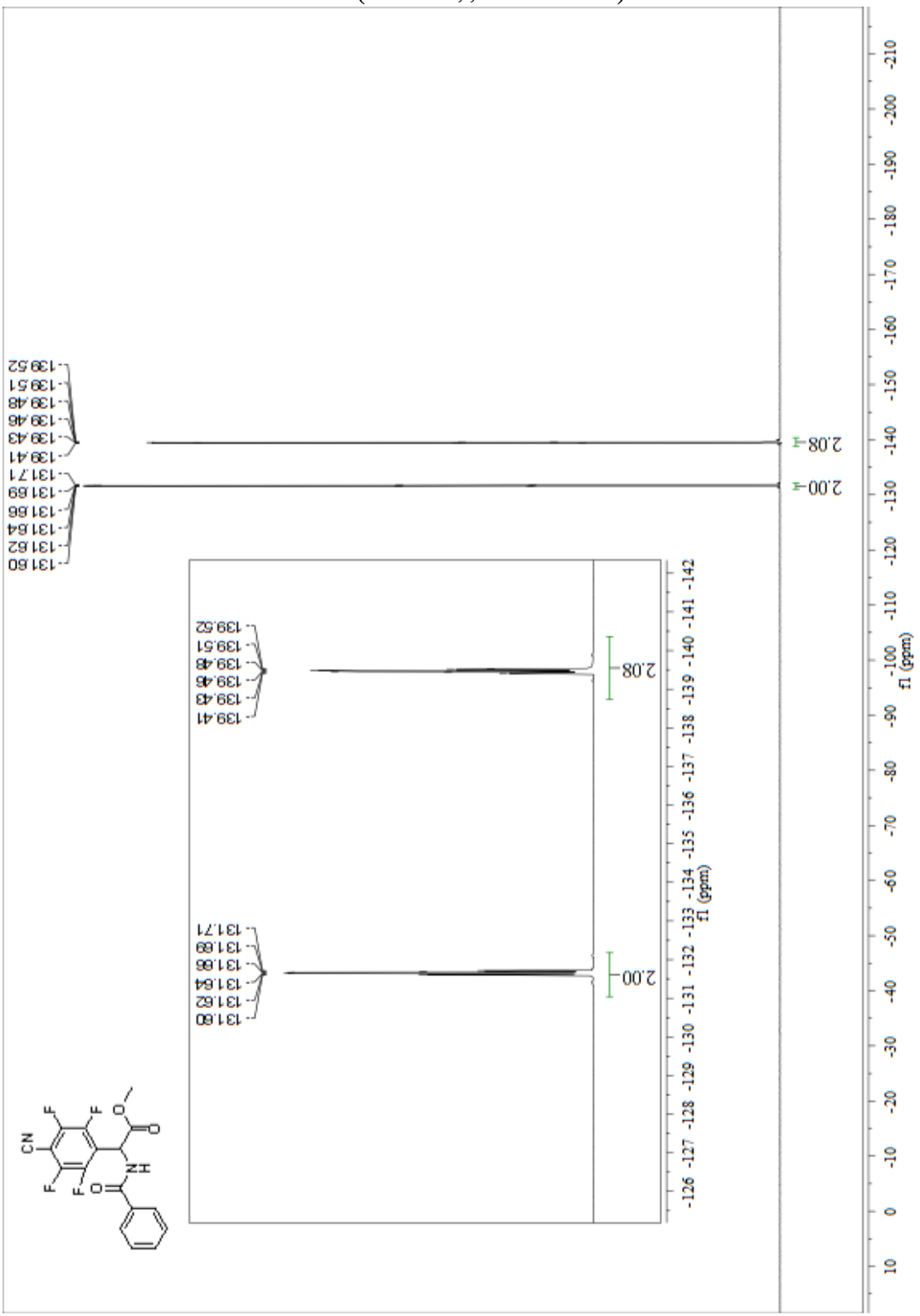

^{13}C NMR (101 MHz , Chloroform-*d*) **6b**

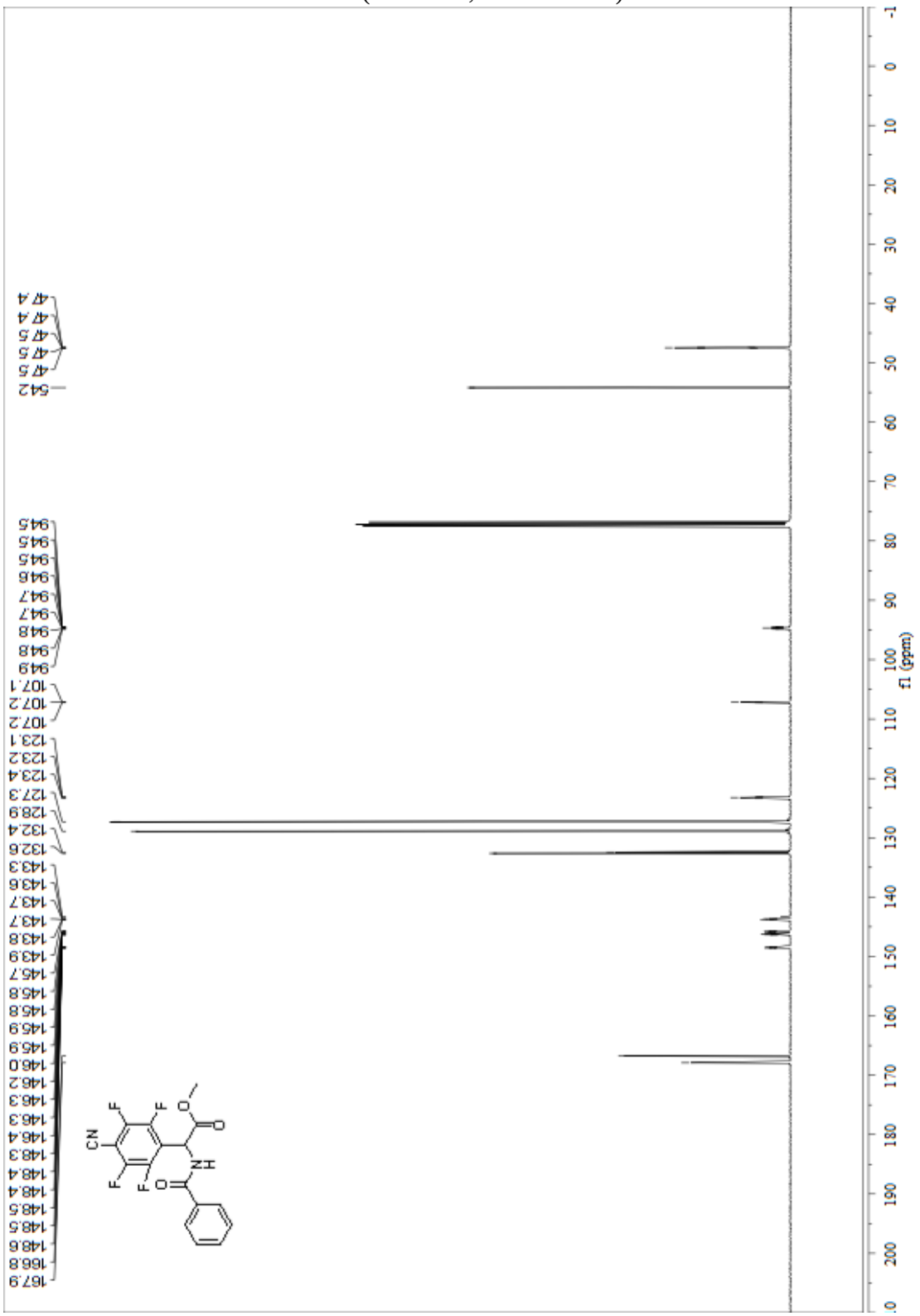

^{1}H NMR (400 MHz, Chloroform-*d*) **methyl 2-(4-acetyl-2,3,5,6-tetrafluorophenyl)-2-benzamidoacetate**

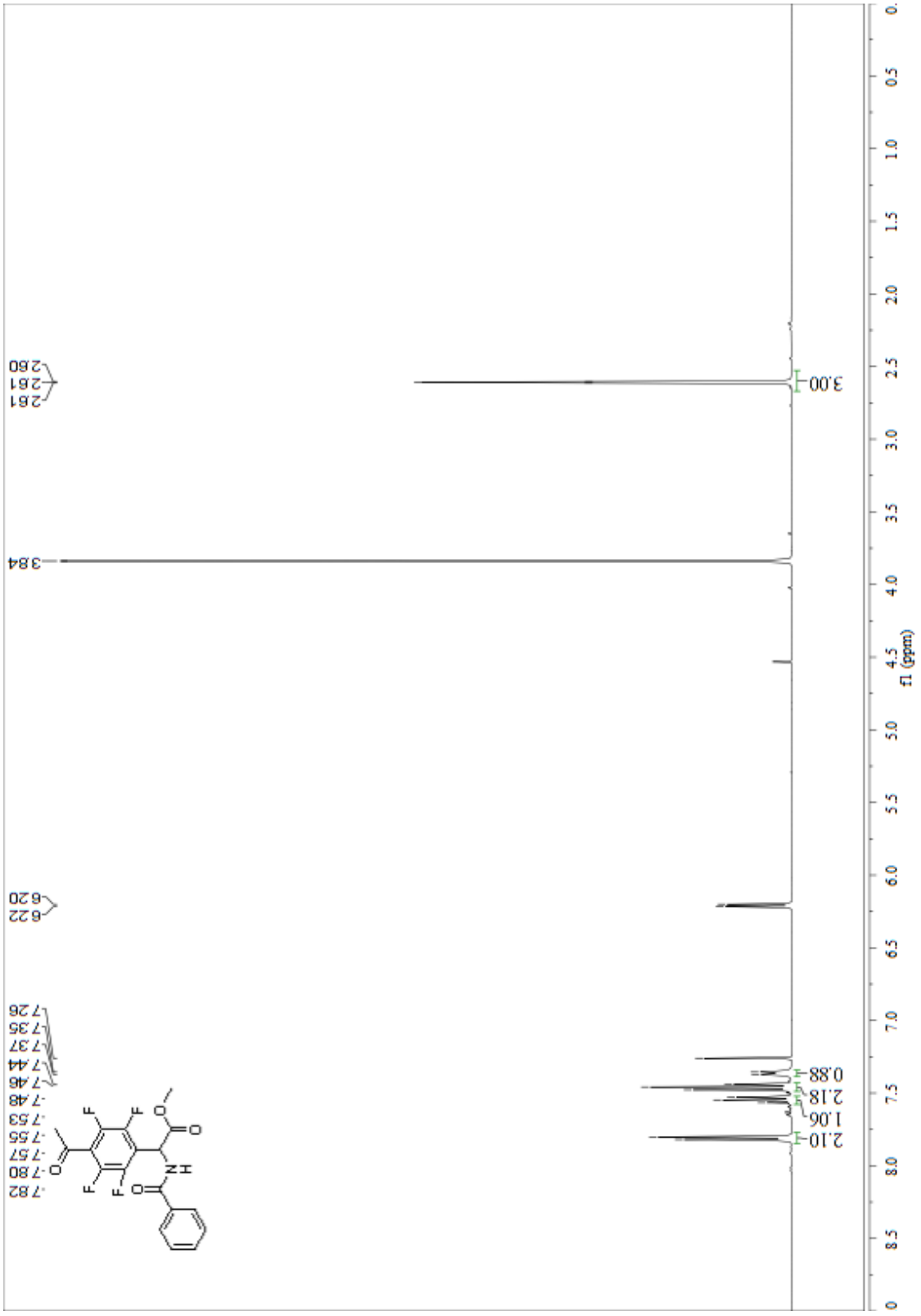

^{19}F NMR (376 MHz, , Chloroform-*d)* **methyl 2-(4-acetyl-2,3,5,6-tetrafluorophenyl)-2-benzamidoacetate**

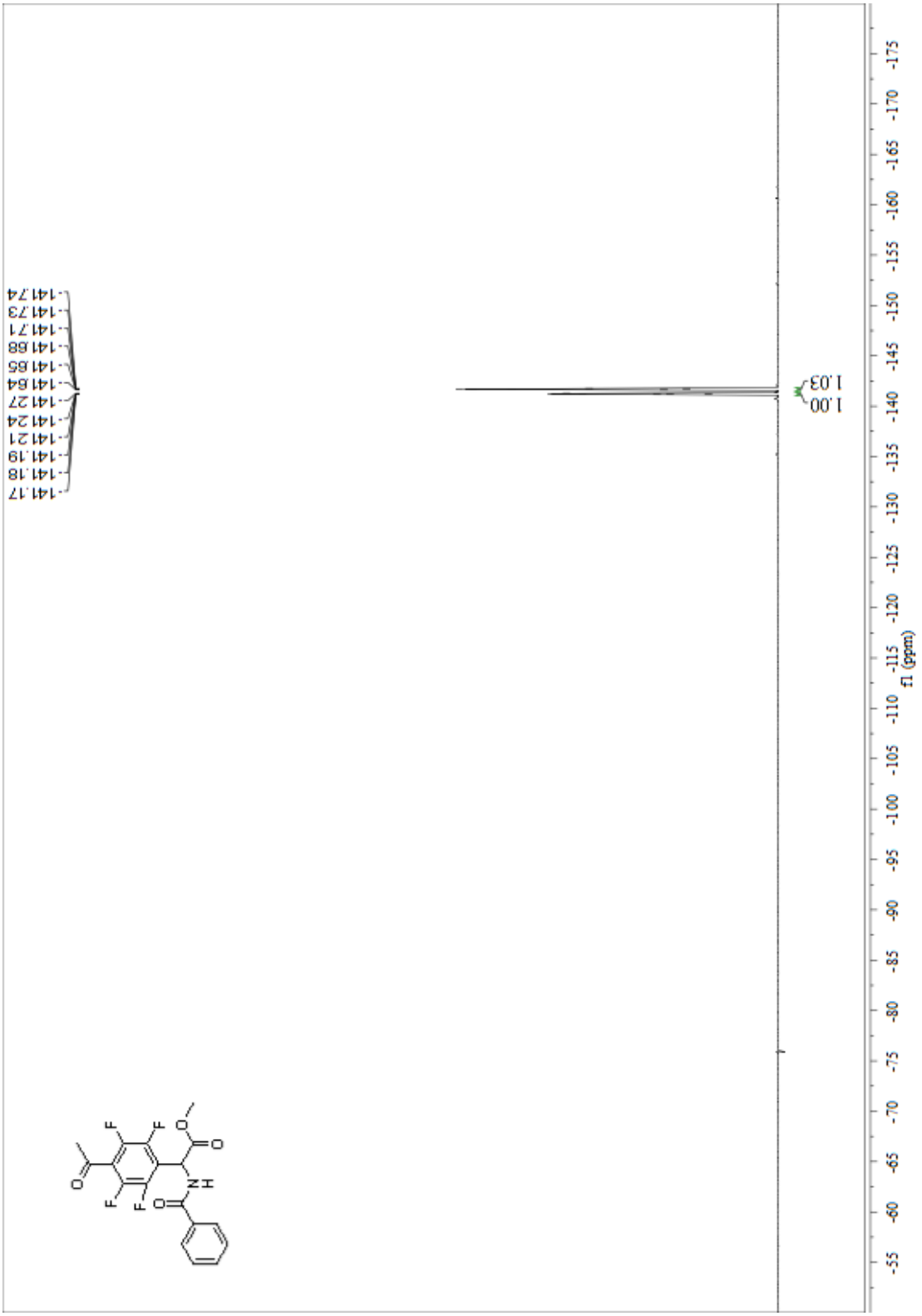

^{13}C NMR (101 MHz , Chloroform-*d*) **methyl 2-(4-acetyl-2,3,5,6-tetrafluorophenyl)-2-benzamidoacetate**

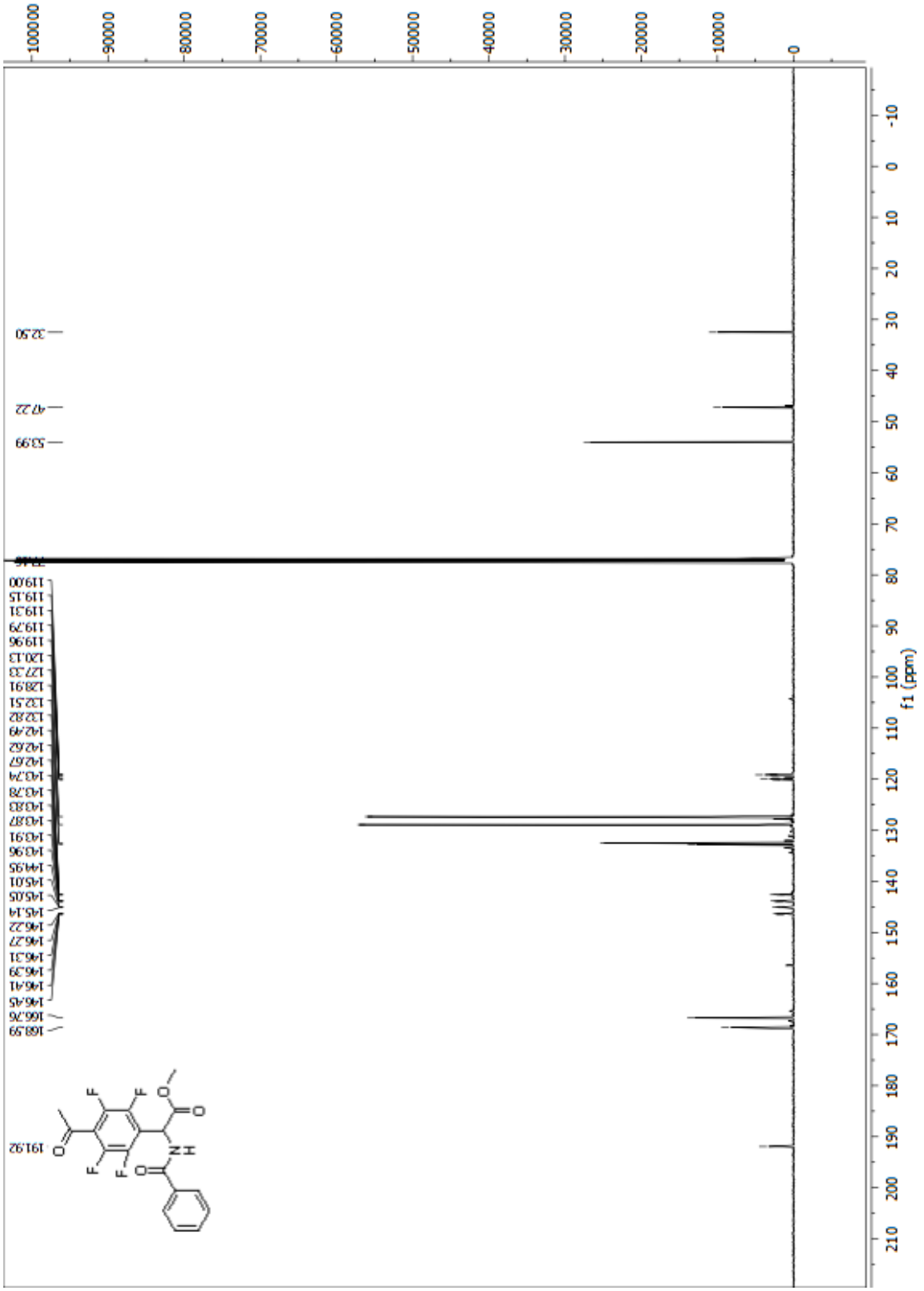

^{1}H NMR (400 MHz, Chloroform-*d*) **methyl 2-benzamido-2-(perfluoronaphthalen-1-yl)acetate**

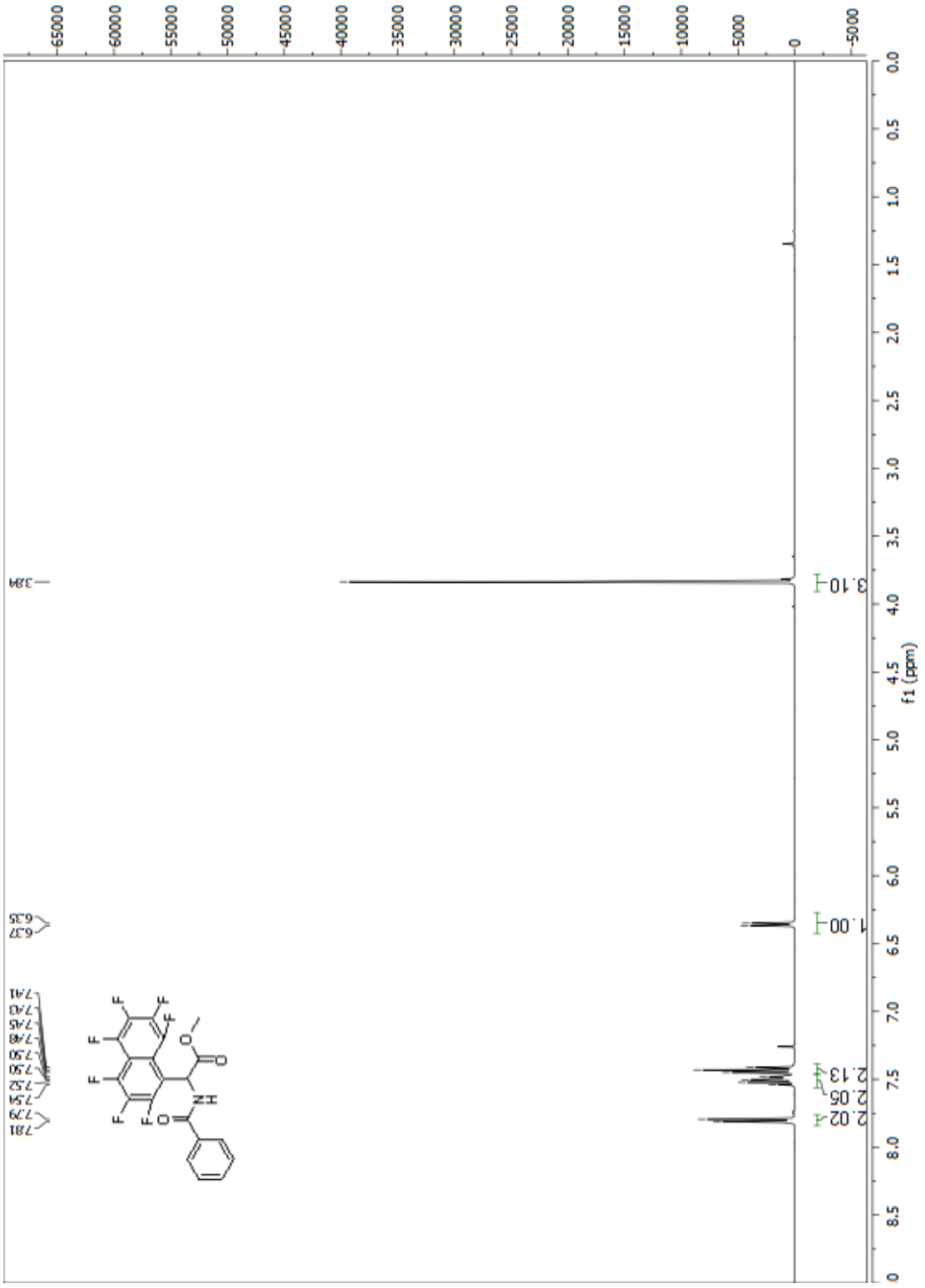

^{19}F NMR (376 MHz, , Chloroform-*d)* **methyl 2-benzamido-2-(perfluoronaphthalen-1-yl)acetate**

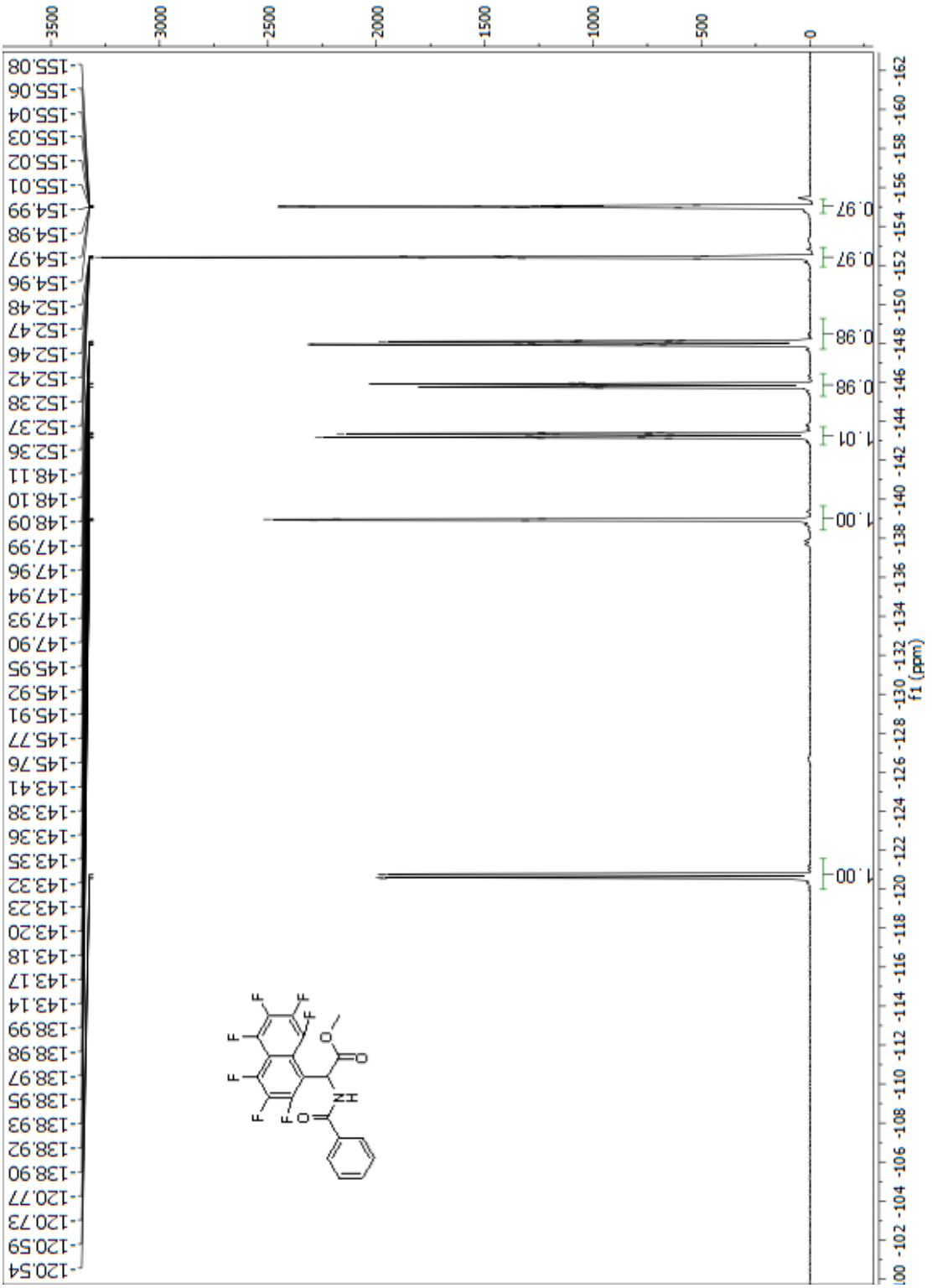

^{13}C NMR (101 MHz , Chloroform-*d*) **methyl 2-benzamido-2-(perfluoronaphthalen-1-yl)acetate**

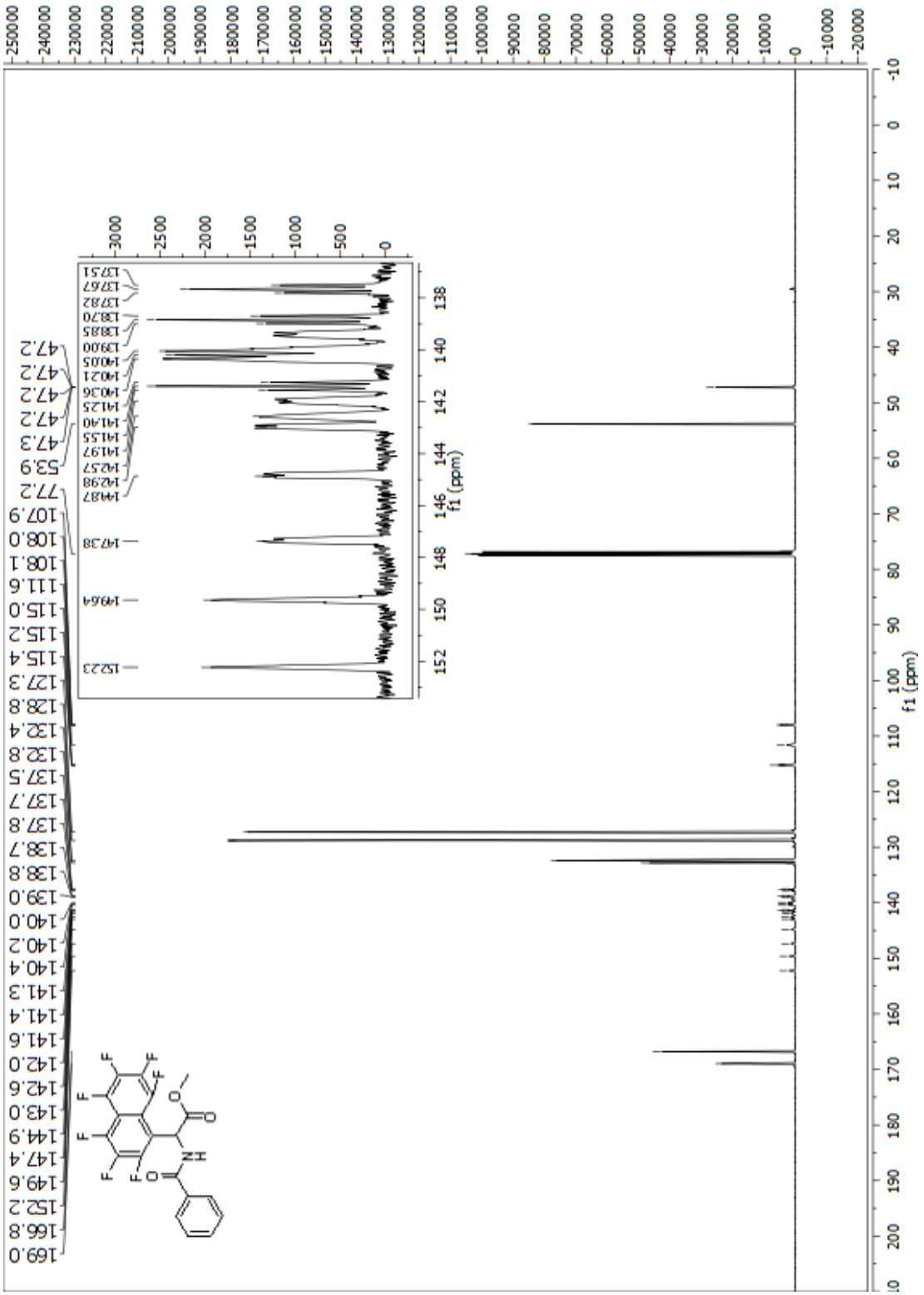

^{1}H NMR (400 MHz, Chloroform-*d)* **2,2,2-trifluoroethyl benzoylalaninate**

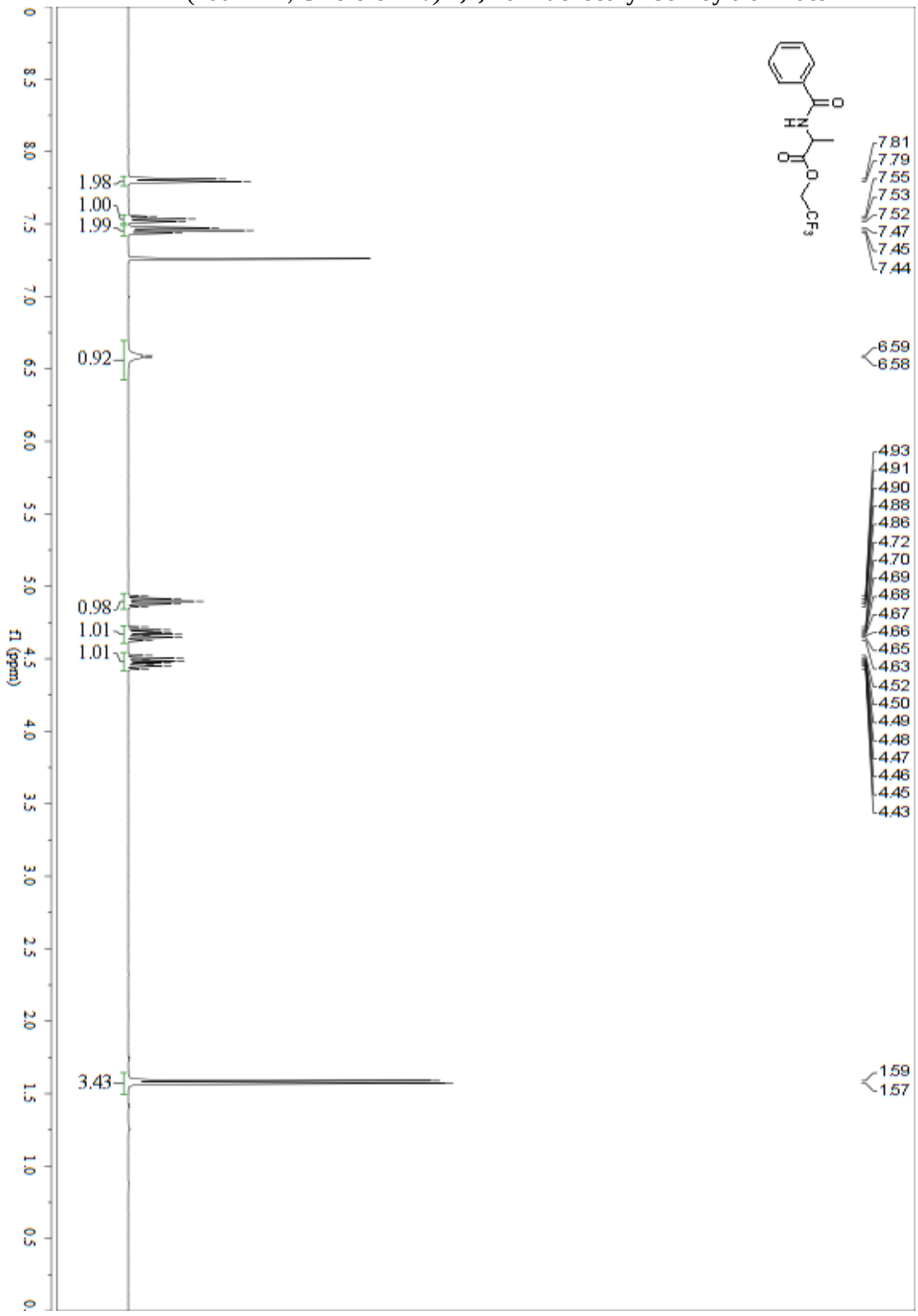

^{19}F NMR (376 MHz, , Chloroform-*d*) **2,2,2-trifluoroethyl benzoylalaninate**

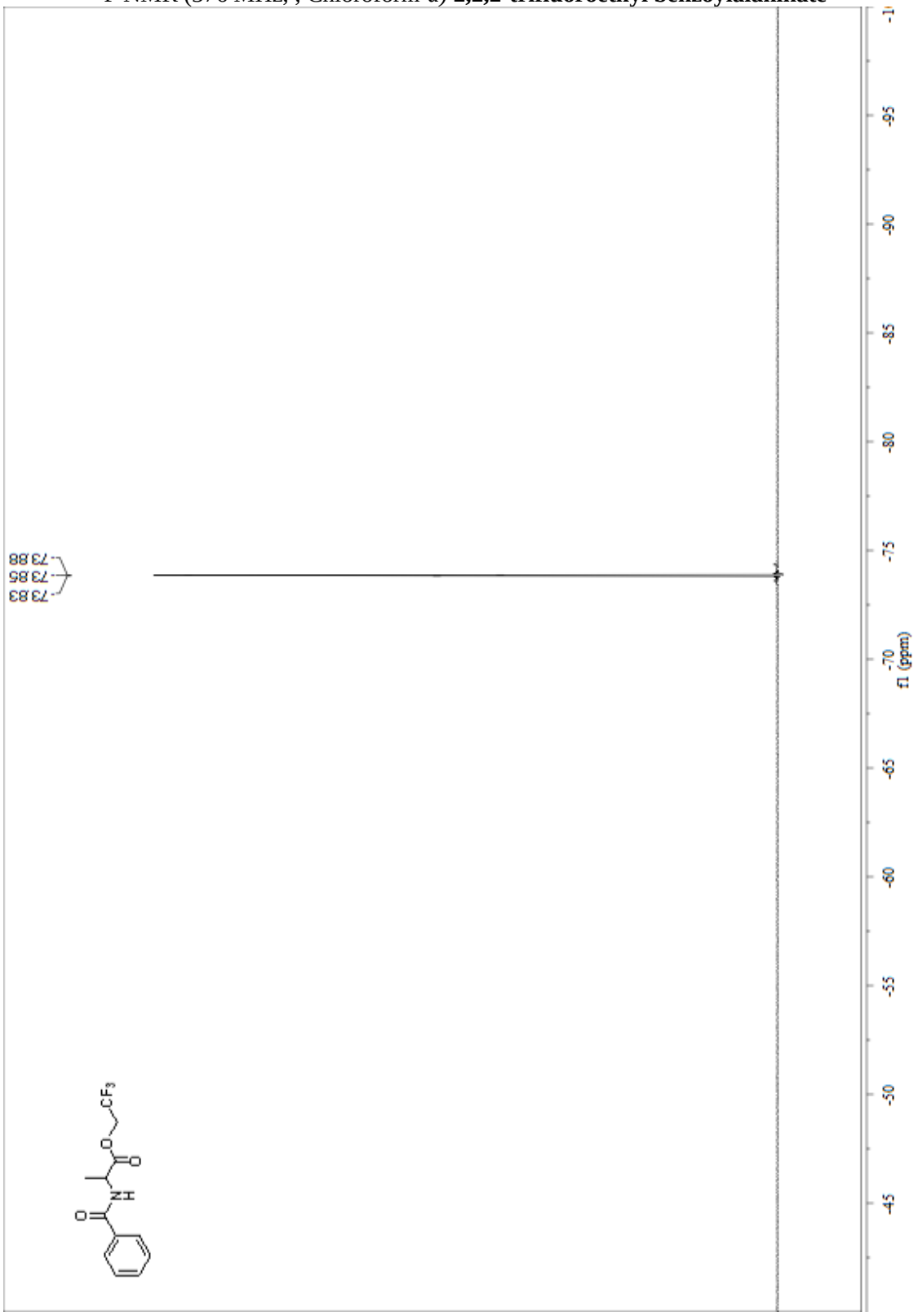

^{13}C NMR (101 MHz , Chloroform-*d*) **2,2,2-trifluoroethyl benzoylalaninate**

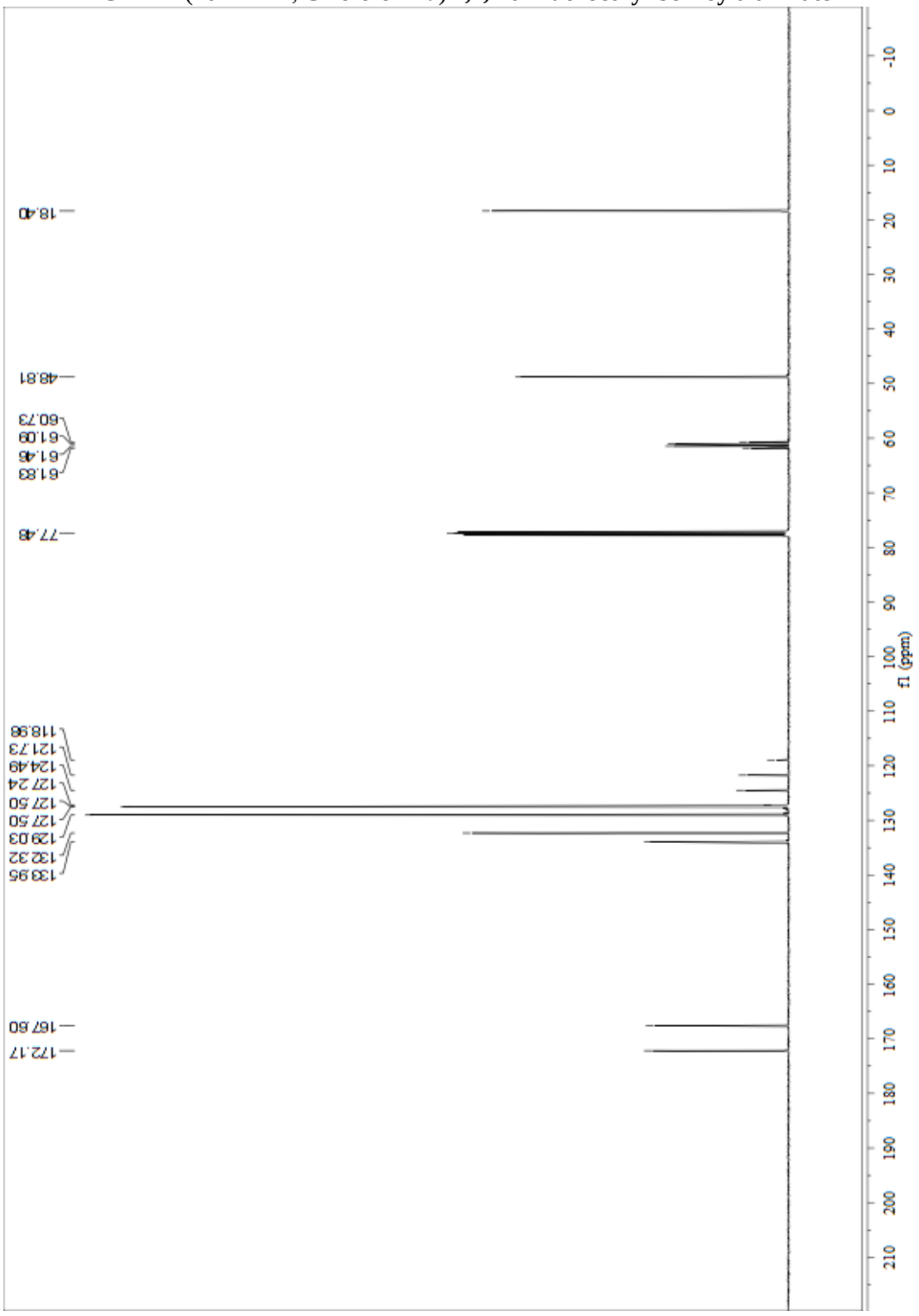

^{1}H NMR (400 MHz, Chloroform-*d*) **, 2,2,2-trifluoroethyl benzoylvalinate**

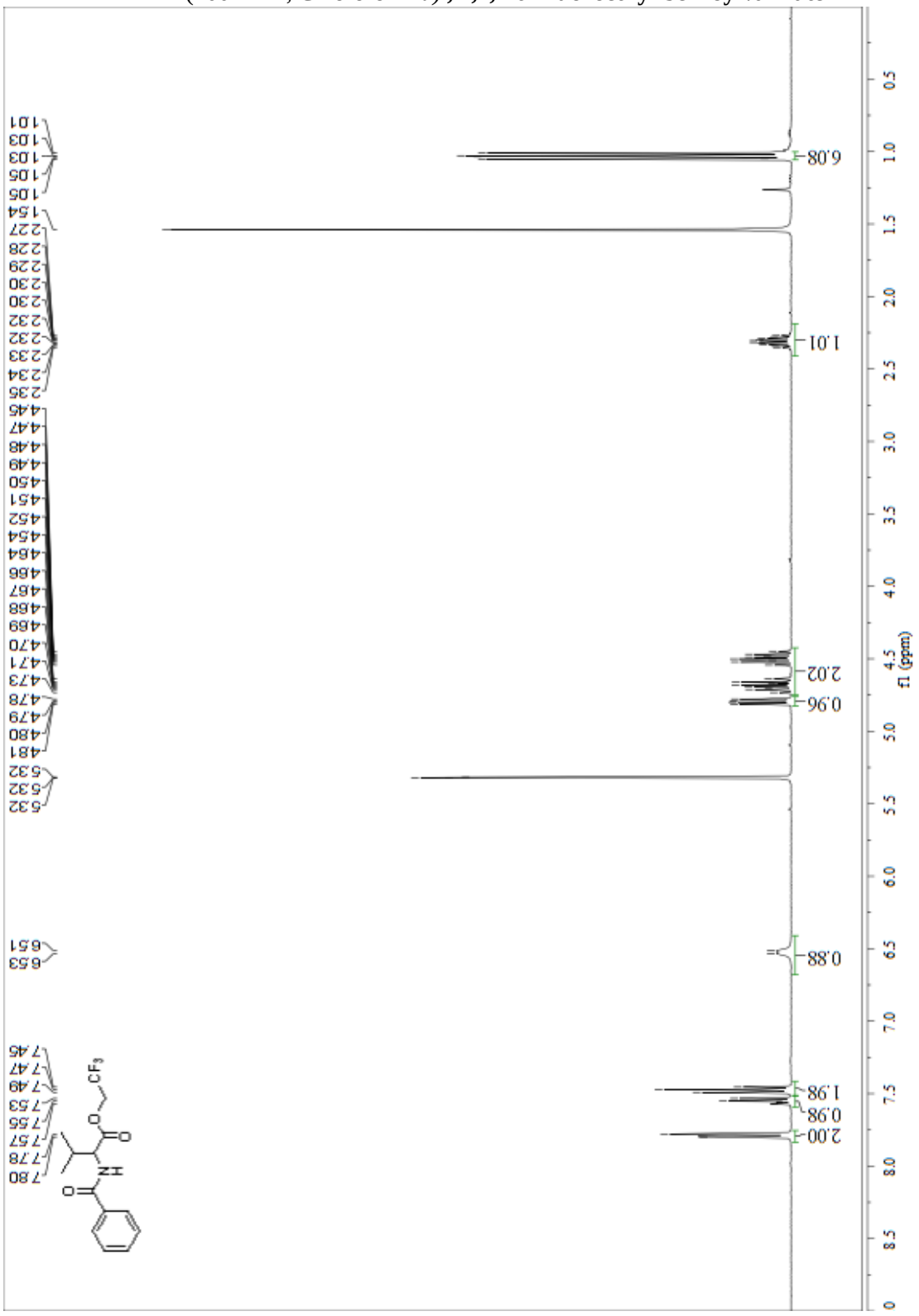

^{19}F NMR (376 MHz, , Chloroform-*d*) **, 2,2,2,2-trifluoroethyl benzoylvalinate**

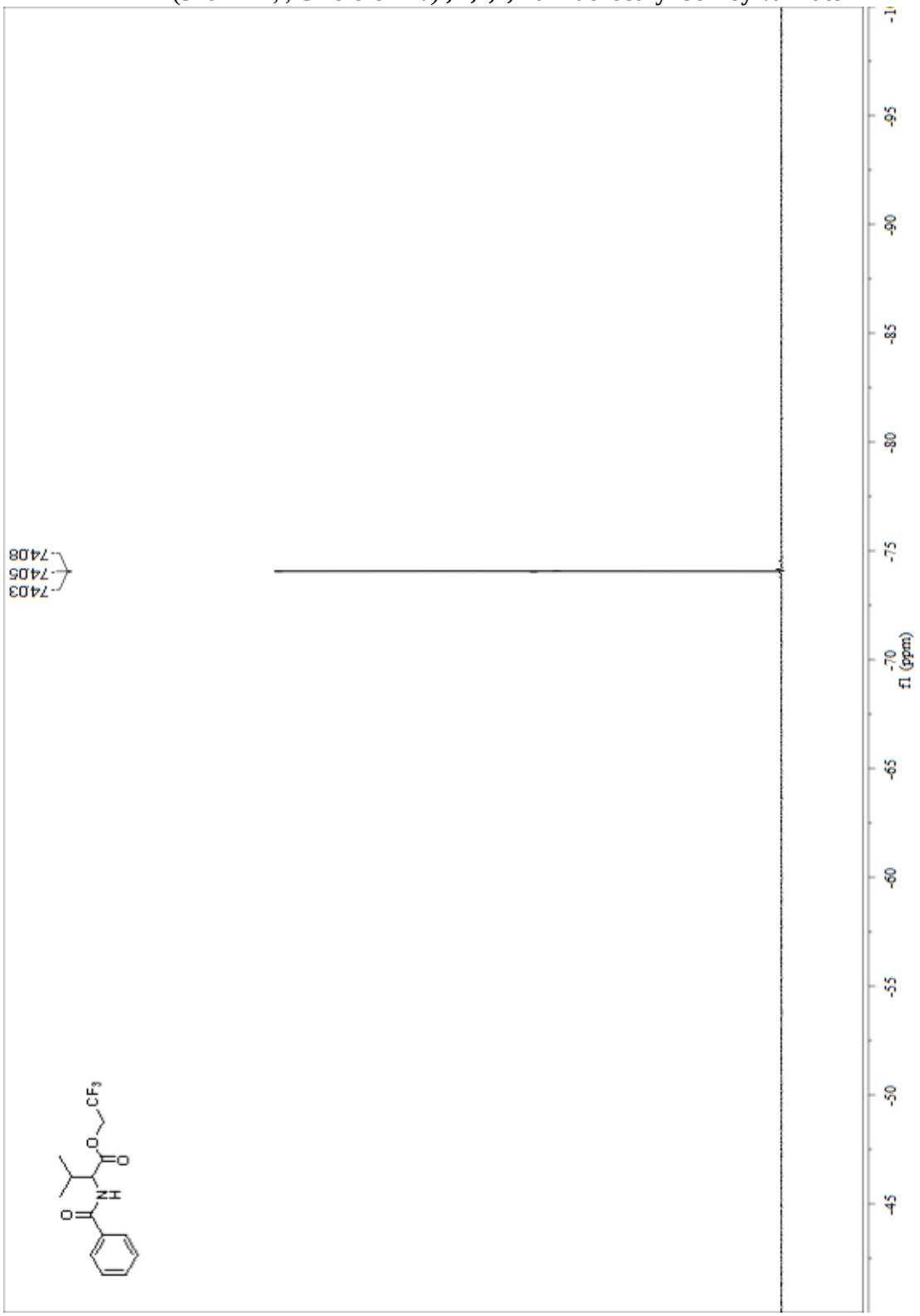

^{13}C NMR (101 MHz , Chloroform-*d*) **,2,2-trifluoroethyl benzoylphenylalaninate**

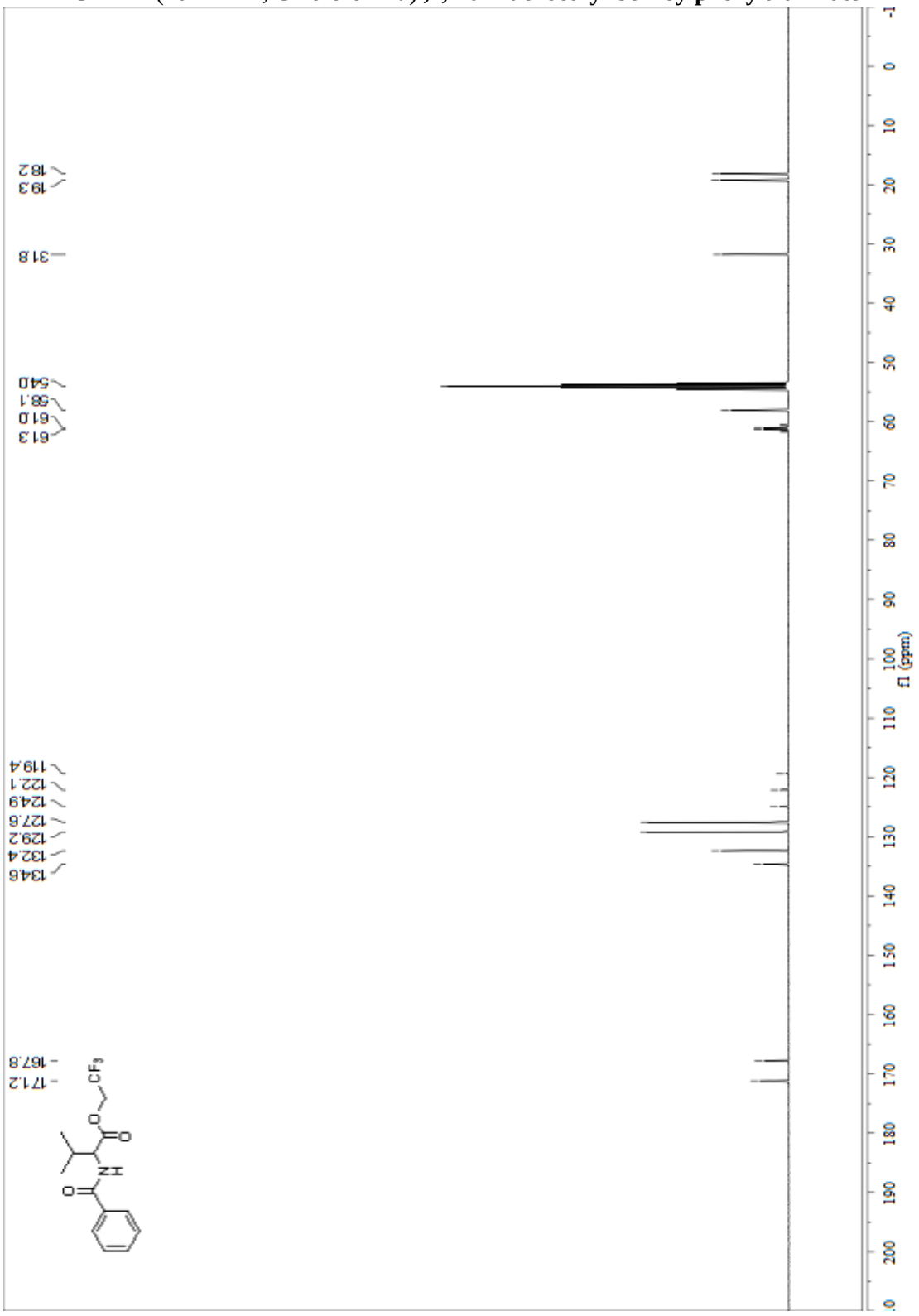

^{1}H NMR (400 MHz, Chloroform-*d)* **2,2,2-trifluoroethyl benzoyl-iso-leucinate**

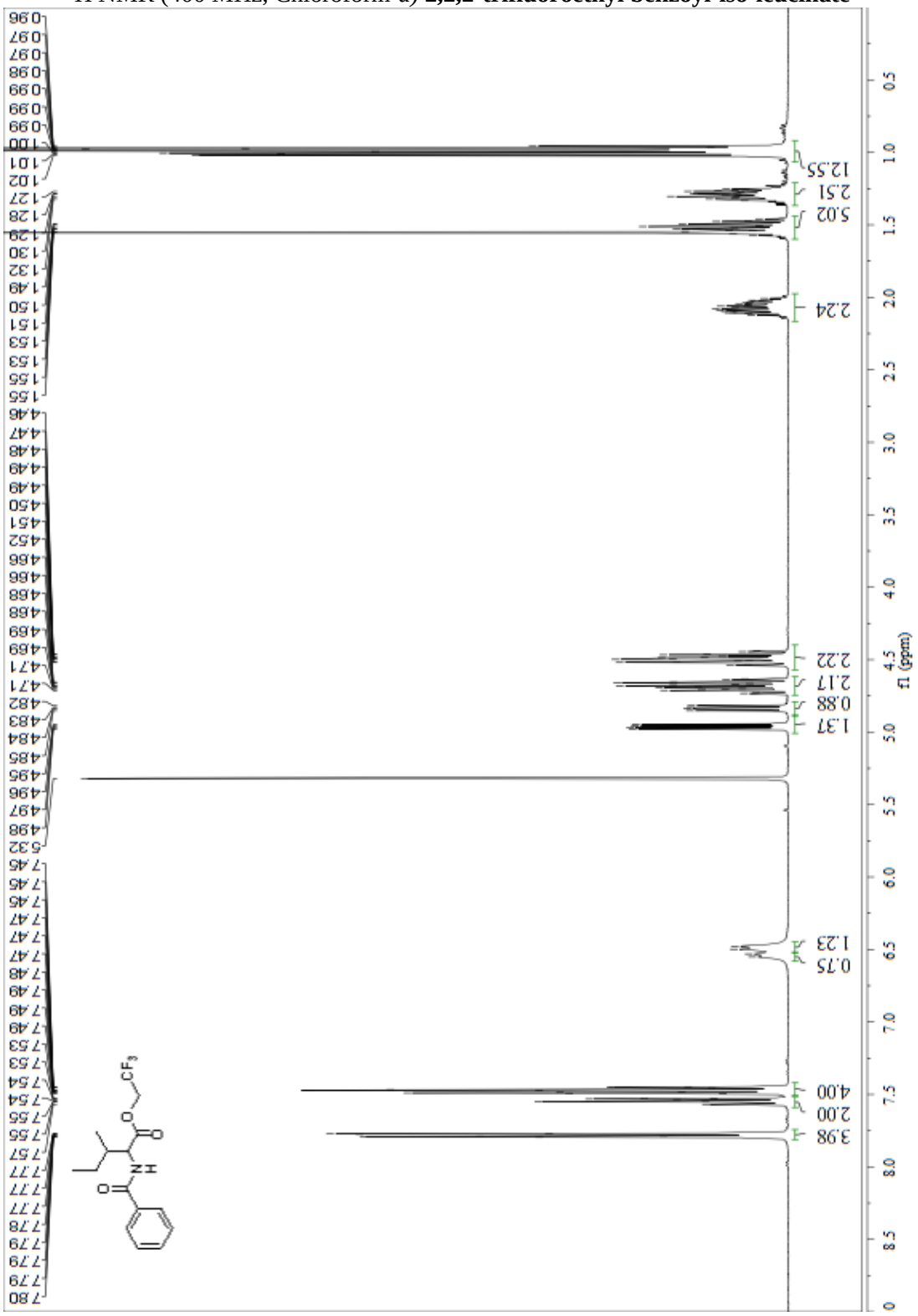

^{19}F NMR (376 MHz, , Chloroform-*d)* **2,2,2-trifluoroethyl benzoyl-iso-leucinate**

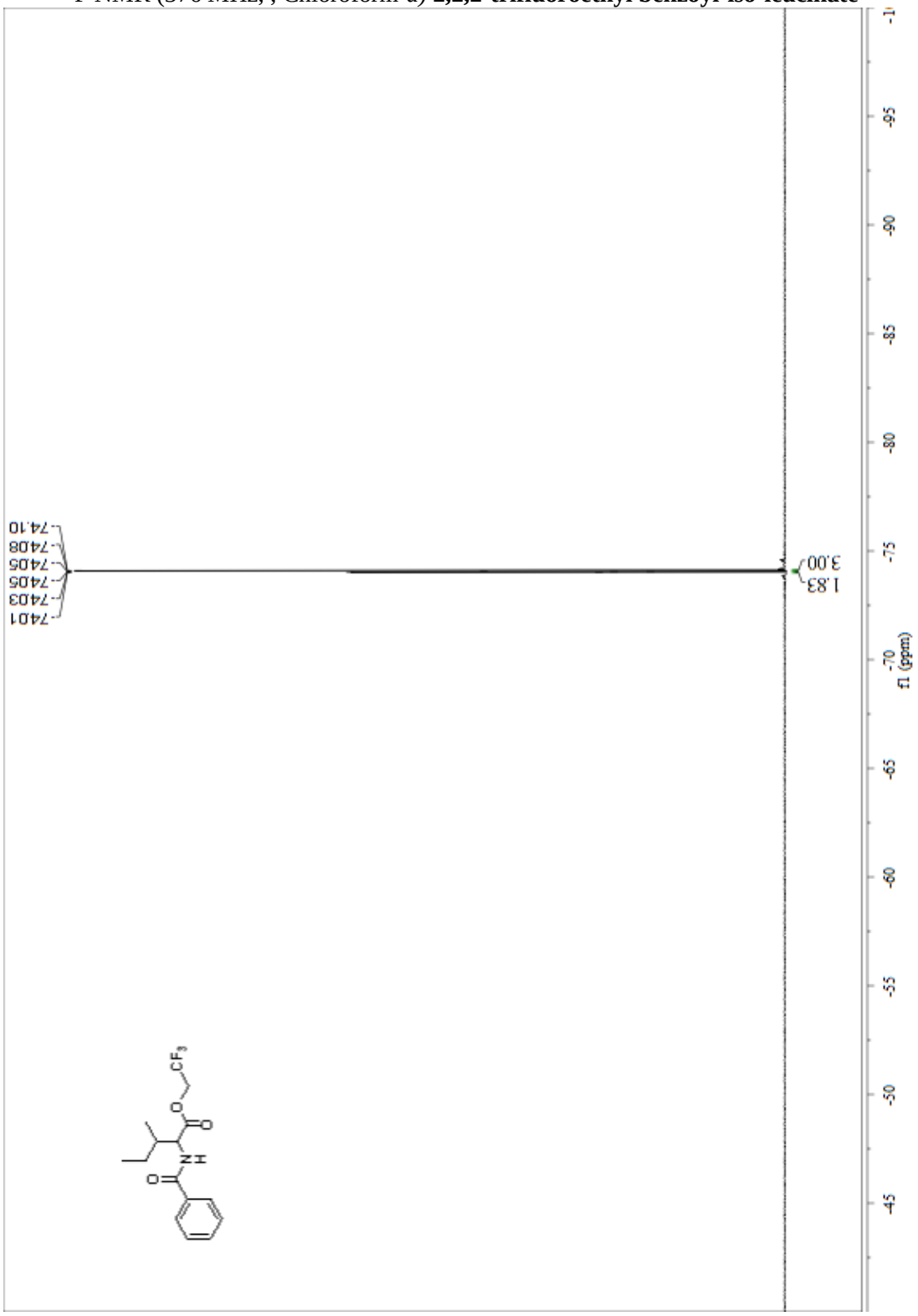

^{13}C NMR (101 MHz , Chloroform-*d*) **2,2,2-trifluoroethyl benzoyl-iso-leucinate**

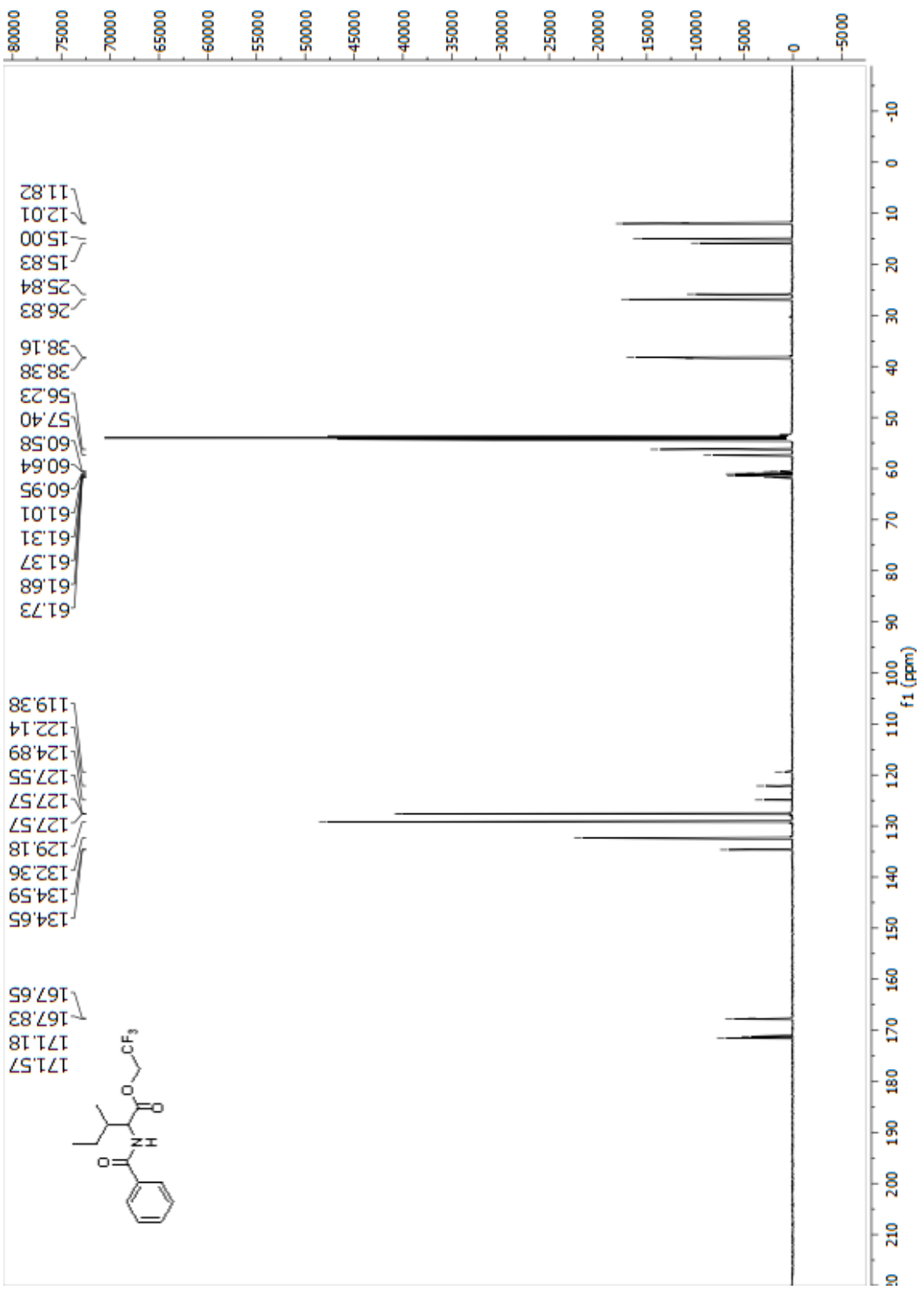

^{1}H NMR (400 MHz, Chloroform-*d*) **2,2,2-trifluoroethyl benzoylmethioninate**

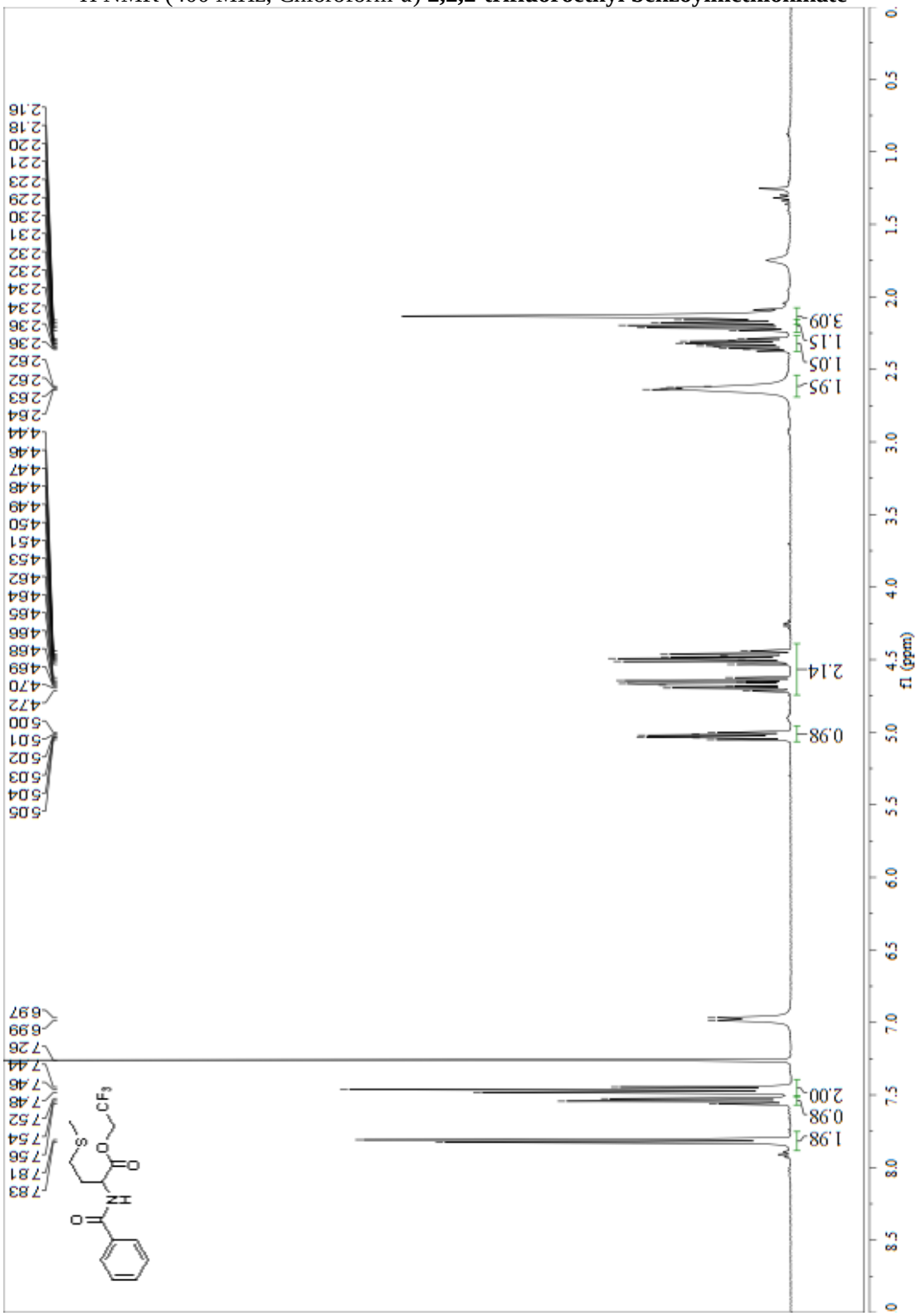

^{19}F NMR (376 MHz, , Chloroform-*d)* **2,2,2-trifluoroethyl benzoylmethioninate**

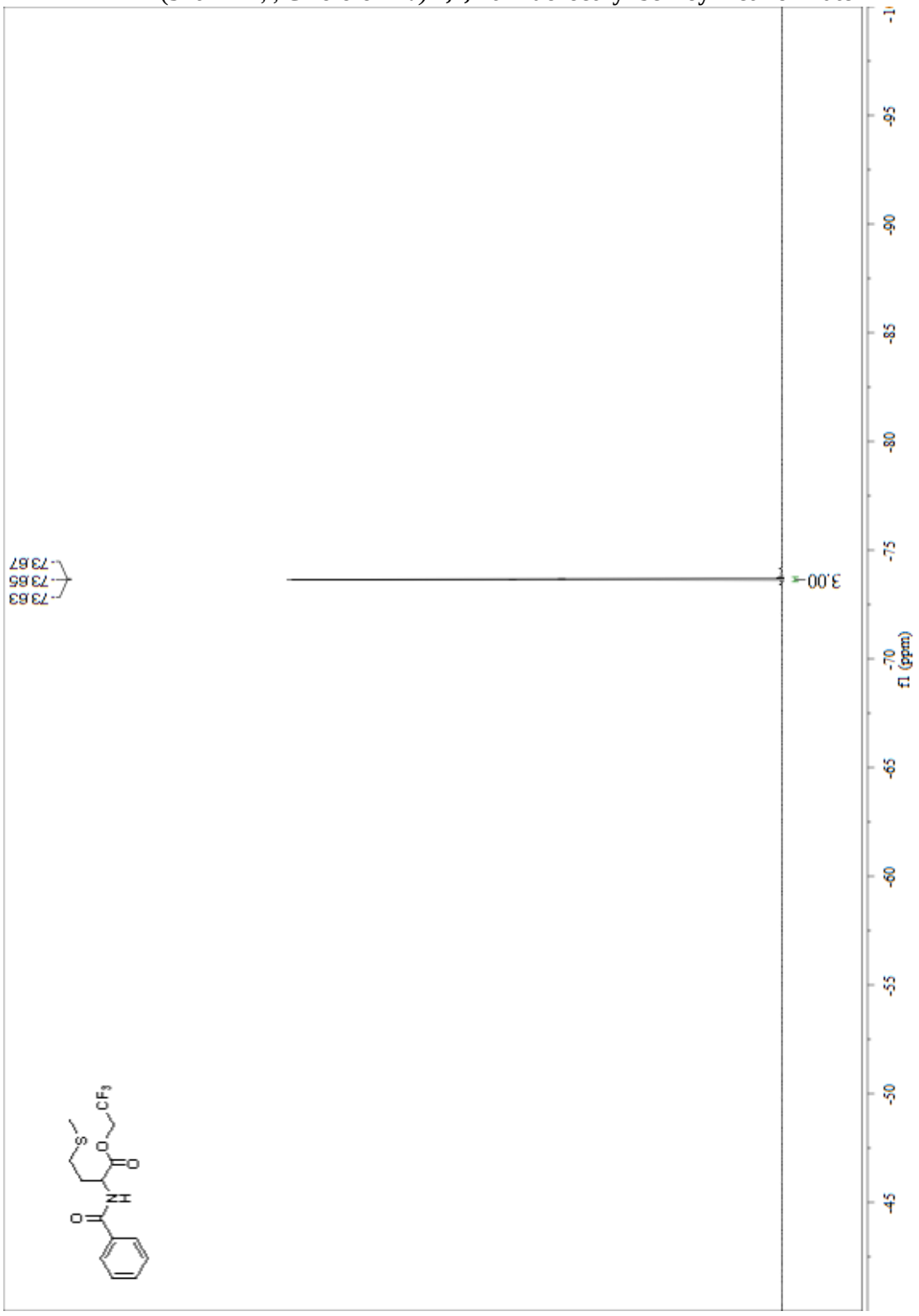

^{13}C NMR (101 MHz , Chloroform-*d*) **2,2,2-trifluoroethyl benzoylmethioninate**

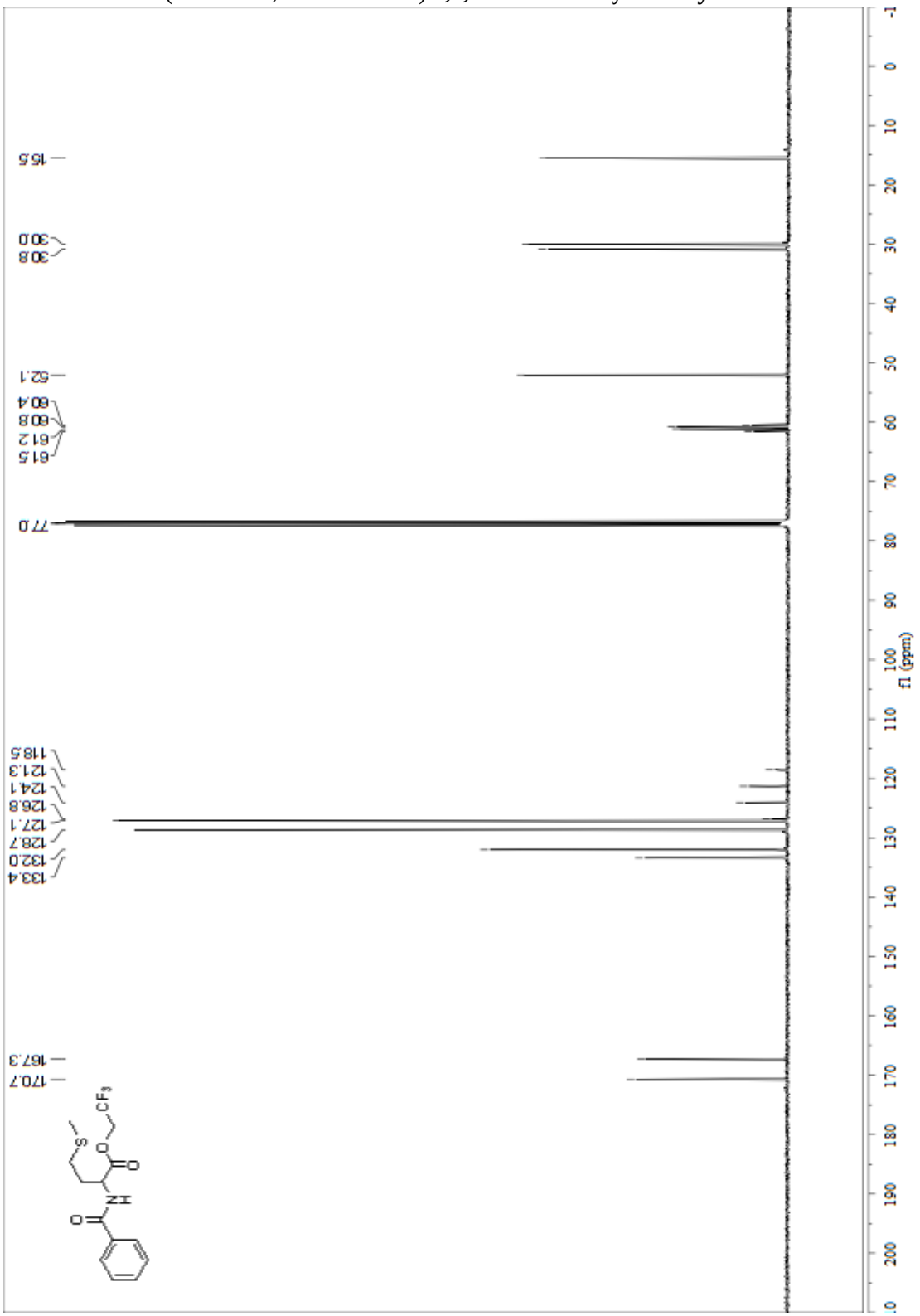

^{1}H NMR (400 MHz, Chloroform-*d*) **methyl 2-benzamido-2-(4-chlorophenyl)acetate**

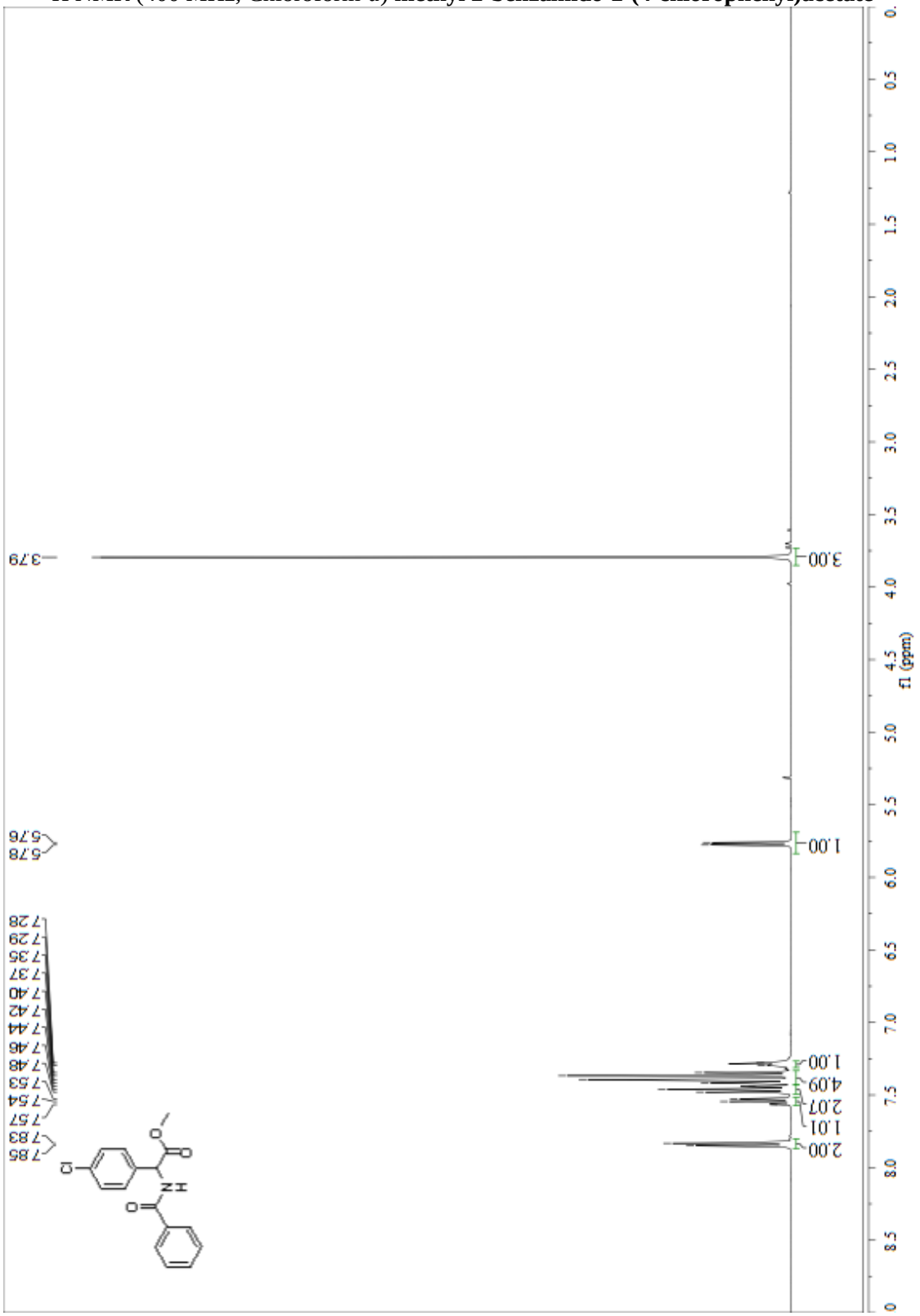

^{13}C NMR (101 MHz , Chloroform-*d*) **methyl 2-benzamido-2-(4-chlorophenyl)acetate**

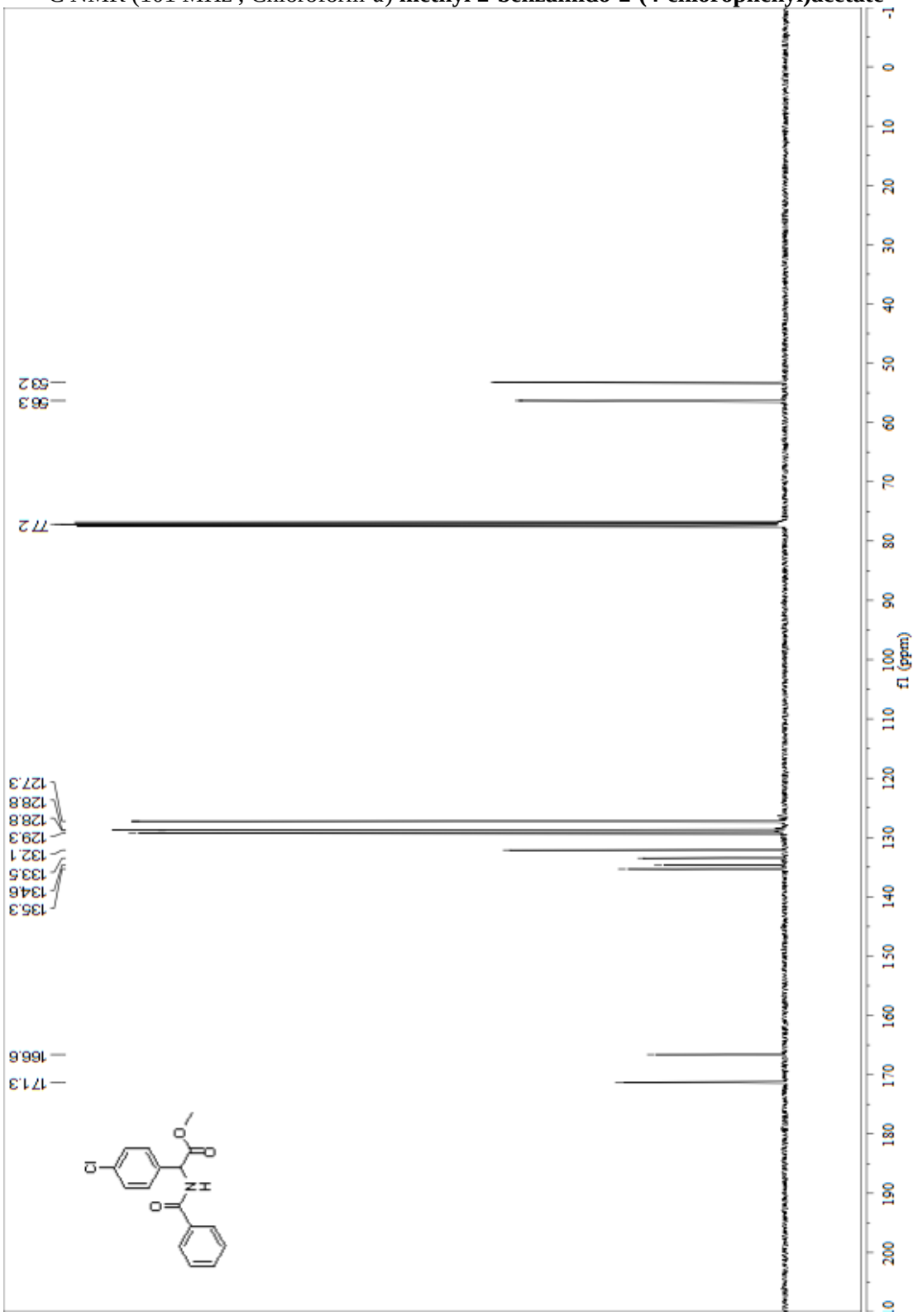

^{1}H NMR (400 MHz, Chloroform-*d)* **methyl 2-benzamido-2-(3,4,5-trifluorophenyl)acetate**

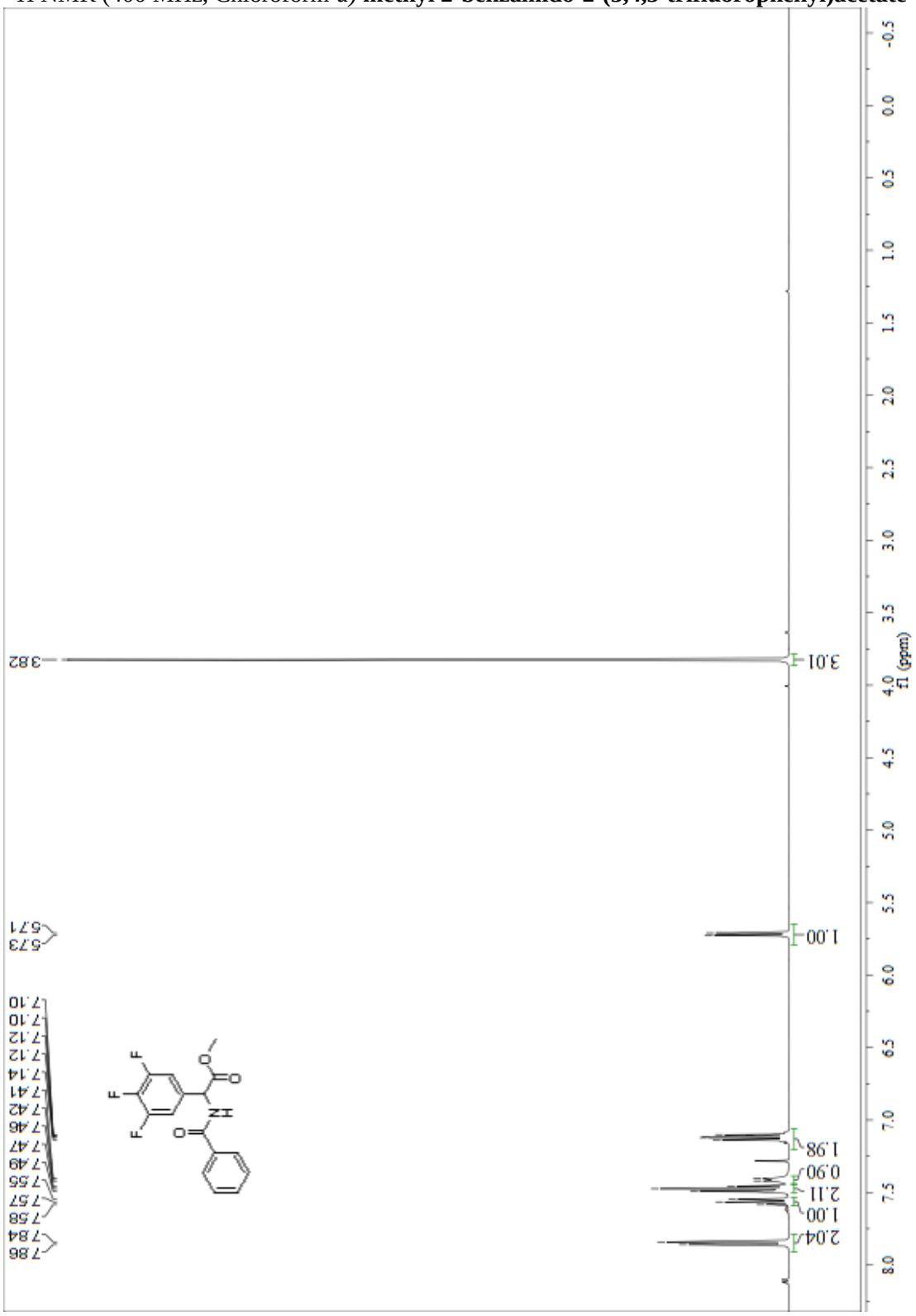

^{19}F NMR (376 MHz, , Chloroform-*d*) **methyl 2-benzamido-2-(3,4,5-trifluorophenyl)acetate**

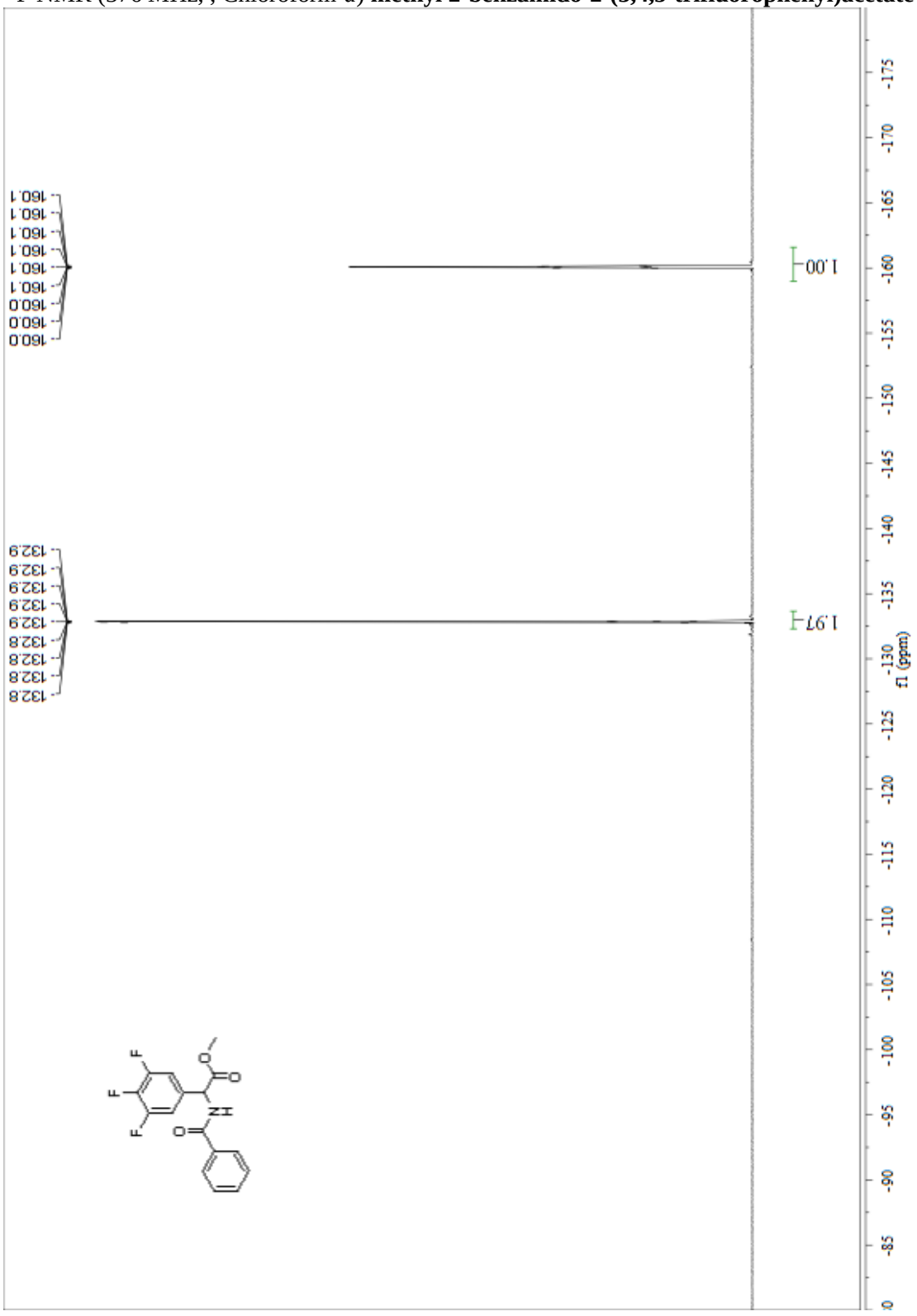

^{13}C NMR (101 MHz , Chloroform-*d*) **methyl 2-benzamido-2-(3,4,5-trifluorophenyl)acetate**

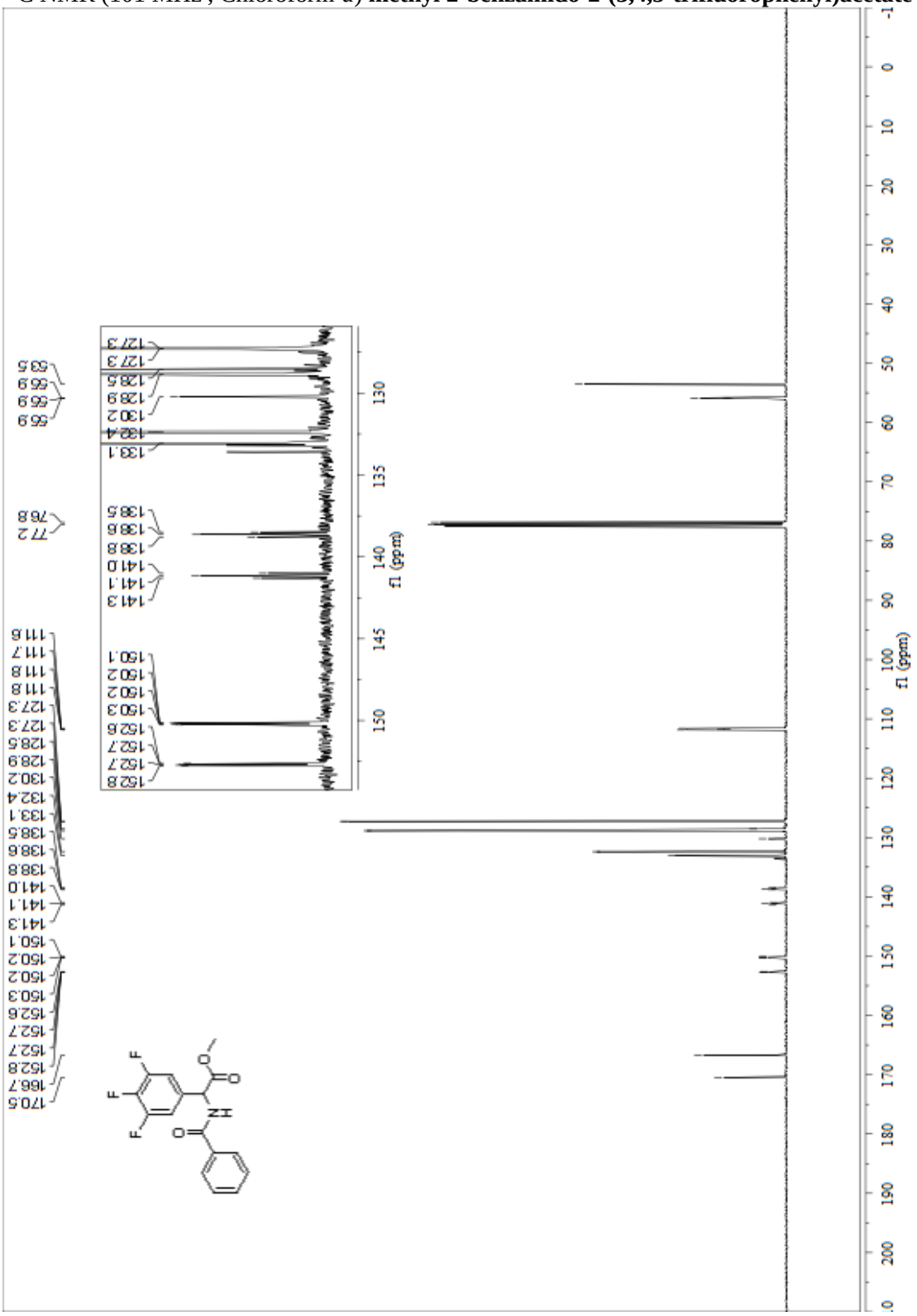

^{1}H NMR (400 MHz, Chloroform-*d)* **,2,2-trifluoroethyl benzoylphenylalaninate**

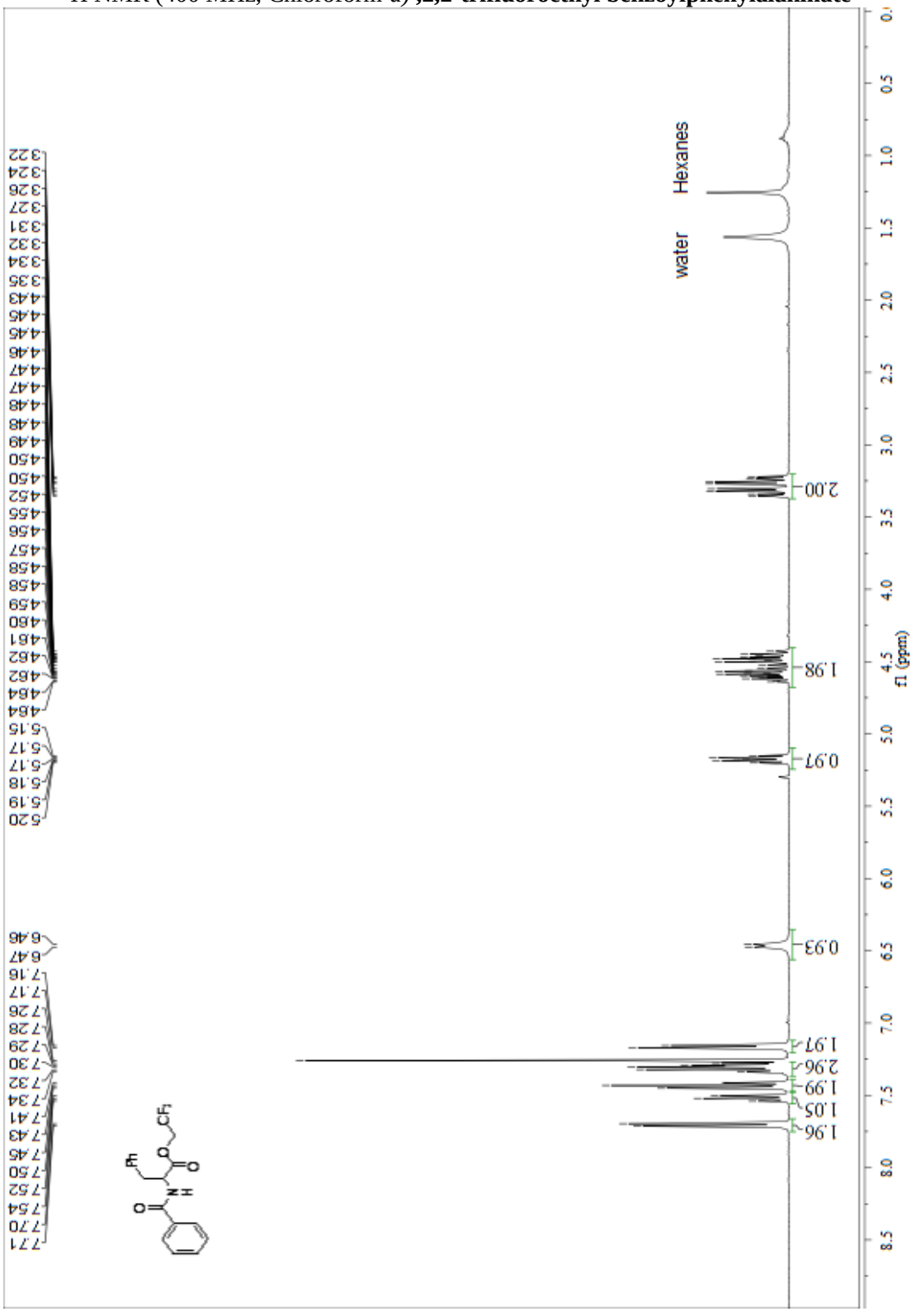

^{19}F NMR (376 MHz, , Chloroform-*d)* **,2,2-trifluoroethyl benzoylphenylalaninate**

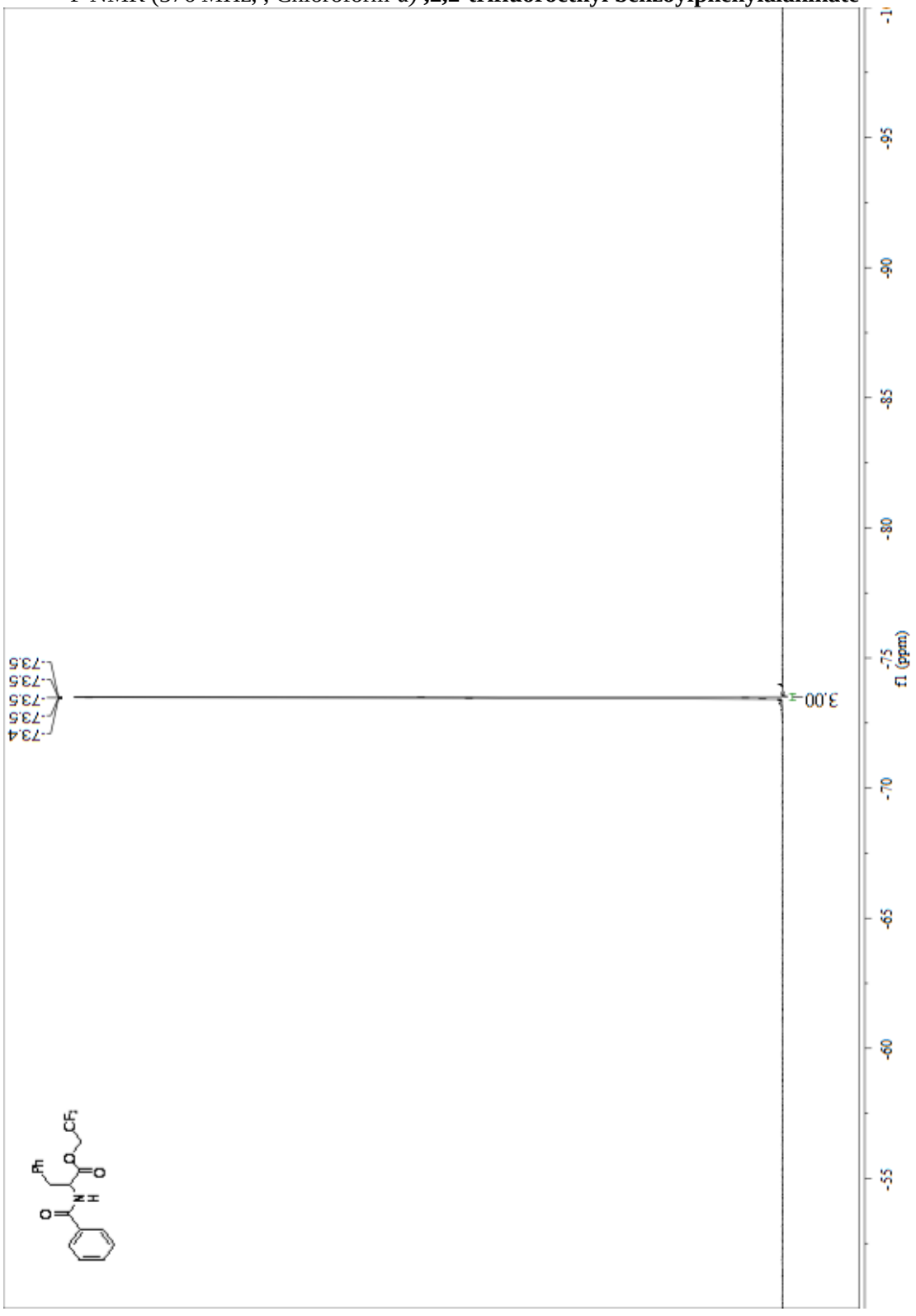

^{1}H NMR (400 MHz, Chloroform- *d)* **2,2,2-trifluoroethyl benzoylleucinate**

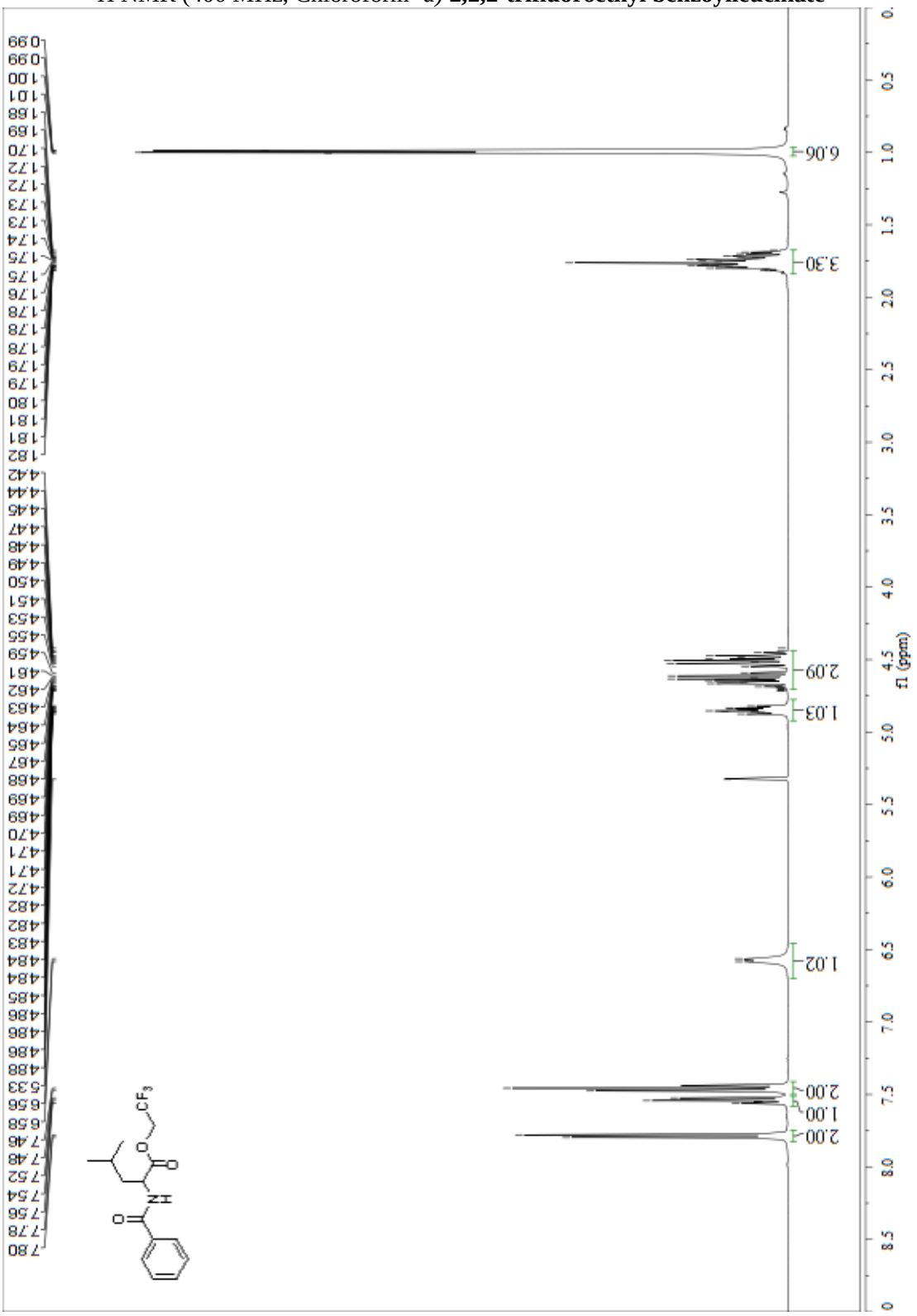

^{19}F NMR (376 MHz, , Chloroform-*d*) **2,2,2-trifluoroethyl benzoylleucinate**

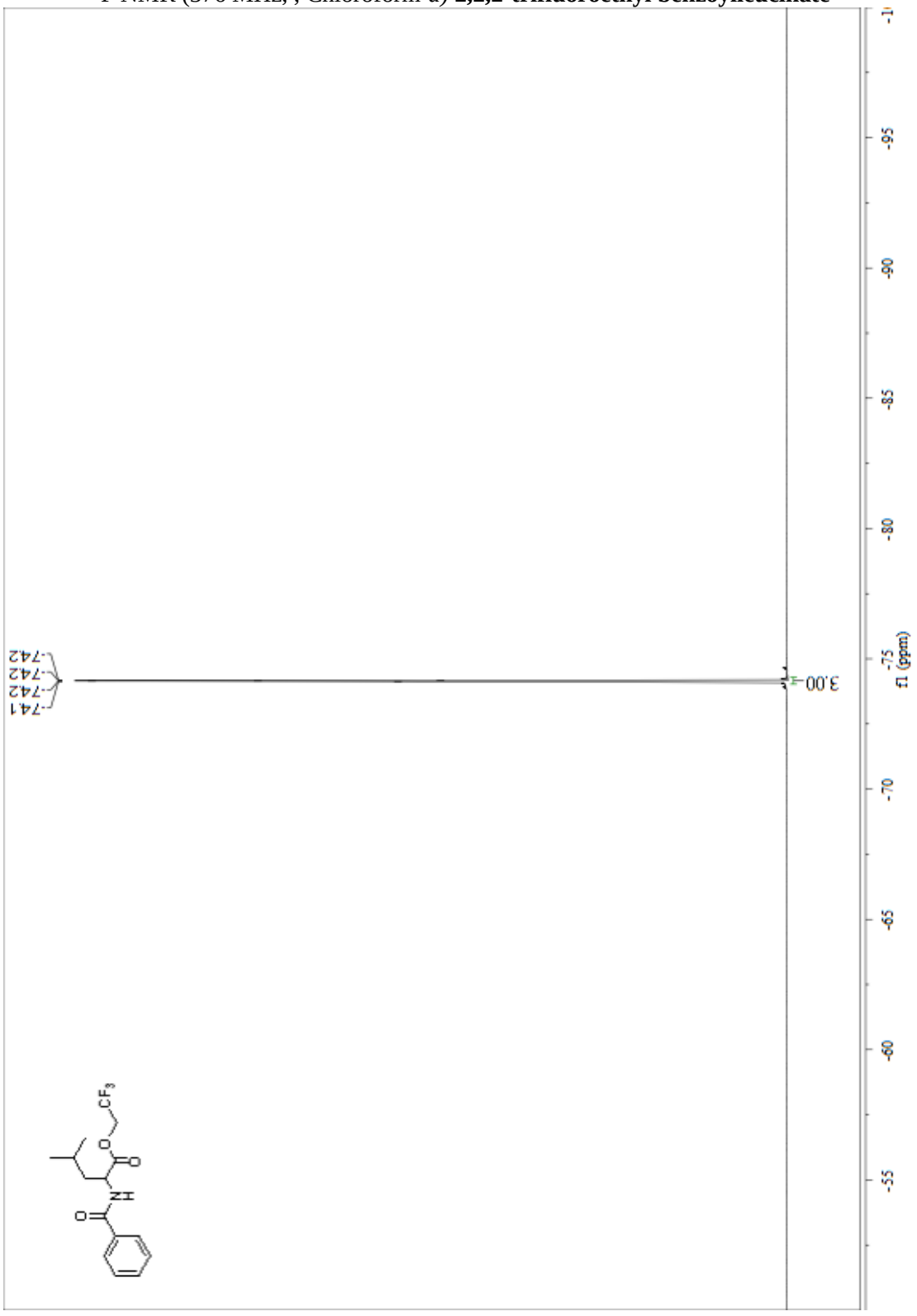

^{13}C NMR (101 MHz , Chloroform-*d*) **, 2,2,2-trifluoroethyl benzoylleucinate**

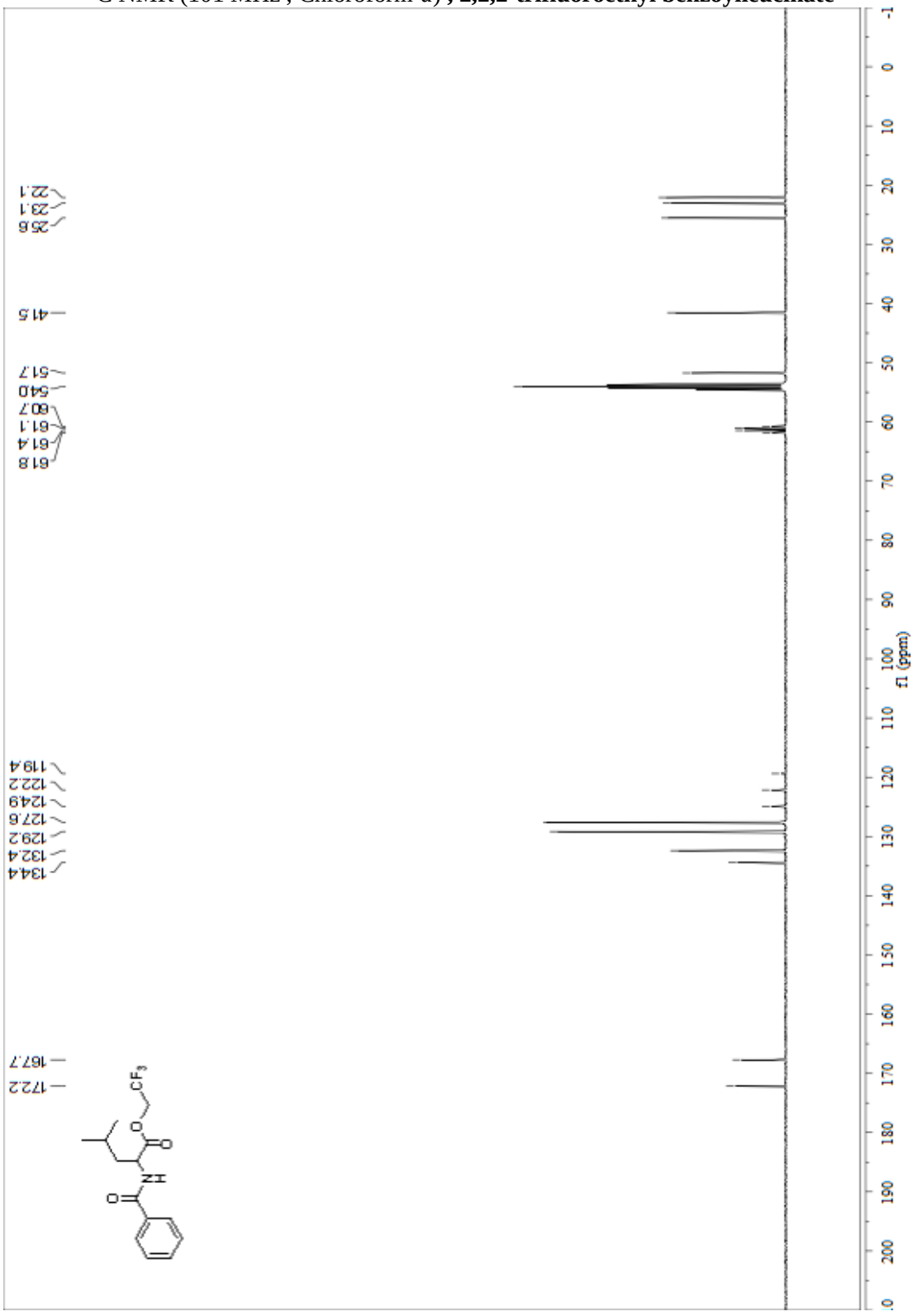

^{1}H NMR (400 MHz, Chloroform-*d*) **methyl 2-benzamido-2-(perfluoropyridin-4-yl)acetate**

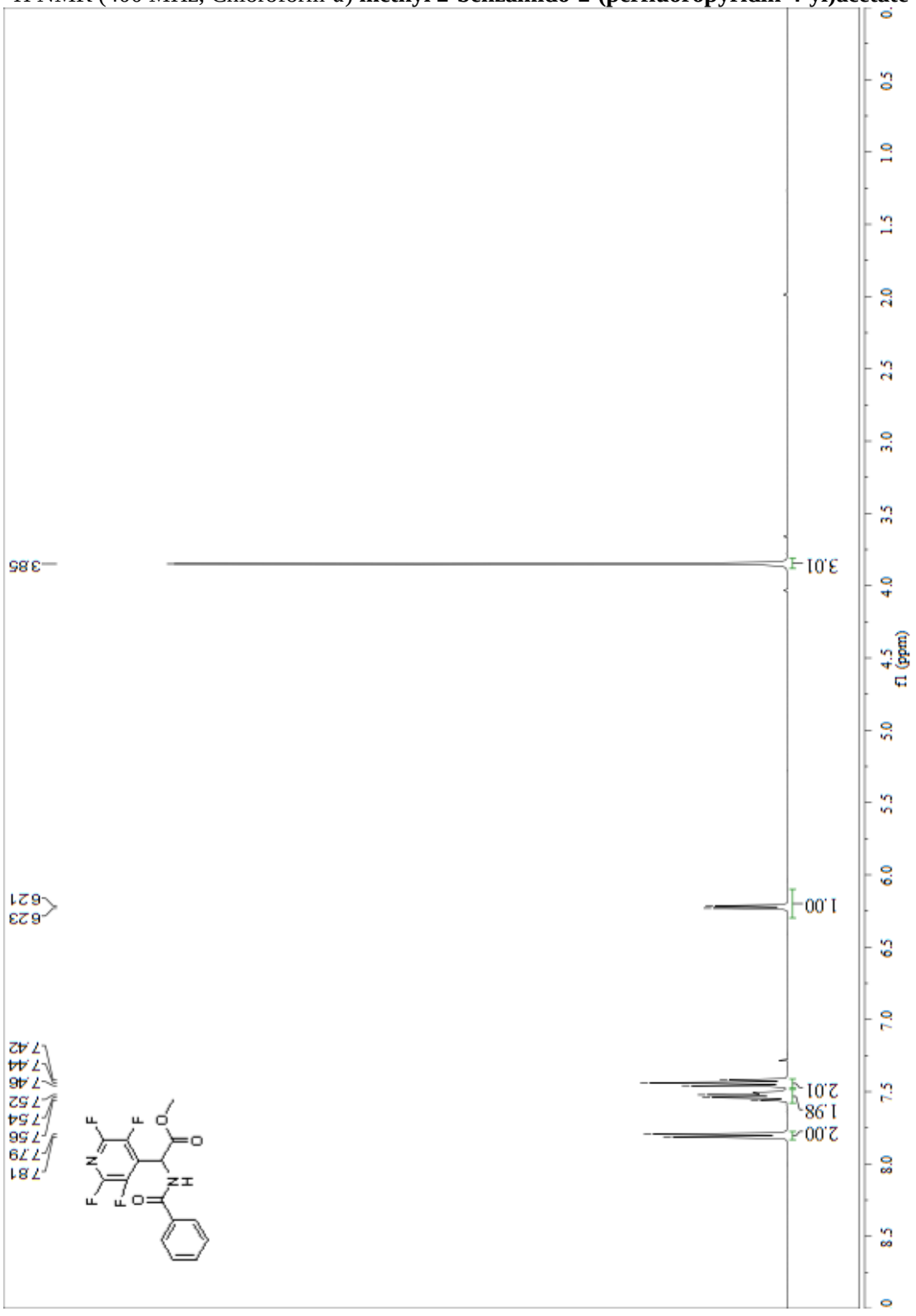

^{19}F NMR (376 MHz, , Chloroform-*d)* **methyl 2-benzamido-2-(perfluoropyridin-4-yl)acetate**

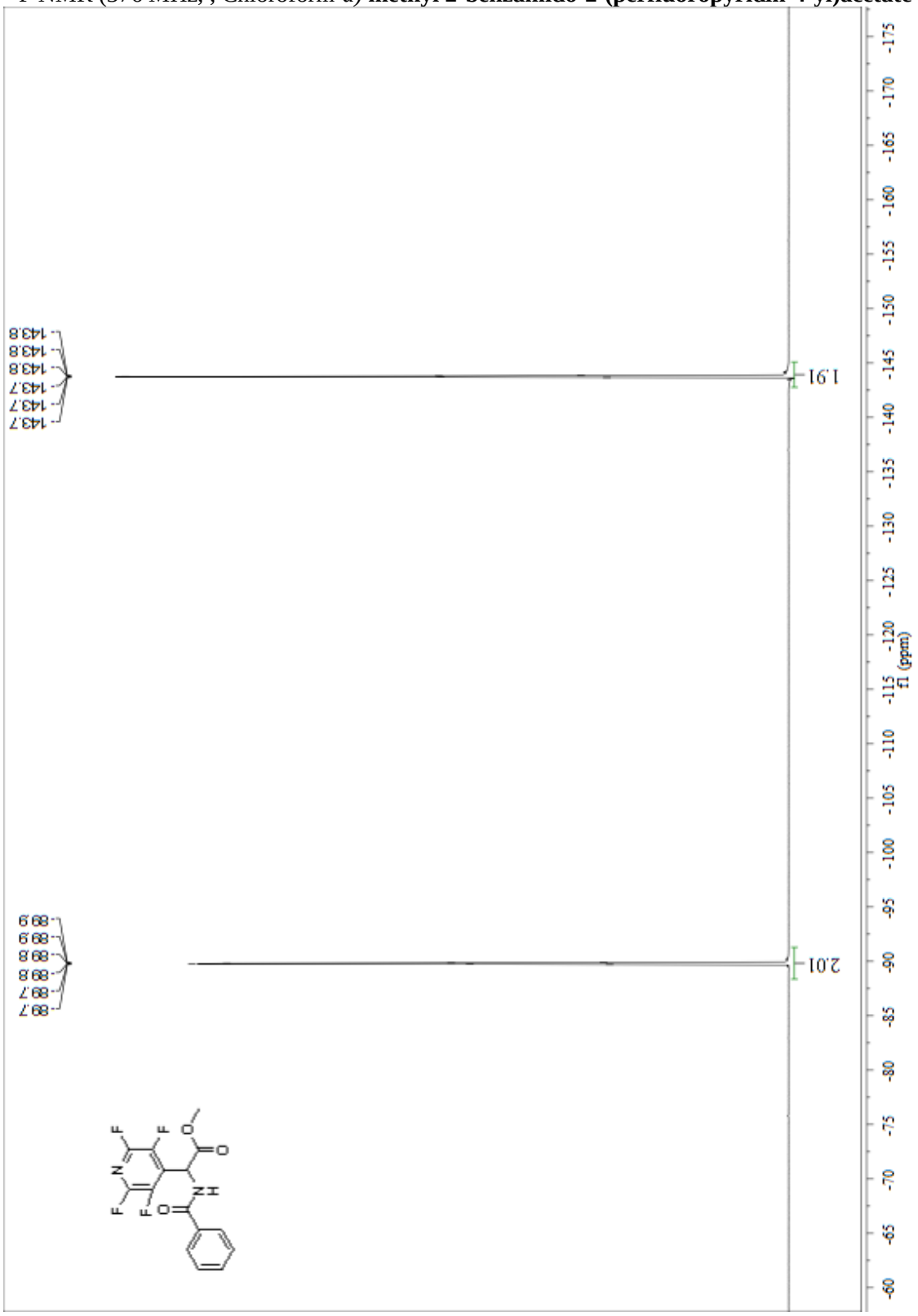

REFERENCES

1. Wang, J.; Sanchez-Rosello, M.; Acena, J. L.; del Pozo, C.; Sorochinsky, A. E.; Fustero, S.; Soloshonok, V. A.; Liu, H., *Chem. Rev.* **2014,** *114* (4), 2432-506.
2. Mast, N.; Zheng, W.; Stout, C. D.; Pikuleva, I. A., *Mol. Pharmacol.* **2013,** *84* (1), 86-94.
3. Ghosh, A.; Banerjee, S., Sulfonated Fluorinated-aromatic Polymers as Proton Exchange Membranes. 2014; Vol. 14, p 227-257.
4. Purser, S.; Moore, P. R.; Swallow, S.; Gouverneur, V., *Chem. Soc. Rev.* **2008,** *37* (2), 320-330.
5. Kiplinger, J. L.; Richmond, T. G.; Osterberg, C. E., *Chem. Rev.* **1994,** *94* (2), 373-431.
6. Savile, C. K.; Janey, J. M.; Mundorff, E. C.; Moore, J. C.; Tam, S.; Jarvis, W. R.; Colbeck, J. C.; Krebber, A.; Fleitz, F. J.; Brands, J.; Devine, P. N.; Huisman, G. W.; Hughes, G. J., *Science* **2010,** *329* (5989), 305.
7. Campbell, M. G.; Ritter, T., *Chem. Rev.* **2015,** *115* (2), 612-633.
8. Lentz, D.; Braun, T.; Kuehnel, M. F., *Angew. Chem. Int. Ed.* **2013,** *52* (12), 3328-3348.
9. Ahrens, T.; Kohlmann, J.; Ahrens, M.; Braun, T., *Chem. Rev.* **2015,** *115* (2), 931-972.
10. Singh, A.; Kubik, J. J.; Weaver, J. D., *Chem. Sci.* **2015**.
11. Amii, H.; Uneyama, K., *Chem. Rev.* **2009,** *109* (5), 2119-2183.
12. Weaver, J.; Senaweera, S., *Tetrahedron* **2014,** *70* (41), 7413-7428.
13. Brooke, G. M., *J. Fluorine Chem.* **1997,** *86* (1), 1-76.
14. Bunnett, J. F.; Zahler, R. E., *Chem. Rev.* **1951,** *49* (2), 273-412.
15. Bunnett, J. F., *Acc. Chem. Res.* **1978,** *11* (11), 413-420.
16. Goldstein, S. W.; Bill, A.; Dhuguru, J.; Ghoneim, O., *J. Chem. Educ.* **2017,** *94* (9), 1388-1390.
17. Bunnett, J. F., *Q. Rev. Chem. Soc.* **1958,** *12* (1), 1-16.
18. Senaweera, S.; Weaver, J. D., *J. Org. Chem.* **2014,** *79* (21), 10466-10476.
19. Zhou, Q.-L., *Angew. Chem. Int. Ed.* **2015,** *55* (18), 5352-5353.
20. Qiu, R.; Chen, Y.; Yin, S.-F.; Xu, X.; Au, C.-T., *RSC Adv.* **2012,** *2* (29), 10774-10793.
21. List, B., *Chem. Rev.* **2007,** *107* (12), 5413-5415.
22. Bai, Y.; Chen, J.; Zimmerman, S. C., *Chem. Soc. Rev.* **2018,** *47* (5), 1811-1821.
23. Lalevee, J.; Blanchard, N.; Tehfe, M.-A.; Morlet-Savary, F.; Fouassier, J. P., *Macromolecules* **2010,** *43* (24), 10191-10195.
24. Kalyanasundaram, K.; Grätzel, M., *Coord. Chem. Rev.* **1998,** *177* (1), 347-414.
25. Lowry, M. S.; Bernhard, S., *Chem. Eur. J.* **2006,** *12* (31), 7970-7977.
26. Nicewicz, D. A.; Nguyen, T. M., *ACS Catalysis* **2014,** *4* (1), 355-360.
27. McCusker, J. K., *Acc. Chem. Res.* **2003,** *36* (12), 876-887.
28. sPac, C.; Ihama, M.; Yasuda, M.; Miyauchi, Y.; Sakurai, H., *J. Am. Chem. Soc.* **1981,** *103* (21), 6495-6497.

29. Fukuzumi, S.; Mochizuki, S.; Tanaka, T., *J. Phys. Chem. A* **1990,** *94* (2), 722-726.
30. Nicewicz, D. A.; MacMillan, D. W. C., *Science* **2008,** *322* (5898), 77-80.
31. Ischay, M. A.; Anzovino, M. E.; Du, J.; Yoon, T. P., *J. Am. Chem. Soc.* **2008,** *130* (39), 12886-12887.
32. King, K. A.; Spellane, P. J.; Watts, R. J., *J. Am. Chem. Soc.* **1985,** *107* (5), 1431-2.
33. Nguyen, J. D.; D'Amato, E. M.; Narayanam, J. M.; Stephenson, C. R., *Nat Chem* **2012,** *4* (10), 854-9.
34. Tang, K.-C.; Liu, K. L.; Chen, I. C., *Chem. Phys. Lett.* **2004,** *386* (4), 437-441.
35. Xu, H.; Chen, R.; Sun, Q.; Lai, W.; Su, Q.; Huang, W.; Liu, X., *Chem. Soc. Rev.* **2014,** *43* (10), 3259-3302.
36. Teegardin, K.; Day, J. I.; Chan, J.; Weaver, J., *Org. Process Res. Dev.* **2016,** *20* (7), 1156-1163.
37. Nguyen, J. D.; D'Amato, E. M.; Narayanam, J. M. R.; Stephenson, C. R. J., *Nat. Chem.* **2012,** *4* (10), 854-859.
38. Prier, C. K.; Rankic, D. A.; MacMillan, D. W. C., *Chem. Rev.* **2013,** *113* (7), 5322-5363.
39. Singh, A.; Arora, A.; Weaver, J. D., *Org. Lett.* **2013,** *15*, 5390-5393.
40. Senaweera, S. M.; Singh, A.; Weaver, J. D., *J. Am. Chem. Soc.* **2014,** *136* (8), 3002-3005.
41. Arora, A.; Teegardin, K. A.; Weaver, J. D., *Org. Lett.* **2015,** *17* (15), 3722-3725.
42. Singh, K.; Staig, S. J.; Weaver, J. D., *J. Am. Chem. Soc.* **2014,** *136* (14), 5275-5278.
43. Singh, K.; Fennell, C. J.; Coutsias, E. A.; Latifi, R.; Hartson, S.; Weaver, J. D., *Chem* **2018,** *4* (1), 124-137.
44. Singh, K.; Trinh, W.; Weaver, J. D., *Org. Biomol. Chem.* **2018**.
45. Day, J. I.; Singh, K.; Trinh, W.; Weaver, J. D., *J. Am. Chem. Soc.* **2018,** *140* (31), 9934-9941.
46. Khaled, M. B.; El Mokadem, R. K.; Weaver, J. D., *J. Am. Chem. Soc.* **2017,** *139* (37), 13092-13101.
47. Flamigni, L.; Barbieri, A.; Sabatini, C.; Ventura, B.; Barigelletti, F., *Top. Curr. Chem.* **2007,** *281*, 143-203.
48. Dedeian, K.; Djurovich, P. I.; Garces, F. O.; Carlson, G.; Watts, R. J., *Inorg. Chem.* **1991,** *30* (8), 1685-1687.
49. Tamayo, A. B.; Alleyne, B. D.; Djurovich, P. I.; Lamansky, S.; Tsyba, I.; Ho, N. N.; Bau, R.; Thompson, M. E., *J. Am. Chem. Soc.* **2003,** *125* (24), 7377-7387.
50. Lee, H. M.; Gong, S. C.; Choi, J. E.; Baek, S. J.; Chang, Y. C.; Chang, H. J., *Mol. Cryst. Liq. Cryst.* **2010,** *530*, 230-238.
51. Dedeian, K.; Shi, J.; Shepherd, N.; Forsythe, E.; Morton, D. C., *Inorg. Chem.* **2005,** *44* (13), 4445-4447.
52. Grushin, V. V.; Herron, N.; LeCloux, D. D.; Marshall, W. J.; Petrov, V. A.; Wang, Y., *Chem. Commun.* **2001,** (16), 1494-1495.
53. Konno, H.; Sasaki, Y., *Chem. Lett.* **2003,** *32* (3), 252-253.
54. Seiple, I. B.; Su, S.; Rodriguez, R. A.; Gianatassio, R.; Fujiwara, Y.; Sobel, A. L.; Baran, P. S., *J. Am. Chem. Soc.* **2010,** *132* (38), 13194-13196.
55. Singh, A.; Teegardin, K.; Kelly, M.; Prasad, K. S.; Krishnan, S.; Weaver, J. D., *J. Organomet. Chem.* **2015,** *776* (0), 51-59.
56. Zuo, Z.; MacMillan, D. W. C., *J. Am. Chem. Soc.* **2014,** *136* (14), 5257-5260.
57. Nonoyama, M., *Bull. Chem. Soc. Jpn. 47*, 467.
58. Lowry, M. S.; Goldsmith, J. I.; Slinker, J. D.; Rohl, R.; Pascal, R. A.; Malliaras, G. G.; Bernhard, S., *Chem. Mater.* **2005,** *17* (23), 5712-5719.

59. Yao, C.; Jiao, B.; Yang, X.; Xu, X.; Dang, J.; Zhou, G.; Wu, Z.; Lv, X.; Zeng, Y.; Wong, W.-Y., **2013,** *2013* (27), 4754-4763.
60. Kapturkiewicz, A.; Chen, T.-M.; Laskar, I. R.; Nowacki, J., *Electrochem. Commun.* **2004,** *6* (8), 827-831.
61. Okada, S.; Okinaka, K.; Iwawaki, H.; Furugori, M.; Hashimoto, M.; Mukaide, T.; Kamatani, J.; Igawa, S.; Tsuboyama, A.; Takiguchi, T.; Ueno, K., *Dalton Trans.* **2005,** (9), 1583-1590.
62. Hay, P. J., *J. Phys. Chem. A* **2002,** *106* (8), 1634-1641.
63. Park, N. G.; Choi, G. C.; Lee, Y. H.; Kim, Y. S., *Current Applied Physics* **2006,** *6* (4), 620-626.
64. Buckley, A., *Organic Light-Emitting Diodes (OLEDs): Materials, Devices and Applications*. Elsevier Science: 2013.
65. Dixon, I. M.; Collin, J. P.; Sauvage, J. P.; Flamigni, L.; Encinas, S.; Barigelletti, F., *Chem. Soc. Rev.* **2000,** *29* (6), 385-391.
66. Cummings, S. D.; Eisenberg, R., *J. Am. Chem. Soc.* **1996,** *118* (8), 1949-1960.
67. Constable, E. C.; Ertl, C. D.; Housecroft, C. E.; Zampese, J. A., *Dalton Trans.* **2014,** *43* (14), 5343-5356.
68. Song, D.-D.; Zhao, S.-L.; Luo, Y.-C.; Aziz, H., *Appl. Phys. Lett.* **2010,** *97* (24), 243304/1-243304/3.
69. Costa, R. D.; Arago, J.; Orti, E.; Pappenfus, T. M.; Mann, K. R.; Matczyszyn, K.; Samoc, M.; Zafra, J. L.; Lopez Navarrete, J. T.; Casado, J., *Chem. - Eur. J.* **2013,** *19* (4), 1476-1488.
70. Zhao, Y.; Sun, J., *Pattern Recognition* **2009,** *42* (5), 837-842.
71. Sengottuvelan, N.; Yun, S. J.; Kang, S. K.; Kim, Y. I., *Bull. Korean Chem. Soc.* **2011,** *32* (12), 4321-4326.
72. Ahmed, K.; Yellamelli Valli Venkata, S.; Mohammed, N. A. K.; Sultana, F.; Methuku, K. R., Recent advances on structural modifications of benzothiazoles and their conjugate systems as potential chemotherapeutics. Taylor & Francis: 2012; Vol. 21, pp 619-635.
73. Yin, Y.; Lin, L.; Ruiz, C.; Cameron, M. D.; Pocas, J.; Grant, W.; Schröter, T.; Chen, W.; Duckett, D.; Schürer, S.; Lograsso, P.; Feng, Y., *Bioorg. Med. Chem. Lett.* **2009,** *19* (23), 6686-6690.
74. Sessions, E. H.; Smolinski, M.; Wang, B.; Frackowiak, B.; Chowdhury, S.; Yin, Y.; Chen, Y. T.; Ruiz, C.; Lin, L.; Pocas, J.; Schröter, T.; Cameron, M. D.; Lograsso, P.; Feng, Y.; Bannister, T. D., *Bioorg. Med. Chem. Lett.* **2010,** *20* (6), 1939-1943.
75. Sessions, E. H.; Yin, Y.; Bannister, T. D.; Weiser, A.; Griffin, E.; Pocas, J.; Cameron, M. D.; Ruiz, C.; Lin, L.; Schürer, S. C.; Schröter, T.; Lograsso, P.; Feng, Y., *Bioorg. Med. Chem. Lett.* **2008,** *18* (24), 6390-6393.
76. Mayo, M. S.; Yu, X.; Zhou, X.; Feng, X.; Yamamoto, Y.; Bao, M., *Org. Lett.* **2014,** *16* (3), 764.
77. Vechorkin, O.; Proust, V.; Hu, X., *Angew. Chem. Int. Ed.* **2010,** *49* (17), 3061-3064.
78. Teng, Q.; Hu, J.; Ling, L.; Sun, R.; Dong, J.; Chen, S.; Zhang, H., *Org. Biomol. Chem.* **2014,** *12* (39), 7721-7727.
79. Zhao, X.; Wu, G.; Zhang, Y.; Wang, J., *J. Am. Chem. Soc.* **2011,** *133* (10), 3296.
80. Xia, J.-D.; Deng, G.-B.; Zhou, M.-B.; Liu, W.; Xie, P.; Li, J.-H., *Synlett* **2012,** *23* (18), 2707-2713.
81. Molander, G. A.; Harring, L. S., *J. Org. Chem.* **1990,** *55* (25), 6171-6176.
82. Junji, I.; Mitsuhiro, I.; Masaru, Y., *Chem. Lett.* **1987,** *16* (7), 1485-1486.
83. Reginato, G.; Catalani, M. P.; Pezzati, B.; Di Fabio, R.; Bernardelli, A.; Curcuruto, O.; Moro, E.; Pozzan, A.; Mordini, A., *Org. Lett.* **2015,** *17* (3), 398.
84. Curran, D. P.; Totleben, M. J., *J. Am. Chem. Soc.* **1992,** *114* (15), 6050-6058.
85. Tan, K. L.; Park, S.; Ellman, J. A.; Bergman, R. G., *J. Org. Chem.* **2004,** *69* (21), 7329.

86. Tan, K. L.; Bergman, R. G.; Ellman, J. A., *J. Am. Chem. Soc.* **2002,** *124* (47), 13964.
87. Singh, A.; Arora, A.; Weaver, J. D., *Org. Lett.* **2013,** *15* (20), 5390-5393.
88. Cahard, E.; Schoenebeck, F.; Garnier, J.; Cutulic, S. P. Y.; Zhou, S.; Murphy, J. A., **2012,** *51* (15), 3673-3676.
89. Todres, Z. V., *Ion-Radical Organic Chemistry: Principles and Applications*. Second Edition ed.; CRC Press: Columbus, Ohio, 2008; p 496.
90. Arora, A.; Weaver, J. D., *Acc. Chem. Res.* **2016,** *49* (10), 2273-2283.
91. Pierini, A. B.; Vera, D. M. A., *J. Org. Chem.* **2003,** *68* (24), 9191-9199.
92. Saveant, J. M., *Acc. Chem. Res.* **1980,** *13* (9), 323-329.
93. Rossi, R. A., *Acc. Chem. Res.* **1982,** *15* (6), 164-170.
94. Rono, L. J.; Yayla, H. G.; Wang, D. Y.; Armstrong, M. F.; Knowles, R. R., *J. Am. Chem. Soc.* **2013**.
95. Ismaili, H.; Pitre, S. P.; Scaiano, J. C., *Catal. Sci. Technol.* **2013,** *3* (4), 935-937.
96. Narayanam, J. M. R.; Tucker, J. W.; Stephenson, C. R. J., *J. Am. Chem. Soc.* **2009,** *131* (25), 8756-8757.
97. Loh, Y. Y.; Nagao, K.; Hoover, A. J.; Hesk, D.; Rivera, N. R.; Colletti, S. L.; Davies, I. W.; MacMillan, D. W. C., *Science* **2017,** *358* (6367), 1182.
98. Srivastava, V. P.; Yadav, A. K.; Yadav, L. D. S., *Synlett* **2013,** (4), 465-470.
99. Carr, A.; Maynard, G.; Kane, J. M.; Cheng, H.; Dudley, M.
100. Chen, H.-J.; Wang, W.-L.; Wang, G.-F.; Shi, L.-P.; Gu, M.; Ren, Y.-D.; Hou, L.-F.; He, P.-L.; Zhu, F.-H.; Zhong, X.-G.; Tang, W.; Zuo, J.-P.; Nan, F.-J., **2008,** *3* (9), 1316-1321.
101. Townsend, L. B.; Devivar, R. V.; Turk, S. R.; Nassiri, M. R.; Drach, J. C., *J. Med. Chem.* **1995,** *38* (20), 4098-4105.
102. Onaran, M. B.; Seto, C. T., *J. Org. Chem.* **2003,** *68* (21), 8136-8141.
103. Tachibana, Y.; Yamahata, M.; Kasuya, K.-i., *Green Chem.* **2013,** *15* (5), 1318-1325.
104. Neuhaus, C. M.; Liniger, M.; Stieger, M.; Altmann, K.-H., **2013,** *52* (22), 5866-5870.
105. Abdel-Magid, A. F.; Carson, K. G.; Harris, B. D.; Maryanoff, C. A.; Shah, R. D., *J. Org. Chem.* **1996,** *61* (11), 3849-3862.
106. Johnson, T. C.; Marsden, S. P., *Org. Lett.* **2016,** *18* (20), 5364-5367.
107. Fisk, J. S.; Mosey, R. A.; Tepe, J. J., *Chem. Soc. Rev.* **2007,** *36* (9), 1432-1440.
108. Hewlett, N. M.; Hupp, C. D.; Tepe, J. J., *Synthesis* **2009,** *2009* (17), 2825-2839.
109. Chai, Z.; Wang, B.; Chen, J.-N.; Yang, G., *Adv. Synth. Catal.* **2014,** *356* (11-12), 2714-2718.
110. Liu, X.; Hartwig, J. F., *Org. Lett.* **2003,** *5* (11), 1915-1918.
111. Wang, T.; Yu, Z.; Hoon, D. L.; Phee, C. Y.; Lan, Y.; Lu, Y., *J. Am. Chem. Soc.* **2016,** *138* (1), 265-271.
112. D'Anello, M.; Erba, E.; Gelmi, M. L.; Pocar, D., *Ber.* **1988,** *121* (1), 67-73.
113. Senaweera, S. M.; Singh, A.; Weaver, J. D., *J. Am. Chem. Soc.* **2014,** *136* (8), 3002–3005.
114. Margetic, D., Physico-Chemical Properties of Organosuperbases. In *Superbases for Organic Synthesis*, John Wiley & Sons, Ltd: 2009; pp 9-48.
115. Lv, H.; Zhan, J.-H.; Cai, Y.-B.; Yu, Y.; Wang, B.; Zhang, J.-L., *J. Am. Chem. Soc.* **2012,** *134* (39), 16216-16227.
116. Gung, B. W.; Amicangelo, J. C., *J. Org. Chem.* **2006,** *71* (25), 9261-9270.
117. Al-Sayyab, A. F.; Lawson, A., *J. Chem. Soc. C* **1968,** (0), 406-410.
118. Alemán, J.; Milelli, A.; Cabrera, S.; Reyes, E.; Jørgensen, K. A., *Chem.—Eur. J.* **2008,** *14* (35), 10958-10966.
119. Cruz, D. S.; Castilho, M. S., *Med. Chem.* **2014,** *10* (2), 162-173.

120. Malamas, M. S.; Erdei, J.; Gunawan, I.; Barnes, K.; Hui, Y.; Johnson, M.; Robichaud, A.; Zhou, P.; Yan, Y.; Solvibile, W.; Turner, J.; Fan, K. Y.; Chopra, R.; Bard, J.; Pangalos, M. N., *Bioorg. Med. Chem. Lett.* **2011,** *21* (18), 5164-5170.
121. Zhou, P.; Li, Y.; Fan, Y.; Wang, Z.; Chopra, R.; Olland, A.; Hu, Y.; Magolda, R. L.; Pangalos, M.; Reinhart, P. H.; Turner, M. J.; Bard, J.; Malamas, M. S.; Robichaud, A. J., *Bioorg. Med. Chem. Lett.* **2010,** *20* (7), 2326-2329.
122. Nowak, P., et al., *Bioorg. Med. Chem. Lett.* **2010,** *20* (2), 632-635.
123. Malamas, M. S.; Robichaud, A.; Erdei, J.; Quagliato, D.; Solvibile, W.; Zhou, P.; Morris, K.; Turner, J.; Wagner, E.; Fan, K.; Olland, A.; Jacobsen, S.; Reinhart, P.; Riddell, D.; Pangalos, M., *Bioorg. Med. Chem. Lett.* **2010,** *20* (22), 6597-6605.
124. Malamas, M. S.; Erdei, J.; Gunawan, I.; Turner, J.; Hu, Y.; Wagner, E.; Fan, K.; Chopra, R.; Olland, A.; Bard, J.; Jacobsen, S.; Magolda, R. L.; Pangalos, M.; Robichaud, A. J., *J. Med. Chem.* **2010,** *53* (3), 1146-1158.
125. Malamas, M. S.; Barnes, K.; Johnson, M.; Hui, Y.; Zhou, P.; Turner, J.; Hu, Y.; Wagner, E.; Fan, K.; Chopra, R.; Olland, A.; Bard, J.; Pangalos, M.; Reinhart, P.; Robichaud, A. J., *Bioorg. Med. Chem.* **2010,** *18* (2), 630-639.
126. Mesaik, M. A.; Rahat, S.; Khan, K. M.; Zia, U.; Choudhary, M. I.; Murad, S.; Ismail, Z.; Atta ur, R.; Ahmad, A., *Biorg. Med. Chem.* **2004,** *12* (9), 2049-2057.
127. Melhado, A. D.; Luparia, M.; Toste, F. D., *J. Am. Chem. Soc.* **2007,** *129* (42), 12638-12639.
128. Badiola, E.; Fiser, B.; Gómez-Bengoa, E.; Mielgo, A.; Olaizola, I.; Urruzuno, I.; García, J. M.; Odriozola, J. M.; Razkin, J.; Oiarbide, M.; Palomo, C., *J. Am. Chem. Soc.* **2014,** *136* (51), 17869-17881.
129. Witkowska, R.; Kaczmarek, K.; Crisma, M.; Toniolo, C.; Zabrocki, J., *J. Pept. Sci.* **2001,** *7* (12), 619-625.
130. Tanaka, K.; Deguchi, M.; Yamaguchi, S.; Yamada, K.; Iwata, S., *J. Heterocycl. Chem.* **2001,** *38* (1), 131-136.
131. Noisier, A. F. M.; Brimble, M. A., *Chem. Rev.* **2014,** *114* (18), 8775-8806.
132. Nájera, C.; Sansano, J. M., *Chem. Rev.* **2007,** *107* (11), 4584-4671.
133. Sorochinsky, A. E.; Aceña, J. L.; Moriwaki, H.; Sato, T.; Soloshonok, V. A., *Amino Acids* **2013,** *45* (4), 691-718.
134. Gokada, M. R.; Hunter, R.; Andrijevic, A.; Petersen, W. F.; Samanta, S.; Venter, G.; Rees-Jones, S., *J. Org. Chem.* **2017,** *82* (19), 10650-10658.
135. Hugelshofer, C. L.; Mellem, K. T.; Myers, A. G., *Org. Lett.* **2013,** *15* (12), 3134-3137.
136. Touzin, P. A. M., *Tetrahedron Lett.* **1975,** *16* (18), 1477-1480.
137. Mkairi, A.; Hamelin, J., *Tetrahedron Lett.* **1987,** *28* (13), 1397-1400.
138. El Achqar, A.; Boumzebra, M.; Roumestant, M.-L.; Viallefont, P., *Tetrahedron* **1988,** *44* (17), 5319-5332.
139. López, A.; Moreno-Mañas, M.; Pleixats, R.; Roglans, A.; Ezquerra, J.; Pedregal, C., *Tetrahedron* **1996,** *52* (24), 8365-8386.
140. Xue, Z.-Y.; Song, Z.-M.; Wang, C.-J., *Org. Biomol. Chem.* **2015,** *13* (19), 5460-5466.
141. Chun-Yan, L.; Wu-Lin, Y.; Xiaoyan, L.; Wei-Ping, D., *Chem. Eur. J.* **2015,** *21* (52), 19048-19057.
142. Koizumi, A.; Harada, M.; Haraguchi, R.; Fukuzawa, S.-i., *J. Org. Chem.* **2017,** *82* (17), 8927-8932.
143. Stork, G.; Leong, A. Y. W.; Touzin, A. M., *J. Org. Chem.* **1976,** *41* (21), 3491-3493.
144. Liu, Z.; Rigger, L.; Rossi, J.-C.; Sutherland John, D.; Pascal, R., *Chem. Eur. J.* **2016,** *22* (42), 14940-14949.

145. R., A. A. N.; Xavier, C.; Guillem, V.; Albert, M.; Ramon, R., *Chem. Eur. J.* **2010,** *16* (18), 5354-5361.
146. Wang, C.-M.; Xiao, J.-A.; Wang, J.; Wang, S.-S.; Deng, Z.-X.; Yang, H., *J. Org. Chem.* **2016,** *81* (17), 8001-8008.
147. Wegmann, H.; Steglich, W., *Chem. Ber.* **1981,** *114* (7), 2580-2594.
148. Jiang, H.; Paixão, M. W.; Monge, D.; Jørgensen, K. A., *J. Am. Chem. Soc.* **2010,** *132* (8), 2775-2783.
149. In fact, we have previously utilized the oxazolone enolate for α-arylation via SNAr addition to a perfluoroarene to give novel non-natural fluorinated amino acids. Unfortunately, attempts to trap the product oxazalone enolate with a secondary electrophile (other than a proton) failed to give a disubstituted oxazaolone
150. McIntosh, J. M.; Thangarasa, R.; Ager, D. J.; Zhi, B., *Tetrahedron* **1992,** *48* (30), 6219-6224.
151. Ackrell, J.; Muchowski, J. M.; Galeazzi, E.; Guzman, A., *J. Org. Chem.* **1986,** *51* (17), 3374-3376.
152. Djuric, S.; Venit, J.; Magnus, P., *Tetrahedron Lett.* **1981,** *22* (19), 1787-1790.
153. Danner, P.; Morkunas, M.; Maier, M. E., *Org. Lett.* **2013,** *15* (10), 2474-2477.
154. Burroughs, L.; Clarke, P. A.; Forintos, H.; Gilks, J. A. R.; Hayes, C. J.; Vale, M. E.; Wade, W.; Zbytniewski, M., *Org. Biomol. Chem.* **2012,** *10* (8), 1565-1570.
155. Lubell, W. D.; Rapoport, H., *J. Am. Chem. Soc.* **1988,** *110* (22), 7447-7455.
156. Lee, J.; Choi, W. B.; Lynch, J. E.; Volante, R. P.; Reider, P. J., *Tetrahedron Lett.* **1998,** *39* (22), 3679-3682.
157. Thompson, C. M.; Green, D. L. C., *Tetrahedron* **1991,** *47* (25), 4223-4285.
158. Krapcho, A. P.; Dundulis, E. A., *Tetrahedron Lett.* **1976,** *17* (26), 2205-2208.
159. Hoye, T. R.; Duff, S. R.; King, R. S., *Tetrahedron Lett.* **1985,** *26* (29), 3433-3436.
160. Teegardin, K. A.; Weaver, J. D., *Chem. Commun.* **2017,** *53* (35), 4771-4774.
161. Kaljurand, I.; Kütt, A.; Sooväli, L.; Rodima, T.; Mäemets, V.; Leito, I.; Koppel, I. A., *J. Org. Chem.* **2005,** *70* (3), 1019-1028.
162. Senaweera, S. M.; Weaver, J. D., *J. Org. Chem.* **2014,** *79* (21), 10466-10476.
163. Day, J. I.; Weaver, J. D., *T J. Org. Chem.* **2017,** *82* (13), 6801-6810.
164. Kaljurand, I.; Saame, J.; Rodima, T.; Koppel, I.; Koppel, I. A.; Kögel, J. F.; Sundermeyer, J.; Köhn, U.; Coles, M. P.; Leito, I., *J. Phys. Chem. A A* **2016,** *120* (16), 2591-2604.
165. Seebach, D.; Bossler, H.; Gründler, H.; Shoda, S. I.; Wenger, R., *Helv. Chim. Acta* **1991,** *74* (1), 197-224.
166. Maetzke, T.; Hidber, C. P.; Seebach, D., *J. Am. Chem. Soc.* **1990,** *112* (23), 8248-8250.
167. O'Neil, I. A.; Bhamra, I., *Tetrahedron Lett.* **2009,** *50* (26), 3635-3638.
168. F., D. H., et al., *J. Neurochem.* **2001,** *76* (1), 173-181.
169. Teodorczyk, M.; Schmidt, M. H. H., *Frontiers in Oncology* **2014,** *4*, 341.
170. Bon, R. S.; Sprenkels, N. E.; Koningstein, M. M.; Schmitz, R. F.; de Kanter, F. J. J.; Domling, A.; Groen, M. B.; Orru, R. V. A., *Org. Biomol. Chem.* **2008,** *6* (1), 130-137.
171. Anderson, Z. J.; Hobson, C.; Needley, R.; Song, L.; Perryman, M. S.; Kerby, P.; Fox, D. J., *Org. Biomol. Chem.* **2017,** *15* (44), 9372-9378.
172. Ma, B.; Luo, W.; Lin, L.; Liu, X.; Feng, X., *Chem. Commun.* **2017,** *53* (29), 4077-4079.
173. Vong Kenward King, H.; Maeda, S.; Tanaka, K., *Chem. Eur. J.T* **2016,** *22* (52), 18865-18872.
174. Karnik, A. V.; Kamath, S. S., *J. Org. Chem.* **2007,** *72* (19), 7435-7438.
175. Thalluri, K.; Nadimpally, K. C.; Chakravarty, M. P.; Paul, A.; Mandal, B., *Adv. Synth. Catal.* **2013,** *355* (2-3), 448-462.

176. Wagner, A. J.; Zubarev, D. Y.; Aspuru-Guzik, A.; Blackmond, D. G., *ACS Central Science* **2017,** *3* (4), 322-328.
177. Mondal, M.; Radeva, N.; Köster, H.; Park, A.; Potamitis, C.; Zervou, M.; Klebe, G.; Hirsch Anna, K. H., *Angew. Chem. Int. Ed.* **2014,** *53* (12), 3259-3263.
178. Banphavichit, V.; Mansawat, W.; Bhanthumnavin, W.; Vilaivan, T., *Tetrahedron* **2009,** *65* (29), 5849-5854.
179. Li, G.; Hu, J.; Zeng, R.; Shi, D.-Q.; Zhao, Y., *Org. Lett.* **2018,** *20* (8), 2454-2458.
180. Bin, X.; Shou-Fei, Z.; Xiu-Lan, X.; Jun-Jie, S.; Qi-Lin, Z., *Angew. Chem. Int. Ed.* **2011,** *50* (48), 11483-11486.
181. Vanfleteren, L.; Anteunis, M. J. O., *Bull. Soc. Chim. Belg.* **1988,** *97* (7), 505-517.
182. Audia, J. E.; Britton, T. C.; Droste, J. J.; Folmer, B. K.; Huffman, G. W.; John, V.; Latimer, L. H.; Mabry, T. E.; Nissen, J. S.; Porter, W. J.; Reel, J. K.; Thorsett, E. D.; Tung, J. S.; Wu, J. Preparation of peptides for inhibiting β-amyloid peptide release and/or its synthesis. US6207710B1, 2001.

APPENDICES

Intersystem crossing (ISC).

Metal Ligand Charge Transfer (MLCT)

Single Electron Transfer (SET)

Regioisomeric ratio (rr)

1,8-Diazabicyclo[5.4.0]undec-7-ene (DBU)

Structure activity relationship (SAR)

Hydrogen atom transfer (HAT)

Diastereoisomeric ratio (dr)

Enantiomeric excess (*ee*)

Trimethylamine (TEA, Et3N)

Di-isoprpylethylamine (DIPEA)

Dichloromethane (DCM)

Acetonitrile (MeCN)

Hydrogen atom transfer (HAT)

Methanol (MeOH)

N, N-Dimethylformamide (DMF)

Tetrahydrofuran (THF)

Thin layer chromatography (TLC)

Phenyl (Ph)

Benzyl (Bn)

Trimethylsilyl (TMS)

tert-Butyloxycarbonyl (Boc)

Methyl (Me)

Starting material (SM)

VITA

Kip Allen Teegardin

Candidate for the Degree of

Doctor of Philosophy

Dissertation: PRACTICAL SYNTHESES OF IRIDIUM COMPLEXES FOR PHOTOCATALYSIS AND THE DEVELOPMENT OF METHODOLOGY TO ACCESS FUNCTIONALIZED AMINO ACIDS

Major Field: Chemistry

Biographical:

Education:

Completed the requirements for the Doctor of Philosophy in Chemistry at Oklahoma State University, Stillwater, Oklahoma in December, 2018.

Completed the requirements for the Bachelor of Science in Chemistry-Biochemistry at University of Arkansas-Fort Smith, Fort Smith, Arkansas in 2012.

Experience:
Lab Technician, University of Arkansas-Fort Smith

Professional Memberships:
American Chemical Society Since 2015
American Chemical Society Division of Organic Chemistry Since 2015